

## The Metallogeny of Volcanic Arcs: Short Course Notes

BCMEMPOR Open File 1998-8

Coordinated by D.V. Lefebure

Open File 1998-8 consists of over 500 pages of notes from the course which consisted of 17 presentations by speakers from government, universities and the private sector. The notes include information concerning the tectonic and structural features of arc deposits, geoenvironmental mineral deposit models, epithermal deposits and their transitions to porphyry settings, porphyry copper and gold deposits, gemstones, unconventional metallic deposits, industrial minerals, skarns and volcanogenic massive sulphides. The following are abstracts of those presentations.

The notes include information concerning the tectonic and structural features of arc deposits, geoenvironmental mineral deposit models, epithermal deposits and their transitions to porphyry settings, porphyry copper and gold deposits, gemstones, unconventional metallic deposits, industrial minerals, skarns and volcanogenic massive sulphides.

## Table of Contents

### INTRODUCTION

- A - Arc Metallogeny - Selected Bibliography: J. Thompson, The University of British Columbia
- B - Tectonic and Structural Features of Arc Deposits: R.V. Kirkham, Geological Survey of Canada
- C - Geoenvironmental Mineral Deposit Models for the Northern Cordillera: R. Goldfarb, E. du Bray, J. Gray, K. Kelley and G. Plumlee, U.S. Geological Survey

### EPITHERMAL AND PORPHYRY

- D - Potential for High Sulphidation Epithermal Gold Deposits in Canada: The Example of the Hope Brook Au Cu Newfoundland: B. Dubé, Geological Survey of Canada and Greg Dunning, Memorial University of Newfoundland
- E - Transitions from Porphyry to Epithermal Environments: A. Panteleyev, XDM Geological Consultants
- F - Porphyry Deposits in Volcanic Arcs with Deposits on the Canadian Cordillera: W.J. McMillan, B.C. Geological Survey
- G - Alkalic Cu-Au-Ag Porphyry Deposits in the Canadian Cordillera: Tectonic Setting, Magmatic Affiliations and Hydrothermal Characteristics: J. Lang, J.F.H. Thompson, and C.R. Stanley, The University of British Columbia
- H - Alkalic-Type Epithermal Gold Deposits: J.P. Richards, University of Alberta

### OTHER DEPOSITS

- I - Unconventional Metallic Deposits in Volcanic Arcs: D.V. Lefebure and G.E. Ray, B.C. Geological Survey
- J - Gemstones in Volcanic Arc Environments: G. Simandl, B.C. Geological Survey
- K - The Relationship Between Intrusion-related Au-(Cu) Sulphide Veins and Mo Breccias: Rosslund: T. Höy, D. Alldrick and K. Dunne, B.C. Geological Survey
- L - Industrial Minerals in Island Arcs: D. Hora, B.C. Geological Survey
- M - Skarns and Skarn Deposits in the Canadian Cordillera: G.E. Ray, B.C. Geological Survey

### VOLCANOGENIC MASSIVE SULPHIDES

- N - Arc-related Volcanogenic Massive Sulphide Deposits: J. Franklin, M.D. Hannington, I.R. Jonasson and C.T. Barrie, Geological Survey of Canada
- O - Geoenvironmental Model of Volcanogenic Massive Sulphide Deposits: C. Alpers and R.A. Zierenberg, U.S. Geological Survey



## MORE EPITHERMAL AND PORPHYRY

P - Geoenvironmental Characteristics of Epithermal and Porphyry Deposits: G.S. Plumlee, U.S. Geological Survey

Q - Porphyry Gold Deposits of the Andean Cordillera: J.L. Muntean, Homestake Mining Company

## A - ARC METALLOGENY - SELECTED BIBLIOGRAPHY

John Thompson, The University of British Columbia

Barton, M.D. (1996): Granitic Magmatism and Metallogeny of Southwestern North America, Geological Society of America, Special Paper 315, p. 261-280.

Carlile, J.C. and Mitchell, A.H.G. (1994): Magmatic Arcs and Associated Gold and Copper Mineralization in Indonesia, in van Leeuwen, T. M., Hedenquist, J.W., James, L.P. and Dow, J.A.S., eds., Mineral deposits of Indonesia; discoveries of the past 25 years., 50; 1-3. Journal of Geochemical Exploration: Amsterdam-New York, International, Elsevier, p. 91-142.

Hamilton (1995): Subduction Systems and Magmatism, Geological Society Special Publication 81, p. 3-28.

Hutchinson, R.W. and Albers, J.P. (1992): Metallogenic Evolution of the Cordilleran Region of the Western United States, in Burchfiel, B. C., Lipman, P. W., and Zoback, M. L., eds., The Cordilleran Orogen; conterminous U.S., United States, Geol. Soc., p. 629-652.

Lang, J.R., Lueck, B., Mortensen, J.K., Russell, J.K., Stanley, C.R. and Thompson, J.F.H. (1995): Triassic-Jurassic Silica-undersaturated and Silica-saturated Alkaline Intrusions in the Cordillera of British Columbia: Implications for Arc magmatism, Geology, Volume 23, p. 451-454.

Lipman, P.W. and Hagstrum, J.T. (1992): Jurassic Ash-flow Sheets, Calderas, and Related Intrusions of the Cordilleran Volcanic Arc in Southeastern Arizona; Implications for Regional Tectonics and Ore Deposits: Geological Society of America Bulletin, v. 104, p. 32-39.

Macdonald, A.J., Lewis, P.D., Thompson, J.F.H., Nadaraju, G., Bartsch, R., Bridge, D.J., Rhys, D.A., Roth, T., Kaip, A., Godwin, C.I. and Sinclair, A. J. (1996): Metallogeny of an Early to Middle Jurassic Arc, Iskut River Area, Northwestern British Columbia: Economic Geology and the Bulletin of the Society of Economic Geologists, v. 91, p. 1098-1114.

Mitchell, A.H.G. and Garson, M.S. (1981) Mineral Deposits and Global Tectonic Settings: London, United Kingdom, Acad. Press, 421 p.

Mitchell, A.H.G. and Leach, T.M. (1991) Epithermal Gold in the Philippines; Island Arc Metallogenesis, Geothermal Systems and Geology: London, United Kingdom, Acad. Press, 457 p.

Sawkins, F.J. (1990): Metal Deposits in Relation to Plate Tectonics. ed: New York, NY, United States, Springer-Verlag, 461 p.

Sillitoe, R.H. (1981): Ore Deposits in Cordilleran and Island-arc Settings, in Dickinson, W.R. and Payne, W.D., eds., Relations of Tectonics to Ore Deposits in the Southern Cordillera., 14. Arizona Geological Society Digest: Tucson, AZ, United States, Arizona Geological Society, p. 49-69.

Sillitoe, R.H. (1987): Copper, Gold and Subduction; A Trans-Pacific Perspective, in Brennan, E., ed., Pacific Rim Congress 87; an international congress on the geology, structure, mineralization and

economics of the Pacific Rim.: Parkville, Victoria, Australia, Australas. Inst. Min. and Metall., p. 399-403.

Sillitoe, R.H. (1988): Epochs of Intrusion-related Copper Mineralization in the Andes, *Journal of South American Earth Sciences*, V. 1, p. 89-108.

Sillitoe, R.H. (1991): Gold Metallogeny in Chile - An Introduction, *Economic Geology*, V. 86, p.1187-1205.

Sillitoe, R.H. (1995): The Influence of Magmatic-hydrothermal Models on Exploration Strategies for Volcano-Plutonic Arcs, *Mineralogical Association of Canada, Short Course*, V. 23, p. 511-525.

Solomon, M. (1990): Subduction, Arc Reversal, and the Origin of Porphyry Copper-gold Deposits in Island Arcs: *Geology (Boulder)*, v. 18, p. 630-633.

Thompson, J.F.H., Mortensen, J.K. and Lang, J.R. (1995): Magma Suites and Metallogeny - Examples from the Cordillera, *Australian Institute of Mining and Metallurgy, Proceedings of the 1995 PACRIM Congress*, p. 569-574.

Titley, S. (1995): Geological Summary and Perspective of Porphyry Copper Deposits in Southwestern North America, *Arizona Geological Society Digest* 20, p. 6-20.

Wolfe, J.A. (1988): Arc Magmatism and Mineralization in North Luzon and its Relationship to Subduction at the East Luzon and North Manila Trenches: *Journal of Southeast Asian Earth Sciences*, v. 2, p. 79-93.

## B - TECTONIC AND STRUCTURAL FEATURES OF ARC DEPOSITS

R.V. Kirkham, Geological Survey of Canada

Kirkham, R.V. (1998): Tectonic and Structural Features of Arcs Deposits; in *Metallogeny of Volcanic Arcs*, B.C. Geological Survey, Short Course Notes, Open File 1998-8, Section B.

### ABSTRACT

Tectonic and structural features of arc deposits can be helpful to the exploration geologist in understanding the distribution and complexity of deposits. Nevertheless, especially in ancient terranes, key tectonic and structural features can be difficult to determine, hence workers often ignore their importance. This talk will consider some tectonic and structural features of arc and other consumptive plate margin deposits and their bearing on exploration.

Arcs are chains of volcanoes that sit above subduction zones along consumptive plate margins in both oceanic and continental margin settings. Arcs can be compressional, extensional, or neutral. Each of these structural states leads to distinctive tectonic settings that control the formation of different types of mineral deposits with different geological features and metal contents. Moreover, some atypical arc and other consumptive plate margin environments were probably of particular importance in the formation of some giant deposits.

In both compressional and neutral arc settings, during and closely following constructive arc volcanism, characteristically porphyry Cu and Au deposits form in the root zones and high- and low-sulphidation epithermal Au(-Ag) deposits form near the tops of andesitic stratovolcanoes (e.g., Batu Hijau, El Teniente, and La Coipa). Such deposits are typically aligned along the traces of former arcs (e.g., the various porphyry belts in northern Chile and southern Peru). Nevertheless, the same deposit types can form in similar volcanic and subvolcanic settings but the deposits are aligned along markedly transverse structures at high angles to the main volcanic arcs (volcanic fronts) (e.g., Bajo de la Alumbrera, Agua Rica, Butte, and Zortman-Landusky). In some cases the transverse trends might be related to the transform fault edge of a flat subducting slab or to the subduction of buoyant aseismic ridges.

In arcs under extension intra-arc rifts can develop and if the rifting is successful deep back-arc rifts can form, both of which are favourable sites for the formation of volcanogenic massive sulphide (VMS) deposits. Kuroko-type VMS deposits related to submarine bimodal felsic and mafic volcanism form in intra-arc to back-arc settings during the dismemberment of arcs (e.g., Hokuroku district and Eskay Creek) and Besshi- and Cyprus-type VMS deposits related to submarine mafic volcanism form in successful back-arc rifts.

An atypical arc environment that could be favourable for the formation of bulk-mineable Au(-Ag) deposits is where oceanic spreading ridges intersect arcs at high angles closely following subduction (e.g., Ladolam and Misima). Also some porphyry Cu-Au and epithermal deposits evidently formed in collision zones closely following termination of subduction in areas with hot metasomatized mantle (e.g., Grasberg and Porgera). Other environments that could be favourable for porphyry Mo and

epithermal Au(-Ag) deposits related to bimodal and calc-alkalic volcanism in areas of slab windows and gaps developed following subduction where spreading ridges intersect subduction zones (e.g., McLaughlin and Kitsault).

Important structural features of deposits can be of two types: those synchronous with magmatic activity (e. g., controlling magmatism, vein orientation, and alignment of deposits along faults) and post-ore structures that severely disrupt and displace deposits. The concern in this talk is mostly with post-ore structures that disrupt the deposits but also can preserve them. Some deposits have undergone penetrative deformation with strong stretching lineation and flattening fabrics and some are cut by thrust faults that have juxtaposed divergent mineral and alteration types (e.g., Sulphurets area, British Columbia). Many parts of the American and Canadian Cordillera, and probably elsewhere, have suffered extension which has tilted and dismembered deposits. In places the tilting has partly protected the deposit from erosion (e.g., San Manuel-Kalamazoo, Ajo, Hall, Ely, Yerington, Endako, and Clark Lake at Chibougamau, Quebec) but in other areas it has completely dismembered the deposits, parts of the deposits being eroded away and other parts being displaced and buried (e.g., Sacaton-Santa Cruz). Knowledge of such deformation and disruption can be useful in exploration and should caution against premature judgement of the geometry and orientation of deposits during the early stages of exploration.

## Introduction

Ten to twenty years ago many people addressed the subject of the relationship of mineral deposits and tectonics but in recent years work in this area has slowed. Some reasons for this decline are that relationships are complex, understanding of tectonic and magmatic processes in continental areas along active plate margins is still incompletely understood, settings of large deposits do not appear to be unique, and applications to old terranes is difficult, if not impossible. Nevertheless, tectonic, magmatic, and hydrothermal processes are fundamental to the formation of many of the world's great ore deposits and we should continue to strive for a better understanding of the processes involved. In this talk I will attempt to discuss tectonic settings and transitions from one tectonic setting to another along consumptive plate margins and their relationships to ore formation and to subsequent structural disruption of deposits. Effective application of mineral deposit models to exploration requires a good understanding of these subjects. In this talk I will take the broad view examining many environments along consumptive plate margins not restricting the discussion to well-documented volcanic arcs.

## Definitions

**Backslip** is reverse motion on a subduction zone and possibly occurs during periods of transtension between converging plates or possibly during the formation of microplates near triple junctions (adapted from Ward, 1991).

**Batholith** is a large, generally discordant plutonic mass that has more than 100 km<sup>2</sup> of surface exposure and no known floor. Its formation is believed by most investigators to involve magmatic processes (Bates and Jackson, 1987).

**Bonanza gold deposits** are those containing greater than 30 metric tonnes of gold averaging at least 30 g/t (1 oz/t) (Sillitoe, 1993).

**Giant gold deposits** are those containing greater than 200 metric tonnes of gold (Sillitoe, 1993).

**Major batholith** is similar to a batholith but has a surface exposure in the order of 10 000 km<sup>2</sup> or larger and is aggregate of several intrusions (Ward, 1991).

**Metamorphic core complexes** are a group of generally domal or archlike, isolated uplifts of anomalously deformed, metamorphic and plutonic rocks overlain by a tectonically detached and distended unmetamorphosed cover (Coney, 1980).

**Slab gap** is a larger, more irregular-shaped slab-free region developed when a spreading ridge and young oceanic crust intersect a subduction zone (Severinghaus and Atwater, 1990).

**Slab window** is a triangular slab-free region developed when a spreading ridge intersects a subduction zone (Dickinson and Snyder, 1979).

**Volcanic arc** is a generally curved linear belt of volcanoes above a subduction zone, and the volcanic and plutonic rocks formed there (Bates and Jackson, 1987).

**World-class copper deposit** is a supergiant or giant copper deposit that is clearly economic.

## COPPER DEPOSIT SIZE GROUPS

Tonnes Contained Cu Metal	Group
>50 000 000	Supergiant
10 000 000 to 50 000 000	Giant
1 000 000 to 10 000 000	Large
100 000 to 1 000 000	Medium
10 000 to 100 000	Small
1000 to 10 000	Very Small

## Some Considerations

Volcanic and plutonic arcs are not necessarily the same.

Major batholiths do not appear to be the root zones of andesitic stratovolcanoes.

Some, if not most, major batholiths appear to form in extensional consumptive plate margin settings related to "continental volcanism" (Ward, 1991).

## Conclusions

- Consumptive plate margin, including arc environments are diverse and can change dramatically in a short period of time (less than a million years) resulting in many different ore-forming settings.
- Important porphyry Cu (Au, Mo), Cu-Au, Au, and Mo deposits and epithermal Au (Ag) deposits form in andesitic stratovolcano environments characteristic of volcanic arcs.
- Kuroko-type VMS deposits form in rifted arcs and Besshi- and Cyprus-type VMS form in successful back-arc rifts.
- Porphyry Cu (Au, Mo), Cu-Au, Au, and Mo deposits; epithermal Au (Ag); Carlin-type Au; manto Pb, Zn, Ag (Cu, Au); and other (eg., Ag, W, U, fluorite, Fe, REE) deposits form in continental extensional magmatic belts that can, in part, be related to subduction along consumptive plate margins. These magmatic belts are not characterized by andesitic stratovolcanoes.
- Porphyry Cu, Mo, Au, epithermal Au (Ag); epithermal Hg; and shear-zone hosted Au deposits (abundant in Precambrian Shield areas) form in slab window and slab gap environments.
- Regional extension is common along consumptive plate margins and can severely disrupt deposits but can also be important in their preservation.

- The great southwestern U.S.A. Laramide porphyry Cu (Mo) cluster, the second most important copper-producing area in the world, would probably have been eroded away without Basin and Range extension and preservation under volcanic and sedimentary cover (Livingston et al., 1968)!

## Acknowledgments

Discussions with many people, unpublished information provided by others, and numerous mine visits are much appreciated and contributed greatly to this analysis. Art Bookstrom and his poster display on the transverse Montana porphyry belt at the 1995 Geological Society of Nevada meeting in Reno renewed my interest in the relationship of mineral deposits with tectonics. The 1997 Society of Economic Geologists research meeting in Elko, Nevada also gave me much better appreciation of the factors involved in the formation of Carlin-type gold deposits. Eric Seedorff's excellent analysis of Cenozoic metallogeny in this part of the United States and many other excellent recent papers on tectonics and mineral deposits were significant factors in this broad metallogenic overview. Slides, as acknowledged, were contributed by other geologists. Tonia Williams, Richard Lancaster, and Antonio Rafer drafted many of the diagrams and Antonio Rafer, Kathryn Dunne, Janet Carrier, and Vitor Pimenta helped with the library research and data compilation.



## Selected Bibliography

### **Armstrong, R.L.**

- 1978: Cenozoic igneous history of the U.S. Cordillera from lat 42° to 49° N; *in* Cenozoic Tectonics and Regional Geophysics of the Western Cordillera, (eds.) R.B. Smith and G.P. Eaton; Geological Society of America, Memoir 152, p. 265-282.

### **Armstrong, R.L., Hollister, V.F., and Harakel, J.E.**

- 1978: K-Ar dates for mineralization in the White Cloud-Cannivan porphyry molybdenum belt of Idaho and Montana; *Economic Geology*, v. 73, p. 94-96.

### **Armstrong, R.L. and Ward, P.L.**

- 1991: Evolving geographic patterns of Cenozoic magmatism in the North American Cordillera: the temporal and spatial association of magmatism and metamorphic core complexes; *Journal of Geophysical Research*, v. 96, p. 13201-13224.
- 1993: Late Triassic to earliest Eocene magmatism in the North American Cordillera: implications for the Western Interior Basin; *in* Evolution of the Western Interior Basin, (eds.) W.G.E. Caldwell and E.G. Kauffman; Geological Association of Canada, Special Paper 39, p. 49-72.

### **Arribas, Jr., A., Hedenquist, J.W., Itaya, T., Okada, T., Concepcion, R.A., and Garcia, Jr., J.S.**

- 1995: Contemporaneous formation of adjacent porphyry and epithermal Cu-Au deposits over 300 ka in northern Luzon, Philippines; *Geology*, v. 23, p. 337-340.

### **Atwater, T.**

- 1989: Plate tectonic history of the northeast Pacific and western North America; *in* The Eastern Pacific Ocean and Hawaii, (eds.) E.L. Winterer, D.M. Hussong, and R.W. Decker; Geological Society of America, The Geology of North America, v. N, p. 21-72.

### **Bartlett, M.W., Enders, M.S., Volberding, J.E., and Wilkinson, W.H.**

- 1996: The geology of the McDonald gold deposit, Lewis and Clark County, Montana; *in* Geology and Ore Deposits of the American Cordillera, (eds.) A.R. Coyner and P.L. Fahey; Geological Society of Nevada Symposium Proceedings, Reno/Sparks, Nevada, April 1995, p. 981-1000.

### **Barton, M.D.**

- 1990: Cretaceous magmatism, metamorphism, and metallogeny in the east-central Great Basin; *in* The Nature and Origin of Cordilleran Magmatism, (ed.) J.L. Anderson; Geological Society of America Memoir 174, Boulder, Colorado, p. 283-302.
- 1996: Granitic magmatism and metallogeny of southwestern North America; *Transactions of the Royal Society of Edinburgh: Earth Science*, v. 87, p. 261-280.

### **Barton, M.D., Sedorff, E., Ilchik, R.P., and Ghidotti, G.**

- 1997: Contrasting siliceous replacement mineralization, east-central Nevada; *in* Carlin-Type Gold Deposits, (eds.) P. Vikre, T.B. Thompson, K. Bettles, O. Christiansen, and R. Parratt; Field Conference, October 16-18, 1997, Society of Economic Geologists, Guidebook Series, v. 28, p. 131-134.

### **Barton, M.D., Staude, J.M.G., Zurcher, L., and Megaw, P.K.M.**

- 1995: Porphyry copper and other intrusion-related mineralization in Mexico; *in* Porphyry Copper Deposits of the American Cordillera, (eds.) F.W. Pierce and J.G. Bolm; Arizona Geological Society Digest 20, p. 487-524.

### **Bates, R.L. and Jackson, J.A. (eds.)**

- 1987: Glossary of Geology; American Geological Institute, Alexandria, Virginia, 788 p.

**Beaty, D.W., Landis, G.P., and Thompson, T.B.**

1990: Carbonate-hosted sulfide deposits of the central Colorado Mineral Belt: introduction, general discussion, and summary; *Economic Geology*, Monograph 7, p. 1-18.

**Benes, V., Scott, S.D., and Binns, R.A.**

1994: Tectonics of rift propagation into a continental margin: western Woodlark Basin, Papua New Guinea; *Journal of Geophysical Research*, v. 99, p. 4439-4455.

**Bennett, E.H.**

1986: Relationship of the trans-Challis fault system in central Idaho to Eocene and basin and range extensions; *Geology*, v. 14, p. 481-484.

**Bird, P.**

1984: Laramide crustal thickening event in the Rocky Mountain foreland and Great Plains; *Tectonics*, v. 3, p. 471-758.

1988: Formation of the Rocky Mountains, western United States: a continuum computer model; *Science*, v. 239, p. 1501-1507.

**Bookstrom, A.A.**

1990: Igneous rocks and carbonated-hosted ore deposits of the central Colorado mineral belt; *Economic Geology*, Monograph 7, p. 45-65.

**Bookstrom, A.A., Carten, R.B., Shannon, J.R., and Smith, R.P.**

1988: Origins of bimodal leucogranite-lamprophyre suite, Climax and Red Mountain porphyry molybdenum systems, Colorado: petrographic and strontium isotopic evidence; in *Cenozoic Volcanism in the Southern Rocky Mountains Revisited*, (eds.) J.W. Drexler and E.E. Larson; Colorado School of Mines, Quarterly, no. 2, p. 1-24.

**Burchfiel, B.C., Cowan, D.S., and Davis, G.A.**

1992: Tectonic overview of the Cordilleran orogen in the western United States; in *The Cordilleran Orogen: Conterminous U.S.*, (eds.) B.C. Burchfiel, P. W. Lipman, and M.L. Zoback; Geological Society of America, Boulder, Colorado, *The Geology of America*, v. G-3, p. 407-479.

**Carlile, J.C. and Mitchell, A.H.G.**

1994: Magmatic arcs and associated gold and copper mineralization in Indonesia; *Journal of Geochemical Exploration*, v. 50, p. 41-142.

**Carten, R.B., White, W.H., and Stein, H.J.**

1993: High grade granite-related molybdenum systems: classification and origin; in *Mineral Deposits Modeling*, (eds.) R.V. Kirkham, W.D. Sinclair, R.I. Thorpe, and J.M. Duke; Geological Association of Canada, Special Paper 40, p. 521-554.

**Carter, N.C.**

1981: Porphyry Copper and Molybdenum Deposits, West-Central British Columbia; British Columbia Ministry of Energy, Mines and Petroleum Resources Bulletin 64, 150 p.

**Christiansen, R.L., Graham, S.A., Niem, W.A., Niem, A.R., and Snavely, Jr., P.D.**

1992: Post-Laramide geology of the U.S. Cordilleran region; in *The Cordilleran Orogen: Conterminous U.S.*, (eds.) B.C. Burchfiel, P.W. Lipman, and M.L. Zoback; Geological Society of America, Boulder, Colorado, *The Geology of North America*, v. G-3 p. 261-406.

**Christiansen, R.L. and Lipman, P.W.**

1972: Cenozoic volcanism and plate-tectonic evolution of the western United States, II. Late Cenozoic; *Philosophical Transactions of the Royal Society of London, A.*, v. 274, p. 249-284.

**Christiansen, R.L., Yeats, R.S., Graham, S.A., Niem, W.A., Niem, A.R., and Snively, Jr., P.D.**

1992: Post-Laramide geology of the U.S. Cordilleran region; in The Cordilleran Orogen: Conterminous U.S., (eds.) B.C. Burchfiel, P. W. Lipman, and M.L. Zoback; Geological Society of America, Boulder, Colorado, The Geology of America, v. G-3, p. 261-406.

**Coney, P.J.**

1980: Introduction; in Cordilleran Metamorphic Core Complexes, (eds.) M.D. Crittenden, Jr., P.J. Coney, and G.H. Davis; Geological Society of America, Memoir 153, p. 3-31.

**Coney, P.J. and Harms, T.A.**

1984: Cordilleran metamorphic core complexes: Cenozoic extensional relics of Mesozoic compression; *Geology*, v. 12, p. 550-554.

**Cooper, P. and Taylor, B.**

1987: Seismotectonics of New Guinea: a model for arc reversal following arc-continent collision; *Tectonics*, v. 6, p. 53-67.

**Cowan, D.S.**

1982: Geological evidence for post-40 m.y. B.P. large-scale northwestward displacement of part of southeastern Alaska; *Geology*, v. 10, p. 309-313.

**Cross, T.A.**

1986: Tectonic controls of foreland basin subsidence and Laramide style deformation, western United States; in Foreland Basins, (eds.) P.A. Allen and P. Homewood; Special Publication No. 8 of International Association of Sedimentologists, Blackwell Scientific Publications, Oxford, p. 15-39.

**Cross, T.A. and Pilger, Jr., R.H.**

1978: Tectonic controls of late Cretaceous sedimentation, western interior, USA; *Nature*, v. 274, August, p. 653-657.

**Crouch, J.K. and Suppe, J.**

1993: Late Cenozoic tectonic evolution of the Los Angeles basin and inner California borderland: a model for core complex-like crustal extension; *Geological Society of America Bulletin*, v. 105, p. 1415-1434.

**Davidson, J. and Mpodozis, C.**

1991: Regional geologic setting of epithermal gold deposits, Chile; *Economic Geology*, v. 86, p. 1174-1186.

**Dawson, K.M., Panteleyev, A., Sutherland Brown, A., and Woodsworth, G.J.**

1991: Regional metallogeny; in *Geology of the Cordilleran Orogen in Canada*, (eds.) H. Gabrielse and C.J. Yorath; Geological Survey of Canada, *Geology of Canada*, no. 4 p. 707-768 (also *Geological Society of America, The Geology of North America*, v. G-2).

**De Cserna, Z.**

1989: An outline of the geology of Mexico; in *The Geology of North America - An Overview*, (eds.) A.W. Bally and A.R. Palmer; Geological Society of America, Boulder, Colorado, *The Geology of North America*, v. A, p. 233-264.

**Dewey, J.F.**

1980: Episodicity, sequence, and style of convergent plate boundaries; in *The Continental Crust and Its Mineral Deposits*, (ed.) D.W. Strangway; Geological Association of Canada Special Paper 20, p. 553-573.

**Dickinson, W.R.**

1997: Tectonic implications of Cenozoic volcanism in coastal California; Geological Society of America Bulletin, v. 109, p. 936-954.

**Dickinson, W.R. and Snyder, W.S.**

1979: Geometry of subducted slabs related to San Andreas transform; Journal of Geology, v. 87, p. 609-627.

**Eaton, P.C. and Setterfield, T.N.**

1993: The relationship between epithermal and porphyry hydrothermal systems within the Tavua Caldera, Fiji; Economic Geology, v. 88, p. 11053-1083.

**Engelbreton, D.C., Cox, A., and Gordon, R.G.**

1985: Relative motions between oceanic and continental plates in the Pacific Basin; Geological Society of America Special Paper 206, 59 p.

**Evenchick, C.A.**

1991: Geometry, evolution, and tectonic framework of the Skeena fold belt, north central British Columbia; Tectonics, v. 10, p. 527-546.

**Ewing, T.E.**

1980: Paleogene tectonic evolution of the Pacific northwest; Journal of Geology, v. 88, p. 619-638.

**Fletcher, J.M., Bartley, J.M., Martin, M.W., Glazner, A.F., and Walker, J.D.**

1995: Large-magnitude continental extension: an example from the central Mojave metamorphic core complex; Geological Society of America Bulletin, v. 107, p. 1468-1483.

**Foster, F. and Childs, J.F.**

1993: An overview of significant lode gold systems in Montana and their regional geologic setting; Exploration and Mining Geology, v. 2, p. 217-244.

**Gabrielse, H.**

1985: Major dextral transcurrent displacements along the northern Rocky Mountain trench and related lineaments in north-central British Columbia; Geological Society of America Bulletin, v. 96, p. 1-14.

1991: Structural styles, Chapter 17; in Geology of the Cordilleran Orogen in Canada, (eds.) H. Gabrielse and C.J. Yorath; Geological Survey of Canada, Geology of Canada, no. 4, p. 571-675. (also Geological Society of America, The Geology of North America, v. G-2)

**Gamble, J.A. and Wright, I.C.**

1995: The southern Havre Trough geological structure and magma petrogenesis of an active backarc rift complex; in Backarc Basins: Tectonics and Magmatism, (ed.) B. Taylor; Plenum Press, New York, p. 29-62.

**Gans, P.B., Mahood, G.A., and Schermer, E.**

1989: Synextensional Magmatism in the Basin and Range Province; a Case Study from the Eastern Great Basin; Geological Society of America, Special Paper 233, 53 p.

**Gehrels, G.E. and Snee, J.B.**

1987: Geologic framework, tectonic evolution, and displacement history of the Alexander terrane; Tectonics, v. 6, p. 151-173.

**Gehrels, G.E. and Berg, H.C.**

1994: Geology of southeastern Alaska; in *The Geology of Alaska*, (eds.) G. Plafker and H.C. Berg; Geological Society of America, Boulder, Colorado, *The Geology of North America*, v. G-1, p. 451-467.

**Goldfarb, R.J., Leach, D.L., Pickthorn, W.J. and Paterson, C.J.**

1988: Origin of lode-gold deposits of the Juneau gold belt, southeastern Alaska; *Geology*, v. 16, p. 440-443.

**Grapes, R.H. Sissons, B.A., and Wellman, H.W.**

1987: Widening of the Taupo volcanic zone, New Zealand, and the Edgecumbe earthquake of March 1987; *Geology*, v. 15, p. 1123-1125.

**Gustafson, L.B.**

1978: Some major factors of porphyry copper genesis; *Economic Geology*, v. 73, p. 600-607.

**Gustafson, L.B. and Hunt, J.P.**

1975: The porphyry copper deposit at El Salvador, Chile; *Economic Geology*, v. 70, p. 857-912.

**Haeussler, P.J., Bradley, D., Goldfarb, R., Snee, L., and Taylor, C.**

1995: Link between ridge subduction and gold mineralization in southern Alaska; *Geology*, v. 23, p. 995-998.

**Harris, N.R., Sisson, V.B., Wright, J.E., and Pavlis, T.L.**

1996: Evidence for Eocene mafic underplating during fore-arc intrusive activity, eastern Chugach Mountains, Alaska; *Geology*, v. 24, p. 263-266.

**Hastings, J.S.**

1987: Gold deposits of Zortman-Landusky, Little Rocky Mountains, Montana; in *Bulk Mineable Precious Metal Deposits of the Western United States*, Symposium Proceedings, (eds.) R.W. Schafer, J.J. Cooper, and P.G. Vikre; *The Geological Society of Nevada*, p. 187-205.

**Haxel, G.B., Tosdal, R.M., May, D.J., and Wright, J.E.**

1984: Latest Cretaceous and early Tertiary orogenesis in south-central Arizona: thrust faulting, regional metamorphism, and granitic plutonism; *Geological Society of America Bulletin*, v. 95, p. 631-653.

**Henderson, L.J., Gordon, R.G., and Engebretson, D.C.**

1984: Mesozoic aseismic ridges on the Farallon plate and southward migration of shallow subduction during the Laramide orogeny; *Tectonics*, v. 3, p. 121-132.

**Henry, C.D. and Aranda-Gomez, J.J.**

1992: The real southern basin and range, mid- to late Cenozoic extension in Mexico; *Geology*, v. 20, p. 701-704.

**Hill, E.J., Baldwin, S.L., and Lister, G.S.**

1992: Unroofing of active metamorphic core complexes in the D'Entrecasteaux Islands, Papua New Guinea; *Geology*, v. 20, p. 907-910.

1995: Magmatism as an essential driving force for formation of active metamorphic core complexes in eastern Papua New Guinea; *Journal of Geophysical Research*, v. 100, p. 10441-10451.

**Hofstra, A.H.**

1997: Isotopic composition of sulfur in Carlin-type gold deposits: implications for genetic models; in *Carlin-Type Gold Deposits*, (eds.) P. Vikre, T.B. Thompson, K. Bettles, O. Christiansen, and R. Parratt; Field Conference, October 16-18, 1997, Society of Economic Geologists, Guidebook Series, v. 28, p. 119-129.

**Hollister, L.S. and Andronicos, C.L.**

1997: A candidate for Baja British Columbia fault system in the Coast Plutonic Complex; *GSA Today*, v. 7, p. 1-7.

**Hynes, A. and Mott, J.**

1985: On the causes of backarc spreading; *Geology*, v. 13, p. 387-389.

**Ilchik, R.P. and Barton, M.D.**

1997: An amagmatic origin of Carlin-type gold deposits; *Economic Geology*, v. 92, p. 269-288.

**Ingram, G.M. and Hutton, D.H.W.**

1994: The Great Tonalite Sill: emplacement into a contractional shear zone and implications for late Cretaceous to early Eocene tectonics in southeastern Alaska and British Columbia; *Geological Society of America Bulletin*, v. 106, p. 715-728.

**Isacks, B.L. and Barazangi, M.**

1977: Geometry of Benioff zones: lateral segmentation and downwards bending of the subducted lithosphere; in *Island Arcs, Deep Sea Trenches and Back-Arc Basins*, (eds.) M. Talwani and W.C. Pitman III; American Geophysical Union, Washington, DC, p. 99-114.

**Keith, S.B. and Swan, M.M.**

1996: The great Laramide porphyry copper cluster of Arizona, Sonora, and New Mexico: the tectonic setting, petrology, and genesis of a world class porphyry metal cluster; in *Geology and Ore Deposits of the American Cordillera*, (eds.) A.R. Coyner and P.L. Fahey; Geological Society of Nevada Symposium Proceedings, Reno/Sparks, Nevada, April 1995, p. 1667-1747.

**Kilgaard, T.H., Fisher, F.S., and Bennett, E.H.**

1986: The trans-Challis fault system and associated precious metal deposits, Idaho; *Economic Geology*, v. 81, p. 721-724.

**Kirkham, R.V.**

1972: Porphyry deposits; in *Report of Activities, Part B; November 1971 to March 1972*; Geological Survey of Canada, Paper 72-1, Part B, p. 62-64.

1997: Giant Cu and Au porphyry deposits: geological parameters and economic importance; in *Pacific Treasure Trove - Copper-Gold Deposits of the Pacific Rim*, Prospectors and Developers Association of Canada, Annual Convention, March 9, 1997, p. 1-30 (abstract and diagrams).

**Kirkham, R.V. and Sinclair, W.D.**

1996: Porphyry copper, gold, molybdenum, tungsten, tin, silver; in *Canadian Mineral Deposit Types*, (eds.) O.R. Eckstrand, W.D. Sinclair, and R.I. Thorpe; Geological Survey of Canada, no. 8, p. 421-446 (also *Geological Society of America, the Geology of North America*, v. P-1).

**Kistler, R.W.**

1990: Two different lithosphere types in the Sierra Nevada, California; in *The Nature and Origin of Cordilleran Magmatism*, (ed.) J.L. Anderson; Geological Society of America Memoir 174, p. 271-281.

**Lasmanis, R.**

1995: Regional geological and tectonic setting of porphyry deposits in Washington State; in *Porphyry Deposits of the Northwestern Cordillera of North America*, (ed.) T.G. Schroeter; Canadian Institute of Mining, Metallurgy and Petroleum, Special Volume 46, p. 77-102.

**Lasmanis, R. and Utterback, W.C.**

1995: The Mount Tolman porphyry molybdenum-copper deposit, Ferry County, Washington; in *Porphyry Deposits of the Northwestern Cordillera of North America*, (ed.) T.G. Schroeter; Canadian Institute of Mining, Metallurgy and Petroleum, Special Volume 46, p. 718-731.

**Livingston, D.E., Mauger, R.L., and Damon, P.E.**

1968: Geochronology of the emplacement, enrichment, and preservation of Arizona porphyry copper deposits; *Economic Geology*, v. 63, p. 30-36.

**MacDonald, G.D. and Arnold, L.C.**

1994: Geological and geochemical zoning of the Grasberg Igneous Complex, Irian Jaya, Indonesia; *Journal of Geochemical Exploration*, v. 50, p. 143-178.

**MacIntyre, D.G., Webster, I.C.L., and Villeneuve, M.**

1997: Babine porphyry belt project: bedrock geology of the Old Fort Mountain area (93M/1), British Columbia; in *Geological Fieldwork 1996*, (eds.) D.V. Lefebure, W.J. McMillan and J.G. McArthur; British Columbia Ministry of Employment and Investment, Paper 1997-1, p. 47-67.

**Martin, M.W., Glazner, A.F., Walker, J.D., and Schermer, E.R.**

1993: Evidence for right-lateral transfer faulting accommodating en echelon Miocene extension, Mojave Desert, California; *Geology*, v. 21, p. 355-358.

**Meldrum, S.J., Aquino, R.S., Gonzales, R.I., Burke, R.J., Suyadi, A., Irianto, B., and Clarke, D.S.**

1994: The Batu Hijau porphyry copper-gold deposit, Sumbawa Island, Indonesia; *Journal of Geochemical Exploration*, v. 50, p. 203-220.

**Miller, E.L. and Gans, P.B.**

1989: Cretaceous crustal structure and metamorphism in the hinterland of Sevier thrust belt, western U.S. Cordillera; *Geology*, v. 17, p. 59-62.

**Miller, L.D., Goldfarb, R.J., Gehrels, G.E., and Snee, L.W.**

1994: Genetic links among fluid cycling, vein formation, regional deformation, and plutonism in the Juneau gold belt, southeastern Alaska; *Geology*, v. 22, p. 203-206.

**Monger, J.W.H. and Nokleberg, W.J.**

1996: Evolution of the northern North American Cordillera: generation, fragmentation, displacement and accretion of successive North American plate-margin arcs; in *Geology and Ore Deposits of the American Cordillera*, (eds.) A.R. Coyner and P.L. Fahey; Geological Society of Nevada Symposium Proceedings, Reno/Sparks, Nevada, April 1995, p. 1133-1152.

**Moyle, A.J., Doyle, B.J., Hoogvliet, H., and Ware, A.R.**

1990: Ladolam gold deposit, Lihir Island; in *Geology and Mineral Deposits of Australia and Papua New Guinea*, (ed.) F.E. Hughes; The Australasian Institute of Mining and Metallurgy, Melbourne, Australia, p. 1793-1805.

**Muller, D. and Grooves, D.I.**

1993: Direct and indirect associations between potassic igneous rocks, shoshonites, and gold-copper deposits; *Ore Geology Reviews*, v. 8, p. 383-406.

**Mutschler, F.E., Larson, E.E., and Bruce, R.M.**

1987: Laramide and younger magmatism in Colorado - new petrologic and tectonic variations on old themes; *Colorado School of Mines, Quarterly*, v. 82, p. 1-47.

**Mutschler, F.E. and Mooney, T.C.**

1993a: A speculative plate kinematic model for central Montana alkalic province and related gold deposits; in *Guidebook of the Central Montana Alkalic Province*, (eds.) D.W. Baker and R.B. Berg; Montana Bureau of Mines and Geology, Special Publication 100, Montana, p. 121-124.

1993b: Precious-metal deposits related to alkalic igneous rocks: provisional classification, grade-tonnage data and exploration frontiers; in *Mineral Deposits Modeling*, (eds.) R.V. Kirkham, W.D. Sinclair, R.I. Thorpe, and J.M. Duke; Geological Association of Canada, Special Paper 40, p. 479-520.

**Nokleberg, W.J., Brew, D.A., Grybeck, D. Yeend, W., Bundtzen, T.K., Robinson, M.S., Smith, T.E**

1994: Metallogeny and major mineral deposits of Alaska; *in* The Geology of Alaska, (eds.) G. Plafker and H.C. Berg; Geological Society of America, Boulder, Colorado, The Geology of North America, v. G-1, p. 855-903.

**Nokleberg, W.J., Bundtzen, T.K., Brew, D.A., and Plafker, G.**

1995: Metallogenesis and tectonics of porphyry copper and molybdenum (gold, silver) and granitoid-hosted gold deposits of Alaska; *in* Porphyry Deposits of the Northwestern Cordillera of North America, (ed.) T.G. Schroeter; Canadian Institute of Mining, Metallurgy and Petroleum, Special Volume 46, p. 103-141.

**O'Neill, J.M. and Lopez, D.A.**

1985: Character and regional significance of Great Falls tectonic zone, east-central Idaho and west-central Montana; American Association of Petroleum Geologists Bulletin, v. 69, p. 437-447.

**Page, R.A., Plafker, G., Fuis, G.S., Nokleberg, W.J., Ambos, E.L., Mooney, W.D., and Campbell, D.L.**

1986: Accretion and subduction tectonics in the Chugach Mountains and Copper River Basin, Alaska: initial results of the Trans-Alaska crustal transect; Geology, v. 14, p. 501-505.

**Peacock, S.M.**

1993: Large-scale hydration of the lithosphere above subducting slabs; Chemical Geology, v. 108, p. 49-59.

**Pierce, F.W. and Bolm, J.G. (eds.)**

1995: Porphyry Copper Deposits of the American Cordillera; Arizona Geological Society Digest 20, 656 p.

**Pilger, R.H.**

1981: Plate reconstructions, aseismic ridges, and low-angle subduction beneath the Andes; Geological Society of America, Bulletin, Part 1, v. 92, p. 448-456.

**Pilkington, D.**

1995: Geology of the Mount Tolman porphyry deposit, Sanpoil District, Ferry County, Washington; *in* Porphyry Copper Deposits of the American Cordillera, (eds.) F.W. Pierce and J.G. Bolm; Arizona Geological Society Digest 20, p. 251-264.

**Plafker, G. and Berg, H.C.**

1994a: Introduction; *in* The Geology of Alaska, (eds.) G. Plafker and H.C. Berg; Geological Society of America, Boulder, Colorado, The Geology of North America, v. G-1, p. 1-16.

1994b: Overview of the geology and tectonic evolution of Alaska; *in* The Geology of Alaska, (eds.) G. Plafker and H.C. Berg; Geological Society of America, Boulder, Colorado, The Geology of North America, v. G-1, p. 989-1021.

**Plafker, G. and Moore, J.C., and Winkler, G.R.**

1994: Geology of southern Alaska margin; *in* The Geology of Alaska, (eds.) G. Plafker and H.C. Berg; Geological Society of America, Boulder, Colorado, The Geology of North America, v. G-1, p. 389-449.

**Price, R.A. and Carmichael, D.M.**

1986: Geometric test for late Cretaceous-Paleogene intracontinental transform faulting in the Canadian Cordillera; Geology, v. 14, p. 468-471.

**Rice, C.M., Harmon, R.S., and Shepherd, T.J.**

1985: Central City, Colorado: the upper part of an alkaline porphyry molybdenum system; Economic Geology, v. 80, p. 1769-1796.



**Richards, J.P**

1997: Controls on scale of Porgera-type porphyry/epithermal gold deposits associated with mafic, alkalic magmatism; Transactions of the Institution of Mining and Metallurgy, v. 106, p. B1-B8.

**Richards, J.P. and Kerrich, R.**

1993: The Porgera gold mine, Papua New Guinea: magmatic hydrothermal to epithermal evolution of an alkalic-type precious metal deposit; Economic Geology, v. 88, p. 1017-1052.

**Rohr, K.M.M. and Currie, L.**

1997: Queen Charlotte basin and Coast Mountains: paired belts of subsidence and uplift caused by a low-angle normal fault; Geology, v. 25, p. 819-822.

**Rostad, O.H.**

1978: K-Ar dates for mineralization in the White Cloud-Cannivan porphyry molybdenum belt of Idaho and Montana - a discussion; Economic Geology, v. 73, p. 1366-1367.

**Rusmore, M.E. and Woodsworth, G.J.**

1991: Coast Plutonic Complex: a mid-Cretaceous contractional orogen; Geology, v. 19, p. 941-944.

**Rytuba, J.J.**

1996: Cenozoic metallogeny of California; in Geology and Ore Deposits of the American Cordillera, (eds.) A.R. Coyner and P.L. Fahey; Geological Society of Nevada Symposium Proceedings, Reno/Sparks, Nevada, April 1995, p. 803-822.

**Shafiqullah, M., Damon, P.E., Lynch, D.J., Reynolds, S.J., Rehrig, W.A., and Raymond, R.H.**

1980: K-Ar geochronology and geologic history of southwestern Arizona and adjacent areas; Arizona Geological Society Digest, v. 12, p. 201-260.

**Schmidt, E.A., Broch, M.J. and White, R.O.**

1982: Geology of the Thompson Creek molybdenum deposit, Cluster County, Idaho; in The Genesis of Rocky Mountain Ore Deposits Changes with Time and Tectonics; Proceedings of Denver Regional Exploration, Geological Society Symposium, p. 79-84.

**Schmidt, E.A., Worthington, J.E., and Thomssen, R.W.**

1979: K-Ar dates for mineralization in the White Cloud-Cannivan porphyry molybdenum belt of Idaho and Montana - a discussion; Economic Geology, v. 74, p. 698-699.

**Schroeter, T.G. (ed.)**

1995: Porphyry Deposits of the Northwestern Cordillera of North America; Canadian Institute of Mining, Metallurgy and Petroleum, Special Volume 46, 888 p.

**Seedorff, E.**

1991: Magmatism, extension, and ore deposits of Eocene to Holocene age in the Great Basin - mutual effects and preliminary proposed genetic relationships; in Geology and Ore Deposits of the Great Basin, (eds.) G.L. Raines, R.E. Little, R.W. Schafer and W.H. Wilkinson; Geological Society of Nevada and U.S. Geological Survey Symposium Proceedings, Reno/Sparks, April 1990, p. 133-178.

**Setterfield, T.N., Eaton, P.C., Rose, W.J., and Sparks, R.S.J.**

1991: The Tavua Caldera, Fiji: a complex shoshonitic caldera formed by concurrent faulting and downsagging; Journal of the Geological Society, v. 148, p. 115-127.

**Shaver, S.A. and McWilliams, M.**

- 1987: Cenozoic extension and tilting recorded in Upper Cretaceous and Tertiary rocks at the Hall molybdenum deposit, northern San Antonio Mountains, Nevada; Geological Society of America Bulletin, v. 99, p. 341-353.

**Sherlock, R.L., Tosdal, R.M., Lehrman, N.J., Graney, J.R., Losh, S., Jowett, E.C., and Kesler, S.E.**

- 1995: Origin of the McLaughlin Mine sheeted vein complex: metal zoning, fluid inclusion, and isotopic evidence; Economic Geology, v. 90, p. 2156-2181.

**Sillitoe, R.H.**

- 1991: Gold metallogeny of Chile - an introduction; Economic Geology, v. 86, p. 1187-1205.  
1992: Gold and copper metallogeny of the central Andes - past, present, and future exploration objectives; Economic Geology, V.87, p. 2205-2216.  
1993a: Gold-rich porphyry copper deposits: geological model and exploration implications; in Mineral Deposit Modeling, (eds.) R.V. Kirkham, W.D. Sinclair, R.I. Thorpe, and J.M. Duke; Geological Association Canada, Special Paper 40, p. 465-478.  
1993b: Giant and bonanza gold deposits in the epithermal environment: assessment of potential genetic factors; in Giant Ore Deposits, (eds.) B.H. Whiting, C.J. Hodgson, and R.Mason; Society of Economic Geologists, Special Publication, no. 2, p.125-156.  
1997: Characteristics and controls of the largest porphyry copper-gold and epithermal gold deposits in the circum-Pacific region; Australian Journal of Earth Sciences, v. 44, p. 373-388.

**Sillitoe, R.H., Graubeger, G.L. and Elliott, L.E.**

- 1985: A diatreme-hosted gold deposit at Montana Tunnels, Montana; Economic Geology, v. 80, p. 1707-1721.

**Sims, P.K., Drake, Jr., A.A., and Tooker, E.W.**

- 1963: Economic Geology of the Central City District, Gilpin County, Colorado; Geological Survey Professional Paper 359, United States Government Printing Office, Washington, 231 p.

**Sinclair, W.D.**

- 1986: Molybdenum, tungsten and tin deposits and associated granitoid intrusions in the northern Canadian Cordillera and adjacent parts of Alaska; in; Mineral Deposits of Northern Cordillera, (ed.) J.A. Morin; The Canadian Institute of Mining and Metallurgy, Special Volume 37, p. 216-233.

**Skewes, M.A. and Stern, C.R.**

- 1994: Tectonic trigger for the formation of late Miocene Cu-rich breccia pipes in the Andes of central Chile, Geology, v. 22, p. 551-554.  
1995: Genesis of giant late Miocene to Pliocene copper deposits of central Chile in the context of Andean magmatic and tectonic evolution; International Geology Review, v. 37, p. 893-909.

**Skulski, T., Francis, D., and Ludden, J.**

- 1991: Arc-transform magmatism in the Wrangell volcanic belt; Geology, v. 19, p. 11-14.

**Snyder, W.S., Dickinson, W.R., and Silberman, M.L.**

- 1976: Tectonic implications of space-time patterns of Cenozoic magmatism in the western United States; Earth and Planetary Science Letters, v. 32, p. 91-106.

**Spencer, J.E. and Reynolds, S.J**

- 1991: Tectonics of the mid-Tertiary extension along a transect through west central Arizona; Tectonics. v. 10, p. 1204-1221.

**Spencer, J.E., Richard, S.M., Reynolds, S.J., Miller, R.J., Shafiqullah, M., Gilbert, W.G., and Grubensky, M.J.**

1995: Spatial and temporal relationships between mid-Tertiary magmatism and extension in southwestern Arizona; *Journal of Geophysical Research*, v. 100, p. 10321-10351.

**Spry, P.G., Paredes, M.M., Foster, F., Tuckle, J.S., and Chadwick, T.H.**

1996: Evidence for a genetic link between gold-silver telluride and porphyry molybdenum mineralization at the Golden Sunlight deposit, Whitehall, Montana: fluid inclusion and stable isotopes studies; *Economic Geology*, v. 91, p. 507-526.

**Stewart, J.H.**

1978: Basin range structure in western North America: a review; *in* *Cenozoic Tectonics and Regional Geophysics of the Western Cordillera*, (eds.) R.B. Smith and G.P. Eaton; Geological Society of America, Inc., Memoir 152, p. 1-31.

**Stout, J.H. and Chase, C.G.**

1980: Plate kinematics of the Denali fault system; *Canadian Journal of Earth Sciences*, v. 17, p. 1527-1537.

**Struik, L. C.**

1993: Intersecting intracontinental Tertiary transform fault systems in the North American Cordillera; *Canadian Journal of Earth Sciences*, v. 30, p. 1262-1274.

**Teal, L. and Jackson, M.**

1997: Geologic overview of the Carlin Trend gold deposits and descriptions of recent deep discoveries; *SEG Newsletter*, no. 31, p. 1, 13-25.

**Thompson, T.B., Trippel, A.D., and Dwelley, P.C.**

1985: Mineralized veins and breccias of the Cripple Creek district, Colorado; *Economic Geology*, v. 80, p. 1660-1688.

**Thorkelson, D.J.**

1996: Subduction of diverging plates and the principles of slab window formation; *Tectonophysics*, v. 255, p. 47-63.

**Thorkelson, D.J. and Taylor, R.P.**

1989: Cordilleran slab windows; *Geology*, v. 17, p. 833-836.

**Titley, S.R.**

1982: *Advances in Geology of the Porphyry Copper Deposits, Southwestern North America*; The University of Arizona Press, Tucson, Arizona, 560 p.

1993a: Characteristics of porphyry copper occurrence in the American southwest; *in* *Mineral Deposits Modeling*, (eds.) R.V. Kirkham, W.D. Sinclair, R.I. Thorpe, and J.M. Duke; Geological Association of Canada, Special Paper 40, p. 433-464.

1993b: Characteristics of high-temperature carbonate-hosted massive sulphide ores in the United States, Mexico and Peru; *in* *Mineral Deposits Modeling*, (eds.) R.V. Kirkham, W.D. Sinclair, R.I. Thorpe, and J.M. Duke; Geological Association of Canada, Special Paper 40, p. 585-614.

**Titley, S.R. and Hicks, C.L. (eds.)**

1966: *Geology of the Porphyry Copper Deposits, Southwestern North America*; The University of Arizona Press, Tucson, Arizona, 287 p.

**Titley, S.R. and Beane, R.E.**

1981: Porphyry copper deposits; *Economic Geology*, 75th Anniversary Volume, p. 214-269.

**Tosdal, R.M., Sherlock, R.L., Nelson, G.C., Enderlin, D.A., and Lehrman, N.J.**

1996: Precious metal mineralization in a fold and thrust belts of McLaughlin hot spring deposit, northern California; in Geology and Ore Deposits of the American Cordillera, (eds.) A.R. Coyner and P.L. Fahey; Geological Society of Nevada Symposium Proceedings, Reno/Sparks, Nevada, April 1995, p. 839-854.

**Tovish, A. and Scubert, G.**

1978: Mantle flow pressure and the angle of subduction: non-Newtonian corner flows; Journal of Geophysical Research, v. 83, p. 5892-5898.

**Van Leeuwen, T.M.**

1994: 25 years of mineral exploration and discovery in Indonesia; Journal of Geochemical Exploration, v. 50, p. 13-90.

**Vikre, P., Thompson, T.B., Bettles, K., Christiansen, O., and Parratt, R. (eds.)**

1997: Carlin-Type Gold Deposits; Field Conference, October 16-18, 1997, Society of Economic Geologists, Guidebook Series, v. 28, 287 p.

**Vila, T. and Sillitoe, R.H.**

1991: Gold-rich porphyry systems in the Maricunga gold-silver belt, northern Chile; Economic Geology, v. 86, p. 1238-1260.

**Ward, P.L.**

1991: On plate tectonics and the geologic evolution of southwestern North America; Journal of Geophysical Research, v. 96, p. 12479-12496.

**Wilkins, Jr., J. and Heidrick, T.L.**

1995: Post-Laramide extension and rotation of porphyry copper deposits, southwestern United States; in Porphyry Copper Deposits of the American Cordillera, (eds.) F.W. Pierce and J.G. Bolm; Arizona Geological Society Digest 20, p. 109-127.

**Wilson, G.I. and Barwick, R.C.**

1991: A case history of the development of the Misima gold-silver mine, Papua New Guinea; Economic Geology, Monograph 8, p. 335-349.

**Wilson, M.R. and Kyser, T.K.**

1988: Geochemistry of porphyry-hosted Au-Ag deposits in the Little Rocky Mountains, Montana; Economic Geology, v. 83, p. 1329-1346.

# PACIFIC RIM SELECTED PORPHYRY Cu, Cu-Au, and Au, and PORPHYRY-RELATED EPITHERMAL Au-Ag DEPOSITS\*

DEPOSIT	AGE (Ma)	CONTAINED COPPER (millions of metric tonnes)	CONTAINED GOLD (tonnes)
Fort Knox	93	-	130
Fish Lake	80	2.5	471
Highland Valley (5 deposits)	205	7.4	-
Zortman-Landusky	2	-	120
Butte	60	17.7	93
Bingham	38	24.0	600
Cripple Creek	28	-	692
Morenci	67	14.0	-
Lone Star	62?	24.4	-
Cananea	54	13.2	-
Cerro Colorado (Panama)	6	13.3	155
Petaquilla	35	7.4	165
Cuajone	51	5.1	-
Toquepala	52	7.0	-
Collahuasi	15	25.4	-
Radomiro Tomic	33	44.0	-
Chuquicamata	33	87.0	-
La Escondida	33	35.0	-
Candelaria	100?	4.4	93
Marte	12	-	62
Lobo	12	-	128
Refugio	22	-	190
Bajo de la Alumbreira	8	3.8	483
Agua Rica (Mi Vida)	4	6.1	265
Andacollo (2 sep. deposits)	105	1.2	63
El Pachon	9	5.5	-
Los Pelambres	9	15.1	-
Rio Blanco-Los Bronces	6	67.0	-
El Teniente	5	109.0	-
Namosi	6	4.0	130
Emperor	4	-	214
Panguna	3.5	5.9	631
Ladolam (Lihir)	0.3	-	677
Misima	10?	-	77
Porgera	6	-	577

B18

Ok Tedi	1	2.7	350
Grasberg	3	23.4	2340
Batu Hijau	1?	5.6	506
Kelian	20	-	180
Atlas	103	4.1	224
Dizon	2.7	0.7	140
Baguio	3	-	400
Santo Tomas II	1.4	1.7	213
Far Southeast-Lepanto	1.35	3.6	550

#### FOR COMPARISON

Witwatersrand (1884-1993 Production)		45068
Bendigo	-	697
Ballarat	-	408
Golden Mile (Kalgoorlie)	-	1800
Hollinger-McIntyre-Coniaurum	-	990
Dome	-	350
Carlin trend	-	3850

\* Figures are general, global, *in situ*, geological resources and include subeconomic as well as economic resources and past production. Modified after Kirkham (1997).

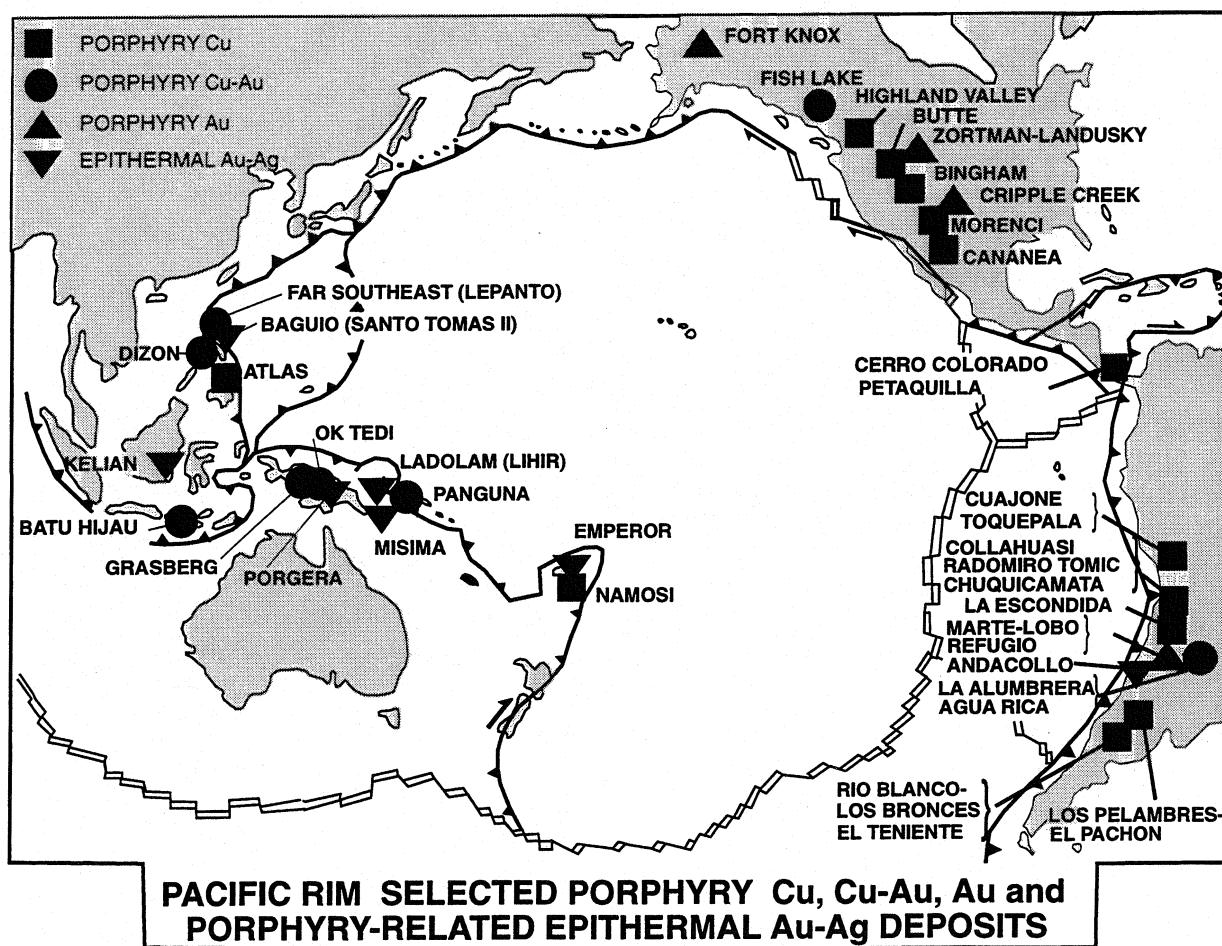
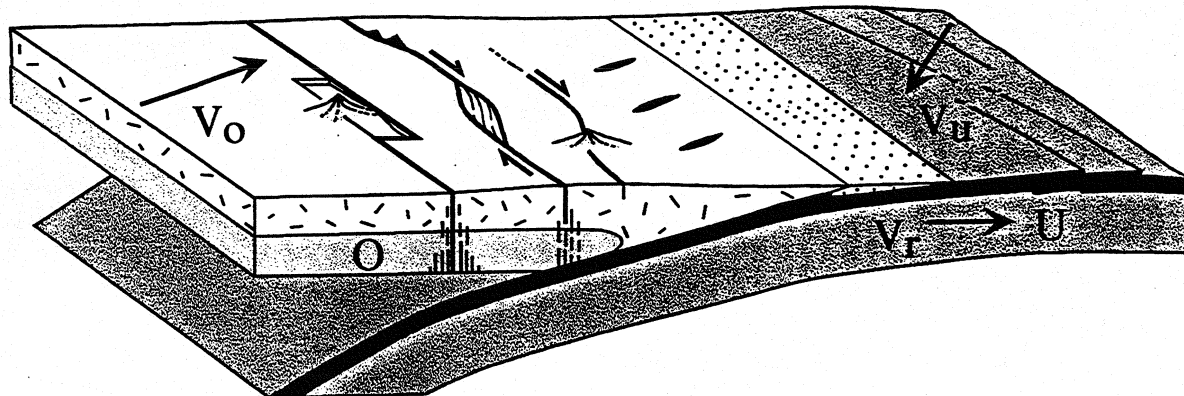
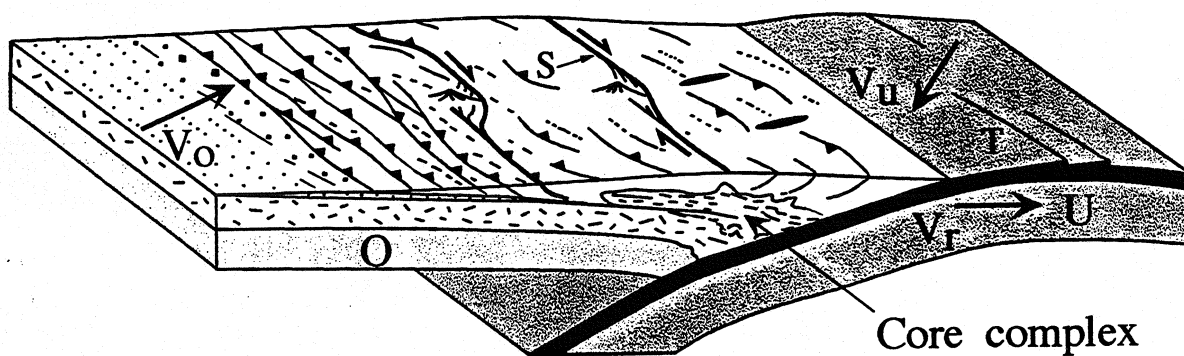


Figure 1. Pacific Rim selected porphyry Cu, Cu-Au, Au and porphyry-related epithermal Au-Ag deposits (modified from Kirkham, 1997).



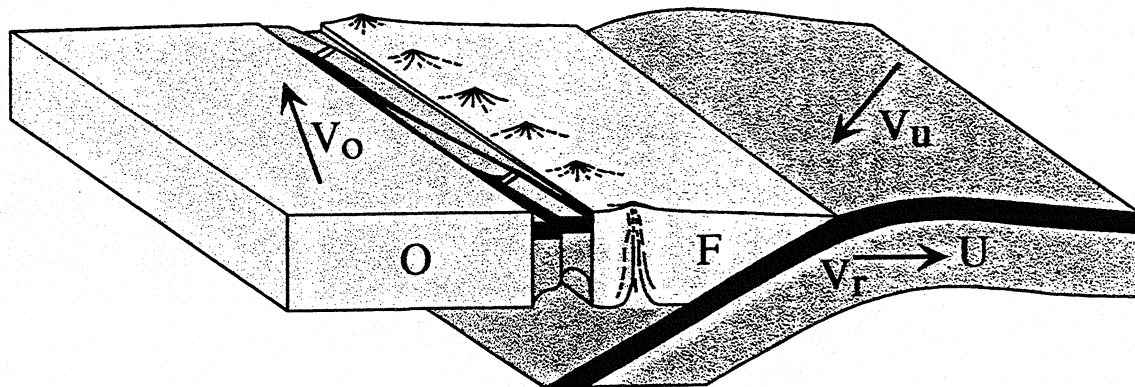
## NEUTRAL ARC



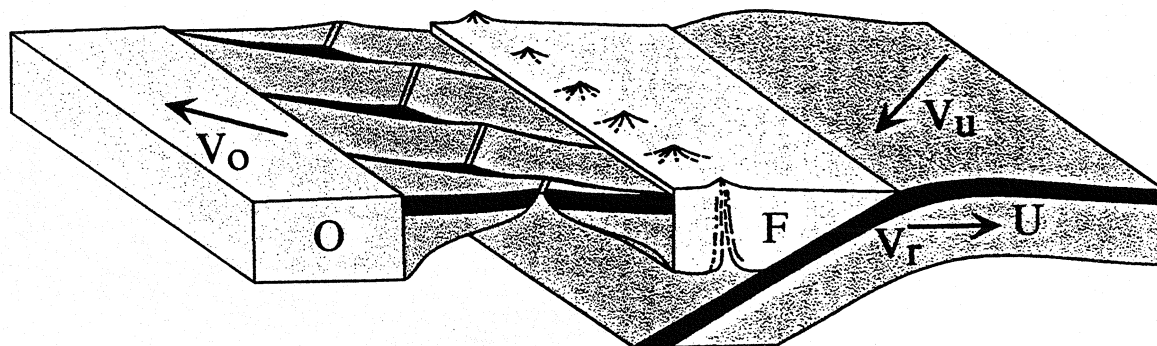
## COMPRESSIVE ARC

Figure 2. Compressive and neutral arcs (after Dewey, 1980).





## EARLY BACK-ARC RIFTING



## ADVANCED BACK-ARC RIFTING

Figure 3. Extensional arc (after Dewey, 1980).

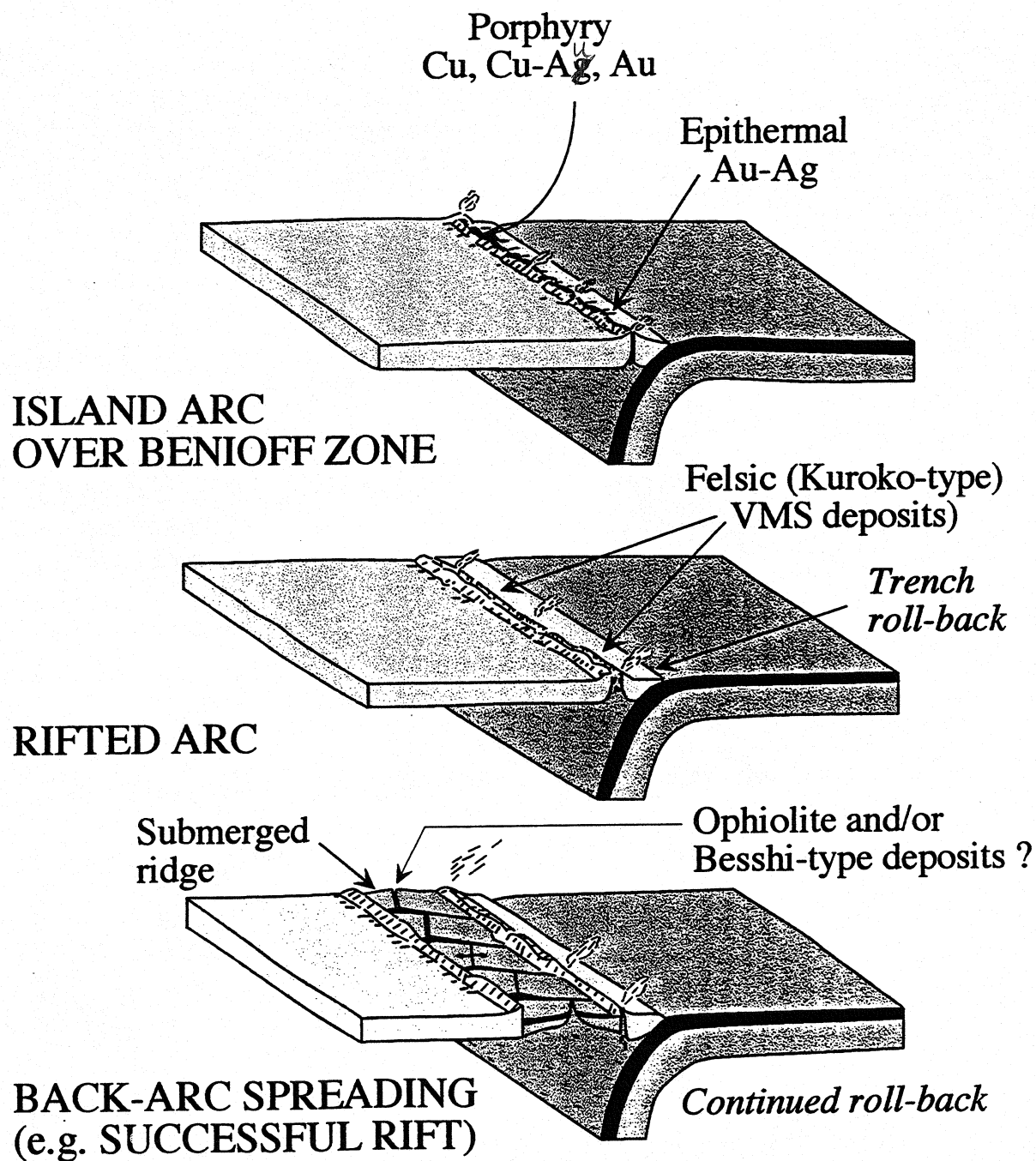


Figure 4. Schematic diagram of different arc types and their related mineral deposits.

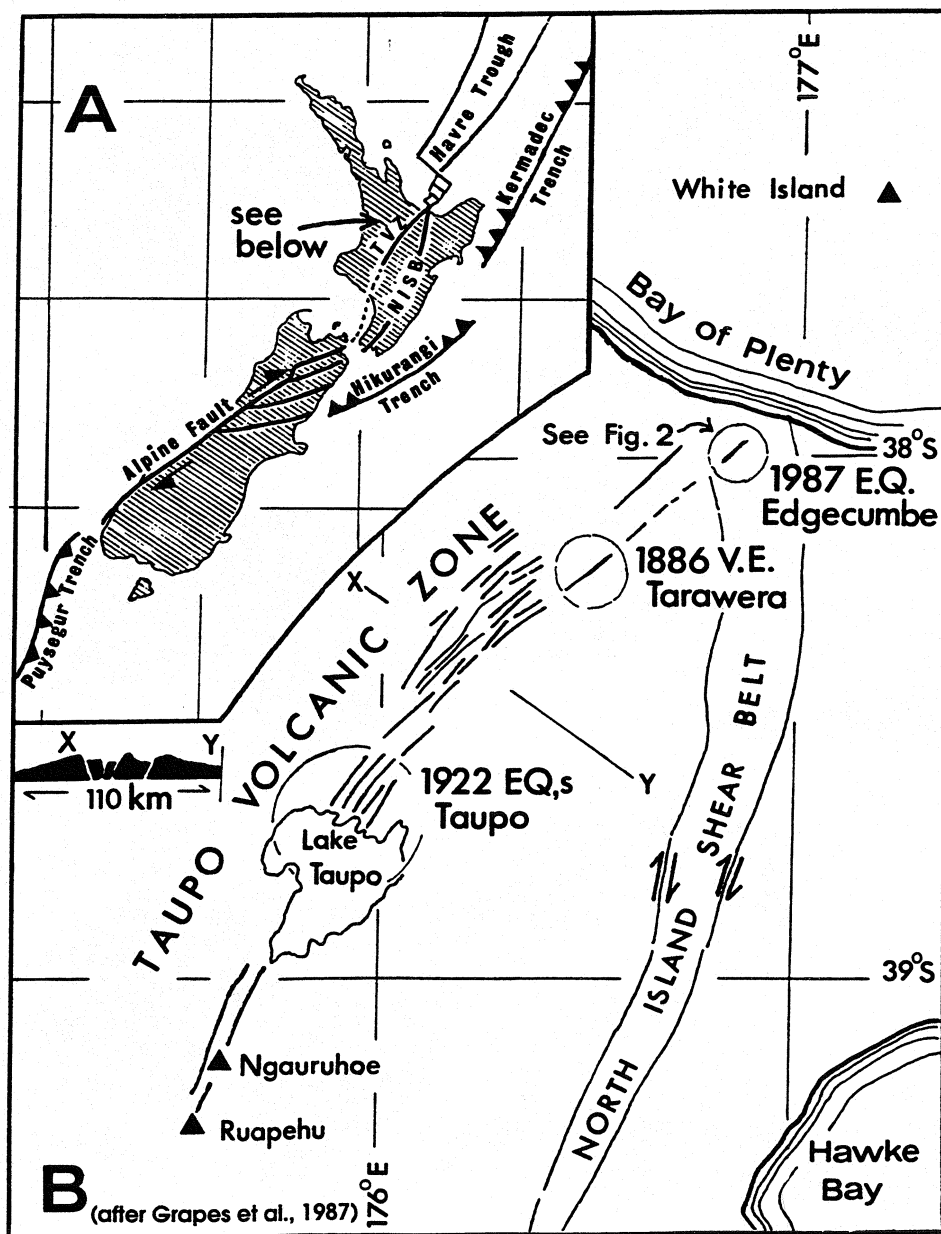


Figure 5. Taupo bimodal volcanic zone in northern New Zealand and its relationship to the Havre trough (after Grapes et al., 1987). Low-sulphidation epithermal gold on land, high-sulphidation epithermal system is active on White Island, and VMS deposits are forming in submarine environments.

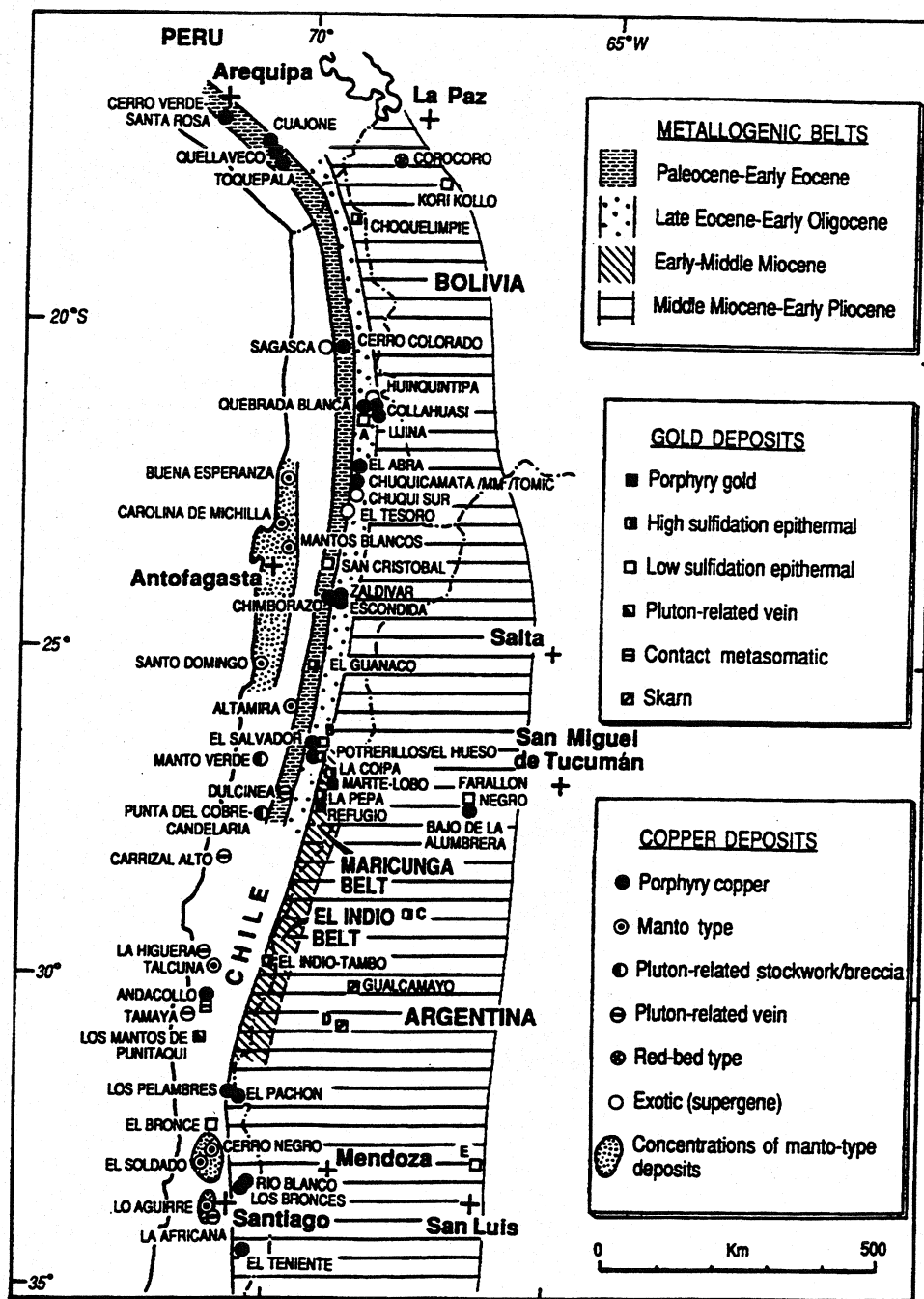


Figure 6: Metallogenic belts in northern Chile illustrating porphyry Cu (Mo) deposits that were probably formed in the root zones of volcanic arcs (after Sillitoe, 1992).

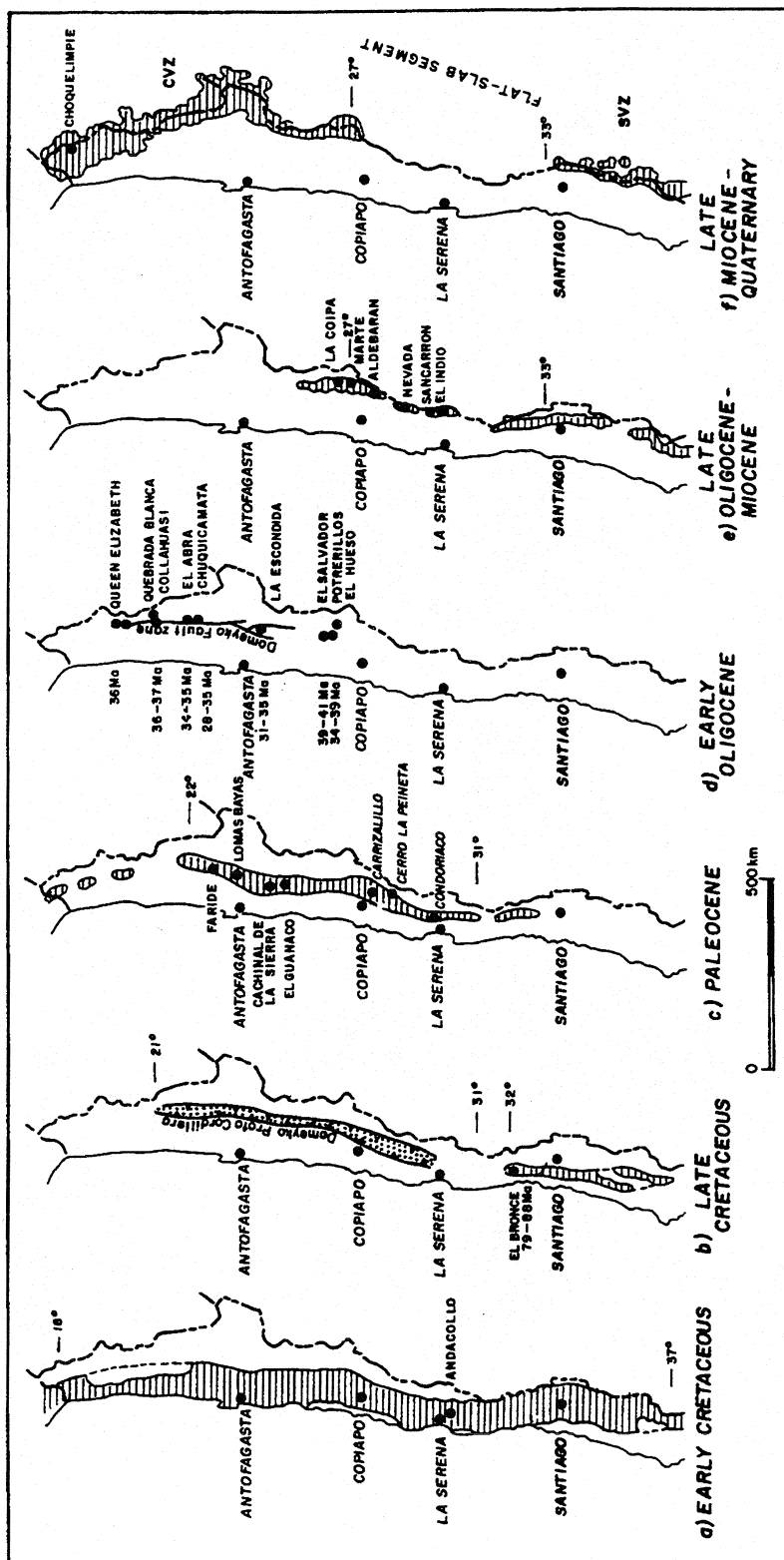
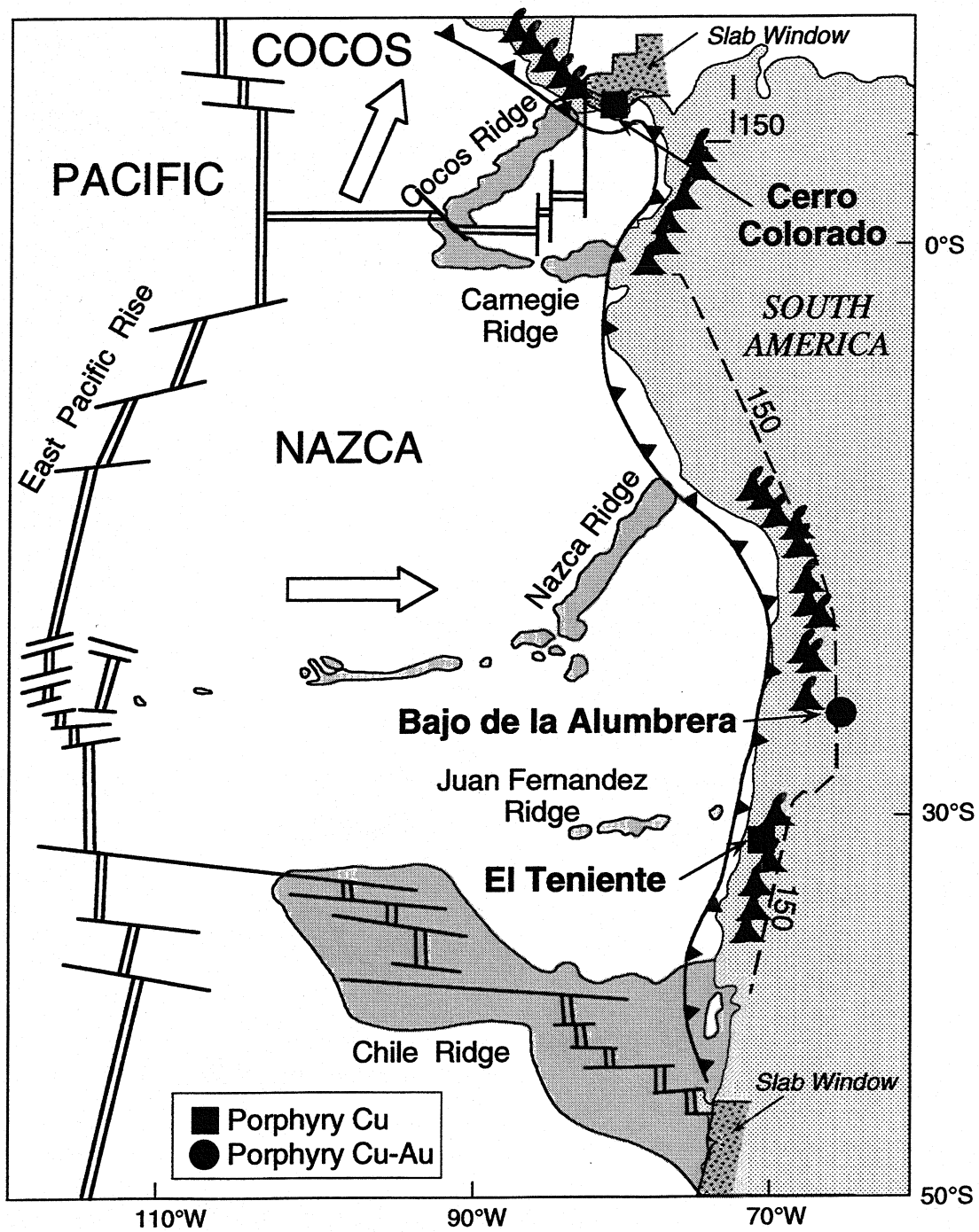


Figure 7. Metallogenic belts of different ages in Chile (after Davidson and Mpodozis, 1991).



(base adapted from Isacks and Barazangi, 1977 and Wollard and Kulm, 1981)

Figure 8. Diagram showing arcs, trenches, spreading and aseismic ridges, and a few young (<10 Ma) porphyry deposits for the southeastern Pacific and South America.

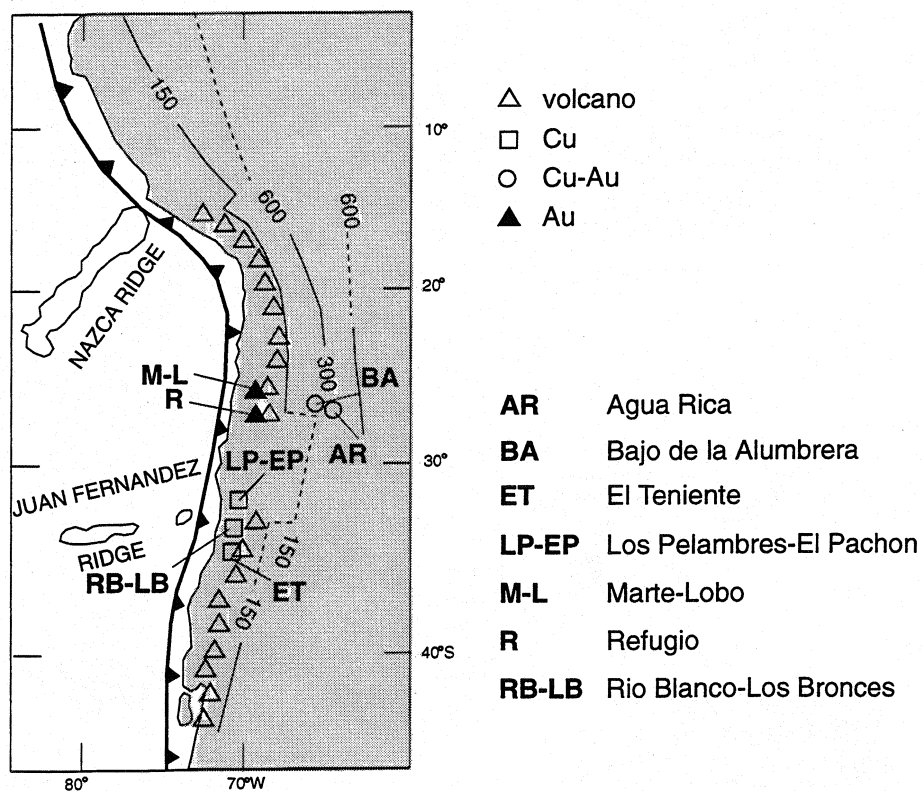


Figure 9. Diagram showing the relationship of the subduction of the aseismic Juan Fernandez ridge and a gap in the volcanic arc over a zone of flat subduction zone (after Pilger, 1981) and the relationship to some important mineral deposits.

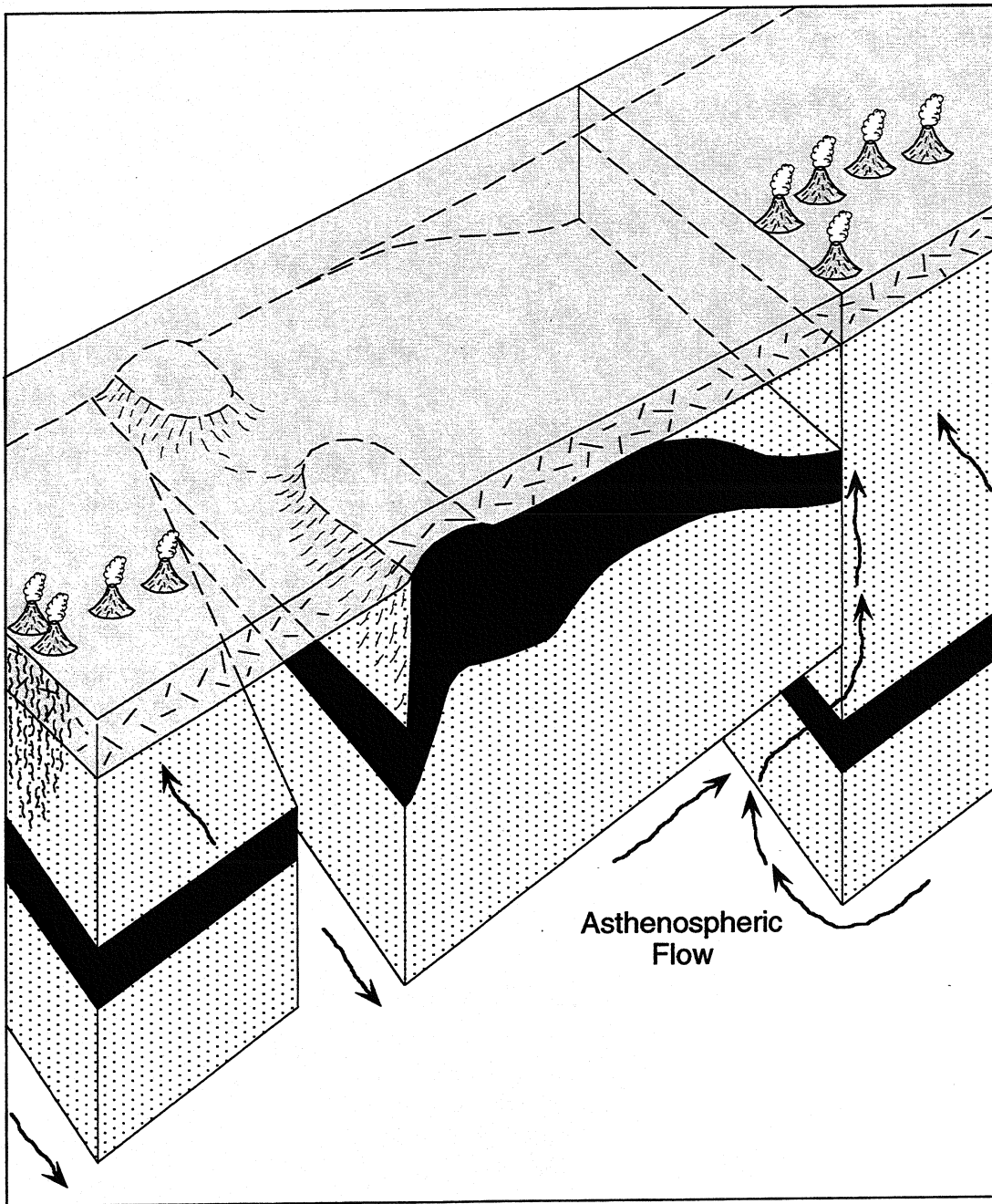
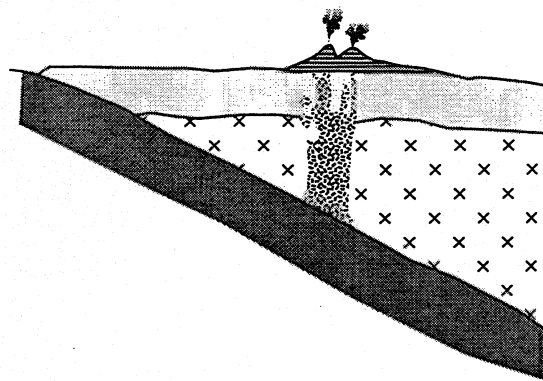


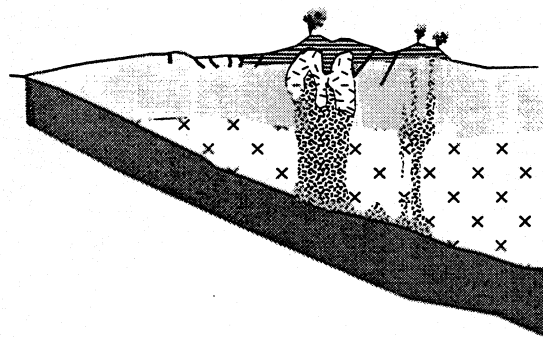
Figure 10. Block diagram illustrating the subduction of a buoyant aseismic ridge.



20-16 Ma peak of Miocene volcanism



16-10 Ma volcanism wanes



10-3 Ma Breccias emplaced

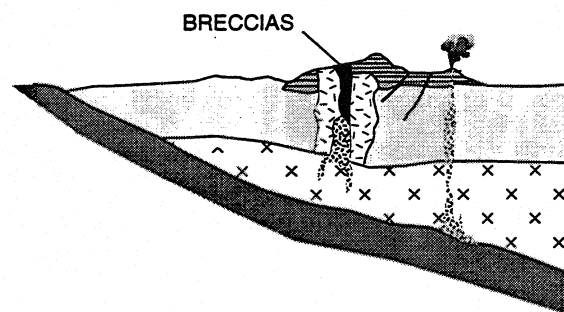


Figure 11. Diagram illustrating the relationship between volcanism, batholith development, and the formation of large, breccia-centred porphyry Cu(Mo) deposits in the El Teniente belt, Chile (after Skewes and Stern, 1994).

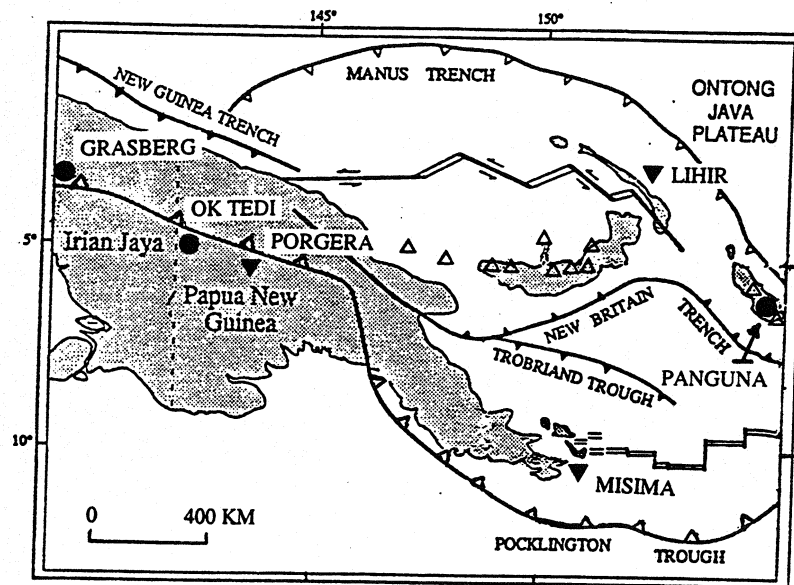


Figure 12. Tectonic setting of large Cu and Au deposits in Papua New Guinea and Irian Jaya.

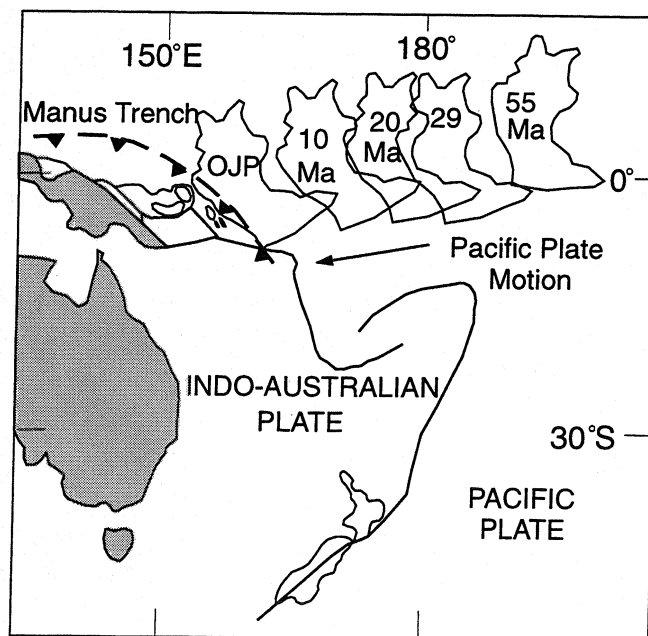


Figure 13. Diagram illustrating the collision of the Ontong Java Plateau with the Manus trench (after McNinnis and Cameron, 1994).

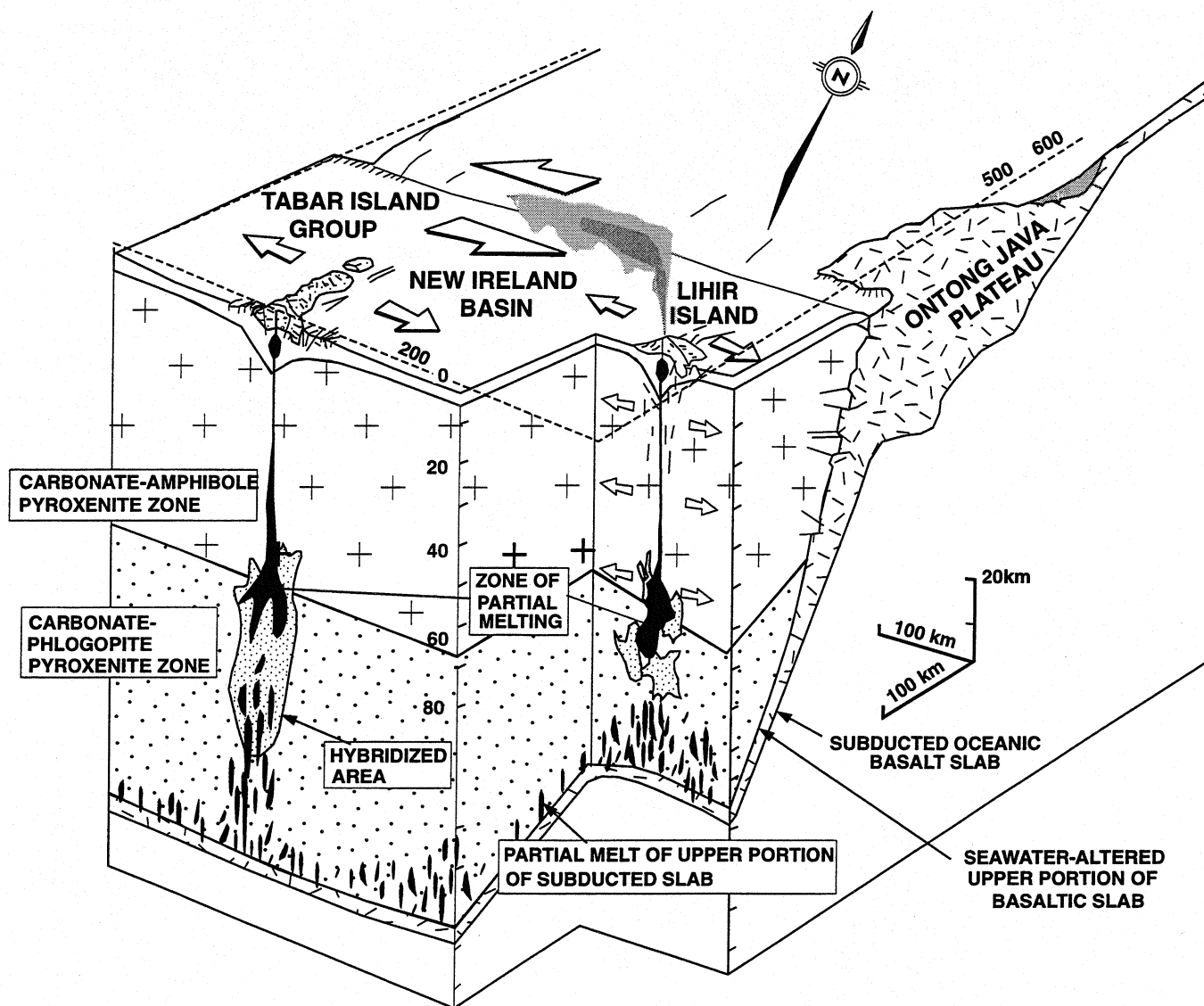


Figure 14. Block diagram illustrating rift reactivation of the Tabar-Feni arc, alkaline magmatism and the formation of the Ladolam Au deposit (after McInnis and Cameron, 1994).

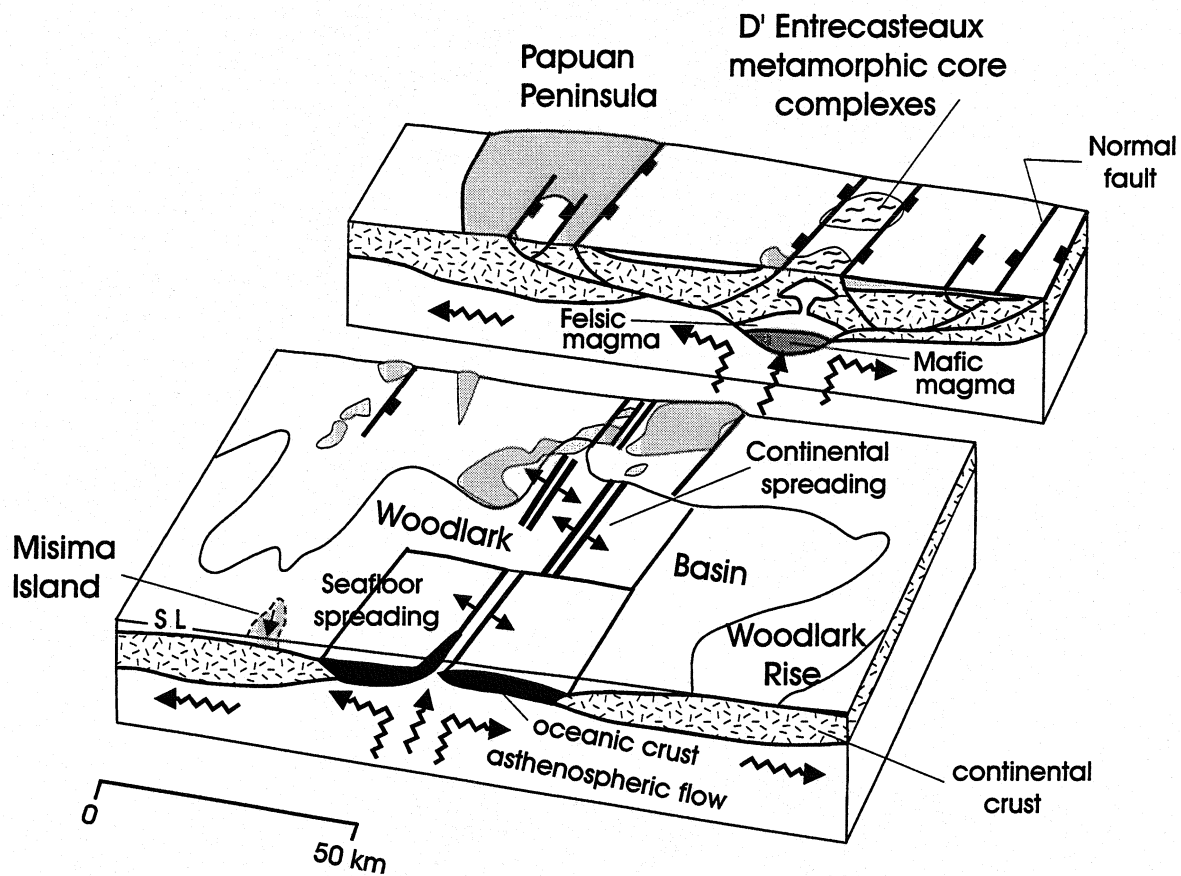


Figure 15. Block diagram illustrating the colinear relationship between the Woodlark spreading ridge and metamorphic core complexes (adapted from Hill et al., 1995). Epithermal and porphyry deposits form in subaerial environments and potential sedex and VMS deposits form in subaqueous spreading environments.

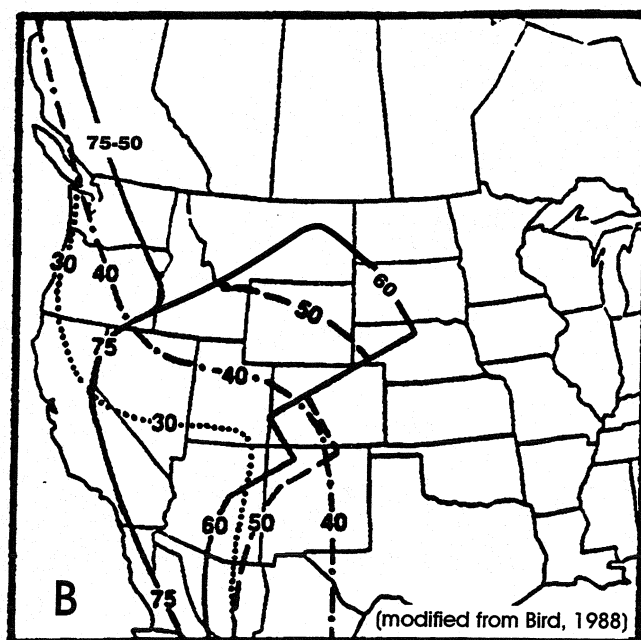
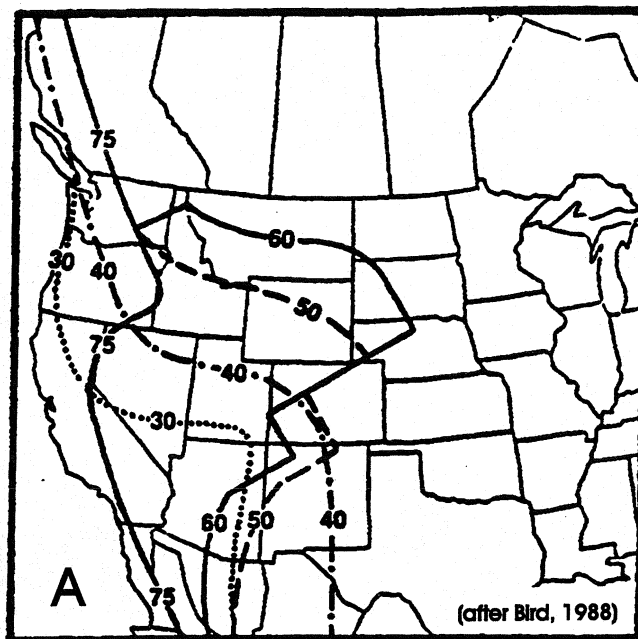


Figure 16. Farallon slab hinge zones 75 to 30 Ma during a period of flat slab subduction in the western United States: a) after Bird, 1988; b) slightly modified from Bird, 1988.

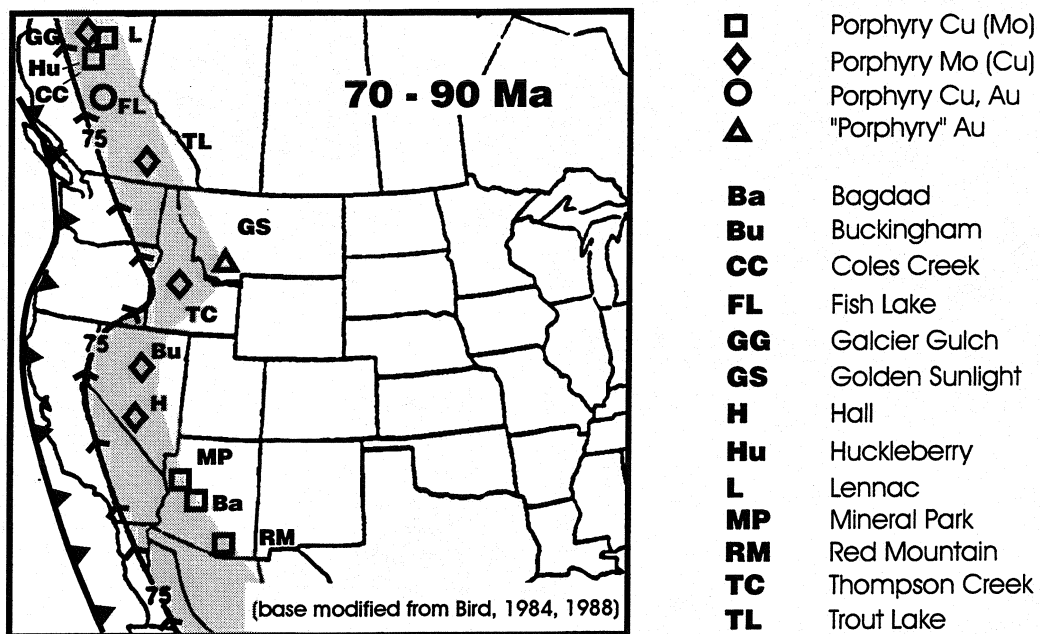
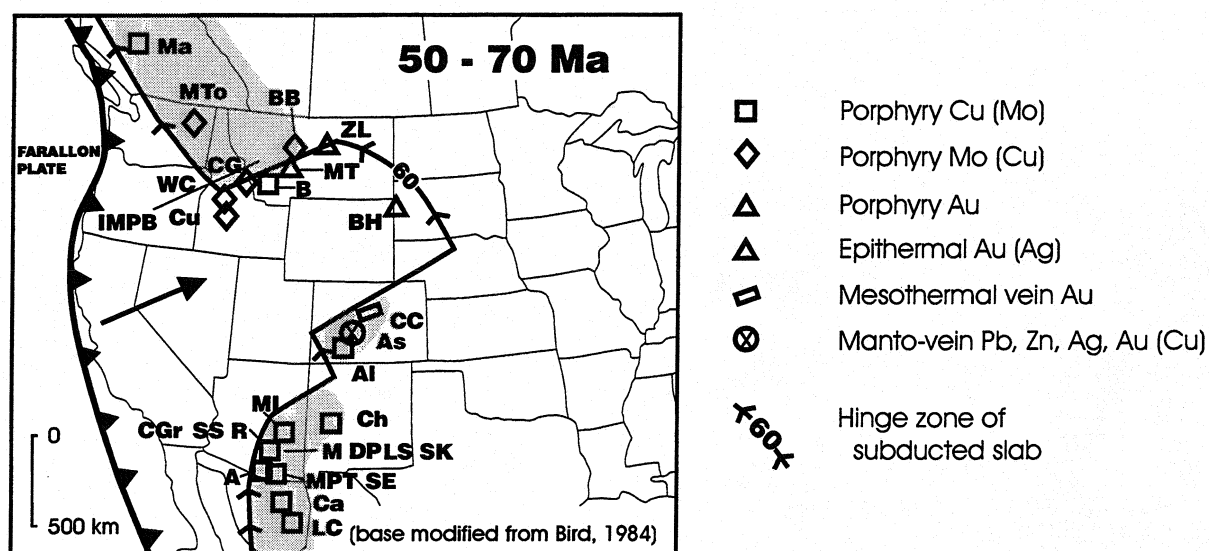


Figure 17. Diagram showing the location of porphyry deposits formed in the central part of the North American Cordillera during a period of relative normal subduction about 70 to 90 Ma.



<b>IMPB</b>	Idaho-Montana porphyry belt	<b>LC</b>	La Caridad
<b>A</b>	Ajo	<b>LS</b>	Lone Star
<b>AI</b>	Allard	<b>M</b>	Morenci
<b>As</b>	Aspen	<b>Ma</b>	Maggie
<b>B</b>	Butte	<b>MI</b>	Miami-Inspiration
<b>BB</b>	Big Ben	<b>MPT</b>	Mission-Pima-Twin Buttes
<b>BH</b>	Black Hills (Gift Edge, Golden Reward, others)	<b>MT</b>	Montana Tunnels
<b>Ca</b>	Cananea	<b>MTo</b>	Mount Tolman
<b>CC</b>	Central City	<b>R</b>	Ray
<b>CG</b>	Cannivan Gulch	<b>SE</b>	Sierrita-Esperanza
<b>CGr</b>	Casa Grande	<b>SK</b>	San Manuel-Kalamazoo
<b>Ch</b>	Chino	<b>SS</b>	Santa Cruz-Sacaton
<b>Cu</b>	Cumo	<b>WC</b>	White Cloud
<b>DP</b>	Dos Pobres	<b>ZL</b>	Zortman-Landusky

Figure 18. Diagram showing the location of deposits formed in the central part of Cordillera during a period of flat slab subduction about 50 to 70 Ma. Note clustering and transverse trends.

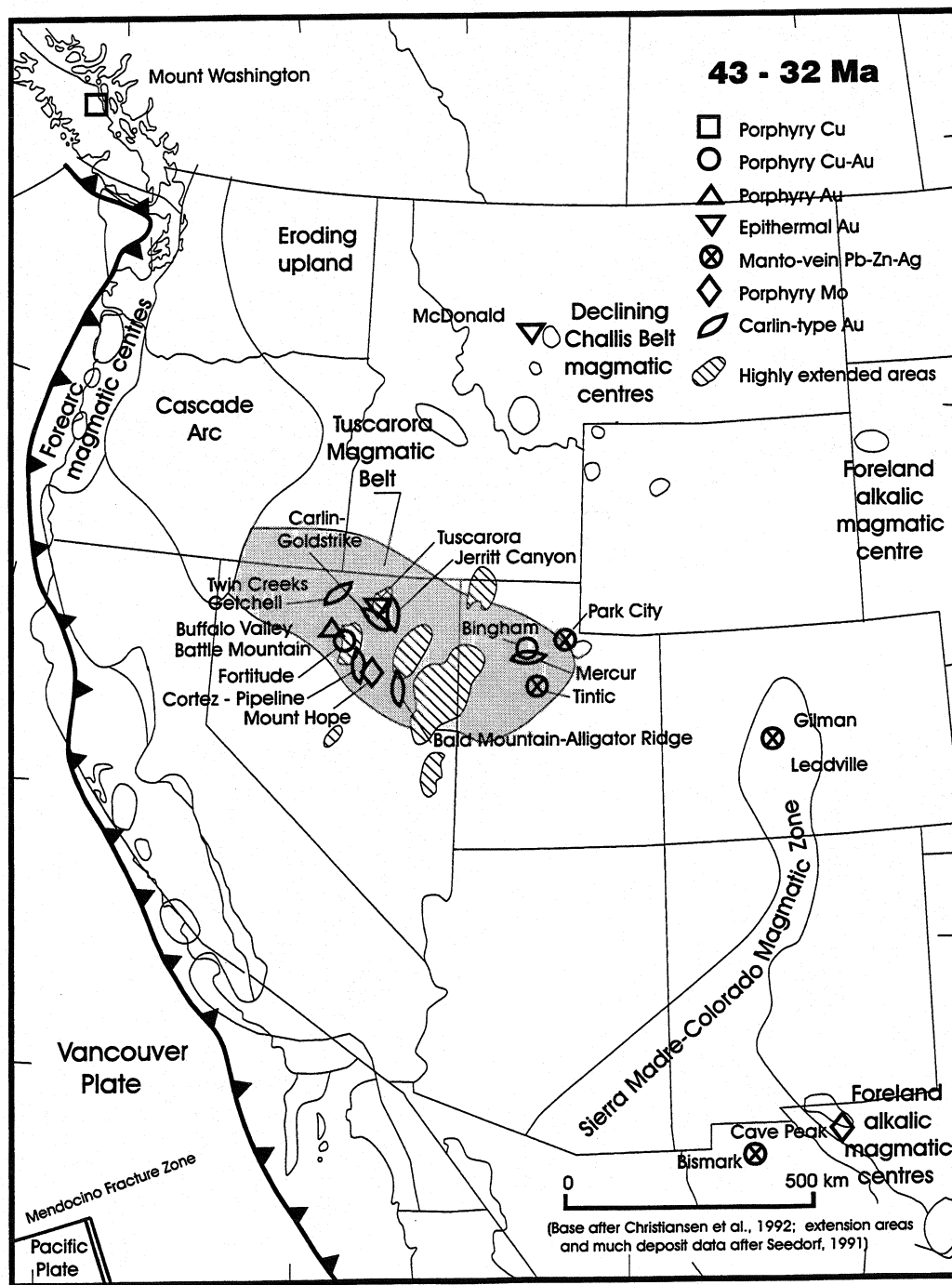


Figure 19. Diagram showing the spatial and temporal relationship of extension and magmatism in the transverse 45 to 32 Ma Tuscarora magmatic belt and the location of many major ore deposits.



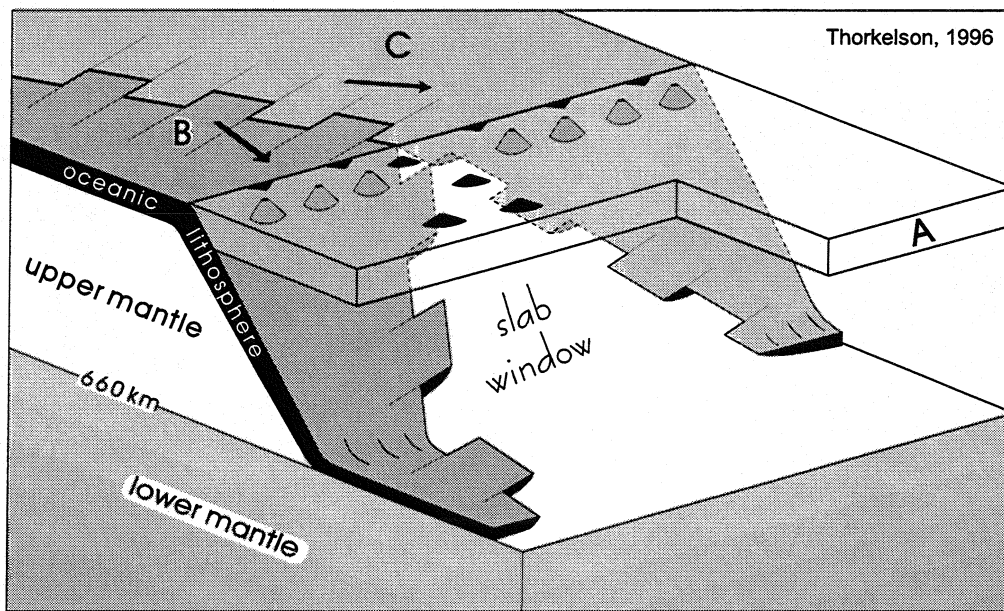


Figure 20. Block diagram illustrating the formation of a slab window and related magmatism (after Thorkelson, 1996).

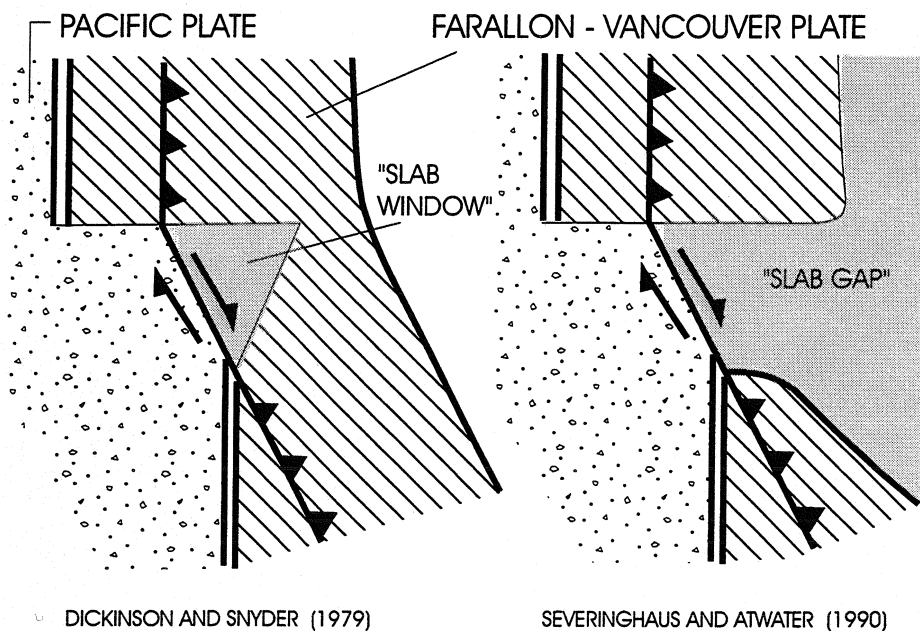


Figure 21. Diagram illustrating the distinction between a slab window and a slab gap.

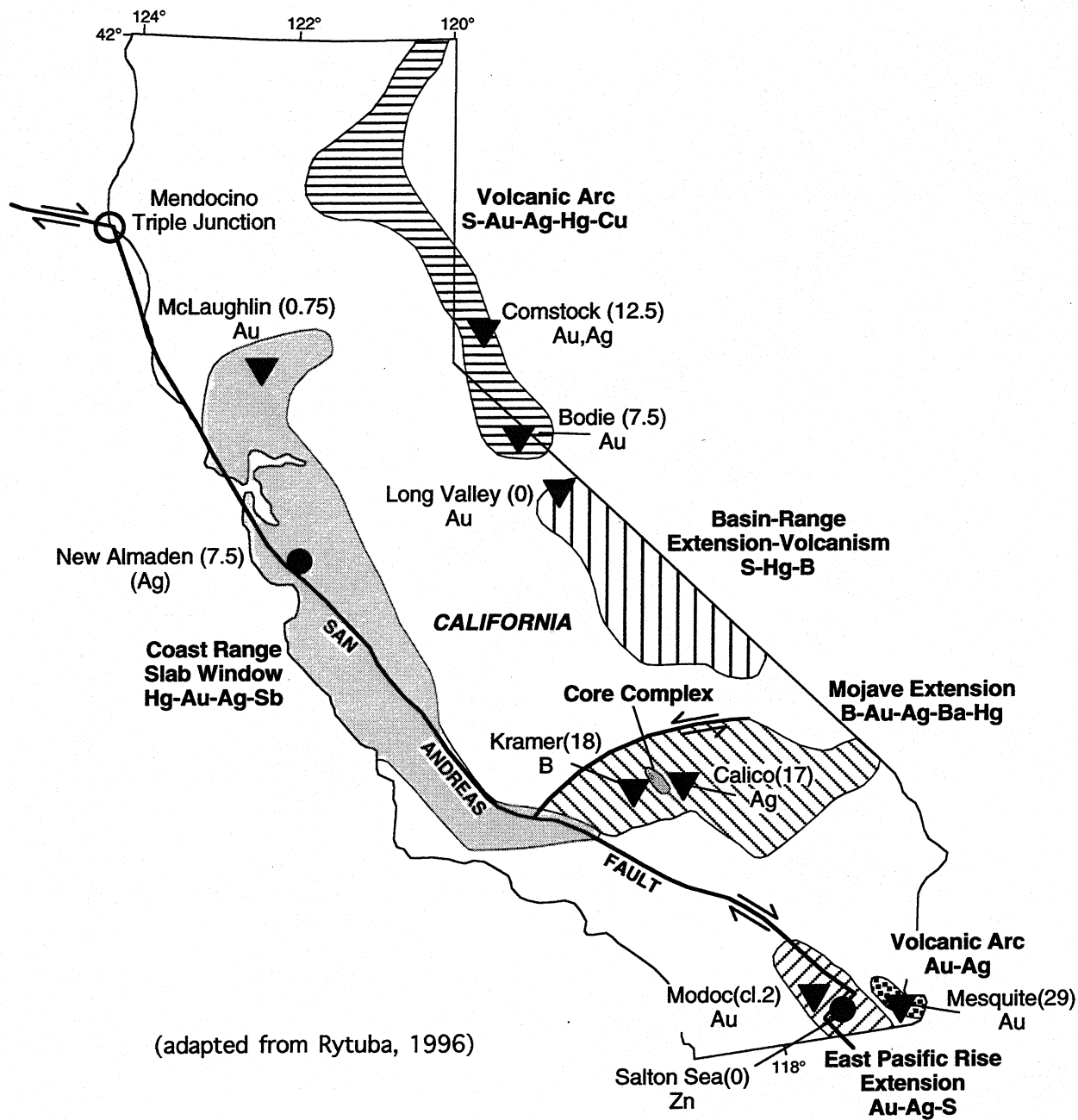


Figure 22. Cenozoic metallogeny of California (adapted from Rytuba, 1996). Arc segments, slab window (gap), and oceanic spreading ridge settings are present.

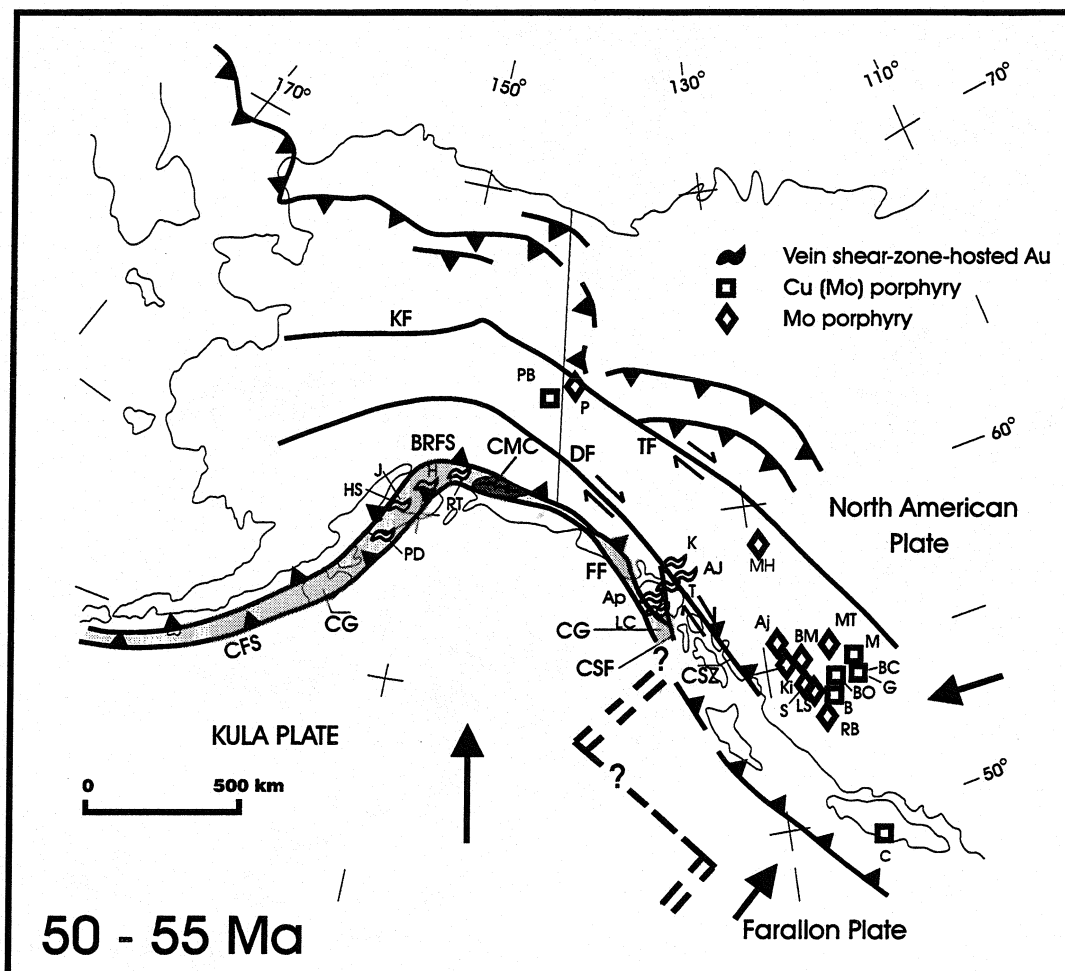


Figure 23. Diagram illustrating tectonic settings and mineral deposit 50 - 55 Ma in the northwestern Cordillera.

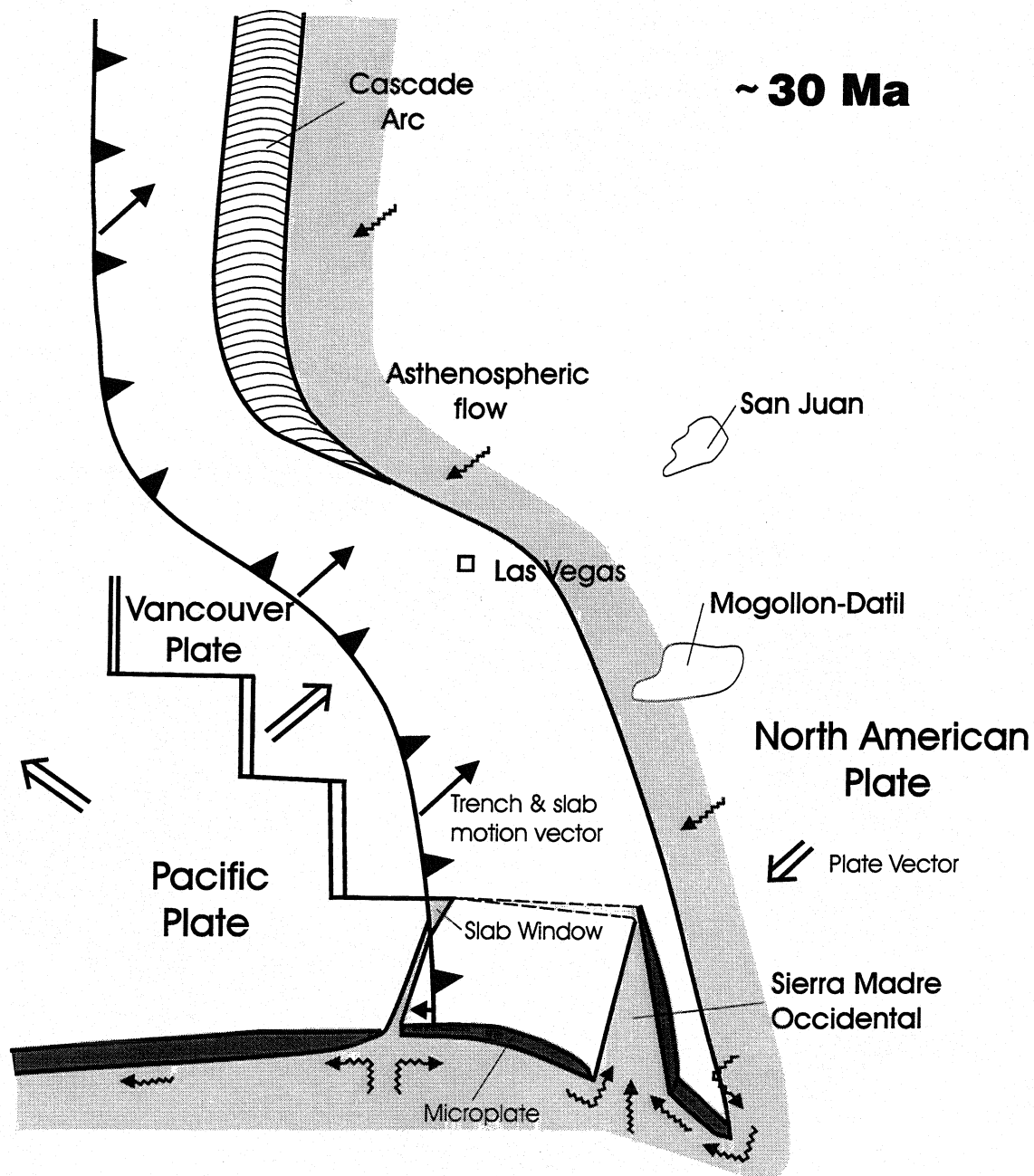
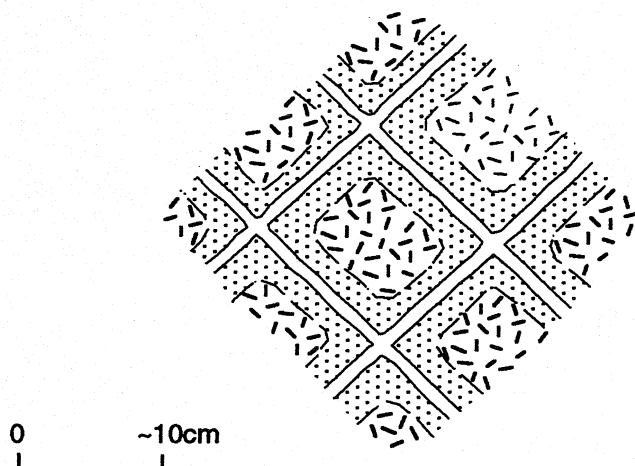


Figure 24. Three dimensional perspective of the subducted slab under North America about 30 Ma trying to illustrating Ward's (1991) concept of a transtensional environment for the large Sierra Madre Occidental batholith and extensive caldera ignimbrite province. Similar transtensional and magmatic environments were soon to follow in the Mogollon-Datil and San Juan areas as the Mendocino triple junction moved to the north. This is viewed to be a characteristic environment for the formation of major batholiths.

## STOCKWORK WITH BIOTITE ALTERATION



## PSUEDOBRECCIA WITH SCHISTOSE BIOTITE

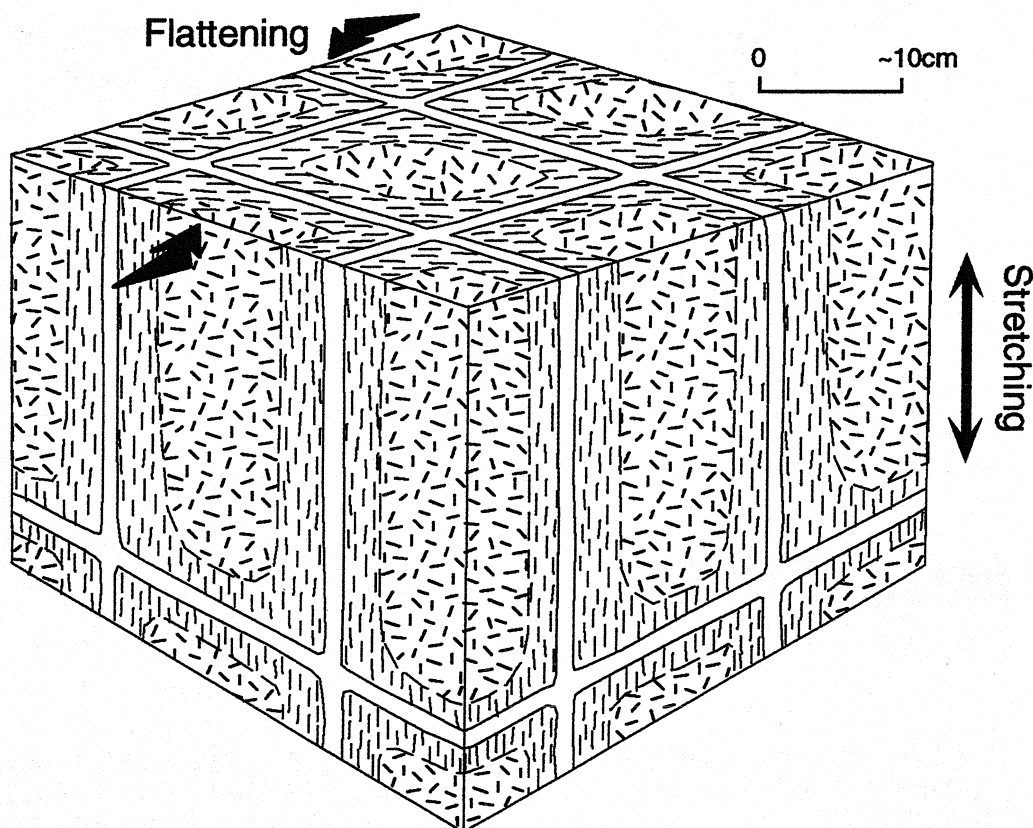


Figure 25. Schematic diagram illustrating tectonic flattening, stretching, and development of a pseudobreccia in an environment of moderate compressional deformation. Modelled after the Troilus porphyry Au (Cu) deposit in the Archean Abitibi greenstone belt, Quebec.

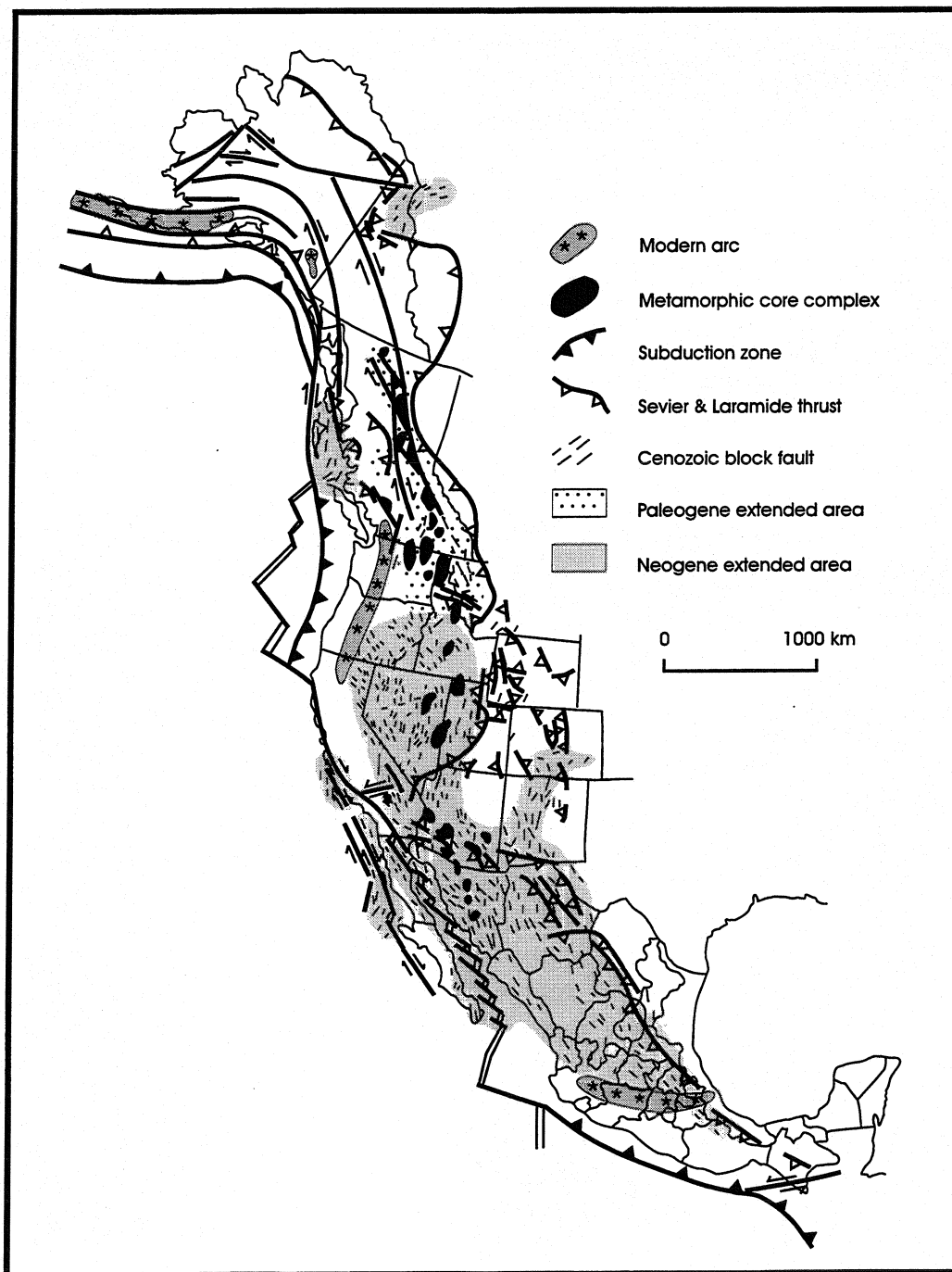


Figure 26. Diagram showing areas and timing of Cordillera extension.

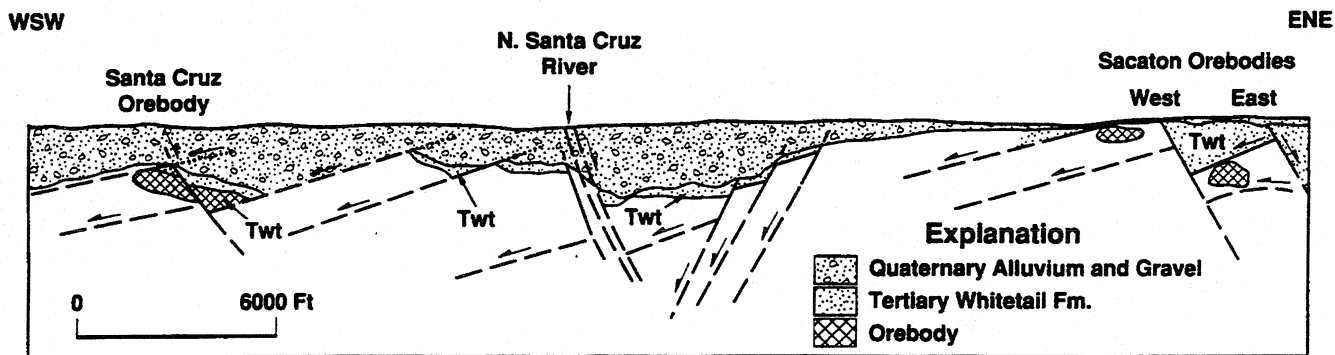
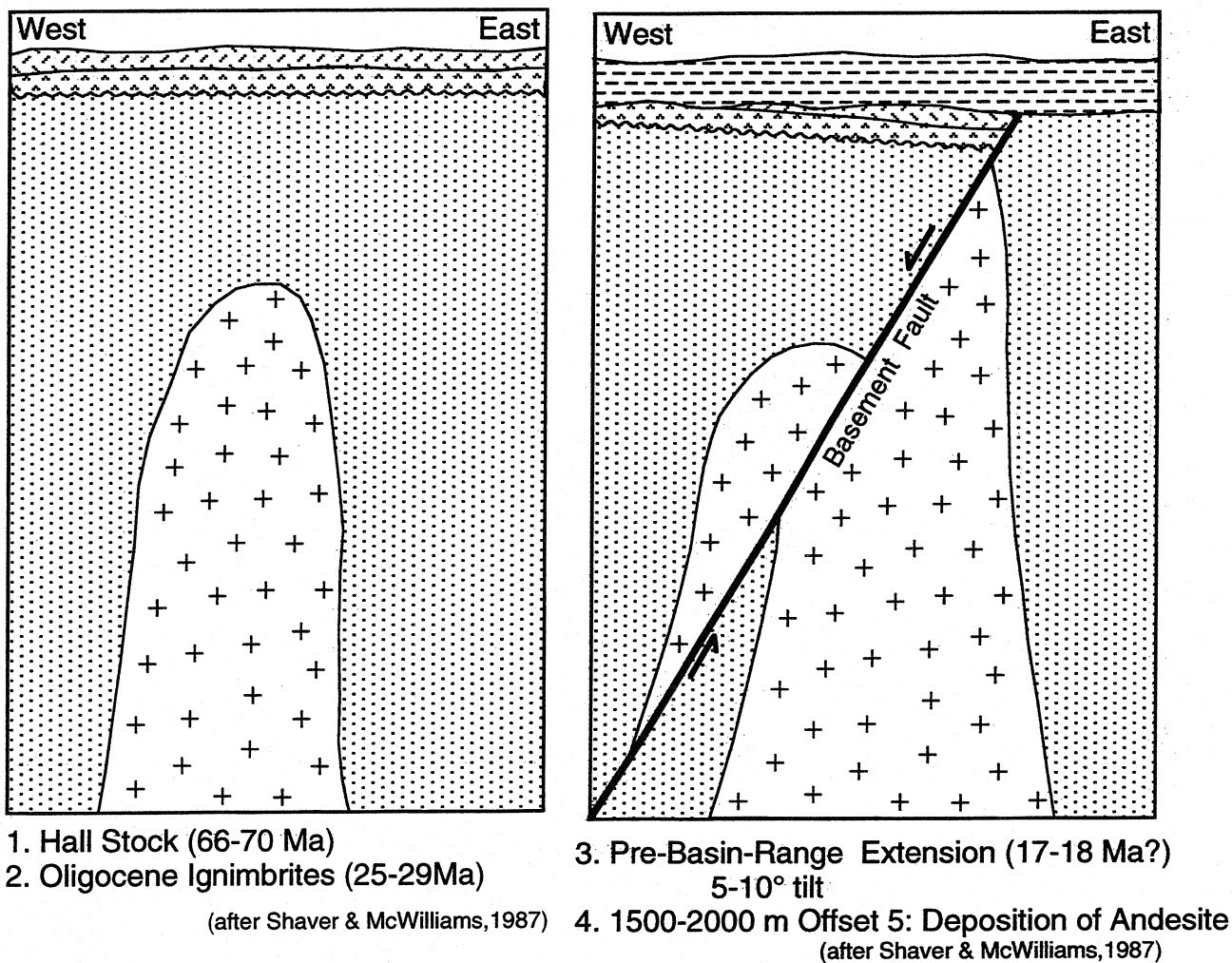
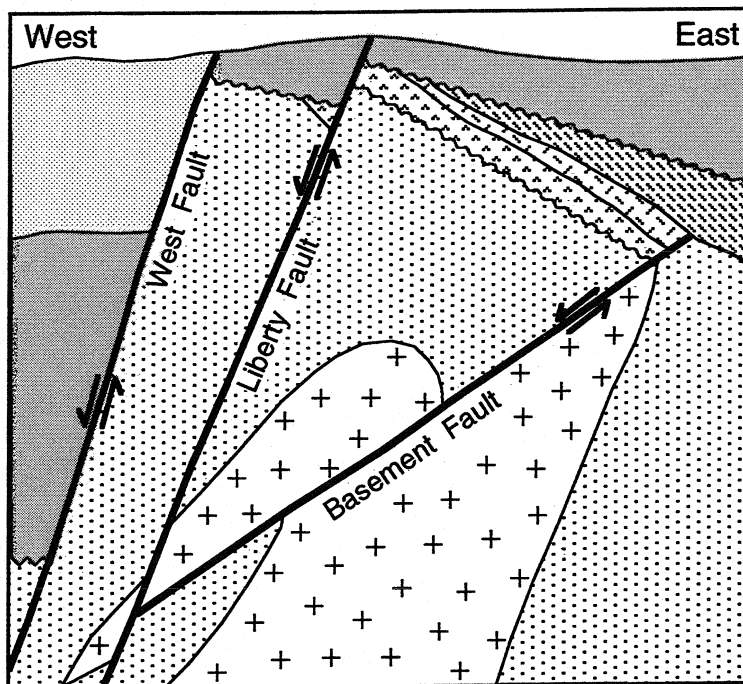


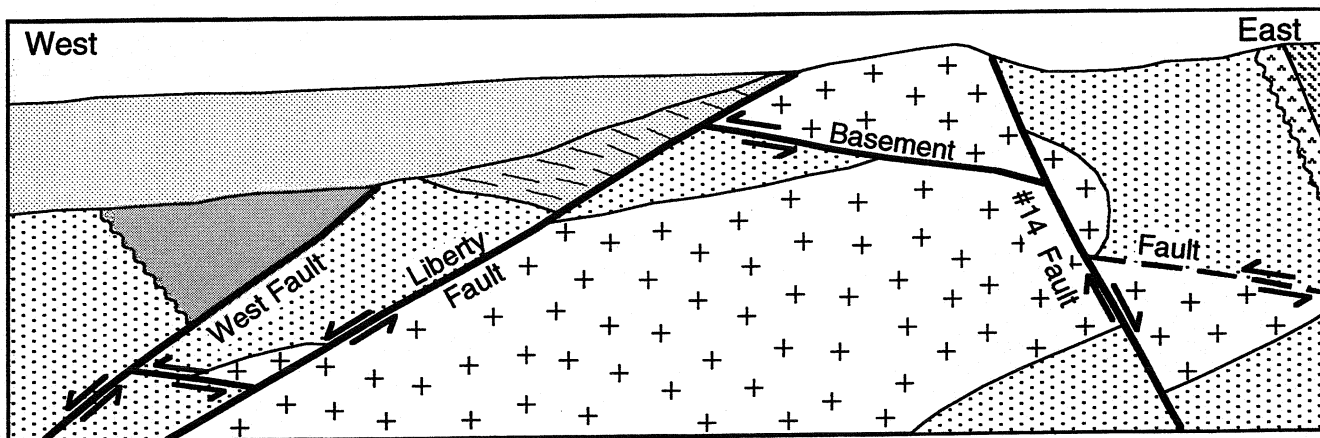
Figure 27. Diagram illustrating the dismemberment and transport of the Santa Cruz - Sacaton deposit, Arizona (after Wilkins and Heidrick, 1994).





8. 20-45° Total Tilt  
10. Initial Liberty Fault

9. West Fault  
(after Shaver & McWilliams, 1987)



14. 70° Total Tilt    15. #14 Fault

16. Erosion Present and Holocene Alluvium  
(after Shaver & McWilliams, 1987)

Figure 28. Diagrams illustrating multiple periods of normal faulting and rotation of the Hall deposit, Nevada (after Shaver and McWilliams, 1987). These diagrams illustrate the difficulty that can be encountered in reconstructing the original geometry of some porphyry deposits.



B 46

## C - GEOENVIRONMENTAL MINERAL DEPOSIT MODELS FOR THE NORTHERN CORDILLERA

Richard Goldfarb, Edward duBray, John Gray, Karen Kelley and Geoffrey Plumlee, U.S. Geological Survey

Goldfarb, R., duBray, E., Gray, G., Kelley, K. and Plumlee, G. (1998): Geoenvironmental Mineral Deposit Models for the, Northern Cordillera; in *Metallogeny of Volcanic Arcs*, B.C. Geological Survey, Short Course Notes, Open File 1998-8, Section C.

Table of Contents pages C6-7

Chapter 29 - Sedimentary Exhalative Zn-Pb-Ag Deposits, pages C8-16

Chapter 34 - Low Sulfide Au Quartz Veins, pages C17-23

Case Studies from the Northern Cordillera, pages C24-49

### ABSTRACT

Empirical mineral deposit models are not only critical in exploring for accumulations of metals and development of ore genesis concepts, but also for understanding geochemical patterns that develop during natural degradation of metal accumulations. These patterns, or environmental signatures, are the result of natural weathering and erosion but may also be affected by human activities.

Environmental signatures are dominantly controlled by the geologic characteristics of ore deposits including size, host rock type, surrounding regional geology, geochemistry of alteration, nature of the ore, trace element geochemistry, mineralogy and mineralogical characteristics, secondary minerals, topography, and geohydrology. Consequently, empirical data that define these signatures can be gathered from waters, sediments, and soils surrounding specific deposit types; these data can then be summarized to produce a comprehensive geoenvironmental mineral deposit model. In theory, a given ore deposit type is characterized by a fairly predictable environmental signature. However, as with any model, other factors can cause deviations. Variables such as climate and mining method can play significant roles in defining environmental signatures associated with individual deposits.

Our recent work in the northern Cordillera has emphasized collection of empirical data that define the environmental signatures of the mineral deposit types commonly associated with accreted terranes and superimposed arcs. Objectives have included establishing estimates for premining geochemical baselines in highly mineralized belts, as well as determining the environmental effects of various mining and processing activities. The influence of geology on natural background concentrations of metals in water is obvious in studies of shale-hosted stratiform Pb-Ag-Zn massive sulfide deposits from the northwestern Brooks Range. Premining surface water draining the Red Dog deposit and water draining the Drenchwater occurrence commonly contained total dissolved metal concentrations between 1-50 ppm at pH values of 3-6; the impact of these deposits is significant for kilometers downstream. In contrast, carbonate rocks in the sedimentary sequence at the Lik occurrence buffer water that drains massive sulfide to neutral to slightly alkaline pH values; this water has much lower metal transport capacity. Similarly in the Wrangell Mountains of eastern Alaska, water draining gold-bearing skarn and

the massive Kennecott-type copper ore has relatively low metal-transport capacity due to thick carbonate sections.

Abandoned Besshi- and Cyprus-type VMS deposits are widespread in the Prince William Sound region of south-central Alaska. Although surface water below these ore deposits is typically acidic and metal-rich, climate plays a major role in defining the extent of metal dispersion in this temperate rainforest climate. Water draining abandoned mine tailings is characterized by pH values as acidic as 2.5 and contains approximately 30 ppm dissolved Fe+Cu+Zn. However, due to the abundance of surface water runoff throughout the region, acid drainage is rapidly diluted to background levels within a few hundred meters of mine workings.

The regional geoenvironmental model for arc-related epithermal vein deposits, which are widespread in southwestern Alaska, emphasizes concerns associated with Hg-enriched mineralogy. The low pyrite content of the veins results in minimal acid mine drainage. But to test the extent that mercury from eroded cinnabar might be naturally converted through biological and chemical processes to more hazardous methylmercury, detailed evaluations were made of stream waters, vegetation, and fish. Results indicate that weathered cinnabar is highly insoluble and is not mobilized through the food chain.

The low sulfide content of mesothermal gold-bearing vein deposits throughout Alaska leads to a model that predicts generally minimal impact on local ecosystems from unmined or mined occurrences. For example, water draining the extensive underground workings of the Alaska-Juneau mine is characterized by concentrations of trace metals that are within the range allowable for safe drinking water. However, the environmental effects of unusually extensive sulfidization of metasedimentary and igneous country rocks that host gold-bearing veins in part of the Fairbanks district exemplify how ore deposit geology can cause significant deviation from a model. Resulting natural dissolved arsenic levels of as much as 500 ppb exceed maximum allowable drinking water standards by an order of magnitude. Also, although mines in this deposit type typically pose little threat to the environment and present milling methods of ore extraction meet strict environmental standards, historic milling methods that concentrated gold-bearing sulfide phases into large abandoned waste piles can lead to metalliferous acid drainage. It is, therefore, critical that our geoenvironmental models clearly indicate the difference in environmental signatures that are likely to result from past and present mining methods.

# **GEOENVIRONMENTAL MINERAL DEPOSIT MODELS FOR THE NORTHERN CORDILLERA**

**Richard Goldfarb, Edward du Bray, John Gray, Karen Kelley, and Geoffrey  
Plumlee  
U.S. Geological Survey**

## **Introduction**

Empirical mineral deposit models are not only critical in exploring for accumulations of metals and development of ore genesis concepts, but also for understanding geochemical patterns that develop during natural degradation of metal accumulations. These patterns, or environmental signatures, are the result of natural weathering and erosion but may also be affected by human activities. Environmental signatures are dominantly controlled by the geologic characteristics of ore deposits including size, host rock type, surrounding regional geology, geochemistry of alteration, nature of the ore, trace element geochemistry, mineralogy and mineralogical characteristics, secondary minerals, topography, and geohydrology. Consequently, empirical data that define these signatures can be gathered from waters, sediments, and soils surrounding specific deposit types; these data can then be summarized to produce a comprehensive geoenvironmental mineral deposit model. In theory, a given ore deposit type is characterized by a fairly predictable environmental signature. However, as with any model, other factors can cause deviations. Variables such as climate and mining method can play significant roles in defining environmental signatures associated with individual deposits.

## **Geoenvironmental Mineral Deposit Models of the U.S. Geological Survey**

Two years ago, the U.S. Geological Survey released a preliminary compilation of descriptive geoenvironmental mineral deposit models (du Bray, 1995). The aim of the volume was to meet a growing demand from many of our own geologists, as well as our outside customers, for geological information that would be most useful in understanding the environmental effects from developed and undeveloped metal accumulations located at and near the earth's surface. The information within the model book is now routinely applied to the USGS' assessment program of public lands (for example, Plumlee et al., 1994). This type of assessment work no longer emphasizes solely the identification of tracts favorable for the occurrence of mineral deposits; rather, it now also includes an important component that assesses the characteristics of environmental effects of mined and unmined mineral occurrences. The data in the model book are also critical for planners and regulators in their need to better identify and prioritize

environmentally hazardous sites, and to predict the environmental signatures from past and future resource development.

Geology and mining/milling methodologies are major controls on the environmental behavior of mineral deposits. Therefore, it is critical that this information be included in any geoenvironmental model. Key factors for each, summarized from Plumlee and Nash (1995), are listed below:

Geologic controls on environmental signatures

1. Ore and gangue mineralogy, and host rock lithogeochemistry--acid-generating vs. acid-consuming
2. Mineral resistance to weathering--susceptibility to oxidation; relative mineral stabilities
3. Major and trace element geochemistry of ores--metal enrichments in soils, waters, and sediments; complexing, sorption, and precipitation reactions; variable mobilities
4. Mineral textures and grain size--fine- vs. coarse-grained; massive vs. euhedral ores
5. Extent of pre-mining oxidation--metals contained in less soluble hydroxides, sulfates, and carbonates; strong climatic control
6. Secondary mineralogy of mine wastes
7. Structure and lithology--controls groundwater access, permeability, etc.

Mining controls on environmental signatures

1. Open pit vs. underground methods--differences in access to weathering agents; evaporative concentration in pits
2. Tailing particle sizes--effects metal adsorption, sulfide oxidation, and dispersion pathways
3. Milling methods--sulfide concentrates, mercury amalgamation, cyanidation, roasting

The U.S. Geological Survey's model guidebook aims to systematically compile this geological and mining information for the more common mineral deposit types. For examples, copies of models for

volcanic-associated massive sulfide, sedimentary exhalative Zn-Pb-Ag, and low-sulfide Au quartz deposits are reproduced in subsequent pages of these short course notes. Models for epithermal-type gold vein deposits are included within a subsequent chapter to this short course by Geoff Plumlee.



## CONTENTS

Geoenvironmental models of mineral deposits--fundamentals and applications, by G.S. Plumlee and J.T. Nash .....	1
Bioavailability of metals, by D.A. John and J.S. Leventhal .....	10
Geophysical methods in exploration and mineral environmental investigations, by D.B. Hoover, D.P. Klein, and D.C. Campbell .....	19
Magmatic sulfide deposits, by M.P. Foose, M.L. Zientek, and D.P. Klein .....	28
Serpentine- and carbonate-hosted asbestos deposits, by C.T. Wrucke. ....	39
Carbonatite deposits, by P.J. Modreski, T.J. Armbrustmacher, and D.B. Hoover .....	47
Th-rare earth element vein deposits, by T.J. Armbrustmacher, P.J. Modreski, D.B. Hoover, and D.P. Klein .....	50
Sn and (or) W skarn and replacement deposits, by J.M. Hammarstrom, J.E. Elliott, B.B. Kotlyar, T.G. Theodore, J.T. Nash, D.A. John, D.B. Hoover, and D.H. Knepper, Jr. ....	54
Vein and greisen Sn and W deposits, by J.E. Elliott, R.J. Kamilli, W.R. Miller, and K.E. Livo .....	62
Climax Mo deposits, by S. Ludington, A.A. Bookstrom, R.J. Kamilli, B.M. Walker, and D.P. Klein .....	70
Porphyry Cu deposits, by L.J. Cox, M.A. Chaffee, D.P. Cox, and Douglas P. Klein .....	75
Cu, Au, and Pb-Zn skarn deposits, by J.M. Hammarstrom, B.B. Kotlyar, T.G. Theodore, J.E. Elliott, D.A. John, J.L. Doebrich, J.T. Nash, R.R. Carlson, G.K. Lee, K.E. Livo, and D.P. Klein .....	90
Fe skarn deposits, by J.M. Hammarstrom, T.G. Theodore, B.B. Kotlyar, J.L. Doebrich, J.E. Elliott, J.T. Nash, D.A. John, and K.E. Livo .....	112
Polymetallic vein and replacement deposits, by G.S. Plumlee, M. Montour, C.D. Taylor, A.R. Wallace, and D.P. Klein .....	121
Au-Ag-Te vein deposits, by K.D. Kelley, T.J. Armbrustmacher, and D.P. Klein .....	130
Volcanic-associated massive sulfide deposits, by C.D. Taylor, R.A. Zierenberg, R.J. Goldfarb, J.E. Kilburn, R.R. Seal, II, and M.D. Kleinkopf. ....	137
Blackbird Co-Cu deposits, by K.V. Evans, J.T. Nash, W.R. Miller, M.D. Kleinkopf, and D.L. Campbell .....	145
Creede, Comstock and Sado epithermal vein deposits, by G.S. Plumlee, K.S. Smith, B.R. Berger, N. Foley-Ayuso, and D.P. Klein .....	152
Epithermal quartz-alunite Au deposits, by G.S. Plumlee, K.S. Smith, J.E. Gray, and D.B. Hoover .....	162
Epithermal Mn deposits, by D.L. Mosier and D.L. Campbell .....	170
Rhyolite-hosted Sn deposits, by E.E. Foord, R.A. Ayuso, D.B. Hoover, and D.P. Klein .....	174
Low-Ti iron oxide Cu-U-Au-REE deposits, by M.P. Foose and V.J.S. Grauch .....	179
Sediment-hosted Au deposits, by A.H. Hofstra, J.S. Leventhal, D.J. Grimes, and W.D. Heran .....	184
Almaden Hg deposits, by J.J. Rytuba and D.P. Klein .....	193
Silica-carbonate Hg deposits, by J.J. Rytuba and M.D. Kleinkopf .....	199
Stibnite-quartz deposits, by R.R. Seal, II, J.D. Bliss, and D.L. Campbell .....	204
Algoma Fe deposits, by W.F. Cannon, D.G. Hadley, and R.J. Horton .....	209
Sediment-hosted Cu deposits, by D.A. Lindsey, L.G. Woodruff, W.F. Cannon, D.P. Cox, and W.D. Heran .....	214
Sedimentary exhalative Zn-Pb-Ag deposits, by K.D. Kelley, R.R. Seal, II, J.M. Schmidt, D.B. Hoover, and D.P. Klein .....	225
Mississippi Valley-type Pb-Zn deposits, by D.L. Leach, J.B. Viets, N. Foley-Ayuso, and D.P. Klein .....	234
Solution collapse breccia pipe U deposits, by K.J. Wenrich, B.S. Van Gosen, and W.I. Finch .....	244
Superior Fe deposits, by W.F. Cannon, D.G. Hadley, and R.J. Horton .....	252
Sedimentary Mn deposits, by E.R. Force, W.F. Cannon, and D.P. Klein .....	257
Low-sulfide Au quartz vein deposits, by R.J. Goldfarb, B.R. Berger, T.L. Klein, W.J. Pickthorn, and D.P. Klein .....	261
Stratabound Au deposits in iron formations, by E.H. DeWitt, W.D. Heran, and M.D. Kleinkopf .....	268



## SEDIMENTARY EXHALATIVE ZN-PB-AG DEPOSITS (MODEL 31a; Briskey, 1986)

by Karen D. Kelley, Robert R. Seal, II, Jeanine M. Schmidt,  
Donald B. Hoover, and Douglas P. Klein

### SUMMARY OF RELEVANT GEOLOGIC, GEOENVIRONMENTAL, AND GEOPHYSICAL INFORMATION

#### Deposit geology

Lens-like bodies of stratiform sulfide minerals (lead, zinc,  $\pm$  iron) as much as a few tens of meters in thickness are interbedded with fine-grained dark clastic and chemical sedimentary rocks. These deposits may have large lateral extent (hundreds of meters to kilometers). Mineralized rock varies from a single layer to numerous bodies that may be vertically stacked or lateral equivalents. The most common associated sulfate mineral is barite which may be peripheral to or stratigraphically above the deposit (Rammelsberg and Meggen, Germany; Tom, Yukon Territory; Lady Loretta, Australia; and Red Dog, Alaska), or it may form crudely segregated mixtures with sulfide minerals (Cirque, British Columbia). Many deposits have no associated barite (HYC, Australia; Sullivan, British Columbia; and Howard's Pass, Yukon Territory). Stockwork, disseminated, or vein-type ore, interpreted as feeder zones to stratiform mineralized rock, are sometimes found underlying or adjacent to stratiform ore and are sometimes accompanied by alteration of footwall rocks (fig. 1). U.S. Bureau of Mines (1993) statistics show that in 1993 the two mines in the United States with greatest zinc output were Red Dog, Alaska and Balmat, N.Y. In 1994, the Red Dog mine produced 533,500 t of zinc concentrate with an average grade of 55.8 weight percent zinc (Mining Journal, 1995). Mines in the Balmat district produced 499,000 t in 1993. Both mines also produce lead and silver.

#### Examples

Red Dog, Lik, and Drenchwater (Alaska); Balmat (N.Y.); Meggen and Rammelsberg (Germany); Faro and other deposits in the Anvil district, Tom, Jason, and Howard's Pass (Yukon Territory); Cirque and Sullivan (British Columbia); Lady Loretta, McArthur River, Mount Isa, HYC, and Broken Hill (Australia); Navan, Silvermines, and

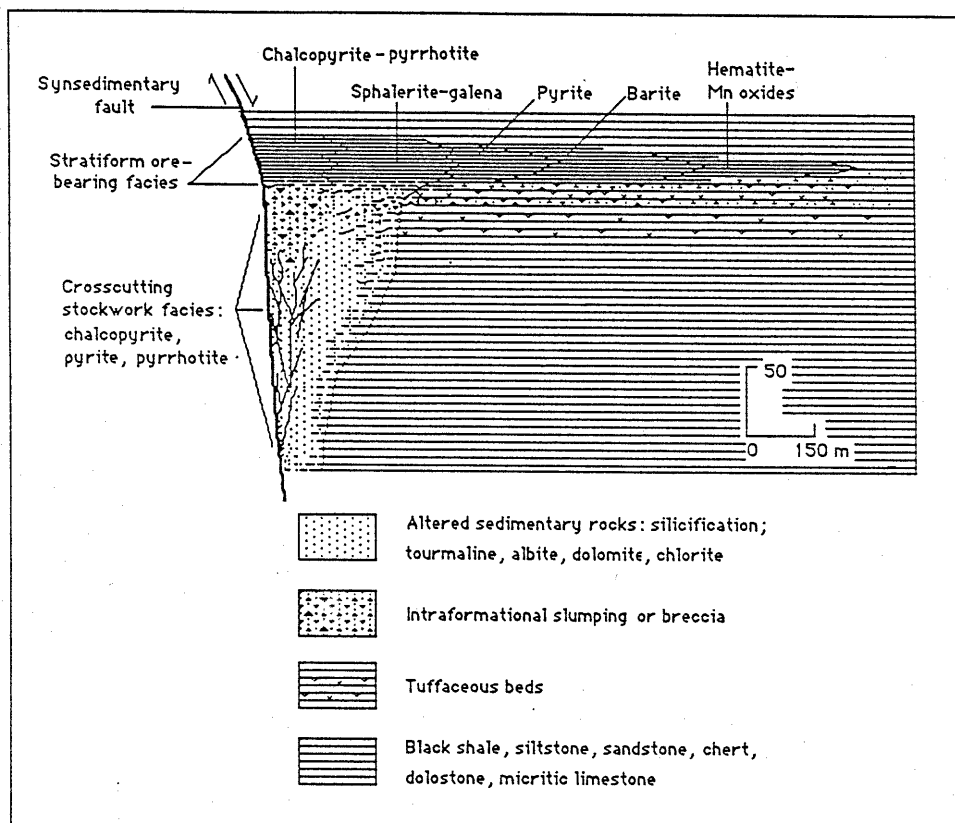
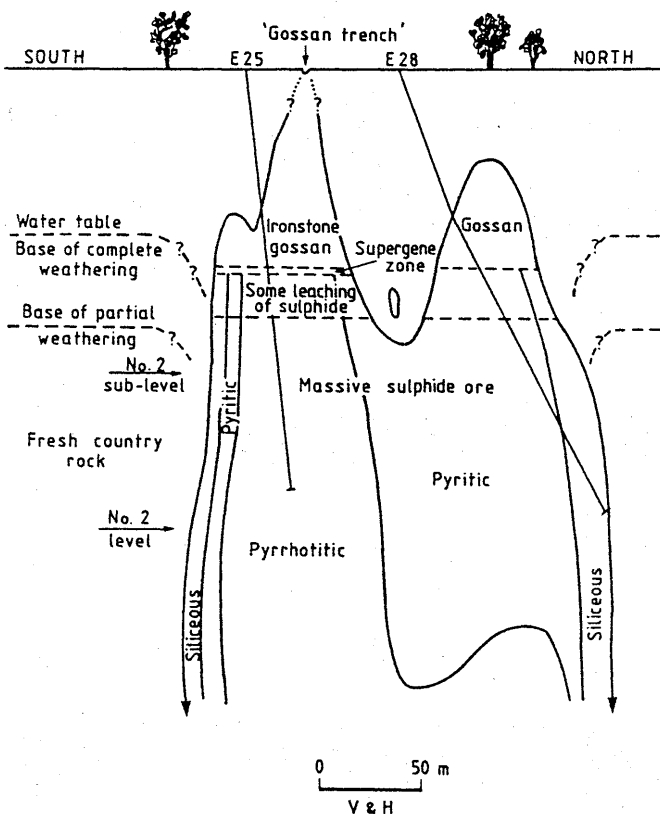


Figure 1. Diagrammatic cross section showing mineral zoning in sedimentary exhalative Zn-Pb deposits (from Briskey, 1986).



**Figure 2.** Longitudinal cross section showing development of supergene zone and iron-rich gossan (based on Elura deposit, Australia; from Taylor and others, 1984).

#### Spatially and (or) genetically related deposit types

Associated deposit types (Cox and Singer, 1986) include bedded barite deposits (Model 31b), stratabound lead-zinc in clastic rocks (Model 30a), Mississippi Valley type lead-zinc (Models 32a,b), sedimentary manganese (Model 34b), sedimentary phosphate (Model 34c), Besshi massive sulfide (Model 24b), Chinese-type black shale (Mo-Ag-As-Zn-Ni-PGE; Pasava, 1993).

#### Potential environmental considerations

- (1) Deposits with no associated carbonate rocks or carbonate alteration minerals may have high potential for generation of natural acid drainage that contains high metal concentrations. Potential for acid-drainage generation may depend on (a) the amount of iron-sulfide present (which may vary from <5 to 80 volume percent among deposits), (b) the type of iron sulfide mineral(s) in the deposit (reactivity decreases from pyrrhotite to marcasite to pyrite) and (c) the extent to which the deposit is exposed to air and water. Water may contain thousands of mg/l sulfate; hundreds of mg/l iron; tens of mg/l aluminum; thousands to tens of thousands of  $\mu\text{g/l}$  zinc; thousands of  $\mu\text{g/l}$  manganese and lead; hundreds of  $\mu\text{g/l}$  cadmium, copper, and nickel; and tens of  $\mu\text{g/l}$  cobalt (Runnells and others, 1992; Kelley and Taylor, in press; EIS for Red Dog).
- (2) Potential downstream environmental effects of natural acid drainage can be significant in magnitude and spatial extent (as far as 30 km downstream), especially if surrounding terrane is composed exclusively of fine-grained clastic rocks and volcanic rocks and no associated carbonate rocks (EIS for Red Dog).
- (3) Deposits with associated carbonate rocks or abundant carbonate alteration minerals have limited potential for acid drainage generation (water pH usually neutral to slightly alkaline), and most metal concentrations are low; exceptions include as much as thousands of  $\mu\text{g/l}$  zinc in some natural water (Kelley and Taylor, in press).
- (4) Iron-rich gossans, formed by oxidation and weathering, may develop above some deposits (fig. 2). Depending on wall-rock buffering capacity, iron content of ore, and metal-sulfur ratios of sulfide minerals, the gossan environment can be acidic ( $\text{pH} < 5$ ). Some gossans may contain a number of secondary lead-manganese minerals as well as secondary sulfates of iron, aluminum, and potassium (Taylor and others, 1984). These minerals are very soluble, can dissolve during periodic storms, and may lead to short term pulses of highly acidic, metal-bearing water.
- (5) High-sulfide ore with elevated abundances of pyrrhotite that is exposed to air and water has potential for spontaneous combustion ("hot muck"), which generates sulfur dioxide (Brown and Miller, 1977; Good, 1977). Hot muck ignition is rare and can be avoided using proper blasting techniques.

### Exploration geophysics

Gravity surveys can be used to identify and delineate the extent of barite-rich zones that may indicate associated base-metal sulfide deposits (Young, 1989; Hoover and others, 1994). Induced polarization methods have proven useful in exploration for some of these deposits (O'Brien and Romer, 1971; Cox and Curtis, 1977). Remote sensing images can be used to help identify associated gossans (Knepper, 1989). Magnetic and electromagnetic methods may help define the presence and extent of massive sulfide deposits, particularly those that contain abundant pyrite and (or) pyrrhotite. Constant source-audiomagnetotelluric methods have been used to help delineate the extent of ore in northwest Alaska (Young, 1989). Other geophysical methods may facilitate geologic mapping of these deposits (Edwards and Atkinson, 1986, p. 245).

### References

Geology: Large (1981), Maynard (1983), Sangster (1983), Moore and others (1986), Turner and Einaudi (1986), Young (1989), Sangster (1990), Maynard (1991), and Schmidt (in press).  
Environmental geology, geochemistry: Lee and others (1984), Runnells and others (1992), Gulson and others (1994), Prusty and others (1994), Sahu and others (1994), Kelley (1995), and Kelley and Taylor (in press).

## GEOLOGIC FACTORS THAT INFLUENCE POTENTIAL ENVIRONMENTAL EFFECTS

### Deposit size

Most deposits are 1.7 (90th percentile) to 130 (10th percentile) million tons; median deposit size is 15 million tons (Menzie and Mosier, 1986).

### Host rocks

Host rocks consist of a variety of marine sedimentary rocks including: carbonaceous shale and chert (Howard's Pass, Yukon Territory; Red Dog and Lik, Alaska; and Sullivan, British Columbia), dolomitic shale or siltstone (HYC and Mount Isa, Australia; and Silvermines, Ireland), and micritic limestone (Meggen, Germany and Tynagh, Ireland). Turbidites and slump breccias are present locally; minor volcanic rocks, usually mafic, may be temporally, but not necessarily spatially, associated. Sangster (1990) indicates that tuff units are present within ore-hosting sequences at a number of deposits, including Meggen and Rammelsberg (Germany), Jason and Faro (Yukon Territory), and HYC (Australia). Many deposits and their host rocks have undergone metamorphism and deformation (Sullivan, British Columbia and Mount Isa and Broken Hill, Australia). Comparisons of host rock chemistry to average abundances in black shale (Vine and Tourtelot, 1970) show that host rocks for these deposits have relatively low sodium-potassium ratios and are characteristically depleted in cobalt, nickel, and copper and enriched in barium and manganese (Maynard, 1991).

### Surrounding geologic terrane

The geologic terrane surrounding these deposits primarily consists of thick sequences of deep-water marine sedimentary rocks that include fine-grained clastic and carbonate rocks. Rocks may be metamorphosed (low to high-grades).

### Wall-rock alteration

Stockwork and disseminated sulfide and alteration minerals (commonly silicified or iron-carbonate altered rocks that rarely contain tourmaline, albite, chlorite), which possibly represent the feeder zones of these deposits, are sometimes present beneath or adjacent to stratiform deposits (fig. 1). In some deposits, silicification is the dominant or only alteration (Meggen, Germany and Red Dog, Alaska). In others, alteration is less extensive and (or) carbonate-rich (Large, 1981). Large (1983) describes more subtle types of alteration near some deposits, including increased dolomite-calcite ratios (McArthur River, Australia; deposits in Ireland) and increased potassium feldspar-albite ratios in tuffs (McArthur River).

### Nature of ore

Within stratiform mineralized rocks, sulfide minerals are generally fine-grained, and commonly form nearly monomineralic laminae several mm to cm thick that have continuity over large parts of the deposits. Some deposits are not laminated (Meggen, Germany and Red Dog, Alaska). Coarse-grained crustiform and comb-textured sulfide minerals may be present in feeder veins associated with stratiform ore. The overall sheet or lens-like morphology of stratiform ore suggests that these deposits formed, in highly restricted basins, by syngenetic to early diagenetic

processes at or below the seawater-sediment interface. Sphalerite, galena, and iron-sulfide minerals (pyrite, marcasite, and pyrrhotite) are the most common sulfide minerals, but chalcopyrite and sulfosalt minerals may also be present in minor amounts (Large, 1981; 1983; Lydon, 1983).

#### Deposit trace element geochemistry

Feeder or stockwork zone (Large, 1983; Lydon, 1983): iron, lead, and zinc ( $\pm$  gold, boron, and copper). Stratiform ore (Large, 1983; Lydon, 1983): lead, zinc (cadmium), with or without barium (zoned laterally outward from feeder zone (fig. 1). Iron may be enriched within and adjacent to the base-metal sulfide zone (Large, 1983); anomalous concentrations of silver  $\pm$  arsenic and antimony in sulfosalt minerals (Cox and Curtis, 1977; Taylor and others, 1984) and manganese (outer halo) are also common (Maynard, 1981). Concentrations of mercury are high in some deposits, where it is primarily in pyrite, sphalerite, or sulfosalt minerals (Ryall, 1981).

#### Ore and gangue mineralogy and zonation

Dominant sulfide ore minerals are sphalerite and galena, although minor chalcopyrite, arsenopyrite, and tetrahedrite are present in some deposits (Large, 1983). The most common gangue minerals are iron sulfide (pyrite or marcasite; less commonly pyrrhotite) and quartz (Meggen, Germany and Red Dog, Alaska). Barite may be present. Numerous other sulfide and sulfosalt minerals have been reported in some deposits (Cox and Curtis, 1977; Large, 1983; Taylor and others, 1994). Relative abundances of major base-metal sulfide minerals vary among deposits and within deposits as a result of zonation. Large (1983) reports that lead-zinc ratios of ore range from approximately 1:1 (Mount Isa, Australia; Sullivan, British Columbia; and Tynagh, Ireland) to 1:8 (Meggen, Germany). The sequence of zonation is generally lead-zinc-(barium-copper) extending outward in laterally zoned deposits and zinc-lead-(barium) extending upward in vertically zoned deposits (Large, 1983; Lydon, 1983). Iron is sometimes enriched at the center of zonation assemblages (for instance, Rammelsberg, Germany and Sullivan, British Columbia) (Large, 1983), or an iron-manganese halo may encircle the base-metal sulfide minerals (Tynagh, Ireland) (Maynard, 1983).

#### Mineral characteristics

Grain size typically ranges from 15 to 400 microns (McClay, 1983). Primary depositional features are dominated by fine-grain size and common layering; framboidal and colloform pyrite with euhedral overgrowths are common; granular sphalerite, galena and barite are typical. Some deposits (Red Dog, Alaska and HYC, Australia) are characterized by very fine-grained intergrowths of silica and sphalerite (individual sphalerite grains are 0.5 to 50 microns) or sphalerite with other sulfide minerals ( $<100$  microns) (McClay, 1983; Moore and others, 1986). Metamorphism partially or completely replaces primary textures and causes grain size increases. Recrystallization causes porphyroblastic textures in pyrite and sphalerite, barite is recrystallized to an elongate habit, and galena may be remobilized to fill fractures (McClay, 1983).

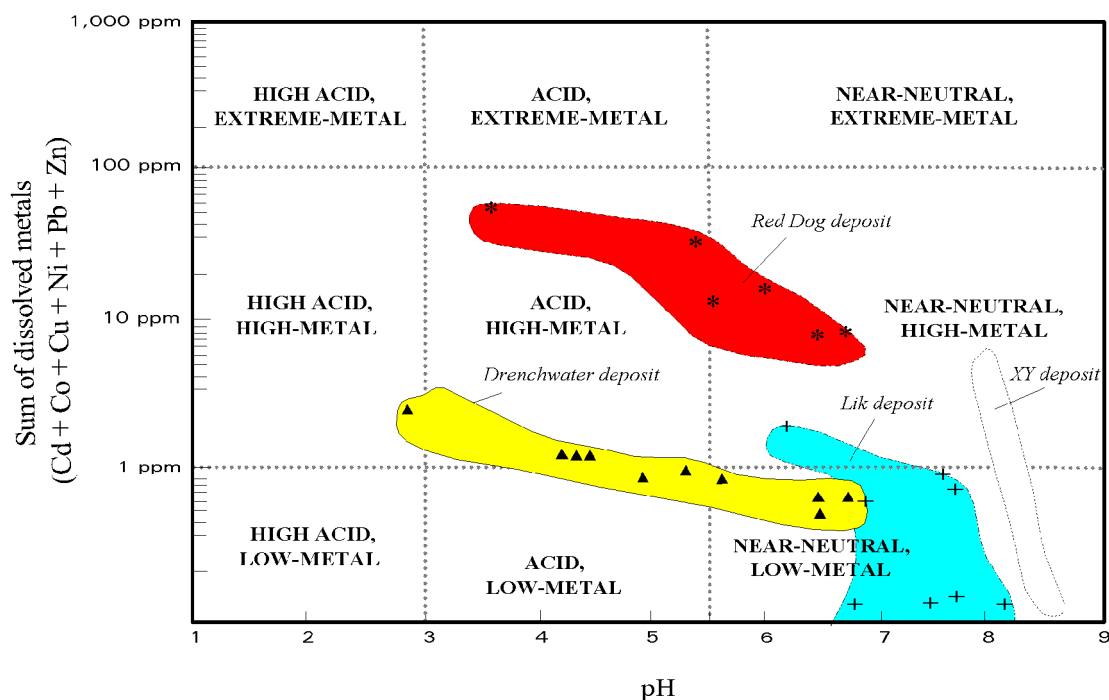
#### Secondary mineralogy

Oxidation of deposits may result in formation of iron-rich gossan and ferruginization of wall rocks (fig. 2). Deposits with low iron-sulfide contents have high metal-sulfur ratios, gangue or wall rocks with high buffering capacity, associated gossans have high pH, and gossan profiles are immature. Ore with high iron content, low metal-sulfur ratios in sulfide minerals, and wall rock with low buffering capacity is likely to be associated with low pH water (Taylor, 1984). Goethite and hematite, with minor quartz, kaolinite, and beudantite, are the main minerals in gossan (Taylor and others, 1984). Anglesite and cerussite are the most abundant secondary lead minerals but coronadite, mimetite, nadorite, pyromorphite, and lanarkite have also been reported. Silver halide minerals may also be present. Secondary zinc minerals are rare. Secondary sulfate minerals include jarosite, barite, and alunite. Native sulfur, produced by oxidation of marcasite, is present at Red Dog, Alaska (R.A. Zierenberg, written commun., 1995). Rock may be oxidized to 100 m below the surface (Australian examples), and may extend to 300 m adjacent to major faults and shear zones. Oxidation depth is controlled partly by fracture density near orebodies and presence of pyrrhotite, which is highly reactive with oxygenated ground water (Taylor and others, 1984).

Secondary zinc minerals hemimorphite, smithsonite, and wurtzite, not found in association with other deposits, are present in lime green mosses and as a cement within talus overlying the XY deposit (Howard's Pass, Yukon Territory) (Jonasson and others, 1983; Lee and others, 1984).

#### Topography, physiography

No generalizations possible. Sedimentary exhalative deposits are widely distributed geographically (from Australia to northern Alaska, to Ireland, for example) and so have completely different physiographies and topographies due



**Figure 3.** Diagram showing the relation between pH and metal content of water draining sedimentary exhalative deposits (modified from Plumlee and others, 1993).

to weathering process variations.

#### Hydrology

Hydrologic conditions associated with sedimentary exhalative deposits are highly variable due to extreme differences of their climate settings. Fine-grained clastic host rocks generally have low permeability. Pre-mineralization and post-mineralization fractures may serve as ground water conduits. However, depth of oxidation is dependant on a number of factors including climate, mineralogy of ore, and (or) host rocks.

#### Mining and milling methods

Underground and open-pit mining have been used historically and in modern times to exploit these deposits. Some sedimentary exhalative deposits contain very fine-grained and intergrown sulfide minerals (for example, Red Dog, Alaska and HYC, Australia) that require fine grinding during ore beneficiation. Base metal sulfide minerals are usually separated by flotation and ore concentrates are smelted. In most cases, concentrates are shipped to custom smelters and therefore do not contribute to environmental impact in the immediate mine vicinity. Large districts, such as Sullivan, British Columbia, are served by nearby smelters (for instance, Trail smelter, British Columbia).

### ENVIRONMENTAL SIGNATURES

#### Drainage signatures

Natural drainage water (Lik, Red Dog, and Drenchwater, Alaska: Dames and Moore, 1983; EIS report for Red Dog; Kelley, 1995; Kelley and Taylor, in press): Cold semi-arid climate--Without carbonate rocks present (Red Dog and Drenchwater), streams draining mineralized areas have low pH (2.8 to 4.7) and elevated dissolved metal abundances, including tens to hundreds of mg/l aluminum and iron and hundreds to tens of thousands of  $\mu\text{g/l}$  Mn, Cd, Co, Cu, Ni, Pb, and Zn. Sulfate concentrations, hundreds to thousands of mg/l, in water draining mineralized areas are also many times higher than background. Sodium and barium may be depleted in water draining mineralized areas. Data for deposits with significant associated carbonate rocks in surrounding geologic terrane (Lik, Alaska) are strikingly different (fig. 3). Water draining these deposits is near-neutral to alkaline (pH 6.2 to 8.1) and contains low metal concentrations, except zinc, whose abundances, thousands of  $\mu\text{g/l}$ , are enriched in streams draining mineralized areas. Sulfate concentrations, hundreds of mg/l, may also be elevated.

Neutral-pH springwater near the XY deposit (Howard's Pass, Yukon Territory) contains elevated dissolved metal abundances, including tens to thousands of  $\mu\text{g/l}$  zinc, tens of  $\mu\text{g/l}$  cadmium, and tens to hundreds of mg/l sulfate.

Mine drainage water (Red Dog, Alaska: Beelman, 1993; unpub. data, Alaska Department of Environmental Conservation, ADEC, 1995; Faro, Yukon Territory: Lopaschuk, 1979; Meggen, Germany: Bergmann, 1971; Broken Hill, South Africa: Gulson and others, 1994): Cold semi-arid climate--Immediately after mining began at Red Dog in the Fall of 1990, water draining the mine was extremely acidic (pH as low as 1.7) and contained elevated metal abundances, including from hundreds to thousands of  $\mu\text{g/l}$  lead, from hundreds to tens of thousands of  $\mu\text{g/l}$  cadmium, and from tens of thousands of  $\mu\text{g/l}$  to thousands of  $\text{mg/l}$  zinc. However, by spring of 1991, these abundances had decreased to pre-mining natural background concentrations (ADEC, 1995). The pulse of metal-enriched mine drainage that followed initial mining was probably the result of dissolution and flushing of a secondary sulfate mineral accumulation that developed as a result of marcasite oxidation in a near surface environment along steep faults (R.A. Zierenberg, written commun., 1995). Mild wet climate--The Meggen, Germany, mine, known in the late 1960s for mine water with high metal ion content and low pH, posed a severe pollution problem (Bergmann, 1971). Elevated metal abundances included hundreds of  $\text{mg/l}$  aluminum, tens of  $\text{mg/l}$  manganese, hundreds to thousands of  $\text{mg/l}$  iron, and hundreds to thousands of  $\text{mg/l}$  zinc.

Potentially economically recoverable elements: Zinc (as zinc hydroxide produced after treatment of mine water) is economically extracted at the Meggen, Germany, mine (Bergmann, 1971).

#### Metal mobility from solid mine wastes

Mine dumps may be a source of lead due to soluble secondary lead minerals common in oxidized material. Some of these dumps have recently been reprocessed, resulting in an increased volume of fine-grained lead-rich dust that contains as much as 3 weight percent lead (Gulson and others, 1994); this dust can be important in arid to semi-arid regions with high wind potential.

Bioavailability studies: The most common lead species in soil and dust associated with the Broken Hill, Australia, deposit was identified as a complex Pb, Fe, Mn, Ca, Al, Si, O material (very soluble), with high bioavailability. Other mining areas may have less soluble, and therefore lower bioavailability forms of lead, including galena, pyromorphite, and anglesite (Gulson and others, 1994).

#### Soil, sediment signatures prior to mining

Cold semi-arid climate: Stream sediment samples (<0.2 mm and <0.5 mm fractions) contain anomalous concentrations of many metals, including as much as ten ppm silver; tens of ppm arsenic, cadmium, and antimony; hundreds of ppm copper and nickel; thousands of ppm manganese, lead, and zinc; and hundreds of thousands of ppm barium (Theobald and others, 1978; Kelley and others, 1992). Soil that overlies mineralized rock contains hundreds to tens of thousands of ppm lead, hundreds to thousands of ppm barium and zinc, tens of ppm silver; and tens to hundreds of ppm copper, but concentrations of other metals, including <2 ppm cadmium, hundreds of ppm manganese, and tens of ppm nickel are low relative to stream sediment abundances (Briggs and others, 1992; Meyer and Kurtak, 1992). The pH of soil directly above mineralized rock may be as low as 3.9 (Briggs and others, 1992).

Warm semi-arid climate (Australia): Soil overlying mineralized rock contains hundreds to thousands of ppm copper, lead, and zinc, and tens of ppm silver (Cox and Curtis, 1977).

#### Potential environmental concerns associated with mineral processing

Mining and milling methods significantly influence potential environmental impacts associated with sedimentary exhalative deposits. Most underground mines dispose of mine waste and mill tailings by backfilling underground workings. Consequently, environmental concerns related to these underground mines may be limited, with exceptions noted below.

Modern mines discharge fine-grained sulfide-mineral-rich tailings into surface tailings ponds that have impermeable linings. Previous tailings discharge methods resulted in significant surface and shallow ground water contamination. Very finely ground, fine-grained and intergrown sulfide minerals may result in highly reactive tailings products.

Until 1967, mine water draining the Meggen, Germany underground mine had a pH as low as 2.5 and contained as much as 1,300  $\text{mg/l}$  zinc; this mine water originates by percolation of surface water through the mine. Acidic, metal-rich water draining the mine caused severe pollution in major river systems draining the area. Modern techniques enabled zinc recovery from mine water; mine effluent ceased to be a pollution source (Bergmann, 1971).

Mining and milling activities at the Zawar, India mine have resulted in contamination of stream sediment and floodplain soil (Prusty and others, 1994; Sahu and others, 1994). Stream sediment samples collected as much as 30 km from the mill site contain elevated metal abundances, including thousands of ppm zinc and iron, hundreds of ppm lead, and tens of ppm cadmium. Floodplain soil contains similarly elevated metal abundances.

"Hot muck" was an environmental concern associated with processing ore from deposits with high pyrrhotite abundances that are exposed to air and water. "Hot muck" is the spontaneous combustion of high sulfide ore in the mine. The primary environmental concern is evolved sulfur dioxide. Fires are ignited by the build-up of heat, caused by ore oxidation, in stock piles, or may be triggered by blasting in areas of previously broken ore. Periodically, air emission can exceed 9.5 ppm SO<sub>2</sub> (Brown and Miller, 1977; Good, 1977); SO<sub>2</sub> release can acidify water in areas downwind from release site. Because hot muck is easily avoided by proper blasting techniques, it does not pose significant risks in modern mining operations.

In some cold climates, it may be necessary to store wet ore, such as that produced from the Faro, Yukon Territory, mine, prior to crushing. If the ore is stockpiled too long, oxidation may ensue (Lopaschuk, 1979), which may cause increased metal concentrations, especially lead, in drainage water.

#### Smelter signatures

Smelting was and is commonly used to process sedimentary exhalative ore. Several studies focus on the correlation between lead in soil near smelters and lead in the blood of children (Gulson and others, 1994). Smelting may produce SO<sub>2</sub>-rich and metal-rich emissions, which may increase acidity and foster accumulation of heavy metals in downwind areas.

#### Climate effects on environmental signatures

Sedimentary exhalative deposits are widely distributed geographically (from Australia to northern Alaska, as well as Ireland) and therefore are in highly variable climatic regimes. The effects of various climate regimes on the geoenvironmental signature specific to sedimentary exhalative deposits are not known. However, in most cases the intensity of environmental impact associated with sulfide-mineral-bearing mineral deposits is greater in wet climates than in dry climates. Acidity and total metal concentrations in mine drainage in arid environments are several orders of magnitude greater than in more temperate climates because of the concentrating effects of mine effluent evaporation and the resulting "storage" of metals and acidity in highly soluble metal-sulfate-salt minerals. However, minimal surface water flow in these areas inhibits generation of significant volumes of highly acidic, metal-enriched drainage. Concentrated release of these stored contaminants to local watersheds may be initiated by precipitation following a dry spell. Although it is commonly assumed that the extent of sulfide mineral oxidation and weathering in cold regions underlain by permafrost are minimal, data from northern Alaska show that metal dispersion from ore deposits in surface water is significant.

#### Geoenvironmental geophysics

Induced polarization methods can provide qualitative estimates of sulfide mineral contents and grain size, which strongly influence potential for generation of acidic, metal-enriched water. Electrical techniques (King and Pesowski, 1993) and ground penetrating radar (Davis and Annan, 1992) can be used to delineate low resistivity anomalies produced by acidic, metal-enriched water that may be associated with this deposit type.

Acknowledgments.--We thank R.A. Zierenberg for helping to clarify this model and also for considerable additional input, especially concerning the Red Dog, Alaska sedimentary exhalative deposit.

#### REFERENCES CITED

- Alaska Department of Environmental Conservation (ADEC), 1995, unpub. data.
- Beelman, Joyce, 1993, Water quality impacts of a lead/zinc mine in northwest Alaska, *in* Magoon, O.T., Wilson, W.S., Converse, H., Tobin, L.T., eds., Coastal zone '93, Proceedings of the eighth Symposium on Coastal and Management: American Society of Civil Engineers, v. 2, p. 1911-1912.
- Bergmann, Artur, 1971, How Meggen purifies mine water and recovers marketable Zn precipitate: *World Mining*, v. 7, no. 10, p. 48-51.
- Briggs, P.H., Motooka, J.M., Bailey, E.A., Cieutat, B.A., Burner, S.A., Kelley, K.D., and Ficklin, W.H., 1992, Analytical results of soil, stream sediment, panned concentrate, and water samples from the Lik deposit, northwestern Brooks Range, Alaska: U.S. Geological Survey Open-File Report 92-15A (paper version) and 92-15B (diskette version).
- Briskey, J.A., 1986, Descriptive model of sedimentary exhalative Zn-Pb, *in* Cox, D.P., and Singer, D.A., eds., Mineral deposit models: U.S. Geological Survey Bulletin 1693, p. 211-212.

- Brown, R.L., and Miller, F.J.L., 1977, Pollution problems associated with Sullivan mine hot muck: Canadian Institute Mining and Metallurgy Bulletin, v. 70, n. 782, p. 89-92.
- Cox, R., and Curtis, R., 1977, The discovery of the Lady Loretta zinc-lead-silver deposit, northwest Queensland, Australia--A geochemical exploration case history: Journal of Geochemical Exploration, v. 8, p. 189-202.
- Cox, D.P., and Singer, D.A., 1986, Mineral deposit models: U.S. Geological Survey Bulletin 1693, 379 p.
- Dames & Moore, 1983, Environmental baseline studies, Red Dog project: Water Quality Report, Chapter 3, by L.A. Peterson and Associates, Inc., for the Red Dog Mine project, Cominco, Alaska, Inc., Anchorage, Alaska.
- Davis, J.L., and Annan, A.P., 1992, Applications of ground penetrating radar to mining, groundwater, and geotechnical projects--selected case histories: Geological Survey of Canada Paper 90-4, p. 49-55.
- Edwards, Richard, and Atkinson, Keith, 1986, Ore deposit geology: London, Chapman and Hall, 466 p.
- EIS (Environmental Impact Statement) for Red Dog.
- Good, B.H., 1977, The oxidation of sulphide minerals in the Sullivan mine: Canadian Institute of Mining and Metallurgy Bulletin, v. 70, no. 782, p. 83-88.
- Gulson, B.L., Mizon, K.J., Law, A.J., Korsch, M.J., Davis, J.J., and Howarth, D., 1994, Source and pathways of lead in humans from the Broken Hill Mining Community--An alternative use of exploration methods: Economic Geology, v. 89, no. 4, p. 889-908.
- Hoover, D.B., Hill, P.L., and Knepper, D.H., Jr., 1994, Geophysical model of bedded barite, in Heran, W.D., ed., Codicil to the Geophysical Expression of Selected Mineral Deposit Models: U.S. Geological Survey Open-File Report 94-174, p. 28-31.
- Jonasson, I.R., Jackson, L.E., and Sangster, D.F., 1983, A Holocene zinc orebody formed by supergene replacement of mosses: Journal of Geochemical Exploration, v. 18, p. 189-194.
- Kelley, K.D., 1995, Natural environmental effects of silver-lead-zinc deposits in the Brooks Range, Alaska: U.S. Geological Survey Fact Sheet 092-95.
- Kelley, K.D., Borden, J.C., Bailey, E.A., Fey, D.L., Motooka, J.M., and Roushey, B., 1992, Geochemically anomalous areas in the west-central part of the Howard Pass Quadrangle, National Petroleum Reserve, Brooks Range, Alaska--Evidence for sediment-hosted Zn-Pb-Ag-Ba mineralization, in Evans, D.C. and Dusel-Bacon, Cynthia, eds., Geologic studies in Alaska by the U.S. Geological Survey during 1991: U.S. Geological Survey Bulletin 2041, p. 60-69.
- Kelley, K.D., and Taylor, C.D., in press, Natural environmental effects associated with the Drenchwater zinc-lead-silver massive sulfide deposit with comparisons to the Lik and Red Dog deposits, Brooks Range, Alaska, in Dumoulin, J.A., and Moore, T.E., eds., Geologic studies in Alaska by the U.S. Geological Survey, 1994: U.S. Geological Survey Bulletin 2152.
- King, A. and Pesowski, M., 1993, Environmental applications of surface airborne geophysics in mining: Canadian Institute of Mining and Metallurgy Bulletin, v. 86, p. 58-67.
- Knepper, D.H., 1989, Mapping hydrothermal alteration with Landsat thematic mapper data, in Lee and others, eds., Mineral deposits of North America, v. 1, Remote sensing in exploration geology; Field trips for the 29th International Geological Congress: Washington, DC, American Geophysical Union, p. 13-21.
- Large, D.E., 1981, Sediment-hosted submarine exhalative lead-zinc deposits--A review of their geological characteristics and genesis, in Wolf, K.H., ed., Handbook of stratabound and stratiform ore deposits: Amsterdam, Elsevier, v. 9, p. 469-508.
- Large, D.E., 1983, Sediment-hosted massive sulfide lead-zinc deposits: an empirical model, in Sangster, D.F., ed., Sediment-hosted stratiform lead-zinc deposits: Mineralogical Association of Canada Short Course Handbook, v. 8, p. 1-30.
- Lee, Julian, Jonasson, I.R., and Goodfellow, W.D., 1984, Metal accumulation by bryophytes in some zinc-rich blanket bogs, Selwyn Mountains, Yukon Territory: Canadian Journal of Botany, v. 62, no. 4, p. 722-728.
- Lopaschuk, R.S., 1979, Drainage control and mine dewatering at Faro open pit mine, in Argall, G.O., Jr., and Brawner, C.O., eds., Mine Drainage: Proceedings of the first international mine drainage symposium, Miller Freeman Publications, p. 233-257.
- Lydon, J.W., 1983, Chemical parameters controlling the origin and deposition of sediment-hosted stratiform lead-zinc deposits, in Sangster, D.F., ed., Sediment-hosted stratiform lead-zinc deposits: Mineralogical Association of Canada Short Course Handbook, v. 8, p. 175-250.
- Maynard, J.B., 1983, Geochemistry of sedimentary ore deposits: Springer-Verlag, New York, New York, 305 p.



- 
- 1991, Shale-hosted deposits of Pb, Zn, and Ba: Syngenetic deposition from exhaled brines in deep marine basins, in Force, E.R., Eidel, J.J., and Maynard, J.B., eds., *Sedimentary and diagenetic mineral deposits: A basin analysis approach to exploration: Society of Economic Geologists Reviews in Economic Geology*, v. 5, p. 177-185.
- McClay, K.R., 1983, Deformation of stratiform lead-zinc deposits, in Sangster, D.F., ed., *Sediment-hosted stratiform lead-zinc deposits: Mineralogical Association of Canada Short Course Handbook*, v. 8, p. 283-309.
- Menzie, W.D., and Mosier, D.L., 1986, Grade and tonnage model of sedimentary exhalative Zn-Pb, in Cox, D.P., and Singer, D.A., eds., *Mineral deposit models: U.S. Geological Survey Bulletin 1693*, p. 212-215.
- Meyer, M.P., and Kurtak, J.M., 1992, Results of the 1991 U.S. Bureau of Mines Colville Mining District study: U.S. Bureau of Mines Open-File Report 75-92, 101 p.
- Mining Journal, 1995, v. 325, no.8344, p. 189.
- Moore, D.W., Young, L.E., Modene, J.S., and Plahuta, J.T., 1986, Geologic setting and genesis of the Red Dog zinc-lead-silver deposit, western Brooks Range, Alaska: *Economic Geology*, v. 81, no. 7, p. 1696-1727.
- O'Brien, M.V., and Romer, D.M., 1971, Tara's zinc-lead discovery at Navan, Republic of Ireland: *Canadian Mining Journal*, v. 92, no. 4, p. 81-82.
- Pasava, J., 1993, Anoxic sediments; an important environment for PGE; an overview: *Ore Geology Reviews*, v. 8, no. 5, p. 425-445.
- Plumlee, G.S., Smith, K.S., Ficklin, W.H., Briggs, P.H., and McHugh, J.B., 1993, Empirical studies of diverse mine drainages in Colorado: implications for the prediction of mine-drainage chemistry, in Munshower, F.F., and Fisher, S.E., Jr., co-chairmen, *Planning, rehabilitation and treatment of disturbed lands, Sixth Billings Symposium, March 21-27, 1993, Reclamation Research Unit Publication No. 9301*, p. 176-186.
- Prusty, B.G., Sahu, K.C., and Godgul, Geeta, 1994, Metal contamination due to mining and milling activities at the Zwar zinc mine, Rajasthan, India I. Contamination of stream sediments: *Chemical Geology*, v. 112, p. 275-291.
- Runnells, D.D., Shepherd, T.A., and Angino, E.E., 1992, Metals in water--determining natural background concentrations in mineralized areas: *Environmental Science Technology*, v. 26, p. 2316-2323.
- Ryall, W.R., 1981, The forms of mercury in some Australian stratiform Pb-Zn-Ag deposits of different regional metamorphic grades: *Mineral Deposita*, v. 16, p. 425-435.
- Sahu, K.C., Prusty, B.G., and Godgul, Geeta, 1994, Metal contamination due to mining and milling activities at the Zwar zinc mine, Rajasthan, India II. Dispersion in floodplain soils: *Chemical Geology*, v. 112, p. 293-307.
- Sangster, D.F., ed., 1983, *Sediment-hosted stratiform lead-zinc deposits: Mineralogical Association of Canada Short Course Handbook*, v. 8, 309 p.
- 1990, Mississippi Valley-type and sedex lead-zinc deposits--a comparative examination: *Transactions of the Institution of Mining and Metallurgy*, section B, v. 99, p. B21-B42.
- Schmidt, J.M., in press, Shale-hosted Zn-Pb-Ag and barite deposits of Alaska, in Goldfarb, R.J., and Miller, L., eds., *Mineral deposits of Alaska: Economic Geology Monograph*.
- Taylor, G.F., 1984, Gossan profiles developed above stratabound sulfide mineralization: *Journal of Geochemical Exploration*, v. 22, p. 351-352.
- Taylor, G.F., Wilmschurst, J.R., Togashi, Y., and Andrew, A.S., 1984, Geochemical and mineralogical halos about the Elura Zn-Pb-Ag orebody, western New South Wales: *Journal of Geochemical Exploration*, v. 22, p. 265-290.
- Theobald, P.K., Barton, H.N., Billings, T.M., Frisken, J.G., Turner, R.L., and VanTrump, G., Jr., 1978, Geochemical distribution of elements in stream sediment and heavy-mineral concentrate samples in the southern half of the National Petroleum Reserve, Alaska: U.S. Geological Survey Open-File Report 78-517, scale 1:500,000.
- Turner, R.J.W., and Einaudi, M.T., 1986, The genesis of stratiform sediment-hosted lead and zinc deposits: *Conference Proceedings: Stanford University Publications in the Earth Sciences Volume XX*, 222 p.
- U.S. Bureau of Mines, 1993, *Minerals Yearbook*.
- Vine, J.D., and Tourtelot, E.B., 1970, Geochemistry of black shales--a summary report: *Economic Geology*, v. 65, p. 253-272.
- Young, L.E., 1989, Geology and genesis of the Red Dog deposit, western Brooks Range, Alaska: *Canadian Institute of Mining and Metallurgy Bulletin*, v. 82, no. 929, p. 57-67.

## LOW SULFIDE AU QUARTZ VEINS (MODEL 36a; Berger, 1986)

by Richard J. Goldfarb, Byron R. Berger, Terry L. Klein, William J. Pickthorn, and Douglas P. Klein

### SUMMARY OF RELEVANT GEOLOGIC, GEOENVIRONMENTAL, AND GEOPHYSICAL INFORMATION

#### Deposit geology

These deposits consist of Archean through Tertiary quartz veins, primarily mined for their gold content, that generally contain no more than 2 to 3 volume percent sulfide minerals, mainly pyrite, in allochthonous terranes dominated by greenstone and turbidite sequences that have been metamorphosed to greenschist facies. Wall rocks contain abundant carbonate and sulfide minerals, quartz, and sericite. Arsenic and antimony are enriched in alteration haloes (fig. 1). These deposits are also known as mesothermal, Mother Lode-type, orogenic, metamorphic rock-hosted, greenstone gold (Archean), turbidite-hosted (Phanerozoic), and slate belt gold (Phanerozoic) deposits.

Low sulfide gold quartz veins in the United States are presently being mined and prospected within rocks of accreted lithotectonic terranes along both continental margins. Development of Paleozoic lode deposits in recent years has been restricted to the South Carolina part of the Carolina slate belt. Open pit mining of the more than 1.5 million oz of gold at the Ridgeway mine, the largest of the deposits, is continuing at a rate of about 100,000 oz/yr. In the Mother Lode region of central California, a few old mines have been reopened in the last 10 to 15 years as open pit operations. Each has been recovering 500,000 to 750,000 oz of gold from low-grade, Early Cretaceous deposits. Production from the Alaska-Juneau and Kensington Eocene vein deposits in southeastern Alaska by underground operations is scheduled to commence during the next few years and will yield about 6 million oz of gold. In the Alaskan interior, open-pit mining will eventually yield 4 million oz of gold from the mid-Cretaceous Fort Knox deposit.

#### Examples

Yilgarn Block, Western Australia; Abitibi Belt, Superior Province, Canada; Yellowknife, Northwest Territory, Canada; Bendigo/Ballarat, Victoria, Australia; Murantau, Uzbekistan; Mother Lode, Calif.; Juneau Gold Belt, Alaska; Otago Schist Belt, South Island, New Zealand.

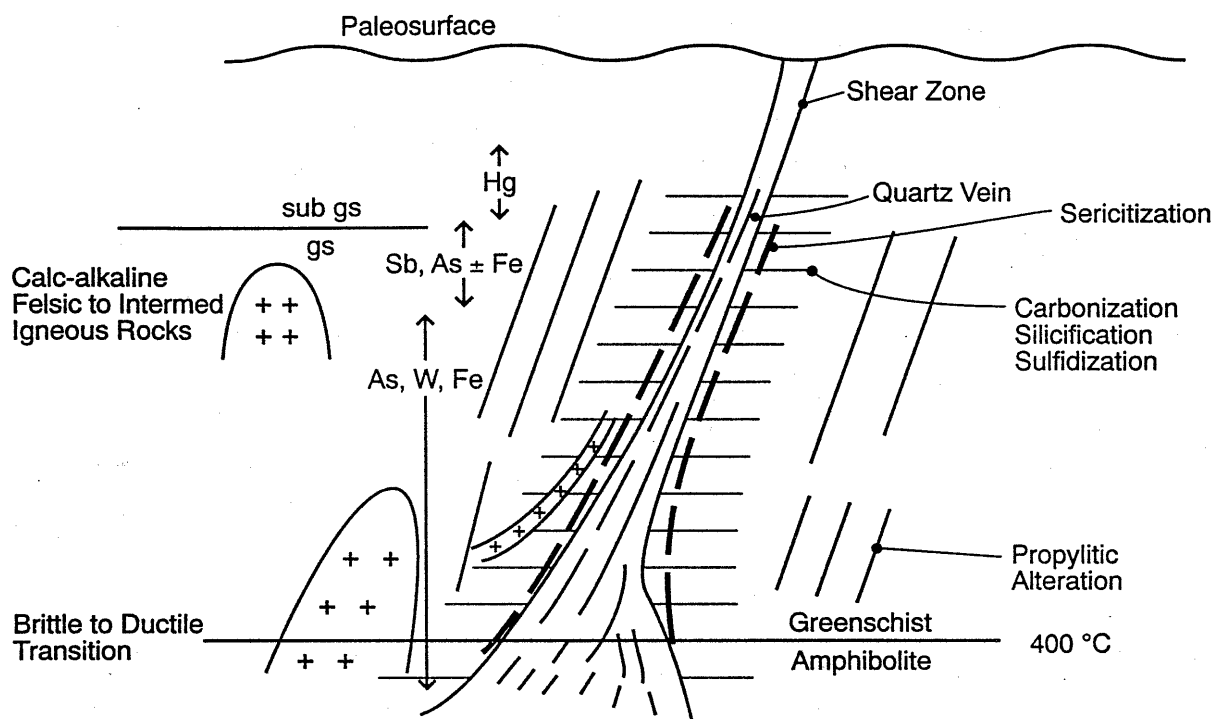


Figure 1. Schematic geologic cross section of a low-sulfide gold deposit.

### Spatially and (or) genetically related deposit types

Associated deposit types (Cox and Singer, 1986) may include silica-carbonate mercury (Model 27c), and gold-antimony (Model 36c), which may reflect shallower exposures of similar hydrothermal systems in areas of limited erosion. In areas of extensive uplift and erosion, gold lodes are reconcentrated in extensive placer accumulations (Model 39a). Low sulfide gold quartz vein deposits subjected to tropical weathering can produce lateritic saprolite (eluvial placer) deposits (Model 38g; McKelvey, 1992). Much older, pre-accretionary Cyprus, Besshi, and Kuroko volcanogenic massive sulfide deposits (Models 24a, 24b, 28a) are spatially associated with gold veins in terranes that contain significant volumes of volcanic rock.

### Potential environmental considerations

- (1) Moderate amounts of acid mine drainage may be present where local, relatively high sulfide mineral concentrations are present in gold ore, where broad zones of sulfidization characterize wall rocks, and (or) where much of the ore is hosted by greenstone that has relatively low acid-buffering capacity.
- (2) Oxidation of mine tailings that contain sulfide minerals, particularly arsenopyrite, or soil formed from unmined, yet sulfide-mineral-bearing rock can release potentially hazardous arsenate, arsenite, and methylarsenic species.
- (3) Increased concentrations of arsenic, antimony, and other trace metals may be present downstream from deposits. Cyanide used for gold extraction at many active mines is a potential additional contaminant in waste water discharge.
- (4) Mercury amalgamation carried out during historic operations may be a source of mercury contamination in aquatic life and in surface sediment. Continued use of mercury amalgamation and roasting for gold extraction in some parts of the world is a direct and very serious health hazard.
- (5) Disposal of tailings from developed deposits can cause sedimentation problems in adjacent waterways.
- (6) Modern open-pit mining methods, allowing for development of previously uneconomic, low-grade gold deposits pose quality-of-life concerns. Potential concerns include mining-related visual impacts, increased traffic and noise, and dust generation. Open-pit mining also produces significantly greater volumes of untreated waste rock.
- (7) Long term exposure to arsenic concentrated in tailings can cause cancer and kidney disease.

### Exploration geophysics

Silicified rock, much of which corresponds to wall rock that contains abundant sulfide minerals, is commonly associated with local resistivity highs. Silicified rock and carbonate minerals along veins increase density and resistivity and may allow indirect sulfide mineral identification using detailed electromagnetic, direct current resistivity, and micro-gravity mapping. Disseminated pyrite, arsenopyrite, and chalcopyrite distributions can be outlined using induced polarization/resistivity surveys. Piezo-electricity may locate sulfide-mineral-bearing quartz veins. Host rocks that contain at least moderate amounts of magnetite may have associated magnetic lows due to magnetite destruction in alteration-halos.

### References

Geology: Berger (1986), Bliss (1986, 1992), Groves and others (1989), Kerrich and Wyman (1990), Kontak and others (1990), Nesbitt (1991), Berger (1993), Goldfarb and others (1993), Phillips and Powell (1993), and Klein and Day (1994).  
Environmental geology and geochemistry: Bowell and others (1994), Callahan and others (1994), Cieutat and others (1994), Azcue and others (1995), and Trainor and others (in press).

## GEOLOGIC FACTORS THAT INFLUENCE POTENTIAL ENVIRONMENTAL EFFECTS

### Deposit size

Deposit size is extremely variable. Archean deposits-mean tonnage is 1.08 million metric tonnes; range is 0.004 to 199 million metric tonnes. The mean tonnage of Phanerozoic deposits is 0.03 million metric tonnes; range is 0.001 to 25 million metric tonnes. The mean tonnage of Chugach-type Phanerozoic deposits is 0.003 million metric tonnes; range is 0.001 to 0.07 million metric tonnes. Because of the high-grade nature of some veins (greater than 30 to 50 g gold/t), many low tonnage deposits (for instance, Chugach-type low sulfide gold deposits; Bliss, 1992) are developed by small, underground workings. Deposits that contain at least 0.5 to 5 million oz gold in low grade ore (generally 2 to 10 g gold/t) have been mined in large, more modern open-pit operations. The largest example of such a deposit is Murantau, Uzbekistan, which contains greater than 140 million oz gold (Berger and others, 1994).

### Host rocks

Archean ore is largely hosted by metamorphosed basalt (greenstone), although ultramafic volcanic rocks (komatiite), felsic volcanic rocks, and granitoid intrusions are locally important hosts. Most of these deposits are in preserved cratonic blocks. Phanerozoic deposits are hosted in slate and graywacke in deformed, continental margin orogenic belts. Where competent, pre-ore igneous bodies are present in metasedimentary sequences, they commonly preferentially host vein-bearing fracture systems.

### Surrounding geologic terrane

Deposits are restricted to medium-grade, generally greenschist facies, metamorphic rocks. High-tonnage deposits, exemplified by Murantau, Uzbekistan, have a spatial association with major structural zones that are commonly believed to be old terrane boundaries. Contemporaneous calc-alkaline dioritic to granitic plutons, sills, and batholiths within a few tens of kilometers of ore indicate that both are products of regional, middle to lower crustal thermal events.

### Wall-rock alteration

Mineral phases vary with host rock lithology; halo width varies with size of hydrothermal system. Alteration zones are poorly developed in metasedimentary host rocks, but are broad and distinct in both felsic and mafic igneous rocks. Silicified rock and carbonate minerals are ubiquitous. Disseminated pyrite and (or) arsenopyrite consistently are present in these broad haloes. Sericite is common, but only close to discrete gold-bearing veins; in some systems, biotite is also present adjacent to veins. Sericite gives way to a chlorite-epidote propylitic zone distal to veins. Talc, chlorite, and fuchsite are also common in alteration zones within ultramafic host rocks; albite is common in granitoid host rocks. Wall rocks are notably enriched in H<sub>2</sub>O, CO<sub>2</sub>, S, K, Au, W, Sb, and As (Nesbitt, 1991).

### Nature of ore

Ore may be present in quartz veins and (or) adjacent sulfidized wall rock. Gold is present as free grains in quartz, as blebs attached to wall rock ribbons, and in veinlets cutting sulfide grains. Individual veins are 1 to 10-m-wide discrete fissure fillings that have strike lengths of less than 100 m. Many veins show ribbon texture or, less commonly, contain brecciated wall rock fragments. In some deposits, ore forms dense stockworks of cm-wide veinlets. Vein swarms at the large deposits can attain 5-km strike lengths, 500 m widths, and extend 2 km down dip. Carbonate minerals may form either (1) restricted alteration zones that range from a few to tens of meters away from small shear zones or (2) may be abundant in rocks within several kilometers of major faults.

### Deposit trace element geochemistry

Abundances of silver, arsenic, gold, and iron are consistently anomalous; tungsten and antimony abundances are much less consistently anomalous; bismuth, copper, mercury, lead, and zinc abundances are anomalous in many deposits; less commonly, anomalous amounts of tellurium and molybdenum are detected.

### Ore and gangue mineralogy and zonation

- (1) Gold is present as native gold and electrum.
- (2) Potentially acid-generating sulfide minerals (in order of abundance) are pyrite, arsenopyrite > stibnite > chalcopyrite, pyrrhotite, galena, sphalerite > telluride minerals, tetrahedrite > bismuthinite > molybdenite.
- (3) Scheelite and graphite are common.
- (4) Potentially acid-buffering carbonate minerals include siderite, ankerite, calcite, magnesite, or ferroan dolomite; the composition of the carbonate species is a function of wall rock chemistry.
- (5) Silicate gangue minerals include quartz, muscovite, chlorite, biotite, fuchsite, tourmaline, rutile, albite, and (or) talc.
- (6) Zoning is uncommon; mineral assemblages and proportions are commonly consistent over depths of greater than 1,000 m. In some systems, shallow levels may contain more abundant stibnite or sulfosalt minerals and native silver (Berger, 1993). Deeper zones may be more pyrrhotite-rich.

### Mineral characteristics

Sulfide minerals are usually present as finely disseminated grains in quartz and wall rocks. In some deposits, massive clots of arsenopyrite, as large as tens of cm, may be present locally. In rare examples, gold-bearing veins may contain massive stibnite (10 to 50 volume percent of the vein material) throughout the deposit (see Berger, 1993).

### Secondary mineralogy

Secondary minerals are not common. Occasionally, some arsenopyrite has weathered to scorodite. Minor limonite is present in many veins.

### Topography, physiography

The deposits do not form distinct topographic features although in some mining districts (for example, Bendigo, Australia) mineralized zones may form distinctive linear ridges. They may have been emplaced along steep and rapidly uplifting mountain belts; many pre-Tertiary low-sulfide gold-quartz veins are present in more tectonically stable zones of moderate relief.

### Hydrology

Veins are generally hosted in permeable fracture zones and hence are also significant local ground water conduits. Mining relatively sulfide-mineral-rich veins of this deposit type could cause discharge of minor volumes of relatively metal-rich ground water. However, seepage from poorly consolidated tailings piles and adits at historic workings is likely to be the most common source of metal contamination of surface water near this type of gold deposit.

### Mining and milling methods

Both underground and open pit mining methods are presently being used to extract ore. In the United States, except for southeastern Alaska, open pit mining is most common. During milling, ore is usually crushed and ground in a ball mill; subsequently, gravity concentration is used to remove the largest gold particles. Remaining ore is reground, classified and thickened, recycled through the gravity concentrator, and then processed in cyanide vats for 48 hours. The slurry is subsequently sent to a carbon-in-pulp circuit where dissolved gold is adsorbed on carbon. Gold is then stripped from carbon and electroplated on steel wool before being refined into bullion in a furnace. Alternatives to vat leaching during cyanidation include *in situ* and heap leaching.

In some parts of the world, mercury amalgamation is still being used to aid gold recovery. Sulfur compounds, which adversely impact the amalgamation process, are eliminated by first roasting ore. Mixing mercury with gold concentrates results in amalgam that leaves gold behind when the mercury is volatilized.

## ENVIRONMENTAL SIGNATURES

### Drainage signatures

For both mined and unmined orebodies, low sulfide mineral contents of ore and acid-buffering capacity of widespread carbonate alteration assemblages generally prevent significant acid-mine drainage and heavy metal contamination associated with this deposit type.

Natural drainage: Limited data (Carrick and Maurer, 1994; Cieutat and others, 1994; Trainor and others, in press) suggest that unmined occurrences have little impact on surface water pH or trace element content. In southern Alaska, data indicate that arsenic abundances increase from <5 to 6 µg/l, iron from <20 to 140 µg/l, and sulfate from <2 to 3 to 5 mg/l where natural water encounters unmined low-sulfide gold quartz vein occurrences.

Mine drainage: Arsenic and iron abundances in water draining small workings may be enhanced by one to two orders-of-magnitude relative to background abundances downstream from unmined occurrences (Cieutat and others, 1994; Trainor and others, in press). Other metals do not exhibit corresponding enrichments. Even water draining directly from major pits and extensive underground workings can have neutral pH and low metal contents; water draining the Alaska-Juneau pit and underground workings, Alaska's largest gold mine, contain <6 µg/l arsenic and <100 µg/l iron at a pH of 8.0; sulfate abundances in this water are as much as 340 mg/l (Echo Bay Mines, unpub. company data). Water flowing out the portal of the Independence, Alaska, mine in the Willow Creek district, the fourth largest past lode gold producer in the state, has a pH of 7.8 and contains <40 µg/l iron, 37 µg/l arsenic, and <4 µg/l cadmium, copper, lead, antimony, tungsten, and zinc (R.J. Goldfard, unpub. data, 1995).

In rare examples, locally high concentrations of sulfide minerals can lead to significant metal-rich and (or) acid mine drainage. Contaminated water that drained from an old adit at the site of an open pit gold mine at Macraes Flat, South Island, New Zealand, which had a pH of 2.9 and elevated dissolved metal abundances, including as much as 77 mg/l zinc and 80 mg/l iron (BHP Gold, New Zealand, unpub. company report, 1988), may reflect this type of situation.

Seepage from poorly consolidated tailings piles may be more acidic. Small volumes of water seeping from tailings in the Cariboo district, British Columbia has a pH of 2.7 and contains 556 µg/l arsenic and elevated abundances of cadmium, copper, lead, and zinc (Azcue and others, 1995). Seepage from sulfide mineral concentrates at an abandoned mill site, of the Treadwell, southeastern Alaska, mines has a pH of 2.9 and contains 330 mg/l iron,

2500 µg/l zinc, 380 µg/l copper, 160 µg/l cobalt, 100 µg/l nickel, 32 µg/l cobalt, and 21 µg/l lead (R.J. Goldfarb, unpub. data, 1995).

Mercury, which is used for gold extraction, is extremely enriched in sediment and fish tissue in drainages downstream from many historic low-sulfide gold mines (Callahan and others, 1994). Down-river from present-day gold mines in Brazil, mercury abundances are as much as 20 ppm in sediment, 2.7 ppm in fish, and 8.6 µg/l in water (Pfeiffer and others, 1989). Down-river from the California Mother lode veins, dredged river sediment contains as much as 37.5 ppm mercury and surface and ground water contains 13 to 300 µg/l mercury (Prokopovich, 1984). Extreme mercury abundances have been documented in sediment in drainages of the Carolina slate belt and the Dolgellau gold belt, Wales, more than 75 years after cessation of mining (Fuge and others, 1992; Callahan and others, 1994). Unfiltered and filtered samples of water draining tailings piles in the Fairbanks, Alaska, district contain as much as 0.58 and 0.11 µg/l mercury, respectively (R.J. Goldfarb, unpub. data, 1995).

#### Metal mobility from solid mine wastes

Acid mine drainage problems are probably restricted to water that infiltrates untreated mine dump piles. In temperate climates, initial spring snow melt draining dumps is likely to contain significant heavy metal abundances, including arsenic, iron, and antimony, and less commonly lead and zinc, mainly due to dissolution of soluble salts accumulated during winter. In most cases, small volume acidic effluent seeping from waste piles is diluted to background abundances upon entering adjacent stream channels; consequently, environmental impact is restricted to surface channels upstream from their intersections with the nearest, major surface waterway.

Arsenic is usually the trace element of greatest environmental concern in soil associated with mine tailings. Inadvertent soil ingestion by young children and arsenic-rich household dust pose potential risks to human health. These risks have become serious public issues in parts of the California Mother Lode belt where housing projects have been developed on soil derived from old mine tailings (Time, September 25, 1995, p. 36). Secondary, arsenic-bearing salt minerals, and to a lesser extent, relatively insoluble arsenic-bearing sulfide minerals, become bioavailable primarily by adsorption from the fluid phase in the small intestine. Geochemical factors that control arsenic bioavailability from soil include the type of arsenic-bearing mineral, the degree of encapsulation of that mineral in an insoluble matrix, the nature of alteration rinds on mineral grains, and the rate of arsenic dissolution in the gastrointestinal tract (Davis and others, 1992).

#### Soil, sediment signatures prior to mining

Arsenic concentrations in soil and sediment are about 50-1,000 ppm near unmined deposits; background abundances elsewhere are typically 10-40 ppm. Antimony levels are commonly >5 ppm near deposits, whereas they are normally <2 ppm in areas unaffected by hydrothermal activity (Bowell and others, 1994; R.J. Goldfarb, unpub. data, 1995).

#### Potential environmental concerns associated with mineral processing

Summarized from Ripley and others (1995).

- (1) Mercury amalgamation, commonly used in historic gold extraction processes, may have deposited significant amounts of mercury in tailings piles. Where amalgamation is still used, volatilized mercury generated by the process may significantly affect air quality because as much as ten percent of the mercury used is lost to the atmosphere.
- (2) Most cyanide used for gold extraction is recovered and recycled, but some inevitably remains in tailings liquor and can leak into regional ground water networks. Any loss of cyanide to the environment is a major concern because it is toxic to a wide variety of organisms. Many mills now use chemical-treatment systems to convert hazardous cyanide compounds to insoluble compounds that are not bioavailable. This is especially critical in cold climates where natural volatilization of cyanide from holding ponds is relatively slow.
- (3) Where heap-leaching methods are employed, environmental risks are greater. Leakage and erosion risks are greatly increased, as are risks to wildlife, because cyanide leaching is usually done outdoors. *In situ* leaching, if applied to relatively impermeable orebodies, could result in local aquifer contamination.
- (4) Roasting ore that contains abundant sulfide minerals emits significant amounts of arsenic trioxide and other metal oxides into the atmosphere.
- (5) Highly acidic effluent is produced during sulfide bio-oxidation. Without proper neutralization or during spills, this effluent can be extremely hazardous.
- (6) Crushing and grinding ore may present noise and dust hazards.

#### Smelter signatures

Ore derived from these deposits is not smelted.

### Climate effects on environmental signatures

In dry and seasonally wet climates, the potential for generating small-volume pulses of significantly metal-enriched acid mine drainage is enhanced by evaporation and soluble salt accumulation. In wet climates, increased surface runoff enhances dilution and may mitigate peak acid and heavy-metal concentrations that characterize mine drainage in dry and seasonally wet climates.

### Geoenvironmental geophysics

Wide-band electromagnetic systems can be used to identify major shears associated with veins that may serve as major ground water conduits. Direct current and electromagnetic resistivity and magnetic surveys can be used to study porous rock associated with faults and shear zones that may control ground water flow. Within and downslope from mine areas, low-resistivity acid- or metal-bearing water can be identified with electromagnetic or direct current induced polarization/resistivity surveys and ground penetrating radar. Structural and stratigraphic features such as bedrock topography, buried channels, and aquitards that affect water flow away from mine areas may be studied with electromagnetic or direct current resistivity, seismic refraction, and gravity surveys. Stratigraphic details in shallow sand and gravel water pathways can be investigated with seismic reflection and ground penetrating radar. Water flow may be monitored using self potential.

### REFERENCES CITED

- Azcue, J.M., Mudroch, A., Rosa, F., Hall, G.E.M., Jackson, T.A., and Reynoldson, T., 1995, Trace elements in water, sediments, porewater, and biota polluted by tailings from an abandoned gold mine in British Columbia, Canada: *Journal of Geochemical Exploration*, v. 52, p. 25-34.
- Berger, B.R., 1986, Descriptive model of low-sulfide Au-quartz veins, *in* Cox, D.P., and Singer, D.A., eds., *Mineral deposit models: U.S. Geological Survey Bulletin 1693*, p. 239.
- Berger, B.R., Drew, L.J., Goldfarb, R.J., and Snee, L.W., 1994, An epoch of gold riches-the Late Paleozoic in Uzbekistan, central Asia: *Society of Economic Geologists Newsletter*, no. 16, p. 1, 7-11.
- Berger, V.I., 1993, Descriptive and grade and tonnage model for gold-antimony deposits: U.S. Geological Survey Open-File Report 93-194, 24 p.
- Bliss, J.D., 1986, Grade and tonnage model of low-sulfide Au-quartz veins, *in* Cox, D.P., and Singer, D.A., eds., *Mineral deposit models: U.S. Geological Survey Bulletin 1693*, p. 239-243.
- \_\_\_\_\_, 1992, Grade and tonnage model of Chugach-type low-sulfide Au-quartz veins, *in* Bliss, J.D., ed., *Developments in mineral deposit modelling: U.S. Geological Survey Bulletin 2004*, p. 44-46.
- Bowell, R.J., Morley, N.H., and Din, V.K., 1994, Arsenic speciation in soil porewaters from the Shanti mine, Ghana: *Applied Geochemistry*, v. 9, p. 15-22.
- Callahan, J.E., Miller, J.W., and Craig, J.R., 1994, Mercury pollution as a result of gold extraction in North Carolina, U.S.A.: *Applied Geochemistry*, v. 9, p. 235-241.
- Carrick, S., and Maurer, M., 1994, Preliminary water resource assessment of the Girdwood area, Alaska: Alaska Division of Geological and Geophysical Surveys, Public Data File 94-51, 36 p.
- Cieutat, B.A., Goldfarb, R.J., Borden, J.C., McHugh, J., and Taylor, C.D., 1994, Environmental geochemistry of mesothermal gold deposits, Kenai Fjords National Park, south-central Alaska, *in* Till, A.B., and Moore, T., eds., *Geological Studies in Alaska by the U.S. Geological Survey, 1993: U.S. Geological Survey Bulletin 2107*, p. 21-25.
- Cox, D.P., and Singer, D.A., eds., 1986, *Mineral deposit models: U.S. Geological Survey Bulletin 1693*, 379 p.
- Davis, A., Ruby, M.V., and Bergstrom, P.D., 1992, Bioavailability of arsenic and lead in soils from the Butte, Montana mining district: *Environmental Science Technology*, v. 26, p. 461-468.
- Fuge, R., Pearce, N.J.G., and Perkins, W.T., 1992, Mercury and gold pollution: *Nature*, v. 357, p. 369.
- Goldfarb, R.J., Snee, L.W., and Pickthorn, W.J., 1993, Orogenesis, high-T thermal events, and gold vein formation within metamorphic rocks of the Alaskan Cordillera: *Mineralogical Magazine*, v. 57, p. 375-394.
- Groves, D.I., Barley, M.E., and Ho, S.E., 1989, Nature, genesis and tectonic setting of mesothermal gold mineralization in the Yilgarn block, Western Australia, *in* Keays, R.R., Ramsey, W.R.H., and Groves, D.I., eds., *The geology of gold deposits--The perspective in 1988: Economic Geology Monograph 6*, p. 71-85.
- Kerrick, R., and Wyman, D., 1990, Geodynamic setting of mesothermal gold deposits--An association with accretionary regimes: *Geology*, v. 18, p. 882-885.

- Klein, T.L., and Day, W.C., 1994, Descriptive and grade-tonnage models of Archean low-sulfide Au-quartz veins and a revised grade-tonnage model of Homestake Au: U.S. Geological Survey Open-File Report 94-250, 29 p.
- Kontak, D.J., Smith, P.K., Kerrich, R., and Williams, P.F., 1990, Integrated model for Meguma Group lode gold deposits, Nova Scotia, Canada: *Geology*, v. 18, p. 238-242.
- McKelvey, G.E., 1992, Descriptive model of laterite-saprolite Au, *in* Bliss, J.D., ed., *Developments in mineral deposit modelling*: U.S. Geological Survey Bulletin 2004, p. 47-49.
- Nesbitt, B.E., 1991, Phanerozoic gold deposits in tectonically active continental margins, *in* Foster, R.P., ed., *Gold metallogeny and exploration*: Blackie, London, p. 104-132.
- Pfeiffer, W.C., DeLacerda, L.D., Malm, O., Souza, M.M., DaSilveira, E.G., and Bastos, W.R., 1989, Mercury concentrations in inland waters of gold-mining areas of Rondonia, Brazil: *The Science of the Total Environment*, v. 87-88, p. 233-240.
- Phillips, G.N., and Powell, R., 1993, A link between gold provinces: *Economic Geology*, v. 88, p. 1084-1098.
- Prokopovich, N.P., 1984, Occurrence of mercury in dredge tailings near Folsom South Canal, California: *Bulletin of the Association of Engineering Geology*, XXI, p. 531-543.
- Ripley, E.A., Redmann, R.E., and Crauder, A.A., 1995, *Environmental effects of mining*: Delray Beach, Florida, St. Lucie Press, 356 p.
- Trainor, T.P., Fleisher, S., Wildeman, T.R., Goldfarb, R.J., and Huber, C., in press, Environmental geochemistry of the McKinley Lake gold district, Chugach National Forest, Alaska, *in* Moore, T., and Dumoulin, J.D., eds., *Geological Studies in Alaska by the U.S. Geological Survey*, 1994: U.S. Geological Survey Bulletin 2152.



## Case Studies from the Northern Cordillera

Our recent work in the northern Cordillera has emphasized collection of empirical data that define the environmental signatures of the mineral deposit types commonly associated with accreted terranes and superimposed arcs (Gray and Sanzolone, 1996). Objectives have included establishing estimates for pre-mining geochemical baselines in highly mineralized belts (fig. 1), as well as determining the environmental effects of various mining and processing activities. These studies are particularly important for this part of North America because numerous mineral deposits exist there that have not yet been developed and resulting data are critical for future mining, monitoring, and remediation programs.

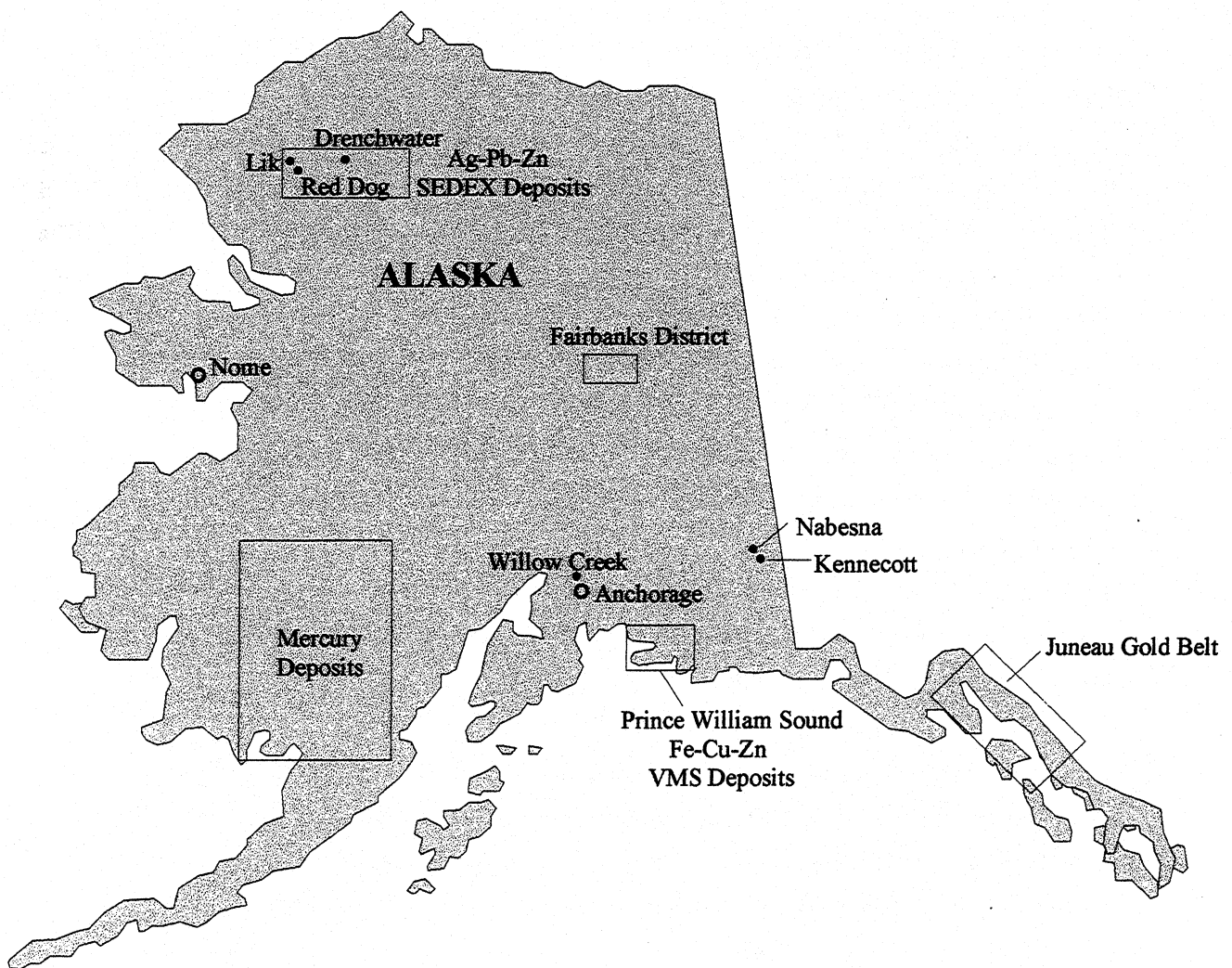
### Shale-hosted massive sulfide (SEDEX) deposits

The influence of geology on natural background concentrations of metals in water is obvious in studies of shale-hosted stratiform Pb-Ag-Zn SEDEX massive sulfide deposits from the northwestern Brooks Range. Natural background concentrations of metals in waters from the undisturbed (unmined) Drenchwater prospect and Lik deposit were compared to pre-mining baseline studies (Dames and Moore, 1983) conducted at Red Dog. Results suggest that the primary factors affecting water chemistry are the extent of exposure of the deposits, the grade of mineralization, the presence of carbonate rocks in the section, and the proportion of Fe-sulfide in the ore (Kelley and Taylor, 1997).

### Red Dog deposit

The Red Dog deposit is hosted by black carbonaceous shale of Mississippian and Pennsylvanian age. The primary ore mineral at Red Dog is sphalerite with lesser amounts of galena, pyrite, or marcasite. Ore minerals were exposed at the surface prior to mining. The deposit was discovered due to the presence of bright red-orange streams draining the deposit. Minus-80-mesh stream-sediment samples collected within 2.5 km of the exposed deposit had extremely high concentrations of Zn (up to 6,000 ppm), Pb (3,400 ppm), Cd (25 ppm), and Ag (7 ppm) (Tailleur, 1970; Theobald and Barton, 1978).

A two-year baseline study conducted by Dames and Moore (1983) for the mining company in the 1980's showed that pre-mining surface waters from the Red Dog deposit area were acidic and metal-rich. For instance, in July of 1981, surface waters from Red Dog Creek immediately draining the deposit area were devoid of fish due to its acidity (pH of 3.5) and metal-rich character (Zn=40,400 ppb; Pb=2,100 ppb; Cd=393 ppb). In Ikalukrok Creek about 14 km below the deposit, elevated concentrations of Pb (50 ppb), Zn (1,100 ppb) and Cd (20 ppb) were also reported. As far as 40 km downstream in Ikalukrok Creek, waters were found to contain a decrease in the number and diversity of fish. Although these waters were more neutral in pH (7.4), they still contained high concentrations of zinc (338 ppb) and Cd (12 ppb). These



**Figure 1.** Locations of environmental case studies from the northern Cordilleran.

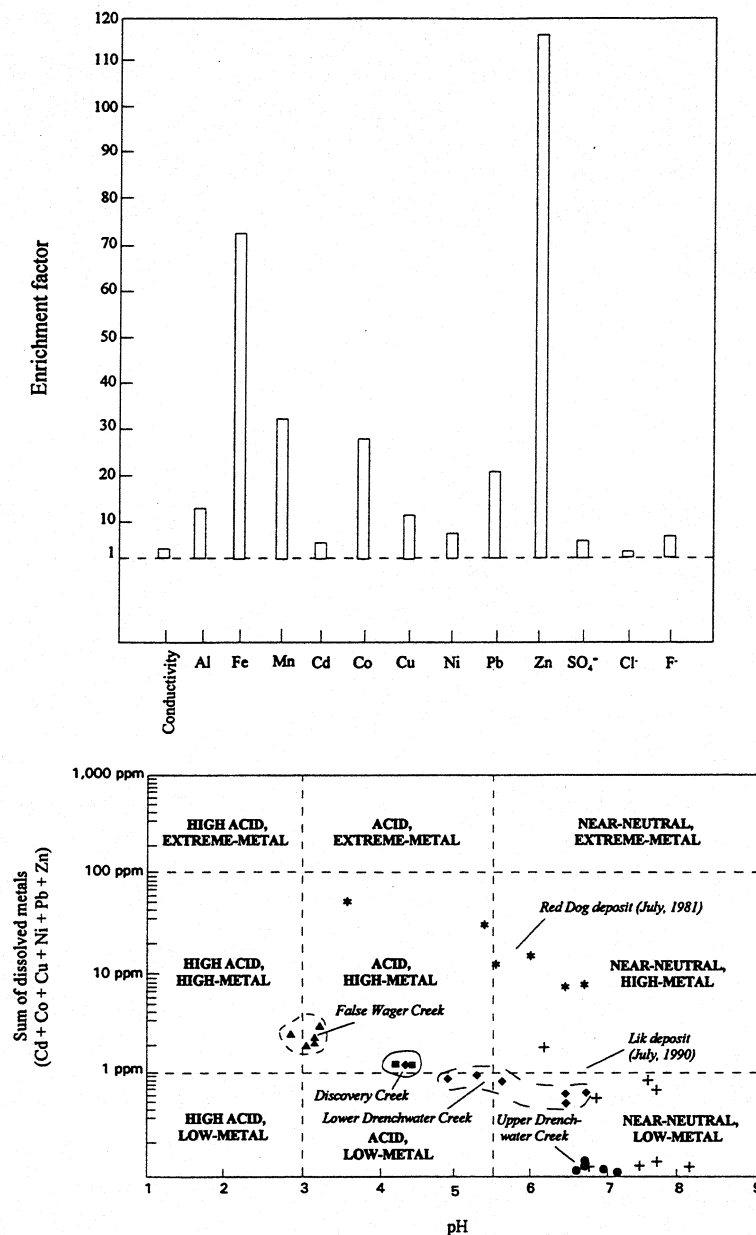
values are many times greater than background concentrations in the area. For example, surface waters draining unmineralized areas contained <0.1-9.2 ppb Pb, 38-190 ppb Zn, and 2-3 ppb Cd (Dames and Moore, 1983).

Seasonal fluctuations in data from Red Dog show that there are significant increases in metal concentrations in late summer and early fall. In May and June, the early months of summer, the metals are relatively low (Dames and Moore, 1983), suggesting that dilution is a major mechanism for attenuation or decreasing metal concentration.

#### Drenchwater prospect

The Drenchwater prospect is similar to Red Dog except that pyrite is the dominant sulfide mineral. Mineralized rocks consist of a broad zone of disseminated sulfides or semi-massive sulfides in black shale and chert of Mississippian and Pennsylvanian age. The sulfides easily weather and oxidize to iron oxides. Stream-sediment geochemical studies indicate that drainages surrounding the Drenchwater prospect contained anomalous concentrations of Ag, As, Ba, Cd, Cu, Mn, Ni, Pb, Sb, and Zn (Kelley et al., 1992). However, except for Zn which occurred in concentrations as high as 1,000 ppm, most elements were relatively lower compared to sediments from Red Dog, evidence of the pyrite-dominant mineralized rock at Drenchwater compared to Red Dog.

In July, 1994, surface water samples from Drenchwater and False Wager Creeks and their tributaries were collected. Both creeks drain mineralized areas. Discovery Creek drains a semi-massive sulfide unit and flows into Drenchwater Creek. Results indicate that Discovery Creek water is enriched in Al, Fe, Mn, Cd, Co, Cu, Ni, Pb, and Zn (fig. 2A; Kelley and Taylor, 1997). Conductivity, pH, and metal concentrations in surface waters from lower Drenchwater Creek, below the confluence with Discovery Creek, also reflect the input of naturally enriched waters from Discovery Creek. The dissolved element profiles for most metals show typical dilution patterns for waters enriched by a single point source. For instance, water from Discovery Creek has low pH (4.5) and high metal concentrations (Zn=1,400 ppb; Cd=6 ppb; Fe=3 ppm), but below the confluence of Discovery Creek with Drenchwater Creek, the concentrations gradually decrease and pH gradually increases with distance downstream from the confluence. The decreasing metal concentrations in lower Drenchwater Creek with distance downstream from the confluence is probably due to adsorption of metals on hydrous Fe oxides. Stream pebbles and cobbles in the stream bed along Drenchwater Creek immediately downstream from the confluence with Discovery Creek are coated with abundant Fe-rich hydrous oxides. Acidic stream waters from Discovery Creek flow into Drenchwater Creek and mix with near neutral waters which typically increases the pH. This increased pH results in adsorption of metals on hydrous Fe-oxides which are present in the sediment and it decreases dissolved metal concentrations.



#### EXPLANATION

- Upper Drenchwater Creek (above confluence with Discovery Creek)
- Discovery Creek
- ♦ Lower Drenchwater Creek (below confluence with Discovery Creek)
- ▲ False Wager Creek
- + Lik deposit (plotted are samples collected from within or downstream from deposit only)
- \* Red Dog deposit (plotted are samples collected from within or downstream from deposit only; from Dames and Moore, 1983)

**Figure 2. (A)** Enrichment factors for stream water samples from the Drenchwater prospect area, with factors representing the ratio of the listed parameter for water below to that directly upstream of the prospect. **(B)** Diagram showing the relation between pH and metal content of stream waters from the shale-hosted massive sulfide deposits, western Brooks Range. Carbonate rocks exposed near the Lik deposit buffer the acidity and limit the metal-carrying capacity of the waters. The relatively high metal content in waters from the Red Dog deposit reflect either a greater extent of surface exposure of sulfide minerals and/or the higher grade of mineralization.

The most acidic waters from the Drenchwater prospect area are those from False Wager Creek which drains the deposit on the southeast side. Natural waters from False Wager Creek have pH values down to 2.8 with up to 95 ppm Al, 230 ppm Fe, 1,180 ppm SO<sub>4</sub>, and 2,600 ppb Zn. Many of the more acidic streams are depositing Fe-oxide coatings on stream sediments, or as a ferricrete cement on the bottom of the creek. Analyses by x-ray diffraction revealed that this material is crystalline jarosite [KFe<sub>3</sub>(SO<sub>4</sub>)<sub>2</sub>(OH)<sub>6</sub>], with variable amounts of quartz, kaolinite, and amorphous Fe oxides (Kelley and Taylor, 1997).

#### Lik deposit

The Lik deposit, which has not been mined but has been extensively drilled, is located 12 km northwest of Red Dog and is similar to Red Dog and Drenchwater in that it is hosted by Mississippian and Pennsylvanian black shale, but unlike these deposits, it has a thick section of carbonate rocks that are exposed upstream or upgradient from the mineralized zone. The dominant ore minerals are pyrite, marcasite, sphalerite, and minor galena. In addition, significant amounts of calcite or sparry dolomite occur in small veins cross-cutting the deposit, and as intergrowths with the sulfides.

Sediment samples from streams draining the deposit contain high Zn (6,000 ppm), Pb (251 ppm), and Cd (23 ppm) (Briggs et al., 1992). Soil also excellently delineates the mineralized zone. Soils collected away from the mineralized zone, or in areas where the mineralized zone is at great depths, had pH values of around 6-7, but immediately overlying the mineralized zone, pH values were as low as 3.9 and corresponding zinc concentrations were as high as 3,470 ppm (Briggs et al., 1992). Similarly, Ag, As, Cu, and Pb all show significant anomalies directly above or slightly displaced from the mineralized zone. For instance, directly overlying mineralized rocks, soils contained maximum concentrations as high as 3.5 ppm Ag, 77 ppm As, 229 ppm Cu, and 4,730 ppm Pb.

In spite of metal-rich sediments and soils from Lik, stream waters draining the deposit are not acidic and contain mostly low dissolved metal concentrations. A diagram of pH versus dissolved metal concentrations illustrates how waters from Lik are mostly near neutral with low concentrations of most elements except Zn which reached 2,000 ppb in a few cases. The presence of carbonate rocks in the section at Lik serves to buffer the acidity of the water and thereby lower its metal-carrying capacity.

#### Summary and comparison of Brooks Range deposits with examples from the Selwyn basin

The geochemistry of surface waters from the three shale-hosted SEDEX deposits in the Brooks Range shows how ore mineralogy and host rock or country rock lithology can affect drainage compositions (fig. 2B). Waters from deposits like Drenchwater and Red Dog, which have no carbonate rocks in the section, have low pH (less than 3 in some cases) and high metal concentrations, particularly Zn, Cd, Fe,

and Pb. The relatively higher concentrations of metals from Red Dog waters compared to Drenchwaters is probably a result of higher zinc grades at Red Dog.

Neutral pH and low dissolved metals except zinc occur in waters from deposits with abundant carbonate rocks in the section, such as the Lik deposit. It is important to note at Lik that only the headwaters of the streams originate in carbonate rocks. With distance downstream (within 400-800 feet of the headwaters), the streams drain almost exclusively shale or chert rather than carbonate. The shale-hosted sulfide deposit is located about 650 m downstream from any exposure of carbonate rock; however, because the stream originates in carbonates, and there are carbonate rocks in float along the stream, the water remains buffered.

A comparison of the Brooks Range deposits with others in the MacMillan Pass area of east-central Yukon Territory show that naturally occurring acidic streams are common in areas draining massive sulfide deposits in that area (Kwong and Whitley, 1991). For example, waters draining sulfide-rich rocks with negligible neutralization potential have pH's down to 2.98 with correspondingly high concentrations of Zn (5,000 ppb), Cd (132 ppb), and  $\text{SO}_4$  (1,610 ppm). As with the Brooks Range examples, Kwong and Whitley (1991) concluded that water chemistry is strongly controlled by local lithology.

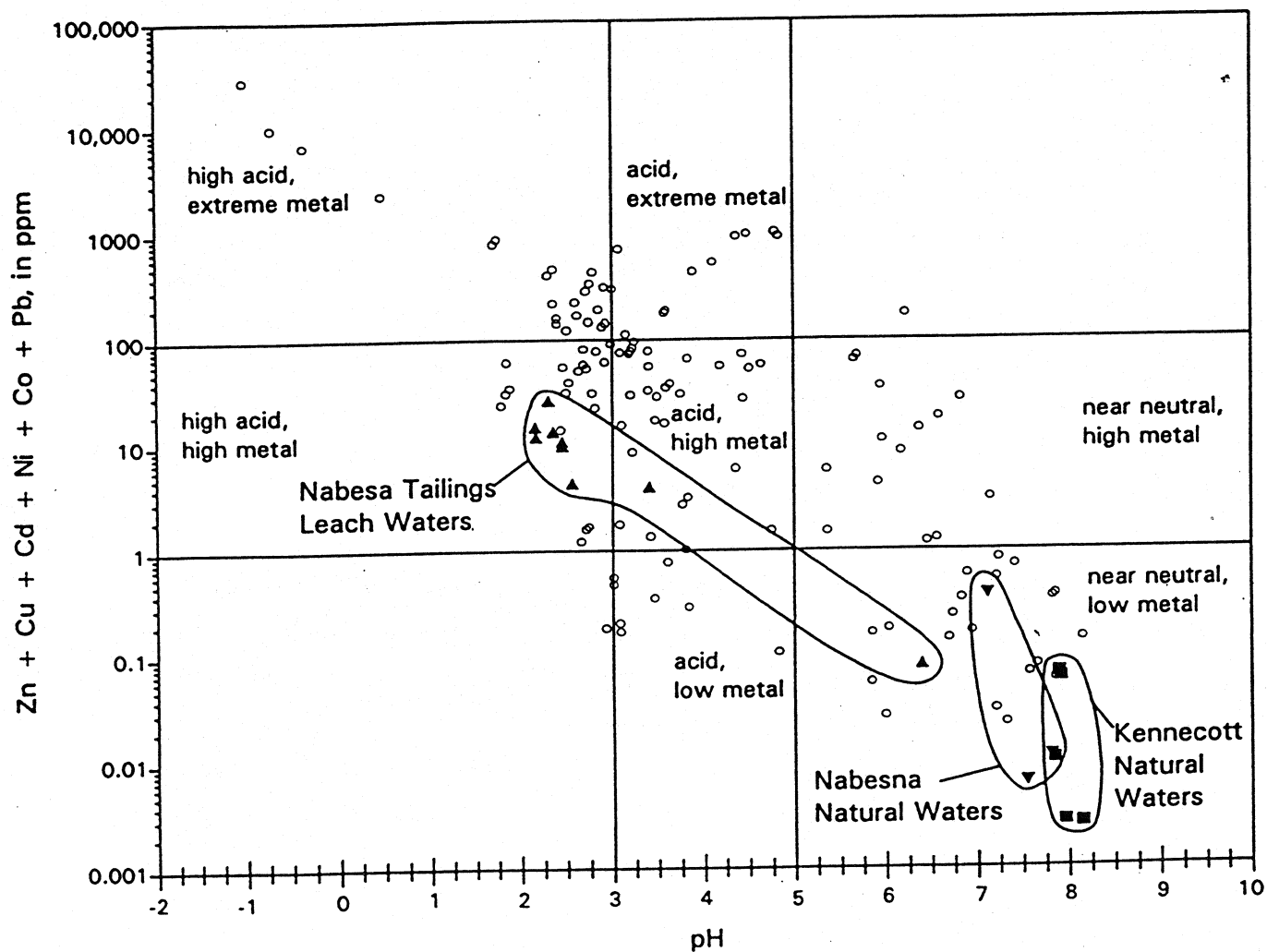
### **Skarn and Kennecott-type deposits of east-central Alaska**

Fe- and Cu-rich sulfide minerals in mineral occurrences and in mine and mill tailings piles in the Wrangell Mountains of eastern Alaska represent a major potential source of acid mine drainage. Oxidation and hydrolysis of metal sulfides from mined and unmined gold-bearing skarn and the massive Kennecott-type ores could release high concentrations of trace metals into the environment. However, as shown by Eppinger et al. (1997), thick carbonate sequences that host most of the mineralization buffer surface waters and hinder significant metal transport (fig. 3). Most of the subsequent discussion is summarized from their study.

#### **Fe-Cu-Au skarn deposits**

Middle Cretaceous calcic Cu and Au skarns occur in Upper Triassic carbonate rocks on the flanks of the Wrangell Mountains. Garnet-chalcopryrite-dominant assemblages in limestone, with significant gold grades, characterize the Nabesna mine. The adjacent Rambler gold mine is developed in pyrrhotite- and pyroxene-rich bodies in dolomite. In addition to the pyrrhotite and chalcopryrite, other metallic minerals at the now abandoned workings include pyrite and magnetite, with lesser galena, sphalerite, arsenopyrite, and stibnite.

Unmined ore, mine waste, and a broad area of fine mill tailings are now scattered below the old workings. X-ray diffraction studies of the tailings identified a variety of secondary iron sulfate minerals



**Figure 3.** Diagram showing the relation between pH and metal content of stream waters from the Kennecott deposits, the Nabesna skarns, and leachates of Nabesna skarn ores, east-central Alaska. Open circles are values for mine drainage waters from other mineral deposit types. Figure taken from Eppinger et al. (1997).

precipitated during dry periods (Eppinger et al., 1997). In the short term, these salts lock up many of the weathered metals and prevent dispersion into the surrounding ecosystem. However, many of the salts such as rozenite ( $\text{FeSO}_4 \cdot 4\text{H}_2\text{O}$ ) and copiapite ( $\text{Fe}_{14}\text{O}_3(\text{SO}_4)_{18}63\text{H}_2\text{O}$ ), are highly soluble. The minerals thus have the potential to release a major flux of acidity and metals into the environment during the sudden onset of wetter conditions.

Laboratory leachate studies of the ores and the mine and mill tailings from the skarns were used to quantify possible mobility of trace metals (Eppinger et al., 1997). Leaching of these solid materials showed resulting discharges often with pH's between 2-3. Under such acidic conditions, surface waters draining both zones of massive ore and oxidized, mined skarn material could typically have conductivities of 5,000-6,000 us/cm. Dissolved metals reached levels of as much as 1,000-3,000 ppm Fe, >20 ppm Cu, >4 ppm Mn, 2.5-3.5 ppm Pb, and 1.8-3.4 ppm Zn.

In the field, however, sampling of springs and streams immediately downstream of all workings and tailings indicated significantly lower dissolved metal concentrations (Eppinger et al., 1997). The carbonate country rocks buffered the waters to neutral to slightly alkaline. Under such conditions, only zinc is highly mobile and runoff below the Nabesna mill tailings contained 0.36 ppm Zn. Conductivities were still relatively high (often 400-900 us/cm regionally), reflecting the abundance of dissolved calcium and bicarbonate. Increased dissolved loads, as shown by conductivities of 1,100-1,300 us/cm in waters below the Nabesna mine and mill tailings, reflects elevated sulfate concentrations of about 400-600 ppm.

#### Kennecott-type deposits

Massive chalcocite and djurleite are stratabound in the lowermost 100 m of the Upper Triassic Chitistone Limestone, which overlies the extensive, Cu-enriched subaerial basalt flows of the Nikolai Greenstone in the Wrangell Mountains. These ore minerals are now widely altered to anilite, covellite, malachite, and azurite. Massive copper ores also contain as much as 700 ppm Ag, 1,000 ppm Pb, 360 ppm Zn, and 2,000 ppm As (MacKevett et al., 1997). The mining of the Kennecott ore essentially ceased in 1938 and the deposits now form an enclave within the Wrangell-Saint Elias National Park and Preserve. Piles of carbonate-rich mine waste rock remain along the hillside below many of the old workings.

The importance of geology on the environmental behavior of mineral deposits is apparent from the drainage signatures below the Kennecott mine workings. All surface waters and springs, even downstream from extensive tailings accumulations, meet the State of Alaska's MCLs for public drinking water (Table 1) and range between 7.7-8.2 in pH (Eppinger et al., 1997). Despite the blocks of massive copper ore in waste piles and any copper enrichments still unexposed in the underground, most sampled waters contain <10 ppb Cu. Iron concentrations are consistently <20 ppb and sulfate levels are <10 ppm throughout the district. The lack of acidity and low metal contents for waters draining the abandoned mine lands of this major mineralized district reflect the buffering due to carbonate host rocks and the lack of unstable sulfide



**Table 1.** Water standards used for reference in these studies.

[concentrations are in µg/L, micrograms per liter (ppb), --, standard has not been established].

Element	EPA criteria maximum concentration (CMC) <sup>1</sup>	State of Alaska maximum contaminant level (MCL) <sup>2</sup>
Arsenic	360	50
Antimony	--	6
Mercury	<sup>3</sup> 2.4	2
Copper	18	1,000
Lead <sup>3</sup>	82	--
Zinc <sup>3</sup>	120	5,000
Cadmium <sup>3</sup>	3.9	5
Iron	--	300
Sulfate	--	250,000

<sup>1</sup>CMC is the Environmental Protection Agency's water quality criteria to protect against acute effects in aquatic life and is the highest instream concentration of a toxic pollutant consisting of a 1-hour average not to be exceeded more than once every 3 years on the average.

<sup>2</sup>MCL is the maximum concentration allowed by the State of Alaska in public drinking water systems. Concentrations listed for copper, zinc, iron, and sulfate are secondary MCL's that are reasonable goals and provide a general guideline for public drinking water systems.

<sup>3</sup>These element standards vary with water hardness. Values listed are for a water hardness of 100, which is similar to that for streams studied here.

minerals such as pyrite. The dominant copper sulfides, chalcocite and djurleite, are relatively stable and do not readily oxidize leading to acidic mine drainage. Therefore, acidic mine drainage is not a problem.

### **Besshi- and Cyprus-type VMS deposits**

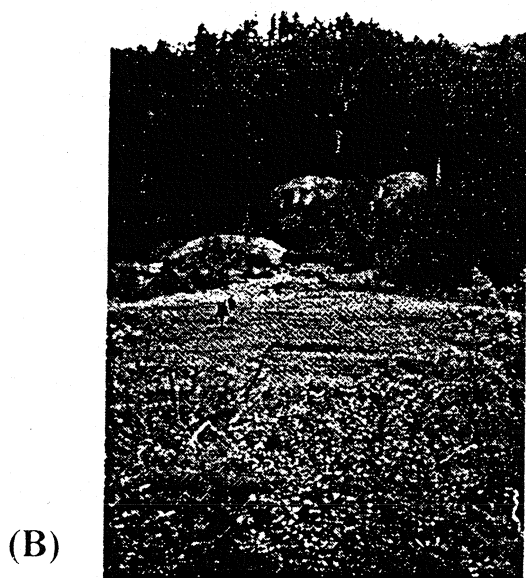
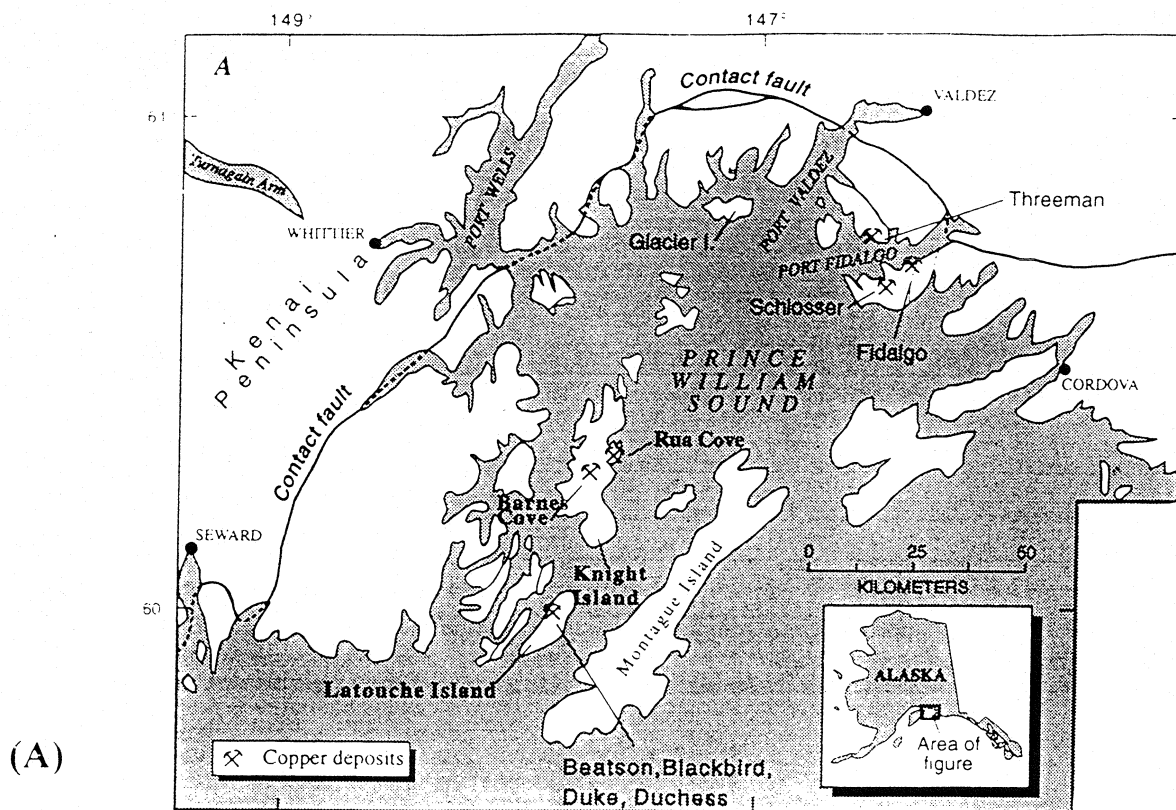
Tertiary Besshi- and Cyprus-type VMS deposits are widespread throughout the Prince William Sound region of south-central Alaska (fig 4A). These Fe-Cu-Zn deposits were mined in the early 1900's and now are reflected by numerous abandoned workings on lands of the Chugach National Forest. Ore mineralogy is dominated by pyrrhotite, pyrite and chalcopyrite, with lesser sphalerite within metasedimentary and mafic metavolcanic host rocks. The Beatson mine on LaTouche Island was Alaska's second largest past copper producer and workings there include a large glory hole that is now filled with water. The mine-waste piles (fig. 4B), underground workings (fig. 4C), and unmined ore zones within the forest have the potential to produce acidic and metal-rich discharge into local drainages. Where such discharge occurs, potential hazards exist for the local vegetation, aquatic life, and wildlife.

### Acid-mine drainage

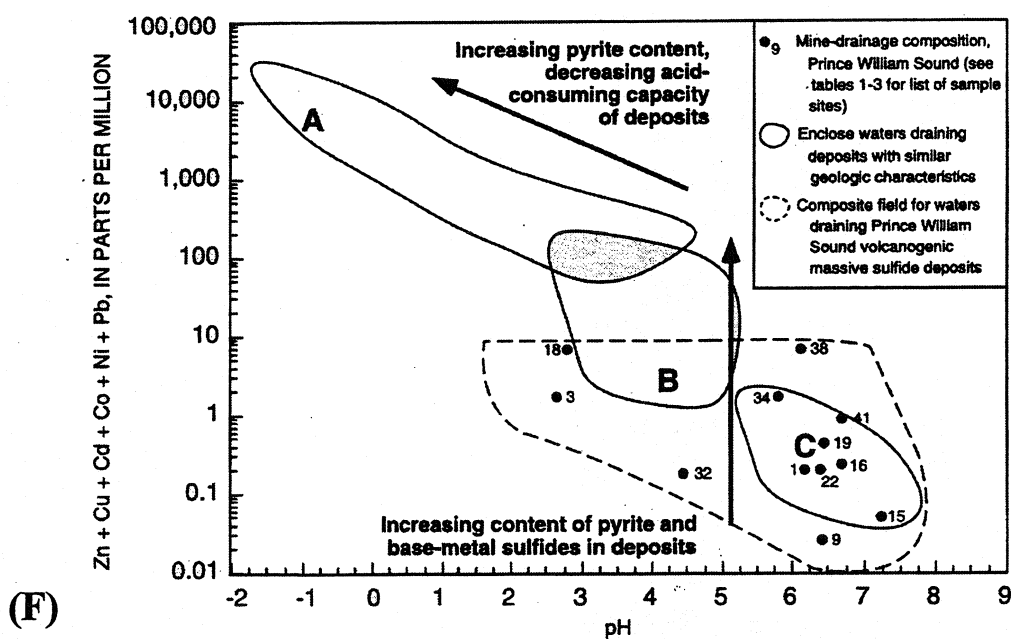
Where unoxidized to weakly oxidized, unmined, metalliferous rocks interact with stream waters, metal levels are little elevated above background concentrations (Goldfarb et al., 1996). Also, waters draining mine adits typically show only slight metal enrichments. These waters have pH values of 6-7 and have maximum dissolved Fe concentrations of 310 ppb and total base metals  $\leq 1$  ppm.

Acid drainage characterizes discharge that has interacted with many of the abandoned and highly oxidized tailing piles at the deposits (Goldfarb et al., 1996). Mine drainage is most acidic at the Duchess and Blackbird metasedimentary rock-hosted deposits on LaTouche Island, where waters with pH=2.6-2.7 drain directly out of bright-green bryophyte mats that surround the bases of the sulfide-rich tailings piles. Less acidic (4.3-6.4) waters are common below other tailings piles within the Chugach National Forest. Under the more acidic conditions, oxygenated surface waters contain dissolved loads of as much as 21,000 ppb Fe, 3,600 ppb Cu, 3,300 ppb Zn, 220 ppb Pb, 30 ppb Co, 150 ppb Ni, 27 ppb Cd, and 311 ppm sulfate. Most of these values exceed the State of Alaska's maximum contaminant levels (Table 1) and thus, at least locally, metals are elevated to concentrations that could potentially be hazardous to wildlife. However, effluent is rapidly diluted to natural background levels for all metals and to alkaline pH's upon entering more major stream channels a few hundred meters below all abandoned mine lands.

### Hydrogeochemistry of the Beatson glory hole



C-34



**Figure 4.** (A) Location map of the major VMS deposits in the Prince William Sound area. (B) Iron-stained tailings adjacent to the Duchess mine, LaTouche Island. (C) Mine discharge from the Schlosser adit in Port Fidalgo. (D) Water-filled glory hole at the Beatson mine, LaTouche Island. (E) Drainage below the Beatson glory hole discharging down to Prince William Sound. (F) Diagram showing the relation between pH and metal content of surface waters from VMS deposits of the Prince William Sound area. Fields A, B, C define waters for the West Shasta VMS deposits, sulfide-rich vein deposits in rocks with low buffering capacity, and sulfide-rich vein deposits in carbonate rocks, respectively (Plumlee et al., 1994). Mine drainage from VMS deposits in the humid Prince William Sound area is typically much less acidic and metalliferous than from VMS' in the more arid West Shasta district.

The water-filled glory hole pit at the Beatson copper mine (fig. 4D) is about 500 m from the shoreline of Prince William Sound. It, therefore, represents a potential significant contaminant source to the marine environment. The water has a blue-green color, which suggests that it contains a significant amount of ferrous sulfate in solution. Discharge from the pit to the Sound (fig. 4E) occurs through an old adit at the pit base at a rate averaging about 10 cfs during the summer.

Water in the pit had a pH of 4.8 when measured in 1957 (Shacklette, 1961); we determined water in the glory hole to have a pH of 7.25 some 40 years later, with discharge at the pit base slightly more acidic with a pH of 6.5 (Goldfarb et al., 1996). The most likely causes for the shift to more alkaline values over time include long-term consolidation of tailings, which hinders significant water/sulfide mineral interaction; flushing of originally more acidic mine waters from the pit; and/or decreased sulfide oxidation in the flooded pit. Iron, Cu, Zn, and sulfate concentrations in waters exiting the pit are only an order of magnitude above natural background levels; the relatively neutral waters hinder more significant metal dissolution.

### Discussion

The weathering of ores from VMS deposits can produce the most acidic, metal-rich mine drainage of any mineral deposit type (Smith et al., 1994). The severity of the acid mine drainage will be dependent on a number of factors, including sulfide concentration, access of oxygen to the sulfides, local hydrology, and acid-neutralizing capacity of the host rock. Study of the Prince William Sound VMS deposits (Goldfarb et al., 1996) indicate that such drainage will most likely be present where surface waters percolate through abandoned tailings piles (fig. 4F). Total dissolved Fe is as much as 21 ppm and base metal contents (Zn+Cu+Cd+Co+Ni+Pb) range between 1-7 ppm in waters with pH <4.5. Under these low pH conditions, all of the heavy metals are relatively mobile and adsorption on iron-rich suspended material is not significant (Smith et al., 1992). In less acidic waters, hydrous iron oxides will sorb many metals, resulting in lower dissolved concentrations.

Both the metasedimentary and metavolcanic host rocks have buffering capacities intermediate between the low capacity of granite and high capacities of carbonate rocks. Slightly calcareous mafic volcanic rocks, such as those at the Rua Cove copper deposit, will have a higher buffering capacity than the metasedimentary rocks. This difference likely explains the more metalliferous and acidic drainage below tailings of the Blackbird and Duchess mines relative to piles at the Rua Cove mines. The relatively less contaminated waters draining the flooded Beatson glory hole and many adits in the region largely reflect more limited oxidation of Fe-sulfides and less interaction between oxidized waters and the sulfides.

Climate plays a major role in defining the severity of acid-mine drainage. In the humid rainforest of Prince William Sound, any acid drainage from abandoned mine workings is rapidly diluted as it typically enters a nearby stream channel with discharge volumes orders of magnitude greater. Much more extreme

and toxic acidic waters are produced from weathering of VMS deposits in more arid environments. Charlie Alpers will describe such conditions from northern California later in the short course.

### **Mercury-rich epithermal vein deposits**

The regional geoenvironmental model for arc-related epithermal vein deposits, which are widespread in SW Alaska, emphasizes concerns associated with Hg-enriched mineralogy. Numerous epithermal deposits and abandoned mercury mines are located throughout the Kuskokwim River basin in southwestern Alaska. The deposits are mainly hosted in sedimentary rocks of the Cretaceous Kuskokwim Group. Formation of these deposits is closely associated with igneous activity of a Late Cretaceous and early Tertiary magmatic arc in southwestern Alaska (Gray et al., 1997). The mineralogy of the deposits is dominated by cinnabar and stibnite with subordinate realgar, orpiment, native mercury, pyrite, gold, and solid and liquid hydrocarbons; quartz, calcite, limonite, dickite, and sericite are alteration gangue minerals. Several of the deposits were mined between the early 1900's and the 1980's, but they are not currently operating because of low prices and low demand for mercury. About 41,000 flasks of mercury (1 flask=76 lb or 34.5 kg) have been produced from the region, which is about 99 percent of the total mercury produced from Alaska. Red Devil is the largest mercury mine in Alaska and it produced about 36,000 flasks of mercury. Most of the deposits consist of small, discontinuous veins that rarely exceed a few meters in width and a few tens of meters in strike length. The deposits generally contain about 1 to 5 percent mercury and less than 1 percent antimony and arsenic, but are base- and precious-metal poor. The presence of the abandoned mercury mines in southwestern Alaska is a potential hazard to residents and wildlife populations because drainage enters streams and rivers that are part of local ecosystems.

### Concerns to the environment

Mercury is a heavy metal of environmental concern because elevated concentrations can be toxic to living organisms. Mercury has no known metabolic purpose, and contaminations are regarded as undesirable and potentially hazardous (National Academy of Sciences, 1978). Most mercury toxicity problems are related to organic mercury compounds, of which methylmercury is the most toxic to humans (Eisler, 1987). Conversion of inorganic forms of mercury (for example, cinnabar) to methylmercury is generally a result of bacterial activity. Methylmercury is volatile, water soluble, and concentrates in tissues (bioaccumulation) of fish and other aquatic organisms. Once mercury is converted to water-soluble forms, like methylmercury, it becomes readily available to biota. Mercury can increase in concentration with increasing trophic position in the food chain (biomagnification), such as fish. Concentration of mercury in fish provides an easy pathway for mercury to enter the food chain (Eisler, 1987).

To evaluate environmental concerns, concentrations of mercury were measured in stream-sediment, stream-water, and fish collected downstream from deposits and mines. Mercury concentrations in fish are used to address the levels of mercury in the food chain that could eventually affect human health. Samples were also collected throughout SW Alaska where there are no known mercury deposits to establish regional backgrounds.

#### Mercury in the environment in SW Alaska

Stream-sediment samples collected downstream from abandoned mines contain as much as 5,000 ppm Hg (Gray, 1994), whereas those collected from streams in unmineralized areas typically contain <1.0 ppm Hg. The high mercury concentrations in the former are due to the presence of the cinnabar (HgS) that is resistant to physical and chemical weathering. But, although these total mercury concentrations in the stream-sediment samples are high, mercury speciation studies indicate that concentrations of the highly toxic methylmercury are low. Methylmercury concentrations rarely exceed 1.0 ppb in stream-sediment samples, and usually comprises <1 percent of the total mercury.

Stream waters below the mercury mines in SW Alaska are slightly alkaline, with pH values of 7.1-8.4 (Gray et al., 1996). Acid formation in streams below the mines is generally insignificant because cinnabar is highly insoluble in water. Cinnabar does not easily form acid drainage during weathering and there is rarely enough pyrite in these deposits to generate any significant acid drainage. Unfiltered stream-water samples collected below mercury mines generally contain <1.0 ppb Hg, but may contain as much as 2.5 ppb Hg. Where corresponding stream-water samples are filtered through a 0.45  $\mu$ m membrane, they contain <0.20 ppb Hg. These stream-water results indicate that suspended material transports most of the mercury downstream from the mines (fig. 5A). Mercury speciation studies indicate that concentrations of methylmercury are low in stream-waters. Methylmercury concentrations are typically <0.10 ppb in filtered and unfiltered stream-water below the mines.

All filtered and unfiltered background stream-water samples collected distal to any known epithermal occurrences in the region contain <0.10 ppb Hg. The mercury concentrations in these stream waters are, therefore, far below both the 2.0 ppb drinking-water standard recommended by the State of Alaska and the 2.4 ppb maximum concentration recommended by the U.S. Environmental Protection Agency (EPA). However, some background data exceed the 0.012 ppb concentration that the EPA indicates may result in chronic effects to aquatic life. When stream water exceeds 0.012 ppb, edible portions of fish are analyzed to determine if they exceed the FDA action level of 1 ppm wet weight.

Muscle samples (edible fillets) of freshwater fish collected downstream from mines contain as much as 0.62 ppm mercury (wet weight). Mercury concentrations for these fish are considered elevated because similar fish collected from background streams contain only about 0.10 ppm mercury (Gray et al.,

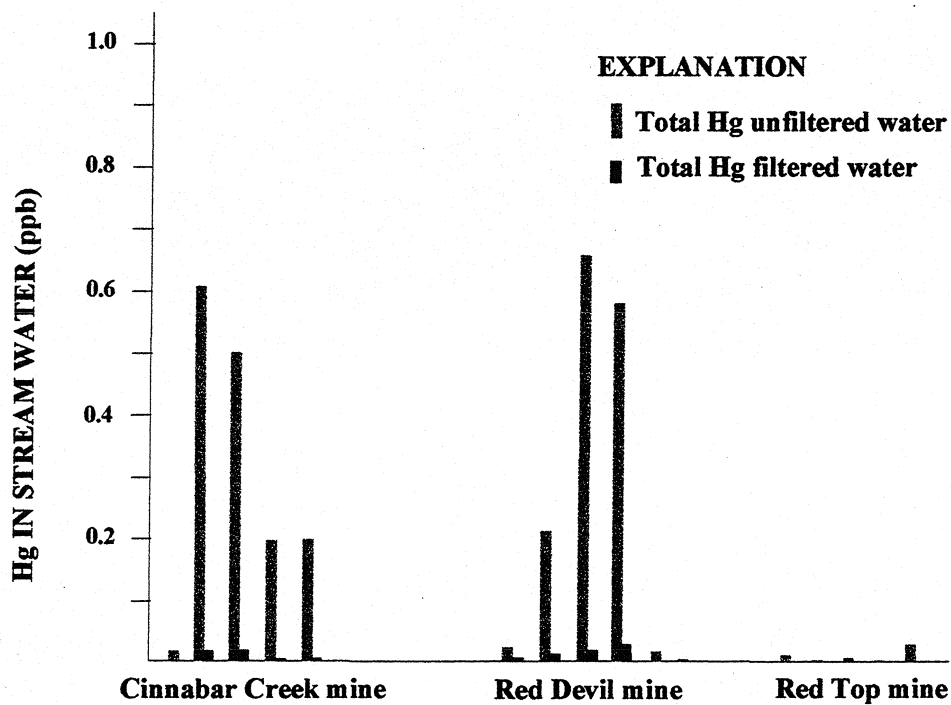


Figure 5. (A) Concentraion of mercury in filtered and unfiltered stream-water samples collected from three mercury mines in SW Alaska.

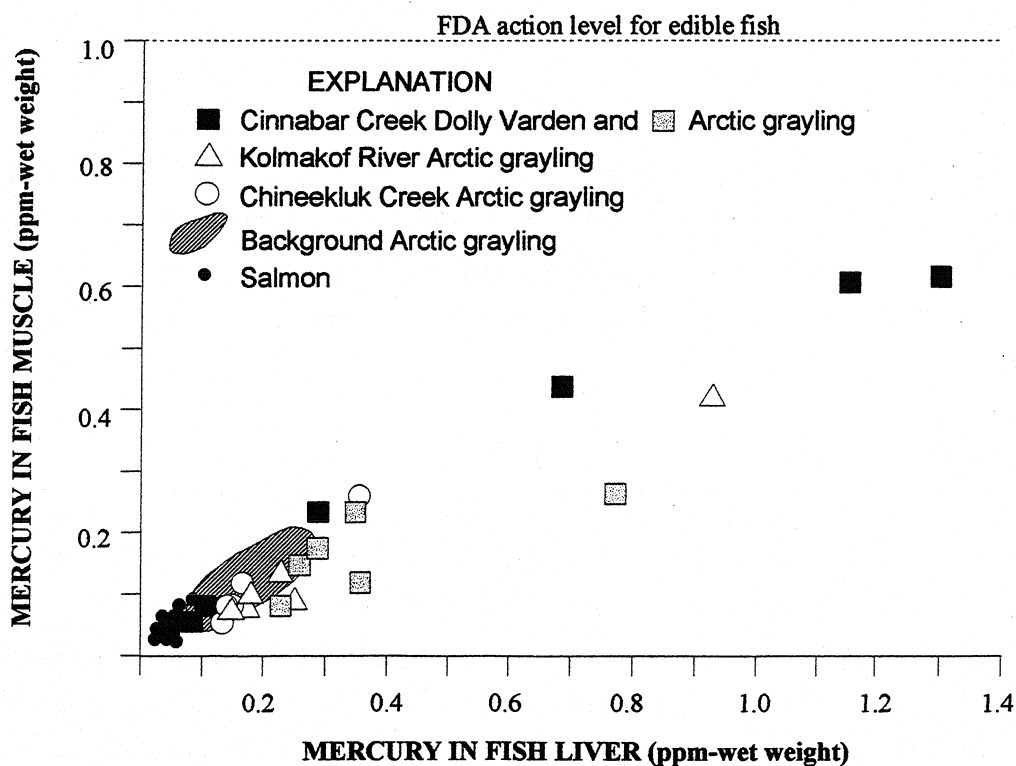


Figure 5. (B) Mercury concentration in fish muscle vs. fish liver for fish collected in SW Alaska.



1996). Generally, methylmercury comprises more than 90 percent of the total mercury in fish muscle, which is typical for freshwater fish. Although fish collected downstream from the mines contain mercury concentrations higher than background samples, the mercury contents in the fish are below the 1.0 ppm FDA action level for edible (fig. 5B). Mercury concentrations were also measured in salmon collected from large rivers in the region because these fish are often consumed by local residents and sportsmen. Mercury concentrations in muscle samples of the salmon are low, <0.10 ppm, and are also below the FDA action level.

### Conclusions

Stream-sediment, stream-water, and fish samples collected downstream from the abandoned mercury mines contain high concentrations of mercury in comparison to regional background concentrations in corresponding samples. Cinnabar, derived from epithermal deposits upstream, is the dominant source of mercury in the stream environment. However, cinnabar is highly insoluble in water and rarely forms acid drainage during weathering, and thus, stream waters below the mercury mines generally have near neutral to slightly alkaline pH.

The low concentrations of methylmercury in stream-sediment and stream-water samples indicates only minor conversion of inorganic mercury in cinnabar to the highly-toxic methylmercury. The elevated mercury concentrations in fish collected near the mines indicate that some biologically available mercury is taken-up by the fish. The fish probably accumulate the mercury through their gills from suspended particulates in stream water or from food sources. When mercury enters the food chain it can be hazardous because mercury tends to concentrate in the highest predators through biomagnification. Mercury concentrations in fish are useful for addressing the levels of mercury in the food chain that can eventually affect human health. However, all of the fish analyzed contain mercury concentrations below the 1.0 ppm action level for edible fish recommended by the FDA. These results represent a case study of the environmental effects of mercury mines that has application to similar mercury-rich mineral deposits worldwide.

### **Orogenic gold vein deposits**

The low sulfide content (generally no more than 1-3 percent of the vein) of mesothermal gold-bearing vein deposits throughout Alaska leads to a model that predicts generally minimal impact on local ecosystems from unmined or mined occurrences. These Cretaceous and early Tertiary vein deposits occur in greenschist facies belts of accreted terranes; host rocks include metasedimentary units and felsic to mafic igneous bodies. The mineralogy of the ore systems plays a major role in determining the chemical character of associated mine drainage (Smith et al., 1994). The sulfide mineral assemblage from one deposit to the

next varies and is dependent upon host rock. In dioritic host rocks in the Willow Creek district and at the Treadwell mine of the Juneau gold belt, pyrite is the dominant sulfide phase. At the Alaska-Juneau mine, where veins lie along metagabbro-phyllite contacts, pyrrhotite, sphalerite, and galena are the dominant sulfide phases. In the schist-dominant part of the Fairbanks district, where we conducted our field investigations, arsenopyrite and stibnite were the most common sulfide minerals in and around the gold lodes; scorodite was a common weathering product of the former mineral. The high CO<sub>2</sub> content of the ore-forming fluids leads to extensive carbonation of the surrounding country rocks. Surface waters have been studied from above and below both abandoned and active mine workings in the Fairbanks, Willow Creek, and Juneau gold districts (Goldfarb et al., 1997).

### Acidity

The formation of acidic waters in association with mesothermal-type gold vein deposits is prevented by the low-sulfide content of the ores and the presence of carbonate alteration minerals that buffer water acidity. Most measured pH values for waters draining gold-mine workings in Alaska are alkaline and similar to waters away from the mines. For example, waters draining the state's largest past lode gold producer, the Alaska-Juneau mine, have a pH of 8.0; those flowing out of the portal of the Independence mine, the most significant working in the Willow Creek district, have a pH of 7.8.

Oxidation of the 2-3 percent sulfide minerals, mainly pyrite, within tailings piles near some of the mines can lead to production of minor amounts of acidity. Waters collected below tailings piles in the different districts (fig. 6A) typically had pH values between 6.7-7.5. Significant acid generation was only noted at two locations. Water flowing through very fine-grained mill tailings in the stream valley adjacent to the Hi-Yu mine (fig. 6B) in the Fairbanks district had a pH of 5.2. Near Juneau, processing of ore in the early 1900's at the Mexican mine on Douglas Island included concentrating sulfide minerals and dumping them in the adjacent forest. Effluent collected downstream from these mine wastes (fig. 6C) had a highly acidic pH of 2.9.

### Dissolved Metals

Data from the Willow Creek gold district (Goldfarb et al., 1997) are typical of those from many low-sulfide, gold-quartz vein districts. The lowest pH value measured in the district was near neutral (pH 6.9), and, as a result, dissolved-ion concentrations draining all workings were below the Alaska and EPA water-quality standards. Total concentrations of 80 ppb As and 3,700 ppb Fe below the Gold Cord tailings piles indicate enhanced transport of ferric hydrous oxides from oxidized, poorly consolidated mine wastes.

All cation concentrations in waters draining workings of the Alaska-Juneau deposit, the state's largest past gold producer, are similar to background concentrations. Formation of sulfate during

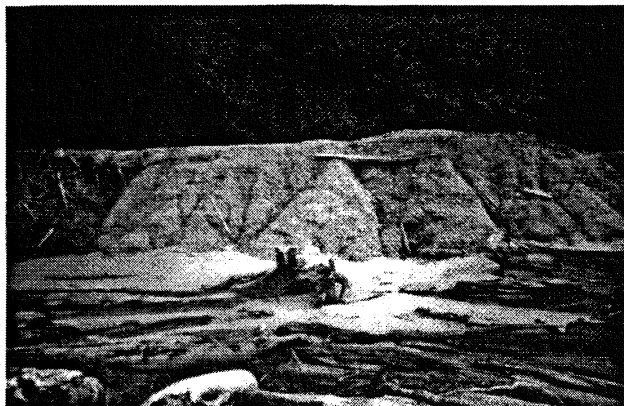
(A)



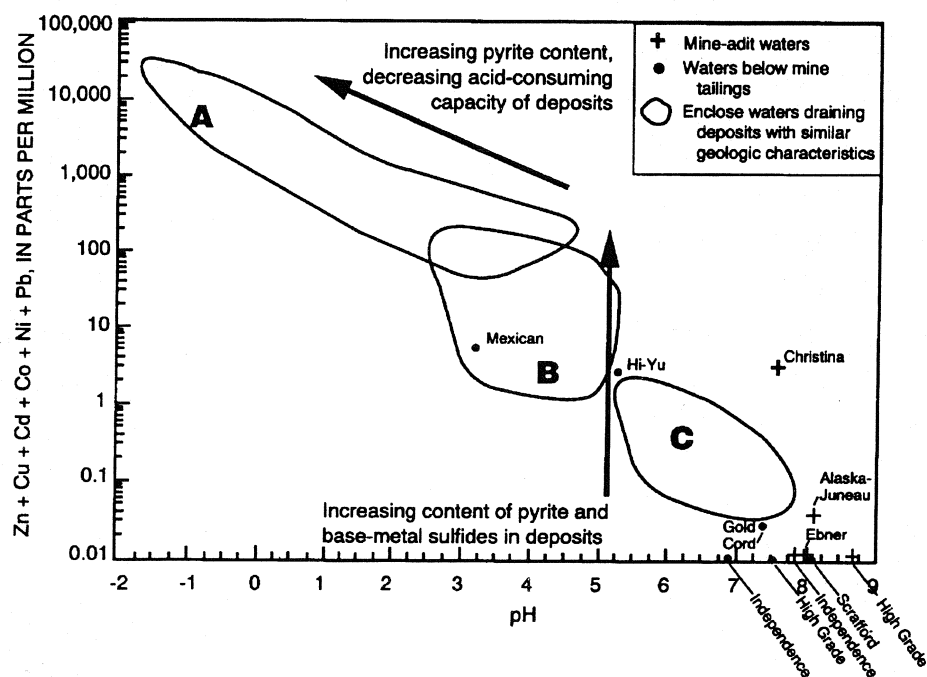
(B)



(C)



(D)



**Figure 6.** (A) Voluminous mine tailings at the Independence mine, Willow Creek district. Water collected at the base of the tailing pile contained dissolved amounts of only 3ppb As, 2.3 ppb Sb, <2ppb Zn, 0.6 ppb Pb, <2ppb Cu, and <40 ppb Fe. (B) Finely ground mine tailings adjacent to the Hi-Yu mine, Fairbanks district. The fine-grained nature to the tailings led to minor amounts of acidity in the waters of Moose Creek. (C) Sulfide-rich mill tailings of the Mexican mine, Treadwell orebody, near Juneau. Water at the base of these tailings had a pH of 2.9 and extremely high metal concentrations. (D) Diagram showing the relation between pH and metal content of surface waters from Alaskan gold deposits. Fields A, B, and C define waters for the West Shasta VMS deposits, sulfide-rich vein deposits in rocks with low buffering capacity, and sulfide-rich vein deposits in carbonate rocks, respectively (Plumlee et al., 1994). Mine waters draining the gold deposits are typically high pH/low metal, except where ore-processing techniques increase sulfide/water interactions.

weathering of sulfide minerals leads to concentrations of as much as 349 ppm sulfate dissolved in mine effluent. At the nearby Treadwell mine glory hole, waters contain cation and anion concentrations similar to water samples collected from background sites. During mining and milling of ore at the Mexican mine, sulfide minerals were likely concentrated. During resultant weathering of the tailings, the acidic waters of pH 2.9 that were produced results in a dissolved load of 330,000 ppb Fe, 7,500 ppb Al, 1,800 ppb Mn, 160 ppb Co, 120 ppb Ni, 380 ppb Cu, 2,500 ppb Zn, 32 ppb Cd, and 1,130 ppm  $\text{SO}_4^{2-}$ .

The Fairbanks district is characterized by waters with variable, but often quite high, natural background levels of dissolved arsenic and dissolved antimony. Some workers have determined naturally occurring concentrations of as much as about 5,000 ppb As dissolved in groundwaters of the district (Hawkins et al., 1982). Measured metal concentrations were as high as 260 ppb As and 23 ppb Sb in surface waters upstream from mine workings (Goldfarb et al., 1997). Dissolved-antimony concentrations were as much as 200 ppb in the Christina adit water samples and 200 ppb in water collected below the stibnite-rich tailings of the Scrafford mine. Total-iron and total-arsenic levels are elevated compared with background levels where abundant oxides form in lode and placer tailings piles. Concentrations of as much as 31,000 ppb Fe and 8,900 ppb As were measured along Too-Much-Gold Creek.

### Discussion

Mining and weathering of low-sulfide, gold-quartz vein deposits typically result in limited environmental contamination relative to the mining of more sulfide-rich deposit types (fig. 6D; du Bray, 1995). Arsenic from oxidized ores and mercury from processing procedures have characteristically been the trace elements of greatest concern. Thermodynamically favored As (V) is the most common inorganic arsenic species dissolved in natural waters, but the human metabolism tends to reduce the species to the more toxic As (III) following ingestion. If As (III) becomes bioavailable and migrates to the kidneys and other vital organs, it poses a major cancer threat in humans (Eisler, 1988; A.H. Smith et al., 1992). Little work has been published on arsenic speciation in Alaska's ground and surface waters. However, a limited amount of data collected by Hawkins et al. (1982) indicates that As (III) makes up a high percentage of the total arsenic dissolved in ground waters in the Fairbanks district. In contrast to the relatively high toxicity of inorganic arsenic, organic forms of mercury (such as methylmercury) are the most toxic, are soluble in water, and are the most serious mercury health concern to humans and other living organisms.

Effluent from gold mine adits in Alaska is generally metal poor and neutral to slightly alkaline in pH (Goldfarb et al., 1997). Waters collected from the adits in the Willow Creek district contained only 5-37 ppb dissolved As, <40 ppb dissolved Fe, 1.6-3.9 ppb dissolved Sb, and 6-38 ppm sulfate; base metals at these sites are also below background levels. Similar low values characterized cations in waters draining the Alaska-Juneau orebody in the Juneau gold belt, although sulfate levels were as great as 349 ppm. In contrast, much higher dissolved-metal levels of 130 ppb Fe, 84 ppb As, 200 ppb Sb, and 1,500 ppb Zn

characterize drainage from the Christina mine in the Fairbanks district. Corresponding total-arsenic and total-iron concentrations are nearly an order of magnitude greater because of either the adsorption and colloidal transport with hydrous oxides or the transport of fine-grained suspended material. The cause for the higher dissolved metal concentrations at the Christina mine is uncertain. An abundance of caved-in vein material within the adit may have enhanced water-rock interaction.

The concentration of mined sulfide-bearing quartz vein and wall rock material stored in abandoned waste piles can be a significant source of hydrous ferric oxides with adsorbed metals and of mercury from ore processing. None of the measured mercury concentrations below Alaskan gold mine workings exceeded EPA-CMC or State of Alaska MCL standards, but the elevated mercury concentrations in waters below tailings at a few mines indicates the need for monitoring of mercury concentrations in waters draining historic mine operations (Goldfarb et al., 1997).

Certain processing techniques used at historic mine workings may increase environmental problems if resulting tailings were abandoned in waste piles. At the Hi-Yu mine near Fairbanks, ore was crushed to fine grain sizes before gold extraction. Hence, the mill tailings that are scattered along adjacent Moose Creek offer a greater total surface area for water-rock interaction. As a result, acidic waters of a measured pH of 5.2 can dissolve and transport greater-than-background metal concentrations. The concentration of sulfide grains prior to gold mining may lead to formation of increased acid mine drainage in association with a deposit type that normally lacks such problems. This is the case at the Mexican mine near Juneau, where water below the milled tailings has a pH of 2.9 and is anomalously metal rich.

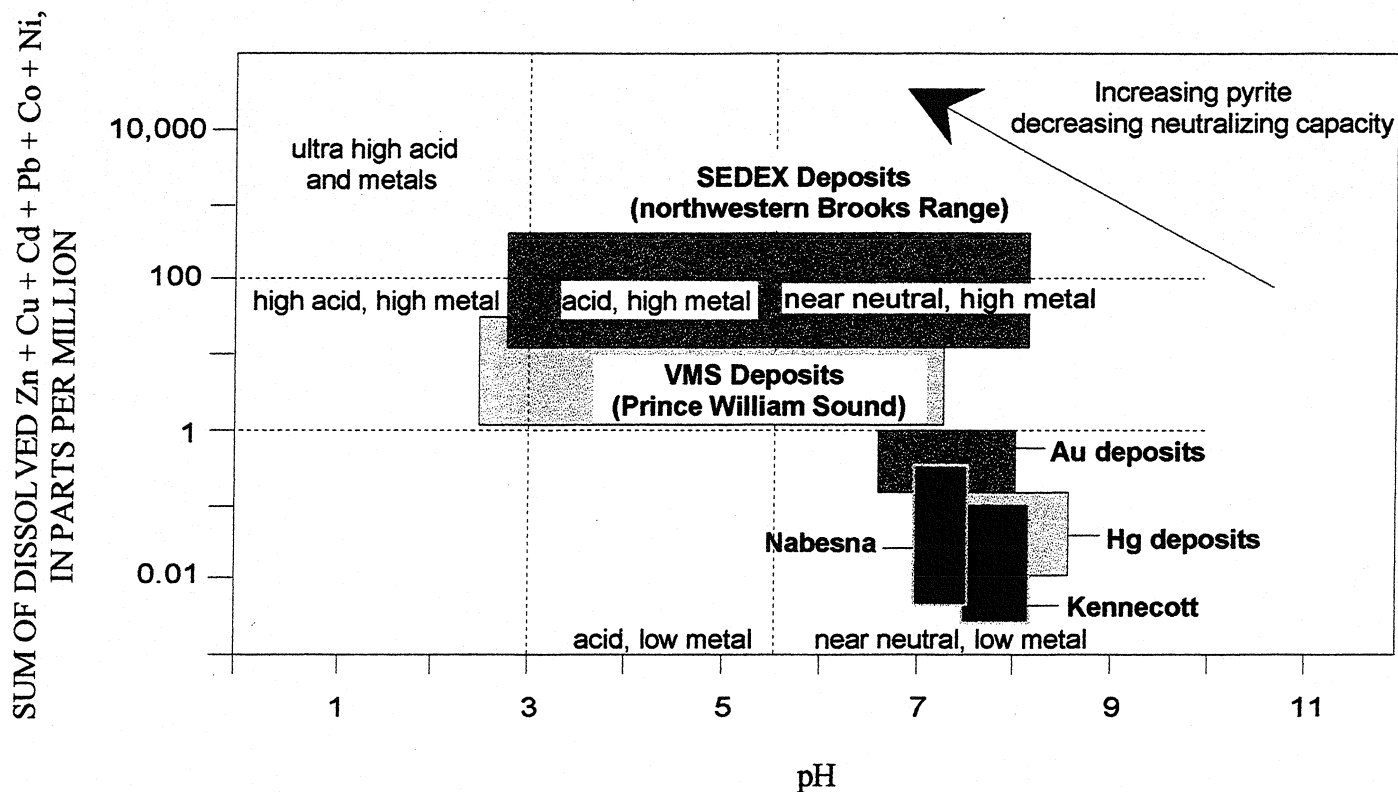
## Summary

The studies of Alaskan mineral deposits presented herein show that various types of mineral deposits have very different geochemical characteristics (table 2) that influence the chemistry of waters draining the mineral deposits (fig. 7). These characteristics are directly related to the mineralogy, geochemistry, and geology of each mineral deposit. For some deposits, downstream water geochemistry may present environmental problems for the local ecosystems. For example, the most adverse effects were observed downstream from the massive sulfide deposits in the northwestern Brooks Range and in Prince William Sound where water samples contain the highest concentrations of metals and lowest pH values of the deposits studied here. Such acid- and metal-rich waters result from the weathering of pyrite and other base-metal sulfide minerals in these deposits that form acid and release heavy metals during the process. Water samples collected near the massive sulfide deposits may contain heavy metal concentrations in excess of State and Federal water standards (table 2). Although waters emanating from these deposits are high in acid and metal content, these waters are rapidly diluted downstream, usually within a few km below the deposits (for example, deposits in the Brooks Range).

Table 2. Geochemical data summary of mineral deposits studied.

Deposit type	Elements of environmental concern	Element concentrations in water exceeding EPA CMC standards <sup>1</sup>	pH range in stream water
Massive sulfides (SEDEX)	Pb, Zn, Cd, Cu	2,250 ppb Pb, 272,000 ppb Zn, 800 ppb Cd, 360 ppb Cu	2.8 - 8.1
Massive sulfides (VMS)	Cu, Pb, Zn, Cd	3,600 ppb Cu, 3,300 ppb Zn, 220 ppb Pb, 27 ppb Cd	2.6 - 7.3
Gold veins	As, Pb, Zn, Cd, Sb		6.4 - 8.0
Gold placers	As, Pb, Zn, Cd, Hg		6.5 - 8.1
Mercury	Hg, Sb, As		7.0 - 8.4
Nabesna Au-Skarn	Cu, As, Pb, Zn, Sb	360 ppb Zn, 615 ppm sulfate	7.1 - 7.8
Kennecott Cu	Cu, As	67 ppb Cu	7.9 - 8.2

<sup>1</sup>CMC is the Environmental Protection Agency's water quality criteria to protect against acute effects in aquatic life and is the highest instream concentration of a toxic pollutant consisting of a 1-hour average not to be exceeded more than once every 3 years on the average.



**Figure 7.** Plot of dissolved metal concentrations in water vs. pH for several mineral deposits in Alaska.

Most of the other Alaskan deposits studied contain low acid and metal concentrations in water collected downstream from the deposits. For example, stream waters collected downstream from mercury deposits in southwestern Alaska have near-neutral pH values and contain low mercury contents, suggesting that these deposits produce only minor amounts of acid and heavy metals upon weathering. The low dissolved mercury concentration is due to the presence of cinnabar, which is resistant to physical and chemical weathering and does not easily form acid water. A greater environmental problem of the mercury deposits is the elevated mercury concentrations in stream sediment samples and fish that were collected downstream from the mines and deposits; however, the mercury concentrations in the fish are below the recommended FDA level for mercury in edible fish, suggesting only minor effects on local food chains. Alaskan gold veins and gold placer deposits contain pyrite and other sulfide minerals capable of producing acid water, but the amount of these sulfide minerals is generally small. Thus, weathering of such deposits does not produce water with significant concentrations of acid or heavy metals.

The case studies presented herein summarize the environmental effects of several types of mineral deposits. The results emphasize the need for additional, well-designed geochemical studies, which are necessary for the classification and understanding of any mineral deposit, but which will also address potential environmental concerns. Environmental geochemical studies are now a common practice in the mining industry, before, during, and subsequent to the mining of mineral deposits. These studies help predict unique effects of mineral deposits on the surrounding environments. Environmental geochemistry can be useful in all phases of mineral exploration, as well as in mine planning, development, and remediation.

## REFERENCES

- Briggs, P. H., Motooka, J. M., Bailey, E. A., Cieutat, B. A., Burner, S. A., Kelley, K. D., and Ficklin, W. H., 1992, Analytical results of soil, stream sediment, panned concentrate, and water samples from the Lik deposit, northwestern Brooks Range, Alaska: U.S. Geological Survey Open-File Report 92-15A (paper version) and 92-15B (diskette version).
- Dames & Moore, 1983, Environmental baseline studies, Red Dog project. Water Quality Report, Chapter 3, prepared by L.A. Peterson and Associates, Inc., for the Red Dog Mine Project, Cominco, Alaska, Inc., Anchorage, Alaska.
- du Bray, E.A., editor, Preliminary compilation of descriptive geoenvironmental mineral deposit models: U.S. Geological Survey Open-file Report 95-381, 272 p.
- Eisler, Ronald, 1987, Mercury hazards to fish, wildlife, and invertebrates: a synoptic review: Fish and Wildlife Service Biological Report 85(1.10), 90 p.
- Eisler, Ronald, 1988, Arsenic hazards to fish, wildlife, and invertebrates--a synoptic review: U.S. Fish and Wildlife Service Biological Report 85(1.12), 92 p.
- Eppinger, R.G., Sutley, S.J., and McHugh, J.B., 1997, Environmental geochemical study of the Nabesna gold skarn and Kennecott strata-bound copper deposits, Alaska, in Dumoulin, J.A., and Gray, J.E.,



- eds., *Geologic studies in Alaska by the U.S. Geological Survey*, 1995: U.S. Geological Survey Professional Paper 1574, p. 19-39.
- Goldfarb, R.J., Nelson, S.W., Taylor, C.D., d'Angelo, W.M., and Meier, A.L., 1996, Acid mine drainage associated with volcanogenic massive sulfide deposits, Prince William Sound, Alaska, in Moore, T.E., and Dumoulin, J.A., eds., *Geologic Studies in Alaska by the U.S. Geological Survey*, 1994: U.S. Geological Survey Bulletin 2152, p. 3-15.
- Goldfarb, R.J., Taylor, C.D., Meier, A.L., d'Angelo, W.M., and O'Leary, R.M., 1997, Hydrogeochemistry of mine-drainage waters associated with low-sulfide, gold-quartz veins in Alaska, in Dumoulin, J.A., and Gray, J.E., eds., *Geologic studies in Alaska by the U.S. Geological Survey*, 1995: U.S. Geological Survey Professional Paper 1574, p. 3-17.
- Gray, J.E., 1994, *Environmental geochemistry of mercury deposits in Alaska*: U.S. Geological Survey Fact Sheet 94-072.
- Gray, J.E., Gent, C.A., Snee, L.W., and Wilson, F.H., 1997, Epithermal mercury-antimony and gold-bearing vein lodes of southwestern Alaska: *Economic Geology Monograph* 9, p. 287-305.
- Gray, J.E., Meier, A.L., O'Leary, R.M., Outwater, C., and Theodorakos, P.M., 1996, Environmental geochemistry of mercury deposits in southwestern Alaska: mercury contents in fish, stream-sediment, and stream-water samples, in Moore, T.E., and Dumoulin, J.A., eds., *Geologic Studies in Alaska by the U.S. Geological Survey*, 1994: U.S. Geological Survey Bulletin 2152, p. 17-29.
- Gray, J.E., and Sanzolone, R.F., editors, 1996, *Environmental studies of mineral deposits in Alaska*: U.S. Geological Survey Bulletin 2156, 40 p.
- Hawkins, D.B., Forbes, R.B., Hok, C.I., and Dinkel, D., 1982, Arsenic in water, soil, bedrock, and plants of the Ester Dome area of Alaska: Institute of Water Resources, University of Alaska, Fairbanks, Report IWR-103, 82 p.
- Kelley, K. D., Borden, J. C., Bailey, E. A., Fey, D. L., Motooka, J. M., and Roushey, B., 1992, Geochemically anomalous areas in the west-central part of the Howard Pass Quadrangle, National Petroleum Reserve, Brooks Range, Alaska--Evidence for sediment-hosted Zn-Pb-Ag-Ba mineralization, in Bradley, D.C. and Dusel-Bacon, C., eds., *Geologic studies in Alaska by the U.S. Geological Survey*, 1991: U.S. Geological Survey Bulletin 2041, p. 60-69.
- Kelley, K.D., and Taylor, C.D., 1997, Environmental geochemistry of shale-hosted Ag-Pb-Zn massive sulfide deposits in northwest Alaska: natural background concentrations of metals in water from mineralized areas: *Applied Geochemistry*, v. 12, p. 397-409.
- Kwong, J.Y.T., and Whitley, W.G., 1991, Assessment of the impact of acid rock drainage on the water quality of the south MacMillan River, Yukon Territory: NHRI Contribution No. 91042 Unpublished report, 20 p.
- National Academy of Sciences, 1978, *An assessment of mercury in the environment*: National Academy of Sciences, Washington, D.C., 185 p.
- Plumlee, G.S., and Nash, J.T., 1995, Geoenvironmental models of mineral deposits--Fundamentals and applications, in du Bray, E.A., editor, Preliminary compilation of descriptive geoenvironmental mineral deposit models: U.S. Geological Survey Open-file Report 95-381, p. 1-9.

- Plumlee, G.S., Smith, K.S., and Ficklin, W.H., 1994, Geoenvironmental models of mineral deposits, and geology-based mineral-environmental assessments of public lands: U.S. Geological Survey Open-file Report 94-203, 7 p.
- Shacklette, H.T., 1961, Substrate relationships of some bryophyte communities on LaTouche Island, Alaska: *The Bryologist*, v. 64, no. 1, p. 1-16.
- Smith, A.H., Hopenhayn-Rich, C., Bates, M.N., Goeden, H.M., Hertz-Picciotto, I., Duggan, H.M., Wood, R., Kosnett, M.J., and Smith, M.T., 1992, Cancer risks from arsenic in drinking water: *Environmental Health Perspectives*, v. 97, p. 259-267.
- Smith, K.S., Ficklin, W.H., Plumlee, G.S., and Meier, A.L., 1992, Metal and arsenic partitioning between water and suspended sediment at mine-drainage sites in diverse geologic settings, in Kharaka, Y.K., and Maest, A.S., eds., *Water-rock interaction: Seventh International Symposium on Water-Rock Interaction*, Park City, Utah, July 13-18, 1992, *Proceedings: Rotterdam, A.A. Balkema*, v. 1, p. 443-447.
- Smith, K.S., Plumlee, G.S., and Ficklin, W.H., 1994, Predicting water contamination from metal mines and mining wastes: U.S. Geological Survey Open-File Report 94-264, 112 p.
- Tailleur, I. L., 1970, Lead-, zinc-, and barite-bearing samples from the western Brooks Range, Alaska, with a section on petrography and mineralogy by G.D. Eberlein and Ray Wehr: U.S. Geological Survey Open-File Report 70-319.
- Theobald, P. K., Barton, H. N., Billings, T. M., Frisken, J. G., Turner, R. L. and VanTrump, George, Jr., 1978, Geochemical distribution of elements in stream sediment and heavy-mineral concentrate samples in the southern half of the National Petroleum Reserve, Alaska: U.S. Geological Survey Open-File Report 78-517.

## D - POTENTIAL FOR HIGH SULFIDATION EPITHERMAL GOLD DEPOSITS IN CANADA: THE EXAMPLE OF THE HOPE BROOK Au Cu DEPOSIT, NEWFOUNDLAND

Benoît Dubé, Geological Survey of Canada and Greg Dunning, Memorial University of Newfoundland

Dubé, B. and Dunning, G. (1998): Potential for High Sulfidation Epithermal Gold Deposits in Canada: The Example of the Hope Brook Au-Cu- Deposit, Newfoundland; in *Metallogeny of Volcanic Arcs*, B.C. Geological Survey, Short Course Notes, Open File 1998-8, Section D.

### ABSTRACT

High-sulfidation epithermal-type gold deposits represent attractive targets for global gold exploration due to their potential to be of giant size (e.g. Pueblo Viejo, Dominican Republic, >600 t Au; Yanacocha, Peru). The Hope Brook gold mine (1.5 M oz Au) is the best Canadian example of such gold mineralization. The deposit is hosted by Late Proterozoic rocks of the Northern Appalachians Avalon Zone. It is located within the Whittle Hill Sandstone intruded by a Late Proterozoic quartz-feldspar porphyry (QFP) sill-dike complex of the Roti Intrusive Suite. A Late Silurian sub-aerial volcanosedimentary cover sequence (La Poile Group) unconformably overlies the Late Proterozoic Avalonian rocks. The unconformity is interpreted to coincide with the Cinq Cerf Fault Zone which was activated in Late Silurian time as a reverse-sinistral fault zone. The fault zone is cut by the Devonian Chetwynd Granite (390 ±3 Ma) and associated contact metamorphism also overprinted the deposit.

The deposit is tabular and enclosed within a zone of hydrothermal alteration more than 3 km long and up to 400m wide. This zone of alteration is characterized by: (1) extensive advanced argillic alteration with pyrophyllite, kaolinite, andalusite, sericite, quartz, diaspore, and alunite which is developed mostly in the structural hanging wall of the ore zone and (2) two stages of massive silicic alteration. A first buff-color massive silicic stage extends for more than 3km laterally away from the deposit, constitutes a barren to weakly auriferous unit and likely results from the pervasive acid leaching of the original hosts. Na<sub>2</sub>O, K<sub>2</sub>O, CaO and MgO were strongly leached in the advanced argillic and silicic alteration zones whereas all the oxides, except silica, are totally depleted in the silicic alteration zones, leaving a residual core of almost pure silica. The gold mineralization is hosted by rocks displaying a second stage of silicic alteration characterized by grey to dark grey color and vuggy silica. The mineralization is characterized by several percent pyrite and lesser amounts of chalcopyrite, bornite and traces of tennantite, either as disseminations, impregnations or veinlets. Besides Au and Cu, other metals in the deposit are minor but geochemically anomalous amounts of Sb, Bi, Pb and As are present.

Precise U-Pb zircon dating of altered (pre-ore) QFP and of an unaltered (post-ore) intermediate dikes cutting altered rocks bracket the age of mineralization/alteration in a relatively short time interval between 574-578 Ma. This temporally and genetically links mineralization/alteration and Roti Intrusive Suite plutonism. The deposit was likely formed by a metal-rich magmatic hydrothermal fluid phase exsolved from the ascending, cooling and degassing subvolcanic sill-dike complex.

Most known high-sulfidation gold deposits are Tertiary in age or younger and Hope Brook, the largest high-sulfidation gold deposit in Canada, differs from type examples by virtue of its Late Proterozoic age.

Its preservation is likely due to its early tilting and a significant extensional event which has most probably buried the deposit and saved it from erosion. Its occurrence highlights the potential for such Au-Cu intrusion-related deposits in older volcanic and magmatic arcs.

The recognition of the two stages of silicic alteration constitutes an important exploration tool in discriminating between potentially mineralized and barren zones and helps in the definition of hydrothermal upflow zone(s). This study emphasizes that the primary characteristics and geological evolution of such high sulfidation gold mineralization in older terranes can only be revealed by cross-cutting relationships established by detailed field mapping of a well exposed area and accurate U-Pb age constraints.

## **POTENTIAL FOR HIGH SULFIDATION EPITHERMAL GOLD DEPOSITS IN CANADA: THE EXAMPLE OF THE HOPE BROOK AU-CU DEPOSIT, NEWFOUNDLAND<sup>1-2-3</sup>**

B. Dubé, Geological Survey of Canada, Quebec Geoscience Center 2535 Boul. Laurier,  
P.O. Box 7500, Ste-Foy, Quebec, Canada, G1V 4C7

and

G. Dunning, Department of Earth Sciences, Memorial University of Newfoundland, St.  
John's, Newfoundland, Canada, A1B 3X5

High-sulfidation epithermal-type gold deposits (e.g. Arribas, 1995; White and Hedenquist, 1995, Panteleyev, 1996) represent attractive targets for global gold exploration due to their potential to be of giant size (eg. Pueblo Viejo, Dominican Republic, >600 t Au; Yanacocha, Peru; El Indio-Tambo, Chile). Most are Tertiary in age or younger and their current distribution is concentrated along the Pacific Rim of Fire (e.g. Arribas, 1995). The Hope Brook gold mine (50 t Au) is the best Canadian example of such gold mineralization. The deposit is hosted by Late Proterozoic rocks of the Northern Appalachian Avalon Zone (Fig. 1). It is located within the Whittle Hill Sandstone intruded by a Late Proterozoic quartz-feldspar porphyry (QFP) sill-dike complex of the Roti Intrusive Suite. A Late Silurian sub-aerial volcano-sedimentary cover sequence (La Poile Group) unconformably overlies the Late Proterozoic Avalonian rocks (O'Brien et al., 1991) (Fig. 1). The unconformity is interpreted to coincide with the Cinq Cerf Fault Zone which was activated in Late Silurian time as a reverse-sinistral fault zone. The deposit is located within Late Proterozoic rocks in the hanging wall of the Cinq Cerf Fault and has been strongly deformed and metamorphosed. The fault zone is cut by the Devonian Chetwynd Granite (390 ± 3 Ma) and associated contact metamorphism also overprinted the deposit (McKenzie, 1986; Dubé, 1990; Yule et al., 1990; O'Brien et al., 1991, Stewart, 1992).

The deposit is tabular and enclosed within a zone of hydrothermal alteration more than 3 km long and up to 400m wide (Fig. 2). This zone of alteration is characterized by: (1) extensive advanced argillic alteration with pyrophyllite, kaolinite, andalusite, sericite, quartz, diaspore, and alunite which is developed mostly in the structural hanging wall of the ore zone (Kilbourne, 1985; McKenzie, 1986; Yule et al, 1990; Stewart, 1992; Dubé et al., 1994; 1995) and (2) two stages of massive silicic alteration. The first stage is represented by a buff-color massive silicic zone which extends for more than 3km laterally away from the deposit, and which constitutes a barren to weakly auriferous unit likely resulting from the pervasive acid leaching of the original hosts. Na<sub>2</sub>O, K<sub>2</sub>O, CaO and MgO were strongly leached in the advanced argillic and first stage silicic alteration zones whereas all the oxides, except silica, are totally depleted in the first stage silicic alteration zones, leaving a residual core of almost pure silica. Although the first silicic and advanced argillic alteration are important in terms of exploration because they constitute the regional scale manifestation of the large hydrothermal system, gold mineralization is only found where the rocks display the second stage of silicic alteration. The latter is characterized by grey to dark grey color, vuggy silica and several percent pyrite with lesser amounts of chalcopyrite, bornite and traces of tennantite, either as

disseminations, impregnations or veinlets as well as local traces of enargite. Besides Au and Cu, other metals in the deposit are minor but geochemically anomalous amounts of Sb, Bi, Pb and As are present.

The primary geological features of such disseminated styles of mineralization in older terranes are commonly obscured by deformation and metamorphism leading to conflicting interpretations and controversies as shown over the years at Hope Brook. Swinden (1984), Kilbourne (1985) and McKenzie (1986) proposed an Ordovician epithermal model for the deposit and suggested that it was related to felsic volcanism and / or high-level magmatism. Dubé (1990) classified Hope Brook as a deformed, pre-Late Silurian, disseminated stratabound sulfide-gold deposit with similarities to Romberger's (1986) disseminated gold sub-type of epithermal deposit. Yule et al. (1990) proposed that Hope Brook represents a pre-metamorphic and pre-shearing, modified mesothermal (sub)volcanic hosted gold deposit of probable Cambrian age which also shares analogies with the acid-sulfate epithermal style. Finally, Stewart (1992) interpreted Hope Brook as a multistage syn-tectonic shear-hosted acid-sulfate-type gold deposit related to a protracted hydrothermal history from Late Precambrian to Devonian times. A similar type of controversy has been discussed about the origin of Temora, Australia, a late Paleozoic high sulfidation deposit in deformed rocks (e.g. Thompson et al., 1986; Allibone et al., 1995).

Establishment of clear cross-cutting relationships combined with U-Pb dating allowed us to determine the age of the mineralization relative to that of other geological elements. New precise U-Pb zircon ages of altered (pre-ore) QFP, weakly to unaltered (syn- to late-ore) QFP cutting the second silicic stage and of unaltered (post-ore) intermediate dike cutting altered rocks bracket the age of mineralization and alteration within a relatively short time interval between 574 and 578 Ma. Combined with the nature and distribution of the lithological and alteration units, these ages temporally and genetically link mineralization and alteration with plutonism of the Roti Intrusive Suite (Dubé and Dunning, submitted). Hope Brook predates both ductile shearing along the Cinq Cerf Fault Zone and thermal metamorphism and is an epithermal high sulfidation-type gold deposit genetically related to a Late Proterozoic subvolcanic sill-dike complex. The deposit was likely formed by a metal-rich magmatic hydrothermal fluid phase exsolved from the ascending, cooling and degassing subvolcanic sill-dike complex.

Most known high-sulfidation gold deposits are Tertiary in age or younger and Hope Brook, the largest high-sulfidation gold deposit in Canada, differs from type examples by virtue of its Late Proterozoic age. It is also atypical when compared to most other gold deposits in Canada. Its preservation is likely due to its early tilting and a significant post-ore extensional event which has most probably buried the deposit and saved it from erosion. Its occurrence highlights the potential for such Au-Cu intrusion-related deposits in older volcanic and magmatic arcs particularly those of the North American Appalachian Avalon Zone. Widespread advanced argillic alteration zones with associated gold mineralization are present elsewhere in Newfoundland's Avalon Zone (O'Brien et al., 1996) and four gold deposits (Brewer, Haile, Ridgeway, Barite Hill; >75 t Au) in the South Carolina Slate Belt within the southern segment of the Avalon Zone (e.g. Spence et al., 1980; Feiss et al., 1993; Ririe, 1990; Zwaschka and Scheetz, 1995) share characteristics with Hope Brook.

High sulfidation epithermal style gold deposits are a single component of larger intrusion-centered hydrothermal systems (e.g. Sillitoe, 1989, 1991; Robert et al., 1997). Consequently, the widespread occurrence of advanced argillic alteration and mineralization clearly emphasizes that the Appalachian Avalon Zone has a significant potential for other types of gold and copper-gold mineralization of epithermal and porphyry styles. These could occur in the vicinity of the already known altered and mineralized areas or elsewhere along strike within this potential gold-copper belt. (e.g. Dubé, 1996; O'Brien et al., 1996) (Fig. 3).

The existence of Hope Brook, along with a few Mesozoic (Pueblo Viejo), Paleozoic (Temora; Australia) and Paleoproterozoic deposits (Enåsen, Sweden), suggests that this deposit type may be an important target for exploration in ancient terranes. Despite their emplacement at high levels in the crust, the potential for preservation of such high sulfidation epithermal gold deposits in older terranes is higher than commonly thought, especially in areas where the tilting of rocks in volcanic/magmatic arcs has occurred early in their geological evolution. This study emphasizes that, where they are preserved, the primary characteristics and geological evolution of such high sulfidation gold deposits in older deformed and metamorphosed terranes can only be revealed by establishing cross-cutting relationships by detailed field mapping of well exposed areas and by linking this with accurate U-Pb age constraints. For example, such an approach could also be used to test the potential presence of high sulfidation Au-Cu deposits in deformed greenstone belts, especially in the vicinity of tilted Archean Au and Cu-Au "porphyry systems", and of the high sulfidation end members of gold-rich volcanogenic massive sulfide deposits (Sillitoe et al. 1996).

Although the nature and distribution of first silicic stage of alteration are critical indications of a large scale hydrothermal system, the ore at Hope Brook is only localized in rocks displaying the second stage of silicic alteration. Consequently, the recognition of the two stages of silicic alteration was critical in understanding the genesis of the Hope Brook deposit and constitutes an important exploration tool in discriminating between potentially mineralized and barren zones and can help in the localization of hydrothermal upflow zone(s) (see also Hedenquist et al., 1994).

Note: This contribution contains excerpts from a detailed study of Hope Brook under review (Dubé and Dunning., submitted). A complete lists of references will accompany this paper.

- 1 Published with the permission of Royal Oak Mines.
- 2 Contribution to the Canada-Newfoundland Agreement on Mineral Development
- 3 **This extended abstract has been published in: The Gangue, Geological Association of Canada-Newsletter, issue No 57.**

#### Figure captions

Figure 1: Simplified geological map of the Hope Brook area. (USA, United States of America; NB, New Brunswick; NS, Nova Scotia; PEI, Prince Edward Island; CBI, Cape Breton Island; NFLD, Newfoundland. CMB, Central Mobile Belt, LPT, Late Proterozoic) Modified from O'Brien et al. (1991) and Stewart (1992). From Dubé and Dunning., (submitted).

Figure 2: Simplified geological map of Hope Brook gold deposit showing the nature and distribution of the alteration and lithotectonic units. . Note: for simplification, the younger and unaltered mafic dikes-sills are not shown. Based on detailed field mapping and surface projection of drill holes. Modified from Stewart (1992) and unpublished BP-Selco and Royal Oak Mines maps. From Dubé and Dunning., (submitted).

Figure 3: Late Paleozoic reconstruction of the circum-North Atlantic area showing location of gold mines. Modified from Murphy et al. (1996) and Keppie and Dallmeyer, 1989.

#### REFERENCES CITED

- Allibone, A.H., Cordery, G.R., Morrison, G.W., Jaireth, S., Lindhorst, J.W., 1995, Synchronous advanced argillic alteration and deformation in a shear zone-hosted magmatic hydrothermal Au-Ag deposit at the Temora (Gidginbung) Mine, New South Wales, Australia: *Economic Geology*, vol. 90, p. 1570-1603.
- Arribas, Jr. A., 1995, Characteristics of high-sulfidation epithermal deposits, and their relation to magmatic fluid: *in* *Magma, fluids, and ore deposits*, J.F.H. Thompson (editor). Mineralogical Association of Canada Short Course Volume 23. P. 419-454.
- Dubé, B., 1990, A preliminary report on contrasting styles of gold-only deposits in western Newfoundland: *Current Research, Part B: Geological Survey of Canada Paper 90-1B*, p. 77-90.
- Dubé, B., 1996, The Hope Brook gold deposit: example of an acid sulfate intrusion-related epithermal gold deposit in Newfoundland and its significance for the Au-Cu potential of the Avalon Zone: *In* *Report of Activities, Newfoundland Department of Mines and Energy, Geological Survey Branch*, p.13-15.
- Dubé, B., and Dunning, G., submitted, *Geology of the Hope Brook Mine, Newfoundland, Canada: a preserved Late Proterozoic high-sulfidation epithermal gold deposit.*
- Dubé, B., Lauzière, K., and Robert, F., 1994, Preliminary report on the alteration and deformation at the Hope Brook Gold deposit: *In* *Report of Activities, Newfoundland Department of Mines and Energy, Geological Survey Branch*, p. 63-64.
- Dubé, B., Lauzière, K., and Boisvert, E., 1995, Preliminary report on the geological setting of the acid-sulfate Hope Brook Gold deposit, SW Newfoundland: *In* *Report of Activities, Newfoundland Department of Mines and Energy, Geological Survey Branch*, p. 49-50.
- Feiss, P.G., Vance, R.K., and Wesolowski, D.J., 1993, Volcanic rock-hosted gold and base-metal mineralization associated with Neoproterozoic-Early Paleozoic back-arc extension in the Carolina terrane, southern Appalachian Piedmont: *Geology*, v. 21, p. 439-442.
- Hedenquist, J.W., Matsuhisa, Y., Izawa, E., White, N.C., Giggenbach, W.F., and Aoki, M., 1994, *Geology, geochemistry and origin of high sulfidation Cu-Au mineralization in*



- the Nansatsu district, Japan: *Economic Geology*, v. 89, p. 1-30.
- Keppie, J.D., and Dallmeyer, R.D., 1989, Tectonic map of Pre-Mesozoic terranes in Circum-Atlantic Phanerozoic orogens. Nova Scotia Department of Natural Resources, Halifax, scale 1:5000000.
- Kilbourne, M.W., 1985, Nature and significance of the quartz-andalusite-pyrophyllite zone Chetwynd gold prospect, southwestern Newfoundland. Unpublished B.Sc thesis, University of Western Ontario, London. 73p.
- McKenzie, C.B., 1986, Geology and mineralization of the Chetwynd deposit, southwestern Newfoundland, Canada: In *Proceedings of Gold'86, an international symposium on the geology of gold*. (A.J. Macdonald, editor). Gold'86, Toronto, p. 137-148.
- Murphy, J.B., Keppie, J.D., Dostal, J., Waldron, J.W.F., and Cude, M.P., 1996, Geochemical and isotopic characteristics of Early Silurian clastic sequences in Antigonish Highlands, Nova Scotia, Canada: constraints on the accretion of Avalonia in the Appalachian-Caledonide Orogen. *Canadian Journal of Earth Sciences*, V. 33, p. 379-388.
- O'Brien, B.H., O'Brien, S.J., and Dunning, G.R., 1991, Silurian cover, Late Precambrian-Early Ordovician basement, and the chronology of Silurian orogenesis in the Hermitage Flexure (Newfoundland Appalachians): *American Journal of Science*, v. 291, p. 760-799.
- O'Brien, S.J., Dubé, B., and O'Driscoll, C.F., 1996, The regional setting of gold mineralization in Neoproterozoic Avalonian rocks of the Newfoundland Appalachians. In *Report of Activities, Newfoundland Department of Mines and Energy, Geological Survey Branch*, p. 19-23.
- Panteleyev, A., 1996: Epithermal Au-Ag-Cu: High Sulphidation; in *Selected British Columbia Mineral Deposit Profiles, Volume 2 - Metallic Deposits*, D.V. Lefebvre and T. Hoy, Editors, British Columbia Ministry of Investment and Employment, Open File 1996-13, pages 37-39.
- Ririe, G.T., 1990, A comparison of alteration assemblages associated with Archean gold deposits in Western Australia and Paleozoic gold deposits in the southeast United States: *Canadian Journal of Earth Sciences*, v. 27, p. 1560-1576.
- Robert, F., Poulsen, K.H., and Dubé, B., 1997, Gold deposits and their geological classification. In Gubins, A.G., (ed), *Proceedings of Exploration 97: Fourth Decennial International Conference on Mineral Exploration*, Toronto septembre 1997. GEO F/X, pp 209-219.
- Romberger, S.B., 1986, Disseminated gold deposits: *Geoscience Canada*, v. 13, p. 23-34.
- Sillitoe, R.H., 1989, Gold deposits in Western Pacific Island Arcs: The magmatic connection: *Economic Geology Monograph 6*: "The geology of gold deposits: the perspective in 1988". pp. 274-291.
- Sillitoe, R.H., 1991, Intrusion-related gold deposits, in Foster, R.P., ed., *Gold Metallogeny and Exploration*: London, Blackie, p. 165-209.
- Sillitoe, R.H., Hannington, M.D., and Thompson, J.F., 1996, High sulfidation deposits in the volcanogenic massive sulfide environment: *Economic Geology*, vol. 91, pp. 204-212.
- Spence, W.H., Worthington, J.E., Jones, E.M., and Kiff, I.T., 1980, Origin of the gold mineralization at the Haile mine, Lancaster County, South Carolina: *Mining Engineering*, v. 32, p. 70-73.

Stewart, P.W., 1992, The origin of the Hope Brook Mines, Newfoundland: a shear-zone-hosted acid sulfate gold deposit. Unpublished Ph.D thesis, University of Western Ontario, 398p.

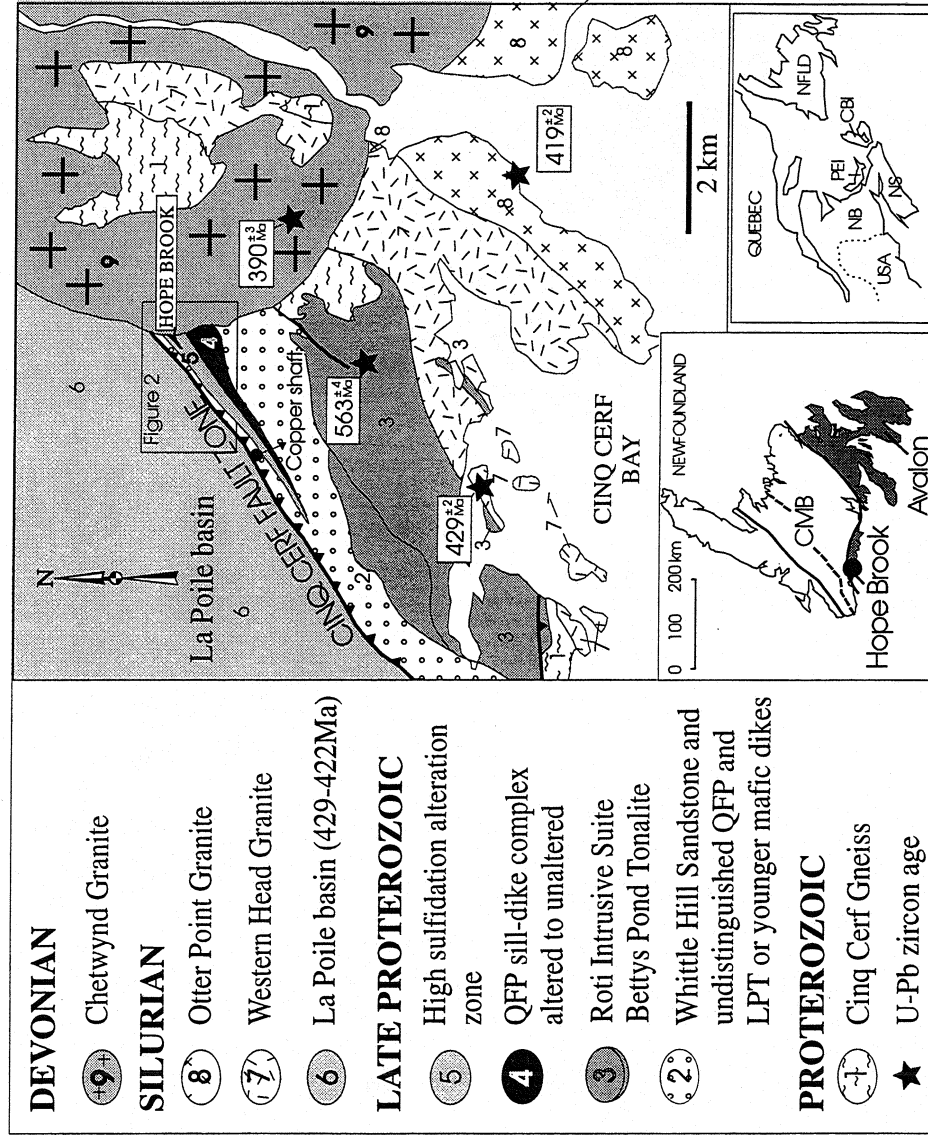
Swinden, H.S., 1984, The Chetwynd prospect, Southwestern Newfoundland. Mineral Development Division, Department of Mines and Energy, Government of Newfoundland and Labrador. Open File (11O/09/148). 10p.

Thompson, J.F.H., Lessman, J., and Thompson, A.J.B., 1986, The Temora gold-silver deposit: A newly recognized style of high sulfur mineralization in the lower Paleozoic of Australia: *Economic Geology*, v. 81, p. 732-738.

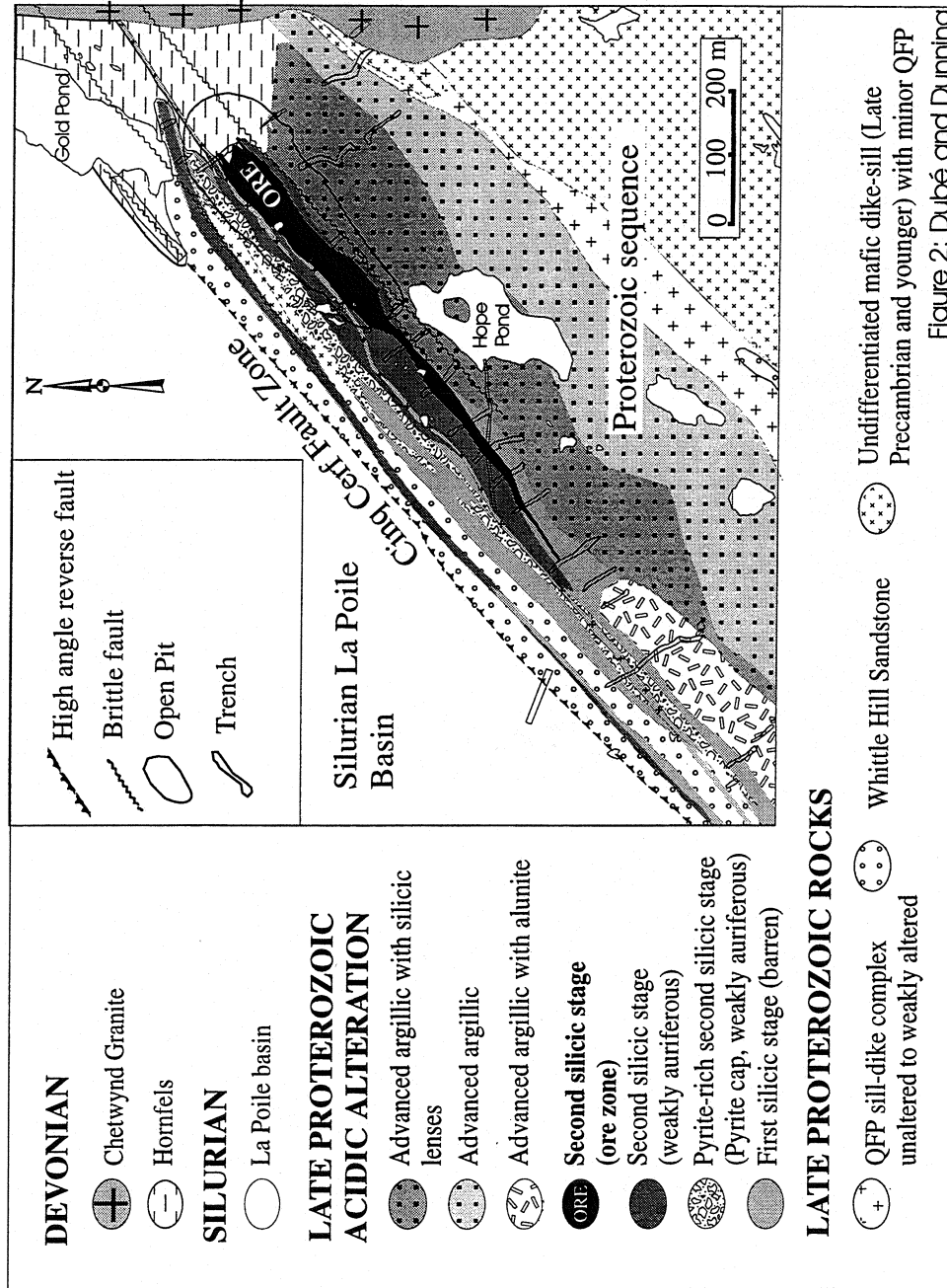
White, N.C., and Hedenquist, J.W., 1995, Epithermal gold deposits: styles, characteristics and exploration: *Society of Economic Geologists Newsletter*, No. 23, p. 1, 9-13.

Yule, A., McKenzie, C., and Zentilli, M., 1990, Hope Brook: a new Appalachian gold deposit in Newfoundland, Canada, and the significance of hydrothermally altered mafic dykes: *Chronique de la Recherche Minière*, no 498, p. 29-42.

Zwaschka, M., and Scheetz, J.W., 1995, Detailed geology of the Brewer Gold Mine, Jefferson, South Carolina: *Society of Economic Geologists, Guidebook Series V*. 24, p. 95-141.



D-10



# Late Paleozoic reconstruction of the circum-North Atlantic area

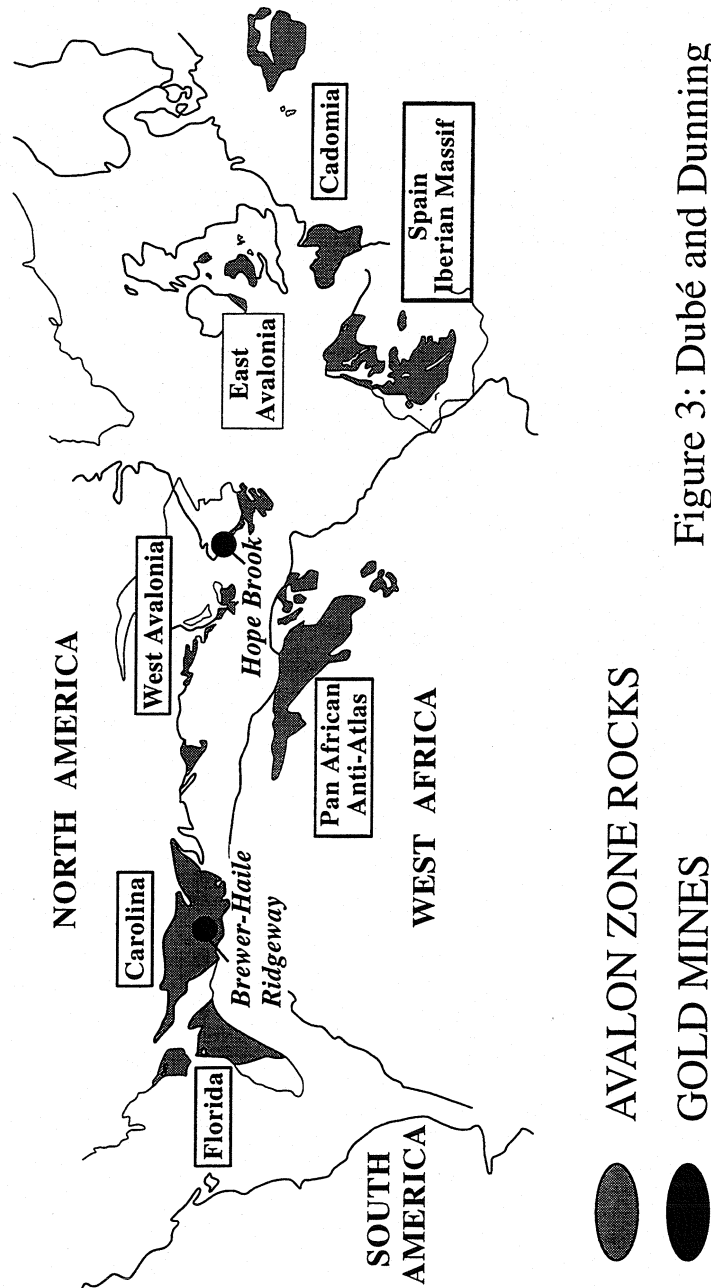


Figure 3: Dubé and Dunning

## E -TRANSITIONS FROM PORPHYRY TO EPITHERMAL ENVIRONMENTS

Andre Panteleyev, XDM Geological Consultants Inc.

A. Panteleyev (1998): Transitions from Porphyry to Epithermal Environments; in Metallogeny of Volcanic Arcs, B.C. Geological Survey, Short Course Notes, Open File 1998-8, Section E.

### ABSTRACTS

Transitions from high level magmatic to hydrothermal conditions account for a variety of mineralization styles. Henley (1990) noted: 'magmatic vapour from crystallizing plutons is critical to (mineralization in) the epithermal environment much as described for porphyry copper-molybdenum-gold deposits' and 'in volcanic terrains the distinction of epithermal from porphyry-type environments of mineralization becomes largely one of convenience for exploration than one of reality'. The recognition that epithermal mineralization occurs in shallow parts of porphyry systems has been known for many years. The high-sulphidation epithermal deposits are generally considered to be intrusion-related. Low-sulphidation deposits are less convincingly so and, if intrusions are present, the deposits tend to occur well away from them.

Lateral and vertical zoning of deposit types and metals centred on intrusive bodies, and their overlying stratovolcanoes, is amply documented. These relationships, and other related styles of mineralization, are particularly well documented in Southwestern Pacific and Andean magmatic arcs. The superimposition, blending and blurring of porphyry and epithermal characteristics can take place in volcano-plutonic arcs when "telescoping" of hydrothermal systems occurs. This is commonly evident as an overprinting of earlier mineralization by lower temperature, more oxidized, advanced argillic alteration assemblages. The telescoping that take place during the late life of the mineralizing hydrothermal systems is commonly due to rapid erosion of volcanic edifices by tropical weathering or glacial erosion, swift degradation of hydrothermally damaged volcanic structures, or cataclysmic decompressional events such as gravitational sector collapse.

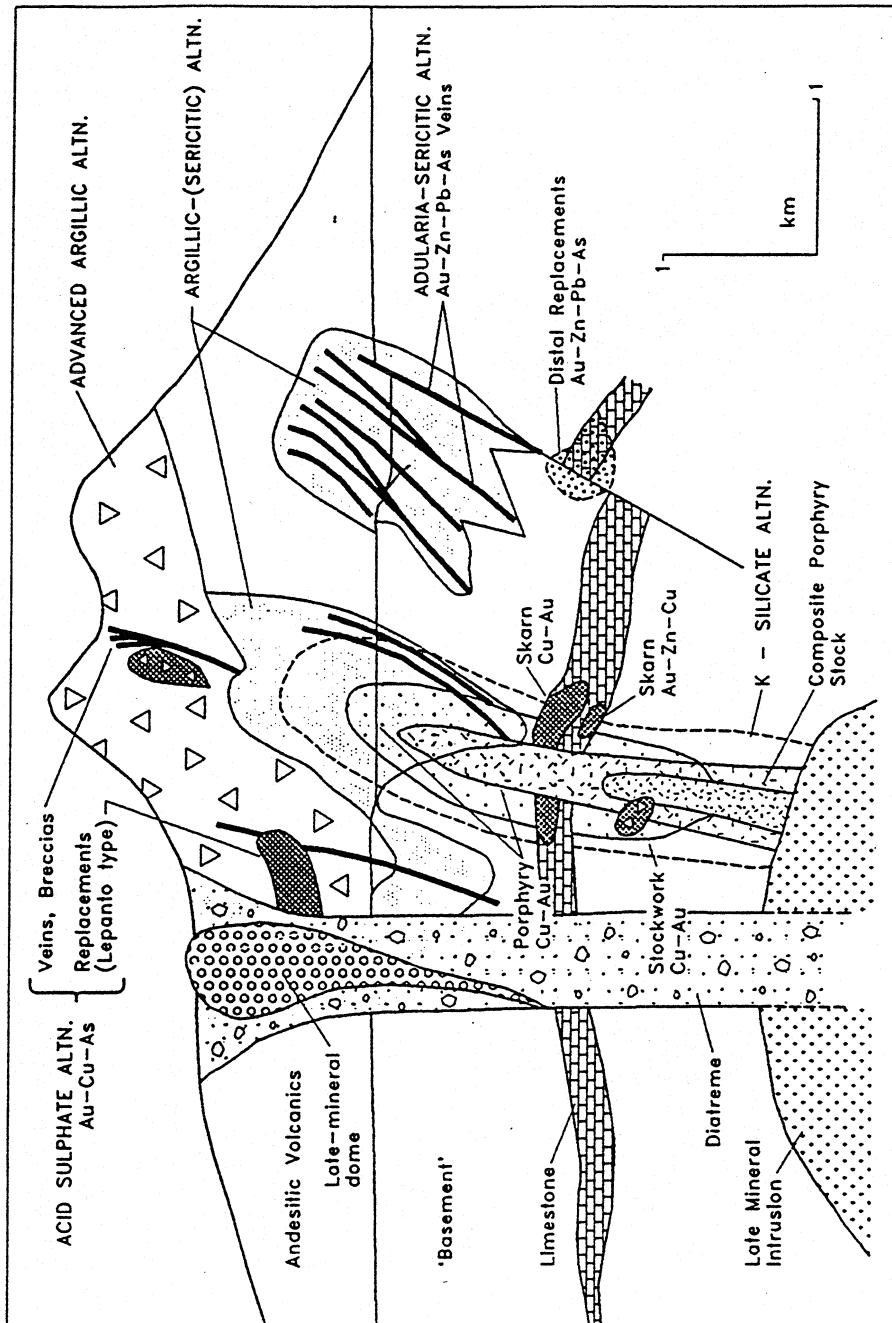
Transitional mineralization can be regarded to be a closely related variant of high-sulphidation systems. The mineralizations are genetically related in as much as the hydrothermal fluids involved are derived from the same, or similar intrusions. However, there are enough significant differences to warrant a separate identity for a 'transitional' deposit type. The high-sulphidation deposits have characteristic copper sulphide (covellite) and Cu-As-Sb minerals (tennantite-tetrahedrite, enargite-luzonite) and advanced argillic (acid sulphate) alteration derived from highly oxidized and highly acidic fluids. The transitional deposits can have similar alteration and mineralization as well but it is generally subordinate and restricted to late, localized acidic fluid flow. The dominant mineralization is by quartz-sericite-pyrite derived from less oxidized, neutral-pH to weakly acidic, relatively high temperature and pressure and highly saline solutions that are more akin to porphyry than epithermal deposits.

The main characteristics of transitional deposits are summarized as follows:

- Mineralization is intrusion-related; (subeconomic) porphyry copper-molybdenum deposits can occur nearby
- The intrusions are emplaced as high-level, subvolcanic stocks; coeval volcanic rocks may, or may not, be present. Quartz-feldspar porphyry domes and flow dome complexes can be mineralized in their interior parts but, overall, they most commonly host typical epithermal and vein deposits
- Cu-Au-Ag and/or Au-Ag ore is associated with polymetallic mineralization, typically with abundant As and Sb
- Pyrite is the dominant sulphide mineral. Chalcopyrite, tetrahedrite/tennantite are common, enargite is rare or absent
- Structural and lithologic permeabilities are the main ore controls
- Sulphide minerals are present in stockworks, veins, breccias and local massive replacement to disseminated zones. The ore stockworks and vein sets are composed of sulphide-bearing fractures; they contain only minor quartz
- Quartz-sericite-pyrite is the dominant alteration, mainly as a pervasive replacement of the ore hostrocks. Advanced argillic alteration forms a locally developed overprint with pervasive kaolinite and veins with quartz-alunite-(jarosite) assemblages. Higher-temperature zones contain andalusite, pyrophyllite, zunyite, diaspore and rare corundum; tourmaline is abundant in some deposits. Propylitic alteration is widespread in the hostrocks surrounding the ore zones
- Vertical zoning is evident and lateral zoning of ore metals may be developed in deposits. From shallow to greater depth there is a progression from Au, Ag with increasing Cu, Zn and Pb, locally Mo, Bi and W and, rarely, Sn
- Mineralization is related to 'robust' high temperature and relatively high pressure fluids emanating from porphyritic intrusions. The ore solutions are highly saline, moderately oxidized and less-acidic than those in high-sulphidation epithermal deposits

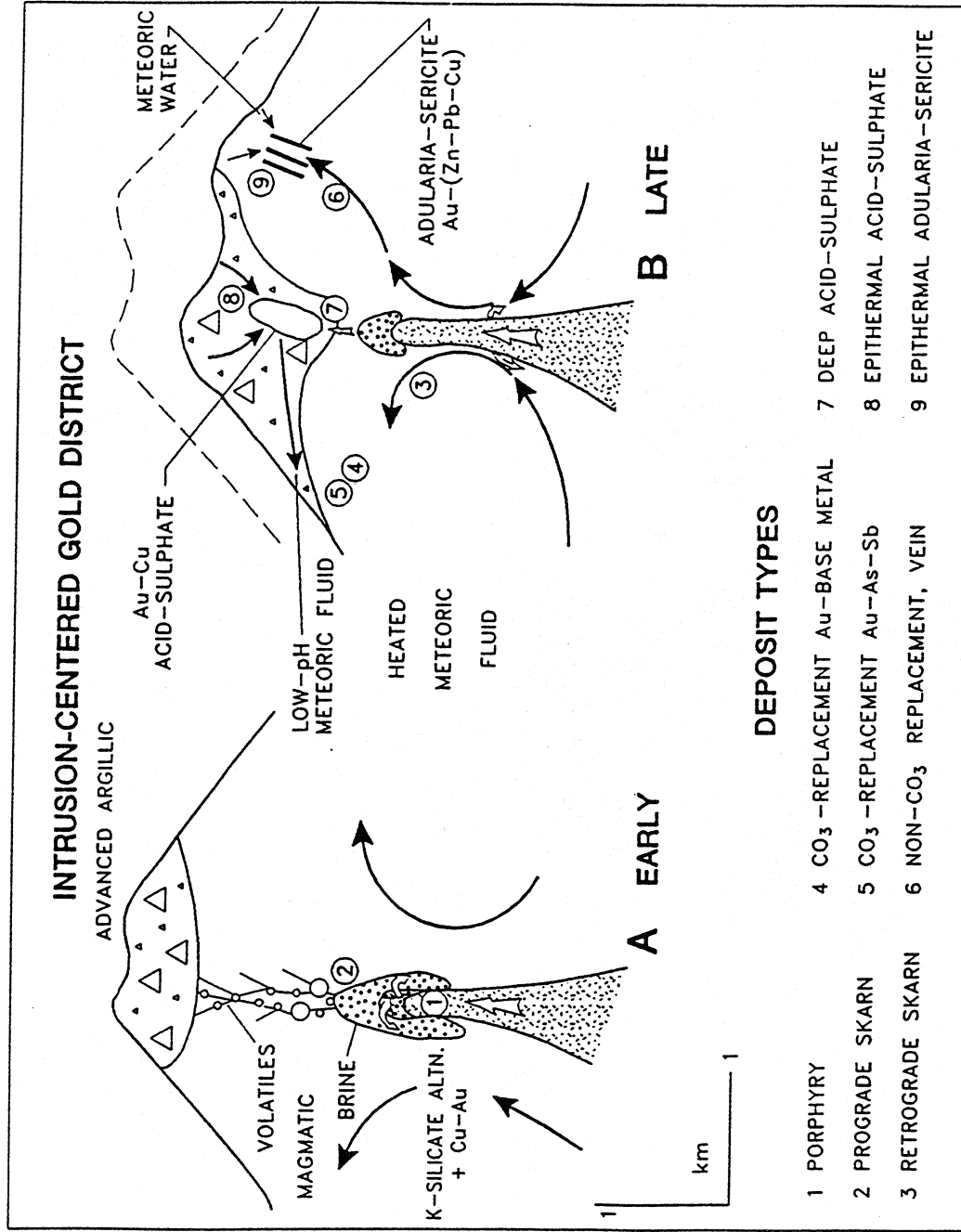
Deposits that will be discussed to exemplify this deposit type are the Kori Kollo mine, Bolivia, and Equity Silver mine, British Columbia.

Linkages between porphyry and epithermal deposits (and probably even Carlin-type jasperoid Au-Ag ores) are now recognized, but are poorly documented. In order to fully define an intrusion-related transitional deposit type, detailed geological deposit studies and careful investigations of alteration, ore and hostrock geochemistry, fluid inclusions and isotopes need to be conducted.



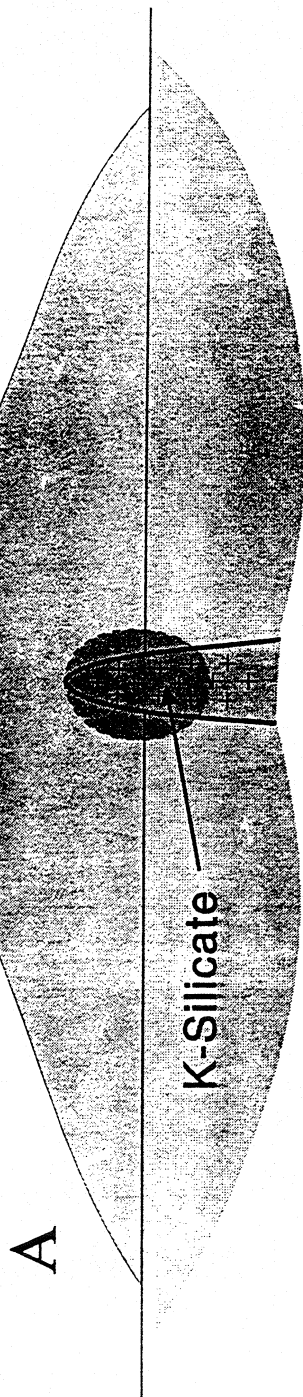
Mineralization in volcano-plutonic arc environments, from Sillitoe (1989, 1991a). The presence in any one deposit of all styles of mineralization is not implied. Environments depicted are transitional upwards from porphyry copper-type to epithermal. Most mineralization typically takes place at depths 1 to 3 km below the paleosurface.





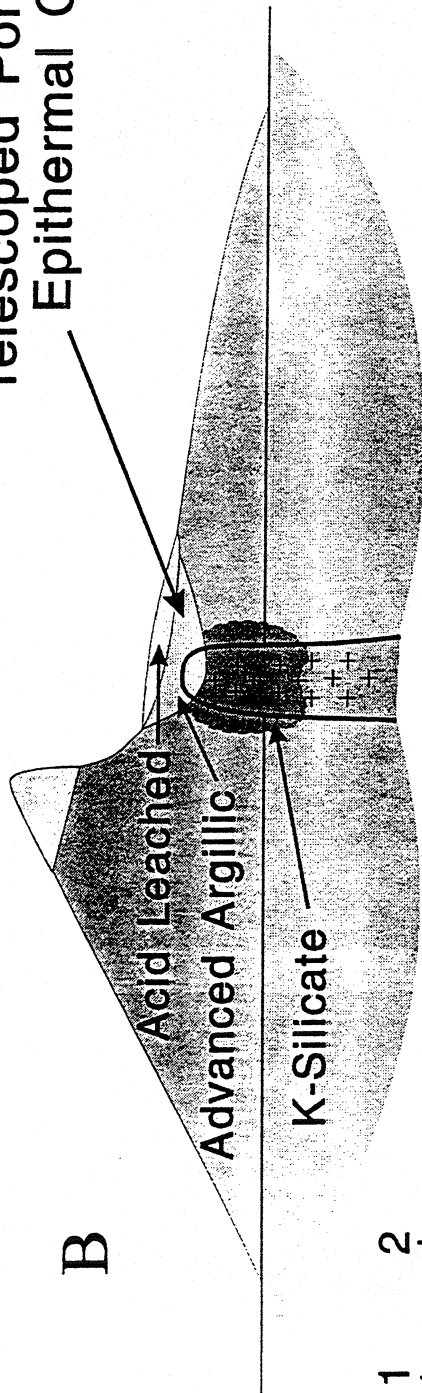
Model for an intrusive-centred gold district, after Sillitoe (1989, 1991). Stippling shows area of magmatic, low salinity two-phase vapour plume with surrounding groundwater system, after Henley and McNabb, 1978. Note that the lapsed time from early to late hydrothermal activity (A to B) is adequate for volcanic collapse and much erosion to take place, especially in island arc environments and late-stage near-surface mineralization may overlap early-stage deep mineralization within a single mineralizing system. The distinctions between hypogene and supergene processes may be indistinct.

Acid Leached  
Advanced Argillic  
Porphyry - Advanced argillic  
(high-sulphidation)  
Separation



0  
1  
2  
km

Telescoped Porphyry -  
Epithermal Gold

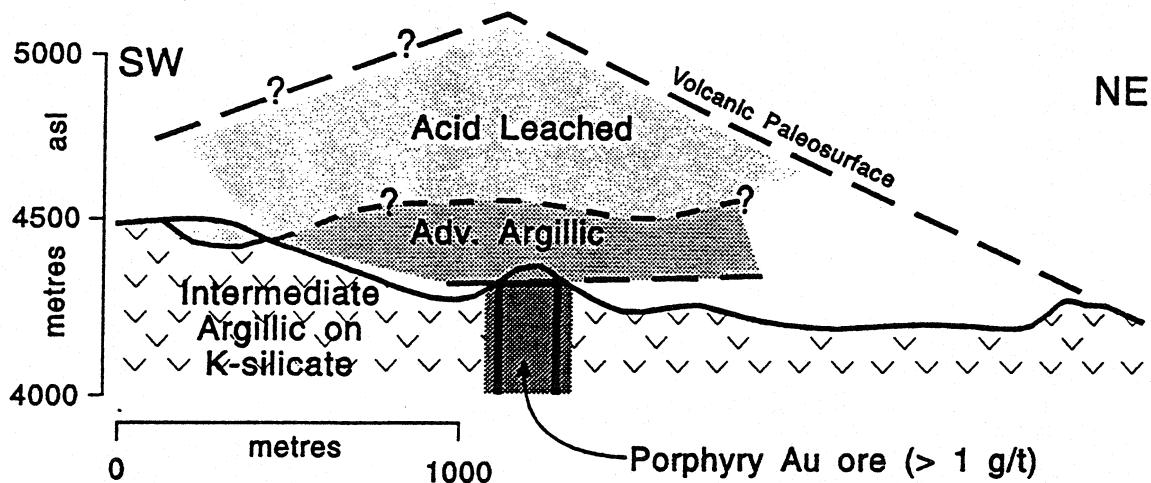


0  
1  
2  
km

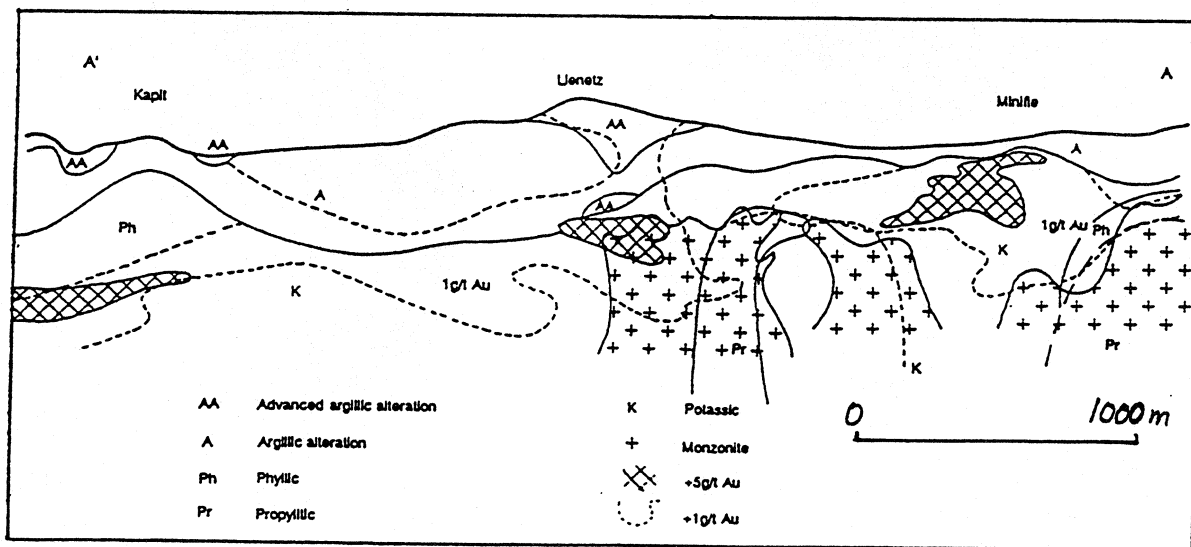
after Sillitoe 1994

E-9

# Marte, Chile



after Sillitoe, 1994



Ladolam deposit, Lihir Island. From Corbett and Leach (1995) after Moyle et al, (1990), in *Geology of the Mineral Deposits of Australia and Papua New Guinea*, Australian Institute of Mining and Metallurgy, pages 1793-1805.

## From Einaudi, 1993; MDRU Short course #14

Captions for Figures a, b, c (adjoining page) - El Salvador Porphyry Copper alteration, sulphide distribution and replacement reactions

**Fig. a.** Wall-rock alteration patterns at the El Salvador porphyry Cu deposit, Chile, based on Gustafson and Hunt (1975). Evolution of alteration is shown as a series of time frames from early (top), to late (middle), to very late (bottom). The early alteration is associated with intrusion of early porphyries and with most of the copper mineralisation. The late alteration is associated with and immediately post-dates the intrusion of Late porphyry. The very late alteration is associated with emplacement of latite dikes and pebble dikes. Arrows denote the presumed direction of hydrothermal fluid circulation, dominated by magmatic water at high temperatures in the early stages, deeply circulating meteoric water in the late stage, and a meteoric hot-spring system in the very late stage. Barbs on zonal boundaries point toward the minerals being replaced (e.g., biotite related to potassic alteration expands outward onto epidote-chlorite related to propylitic alteration in upper figure; sericite-quartz replaces minerals of the early potassic event in middle figure; and pyrophyllite of the advanced argillic assemblage replaces sericite during the very late event.

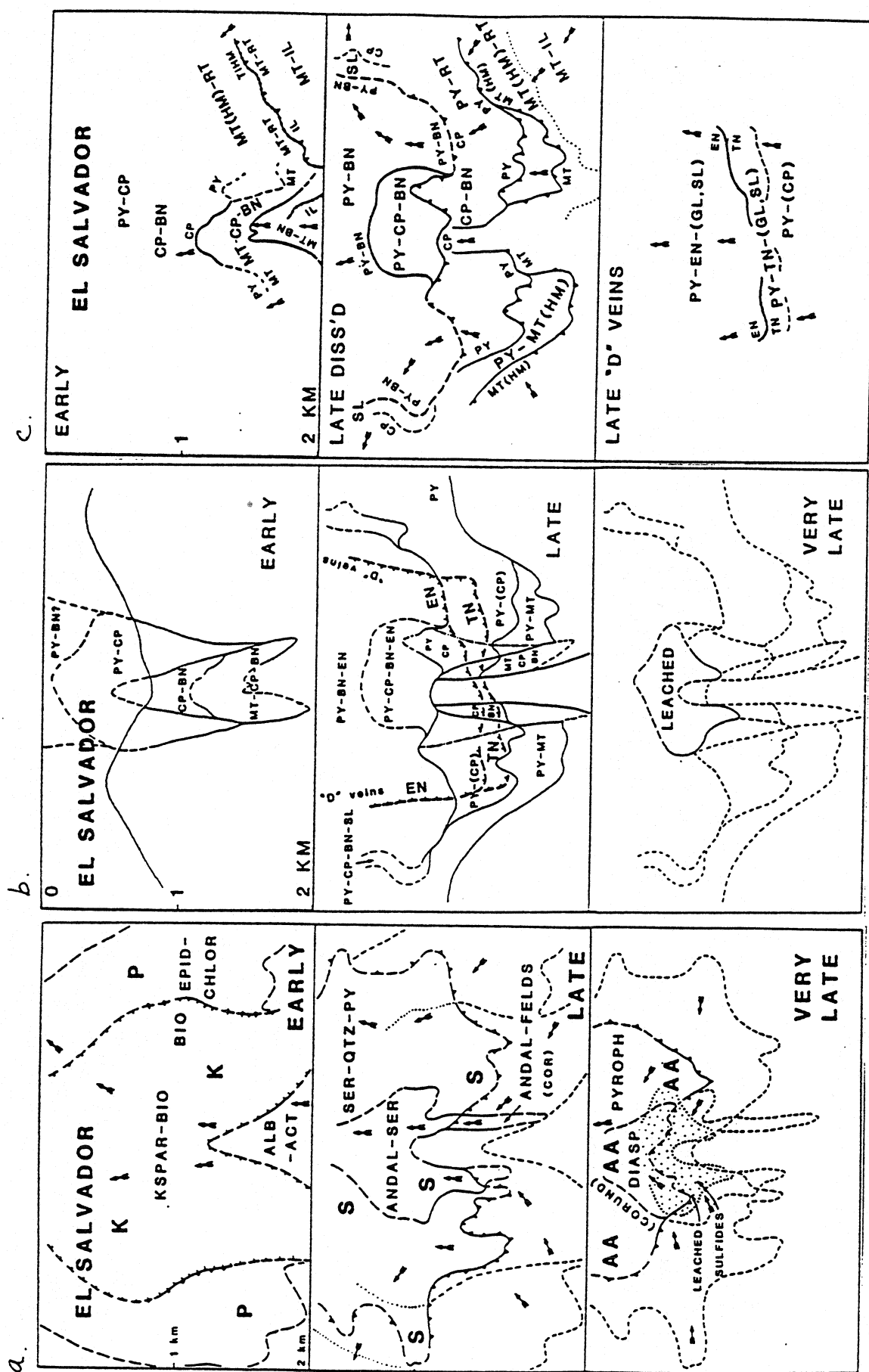
**Fig. b.** Patterns of sulfide distribution at the El Salvador porphyry Cu deposit, Chile, based on Gustafson and Hunt (1975). Compare with Fig. 3 for correlation of sulfide associations with wall-rock alteration. Broad zones of disseminated and veinlet sulfides are denoted by thin black lines; zones of vein sulfides (late "D" veins) shown by heavy dashed lines. Note vertical zoning within late D veins is from deep PY-TN to shallow PY-EN. The uppermost portion of the late pattern bears considerable resemblance to zoning of sulfides and wall-rock alteration at Butte, Montana, during Main Stage (see Fig. ), and at Magma, Arizona (see Fig.

**Fig. c.** Location of univariant sulfidation and sulfidation-oxidation reactions at El Salvador, Chile, based on Gustafson and Hunt (1975) and Gustafson (unpub'd data, 1980), as a function of time and space. Barbs on reaction lines point toward the mineral(s) being replaced (e.g., TiHM replaces MT-RT and MT-RT replaces IL in upper figure; PY-BN replaces CP in the middle figure). Arrows denote interpreted direction of hydrothermal fluid flow.

E-11

From Einaudi, 1993; MDRU Short course #14

E-12



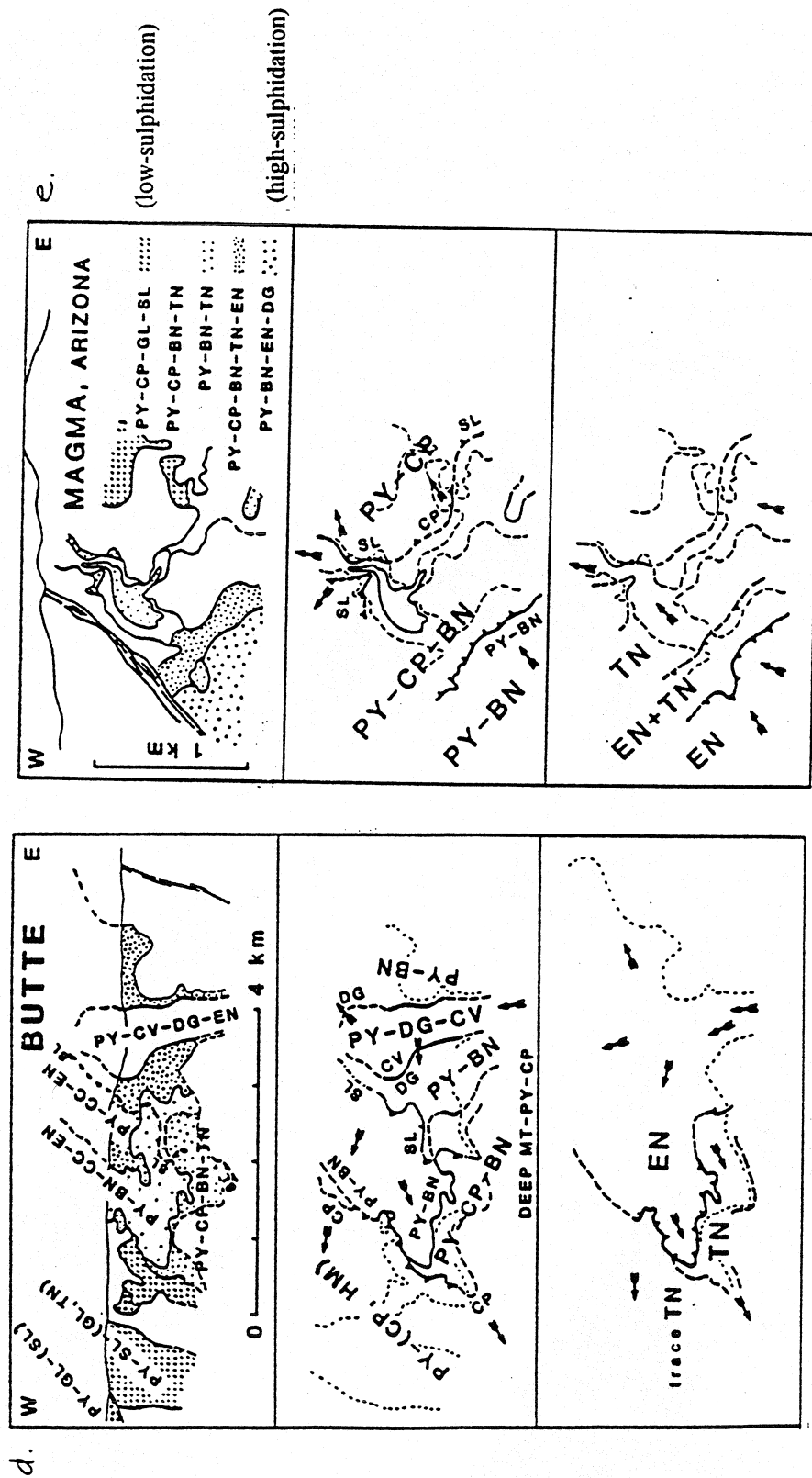


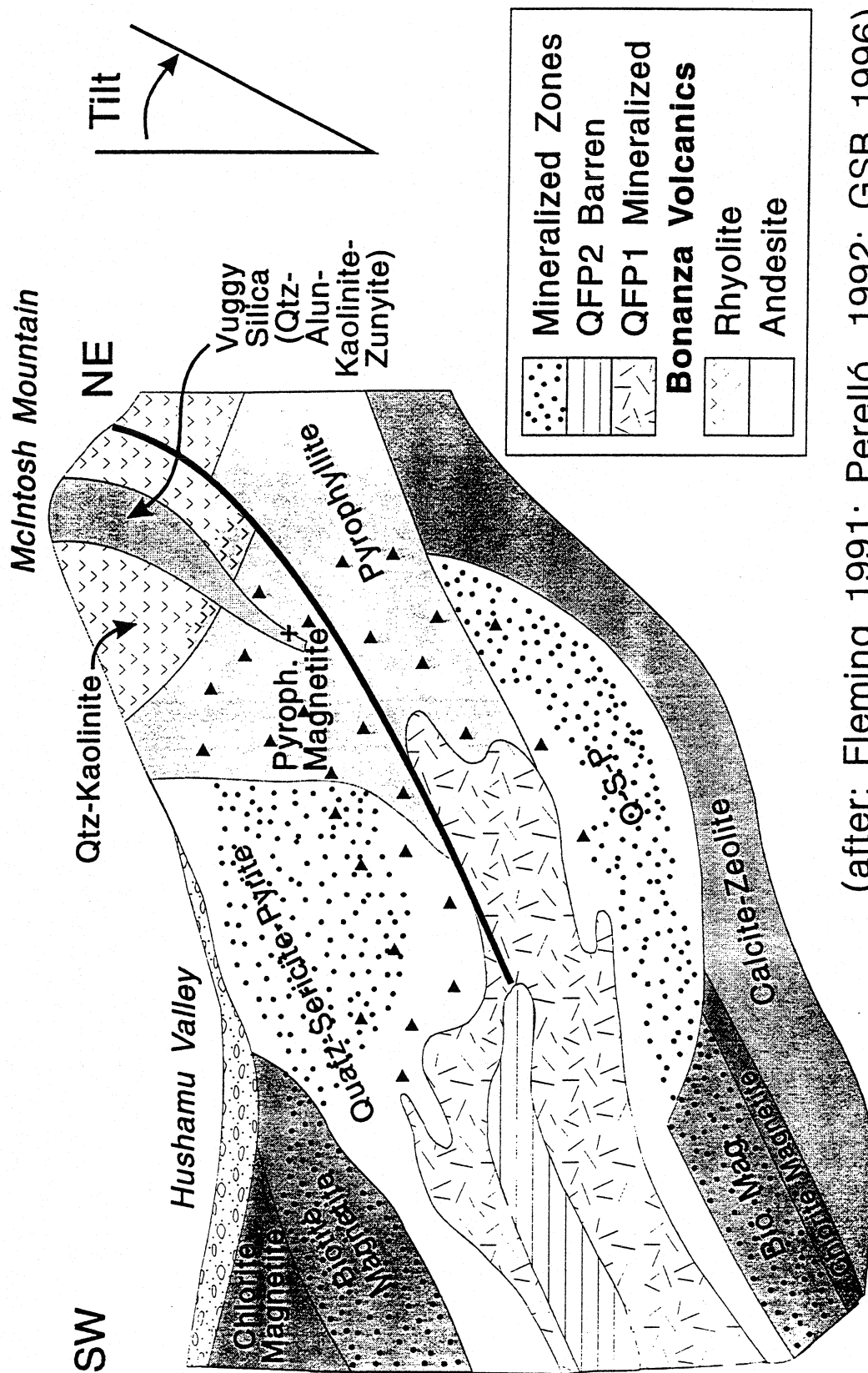
Figure d . Butte, Montana. Patterns of sulphide distribution during Main Stage mineralization, based on Proffett (1979). Upper figure shows the distribution of Cu-Fe-As sulphides in the intermediate and central zone (east side), and the location of the Pb-Zn-Ag peripheral zone (west side). Lower two figures show the location of univariant sulphidation reactions as a function of space; barbs point towards the mineral being replaced (e.g., Cu-Fe-sulphides replace sphalerite in middle figure; tennantite (TN) replaces enargite (EN) in lower figure). Arrows denote the interpreted direction of hydrothermal fluid circulation.

Figure e . Magma, Arizona. Patterns of sulphide distribution based on Gustafson (1961) and Hammer and Peterson (1968).

Fluid flow paths (arrows) are interpreted from sulphide replacement and cross-cutting relationships.

E-14

# Hushamu - Mt. McIntosh



(after: Fleming 1991; Perelló, 1992; GSB 1996)

**Porphyry Cu Overprints  
Structurally controlled, acidic fluids**

**Butte, Chuquicamata, Collahuasi  
[El Salvador, Ely, Bisbee, Yauricocha, Co. de Pasco, Tintic]**

**Porphyry Cu - Epithermal Transitions  
High and low sulphidation, jasperoid in CO<sub>3</sub> hostrocks  
Aldebaran, La Pepa, La Grande (Rosario), El Hueso;  
Baguio district - Kelly, Acupan; Lepanto  
PNG - Nena, Kabang; Ladolam (Lihir)  
Bor, Resck  
others**

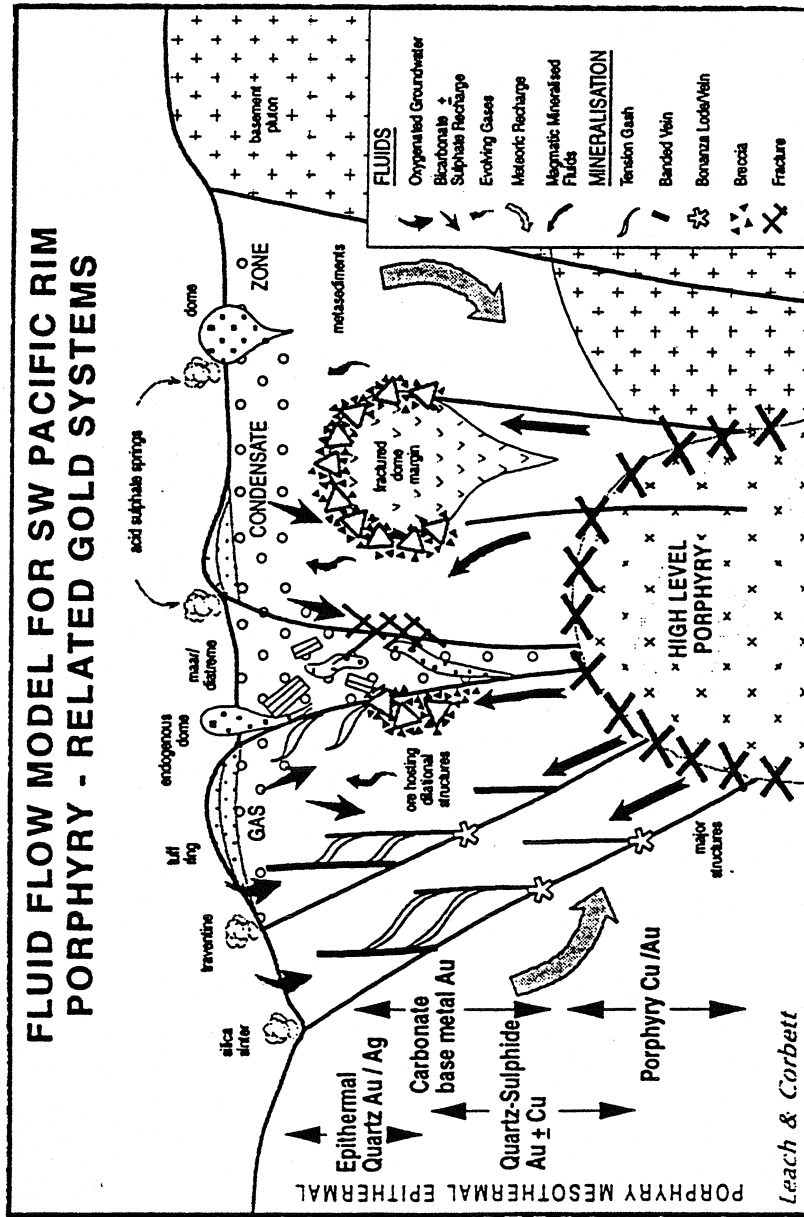
**From Einaudi, 1993; MDRU Short course #14**

**B.C. - Hushamu, Taseko, Equity Silver, Thorn**

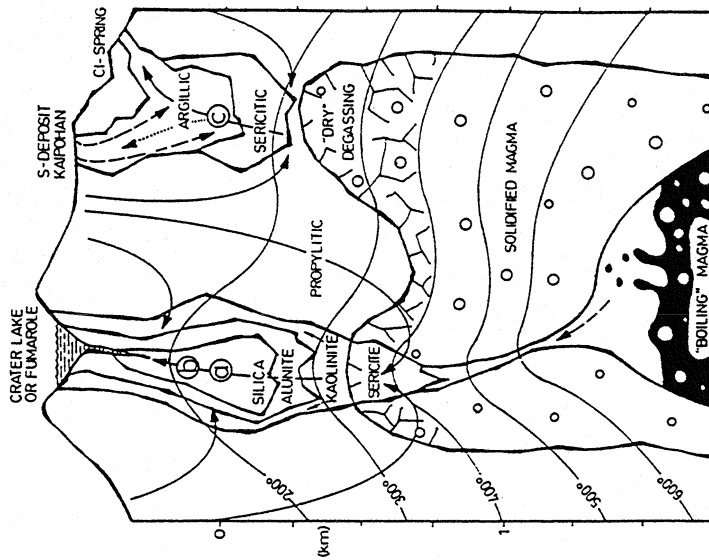
E-15



E-16



Fluid flow model, from Corbett and Leach, 1995. 'hot mineralized fluids evolve from cooling shallow level porphyry intrusives and rise along permeable zones provided by regional structures, diatreme margins or other lithological contacts such as feeder dykes or domes, or basement plutons. At depth, these fluids mix with circulating meteoric waters within splay or dilational structures and form gold mineralization. (in vein systems). .... gases evolving from the upwelling fluids form gas condensate zones at surficial levels and which are dominated by bicarbonate waters, with a minor acid sulphate component. Cycling of the hydrothermal system facilitates periodic descent of these cool, oxygenated, moderately low pH bicarbonate fluids deep into the hydrothermal system. ....'



Schematic models of hydrothermal systems responsible for the formation of "high sulfidation" (paths a and b) and "low sulfidation" (path c) epithermal mineral deposits. The low sulfidation system, on the right, is assumed to be situated on the flanks of a volcanic structure. The dotted line represents the path of gas-charged vapors, the dashed lines that of downward-percolating air-oxidized, acid sulfate waters.

From Gigganbach, 1992

## KORI KOLLO (Gold Hill) DEPOSIT, La Joya Mining District

42 km NW of Oruro, Bolivia

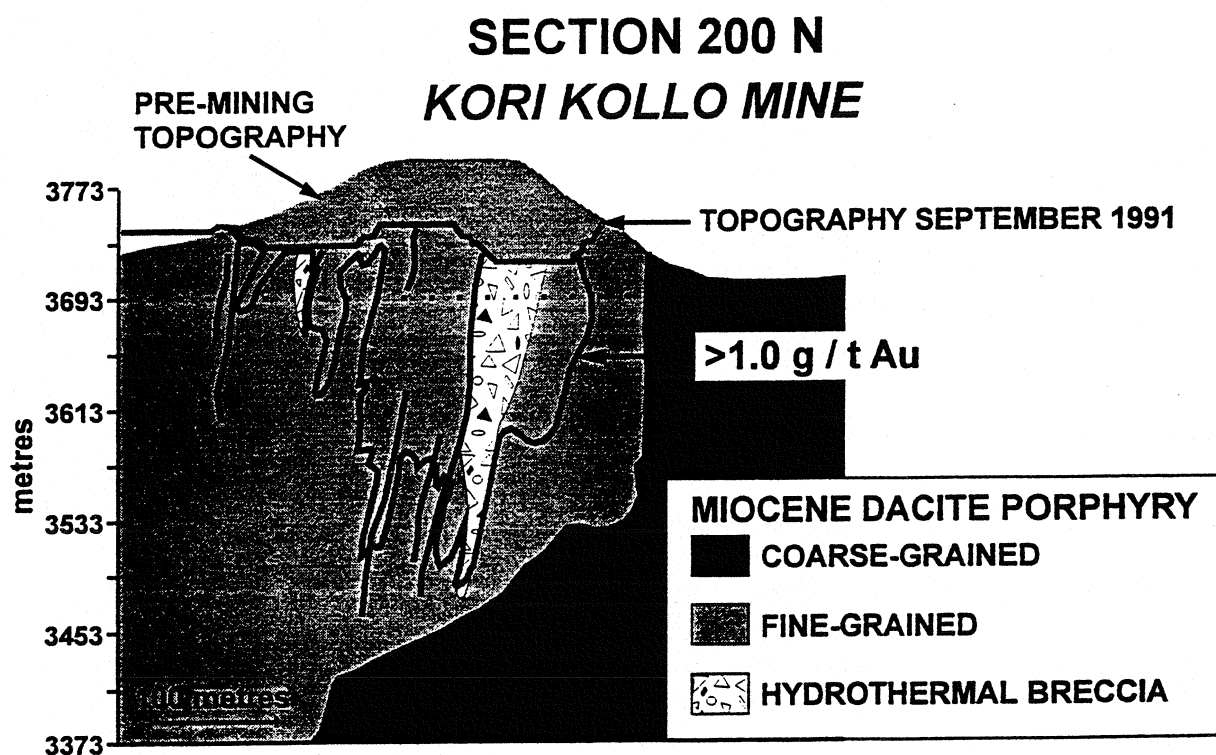
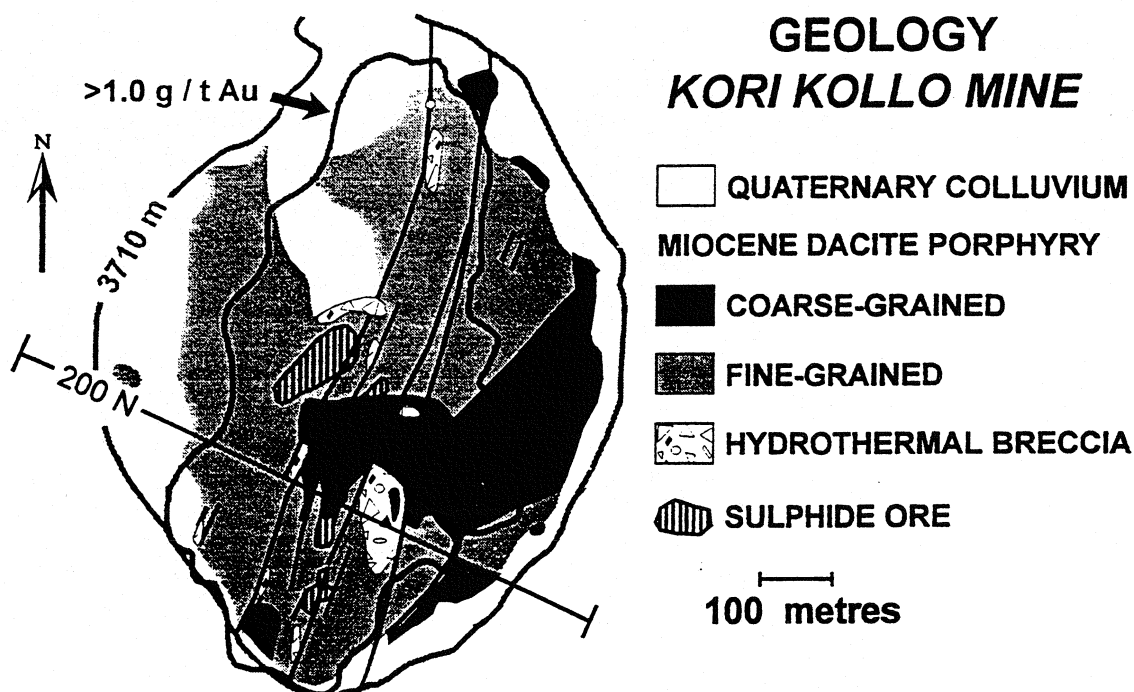
1700's	exploitation of veins around porphyry stocks for gold and copper
1960's	exploration adit, minor high-grading of breccia ore by local claim owners
1972	Canadian company (Prospection Ltd., and associates) sampled surface outcrops of porphyry and recognized widespread nature of mineralization; underground sampling of refractory sulphide ore in adit
1976 (1980?)	Empresa Minera Unificada (EMUSA) became involved
1982	Empresa Minera Inti Raymi S.A. founded
1983	estimated oxide reserves 9.4 mt @ 1.7 g/t Au, 25 g/t Ag. (The exploited oxide reserves were 10.1 mt @ 1.61 g/t and 24.7 g/t Ag [Sillitoe, 1995])

<u>Production</u>		<u>Ounces</u>
1985	production starts (heap leaching oxide ore)	5,176 oz
1986-87		26,910
1988-89	Battle Mtn. Gold Corp. (88% interest in 1995)	72,500
1990-91	Reserves 53.1 mt @ 2.32 g/t Au, 14.5 g/t Ag	98,478
1992	Oxide ore ends	53,852
1993	Sulphide 'refractory' ore starts @ us\$169/oz Cyanide/carbon in leach (CIL) process Sulphide reserves 59.2 mt @ 2.26 g/t Au (or 64 mt @ 2.26 g/t Au and 13.8 g/t Ag with 1.15 g/t cut-off [Sillitoe, 1995])	211, 037
1994		265,000
1995		339,000
1996		353,000 (estimated)
First 10-year (expected) production from sulphide ore	gold (79, 067 kg) silver (231,498 kg)	2,542,067 oz 7,442,315 oz

Recent exploration at Llallagua, near Kori Kollo - Nueva Esperanza deposit, by Battle Mountain (Aug. 14/'95 *Northern Miner*)  
oxide ore - 4.7 mt @ 1.26 g/t Au, 14.6 g/t Ag  
additional sulphide mineralization

### **Key References:**

1. Columba C., M. and Cunningham, C.G. (1993): Geologic Model For the Mineral Deposits of the La Joya District, Oruro, Bolivia; *Economic Geology*, Volume 88, pages 701-708.
2. Empresa Minera INTI RAYMI S.A. (1994):, 1994 Company Report
3. Long, K. R., Ludington, S., du Bray, E.A., André-Ramos, O and McKee, E.H. (1992): La Joya District, in *Geology and Mineral Resources of the Altiplano and Cordillera Occidental, Bolivia; U.S. Geological Survey, Bulletin 1975*, pages 131-236. (Same article is published in SEG Newsletter, Number 10, July 1992).
4. R.H. Sillitoe (1995): Exploration and Discovery of Base- and Precious Metal Deposits in the Circum-Pacific Region During the Last 25 Years; *Metal Mining Agency of Japan*, Special Report, 128 pages.



Source: Empresa Minera INTI RAYMI S.A, 1994 Report

# Geology and Mineralization at Equity Silver Mine

J.B. CYR, R.B. PEASE

*Equity Silver Mines Limited, P.O. Box 1450, Houston, British Columbia, V0J 1Z0*

AND T.G. SCHROETER

*British Columbia Ministry of Energy, Mines and Petroleum Resources, Bag 5000, Smithers, British Columbia V0J 2N0, Canada*

**in *Economic Geology* Volume 79, 1984, pages 947-968**

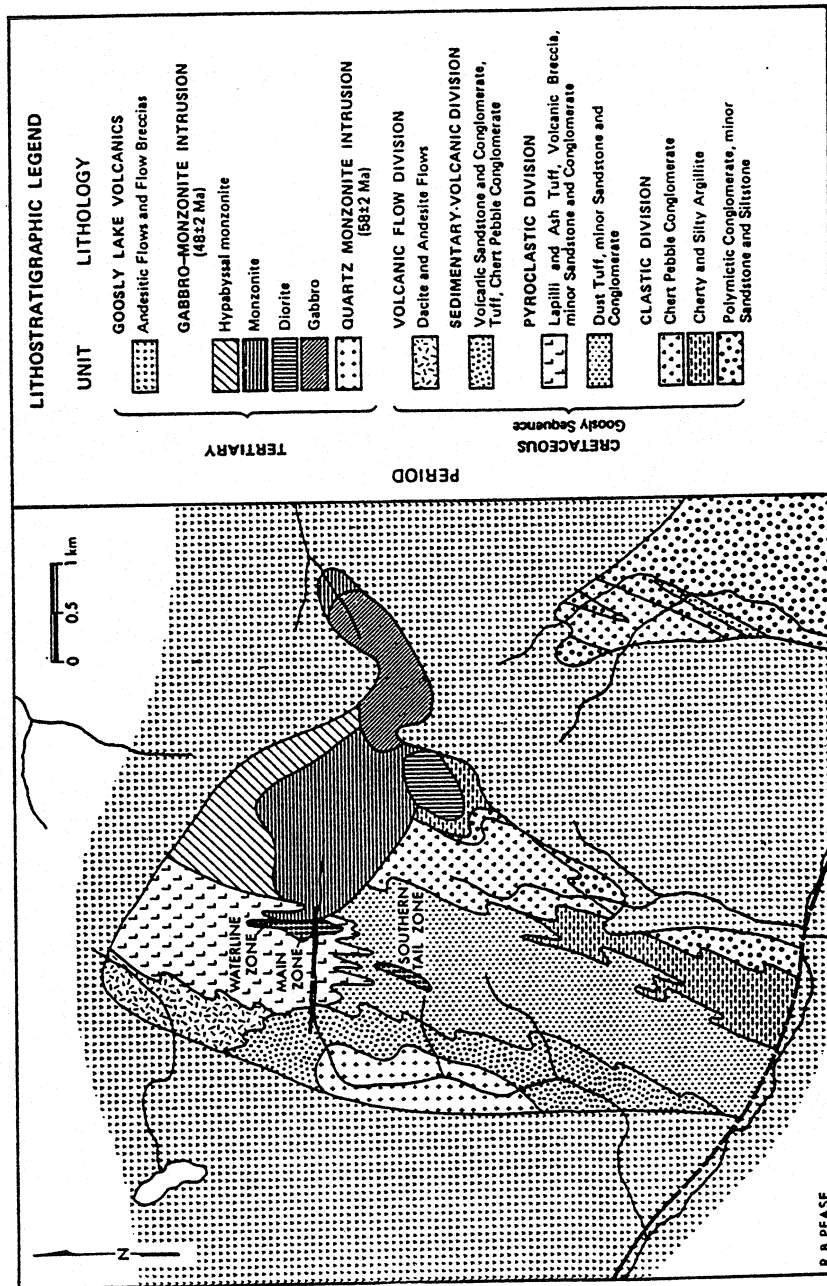
## Abstract

Equity Silver mine occurs in a homoclinal Upper Jurassic to Cretaceous inlier consisting of sedimentary, pyroclastic, and volcanic rocks plus intrusions overlain and surrounded by younger, unconformable Tertiary andesitic to basaltic flows and flow breccias. Four stratigraphic conformable subdivisions, termed the Goosly sequence, are recognized in the inlier and consist of a basal conglomerate and minor argillite (clastic division); intercalated subaerial tuffs breccias and minor reworked pyroclastic debris (pyroclastic division); interbedded volcanic conglomerate, sandstone, and tuff (sedimentary-volcanic division); and bedded andesitic to dacitic flows (volcanic flow division). A quartz monzonite stock with an approximate age of 58 m.y., and a gabbro-monzonite complex with an approximate age of 49 m.y. intrude the Goosly sequence. Postmineral andesitic and quartz latitic dikes with an approximate age of 49 m.y. crosscut the Goosly sequence and the gabbro-monzonite complex. Copper-silver-antimony sulfides and sulfosalts with associated gold occur as tabular zones with attitudes grossly conformable to the Goosly sequence. Sulfides were deposited as disseminations, open-space fracture fillings, veins, and crackle and breccia zones with an associated advanced argillic alteration suite including andalusite, corundum, pyrite, quartz, tourmaline, and scorzalite; they are believed to have developed at a high elevation in the porphyry system. Potassium-argon age dating indicates a main pulse of mineralization and hydrothermal alteration around 58 m.y. and a younger postmineral event at around 49 m.y.

Mining of the Southern Tail orebody commenced in April 1980 with a current mill feed rate of 5,400 metric tons/day. Production to December 1982 totaled 4.3 million metric tons of ore grading 135 g/metric ton Ag, 0.45 percent Cu, and 1.3 g/metric ton Au. Antimony and arsenic are leached from concentrate and recovered as by-products. The Main zone orebody, with reserves of 21.6 million metric tons grading 109 g/metric ton Ag, 0.35 percent Cu, and 0.85 g/metric ton Au, commenced production in late 1983. A smaller tonnage with similar grades is defined in the Waterline zone. Elsewhere, weak copper-molybdenum sulfides are associated with the quartz monzonite stock, and intense, irregularly distributed brecciation and tourmalinization with minor chalcopyrite, tetrahedrite, galena, and sphalerite occur in the northern part of the property, indicating that a mineralizing hydrothermal system was present in the proximity of known sulfide deposits.

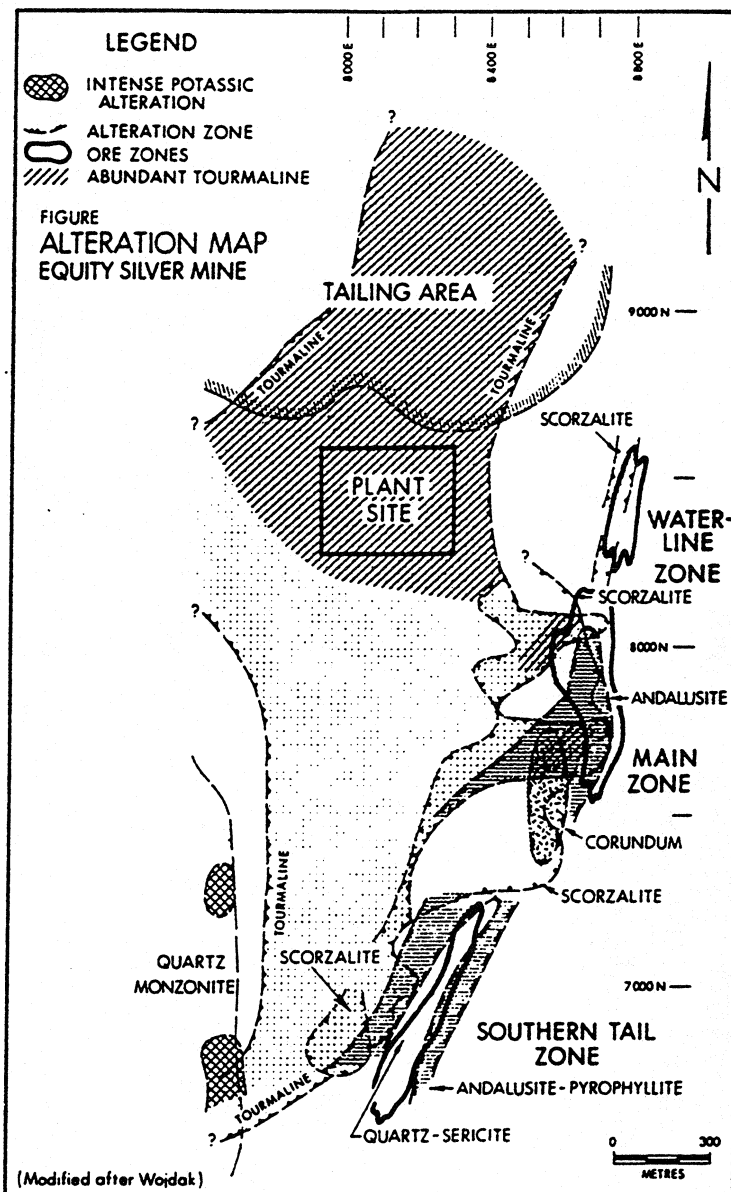
Alteration and mineralization are compatible with an advanced argillic alteration, possibly related to base leaching associated with fluid circulation at a high level in a developing porphyry system.

E20



Geologic setting of the Equity Silver mine.

From Cyr et al., 1984



Alteration map, Equity Silver mine.

From Cyr et al. (1984) after Wojdak, P.J. (1974): Alteration at the Sam Goosly Copper-Silver Deposit, British Columbia; Unpublished M.Sc. thesis, The University of British Columbia, 116 pages.

See also: Wojdak, P.J. and Sinclair, A.J. (1984): Equity Silver-Copper-Gold Deposit: Alteration and Fluid Inclusion Studies, *Economic Geology*, Volume 79, pages 969-990.

E-22

## Summary - Transitional Deposits

Setting: High-level stocks ('domes')

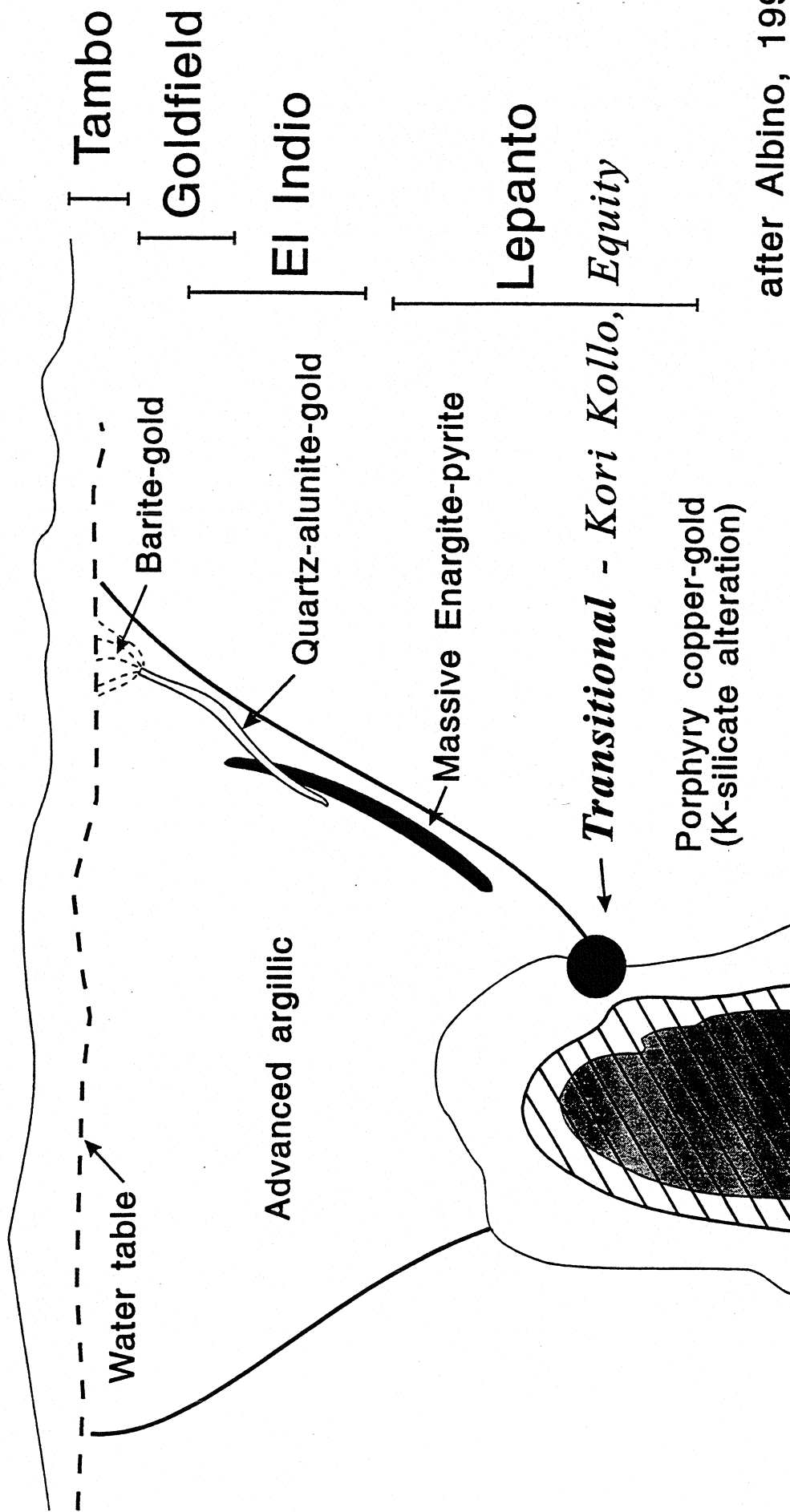
Alteration: QSP  $\pm$  tourmaline

Mineralization: polymetallic

\*Fluids: 'Robust' - high salinity, T, P

Long et.al. 1992    Re: La Joya (Kori Kollo)  
, ... these deposits did not form near the surface in a volcanic environment, but at considerable pressure and depth, in an environment more akin to that of porphyry copper deposits than to that of epithermal precious metal deposits.

# Porphyry Copper and Related Gold Deposits





## SELECTED REFERENCES

- Albino, G.V. (1994): Time-pH-fO<sub>2</sub> Paths of Hydrothermal Fluids and the Origin of Quartz-Alunite-Gold Deposits; *in* Advances in Research on Mineral Resources, U.S. Geological Survey, Bulletin 2081, pages 33-42.
- Arribas, Antonio Jr. (1995): Characteristics of High-sulphidation Epithermal Deposits, and Their relation to Magmatic Fluid; *in* Magmas, Fluids, and Ore Deposits, J.F.H. Thompson, Editor, *Mineralogical Association of Canada*, Short Course Volume 23, pages 419-454.
- Columba C. M. and Cunningham, C.G. (1993): Geologic Model for the Mineral Deposits of the La Joya District, Oruro, Bolivia; *Economic Geology*, Volume 88, pages 701-708.
- Corbett, G.J. and Leach, T.M. (1995): S.W. Pacific Rim Au/Cu Systems: Structure, Alteration and Mineralization; *Mineral Deposit Research Unit*, MDRU Short Course 17, 150 pages.
- Cyr, J.B., Pease, R.P. and Schroeter, T.G. (1984): Geology and Mineralization at Equity Silver Mine; *Economic Geology*, Volume 79, pages 947-968.
- Einaudi, M.T. (1993): Porphyry Cu Systems: Volcanic Roots?; *in* Volcanoes and Ore Deposits, *Mineral Deposit Research Unit*, MDRU Short Course 14, 62 pages.
- Giggenbach, W.F. (1992): Magma Degassing and Mineral Deposition in Hydrothermal Systems Along Convergent Plate Boundaries; *Economic Geology*, Volume 87, pages 1927-1944.
- Gustafson, L.B. and Hunt, J.P. (1975): The Porphyry Copper Deposit at El Salvador, Chile, *Economic Geology*, Volume 70, pages 875-912.
- Hedenquist, J.W. (1993): Environments of Volcanic-hosted Epithermal Mineralization: Recent Advances in Understanding the Variable Nature of Near-surface Hydrothermal Systems; *in* Volcanoes and Ore Deposits, *Mineral Deposit Research Unit*, MDRU Short Course 14, 31 pages.
- Hedenquist, J.W. (1995): The Ascent of Magmatic Fluids: Discharge Versus Mineralization; *in* Magmas, Fluids, and Ore Deposits, J.F.H. Thompson, Editor, *Mineralogical Association of Canada*, Short Course Volume 23, pages 263-289.
- Hedenquist, J.W. and Lowenstern, J.B. (1994): The Role of Magmas in the Formation of Hydrothermal Ore Deposits; *Nature*, Volume 370, pages 519-527.
- Hedenquist, J.W., Izawa, E., Arribas, A., Jr. and White, N.C. (1996): Epithermal Gold Deposits: Styles, Characteristics and Exploration; *Society of Resource Geology*, Special Publication number 1, wall poster with text and figures.
- Long, K. R., Ludington, S., du Bray, E.A., André-Ramos, O. and McKee, E.H. (1992): La Joya District, *in* Geology and Mineral Resources of the Altiplano and Cordillera Occidental, Bolivia; *U.S. Geological Survey*, Bulletin 1975, pages 131-236.
- Long, K. R., Ludington, S., du Bray, E.A., André-Ramos, O. and McKee, E.H. (1992): Geology and Mineral Deposits of the La Joya District, Bolivia; *Society of Economic Geologists*, SEG Newsletter, Number 10, July 1992.
- Panteleyev, A. (1991): Gold in the Canadian Cordillera - A Focus on Epithermal and Deeper Environments; *in* Ore Deposits, Tectonics and Metallogeny in the Canadian Cordillera, *B.C. Ministry of Energy, Mines and Petroleum Resources*, Paper 1991-4, pages 163-212.
- Sillitoe, R.H. (1989): Gold Deposits in Western Pacific Island Arcs: The Magmatic Connection; *in* The Geology of Gold Deposits: The Perspective in 1988; *Economic Geology*, Monograph 6, pages 274-292.

- Sillitoe, R.H. (1991): Intrusion-related Gold Deposits; *in* Gold Metallogeny and Exploration; R.P. Foster, Editor, *Blackie and Sons Ltd.*, pages 165-209.
- Sillitoe, R.H. (1992): The Porphyry-epithermal Transition; *in* Magmatic Contributions To Hydrothermal Systems, *Geological Survey of Japan*, Report No. 279, pages 156-160.
- Sillitoe, R.H. (1993): Epithermal Models: Genetic Types, Geometrical Controls and Shallow Features; *in* Mineral Deposit Modeling, *Geological Association of Canada*, Special Paper 40, pages 403-418.
- Sillitoe, R.H. (1994): Erosion and Collapse of Volcanoes: Causes of Telescoping in Intrusion-centered Ore Deposits; *Geology*, Volume 22, pages 945-948.
- Simmons, Stuart S. (1995): Magmatic Contributions To Low-sulphidation Epithermal Deposits; *in* Magmas, Fluids, and Ore Deposits, J.F.H. Thompson, Editor, *Mineralogical Association of Canada*, Short Course Volume 23, pages 455-477.
- White, N.C. and Hedenquist, J.W. (1990): Epithermal Environments and Styles of Mineralization: Variations and Their Causes, and Guidelines for Exploration, *Journal of Geochemical Exploration*, Volume 36, pages 445-474.
- White, N.C. and Hedenquist, J.W. (1995): Epithermal Gold Deposits: Styles, Characteristics and Exploration; *Society of Economic Geologists*, SEG Newsletter, Number 21, October 1995.
- White, N.C., Leake, M.J., McCaughey, S.N. and Parris, B.W. (1995): Epithermal Deposits of the Southwest Pacific; *Journal of Geochemical Exploration*, Volume 54, pp 87-136.

E26

## F - PORPHYRY DEPOSITS IN VOLCANIC ARCS WITH EMPHASIS ON THE CANADIAN CORDILLERA

W.J. McMillan, British Columbia Geological Survey

McMillan, W.J. (1998): Porphyry Deposits in Volcanic Arcs with Emphasis on the Canadian Cordillera; in Metallogeny of Volcanic Arcs, B.C. Geological Survey, Short Course Notes, Open File 1998-8, Section F.

See also, CIM Special Volume 46, Regional Geological and Tectonic Setting of Porphyry Deposits in British Columbia and Yukon Territory by W.J. McMillan, BC Ministry of Energy, Mines and Petroleum Resources; J.F.H. Thompson, MDRU, University of British Columbia and C.J.R. Hard and S.T. Johnston, Canada/Yukon Geoscience Office, Whitehorse, Yukon Territory

### ABSTRACT

Porphyry deposits commonly formed at convergent plate margins in volcanic arcs. They are related to the emplacement intermediate to felsic, hypabyssal, generally porphyritic intrusions. These large tonnage low grade mineral deposits have metal assemblages that may contain varying proportions of copper, molybdenum, gold and silver. Arc-related porphyry deposits, as exemplified by those in the Canadian Cordillera, occur in association with two distinctive calc-alkalic and alkalic intrusive suites. These deposits show the full range of morphological and depth relationships found in porphyry deposits worldwide. In addition, alkalic suite deposits, which are rare worldwide, are common; there are unusual, possibly syntectonic deposits (Gibraltar); and also end-member gold-rich granite-hosted deposits, such as Ft. Knox in Alaska.

In the Canadian Cordillera, porphyry deposits formed during two separate time periods: Late Triassic to Middle Jurassic (Early Mesozoic), and Late Cretaceous to Eocene (Mesozoic-Cenozoic). Most Early Mesozoic deposits occur in volcanic arc terranes, Wrangellia, Stikinia and Quesnellia, but one, Gibraltar occurs in the oceanic Cache Creek terrane. Like deposits in the southeast Pacific, most of the early Mesozoic Cordilleran porphyry deposits formed while the host terranes were located outboard from continental North America. Other deposits, formed during this early period may have been emplaced during terrane collisions. Metal assemblages in deposits of the calc-alkalic suite, with Cordilleran examples, include Mo-Cu (Brenda), Cu-Mo (Highland Valley, Gibraltar), and Cu-Mo-Au-Ag (Island Copper, Schaft Creek) and Cu-Au (Kemess, Kerr). Cordilleran alkalic suite deposits are restricted to the Early Mesozoic and display distinctive petrology, alteration and mineralization that suggest a similar tectonic setting for both Quesnellia and Stikinia in Early Jurassic time. These deposits are characterized by a Cu-Au assemblage (Copper Mountain, Afton-Ajax, Mt. Milligan, Mount Polley, Galore Creek).

Late Mesozoic to Cenozoic deposits in the Canadian Cordillera formed in an continental arc setting, after the terranes in which they occur had been accreted to the western margin of North America and are related to small stocks that intrude unrelated country rock. Individual deposits show a spectrum of metal associations Cu-Mo (Huckleberry, Berg), Cu-Au(-Mo) (Bell, Granisle, Fish Lake, Casino), Mo (Endako, Boss Mountain, Kitsault, Quartz Hill), Mo-W (Logtung), Au-W (Dublin Gulch) and Au (Ft. Knox). There may be a continuum between Mo, Mo-W, Au-Mo-W and Au deposits. The distribution and timing of these post-accretion deposits likely reflect major crustal structures and subduction geometry.

Porphyry mineralization is genetically related to plate tectonic processes and mineralization is episodic. Many deposits have clear linkages to subduction but the effects of collisional events also appear to have been important. The latest Triassic alkalic porphyry deposits of Stikinia illustrate this concept. Alkaline intrusions appear to be coeval with the tectonic hiatus may have resulted from collision of part of the Yukon-Tanana terrane with Stikinia. This event caused a lull in subduction, cessation of Triassic Stuhini Group volcanism, and at least local deformation of the Stuhini arc. Volcanism related to subsequent reactivation of subduction produced the Jurassic Hazelton arc. Other porphyry deposits that may have formed in response to collisional events include the Minto and Williams Creek deposits in Yukon Territory. These are controlled by brittle-ductile shear zones that formed during imbrication of the Yukon-Tanana terrane with oceanic strata of the Slide Mountain terrane along regional thrust faults. The Gibraltar deposits show similar structural features. Finally, the Mt. Milligan and Rossland area deposits also may be syn-collisional in timing.

**Cordilleran-Roundup/Pathways**  
**Short Course: Arc Related Mineral Deposits**

**Calc-Alkalic Porphyry Deposits With Emphasis on the Canadian Cordillera**

**January 1998**

**OPENING STATEMENT**

Porphyry deposits are intimately linked with subduction and consuming margin plate tectonic processes but occur in both island arc and continental arc settings

**TALK PLAN OUTLINE**

1. The importance of porphyry deposits
2. The tectonic settings of porphyry deposits
3. Types of porphyry deposits and their classification
4. Examples of various deposit types with emphasis on gold-bearing porphyry systems
6. Conclusion

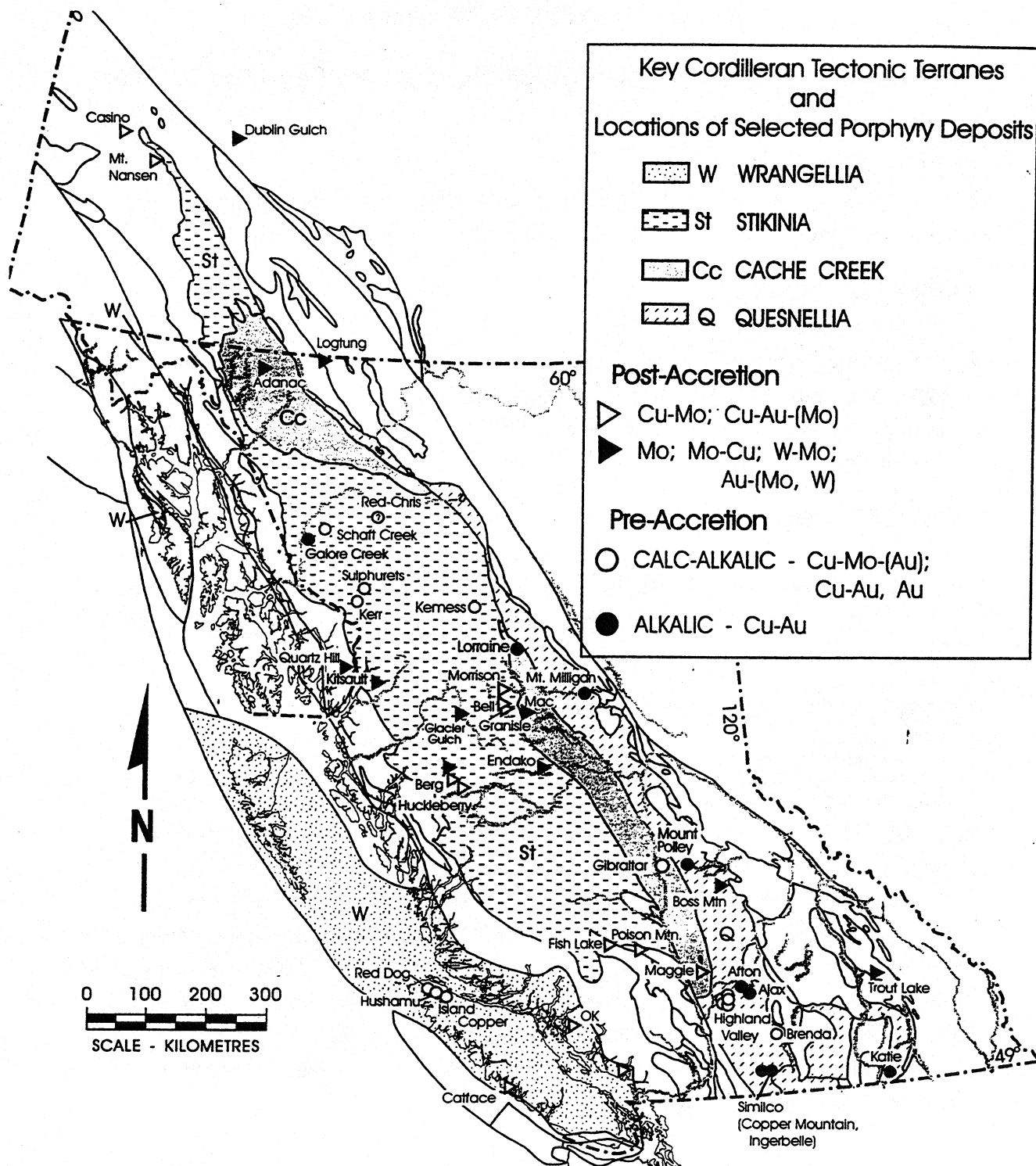
**INTRODUCTION**

I will only discuss calc-alkalic deposit types here and key on copper +/- molybdenum +/- gold porphyries, molybdenum porphyries and gold porphyries. Jim Lang, in the following presentation, will discuss alkalic varieties.

**ECONOMIC IMPORTANCE TO B.C.**

**Slide: ECONOMIC IMPORTANCE DIAGRAM**

During most of the twentieth century, copper has been the most important metal produced in British Columbia, and since the 1960s, it has come largely from porphyry deposits. Further, many of the porphyry copper deposits produced significant amounts of molybdenum, gold and silver. In addition, reserve statistics compiled by Schroeter and Lane (1991) indicate that more than 80 per cent of British Columbia's copper reserves and half the province's gold reserves were in porphyry deposits. About 90% of B.C.'s copper production each year is from porphyries; they also produce major amounts of gold and silver and account for all the molybdenum production. The value of production exceeded \$800 million last year. The province's mines are generally processing hypogene ore and grades in the 0.3 to 0.5% copper range are characteristic.



**FIGURE 2.** Locations of selected Cordilleran porphyry deposits in their tectonic settings. Key terranes are highlighted. Pre- and post-accretion deposits and their characteristic metal associations are distinguished.

## **TECTONIC SETTING OF PORPHYRY DEPOSITS IN THE CORDILLERA**

**Slide: Porphyry deposit locations and tectonic belts**

### **Elements of the Tectonic Evolution of the Canadian Cordillera**

Tectonic models describing the formation of the northwestern North American Cordillera have evolved dramatically from fixist geosynclinal belt models developed in the first part of the century to more recent models based upon the accretion of numerous disparate crustal fragments. Monger et al. (1972) argued that although rocks of the eastern Canadian Cordillera have ties to North America, the western Cordillera consists largely of island arc and oceanic assemblages that are generally allochthonous with respect to North America.

From a metallogenic perspective, we have long suspected that the early Mesozoic island-arcs of Stikinia and Quesnellia were correlative. Both pre- or syn-accretion calc-alkalic and the more unusual alkalic porphyry deposits occur in both terranes, and the host volcanic packages for the deposits are largely pyroxene-bearing basalts of similar age - the Nicola, Takla and Stuhini Groups (McMillan, 1991). These arcs began to form in Late Triassic (Carnian) time, and magmatism ended in Early Jurassic (Pleinsbachian-Toarcian) time in Quesnellia and in Middle Jurassic (Bajocian) time in Stikinia (Nelson, 1991). Similarly, new isotopic dating of mineral deposits confirms that deposits in the two terranes have nearly identical age ranges (Mortensen, 1995). However, Quesnellia and Stikinia now form parallel belts that are separated by the oceanic Cache Creek terrane, which contains equatorial fauna. Recent models have attempted to explain this relationship through either fault offset (Wernicke and Klepaki, 1988) or counter-clockwise rotation of Stikinia (Mihalynuk et al., 1994). Geochronology and field relationships presented by Nixon and others (1993) provide convincing constraints on the timing of final closure and accretion with North America at between 186 and 180 Ma. Despite variances in the tectonic interpretations, there is a degree of agreement that no significant accretion occurred prior to the late Early Jurassic. Hence porphyry deposits that were formed prior to this time in Quesnellia and other terranes to the west, Stikinia and Wrangellia, are termed pre- to syn-accretion and are inferred to have been generated in volcanic arcs that were outboard from ancestral North America. The post-180 Ma in Stikinia and Quesnellia and post-100 Ma porphyry deposits in Wrangellia formed are termed post-accretion deposits.

Although uncertainties in terrane accretion models remain, much of the debate now involves the timing of collisional events for different terranes in the mid-Jurassic to mid-Cretaceous period. For example, both paleomagnetic (Irving and others, 1980; Irving and Wynne, pers. Comm., 1994; and others) and fossil data (Tipper, 1984) indicate northward translation of some terranes in Middle to Late Cretaceous time. However, because



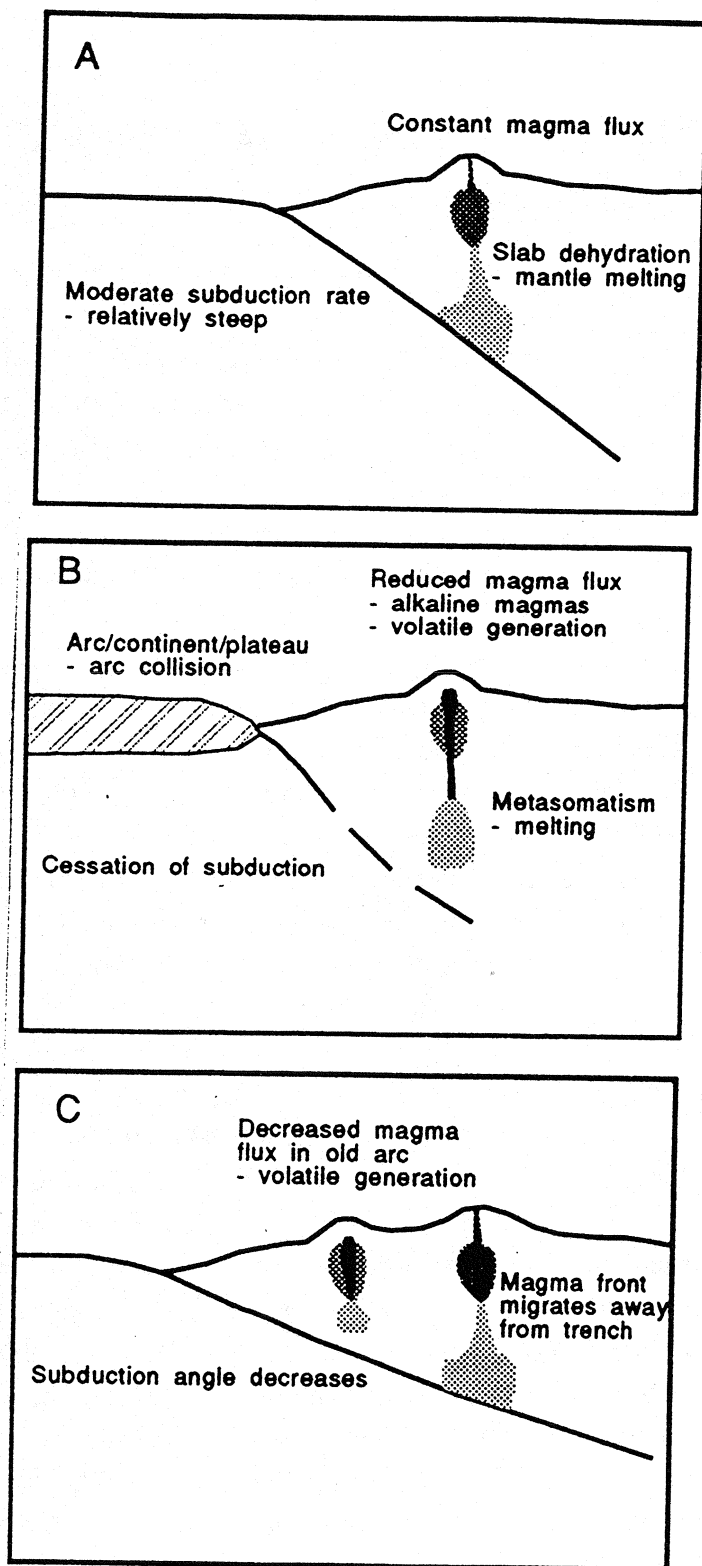


FIGURE 4. Three schematic cross-sections through convergent plate margins (not drawn to scale): (A) Constant tectonic processes and magma flux, conditions that may not be suited to the formation of porphyry deposits; (B) collision of an arc, continent or oceanic plateau with the active arc, resulting in cessation of subduction, slab melting, mantle metasomatism or hybridization and the formation of unusual (alkaline) magmas suited to the formation of gold-rich porphyry deposits (based on the model for the Tabar-Feni chain post-collision with the Ontong-Java plateau by McInnes and Cameron, 1994); (C) shallowing of the angle of subduction relative to A, possibly due to an increased rate of convergence or an approaching mid-ocean ridge in the subducting plate; active arc magmatism moves away from the trench, the magma flux in the old arc declines and large magma bodies fractionate, form volatile phases and associated mineralization (based on the model for central Chile by Skewes and Stern, 1994).

porphyry deposits formed mainly before or after this period, the division into pre- and post-accretion deposits is not affected by resolution of these debates. The general conclusion is that Mesozoic Cordilleran porphyry deposits formed in response to island arc processes that took place before their volcano-sedimentary host terranes accreted with North America, whereas the Late Cretaceous and Tertiary porphyry deposits formed after accretion.

### **INITIAL SR ISOTOPE DATA**

**Slides: Initial Sr ratio plots**

Initial strontium ratios from Early Jurassic and Early Tertiary granitic rocks in the Canadian Cordillera were plotted (Armstrong, 1988). Many porphyry-related plutons lie close to the line that marks intrusions with initial  $^{87}\text{Sr}/^{86}\text{Sr}$  values below 0.704, that is, I-type granites derived from the mantle or subducted oceanic crust. Thus porphyry deposits are virtually confined to areas where intrusions have primitive strontium ratios and are hosted by granitic rocks that show no signs of crustal contamination.

---

---

### **Subduction Processes Favoring Porphyry System Development**

**Slide: Thompson - Subduction rate and angle**

The diagram shows three hypothetical sections through a converging plate margin:

- A. constant tectonic processes and magma flux - no porphyries likely
- B. collision of an arc, continent or plateau with an active arc leads to cessation of subduction. This causes slab melting and mantle metasomatism. Conditions are right for alkaline magmas formation, volatile evolution and gold-rich porphyry mineralization (i.e. Tabar-Feni Chain after collision with the Ontong-Java plateau)
- C. shallowing of the subduction zone (relative to that in A) caused by increased rate of convergence, or approach of a mid-ocean ridge in the subducting plate. Leads to migration of the active arc magmatic front away from the trench, decline in the rate of magma flux in the old arc and fractionation in large bodies of magma that lead to volatile evolution and porphyry mineralization (i.e. central Chile)

**Message: mineralization reflects specific conditions within the magmatic cycle and specific conditions within the process of subduction.**

---

---

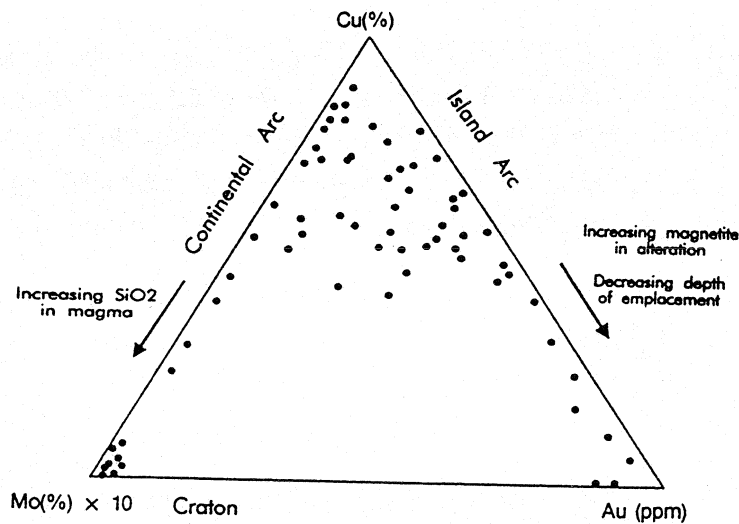


FIGURE 3. Plot of relative abundances of copper (in per cent), molybdenum (per cent  $\times 10$ ) and gold (in grams per tonne) for various porphyry deposits from around the world [after Cox and Singer (1988) and Sillitoe (1993)].

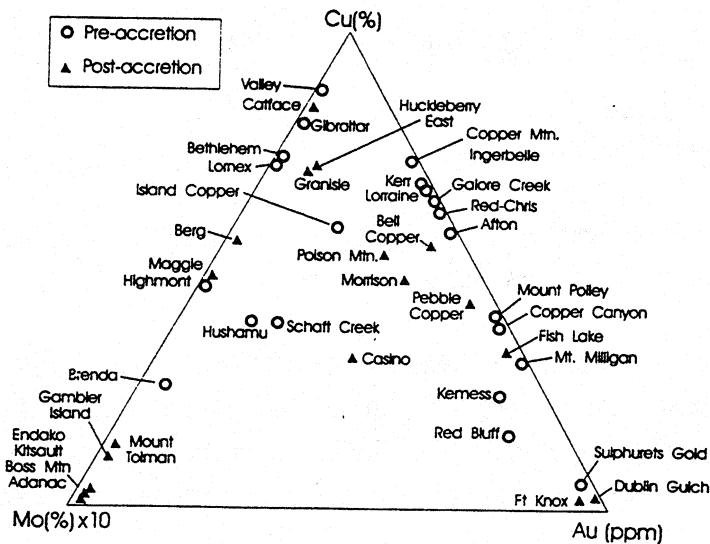


FIGURE 4. Plot of relative abundances of copper (in per cent), molybdenum (per cent  $\times 10$ ) and gold (in grams per tonne) for selected Cordilleran porphyry deposits. Pre- to syn- and post-accretion deposits are distinguished by open circles and filled triangles respectively. Data are plotted based on reported reserves, thus some non-economic quantities of copper, molybdenum or gold may have been omitted. Some data points would shift slightly if data were complete.

## **TYPES OF PORPHYRY DEPOSITS:**

### **CLASSIFICATION BY METAL SIGNATURES**

(Cu only; Cu-Mo; Cu-Au; Cu-Au-Mo; Mo-W; Au only)

### **Slide: CU-MO-AU TRIANGLE DIAGRAM - WORLD**

The spectrum of porphyry deposit types ranges from copper only, through copper-molybdenum, to copper-gold-molybdenum, to gold or molybdenum only. Generally, gold and molybdenum are negatively correlated, but Cox and Singer (1988) and Sillitoe (1991) documented transitional deposits. Cordilleran examples are Pebble, Island Copper and Poison Mountain.

### **Slide: CU-MO-AU TRIANGLE DIAGRAM - CORDILLERA**

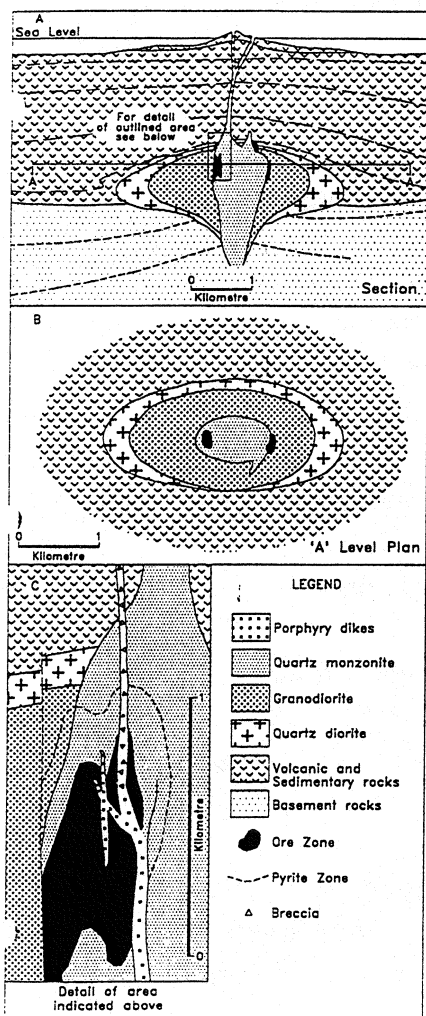
Classification of porphyry deposits in the Cordillera can be based on metal budgets using the same subdivisions as for world-wide deposits. Deposits enriched in both commodities occur in the Cordillera. In the new porphyry volume, CIM Special Volume 46, we divided deposits into copper, copper-molybdenum (with a cutoff at 0.1% Mo), copper-gold-molybdenum, copper-gold (with cutoff at 0.15g/T Au), gold, molybdenum-tungsten and molybdenum subclasses.

Precise tectonic reconstruction for deposits that were emplaced in the early Mesozoic time in the Cordillera is difficult, and in many cases the composition of the crust or basement is still uncertain. As mentioned previously, rather than show arbitrary affiliations, deposits are divided into pre- and post-accretion groups.

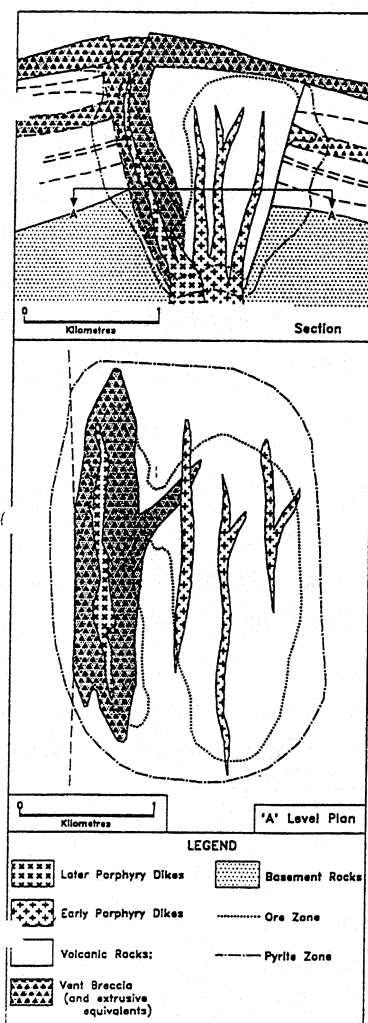
- **Pre-accretion deposits** were emplaced into terranes that were separated from continental North America. At the time the porphyry deposits were forming, these terranes were probably involved in subduction-related tectonic processes in discrete island arcs, although there is evidence that at least some of these arcs had basements of older continental material.
- **Post-accretion deposits** were emplaced during Cretaceous and Tertiary time, after the allochthonous terranes had been added to the western margin of North America. Post-accretion deposits are hosted by several of the older terranes, and therefore, the composition of the basement varies considerably.

The metal budgets of porphyry copper deposits, enrichment of Mo versus Au, and copper:gold ratios do not correlate directly with terrane or timing of emplacement (pre-versus post-accretion). There are, however, several generalizations that can be made:

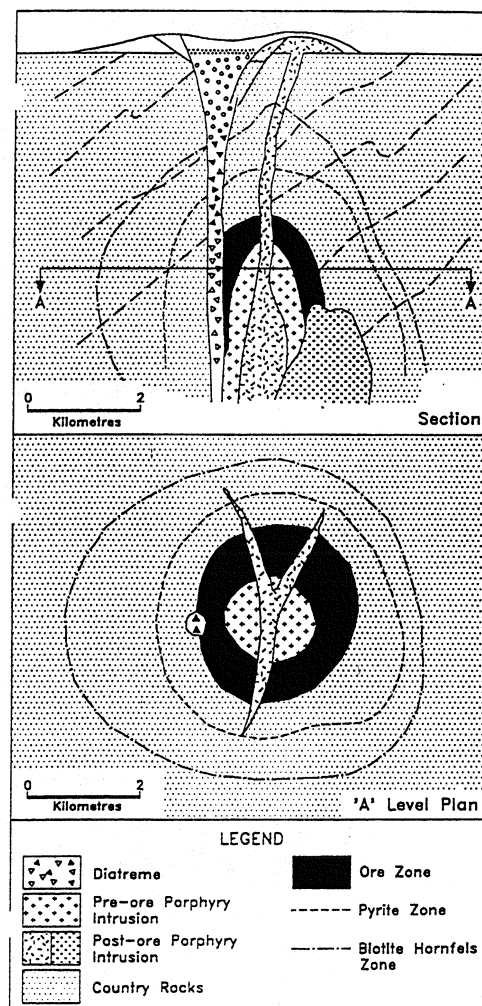
- Porphyry copper-gold deposits of the alkaline suite (Barr et al., 1976) were emplaced in two different terranes prior to accretion.
- Porphyry molybdenum deposits are restricted to the post-accretion setting.



PLUTONIC



VOLCANIC



CLASSIC

- Porphyry gold deposits related to granites (Fort Knox and Dublin Gulch) also appear to be restricted to post-accretion time, although other porphyry gold deposits related to more conventional porphyry environments (e.g., Sulphurets Gold) predate accretion.

The breakdown of deposits into pre- and post-accretion ages is used as the major division in the remainder of this presentation. Cordilleran deposits are further subdivided on the basis of petrology, into the **CALCALKALINE** and distinctive **ALKALINE** suites, and by principal commodities. Calcalkaline types are here reviewed in terms of their distribution, settings and general characteristics.

### **General Porphyry Models**

Deposits emplaced into various geological settings were classified by Sutherland Brown (1976) and McMillan and Panteleyev (1981) as plutonic, volcanic and "classic" types. That is, those formed within plutons; in the root zones of volcanoes; and both in and adjacent to shallow stocks. Within a general porphyry model, deposits from specific depths and settings within the overall system are distinctive.

**Slides: GENERAL MODEL(S) - PLUTONIC VOLCANIC CLASSIC**

#### **Plutonic**

Plutonic deposit types formed at relatively deep levels and are hosted by plutonic rocks. Dikes and breccia bodies may be abundant. Alteration patterns are similar to those described for deposits in the southwest United States. They tend to be copper-molybdenum deposits with low gold values. Gold values tend to be low, commonly less than 0.1g/tonne. Examples are the Highland Valley, Brenda and Gibraltar.

#### **Volcanic**

Volcanic deposit types formed in the root zones of ancient volcanoes of both calc-alkalic and alkalic character in association with subvolcanic stocks, plugs, sills and dike swarms. The rocks, which host most of the ore, are largely volcanic rocks, breccias and dikes.

Early developed biotite, which McMillan and Panteleyev (1988) argue may be hornfelsing, is typical, and propylitic alteration extends well out into the country rock from the deposits.

Calc-alkalic Cordilleran examples are Island Copper and Schaft Creek. Alkalic examples are Galore Creek, Afton, Copper Mountain-Ingerbelle, and Mount Milligan. It is important to note that calc-alkalic phases often occur within the suites of intrusive rocks that contain both alkalic members and alkalic porphyry deposits (Hollister, personal communication, 1991).

#### **Classic**

The classic deposit types are related to multiple subvolcanic plutons. Host-rocks may be volcanic or sedimentary; dikes and breccias are common. Early developed biotite is characteristic and the change of biotite colour from green in the aureole to brown in the ore zone may provide a "vector" for exploration (Carson and Jambor, 1974). These deposits are close analogues of Tertiary porphyries in the southwest United States. Examples are Granisle, Morrison, Bell and Berg. Late Cretaceous to Tertiary deposits are mainly of the classic type. At Granisle, for example, Fahrni et al (1976) associate the porphyry copper deposit with multiple porphyry intrusions of Eocene age that cut Jurassic volcanic and sedimentary country rocks.

Copper mineralization is centered on the contact between biotite-feldspar porphyry and an earlier quartz diorite porphyry. The main zone consists of chalcopyrite and bornite in quartz-filled fractures and is enclosed in a pyritic halo. Alteration zoning is well developed, from a potassic core, with secondary biotite, through a flanking phyllic zone, characterized by quartz-sericite-carbonate-pyrite assemblages, to a propylitic fringe with chlorite, carbonate and epidote alteration.

Gold-enhanced porphyry deposits fall within the volcanic and classic deposit types, whereas the gold-poor deposits fall in the plutonic deposit type. Gold values in the volcanic and classic deposits can be significant, in the 0.3 to 0.7 gram per tonne range.

#### **Alteration in Calcalkaline Porphyry Deposits**

Calcalkaline porphyry copper deposits have alteration patterns like those described from the southwestern United States; central potassic alteration zones, defined by secondary biotite or metasomatic potassium feldspars, pass outward through successive envelopes of phyllic alteration, defined by the presence of sericite, pyrite and quartz, then propylitic alteration, defined by epidote, chlorite and albite, into unaltered rock. Molybdenum and gold porphyries have similar assemblages but the patterns and relatives of alteration types varies. These variations are discussed further later in this report.

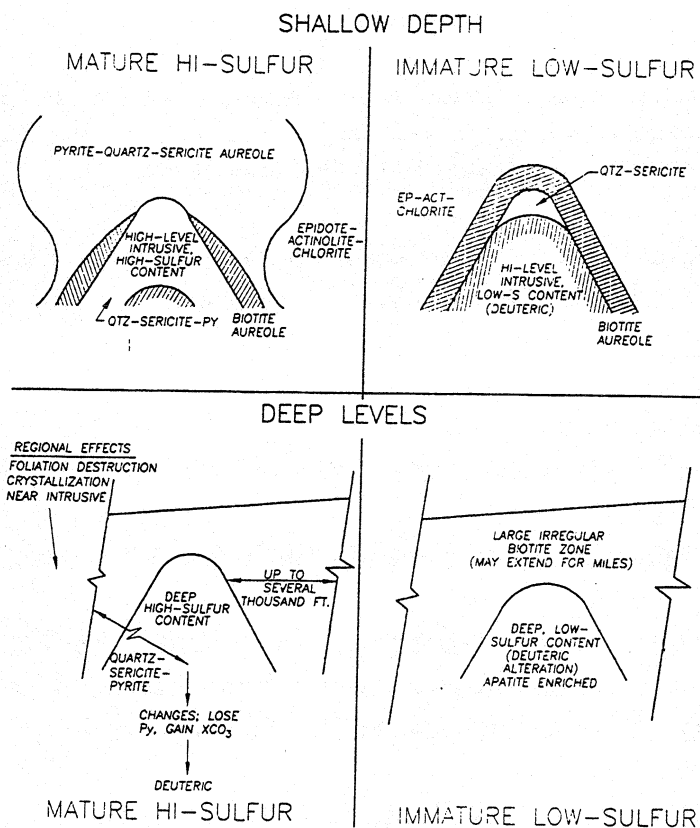


Figure 1. Changes in alteration zonation with variations in maturity, sulfur content, and depth of intrusion.

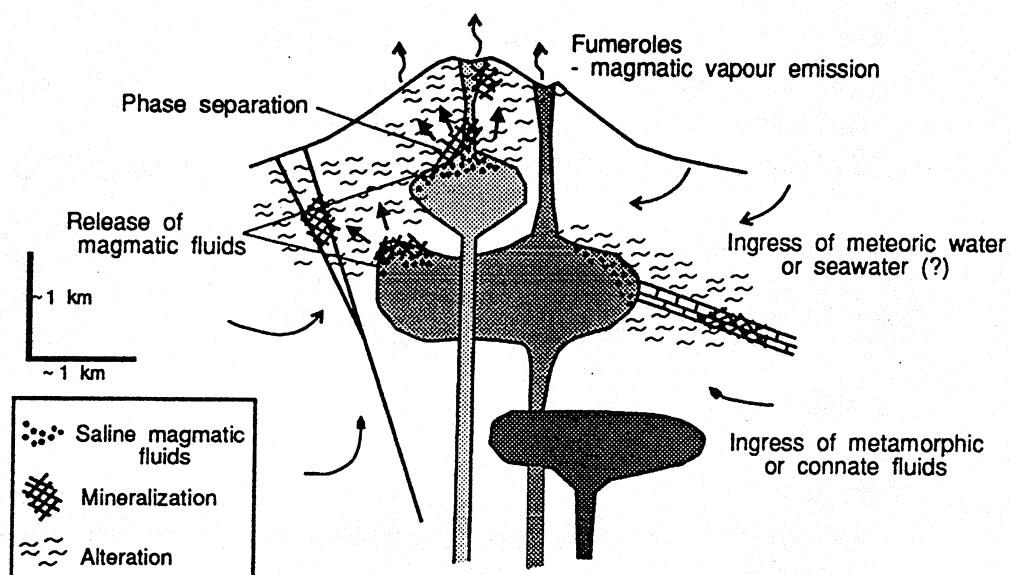


FIGURE 6. Magmatic-hydrothermal complex forming several discrete zones of mineralization within extensive areas of alteration. The potential contribution of external fluids from different sources, magmatic fluids, and hydrothermal processes are shown; see text for discussion.



---

---

**Slide: Williams and Forrester, Sulphur, depth and maturity**

Some of the causes of variability in alteration patterns in copper porphyries are discussed by Williams and Forrester (1995) for deposits in the southwest United States.

They relate them to:

- compositional maturity-
  - Tonalite (immature) through Granodiorite to Quartz monzonite (mature)
- sulphur content -
  - generally increases with maturity and higher crustal level - reaches 8% in some magmas

\*High sulphur promotes broad alteration halos and retards thermal alteration - sulphur seems to break up silicate structures of mafic minerals, capture iron and cause release of potassium, water, silica and aluminum. Sericite formation results.

- A: MATURE HIGH SULPHUR, SHALLOW end member
  - broad alteration (dominantly phyllic), narrow thermal alteration
- D: IMMATURE, LOW SULPHUR DEEP
  - broad thermal halo, narrow alteration zones

These authors also plotted maturity against sulphur:

- low sulphur contents links with only minor sericite development; high sulphur leads to a systems with chalcopyrite but no bornite
- they argue that an ideal porphyry system has a vertical range of about 8000 feet

---

---

**Slide: Thompson - Magmatic-hydrothermal complex**

Advances in understanding:

Alteration:

- widespread overprinting of early K-silicate alteration by SCC - sericite-chlorite-clay (relatively late, low temperature) i.e. Philippines, Galore Creek
- high level advanced argillic alteration over porphyries i.e. Island Copper; in deposits with telescoping, this alteration may be superimposed on deeper types (SLIDE - Sillitoe, 1994) sodic-calcic alteration is important in some deposits i.e. Yarrington - ingress of formation waters?. Also seen with Cordilleran alkalic deposits and Island Copper has sodic amphiboles alteration in the core of the deposit.

- the distribution of gold relative to other sulphides, oxides and alteration minerals has been studied. In many deposits, gold and copper grades correlate and elevated gold is associated with bornite, magnetite and potassic alteration (there are exceptions i.e. Copper Mountain). In some deposits, elevated gold may have been remobilized or introduced at late stages.
- metals are derived from the magma and transport in brines or even the vapor phase. Magmatic fluid inclusions have been shown to carry not only copper minerals but also have elevated contents of zinc, lead, manganese and iron (Bodnar, 1995).
- depth of emplacement from about 10 km (Butte) to 5 km (Sierrita, Morenci, Santa Rita) to 1.5 to 3 km below the summits of associated strata volcanoes (Red Mountain). The depth range influences (Bodnar, 1995) the kinds of fluid inclusions formed
- Bodnar (1995) argues that metals are transported by the magmatic fluids and deposited in the magmatic/meteoric transition zone.
- magmatic fluids are critical but stable isotopes indicate that many other fluids may become involved, meteoric water, evolved groundwater, formation water, or even sea water, and may cause distinctive alteration zones. The other fluids do not seem to have been major sources of metals (Thompson, 1995)

---

### **Hypogene Mineralization and Metal Patterns in Copper Porphyries**

Typical calcalkaline hypogene sulphides are pyrite, bornite, chalcopyrite and molybdenite; hypogene chalcocite occurs locally. Gold may or may not be an important component of the system. Hypogene ore minerals generally occur on fractures, in veins and as disseminations. Quartz is an abundant gangue mineral but chlorite and sericite are also common.

In these deposits, a weakly mineralized or barren, often silicified core zone is rimmed by first a zone with bornite as the dominant sulphide (with molybdenite), then a zone in which chalcopyrite dominates (with molybdenite).

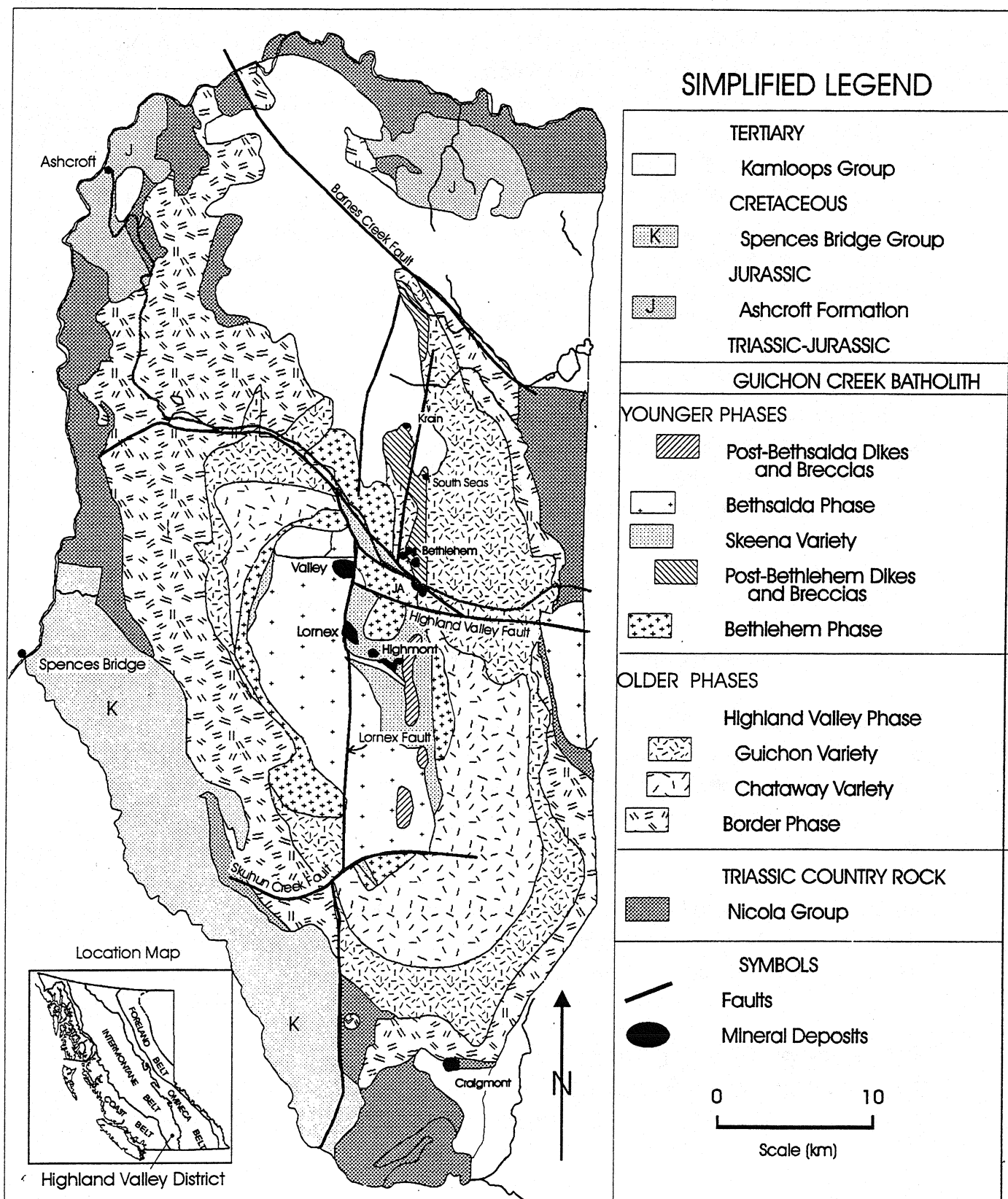
---

### **PRE-ACCRETIONARY DEPOSITS**

Deposited in Mesozoic island arc settings in what are now Quesnellia, Stikinia and Wrangellia, all are plutonic or volcanic deposit types and all are Cu +/- Mo +/- gold deposits.

#### **Calc-Alkalic: Plutonic**

Examples: Highland Valley deposits, Gibraltar, Brenda



## Highland Valley Porphyry District

### Setting - within the Guichon Creek batholith

- the batholith is 210 Ma and mineralization followed soon after emplacement
- the batholith is multiphase and zoned from edge to core: mafic quartz diorite at the border to leucocratic porphyritic granodiorite in the core
- dimensions are about 80 by 60 kilometres
- mineralization apparently occurred in two main episodes. The first is related to an intermediate phase of the batholith (Bethlehem phase biotite-hornblende granodiorite), and the second to the youngest major phase of the batholith (Bethsaida phase biotite granodiorite)
- there is presently two producing deposits, Valley and Lornex, and several past producers (Highmont, Bethlehem) as well as one large subeconomic deposit (JA) and several Bethlehem-type deposits (for example Krain (now Getty North) which is being actively explored, especially for its oxide ore potential)

### Example: Valley mine

#### General Characteristics:

##### Mineralization:

- the deposit has produced \*\* and has remaining reserves of \*\*
- the ore is hosted entirely by Bethsaida granodiorite
- mineralization consists mainly of bornite and chalcopyrite; molybdenite is locally recoverable
- almost all the mineralization is in fractures and veins or disseminated in altered zones; grades are best where several mineralized fracture sets overlap

##### Alteration:

- There is a quart-flooded and quartz vein-rich core zone in the deposit
- The flanking potassic zone is well-defined by potassic feldspar in and adjacent to quartz veins and gives way to
- a strongly developed replacement and vein quartz-sericitic (phyllic) alteration (Osatenko and Jones, 1976).
- There is a weakly developed peripheral propylitic zone.
- Alteration is regionally developed in these large hydrothermal systems and can be used to vector in toward mineralization (Casselman et al., 1995)

##### Metal Zoning

- Metal zoning at Valley copper is from bornite through chalcopyrite to a weak pyrite halo in the relatively leucocratic granodiorite to quartz monzonite host rock.
  - Molybdenite is most abundant away from the bornite zone.
-

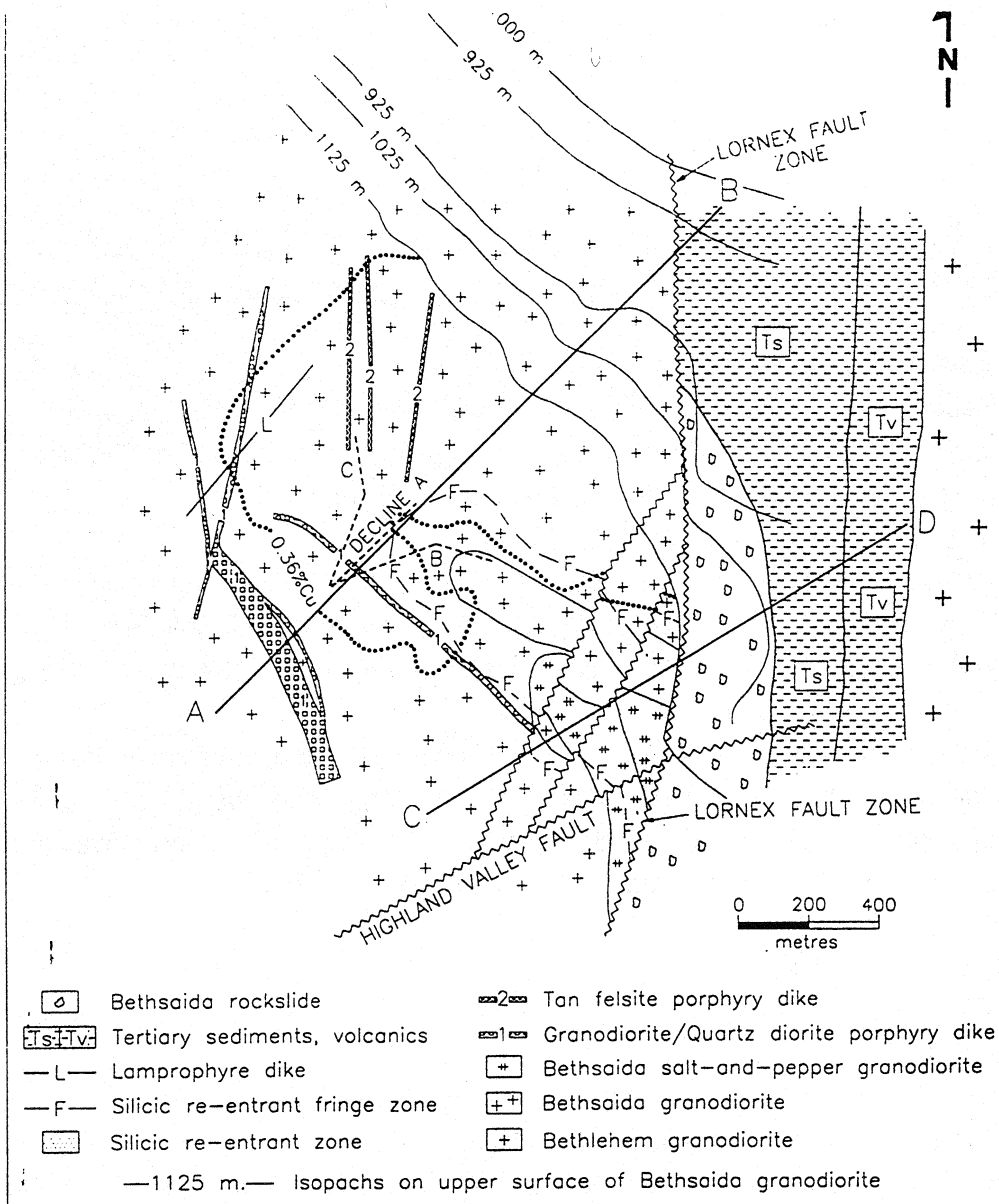


FIGURE 2a. Geology of the Valley deposit on the 1125 m level showing the location of former underground workings (bulk sampling and grade testing) for reference, as well as vertical sections A-B and C-D.

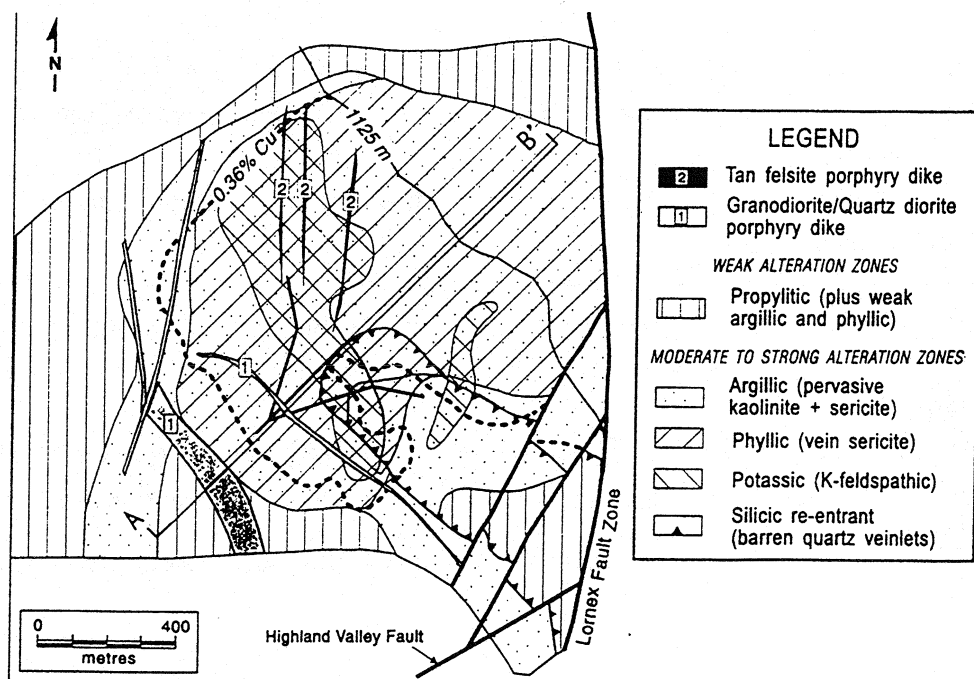
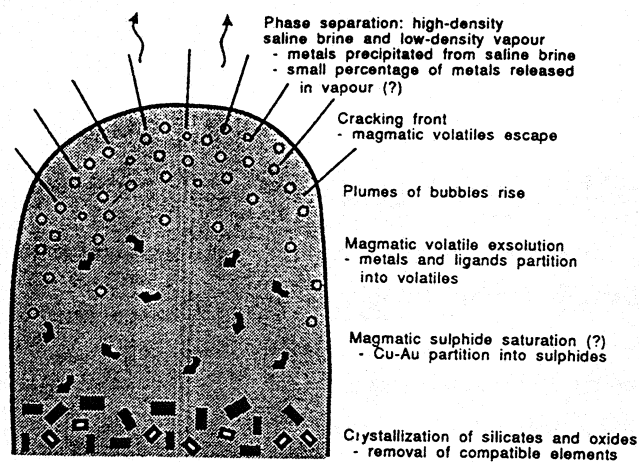
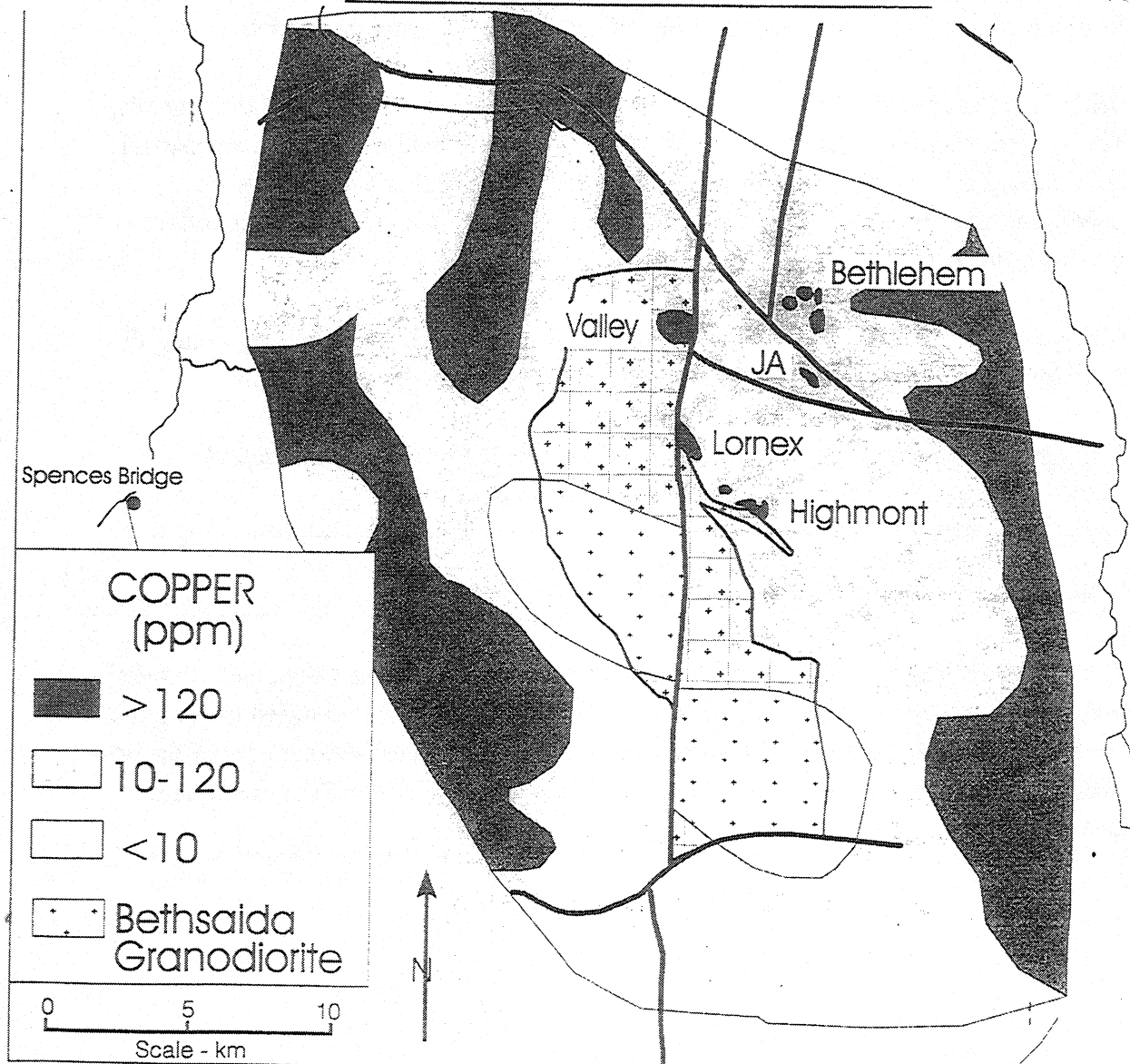


FIGURE 17a. Plan view showing the distribution of major alteration types in the Valley deposit projected to 1125 m level (modified after Osatenko and Jones, 1976).



**FIGURE 5.** Schematically illustrated processes operating in a magma chamber that may affect the concentration of metals. The timing and extent of crystallization relative to the timing of volatile saturation are critical to determining the availability of metals and ligands, particularly chlorine and sulphur (e.g., Candela, 1989a, 1989b) and their escape via plumes or bubbles to the cracking front at the margin of the intrusion (Candela, 1991). If magmatic sulphides form early, copper and gold will partition preferentially into the sulphide which, if it is removed, will result in a magma depleted in metals. If magmatic sulphides form late, sulphides may be resorbed during volatile saturation, returning metals to the magma and the volatile phase (Candela, 1989b; Keith et al., 1991); see text for further discussion.



## **ORTHOMAGMATIC SOURCE OF METALS**

**Slide: Thompson - magma chamber processes: considered in light of data from the Guichon batholith; note timing of mineralization and copper depletion in the core**

Metals in porphyry deposits are interpreted to have been derived from the magma after crystallization caused the melt to become saturated in fluids and allowed a volatile phase to separate.

Thompson discussed processes that are involved:

**Controlling factors:** bulk composition, oxygen fugacity;  $H_2O$ , S, Cl and  $CO_2$  contents of the magma; depth of emplacement (pressure). These control the timing and nature of volatile saturation relative to the degree of fractionation and the potential removal of more compatible metals by crystallizing phases. NOTE: selective assimilation of  $H_2O$  from the country rock could significantly alter the timing of volatile saturation.

Schematic illustration of processes in a magma chamber that might concentrate metals. Timing and extent of crystallization relative to timing of volatile saturation are critical in determining the availability of metals and elements like sulphur and chlorine. If conditions are right, these escape via plumes or bubbles to the cracking front at the margin of the intrusion.

If magmatic sulphides form early, then copper and gold partition preferentially into the sulphides. If these are removed, then the magma becomes depleted in metals.

If magmatic sulphides form late, then sulphides may be resorbed during volatile saturation, returning metals to the magma and the volatile phase.

---

---

**Slide: copper geochemistry from the Guichon Creek batholith**

Lithogeochemical analyses of samples collected from the Guichon Creek batholith define a pronounced zone of copper depletion in the southern part of the youngest major phase of the batholith. We interpret this to mean that the copper was partitioned out of the host rock and moved northward where it deposited in structural traps to form the mineral deposits.

---

---

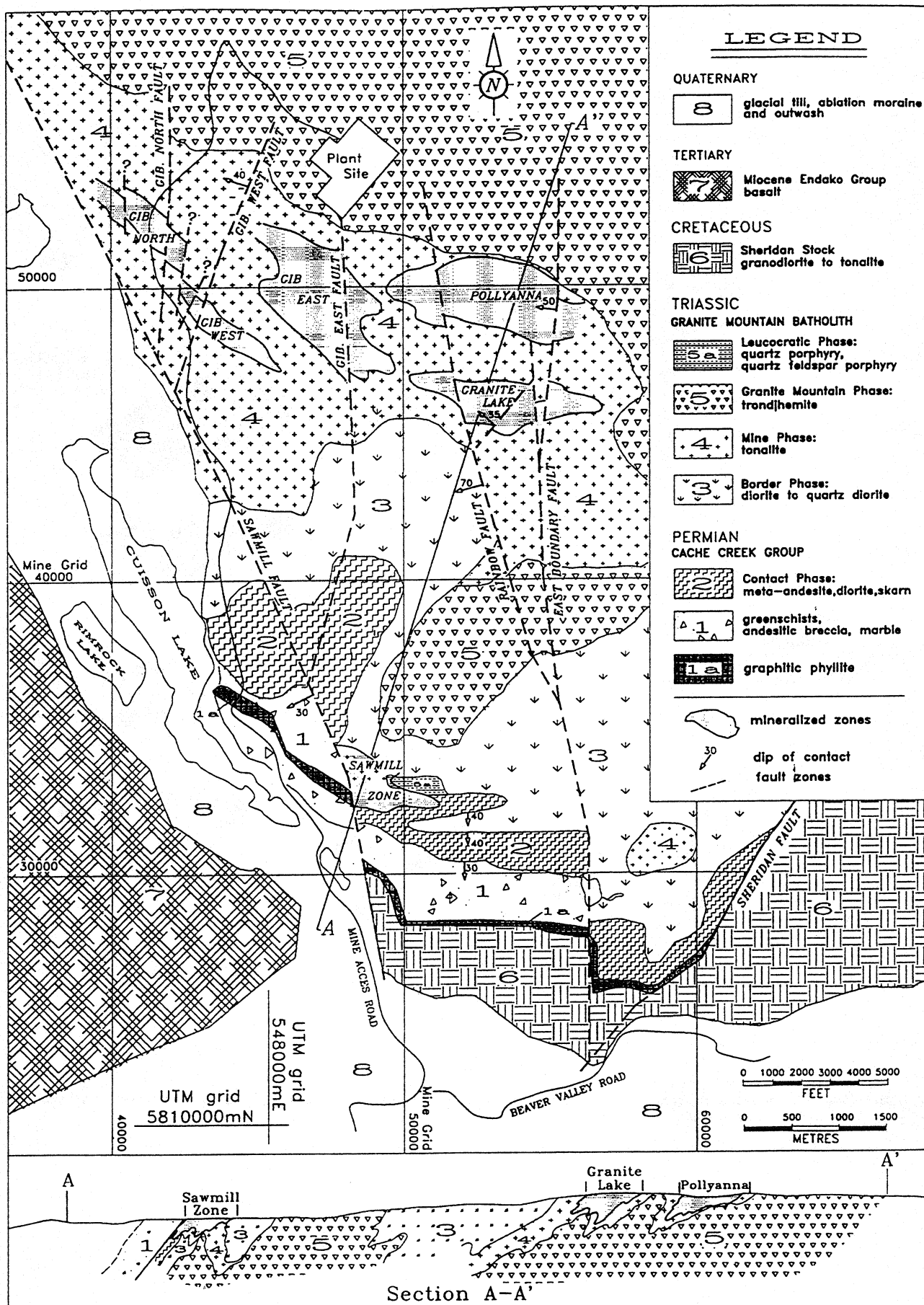


FIGURE 3. Gibraltar mine area geology.

F-39 10a



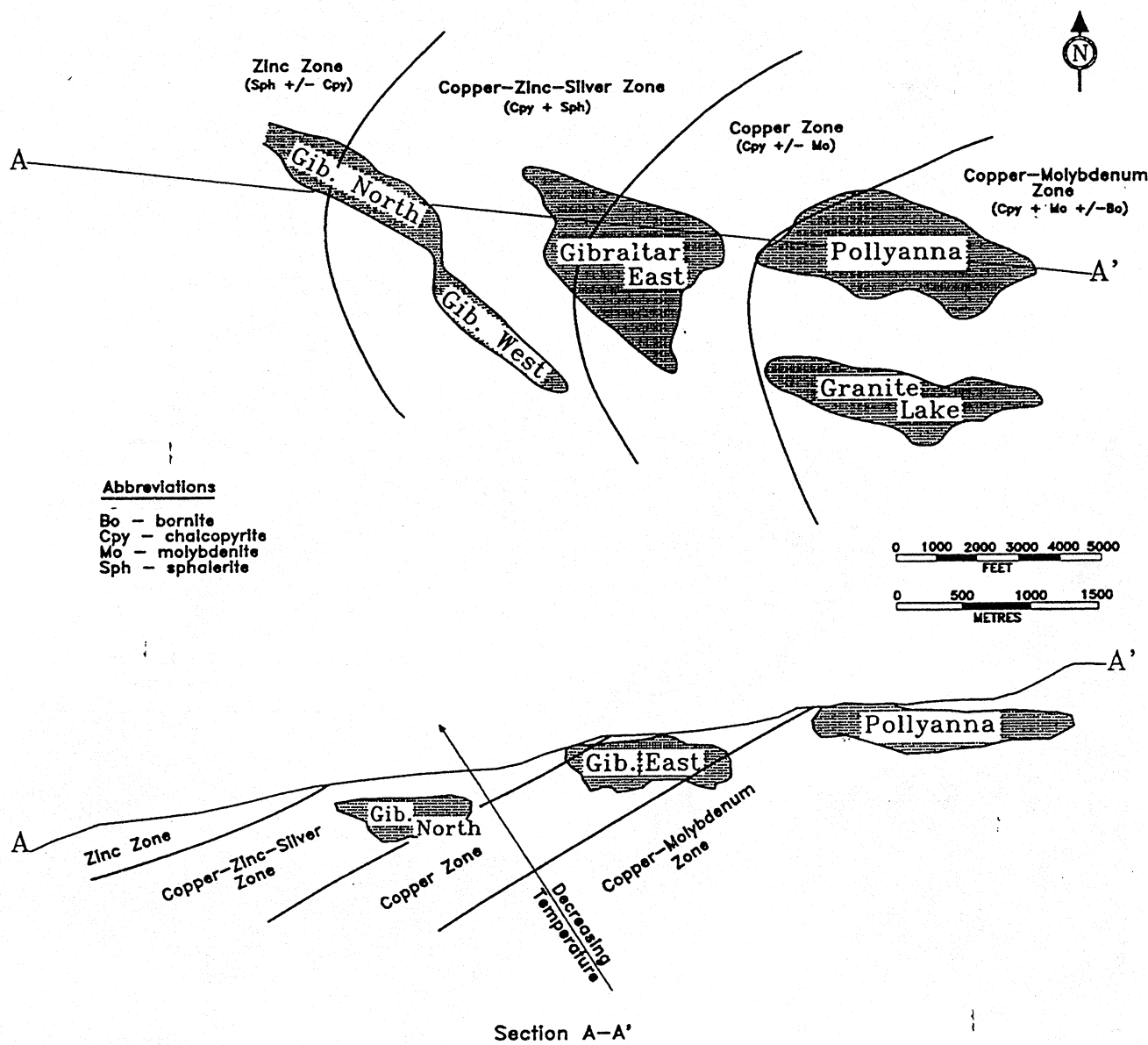


FIGURE 10. Section and plan of the Gibraltar mineralized system showing hydrothermal metal zonation and inferred orientation of temperature controls. Pyrite is widespread throughout all zones. Silver is hosted primarily by chalcopyrite.

<b>Example: Pre-accretionary plutonic type - Gibraltar Cu-Mo deposit</b>
--

**Mineralization:**

- is syntectonic, so in a sense it is a “shear zone copper deposit”
- is related to a zoned tonalite to trondhjemite batholith that intrudes oceanic Cache Creek country rocks
- the batholith is 217 Ma and is penetratively foliated
- overlaps and follows the emplacement of the trondhjemite, which is Late Triassic to Jurassic in age
- the deposit comprises 6 orebodies that plunge southward. There were 241 million tonnes mined to the end of 1992 and mining reserves remaining were 147 million tonnes at 0.301% Cu as well as a much larger mineral resource
- major sulphide minerals are pyrite and chalcopyrite; molybdenite is economically important
- metal zoning occurs between the deposits from the east, where chalcopyrite + molybdenite predominate, through chalcopyrite, then chalcopyrite + sphalerite to sphalerite-dominated mineralization in the west. This may represent shallower zones being exposed to the west due to tilting and erosion.

**Alteration:**

- is propylitic and phyllic. Quartz and chalcopyrite in chlorite folia are typical. Alteration minerals are quartz, sericite, chlorite, epidote and carbonate.

**Recovery of Metals from Waste Dumps**

- waste dumps are acid-leached and copper recovered in a SXEW plant

**Conclusion:**

**Mineralization is apparently syntectonic and may have developed during subduction of Cache Creek rocks under Quesnellia.**

---

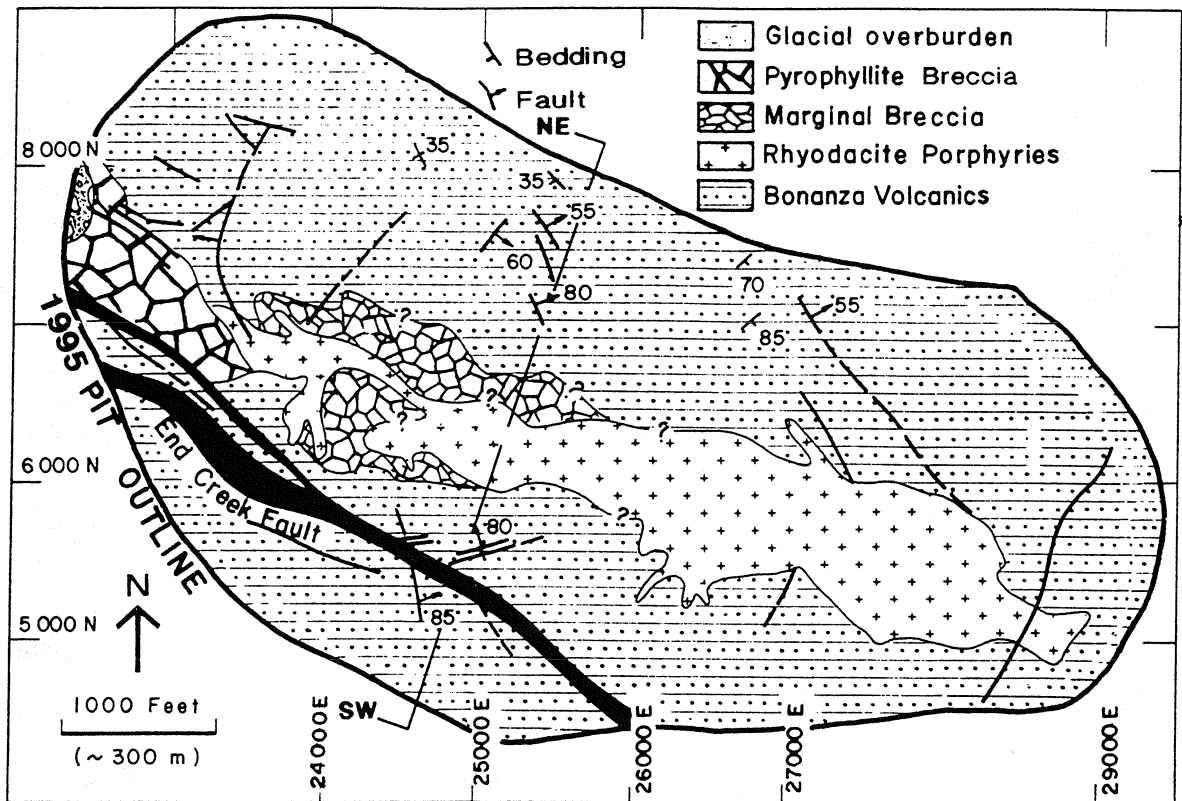


FIGURE 6. Composite plan: Geology of the Island Copper deposit.

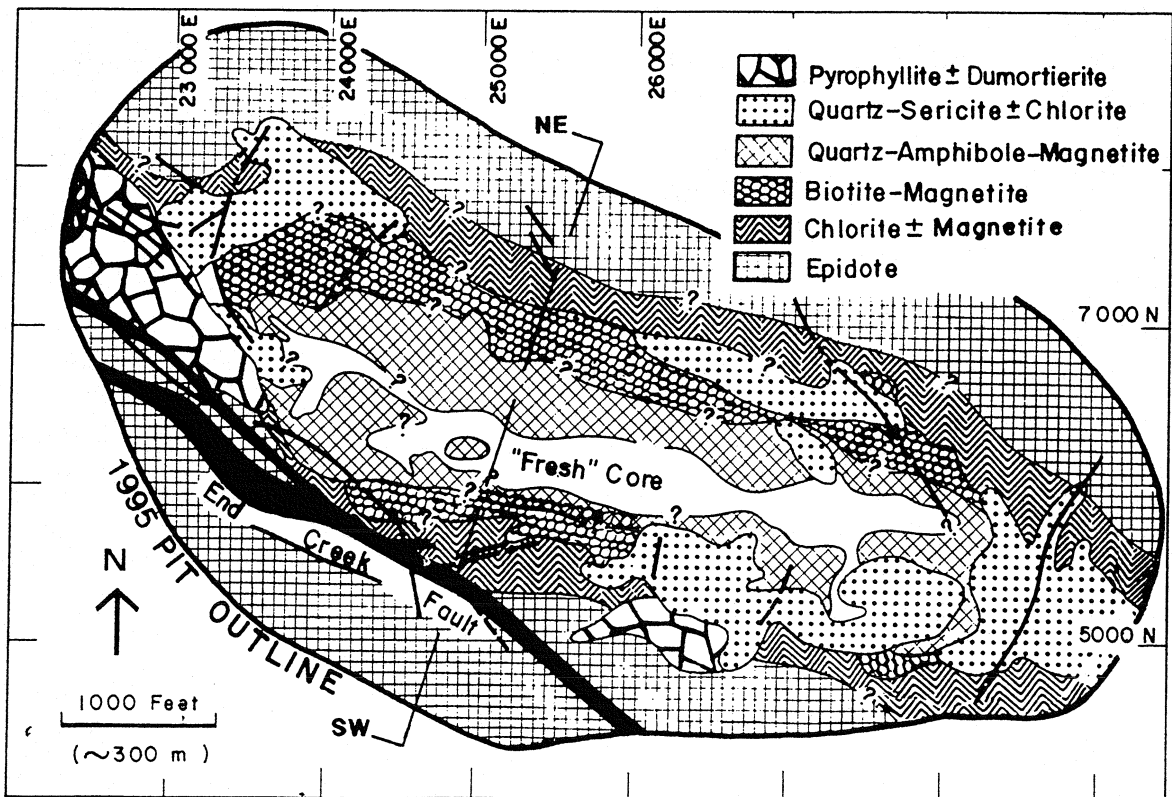


FIGURE 12. Composite plan: Alteration types of the Island Copper deposit.

## **Pre-accretionary Volcanic Type Deposits**

**Example: Island Copper**

**Slides: geology and alteration**

### **General Features:**

- The host terrane is Wrangellia and the deposit is dated at 167 Ma.
- Intruded into a high level in the crust: Cu-Mo-Au mineralization is related to dikes and a dike-like multiphase rhyodacite stock
- the country rocks are Jurassic volcanics of the Bonanza Group - andesites, basalts and volcaniclastics
- marginal breccias developed at the plunging west end of the stock
- advanced argillic alteration (acid sulphate) with dumortierite-pyrophyllite breccia is developed high on the pit wall, in the shallower part of the system
- Alteration and mineralization are multiphased
- Main ore stage assemblages are:
  - central barren with quartz-magnetite-albite-amphibole assemblage
  - intermediate mineralized with biotite-magnetite-chalcopyrite-pyrite-molybdenite
  - fringing mineralized chlorite-pyrite +/- chalcopyrite
  - outer barren epidote
- These are overprinted by phase II:
  - quartz-sericite alteration
  - sericite-clay-chlorite (SCC) alteration with some sulphides
  - breccias
- Phase III produced pyrophyllite breccia with pyrite but no copper. Also present are dumortierite, kaolinite and sericite.

NOTE: gold values are higher in the zone just north of the breccias.

### **Synopsis:**

- emplacement of the rhyodacite dike produced biotite alteration in the volcanic country rock (early developed biotite - EDB)
  - the deposit is calc-alkalic but average gold mill head grades were 0.22 g/T and large areas exceeded 0.4 g/T
  - as is characteristic in many gold porphyries, gold and copper are positively correlated, magnetite is abundant and gold is predominantly in the potassic alteration zone
-

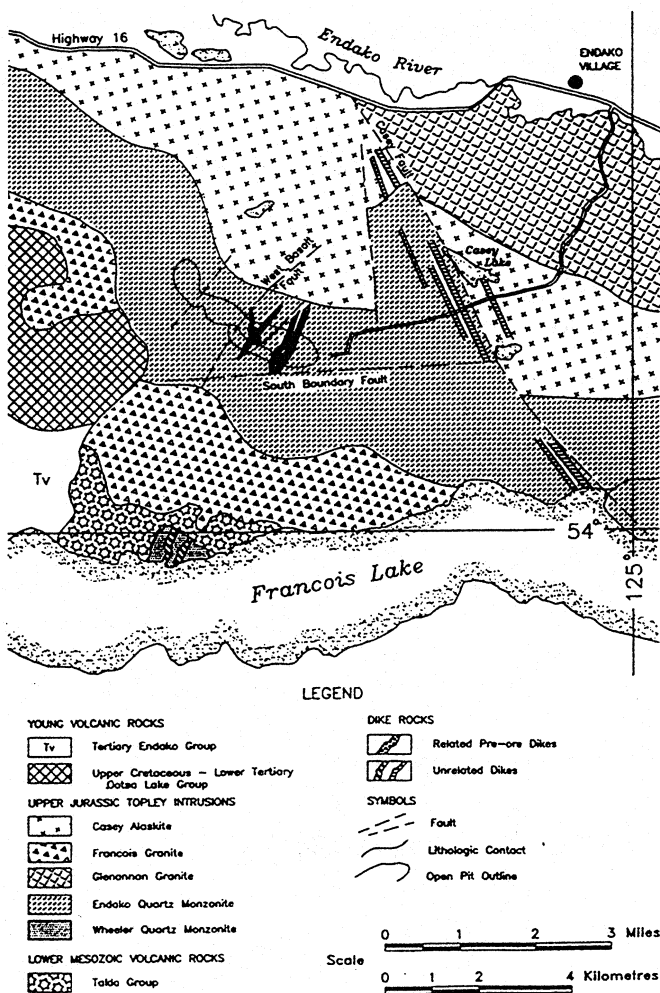


FIGURE 4. Local geology of the Endako Mine (from Kimura, Bysouth and Drummond, 1976).

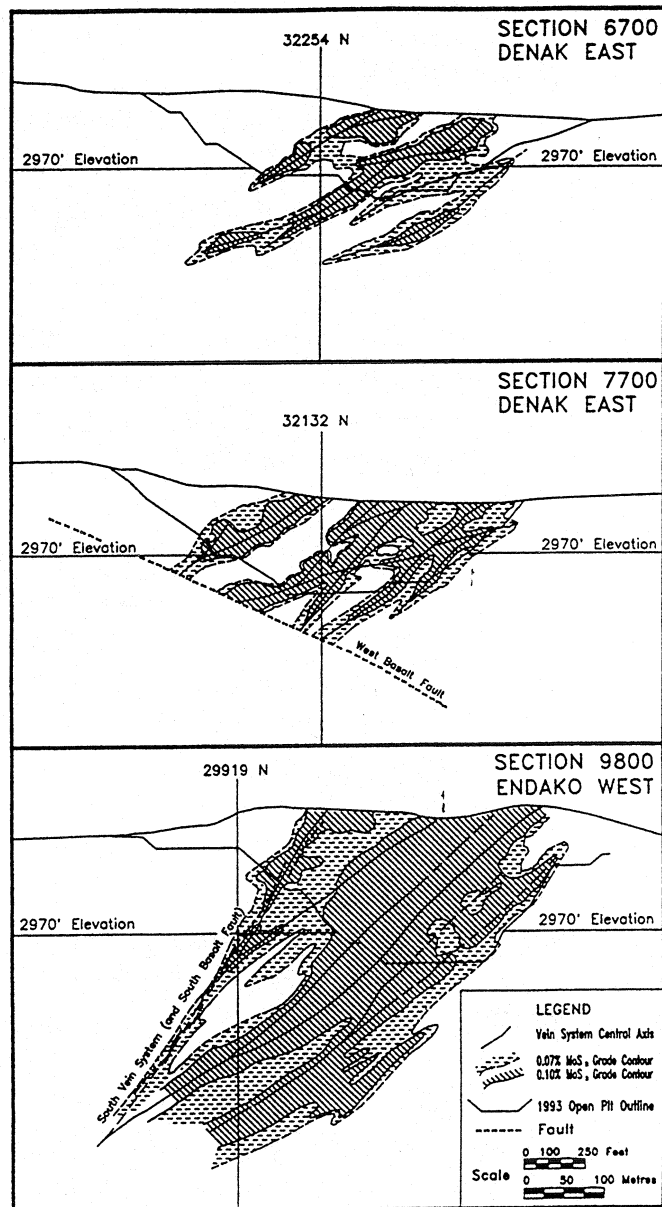


FIGURE 6. Geological cross-sections showing the linking pattern of controlling vein systems.

Looking West

## POST-ACCRETIONARY DEPOSITS

Emplaced into older country rock in continental arc settings. Most are classic but deposits range from Cu-Mo to Cu-Au +/- Mo to Mo +/- W to W +/- Mo to Au only types. Some are related to calc-alkalic intrusions along transverse structural zones like the Stikine and Skeena arches, or are in Tertiary extensional settings; examples are Bell and Granisle in Central British Columbia.

Examples of post-accretionary deposits follow.

### **Molybdenum Deposits**

Examples: Endako 142Ma; Boss Mountain 102Ma; Hudson Bay Mountain 65Ma, Kitsault (52 Ma), Adanac (71 Ma), and Mt. Tolman (57 Ma) in Washington State

### **Classification**

Different classification schemes for porphyry molybdenum deposits have been proposed by various authors. The most widely accepted is based on the petrology of the related intrusions, granite porphyry or alkali rhyolite versus quartz monzonite (White et al., 1981). The former are commonly referred to as Climax-type deposits after the Climax mine, the latter Quartz Monzonite type. Characteristic of the Climax versus Quartz monzonite type are given in the table. Carten et al. (in press\*) modified this classification scheme to define three groups of deposits: a high-silica rhyolite-alkaline suite, a differentiated monzogranite suite, and a granite-related Mo-Cu suite with Mo>0.05%. **All the known porphyry molybdenum deposits in the Canadian Cordillera fall in the differentiated monzogranite suite.**

\* was not able to find a reference to a published source

**Examples of Cretaceous Post-Accretionary Deposits: Endako, Fish Lake, Casino, Taurus?, Pebble**

**At Endako:**

### **Slides: Location, geology, section**

- mining began in 1965; since then 188 million tonnes averaging 0.15% MoS<sub>2</sub> have been milled and remaining reserves exceed 100 million tonnes at 0.136% MoS<sub>2</sub>.

**New Ar/Ar and U/Pb age dates by the Nechako NATMAP GSC crew has broken the Francois Lake intrusions into 4 suites:**

- Boer diorites and gabbros at 219Ma;
- Stag Lake hornblende +/- biotite diorite to granodiorite at 163 to 170Ma;

- Francois Lake granites and quartz monzonites at 145 to 147 and 154 to 156Ma; and
- Fraser Lake suite at 112Ma (K-Ar).

#### **Mineralization:**

- is entirely within the Endako Quartz Monzonite, a middle stage Francois Lake intrusion
- pre-ore K-feldspar porphyritic granite dikes have been dated at 147 Ma and the late stage Casey Alaskite, to the northeast, has been dated at 145 Ma. There are also younger Granite intrusions on the north and south
- the younger intrusions are dike-like, implying WNW and NW structural control
- in the mine area there are also post-ore Tertiary? mafic dikes that are associated with faulting.

#### **Hydrothermal alteration** comprises three phases:

- K-feldspar forms envelopes on quartz-MoS<sub>2</sub> veins in the orebody and barren quartz veins to the north
- sericite forms envelopes on quartz-magnetite veins in the orebody and quartz-pyrite veins in the pyrite zone
- kaolinite (argillic) alteration is the dominant alteration in the orebody, K-feldspar (potassic) in the footwall and sericite-pyrite-quartz (phyllic) in the hanging wall

#### **Metal zoning** is defined by:

- pyrite (0.5 to 1.5%) with minor magnetite and molybdenite which forms a zone along the south side or hanging wall of the deposit. It also occurs within the ore zone.
- molybdenite which occurs in quartz veins that are often ribboned. It is accompanied by magnetite, minor chalcopyrite and rare bornite, bismuthinite, scheelite and specularite. Locally there are galena inclusions in the molybdenite.

#### **In the ore zone:**

- ore veins occur as simple, parallel or en echelon veins, or complex, branching meshworks of veins, systems.
- the ore zone is elongated WNW, 3360m long, 370m wide and maximum 370m deep and comprised of four zones. Mineralization occurs in intersecting sets of veins
- the vein systems define ore zones that are relatively shallow dipping. Preliminary new paleomagnetic data (NATMAP) suggests that rotation occurred during Tertiary extension and accords with field relationships.

#### **TUNGSTEN-Molybdenum**

EXAMPLES: Logtung, Yukon (118 Ma) - reference CIM Special Volume 46.

Not illustrated

## **CU-MO-AU**

Examples: Fish Lake (77 Ma), Casino in Yukon (70 Ma), and Pebble (91 to 95 Ma) and Taurus (Tertiary) in Alaska; Huckleberry (82 Ma) and the Babine Camp in B.C. (50 Ma most important)

## **Prosperity (Fish Lake) - Taseko Mines Ltd.**

### **General**

- reserves are now estimated at 675 million tonnes 0.236% copper, 0.435 g/T gold

## **Slides: geology and alteration**

### **Features:**

- Potassium argon dating indicates an age of 77MA
- mineralization is related to the Fish Lake complex, a steep, lenticular body of quartz diorite surrounded by an east-west elongated quartz feldspar porphyry dike complex; some of the dikes are mineralized
- the country rock consists of
  - Late Cretaceous, flows and tuffs
  - coeval?, subvolcanic diorite porphyry
- most of the mineralization is in volcanic flows and volcanoclastics adjacent to the Fish lake complex

### **Alteration:**

- mineralization is associated with a biotite core zone partly overprinted by chlorite alteration
- the central quartz diorite has widely developed K-feldspar in microfractures and quartz veinlets
- texture-destructive phyllic alteration overprints the northern and eastern borders of the deposit

### **Synopsis:**

The best mineralization in the deposit is related to pervasive potassic alteration in and adjacent to the quartz diorite, and extends into flanking propy-argillic or intermediate argillic (Sillitoe, 1991) alteration that consists of sericite, quartz, carbonate and clays (Wolfhard, 1976). The propy-argillic zone partly laps onto the earlier potassic zone and is flanked by a propylitic zone. Earliest veins carry quartz, magnetite, hematite, sulphides and chlorite; during main stage mineralization, sulphides were deposited along with quartz, biotite, chlorite and sericite. Later veins are quartz, quartz with sulphides, carbonate, hematite and gypsum with chlorite or pyrite.

### **Conclusion:**

- this may be a volcanic-type deposit



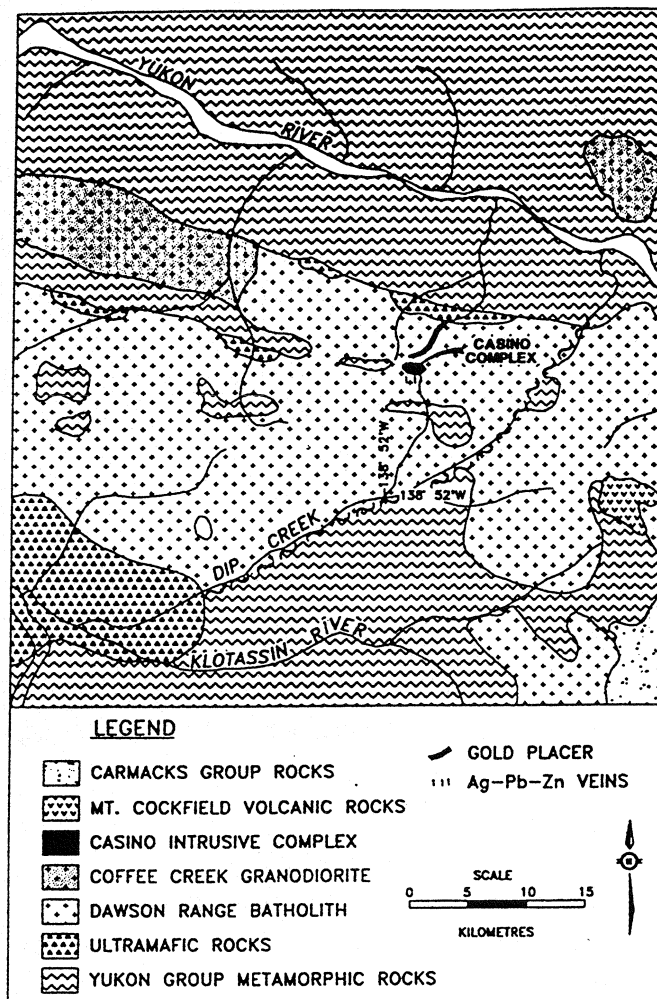


FIGURE 4. Regional geology (modified after Payne et al., 1987).

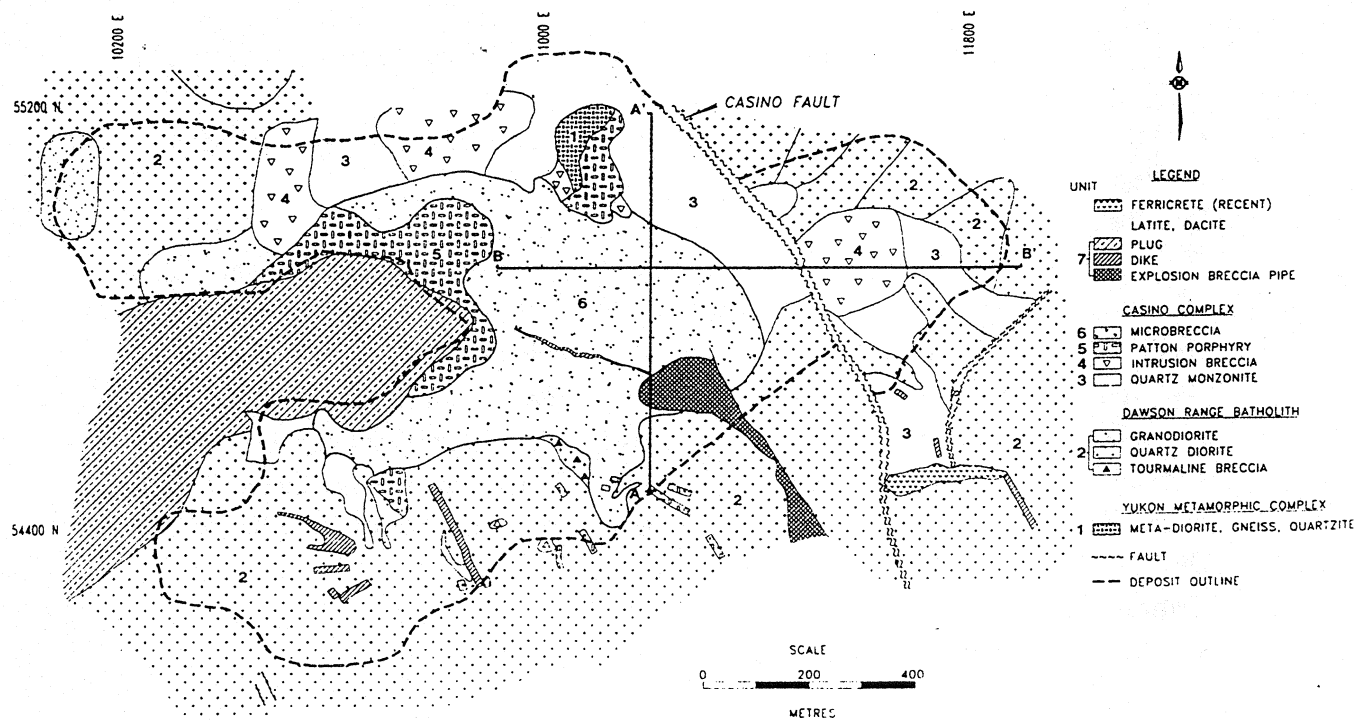


FIGURE 5. Subsurface property geology.

## **Yukon Example**

### **Casino Deposit**

The following is largely based on work by Colin Godwin

#### **Setting:**

- It is a porphyry copper-molybdenum deposit
- Country rock is the Yukon metamorphic complex
- These were intruded by mid-Cretaceous granitic rocks of the Klotassin batholith, which has a K-Ar age of 99.3 Ma
- This is in turn cut by the Casino complex, dated at 70 MA. This complex cuts the Klotassin but is cogenetic with the casino deposit
- Subvolcanic feldspar porphyry plug emplaced was followed by an explosive event that produced a conical breccia pipe (700 x 400 metres at surface)

#### **Alteration:**

- Potassic core: magnetite, biotite and K-feldspar
- Phyllic rim: quartz, sericite, sulphides (extends 300 metres into rocks of the batholith)
- Outer weak argillic and propylitic zones are developed

#### **Metals:**

- Chalcopyrite and molybdenite are mainly in the phyllic zone as disseminations and veins
- There is an outer pyrite halo

#### **Supergene:**

- Area is unglaciated so supergene is preserved
- Leached CAP averages 75 metres; supergene blanket averages 25 metres of oxide and 70 metres of sulphide mineralization
- grades are increased in the subhorizontal chalcocite - enriched zone by about 1.65 times the protore grades

#### **Conclusion:**

This is either a classic or a plutonic-type deposit; I favor classic because of the time gap.

## Alaskan Examples

### Taurus

The property is in Alaska, 10 miles west of the Yukon border. Area not glaciated - Yukon-Tanana Upland.

Looking west across the east Taurus airstrip, the "bald" area at the back is the west Taurus area. Thanks, Peter Leriche and Tom Peevers.

- Metamorphic rocks - Precambrian to early Paleozoic
- Gneiss, Schist and quartzite intruded by granodiorite to quartz monzonite
- Cretaceous to Tertiary volcanic activity at the same time: tuffs and lavas
- Cretaceous granodiorite; disseminated pyrite and magnetite
- Tertiary; main hosts to mineralization
  - quartz monzonite mainly at east and west Taurus zones. porphyritic, biotite, hornblende, plagioclase
  - quartz lattice - peripheral to and grades into the quartz monzonite porphyry - often as monomictic breccia
  - feldspar-quartz porphyry (orange) - plagioclase has argillic alteration, matrix silicified
  - intrusive breccia (blue) - QFP fragments in dacitic groundmass
- "classic" or Arizona-type; similar to casino and pebble according to Peter Leriche.
- \*??supergene??

---

### Pebble

#### General Information

- calc-alkalic porphyry copper-gold system
- north of Bristol Bay, area not glaciated, low rolling topography and less than 1% outcrop
- general geology: late Cretaceous granodiorite porphyries cut and hornfelsed Jura-Cretaceous graywackes
- post-mineral Tertiary volcanics lie to the east
- biotite diorite with magnetite veinlets (intense alteration?)
- early biotite alteration of graywackes dominates; is cut by K-feldspar alteration
- other alteration minerals: albite, iron carbonates, sericite, anhydrite, apatite and rutile
- copper is associated with the biotite alteration
- gold and copper are closely correlated

**Timing:**

K-AR dates: (Cretaceous)  
fresh primary K-feldspar - 95MA  
biotite in biotite pyroxenite - 96MA  
secondary K-feldspar - 91 MA Cenomanian

**Multiple intrusions:**

diorite  
then quartz monzonite  
then biotite pyroxenite  
mineralization and intrusive breccias  
then porphyritic granodiorite

**Drill indicated reserves:** February 1992:

50 million short tons at 0.35% copper and 0.012 ounces/ton gold; a higher grade core zone runs 0.5% copper and 0.015 ounces per ton gold (0.44 grams/tonne).

Note: there are two higher grade "bullseyes" at the margin of the equigranular granodiorite - copper exceeds 1% and there is 0.025 ounces per ton gold.

**Exploration tools:**

- soil geochemistry - copper and gold anomaly more than five square kilometres in size
  - on the "shoulder" of an IP chargeability high
  - there is a coil colour anomaly
- 

**Examples of Tertiary Post-Accretionary Deposits**

note: Cascades examples - 6.2 to 24.0 MA

**Example:****Berg Copper-Molybdenum Porphyry****Features:**

- reserves 400 million tonnes 0.4% copper, 0.05% molybdenite
- a middle Eocene composite, 4-phase porphyritic quartz monzonite to granodiorite stock cores the deposit
- the stock cuts Middle Jurassic Hazelton volcanics and an older quartz diorite stock
- Mineralization forms an annular zone within and around the composite stock

**Alteration:**

- Country rock Hornfelsed (EDB) - zone wide relative to size of stock

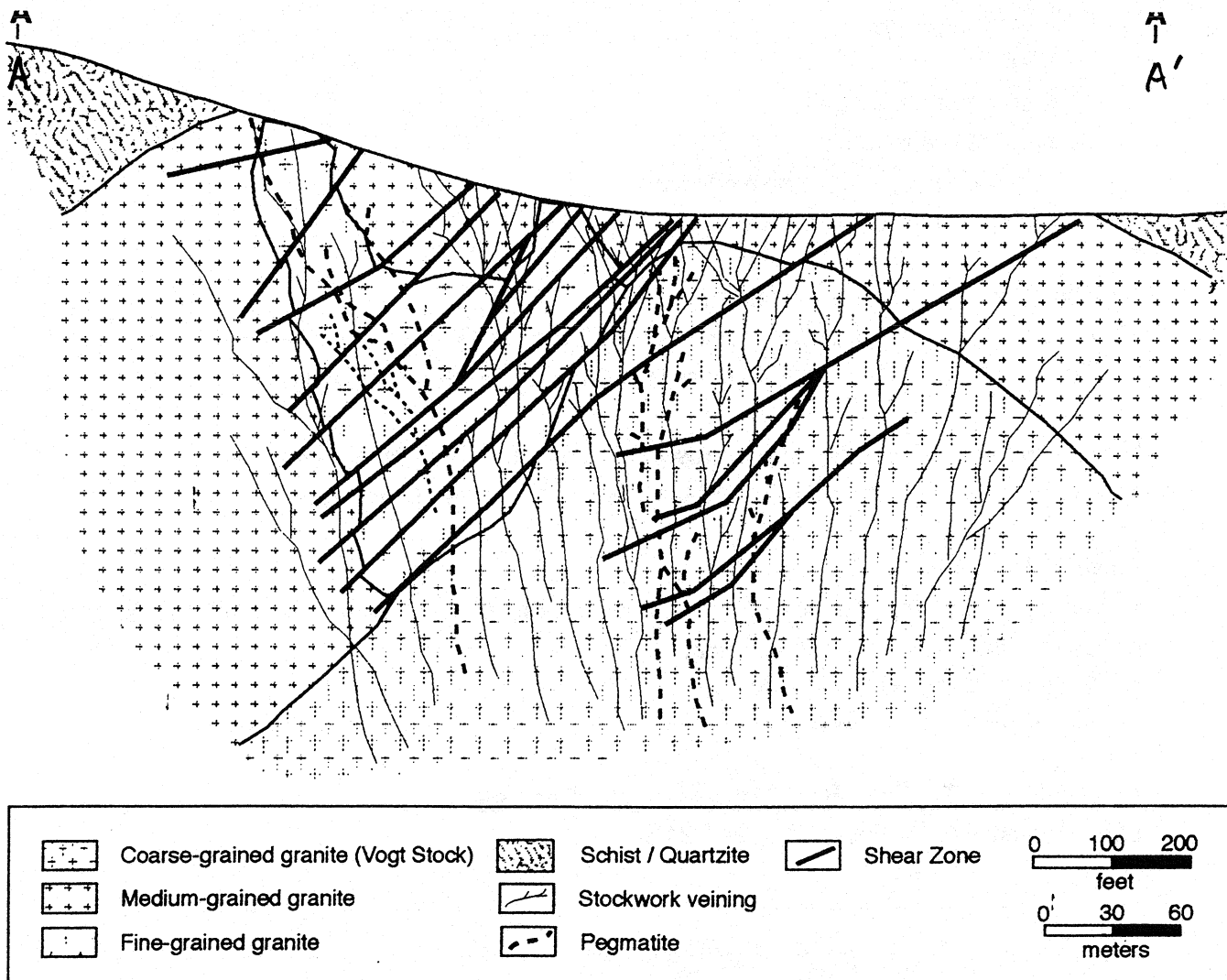


FIGURE 4. Section A-A' (looking west) — Fort Knox.

18a

F-52

- quartz-sericite envelopes are developed on quartz sulphide veins with less common quartz-chlorite and rare K-feldspar
- stock has biotite, kaolinite alteration, then quartz-sericite-pyrite, then propylitic alteration

### **Sulphides:**

Three separate but overlapping concentric, cylindrical shells:

- Inner molybdenite - narrow, 100-135 M from contact
- Inner copper - chalcopyrite - wider - to more than 260 M
- pyrite halo up to 700 m out from the stock
- Peripheral lead-zinc-copper-silver veins

Supergene: leached cap - supergene zone enriched 1.25 times over hypogene grades

Other examples: Morrison - Huckleberry, etc.

### **Interpretation:**

- classic-type probably, calc-alkalic copper-gold-molybdenum type; possible peripheral precious metal deposits (8 kilometres), has multiple intrusions, EDB and breccias; possibly subduction-related

### **Post-Accretionary Gold Porphyry Deposits**

Sillitoe (1979) predicted the existence of porphyry deposits where gold could be the principal or sole economic commodity. Several discoveries have been made since then that can be classified as porphyry gold deposits. The Marte and Lobo gold deposits in Chile (Villa et al., 1991), which show many features typical of porphyry deposits associated with calcalkaline diorite intrusions, contain only minor amounts of copper and molybdenum. In the Cordillera, discoveries at Fort Knox (Bakke, 1995) and Dublin Gulch (Hitchins and Orssich, 1995) are apparently porphyry gold deposits with characteristics similar to some porphyry molybdenum deposits.

EXAMPLES: Fort Knox, Dublin Gulch

**Slides: (3) Bakke Ft. Knox gold**

**Slide (location):** The deposit is located north of Fairbanks in Alaska within a Late Cretaceous (90-93 Ma) granite body that cuts the Fairbanks schists, which are part of the Yukon-Tanana terrane. The intrusion is in an east-west panel of Yukon Tanana rocks that is bounded by the Tintina and Denali fault zones.

Figure 1. A: Nontelescoped porphyry Cu-Mo system at Red Mountain, Arizona (after Quinlan, 1981), showing 600 m separation between K-silicate core and advanced argillic-sericitic zone of high-sulfidation type. Undocumented thickness of advanced argillic alteration and surficial, supra-water table acid-leached zone have been lost to erosion. B: Telescoped porphyry Au system at Marte, Chile (after Vila et al., 1991), showing advanced argillic zone of high-sulfidation type juxtaposed with Au-bearing quartz veinlet stockwork (of K-silicate parentage) developed in diorite porphyry stock. Acid-leached rock generated above paleo-water table is nearby. C: Extremely telescoped porphyry Cu-Mo-Au system at Ladolam, Lihir Island, Papua New Guinea (after Moyle et al., 1990), showing overprinting of K-silicate-altered, monzonitic intrusion and tabular zone of low-sulfidation epithermal Au mineralization. Acid leaching, locally still active, affects intrusive rocks and is believed to overprint Au mineralization.

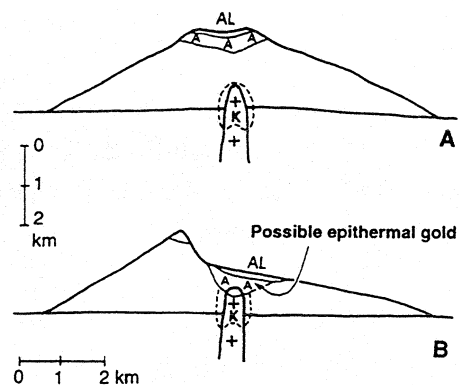
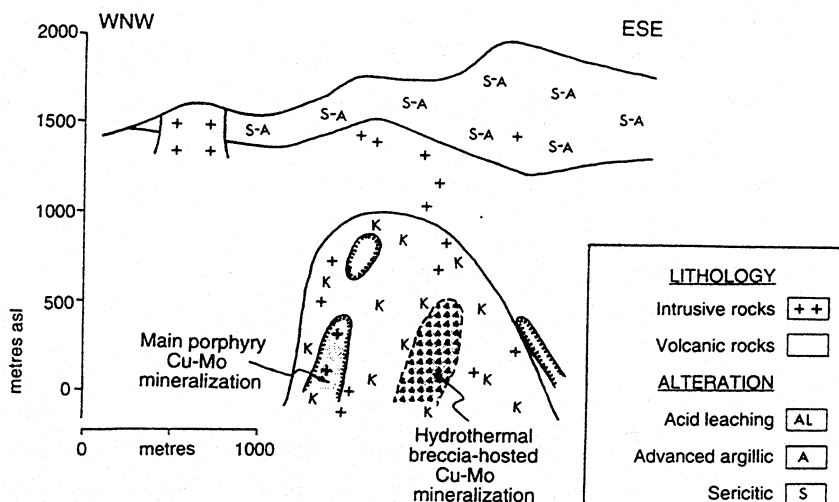


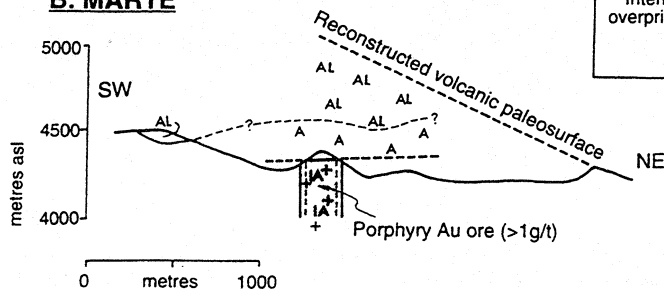
Figure 2. A: Stratovolcano during early stages of development of porphyry Cu and/or Au deposits at depth. High-sulfidation epithermal environment, including surficial acid-leached zone, is present high in system. B: Telescoping of epithermal environment and porphyry Cu and/or Au deposit as result of sector collapse. Epithermal Au ± Cu mineralization may develop in telescoped high-sulfidation zone. Legend as in Figure 1.

GEOLOGY  
GEOLOGY

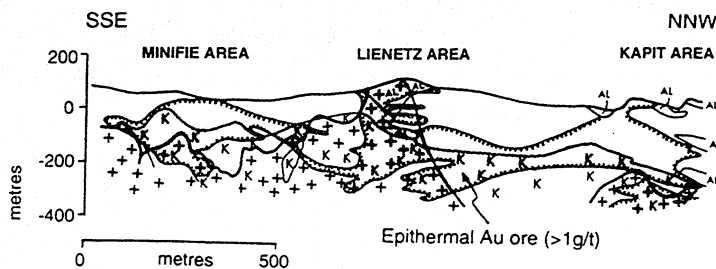
### A. RED MOUNTAIN



### B. MARTE



### C. LADOLAM



**Slide (plan):** The intrusion, which is small, 600 by 1100 metres at surface, has sharp contacts with the schists and forms an east-west elongated dome. Swarms of narrow, irregular aplite dikes cut all phases and are in turn cut by swarms of near-vertical, east-west oriented, 2 to 15 cm pegmatite (grey and white quartz with grains and clots of K-Feldspar, biotite and hornblende that grade into grey quartz veins).

**Slide (composition, texture):** The stock is multiphase with 3 main phases: fine grained, medium grained, porphyritic and coarse grained seriate textured porphyritic granite.

**Slide (section):** In cross section it is clear that the medium grained granite, which predominates in map view, is a narrow carapace on the coarse grained granite stock. that hosts the gold mineralization. There is pervasive propylitic alteration and weak structurally controlled porphyry alteration that occurs along the two main structural trends: east-west, related to doming, and southeast-northwest shear zones. Alteration consists of 0.5 to 3 cm potassic, albitic and phyllic envelopes. Shear zones have mixed phyllic and argillic alteration.

The system is sulphide-poor but there are related bismuth minerals, and some iron sulphides, molybdenite and scheelite. The deposit has a weak pyrite halo.

Gold occurs in quartz veins in the granite, in quartz-filled shears, at the margins of milky-white stockwork veins ( east-west strike, variable dips) and along fractures. It also occurs in the pegmatites where they grade to gray quartz veins.

Reserves are 158 mT of 0.83 g/t gold.

Structural control: doming of the granite followed by subsidence at the apex of the stock that formed subsidiary shears and structures.

Soil geochemistry has been the main exploration tool, mainly using gold but also bismuth, tellurium, molybdenum, and tungsten.

---

---

#### **Newer Ideas: Telescoped Alteration and Gold Porphyries**

---

#### **Slide: Sillitoe Erosion and alteration overprinting**

A complication seen in some porphyry systems is telescoping. Telescoping is the process of overprinting early, deep mineralization with shallow, possibly even epithermal styles of precious and base metal mineralization.

- it can be caused by rapid, syn-hydrothermal erosion or sector collapse of the volcanic edifices (stratovolcanoes or large flow dome complexes).
- Sillitoe (1994) estimates that in elevated terrain 1 km of erosion is easily feasible during the life span of a hydrothermal system with resultant compression of any contained ore deposits.



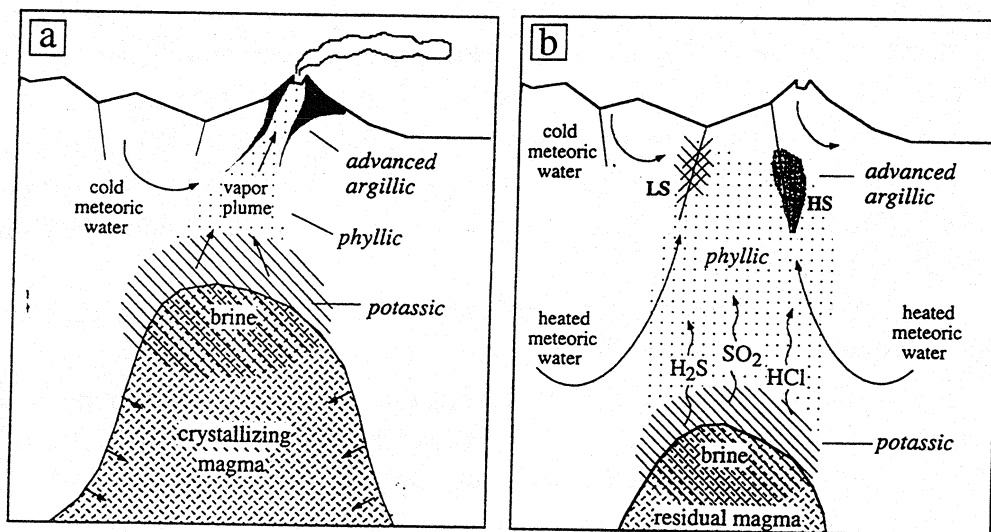


FIG. 11. Schematic diagrams summarizing two stages in the evolution of a porphyry-epithermal system. In (a), fresh magma has intruded to a shallow depth, causing fumarolic activity at the surface and intermittent volcanic eruptions. Orthomagmatic fluids exsolve from the crystallizing melt and make their way upward until the zone of boiling and potassic alteration is reached. Gold partitions into the dense, saline brine as  $\text{AuCl}_2^-$  and precipitates in the potassic zone due to cooling, dilution, and/or pH changes accompanying boiling. Meanwhile, a rising plume of  $\text{H}_2\text{S}$ -rich steam causes phyllic alteration of the overlying rocks, as well as sulfidation of ferrous iron to pyrite. At shallow depths, mixing with cool meteoric waters causes the vapor plume to condense along its margins, with local advanced argillic alteration. In (b), the water-saturated melt has retreated to deeper levels, allowing invasion of heated meteoric water and widespread phyllic overprinting of earlier potassic alteration.  $\text{H}_2\text{S}$  and other magmatic volatiles are no longer vented to the surface, but are condensed into the potassic zone (a). Migration of metal- and  $\text{H}_2\text{S}$ -enriched meteoric waters may ultimately form a low sulfidation (LS) or high sulfidation (HS) deposit, depending on whether or not the fluids and surrounding country rocks are capable of neutralizing acidic volatiles such as  $\text{HCl}$  and  $\text{SO}_2$ .

20a

F-56

- the slide shows the effect of sector collapse, such as debris avalanches, that may be triggered by volcanic swelling due to synmineralization intrusion and facilitated by hydrothermal weakening of volcanic edifices. Telescoping of the hydrothermal system results.
- collapse leads to rapid influx of meteoric and/or ocean water into the hydrothermal environment and a drop in confining pressure
- the lower pressure may induce boiling, hydrothermal brecciation, and possibly epithermal gold precipitation.
- it may also lead to rapid influx of magmatic fluids
- these systems may have potential to create shallower than normal porphyry deposits that may be giants.

**Slide: Sillitoe example of telescoped alteration overprinting**

- Red Mountain represents a non-telescoped deposit with about 600m separating the K-silicate core and the advanced argillic-sericite zone of high sulphidation type (everything above has been eroded)
- Marte, Chile is a telescoped porphyry gold system developed in diorite porphyry. High sulphidation advanced argillic alteration (A) is juxtaposed against a gold-bearing quartz veinlet stockwork of K-silicate parentage. (with an intermediate argillic (IA) overprint). Acid leached rock (AL) generated above the paleo-water table is nearby

Ladolam, Papua New Guinea, is an extreme example of telescoping in which -silicate-altered monzonite is overprinted by a tabular zone of low sulphidation epithermal gold mineralization. Acid leaching, which is still locally active, affects the monzonite and may overprint the gold mineralization.

**Theoretical Aspects of Gold Distribution in Porphyry and Related Deposits**

**Slide: Gammons and Williams-Jones theoretical treatment - gold porphyry**

Two stages of evolution of a porphyry-epithermal system are shown.

A. fresh magma intruded to shallow depth causing fumarolic activity at surface and episodic volcanic eruptions. Orthomagmatic fluids evolve migrate upward until reaching a zone of boiling and potassic alteration. Gold partitions into the dense, saline brine as  $\text{AuCl}_2$  and precipitates in the potassic zone due to cooling, dilution or pH changes during boiling. At the same time a plume of  $\text{H}_2\text{S}$ -rich steam causes phyllic alteration in the overlying rocks and sulphidation of ferrous iron to pyrite. At shallow depth, mixing with cool meteoric water condenses the edges of the vapor plume leading to local advanced argillic alteration.

B. the water saturated melt has retreated to deeper levels, allowing invasion of heated meteoric water that causes widespread phyllic overprinting of earlier potassic alteration.  $H_2S$  and other magmatic volatile are no longer vented to surface but condensed into the meteoric waters, which increases their capacity to remobilize gold that was previously deposited in the potassic zone developed during stage A. Migration of metal and  $H_2S$ -enriched waters can lead to low sulphidation (LS) or high sulphidation (HS) mineralization if the country rock is able to neutralize these waters.

Key comments in the paper are that:

- magmatic fluids can transport significant quantities of dissolved gold ( $>0.1$  ppm)
- gold is dissolved mainly as  $AuCl_2$  at high temperatures and solubility drops as temperature drops. At lower temperature, the dominant complex becomes  $Au(HS)_2$ , and solubility may increase with cooling. Hence gold in  $H_2S$ -rich fluids tends to be flushed away from the parent intrusion whereas  $H_2S$ -poor fluids tend to deposit gold close to the parent melt.
- the temperature of the transition depends on pH and  $H_2S/Cl$  ratio of the original fluid and whether boiling occurs
- downward collapse of an evolving porphyry system may lead to overprinting of original gold-rich magnetite and potassic alteration zones by retrograde pyrite-rich phyllic alteration. This can result in widespread remobilization of previously deposited gold as bisulphide complexes
- porphyry systems may link to later epithermal gold deposition by providing a large amount of low grade gold protore, by increasing secondary permeability and because of abundant pyrite developed.

---

---

**Slide: Thompson magmatic hydrothermal complex**

Fluid processes affect porphyry mineralization. Although research supports a magmatic-hydrothermal or orthomagmatic model for ore-forming fluids, external fluids play a role. They may be metamorphic or connate waters, meteoric or sea water.

---

---

**Slide: Thompson multi-phase system**

**Porphyry and Related Mineral Deposits**

A wide variety of deposits occur peripherally to porphyry deposits. Deeper types are base +/- precious metal skarns, mantos and replacement bodies. Gold skarns have been targets recently (Gerry Ray will talk about skarns later). Replacement or disseminated styles of gold deposits are spatially associated with porphyry systems, perhaps even Carlin-type

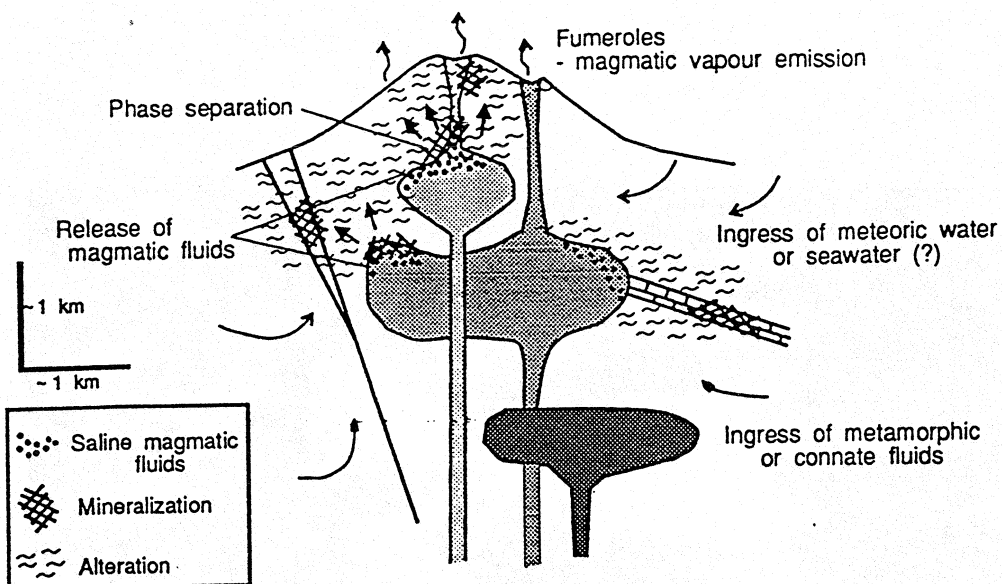
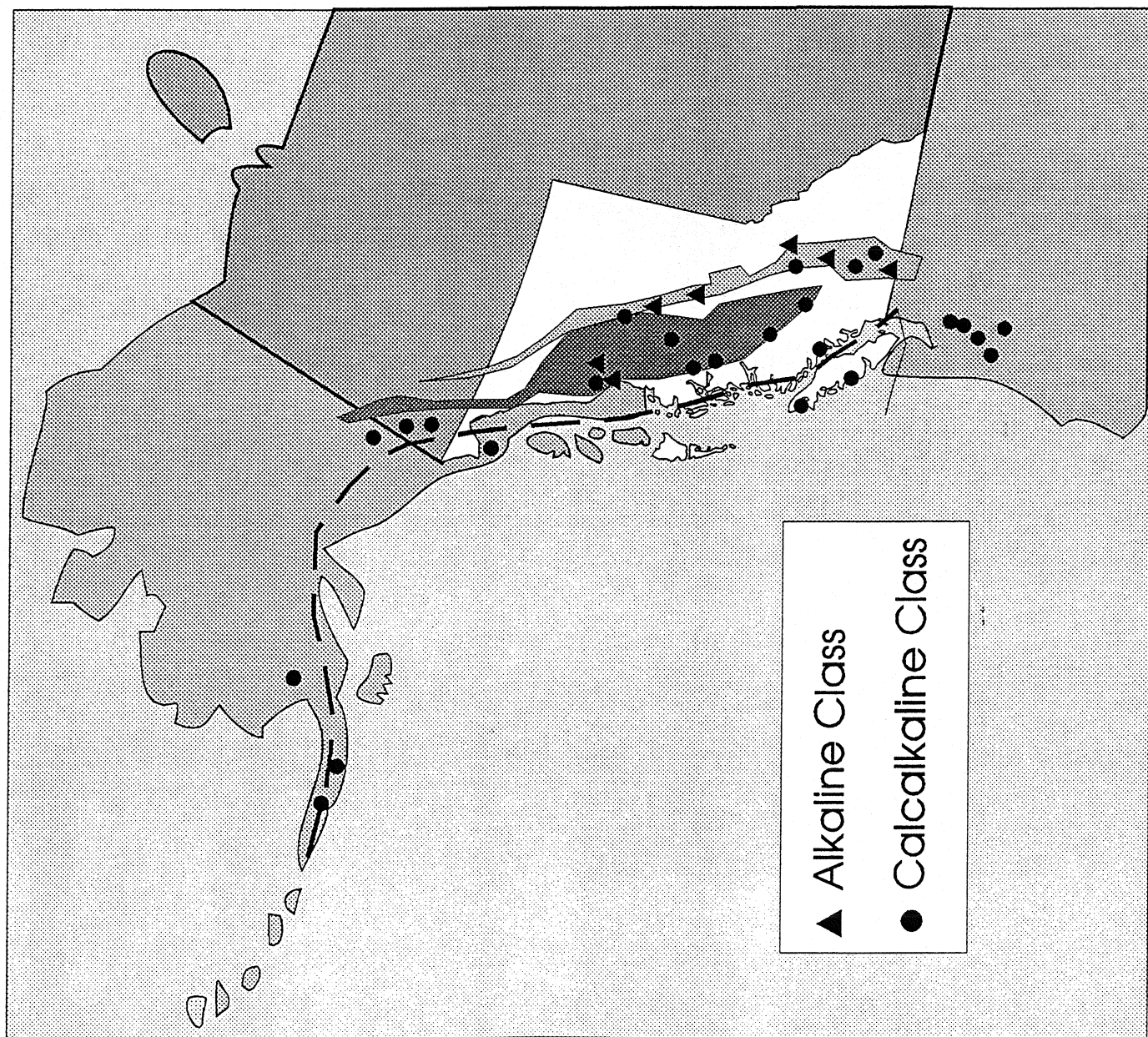


FIGURE 6. Magmatic-hydrothermal complex forming several discrete zones of mineralization within extensive areas of alteration. The potential contribution of external fluids from different sources, magmatic fluids, and hydrothermal processes are shown; see text for discussion.

21a

F-59



deposits. Precious metal-bearing veins also occur, an example being the gold-copper-rich brittle-ductile Twin Zone (Snip Mine) which is adjacent to the Red Bluff porphyry system in the Iskut area of northwestern British Columbia. Nearby precious metal veins on Johnny Mountain, have only brittle textures and formed at shallower depths. Paragenetically late copper-gold veins in the upper parts of many porphyry deposits commonly have high sulphidation mineral assemblages with advanced argillic alteration envelopes. Deposits on the north end of Vancouver Island illustrate these relationships. In summary, there are a continuum of deposit types related to porphyry systems.

---

## **CONCLUSION**

There are a wide variety of calc-alkaline porphyry deposits, and these are mainly related to destructive margin plate tectonic processes. In the Canadian Cordillera, the development of Mesozoic SW Pacific type island arcs played a key role but Eocene continental arcs were also important for development of copper +/- molybdenum +/- gold, molybdenum and gold porphyries.

## **Bibliography and References**

Most references cited can be found in the listing in the accompanying paper: Regional Geological and Tectonic Setting of Porphyry Deposits in British Columbia and Yukon Territory.

In addition are the following:

Armstrong, R.L., 1988. Mesozoic and Early Cenozoic magmatic evolution of the Canadian Cordillera. *in* Rogers Symposium Volume, *Geological Society of America*, Special Paper 218, p. 55-91.

Bodnar, R.J., 1995. Fluid-inclusion evidence for a magmatic source for metals in porphyry copper deposits. *in* Magmas, Fluids and Ore Deposits, J.F.H. Thompson, Editor, *MDRU Short Course* volume 23, p. 139-152.

Gammons, C.H. and Williams-Jones, A.E., 1997. Chemical mobility of gold in the porphyry epithermal environment. *Economic Geology*, vol. 92, p. 45-59.

Sillitoe, R.H., 1994. Erosion and collapse of volcanoes: Causes of telescoping in intrusion-centered ore deposits. *Geology*, Vol. 18, p. 945-948.

Williams, S.A. and Forrester, J.D., 1995. Characteristics of porphyry copper deposits. *in* Porphyry Copper Deposits of the American Cordillera, F.W. Pierce and J.G. Bolm, Editors, *Arizona Geological Society Digest*, 20, p. 21-34.

F-62

## G - ALKALIC Cu-Au-Ag PORPHYRY DEPOSITS IN THE CANADIAN CORDILLERA: TECTONIC SETTING, MAGMATIC AFFILIATIONS AND HYDROTHERMAL CHARACTERISTICS

James R. Lang, John F.H. Thompson, and Clifford R. Stanley, The University of British Columbia

Lang, R.R., Thompson, J.F.H. and Stanley, C.R. (1998): Alkalic Cu-Au-Ag Porphyry Deposits in the Canadian Cordillera: Tectonic Setting, Magmatic Affiliations and Hydrothermal Characteristics; in *Metallogeny of Volcanic Arcs*, B.C. Geological Survey, Short Course Notes, Open File 1998-8, Section G.

### ABSTRACT

Porphyry ore systems are widespread in the Canadian Cordillera and formed during two major episodes in the Early Mesozoic and Late Cretaceous to Early Tertiary. Most of these deposits are calc-alkalic, Cu-Mo-Ag-Au systems, but a subset of distinctive Cu-Au deposits is associated with alkaline igneous rocks which were emplaced mostly between 210 and 200 Ma. The alkaline deposits are spatially restricted to primitive volcanic arc sequences of the Stuhini, Takla and Nicola Groups in the Quesnel and northern Stikine terranes and comprise two K-rich magmatic affiliations. The first group (e.g., Galore Creek, Rayfield River) is associated with silica-undersaturated alkaline magmatic complexes and is found in both Quesnellia and Stikinia. The second group (e.g., Copper Mountain, Mt. Milligan) is associated with silica-saturated alkaline complexes and is located mostly in Quesnellia. The intrusions of both groups have primitive  $^{87}\text{Sr}/^{86}\text{Sr}$  (0.70330.0003) and NdT (+2.7 to +7.9) signatures, and a petrogenetic link between the two types is suggested by the coexistence of saturated and undersaturated igneous rocks in some systems (e.g., Lorraine, Mount Polley).

Saturated complexes are hosted by augite and plagioclase phyric shoshonitic basalt and andesite and cut by multiphase intrusive complexes. Intrusions vary in size from small batholiths to plutons and dike swarms, and comprise equigranular to porphyritic diorite to monzonite with rare syenite. Phenocrysts include major augite and plagioclase, more variable magnetite, hornblende, biotite and apatite, and rare titanite. K-feldspar is abundant in the matrix and the intrusions contain up to 15% total magnetite. Trace quartz is observed in only a few stocks. Most recognized saturated complexes contain Cu-Au mineralization.

Mineralization in undersaturated complexes is less consistently developed. Strongly mineralized systems are related to emplacement of multiphase intrusive complexes into shoshonitic basalts and/or feldspathoid-bearing phonolites. Intrusions are dominated by porphyritic to megacrystic syenite with K-feldspar megacrysts (to 25 cm) accompanied by augite, biotite, magnetite and apatite, and more rarely by plagioclase, titanite, pseudoleucite and/or melanite garnet phenocrysts. Undersaturated systems with little to no mineralization are characterized by coexisting syenite and lesser pyroxenite, typically in smaller, concentrically zoned or layered bodies; mineralization is erratic and restricted to small skarn or veinlet-controlled Cu-Au zones.

The characteristics of alteration correspond to the range in magmatic composition from strongly undersaturated to saturated. Alteration is quartz-absent and is characterized by distinctive Na-rich (albite, scapolite, analcite) and Ca-rich (andradite, diopside, actinolite, calcite, anhydrite) mineral



assemblages, in addition to magnetite-rich potassic assemblages (biotite, K-feldspar). Mineralization may be associated with Ca-, Na- and/or K-rich assemblages. Propylitic alteration is typically early and peripheral, but spatial and temporal relationships among other assemblages vary. Sericitic and argillic assemblages are generally absent to minor, and trace quartz is found only in late stage alteration in a few saturated systems.

Alkalic deposits range up to 400M tonnes but are generally smaller, and typical grades are 0.25-0.5% Cu and 0.35-0.75 ppm Au with locally higher grade subzones. The characteristic metal assemblage is Cu-Au-Ag, with no significant Mo. Mineralization is low in total sulphide, and is both disseminated and fracture controlled. Chalcopyrite and lesser bornite are the main ore minerals and have high ratios to pyrite. Cu and Au are usually well correlated, but Cu/Au ratios vary between and locally within deposits, and may be spatially zoned. Local disruption of the Cu to Au correlation reflects preferential redistribution of Au during late, low temperature overprints in some systems. The low pyrite and high carbonate concentrations in the ores inhibited secondary Cu enrichment.

Hydrothermal P-T conditions were generally similar to calc-alkalic deposits. Early fluid inclusions at Galore Creek homogenize at up to 650°C, have salinities to 77 wt% NaCl equiv., compositions in the H<sub>2</sub>O-KCl-NaCl-CaCl<sub>2</sub> system and formed at P<650bars; later fluids were cooler and less saline but of similar composition. Mineralogical, fluid inclusion and stable isotope data support a magmatic origin for the hydrothermal fluids. Fluids were released from magmas in undersaturated complexes both earlier and more passively than in saturated complexes, and fracture densities are much lower in both alkalic subtypes than in calc-alkalic deposits.

High-K calc-alkalic Cu-Mo-AgAu, saturated alkalic Cu-Au and undersaturated alkalic Cu-Au deposits form a continuum across the alkalic end of the porphyry deposit spectrum. Alkalic intrusive rocks similar to those which host Cu-Au deposits in British Columbia have been described from several widespread shoshonitic volcanic belts, suggesting that they may also be prospective for Cu-Au deposits. Successful exploration models for these belts must recognize and incorporate the magmatic, hydrothermal and tectonic characteristics which distinguish alkalic from calc-alkalic porphyry systems.

## Chapter 16

# Na-K-Ca MAGMATIC-HYDROTHERMAL ALTERATION IN ALKALIC PORPHYRY Cu-Au DEPOSITS, BRITISH COLUMBIA

James R. Lang, Clifford R. Stanley, John F. H. Thompson, Kathryn P. E. Dunne

*Mineral Deposit Research Unit, Department of Geological Sciences, University of British Columbia,  
Vancouver, British Columbia, Canada V6T 1Z4*

### INTRODUCTION

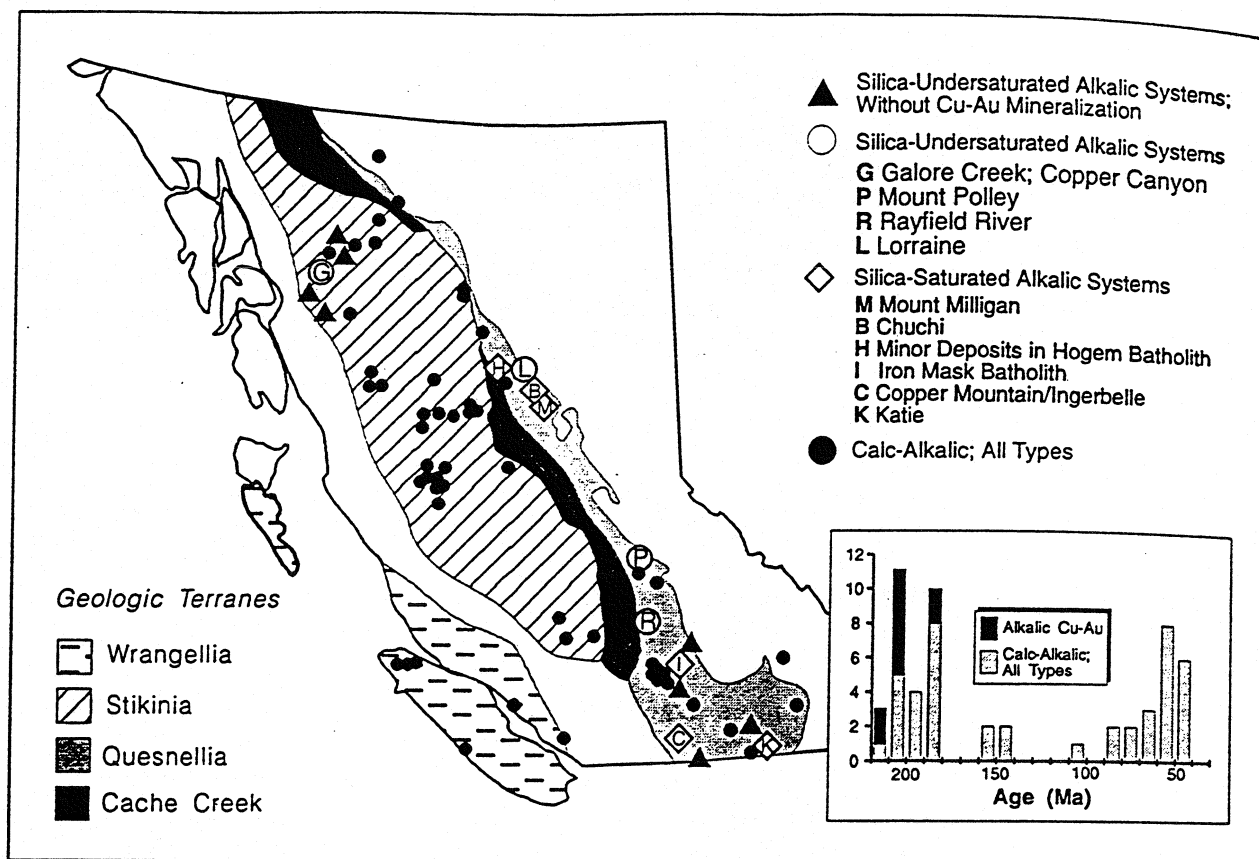
In the Canadian Cordillera, porphyry ore deposits formed within several tectonostratigraphic terranes, and along the margin of ancestral North America, between Late Triassic and Eocene time (Fig. 1). Most of these porphyry systems contain Cu-Mo  $\pm$  Au deposits that formed in response to emplacement of low- to high-K<sub>2</sub>O calc-alkalic intrusive complexes in magmatic arc settings and are typical of the class worldwide (McMillan & Panteleyev 1994; McMillan *et al.* 1995; Sutherland Brown 1976). Among these deposits, Barr *et al.* (1976) recognized the alkaline suite of porphyry deposits (Fig. 1), a subgroup that is temporally restricted to the Early Mesozoic Quesnel and Stikine terranes in British Columbia and which is distinguished by: (1) an association with alkalic igneous rocks, (2) a metal assemblage of Cu-Au-Ag with no significant Mo, and (3) distinctive alteration, including assemblages characterized by Na- and Ca-bearing minerals (Na-rich and Ca-rich assemblages hereafter), accompanied by magnetite-rich potassic alteration and typical propylitic alteration, with a near-absence of sericitic, argillic and advanced argillic assemblages. In this paper we consider the hydrothermal characteristics of alkalic Cu-Au porphyry deposits, including: (1) the mineralogy, paragenetic sequence, and zoning relationships among the major alteration assemblages, (2) the constraints on fluid composition, and (3) a comparison of Na-rich and Ca-rich alteration assemblages in alkalic systems to similar assemblages described from other hydrothermal environments. We conclude by presenting a model that describes the relationship between the major alteration assemblages and the composition

and evolution of the associated alkalic magmas.

### TECTONIC SETTING AND MAGMATIC ASSOCIATIONS

The alkalic Cu-Au deposits are restricted to Quesnellia and northern Stikinia (Fig. 1). These terranes are dominated by volcanic rock sequences that formed in an intraoceanic island-arc environment (Souther 1991; Gabrielse *et al.* 1991). The volcanic sequences comprise the Nicola and eastern Takla groups in Quesnellia, and the Stuhini and western Takla groups in northern Stikinia. Each sequence includes suites of both alkalic and calc-alkalic composition (Mortimer 1987; Preto 1977) overlain unconformably by Middle Jurassic volcanic sequences. Recent U-Pb dating by Mortensen *et al.* (1995) has shown that the majority of the alkalic deposits formed between 211 and 200 Ma. This age range corresponds to the unconformity between Late Triassic and Early to Middle Jurassic volcanic sequences and may reflect a volcanic hiatus or a period of restricted magmatic activity resulting from a change in subduction-zone dynamics or morphology (Lang *et al.* 1995). Two deposits are significantly younger, Mount Milligan (183 to 189 Ma) and Katie (an inferred age of about 185 Ma; Cathro *et al.* 1993), with ages that coincide with the collision of the Quesnel terrane, host to the deposits, with ancestral North America.

The alkalic suite magmatic-hydrothermal complexes in British Columbia have been subdivided by Lang *et al.* (1994) into silica-saturated and silica-undersaturated types (Fig. 1). Silica-saturated complexes in British Columbia are characterized by: (1) alkalic igneous rocks that typically either lack, or have very minor,



**Figure 1.** Location of alkalic Cu-Au porphyry deposits in British Columbia. Inset shows reported radiometric ages for porphyry deposits in British Columbia; data for alkalic deposits are from Mortensen *et al.* (1995).

normative quartz or feldspathoid, and only rarely contain very minor modal quartz (usually restricted to late-stage intrusions); (2) diorite/gabbro to monzonite compositions only rarely accompanied by minor pyroxenite and syenite; (3) equigranular to porphyritic igneous textures; and (4) associated volcanic rocks of the Takla or Nicola groups that are augite-phyric and mafic to intermediate in composition. Although individual silica-saturated magmatic complexes typically include 'barren' intrusions which are not directly related to hydrothermal mineralization, Cu-Au mineralization is genetically related to at least one intrusive stage in each complex identified to date. Silica-saturated systems (Fig. 1) include Copper Mountain/Ingerbelle (Stanley *et al.* 1995), Katie (Cathro *et al.* 1993), the Iron Mask batholith (Lang & Stanley 1995; Ross *et al.* 1995), and Mount Milligan (Barrie 1993; Sketchley *et al.* 1995).

Silica-undersaturated systems in British Columbia are characterized by: (1) alkalic intru-

sions with ubiquitous normative feldspathoids, and commonly modal feldspathoids or other silica-undersaturated mineral phases (*e.g.*, melanite garnet); (2) intrusions dominated by syenite with lesser but significant pyroxenite, which in several complexes form zoned plutons with textural evidence for gravitational segregation of pyroxenite; (3) variable amounts of igneous rocks of intermediate composition that are magmatic or mineralogical combinations of the syenite and pyroxenite end-members (Lueck & Russell 1994); (4) megaporphyritic igneous textures; and (5) associated volcanic rocks that, where preserved, commonly include feldspathoid-bearing sequences in addition to augite-phyric units similar to those that host silica-saturated intrusions. In contrast to silica-saturated complexes, the silica-undersaturated systems include a group that hosts major Cu-Au mineralization, including Rayfield River, Galore Creek (Enns *et al.* 1995), and Copper Canyon (Bottomer & Leary 1995), and a second group of petrologically

Table 1. Reserves in alkalic porphyry Cu-Au deposits

	Million Tonnes	Cu %	Au ppm	Ag ppm	Reserve Type	Source
Mount Milligan	299	0.22	0.450		mineable	Sketchley <i>et al.</i> (1995)
BP-Chuchi	50	0.21-0.4	0.21-0.44		geologic	Nelson <i>et al.</i> (1991)
Lorraine	10	0.70	0.343		geologic	Bishop <i>et al.</i> (1995)
Copper Mtn Ca	167.7	0.46	0.127	1.72	production	Stanley <i>et al.</i> (1995)
Afton	30.8	0.77	0.580	4.2	mineable/prod	Kwong (1987)
Ajax	20.7	0.45	0.340		mineable/prod	Ross <i>et al.</i> (1995)
Pothook	3.26	0.35	0.770		production	L. Bond (pers. comm.)
Big Onion	2.4	0.84	0.400	8	mineable	Vollo (1985)
DM	2.685	0.38	0.270		geologic	L. Bond (pers. comm.)
Crescent	1.448	0.44	0.180		production	L. Bond (pers. comm.)
Katie	small	0.04-1	low 0.x			Cathro <i>et al.</i> (1993)
Galore Creek	125	1.06	0.400	7.7	proven	Kennecott (pers. comm.)
Mount Polley	48	0.44	0.583	4.5	mineable	Fraser <i>et al.</i> (1995)

similar complexes (Lueck & Russell 1994) that have no associated Cu-Au mineralization (Fig. 1).

Several alkalic complexes contain both silica-saturated and silica-undersaturated igneous rocks. Within the Hogem batholith (Fig. 1), the Lorraine deposit (Bishop *et al.* 1995) is located within the Duckling Creek complex which includes silica-undersaturated syenite and melanite-bearing biotite pyroxenite, and silica-saturated rocks of intermediate composition. Mineralization at Mount Polley (Fraser 1994a,b; Fraser *et al.* 1995) is hosted by the silica-saturated Mount Polley diorite and monzonite complex that is adjacent to an intrusion dominated by pseudoleucite-bearing syenite. Several unmineralized complexes also contain silica-undersaturated and silica-saturated to oversaturated rocks that are temporally and spatially coincident (Lang *et al.* 1995).

#### HYDROTHERMAL CHARACTERISTICS AND RELATIONSHIPS

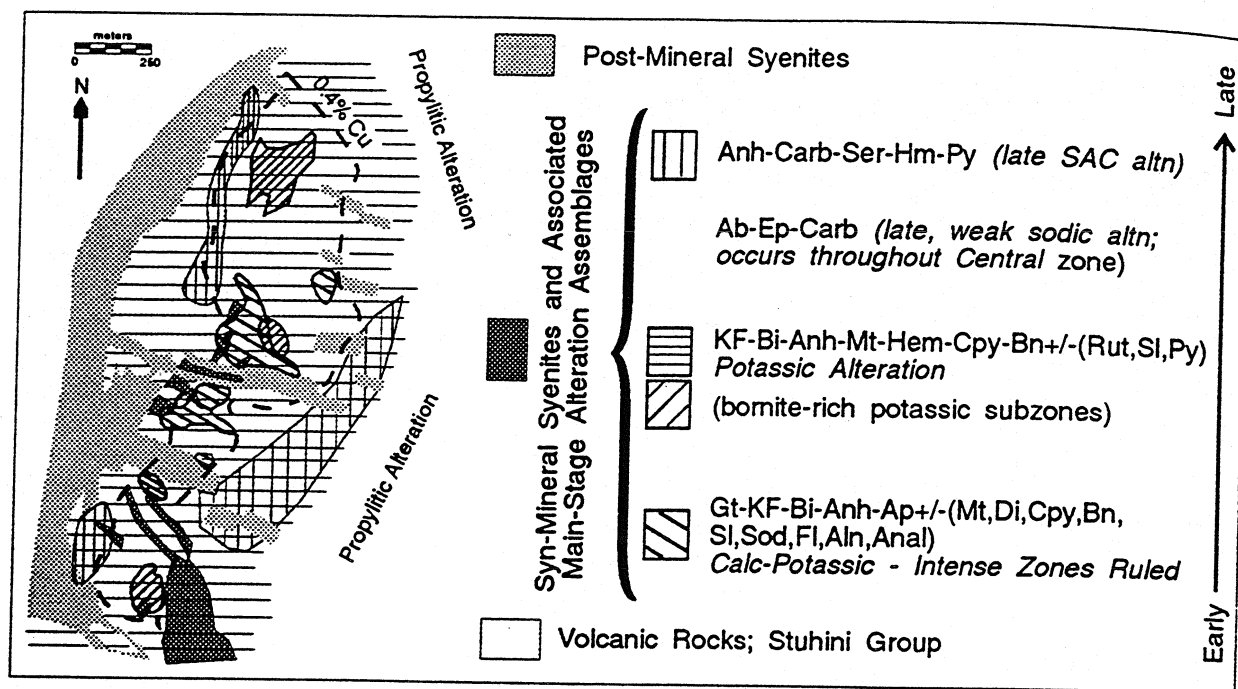
Documentation of the relationship of Na-rich and Ca-rich alteration assemblages to magmatic events and other hydrothermal alteration assemblages is prerequisite to understanding the origin and evolution of the hydrothermal fluids. The following sections summarize the field and petrographic characteristics of hydrothermal alteration and mineralization at Galore Creek, Mount Polley, Copper Mountain, and in the Iron Mask batholith, for which our documentation of

these relationships is most complete. Na-rich alteration also occurs at Mount Milligan, but its relationship to other alteration assemblages is not well-constrained and it is not described further. Grade and tonnage of the alkalic deposits are summarized in Table 1.

#### Galore Creek

The geology of Galore Creek has been described most recently by Enns *et al.* (1995). Hydrothermal alteration is developed within a silica-undersaturated, multiphase complex of at least twelve stages of syenite intrusion which cut alkalic, augite-phyric intermediate volcanic rocks and pseudoleucite-bearing phonolites. The district includes twelve zones of Cu-Au mineralization. The largest deposit, and the focus of this description, is the northerly-elongated Central zone, in which mineralization formed within and adjacent to syenites that intruded early in the sequence of magmatic events. However, hydrothermal activity continued, perhaps episodically, until the very latest stages of intrusive activity, and this later mineralization is found most commonly in the matrix of, and in fragments within, orthomagmatic and diatreme breccias. The distribution and paragenetic sequence of the major alteration assemblages in the Central zone are summarized in Figure 2.

Alteration in the core of the Central zone is dominated by an assemblage that is characterized both by Ca-bearing and K-bearing minerals,



**Figure 2.** Geology (simplified from Enns *et al.* 1995) and alteration paragenesis for the Central zone, Galore Creek. Mineral abbreviations in this and subsequent diagrams are: ab albite; act actinolite; aeg aegerine; aln allanite; anal analcime; anh anhydrite; ap apatite; arfved arfvedsonite; bi biotite; bn bornite; cal calcite; carb carbonate; chl chlorite; cpy chalcopyrite; di diopside; dolo dolomite; ep epidote; fl fluorite; gl galena; gt garnet; hem hematite; KF potassium feldspar; mt magnetite; py pyrite; qtz quartz; rieb riebeckite; rut rutile; scap scapolite; ser sericite; sl sphalerite; sod sodalite; tim titanite; tour tourmaline; verm vermiculite. Parenthesized phases indicate minor occurrence.

which we hereafter refer to as a calc-potassic assemblage. The calc-potassic alteration is intense and is characterized by disseminations and massive replacements, and to a lesser degree by veins and envelopes around fractures, in both the syenites and their volcanic wallrocks. The paragenetic sequence of this early alteration includes an initial stage of apatite and strongly zoned andradite garnet precipitation, an intermediate stage in which apatite, garnet, biotite and K-feldspar are the major stable assemblage, and a later stage in which garnet is partly replaced by biotite and K-feldspar. The garnets typically have compositions of  $Ad_{75-90}$  and  $TiO_2$  concentrations between 0.1 and 4.9 wt.% (Lang *et al.* 1993; Lang 1994), but a few grains contain minor, sharply-bounded grossular zones. Anhydrite is locally intergrown with, but is more commonly interstitial to or replaces the garnet, and is also found as fill in dilatant fractures. Minor minerals that are difficult to place in a definite temporal sequence,

but which seem to be mostly later than garnet, include chalcopyrite, bornite, sphalerite, galena, diopside, albite, carbonate, analcime, sodalite, scapolite, allanite, and fluorite.

Toward the northern and southern ends of the Central zone, the calc-potassic core yields to a potassic assemblage of K-feldspar - biotite - anhydrite-magnetite-hematite-chalcopyrite-bornite  $\pm$  rutile  $\pm$  sphalerite  $\pm$  pyrite. The style and intensity of this potassic alteration are similar to those observed in the calc-potassic core, but the precise timing between these two assemblages has not been fully resolved. Locally, albite-epidote veins are found within the areas affected by calc-potassic and potassic alteration. All alteration assemblages are locally overprinted by a sericite-anhydrite-carbonate assemblage.

Throughout the Central zone, mineralization is found in disseminated and minor fracture-controlled styles. Chalcopyrite is the major sulfide throughout the deposit, but is accompanied by

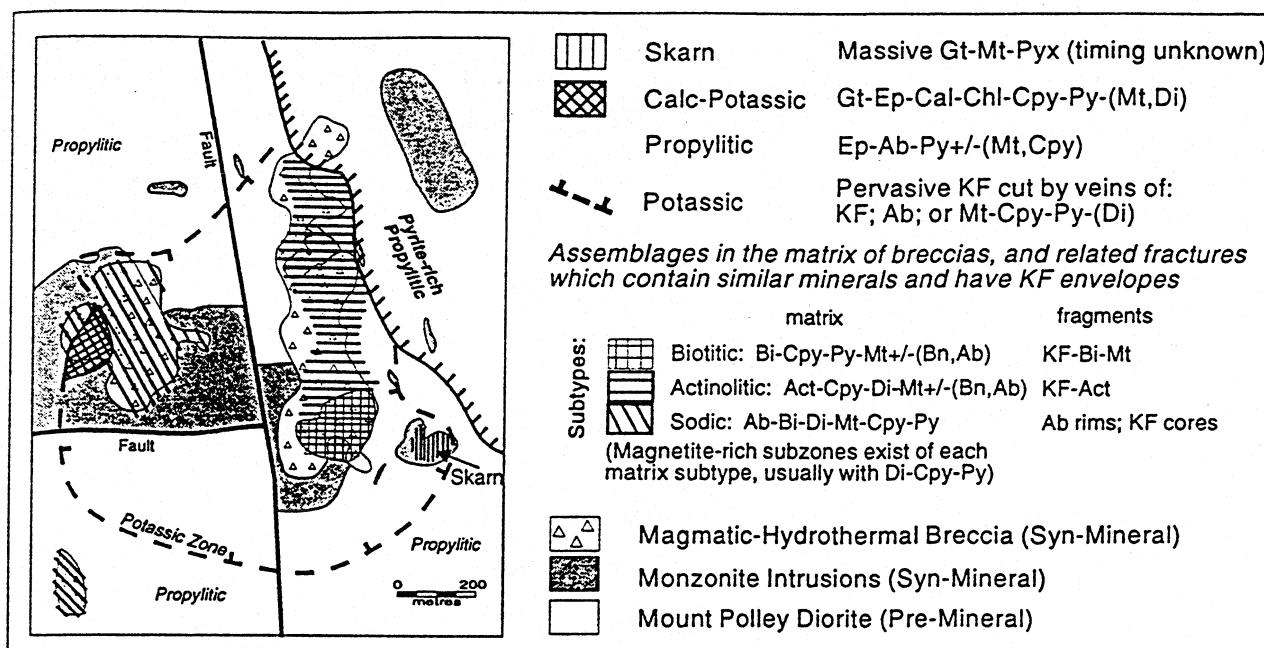


Figure 3. Simplified geology and alteration paragenesis in the Mount Polley deposit. Distribution of units is simplified from Fraser (1994b). See Figure 2 for abbreviations.

significant bornite in the northern and southern ends of the deposit (Fig. 2). Within the ore zone pyrite is minor to absent, but it increases to 5% in calcite-chlorite-pyrite propylitic alteration to the north and east. The Cu grade is relatively constant throughout the Central zone, but the Au grade increases slightly toward both the north and south.

### Mount Polley

The Mount Polley system has been described most recently by Fraser (1994a,b) and Fraser *et al.* (1995). Mineralization at Mount Polley is hosted by a silica-saturated diorite intrusion but, on the basis of crosscutting relationships and zoning of alteration, is temporally related to younger, silica-saturated monzonite plugs and dykes. The district also contains a pseudoleucite-bearing syenite intrusion and volcanic rocks both with and without feldspathoids, but the petrogenetic relationship between the silica-undersaturated rocks and the silica-saturated intrusions has not been established.

Hydrothermal effects at Mount Polley are associated with magmatic-hydrothermal breccias that formed adjacent to the plagioclase-phyrlic

monzonite porphyry intrusions (Fig. 3). Alteration and mineralization are found in the matrix of the breccias, in altered fragments within the breccias, and in veins and vein swarms distributed around the breccias. The breccias have been subdivided into four types on the basis of the major mineral in the matrix: (1) actinolite (with chalcopryrite-diopside-magnetite-calcite-pyrite  $\pm$  bornite); (2) biotite (with chalcopryrite-pyrite-magnetite  $\pm$  bornite  $\pm$  albite); (3) magnetite (with diopside-chalcopryrite-pyrite); and (4) albite (with biotite-diopside-magnetite-chalcopryrite-pyrite). The actinolite breccias commonly have fragments with relatively unaltered cores and pervasively K-feldspar-altered margins, whereas fragments in the biotite and magnetite breccias are pervaded by K-feldspar-biotite-magnetite alteration. Fragments in albite breccias commonly grade from albitized margins ( $An_{01-02}$ ; Fraser 1994b) to K-feldspar-altered cores, and this pattern may represent a Na-rich overprint on preexisting potassic alteration, or mineralogical zoning during a single episode of hydrothermal alteration.

The hydrothermal breccias yield outward to rocks cut by veins. Sinuous veins dominated by actinolite with K-feldspar envelopes are found

near and within the actinolite breccias. Discontinuous stringers of magnetite-chalcopyrite  $\pm$  diopside  $\pm$  pyrite with K-feldspar envelopes and sinuous, unfilled fractures with K-feldspar envelopes are found throughout the core of the system. The early, irregular veins are cut by planar, dilatant fractures filled with magnetite-chalcopyrite-bornite which grade outward to magnetite-chalcopyrite-pyrite veins. Near the albite breccias, veins with K-feldspar envelopes are crosscut by albite-diopside veins. Locally, the alteration envelopes coalesce to form pervasive alteration.

The area that encompasses alteration dominated by K-feldspar and the magmatic-hydrothermal breccias is surrounded by low- to high-sulfide, fracture-controlled propylitic alteration consisting of epidote-albite-chlorite-pyrite  $\pm$  magnetite  $\pm$  trace chalcopyrite which is interpreted from crosscutting relationships to have formed at approximately the same time as potassic alteration. Near the contact between the potassic and propylitic assemblages is a zone of pervasive and fracture-controlled andradite-K-feldspar-albite-epidote-chalcopyrite-pyrite  $\pm$  magnetite  $\pm$  diopside alteration. This calc-potassic alteration overprints the potassic and propylitic assemblages and an albite breccia. A zone of massive andradite-clinopyroxene-magnetite skarn with minor chalcopyrite and trace pyrite is located in the southeastern part of the deposit (Fig. 3), but its timing relative to other alteration assemblages is unknown.

### ***Iron Mask Batholith***

The Iron Mask batholith is a composite, alkalic intrusive complex hosted by Nicola Group volcanic rocks. The magmatic rocks in the batholith (Fig. 4), described in detail by Snyder & Russell (1995), were emplaced in the following sequence: (1) the Pothook clinopyroxene diorite, and the Hybrid clinopyroxene diorite, the latter an intrusion breccia phase of the Pothook diorite; (2) the Cherry Creek clinopyroxene monzodiorite to monzonite; and (3) the hornblende-phyric Sugarloaf diorite. On the basis of Pearce element-ratio analysis (Snyder & Russell 1995), the Pothook and Cherry Creek phases are interpreted

to have a direct petrogenetic relationship to each other, whereas the geochemical composition of the Sugarloaf diorite cannot be directly derived from the earlier intrusions.

Three distinct styles of hydrothermal alteration and mineralization formed in association with intrusion of the Pothook, Cherry Creek, and Sugarloaf phases of the batholith, respectively, and one or all may be present in the numerous zones of Cu-Au mineralization (Fig. 4). Within the Pothook diorite, hydrothermal fluids formed large, dilatant magnetite-apatite-amphibole veins which do not contain significant Cu or Au (Cann 1979). The second hydrothermal event formed zones of pervasive K-metasomatism along both sides of the contact between the Cherry Creek and Pothook phases where either intrusion breccias or intense fracturing focussed fluid flow (Lang & Stanley 1995). This alteration, which forms the major assemblage in the Crescent and DM deposits, and is also present in the Afton and Pothook deposits, comprises K-feldspar  $\pm$  biotite  $\pm$  magnetite. Sulfides in this assemblage are disseminated or in microfractures, and the sulfide concentration is highest in zones characterized by secondary biotite; additional Cu-Au mineralization precipitated during several subsequent stages of vein formation (Lang & Stanley 1995). In addition, many similar but sulfide-barren zones of K-metasomatism are found along the margins of intrusions of the Cherry Creek phase throughout the northern end of the batholith (Lang & Stanley 1995). Minor quartz accompanies pervasive alteration at Crescent. In the DM zone, quartz-sulfide veins are common and are the only example of significant silica precipitation among the alkalic porphyry deposits investigated. The third major hydrothermal episode resulted in Na-rich alteration in the Big Onion, Afton, Galaxy, Pothook, and Ajax East and West deposits, and is spatially and temporally associated with intrusions of Sugarloaf diorite (Lang & Stanley 1995; Ross *et al.* 1995). A critical characteristic of alteration in the batholith is that Na-rich alteration is never associated with intrusions of the Cherry Creek phase, whereas Sugarloaf intrusions, varying from large stocks to dykes less than one meter in width and located throughout the batholith, are almost

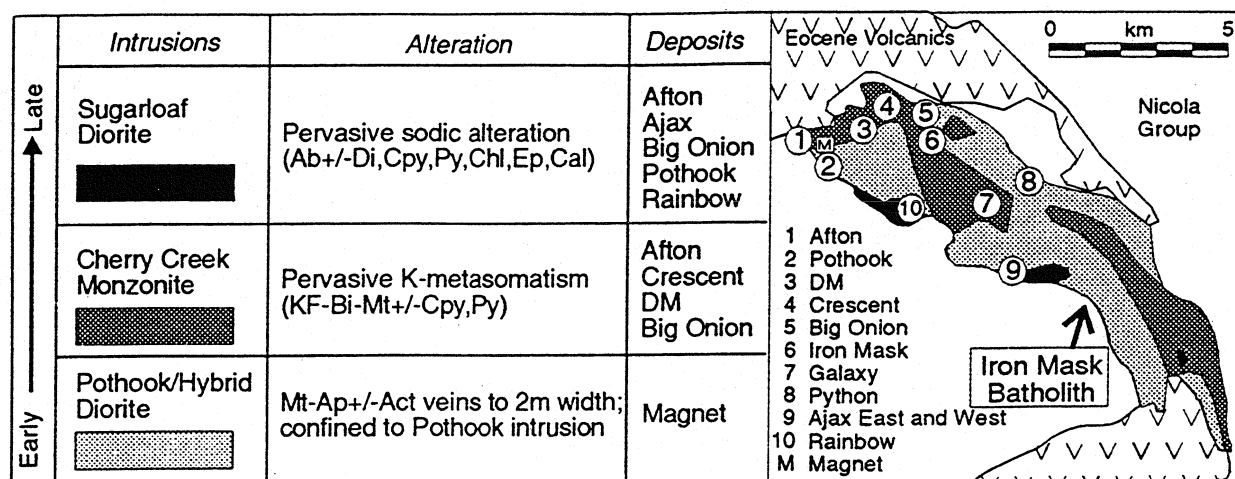


Figure 4. Location of Cu-Au deposits and the sequence of magmatic and hydrothermal events in the Iron Mask batholith. The geology is simplified from Snyder (1994); intrusions and dykes of Sugarloaf diorite occur throughout the batholith but are too small to show. See Figure 2 for abbreviations.

invariably affected by Na-rich alteration without accompanying K-rich alteration.

In the Ajax East and West deposits (Ross *et al.* 1995), Na-rich alteration (Fig. 5) is characterized by selectively pervasive replacement of plagioclase by chessboard-twinned albite, and by diopside after igneous hornblende and clinopyroxene. Na-rich alteration varies from incipient to intense, and its pervasive character commonly results from coalescence of alteration

envelopes around dilatant albite-diopside-epidote-pyrite-chalcopryrite veins which comprise 0 to 15 vol. % in zones of intense Na-rich alteration. In intensely altered zones, titanite with magnetite inclusions replaced diopside. Na-rich assemblages are locally replaced by prehnite and are crosscut by sulfide-bearing pumpellyite and calcite veins. The Cu and Au grades have a strong statistical correlation with Na-rich alteration of moderate intensity, but grades of both metals diminish

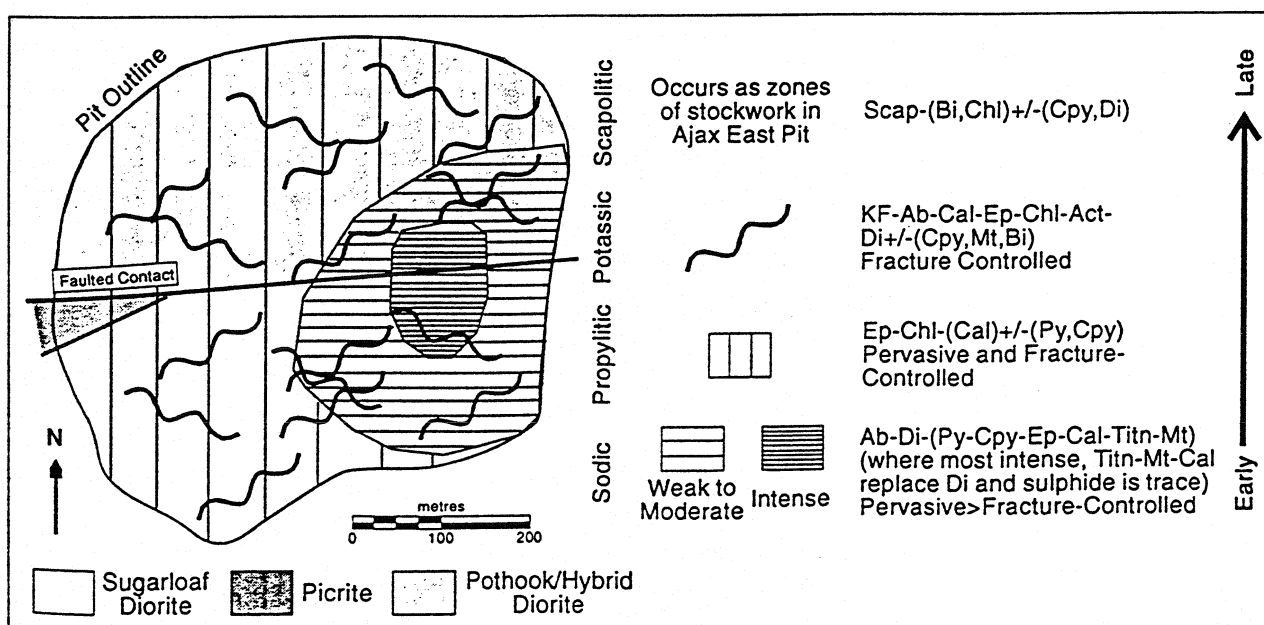


Figure 5. Simplified geology and alteration paragenesis in the Ajax West deposit, Iron Mask batholith. Geology and alteration have been simplified from Ross *et al.* (1995). See Figure 2 for abbreviations.



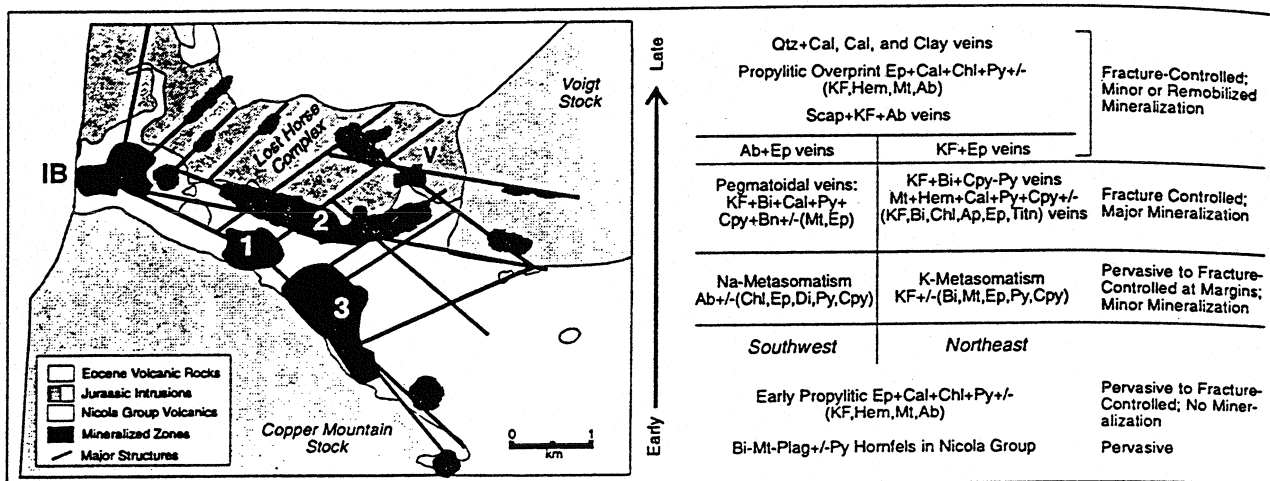


Figure 6. Simplified geology of the Copper Mountain district. Geology simplified from Preto (1972). See Figure 2 for abbreviations.

sharply as the intensity increases (Ross 1993). On the basis of mutual crosscutting relationships, the Na-rich alteration has been interpreted as generally coeval with the propylitic alteration which surrounds it (Ross *et al.* 1995). Potassic alteration is expressed as swarms of sub-parallel veins that cut both pervasive Na-rich and propylitic alteration. Potassic veins contain K-feldspar, minor albite, calcite, epidote, and diopside, and trace chalcopyrite. The veins commonly have selvages of chlorite, calcite, and actinolite and envelopes of K-feldspar and actinolite. (In this paper, selva is defined as a mineral coating on the inside wall of a dilatant vein, whereas an envelope is alteration in the wallrock of the vein). Minor disseminated biotite occurs locally. Younger marialitic scapolite alteration occurs as minor stockworks in the Ajax East pit, and is accompanied by minor biotite, chlorite, chalcopyrite and diopside. The average composition of 23 electron microprobe analyses of scapolite (Ross 1993) is  $(\text{Na}_{2.6}\text{Ca}_{0.9}\text{K}_{0.2}\text{Fe}_{0.01})\text{-(Al}_{1.7}\text{Si}_{7.6})\text{(O}_{23.1}\text{Cl}_{0.9}\text{OH}_{0.1})$ .

The composition of secondary feldspars has been reported by Ross (1993). A feldspar grain in a potassic vein which cuts the propylitic zone has an albite core ( $\text{An}_{06}$ ) and a margin of orthoclase ( $\text{Or}_{96}$ ). Veins that cut pervasively albitized Sugarloaf diorite contain albite ( $\text{An}_{03}$ ), orthoclase ( $\text{Or}_{96}$ ), and a feldspar of intermediate composition ( $\text{Or}_{30}\text{Ab}_{69}\text{An}_{01}$ ). Feldspar from pervasive Na-rich

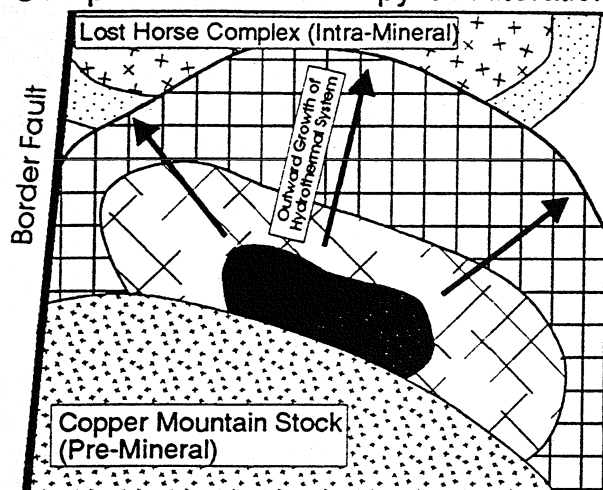
alteration in Sugarloaf diorite is  $\text{An}_{<06}$ .

The recently discovered Rainbow zone (Fig. 4) contains significant Cu-Au mineralization hosted by an intrusion of Sugarloaf diorite. Although we have not yet examined this zone, J. Oliver (personal comm. 1995) reports that, in contrast to other examples of altered and mineralized Sugarloaf diorite, this intrusion has been only weakly affected by Na-rich alteration. More importantly, the zone contains distinctive alteration that is largely confined to the intrusion and that is defined by Ca-bearing minerals which include zoned andradite garnet accompanied by, or zoning outward to, a diopside-hedenbergite-actinolite assemblage. K-feldspar and chlorite (after biotite?) are also present, but their relationship to the Ca-rich assemblage is not yet known. This alteration may be similar to the calc-potassic assemblage at Mount Polley and Galore Creek.

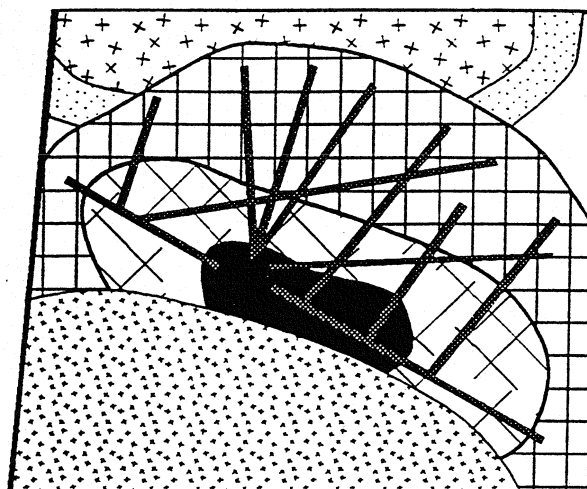
### Copper Mountain/Ingerbelle

In the Copper Mountain district (Stanley *et al.* 1995; Fig. 6), Nicola Group volcanic rocks were intruded by the Copper Mountain stock, a large intrusion that is concentrically zoned from a margin of diorite to a core of syenite, and by the Smelter Lake and Voigt stocks which are petrographically similar to the diorite phase of the zoned stock. The plutons and volcanic rocks were subsequently intruded by diorite to monzonite

- ① Pervasive Propylitic; Overprints Hornfels
- ② Pervasive Sodic + Potassic Alteration Overprint Pervasive Propylitic Alteration



- ③ Potassic Veins and Main Mineralization



- ④ Collapse; Propylitic Assemblage Veins

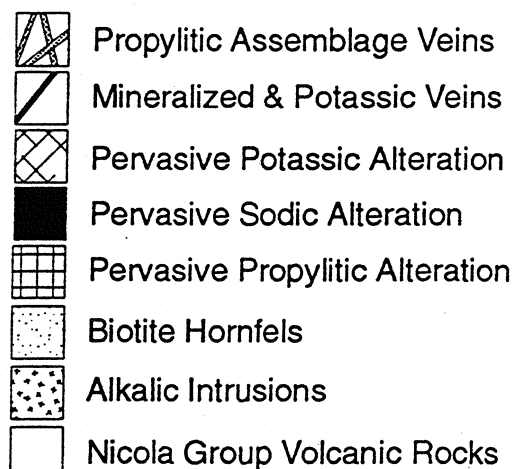
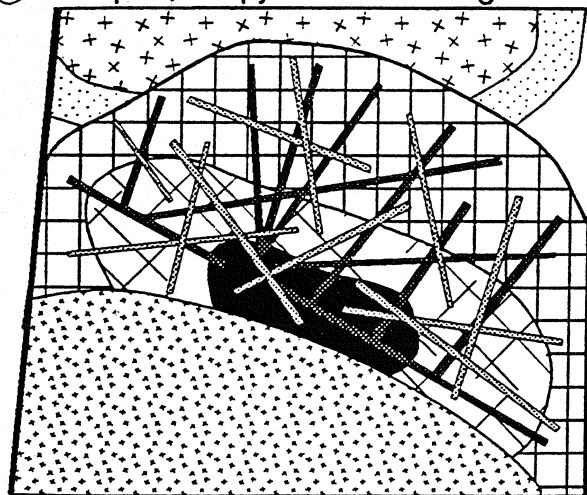


Figure 7. Schematic model for the evolution of the hydrothermal system at Copper Mountain.

dykes, sills, and plugs of the Lost Horse intrusive complex. The youngest phase of the Lost Horse complex is a porphyritic monzodiorite to monzonite that is temporally and spatially associated with alteration and Cu-Au mineralization (Huyck 1991).

Hydrothermal activity in the district has produced a complex distribution of alteration assemblages that exhibit significant spatial and temporal variation in mineralogy (Figs. 6 and 7). The main occurrence of the Lost Horse complex is on the north side of the district, but zoning patterns of alteration and mineralization are more consistent with a thermal center on the south side

of the camp. Locally in the south part of the district, there is an early stage of pervasive propylitic alteration that is overprinted by Na-rich and potassic assemblages. This sequence has been interpreted to reflect an initial stage of prograde propylitic alteration that expanded outward over time, followed by formation of pervasive Na-rich and pervasive potassic alteration. The Na-rich alteration is dominated by albite ( $An_{<5}$ ) with variable amounts of diopside, chlorite, and epidote, and minor pyrite and chalcopyrite. Pervasive potassic alteration is dominated by K-feldspar, and also contains biotite, minor magnetite, epidote, and chalcopyrite, and trace

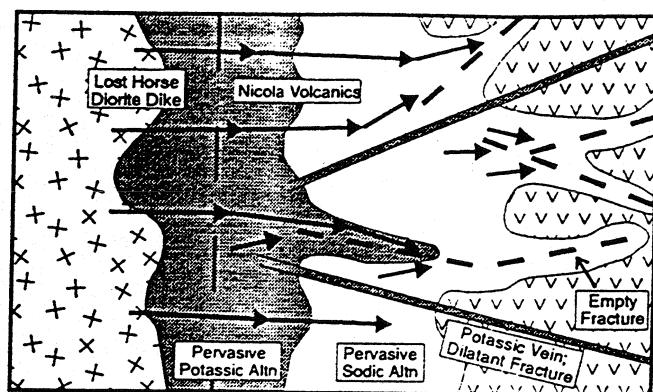


Figure 8. Schematic depiction of the relationship between pervasive Na-rich and pervasive potassic alteration associated with dykes of the Lost Horse intrusive complex, Copper Mountain. Arrows indicate fluid flow-paths.

pyrite. The pervasive Na-rich and potassic alteration hosts potassic-assemblage veins which introduced most of the Cu-Au mineralization and which comprise pegmatoidally-textured K-feldspar-biotite-calcite-pyrite-chalcopryrite-bornite  $\pm$  magnetite  $\pm$  epidote veins in the south and magnetite-hematite-calcite-pyrite-chalcopryrite  $\pm$  K-feldspar  $\pm$  biotite  $\pm$  chlorite  $\pm$  apatite  $\pm$  titanite veins in the north. These veins are cut by barren to weakly mineralized albite-epidote and K-feldspar-epidote veins in the south and north, respectively. In the Ingerbelle and Pit 3 areas, late-stage veins of barren scapolite-albite-K-feldspar formed which, together with the albite-epidote veins, may represent a second stage of Na-rich alteration. Fracture-controlled propylitic alteration and several stages of post-mineralization veining overprinted the early pervasive and veinlet-controlled alteration assemblages during thermal collapse (Stanley *et al.* 1995). Minor, early-stage alteration which includes garnet and diopside has been reported from the Copper Mountain camp (Preto 1972), but its temporal and spatial relationship to other alteration assemblages is unknown.

Pervasive Na-rich alteration is most abundant in the south part of the district, but minor occurrences are present throughout the camp. Pervasive potassic alteration is also widely distributed, but is most abundant and intense in the north. The relationship between these pervasive assemblages is more clearly displayed around individual dykes of the Lost Horse complex (Fig. 8). Dykes of Lost Horse monzonite commonly have an interior zone of pervasive potassic alteration which may affect both the outer

portion of the dyke and the wallrocks, and an outer zone of pervasive Na-rich alteration that is usually confined to the wallrocks. Farther from the dyke, the Na-rich alteration commonly has albite envelopes around fractures that channeled fluid flow. The zones of both pervasive Na-rich and potassic alteration also commonly contain dilatant potassic veins. In Pit 3, a Lost Horse dyke has sections affected by K-metasomatism and Na-metasomatism which are separated by only a few meters along strike. Individual veins with envelopes of K-feldspar adjacent to the vein and envelopes of albite farther from the vein have also been observed.

#### SUMMARY OF ALTERATION AND MINERALIZATION ASSEMBLAGES

The general characteristics of the major alteration assemblages in alkalic porphyry deposits are summarized in Table 2. Potassic alteration is dominated by K-feldspar and/or biotite, is commonly magnetite-rich, and is an important or principal assemblage in all alkalic deposits. Na-rich alteration is a widespread, strongly-developed assemblage in the silica-saturated Iron Mask and Copper Mountain systems, is well-developed locally in the silica-saturated Mount Milligan complex and in the mixed saturated/undersaturated system at Mount Polley, but is absent to trace at Galore Creek, Lorraine, and Rayfield River. It is probable that Na-rich alteration in alkalic porphyry deposits will eventually be subdivided into several different sub-assemblages, but we are not yet prepared to do so here. Alteration characterized by Ca-bearing

Table 2. Summary of the characteristics of major alteration assemblages in alkalic porphyry Cu-Au deposits

Alteration Assemblage	Deposits	Defining Minerals <sup>1</sup>	Host Rocks <sup>2</sup>	Style <sup>3</sup>	Depth	Temp (°C)	Location <sup>4</sup>	Association with Mineralization
Potassic	All	KF and/or bi ± mt	diorite to syenite (I>V,Bx)	P,F	shallow, subvolcanic	>350?	core	weak to strong
Sodic	Copper Mountain Iron Mask System Mount Polley Mount Milligan	ab-di ± (chl,ep)	diorite to monzonite (I>>V>Bx)	P,F	shallow, subvolcanic	350<T<670	core	weak to strong
Calc-Potassic	Galore Creek Mount Polley Rainbow Zone Lorraine?	t-KF-bi ± (ap,anh)	syenite to monzonite I,V,Bx	P	shallow, subvolcanic	400 to 650	core and intermediate	weak to moderate
Propylitic	All	al-chl-py ± (ep,ab)	diorite to syenite I,V	F>P	shallow, subvolcanic	<200 to 300 <sup>5</sup>	peripheral or overprint	none

<sup>1</sup> Abbreviations listed in Figure 2<sup>2</sup> i = intrusion; V = volcanic; Bx = orthomagmatic breccia<sup>3</sup> P = pervasive; F = fracture-controlled<sup>4</sup> Relative position within the hydrothermal system<sup>5</sup> Unpublished fluid-inclusion data of Lang

minerals, usually also contains abundant K-bearing minerals and is herein considered to be a calc-potassic assemblage; this alteration type is most strongly developed in the silica-undersaturated system at Galore Creek, is an important assemblage in the mixed silica-saturated/undersaturated systems at Mount Polley and Lorraine, and is a minor assemblage in the silica-saturated Iron Mask and Copper Mountain systems. On the basis of the above review, calc-potassic and Na-rich assemblages may be earlier, later, or contemporaneous with potassic assemblages, and the three assemblages exhibit variable spatial relationships to each other. The style of each of these early assemblages is most commonly pervasive and microfracture-controlled, accompanied by only minor and discontinuous dilatant fractures. Later stages of alteration are more commonly characterized by the presence of planar, tight to dilatant fractures, although these veins are never observed in the density typical of stockworks in calc-alkalic porphyry systems. Propylitic alteration is limited and weak in many deposits, but forms a halo up to 3 km in width at Mount Milligan. Propylitic alteration is found mostly on the periphery of the hydrothermal systems, but our working hypothesis, which is based on crosscutting vein relationships in several deposits, is that propylitic alteration formed in approximate contemporaneity with the Na-rich, Ca-rich, and/or K-rich assem-

blages, although it is common to locally find propylitic overprints on the other assemblages.

The main ore mineral in each of the deposits is chalcopyrite. Bornite is common and may locally exceed chalcopyrite in abundance. Trace to minor sphalerite and galena are present in some systems, but their timing and distribution are erratic and only poorly known. Molybdenite is very rare and Mo concentrations are usually <20 ppm. Gold occurs as inclusions in Cu sulfide minerals, and Cu and Au are usually well-correlated within individual deposits or zones (Stanley, work in progress). Within the ore zones, sulfide concentration is invariably low and Cu sulfides greatly exceed pyrite, whereas in propylitic zones pyrite concentration ranges up to several percent. Na-rich, Ca-rich, and potassic alteration are all associated, at least locally, with Cu-Au mineralization.

Alteration and mineralization in each of the alkalic systems is interpreted to have formed at depths which did not exceed a few kilometers. Data on primary fluid inclusions in garnet from Galore Creek (Dunne *et al.* 1994; Thompson *et al.*, work in progress) indicate pressures between 200 and 650 bars. This is consistent with the interpretation of Enns *et al.* (1995) that the syenites at Galore Creek intruded a volcanic pile to which they are genetically related, and with the presence, in late-stage syenites, of deuteric garnet-epidote alteration that filled miarolitic cavities.

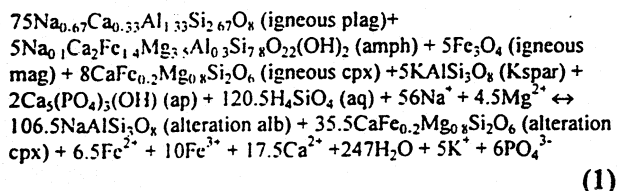
Most deposits contain planar, dilatant veins and magmatic-hydrothermal breccias with textural evidence for abundant open space, both of which are consistent with relatively shallow depths.

### PROCESSES OF HYDROTHERMAL ALTERATION

The formation of Na-rich or calc-potassic assemblages, and their temporal and spatial relationship to potassic alteration, may be a consequence of: (1) magmatic fluid composition, which may vary between individual magmas or may evolve within a single magma in response to differentiation; (2) changes and gradients in temperature and pressure across, and during the evolution of, the hydrothermal system; and (3) changes in fluid chemistry because of mineral precipitation, wallrock reactions, or mixing with externally-derived fluids. Field relationships, alteration parageneses, and the variation in zoning relationships among alteration assemblages, as described above, indicate that all of these controls have influenced the formation of Na-rich and, to a lesser extent, calc-potassic alteration in alkalic porphyry deposits. The relative importance of these controls is discussed with reference to each style of alteration in the following sections.

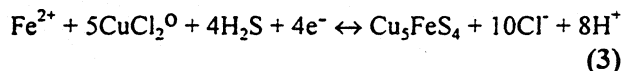
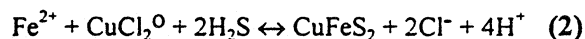
#### Sodium-rich (Sodic) Alteration

In the Iron Mask batholith, Na-rich alteration of the Sugarloaf diorite in the Ajax East and West deposits, which will be suggested in later sections to be controlled by the composition of magmatic fluids emanating from the Sugarloaf diorite, can be represented by the following equation:



The reaction is balanced on Al, which Pearce element-ratio analysis indicates is conserved (Stanley, work in progress), and is constrained to produce a molar ratio of albite to diopside of 3:1, consistent with field observation. Based on an

average modal composition of fresh Sugarloaf diorite (70plag 15hbl 5cpx 5Kspar 2.5mag 2.5ap; Snyder 1994; Ross 1993), the respective calculated reactant and product densities of 2.837 g/cm<sup>3</sup> and 2.772 g/cm<sup>3</sup> are very similar to average measured densities of 2.828 g/cm<sup>3</sup> and 2.754 g/cm<sup>3</sup>, with a similar magnitude of change. The reaction produces a molar volume decrease of 12.8% (from 105.22 cm<sup>3</sup> to 91.47 cm<sup>3</sup>), which compares favorably with the proportion of dilatant veins observed in the intensely altered zones (Ross 1993). The modelled composition of altered Sugarloaf diorite compares favorably with the measured compositions. Furthermore, the effects of reaction (1) are consistent with petrographic observations, including: (1) Fe<sup>3+</sup> and Ca<sup>2+</sup> are liberated for precipitation of epidote; (2) Ca<sup>2+</sup> may also be fixed in diopside, and possibly calcite and trace anhydrite; (3) minor K<sup>+</sup> is produced for precipitation in K-feldspar veins that may crosscut the Na-rich alteration; and (4) both H<sup>+</sup> and H<sub>4</sub>SiO<sub>4</sub> (aq) are consumed, which inhibits quartz precipitation, in spite of cooling. The transport of Cu in porphyry systems has usually been ascribed to chloride complexes (e.g., Barnes 1979). In the alkalic porphyry systems, dissociation of these complexes may have been induced by the Fe<sup>2+</sup> liberated in reaction (1) by equations similar to the following:



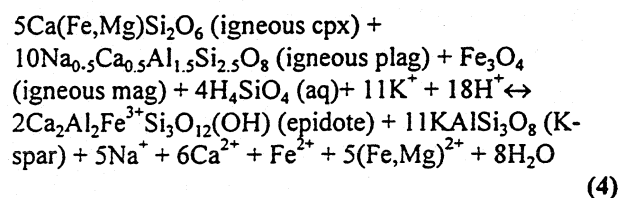
The observed decrease in grades of Cu and Au with increasing intensity of Na-rich alteration at the Ajax deposit (Ross 1993) may reflect either leaching of previously precipitated sulfides or their non-precipitation because of the reduced availability of Fe<sup>2+</sup> to drive Reactions 2 and 3.

In the Copper Mountain system, pervasive Na-rich and pervasive potassic alteration are zoned at the district scale. The spatial relationship between these assemblages may reflect both district-scale temperature gradients and local modification of fluid composition by reaction with minerals, rather than control by the composition of fluids evolved from chemically distinct

magmas. Albitization of plagioclase or K-feldspar requires a fluid with low ratios of  $m\text{CaCl}_2/(m\text{CaCl}_2 + m\text{NaCl})$  and  $m\text{KCl}/(m\text{KCl} + m\text{NaCl})$  (where  $m$  is the molality of species in solution; Orville 1963, 1972). At 2 kb pressure, the molar  $\text{K}/(\text{K}+\text{Na})$  ratio of a fluid in equilibrium with two alkali feldspars is 0.25 at 650 °C, but drops to  $\leq 0.16$  at 400 °C (Orville 1963); thus, with increasing temperature a Cl-bearing fluid with both K and Na will cause albitization, whereas cooling of this fluid will result in K-feldspathization. The effect of high F concentrations on the direction of change in the molar  $\text{K}/(\text{K}+\text{Na})$  ratio with temperature is uncertain, as the experimental studies of Kovalenko (1976) and Doherty (1990) indicate a reverse and a similar relationship, respectively, to that observed in Cl-rich fluids; in either case there is, except for minor fluorite at Galore Creek, little evidence for F-rich fluids in alkalic porphyry deposits. Cooling of a Cl-rich fluid in the presence of only plagioclase will cause a decrease in the molar  $\text{Na}/(\text{Na}+\text{Ca})$  ratio and will result in albitization, but in the alkalic systems two alkali feldspars are usually present. Control of feldspathization by temperature gradients has been documented at Yerington, Nevada, where sodic-calcic alteration formed in a prograde temperature regime at depth and was contemporaneous with potassic alteration which formed in a retrograde temperature regime at shallower levels (Carten 1986; Dilles & Einaudi 1992). Stanley *et al.* (1995) have suggested that although the main mass of the syn-mineral Lost Horse intrusions lies in the northern part of the Copper Mountain district, zoning of alteration and mineralization indicates that the thermal center of the system was located in the south, probably as a consequence of the channelling of fluids along major structures and of the morphology of the Lost Horse complex at depth. This model, in which pervasive Na-rich alteration formed early in the centre of the hydrothermal system whereas pervasive potassic alteration is more abundant and intense, but contemporaneous with Na-rich alteration, in the more peripheral part of the system, permits the interpretation that Na-rich and potassic assemblages formed in prograde and retrograde temperature regimes, respectively. The

spatial relationship between Na-rich and potassic alteration may therefore reflect either deeper erosion of the southern part of the district, or lateral temperature gradients, or both. Intense replacement of either the intrusions or the chemically similar volcanic rocks by albite would have effects similar to Reaction 1 and could liberate significant amounts of K; the K could be transported to the more peripheral parts of the system for pervasive potassic alteration or, as a more reasonable alternative, could be retained locally for precipitation in overprinting, fracture-controlled potassic alteration. Precipitation of Ca-bearing minerals during both pervasive Na-rich and pervasive potassic alteration would maintain the  $m\text{CaCl}_2/(m\text{NaCl} + m\text{CaCl}_2)$  ratio in the fluid at the low values necessary for continued feldspathization of either type (Orville 1972).

Locally superimposed upon the district-scale zoning at Copper Mountain is the outward zoning from pervasive potassic to pervasive Na-rich alteration around individual Lost Horse dykes (Fig. 8), and in alteration envelopes adjacent to individual veins. This style of albitization is interpreted to have accompanied decreasing temperatures. Albitization may be induced in preference to K-feldspathization in a retrograde temperature environment by a large decrease in fluid pressure (Orville 1963), but such a pressure change or gradient is unreasonable here. More plausibly, the zoning pattern illustrates that, at least locally, Na-rich alteration formed in response to the liberation of Na and a decrease in the molar  $\text{K}/(\text{K}+\text{Na})$  ratio resulting from K-metasomatism by a reaction similar to the following:



Reaction 4 would have results similar to reaction 1 and would: (1) liberate  $\text{Ca}^{2+}$  for precipitation in epidote, which is common in potassic alteration at Copper Mountain, or as epidote in the Na-rich alteration zone; (2) effect

the commonly observed destruction of magnetite in the potassic zone, and yield both  $\text{Fe}^{3+}$  for epidote precipitation as well as  $\text{Fe}^{2+}$ ; (3) consume  $\text{H}^+$  and promote formation of calcite; (4) consume  $\text{H}_4\text{SiO}_4$  (aq) and inhibit quartz precipitation; and (5) lower the molar  $\text{K}/(\text{K}+\text{Na})$  ratio in the fluid and promote albitization. The resulting albitization would, in turn, liberate small amounts of K which could be incorporated in crosscutting potassic-assemblage veins that fill fractures formed by volume loss, as described above. At Mount Polley, a similar but reversed relationship between Na-rich and potassic alteration in breccia fragments may have formed in the same fashion, with the K necessary for potassic alteration in the cores of the fragments being liberated by albitization along the margins.

The temperature range attending Na-rich alteration in alkalic systems is poorly constrained. The albite commonly has chessboard twinning but is not antiperthitic, indicating temperatures below about 670 °C (Orville 1963); one feldspar composition ( $\text{Or}_{30}\text{Ab}_{69}\text{An}_{01}$ ) obtained from a vein within albitically altered Sugarloaf diorite in the Ajax deposit, however, is compatible with hypersolvus temperatures. Although minerals suitable for fluid-inclusion analysis are largely absent, Pan *et al.* (1994; personal comm. 1994) reported temperatures of  $\geq 350$  °C and salinities of about 40 equiv. wt.% NaCl for primary fluid inclusions in a single sample of scapolite from a late-stage scapolite-K-feldspar-albite vein in the Ingerbelle deposit at Copper Mountain. This late-stage Na-rich alteration is interpreted to have formed during thermal collapse of the hydrothermal system (Stanley *et al.* 1995), and the fluid-inclusion data may therefore place a (poor) minimum temperature on the earlier pervasive alteration assemblages. High temperatures are consistent with the formation of pervasive alteration within and immediately adjacent to Lost Horse and Sugarloaf intrusions, and with the sinuous, discontinuous character of associated fractures.

#### **Potassium-rich (Potassic) Alteration**

Potassic alteration in alkalic deposits is dominated by K-feldspar and/or biotite, is

commonly accompanied by abundant magnetite, and usually has associated Cu-Au mineralization. The style and mineralogy of potassic alteration in alkalic deposits are very similar to those observed in calc-alkalic porphyry environments, particularly in comparison to Au-rich calc-alkalic systems which also have high concentrations of hydrothermal magnetite (Sillitoe 1979). The common presence of epidote in the potassic assemblage of alkalic systems, however, differs from the typical potassic assemblage in calc-alkalic deposits in which anhydrite is more common as a major Ca-bearing phase. Anhydrite is abundant only in potassic assemblages in the Big Onion and Galore Creek deposits. In calc-alkalic deposits, it has commonly been demonstrated that potassic alteration formed at temperatures in excess of 400 °C from fluids with a large magmatic component. In the current absence of applicable fluid-inclusion data, we infer that potassic alteration in alkalic deposits formed under generally similar conditions.

#### **Calcium-rich (Calc-Potassic) Alteration**

Calcium-rich alteration is most strongly developed as a calc-potassic assemblage in the core of the Central zone at Galore Creek, where it grades outward to broadly coeval potassic alteration (Enns *et al.* 1995). A similar but more weakly developed relationship is found at Lorraine (Bishop *et al.* 1995). In the Mount Polley system, calc-potassic alteration overprints early potassic and Na-rich alteration (Fraser 1994a,b). Although the Ca-rich assemblage in the Rainbow zone in the Iron Mask system has not been examined in detail, it may be similar to calc-potassic alteration at Galore Creek and Mount Polley. The following discussion focusses on Galore Creek, for which alteration parageneses and relationships have been most completely documented.

At Galore Creek, alteration in the Central zone is strong to intense and typically obliterates primary minerals and texture. The uncertainty in identifying protolith composition and unaltered equivalents among the many intrusive phases, and poor constraints on mineral replacement relationships, have prevented quantitative treatment of mass transfer. Qualitatively, it is apparent that Ca



has been introduced, at least in the most intensely altered zones, and that the K/Na ratio in altered syenite is elevated relative to the average value in fresh syenite from outside the Central zone.

Primary fluid inclusions in garnet from Galore Creek have been analyzed by Dunne *et al.* (1994). The results are summarized below, and a more complete discussion will be presented elsewhere (Thompson *et al.*, work in progress). Although data have not yet been acquired from other alkalic systems, fluid inclusions that are petrographically similar to those in garnet at Galore Creek have been observed in andradite from Mount Polley and the Rainbow zone (J. Oliver, personal comm. 1995).

Primary fluid inclusions in garnet at Galore Creek occur along and parallel to growth-zone boundaries. Type I inclusions contain only aqueous liquid and a small vapor bubble, whereas type III inclusions contain a halite cube in addition to liquid and vapor. Approximately 80% of primary inclusions are type III, and 20% are type I; both inclusion types are also found in secondary and pseudo-secondary habits. Individual type III inclusions contain up to nine mineral phases: halite, sylvite, anhydrite, and hematite have been identified optically. SEM analysis identified a possible alkali feldspar in one opened inclusion and a Na-K-Cl salt in two others, and the remaining minerals have not yet been identified.

Homogenization temperatures for primary and secondary type I and type III inclusions range from 250 to 650 °C, but primary type III inclusions display a distinct mode between 450 and 500 °C. No consistent spatial variations in temperature have been observed (Dunne *et al.* 1994). The shallow interpreted depth of formation of the Central zone (Enns *et al.* 1995) limits the trapping temperatures of these inclusions to values no more than about 30 °C higher than the measured homogenization temperatures.

When frozen inclusions are heated, three distinct melting events are observed. These have been interpreted to correspond to: (1) melting of a Ca-bearing salt hydrate such as antarcticite (-70 to -35 °C); (2) ice melting (-25 to -20 °C); and (3) dissolution of metastable hydrohalite (>0 °C). These phase changes have been observed both in

type III and type I primary inclusions and suggest that types III and I represent strongly oversaturated to slightly undersaturated examples of a compositionally similar fluid. The presence of halite, sylvite, and a Ca hydrate demonstrates that fluid composition must be described, at a minimum, by the NaCl-KCl-CaCl<sub>2</sub>-H<sub>2</sub>O compositional system. Data on this system, however, are limited to temperatures below 100 °C (Linke 1965), and salinity and cation ratios have therefore been estimated from the NaCl-CaCl<sub>2</sub>-H<sub>2</sub>O system (Williams-Jones & Samson 1990) and the NaCl-KCl-H<sub>2</sub>O system (Roedder 1984). Using these chemical systems, type III inclusions with halite have NaCl concentrations of 26 to 60 wt.%, and CaCl<sub>2</sub> between 0.5 and 12 wt.%; type III inclusions with both halite and sylvite have 26 to 55 wt.% NaCl and 19 to 47 wt.% KCl. The molar K/(K+Na) ratio from seven inclusions that contain both halite and sylvite ranges from 0.43 to 0.69, with one value of 0.27, and total equivalent NaCl salinities are 45 to 77 wt.%. Type I inclusions have 10 to 26 wt.% NaCl and 0 to 15 wt.% CaCl<sub>2</sub>, but no estimates of KCl concentration are available.

The fluid-inclusion data from Galore Creek indicate that calc-potassic alteration formed between 450 and 650 °C. Sulfur-isotope fractionation between coexisting anhydrite and pyrite, which paragenetically overlapped with but largely succeeded garnet precipitation, yields temperatures of 399 to 437 °C ( $n = 5$ ), with one value of 482 °C ( $\pm 20$  °C; equation of Ohmoto & Lasaga 1982), that probably establish a minimum temperature for earlier calc-potassic alteration. High temperatures are consistent with the formation of calc-potassic alteration in association with syenites that intruded very early in the sequence of intrusion emplacement at Galore Creek.

## DISCUSSION

The alkalic porphyry Cu-Au deposits in British Columbia comprise an important and distinct subtype of magmatic-hydrothermal mineral deposit on the basis of the composition of the associated igneous rocks, the metal assemblage, and the paragenesis, style, and relationship among alteration assemblages.



Critical features of genesis which must be resolved include: (1) the source(s) of hydrothermal fluids which formed the alteration assemblages; (2) the relationship among these fluids; and (3) the nature of controls exerted by the composition and/or differentiation history of the associated intrusions. Improved understanding of these processes will permit development of better models, and will provide increased confidence in their possible application to similar alteration assemblages in other magmatic-hydrothermal systems.

### *Source of the Hydrothermal Fluids*

#### *Calc-Potassic Alteration.*

The calc-potassic assemblage at Galore Creek forms an assemblage that has not been previously described from within porphyry metal deposits, with the possible exceptions of alteration in the Shamrock batholith, Nevada (D. Battles, personal comm. 1995) and in the Willa porphyry-related breccia deposit in southern British Columbia (Wong & Spence, unpublished). This style of Ca-rich alteration, as well as garnet-bearing alteration in the western part of Mount Polley and in the Rainbow zone in the Iron Mask batholith, differs from the more commonly described examples of calcic skarns. Near the northern margin of the Central zone at Galore Creek, minor augite-bearing volcanoclastic units with a calcareous matrix are altered to a calc-silicate mineral assemblage in zones a few meters wide (Enns *et al.* 1995) in which early garnet-diopside alteration was overprinted by a biotite-epidote-carbonate assemblage. The formation of the calc-silicate minerals in the matrix of the volcanoclastics prior to K-silicate alteration and mineralization distinguish these skarns from the intense, pervasive, calc-potassic alteration in the core of the Central Zone, in which the zonation from the calc-potassic core to the potassic margins is the reverse of expectations in a zoned porphyry-skarn system. At Mount Polley, the massive garnet-magnetite-diopside zone in the southeastern part of the deposit is similar to a calcic skarn, but is mineralogically distinct from the calc-potassic alteration to the west.

At Galore Creek, the dominance of magmatic

waters in the early hydrothermal fluids is suggested by the fluid-inclusion data described above and by the oxygen-isotope composition of hydrothermal minerals. Oxygen-isotope analyses were obtained from biotite, magnetite, and andradite from the calc-potassic alteration in the Central zone at Galore Creek (F. Longstaffe, work in progress). Measured ranges in  $\delta^{18}\text{O}$  for biotite, magnetite, and garnet, are 5.5 to 6.9 per mil, 2.8 to 3.3 per mil, and 3.9 to 4.9 per mil., respectively. Between 400 and 600 °C, the calculated isotopic composition of water in equilibrium with biotite ranges from 7.9 to 9.5 per mil (using data from O'Neil & Taylor 1967; Bottinga & Javoy 1975; and Chiba *et al.* 1989), water in equilibrium with magnetite ranges from 12.1 to 9.4 per mil (data of O'Neil & Taylor 1967 and Chiba *et al.* 1989), and fluids in equilibrium with garnet are between 6.5 and 7.8 per mil (data of Matthews 1994, using a mole fraction of 0.9 of andradite in garnet). These isotopic compositions are consistent with precipitation from a fluid dominated by magmatic water.

At Galore Creek, several phases of post-mineral syenite have been affected by alteration that is dominated by garnet and epidote, and locally includes pyrite, anhydrite, calcite, and trace albite. This alteration does not affect the wallrocks; rather it is confined within the intrusions, occurring as clotty replacements and as fill inmiarolitic cavities. This style of alteration has been observed in dykes as small as one meter in width. We interpret this phenomenon as a classic deuteric alteration assemblage. The general similarity of this alteration to the calc-potassic assemblage in the Central zone, and its restriction to the interiors of syenite intrusions, demonstrates that the Ca necessary for alteration may be readily derived from, or redistributed within, the intrusions themselves and does not require influx of external fluids.

#### *Sodium-rich alteration*

In contrast to calc-potassic alteration, Na-rich alteration has been recognized in many magmatic-hydrothermal and regional alteration environments (Table 3). Na-rich alteration in alkalic Cu-Au porphyry deposits is similar, in at least some

Table 3. Selected examples of sodium-rich alteration in magmatic-hydrothermal systems

Type	Igneous Rocks	Sodic Assemblage <sup>1</sup>	Temp. (°C)	Salinity <sup>2</sup>	Fluid Source	Mineralization	Relationship to Potassic Alteration	References
Fenites (general)	carbonatites	ab-arfved-aeg	near solidus	n.a.	magmatic		Inner K-rich; outer Na-rich zones K-rich always overprints Na-rich	Woolley (1982)
Albite-U Deposits Metasediment-hosted Ukraine	anorthositic rapakivi syenogranite metamorphic rocks	oligoclase-KF- chl-ep-hem	>350	n.a.	metamorphic	U	No related potassic alteration	Shmurayeva (1985) Oncl'yanenko & Mineyeva (1982)
Albite-U Deposits Intrusion-hosted Ukraine	rapakivi syenogranite		n.a.	n.a.	magmatic	none	No related potassic alteration	Shmurayeva (1985) Oncl'yanenko & Mineyeva (1982)
Albite-U Deposits Metasediment-hosted Otish Basin, Quebec	gabro				basin brines	U-(Te,Se)	No related potassic alteration	Ruhmann <i>et al.</i> (1986)
Caucasus Mtns	diabase	oligoclase	n.a.	n.a.	magmatic	trace Cu	No related potassic alteration	Beridze & Akhylediani (1980)
Wernecke Breccias Yukon	diorite/gabbro	ab-chl-carb-hem-par dolo-qtz <sup>+</sup> /ser	n.a.	n.a.	magmatic?	Cu-U-(Co)	Sodic core yields progressively to Na-phyllic, K-phyllic, propylitic and carbonatization	Laznika & Edwards (1979)
Bristol Mountains California	granodiorite	ab-chl	? to >600	n.a.	meteoric or formation magmatic possible	none, or Fe skarns	Local potassic overprints	Fox (1987a,b); Hall <i>et al.</i> (1988)
Melones Fault Zone California	intermediate dikes	ab-riebe-aeg-(titn- chl- mt-hem <sup>+</sup> / scap,apa,anal ab-(act or di)/+qtz scap-act ab <sup>+</sup> /-chl,qtz	n.a.	n.a.	n.a.	pyrite only	No related potassic alteration	Albino (1986)
Great Basin, Nevada Sodic and Sodic- Calcic	felsic to mafic		n.a.	moderate to high	seawater, formation meteoric +/- magmatic	Fe and Cu skarns; porphyry Cu	Usually deeper, more peripheral sodic and sodic-calcic	Battles & Barton (in review)
Great Basin, Nevada Sodic-Potassic	peraluminous, 2-mica granites	ab-musc <sup>+</sup> /(qtz,fl)		moderate to low	magmatic +/- meteoric	W,Bc,Zn <sup>+</sup> / Mo,Pb	After minor potassic; before greisenization	Battles & Barton (in review); Barton (1987)
Emuford Deposit Queensland	peraluminous bt-granites	ab	to 428	30 to 50	magmatic +/- meteoric	Sn-W	No related potassic alteration	Charoy & Pollard (1989)
Coolgarra Batholith Queensland	peraluminous bt-granites	ab-musc	to 650	to 70	magmatic	Sn-W	Sequence: early potassic, sodic, greisenization, late potassic, argillitic	Witt (1988)
Yerington Porphyry System Nevada	intermediate granitoids	oligoclase-act-titn	360 to 480	31-41	formation water	Cu w/ potassic (but leaches Cu)	Early, shallow level potassic at same time as early, deeper sodic- calcic; then later shallow sodic.	Carten (1986) Dilles <i>et al.</i> (1992)
Yerington Porphyry System Nevada Late Sodic	intermediate granitoids	ab-chl-verm-ser <sup>+</sup> / tour	175-250	unknown	meteoric	post Cu	See above	Carten (1986) Dilles <i>et al.</i> (1992)

<sup>1</sup>Mineral abbreviations in caption of Figure 2. <sup>2</sup>Equivalent wt.% NaCl

respects, to many of these other examples but, more importantly, significant departures exist which distinguish Na-rich alteration in the alkalic environment. We ascribe many of the differences to variation in the sources and/or compositions of the fluids present in the different environments.

Albitization in peraluminous granite systems (e.g., Charoy & Pollard 1989; Witt 1988; Barton 1987) and carbonatites (Woolley 1982) has been attributed to magmatic fluids. In peraluminous granite systems, fluid-inclusion evidence, mineralogical relationships and assemblages, and an alteration sequence from early K-feldspathization to albitization to greisenization demonstrate that the fluids were F-rich. In carbonatites, Woolley (1982) documented a consistent sequence of early Na fenites, overprinted by K fenites which he attributed to changes in composition of CO<sub>2</sub>-rich magmatic fluids emanating from a differentiating carbonatite intrusion. Regardless of their origin, the fluids that effected albitization in alkalic porphyry systems were Cl-rich and compositionally distinct from the F-rich and CO<sub>2</sub>-rich fluids in peraluminous granites and carbonatites. Na-rich alteration in alkalic porphyry deposits formed in an environment distinct from spilitization caused by seawater circulation, and distinct from albitization that formed from metamorphic fluids or formation waters in albite-uranium  $\pm$  Cu deposits (e.g., Shmurayeva 1985; Ruhlmann *et al.* 1986; Laznicka & Edwards 1979). Regional-scale Na-rich alteration is common within and adjacent to Jurassic granitoids in southern California; Fox (1987a,b) attributed this alteration to circulation of meteoric or formation waters at poorly constrained, but probably high, temperatures, although Hall *et al.* (1988) have noted in this same region the possible presence of a magmatic water component in hydrothermal fluids that caused albitization in the Iron Hat skarn deposit.

The closest analog to Na-rich alteration in alkalic porphyry deposits is albite-dominated alteration in calc-alkalic porphyry systems. Dilles & Einaudi (1992) list nine calc-alkalic examples, including Ajo and Sierrita-Esperanza, Arizona, Ox Lake, British Columbia, Yandera, Papua New Guinea, the Drammen district, Norway, Cuddy Mountain, Idaho, Yerington and Royston, Nevada,

and the Lights Creek district, California, to which we add the Island Copper deposit in British Columbia (Perello *et al.* 1995). Although Na-rich alteration in calc-alkalic systems varies both in intensity and in timing relative to other alteration assemblages, Dilles & Einaudi (1992) have suggested that it may have formed by processes generally similar to those documented at Yerington, at which sodic-calcic alteration is attributed to influx and heating of evolved, highly-saline formation waters. The Yerington model is consistent with that proposed by Battles & Barton (in review), who have observed that sodic and sodic-calcic alteration in the Great Basin of the western United States is very common (40 examples cited, including Yerington) in Permian to Jurassic igneous rocks which formed in a marine and/or arid rifted arc setting, but is rare in Cretaceous and younger rocks which formed in a fully-emergent continental arc. Battles & Barton (in review) have further proposed that Na-rich alteration in the older igneous complexes was effected by moderately to highly saline brines of marine formation (equilibrated with evaporites) or meteoric origin, with or without a magmatic component, that were readily available in their paleogeographic environment. Similar fluids were less available to magmatic systems in the younger emergent arc, and Na-rich alteration in these systems is restricted to small volumes of sodic-potassic alteration formed by magmatic waters, with or without a meteoric component, evolved from peraluminous granites. In British Columbia, paleogeography was probably not an important control on the formation of Na-rich alteration. The alkalic volcanic sequences and related intrusive complexes formed in a (possibly rifted) intraoceanic arc setting (Souther 1991), and are interpreted as both subaerial and submarine (e.g., Nelson *et al.* 1991). Although seawater or meteoric waters were probably available in this environment, evaporites were not; thus, in the absence of evidence for boiling, the extremely saline fluids at Galore Creek, Mount Polley, and in the late-stage Na-rich alteration at Copper Mountain, are unlikely to have originated as <sup>18</sup>O-enriched marine, formation, or meteoric waters. Furthermore, the several calc-alkalic porphyry systems in British Columbia (e.g., Highland

Valley) that are contemporaneous with and formed in a paleogeographic setting similar to that of the alkalic systems, do not exhibit Na-rich alteration; included in these systems is the Sulphurets deposit, for which Margolis (1993) has documented a large seawater component in the hydrothermal fluids.

The Na-rich alteration that developed adjacent to Lost Horse dykes at Copper Mountain is more plausibly related to magmatic fluids than to influx of external fluids, but a component of exogenous water cannot be discounted for the camp-scale Na-rich alteration. In the Iron Mask batholith, the formation of Na-rich alteration within and adjacent to all known exposures of Sugarloaf diorite, including very small dykes which did not have the thermal capacity to effect substantial mobilization of external fluids, and the complete dissociation of Na-rich alteration from other intrusive types, also suggest a dominant role for intrusion-specific magmatic fluids. Preferential availability of an external, Na-rich fluid to Sugarloaf intrusions is very unlikely as albitization affects stocks and dykes that are found both near the margin of the batholith and well within its interior; moreover, Na-rich alteration is absent from the Cherry Creek intrusions, which are most common at the margins of the batholith, where external fluids would be most readily available. The composition of hydrothermal fluids derived from alkalic magmas in British Columbia was likely a more important control on the formation of Na-rich alteration, and by analogy calc-potassic alteration, than either paleogeographic setting or influx of externally-derived fluids.

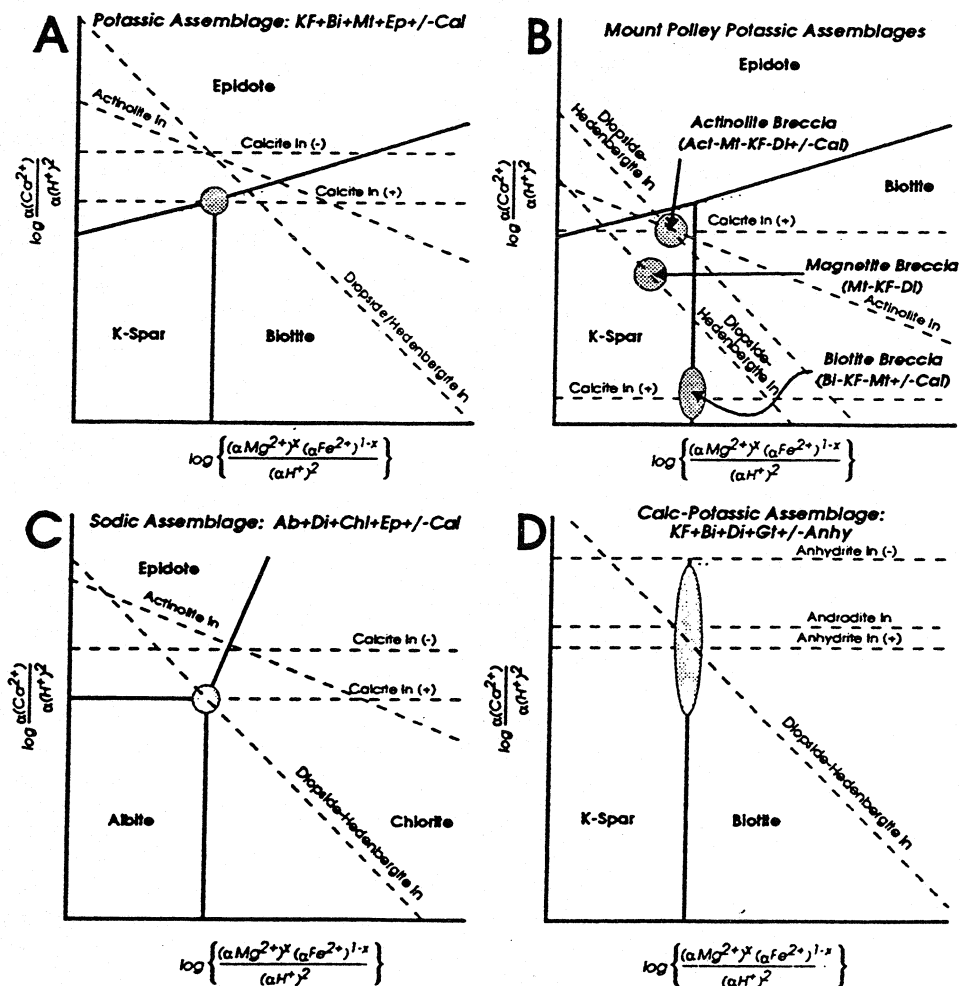
#### *Relationship to Magmatic Composition and Processes*

Na-rich, potassic, and calc-potassic alteration assemblages in alkalic porphyry deposits exhibit variable temporal and spatial relationships to each other. However, although potassic assemblages are present in all systems and, in general, Na-rich and calc-potassic assemblages are best developed in silica-saturated and silica-undersaturated alkalic systems, respectively, we think that the occurrence of all three assemblages at Mount Polley and in the Iron Mask batholith is a

critically important feature of alkalic porphyry systems.

The chemical similarities among potassic, Na-rich and calc-potassic alteration are illustrated in Figure 9. This diagram utilizes observed mineral-replacement reactions (Table 4) and suggests that the major alteration assemblages may have formed under broadly similar chemical conditions. The mineralogical variation in potassic alteration assemblages in the matrix of breccias at Mount Polley (Fig. 9B), for example, may reflect only minor changes in fluid composition. We recognize that the alteration assemblages depend on many factors, including temperature, pressure, and the activity of cations and anions, but from consideration of Figure 9 and field evidence, only small changes in physical or chemical conditions may be necessary to shift between major alteration assemblages. Lang *et al.* (1995) have suggested that Early Mesozoic silica-undersaturated and silica-saturated alkalic complexes in Quesnellia and Stikinia are related through variations along a petrogenetic continuum, and in this light the subtle but consistent variations observed in alteration associations may be anticipated.

Magmatic characteristics and processes were the major influence on variation among the alteration assemblages. As an example, the absence of early, pervasive Na-rich alteration in the Galore Creek system may be a consequence of a high molar  $K/(K+Na)$  ratio in the hydrothermal fluid. Barsukov & Klintsova (1969) effected albitization (as opposed to K-feldspathization) of plagioclase by fluids with 15 to 35 wt.% total salinity and molar  $K/(K+Na)$  ratios of 0.10 to 0.24, consistent with the experimentally determined molar  $K/(K+Na)$  ratio of 0.25 for fluids in equilibrium with two alkali feldspars at 2 kb and 650 °C (Orville 1963). The molar  $K/(K+Na)$  ratios of fluids in primary fluid inclusions at Galore Creek (0.27 to 0.69) are consistent with K-feldspathization rather than albitization. Precipitation of garnet and apatite, and later anhydrite, apparently buffered the fluid at  $mCaCl_2/(mKCl + mCaCl_2)$  ratios compatible with continued K-feldspathization. Although most of the syenites at Galore Creek have been affected by potassic alteration, the least altered samples have high



**Figure 9.** Empirical activity-ratio diagrams constrained topologically by the major alteration assemblages in alkalic Cu-Au porphyry deposits; Figures constructed in the absence of quartz. Equations used in the construction of the diagrams are listed in Table 4. Diagrams (A) and (B) are projected from magnetite, and reactions are balanced on Al and  $\text{Fe}^{3+}$ . Reactions for diagrams (C) and (D) are balanced on Al. Shaded areas indicate possible positions of the indicated alteration assemblage. Saturation curves for calcite and anhydrite fixed arbitrarily as a schematic illustration of presence (+) or absence (-) from the assemblage; actual position is dependent on  $T$ ,  $P$ , and the activities of  $(\text{CO}_3)^{2-}$  or  $(\text{SO}_4)^{2-}$ . The location of the andradite, diopside, and actinolite saturation lines, relative to other Al-bearing mineral-stability fields, are dependent on  $\text{Fe}^{3+}$  and  $\text{H}_4\text{SiO}_4$  activities,  $\text{H}_4\text{SiO}_4$ , and  $\text{H}_4\text{SiO}_4$  and  $\text{H}_2\text{O}$  activities, respectively, in addition to  $T$  and  $P$ .

$\text{K}_2\text{O}/\text{Na}_2\text{O}$  ratios which may have buffered fluid composition at relatively higher  $\text{K}_2\text{O}/\text{Na}_2\text{O}$  ratios than would be present in fluids associated with relatively more Na-rich, silica-saturated diorite to monzonite (Fig. 10).

Although variation in primary magmatic  $\text{K}_2\text{O}/\text{Na}_2\text{O}$  ratios (Fig. 10) may broadly influence the ability of intrusions to form Na-rich alteration, this simple observation cannot account for the strong preference in the Iron Mask batholith for

Na-rich and potassic alteration to form in association only with the Sugarloaf and Cherry Creek suites, respectively, because the Cherry Creek phase has the lower average  $\text{K}_2\text{O}/\text{Na}_2\text{O}$  ratio. Burnham (1979) demonstrated that calc-alkalic granitoids with biotite, hornblende, and plagioclase will have a molar  $\text{KCl}/\text{NaCl}$  ratio in the associated fluid phase near unity, but this value decreases if K becomes buffered by biotite without hornblende on the liquidus, and increases

Table 4. Reactions used in construction of Figure 9

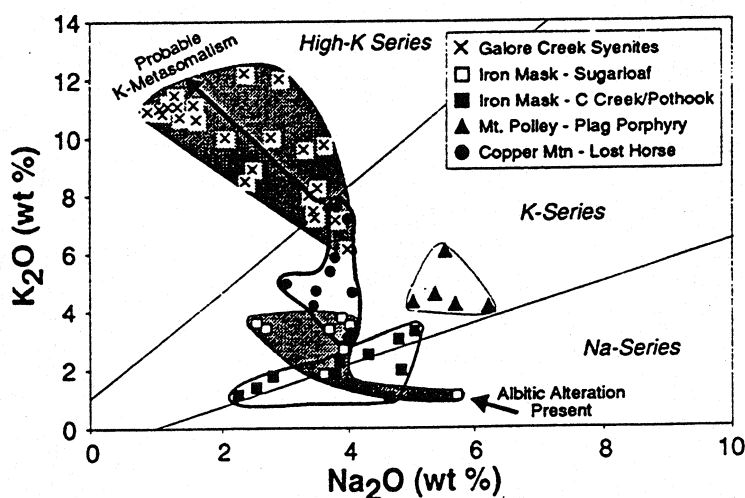
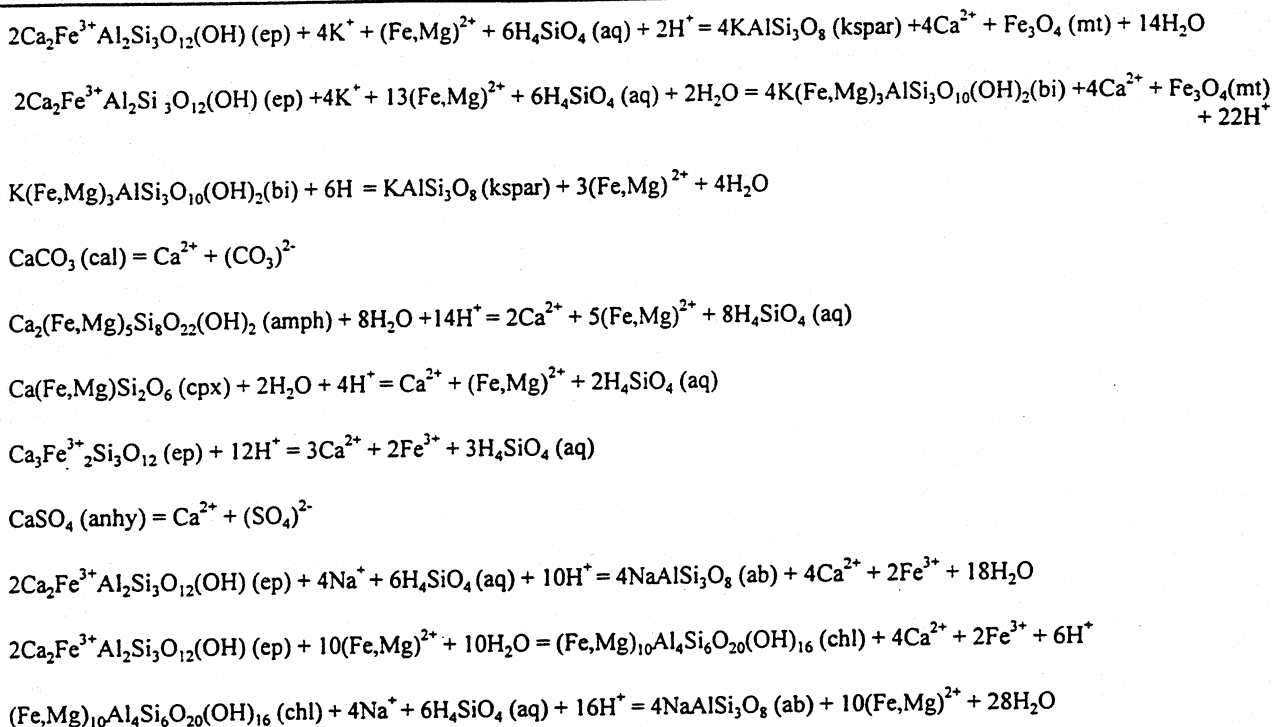


Figure 10. Plot of  $\text{Na}_2\text{O}$  versus  $\text{K}_2\text{O}$  for unaltered and least altered samples of selected intrusive units associated with potassic, calc-potassic, and Na-rich alteration. Note that most samples of syenite from Galore Creek have been affected by potassic alteration.

if Na is buffered by hornblende crystallization without accompanying biotite. Witt (1988) proposed that albitization in the peraluminous Coolgarra batholith resulted from buffering of fluid composition at a low  $\text{KCl}/\text{NaCl}$  ratio by biotite without accompanying hornblende. In the Iron Mask batholith, however, the relationship between alteration and the modal igneous mineral assemblage (Snyder & Russell 1995) of the Sugarloaf (abundant hornblende, no biotite) and Cherry Creek intrusions (abundant biotite, no

hornblende) is exactly opposite to this model.

Figure 11 presents a model that may partly explain the consistent magmatic associations of Na-rich and potassic alteration in the Iron Mask batholith. The experimental data of Holland (1972) demonstrate that the molar partition coefficients of Na and K between melt and aqueous fluid in granites are linear functions of fluid salinity. On the basis of these data, the calculated  $(\text{Na}/\text{K})_{\text{fluid}}/(\text{Na}/\text{K})_{\text{melt}}$  partition coefficient is 1.375 and is independent of salinity. [We

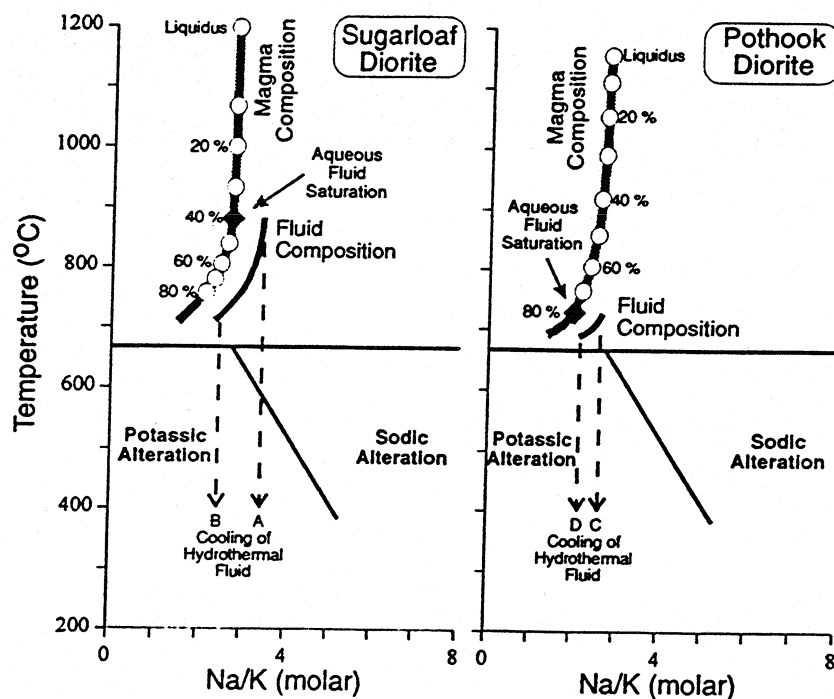


Figure 11. Models illustrating the relationship between the degree of crystallization of the Sugarloaf and Pothook diorites in the Iron Mask batholith versus the molar Na/K ratio of the melt and coexisting aqueous magmatic fluid. On the crystallization paths (widest lines), open circles show the percentage of crystallization, and black triangles mark the degree of crystallization at which aqueous fluid saturation occurs (see text for explanation). The initial molar Na/K ratio selected for each diorite melt has been taken as the value of the individual sample whose composition is closest to the average molar Na/K ratio measured in a suite of unaltered diorite samples (Snyder 1994). Crystallization

paths have been defined with the MELTS modelling program of Ghiorso & Sack (1995). The composition of the magmatic fluids (thick curved lines, adjacent to Fluid Composition) has been calculated from the experimental data compiled in Holland (1972). The boundary between fields of sodic and potassic feldspar alteration has been defined using the data of Orville (1963). Dashed lines with arrows are cooling paths for magmatic-hydrothermal fluids evolved from the magmas at the indicated position along the crystallization path.

note, however, that the experimental data have been obtained largely from haplogranite and rhyolite compositions (Candela & Piccoli this volume), and therefore may not be directly analogous to the low-silica, alkalic intrusions of interest here]. With knowledge of the molar Na/K ratio in a granitic melt at the time of aqueous fluid saturation, the molar Na/K ratio in the aqueous fluid can be determined. The experimental data of Orville (1963) may be used to determine whether albite or K-feldspar would be in equilibrium with the aqueous fluid at a given temperature, and this will indicate whether Na-rich or potassic alteration will result from the interaction of the magmatic fluid and wallrocks. The critical molar Na/K ratio that separates Na-rich alteration from potassic alteration is temperature-dependent, with lower temperatures favoring potassic alteration for any given molar Na/K ratio (Fig. 11).

We have used these data to model the relationship between the intrusions and their associated alteration in the Iron Mask batholith

(Fig. 11). The Pothook diorite is a fine- to medium-grained equigranular pyroxene diorite that characteristically contains blebs, schlieren, breccias, and veins of magnetite  $\pm$  actinolite  $\pm$  epidote; the veins typically have potassic alteration envelopes, although albitic envelopes have also been observed in rare cases. We use the Pothook diorite as a proxy for modelling the abundant potassic alteration associated with the Cherry Creek phase; the proxy is necessary because samples that are definitely unaltered are readily available from the Pothook phase, and it is valid because Snyder & Russell (1995) have shown that these intrusive phases are compositionally similar and have a direct genetic relationship. Volume and textural constraints (Snyder 1994) indicate that aqueous fluid saturation took place very late in the crystallization history of the Pothook diorite, and we have chosen to model saturation at  $\geq 80\%$  crystallization in Figure 11. Using geochemical and mineralogical constraints from Snyder (1994),



we have modelled the evolution of the molar Na/K ratio of the melt, assuming an equilibrium crystallization path, and the molar Na/K ratio of an aqueous fluid that evolves from the melt at any stage in after initial fluid saturation. The molar Na/K ratio of an aqueous fluid evolved from the Pothook diorite at any stage subsequent to saturation (paths C and D, Fig. 11) would have been too low to produce Na-rich alteration.

An analogous model is presented for the Sugarloaf hornblende diorite (Fig. 11). Volume and textural constraints indicate that fluid saturation took place relatively early in the crystallization history of the Sugarloaf diorite (Snyder 1994), and we have chosen to saturate at 40% crystallization in our model. The molar Na/K ratio for the aqueous fluid evolving from the Sugarloaf diorite is much higher than the corresponding ratio for the aqueous fluid that was derived from the Pothook diorite. Early fluid saturation of the Sugarloaf diorite at high temperatures would result in Na-rich alteration (path A, Fig. 11), and the model can also accommodate the observed formation of the fracture-controlled potassic alteration which overprints the pervasive Na-rich alteration, if the fluids are allowed either to cool significantly (path A, Fig. 11) or to be lost from the magma at a very late stage of crystallization (path B, Fig. 11).

The contrast between these two diorites, in terms of initial composition, fractionation history, and hydrothermal alteration, illustrates why Na-rich and potassic alteration may exhibit variable relationships in alkalic porphyry systems. Subtle changes in geochemical, petrological, or hydrothermal parameters can readily change the style of alteration associated with an aqueous fluid that evolved from a particular intrusion. The temperature of water/rock reaction can also influence the alteration assemblage.

At Galore Creek the probable intrusive rocks that generated the intense calc-potassic alteration have been recognized, but alteration has obliterated primary textural and chemical characteristics to the point that the data are insufficient to generate a model for crystallization similar to that presented above. The role of  $\text{Ca}^{2+}$ , however, may be postulated from the data of Holland (1972). Holland (1972) presented

experimental data describing the relationship between salinity and melt-fluid partition coefficients for  $\text{Ca}^{2+}$ ,  $\text{Mg}^{2+}$ ,  $\text{Mn}^{2+}$ , and  $\text{Zn}^{2+}$ , and the melt-fluid partition coefficient ratios for the divalent cations to K,  $(\text{Me}^{2+}/\text{K})_{\text{fluid}}/(\text{Na}/\text{K})_{\text{melt}}$ , may therefore be calculated. The curves describing the relationship between salinity and partition coefficient for divalent cations are quadratic rather than linear, and the partition coefficient ratios are, therefore, linear functions of salinity. As salinity increases, divalent cations will show increasingly strong partitioning into the fluid. Furthermore, divalent cations with lower overall concentrations ( $\text{Mn}^{2+}$  and  $\text{Zn}^{2+}$ ) partition more strongly into the fluid phase with increasing salinity than do divalent cations with high concentrations ( $\text{Ca}^{2+}$  and  $\text{Mg}^{2+}$ ).

The favorable partitioning of a divalent cation such as  $\text{Ca}^{2+}$  into a high-salinity aqueous fluid evolving from a melt may thus be responsible for the observed calc-potassic alteration related to high-salinity hydrothermal fluids present in alkalic porphyry Cu-Au deposits. Fluid inclusions document a significant Ca concentration in the fluids at Galore Creek (up to 15 wt. %  $\text{CaCl}_2$ ; Dunne *et al.* 1994). Thus, calc-potassic alteration in alkalic porphyry Cu-Au deposits may be a result of the evolution of high-salinity aqueous fluids from a melt.

At Galore Creek, late-stage fluid saturation during crystallization of the early syenite intrusions may have generated fluids with very high concentrations of Ca which may have contributed to the formation of calc-potassic alteration. Magmatic-hydrothermal fluids associated with calc-potassic alteration have measured salinities of up to 77 equiv. wt. % NaCl in fluid inclusions at Galore Creek, and were probably substantially more saline than fluids related to Na-rich alteration in silica-saturated deposits. Another factor that may contribute to the formation of calc-potassic alteration in silica-undersaturated magmatic systems is that the hydrothermal fluids were also undersaturated in silica (Lueck & Russell, in review), particularly in comparison to fluids in silica-saturated alkalic complexes.

In conclusion, although we are not yet prepared to propose specific mechanisms or



controls to account for the observation that calc-alkalic porphyry deposits most commonly form only potassic alteration, whereas alkalic deposits contain Na-rich and calc-potassic alteration with variable relationships to potassic alteration, our models suggest that the differences may be controlled by the composition and petrogenetic evolution of the associated magmas. The controls may include: (1) differences in temperature of the magmatic fluids; (2) different timing of fluid loss from the magmas, particularly in relation to the extent or style of magmatic differentiation; and (3) differences in the composition of fluids buffered by magmas of different mineral assemblage or different bulk composition. Future and ongoing comparative studies of the petrogenetic history of alkalic and calc-alkalic intrusive complexes associated with porphyry mineralization will address these fundamental questions.

#### ACKNOWLEDGMENTS

This paper is part of the Cu-Au Porphyry project of the Mineral Deposit Research Unit and has been supported by Placer-Dome, Inc., Teck Corp., Kennecott Canada, Inc., BP Minerals, Princeton Mining Corp., Rio Algom Exploration, Homestake Canada, Inc., the University of British Columbia, the Science Council of British Columbia, and the Natural Science and Engineering Research Council. The final manuscript was greatly improved by the reviews of Drs. Mark Reed, John Dilles, and Denise Battles. This paper is MDRU Contribution 63.

#### REFERENCES

- ALBINO, G.V. (1986): Sodium metasomatism and 'fenitization' along the Melones fault, Sierra Nevada foothills, California. *Geol. Soc. Am. Abstr. Programs* 18, 624.
- BARNES, H.L. (1979): Solubilities of ore minerals. In *Geochemistry of Hydrothermal Ore Deposits* (H.L. Barnes, ed.). John Wiley & Sons, New York, 404-460.
- BARR, D.A., FOX, P.E., NORTHCOTE, K.E. & PRETO, V.A. (1976): The alkaline suite porphyry deposits – a summary. In *Porphyry Deposits of the Canadian Cordillera* (A. Sutherland Brown, ed.). *CIM Special Vol.* 15, 359-367.
- BARRIE, T.C. (1993): Petrochemistry of shoshonitic rocks associated with porphyry copper-gold deposits of central Quesnellia, British Columbia, Canada. *J. Geochem. Explor.* 48, 225-258.
- BARSUKOV, V.L. & KLINTSOVA, A.P. (1969): Experimental modelling of post-magmatic alteration of granite. *Geochem. Internat.* 6, 310-315.
- BARTON, M.D. (1987): Lithophile element mineralization associated with Late Cretaceous two-mica granite in the Great Basin. *Geology* 15, 337-340.
- BATTLES, D.A. & BARTON, M.D. (in review): Arc-related sodic hydrothermal alteration in the western United States. *Geology*.
- BERIDZE, M.A. & AKHVLEDIANI, R.A. (1980): Origin of soda metasomatites associated with Jurassic basaltoid volcanics of the southern slope of the Greater Caucasus. *Internat. Geol. Review* 22, 926-936.
- BISHOP, S.T., HEAH, T.S., STANLEY, C.R. & LANG, J.R. (1995): Lorraine – an example of comagmatic copper-gold mineralization. In *Porphyry Deposits of the Northwestern Cordillera of North America* (T.G. Shroeter, ed.). *CIM Special Vol.* 46 (in press).
- BOTTINGA, Y. & JAVOY, M. (1975): Oxygen isotope partitioning among the minerals in igneous and metamorphic rocks. *Reviews Geophys. Space Physics* 13, 401-418.
- BOTTOMER, L. & LEARY, G. (1995): Geology of the Copper Canyon porphyry Cu-Au deposit, northwestern British Columbia. In *Porphyry Deposits of the Northwestern Cordillera of North America* (T.G. Shroeter, ed.). *CIM Special Vol.* 46 (in press).
- BURNHAM, C.W. (1979): Magmas and hydrothermal fluids. In *Geochemistry of Hydrothermal Ore Deposits* (H.L. Barnes, ed.). John Wiley & Sons, New York, 71-136.
- CANN, R.M. (1979): *Geochemistry of Magnetite and the Genesis of Magnetite-Apatite Lodes in the Iron Mask batholith, British Columbia*. M.Sc. thesis,

- Univ. British Columbia, Vancouver, British Columbia.
- CARTEN, R.B. (1986): Sodium-calcium metasomatism: Chemical, temporal and spatial relationships at the Yerington, Nevada, porphyry copper deposit. *Econ. Geol.* **81**, 1495-1519.
- CATHRO, M.S., DUNNE, K.P.E. & NACIUK, T.M. (1993): Katie – an alkaline porphyry copper-gold deposit in the Rossland Group, southeastern British Columbia. In *Geological Fieldwork 1992* (B. Grant & J. Newell, eds.). *Brit. Col. Ministry Energy Mines Petroleum Resources Paper 1993-1*, 233-248.
- CHAROY, B. & POLLARD, P.J. (1989): Albite-rich, silica-depleted metasomatic rocks at Emuford, northeast Queensland: Mineralogical, geochemical, and fluid inclusion constraints on hydrothermal evolution and tin mineralization. *Econ. Geol.* **84**, 1850-1874.
- CHIBA, H., CHACKO, T., CLAYTON, R.N. & GOLDSMITH, J.R. (1989): Oxygen isotope fractionations involving diopside, forsterite, magnetite, and calcite: application to geothermometry. *Geochim. Cosmochim. Acta* **53**, 2985-2995.
- DILLES, J.H. & EINAUDI, M.T. (1992): Wall-rock alteration and hydrothermal flow paths about the Ann-Mason porphyry copper deposit, Nevada – a 6-km vertical reconstruction. *Econ. Geol.* **87**, 1963-2001.
- DILLES, J.H., SOLOMON, G.C., TAYLOR, H.P. & EINAUDI, M.T. (1992): Oxygen and hydrogen isotope characteristics of hydrothermal alteration at the Ann-Mason porphyry copper deposit, Yerington, Nevada. *Econ. Geol.* **87**, 44-63.
- DOHERTY, J. (1990): *An Experimental Investigation of Supercritical Alkali Halide-Mineral Exchange Equilibria*. M.Sc. thesis, University of California at Los Angeles, Los Angeles, California.
- DUNNE, K.P.E., LANG, J.R. & THOMPSON, J.F.H. (1994): Fluid inclusion studies of zoned hydrothermal garnet at the Galore Creek Cu-Au porphyry deposit, northwestern British Columbia. *Geol. Assoc. Can. – Mineral. Assoc. Can. Program Abstr.* **19**, A31.
- ENNS, S., THOMPSON, F.H.T., STANLEY, C.R. & YARROW, E. (1995): The Galore Creek porphyry Cu-Au deposits, northwestern British Columbia. In *Porphyry Deposits of the Northwestern Cordillera of North America* (T.G. Shroeter, ed.), *CIM Special. Vol. 46* (in press).
- FOX, L.K. (1987a): Sodium metasomatism of Jurassic plutons, east-central Mohave Desert, California. *Geol. Soc. Am. Abstr. Programs* **19**, 379.
- FOX, L.K. (1987b): Mineralogical and chemical effects of late-magmatic albitization of Jurassic plutons, Bristol Mountains, California: Implications for fluid composition. *Geol. Soc. Am. Abstr. Programs* **19**, 667.
- FRASER, T.M., (1994a): Hydrothermal breccias and associated alteration of the Mount Polley copper-gold deposit. In *Geological Fieldwork 1993* (B. Grant & J. Newell, eds.). *Brit. Col. Ministry Energy Mines Petroleum Resources Paper 1994-1*, 259-268.
- FRASER, T.M. (1994b): *Geology, Alteration and Origin of Hydrothermal Breccias at the Mount Polley Alkalic Porphyry Copper-Gold Deposit, South-Central British Columbia*. M.Sc. thesis, Univ. British Columbia, Vancouver, British Columbia.
- FRASER, T.M., NIKIC, Z.T., PESALJ, R., GORC, D. & STANLEY, C.R. (1995): The geology of the Mount Polley alkalic porphyry Cu-Au deposit. In *Porphyry Deposits of the Northwestern Cordillera of North America* (T.G. Shroeter, ed.). *CIM Special. Vol. 46* (in press).
- GABRIELSE, H., MONGER, J.W.H., WHEELER, J.O. & YORATH, C.J. (1991): Morphogeologic belts, tectonic assemblages, and terranes; Chapter 2, Part A. In *Geology of the Cordilleran Orogen in Canada* (H. Gabrielse & C.J. Yorath, eds.). *Geol. Soc. Am., Geol. North Am. Series G-2*, 457-490.
- GHIORSO, M.S. & SACK, R.O. (1995): Chemical mass transfer in magmatic processes IV. A revised and internally consistent thermodynamic model for the interpolation and extrapolation of liquid-solid equilibria in magmatic systems at elevated temperatures and pressures. *Contrib. Mineral. Petrology* (accepted).
- HALL, D.L., COHEN, L.H. & SCHIFFMAN, P.

- (1988): Hydrothermal alteration associated with the Iron Hat iron skarn deposit, eastern Mohave Desert, San Bernardino County, California. *Econ. Geol.* **83**, 568-587.
- HOLLAND, H.D. (1972): Granites, solutions, and base metal deposits. *Econ. Geol.* **67**, 281-301.
- HUYCK, H.L.O. (1991): *Recent Insights about Mineralization at Copper Mountain*. Unpublished Report to Princeton Mining Corporation, Princeton, British Columbia, 7 p.
- KOVALENKO, V.I. (1976): The reaction between granite and aqueous hydrofluoric acid in relation to the origin of fluorine-bearing granites. *Geochem. Internat.* **14**, 108-118.
- KWONG, Y.T.J. (1987): Evolution of the Iron Mask batholith and its associated copper mineralization. *Brit. Col. Ministry Energy Mines Petroleum Resources Bull.* **77**.
- LANG, J.R. (1994): Major and trace element compositional zoning in hydrothermal and igneous garnets from alkalic intrusive complexes in British Columbia. *Geol. Soc. Am. Abstr. Programs* **25**, A369.
- LANG, J.R. & STANLEY, C.R. (1995): Contrasting styles of alkalic porphyry Cu-Au deposit in the northern part of the Iron Mask batholith, Kamloops, British Columbia. In *Porphyry Deposits of the Northwestern Cordillera of North America* (T.G. Shroeter, ed.). *CIM Special Vol.* **46** (in press).
- LANG, J.R., LUECK, B., MORTENSEN, J.K., RUSSELL, J.K., STANLEY, C.R. & THOMPSON, J.F.H. (1995): Triassic-Jurassic silica-undersaturated and silica-saturated alkalic intrusions in the Cordillera of British Columbia: Implications for arc magmatism. *Geology* **23** (in press).
- LANG, J.R., THOMPSON, J.F.H. & DUNNE, K.P.E. (1993): Hydrothermal garnets from the Galore Creek copper-gold porphyry deposit, B.C., Canada. *Geol. Soc. Am. Abstr. Programs* **24**, A143.
- LANG, J.R., THOMPSON, J.F.H. & STANLEY, C.R. (1994): Porphyry copper-gold deposits related to alkalic igneous rocks in the Triassic-Jurassic arc terranes of British Columbia. *Arizona Geol. Soc. Digest* **20** (in press).
- LAZNICKA, P. & EDWARDS, R.J. (1979): Dolores Creek, Yukon - a disseminated copper mineralization in sodic metasomatites. *Econ. Geol.* **74**, 1352-1370.
- LINKE, W.F. (1965): Solubilities, inorganic and metal-organic compounds. *Am. Chem. Soc.* **2**, 117 p.
- LUECK, B.A. & RUSSELL, J.K. (1994): Silica-undersaturated, zoned alkaline intrusions within the British Columbia Cordillera. In *Geological Fieldwork 1993* (B. Grant & J. Newell, eds.). *Brit. Col. Ministry Energy Mines Petroleum Resources Paper* **1994-1**, 311-315.
- LUECK, B.A. & RUSSELL, J.K. (in review): Substitution mechanisms within igneous melanite garnets: implications for the petrogenesis of silica-undersaturated alkaline plutons. *Can. Mineral.*
- MARGOLIS, J. (1993): *Geology and Intrusion-related Copper-Gold Mineralization, Sulphurets, British Columbia*. Ph.D thesis, Univ. of Oregon, Eugene, Oregon.
- MATTHEWS, A. (1994): Oxygen isotope geothermometers for metamorphic rocks. *J. Metamorphic Geol.* **12**, 211-219.
- MCMILLAN, W.J. & PANTELEYEV, A. (1994): Porphyry copper deposits of the Canadian Cordillera. *Arizona Geol. Soc. Digest* **20** (in press).
- MCMILLAN, W.J., THOMPSON, J.F.H., HART, C. & JOHNSTON, S. (1995): Regional geological and tectonic setting of porphyry deposits in British Columbia and the Yukon. In *Porphyry Deposits of the Northwestern Cordillera of North America* (T.G. Shroeter, ed.). *CIM Special Vol.* **46** (in press).
- MORTENSEN, J.K., GHOSH, D. & FERRI, F. (1995): U-Pb geochronology of intrusive rocks associated with Cu-Au porphyry deposits in the Canadian Cordillera. In *Porphyry Deposits of the Northwestern Cordillera of North America* (T.G. Shroeter, ed.). *CIM Special Vol.* **46** (in press).
- MORTIMER, N. (1987): The Nicola Group: Late Triassic and Early Jurassic subduction-related volcanism. *Can. J. Earth Sci.* **24**, 2521-2536.
- NELSON, J., BELLEFONTAINE, K., GREEN, K. &

- MACLEAN, M. (1991): Regional geological mapping near the Mount Milligan deposit. In Geological Fieldwork 1990 (B. Grant & J. Newell, eds.). *Brit. Col. Ministry Energy Mines Petroleum Resources Paper* 1991-1, 269-283.
- OHMOTO, H. & LASAGA, A.C. (1982): Kinetics of reactions between aqueous sulfates and sulfides in hydrothermal systems. *Geochim. Cosmochim. Acta* 46, 1727-1745.
- OMEL'YANENKO, B.I. & MINEYEVA, I.C. (1982): Pre- and syn-ore vertical zonation in Precambrian uraniferous sodic metasomatites. *Internat. Geol. Review* 24, 422-430.
- O'NEIL, J.R. & TAYLOR, H.P., JR. (1967): The oxygen isotope and cation exchange chemistry of feldspars. *Amer. Mineral.* 52, 1414-1437.
- ORVILLE, P.M. (1963): Alkali ion exchange between vapor and feldspar phases. *Am. J. Sci.* 261, 201-237.
- ORVILLE, P.M. (1972): Plagioclase cation exchange equilibria with aqueous chloride solution: Results at 700°C and 2000 bars in the presence of quartz. *Am. J. Sci.* 272, 234-272.
- PAN, Y., FLEET, M.E. & RAY, G.E. (1994): Chlorine-rich scapolite in gold skarn and Cu-Au porphyry deposits, B.C. *Geol. Assoc. Can. - Mineral. Assoc. Can. Program Abstr.* 19, A85.
- PERELLO, J.A., FLEMING, J.A., O'KANE, K.P., BURT, P.D., CLARKE, G.A., HIMES, M.D. & REEVES, A.T. (1995): Porphyry copper-gold-molybdenum mineralization in the Island Copper cluster, Vancouver Island. In *Porphyry Deposits of the Northwestern Cordillera of North America* (T.G. Shroeter, ed.). *CIM Special Vol.* 46 (in press).
- PRETO, V.A.G. (1972): Geology of Copper Mountain, B.C. *Brit. Col. Ministry Energy Mines Petroleum Resources Bull.* 59.
- PRETO, V.A.G. (1977): The Nicola Group: Mesozoic volcanism related to rifting in southern British Columbia. In *Volcanic Regimes in Canada* (W.R.A. Baragar, L.C. Coleman & J.M. Hall, eds.). *Geol. Assoc. Can. Special Paper* 16, 39-57.
- ROEDDER, E., editor (1984): Fluid Inclusions. *Reviews Mineral.* 12, 644 p.
- ROSS, K.V. (1993): *Geology of the Ajax East and Ajax West Copper-Gold Porphyry Deposits, Kamloops, South-Central British Columbia*. M.Sc. thesis, Univ. British Columbia, Vancouver, British Columbia.
- ROSS, K.V., GODWIN, C.I., BOND, L. & DAWSON, K.M. (1995): Geology of the Ajax copper-gold alkalic porphyry deposits, Kamloops, south-central British Columbia. In *Porphyry Deposits of the Northwestern Cordillera of North America* (T.G. Shroeter, ed.). *CIM Special Vol.* 46 (in press).
- RUHLMANN, F., RAYNAL, M. & LAVOIE, S. (1986): An example of albite-uranium alkaline metasomatism in the Otish Basin, Quebec. *Can. J. Earth Sci.* 23, 1742-1752.
- SHMURAYEVA, L.Y. (1985): Distinguishing features of two varieties of sodium metasomatism. *Internat. Geol. Review* 27, 1230-1237.
- SILLITOE, R.H. (1979): Some thoughts on gold-rich porphyry copper deposits. *Mineral. Deposita* 14, 161-174.
- SKETCHLEY, D., REBAGLIATI, M. & DELONG, C. (1995): Geology of the Mount Milligan alkalic porphyry Cu-Au deposits. In *Porphyry Deposits of the Northwestern Cordillera of North America* (T.G. Shroeter, ed.). *CIM Special Vol.* 46 (in press).
- SNYDER, L.D. (1994): *Petrological Studies within the Iron Mask Batholith, South Central British Columbia*. M.Sc. thesis, Univ. British Columbia, Vancouver, British Columbia.
- SNYDER, L.D. & RUSSELL, J.K. (1995): Petrogenetic relationships and assimilation processes in the alkalic Iron Mask batholith, south-central British Columbia. In *Porphyry Deposits of the Northwestern Cordillera of North America* (T.G. Shroeter, ed.). *CIM Special Vol.* 46 (in press).
- SOUTHER, J.G. (1991): Volcanic regimes. In *Geology of the Cordilleran Orogen in Canada* (H. Gabrielse & C.J. Yorath, eds.). *Geol. Soc. Am., Geol. North Am. Series G-2*, 457-490.
- STANLEY, C.R., HOLBECK, P.M., HUYCK, H.L.O., LANG, J.R., PRETO, V.A.G., BLOWER, S. &

- BOTTARO, J.C. (1995): Geology of the Copper Mountain alkalic copper-gold porphyry deposits, Princeton, British Columbia. In *Porphyry Deposits of the Northwestern Cordillera of North America* (T.G. Shroeter, ed.). *CIM Special Vol. 46* (in press).
- SUTHERLAND BROWN, A., editor (1976): Porphyry deposits of the Canadian Cordillera. *CIM Special Vol. 15*, 510 p.
- VOLLO, N.B. (1985): *Report on the CID Claim Group, Iron Mask Area, Kamloops, B.C.* Report to Comet Industries Ltd., Initial Developers Ltd., and Davenport Industries Ltd., 7 p.
- WILLIAMS-JONES, A.E. & SAMSON, I.M. (1990): Theoretical estimation of halite solubility in the system  $\text{NaCl-CaCl}_2\text{-H}_2\text{O}$ : applications to fluid inclusions. *Can. Mineral.* **28**, 299-304.
- WITT, W.K. (1988): Evolution of high-temperature hydrothermal fluids associated with greisenization and feldspathic alteration of a tin-mineralized granite, northeast Queensland. *Econ. Geol.* **83**, 310-334.
- WOOLLEY, A.R. (1982): A discussion of carbonatite evolution and nomenclature, and the generation of sodic and potassic fenites. *Mineral. Mag.* **46**, 13-17.

## H - ALKALIC-TYPE EPITHERMAL GOLD DEPOSITS

Jeremy P. Richards, University of Alberta

Richards, J.P. (1998): Alkalic-Type Epithermal Gold Deposits; in *Metallogeny of Volcanic Arcs*, B.C. Geological Survey, Short Course Notes, Open File 1998-8, Section H.

### ABSTRACT

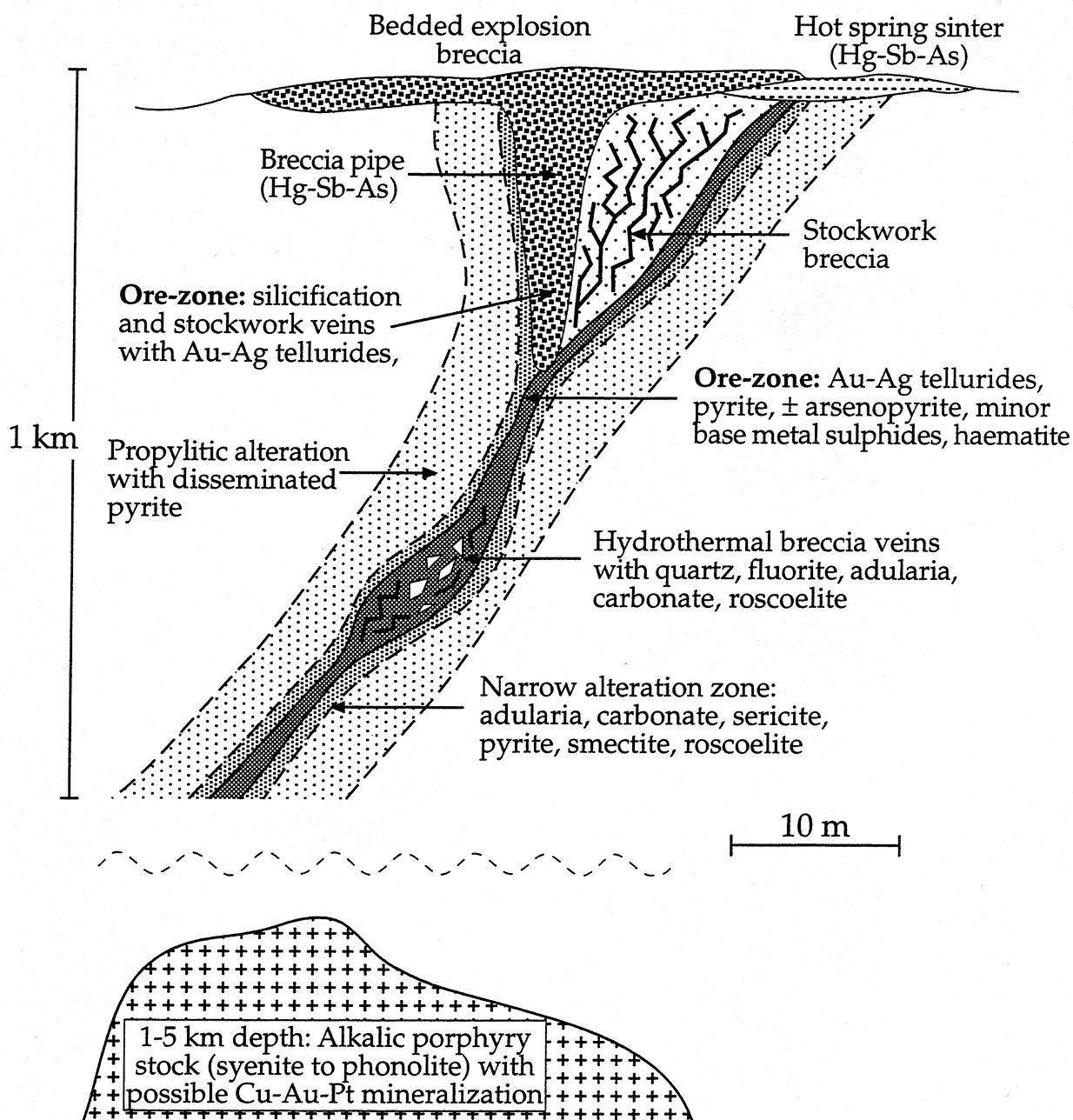
Alkalic-type epithermal gold deposits are part of a spectrum of igneous-related ore-forming hydrothermal systems, which probably stretches as a continuum from porphyry-type magmatic-hydrothermal, through high- and low-sulfidation epithermal, to meteoric water-dominated hot spring deposits in volcanic terrains. Commonly repeated combinations of certain variables, such as magma composition, fluid composition, depth, and temperature, lead to the formation of certain characteristic deposit types and deposit associations. For example, in calc-alkalic terrains, porphyry Cu deposits hosted at moderate depths within or near a parental pluton are commonly associated with shallow-level high-sulfidation, and/or more distal low-sulfidation epithermal Au deposits. Recognition of this continuum has been slow to gain acceptance because of the rare preservation of both porphyry and epithermal mineralization in the same deposit (due to erosion levels), and the difficulties with demonstration of their contemporaneity where preservation has occurred. However, recent careful studies, such as that conducted at the Lepanto Cu-Au epithermal and adjacent Far Southeast Cu-Au porphyry deposits in the Philippines by Arribas et al. (1995: *GEOLOGY*, v. 23, p. 337–340), have convincingly demonstrated the genetic nature of this spatial relationship.

In many respects, alkalic-type epithermal deposits associated with alkalic magmatism are little different from low-sulfidation epithermal deposits associated with calc-alkalic magmas. The most distinctive features of alkalic systems, apart from the igneous geochemical association, are details of mineralogy, such as the common presence of Au-Ag-tellurides, vanadium-micas (roscoelite), and fluorite, and their tectonic settings (atypical destructive margin settings, such as arc-collisional, post-subduction, and back-arc environments). From an economic point of view, however, the most important characteristic, which is shared by both deposit types, is the occurrence of structurally controlled, quartz-rich, vein and hydrothermal breccia systems that potentially host bonanza grades of gold mineralization (frequently measured in kg/tonne Au over several metres, and locally up to weight percent concentrations). Ore deposition occurs during explosive discharge of overpressured fluids along hydrologically convenient conduits (often normal faults or volcanic structures that offer high-permeability pathways to shallower, lower pressure levels).

Overpressuring of the fluid to some degree is required for vertical flow, and a common consequence of depressurization during ascent is fluid phase separation. Gold is thought to be dissolved as a Au-bisulfide complex in epithermal fluids, but phase separation causes the loss of the bisulfide ligand to the vapor phase as H<sub>2</sub>S, resulting in precipitation of the metal. If hydrostatic pressures are maintained in the conduit and the fluid is gas-poor, then the fluid will boil along a classic boiling-point–depth curve as it rises to relatively shallow levels (within a kilometre of the surface in typical low-sulfidation calc-alkalic epithermal systems). However, if the fluid contains dissolved gases, such as CO<sub>2</sub> and CH<sub>4</sub>, then

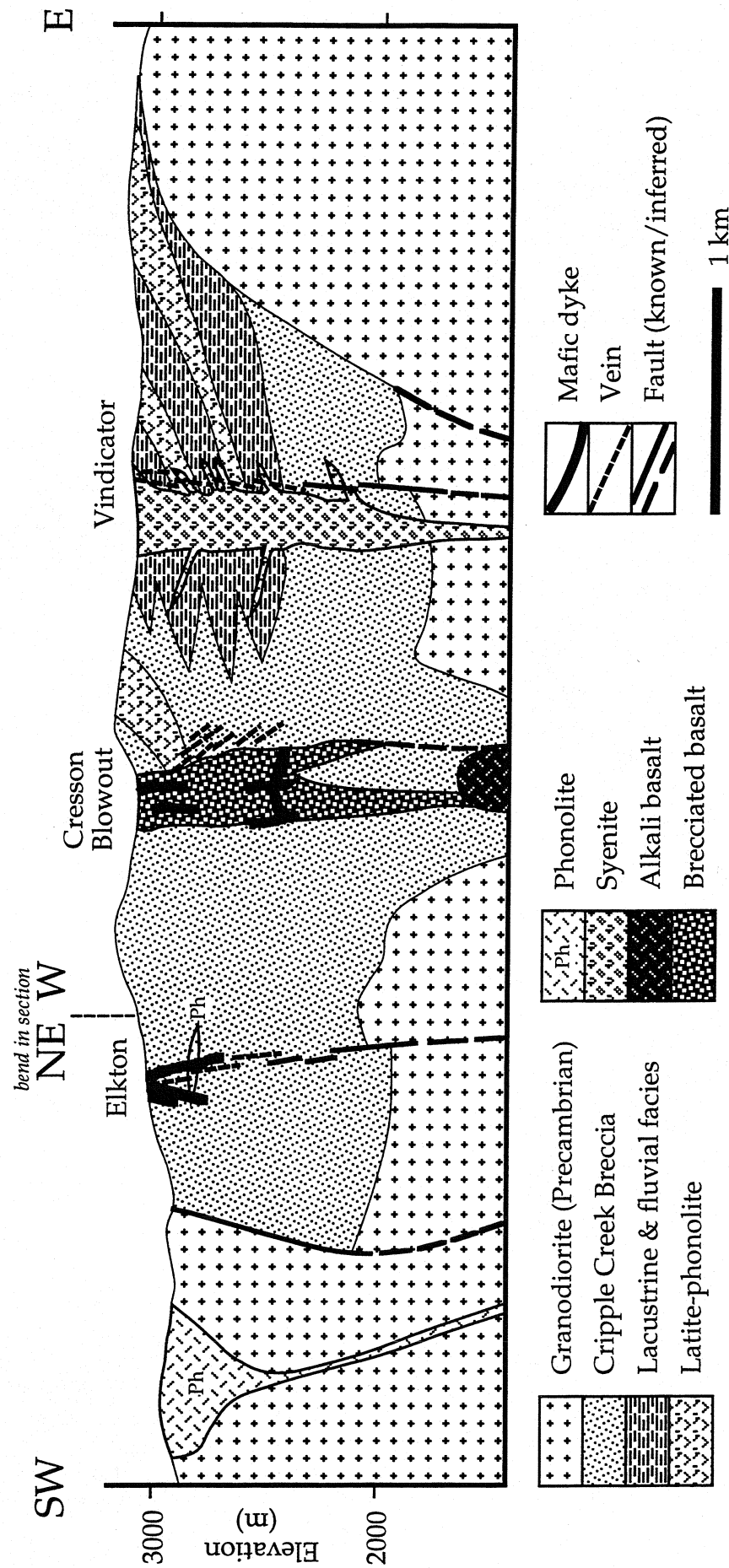
effervescence will occur at either higher pressures or greater depths than in gas-poor systems at a given temperature, thus extending the range of epithermal-style mineralization (in terms of ore textures and fluid temperatures) closer to the locus of the source igneous activity. Herein lies one difference commonly observed between typical calc-alkalic low-sulfidation systems and alkalic-type epithermal systems: the former are commonly distal to potential source intrusions, and are often thought to be unrelated to magmatic hydrothermal activity as a consequence. In contrast, many alkalic-type epithermal deposits, such as Cripple Creek (Colorado), Emperor (Fiji), and Porgera (Papua New Guinea), are hosted within or adjacent to alkalic intrusive rocks and related volcanic structures (diatremes or calderas). Few data exist relating to the gas-content of the ore-forming fluids in these systems, but at Porgera there is evidence that combined concentrations of CO<sub>2</sub> and CH<sub>4</sub> were sufficient to cause phase separation in relatively cool fluids (200–150°C) at depths of at least two kilometres, and over vertical intervals in excess of one kilometre. These fluids are believed to have been derived during relatively late-stage fractionation and devolatilization of a magma chamber located beneath the currently exposed hydrothermal system. Current research at Porgera is aimed at investigating the transition from early higher-temperature base-metal-rich mineralization to this later style of alkalic-type epithermal mineralization, and exploring the potential for porphyry-type Cu-Au mineralization related to the source intrusion at greater depth.

Finally, some speculations will be offered regarding tectonic and petrogenetic controls on metal inventory in alkalic and calc-alkalic ore-forming systems. Typical calc-alkalic metalliferous provinces associated with arc magmatism are Cu-rich, with porphyry Cu deposits containing by-product Au at various levels of economic importance. In contrast, alkalic-type deposits appear to be dominated by Au, with little associated economic Cu mineralization. It is proposed that this distinction relates directly to melting processes in the mantle, and specifically to the role of sulfides in this source region.

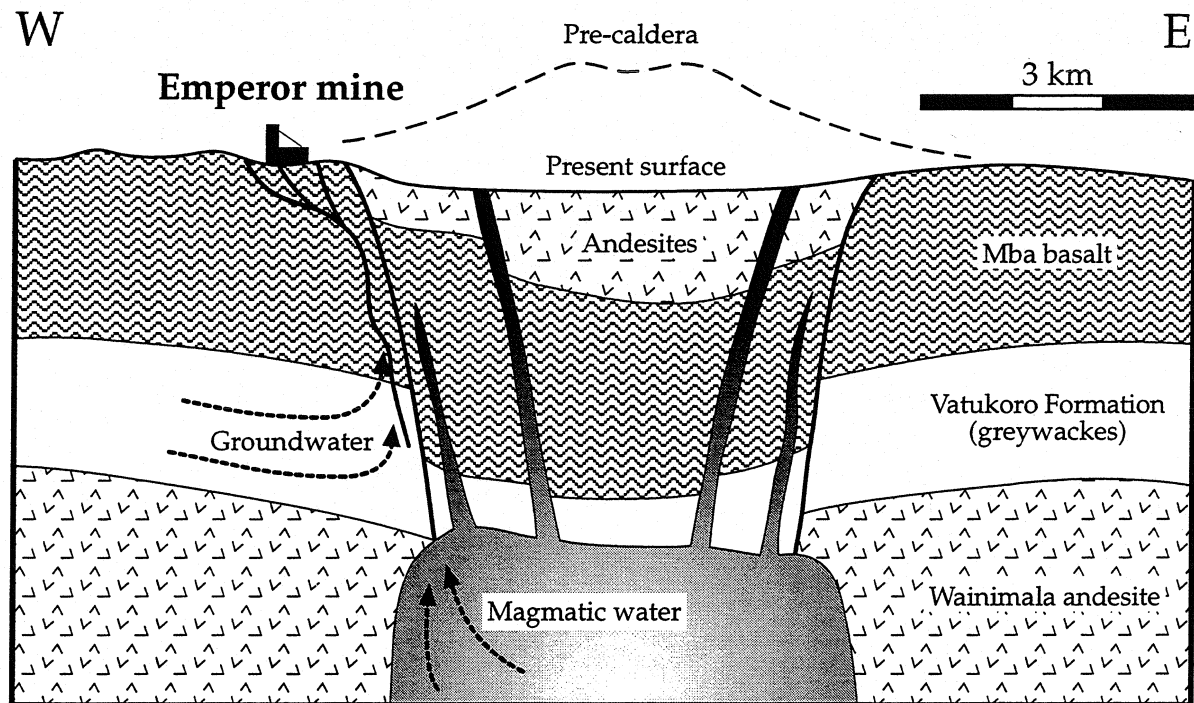


**Schematic model of an alkalic-type epithermal Au system.** Modified from Richards, 1995 (Alkalic-type epithermal gold deposits—a review, in Thompson, J.F.H. (ed.), *Magma, Fluids, and Ore Deposits*: Mineralogical Association of Canada, Short Course Series, v. 23, ch. 17, p. 367–400), after Bonham, 1986 (Models for volcanic-hosted epithermal precious metal deposits; a review. Proceedings of Symposium 5, Volcanism, hydrothermal systems and related mineralization, in International Volcanological Congress, Univ. Auckland, New Zealand, 13-17).

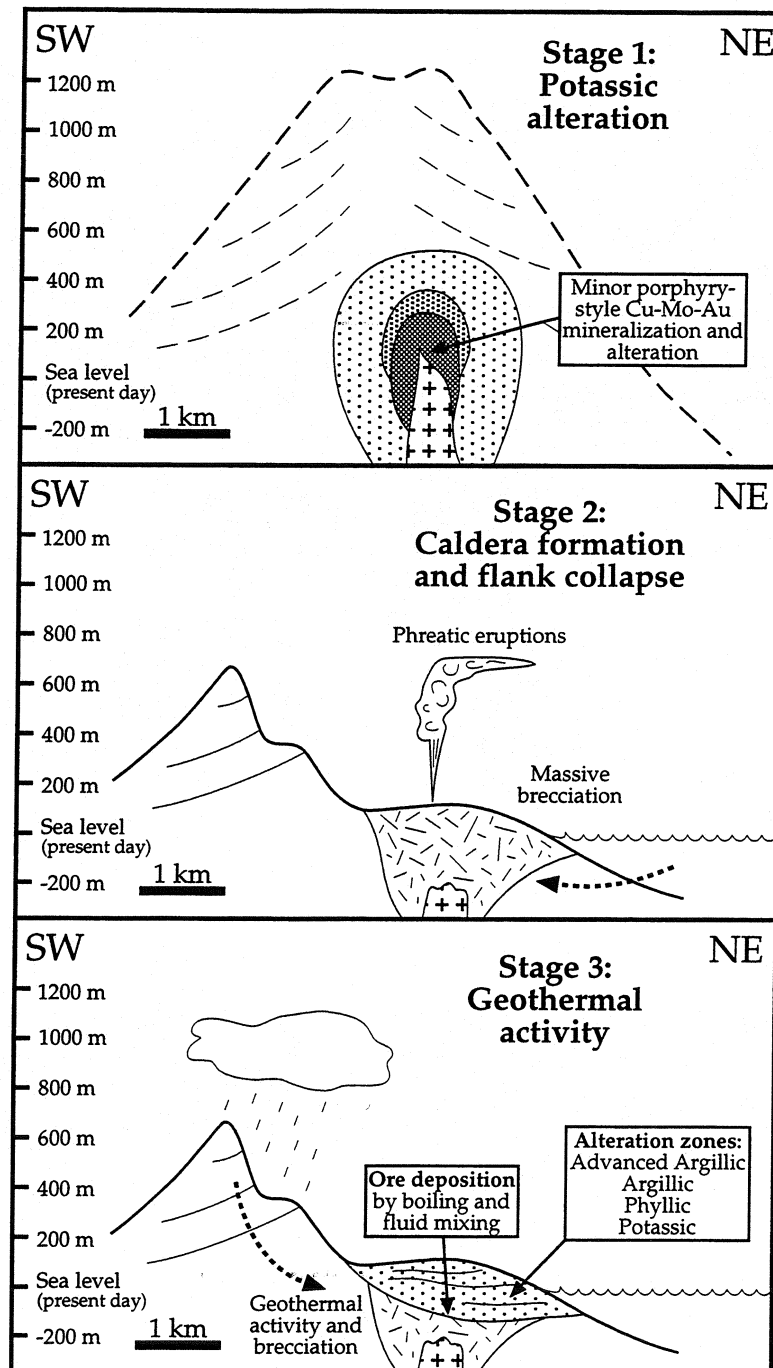




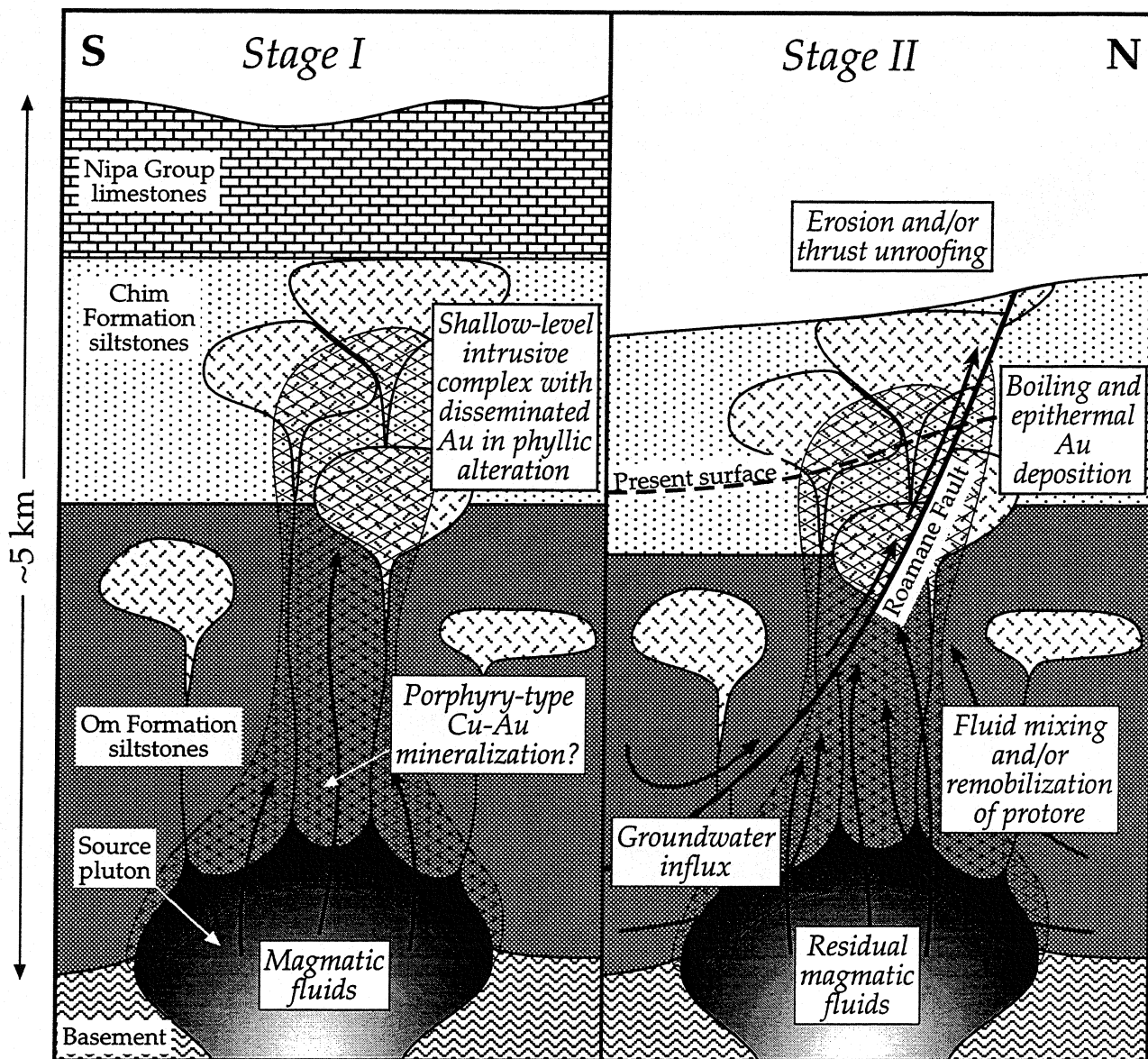
**Geological cross-section through the Cripple Creek volcanic complex.** Modified from Richards, 1995 (Alkaline-type epithermal gold deposits—a review, in Thompson, J.F.H. (ed.), *Magma, Fluids, and Ore Deposits: Mineralogical Association of Canada, Short Course Series*, v. 23, ch. 17, p. 367–400), after Thompson et al., 1985 (Mineralized veins and breccias of the Cripple Creek District, Colorado. *Econ. Geol.* **80**, 1669–1688).



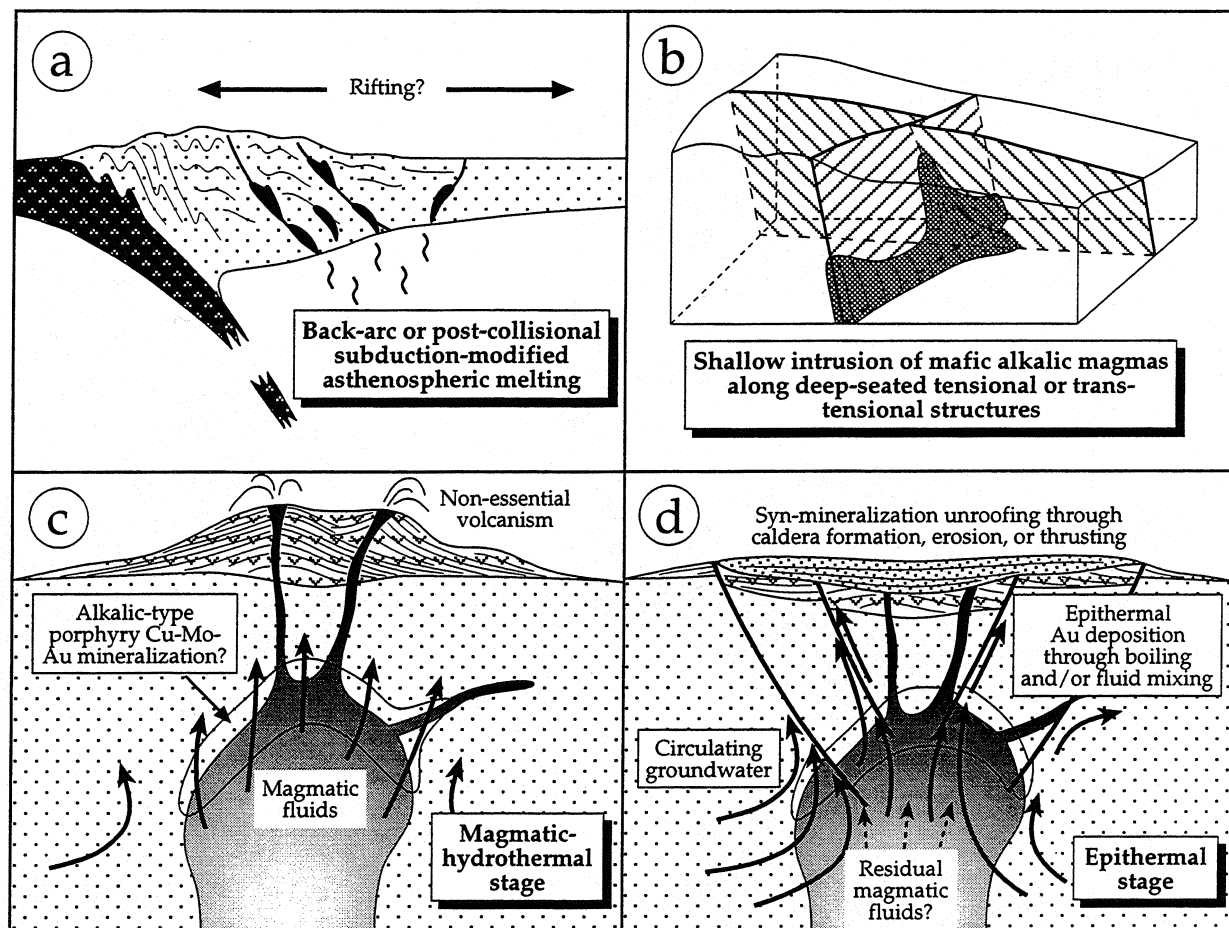
**Schematic section through the Emperor Au deposit, Fiji.** Modified from Richards, 1995 (Alkalic-type epithermal gold deposits—a review, in Thompson, J.F.H. (ed.), *Magma, Fluids, and Ore Deposits*: Mineralogical Association of Canada, Short Course Series, v. 23, ch. 17, p. 367–400), after Ahmad et al., 1987 (Mineralogical and geochemical studies of the Emperor gold telluride deposit, Fiji: *Econ. Geol.* 82, 345–370.).



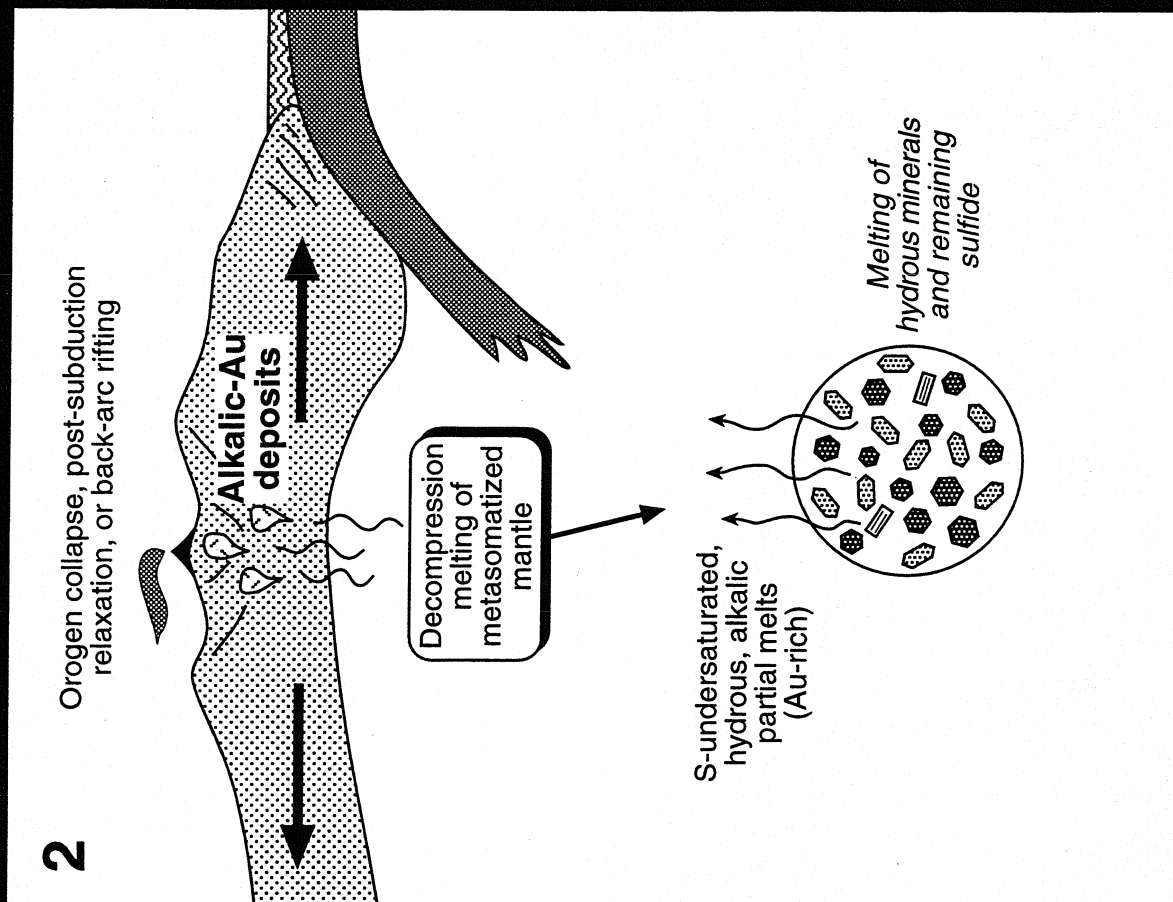
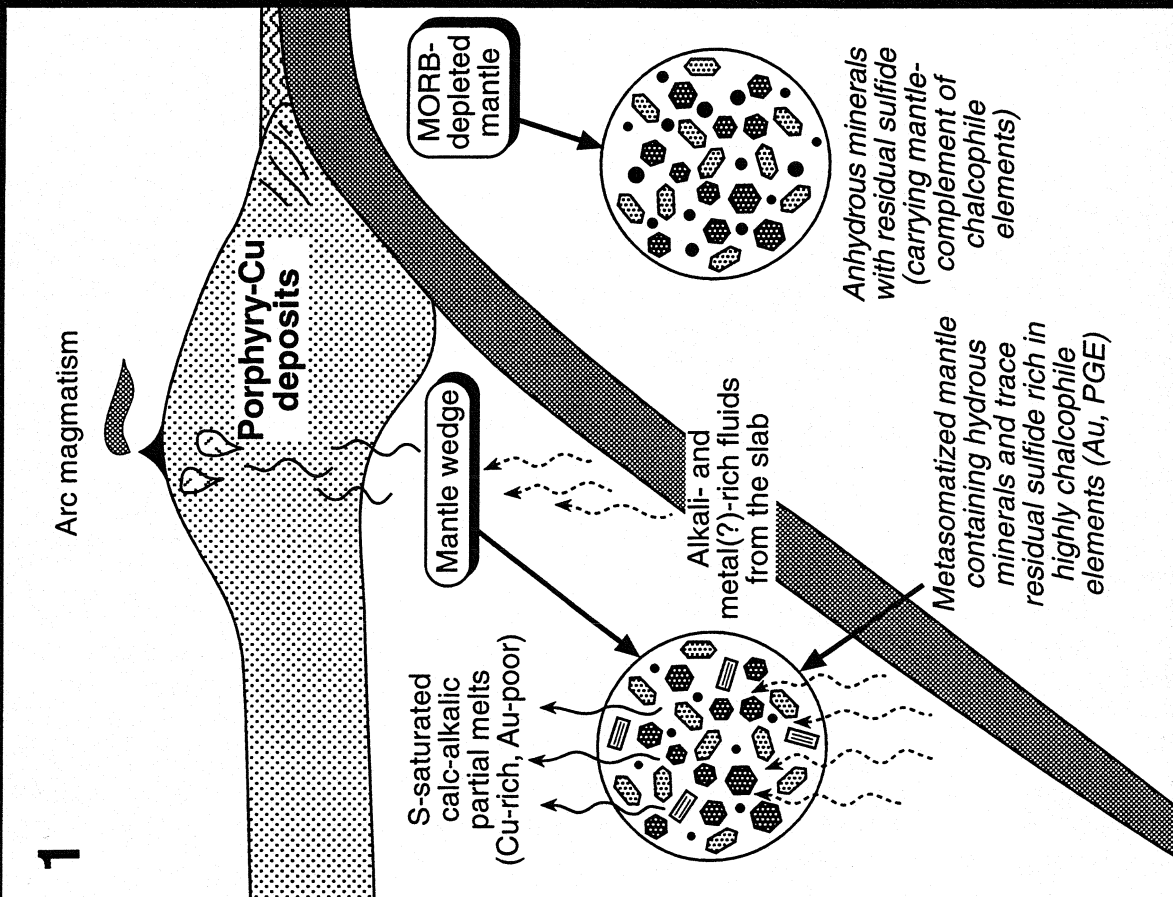
**Schematic model for formation of the Ladolam Au deposit, PNG.** Modified from Richards, 1995 (Alkalic-type epithermal gold deposits—a review, in Thompson, J.F.H. (ed.), *Magma, Fluids, and Ore Deposits*: Mineralogical Association of Canada, Short Course Series, v. 23, ch. 17, p. 367–400), after Moyle et al., 1990 (Ladolam gold deposit, Lihir Island, in *Geology of the mineral deposits of Australia and Papua New Guinea* (F.E. Hughes, ed.). *Austral. Inst. Mining & Metall.*, 1793–1805).



**Schematic model for formation of the Porgera Au deposit.** Modified from Richards, 1995 (Alkalic-type epithermal gold deposits—a review, in Thompson, J.F.H. (ed.), *Magma, Fluids, and Ore Deposits*: Mineralogical Association of Canada, Short Course Series, v. 23, ch. 17, p. 367–400).



**Generalized model depicting the development of alkalic-type epithermal gold deposits in association with alkalic intrusive complexes.** Modified from Richards, 1995 (Alkalic-type epithermal gold deposits—a review, in Thompson, J.F.H. (ed.), *Magmas, Fluids, and Ore Deposits: Mineralogical Association of Canada, Short Course Series*, v. 23, ch. 17, p. 367–400).



## Chapter 17

# ALKALIC-TYPE EPITHERMAL GOLD DEPOSITS – A REVIEW

Jeremy P. Richards

Department of Geology, University of Leicester,  
University Road, Leicester, LE1 7RH, UK

### INTRODUCTION

The term “alkalic-type” is a less than wholly satisfactory label for a variety of epithermal gold-rich deposits that are associated with igneous rocks of alkalic affinity. The problem is immediately apparent: how do we define “alkalic” in this context? Even igneous petrologists cannot agree on a single definition for this term, and competing classification schemes use various measures of silica content, alkali content, or discriminants based on trace elements, to distinguish alkalic rocks from other igneous suites. What is almost certain, however, is that the limits of the range of alkalic rocks as surveyed by the petrologist will have only limited relevance to the range of rock types associated with alkalic-type gold deposits. In the context of epithermal deposits, therefore, the term ‘alkalic’ is used simply in recognition of a broad association of gold deposits with igneous rocks of relatively high alkali-element content and also, typically, relatively high volatile content.

In the following discussions, the existence of a direct genetic relationship between alkalic-type epithermal gold deposits and the associated alkalic magmatism is taken as a working premise. Perhaps alone among the epithermal deposit types, the alkalic group can support this argument with least question.

This contribution firstly summarizes the characteristics of some well-known examples of alkalic-type epithermal mineralization (Cripple Creek, Colorado; Colorado mineral belt; Montana alkalic province; Porgera, Mt. Kare, and Ladolam, Papua New Guinea; Emperor, Fiji). The relative importance of some of these characteristics is then discussed, with a view to isolating unifying factors in the process of ore genesis.

### HISTORY OF MODEL DEVELOPMENT

Bonham & Giles (1983) first drew attention to an association between Au-Te-rich epithermal deposits and alkalic rocks. This paper was followed by the simultaneous publication of abstracts by Bonham (1984) and Mutschler *et al.* (1984), who elaborated on the theme and listed several important characteristics of the deposits (Table 1). These characteristics included the presence of quartz-carbonate-fluorite-orthoclase (“adularia”) alteration, high Au/Ag ratios with Au commonly present in Au-Ag tellurides, and relatively low sulfur and base-metal abundances. Mutschler *et al.* (1984) and Werle *et al.* (1984) further suggested that such epithermal systems may grade downwards into porphyry-type Cu – precious-metal deposits associated with alkali gabbros and syenites, an idea ventured earlier by Bonham & Giles (1983). The contrast between these types of deposit and the more clearly defined acid-sulfate and adularia-sericite epithermal systems was recognized by Heald-Wetlaufer *et al.* (1983), and later by Hayba *et al.* (1985) and Heald *et al.* (1987), but no detailed comparison of mineralization styles was offered. Both Mutschler *et al.* (1985) and Bonham (1986) subsequently expanded on their theses, and it was then that Bonham first coined the term “alkalic-type” to describe this mineral-deposit association. The model was further refined to acknowledge the common presence of the vanadium-mica roscoelite in vein and alteration assemblages, and potential association with alkalic rocks as diverse as syenites, trachytes, phonolites, and shoshonites. A schematic cross-section (Bonham 1986; Fig. 1) emphasized the importance of stockwork veins and hydrothermal breccias in the deposit structure, with a locus of

Table 1. Development of models for alkalic-type epithermal gold deposits

Feature	Bonham (1984)	Mutschler <i>et al.</i> (1984)	Mutschler <i>et al.</i> (1985)	Bonham (1986)	Cox & Bagby (1986)	Jaireth (1991)
Type name	Epithermal Au characterized by quartz-fluorite-adularia alteration Au tellurides	Epithermal Au related to alkaline rocks	Epithermal Au related to alkaline rocks	Alkalic Au-Ag epithermal deposits	Au-Ag-Te vein deposits related to hypabyssal/-extrusive alkalic rocks	Te-bearing epithermal gold-silver deposits
Main ore minerals		Au tellurides	Pyrite, Au-Ag tellurides	Au-Ag tellurides, electrum, Au <sup>0</sup> in Py	Au-Ag tellurides, pyrite	Au <sup>0</sup> , Au-Ag tellurides
Other ore minerals				Base-metal & Mo, As, Hg, Sb sulfides	Hg tellurides, base-metal sulfides, tetrahedrite, stibnite	Base-metal sulfides & sulfosalts, Hg-, Ni-, Pb-tellurides, Te <sup>0</sup>
Main gangue minerals	Quartz, fluorite, adularia	Carbonate, fluorite, quartz	K-feldspar, quartz, carbonate, fluorite	Quartz, carbonate, roscocelite, fluorite, adularia	Quartz, calcite, fluorite, barite, celestite, roscocelite, adularia	Quartz, barite
Mineralization style		Veins, disseminations	Veins	Veins, stockworks, breccias	Veins, breccias	
Alteration style	Quartz, fluorite, adularia	K-metasomatism, carbonate, Fe-oxidation	K-metasomatism, phyllic alteration, pyritization, carbonate, roscocelite, fluorite, or adularia alteration halos around veins	Regional propylitic alteration; narrow quartz, carbonate, roscocelite, fluorite, or adularia alteration halos around veins	Propylitic with carbonates & pyrite; sericitization of wallrocks, rare silicification	Regional propylitic alteration; local sericitic, silicic & argillic alteration around veins
Geochemical indicators	Au > Ag; anomalous F, Te; minor Cu, Pb, Zn	Low S; Au > Ag; anomalous Ag, As, Bi, Hg, La, Mo, Nb, Pb, Sb, Te, Ti, U, V	Anomalous Ag, As, Bi, Ce, Cu, F, Hg, La, Mo, Nb, Pb, S, Sb, Te, Ti, U, V	As for Mutschler <i>et al.</i> (1984)	Au, Ag, Te, Cu, Pb, Zn, Sb, Hg, F, Ba, PGE	
Associated igneous rocks	Alkalic	Unsaturated syenite, trachyte, phonolite	Unsaturated felsic syenite - differentiates of alkali basalts; late lamprophyre, alkali basalt intrusions	Syenite, trachyte, phonolite, shoshonite	Syenite, monzonite, diorite, phonolite, monchiquite, vogesite, shoshonite	Syenite, monzonite, diorite, phonolite, latite, trachyandesite, alkali basalt, lamprophyre
Geochemistry of igneous rocks		SiO <sub>2</sub> > 45 wt % unless CO <sub>2</sub> > 5 wt %, Na <sub>2</sub> O + K <sub>2</sub> O > 8.0 wt %; Na <sub>2</sub> O/K <sub>2</sub> O < 1; Fe <sub>2</sub> O <sub>3</sub> > 1.7 × FeO; high Ba/Rb; Au > 10 ppb	Na <sub>2</sub> O + K <sub>2</sub> O > 10.0 wt %; Na <sub>2</sub> O > K <sub>2</sub> O; CO <sub>2</sub> & F saturated upon eruption	As for Mutschler <i>et al.</i> (1984)		
Style of magmatism		Epizonal intrusions & vent complexes	Subvolcanic complexes	Maar-diatreme complexes, calderas	Volcanic centers, calderas	Calderas, diatremes, breccia pipes
Comments		May grade downwards into porphyry Cu-precious metal deposits	Zonation from Au-rich epithermal deposits downwards to Cu-Ag-(PGE)-rich porphyries	As for Mutschler <i>et al.</i> (1984)	Veins may follow porphyry dykes	Recognition of magmatic fluid involvement; ore deposition by boiling and/or mixing
Examples	Cripple Creek (Colorado); Zortman-Landusky (Montana)		Cripple Creek (Colorado); Bear Lodge Mts. (Wyoming)	Cripple Creek (Colorado); central Montana alkalic province; Emperor (Fiji)	Cripple Creek, La Plata (Colorado); Montana alkalic province; Emperor (Fiji)	Cripple Creek & Colorado mineral belt; Golden Sunlight (Montana); Emperor (Fiji); Queensland; Kochbulak (Kazakhstan)



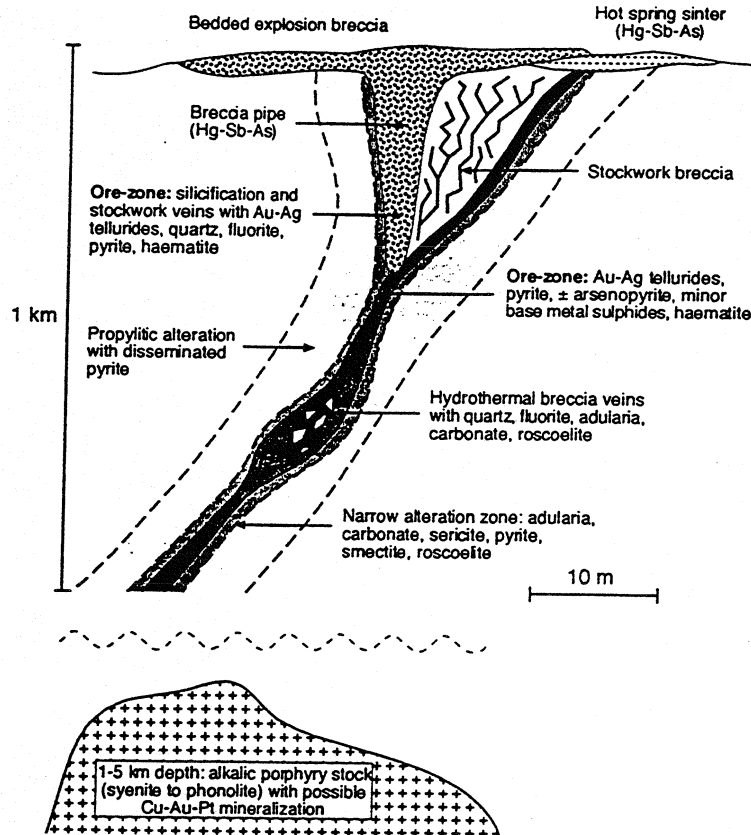


Figure 1. Schematic model of an alkalic-type Au-Ag deposit (after Bonham 1986).

ore deposition intermediate between deeper alkalic porphyry-type activity, and shallow volcanism. Many of these characteristics were summarized by Cox & Bagby (1986) in their descriptive model for Au-Ag-Te veins, with further expansion of the range of associated igneous rocks to include diorites and certain lamprophyres. Finally, a recent review of selected deposit characteristics by Jaireth (1991) included summaries of stable isotopic and fluid-inclusion data pertaining to fluid sources and depositional mechanisms (Table 1).

As with all such models, the setting up of criteria invites the recognition of exceptions, and with each new discovery further 'permitted' criteria have been added. Given the wide diversity of potential source-rock compositions for deposits in this class, this expansion of the classification is hardly surprising.

#### EXAMPLES OF ALKALIC-TYPE EPITHERMAL GOLD DEPOSITS

The early models of alkalic-type epithermal

Au systems were based largely on the Cripple Creek (Colorado) and Emperor (Fiji) deposits, and mines in the central Montana alkalic province. Since then, a number of other deposits have been recognized as belonging to this suite, including the Porgera, Mt. Kare, and Ladolam deposits in Papua New Guinea. It is, however, difficult to know where to draw the boundary between alkalic-type and other epithermal mineralization styles. For the purposes of this review, therefore, the characteristics of a selection of well-studied deposits that fall well within the bounds of the alkalic category are summarized below.

##### *Cripple Creek, Colorado*

The Cripple Creek gold deposit was the subject of early studies by Cross & Penrose (1895), Lindgren & Ransome (1906), and Loughlin & Koschmann (1935), who focussed on detailed description and petrography. The few papers published since then have addressed the more modern subjects of geochemistry and fluid evolution (Gott *et al.* 1969; Boyle 1979; Thompson *et al.* 1985; Thompson 1992).

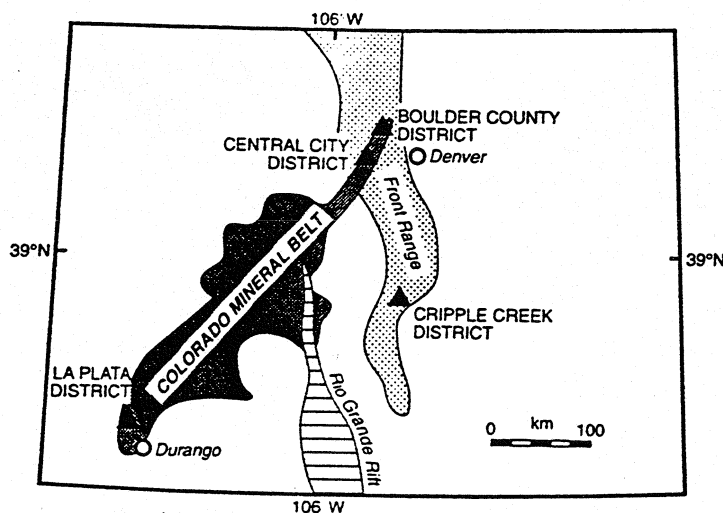


Figure 2. Sketch map showing the location of the Colorado mineral belt and Cripple Creek (after Saunders 1991).

The Cripple Creek deposit is hosted by an alkalic volcanic center related to extensional tectonism associated with the Rio Grande rift, and has K-Ar ages ranging from 34 to 28 Ma (cited in Thompson *et al.* 1985; Fig. 2). The volcanic center is represented by a brecciated mass of Precambrian country rocks and Tertiary volcanic fragments, interdigitated with phonolitic pyroclastics, and lacustrine and fluvial sediments. Deposition of this breccia occurred in subsiding basins related to the development of three coalescing diatremes. The breccia and diatremes were subsequently cut by a series of penecontemporaneous alkalic intrusions (Fig. 3) ranging from early stocks of phonotephrite, phonolite, and trachyte, to later alkali basalt and lamprophyre dykes (monchiquite and vogesite). Thompson *et al.* (1985) proposed that the range in magmatic compositions resulted from mixing between phonolitic and alkali basaltic magmas. A small diatreme body, the "Cresson blowout", appears to be coeval with late dyke emplacement as it contains a high proportion of basaltic fragments, as well as being crosscut by dykes. It has been suggested that the blowout may be phreatomagmatic in origin, resulting from interaction between groundwaters and the mafic magmas (Thompson *et al.* 1985).

Four main types of mineral deposit have been recognized by Thompson (1992): vein deposits, which occur throughout the complex; diatreme-hosted deposits, such as those hosted by the Cresson blowout; hydrothermal breccia deposits,

common in the northern diatreme; and stratiform deposits hosted by tuffs and sediment horizons mainly within the eastern diatreme.

Vein-type deposits (*e.g.*, Elkton, Vindicator, Ajax) occur in sheeted sets of narrow veinlets, and are characterized by unusual vertical continuity of up to 1 km. The veins display five stages of mineralization (Thompson *et al.* 1985). Stage 1 quartz-fluorite-adularia-pyrite deposition was associated with hot, saline, CO<sub>2</sub>-bearing fluids (fluid-inclusion homogenization temperatures  $T_h$  from 206° to 510 °C; salinities from 33 to 40 eq. wt.% NaCl). Stage 2 base-metal sulfide-quartz-pyrite, and stage 3 quartz-fluorite-pyrite-hematite-rutile deposition was accompanied by more dilute fluids (0-8.3 eq. wt.% NaCl), with steadily decreasing temperatures falling to ~140 °C ( $T_h$ ) by stage 4. During this last stage, Au was deposited as calaverite along with quartz, pyrite, rutile, and acanthite. Thompson *et al.* (1985) suggested that boiling occurred during all four stages with a coupled fall in temperature and salinity, and that pressures during stage 4 were 360-400 bars. Final vein filling was characterized by low-temperature quartz-fluorite-dolomite deposition. Limited wallrock alteration associated with these veins consists of adularia, roscoelite, sericite, pyrite, and Fe-Ti oxides.

In the Cresson blowout, hydrothermal minerals were precipitated interstitially to the heterolithic breccia fragments of the diatreme. These breccia cements are characterized by an early adularia-quartz-pyrite-hematite-marcasite

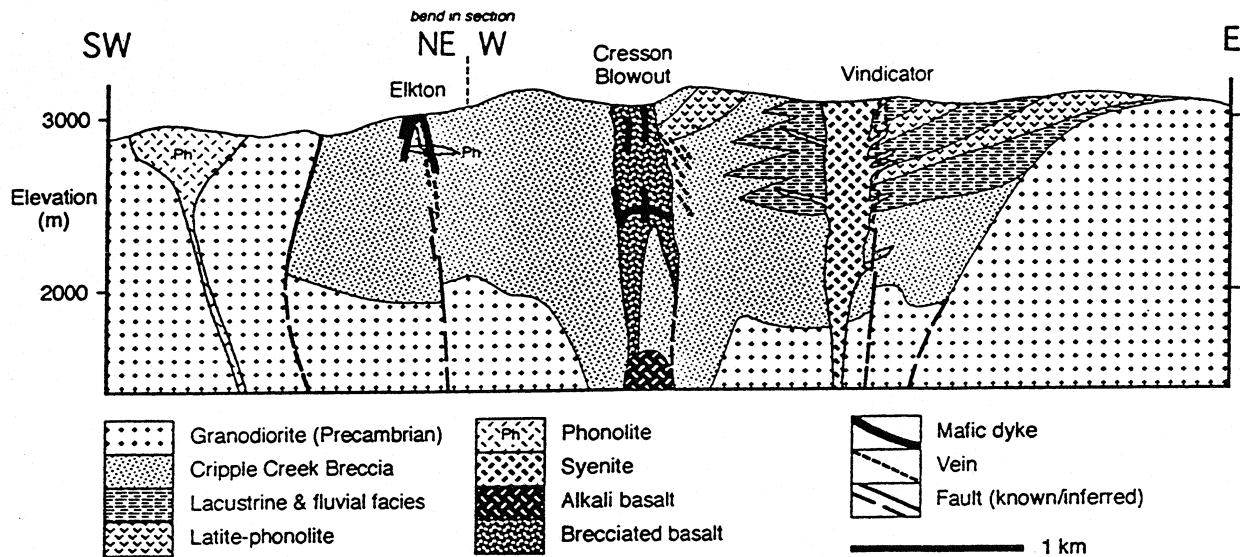


Figure 3. Geological cross-section through the Cripple Creek volcanic complex (after Thompson *et al.* 1985).

assemblage, intermediate celestine-dolomite-quartz-fluorite and base-metal sulfides, and late quartz/chalcedony/opal with native gold and Au-Ag tellurides. Fluid temperatures and salinities ranged from 131° to 175 °C and <3 eq. wt.% NaCl, with periodic boiling (Thompson 1992). Propylitic alteration of the breccia wallrocks seems to pre-date mineralization.

Hydrothermal breccia deposits seem to be restricted to areas capped by intrusive plagioclase phonolite, which may have acted as a permeability barrier causing build-up of fluid pressure. The breccias formed at shallow levels and involved oxidized fluids. The heterolithic clasts are cemented by quartz, Fe and Mn oxides, celestine, barite, anhydrite, and carbonates, with base-metal sulfides, native gold, and minor calaverite. At least some of the oxidation is secondary, and may have resulted in break down of tellurides to leave native gold. Thompson (1992) interpreted the breccias as near-surface equivalents of the deeper vein systems, and reported fluid-inclusion temperatures and salinities of <190 °C ( $T_h$ ) and <8 eq. wt.% NaCl, plus significant CO<sub>2</sub>.

Stratiform deposits hosted by sedimentary and tuffaceous sequences within the Cripple Creek diatreme have not been studied as extensively as the previous types, perhaps because of their lower gold productivity. Thompson (1992) suggested, however, that Au values associated with extensive silicic, potassic, and argillic alteration assem-

blages resulted from lateral flow of hydrothermal fluids along these relatively permeable strata where they were intersected by vein systems.

#### Colorado Mineral Belt

Gold-telluride mineralization was first discovered in the Boulder and La Plata counties of Colorado during the 1870s and 1880s, and the intensely mineralized stretch of ground between these two districts has become known as the Colorado mineral belt (Fig. 2). This ~425-km-long NE-SW-trending belt marks a zone of intense Late Cretaceous-Tertiary (Laramide) igneous activity that cuts across the main N-S grain of the Colorado mountains, and has been interpreted as a reactivated shear zone in the Precambrian basement (Tweto & Sims 1963; Warner 1978). Magmatism was long-lived, widespread, and varied throughout this region, but gold-telluride mineralization seems to be most closely associated with the later phases of this activity (e.g., 44-59 Ma in the Boulder district, 54-59 Ma in Central City, and 65-70 Ma in La Plata; Rice *et al.* 1982; Gable 1985; Saunders & May 1986, and references therein; Spry 1987).

These late intrusive phases are dominantly of alkalic affinity, and consist of syenite and alkali syenite, diorite, monzonite, trachyte, bostonite (alkali feldspar syenite), and biotite latite (e.g., Simmons & Hedge 1978). In addition to the gold-telluride deposits, fluorite breccia pipes,

stockwork Mo-Au deposits, and pyritic gold veins are also closely associated with these intrusions (Kelly & Goddard 1969; Rice *et al.* 1985; Saunders 1991).

An extensive literature exists on the Colorado mineral belt, but for brevity only the Boulder County deposits, which seem to be representative of the belt as a whole, are discussed in detail here. The reader is referred to papers by Werle *et al.* (1984) and Saunders & May (1986) for useful descriptions of deposits in the La Plata district, and to Rice *et al.* (1985), Dickin *et al.* (1986), and Spry (1987) for deposits in the Central City district.

Gold deposits of the Boulder County district have been described by Lovering & Goddard (1950), Kelly & Goddard (1969), and more recently by Saunders (1991). Among the best known of these deposits are the Gold Hill, Jamestown, and Magnolia gold-telluride mines which operated extensively prior to 1900, but which still provoke occasional exploration interest (Fig. 4). With the exception of Magnolia, at which no intrusive rocks are exposed, each of these deposits is closely associated with Tertiary alkalic stocks: examples are the 54-44 Ma alkali syenite Sunset Stock near Gold Hill, and the 45 Ma syenite Porphyry Mountain stock near Jamestown (Gable 1985; Saunders 1991). The locus of intrusion and subsequent mineralization seems to be controlled in the first order by a prominent series of NW-trending normal and strike-slip faults ("breccia reefs" of Lovering & Goddard 1950), but in detail the gold deposits are localized by a set of younger NE-trending brecciated cross-faults. Lovering & Goddard (1950) proposed that the breccia reefs acted as primary conduits for the ore fluids, but that their sheared and quartz-sealed nature prevented significant ore deposition. In contrast, where these fluids flowed into the more open NE faults, ore minerals were deposited as breccia cements and open-space fillings. Optimal settings for ore deposition were intersections of the veins with other structures or brittle wallrocks (e.g., granite), where maximum brecciation and cavity formation was achieved.

Paragenetic studies by Kelly & Goddard (1969) revealed a complex sequence of sixty-seven vein minerals, including the main ore

minerals sylvanite, petzite, hessite, and native gold, plus ten other tellurides and various sulfides and sulfosalts. Gangue minerals are predominantly quartz, locally with adularia, roscoelite, fluorite, barite, ankerite, and calcite. Wallrock alteration is characterized by sericitization, silicification, pyritization, and distal argillization. In broad terms, mineral deposition began with quartz, and was followed by base-metal sulfides with adularia, roscoelite, fluorite, and barite. Sulfosalts were deposited at the end of the sulfide stage, and preceded the main telluride ore stage. The occurrence of native Te among the telluride minerals, followed by a stage of native gold deposition, is notable. Final vein-fillings consist of carbonates and chalcedony, plus late (possibly supergene) gypsum and opal. Overall, the veins represent anomalous enrichments in Au, Ag, Te, Hg, As, Sb, Mo, Cu, Pb, Zn, F, V, and Ni (Saunders 1991).

Fluid-inclusion studies (Kelly & Goddard 1969; Nash & Cunningham 1973; Geller & Atkinson 1991; Saunders 1991, and references therein) have shown that early vein fluids may have had temperatures as high as 375 °C and salinities between 20 and 28 eq. wt.% NaCl; in addition, CO<sub>2</sub>-rich fluid inclusions (II-23 mole % CO<sub>2</sub>) have been reported in early fluorite veins. Temperatures and salinities fell progressively to <250 °C and 3 to 6 eq. wt.% NaCl by the start of the main telluride stage, and continued to fall, perhaps to below 100 °C during deposition of native gold. Carbon dioxide concentrations also fell progressively over this period. Pressures are estimated to have been between 200 and 360 bars (650 to 1300 m in depth). Although Nash & Cunningham (1973) reported the presence of early vapor- and CO<sub>2</sub>-rich fluid inclusions suggestive of phase separation, Saunders (1991) reported no fluid-inclusion evidence for boiling during gold and telluride deposition. Nevertheless, the brecciated nature of the veins and the high CO<sub>2</sub> content of the early fluids are strongly suggestive that phase separation, perhaps promoted by depressurization as fluids flowed out of the breccia reefs and into the open NE faults (Kelly & Goddard 1969), was an important precipitation mechanism. Saunders (1991) proposed that the telluride deposits are the distal products of

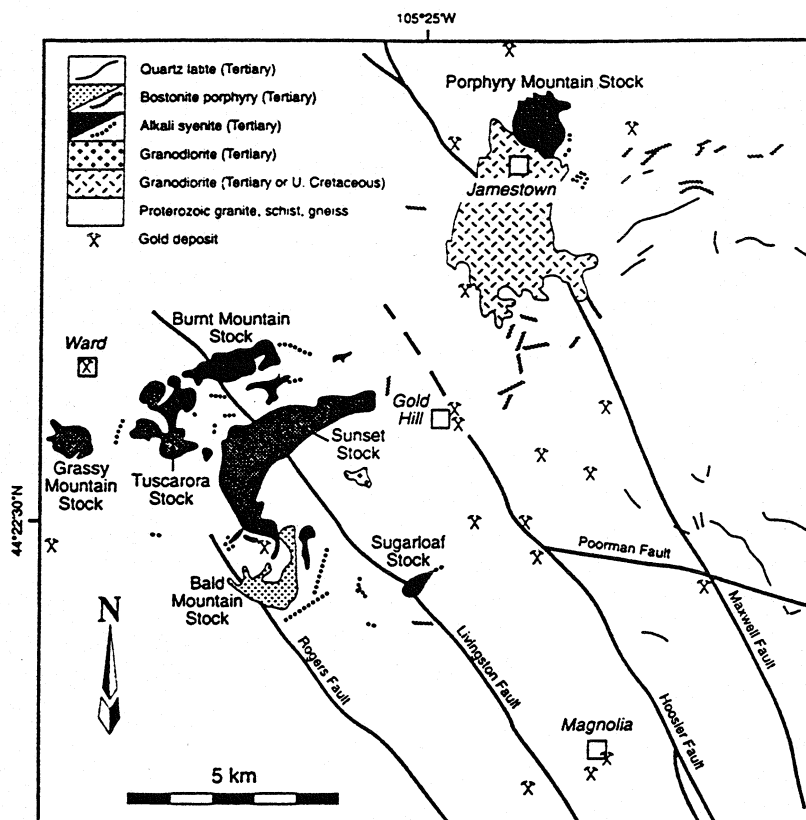


Figure 4. Geological sketch map of the Boulder County gold district (after Saunders 1991).

magmatic-hydrothermal systems associated with coeval monzonitic and syenitic intrusions, the fluorite breccia pipes and stockwork Mo-Au deposits representing more proximal facies of this activity (Fig. 5). Werle *et al.* (1984) proposed that the parental magma for these intrusions was alkali basaltic in composition, with differentiation in a crustal magma chamber giving rise to volatile-enriched monzonite-syenite melts from which the mineralizing fluids were derived.

#### **Central Montana Alkalic Province**

Gold mineralization in the central Montana alkalic province has been reviewed by Giles (1982; Fig. 6). The province is one of several manifestations of Cretaceous Tertiary back-arc or flat-slab magmatism located along the Rocky Mountain foreland, which peaked in activity at ~50 Ma (Dudas 1991; O'Brien *et al.* 1991; Baker 1992). Magmatism is characterized by scattered, small intrusive centers consisting of dioritic or monzonitic stocks, laccoliths or phacoliths of mafic syenite and granite, lamprophyric sills and dykes, and kimberlitic diatremes and ultramafic dyke swarms. Localization of these igneous

centers may have been controlled by the intersection of major WNW- and NNE-trending lineaments (e.g., Smith 1965; Zhang & Spry 1994). Several of the centers show intrusive activity spanning 3 to 4 Ma or longer, as in the cases of the Judith, Moccasin, and Little Rocky Mountains. In each district, Au mineralization is related to the final stages of igneous activity, and there is a correlation between the magnitude and longevity of intrusive activity, and the abundance and diversity of the associated mineralization.

Three main types of Au deposit occur in the province (Giles 1982): (1) intrusion-hosted disseminated auriferous pyrite (e.g., Zortman-Landusky, Little Rocky Mountains; Neihart, Little Belt Mountains); (2) stockworks and brecciated veins of auriferous quartz-pyrite at intrusive contacts (e.g., Gies and Spotted Horse mines, Judith Mountains); and (3) limestone- and dolomite-hosted disseminated replacement deposits adjacent to porphyry contacts (e.g., Kendall mine, North Moccasin Mountains; Gilt Edge mine, Judith Mountains). No single mineralization style is unique to any given district, and more than one style may be present in any

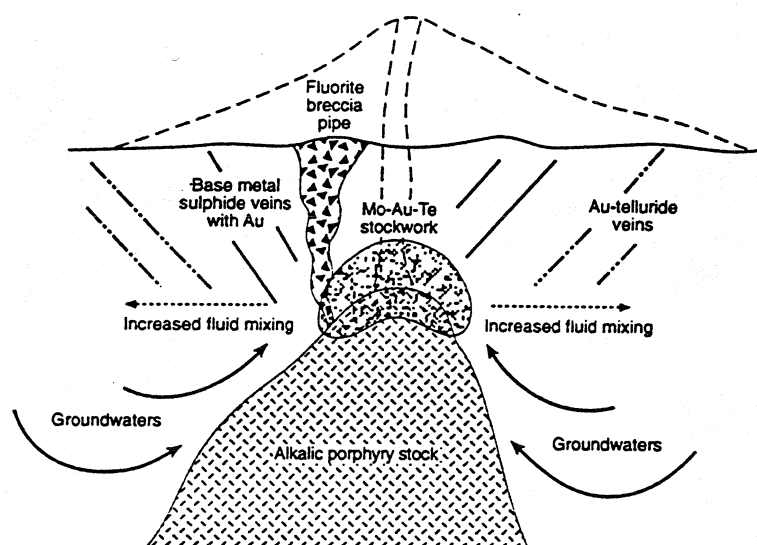


Figure 5. Schematic model for gold deposition in the Jamestown sub-district of the Colorado mineral belt (after Saunders 1991).

individual deposit.

The Zortman and Landusky deposits have been described by Giles (1982), Hastings (1988), Wilson & Kyser (1988), Ryzak (1990), and Russell (1991). Mineralization occurs in stockworks, brecciated shear zones, and disseminations in altered and fractured intrusions of syenite porphyry. These intrusions form part of the Little Rocky Mountains complex, which consists of porphyritic syenites and trachyte dykes, plus rhyolites, quartz latites, and rhyodacites. The complex has been dated at between 61 and 64 Ma (quoted in Hastings 1988). Early silicification, argillization, and pyritization of the host rocks was followed by deposition of quartz with base-metal and silver sulfides, native gold, and Au-Ag tellurides (petzite, hessite, sylvanite, krennerite, and calaverite) in veins and breccias. The ore stage was followed by widespread potassic alteration (K-feldspar) and quartz veining, with introduction of fluorite (Ryzak 1990). Although Wilson & Kyser (1988) have argued on the basis of Sr isotopic signatures that Au was derived from the Precambrian basement, most other workers hold to the traditional view that the ore-forming systems were genetically related to the spatially and temporally associated magmatic activity. Russell (1991) proposed that Au was deposited during mixing between oxidized meteoric groundwaters and highly reduced metalliferous fluids of probable magmatic origin, at temperatures below 250 °C

(see also White & Lawless 1989).

In a recent study of the Gies Au-Ag-telluride deposit in the Judith Mountains, Zhang & Spry (1994) came to similar conclusions about the origin of this deposit. Mineralization occurs in quartz veins near the sedimentary contacts with syenite and quartz monzonite stocks, and tinguaitite (aegirine-phonolite) dykes, which have been dated variably between 54 and 69 Ma. There is a particularly close association between the veins and tinguaitite dykes, which show mutually crosscutting relationships. A preferred age estimate of ~59 Ma for mineralization is proposed by Zhang & Spry (1994), based on the age of roscoelite at the nearby Spotted Horse deposit. Fluid-inclusion and stable isotopic data indicate progressive mixing between magmatic and evolved meteoric waters, resulting in a fall in temperature from ~300 °C during early quartz-pyrite-roscoelite-carbonate deposition, to ~225 °C during the main stage of Au-Ag-telluride and base-metal sulfide mineralization. Subsequent native gold deposition with sulfides and sulfosalts probably occurred at even lower temperatures (170-180 °C). Fluid salinities ranged between 5.7 and 8.0 eq. wt.% NaCl.

#### *Porgera and Mt. Kare Deposits, Papua New Guinea*

Low-grade occurrences of disseminated gold have been known in the Porgera area since 1945, but the deposit only became of economic interest

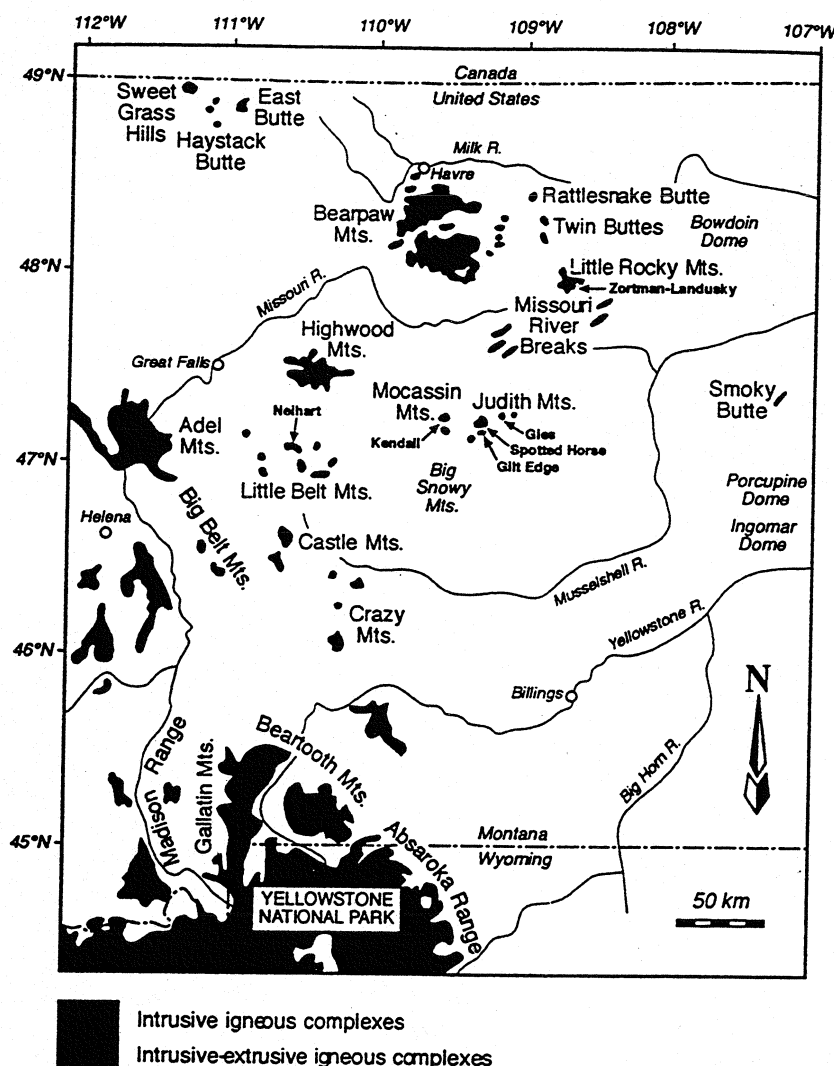


Figure 6. Sketch map of the central Montana alkalic province (after Giles 1982).

after the discovery of high-grade vein-hosted mineralization in 1982-1983 (Fleming *et al.* 1986; Handley 1987; Handley & Henry 1990). The deposit is spatially and temporally associated with a Late Miocene hypabyssal mafic alkalic intrusive complex, emplaced in poorly consolidated Jurassic-Cretaceous shelf sediments of the northeastern Australasian palaeo-plate margin (Fig. 7). These supracrustal rocks were involved in collision orogenesis prior to and following emplacement of the Porgera magmas at  $6.0 \pm 0.3$  Ma, which resulted in thin-skinned folding and thrusting, with no penetrative deformation or metamorphism at currently exposed levels. Porgera lies ~25 km from a major Oligocene-age suture zone (the Stolle-Lagaip Fault; Fig. 7), but its location, and that of the nearby Mt. Kare

deposit, may be controlled in detail by deep cross-orogen (NE-SW) structures. Potassium-argon dating of alteration minerals associated with Au mineralization at Porgera indicates an age range from 5.1 to 6.1 Ma. This range may have been broadened by loss or inheritance of radiogenic Ar, however, and it is thought that hydrothermal activity probably occurred within 0.5 Ma of the time of magmatic emplacement (Richards & McDougall 1990).

The Porgera intrusive complex comprises a suite of small spheroidal stocks (typically <500 m in diameter) and rare dykes, which were emplaced into the soft carbonaceous and calcareous siltstone sequences above a larger mid-crustal magma chamber (Fig. 8). The existence of this source pluton is inferred from geophysical and

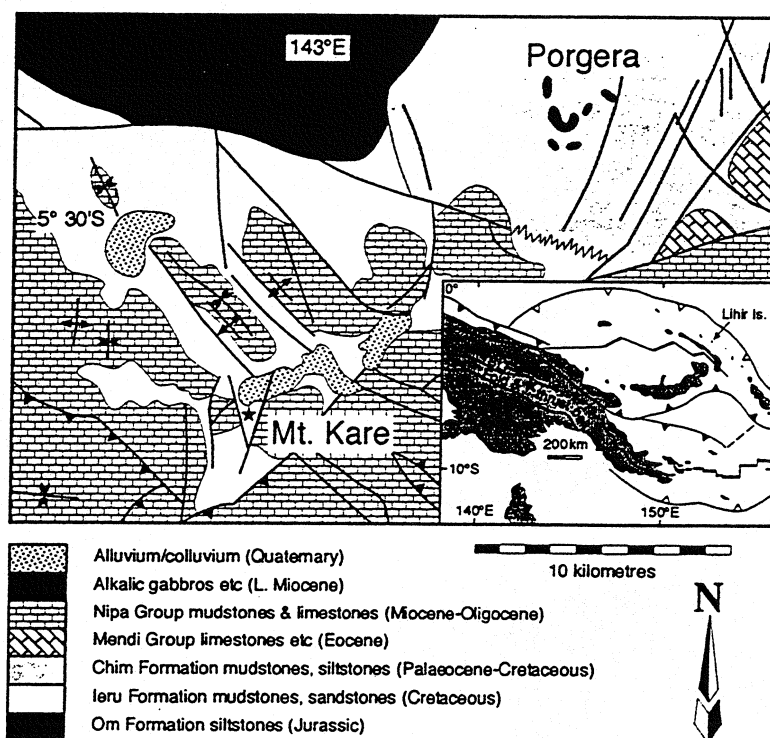


Figure 7. Geological map of the Porgera - Mt. Kare region, with inset showing the location within Papua New Guinea marked by a star (after Brunner & Caithness 1990; Richards *et al.* 1990). SLF = Stolle-Lagaip fault.

geochemical observations, which indicate a large 5-km-wide aeromagnetic anomaly over the complex, and progressive fractionation of a common parental magma to supply the shallow-level apophyses (Henry 1988; Richards 1990a; Richards *et al.* 1990). Compositionally, the

intrusions range from alkali gabbro or alkali basalt, through hawaiite to mugearite; most rock types are nepheline-normative, and all are silica-undersaturated. This classification is based on the TAS scheme, and reflects the sodic, alkalic nature of the suite. The rocks are gabbroic to porphyritic in texture, with phenocrysts of olivine or hornblende, chromite, clinopyroxene, and plagioclase, and interstitial biotite/phlogopite and titanite magnetite. The entire complex is affected to various degrees by propylitic alteration, which may be in part deuteric.

Gold mineralization occurs in two main stages at Porgera, the first resembling porphyry-type activity, and the second bearing all the hallmarks of a classic alkalic-type epithermal deposit. Stage I consists of relatively low-grade, refractory mineralization, disseminated as auriferous pyrite in phyllic alteration zones in both igneous and sedimentary rocks. Rare hypersaline fluid inclusions have been found in secondary quartz eyes in the altered intrusive rocks, and represent the earliest ore-forming fluids in the system. These fluids are interpreted to have evolved from an original magmatic-hydrothermal fluid, trapped under halite-saturated conditions between 200° and 210 °C, and with ~32 eq. wt.% NaCl

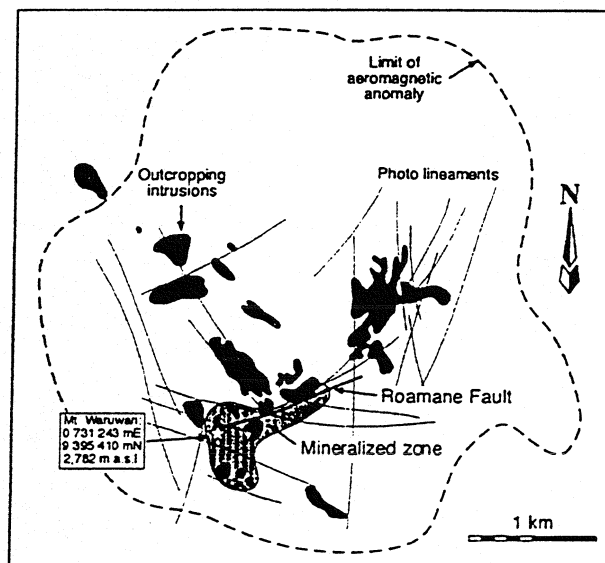


Figure 8. Sketch map of the Porgera intrusive complex and gold deposit, showing the limit of the large aeromagnetic anomaly associated with the complex (after Henry 1988; Richards 1990a).



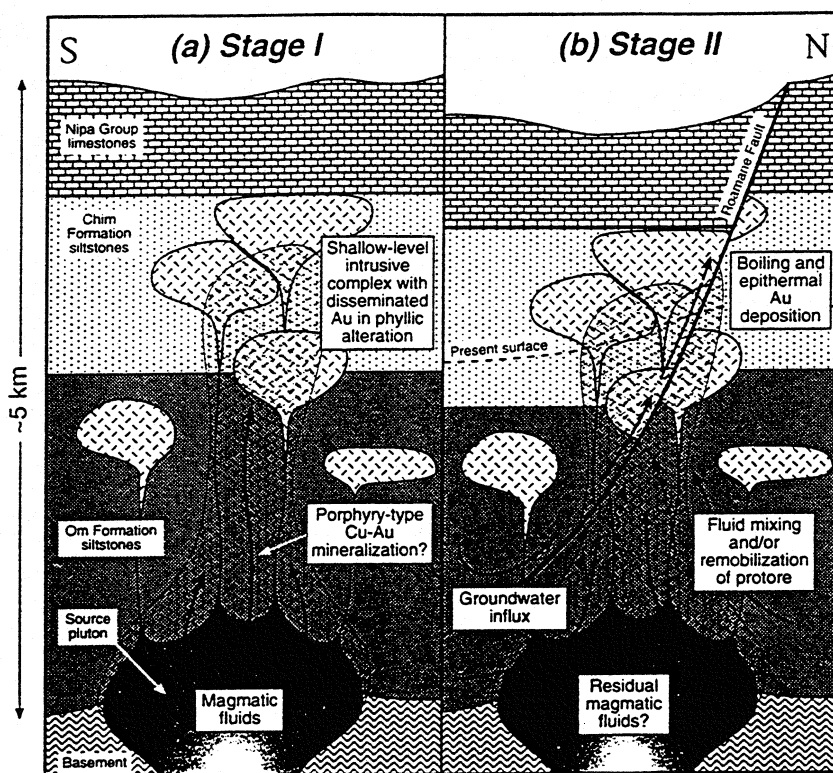


Figure 9. Schematic model for gold deposition at Porgera. (a) Stage I magmatic-hydrothermal mineralization; (b) stage II epithermal mineralization.

(Richards & Kerrich 1993). Associated with this alteration at a late stage is a suite of base-metal sulfide veins with minor early quartz and late Mn-Fe-Ca-Mg carbonates. Free gold occurs as small grains (1-10  $\mu\text{m}$ ) interstitial to early pyrite, or intergrown with later sphalerite and galena in these veins. Other ore minerals include arsenopyrite, tetrahedrite, chalcopyrite, pyrrhotite, and freibergite, the Cu-bearing minerals being sparse in comparison with galena and sphalerite. Fluid inclusions observed in early quartz and later sphalerite indicate a fall in trapping temperature from  $\sim 345^\circ$  to  $\sim 300^\circ\text{C}$ , but uniform salinity averaging 9.5 eq. wt.% NaCl with up to 3.1 mole %  $\text{CO}_2$  (Richards & Kerrich 1993; Richards, Bray, Channer & Spooner, unpublished data). Ore deposition in the veins may have been mainly a function of cooling, therefore, as the hot ascending fluids contacted relatively cool wallrocks (Fig. 9a).

The second stage of mineralization is characterized by vuggy veins and hydrothermal breccias, locally containing bonanza concentrations of gold. The veins are structurally associated with a late NE-trending normal fault,

the Roamane Fault, which cuts the southern end of the intrusive complex (Figs. 8, 9b). Mineralization is open at depth, with vertical continuity exceeding 700 m (B. Fulton, personal commun. 1994). The brecciated and layered nature of the veins suggests explosive pressure release accompanying vein formation, and phase separation is thought to be the controlling ore depositional mechanism. The vein paragenesis is characterized by precipitation of early fine-grained (perhaps originally amorphous) silica, followed by slightly coarser but anhedral quartz, intergrown with roscoelite, pyrite, native gold, Au-Ag tellurides, and tetrahedrite; minor chalcopyrite is present locally, and Hg- and Pb tellurides have been detected. Fluid-inclusion data indicate uniform trapping temperatures averaging  $\sim 165^\circ\text{C}$  at pressures of  $\sim 250$  to  $\sim 450$  bars, and salinities ranging between 3.4 and 9.6 eq. wt.% NaCl in a bimodal population (Richards 1992; Richards & Kerrich 1993). There is little evidence for fluid mixing, or petrographic evidence for boiling, but recent gas chromatographic analyses of inclusion fluids suggest that phase separation did occur in the early vein fluids. Depressurization resulting

from coeval fault movement is thought to have triggered exsolution of a  $\text{CO}_2\text{-CH}_4\text{-H}_2\text{S}$ -rich vapor phase from the ore fluid, with subsequent oxidation and destabilization of dissolved gold-bisulfide complexes.

Richards *et al.* (1991) used Sr and Pb isotopes to show that the source of these components was identical in both stages of mineralization, and proposed that stage II ores were derived by remobilization of earlier disseminated metals from deeper levels in the system. The isotopic data indicate a mixed magmatic-sedimentary source for both Pb and Sr, reflecting the scale of operation of the hydrothermal system beyond the confines of the intrusions themselves. Although Au itself cannot be isotopically traced, it is thought likely that the bulk of the precious-metal content of the ore deposit was of magmatic origin, introduced into the ore-forming system by magmatic-hydrothermal fluids.

For several years it was thought that Porgera was unique in terms of igneous rocks and mineralization in Papua New Guinea, but in 1986 the Mt. Kare deposit was discovered 18 km to the southwest (Fig. 7). This occurrence is closely similar to the Porgera intrusive and hydrothermal system, albeit on a smaller scale, and consists of a cluster of mafic alkalic intrusions locally overprinted by auriferous phyllic alteration and hydrothermal breccia zones containing the assemblage quartz-roscoelite-tetrahedrite-native gold (Brunker & Caithness 1990; Bartram *et al.* 1991; Richards & Ledlie 1993); telluride minerals have not been discovered to date on the property. Potassium-argon ages of the intrusive rocks ( $6.0 \pm 0.1$  Ma) and alteration ( $5.5 \pm 0.1$  Ma) are identical to those at Porgera, and geochemical and isotopic studies suggest that the two magmas were cogenetic at mantle source levels. The similarity of magmatism and mineralization styles at these localities demonstrates the repeatability of the ore-forming process, with obvious implications for mineral exploration.

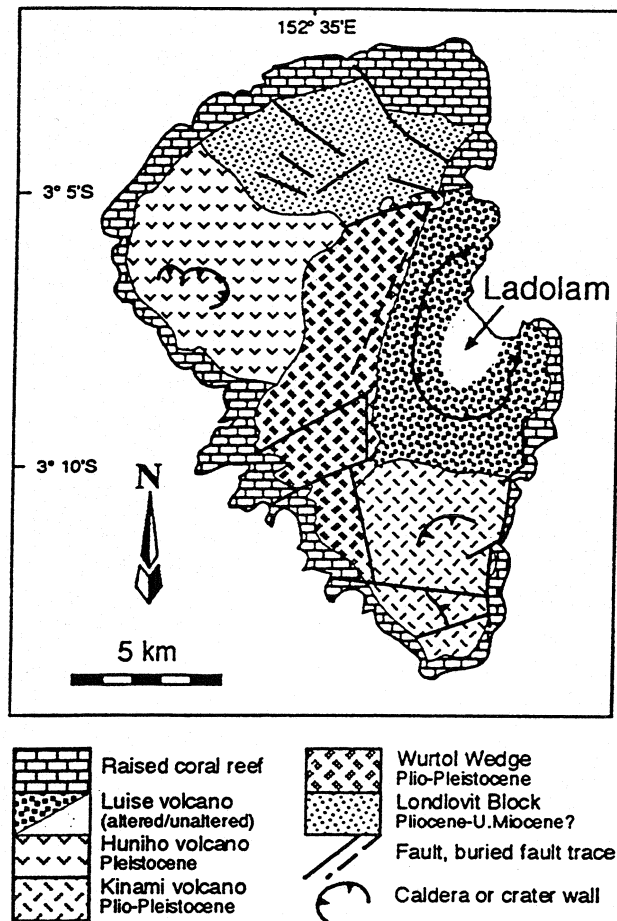
#### **Ladolam Deposit, Lihir Island, Papua New Guinea**

Ladolam is one of the largest unexploited gold deposits in the world, with mineable reserves of 188 Mt grading 3.6 g/t (1.6 g/t cutoff; *Mining*

*Journal*, December 3, 1993). The deposit is located on Lihir Island, one of the Tabar to Feni chain of islands off the northeastern coast of New Ireland, Papua New Guinea (see inset in Fig. 7). These Pliocene to Pleistocene volcanic islands are distinctive in their silica-undersaturated, sodic, alkalic nature, which contrasts with the more generally silica-oversaturated, potassic compositions of arc rocks elsewhere in Papua New Guinea and the Solomon Islands (Johnson *et al.* 1976; Wallace *et al.* 1983). Recent studies of the petrogenesis of the Lihir Island volcanics by Kennedy *et al.* (1990a,b) and McInnes & Cameron (1994) indicate that, although the suite has trace-element and isotopic signatures typical of island-arc lavas, the volcanics were not produced in response to coeval subduction. Rather, they seem to have been derived from mantle that was enriched in alkali and alkali-earth elements during earlier subduction episodes along the Miocene New Britain and Bougainville trenches. A change to extensional tectonics, following cessation of subduction activity in the Late Miocene, resulted in small degrees of melting of this enriched mantle, and the eruption of undersaturated, alkalic lavas.

Lihir Island is built from a complex of Pliocene to Pleistocene stratovolcanoes, composed mainly of alkali basalts, trachybasalts, and trachyandesites (Wallace *et al.* 1983; Kennedy *et al.* 1990b; Moyle *et al.* 1990). It is the youngest of these structures, the Luise volcano (0.35 to 0.9 Ma; Davies & Ballantyne 1987), that is host to the Ladolam Au deposit (Fig. 10). The original volcanic edifice collapsed to form a  $5.5 \times 3.5$  km caldera filled by lavas, pyroclastics, and breccias of latite, andesite, trachyte, and trachybasalt composition. These volcanics were then intruded by a monzonitic stock and a varied suite of smaller andesitic to latitic porphyry bodies (Moyle *et al.* 1990).

Gold mineralization occurs in four main areas within the caldera, and is associated with two distinct phases of alteration (Moyle *et al.* 1990). An early stage of potassic and propylitic alteration, possibly as old as 0.7 Ma, is encountered at depth, and is associated with weak porphyry-style Cu, Mo, and Au mineralization. This stage of activity probably occurred prior to



**Figure 10.** Geological map of Lihir Island (after Wallace *et al.* 1983; Moyle *et al.* 1990).

caldera formation at ~0.35 Ma, and seems to have involved magmatic-hydrothermal fluids. Collapse of the northeastern flank of the volcano resulted in sudden unroofing of the high-temperature hydrothermal core, with extensive brecciation and anhydrite veining (deposited from inflowing seawater), and the superimposition of a meteoric-water-dominated epithermal system (Fig. 11). This system is still active, and geothermal fluids with temperatures up to 231 °C have been encountered at 750 m in one geothermal well (Moyle *et al.* 1990).

Epithermal activity has resulted in the generation of phyllic, argillic, and advanced argillic alteration, which overprint the earlier porphyry-style alteration zones in a complex way. The highest Au grades are found where this system overprints the early potassic zone, whereas propylitic zones are generally barren. Vertical

zoning of the epithermal alteration is thought to reflect a boiling water table, with advanced argillic alteration assemblages, including enargite, alunite, and sulfur, occurring above this level, and argillic and phyllic assemblages occurring below. Preliminary fluid-inclusion data reported by Moyle *et al.* (1990) indicate the presence of hypersaline liquids and CO<sub>2</sub>-H<sub>2</sub>S-CH<sub>4</sub>-rich vapors in early anhydrite veins, and lower salinity (~3.8 eq. wt.% NaCl) fluids at between 120° and 340 °C ( $T_h$ ) in veins from the epithermal system. These data may be interpreted to indicate the presence of early boiling magmatic fluids, and later meteoric- or seawater-dominated epithermal fluids. Stable-isotope data indicate that meteoric waters dominate the near-surface geothermal system today (Moyle *et al.* 1990; Nedachi & Taguchi 1992).

Two main ore types are present, represented by sulfide and oxide facies. Sulfide ore in the phyllic and argillic zones is highly refractory, with sub-micrometer gold particles mainly contained in pyrite, and associated with marcasite, base-metal sulfides, and sulfosalts; molybdenite is locally present in potassic alteration zones. Free gold, with grain size up to 20 µm, occurs with sulfosalts (tetrahedrite, tennantite, luzonite, enargite) and rare tellurides (including sylvanite) in advanced argillic alteration. Oxide ore, which is developed above sea level, contains free gold grains up to 100 µm across (Davies & Ballantyne 1987; Moyle *et al.* 1990).

#### *Emperor Deposit, Vatukoula, Fiji*

The Emperor gold-telluride deposit is located on the western edge of the shoshonitic Tavua caldera, on the island of Viti Levu, Fiji (Fig. 12). Like the Tabar-Feni island chain which hosts the Ladolam deposit, the Fijian islands have had an unconventional recent geological history following their isolation from subduction processes in the Late Miocene, and subsequent rifting and fragmentation of the arc. Magmatic compositions changed from island-arc tholeiites and calc-alkaline andesites to shoshonitic at ~5.5 Ma (Gill 1970; Kroenke & Rodda 1984; Gill & Whelan 1989).

Recent studies of volcanism at Tavua (Setterfield *et al.* 1991, 1992) documented the

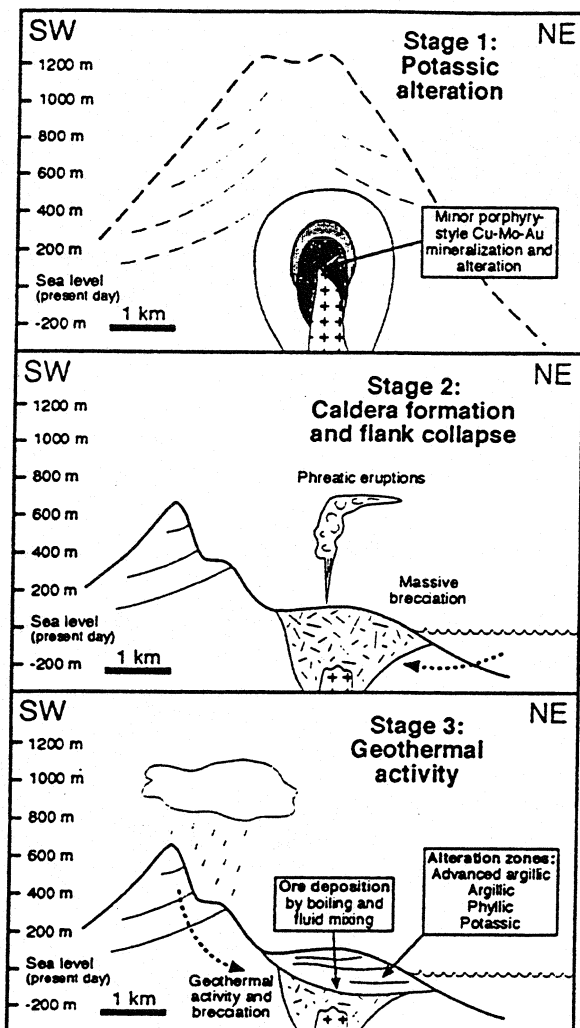


Figure 11. Schematic model for development of the Ladolam gold deposit within the Luise caldera (after Moyle *et al.* 1990).

early presence of mafic volcanics (absarokites) forming the relict volcanic edifice, followed by the eruption of more evolved shoshonites and banakites to fill the caldera. The original volcano has been dated at  $\sim 4.7$  Ma, with caldera collapse at 4.6–4.5 Ma. Post-collapse intrusion of monzonitic bodies into the volcanic pile occurred at  $\sim 4.5$  Ma, and is associated with weak porphyry Cu-Au mineralization in the Nasivi 3 deposit (Eaton & Setterfield 1993). Epithermal Au-Te mineralization was developed some time after the main stage of volcanic activity, at  $\sim 3.7$  Ma. The location of the caldera is defined by the intersection of two regional-scale structures, the NE-trending Viti Levu lineament, and a set of NW-trending shear zones. One of the latter, the

Nasivi shear zone, was responsible for controlling subsidence within the caldera, emplacement of monzonite intrusions, and possibly also provided a fluid conduit for later epithermal activity at Emperor (Anderson *et al.* 1987; Setterfield *et al.* 1991; Eaton & Setterfield 1993).

Gold was first discovered at Vatukoula in 1932, and the structural control of orebodies by intersections between NW-trending faults and the caldera fault system was recognized at an early stage. These intersections gave rise to shattered zones in which flat-dipping tensional structures (flatmakes) acted as important hosts to mineralization (Denholm 1967; Anderson *et al.* 1987; Anderson & Eaton 1990). Within these structures, multi-stage vein fillings developed with crustiform, vuggy textures and weak marginal alteration [silicification, pyritization, sericitization, carbonatization, feldspathization (adularia)]. Quartz is the main gangue mineral in the veins, accompanied by adularia, carbonates, sericite, and roscoelite. Ore minerals, commonly intergrown with roscoelite, include Au-Ag tellurides, auriferous pyrite, and minor native gold, plus base-metal sulfides, sulfosalts, and native silver and tellurium (Anderson *et al.* 1987).

Ore depositional mechanisms at Emperor have been the subject of a number of recent

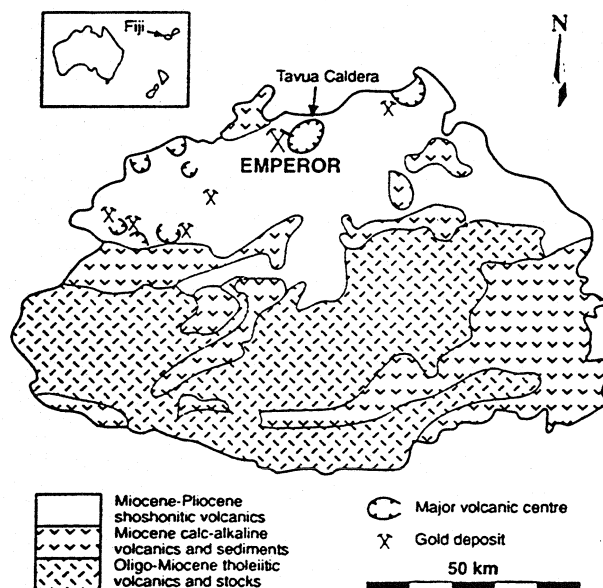


Figure 12. Geological sketch map of Fiji, showing the location of the Tavua caldera (after Anderson & Eaton 1990).

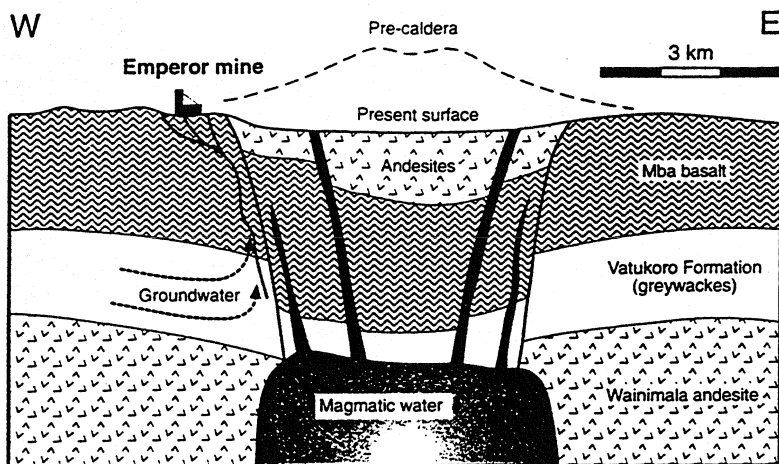


Figure 13. Schematic model for development of the Emperor gold deposit within the Tavua caldera (after Ahmad *et al.* 1987b).

studies, including Ahmad *et al.* (1987a,b), Ahmad & Walshe (1990), Anderson & Eaton (1990), and Kwak (1990). With the exception of Kwak (1990), who prefers a fluid-mixing mechanism, all other investigators conclude that boiling in response to depressurization was the main control on ore deposition. There is general consensus from stable-isotope studies that regional propylitic alteration which preceded epithermal mineralization was caused by heated seawater, whereas the ore fluids consisted of a mixture of magmatic water with meteoric and/or seawater. Vein fluid temperatures varied from 300 to 250 °C during early stages of barren quartz deposition, and down to 160 °C during later ore stages. Salinities were quite uniform, however, averaging 5.5 eq. wt.% NaCl, and pressures are estimated to have been below 40 bars (Ahmad *et al.* 1987b). However, the observation of rare CO<sub>2</sub>-bearing fluid inclusions by Kwak (1990) may indicate that actual fluid pressures were considerably higher than this.

Several authors have alluded to a relationship between the early porphyry-style mineralization within the caldera and the later epithermal activity at its rim. The isotopic evidence for a magmatic component in the epithermal ore fluids argues for such a connection, and further support is given by the recent discovery of Au tellurides and vanadiferous sulfides in anhydrite veins associated with the porphyry deposit (Eaton & Setterfield 1993). A summary model for metallogenesis at Emperor is shown in Figure 13 (from Ahmad *et al.* 1987b).

#### SUMMARY OF DEPOSIT CHARACTERISTICS

Key characteristics displayed by the deposits discussed above are presented in Tables 2 and 3, along with data from other lesser known deposits and regions such as Golden Sunlight, Montana (Porter & Ripley 1985; Spry *et al.* 1994), the Black Hills, Dakota (Paterson *et al.* 1989; Paterson 1990), Tongyoung, Korea (Shelton *et al.* 1990), and Acupan, Philippines (Cooke & Bloom 1990; Mitchell & Leach 1991). It will be seen that, despite a great variation in superficial appearance, all of these deposits share some strong fundamental characteristics. Many of these features, such as the relationship to alkalic magmatism (Table 2) and the presence of Au-telluride and V-bearing minerals, formed the basis for the early classification schemes summarized in Table 1. Subsequent investigations have not only strengthened these relationships, but have revealed further traits, such as evidence for the role of early magmatic-hydrothermal fluids, the involvement of externally-derived groundwaters during the later epithermal phase, clear relationships with alkalic porphyry-type activity, and large-scale structural control on emplacement and mineralization. The variations which still remain among the deposits are due to the wide range not only of potential host rocks and structures, but also of the associated magmatic source rocks. Some of these parameters are discussed in detail below, with a view to exploring their effects on the characteristics of the alkalic epithermal group as a whole.

Table 2. Characteristics of magmatism associated with alkalic-type epithermal gold deposits

Deposit or district	Associated igneous rocks (TAS classification)	SiO <sub>2</sub> (wt. %)	Na <sub>2</sub> O + K <sub>2</sub> O (wt. %)	(Na <sub>2</sub> O - 2.0) - K <sub>2</sub> O	Proposed parental magma	Proposed tectonic setting
Cripple Creek, Colorado	Phonolite, trachyte, tephriphonolite, and phonotephrite volcanics; alkali basalt and lamprophyre dykes	avg = 55.5 max = 62.8 min = 44.1 n = 21	avg = 11.5 max = 15.3 min = 6.3 n = 21	avg = -0.1 max = 2.7 min = -2.3 n = 21	Two magmas which mixed - phonolite and alkali basalt	Back-arc rifting. Regional-scale structural control on location
Colorado Mineral Belt	Alkali feldspar syenite (including bostonite), monzonite, and biotite-quartz latite intrusions	avg = 61.3 max = 74.8 min = 49.7 n = 69	avg = 10.5 max = 15.3 min = 6.9 n = 69	avg = -4.6 max = 0.7 min = -15.9 n = 69	Alkali basalt	Back-arc? Location controlled by reactivated Precambrian basement structures
Montana alkalic province	Monzonite, syenite, diorite, phonolite (including tinguaita), and alkali granite intrusions; trachyte and lamprophyre dykes	avg = 61.9 max = 69.1 min = 56.7 n = 24	avg = 10.5 max = 15.6 min = 8.1 n = 24	avg = -2.9 max = 0.7 min = -9.5 n = 24	Alkali basalt	Back-arc, perhaps related to flat-slab tectonics. Location controlled by basement structures
Porgera and Mt. Kare, PNG	Sodic alkali basalt/gabbro, hawaiite, mugearite intrusions; late plagioclase porphyry dykes	avg = 46.7 max = 53.4 min = 41.5 n = 45	avg = 5.6 max = 8.3 min = 3.1 n = 45	avg = 0.8 max = 2.4 min = -1.5 n = 45	Sodic alkali basalt	Continent-arc collision zone. Location controlled by basement structures?
Ladolam (Luise caldera), PNG	Alkali basalt, trachybasalt, trachyandesite, latite, and trachyte volcanics; intruded by monzonitic stock	avg = 49.6 max = 51.6 min = 46.6 n = 13	avg = 5.5 max = 6.3 min = 4.9 n = 13	avg = -1.2 max = -0.2 min = -1.9 n = 13	Alkali basalt	Post-subduction rifting
Emperor (Tavua caldera), Fiji	Absarokite, shoshonite, and banakite volcanics; intruded by monzonitic stocks	avg = 50.1 max = 55.6 min = 46.8 n = 8	avg = 4.9 max = 9.1 min = 2.6 n = 8	avg = -2.4 max = -1.4 min = -3.2 n = 8	Shoshonitic alkali basalt	Post-subduction rifting of arc. Location controlled by basement structures

Data summarized from Lindgren & Ransome (1906), Johnson *et al.* (1976), Simmons & Hedge (1978), Wallace *et al.* (1983), Werle *et al.* (1984), Rice *et al.* (1985), Ahmad & Walshe (1990), Moyle *et al.* (1990), Richards (1990a,b), Richards *et al.* (1990), Dudás (1991), O'Brien *et al.* (1991), Russell (1991), Saunders (1991), Eaton & Setterfield (1993), Richards & Ledlie (1993), Zhang & Spry (1994).

## DISCUSSION

### Characteristics and Role of Associated Magmatism

Perhaps the most noticeable feature of the examples of alkalic epithermal Au deposits given above is the extraordinary compositional diversity of the associated igneous rocks (Table 2). These vary from alkali basalts and related lamprophyres, through intermediate compositions, to evolved

quartz bostonites. Silica contents span a range from 41.5 to 74.8 wt.%, encompassing highly undersaturated to quartz-normative compositions, and trace-element signatures suggest tectono-magmatic affinities from island-arc to intraplate. Without exception, however, the suites are characterized by high levels of alkalis (Na<sub>2</sub>O + K<sub>2</sub>O) at any given level of silica content (Fig. 14; see also Muller & Groves 1993), and relatively high levels of water (as indicated by the presence

Table 3. Summary of characteristics of alkalic-type epithermal gold deposits

Feature	Early magmatic-hydrothermal system	Epithermal system
Geodynamic setting	Back-arc, post-subduction, or arc-arc collision zone; rifting may be important	
Associated igneous rocks	Alkali basalt, phonolite, monzonite, tinguaita, syenite, trachyte, latite; shoshonites, lamprophyres; variable Na/K ratio, but high alkali/silica ratio; porphyritic	
Style of magmatism	Volcanic/intrusive complexes, breccia pipes, calderas	
Form of hydrothermal system	Disseminations, stockworks, breccias, veins	Fault-related veins, shears, hydraulic breccias, shatter zones; veins are layered, vuggy
Wallrock alteration	Potassic, phyllic, propylitic. (rare skarn); magnetite often present	Phyllic, propylitic, argillic, potassic, silicic, pyritic; commonly of limited extent around mineralized structures
Ore minerals	Disseminated auriferous pyrite, base metal sulfides commonly including molybdenite; refractory Au	Au <sup>0</sup> , electrum, Au-Ag tellurides, Pb/Hg tellurides, rare Te <sup>0</sup> and Ag <sup>0</sup> ; base-metal sulfides, sulfosalts, stibnite, rutile, local hematite
Gangue minerals	Quartz, calcite, K-feldspar, sericite, fluorite	Quartz, chalcedony, roscoelite, barite, fluorite, adularia, carbonates, celestine, kaolinite
Temperature, pressure, and composition of hydrothermal fluids	200° to > 600°C; 400 to 750 bars; 2 to 74 equiv. wt. % NaCl; ≤13 mole % CO <sub>2</sub> (few data)	150° to 320°C (commonly ≤200°C); ≤500 bars; 0 to 10 equiv. wt. % NaCl; ≤2 mole % CO <sub>2</sub> , plus minor CH <sub>4</sub> , N <sub>2</sub> , or H <sub>2</sub> S (few data)
δ <sup>18</sup> O, δD of hydrothermal fluids	δ <sup>18</sup> O <sub>H<sub>2</sub>O</sub> = 4.7 to 11.4 ‰; δD <sub>H<sub>2</sub>O</sub> = -50 to -32 ‰	Data fall between meteoric water line or isotopically exchanged meteoric waters, and typical magmatic waters; individual deposits well-grouped
δ <sup>34</sup> S of sulfides	δ <sup>34</sup> S = -7.9 to +5.5 ‰	δ <sup>34</sup> S = -15 to +8 ‰ (typically < 0 ‰)
δ <sup>13</sup> C of carbonates	δ <sup>13</sup> C = -7 to -3.5 ‰ (Porgera)	δ <sup>13</sup> C = -8 to 0 ‰
Sources of ore fluids	Magmatic	Dominantly exchanged meteoric waters (seawater at Emperor?) with minor magmatic component
Source of carbon and sulfur	Dominantly magmatic	Magmatic and/or country rock
Suggested source of ore components	Magmatic	Magmatic/remobilized magmatic
Depositional mechanism	Phase separation, wallrock interaction, cooling, fluid mixing	Phase separation, fluid mixing, cooling

Data summarized from Lindgren & Ransome (1906), Loughlin & Koschmann (1935), Kelly & Goddard (1969), Casadevall & Ohmoto (1977), Sawkins *et al.* (1979), Giles (1982), Werle *et al.* (1984), Mutschler *et al.* (1985), Porter & Ripley (1985), Rice *et al.* (1985), Thompson *et al.* (1985), Cox & Bagby (1986), Saunders & May (1986), Ahmad *et al.* (1987a,b), Anderson *et al.* (1987), Spry (1987), Afifi *et al.* (1988), Bonham (1986), Hastings (1988), Wilson & Kyser (1988), White & Lawless (1989), Ahmad & Walshe (1990), Anderson & Eaton (1990), Cooke & Bloom (1990), Kwak (1990), Moyle *et al.* (1990), Ryzak (1990), Shelton *et al.* (1990), Geller & Atkinson (1991), Russell (1991), Saunders (1991), Richards (1992), Eaton & Setterfield (1993), Richards & Kerrich (1993), Zhang & Spry (1994).

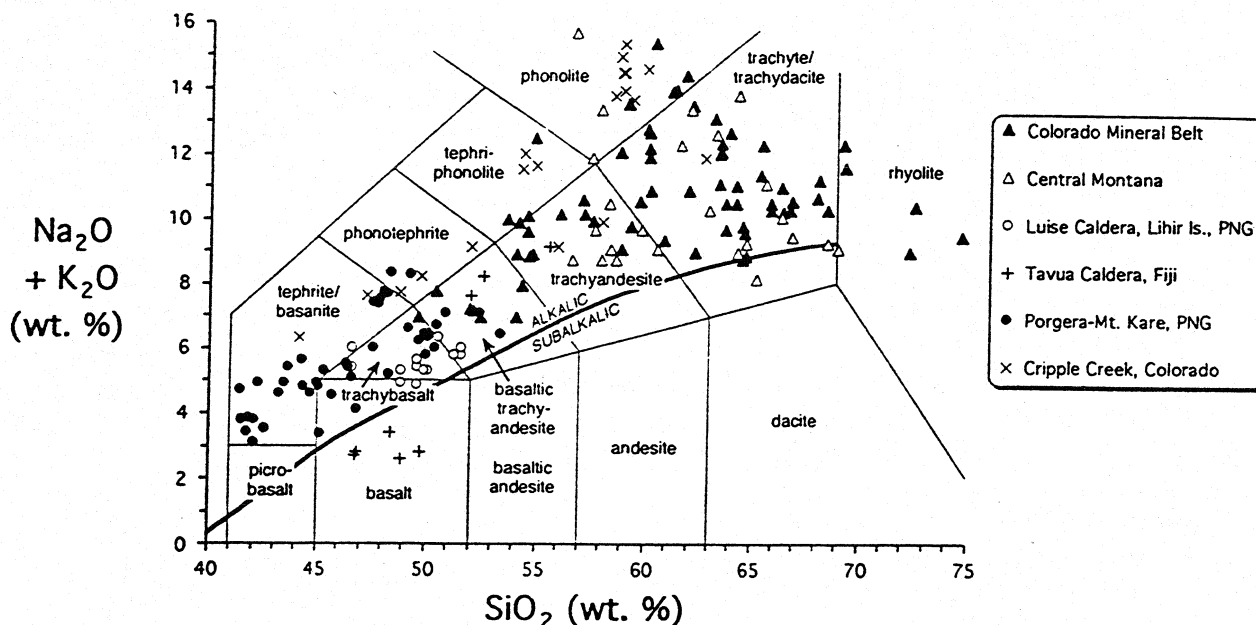
of hydrous phenocryst phases). Furthermore, in all of the examples cited above, there are indications that alkali basalts were the parental magmas to the igneous suites (Table 3).

There is, therefore, a clear connection between these types of mineral deposit and hydrous, alkalic igneous lithologies. The question which then begs to be asked is: why might this be? What is it about alkalic magmas that gives them the potential to generate Au-rich hydrothermal ore deposits, whereas calc-alkaline magmatic-hydrothermal systems very efficiently

concentrate copper?

Many investigators have looked for an answer to this question in the primary metal content of the magmas, despite the long-recognized ambiguity that high levels of an element in an igneous rock may simply reflect contamination during the ore-forming process, rather than a primary enrichment. Similarly, low levels do not necessarily mean that the rock was not the source lithology, but may instead reflect depletion during leaching or partitioning of metals into an ore-forming fluid. The conclusions of Tilling *et al.*





**Figure 14.** Total alkali-silica diagram (Le Bas *et al.* 1986) showing compositions of various intrusive and extrusive lithologies associated with alkalic-type epithermal Au deposits. The dashed line is the division between alkalic and tholeiitic suites defined by Irvine & Baragar (1971). Sources of data as in Table 2.

(1973) still seem valid, therefore – they found that there is no such thing as an inherently Au-rich magma, beyond a broad enrichment (by a factor of ~2) of mafic over felsic compositions (see also Connors *et al.* 1993). Furthermore, this contrast may be more a function of depletion in evolved magmas rather than enrichment in primitive ones.

What, then, is the fate of this small concentration of Au in a differentiating magmatic system? Bornhorst & Rose (1986) showed that crystal-liquid partition coefficients for Au were  $<1$  for most major phenocryst phases in a calc-alkaline volcanic suite, yet Au was depleted in more evolved magmas. They attributed this behavior to the partitioning of Au into an immiscible sulfide melt, which progressively fractionated from the differentiating silicate magma (see also Campbell *et al.* 1983; Hamlyn *et al.* 1985; Keays 1987; Barnes *et al.* 1988). An extensive literature now exists on the behavior of sulfur in magmas, spurred by the recognition that immiscible sulfide melts act as collectors for base- and precious metals (platinum-group elements [PGE], Au, Ag). Segregation of these melts from the parental silicate magma is thought to give rise

to orthomagmatic Cu-Ni-PGE-Au deposits (see recent reviews by Naldrett 1989a,b).

An alternative fate for precious metals dissolved in a fractionating magma is that sulfur saturation does not occur, and the metals become progressively enriched in the residual melt. Studies of silicate magmas have shown that sulfide solubility is a complex function of magmatic composition (increases with FeO content), temperature (decreases as temperature falls), oxidation state (generally decreases with increasing  $fO_2$ ), and sulfur fugacity (increases with increasing  $fS_2$ ; e.g., Haughton *et al.* 1974; Shima & Naldrett 1975; Wallace & Carmichael 1992). Sulfur and chalcophile-element concentrations will thus be highest in primary mantle-derived magmas, but will fall rapidly if sulfur saturation and sulfide-liquid segregation occur. Such fractionated magmas will not be strong candidates for subsequent generation of chalcophile-element deposits. From the aforementioned studies, however, it is apparent that sulfur saturation can be delayed under certain conditions, thus retaining chalcophile elements in the melt until later in the fractionation history.



Perhaps the most effective variable in this respect is oxidation state. Under conditions of relatively high  $fO_2$ , sulfide species become unstable with respect to sulfates in the magma, and segregation of an immiscible sulfide-melt phase will no longer be possible. Instead, partitioning of sulfur into a volatile phase (as  $SO_2$ ) may become the dominant process (e.g., Burnham & Ohmoto 1980; Carroll & Rutherford 1985; Mathez 1989). Chalcophile elements would therefore behave as incompatible components in the magma, and would become steadily enriched during fractionation, or at least would not be depleted (Richards *et al.* 1991). Furthermore, if sulfur saturation was delayed until after the onset of volatile saturation, we have the potential to generate chalcophile-element-enriched magmatic-hydrothermal fluids (Candela 1992; Richards & Kerrich 1993; Spooner 1993). The recent observation of sulfide globules in a felsite dyke associated with a differentiated quartz monzonite intrusive complex in Malasia suggests that sulfur saturation can indeed be delayed well into the felsic range of igneous rock compositions (Imai 1994). The reason for the association between Au deposits and mantle-derived igneous rocks of alkalic affinity may therefore lie in the relatively high oxidation state (e.g., Sack *et al.* 1980) and volatile content of such magmas, which act to retain chalcophile elements in the melt until or after the onset of volatile saturation.

Wyborn & Sun (1994) have recently taken this model one step further. They proposed the mantle lithosphere as a source for potential ore-forming magmas, as this region of the Earth has already undergone melting to form sulfur-saturated basaltic magmas (see also Solomon 1990). The small amounts of sulfide remaining in the basalt-depleted residue would be highly chalcophile-element enriched. Subduction-related metasomatism would lower the solidus of this material, such that chalcophile-element-rich alkalic magmas could be generated during subsequent tectonically-induced melting events. These magmas would be sulfur-poor and would not reach saturation in sulfur until a late stage of fractionation, thus potentially retaining precious metals in the melt until the onset of volatile saturation. Possible examples of such precious-

metal-rich magmas from the Lachlan Fold Belt, Australia, have been described by Wyborn (1992). Nevertheless, it is noted that these enrichments are only one to five times greater than average mantle values for Pt and Au, and fall within the range of typical igneous rocks recognized by Tilling *et al.* (1973).

### *The Role of Tectonic and Structural Setting*

If a direct relationship between epithermal Au deposits and hydrous alkalic magmatism is accepted, then the choice of tectonic setting for such systems becomes fairly well-constrained. Such magmas, for example, are not generated in standard island- or continental-arc settings, nor typically in stable intraplate settings. Alkalic rocks as a broad group, however, are commonly associated with crustal-scale rifting, and are characterized by relatively low volumes of magma. In other words, such systems typically appear in isolation or as clusters of magmatic centers, but not as regionally extensive batholithic provinces. The field can be narrowed further by eliminating rocks of the highly silica-undersaturated alkalic suite, such as carbonatites, kimberlites, and lamproites, which are not associated with the deposits under discussion. The parental magmas to these latter rock types are commonly  $CO_2$ -rich rather than hydrous, which in part results in their trend of fractionation towards ever more undersaturated compositions, compared with the silica-saturation trend of hydrous alkalic magmas.

In all of the cases discussed above, some association with subduction-zone activity can be demonstrated, although a displacement either in space or time from the active magmatic arc is evident. Indeed, the high water content of these magmas compared with other alkaline rocks argues strongly for at least an indirect relationship to subduction. The alkalic, rather than calc-alkalic character of the suite, however, is more consistent with back-arc or post-subduction magmatism, and this is the pattern which emerges in Tables 2 and 3. In these settings, the driving force responsible for voluminous arc magmatism is not present or has ceased, and melting which does occur in the mantle is usually small in extent and volume, occurring in response to distal effects or post-

subduction tectonic readjustments. The exact mechanisms and triggers for mantle melting in such settings are diverse and poorly understood, and the heterogeneity expected in the back-arc and deactivated sub-arc mantle can be expected to give rise to a compositionally diverse range of magmas under low degrees of melting.

It is concluded, therefore, that a typical tectonic setting for alkalic epithermal deposits is not to be found. Instead, we should be looking for more peripheral settings (in terms of both space and time) within the broader arc environment, and in particular in back-arc or post-subduction domains.

In a number of the deposits discussed above, deep-seated structures of regional extent have been implicated in the localization of magmatic complexes, and also in subsequent faulting and caldera formation. Many of these structures seem to pre-date arc activity and commonly run at an angle to the orogen, suggesting tensional reactivation of older lithospheric features (e.g., the Montana alkalic province, Colorado mineral belt, Porgera-Mt. Kare, and the Tavua caldera, Fiji). This dependence on deep structure might be expected for magmas that are derived ultimately from the mantle, and which will therefore follow high-permeability pathways through the lithosphere to the shallow crust. Initial generation of these magmas will not be dependent on shallow structure, but if structural pathways through the crust are not present, the melts will remain trapped at lower crustal or mantle levels and will be of no economic interest.

On the deposit scale, as with most volcanic-related epithermal systems, economic mineralization is restricted to a highly localized part of the overall intrusive complex. Invariably the main control on the focus of hydrothermal activity is structural, and caldera or post-intrusive faults and breccias feature large in these considerations (e.g., the Tavua caldera Fault at Emperor, the Roamane fault at Porgera, and the Cresson Blowout at Cripple Creek). This relationship again reflects a permeability control, and efficient hydrothermal ore-forming systems are presumably those which focus their activity in one place rather than across several different structures.

### *The Porphyry – Epithermal Connection*

In all of the examples of alkalic gold deposits discussed above, suggestions of a link between the epithermal mineralization and earlier porphyry-style magmatic-hydrothermal activity have been made. The basis for these suggestions has varied from a general spatial and temporal association between the two types of mineralization (e.g. Bonham & Giles 1983; Mutschler *et al.* 1984, 1985; Werle *et al.* 1984; Bonham 1986; Handley & Bradshaw 1986; Paterson 1990; Ryzak 1990; Russell 1991; Saunders 1991; Setterfield *et al.* 1992), to direct evidence for the involvement of magmatic fluids (e.g. Nash & Cunningham 1973; Porter & Ripley 1985; Rice *et al.* 1985; Thompson *et al.* 1985; Ahmad *et al.* 1987a,b; Anderson & Eaton 1990; Cooke & Bloom 1990; Moyle *et al.* 1990; Richards 1992; Eaton & Setterfield 1993; Zhang & Spry 1994). In very few of these examples, however, is the porphyry-type mineralization of economic interest, and even at Porgera, where relatively low-grade disseminated ore is being mined on a large scale, this has only been economically possible because of the additional presence of high-grade epithermal ore. What, then, is meant by a relationship between porphyry-type and alkalic epithermal activity?

In the case of the deposits discussed here, there is clear evidence for the release of volatiles from the magmas most closely associated with the epithermal mineralization, and in many cases these early magmatic-hydrothermal systems were auriferous. They rarely generated ore-grade mineralization, but their existence is evidence for a process of magmatic-to-hydrothermal transfer of metals. Moreover, that process, involving high-salinity, high-temperature liquids plus vapors, and resulting in disseminated mineralization, multiple alteration zones, and leaving porphyritic host rocks as evidence of devolatilization, is substantially similar to the mechanism of ore formation in classic porphyry-type Cu/Mo deposits. A major difference, however, is the general paucity of copper (low Cu:Au ratio) and other base metals in the alkalic epithermal-related systems.

Fluid-inclusion and stable-isotope data therefore support a magmatic origin for early

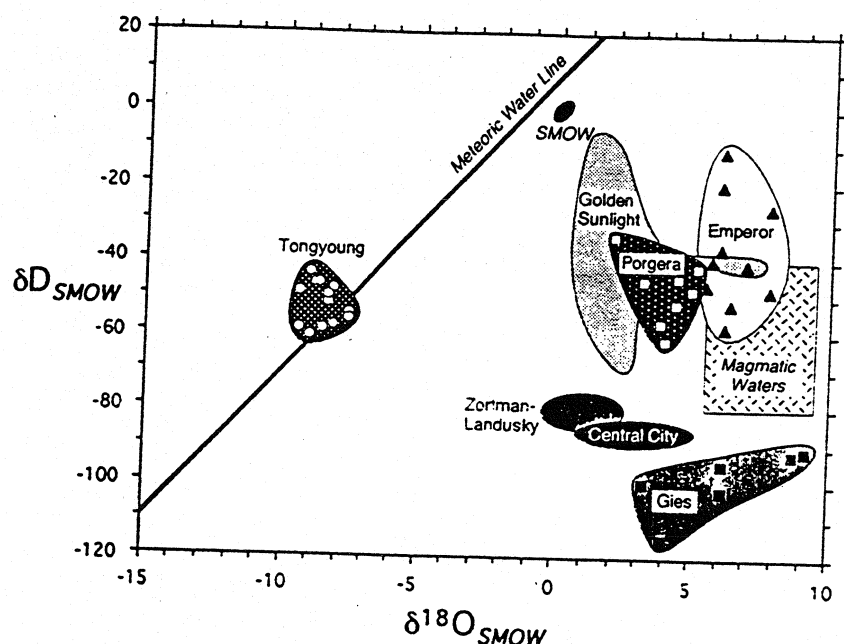


Figure 15. Plot of oxygen versus hydrogen isotopic compositions of fluids involved in alkalic-type epithermal Au deposition. The data are interpreted to reflect variable degrees of mixing between magmatic fluids and isotopically exchanged meteoric groundwaters (or perhaps seawater in the case of Emperor). Data are taken from Porter & Ripley (1985), Rice *et al.* (1985), Ahmad *et al.* (1987a,b), Wilson & Kyser (1988), Shelton *et al.* (1990), Richards & Kerrich (1993), Spry *et al.* (1994), and Zhang & Spry (1994). The compositional range of magmatic waters is from Sheppard (1986).

fluids and volatiles in alkalic-type hydrothermal systems, but it is rare to find evidence for such fluids within the main epithermal stage of mineralization. The latter activity is invariably dominated by cooler, lower salinity fluids (Table 3).

A number of studies have addressed the origin of these epithermal fluids using O and H isotopic data from fluid inclusions and vein minerals. In all cases, the interpreted fluid compositions fall between the range for magmatic waters and the meteoric water line (Fig. 15). Commonly, however, the data do not fall on a direct mixing line between magmatic waters and the inferred meteoric waters at the time of ore deposition; rather, the data indicate that the epithermal fluids were dominated by isotopically evolved groundwaters. In other words, the fluids had exchanged with the country rocks prior to involvement in the ore-forming system (*e.g.* Richards & Kerrich 1993; Zhang & Spry 1994). The data are not usually coherent enough to permit further interpretation, leaving open the question of in-mixing of minor amounts of magmatic fluid into the epithermal reservoir. Zhang & Spry (1994), however, presented evidence for just such a process at the Gies deposit, Montana, with the implication that mixing between these fluids may have been an important control on ore deposition.

These data imply a more-or-less continuous transition from early magmatic-hydrothermal fluid activity to later, lower temperature epithermal activity dominated by externally derived groundwaters.

Stable-isotope evidence for the source of other volatile components such as sulfur and carbon in the epithermal stage is less conclusive. Sulfide minerals, for example, yield values of  $\delta^{34}\text{S}$  ranging from -15 to +8‰, and carbonates yield  $\delta^{13}\text{C}$  values from -8 to 0‰ (Table 3). These data overlap accepted values for magmatic compositions, but the broadening of the ranges from those observed in the earlier magmatic-hydrothermal stage suggests either mixing with other isotopic reservoirs such as the country rocks, or the operation of redox processes during epithermal mineralization (affecting sulfur isotopes in particular; *e.g.* Richards & Kerrich 1993).

In conclusion, a magmatic signature is carried through from the early stages of hydrothermal activity to the later epithermal stage, but it seems to be variably diluted by externally derived components. Most notably, the ore fluid itself is dominated by groundwaters, with only occasional indications of magmatic fluid in-mixing. It seems likely, therefore, that the chemistry of these groundwaters and the rocks with which they have

interacted will have a profound effect on the nature of the resultant epithermal system.

As a final point for consideration, a number of authors have alluded to the characteristic enrichments of Te and V (and in some cases, F) in these deposits, and have suggested that they reflect the specific involvement of mafic alkalic magmas, which commonly contain elevated concentrations of these components (e.g. Sindeeva 1964; Carmichael *et al.* 1974; Mutschler *et al.* 1985, 1990; Afifi *et al.* 1988; Bailey & Hampton 1990; Eaton & Setterfield 1993; Stanton 1994). Arguments such as these are based on purely circumstantial evidence, however, and can only be considered as supportive of a link with alkalic magmatism, rather than providing definitive proof.

### ***Mechanisms for Hydrothermal Gold Transport and Deposition***

#### ***Magmatic-hydrothermal stage***

Transfer of Au from alkalic magmas to a hydrothermal fluid phase is suggested by the close association of alkalic-type epithermal deposits with porphyry-type mineralization. Unfortunately, there is little information available on the melt-fluid partitioning of Au, despite an extensive literature for Cu and Mo (e.g. Henley & McNabb 1978; Candela & Holland 1984, 1986; Cline & Bodnar 1991; Candela 1992). Two recent studies suggest, however, that Au behaves in an analogous manner to Cu (Candela 1989; Ballhaus *et al.* 1994). Copper and Au should therefore be preferentially partitioned into the volatile phase during magmatic devolatilization, and both metals would be dissolved in that phase as chloride complexes (Seward 1984; Hayashi & Ohmoto 1991). Because of the requirement of non-saturation of sulfide in the melt that conditions be relatively oxidizing, S would be dominantly present in the early fluid phase as SO<sub>2</sub>, and Cu could therefore be carried at relatively high concentrations. Cooling will eventually result in disproportionation of the SO<sub>2</sub> to sulfate and sulfide species, however, and this and related processes will lead to deposition of Cu-bearing sulfide minerals (*i.e.*, typical disseminated porphyry-type mineralization. Some Au may also

be deposited with these sulfides, but much of it may remain in solution by conversion from chloride to bisulfide complexing (Hayashi & Ohmoto 1991). The potential thus exists for separating the deposition of Cu and Au in magmatic-hydrothermal systems, with Au being deposited at a later stage, and perhaps at shallower levels, through processes different from those affecting the solubility of base metals. A mechanism exists, therefore, for maintaining Au in solution beyond the depositional front of porphyry ore, and hence potentially into the epithermal environment. This model predicts that Au-rich systems should grade downwards into a zone of Cu-rich mineralization, as was originally proposed by Bonham & Giles (1983), Mutschler *et al.* (1984), and Werle *et al.* (1984); see also Titley (1978) and Jones (1992). That few economic examples of such porphyry-type mineralization have been found associated with alkalic epithermal deposits is of little importance compared to the fact that such a process does operate (e.g. Allard stock, Colorado; Ladolam, Papua New Guinea; Emperor, Fiji).

#### ***Epithermal Au transport***

The nature of the magmatic – epithermal transition has attracted a great deal of recent interest (e.g. Cooke & Bloom 1990; Hedenquist & Aoki 1991; Hedenquist 1992; Richards 1992; Rye 1993; Hedenquist & Lowenstern 1994). Transfer of materials between the two phases of activity can occur either directly, by mixing of magmatic-hydrothermal vapors or liquids with externally derived fluids, or indirectly by leaching of early alteration and mineralization products. Evidence for magmatic vapor-phase involvement is clearly found in the acid-sulfate-type epithermal deposits, at which near-surface condensation of acidic volatiles results in intense silicification and advanced argillic alteration (Hayba *et al.* 1985; Heald *et al.* 1987; Stoffregen 1987; Rye *et al.* 1992; Hedenquist *et al.* 1994a,b). Hedenquist *et al.* (1994a) found, however, that the metal load of these vapors at shallow levels was insufficient to account for the subsequent inventory in acid-sulfate epithermal deposits, despite the potential for such vapors to carry significant metal concentrations at high temperatures (e.g.

Lowenstern *et al.* 1991). Hedenquist *et al.* (1994a) concluded that ore was deposited by subsequent ingress of metal-rich liquids, and that the early acidic fluids acted merely to prepare the ground. The subsequent metalliferous fluids were thought to represent the condensed saline component of the original magmatic fluid phase, after extensive dilution by externally-derived groundwaters. Similar mechanisms are proposed for the origin of metalliferous fluids in adularia-sericite-type epithermal deposits (*e.g.* Heald *et al.* (1987).

Richards *et al.* (1991) proposed, on the basis of isotopic studies, that metals in the Porgera epithermal system were derived largely by leaching of earlier disseminated ore at depth. The latter mineralization, perhaps represented in part by stage I ore exposed at current mining levels, was deposited by the early magmatic-hydrothermal system above an unexposed source pluton. In the light of the need for efficiency in ore-forming systems, however, it may not in fact be necessary to propose a two-stage precipitation-redissolution mechanism to explain the isotopic composition of the later ores. Instead, direct transfer of ore components to the circulating groundwater system may have been achieved by mixing with late-stage magmatic fluids, as suggested for other epithermal systems discussed above. This mechanism may be particularly effective for the transfer of Au into the epithermal environment, due to the potential for Au to be dissolved as bisulfide complexes in otherwise relatively dilute solutions. Copper and other base-metal concentrations, on the other hand, would be low in these groundwater-dominated fluids. This effect would be compounded if the fluids concerned were mildly reducing, thus raising the activity of sulfide in solution to the detriment of base-metal solubility, but to the advantage of precious metals. The isotopic composition of the minor amounts of Pb found in stage II ores may indeed have been inherited from the earlier relatively Pb-rich mineralization, but Au, perhaps along with V and Te, could have been derived dominantly from fresh influxes of residual magmatic fluids.

Although few direct measurement of oxidation state in epithermal fluids involved in alkalic systems currently exist, a glance at the

typical mineralogy of such deposits (Table 3) indicates the dominance of sulfide minerals over sulfates and oxides (although the latter minerals may be important during later stages of ore deposition). A condition for the formation of epithermal deposits high in Au:Cu may therefore be the involvement of relatively reducing, perhaps deeply circulating groundwaters, as opposed to the oxidized surface fluids involved in acid-sulfate systems. Furthermore, the nature of the country rocks may play an important role in this regard. Porgera and Mt. Kare, for example, are emplaced in carbonaceous and pyritic black mudstones and siltstones. Thus, the local groundwaters circulating around the intrusive system would be expected to have been reducing, and probably sulfide-rich. They would therefore represent ideal solvents for Au during its transfer from the magmatic-hydrothermal system, either by fluid mixing or leaching. Furthermore, if much of the dissolved sulfide in these epithermal fluids was indeed derived from the sedimentary country rocks, this might explain the negative sulfur-isotopic compositions of sulfide minerals in stage II ore compared with the 'magmatic' values of the earlier base-metal sulfide veins (*cf.* Richards & Kerrich 1993).

Gold solubility may also have been enhanced in these late fluids by the action of other complexing agents, such as telluride species (*e.g.* Saunders & May 1986; Seward 1993). Although no experimental data exist for the solubility of such complexes, Saunders & May (1986) suggested that ditelluride species ( $\text{AuTe}_2^-$ ) could be significantly soluble under some epithermal conditions.

#### *Epithermal Au deposition*

It is remarkably difficult to determine unequivocally the dominant mechanism of ore deposition in epithermal systems. This is due in large part to the generally observed inverse relationship between ore-stage minerals and fluid inclusions. Thus, despite boiling being a commonly proposed method for precipitating gold (*e.g.* Drummond & Ohmoto 1985; Seward 1989; Bowers 1991), the observation of classic boiling fluid-inclusion assemblages in direct association with ore is relatively rare. Indeed, Hedenquist &

Henley (1985a, p. 1394) noted that calcite deposited from boiling fluids in a geothermal well contained only liquid-rich fluid inclusions, with no evidence of the vapor phase.

The Porgera Au deposit is a case in point (Richards 1992; Richards & Kerrich 1993). Gold deposition in the epithermal veins occurs at an early stage in the vein paragenesis, and is associated with fine-grained silica. This material contains few fluid inclusions, although later vuggy quartz radiating from these ore layers is rich in large, liquid-rich inclusions. Notwithstanding this lack of direct evidence for boiling, these authors proposed that the earliest materials to be deposited in the veins were associated with a brief period of catastrophic phase separation, or flashing, resulting from depressurization during hydrothermal fracturing and brecciation. Sudden supersaturation of the fluid with respect to ore and gangue components resulted in rapid deposition of fine-grained ore and gangue minerals, in which few visible fluid inclusions were trapped. Only when conditions stabilized following resealing of the fracture system were large inclusions trapped in more slowly grown vuggy quartz, but by this time ore deposition had ceased.

Similar ambiguities are found in the majority of epithermal deposits, of any kind, studied to date. However, the widespread occurrence of hydraulic fracturing and brecciation attest to sudden fluid-pressure and volume changes, which can reasonably be explained in the epithermal environment only by phase-separation mechanisms (e.g. Hedenquist & Henley 1985b; Nelson & Giles 1985; Sibson 1987; Parry & Bruhn 1990). Moreover, evidence from many active and fossil geothermal systems indicates that fluid conditions closely adhere to the two-phase curve on pressure-temperature diagrams, implying that vapor saturation is a widespread condition in such settings.

An additional factor that may enhance the potential for boiling is the presence of dissolved gases in the epithermal fluid. No shortage of such components is to be expected in the deep fluid reservoir, because, as we have seen, these waters contain a significant contribution from magmatic-derived volatile phases. The effect of dissolved gases on aqueous fluids is to expand the field of

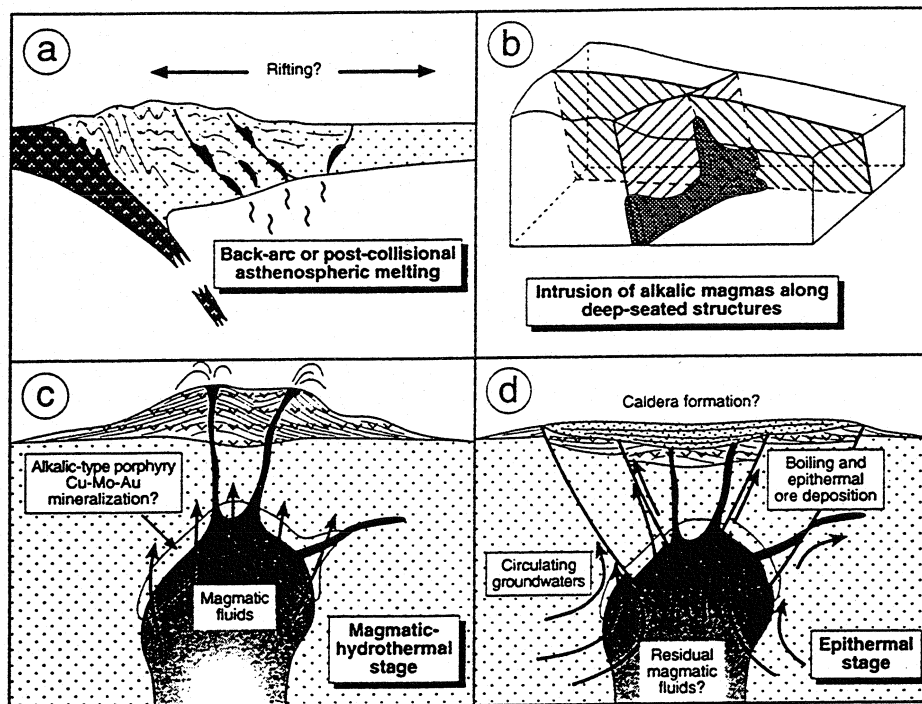
liquid-vapor immiscibility, thereby increasing the depth, or pressure, at which phase separation will first occur (Drummond & Ohmoto 1985; Bodnar *et al.* 1985). Alternatively, for any given depth or pressure, the temperature at which a fluid will start to unmix will be reduced.

The paucity of ore-related fluid inclusions in alkalic-type epithermal deposits means that measurements of gas content in the primary ore fluids are similarly rare. Nevertheless, the few data that exist in the literature suggest that low but significant concentrations of CO<sub>2</sub> and perhaps other gases are the norm (up to 2 mole % CO<sub>2</sub>, plus minor CH<sub>4</sub>, N<sub>2</sub>, or H<sub>2</sub>S; Table 3). Gas-chromatograph analyses of fluid inclusions in post-ore-stage vuggy quartz from Porgera indicate that volatile saturation could indeed have occurred in these fluids, despite their relatively low temperatures and greater depths of formation compared with other types of epithermal deposits. These characteristics seem to be typical of the alkalic epithermal group as a whole (temperatures commonly  $\leq 200$  °C and pressures up to 500 bars; Table 3), and mark these deposits apart from the classic near-surface adularia-sericite and acid-sulfate epithermal systems (e.g. 200-300 °C and 100 bars; Hayba *et al.* 1985; Heald *et al.* 1987).

Gas-enhanced phase separation therefore seems to be a viable mechanism for ore deposition in alkalic-type epithermal systems, and has been invoked for the majority of deposits considered above. Almost certainly, however, this is not the exclusive control on Au precipitation, and other processes such as wallrock interaction and fluid mixing may be important locally (e.g. the stratiform replacement deposits at Cripple Creek and in the Montana alkalic province; vein deposition at Emperor, as proposed by Kwak 1990). Moreover, fluid mixing at depth has been invoked as a fundamental step in the transfer of components from the magmatic to the epithermal environment.

#### A GENERAL MODEL FOR ALKALIC-TYPE EPITHERMAL GOLD DEPOSITS

Alkalic epithermal gold deposits have been distinguished from other epithermal deposit types principally on the basis of their distinct



**Figure 16.** Four-stage generalized model depicting the development of alkalic-type epithermal gold deposits in association with alkalic intrusive complexes. (a) Generation of alkalic magmatism in back-arc, post-subduction, or arc collisional settings. (b) Emplacement of magmas at shallow levels in the crust, by intrusion along trans-lithospheric fractures, and particularly their intersections. (c) Possible development of porphyry-style Cu-Mo-Au mineralization from magmatic-hydrothermal fluids exsolved from the intrusions. (d) Groundwater-dominated hydrothermal convection system, with epithermal Au-Te mineralization developed where these fluids are channelled to the surface along late structural conduits.

association with alkaline igneous rocks. In the process of reviewing the current literature on these deposits, a number of other common features have been revealed, including consistent evidence for the nature and sources of fluids and volatiles involved in ore deposition, and a consensus that the ore metals were ultimately derived from the associated igneous intrusions by magmatic-hydrothermal processes. In an attempt to fulfil the objectives set out at the beginning of this review, therefore, the main features that seem to control the development of alkalic-type epithermal systems are depicted in Figure 16 and summarized below.

1. The associated hydrous alkalic magmas are generated through processes indirectly related to subduction, but not within active arcs. The magmas seem to be products either of post-subduction tectonic readjustments, or back-arc activity. Low degrees of melting of subduction-

modified (*i.e.*, metasomatized) mantle in such settings may result in the generation of small volumes of water-bearing, relatively oxidized alkaline magmas.

2. Emplacement of these small-volume melts at shallow crustal levels is facilitated where extensive trans-crustal or trans-lithospheric faulting exists within the orogen. Intersections of such structures are particularly favorable loci for intrusion, and commonly involve the reactivation of old cross-orogen lineaments. Such structures may be oriented obliquely to the prevailing stress direction, and may be the focus for tensional stress release in the form of pull-aparts and rifts. The tensional regime extant during formation of many deposits, despite the large-scale collisional or convergent setting, is demonstrated by their common association with caldera structures and normal faults.

3. A key requisite for the hydrothermal



extraction of Au from the magma is that removal of chalcophile elements from the melt by sulfide-liquid segregation should not occur before volatile saturation. This condition may be achieved by suppression of sulfur saturation through the relatively oxidizing state of the magma (sulfur is then mostly present in the melt as sulfate, not sulfide), and promotion of volatile saturation through its relatively high primary water content. Alternatively, or additionally, the magmas may have been derived from a sulfur-depleted mantle lithosphere source. Thus, the magmas are emplaced at shallow crustal levels bearing their full mantle-derived complement of chalcophile elements, which can then be partitioned into an exsolving magmatic volatile phase.

4. The process of magmatic-hydrothermal metal partitioning is thought to be analogous to that operating in typical porphyry-type systems, with Au segregating into a chloride-rich volatile phase, along with Cu and other base metals. Deposition of ore-grade mineralization from this high-temperature hydrothermal system is not a prerequisite for the subsequent development of an epithermal deposit, and indeed, these two ore types may be to some extent mutually exclusive. Thus, Au may either precipitate early along with base metals to form a disseminated Cu-Au orebody, or may remain in solution until deposition at lower temperatures and shallower levels to form an epithermal deposit. A control on the separation of Au from base metals by this process may be the oxidation state and sulfide content of the hydrothermal fluids. After disproportionation of magmatic  $\text{SO}_2$  as the early fluids cool, the activity of dissolved sulfide will increase dramatically and base metals will tend to precipitate. Gold, on the other hand, may remain in solution by conversion from chloride to bisulfide (or possibly telluride) complexing.

5. Following the main magmatic-hydrothermal stage of activity, the system becomes progressively flooded by heated, evolved, relatively reducing groundwaters. Two possible routes are then envisaged for the transfer of ore components from the magmatic-hydrothermal stage to these epithermal fluids. First, if Au has already been precipitated from solution, perhaps along with Cu in a porphyry-

type protore, then selective leaching by sulfide-rich, chloride-poor waters may yield an Au-rich solution. Alternatively, if Au remains in solution during the magmatic-hydrothermal stage, these residual auriferous fluids will mix with the circulating groundwater system. From an efficiency standpoint, the latter mechanism seems preferable, as it obviates the necessity for a two-stage precipitation-redissolution process. It may also explain the enrichments in V and Te seen in these deposits, these elements being concentrated in late-stage magmatic differentiates and emanations.

6. For the resulting groundwaters to precipitate economic concentrations of precious metals, and in particular the bonanza concentrations commonly found in these deposit types, an extremely effective depositional mechanism must operate. Characteristically, the epithermal ores are found in structurally-related veins and hydrothermal breccias, indicating rapid, perhaps explosive ascent of fluids from depth. These fluids are also commonly gaseous (higher average  $\text{CO}_2$  content than in other epithermal deposit types), and although the fluid-inclusion record rarely preserves unequivocal evidence, it is thought that phase separation is an integral factor in vein formation and ore deposition. The rapid ascent of the fluids and subsequent violent unmixing may be promoted by coeval movement on the related fault structures, causing depressurization of the fluid reservoir and effervescence at relatively deep levels. The volume change resulting from vapor exsolution would cause further brecciation and hydraulic fracturing, leading to the generation of cavity space for subsequent mineralization. It is envisaged that brecciation and phase separation are marked only by the deposition of fine-grained, perhaps amorphous silica. During reequilibration of the fluid to the new degassed conditions, however, gold and Au-Ag tellurides would precipitate as a consequence of the breakdown of bisulfide complexes through loss of  $\text{H}_2\text{S}$  to the vapor phase and coupled oxidation of the remaining liquid.

To conclude on a cautionary note, it is suggested that care must be taken not to over-emphasize the boundary between 'alkalic' and other types of epithermal deposits. In this review



attention has been focussed on a set of characteristics that are distinctive of a certain group of epithermal deposits, but many of these features can be found, either individually or as a subset, in other deposits that might be classified as adularia-sericite or acid-sulfate types. None of the mechanisms outlined in the above paragraphs, including those relating to magmatic-hydrothermal systems, is exclusive to the alkalic epithermal group, and it is therefore likely that we are dealing with a complete spectrum of products derived from subtle variations in a global ore-forming process – that of hydrothermal concentration of metals from silicate magmas.

#### ACKNOWLEDGMENTS

This contribution is dedicated to those killed at Porgera in an explosion on the minesite in August 1994. I thank John Thompson for providing the motivation to write this review, and Jeff Hedenquist, Paul Spry, Shen-Su Sun, and my wife Lee Ewert for additional information and encouragement to complete the job. Paul Spry, Brent McInnes, and John Thompson are also thanked for perceptive reviews, but responsibility for omissions and oversimplifications remains with me.

#### REFERENCES

- AFIFI, A.M., KELLY, W.C. & ESSENE, E.J. (1988): Phase relations among tellurides, sulfides, and oxides: II. Applications to telluride-bearing ore deposits. *Econ. Geol.* **83**, 395-404.
- AHMAD, M., SOLOMON, M. & WALSHE, J.L. (1987a): The formation of the quartz – gold-telluride veins of the Emperor mine, Fiji. *In Pacific Rim Congress 87, Proceedings: The Geology, Structure, Mineralization and Economics of the Pacific Rim.* Austral. Inst. Mining Metall., 1-4.
- AHMAD, M., SOLOMON, M. & WALSHE, J.L. (1987b): Mineralogical and geochemical studies of the Emperor gold telluride deposit, Fiji. *Econ. Geol.* **82**, 345-370.
- AHMAD, M. & WALSHE, J.L. (1990): Wall-rock alteration at the Emperor gold-silver telluride deposit, Fiji. *Austral. J. Earth Sci.* **37**, 189-199.
- ANDERSON, W.B., ANTONIO, M., DAVIS, B., JONES, G.F.P., SETTERFIELD, T.N. & TUA, P. (1987): The Emperor epithermal gold deposit, Vatukoula, Fiji. *In Pacific Rim Congress 87, Proceedings: The Geology, Structure, Mineralization and Economics of the Pacific Rim.* Austral. Inst. Mining Metall., 9-12.
- ANDERSON, W.B. & EATON, P.C. (1990): Gold mineralization at the Emperor mine, Vatukoula, Fiji. *J. Geochem. Explor.* **36**, 267-296.
- BAILEY, D.K. & HAMPTON, C.M. (1990): Volatiles in alkaline magmatism. *Lithos* **26**, 157-165.
- BAKER, D.W. (1992): Central Montana alkaline province: critical review of Laramide plate tectonic models that extract alkaline magmas from abnormally thick Precambrian lithospheric plate. *Northwest Geology* **20/21**, 71-95.
- BALLHAUS, C., RYAN, C.G., MERNAGH, T.P. & GREEN, D.H. (1994): The partitioning of Fe, Ni, Cu, Pt, and Au between sulfide, metal, and fluid phases: A pilot study. *Geochim. Cosmochim. Acta* **58**, 811-826.
- BARNES, S.-J., BOYD, R., KORNELIUSSEN, A., NILSSON, L.-P., OFTEN, M., PEDERSEN, R.B. & ROBINS, B. (1988): The use of mantle normalization and metal ratios in discriminating between the effects of partial melting, crystal fractionation and sulphide segregation on platinum-group elements, gold, nickel and copper: examples from Norway. *In Geo-Platinum 87* (H.M. Prichard, P.J. Potts, J.F.W. Bowles & S.J. Cribb, eds.). Elsevier, Amsterdam, 113-143.
- BARTRAM, J.A., HEAPE, J.M.T. & CAITHNESS, S.J. (1991): The Mount Kare gold project. *In Proceedings, PNG Geology, Exploration and Mining Conference, Rabaul, 1991, Melbourne.* Austral. Inst. Mining Metall., 96-100.
- BODNAR, R.J., REYNOLDS, T.J. & KUEHN, C.A. (1985): Fluid inclusion systematics in epithermal systems. *Reviews Econ. Geol.* **2**, 73-97.
- BONHAM, H.F. (1984): Three major types of epithermal precious-metal deposits. *Geol. Soc. Am. Abstr. Programs* **16**, 449.

- BONHAM, H.F. (1986): Models for volcanic-hosted epithermal precious metal deposits; a review. In Proceedings of Symposium 5, Volcanism, Hydrothermal Systems and Related Mineralization. Internat. Volcanol. Congress, Univ. Auckland, New Zealand, 13-17.
- BONHAM, H.F. & GILES, D.L. (1983): Epithermal gold/silver deposits: the geochemical connection. *Geothermal Resources Council, Special Report* 13, 257-262.
- BORNHORST, T.J. & ROSE, W.I. (1986): Partitioning of gold in young calc-alkaline volcanic rocks from Guatemala. *J. Geol.* 94, 412-418.
- BOUDREAU, A.E. & MCCALLUM, I.S. (1992): Concentration of platinum-group elements by magmatic fluids in layered intrusions. *Econ. Geol.* 87, 1830-1848.
- BOWERS, T.S. (1991): The deposition of gold and other metals: Pressure-induced fluid immiscibility and associated stable isotope signatures. *Geochim. Cosmochim. Acta* 55, 2417-2434.
- BOYLE, R.W. (1979): The geochemistry of gold and its deposits. *Geol. Surv. Can. Bull.* 280.
- BRUNKER, R.L. & CAITHNESS, S.J. (1990): Mount Kare gold deposit. In *Geology of the Mineral Deposits of Australia and Papua New Guinea* (F.E. Hughes, ed.). Australasian Inst. Mining Metall. 1755-1758.
- BURNHAM, C.W. & OHMOTO, H. (1980): Late-stage processes in felsic magmatism. *Mining Geol. Special Issue* 8, 1-11.
- CAMPBELL, I.H., NALDRETT, A.J. & BARNES, S.-J. (1983): A model for the origin of the platinum-rich sulfide horizons in the Bushveld and Stillwater complexes. *J. Petrology* 24, 133-165.
- CANDELA, P.A. (1989): Felsic magmas, volatiles, and metallogenesis. *Reviews Econ. Geol.* 4, 223-233.
- CANDELA, P.A. (1992): Controls on ore metal ratios in granite-related ore systems: an experimental and computational approach. *Trans. Royal Soc. Edinburgh, Earth Sci.* 83, 317-326.
- CANDELA, P.A. & HOLLAND, H.D. (1984): The partitioning of copper and molybdenum between silicate melts and aqueous fluids. *Geochim. Cosmochim. Acta* 48, 373-380.
- CANDELA, P.A. & HOLLAND, H.D. (1986): A mass transfer model for copper and molybdenum in magmatic hydrothermal systems: the origin of porphyry-type ore deposits. *Econ. Geol.* 81, 1-19.
- CARMICHAEL, I.S.E., TURNER, F.J. & VERHOOGEN, J. (1974): *Igneous Petrology*. McGraw-Hill, New York, 739 p.
- CARROLL, M.R. & RUTHERFORD, M.J. (1985): Sulfide and sulfate saturation in hydrous silicate melts. *J. Geophys. Research* 90, Supplement, C601-C612.
- CASADEVALL, T. & OHMOTO, H. (1977): Sunnyside mine, Eureka mining district, San Juan County, Colorado: geochemistry of gold and base metal ore deposition in a volcanic environment. *Econ. Geol.* 72, 1285-1320.
- CLINE, J.S. & BODNAR, R.J. (1991): Can economic porphyry copper mineralization be generated by a typical calc-alkaline melt? *J. Geophys. Research* 96, 8113-8126.
- CONNORS, K.A., NOBLE, D.C., BUSSEY, S.D. & WEISS, S.I. (1993): Initial gold contents of silicic volcanic rocks: bearing on the behavior of gold in magmatic systems. *Geology* 21, 937-940.
- COOKE, D.R. & BLOOM, M.S. (1990): Epithermal and subadjacent porphyry mineralization, Acupan, Baguio District, Philippines: a fluid inclusion and paragenetic study. *J. Geochem. Explor.* 35, 297-340.
- COX, D.P. & BAGBY, W.C. (1986): Descriptive model of Au-Ag-Te veins. In *Mineral Deposit Models* (D.P. Cox & D.A. Singer, eds.). *U.S. Geol. Surv. Bull.* 1693, 124.
- CROSS, W. & PENROSE, R.A.F., JR. (1895): Geology and mining industries of the Cripple Creek district, Colorado. *U.S. Geol. Surv. 16th Ann. Report*, Pt. 2, 1-209.
- DAVIES, R.M. & BALLANTYNE, G.H. (1987): Geology of the Ladolam gold deposit, Lihir Island, Papua New Guinea. In *Pacific Rim Congress* 87.

- Papua New Guinea. *In* Pacific Rim Congress 87, Proceedings: The Geology, Structure, Mineralization and Economics of the Pacific Rim. Austral. Inst. Mining Metall., 943-949.
- DENHOLM, L.S. (1967): Lode structures and ore shoots at Vatukoula, Fiji. *Austral. Inst. Mining Metall. Proceedings* 222, 73-83.
- DICKIN, A.P., RICE, C.M. & HARMON, R.S. (1986): A strontium and oxygen isotope study of Laramide magmatic and hydrothermal activity near Central City, Colorado. *Econ. Geol.* 81, 904-914.
- DRUMMOND, S.E. & OHMOTO, H. (1985): Chemical evolution and mineral deposition in boiling hydrothermal systems. *Econ. Geol.* 80, 126-147.
- DUDÁS, F.Ö. (1991): Geochemistry of igneous rocks from the Crazy Mountains, Montana, and tectonic models for the Montana alkalic province. *J. Geophys. Research* 96, 13,261-13,277.
- EATON, P.C. & SETTERFIELD, T.N. (1993): The relationship between epithermal and porphyry hydrothermal systems within the Tavua calderaru, Fiji. *Econ. Geol.* 88, 1053-1083.
- FLEMING, A.W., HANDLEY, G.A., WILLIAMS, K.L., HILLS, A.L. & CORBETT, G.J. (1986): The Porgera gold deposit, Papua New Guinea. *Econ. Geol.* 81, 660-680.
- GABLE, D.J. (1985): Geologic setting and petrochemistry of the Late Cretaceous - Early Tertiary intrusives in the Front Range mineral belt, Colorado. *U.S. Geol. Surv. Prof. Paper* 1280.
- GELLER, B.A. & ATKINSON, W.W. (1991): Paragenetic sequence of telluride and related mineral stages in the Boulder County telluride belt, Colorado. *Geol. Soc. Am. Abstr. Programs* 23, A417.
- GILES, D.L. (1982): Gold mineralization in the laccolithic complexes of central Montana. *In* Symposium Proceedings, The Genesis of Rocky Mountain Ore Deposits: Changes with Time and Tectonics. Denver Region Exploration Geologists Soc., Denver, Colorado, 157-162.
- GILL, J.B. (1970): Geochemistry of Viti Levu, Fiji, and its evolution as an island arc. *Contrib. Mineral. Petrology* 27, 179-203.
- GILL, J.B. & WHELAN, P. (1989): Early rifting of an oceanic island arc (Fiji) produced shoshonitic to tholeiitic basalts. *J. Geophys. Research* 94, 4561-4578.
- GOTT, G.B., MCCARTHY, J.H., VANSICKLE, G.H. & MCHUGH, J.B. (1969): Distribution of gold and other metals in the Cripple Creek district, Colorado. *U.S. Geol. Surv. Prof. Paper* 625-A, 1-17.
- HAMLYN, P.R., KEAYS, R.R., CAMERON, W.E., CRAWFORD, A.J. & WALDRON, H.M. (1985): Precious metals in magnesian low-Ti lavas: implications for metallogensis and sulfur saturation in primary magmas. *Geochim. Cosmochim. Acta* 49, 1797-1811.
- HANDLEY, G.A. (1987): Exploration of the Porgera gold deposit. *In* Pacific Rim Congress 87, Proceedings: The Geology, Structure, Mineralization and Economics of the Pacific Rim. Austral. Inst. Mining Metall., 145-149.
- HANDLEY, G.A. & BRADSHAW, P.M.D. (1986): The Porgera gold deposit, Papua New Guinea. *In* Proceedings Gold '86 (A.J. Macdonald, ed.). Konsult International, Willowdale, Ontario, 416-424.
- HANDLEY, G.A. & HENRY, D.D. (1990): Porgera gold deposit. *In* Geology of the Mineral Deposits of Australia and Papua New Guinea (F.E. Hughes, ed.). Austral. Inst. Mining Metall., 1717-1724.
- HASTINGS, J.S. (1988): Gold deposits of Zortman-Landusky, Little Rocky Mountains, Montana. *In* Bulk Mineable Precious Metal Deposits of the Western United States (R.W. Schafer, J.J. Cooper & P.G. Vikre, eds.). Geol. Soc. Nevada, Reno, Nevada, 187-205.
- HAUGHTON, D.R., ROEDER, P.L. & SKINNER, B.J. (1974): Solubility of sulfur in magmas. *Econ. Geol.* 69, 451-462.
- HAYASHI, K.-I. & OHMOTO, H. (1991): Solubility of gold in NaCl- and H<sub>2</sub>S-bearing aqueous solutions at 250-350 °C. *Geochim. Cosmochim. Acta* 55, 2111-2126.

- HAYBA, D.O., BETHKE, P.M., HEALD, P. & FOLEY, N.K. (1985): Geologic, mineralogic, and geochemical characteristics of volcanic-hosted epithermal precious-metal deposits. *Reviews Econ. Geol.* 2, 129-167.
- HEALD, P., FOLEY, N.K. & HAYBA, D.O. (1987): Comparative anatomy of volcanic-hosted epithermal deposits: acid-sulfate and adularia-sericite types. *Econ. Geol.* 82, 1-26.
- HEALD-WETLAUFER, P., HAYBA, D.O., FOLEY, N.K. & GOSS, J.A. (1983): Comparative anatomy of epithermal precious- and base-metal districts in volcanic terranes. *Geol. Assoc. Can. - Mineral. Assoc. Can. Program Abstr.* 8, 1.
- HEDENQUIST, J.W., editor (1992): Magmatic contributions to hydrothermal systems. *Geol. Surv. Japan Report* 279, 199 p.
- HEDENQUIST, J.W. & AOKI, M. (1991): Meteoric interaction with magmatic discharges in Japan and the significance for mineralization. *Geology* 19, 1041-1044.
- HEDENQUIST, J.W., AOKI, M. & SHINOHARA, H. (1994a): Flux of volatiles and ore-forming metals from the magmatic-hydrothermal system of Satsuma Iwojima volcano. *Geology* 22, 585-588.
- HEDENQUIST, J.W. & HENLEY, R.W. (1985a): The importance of CO<sub>2</sub> on freezing point measurements of fluid inclusions: evidence from active geothermal systems and implications for epithermal ore deposition. *Econ. Geol.* 80, 1379-1406.
- HEDENQUIST, J.W. & HENLEY, R.W. (1985b): Hydrothermal eruptions in the Waiotapu geothermal system, New Zealand: their origin, associated breccias, and relation to precious metal mineralization. *Econ. Geol.* 80, 1640-1668.
- HEDENQUIST, J.W. & LOWENSTERN, J.B. (1994): The role of magmas in the formation of hydrothermal ore deposits. *Nature* 370, 519-527.
- HEDENQUIST, J.W., MATSUHISA, Y., IZAWA, E., WHITE, N.C., GIGGENBACH, W.F. & AOKI, M. (1994b): Geology, geochemistry, and origin of high sulfidation Cu-Au mineralization in the Nansatsu district, Japan. *Econ. Geol.* 89, 1-30.
- HENLEY, R.W. & McNABB, A. (1978): Magmatic vapor plumes and ground-water interaction in porphyry copper emplacement. *Econ. Geol.* 73, 1-20.
- HENRY, D.D. (1988): Porgera - the first fifty years. In *Bicentennial Gold '88, Extended Abstracts, Oral Programme. Geol. Soc. Austral. Abstracts* 22, 144-149.
- IMAI, A. (1994): Sulfide globules associated with a felsite intrusion in the Mount Kinabalu quartz monzonite, Sabah, East Malaysia; sulfide melt immiscibility in a highly silicic melt. *Econ. Geol.* 89, 181-185.
- IRVINE, T.N. & BARAGAR, W.R.A. (1971): A guide to the chemical classification of the common volcanic rocks. *Can. J. Earth Sci.* 8, 523-548.
- JAIRETH, S. (1991): Hydrothermal geochemistry of Te, Ag<sub>2</sub>Te and AuTe<sub>2</sub> in epithermal precious metal deposits. *Econ. Geol. Research Unit, James Cook Univ., Queensland, Contrib.* 37, 20 p.
- JOHNSON, R.W., WALLACE, D.A. & ELLIS, D.J. (1976): Feldspathoid-bearing potassic rocks and associated types from volcanic islands off the coast of New Ireland, Papua New Guinea: a preliminary account of geology and petrology. In *Volcanism in Australasia* (R.W. Johnson, ed.). Elsevier, Amsterdam, 297-316.
- JONES, B.K. (1992): Application of metal zoning to gold exploration in porphyry copper systems. *J. Geochem. Explor.* 43, 127-155.
- KEAYS, R.R. (1987): Principles of mobilization (dissolution) of metals in mafic and ultramafic rocks - the role of immiscible magmatic sulphides in the generation of hydrothermal gold and volcanogenic massive sulphide deposits. *Ore Geol. Reviews* 2, 4763.
- KELLY, W.C. & GODDARD, E.N. (1969): Telluride ores of Boulder County, Colorado. *Geol. Soc. Am. Memoir* 109.
- KENNEDY, A.K., GROVE, T.L. & JOHNSON, R.W. (1990a): Experimental and trace element constraints on the evolution of lavas from Lihir Island, Papua New Guinea. *Contrib. Mineral. Petrology* 104, 722-734.
- KENNEDY, A.K., HART, S.R. & FREY, F.A.

- (1990b): Composition and isotopic constraints on the petrogenesis of alkaline arc lavas: Lihir Island, Papua New Guinea. *J. Geophys. Research* 95, 6929-6942.
- KROENKE, L.W. & RODDA, P. (1984): Cenozoic tectonic development of the southwest Pacific. *United Nations Econ. Social Commission for Asia and the Pacific, CCOPISOPAC Tech. Bull.* 6, 122 p.
- KWAK, T.A.P. (1990): Geochemical and temperature controls on ore mineralization at the Emperor gold mine, Vatukoula, Fiji. *J. Geochem. Explor.* 36, 297-337.
- LE BAS, M.J., LE MAITRE, R.W., STRECKEISEN, A. & ZANETTIN, B. (1986): A chemical classification of volcanic rocks based on the Total Alkali-Silica diagram. *J. Petrology* 27, 745-750.
- LINDGREN, W. & RANSOME, F.L. (1906): Geology and gold deposits of the Cripple Creek district, Colorado. *U.S. Geol. Surv. Prof. Paper* 54.
- LOUGHLIN, G.F. & KOSCHMANN, A.H. (1935): Geology and ore deposits of the Cripple Creek district, Colorado. *Colorado Sci. Soc. Proceedings* 13 (6), 217-435.
- LOVERING, T.S. & GODDARD, E.N. (1950): Geology and ore deposits of the Front Range Colorado. *U.S. Geol. Surv. Prof. Paper* 223.
- LOWENSTERN, J.B., MAHOOD, G.A., RIVERS, M.L. & SUTTON, S.R. (1991): Evidence for extreme partitioning of copper into a magmatic vapor phase. *Science* 252, 1405-1409.
- MATHEZ, E.A. (1989): Vapor associated with mafic magma and controls on its composition. *Reviews Econ. Geol.* 4, 21-31.
- MCINNES, B.I.A. & CAMERON, E.M. (1994): Carbonated, alkaline hybridizing melts from a sub-arc environment: mantle wedge samples from the Tabar-Lihir-Tanga-Feni arc, Papua New Guinea. *Earth Planet. Sci. Lett.* 122, 125-141.
- MITCHELL, A.H.G. & LEACH, T.M. (1991): *Epithermal Gold in the Philippines: Island Arc Metallogenesis, Geothermal Systems and Geology*. Academic Press, New York, 457 p.
- MOYLE, A.J., DOYLE, B.J., HOOGVLIET, H. & WARE, A.R. (1990): Ladolam gold deposit, Lihir Island. In *Geology of the Mineral Deposits of Australia and Papua New Guinea* (E. Hughes, ed.). Austral. Inst. Mining Metall., 1793-1805.
- MÜLLER, D. & GROVES, D.I. (1993): Direct and indirect associations between potassic igneous rocks, shoshonites and gold-copper deposits. *Ore Geol. Reviews* 8, 383-406.
- MUTSCHLER, F.E., GRIFFIN, M.E., STEVENS, D.S. & SHANNON, S.S. (1984): Precious metal deposits related to alkaline rocks in the North American Cordillera. *Geol. Soc. Am. Abstr. Programs* 16, 606.
- MUTSCHLER, F.E., GRIFFIN, M.E., STEVENS, D.S. & SHANNON, S.S. (1985): Precious metal deposits related to alkaline rocks in the North American Cordillera - an interpretive review. *Trans. Geol. Soc. S. Africa*, 88, 355-377.
- MUTSCHLER, F.E., MOONEY, T.C. & JOHNSON, D.C. (1990): Precious metal deposits related to alkaline igneous rocks - a space-time trip through the Cordillera. In *Fourth Western Regional Conference on Precious Metals and the Environment, Proceedings, September 19-22, 1990, Lead, South Dakota*. Soc. Mining Metall. Explor., 43-59.
- NALDRETT, A.J. (1989a): Magmatic Sulfide Deposits. *Monographs on Geology and Geophysics* 14. Oxford University Press, Oxford, 186 p.
- NALDRETT, A.J. (1989b): Stratiform PGE deposits in layered intrusions. *Reviews Econ. Geol.* 4, 135-165.
- NASH, J.T. & CUNNINGHAM, C.G. (1973): Fluid-inclusion studies of the fluorspar and gold deposits, Jamestown District, Colorado. *Econ. Geol.* 68, 1247-1262.
- NEDACHI, M. & TAGUCHI, S. (1992): Geochemistry of hot spring waters in the Ladolam gold deposit, Lihir Island, Papua New Guinea. *Geol. Soc. Am. Abstr. Programs* 24, A316.
- NELSON, C.E. & GILES, D.L. (1985): Hydrothermal eruption mechanisms and hot spring gold deposits. *Econ. Geol.* 80, 1633-1639.

- O'BRIEN, H., IRVING, A.J. & MCCALLUM, S. (1991): Eocene potassic magmatism in the Highwood Mountains, Montana: petrology, geochemistry, and tectonic implications. *J. Geophys. Research* 96, 13237-13260.
- PARRY, W.T. & BRUHN, R.L. (1990): Fluid pressure transients on seismogenic normal faults. *Tectonophysics* 179, 335-344.
- PATERSON, C.J. (1990): Magmatic-hydrothermal model for epithermal-mesothermal Au-Ag deposits in the northern Black Hills. In *Proceedings, Fourth Western Regional Conference on Precious Metals and the Environment, September 19-22, 1990, Lead, South Dakota. Soc. Mining Metall. Explor.*, 89-102.
- PATERSON, C.J., UZUNLAR, N., GROFF, J. & LONGSTAFFE, F.J. (1989): A view through an epithermal - mesothermal precious metal system in the northern Black Hills, South Dakota: a magmatic origin for the ore-forming fluids. *Econ. Geol. Monogr.* 6, 564-570.
- PORTER, E.W. & RIPLEY, E. (1985): Petrologic and stable isotope study of the gold-bearing breccia pipe at the Golden Sunlight deposit, Montana. *Econ. Geol.* 80, 1689-1706.
- RICE, C.M., HARMON, R.S. & SHEPHERD, T.J. (1985): Central City, Colorado: the upper part of an alkaline porphyry molybdenum system. *Econ. Geol.* 80, 1769-1796.
- RICE, C.M., LUX, D.R. & MACINTYRE, R.M. (1982): Timing of mineralization and related intrusive activity near Central City, Colorado. *Econ. Geol.* 77, 1655-1666.
- RICHARDS, J.P. (1990a): Petrology and geochemistry of alkalic intrusives at the Porgera gold deposit, Papua New Guinea. *J. Geochem. Explor.* 35, 141-199.
- RICHARDS, J.P. (1990b): *The Porgera Gold Deposit, Papua New Guinea: Geology, Geochemistry and Geochronology*. Ph.D. thesis, Australian National University, Canberra, Australia.
- RICHARDS, J.P. (1992): Magmatic-epithermal transitions in alkalic systems: Porgera gold deposit, Papua New Guinea. *Geology* 20, 547-550.
- RICHARDS, J.P., CHAPPELL, B.W. & MCCULLOCH, M.T. (1990): Intraplate-type magmatism in a continent-island-arc collision zone: Porgera intrusive complex, Papua New Guinea. *Geology* 18, 958-961.
- RICHARDS, J.P. & KERRICH, R. (1993): The Porgera gold mine, Papua New Guinea: Magmatic-hydrothermal to epithermal evolution of an alkalic-type precious metal deposit. *Econ. Geol.* 88, 1017-1052.
- RICHARDS, J.P. & LEDLIE, I. (1993): Alkalic intrusive rocks associated with the Mount Kare gold deposit, Papua New Guinea: Comparison with the Porgera intrusive complex. *Econ. Geol.* 88, 755-781.
- RICHARDS, J.P., MCCULLOCH, M.T., CHAPPELL, B.W. & KERRICH, R. (1991): Sources of metals in the Porgera gold deposit, Papua New Guinea: Evidence from alteration, isotope, and noble metal geochemistry. *Geochim. Cosmochim. Acta* 55, 565-580.
- RICHARDS, J.P. & MCDOUGALL, I. (1990): Geochronology of the Porgera gold deposit, Papua New Guinea: resolving the effects of excess argon on K-Ar and  $^{40}\text{Ar}/^{39}\text{Ar}$  age estimates for magmatism and mineralization. *Geochim. Cosmochim. Acta* 54, 1397-1415.
- RUSSELL, C.W. (1991): Gold mineralization in the Little Rocky Mountains, Phillips County, Montana. In *Guidebook to the Central Montana Alkalic Province; Geology, Ore Deposits and Origin* (D.W. Baker & R.B. Berg, eds.). *Montana Bureau Mines Geol. Special Publication* 100, 1-18.
- RYE, R.O. (1993): The evolution of magmatic fluids in the epithermal environment. The stable isotope perspective. *Econ. Geol.* 88, 733-753.
- RYE, R.O., BETHKE, P.M. & WASSERMAN, M.D. (1992): The stable isotope geochemistry of acid sulfate alteration. *Econ. Geol.* 87, 225-262.
- RYZAK, D. (1990): Gold deposits of active mining areas, Little Rocky Mountains, Montana. In *Proceedings, Fourth Western Regional Conference on Precious Metals and the Environment, September 19-22, 1990, Lead, South Dakota. Soc. Mining Metall. Exploration*, 61-75.

- SACK, R.O., CARMICHAEL, I.S.E., RIVERS, M. & GHIORSO, M.S. (1980): Ferric-ferrous equilibria in natural silicate liquids at 1 bar. *Contrib. Mineral. Petrology* 75, 369-376.
- SAUNDERS, J.A. (1991): Gold deposits of the Boulder County gold district, Colorado. *U.S. Geol. Surv. Bull.* 1857-1, 137-148.
- SAUNDERS, J.A. & MAY, E.R. (1986): Bessie G: a high-grade epithermal gold telluride deposit, La Plata County, Colorado, U.S.A. In *Proceedings, Gold '86* (A.J. Macdonald, ed.). Konsult International, Willowdale, Ontario, 436-444.
- SAWKINS, F.J., O'NEIL, J.R. & THOMPSON, J.M. (1979): Fluid inclusion and geochemical study of vein gold deposits, Baguio district, Philippines. *Econ. Geol.* 74, 1420-1434.
- SETTERFIELD, T.N., EATON, P.C., ROSE, W.J. & SPARKS, R.S.J. (1991): The Tavua caldera, Fiji: a complex shoshonitic caldera formed by concurrent faulting and downsagging. *J. Geol. Soc. London*, 148, 115-127.
- SETTERFIELD, T.N., MUSSETT, A.E. & OGLETHORPE, R.D.J. (1992): Magmatism and associated hydrothermal activity during the evolution of the Tavua caldera:  $^{40}\text{Ar}/^{39}\text{Ar}$  dating of volcanic, intrusive, and hydrothermal events. *Econ. Geol.* 87, 1130-1140.
- SEWARD, T.M. (1984): The transport and deposition of gold in hydrothermal systems. In *Proceedings, Gold '82, The Geology and Geochemistry and Genesis of Gold Deposits* (R.P. Foster, ed.). Balkema, Rotterdam, 165-181.
- SEWARD, T.M. (1989): The hydrothermal chemistry of gold and its implications for ore formation: boiling and conductive cooling as examples. *Econ. Geol. Monogr.* 6, 398-404.
- SEWARD, T.M. (1993): The hydrothermal geochemistry of gold. In *Gold Metallogeny and Exploration* (R.P. Foster, ed.). Chapman & Hall, London, 37-62.
- SHELTON, K.L., SO, C.-L., HAEUSSLER, G.T., CHI, S.-J. & LEE, K.-Y. (1990): Geochemical studies of the Tongyoung gold-silver deposits, Republic of Korea: evidence of meteoric water dominance in a Te-bearing epithermal system. *Econ. Geol.* 85, 1114-1132.
- SHEPPARD, S.M.F. (1986): Characterization and isotopic variations in natural waters. *Reviews Mineral.* 16, 165-183.
- SHIMA, H. & NALDRETT, A.J. (1975): Solubility of sulfur in an ultramafic melt and the relevance of the system Fe-S-O. *Econ. Geol.* 70, 960-967.
- SIBSON, R.H. (1987): Earthquake rupturing as a mineralizing agent in hydrothermal systems. *Geology* 15, 701-704.
- SIMMONS, E.C. & HEDGE, C.E. (1978): Minor-element and Sr-isotope geochemistry of Tertiary stocks, Colorado mineral belt. *Contrib. Mineral. Petrology* 67, 379-396.
- SINDEEVA, N.D. (1964): *Mineralogy and Types of Deposits of Selenium and Tellurium*. Wiley & Sons, New York, 363 p.
- SMITH, J.G. (1965): Fundamental transcurrent faulting in the northern Rocky Mountains. *Am. Assoc. Petroleum Geol. Bull.* 49, 1398-1409.
- SOLOMON, M. (1990): Subduction, arc-reversal, and the origin of porphyry copper-gold deposits in island arcs. *Geology* 18, 630-633.
- SPOONER, E.T.C. (1993): Magmatic sulphide/volatile interaction as a mechanism for producing chalcophile element enriched, Archean Au-quartz, epithermal Au-Ag and Au skarn hydrothermal ore fluids. *Ore Geol. Reviews* 7, 359-379.
- SPRY, P.G. (1987): A fluid inclusion and sulfur isotope study of precious and base metal mineralization spatially associated with the Patch and Gold Cup breccia pipes, Central City, Colorado. *Econ. Geol.* 82, 1632-1639.
- SPRY, P.G., PAREDES, M.M., FOSTER, F., TRUCKLE, J. & CHADWICK, T.H. (1994): Evidence for magmatic hydrothermal to epithermal origin for the Golden Sunlight gold-silver telluride deposit, Whitehall, Montana. *Geol. Soc. Am. Abstr. Programs* 26, A-311.
- STANTON, R.L. (1994): Ore Elements in Arc Lavas. *Oxford Monographs on Geology and Geophysics* 29. Oxford University Press, Oxford, U.K. 391 p.

- STOFFREGEN, R. (1987): Genesis of acid-sulfate alteration and Au-Cu-Ag mineralization at Summitville, Colorado. *Econ. Geol.* 82, 1575-1591.
- THOMPSON, T.B. (1992): Mineral deposits of the Cripple Creek district, Colorado. *Mining Eng.* 44, 135-138.
- THOMPSON, T.B., TRIPPEL, A.D. & DWELLEY, P.C. (1985): Mineralized veins and breccias of the Cripple Creek District, Colorado. *Econ. Geol.* 80, 1669-1688.
- TILLING, R.I., GOTTFRIED, D. & ROWE, J.J. (1973): Gold abundance in igneous rocks: bearing on gold mineralization. *Econ. Geol.* 68, 168-186.
- TITLEY, S.R. (1978): Copper, molybdenum, and gold content of some porphyry copper systems of the southwestern and western Pacific. *Econ. Geol.* 73, 977-981.
- TWETO, O. & SIMS, P.K. (1963): Precambrian ancestry of the Colorado mineral belt. *Geol. Soc. Am. Bull.* 74, 991-1014.
- WALLACE, D.A., JOHNSON, R.W., CHAPPELL, B.W., ARCULUS, R.J., PERFIT, M.R. & CRICK, I.H. (1983): Cainozoic volcanism of the Tabar, Lihir, Tanga, and Feni islands, Papua New Guinea: geology, whole-rock analyses, and rock-forming mineral compositions. *Bureau Mineral Resources, Geol. Geophys. (Australia), Report* 243.
- WALLACE, P. & CARMICHAEL, I.S.E. (1992): Sulfur in basaltic magmas. *Geochim. Cosmochim. Acta* 56, 1863-1874.
- WARNER, L.A. (1978): The Colorado Lineament – a middle Precambrian wrench fault system. *Geol. Soc. Am. Bull.* 89, 161-171.
- WERLE, J.L., IKRAMUDDIN, M. & MUTSCHLER, F.E. (1984): Allard stock, La Plata Mountains, Colorado – an alkaline rock-hosted porphyry copper – precious metal deposit. *Can. J. Earth Sci.* 21, 630-641.
- WHITE, P.J. & LAWLESS, J.V. (1989): Geochemistry of porphyry-hosted Au-Ag deposits in the Little Rocky Mountains, Montana – a discussion. *Econ. Geol.* 84, 970-971.
- WILSON, M.R. & KYSER, T.K. (1988): Geochemistry of porphyry-hosted Au-Ag deposits in the Little Rocky Mountains, Montana. *Econ. Geol.* 83, 1329-1346.
- WYBORN, D. (1992): The tectonic significance of Ordovician magmatism in the eastern Lachlan Fold Belt. *Tectonophysics* 214, 177-192.
- WYBORN, D., & SUN, S.-S. (1994): Sulphur-undersaturated magmatism – a key factor for generating magma-related copper-gold deposits. *AGSO Research Newsletter* 21, 7-8.
- ZHANG, X. & SPRY, P.G. (1994): Petrological, mineralogical, fluid inclusion, and stable isotope studies of the Gies gold-silver telluride deposit, Judith Mountains, Montana. *Econ. Geol.* 89, 602-627.





## I - UNCONVENTIONAL METAL DEPOSITS IN VOLCANIC ARCS

David V. Lefebure and Gerald E. Ray, British Columbia Geological Survey

Lefebure, D.V. and Ray, G.E. (1998): Unconventional Metal Deposits in Volcanic Arcs; in Metallogeny of Volcanic Arcs, B.C. Geological Survey Branch, Short Course Notes, Open File 1998-8, Section I.

Section I:

Volcanic Redbed Cu - Profile D03

Carbonate-Hosted Disseminated Au-Ag - Profile E03

Iron Oxide Breccias and Veins P-Cu-Au-Ag-U - Profile D07

[View pages I15-28](#)

### ABSTRACT

The wide variety of deposit types formed in volcanic arcs reflects a number of factors favourable to ore generation which include differentiated magmas, enhanced heat flow, major structures and favourable host rocks. In recent years, exploration companies have concentrated on the better known metallic deposit types that occur in volcanic arcs, such as porphyries, skarns, epithermal veins and volcanogenic massive sulphides (VMS). Many new mines have been discovered by this strategy and more will be found, particularly in the poorly prospected areas. However, there are other less well known types of metallic deposits that occur in volcanic arcs which are also attractive exploration targets. These include: volcanic redbed Cu (basaltic Cu), iron-oxide breccias and veins (Olympic Dam-type), carbonate-hosted disseminated Au-Ag (Carlin-type), Algoma-type iron-formation, volcanogenic manganese beds, epithermal manganese veins, Sn-Ag veins, alkalic intrusion-related Au, polymetallic veins, and Alaskan-type Pt. Some of these deposits are fairly common (volcanic redbed Cu, Algoma-type iron-formation, volcanogenic manganese beds, epithermal manganese veins and polymetallic veins), but currently are attracting less attention.

Unconventional deposits belong to two types: (1) styles of mineralization which are found in other environments but are not yet widely recognized to occur within volcanic arcs, and (2) unique deposits which are not easily classified. Carlin-type and Olympic Dam-type deposits are examples of the first category. They are believed by many geologists to be restricted to marginal continental sediments; however, examples have been identified in volcanic arcs. An improved understanding of the second type can lead to identification of new deposit types. For example, Eskay Creek is a precious metal-rich deposit that initially appeared unique because of its unusual mineralogy and setting. Further work suggested it was transitional between an epithermal and VMS system. Subsequent studies of modern, shallow submarine hot springs on the seafloor now suggest that Eskay Creek formed in a similar environment and may be regarded as a new type of VMS deposit (Alldrick, 1995, Hannington, 1997).

Disseminated, sediment-hosted Au deposits of the Carlin or Nevada-type are currently an attractive exploration target because of their large quantities of contained gold and their low-cost, bulk tonnage mining potential. Until recently, these deposits were thought to be confined to Nevada due to unique, but poorly understood geological controls. However, recent studies and continuing exploration of the deposits has revealed a variety of deposit styles, including the presence of higher grade, structurally-controlled mineralization that commonly underlies the bulk tonnage ore zones. Thus geologists are re-examining the potential for Carlin-type deposits in other regions, including island arcs. The Mesel deposit in Indonesia (Turner et al., 1994) and the Bau district of Malaysia (Sillitoe and Bonham, 1990; Christensen et al., 1996) have been identified as being limestone-hosted, Carlin-type deposits in younger island arcs. The Golden Bear deposit in northern British Columbia, which is hosted by arc rocks, exhibits many characteristics of the Carlin-type. The micron-sized gold occurs within arsenian rims on pyrite grains hosted by pervasively decalcified and silicified limestones associated with a regional fault zone.

Another poorly understood deposit type consists of magnetite and/or hematite breccia zones, veins, pipes and tabular bodies which span a spectrum between two end members - Kiruna-type monometallic (Fe P) and Olympic Dam type polymetallic (Fe Cu U Au REE). Kirunavaara in Sweden is the world's largest Fe deposit containing more than 2.5 billion tonnes grading 60% Fe, while Olympic Dam has a resource of 2 billion tonnes grading 35 % Fe, 1.6% Cu, 0.06% U<sub>3</sub>O<sub>8</sub>, 0.6 g/t Au and 0.6 g/t Ag. The polymetallic end members are less common and can be associated with a larger number of Fe occurrences containing little or no Cu and Au. The Kiruna district (Sweden), Pea Ridge and Boss-Bixby (Missouri) and Sue-Dianne (Northwest Territories) deposits are hosted by Precambrian volcanic rocks. There are also a number of Fe-Cu deposits in Chile which occur in a Paleozoic arc environment that have been assigned to the Olympic Dam-type by Hitzman et al. (1992, personal communication, 1998), including Candelaria and El Romeral. This interpretation is controversial because skarn minerals occur in these deposits and they have also been interpreted as Fe or Cu skarns. A more all encompassing interpretation has been offered by Marschik et al. (1997) for the Punta del Cobre district which relates the mineralization to intrusions which generate iron oxide-rich zones adjacent to possible porphyry systems in a skarn environment. However, the existence of magnetite lavas at El Lago and Magnetita Pedernales (Grez et al., 1991) demonstrate that intrusive-magmatic Kiruna-type deposits occur in Tertiary volcanic rocks in the Andes. Further research and exploration will clarify the potential for polymetallic iron-oxide deposits (Olympic Dam-type) in island arcs.

# Unconventional Metal Deposits in Volcanic Arcs

by David V. Lefebure and Gerald E. Ray  
B.C Geological Survey

## Introduction

The wide variety of deposit types formed in volcanic arcs includes the well known porphyry, skarn, epithermal vein and volcanogenic massive sulphide deposits. However, there are a number of other metallic deposits that occur in volcanic arcs, including volcanic redbed copper, iron-oxide breccias and veins (Olympic Dam-type), Carlin-type, Algoma-type iron-formation, volcanogenic manganese beds, epithermal manganese veins, silver-tin veins, alkalic intrusion-related gold, polymetallic veins and Alaskan-type platinum (Table 1). Some of these deposits warrant consideration as potential exploration targets, particularly volcanic redbed copper, iron oxide breccia and vein and Carlin-type deposits which are discussed in more detail below.

## Volcanic Redbed Copper

Volcanic redbed copper deposits occur near intracontinental rifts with subaerial flood basalt sequences and at plate margins with island arc and continental arc volcanics. Although not attracting much exploration interest at the present time, these deposits can contain substantial quantities of copper and silver (Table 2, Figure 1). For example, the Sustut Copper deposit in northern British Columbia contains 43.5 Mt grading 0.81% Cu and Mantos Blancos in Chile had initial hypogene ore reserves of 1.60 % Cu and 17g/t Ag (unpublished field trip guide) Chile has a several producing deposits, including Mantos Blancos, which are commonly included in a group of deposits referred to as copper mantos based on their blanket-shaped morphology (Sato, 1984). Some of the Chilean deposits have substantial oxide zones (e.g. Mantos Blancos with 91 Mt grading 1.40% soluble Cu, unpublished field trip guide) which reflects the prolonged arid climate in the region.

Table 1. Less Conventional Metalliferous Deposit Types Found in Volcanic Arcs.\*

Deposit Type	Commodities	Examples
volcanic redbed copper	Cu, Ag	Sustut Copper (B.C.); Mantos Blancos, El Soldado (Chile)
iron-oxide breccias and faults	Fe, P, Cu, Au, Ag, U, REE?	El Romeral, Candelaria? (Chile)
Carlin-type	Au, Ag	Mesel (Indonesia), Golden Bear (B.C.)
Algoma-type iron formation	Fe, Mn	Austin Brook (New Brunswick), Falcon (B.C.)
volcanogenic Mn	Mn	Cuba
shallow submarine hot spring	Au, Ag, Cu, Pb, Zn	Eskay Creek (B.C.); Kagoshima Bay (Japan)
epithermal Mn	Mn	Talamantes (Mexico); Gloryana (New Mexico)
alkalic intrusion associated Au	Au, Ag, Zn, Pb	Emperor (Fiji); Porgera (Papua New Guinea)
Sn-Ag veins	plus Zn, Cu, Pb, Cd, In, Bi, W	Cerro Rico de Potosi, Oruro (Bolivia)
polymetallic veins	Pb, Zn, Ag, Au	Silver Queen, Duthie (B.C.); Creede (Colorado)
Alaskan-type Pt	Pt, magnetite	Tulameen Complex (B.C.)

\* This list excludes porphyry, skarn, vms and most epithermal deposits.

Table 2. Production and Reserves of Selected Volcanic Redbed Copper Deposits (from Kirkham, 1995)

Deposit	Production/Reserves
Coppercorp (Mamainse Point), Ontario	0.85 Mt; 1.15% Cu, g/t Ag, 0.06 g/t Au
47 Zone, Coppermine River area, Northwest Territories	3.2 Mt; 3.44% Cu
Sustut, British Columbia	43.5 Mt; 0.81% Cu
Bleida, Morocco	5.2 Mt; 4.1% Cu
Carolina de Michilla district, Chile	~40 Mt; 2% Cu
Ivan, Chile	5.3 Mt; 2.3% Cu
Sierra Valenzuela, Chile	10-15 Mt; 1.75% Cu
San José de Tuina, Chile	4.4 Mt; 1.5% Cu
Mantos Blancos, Chile	220 Mt; 1.2% Cu
Cateta del Cobre, Chile	11 Mt; 2.2% Cu
Jardin, Chile	Mt; 1.4% Cu, 80 g/t Ag
Amolanas, Chile	10 Mt; ~1.8% Cu, ~20 g/t Ag
Talcuna, Chile	4.3 Mt; 1.47% Cu, 38 g/t Ag
El Soldado, Chile	136 Mt; 1.6% Cu, 6-10 g/t Ag
Cerro Negro, Chile	Mt; 2% Cu, 20 g/t Ag
Mantos de Catemu, Chile	2.0 Mt; 1.75% Cu, 20 g/t Ag
El Salado, Chile	1.0 Mt; 1.25% Cu
Lo Aguirre, Chile	11 Mt; 2.24% Cu
Altamira, Chile	Mt; 1.7% Cu, 41 g/t Ag
Calumet-Hecla, Michigan	114 Mt; 2.4% Cu
Kingston, Michigan	5.4 Mt; 1.2% Cu
Kearsarge, Michigan	161 Mt; 1.0% Cu
Pewabic, Michigan	38.9 Mt; 1.26 % Cu
Allouez, Michigan	41.3 Mt; 0.77% Cu
Isle Royale, Michigan	17.1 Mt; 0.90% Cu
Baltic, Michigan	55.6 Mt; 1.5% Cu
Osceola, Michigan	37.7 Mt; 0.92% Cu

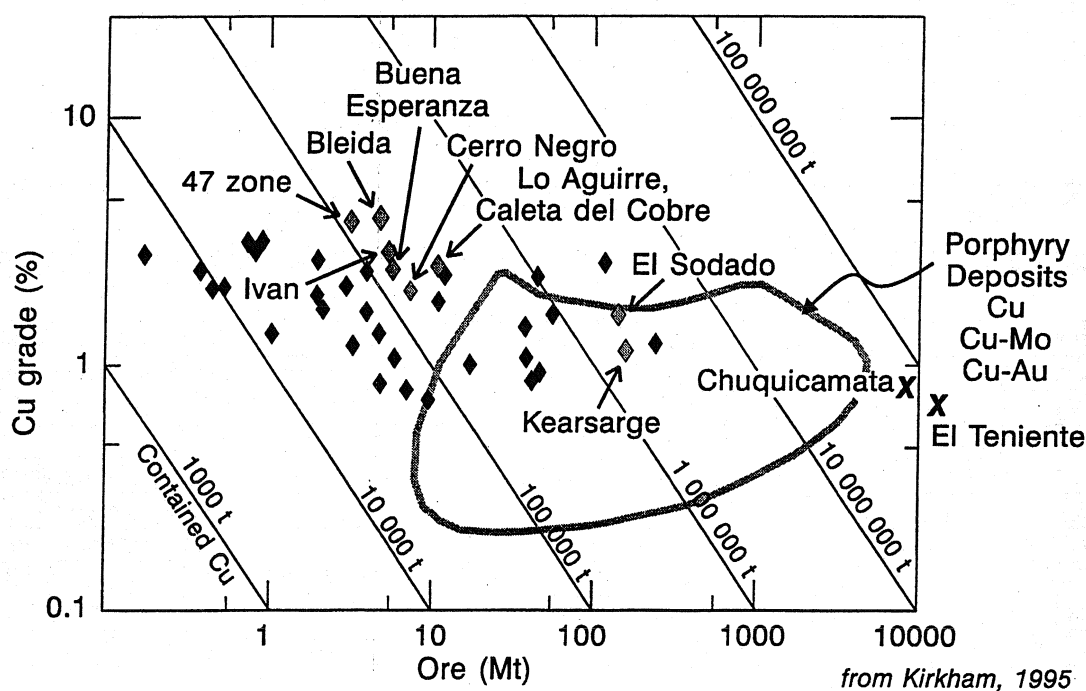


Figure 1. Grade and Tonnage Characteristics of Volcanic Redbed Copper Deposits

Typically chalcocite, bornite and chalcopyrite occur in mafic to felsic volcanic flows, tuff and breccia and related clastic sedimentary rocks as disseminations, veins and infilling amygdulites, fractures and flow top breccias. Some deposits are zoned from chalcocite through bornite and chalcopyrite to fringing pyrite. Silver minerals are not always obvious, although digenite is found in some deposits. Deposits can be tabular, stratabound zones from a few to several tens of metres thick or controlled by structures and crosscut stratigraphy (Figure 2). For a more complete description of volcanic redbed copper deposits see the deposit profile (page A-3).

Most authors have favoured metamorphism of copper-rich, mafic volcanic rocks at greater depth for the source of the metal-bearing fluids, and subsequent deposition higher in the stratigraphic sequence, in oxidized subaerial hostrocks at lower metamorphic grade (Sato, 1984). More recently analogies have been drawn to diagenetic models for sediment-hosted Cu deposits which predate the metamorphism. Low-temperature fluids migrating updip along permeable strata to the margins of basins, or along structures, deposit copper upon encountering oxidized rocks (Kirkham, 1995). These rocks are typically shallow-marine to subaerial volcanic rocks which formed in "low to intermediate latitudes" with arid to semi-arid environments. Both models require oxidized rocks as traps, which requires the presence of an oxygen-rich atmosphere; therefore, all deposits must be younger than ~2.4 Ga. Recent studies of some of the Chilean deposits by Zentilli *et al.* (1997) and Wilson and Zentilli (1998) identify a correlation between solid bitumen, representing residual migrated hydrocarbons, and the copper ores. Initially pyrite formed within the petroleum reservoir, then iron sulphides were replaced by copper sulphides Wilson and Zentilli (1998). Sediment-hosted copper deposits often occur in the same stratigraphic sequences.

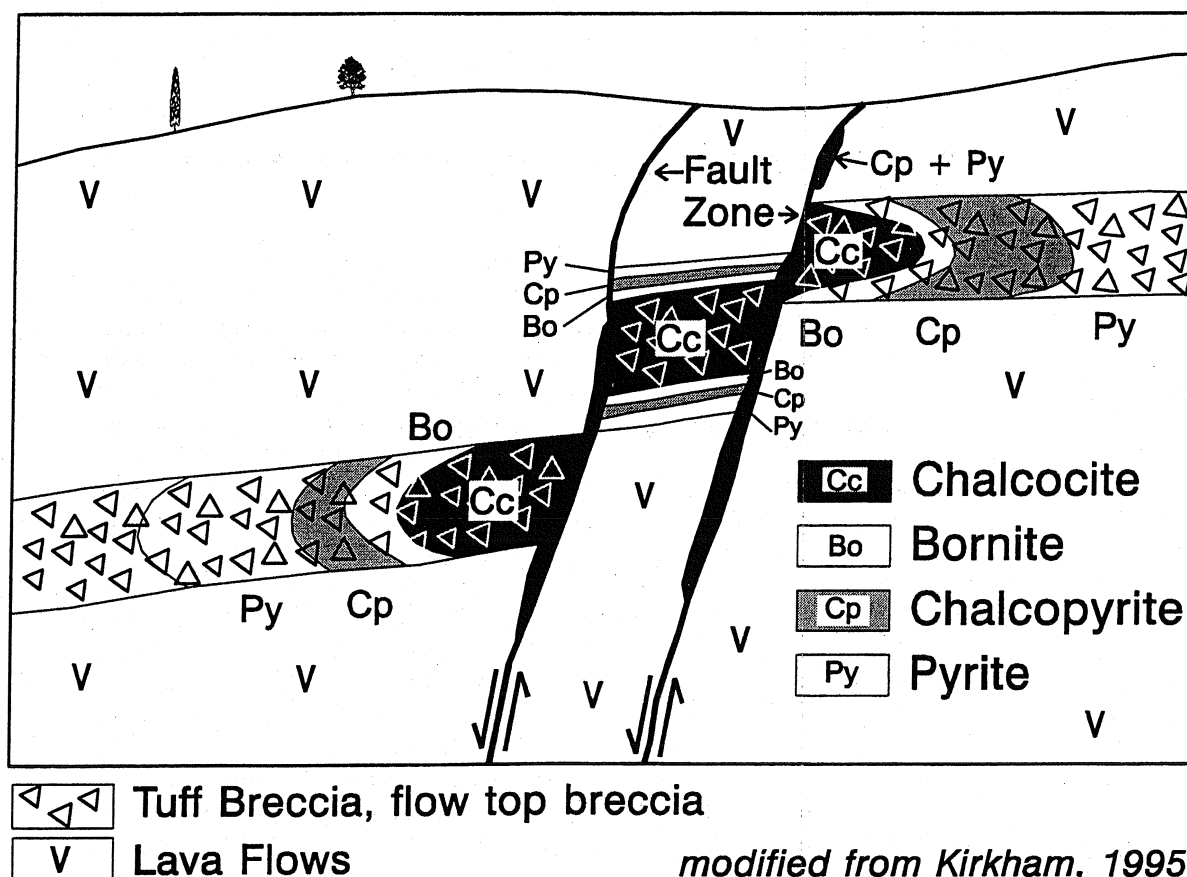


Figure 2. Schematic Diagram Showing Typical Mineral Zoning of Volcanic Redbed Copper Deposits

## Carlin-type Deposits

The Carlin Trend is the most prolific gold belt in North America with a current resource of more than 100 million ounces (Teal and Jackson, 1997). Despite the numerous deposits and mines located along the trend, the genesis of these deposits remains controversial and potential for finding similar deposits in other regions poorly understood. This is clearly underlined by the fact some very large deposits exposed at the surface went undiscovered until the past 15 years because the gold was not visible and alteration inconspicuous (Christensen, 1994). Exploration for Carlin-type deposits has tended to draw on empirical relationships observed along the Carlin and Getchell trends in Nevada (Figure 3), such as the presence of a thick sedimentary sequence along a paleo-continental margin, the presence of significant thicknesses of impure carbonate beds and presence of realgar, orpiment and stibnite (see Table 3). Gold is usually the only metal recovered from Carlin deposits, although gold to silver ratios are roughly 1:1 to for many low grade deposits. While sphalerite and galena are noted in some zones, the deposits rarely have any copper minerals.

Despite the attractiveness of the target, relatively few Carlin-type deposits have been identified outside the western USA. This may indicate some unique aspect to the geology found along the Carlin and Getchell trends or perhaps a lack of understanding of the critical factors in forming these deposits.

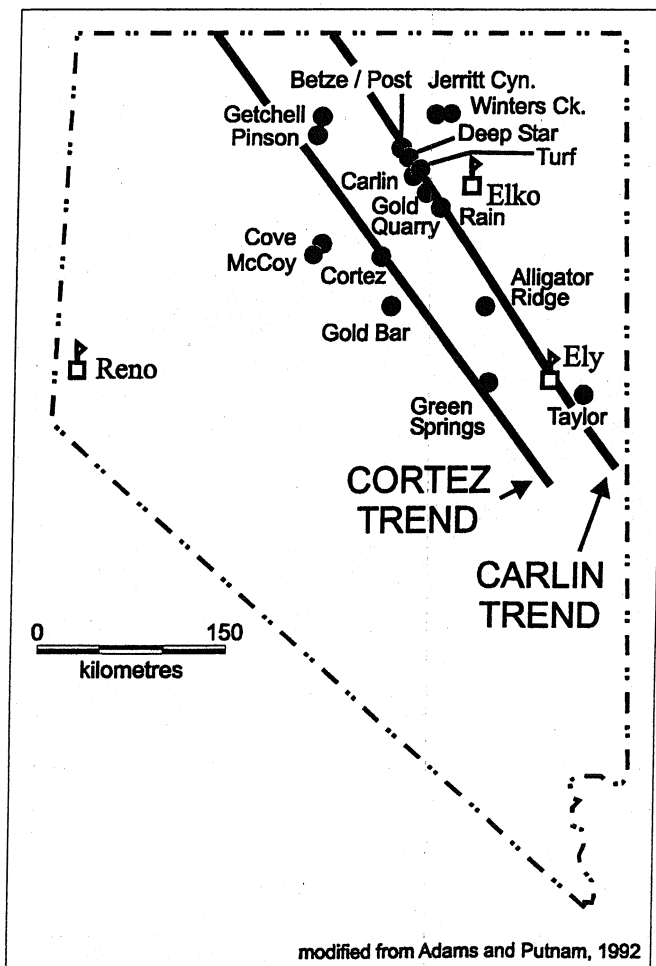


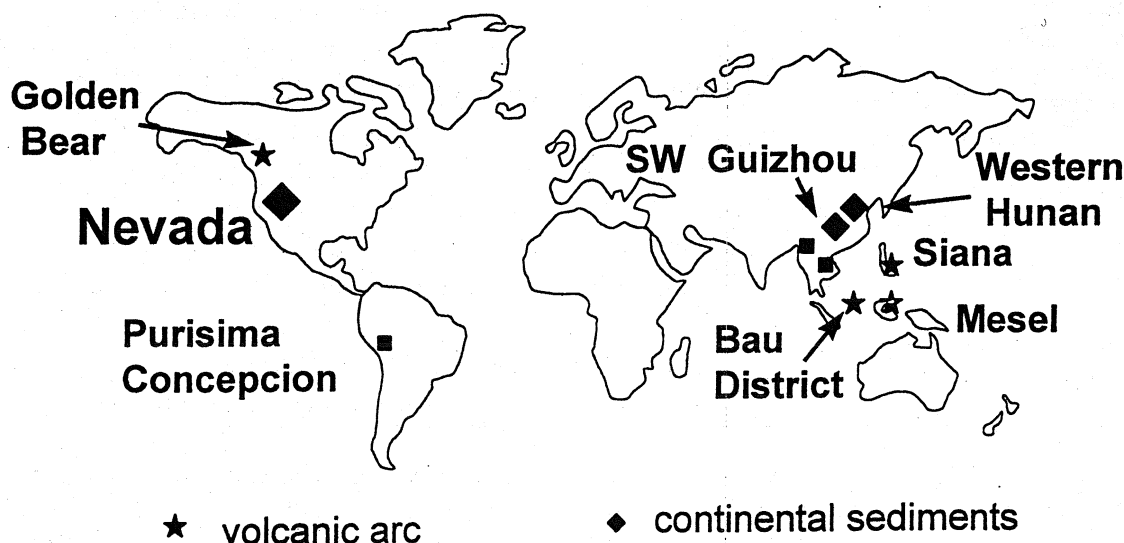
Figure 3. Selected Sediment-hosted Gold Deposits in Nevada.

**Table 3 Key Characteristics of Carlin-type Deposits.**

- hosted by sedimentary sequences containing carbonate
- most favourable host silty carbonate or calcareous siltstone
- non-visible, micron Au occurs in arsenical pyrite rims or pyrite
- gold cannot be panned
- can have realgar, orpiment and/or stibnite
- anomalous values of Ag, As, Hg, Sb (Te, Thallium, B, W)
- alteration is often inconspicuous and assemblages are:
  - carbonate dissolution (decalcification)
  - silica replacement and deposition
  - alteration of aluminosilicates to clay
  - sulphidation of iron to pyrite

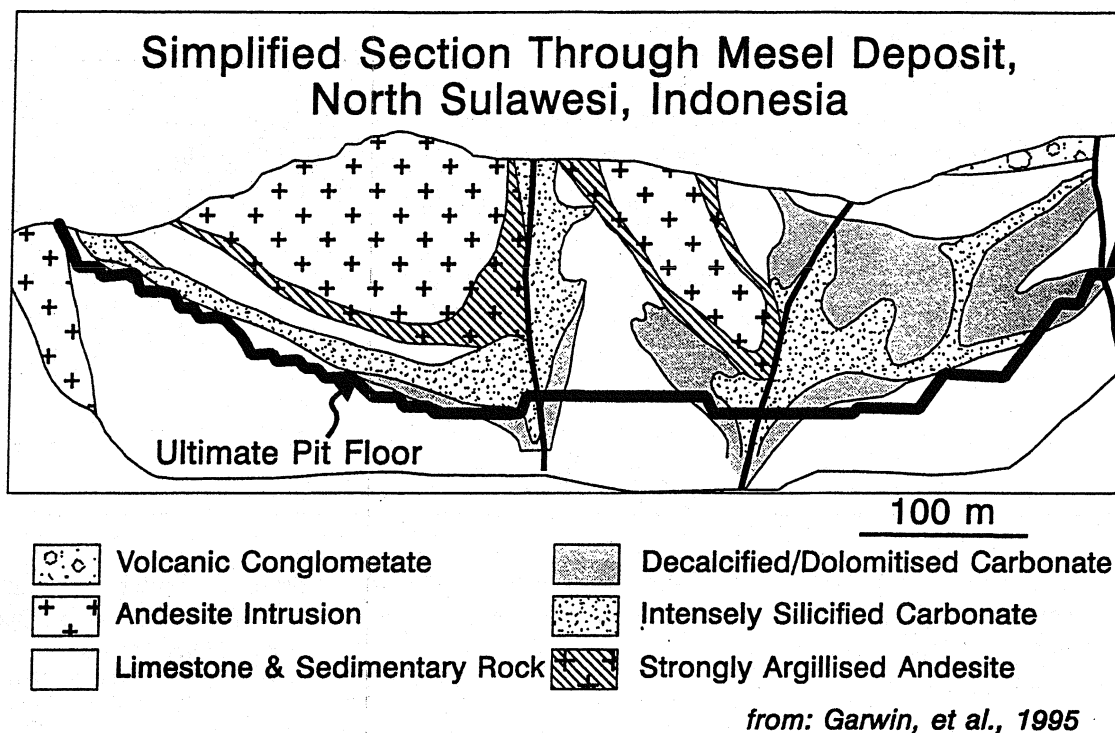
Outside of Nevada, the only region with a large number of Carlin-type deposits is southeastern China in the southwest Guizhou and western Hunan regions (Cunningham *et al.*, 1988; Figure 3). The gold mineralization is hosted by Upper Permian to Middle Triassic shelf carbonates which have experienced broad, open folding and some high angle faulting (Christensen *et al.*, 1996). Igneous rocks are notable by their absence in the Guizhou area.

There are relatively few Carlin-type deposits hosted by volcanic arc sequences. The best known examples, are the Bau District of Sarawk, Malayasia (Sillitoe and Bonham, 1990) and the Mesel deposit of North Sulawesi, Indonesia (Garwin *et al.*, 1995) which occur in the southwest Pacific (Figure 3). The Mesel deposit was discovered by Newmont geologists in 1988. It contains a mineable reserve of 7.8 Mt grading 7.3 g/t Au and is currently in production. The Mesel deposit exhibits many of the distinctive characteristics of Carlin-type deposits, including decalcification, dolomitization and jasperoid development accompanied with gold in disseminated fine-grained arsenian pyrite (Sillitoe, 1995). In British Columbia recent work by Howard Poulsen and Gerry Ray has shown that the Golden Bear deposit, which is hosted by arc rocks, can be classified as a Carlin-type deposit as first suggested informally by Tom Schroeter.



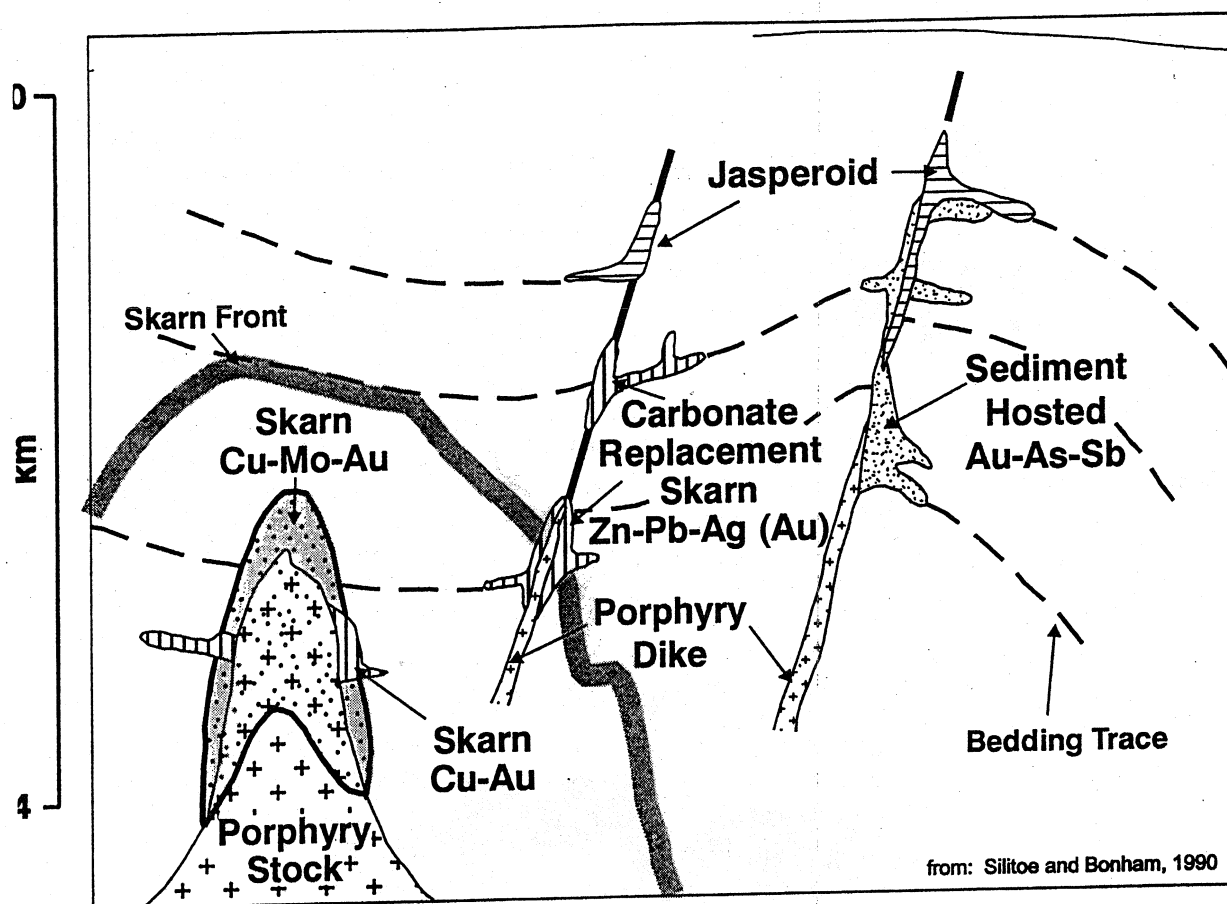
**Figure 3. Location of Carlin-type Deposits and Districts (modified from Christensen *et al.*, 1996).**





**Figure 5. Simplified Section of the Mesel Deposit, North Sulawesi, Indonesia.**

Three general models have been proposed to explain Carlin-type deposits in the western United States - epithermal, distal products of magmatic-hydrothermal systems and deep crustal fluids. The epithermal model was once widely accepted but is now discounted for most deposits. Mineralization was thought to result from shallow Miocene magmatism related to basin and range extension. Sillitoe and Bonham (1990) popularized the importance of porphyry-type magmatic-hydrothermal systems to generate deposits akin to distal skarns. Many deposits do occur near intrusions, skarns and calc-silicate rocks. This model cannot explain all deposits because several districts (e.g., Jerritt Canyon; Guizhou, China) have no related magmatism (Schroeter and Poulsen, 1996). Deep crustal fluids or an amagmatic model has been proposed by some to account for inferred deep mixing of different fluids from different reservoirs (most recently Arehart, 1996). While ultimately a true understanding of the genesis of Carlin-type deposits will result in more effective ore search, most exploration geologists will continue to place more emphasis on their favoured empirical relationships. Therefore, it is important for those of us not working in the western United States to stay current with the results of recent exploration and research.

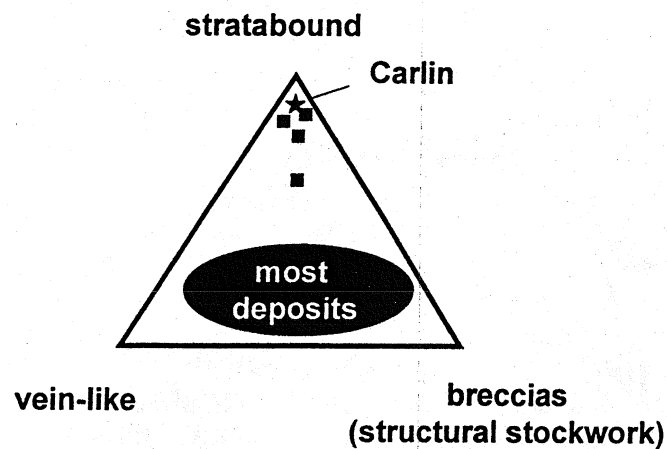


**Figure 6. Intrusion-related Model for Sediment-hosted Gold Deposits from Sillitoe and Bonham (1990). Note the strong structural controls on the deposits and the distal position of the sediment-hosted or Carlin-type mineralization.**

The discovery of deep deposits along the Carlin Trend in the last ten years (Teal and Jackson, 1997) has expanded the definition of Carlin -type deposits to include deposits with very different tenors and geology. As a result of these new discoveries, the first underground mining on the Carlin Trend started in 1996. Since these are hypogene ore deposits, they are possibly more relevant to exploration in other parts of the world than the classic stratabound, low grade, oxidized ore recovered from the Carlin mine and other similar deposits in Nevada.

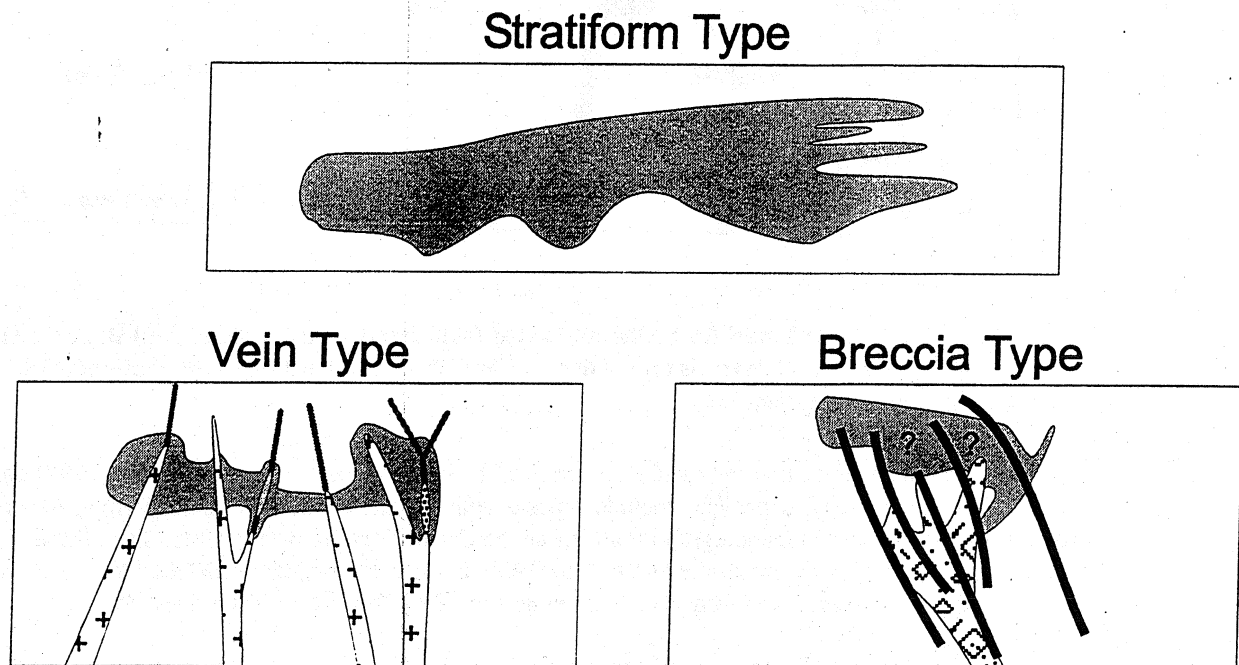
Along the Carlin Trend, different styles of mineralization have been defined by Christensen *et al*, 1993, Groves (1996) and Teal and Jackson (1997). The traditional style of mineralization, stratabound replacement, is found in the Carlin deposit. These large zones of altered rocks contain relatively low grade gold zones which have experienced limited structural disruption of beds. They can be particularly attractive deposits in Nevada because the climate in the region has been arid since the Cretaceous and the primary refractory ore has been oxidized in the near surface environment which makes the deposits amenable to heap leaching and bulk mining techniques. Other

examples of the stratabound replacement style of mineralization are the Pete and Deep West portion of Gold Quarry. Exploration along the Carlin Trend has shown that there are a variety of other styles of mineralization which can be grouped as either as "vein-like" or "breccias". Many of these deposits sit at deeper levels in the surface and have only been found relatively recently. However, data collected by Teal and Jackson (1997) as portrayed in Figure 5 shows that orebodies that are solely stratabound replacement style are relatively uncommon compared to the other types.



**Figure 7. Mineralization Styles of the Carlin Trend.** See text for sources of information.

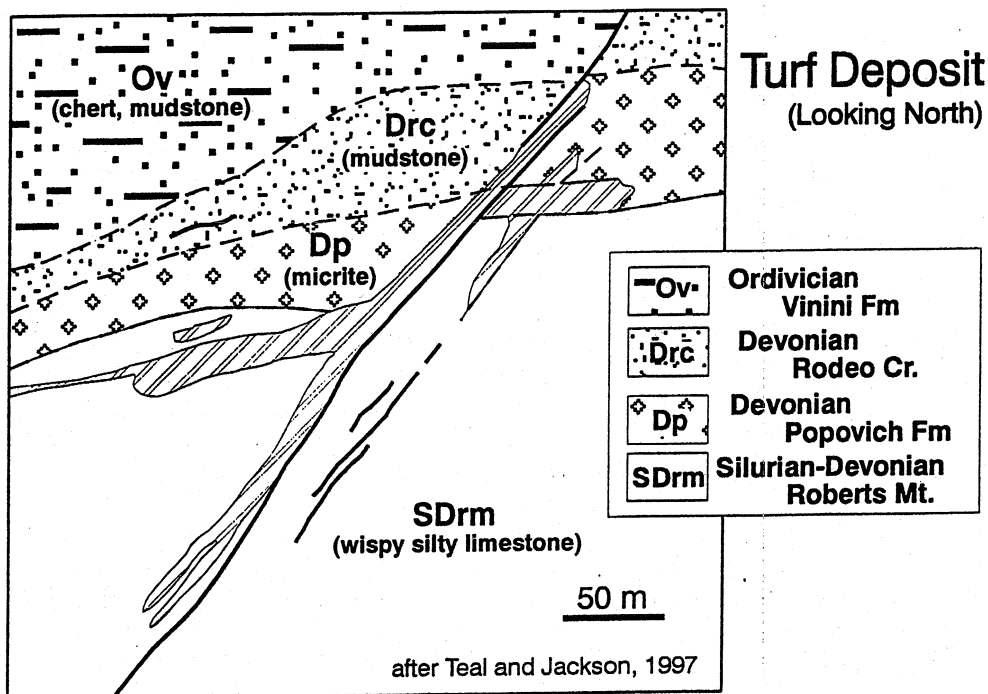
The vein-like mineralization contains zones with higher grade gold than the stratabound type. It occurs within and adjacent to faults which are typically at a high-angle in Nevada, although some deposits are believed to be associated with the Roberts Mountain thrust fault. The gold is fairly restricted which may reflect intense silicification sealing the system or less permeable host rocks. Examples of this style of mineralization are Meikle and Boot Strap, Capstone, in the northern Carlin trend. The structures are often dyke-filled, igneous rock intensely altered and contain relatively higher grade gold.



from Christensen, 1993

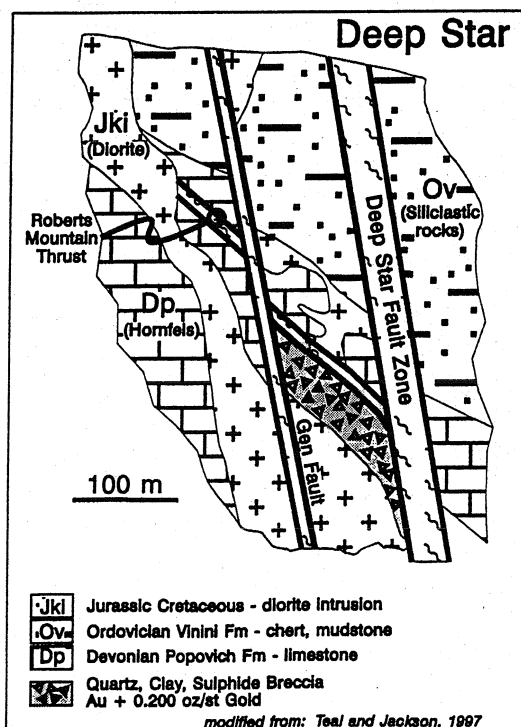
**Figure 8. Three Common Styles of Mineralization Found in Carlin-type Deposits along the Carlin Trend.**

The third style of mineralization is called stockwork (Christensen, 1993) or breccia (Groves, 1996) ore. This type of ore is found near structural intersections which can produce complex structural and lithological relationships. Christensen points out that the gold mineralization appears to be disseminated deposit at the deposit scale, however, gold is structurally controlled at all scales. An example of this deposit type is the Main Gold Quarry deposit which has a variety of lithologies, including thin bedded siltstone, shale, chert and limestone.



**Figure 9. Section of Turf, a vein style deposit which contains a drill indicated resource of 2.5 Mt grading 0.432 oz/t Au.**

**Figure 10 (below). Section of the Deep Star Deposit.**

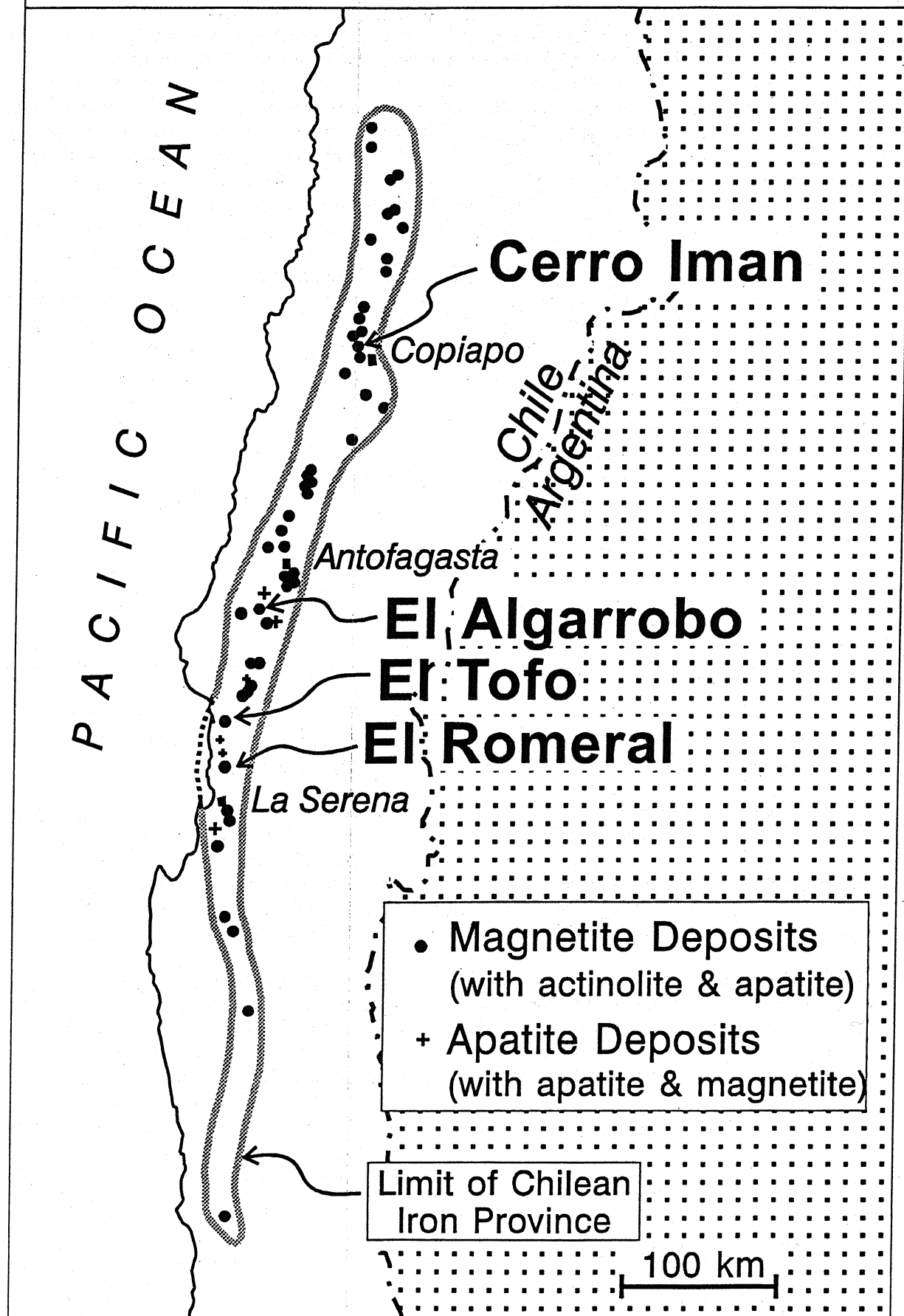


## References

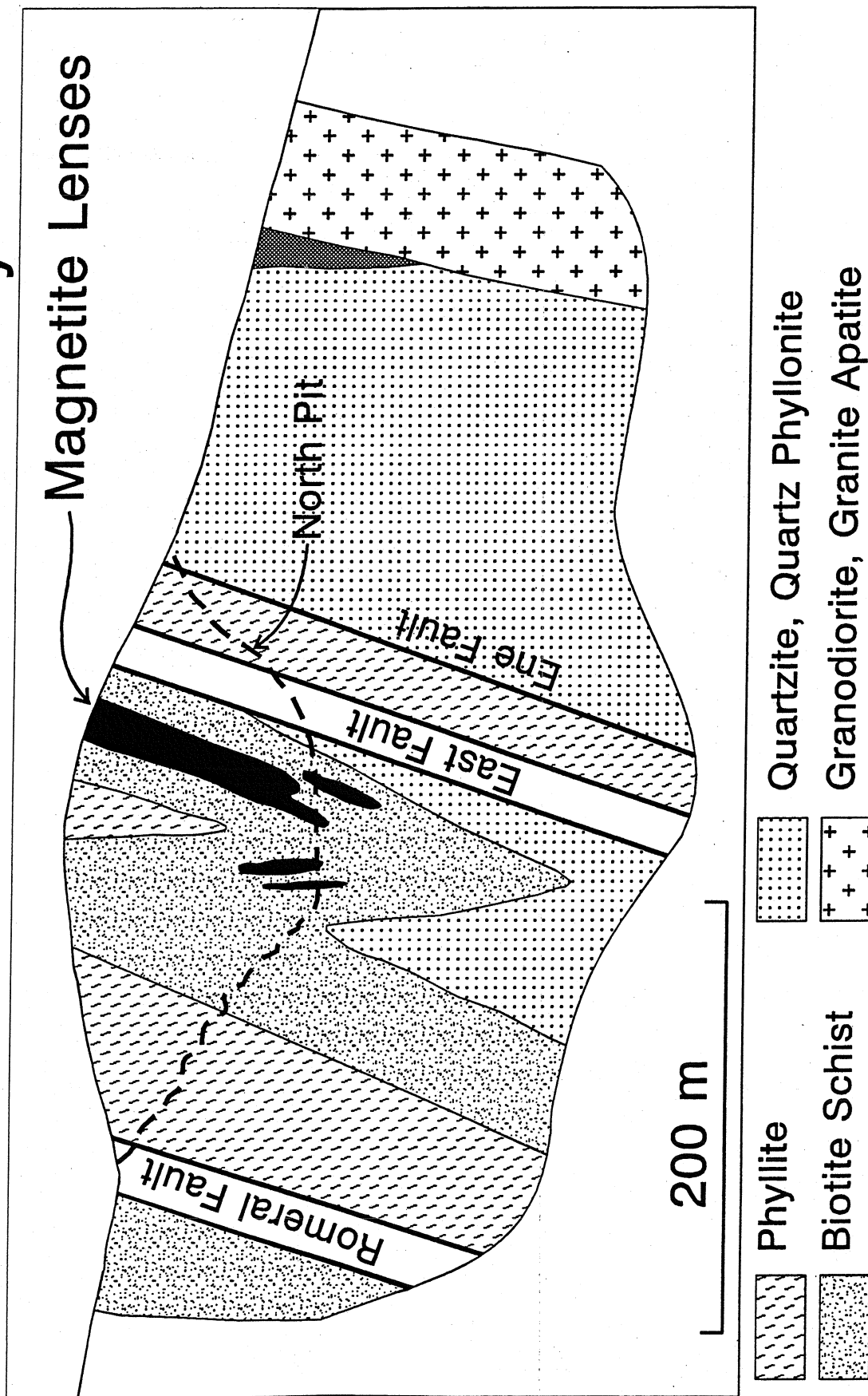
- Arehart, G.B. (1996): Characteristics and Origin of Sediment-hosted Disseminated Gold Deposits: a Review; *Ore Geology Reviews*, Volume 11, pages 383-403.
- Alvarez, A., A. and Noble, D.C. (1988): Sedimentary Rock-Hosted Disseminated Precious Metal Mineralization at Purisima Concepción, Yauricocha District, Central Peru; *Economic Geology*, Volume 83, pages 1368-1378.
- Christensen, O.D., Editor (1993): Gold Deposits of the Carlin Trend, Nevada; *Society of Economic Geologists*, Guidebook Series, Volume 18, 95 pages.
- Christensen, O.D. (1994): Wall Rock Alteration in Carlin-type Sedimentary-Rock-Hosted Gold Deposits; *Northwest Mining Association*, Short Course, Models in Base and Precious Metals, 11 pages.
- Christensen, O., Garwin, S.L. and Mitchell, P.A. (1996): Carlin-type Sedimentary Rock-Hosted Disseminated Gold Deposits Around the Pacific; in *New Mineral Deposit Models for the Cordillera*; *Northwest Mining Association*, Short Course Notes, pages E1-E34.
- Cunningham, C.G., Ashley, R.P., Chou, I., Zushu, H., Chaoyuan, W. and Wenkang, L. (1988): Newly Discovered Sedimentary Rock-Hosted Disseminated Gold Deposits in the People's Republic of China; *Economic Geology*, Volume 83, pages 1462-1467.
- Garwin, S.L., Hendri, D. and Lauricella, P.F. (1995): The Geology of the Mesel Sediment-hosted Gold Deposit, North Sulawesi, Indonesia; *Proceedings of the PACRIM Congress 1995*, Australian Institute of Mining and Metallurgy.
- Groves, D.A. (1996): End Members of the Deposit Spectrum on the Carlin Trend: Examples from Recent Discoveries; in *New Mineral Deposit Models for the Cordillera*; *Cordilleran Roundup*, Short Course Notes, pages D1-D35.
- Hitzman, M. W., Oreskes, N. and Einaudi, M. T. (1992): Geological Characteristics and Tectonic Setting of Proterozoic Iron Oxide (Cu-U-Au-REE) Deposits; *Precambrian Research*, Volume 58, pages 241-287.
- Ilchik, R.P. and Barton, M.D. (1997): An Amagmatic Origin of Carlin-type Gold Deposits; *Economic Geology*, Volume 92, pages 269-288.
- Jackson, M. (1996): Geology of the West Leeville Deposit: a High Grade Refractory Gold Deposit on the Carlin Trend, Nevada; in *New Mineral Deposit Models for the Cordillera*; *Northwest Mining Association*, Short Course Notes, pages C1-C25.
- Kirkham, R.K. (1995): Volcanic Redbed Copper; in *Geology of Canadian Mineral Deposit Types*, Eckstrand, O.R., Sinclair, W.D. and Thorpe, R.I., Editors, *Geological Survey of Canada*, Geology of Canada, Number 8, pages 243-254.
- Lefebure, D.V. (1995): Iron Oxide Breccias and Veins P-Cu-Au-Ag-U; in *Selected British Columbia Mineral Deposit Profiles*, Volume 1, *Metallics and Coal*, Lefebure, D.V. and Ray, G.E., Editors, *British Columbia Ministry of Employment and Investment*, Open File 1995-20, pages 33-36.
- Lefebure, D.V. and Church, B.N. (1996): Volcanic Redbed Copper; in *Selected British Columbia Mineral Deposit Profiles*, Volume 2, *More Metallics*, Lefebure, D.V. and Hoy, T., Editors, *British Columbia Ministry of Employment and Investment*, Open File 1996-13, pages 5-7.
- Poulsen, K.H. (1996): Carlin-type Gold Deposits and their Potential Occurrence in the Canadian Cordillera; in *Current Research 1996-A*, *Geological Survey of Canada*.
- Poulsen, K.H. (1996): Carlin-type Gold Deposits: Canadian Potential?; Short Course Notes in *New Mineral Deposit Models for the Cordillera*; *Northwest Mining Association*, Short Course Notes, pages E1-E34.
- Sato, T. (1984): Manto type Copper Deposits in Chile - a Review; *Bulletin Geological Survey of Japan*, Volume 35, pages 565-582.
- Schroeter, T.G. (1986): Muddy Lake Project; in *Geological Fieldwork, 1985*, B. C. Ministry of Energy, Mines and Petroleum Resources, Paper 1986-1, pages 175-183.
- Schroeter, T.G. and Poulsen, K.H. (1996): Carbonate-hosted disseminated Au-Ag; in *Selected British Columbia Mineral Deposit Profiles*, Volume 2, *More Metallics*, Lefebure, D.V. and Hoy, T., Editors, *British Columbia Ministry of Employment and Investment*, Open File 1996-13, pages 9-12.
- Sillitoe, R.H. (1995): Exploration and Discovery of Base- and Precious-Metal Deposits in the Circum-Pacific Region During the Last 25 Years; *Metal Mining Agency of Japan*, 127 pages.

- Sillitoe, R.H. and Bonham, H.F. Jr. (1990): Sediment-hosted Gold Deposits: Distal Products of Magmatic-Hydrothermal Systems; *Geology*, Volume 18, pages 157-161.
- Teal, L. and Jackson, M. (1997): Geologic Overview of the Carlin Trend Gold Deposits and Descriptions of Recent Deep Discoveries; *Society of Economic Geologists*, Newsletter, Number 31, pages 1, 13-25.
- Turner, S.J., Flindell, P.A., Hendri, D.; Hardjana, I., Lauricella, P.F., Lindsay, R.P., Marpaung, B., and White, G.P. (1994): Sediment-hosted Gold Mineralisation in the Ratatotok District, North Sulawesi, Indonesia; in Mineral Deposits of Indonesia; Discoveries of the past 25 years, van-Leeuwen, Theo-M., Hedenquist, J.W., James, L.P. and Dow, J.A.S., Editors, *Journal of Geochemical Exploration*, Volume 50, pages 317-336.
- Wilson, N. and Zentilli, M. (1998): The Formation of Stratabound Copper Deposits in Degraded Petroleum Reservoirs, Central Chile; Geological Association of Canada, Mineral Deposits Division Newsletter, The Gangue, No. 57, pages 1617.
- Zentilli, M., Munziaga, F., Graves, M.C., Boric, R., Wilson, N.S.F., Mukhopadhyay, P.K. and Snowden, L.R. (1997): Hydrocarbon Involvement in the Genesis of Ore Deposits: an Example in Cretaceous Stratabound (Manto-type) Copper Deposits of Central Chile, *International Geology Review*, Volume 39, pages 1-21.

# Chilean Iron Province



# El Romeral - North Ore Body



modified from Bookstrom, 1977





## J - GEMSTONES IN VOLCANIC ARC ENVIRONMENTS

George J. Simandl, British Columbia Geological Survey

Simandl, G.J. (1998): Gemstones in Volcanic Arc Environments in Metallogeny of Volcanic Arcs, B.C. Geological Survey, short Course Notes, Open File 1998-8, Section J.

### ABSTRACT

Gemstone exploration by major and mid-size mining companies is strongly cyclical. Grass root discoveries, such as the discovery of the Ekati Mine, Northwest Territories, Canada result in surges of staking, prospecting and exploration activities. However, recently a broader interest in gemstones, may be attributed to low precious and base metal prices and to a need of the exploration companies to find sound and "sexy" exploration plays, that would meet underwriter's criteria and investor's expectations.

This presentation addresses selected precious, semi-precious and ornamental stone deposit-types such as precious opal, jadeite, nephrite, rhodonite, emeralds, sapphires and rubies and possibly diamonds, that may be found in, but are not restricted to volcanic arcs.

Precious opal deposits, similar to the Erandique fields in Western Honduras, the historic Santa Maria "Iris" mine, located near Queretaro, Mexico and the Klinker deposit in British Columbia, are associated with relatively pristine volcanic rocks that occur in variety of tectonic environments including young volcanic arcs. Although there is no consensus, commonly these deposits are interpreted as hydrothermal in origin. Number of these deposit are the source of "specimen-type" materials, however, precious opal deposits in volcanic rocks, supplying "stable" high-quality precious opal on commercial scale, are not common. The current low profile of the volcanic-hosted precious opal deposits is in partly due to past marketing of "crazing" unstable opal for gemological applications, and to some extent, to a well orchestrated continuous marketing effort of the companies that mine Australian opal from the renown sedimentary-hosted deposits.

Jade (jadeite or nephrite) deposits are hosted by metamorphosed, mafic and ultramafic rocks associated with ancient volcanic arcs. Jadeite deposits, such as that of the Clear Creek Area, San Benito County California, USA are restricted to blueschist (high pressure/low temperature) metamorphic facies. Nephrite deposits, such as the Polar and Kutcho deposits in Dease Lake area of British Columbia, Canada are more widespread because they form under relatively common pressure-temperature conditions.

Some rhodonite deposits, such as Hollings and occurrences in the Cowichan Lake area, British Columbia, are interpreted as metamorphosed distal exhalative equivalents of volcanogenic massive sulphide deposits associated with arc environments.

Most of the major emerald deposits are either "schist-hosted" or "Colombia-type". Number of "schist-hosted" emerald deposits occur along or near suture zones where mafic/ultramafic rocks of ancient arcs are juxtaposed against or intruded by felsic, continental rocks containing beryllium. Examples to consider are Mingora mines and Gujar Killi deposit of the Swatt district, northern Pakistan, where deposits are located within a ophiolitic melange zone. Colombia-type deposits are much less common

than schist-hosted variety. The famous Muzo and Chivor deposits in Colombia, are the type localities. They are hosted by sedimentary rocks interpreted to be part of a back arc basin.

Corundum forms under variety of geological conditions, including assimilation of pelitic or other high alumina rocks by igneous rocks, high-grade metamorphism or partial melting of aluminous rocks resulting in corundum-bearing pegmatites, syenites, and mica schists, subduction-related prograde metamorphism of aluminous sediments and by desilication of granitic intrusions and pegmatites in contact with marbles or ultramafic rocks. Gem-quality corundum, formed in high-grade metamorphic settings, may be exposed at the surface by tectonic movements (uplift and erosion) , such as the Blu Star deposit currently explored in Southeast British Columbia. Alternatively, it may be transported by alkaline basalts or basaltic volcanoclastic rocks as documented in New South Wales, eastern Australia, by lamprophyres Yogo dike, Montana, USA or it may be brought up by alkaline diatremes (Mark diatreme, British Columbia). The Corundum is also known to occur in alteration zones of epithermal and shallow porphyry Cu type- mineralization. The Empress deposit in British Columbia, Canada is an excellent example of the later type, however it remains to be established if it, or any of similar occurrences, contain stones of gem-quality. Any of these primary gem corundum-bearing protoliths may be eroded and further concentrated by natural processes to form placer deposits.

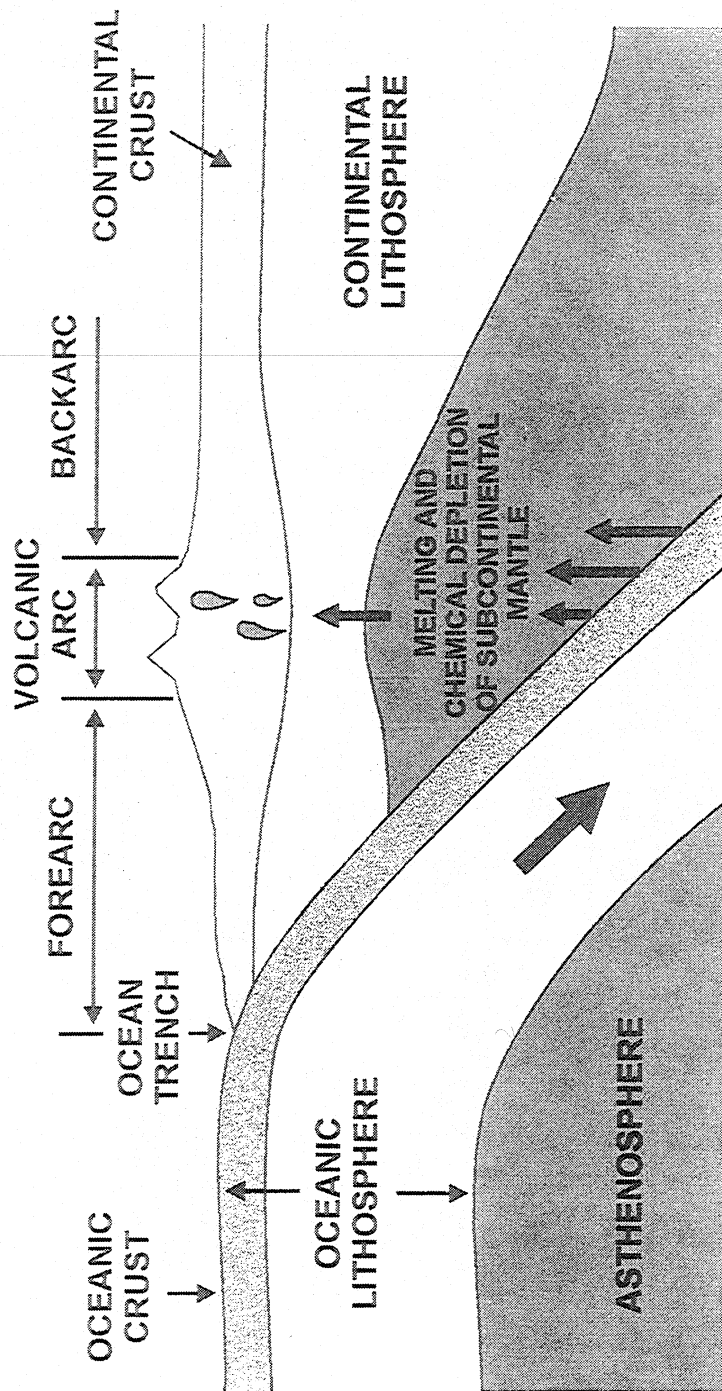
Economic, stable intracratonic, kimberlite -hosted diamond deposits, such as those of the Lac de Grass area, Northwest Territories, Canada or lamproid-hosted diamond deposits, such as Argyle and Ellendale deposits of Western Australia, are now considered as classics and familiar to any exploration geologist. However, several speculative and highly provocative papers published since the mid seventies suggest the possibility of diamond formation in other more exotic geological environments. The most publicised, highly controversial "Subduction model" (S-model) was proposed to explain source of the alluvial diamonds- sapphires deposits of eastern New South Wales, Australia. The S- model ties genetically the suspected diamond protolith to the subduction zone. If this model is correct, a number of areas traditionally considered unfavourable in terms of the diamond exploration, because of a thin continental crust, such as western North America, may require re-evaluation.

As in the case of industrial minerals, the quality of the product, the technical parameters of raw material, the response to upgrading methods, the size and knowledge of the market and successful test-marketing are essential elements in decision-making, when the development of a specific deposit is under consideration. However, unlike most industrial minerals, gemstones have very high unit-value. Therefore, even modest gemstone deposits, in areas lacking infrastructure, may be developed on the commercial scale or as cottage-type industry and marketed world-wide. From the environmentalists view, most gemstone deposits are benign in terms of acid drainage generation, which is in some cases related to base metal and gold mining. Atmospheric discharges are also limited, because no smelting is involved in the extractive process.

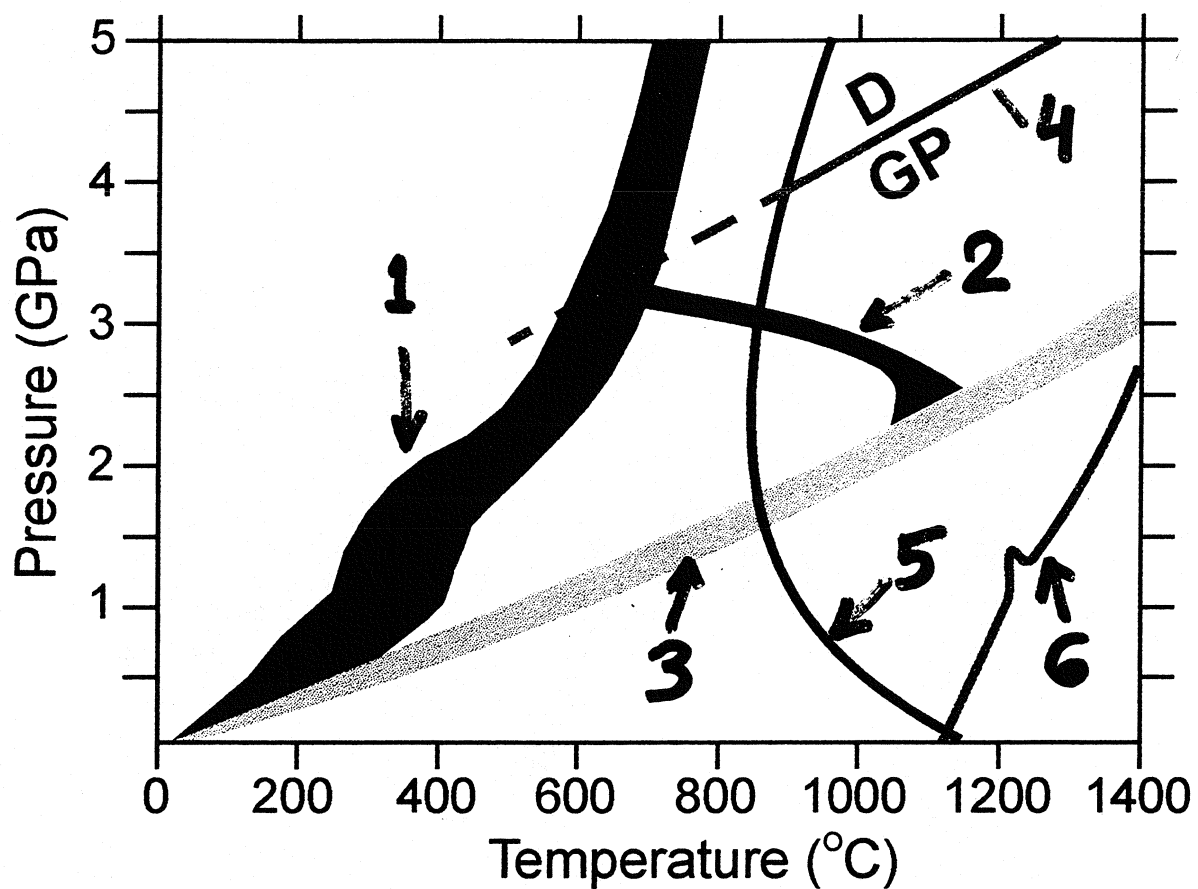
**U.S. IMPORTS OF GEMSTONES (1996)**  
(Thousand carats and million dollars U.S.)

STONE			VALUE
DIAMOND	ROUGH OR UNCUT	1,450	731.0
	CUT BUT UNSET	12,300	5830.0
EMERALDS	CUT BUT UNSET	9,930	203.0
RUBIES/ SAPPHIRES	CUT BUT UNSET	14,400	181.0
OTHER PRECIOUS & SEMIPRECIOUS STONES	ROUGH, UNCUT	1,610,000	37.4
	CUT, SET & UNSET	NA	105.0
SYNTHETICS	CUT BUT UNSET	174,000	40.7
	OTHER	NA	3.8
IMITATION GEMSTONE		NA	66.8
CORAL  PEARLS	UNWORKED	NA	6.3
	NATURAL	NA	1.1
	CULTURED	NA	31.8
	IMITATION	NA	1.7
TOTAL		NA	7,240.0

source:USGS

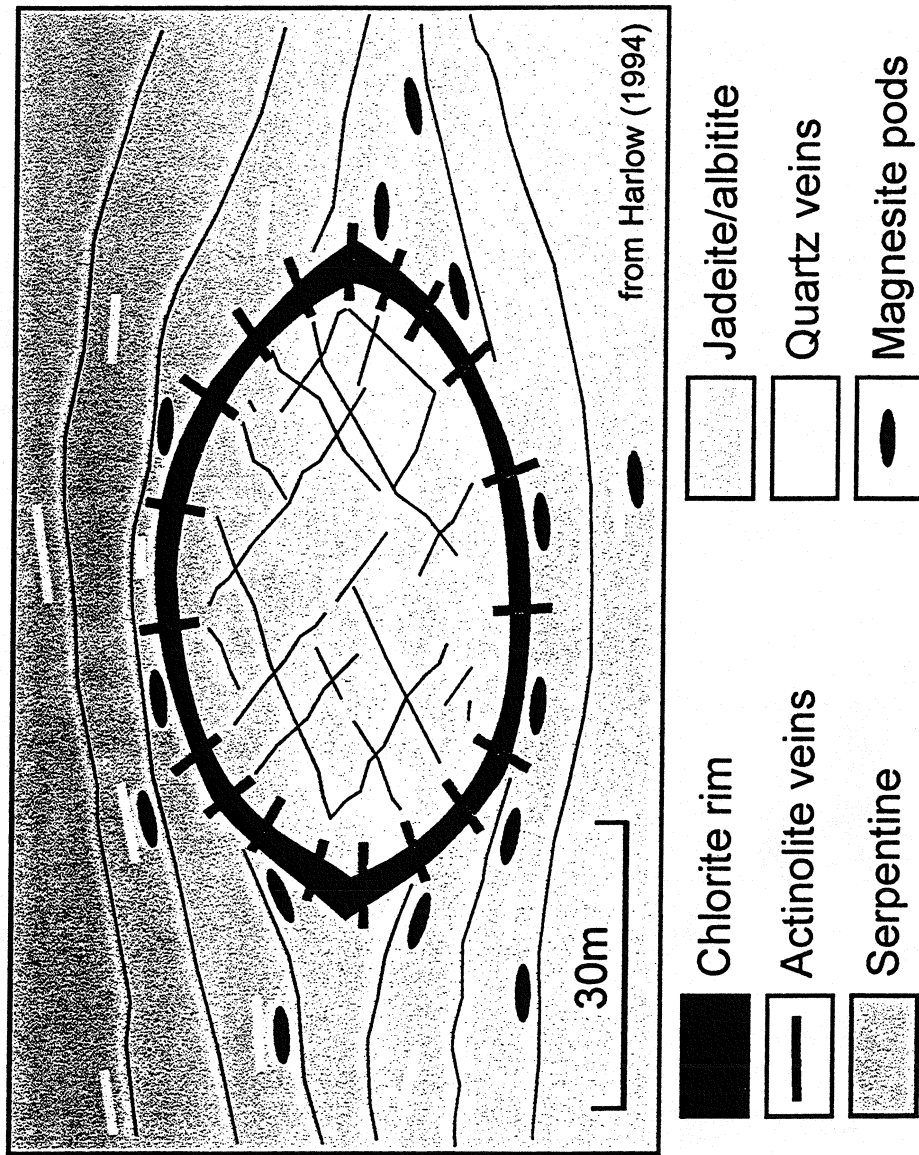


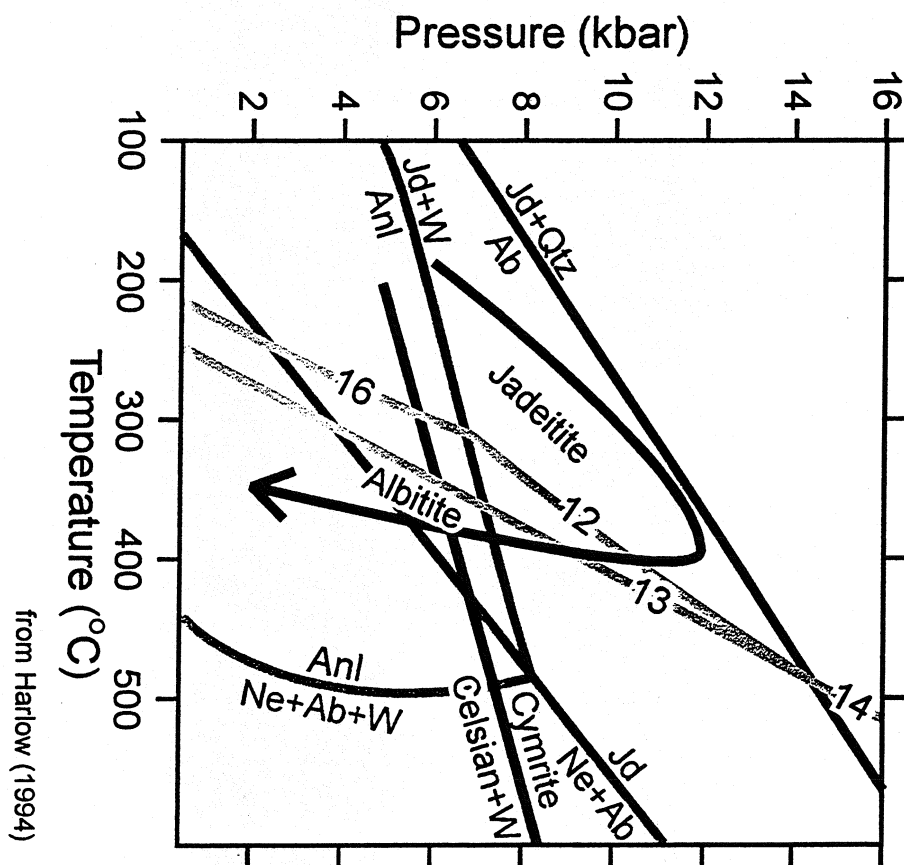
Francis (1994)



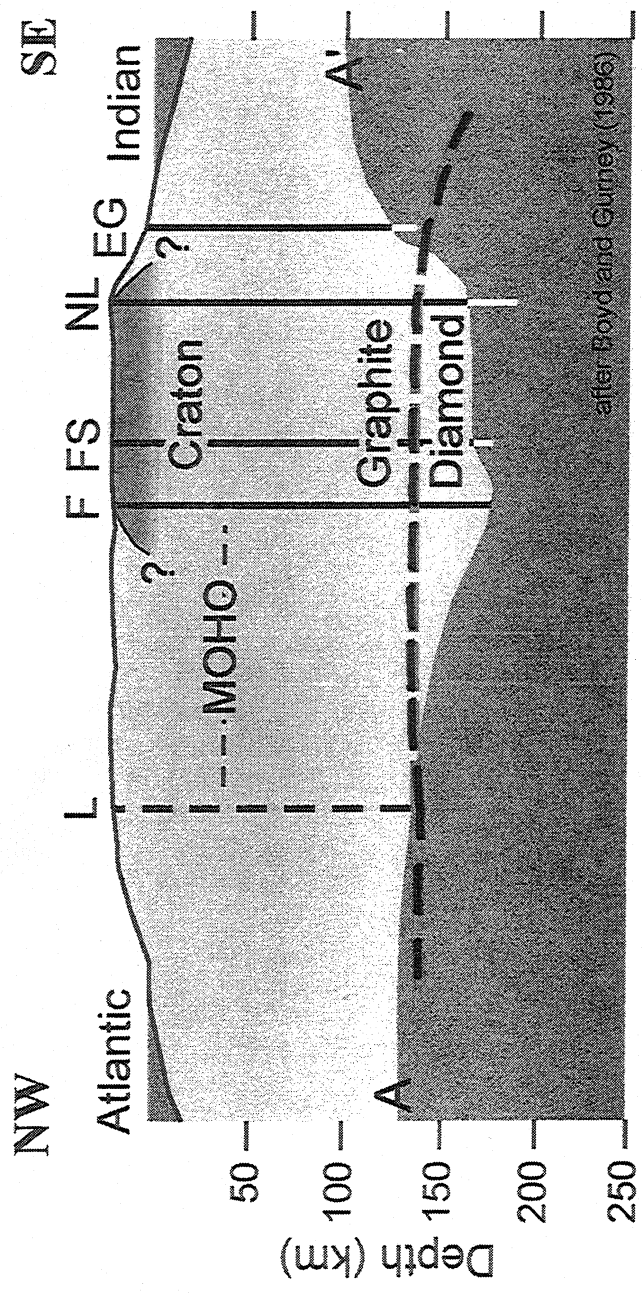
- 1** ■ PT - Top of subducting slab
- 2** ■ Sub - arc geotherm
- 3** ■ Upper plate geotherm
- 4** — Diamond/graphite
- 5** — Wet solidus peridotite
- 6** — Dry solidus peridotite

modified from Panco and Peacock (1995)

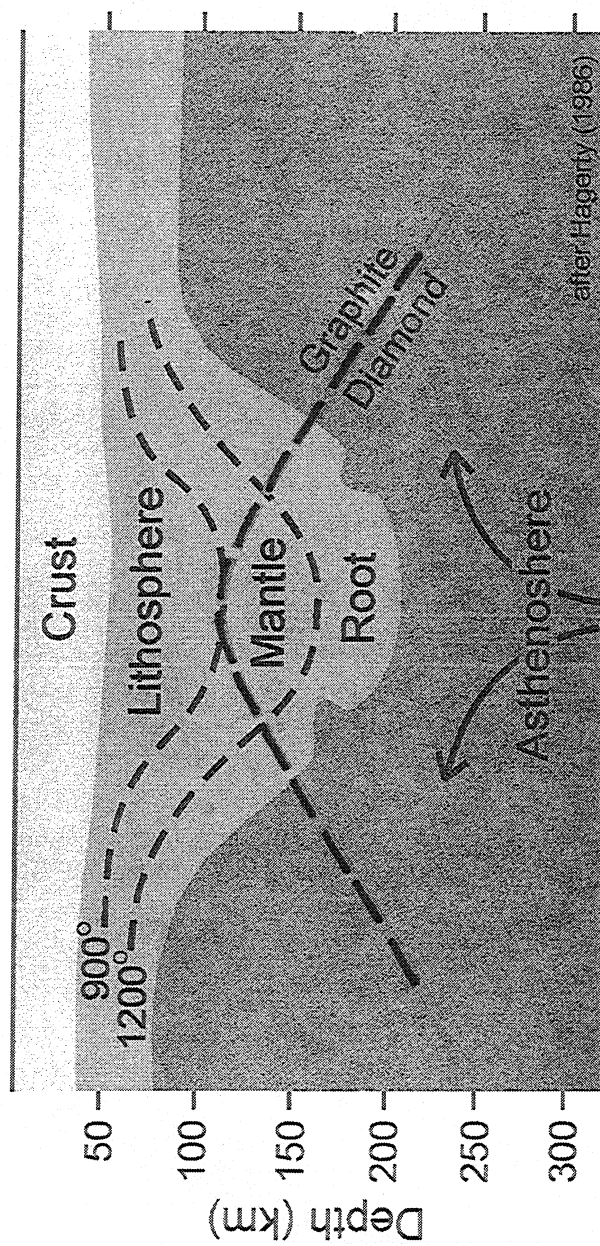




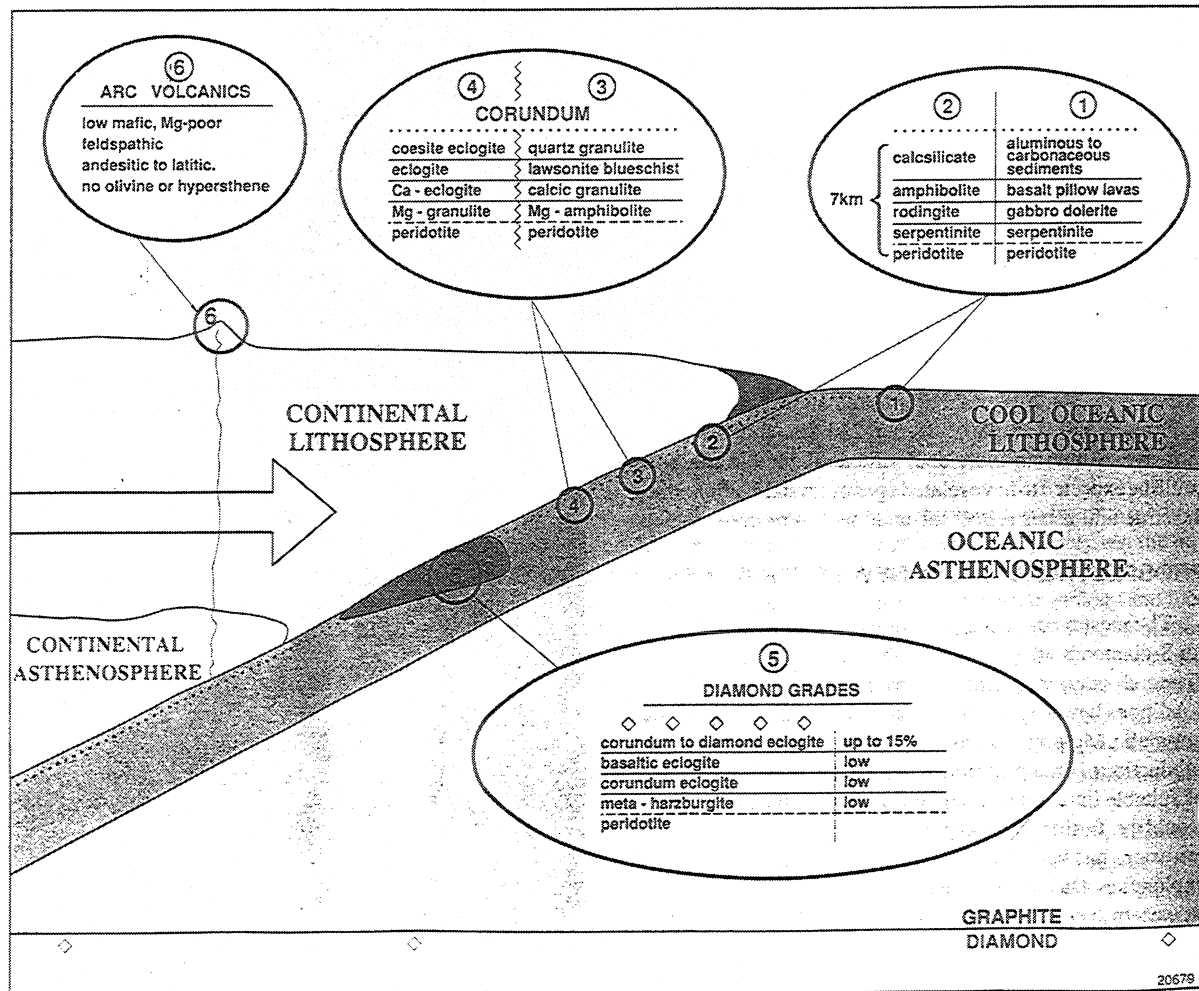
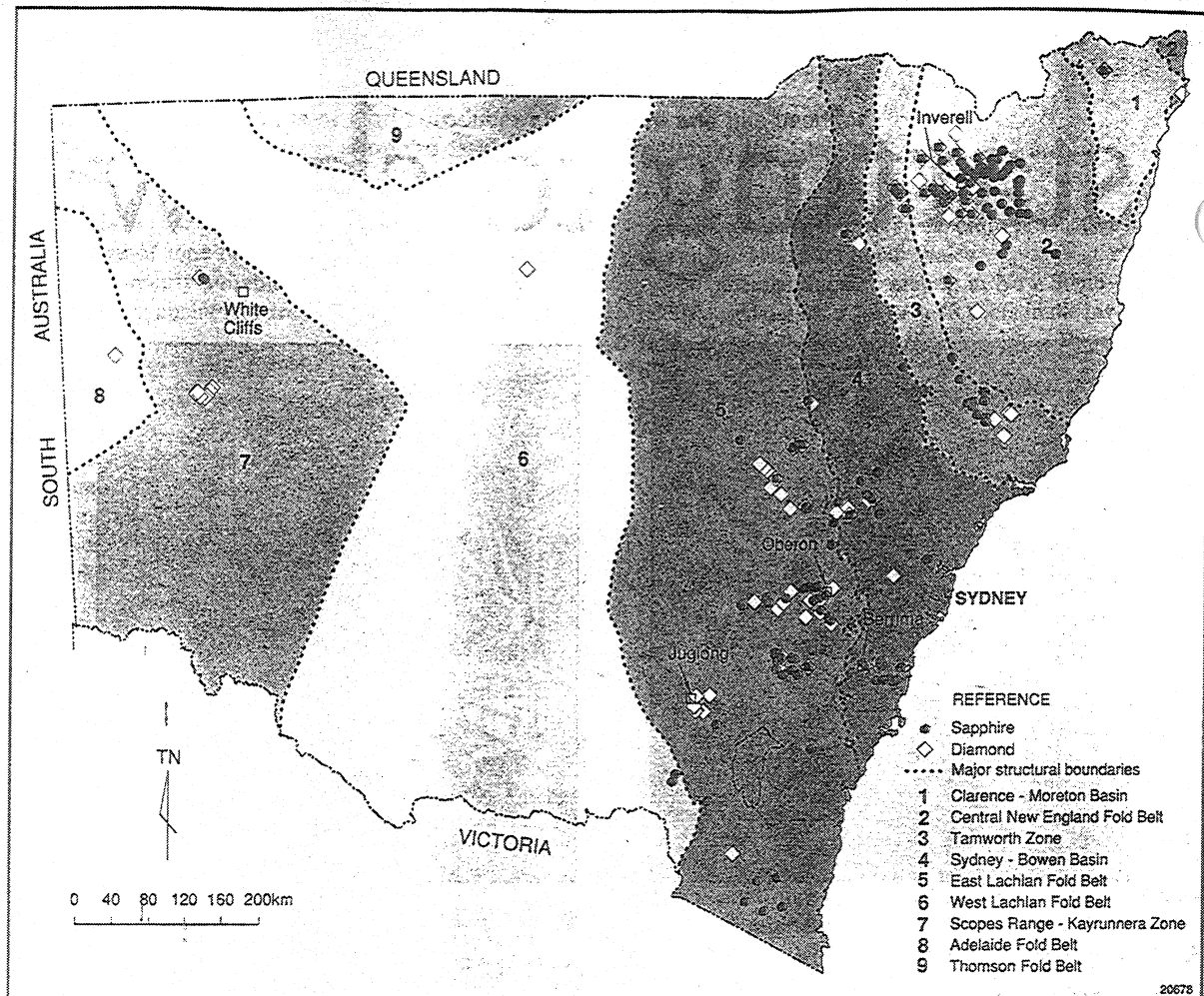


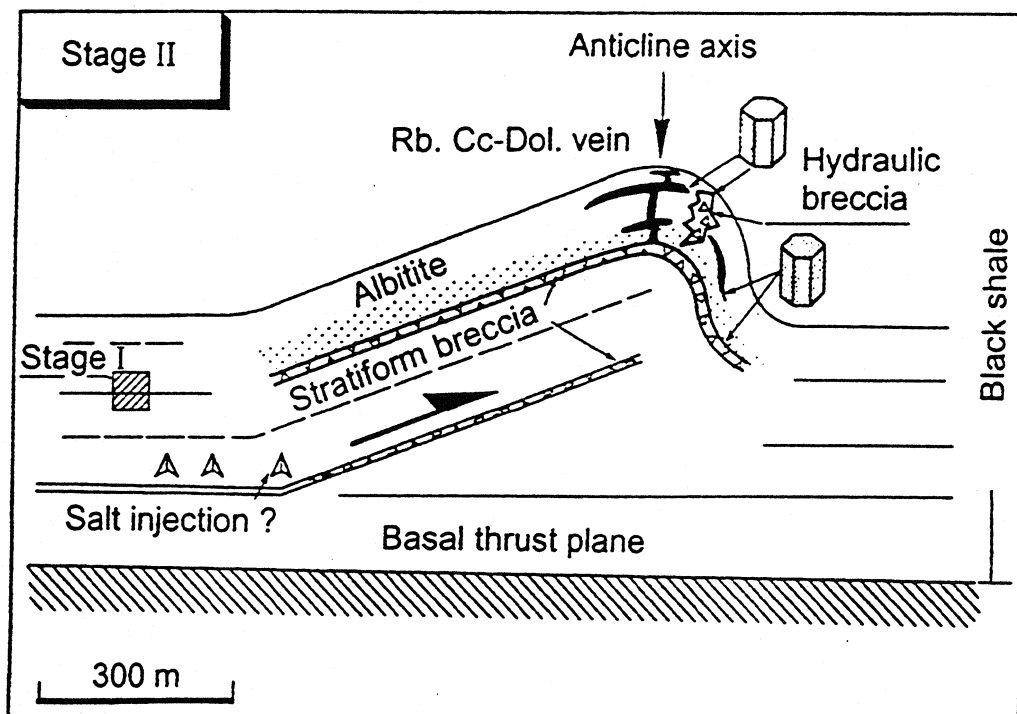
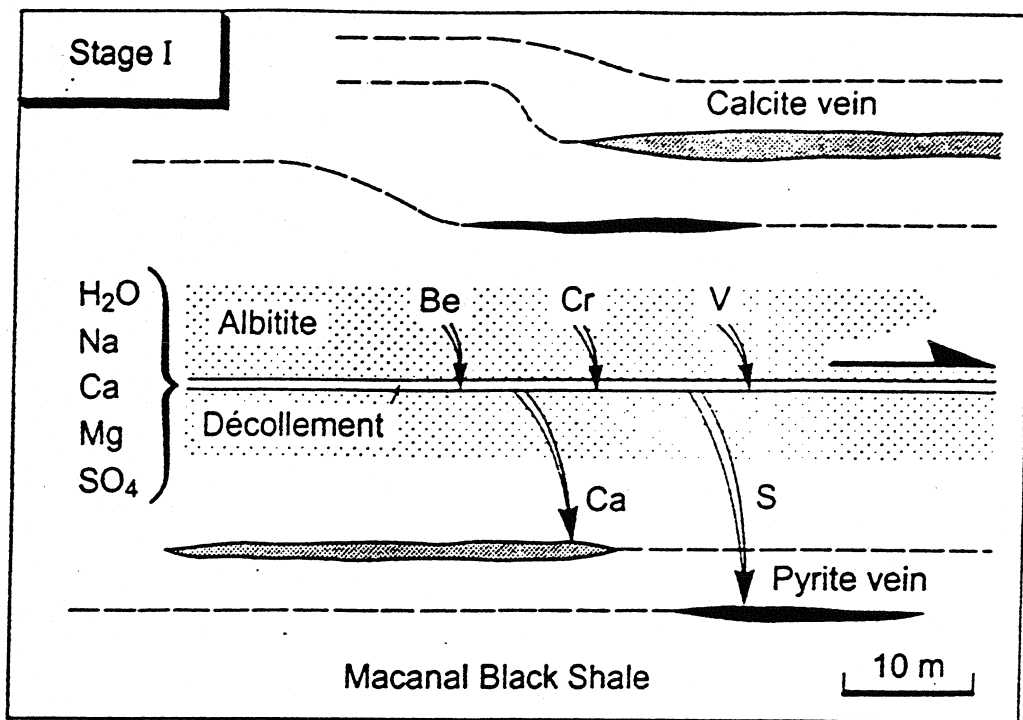


# DIAMONDIFEROUS MANTLE ROOT



BARRON (1995), Minfo





**Fig. 3.** The two-stage model of formation of the Colombian emeralds. Stage I is characterized by decollement plane within the black shale series, hydrothermal fluid infiltration and wall-rock metasomatic alteration. Albitite and fibrous calcite and pyrite veins are illustrated in Fig. 2a, e. Stratiform albitite layers of stage I are well preserved in the eastern mining districts (Chivor). Stage II corresponds to the mineralizing episode. Thrust-related folds synchronous to emerald deposition (Fig. 2b, d) characterize the western emerald districts whereas stage I structures are better preserved in the eastern districts

CHEILLETZ & GIULIANI (1996)

J-12

## K - THE RELATIONSHIP BETWEEN INTRUSION-RELATED Au-(Cu) SULPHIDE VEINS AND Mo BRECCIAS: ROSSLAND

Trygve Höy, Dani Aldrick and Kathryn Dunne, British Columbia Geological Survey

Höy, T., Aldrick, D. and Dunne, K. (1998): The Relationship Between Intrusion-related Au-(Cu) Sulphide Veins and Mo Breccias: Rossland; in *Metallogeny of Volcanic Arcs*, B.C. Geological Survey, Short Course Notes, Open File 1998-8, Section K.

Section K:

Intrusion-Related Au-(Cu) Sulphide Veins Profile

### ABSTRACT

Intrusion-related gold-bearing pyrrhotite/pyrite veins occur as a series of parallel, tabular to cymoid veins of massive iron and copper sulphides. They are generally emplaced around the margins of synvolcanic quartz diorite to granodiorite plutons, commonly in en echelon fracture sets. Examples occur in some of the historical as well as recently discovered gold camps of British Columbia, including Rossland, Scottie Gold, Snip and Johnny Mountain, Chib-Kayrnan and mines and other deposits in the Chibougamau camp in Quebec, and (?) Keating and Ohio-Keating mines in Montana. These are attractive exploration targets because of their high grades, ease of mining, relative ease of exploration and close associations with other important mineral deposit types. Locally, these veins may be associated with either Mo breccia or porphyry deposits.

Veins are typically composed of massive pyrrhotite and/or pyrite and chalcopyrite, variable but generally minor quartz, chlorite, calcite and biotite and minor to accessory disseminations, knots and crystal aggregates of sulphides. Gold and copper are the primary commodities, but important concentrations of Pb, Zn, Ag, Mo and Bi also occur.

Massive pyrrhotite-chalcopyrite veins in the historical Rossland gold camp are examples. They produced more than 84 tonnes of gold and 105 tonnes of silver between 1894 and 1941. Veins are preferentially located along the margins of a synvolcanic intrusion, the Rossland monzonite, within a thick pile of Early Jurassic volcanic rocks. The camp provides an excellent study of this deposit type as Tertiary faulting has tilted the vein system producing surface exposures that extend from deeper to more shallow structural and intrusive levels from east to west. At deeper levels, the veins are associated with K and Si skarn wallrock alteration and disseminated sulphides. At higher levels, these grade to massive pyrrhotite-chalcopyrite veins with only minor gangue and alteration envelopes. In uppermost brittle zones, thin, discontinuous fracture controlled veins and veinlets, with mainly Pb-Zn-Ag and with quartz-carbonate gangue, predominate. This zonation is critical in deposit and camp evaluation as the massive Au-rich veins are concentrated near or within the ductile-brittle transition zone.

Farther west, and at higher stratigraphic levels, veins are overprinted by a Mo breccia complex. This complex is associated with quartz diorite dykes and breccias, and intense hornfelsing and locally skarn alteration. Anomalous concentrations of Co, Bi, As and U occur with the Mo mineralization.

The subvolcanic setting of these deposits is transitional between the deeper level of porphyry copper or skarn systems and the shallower setting of epithermal systems. Mineralization is synvolcanic and syn-intrusive, and commonly forms along the thermal "brittle-ductile transition envelope" surrounding subvolcanic intrusions. Late magma movement generates local shearing and open space fracturing. Circulating hydrothermal fluids then precipitate gold-rich iron sulphides and gangue as vein sets. Late-stage higher level intrusions produced the Mo breccia complex.

Intrusion-related gold-copper veins are emplaced in both oceanic and continental volcanic arc environments. They have close associations with other ore deposits that are typical of arc environments. Consequently, they should provide new exploration targets within established arc-related porphyry, skarn and epithermal camps.

## INTRODUCTION

### **Examples of Intrusion-related gold-(copper) sulphide veins**

#### Definite

Rossland, B.C.  
Snip, B.C.  
Scottie Gold, B.C.  
Johnny Mountain, B.C.

#### Probable

Red Cliff  
Cambria

#### Possible

Baker  
Brucejack Lake  
(West zone)

Copper Rand, Chip Kayrand, Chibougamau, Quebec

### **Resources Intrusion-related gold-(copper) sulphide veins**

Rossland	5.4 m tonnes	15.7 g/t	2.6 m oz Au
Snip	1.3 m tonnes	27.9 g/t	1.1 m oz Au
Scottie Gold	0.3 m tonnes	17.6 g/t	0.16 m oz Au
Johnny Mountain	0.2 m tonnes	18.1 g/t	0.11 m oz Au



## VEIN CHARACTERISTICS

### Vein forms

#### Intrusion-related gold-(copper) sulphide veins

en echelon veins  
extension veins  
tension gashes  
ladder veins

shear veins  
cymoid veins  
cymoid loops  
sigmoidal veins

### Principal vein minerals

#### Intrusion-related gold-(copper) sulphide veins

##### Massive Sulphide Veins

pyrrhotite  
pyrite  
chalcopyrite  
  
sphalerite  
galena  
arsenopyrite  
  
molybdenite

##### (Bull Quartz Veins)

quartz  
  
pyrite  
pyrrhotite  
  
chalcopyrite  
galena  
sphalerite  
calcite

### Gangue and alteration mineralogy

#### Gangue

quartz	<i>sericite</i>
calcite	<i>rhodocrosite</i>
ankerite	<i>k-feldspar</i>
chlorite	<i>biotite</i>

#### Alteration

chlorite	<i>rhodocrosite</i>
sericite	<i>biotite</i>
pyrite	<i>epidote</i>
carbonate	<i>K-feldspar</i>
	<i>ankerite</i>

## SETTING

### Host rocks

#### Intrusion-related gold-(copper) sulphide veins

Rosslund	Early Jurassic	mafic tuffs, intrusions
Johnny Mountain	Early Jurassic	andesitic tuffs, volcanic conglomerates
Scottie Gold	Early Jurassic	andesitic tuffs
Snip	Early Triassic	greywacke

### Associated Deposit Types

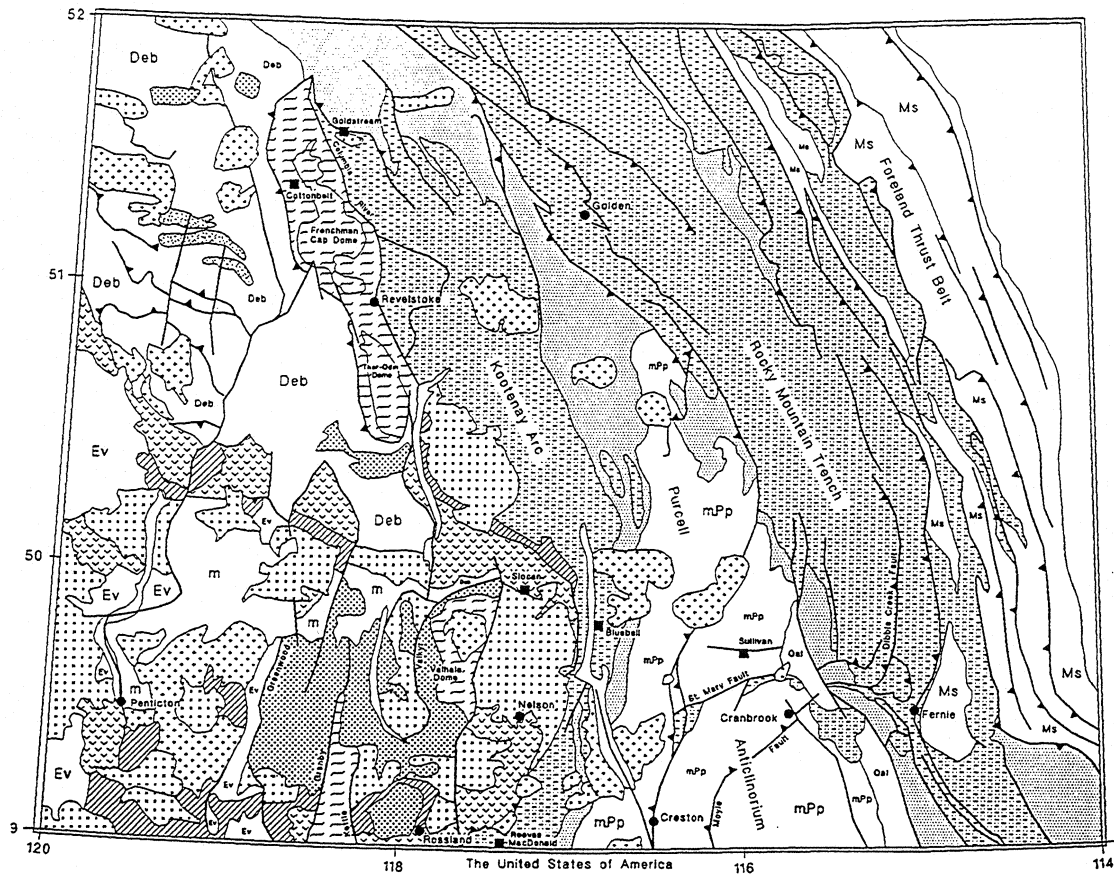
fumarolic hot springs	H03	
epithermal veins/breccias	H04, H05	Au, Ag, Cu
exhalative deposits	G06	Cu,Pb,Zn,Ag,Au
polymetallic veins	I05	Ag,Pb,Zn,Au
transitional deposits	L01	Cu,Au,Ag
porphyries	L03, L04	Cu,Au,Mo
skarn	K01, K04	Cu,Au

## EXPLORATION

### Exploration Guides

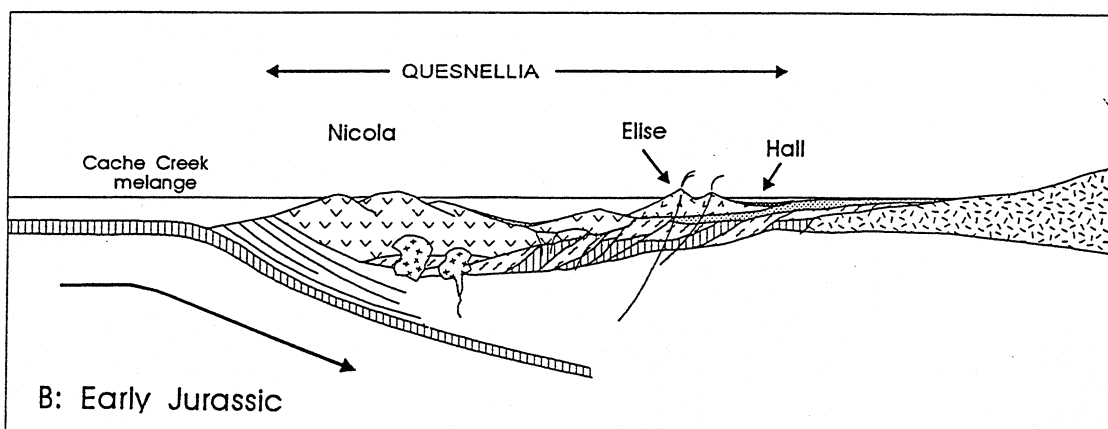
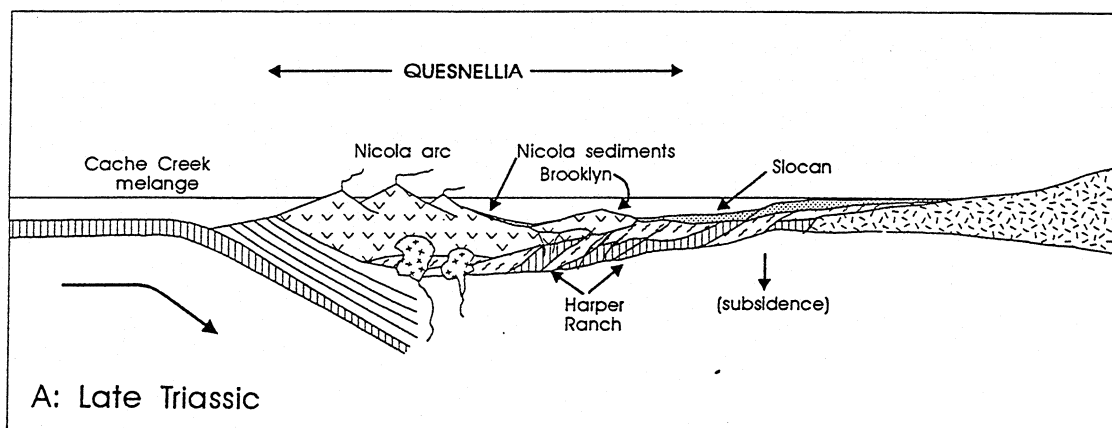
Tectonic setting	volcanic arcs
Geological setting	subvolcanic peripheral to intrusions
Deposit geometry	en echelon vein sets
Associated deposits	deposit suite of volcanic arcs
Geophysics	magnetic signatures moderate to strong EM response
Geochemistry	Au, Ag, Cu, <i>Pb</i> , <i>Zn</i> , <i>Mo</i> , <i>Bi</i>

# THE ROSSLAND GOLD CAMP, QUESNELIA

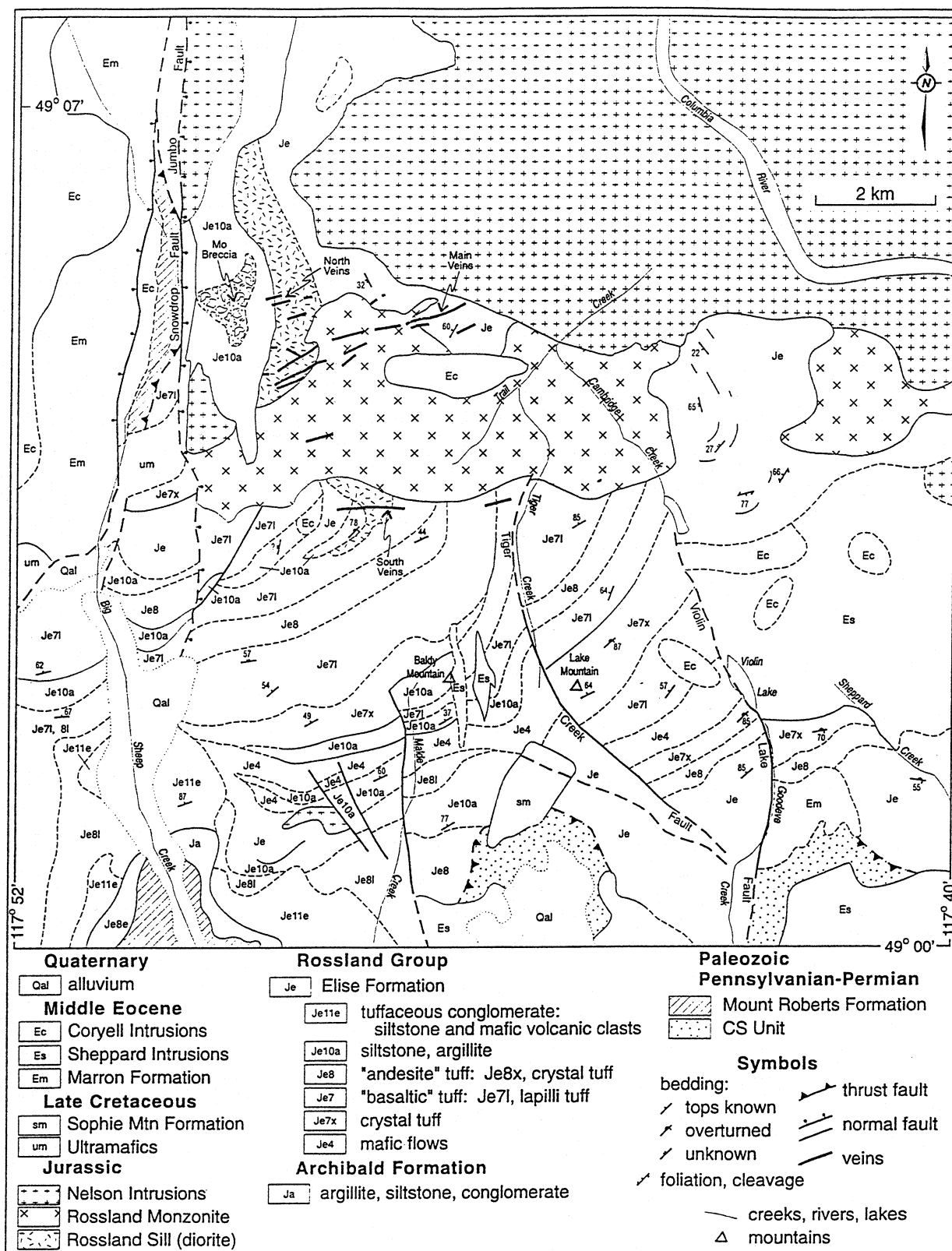


	Slide Mtn	Quesnellia	Kootenay	North America	Intrusive
Cenozoic				Ev volcanic	Eocene (Paleocene)
Mesozoic		Rosland Group Nicola Group (Slocan, Kaslo)		Ms sedimentary	Middle Cretaceous Middle Jurassic
Paleozoic	Anarchist, Harper Ranch Mt. Roberts (Kaslo)		Deb Eagle Bay Arc Lardeau meta-sedimentary	sedimentary	
Proterozoic				upper Windermere middle Purcell mPp	

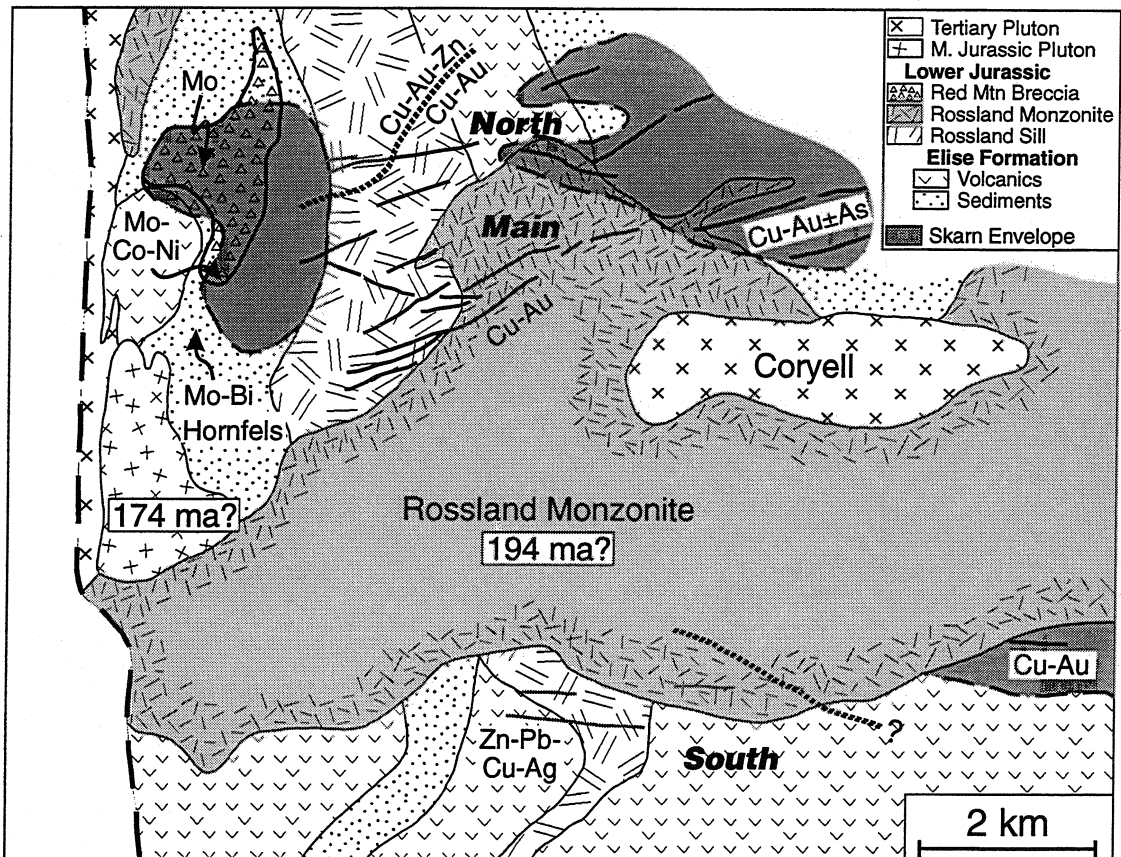
Tectonic synthesis map, southern British Columbia, showing location of Rossland Group along the eastern margin of Quesnellia; (after Wheeler and McFeely, 1991)



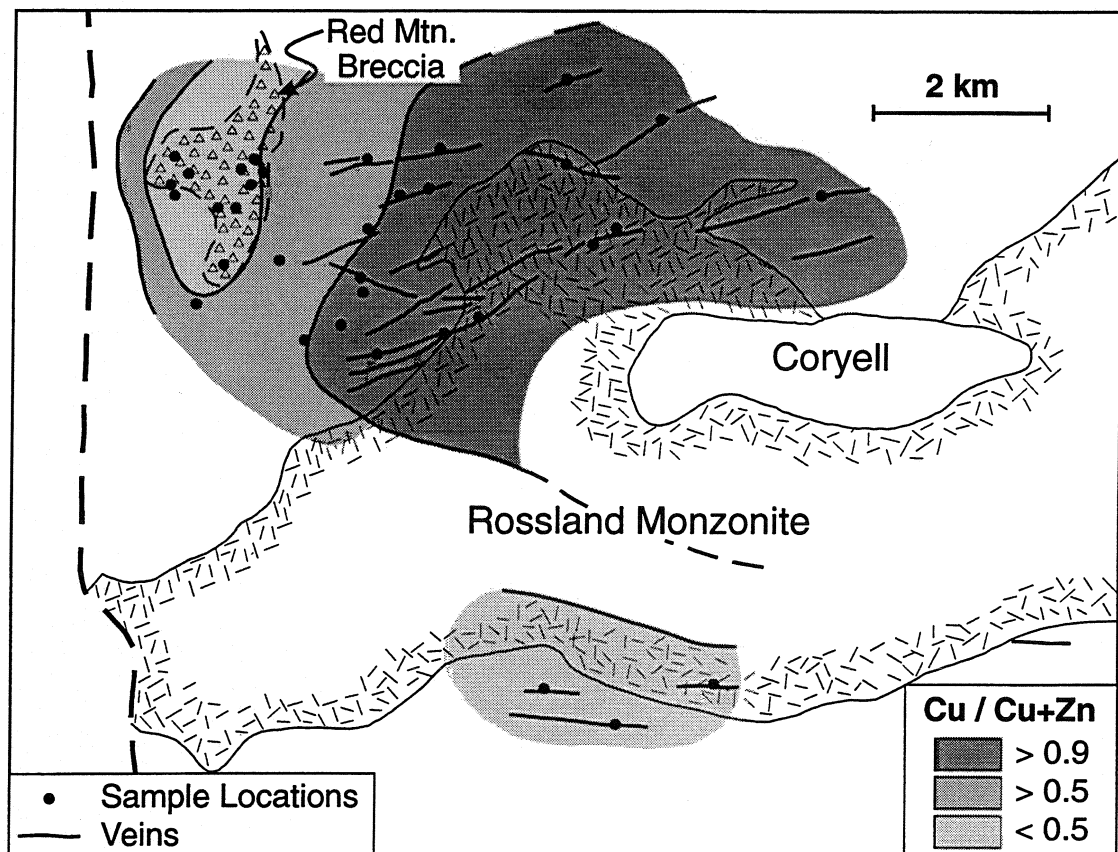
Evolution of the Rossland-Nelson area in southern British Columbia in (a) Late Triassic and (b) Early Jurassic time (after Höy and Andrew, 1997)



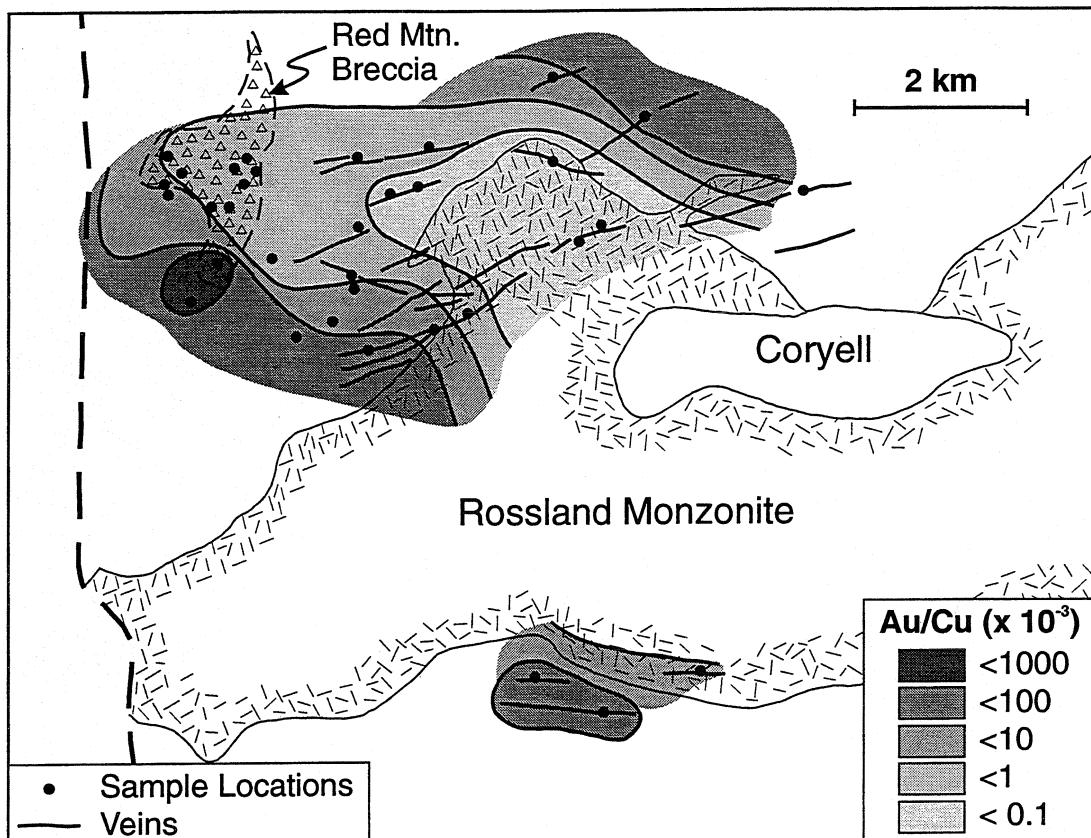
Geological map of the Rossland area, southeastern British Columbia (after Höy and Andrew, 1997)



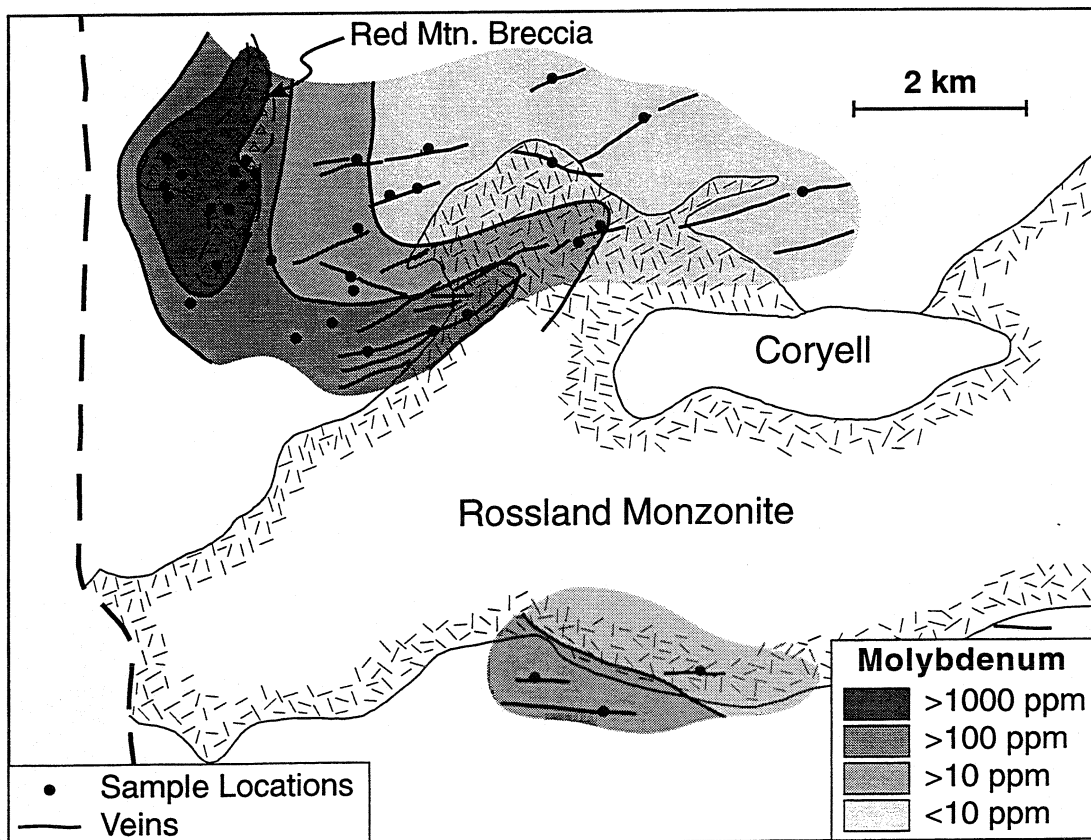
Geological map of the Rossland area, showing North, Main and South belt veins (after Höy and Andrew, 1997; Fyles, 1984; and Drysdale, 1915).



Copper-zinc zoning in the veins of the Rossland camp (from assays of hand samples), (Höy and Andrew, 1998).

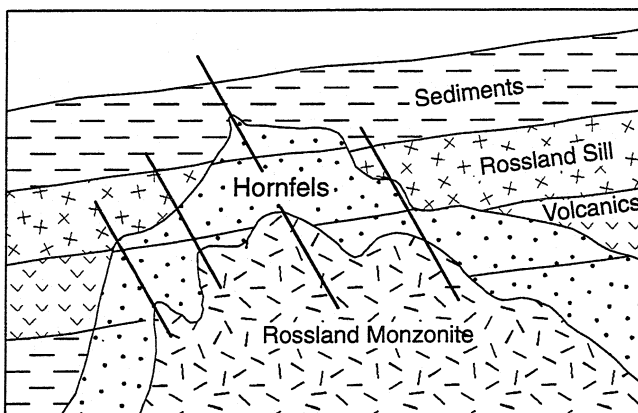


Gold-copper zoning in the veins of the Rossland camp (from assays of hand samples), (Höy and Andrew, 1998).



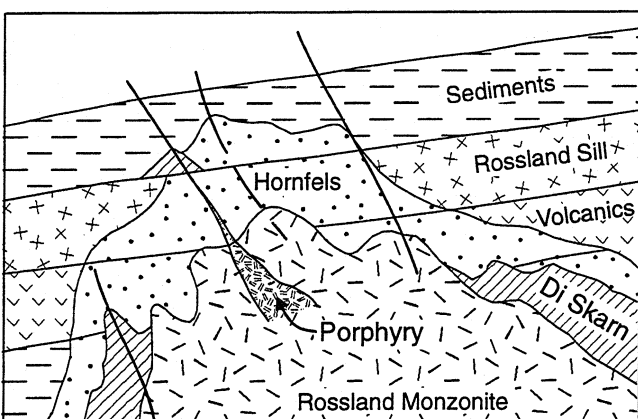
Molybdenite zoning in the veins (and skarns) of the Rossland camp (from assays of hand samples), (Höy and Andrew, 1998).



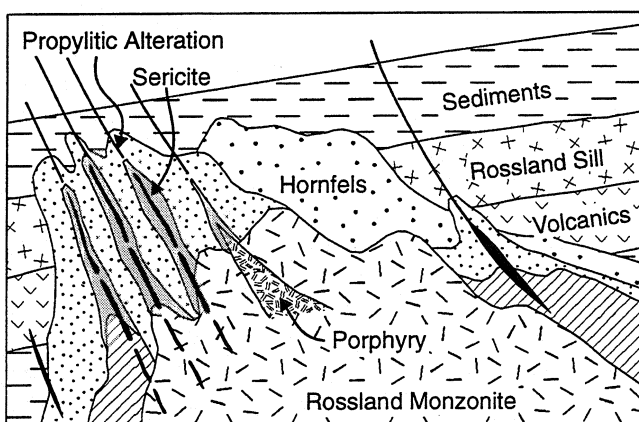


Schematic model for the evolution of the "intrusion related gold-(copper) sulphide veins" and related mineralization in the Rossland camp, southern British Columbia (Hoy and Andrew, 1998).

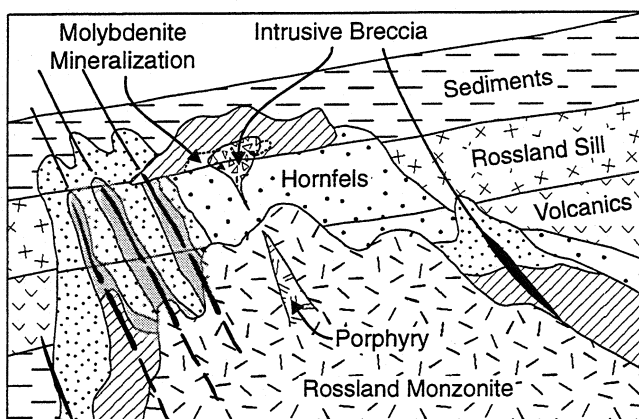
1. Intrusion of Rossland monzonite; hornfelsing.



2. Prograde skarn alteration; intrusion of "porphyrite dykes".

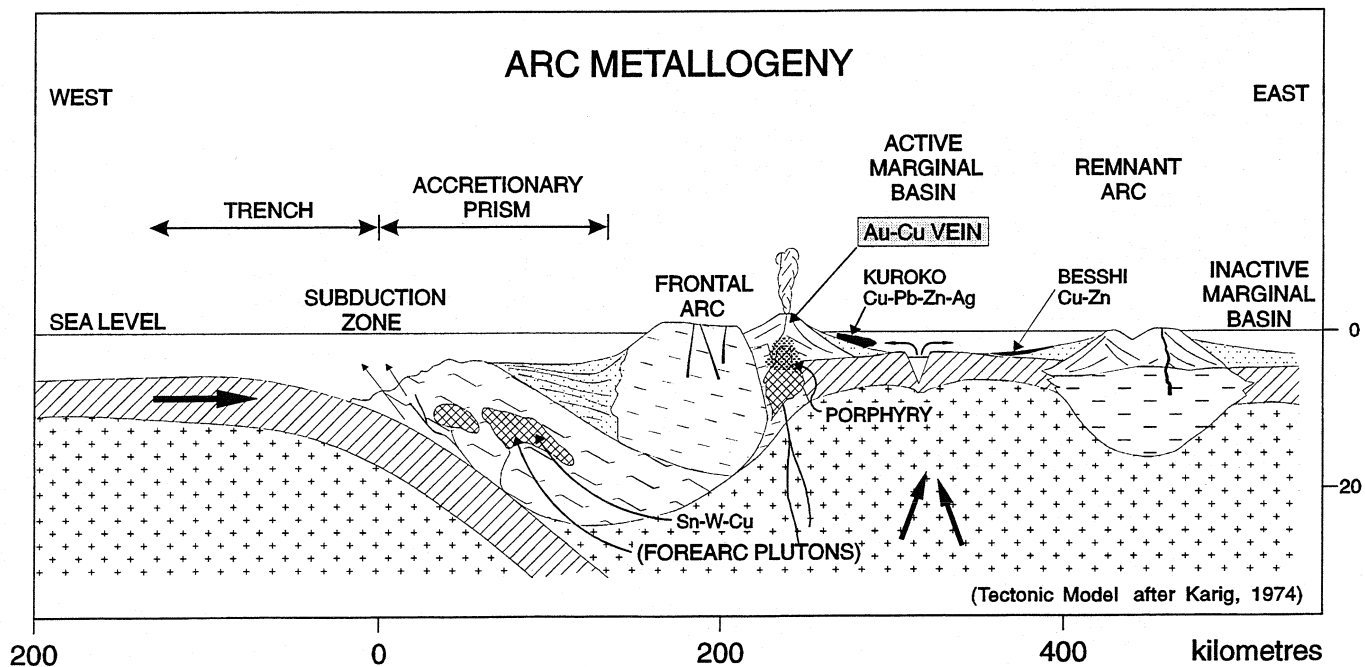
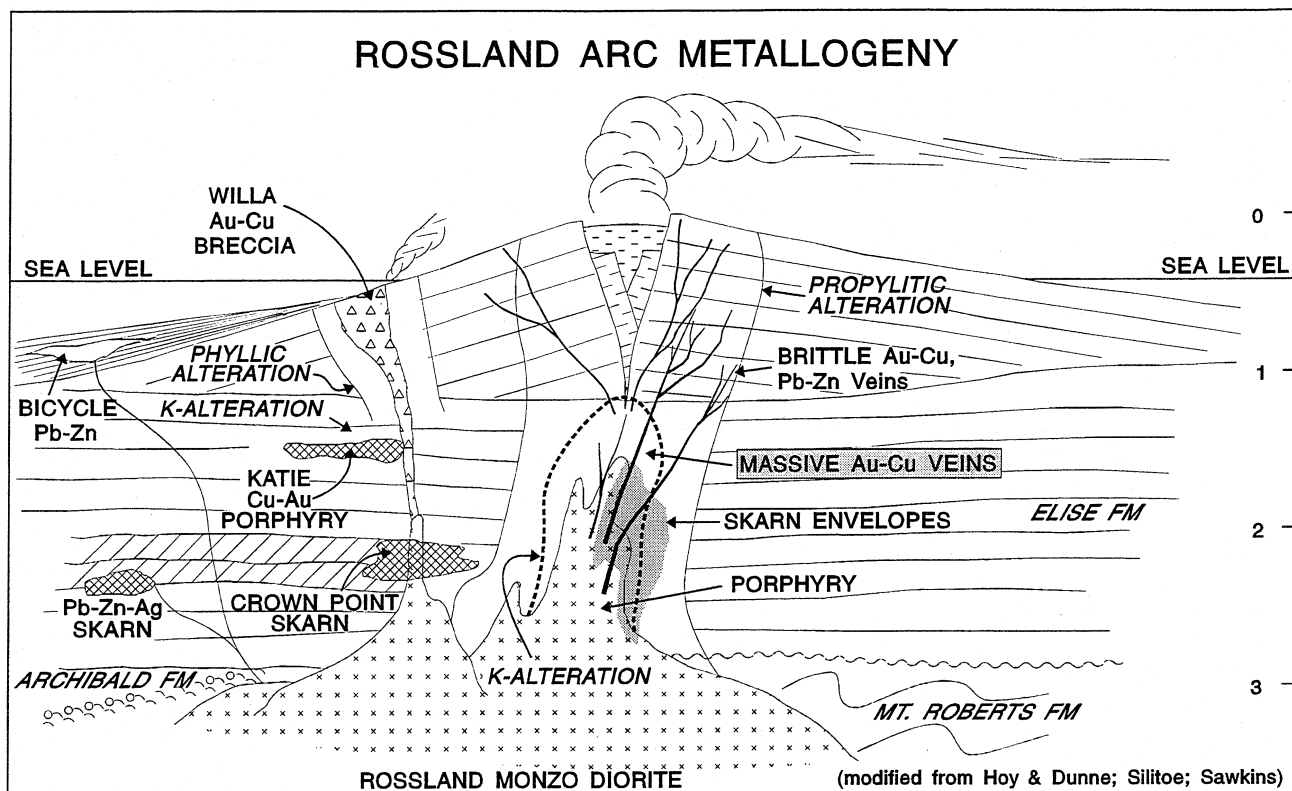


3. Gold-copper veins; peripheral lead-zinc silver veins; retrograde alteration.

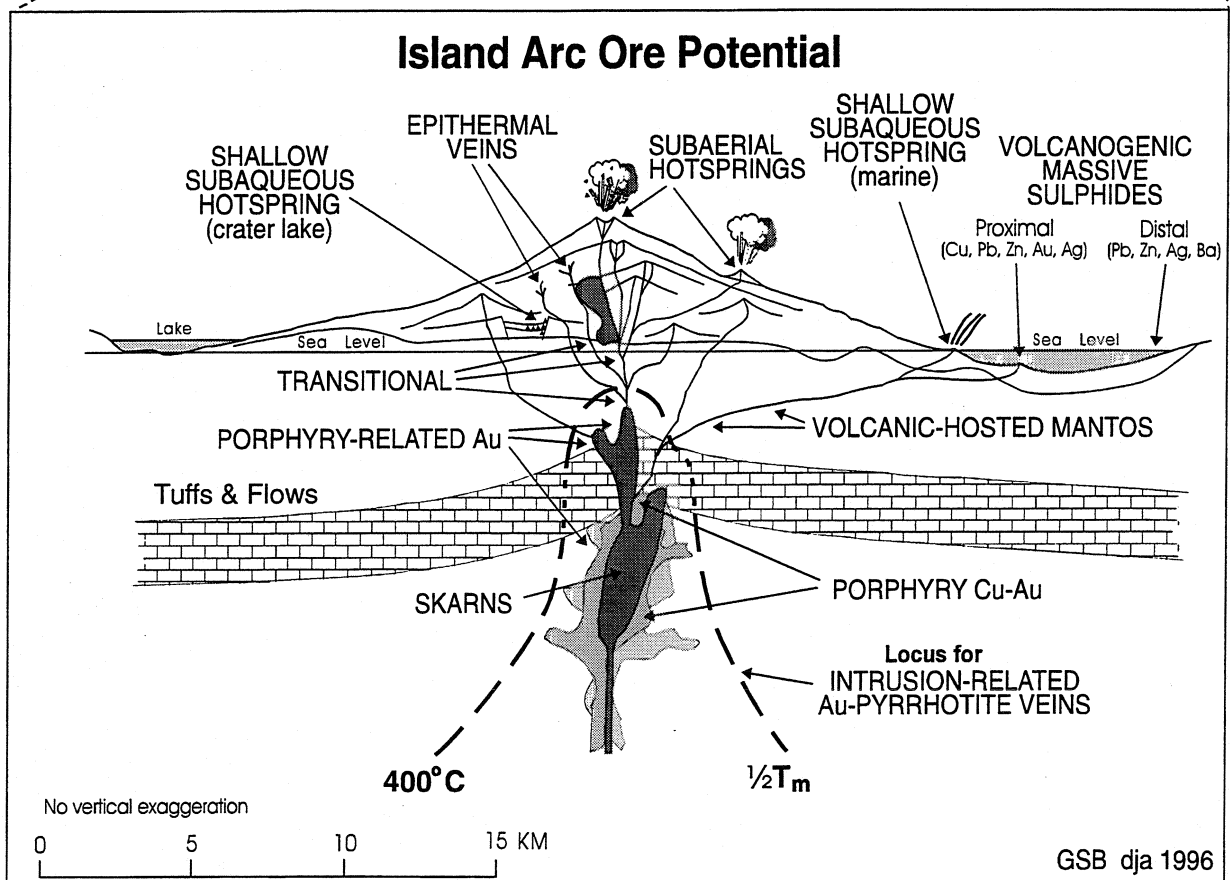
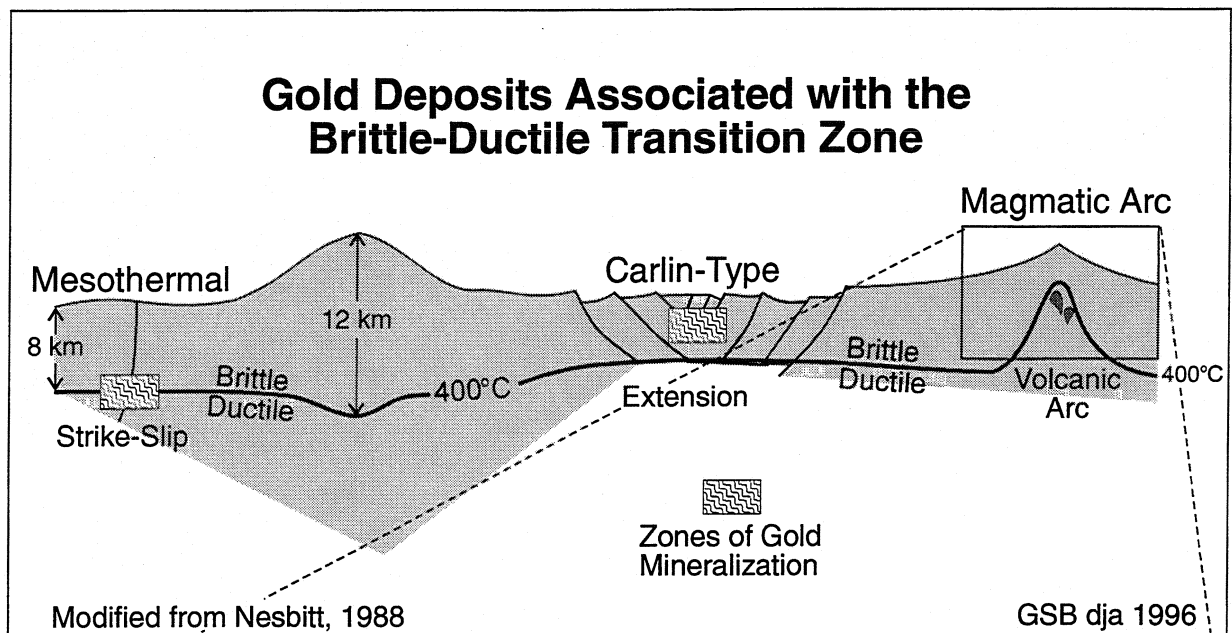


4. Intrusive breccia; skarn alteration, molybdenite mineralization.

## TECTONIC SETTING



## TECTONIC SETTING





## L - INDUSTRIAL MINERALS IN ISLAND ARCS

Z.D. Hora, British Columbia Geological Survey

Hora, Z.D. (1998): Industrial Minerals in Island Arcs; in Metallogeny of Volcanic Arcs, B.C. Geological Survey, Short Course Notes, Open File 1998-8, Section L.

### ABSTRACT

Island arcs are host to a variety of important industrial minerals deposit types. These deposits can be attractive exploration targets on their own, but many are found in association with metallic ores. Globally, island arcs have or had been important producers of halloysite, kaolin, bentonite, calcium carbonate, zeolites, manganese oxides, anhydrite and gypsum, barite, pumice, perlite, pyrophyllite, diatomite and are favourable geological environment for deposits of wollastonite and garnet.

Geothermal fields with thermal waters and ore fluids related to epithermal, porphyry and volcanogenic massive sulphides deposits circulating through favourable geological environments can produce deposits of industrial clays. Hydrothermal alteration in island arc settings may be the product of both low pH, high sulphate fluids or rather neutral pH reservoir fluids. Individual deposits often develop typical temperature-controlled zonation as a result of the stability fields for individual minerals. At low temperatures of some 50-80°C halloysite is the main product, at moderate temperatures kaolinite and dickite form, and when the temperature rises to 300°C range, pyrophyllite is the main alteration product. Presence or absence of alunite may be primarily the result of hydrothermal fluid composition. Deposits of hydrothermal halloysite are exploited in Northland, New Zealand at a rate of some 25 000 tonnes per year. Small producers are known in Philippines, Indonesia, Vietnam and Japan. Hydrothermal pyrophyllite is an important product in South Korea and Japan. The mines are located mostly in southwestern Honshu, Japan and produce some million tonnes yearly. In South Korea, the deposits are located along the southern coast of the peninsula and produce approximately 650 000 tonnes annually. In British Columbia, alteration zones with pyrophyllite-alunite are known from Vancouver Island in a belt that extends from Kyuquot Sound to Pemberton Hills area on Holberg Inlet. Regional metamorphism may transform zones of hydrothermal alteration into deposits of mica (sericite) and/or kyanite. The large sericite envelope of the Homestake VMS deposit near Kamloops is an example of a metamorphosed alteration zone in British Columbia. Some geologists interpret the kyanite deposits of Virginia, U.S.A. as a metamorphosed hydrothermal alteration zone. Thermal recrystallization of alteration zones under low pressure conditions will result in andalusite hornfels, sometimes with corundum. The Empress zone of the Taseko deposit is an example of such mineral association.

Volcanogenic massive sulphide (VMS) deposits contain barite and anhydrite as common constituents. Barite is frequently a minor component of Kuroko orebodies, like Myra Falls, Britannia mine, Adams Plateau occurrences or Tulsequal Chief in British Columbia. In some deposits, however, barite is a major component of the ore, such as the Homestake deposit near Kamloops, or the Buchans mining camp of Newfoundland. The Buchans camp contains an estimate of 350 000 tonnes of barite in tailings and since 1971 has produced 10-15 000 tonnes annually for oil and gas exploration on the Canada east coast.

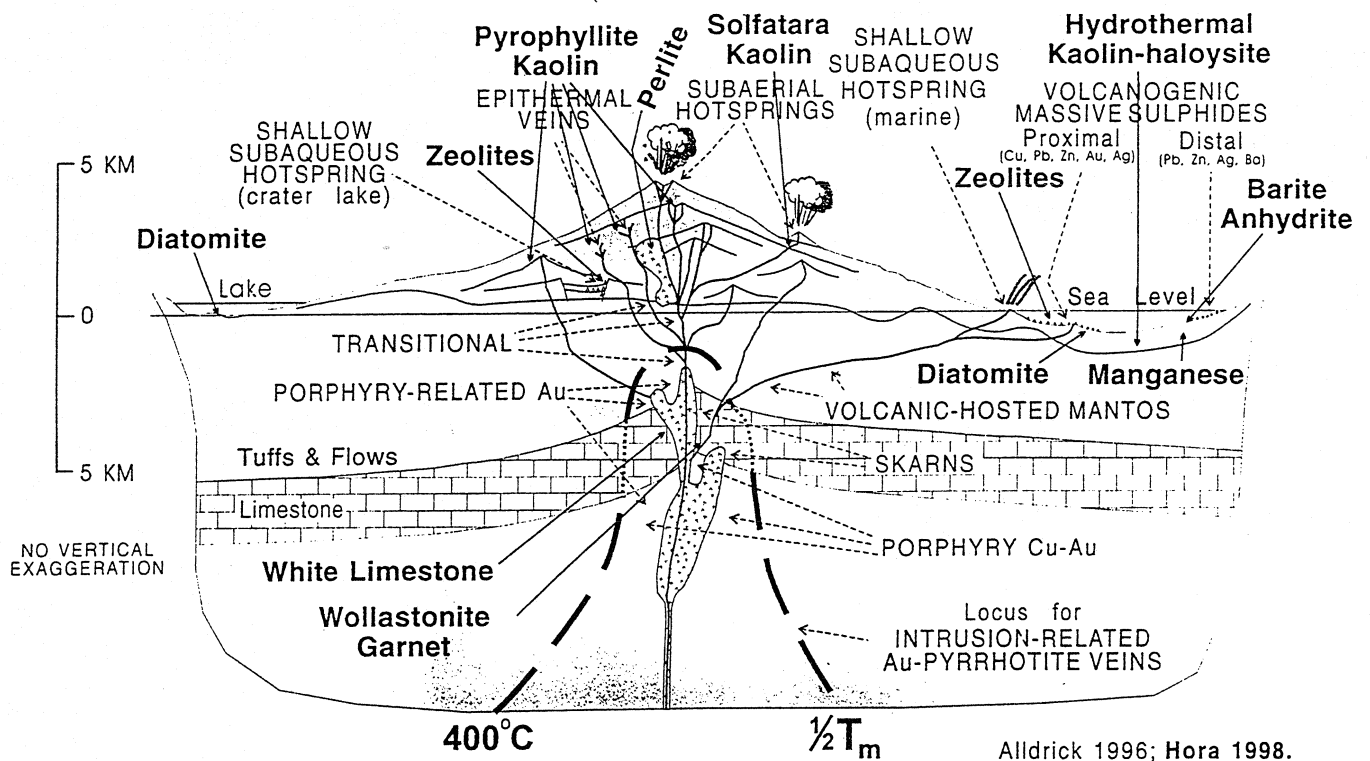
There is also the possibility of finding separate lenses and beds of barite towards the top of Kuroko-type VMS and deposits distal to the metal rich orebodies.

Anhydrite and gypsum have many similarities to barite in their distribution in VMS deposits. They have been described from many deposits in Japan and in B.C. are known from the Britannia mine and the Tulsequah Chief. The recent studies of black smokers indicate that anhydrite can occur with base metals but is more likely than barite to produce also distal accumulations barren of base metals. Two anhydrite/gypsum deposits in B.C. may be interpreted to be of this type. The Falkland deposit, located northwest of Vernon, produced a little over 1 million tonnes of gypsum between 1926 and 1956. Since 1974, this deposit has been supplying an anhydrite-gypsum mixture for the cement plant in Kamloops. O'Connor River gypsum deposit in northwestern B.C. has a 10 million tonne gypsum resource.

Manganese oxide deposits in waterlain pyroclastic deposits of basaltic, andesite and dacitic deposition are known from Cuba, Hispaniola and Puerto Rico. Particularly the deposits in the Cobre Formation of eastern Cuba were mined extensively in 1940's and 1950's. The length of the ore lenses may be up to 2 kilometres and the thickness up to 5 metres. The orebodies are frequently underlain by massive, several metres thick lenticular bodies of siliceous, jasper-like rocks up to several metres thick. The manganese deposits are considered coeval with vein and stockwork copper deposits associated with sub-volcanic intrusions abundant in the lower part of the Cobre Formation. In B.C., the Big Bull mine on Taku River has lenses of massive Mn minerals braunite and piemontite within andesite tuff which are stratigraphically above the VMS orebody and up to 31 metres thick.

Deposits of zeolites in island arcs are very common and widespread. Zeolites are a product of devitrification of volcanic glass under a variety of conditions. Burial diagenesis and low temperature hydrothermal alteration of pumice and volcanic ash deposits in sea water environment have produced massive deposits of zeolites, such as those known from Japan, Italy or Cuba. Mordenite and clinoptilolite are the most common zeolites commercially produced, with smaller quantities of chabasite, erionite and phillipsite. Japan, probably, has been the most successful in developing a variety of industrial applications for natural zeolites with annual consumption of over 100 000 tonnes per year.

# ISLAND ARC ORE POTENTIAL and INDUSTRIAL MINERALS



Hydrothermal kaolin

Hydrothermal halloysite

Calcium carbonate

Anhydrite/gypsum

Manganese

Zeolites

Pumice

Pyrophyllite

Solfatara kaolin

Perlite

Marine diatomite

Lacustrine diatomite

Barite

Wollastonite

Garnet

## EPITHERMAL MODEL

Halloysite

Kaolin

Pyrophyllite

Zeolites

## VMS MODEL

Anhydrite

Kaolin

Manganese

Barite

## EPITHERMAL MODEL

Halloysite

Kaolin

Pyrophyllite

Zeolites

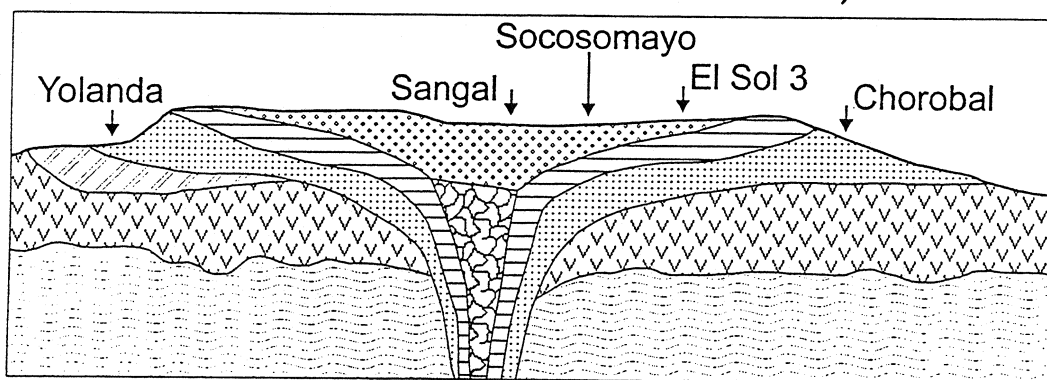


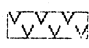
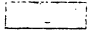
# HYPOGENE KAOLIN DEPOSITS, PERU


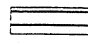
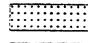
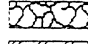
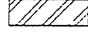
Minerals	Diatreme fill near vent facies		Hot spring facies of maar lake
alunite			
pyrophyllite			
dickite			
kaolinite			
halloysite			
smectite			
quartz			
silica			
compounds			
barite			
TEMPERATURE	< 400°C	< 300°C	< 200°C
pH	appx 3.5	appx 3.5-4.5	> 5
DEPOSIT	La Noemia	Sangal	Socosmayo El Sol 3

after Dill et al., 1997

# HYPOGENE KAOLIN DEPOSITS, PERU

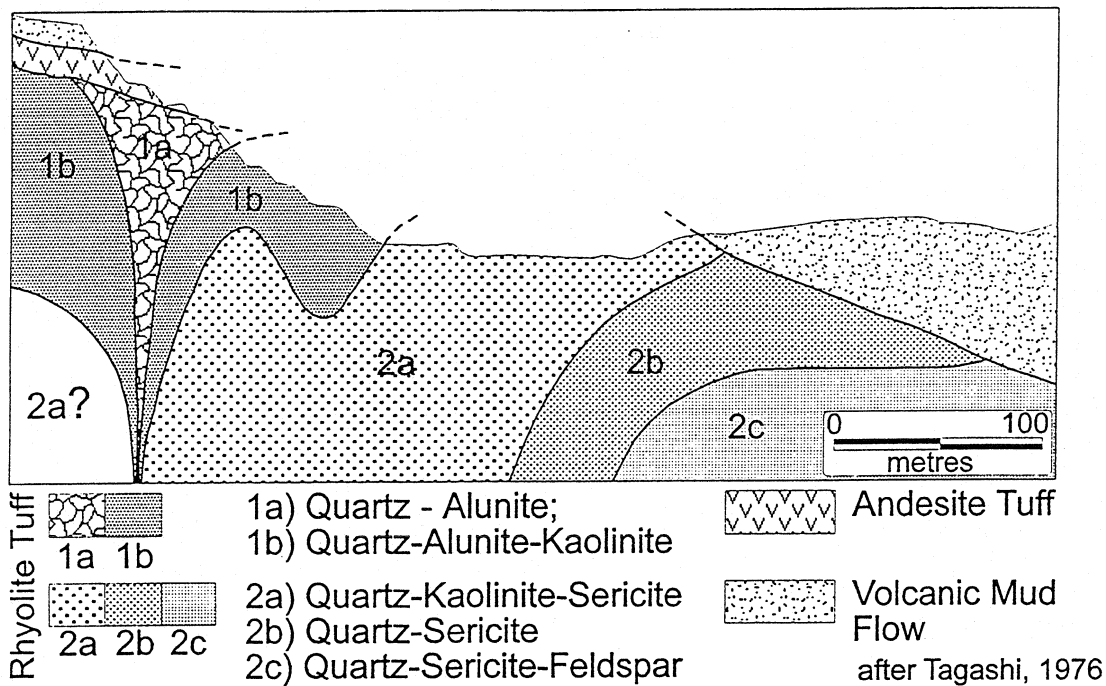


 Volcanic /  
Volcaniclastic rocks  
 Bedrock (undiff.)

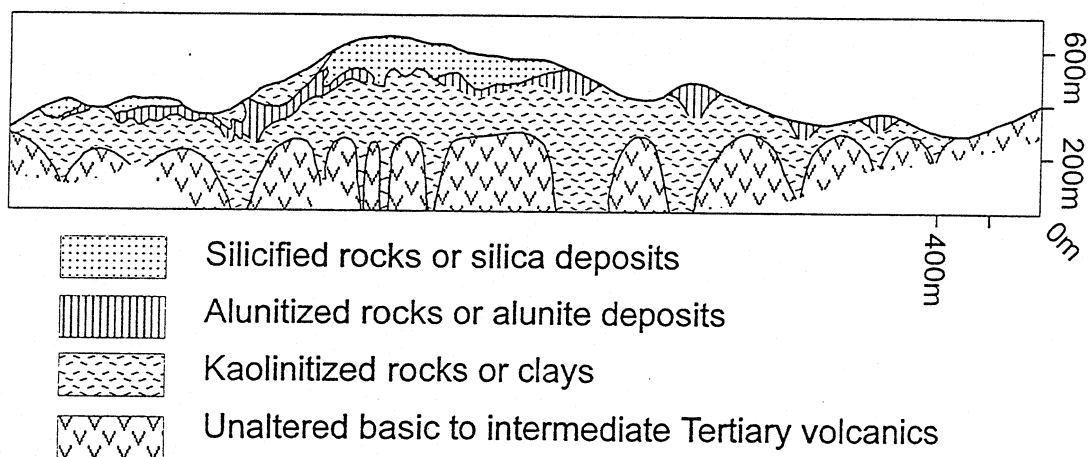
 Halloysite + opaline silica  
 Alunite  
 Dickite + Kaolinite  
 Quartz + Alunite  
 Smectite

after Dill et al., 1997

# ITAYA KAOLIN DEPOSIT, JAPAN

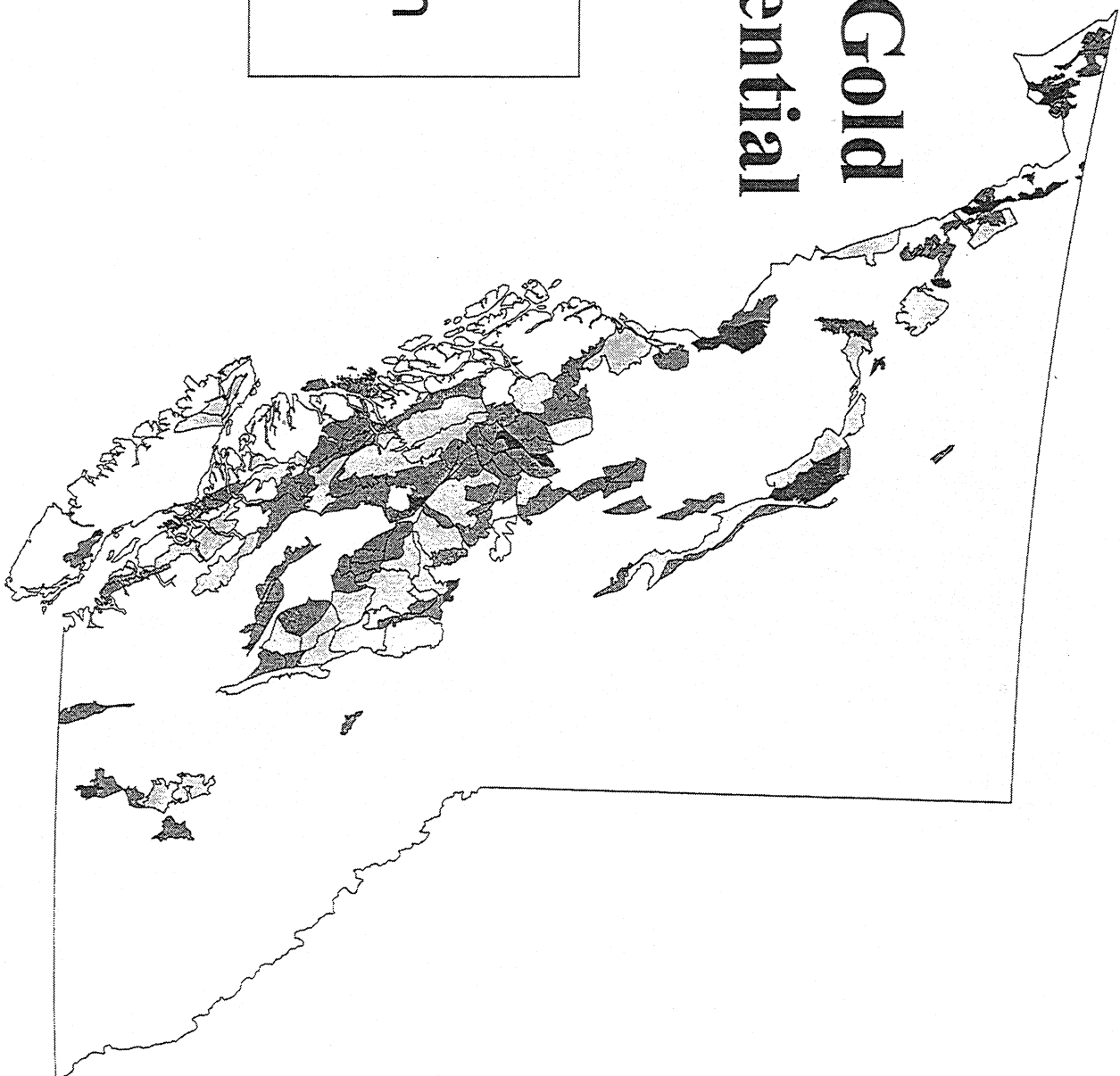
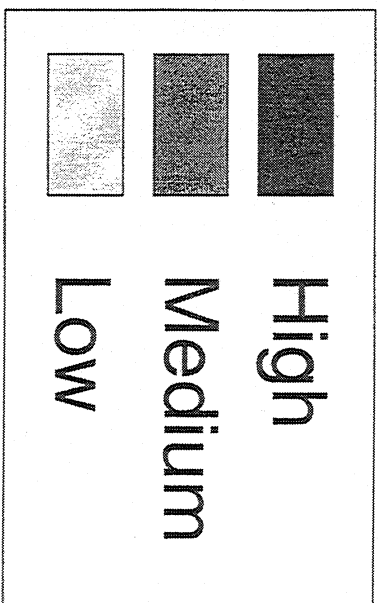


# UGUSU, JAPAN: DEPOSITS OF KAOLIN, ALUNITE AND SILICA



after Iwao, 1968

# Epithermal Gold Mineral Potential in B.C.

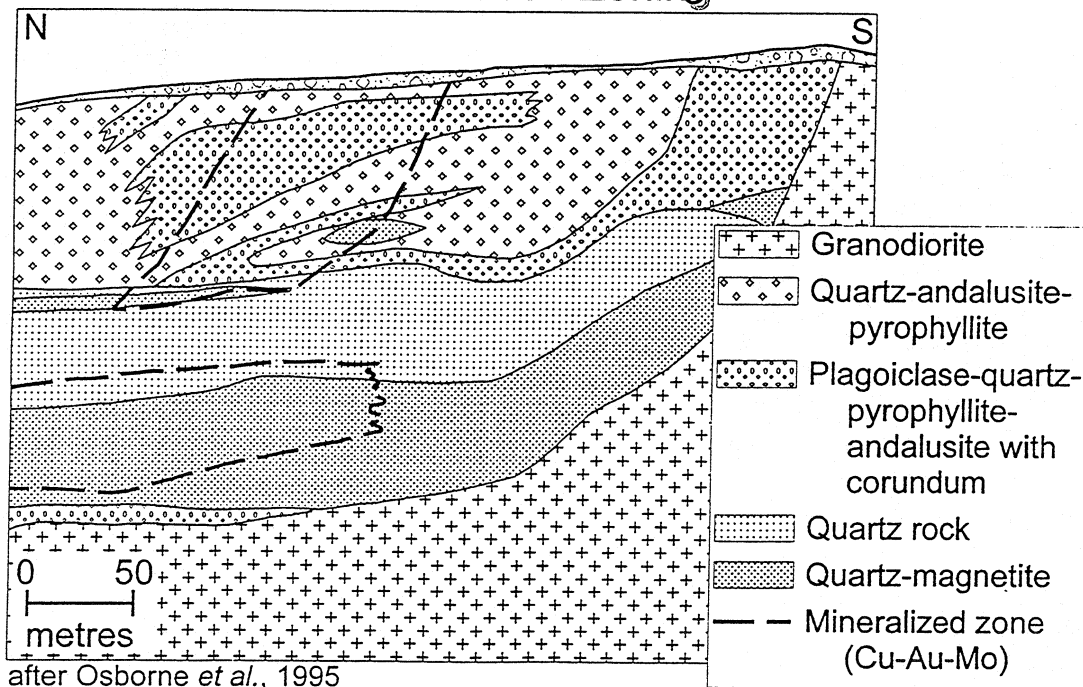


# PORPHYRY MODEL

Pyrophyllite

Kaolin

## EMPRESS AREA, TASEKO DEPOSIT, B.C. Alteration Zoning



# CLAY DEPOSIT

High temperature -  
Low pressure

Regional  
metamorphism

Andalusite

Mica

Corundum

Kyanite

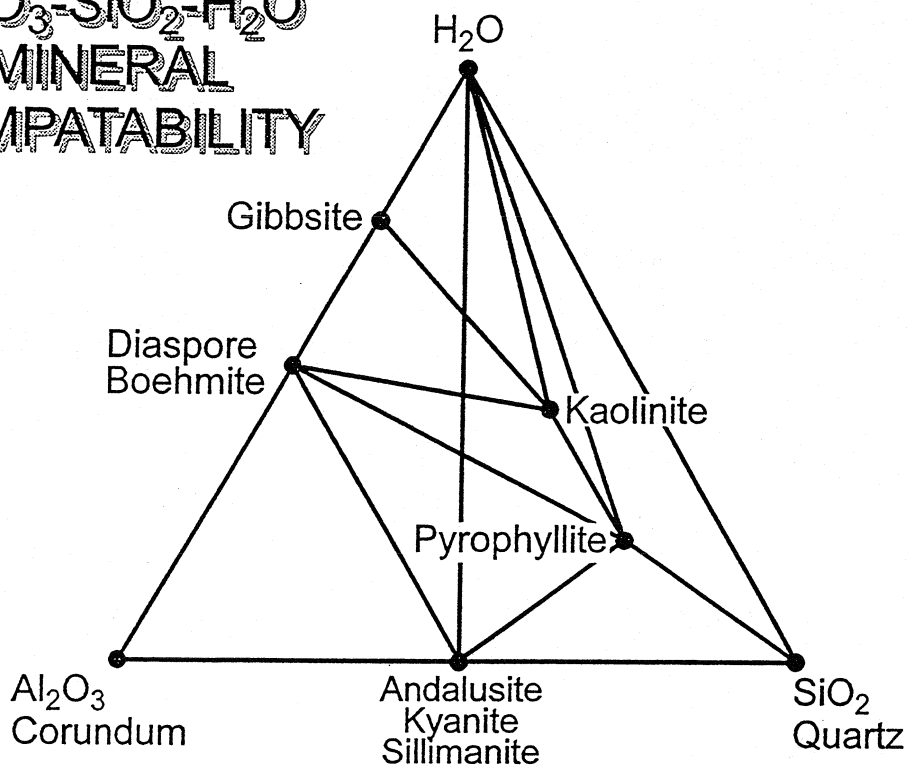
Emery

Muscovite + Quartz =  
Andalusite + Feldspar + H<sub>2</sub>O

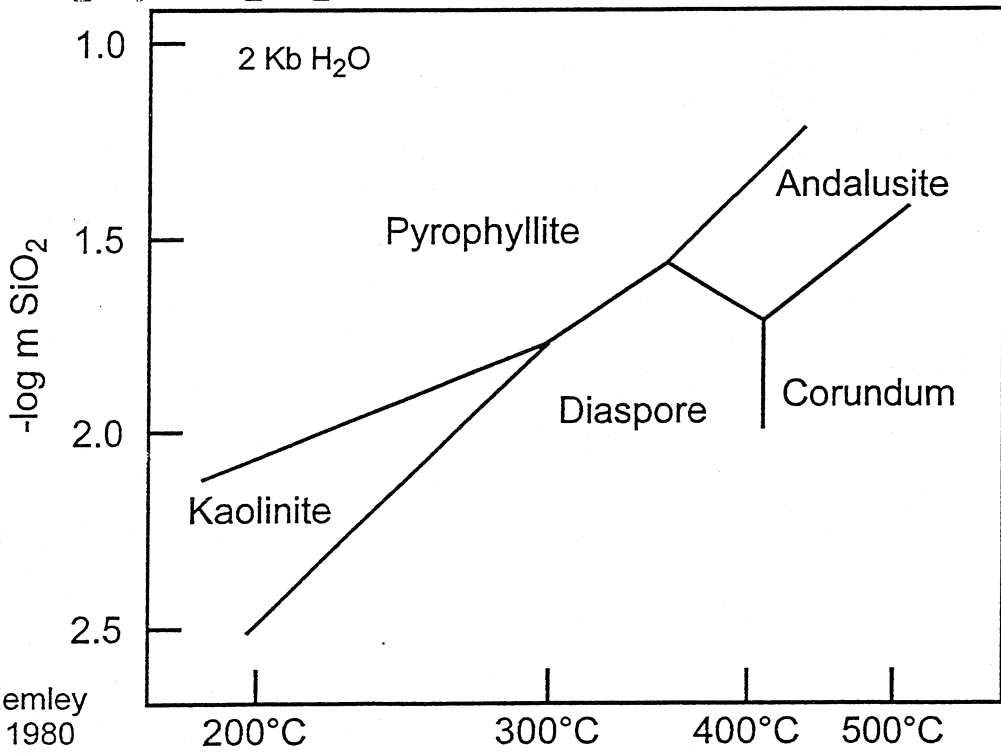
Muscovite =  
Corundum + Feldspar + H<sub>2</sub>O

# $\text{Al}_2\text{O}_3$ - $\text{SiO}_2$ - $\text{H}_2\text{O}$ MINERAL COMPATABILITY

after Hemley et al., 1980



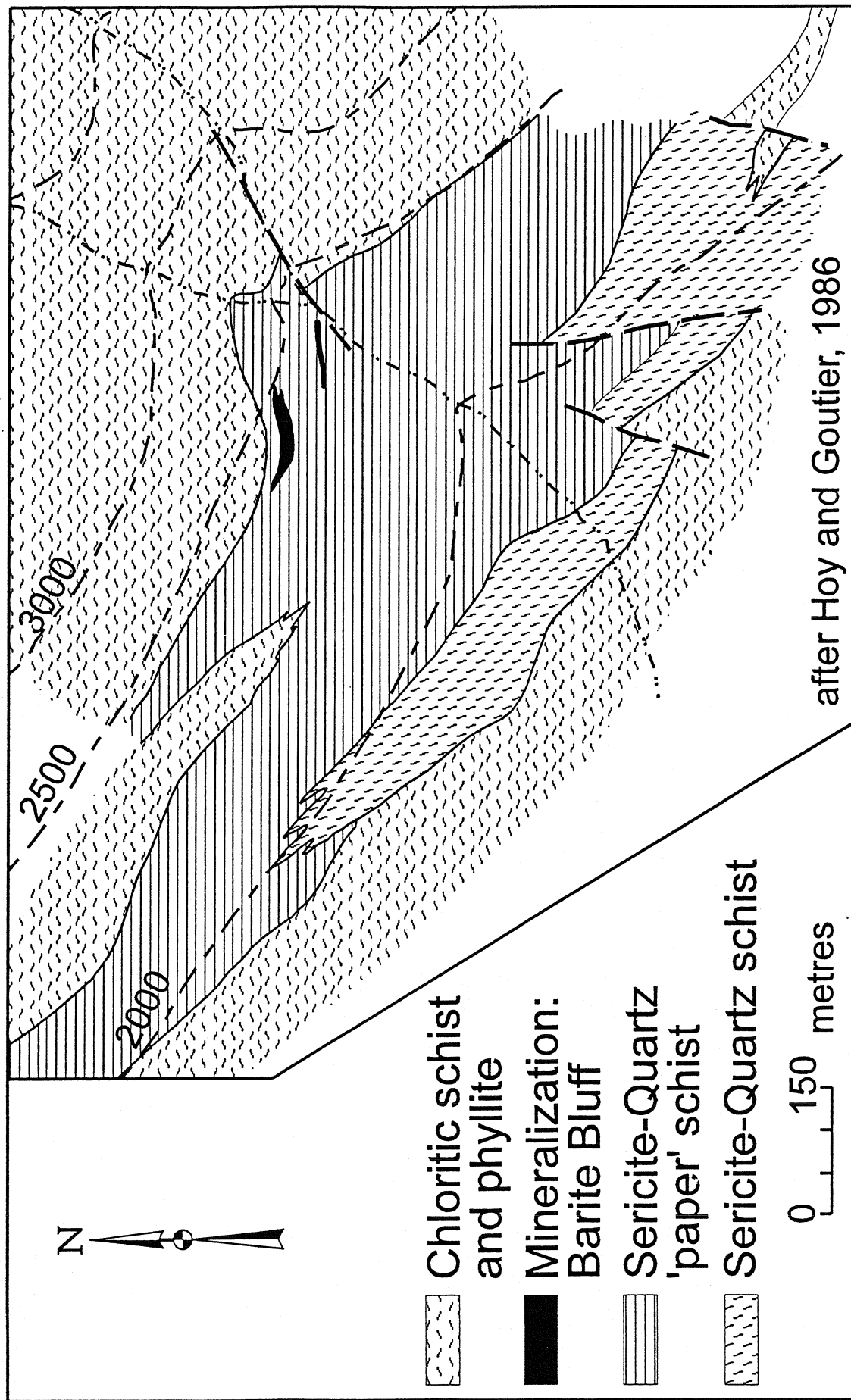
## $\text{Al}_2\text{O}_3$ - $\text{SiO}_2$ - $\text{H}_2\text{O}$ STABILITY RELATIONSHIPS



after Hemley  
et al., 1980

210

# HOMESTAKE PROPERTY, B.C.



# VMS MODEL

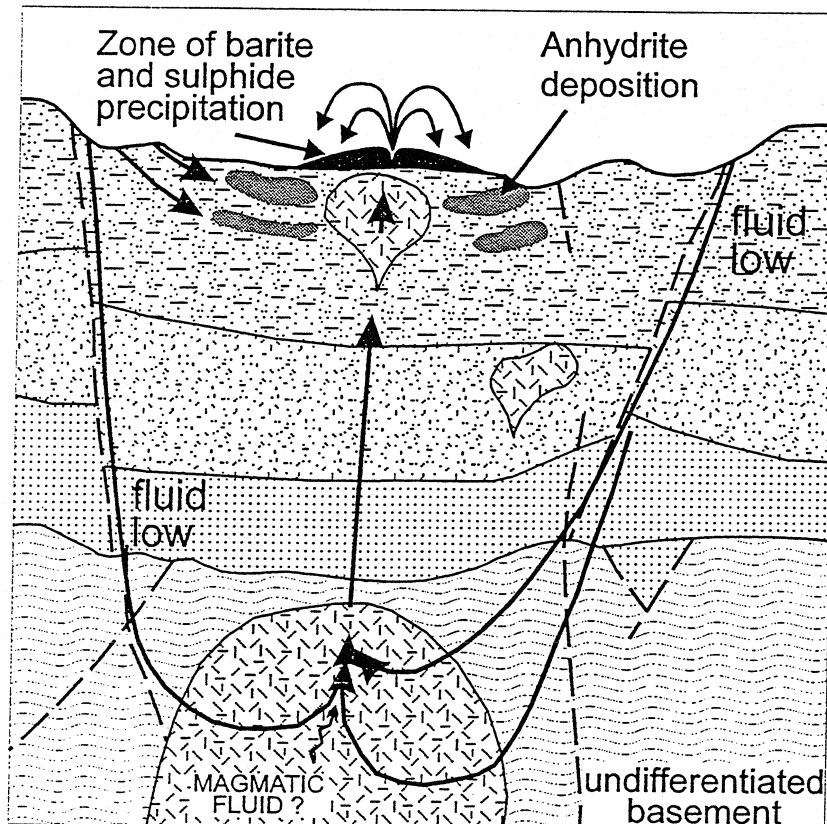
Anhydrite

Kaolin

Manganese

Barite

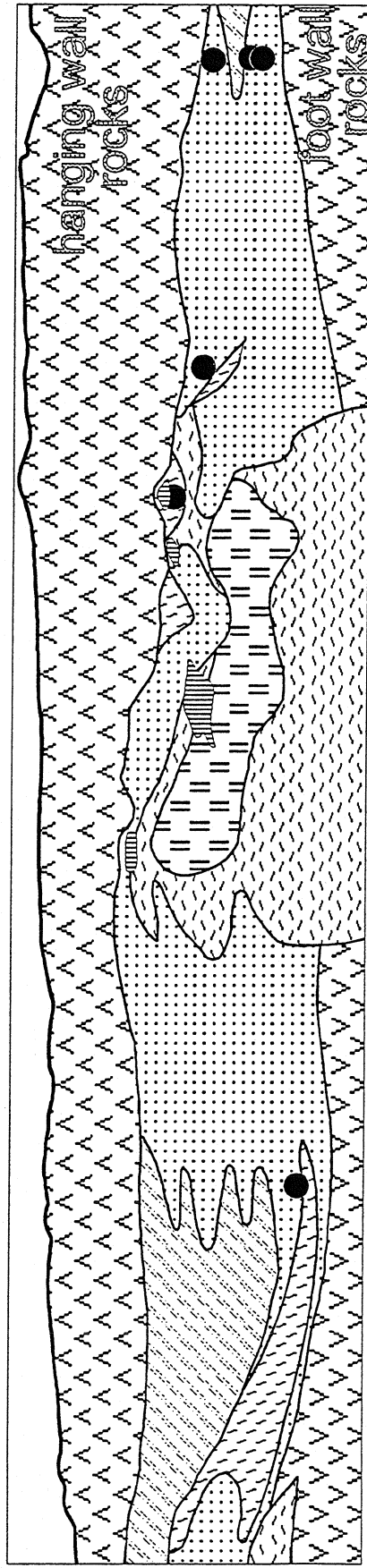
## CONCEPTUAL MODEL FOR KUROKO GENESIS



after Farrell  
et al., 1983



# KOSAKA MINE, JAPAN



0 500  
metres

Massive ore Gypsum

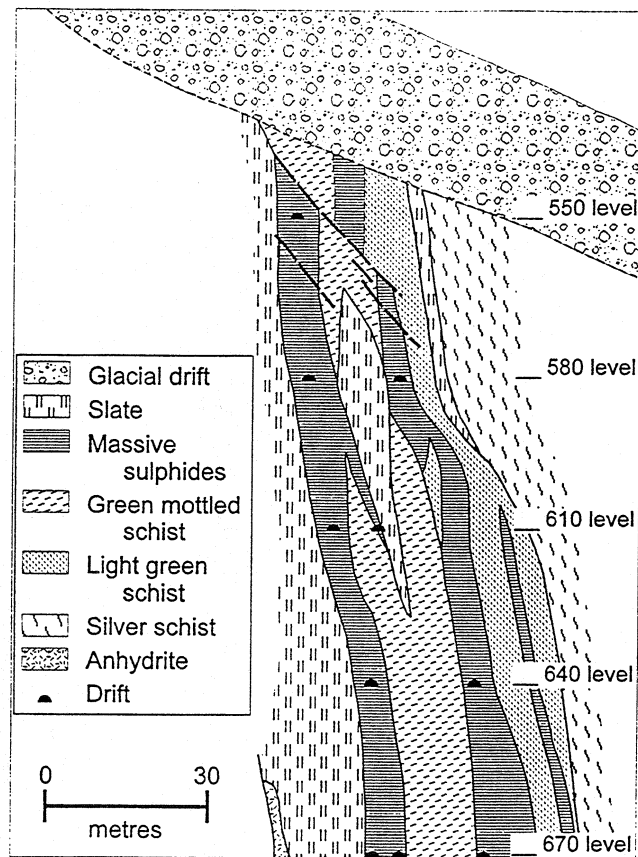
Sasahasta Fm.

## ALTERATION ZONES IN FELSIC LAVA AND TUFF BRECCIA

- Quartz + Sericite
- Sericite + Chlorite + Quartz
- Mixed-layer clay + Chlorite + Quartz
- Albite + Sericite + Quartz
- Kaolinite + Quartz + Sericite

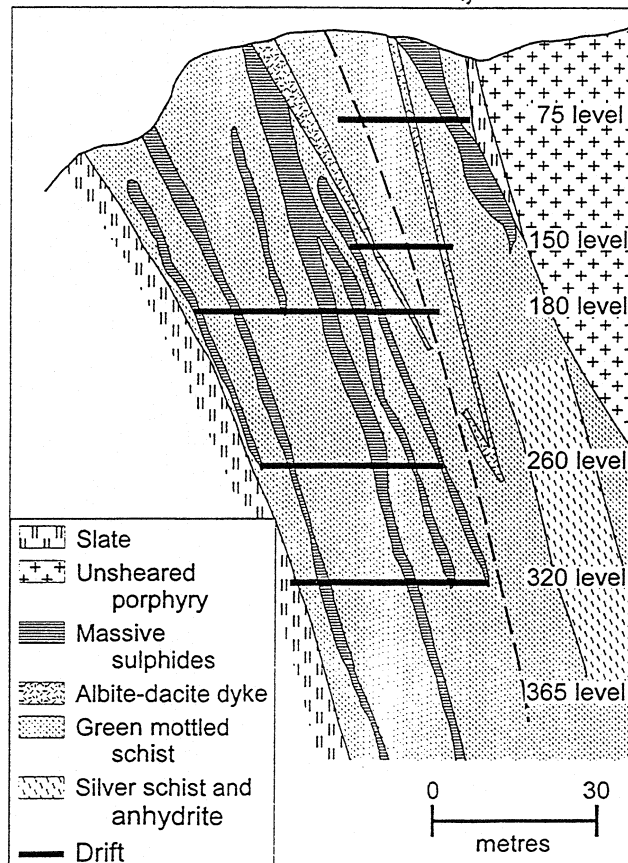
after Urabe *et al.*, 1983

# BRITANNIA MINE, B.C.



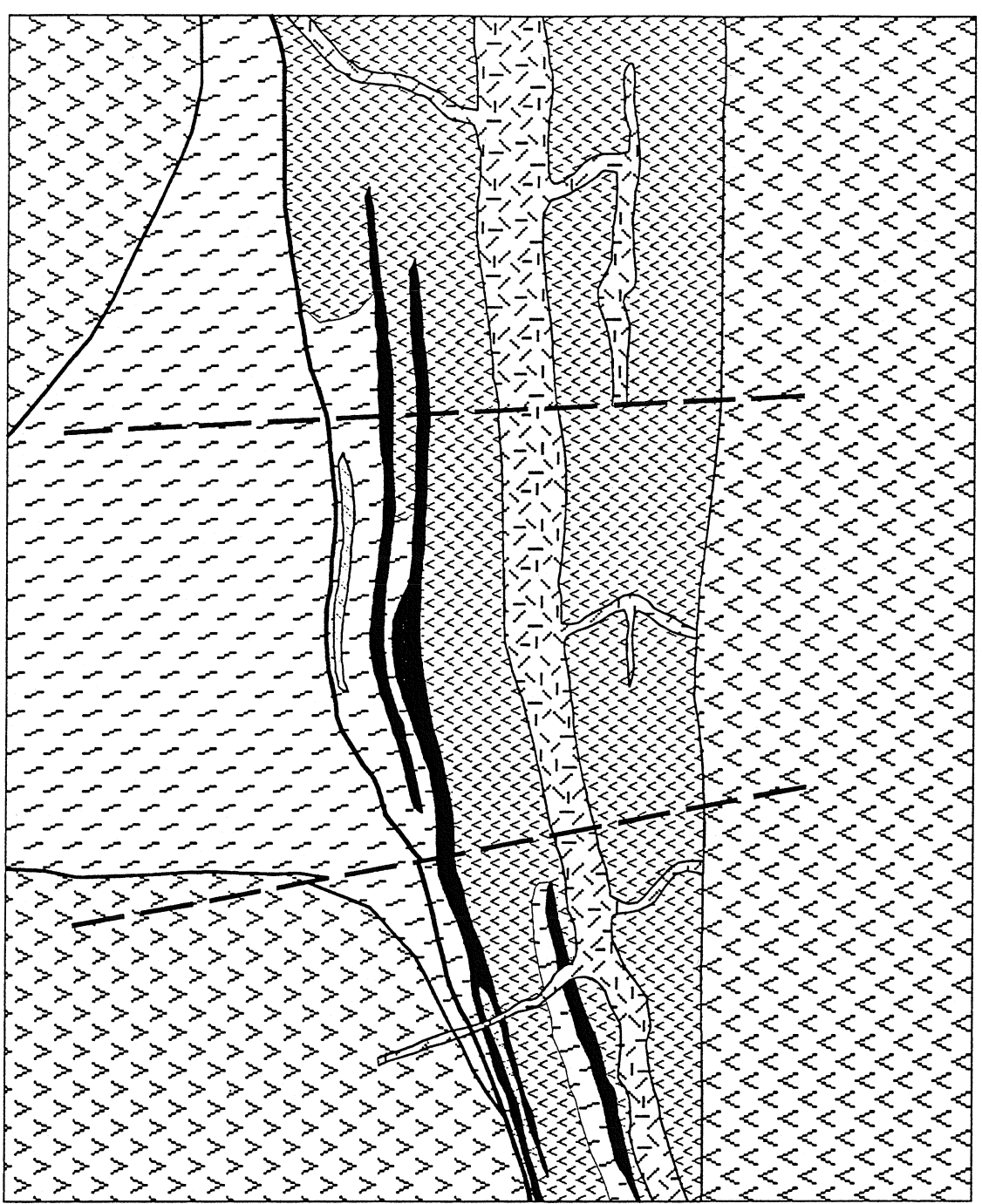
after Sutherland-Brown, 1974




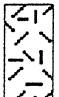



# BRITANNIA MINE, B.C.



after Sutherland-Brown, 1974

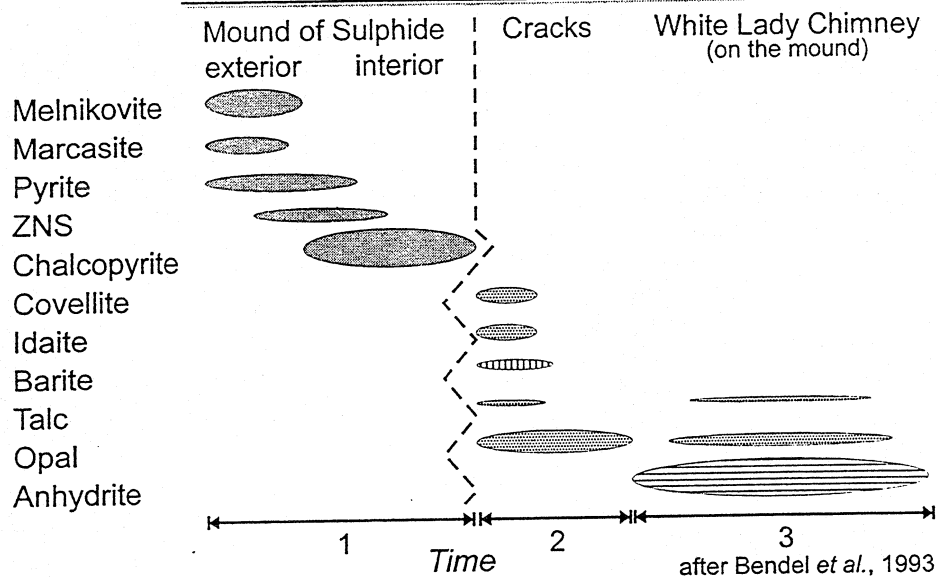
# TULSEQUAH CHIEF MINE, B.C.



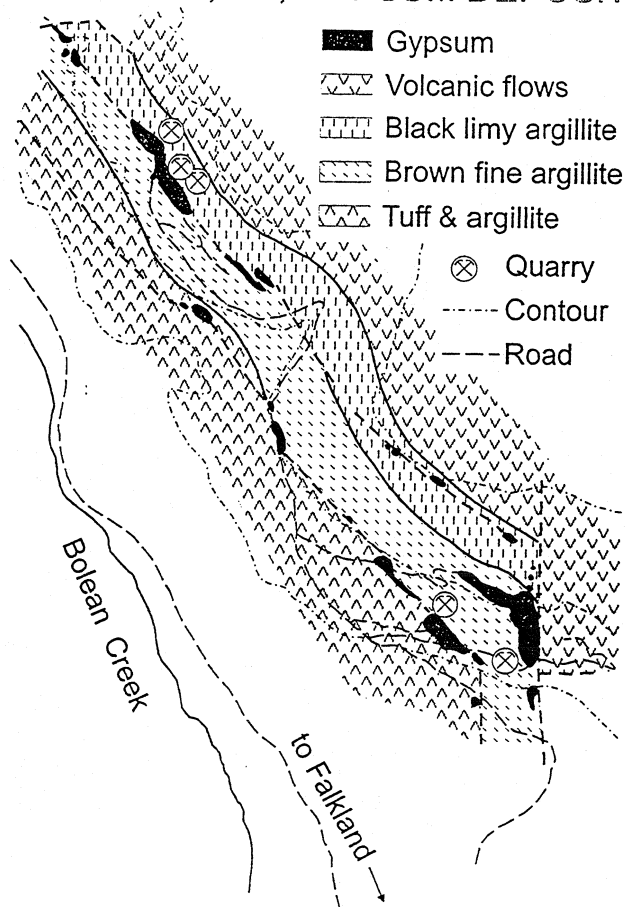
-  Mafic volcanics
-  Felsic volcanics
-  Andesite
-  Gabbro
-  Sericite alteration
-  Anhydrite
-  Pb-Zn-Cu-Ba ore

from Redfern  
Resources, 1995

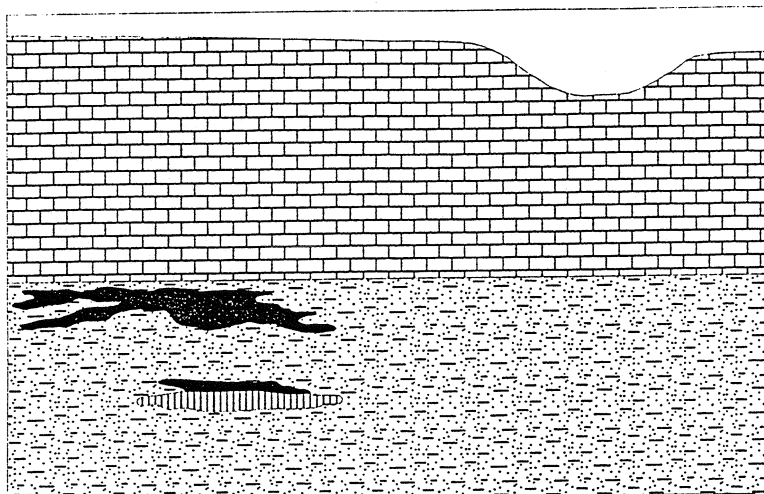
## WHITE LADY SMOKER, FIJI

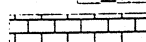
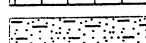
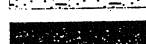



## FALKLAND, BC, GYPSUM DEPOSIT



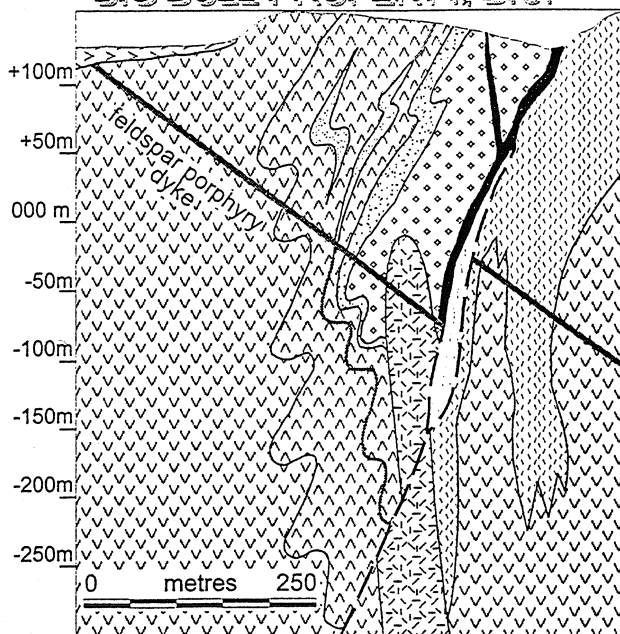
## EL COBRE FORMATION, CUBA

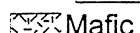

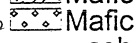
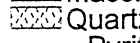

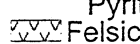
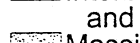
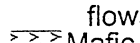

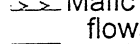
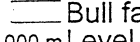


- |   |   |
|---|---|
|  | Limestone   |
|  | Water-lain pyroclastics (basaltic, andesitic and dacitic) |
|  | Manganese oxides  |
|  | Jasper  |

after Kesler et al., 1990

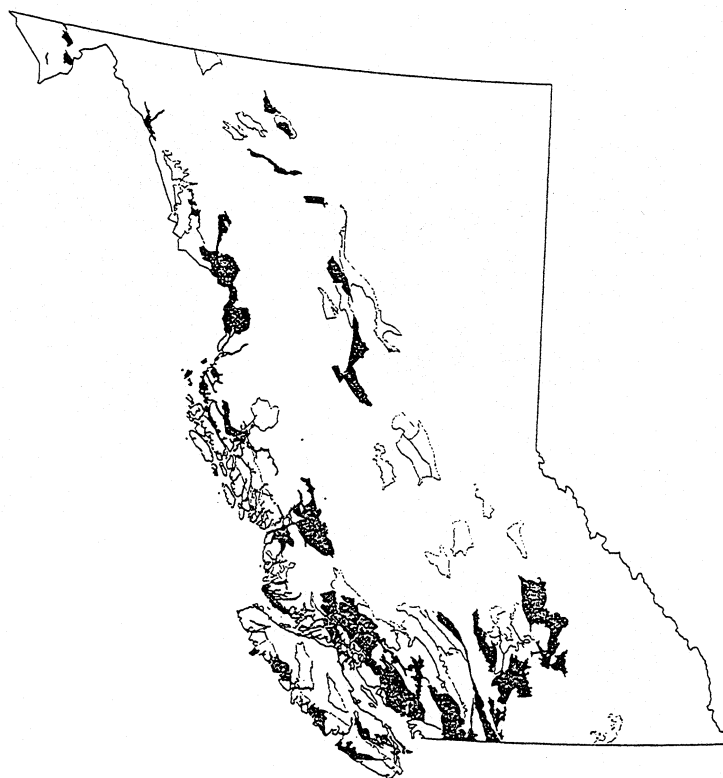
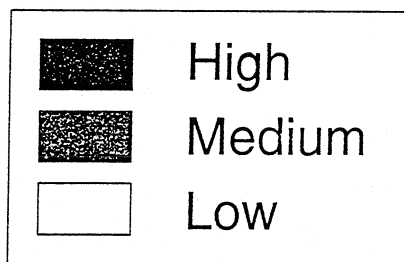
## BIG BULL PROPERTY, B.C.



- |   |                                   |   |                                   |
|---|-----------------------------------|---|-----------------------------------|
|  | Mafic intrusives                  |  | Massive sulphides                 |
|  | Mafic lapilli tuff and ash tuff   |  | Quartz-Sericite-Pyrite alteration |
|  | Interbedded tuff and Mn-silicates |  | Felsic tuffs, minor flows         |
|  | Massive braunite and piemontite   |  | Mafic tuffs and flows             |
|  | Maroon andesite tuffs             |  | Bull fault zone                   |
|   |                                   |  | 000 m Level                       |

Manganese

# Kuroko Mineral Potential in B.C.



## SKARN MODEL

Wollastonite

Garnet

White limestone

# OPEN SYSTEM ZEOLITE

# CLOSED SYSTEM ZEOLITE

Percolating  
groundwater

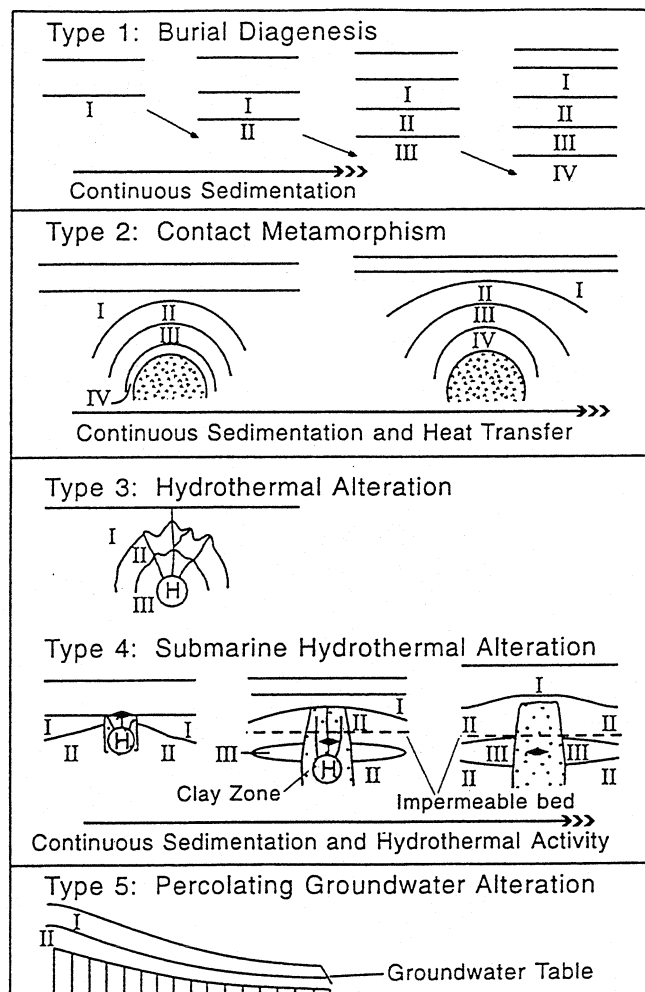
metamorphism

Alkaline lake

Hydrothermal

Sea water

Burial

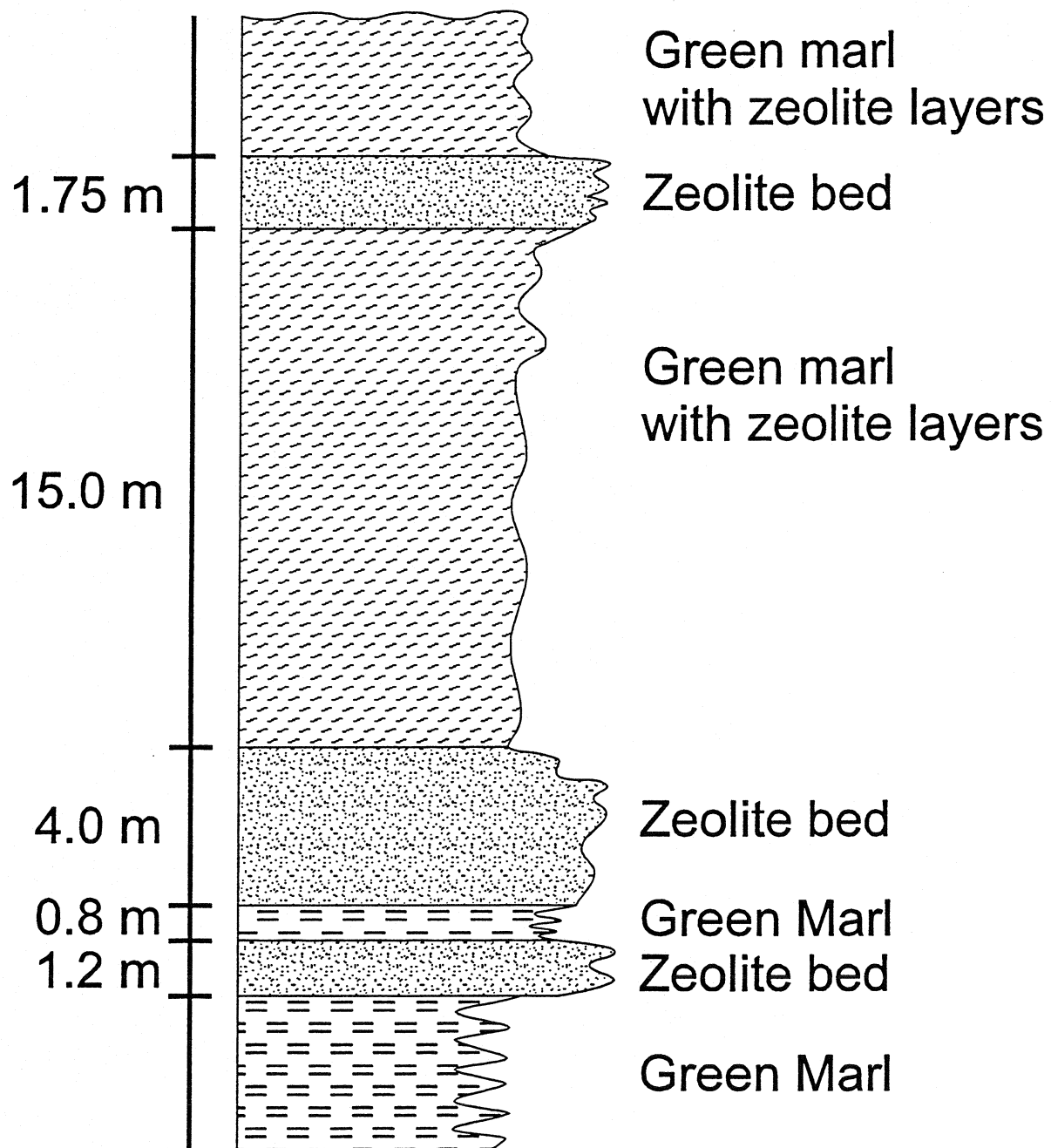


41-49°C I Unaltered Glass  
84-91°C II Clinoptilolite-mordenite zone  
120-125°C III Analcime zone (with heulandite or laumontite)  
IV Albite zone  
H Hydrothermal source

after Ijima 1978

# GARBAGNA, ITALY

## ZEOLITE DEPOSIT





# Industrial clays in the 21st century: A perspective of exploration, technology and utilization

Colin C. Harvey \*, Haydn H. Murray

## 3.1.3. Hydrothermal kaolins in island arc settings

In contrast to the low temperature, slow alteration of granitic rocks in England, hydrothermal alteration in Island Arc settings is relatively short-lived. Table 5 describes the range in mineralogy and fluid chemistries typically associated with hydrothermal kaolin resources. Two types of fluids may be involved: acid (sulfate) fluids produced from condensates of ascending hydrogen sulfide, or neutral pH reservoir fluids. At

Table 3  
Models of kaolin resources

Category	Model	Criteria
Residual	weathering	Kaolinization caused by weathering. Kinetics depend on climate, rock type and topography.
	arkose-derived kaolin	In situ alteration of arkosic sediments.
Hydrothermal	Cornwall Model	The heat source for the hydrothermal alteration of granites is long term radioactive decay. In Cornwall it was followed by the weathering.
	Island Arc Model	The heat source for hydrothermal alteration is a cooling pluton at depth or a near surface magmatic source.
Secondary (sedimentary)	transported kaolin	The eroded kaolins have been transported mechanically sorted and deposited in sedimentary basins.

higher temperatures, dickite may replace kaolinite or may be found in association with kaolinite, while at still higher temperatures pyrophyllite may be the stable phase. Deposits have been recorded in which pyrophyllite, dickite and kaolinite occur in temperature-controlled zonations in hydrothermal environments (Swindale and Hughes (1968). At low temperatures (typically less than 80°C) halloysite may be the preferred stable phase. For example, the formation of the Northland halloysite deposits in New Zealand is the result of the low temperature but rapid alteration of glassy rhyolites. In these deposits the volcanic glass has altered to halloysite rather than kaolinite (Murray et al., 1977; Harvey, 1980; Harvey and Murray, 1993). The resulting halloysite has an elongate structure and because of its very low iron and titania content, it is in world demand as a ceramic raw material.

Table 4  
Criteria for field recognition of kaolin resources

Category	Field relationships		Description
Residual weathering	regional	penetration	Horizontal or tilted conformity of alteration profiles.
	local	depth relationships remnant textures compositional studies	Decreasing alteration with increasing depth. Remnant textures of parent material. Progressive changes in alkalies, metals, hydration, etc.
Hydrothermal Cornwall Model	regional	granite terrain tectonic history mineralization history distribution of kaolinization	Source rocks having potential for radioactive decay. History of uplift and fracturing. Associated hydrothermal mineral assemblages. Possibly restricted at the surface zones of intense fracturing.
Hydrothermal Island Arc Model	regional	volcanic terrain current fossil	Evidence of current or recent volcanic activity. Evidence of current or recent hydrothermal alteration (altered ground, silification and hot springs). Structural control of thermal features.
	local	tectonic history textural mineralogy	May indicate low primary permeability in host rocks. Alunite indicative of acid sulfate alteration. Absence of alunite supporting evidence for neutral pH outflows kaolins.
Sedimentary (secondary)	regional	sedimentary terrain	Proximity of coal, carbonates or other sedimentary units may assist in defining sedimentary environment.
	local	fossils, organics, etc., textural	Presence of fossils, organic components, textural features and other sedimentary features may assist in characterizing the sedimentary environment.

Table 5  
Categorization of Island Arc hydrothermal systems

	Acid sulfate condensate clays	Neutral pH outflow clays
Water chemistry	Condensate formed from rising steam, $H_2S$ and $CO_2$ condensing into groundwater.	Neutral pH reservoir fluid which has undergone boiling and cooling on its way to the surface. Fluid salinity is related to extent of water-rock interaction and reservoir temperature.
Mineral saturation	Typically saturated in respect to cristobalite saturated in respect to sulfates, carbonates and other minerals.	Saturated or supersaturated in respect to quartz or lower temperature phases of silica.
Alteration mineral assemblages	Kaolinite (halloysite), dickite, alunite + cristobalite; silification, iron sulfates, possibly carbonates; pyrophyllite at higher temperatures.	Saturated in respect to other minerals. Kaolinite (halloysite), cristobalite and/or quartz silification possibly carbonates.
Requirements for a commercial deposit	Low sulfidation state hydrothermal system, location remote from the upflow zone, high uniform permeability in host rocks (such as tuffs or perhaps breccias). Soluble salts, variable iron content, very fine silica or silica cement.	High permeability host rocks such as tuffs and perhaps breccias.
Typical limitations	No known large kaolin resources, many small mines in Indonesia, Philippines and Vietnam. Pyrophyllite mines in Japan.	Fine silica or silification. Inconsistent alteration if the host rock has fracture controlled permeability.
Exploited commercially significant deposits		N.Z. China clays halloysite, small mines in the Philippines and Indonesia.

### *3.3. Exploration model for bentonite deposits*

Two of the largest known deposits in the developed world, one in the Western US and the other in Greece, are derived from the alteration of volcanoclastics. The most extensive and well studied bentonite resources in the US occur in a 1000 m thick section of marine marls, shales and argillaceous sandstones of Cretaceous age in the Black Hills which extend over several hundred kilometers in Wyoming, South Dakota and Montana (Patterson, 1955). The bentonite has formed by the in situ alteration of volcanic ash in seawater (Elzea, 1990). The bentonite beds are underlain by a siliceous horizon which increases in thickness with increasing thickness of bentonite. The overlying beds are non-siliceous shales. The volcanic origin for the ash is evidenced by the presence of unaltered glass shards in some of the bentonite horizons (Elzea, 1990). Both sodium and calcium bentonite are present in the deposit but this deposit has possibly the most extensive known resources of sodium bentonite in the world. Grim and Guven (1978) propose that the sodium bentonite has in places transformed to calcium bentonite by exchange with the calcium in circulating groundwater. The bentonite resources of Milos, Greece, are considered to have formed from seawater interaction with Lower Pleistocene volcanoclastic rocks (Christidis et al., 1995) with no specific contribution from associated hydrothermal activity. It has been previously suggested that there also may be a low temperature hydrothermal component to the alteration (Grim and Guven, 1978).

The requirements for economic resources of bentonites are therefore a source of volcanoclastic rocks or volcanic ash and a suitable environment in which alteration can take place. Such environments may include freshwater or marine sedimentary basins, submarine alteration or low temperature hydrothermal alteration. Known commercial deposits are restricted to late Cretaceous or younger rocks.

### *3.5. Exploration model for pyrophyllite*

The major exploited pyrophyllite resources are hydrothermal in origin (Ciullo and Thompson, 1994) with Japan and Korea producing over 80% of the world's pyrophyllite (Virta, 1991) from hydrothermally-altered volcanic rocks. These two countries also are the largest users of pyrophyllite. Several metamorphic pyrophyllite resources are known (Zaykov et al., 1988) but they are typically of low purity. In the exploration for pyrophyllite, fault zones associated with high temperature hydrothermal systems are considered to offer the most attractive exploration targets.

# Kaolin Deposits of Japan

N. FUJII, T. OKANO and Y. SHIMAZAKI

## Geologic conditions

The number of kaolin deposits in Japan is very large, and the geologic conditions of the representative deposits of various types are presented below.

### Hydrothermal deposits—I (in volcanic rocks)

These deposits were formed by the hydrothermal alteration of volcanic and pyroclastic rocks of Cretaceous to Quaternary period. Many of these are closely associated with metallic deposits of gold, mercury, iron sulphides, iron, and others.

Some of these deposits have vein forms such as those of the Seta mine, but most of them are irregular beds or massive deposits. The scale of these deposits is mostly small.

Itaya mine consists of exceptionally large deposits of this type and the monthly production is about 15,000 tons. There are three major deposits and the largest one has the confirmed dimensions of 350 m east-west, 300 m north-south, and the depth is over 100 m. The deposits are the hydrothermal alteration product of andesitic lava and pyroclastics of Quaternary eruption. The occurrence is complex as the silicified and kaolinized zones are intricately interwoven. Montmorillonitized zone is developed in the fringes of the deposits. Many parts of the kaolinized zone contain sericite.

### Hydrothermal deposits—II (in granitic rocks)

There are hydrothermal kaolin deposits formed in the acidic intrusives such as granite and quartz porphyry of Cretaceous to early Tertiary age. Most of them are of massive or vein form.

The deposit of the Taishu mine is well known in this group. The deposit of this mine was formed by halloysitization of quartz porphyry which intruded almost concordantly into Paleogene strata. There are scores of deposits of this type with various dimensions and the largest ones are in the order of 100 m × 200 m. Similar deposits are Kanpaku, Okutsu, Komaki and others.

L25

# GYPSUM IN BRITISH COLUMBIA

By S.B. Butrenchuk

## FALKLAND - MINFILE 082LNW001

Latitude: 50°31'00" Longitude: 119°34'00" NTS: 82L/12E

The Falkland gypsum deposits comprise a series of lenses along the northeast side of Bolean Creek valley north of Falkland (Figure 21). They were first staked in 1894 with production beginning in 1926. Production was continuous through to 1956 during which time 1 125 000 tonnes were produced. During the period 1976-1980 gypsum and anhydrite were mined intermittently from seven quarries and trucked to the Canada Lafarge Cement plant 18 kilometres east of Kamloops. There is still intermittent production from these quarries although gypsum reserves are virtually mined out. Anhydrite is still present in the deeper part of the quarries.

The deposits have been described by various authors (Baird, 1964; Cummings, 1940; Jones, 1959). Gypsum occurs along two parallel shear zones that are slightly discordant with a northwesterly striking and northeast-dipping sequence of interbedded volcanic and argillaceous rocks. These rocks belong to the Cache Creek Group of Carboniferous to Permian age.

Volcanic rocks consist of a series of flows that are dark green to grey to black, medium grained, slightly schistose and composed primarily of amphibole. Beneath the flows are thin-bedded, fine-grained, limy argillites. Alteration of the argillite close to the gypsum is manifest by colour changes from black to reddish brown. Pyrite and quartz stringers and veinlets are common within the alteration zone. Underlying this unit are thin-bedded, light green to greyish brown, brown-weathering argillites. The oldest rocks consist of bedded tuffs and a lower sequence of interbedded black argillite and tuff.

Gypsum is conformable with the enclosing rocks and occurs in a series of irregular, discontinuous lenses along a strike length of 2.4 kilometres (Figure 21). The irregular shape of these lenses, both in plan and section, is partly attributed to displacement along the shear zones. The

gypsum varies in colour from pure white through various shades of grey, grey-and-white banded and brown-and-white banded to reddish brown. Locally, the siliceous and argillaceous component reaches significant proportions especially in certain banded and brecciated material. Variations are sharp but generally unpredictable. Inclusions of dark red-brown to orange-brown, severely fractured argillaceous rocks, ranging in size from masses measuring 10 by 15 metres down to dust size, are present within the gypsum. These inclusions consist of fine-grained aggregates of quartz and albite, pyrite cubes, tiny tourmaline prisms and calcite in masses and small rhombs. At depths ranging between 20 and 35 metres gypsum grades abruptly into anhydrite. Mineable gypsum was generally confined to depths less than 25 metres.

In thin section the gypsum is seen to consist of sub-hedral crystals, fibrous masses and aggregates of gypsum with various impurities. Replacement of anhydrite by gypsum has also been observed (McCammon, 1952). The gypsum remaining appears to be of high purity (Table 7).

McCammon (1952) believed that the gypsum formed by the hydrothermal replacement of argillites and tuffs along shear zones. In thin section he observed that gypsum was the last mineral to form and that it replaces all other minerals. The mineral assemblage observed was at least partially a hydrothermal suite. Cummings (1940) interpreted the gypsum to have formed by the replacement of limestone by sulphate solutions. This replacement was believed to have been related to volcanic activity. Baird (1964) concluded that the gypsum-anhydrite bodies were deposited pre-Cache Creek as part of a sedimentary sequence and were later squeezed into their present position by plastic flow. The author favours a volcanogenic origin for these deposits although evidence, other than an association with volcanic rocks, is lacking.

TABLE 7  
CHEMICAL ANALYSES OF GYPSUM - FALKLAND DEPOSITS

Lab No.	SiO <sub>2</sub> %	CaO %	Na <sub>2</sub> O %	K <sub>2</sub> O %	MgO %	H <sub>2</sub> O %	SO <sub>3</sub> %	S %	Sr ppm
37651	2.58	30.89	0.30	0.02	0.22	18.60	42.51	17.3	1200
37652*	0.38	38.85	0.05	0.01	0.15	0.32	59.02	23.6	1300
37653	0.47	31.15	0.02	0.01	0.14	20.40	46.69	18.6	1000
38427	0.57	40.08	0.14	0.04	0.07			23.4	1400

\*Denotes anhydrite.

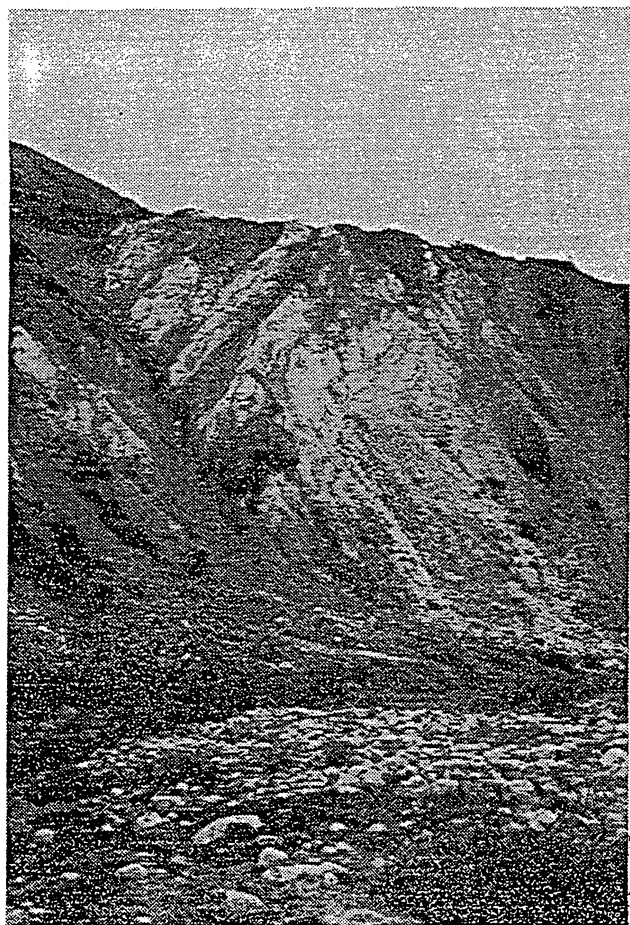


Plate 8. Exposure of gypsum in the O'Connor River area.

#### O'CONNOR RIVER GYPSUM - MINFILE 114P 005

Latitude: 59°39'00" Longitude: 136°34'00" NTS: 114P/10E

The O'Connor River gypsum deposit (Plate 8) is located in northwestern British Columbia, 96 kilometres northwest of Haines, Alaska. Gypsum occurs in rugged terrain above tree line on both sides of the river near the headwaters of its north fork. The nearest major transportation route is the Haines Road 12 kilometres east of the deposit. A haul distance of 104 kilometres will be required to transport the gypsum to tidewater at Haines.

This deposit was discovered in 1958 by J.J. McDougall while working for Ventures Ltd. A little work was done on the property in 1959 and again in 1964 when Falconbridge Limited did some trenching. Some drilling was done in 1965. In 1984 a bulk sample was taken by

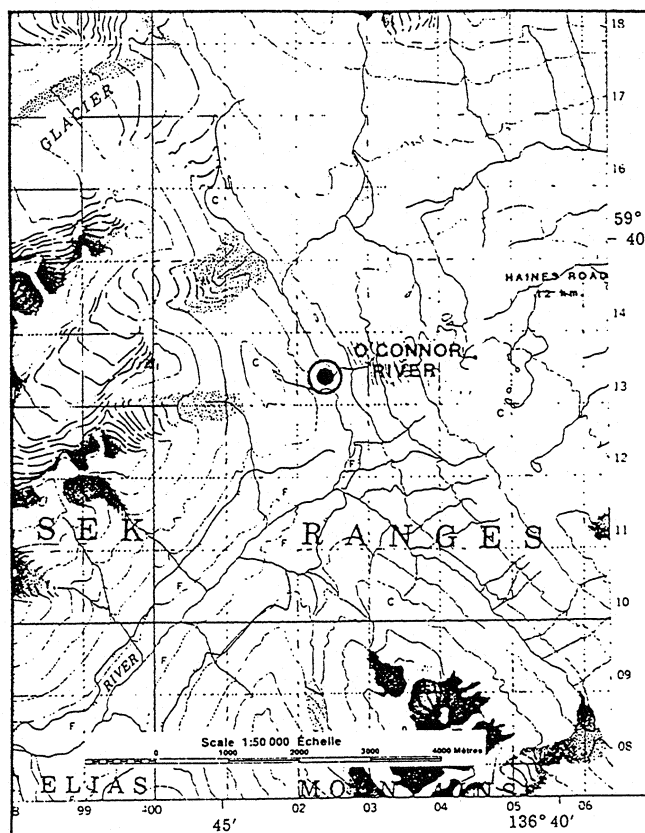


Figure 22. Location of the O'Connor River gypsum deposit.

Haines Gypsum Inc. and further drilling was completed in 1986 by Queenstake Resources Ltd.

Gypsum occurs in complexly deformed Paleozoic sedimentary rocks and Triassic basic flows and related volcanoclastic rocks within the Alexander Terrane of the Insular tectonic belt (Figure 22). The following description is summarized from White (1986), McDougall (1959) and Kootenay Geo-Services (1986).

Hostrocks to the gypsum are limestone, limestone breccia and black calcareous argillite. Sill-like dioritic intrusions are also present in the area. Sediments adjacent to these sills have been silicified and metamorphosed. Better quality gypsum is described as snow white with no visible impurities and occurring in massive continuous beds. Traces of anhydrite may be present. Brown or buff-coloured gypsum or gypsiferous carbonate is present near the edges of the pure white material (McDougall, 1959). A sample of pure-white gypsum taken by G.V. White indicates a purity in excess of 90 per cent gypsum (Table 8).

TABLE 8  
CHEMICAL ANALYSIS OF GYPSUM - O'CONNOR RIVER

Lab No.	SiO <sub>2</sub> %	CaO %	Na <sub>2</sub> O %	K <sub>2</sub> O %	MgO %	H <sub>2</sub> O %	SO <sub>3</sub> %	S %	Sr ppm
37650	0.47	31.06	0.01	0.02	0.62	19.50	45.77	17.9	1300

Tuffaceous layers consisting of biotite, chlorite, amphibole and sericite are commonly found concordant with bedding within the gypsum. Other impurities include strontianite, siderite, ankerite, limonite and scapolite. There are remnants of anhydrite the size and shape of footballs within the gypsum at surface. Hydration is estimated to have taken place to a depth of 40 metres from the paleosurface. The absence of enterolithic folding implies a recent origin with unconfined swelling.

Gypsum is exposed in three zones (Figure 23) of which two may in fact be the same, with the central portion eroded away by the O'Connor River. Zone 1, described as irregular in shape, is exposed along strike for 400 metres over a vertical height (Plate 8) of 122 metres (White, 1986). It strikes northwest with steep dips to the northeast. The gypsum is generally pure containing only minor anhydrite. Contacts with the surrounding rocks are sharp. Locally it appears that the gypsum crosscuts the sedimentary rocks. Sinkholes, 10 to 20 metres in diameter and 10 to 15 metres deep, are present at the southeast end of zone; gypsum is exposed in the walls of some of them.

Zone 2 or West zone is believed to be an extension of Zone 1. It is exposed along strike for 220 metres across widths of 60 to 100 metres and a vertical component of

200 metres. The gypsum is white, massive and finely crystalline. There is a 30-metre-wide argillaceous limestone exposed within the gypsum at the southeast end of the zone. Contacts are sharp although there are a few inclusions of argillaceous limestone, up to 15 centimetres in size, in the gypsum.

Zone 3, located 1200 metres south of Zone 2, strikes east and dips to the north. It is exposed along strike for 550 metres across widths of 50 to 110 metres and a height of 120 metres. The gypsum is white and is in sharp contact with a limestone unit. Sinkholes are present along the entire length of the zone.

Reserves for Zone 1 are estimated to be 2.5 million tonnes grading 79 per cent gypsum (Kootenay Geo-Services, 1986). The  $\text{SO}_3$  content averages 40 per cent and the oxide and insoluble content is fairly high making the gypsum suitable for wallboard manufacture but not for the cement industry. There is a potential for 10 million tonnes in the three zones combined.

Other areas containing sinkholes occur between the O'Connor River gypsum deposit and the Haines Road and east of the Haines Road (J.J. McDougall, oral communication, 1989). Both localities contain no outcrop.



# REA GOLD (HILTON) AND HOMESTAKE VOLCANOGENIC SULPHIDE-BARITE DEPOSITS SOUTHEASTERN BRITISH COLUMBIA (82M/4W)

By T. Höy  
Ministry of Energy, Mines and Petroleum Resources  
and  
F. Goutier  
Department of Geological Sciences, University of British Columbia

## HOMESTAKE

### INTRODUCTION

Homestake is a polymetallic base and precious metal deposit in intensely altered and sheared sericite schists of the Eagle Bay Formation (Schiarrizza and Preto, 1984). Mineralization is generally contained in barite lenses or, locally, it is in quartz veins. Access to the property is provided by a switchback road that leaves the main road 5 kilometres northwest of Squaam Bay.

### HISTORY

The property, as recorded in *Minister of Mines* Annual Reports (1927, 1936), was discovered in 1893 and first developed between 1893 and 1895. Work on the property was intermittent and shipments of ore occurred sporadically until 1927. The mine was reopened by Kamloops Homestake Mines Ltd. in 1935; workings at

TABLE 7-1  
STRATIGRAPHIC SECTION OF THE EAGLE BAY  
FORMATION AT THE HOMESTAKE DEPOSIT

Map Unit	Description	Possible Primary Source Rock
	Greenstone	Basalt
5	Tuffaceous chlorite schist	Intermediate tuff
3/4	Chloritic schist/ankeritic phyllite	Andesitic volcanic rocks/sedimentary rocks
2b	Sericite-quartz paper schist	Felsic tuff
2a	Sericite-quartz schist	Felsic volcanic rocks
1	Chlorite phyllite	Intermediate volcanic rocks

that time consisted of four adits and more than 455 metres of crosscuts, drifts, raises, and a winze. A 50-tonne per day flotation mill was installed on the site. Recorded production between 1935 and 1941 totalled approximately 6 965 tonnes from which 12 400 grams of gold, 9 565 900 grams of silver, 11 080 kilograms of copper, 171 325 kilograms of lead, and 246 520 kilograms of zinc were recovered. In the early 1970's, work on the property was resumed with geophysical and geochemical surveys, diamond drilling, and drifting to gain access to the old workings and to provide underground diamond-drill sites. Proven reserves were, at that time, estimated to be 1 010 800 tonnes with an average grade of about 240 grams silver per tonne, 2.5 per cent lead, 4.0 per cent zinc, 0.55 per cent copper, and 28 per cent barite (The Financial Post, Jan. 13, 1973). Since 1982 work by Kamad Silver Company Ltd. has confirmed and improved previous grade estimates but the deposit is considered difficult to mine, mainly because of the poor strength of the host rocks.

#### ROCK UNITS

The mineralized barite lenses are overlain by a siderite phyllite that contains interbedded argillite and by a tuffaceous chlorite schist unit. A wide zone of altered rock occurs below the mineralized

lenses. Regional metamorphism and local hydrothermal alteration have obscured the primary composition of the host rocks; consequently, the following unit descriptions are based on mineral assemblages. Primary compositions are tentatively inferred from these assemblages (Table 7-1), and chemical analyses in progress will better characterize the original host rocks.

A poorly exposed chlorite phyllite (unit 1) occurs in the southern part of the map-area (Fig. 7-7). It is a thinly laminated brownish green chlorite phyllite that is noticeably less foliated than the overlying schists.

Unit 2 comprises dominantly sericite-quartz schist with abundant disseminated pyrite throughout. Unit 2a is a more massive phase of the 'paper' schist of unit 2b and contains lenticular, silica-rich segregations up to 6 centimetres in length. Unit 2b, referred to as a sericite-quartz 'paper' schist (Table 7-1, Fig. 7-7), is the most conspicuous unit in the map-area. In outcrop, the paper schist unit is easily discernible by its fissile appearance and by its weathered coating of yellow ferric sulphate. It is the host and the footwall to the barite-sulphide lenses and is interpreted to be a highly altered, predominantly felsic tuff unit. A number of quartz veins up to a

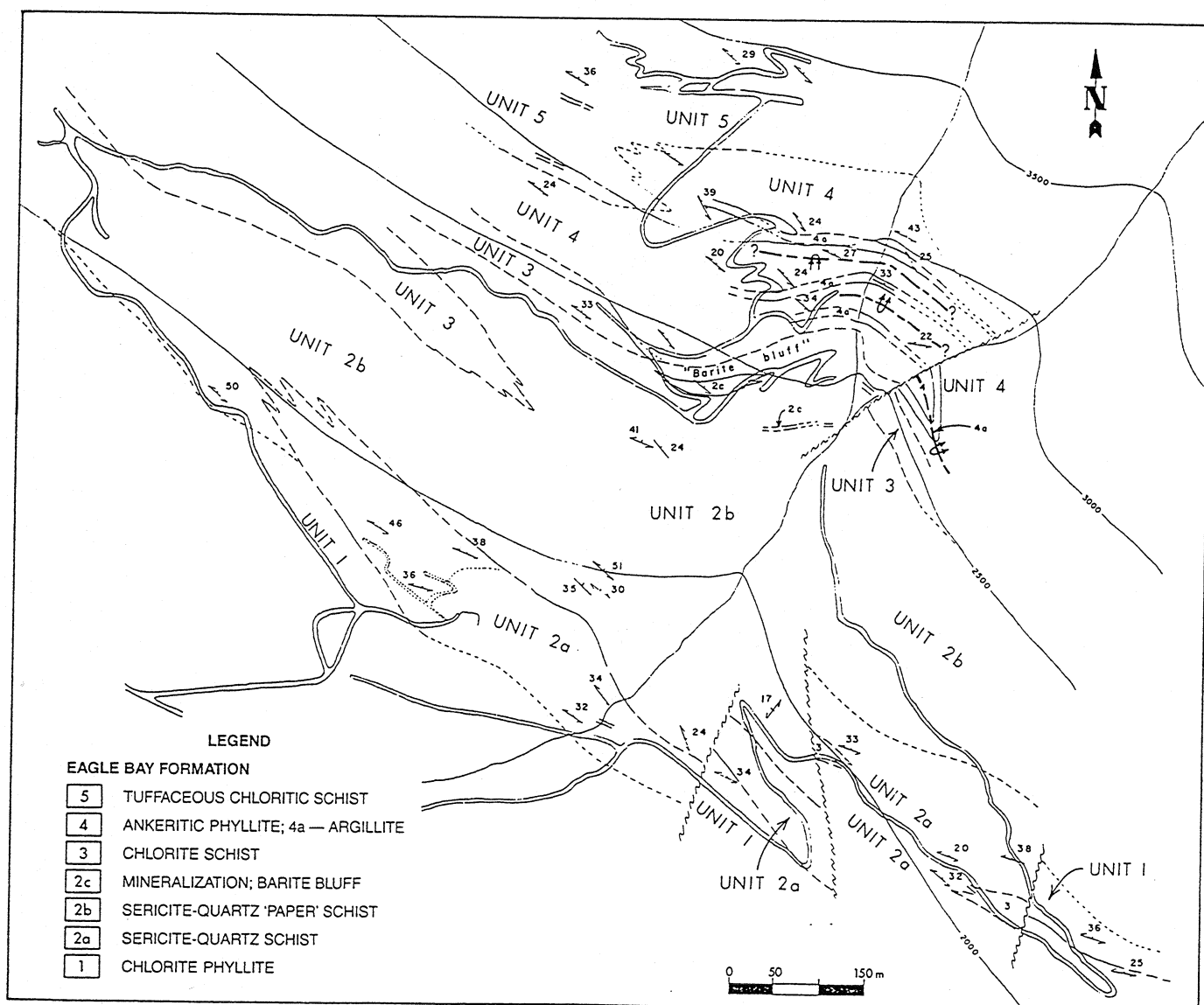


Figure 7-7. Map of the Homestake property showing geology and access roads.

L30

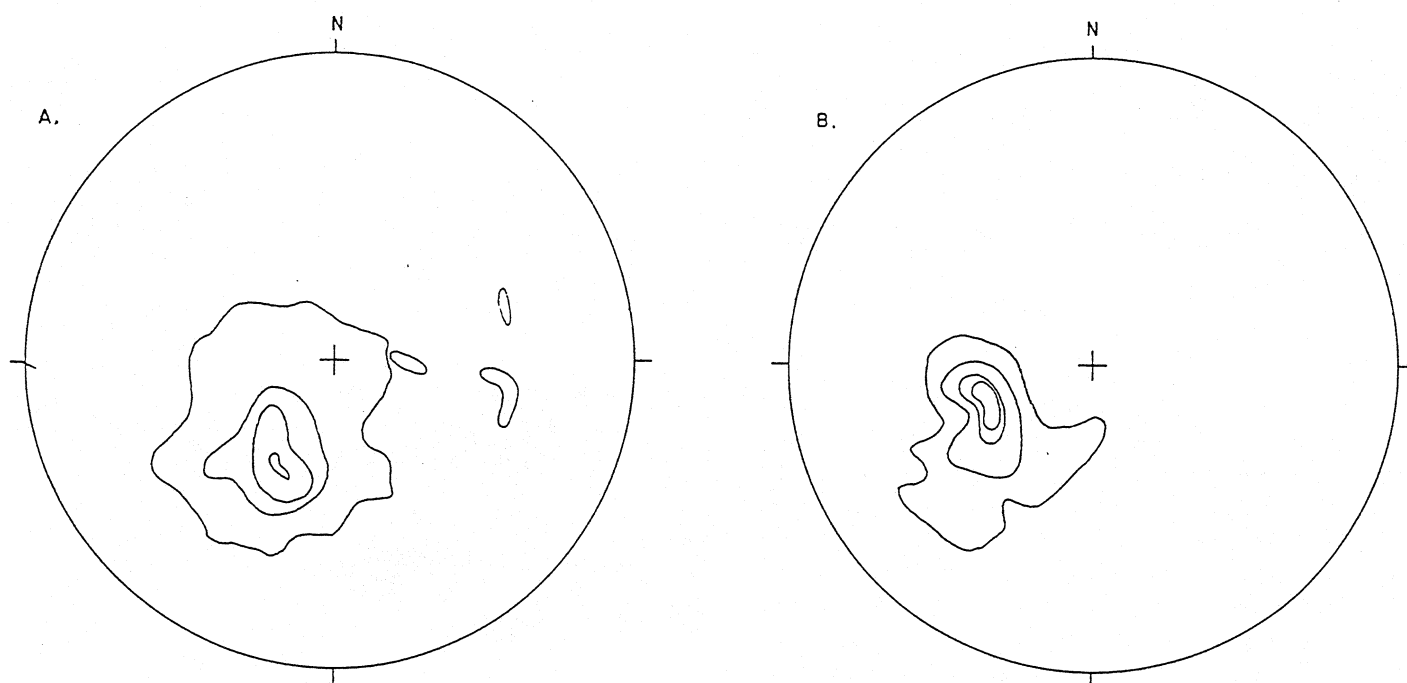


Figure 7-8. Lower hemisphere equal area projections of structural elements, Homestake deposit area. A — poles (92) to foliation, maximum concentration — 30%; B — poles (15) to compositional layering, maximum concentration — 33%; contour intervals — 1, 10, 20, 30%.

metre thick are found within the paper schist below the barite lenses; they contain pyrite but are generally barren of other sulphides.

A dark green laminated chlorite schist (unit 3, Table 7-1; Fig. 7-7) occurs stratigraphically above and laterally west of unit 2b. It consists of carbonate phenocrysts within a fine-grained chlorite-feldspar matrix. These phenocrysts, which may be pseudomorphic after plagioclase, are rimmed and partially replaced by chlorite. This unit is probably altered andesite tuff; its contact with unit 2b is in part an interfingering of felsic and intermediate tuffs but may also reflect an irregular pervasive potassic and silicic alteration boundary.

A fine-grained ankeritic phyllite (unit 4) composed of interbedded layers of ankerite-bearing chlorite phyllite occurs above units 2b and 3. In outcrop, limonite pseudomorphs after iron-rich carbonate give the rock a characteristic brown tinge. Some fine-grained pyritic argillites within the phyllite package are the most continuous and reliable marker units at Homestake. These argillite layers contain elongate quartz eyes or augen-shaped clasts up to 0.8 millimetre in diameter. The quartz eyes have cores of euhedral pyrite crystals and are set in a fine-grained pyritic and carbonaceous matrix of phyllosilicates, quartz, and feldspar. Unit 4 is interpreted to be largely a sedimentary clastic rock with interbedded chloritic tuff layers.

A tuffaceous chlorite schist (unit 5) occurs on the steep cliffs in the upper, northern portion of the Homestake area. The rock contains massive and tuffaceous zones composed of chlorite and carbonate, probably developed from regional metamorphism of rocks of intermediate composition such as andesite. Relict flattened felsic clasts imply a pyroclastic origin for at least part of this unit. Pyritic quartz veins and calcite stringers occur throughout the schist and, in several places, cut the foliation. Locally, cherty pods and argillite layers are interbedded with the schist. This unit is overlain by a thick greenstone sequence (V. A. Preto, pers. comm., 1985).

#### SULPHIDE-BARITE LENSES

A number of barite lenses with variable amounts of sulphides occur within the upper part of unit 2b. They are described in detail in

early *Minister of Mines* Annual Reports (1927, 1936) and will be briefly reviewed here. At least three lenses, separated by sericite schist, are recognized. They range in thickness from less than a metre to at least 10 metres and underground some have been traced several hundred metres. Metallic minerals within these lenses include tetrahedrite, galena, sphalerite, pyrite, chalcopyrite, argentite, minor native silver, and trace ruby silver and native gold.

The lenses may consist either of massive to banded barite with only scattered metallic minerals throughout, or interlayered barite, schist, and sulphides. Two lenses are exposed on surface. The largest, referred to as the 'barite bluff' (unit 2c, Fig. 7-7), has an exposed thickness of 5 to 6 metres. It pinches out rapidly along strike, has a sharp hangingwall contact with sericite schist, and grades down into massive sericitic chert. A smaller lens, 1 to 2 metres thick, occurs below the 'barite bluff' unit (Fig. 7-7); it is banded but contains only minor sulphides.

# Metallogenic evolution of the Caribbean region

Stephen E. Kesler

Department of Geological Sciences, University of Michigan, Ann Arbor, Michigan 48109

Enrique Levy

25 Calle "A" 12-03, Zona 11, Guatemala, Guatemala

Cecilia Martín F.

Avenida Principal de Cumbres de Curumo, Residencia 680 PH, Caracas 1080, Venezuela

A distinct type of manganese deposit is found in the Upper Cretaceous(?)–middle Eocene Cobre Formation in eastern Cuba, which consists largely of water-laid pyroclastic material of basaltic, andesitic, and dacitic composition (Lewis and Straczek, 1958). The largest manganese deposits in the Cobre Formation are stratiform oxide lenses in tuff (Fig. 4), which are commonly associated with jasper, known as bayate, or similar stratiform lenses in limestone (Woodring and Daviess, 1944; Simons and Straczek, 1958). They are found at and just below the lower contact of the middle Eocene Charco Redondo limestone-tuff, the uppermost unit of the Cobre Formation (Park, 1942). Similar deposits are found in Haiti (Butterlin, 1960) and Puerto Rico (Cox and Briggs, 1974). Closely related copper mineralization, in the form of vein and stockwork deposits associated with subvolcanic intrusions, is abundant in the lower part of the Cobre Formation in Cuba. These deposits, which include Eureka (Bogdanov and others, 1966) and the historic El Cobre mine mentioned above (Ansted, 1856; Lawrence, 1910), are probably coeval with the manganese and could occupy the deeper parts of the manganese depositing systems. Probably related hot spring, epithermal vein, and replacement base and precious-metal mineralization is also found in the Wagwater trough of Jamaica, as discussed in a later section.

The Cobre-type manganese deposits clearly formed from submarine hydrothermal activity rather than as hydrogenous sediments, but they differ significantly from the ophiolite-related manganese deposits in both depth of formation and composition. Whereas most submarine manganese deposits are associated with pillow basalt and abundant radiolarian and chemical cherts, the Cobre deposits are closely associated with pyroclastic rocks and shallow-water limestone (Lewis and Straczek, 1958). Secondly, the Cobre-type deposits plot in conflicting fields on the main chemical diagrams used to classify submarine manganese deposits (Fig. 5). In particular, they have too much Al and Si, and their Mn:Fe ratio is too low (Sokolova, 1977). The abundance of Al and Si is likely due to the location of these deposits in a region where relatively large amounts of detrital sediments contaminated the manganese lenses as they formed, and the relative abundance of Fe could reflect shallower, more oxidizing waters into which the solutions exhaled.

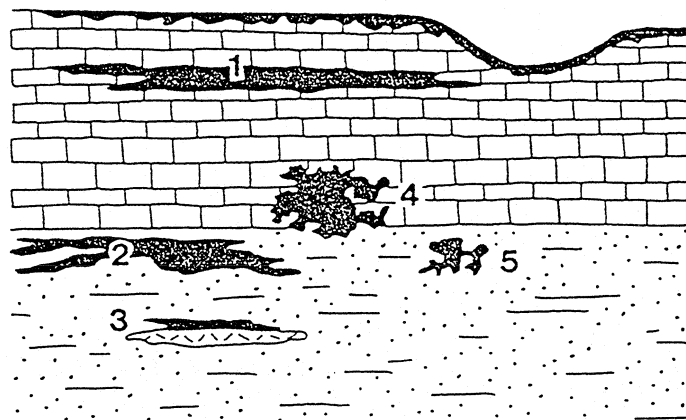


Figure 4. Schematic illustration of types of primary manganese deposits in the Cobre Formation of eastern Cuba (modified from Woodring and Daviess, 1944). 1, bedded ore in limestone; 2, bedded ore in tuff (not associated with bayate); 3, bedded ore in tuff (associated with bayate); 4, nonbedded ore in limestone; 5, nonbedded ore in tuff.

Manganese ores in stratiform deposits are predominantly oxides. The chief mineral is todorokite, which is locally replaced by supergene (partly hypogene?) pyrolusite.\* Productive benches in most of the ore deposits include two or three ore "seams," which are located one above the other and are separated by barren rocks. In plan the ore deposits, with an overall elliptical, or less commonly roughly circular shape, have a slightly sinuous outline. Their length is usually hundreds of meters, and in the large deposits up to 1 km. Only in the Charco Redondo deposit does the length of the ore seam reach 2 km (including noncommercial ore). The thickness of the ore-bearing horizons ranges within wide limits, changing from a few tens of centimeters up to 1-5 m. In certain cases it exceeds 10 m: For example, the ore "seam" in the Sultana deposit is 11 m thick, and in the Quinto deposit, 15 m. The nature of the pinchouts and aspects of the contacts of the ore bodies will be discussed below, followed by a description of the textural features of the ore.

As mentioned, above, the overwhelming majority of stratiform ore bodies are localized in the upper part of the El Cobre Formation within the volcanogenic-fragmental and carbonate (Charco Redondo Limestone) rock associations. In a large part of the area under consideration the Charco Redondo Limestone lies directly on rocks of the volcanogenic-fragmental association, and grades upward into terrigenous deposits of the San Luis Formation. Only in the El Cristo area (approximately on the longitude of the city of Santiago de Cuba) are limestones completely absent, and the San Luis Formation rests directly on rocks of the volcanogenic-fragmental association. The thickness of the limestones within the manganese-bearing part of the El Cobre Formation ranges from 100-110 m in the west to 5-10 m in the east. Among the volcanogenic-fragmental rocks underlying the Charco Redondo association there are often thin interbeds of limestone, just as in the carbonate unit individual seams of tephroid and tuffites are encountered.

Stratiform mineralization, apart from its dependence on localization within the volcanogenic-fragmental or carbonate associations, is invariably associated with the clastic deposits. Thus, in the carbonate Charco Redondo unit the ore-bearing beds are volcanogenic-fragmental rocks enclosed within limestones. As regards the limestones, they themselves contain only insignificant ore shows, which are either pocket-like deposits of manganese oxides or fracture zones mottled with ore veinlets. An interesting pattern should be noted, however; limestones, which are not ore-bearing, often occur in the productive benches of ore deposits, usually being located above the ores. A similar relationship of carbonate rocks and ores has often been observed in deposits associated with the volcanogenic-fragmental association. In this case the ore-bearing seams are clastic rocks underlying limestones and occurring either in the Charco Redondo unit or in thin interbeds within the volcanogenic-fragmental deposits. Limestones may lie directly upon ore or may be separated from it by thin interbeds of barren clastic rocks. In some cases the limestone caprock is completely absent and the productive seam is underlain and overlain by about the same type of clastic rocks. To illustrate this, we present a brief description of the productive units in specific ore deposits. Columnar sections of these units are shown in Fig. 1.

1. Charco Redondo Deposit. The mineralization is associated with three beds of volcanogenic-fragmental rocks: basal, lower, and upper. The basal ore "bed" corresponds to the

\*The composition of Cuban manganese ores has been studied by a number of investigators, including Hewett and Shannon (1921), Fleisher and Richmond (1943), Frondel et al., (1969), Straczek et al., (1960), Faulring (1962), and Richmond et al., (1969). As a result of these studies, there have been established in manganese ores of the El Cobre Formation (occurring in both the stratiform deposits and the irregularly shaped bodies) the following minerals: braunite, pyrolusite, manganite, hausmannite, romanèchite, cryptomelane, ramsdellite, todorokite, neotocite, bementite, orientite, inesite, piemontite, and rhodonite. Of these minerals, only todorokite and pyrolusite and to a lesser degree braunite form commercial concentrations.

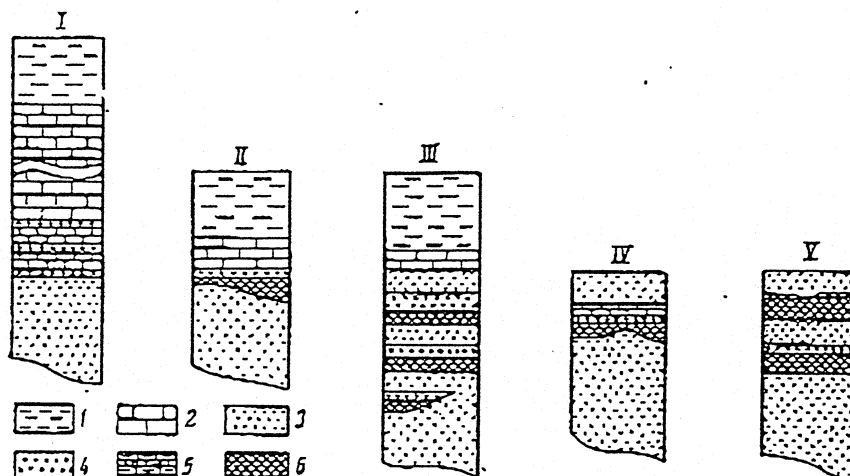


Fig. 1. Schematic sections of the productive horizons in the El Cobre Formation. 1) San Luis Formation; 2-6) El Cobre Formation: 2) Charco Redondo Limestone, 3) volcanogenic-fragmental rocks, 4) manganese ore in volcanogenic-fragmental rocks, 5) limestone interbeds in volcanogenic-fragmental rocks, 6) siliceous rocks; deposits: I) Charco Redondo, II) Ponupo, III) Quinto, IV) Boston, V) Espania.

uppermost horizon of the volcanogenic-fragmental section (volcanogenic-fragmental association) and directly underlies the Charco Redondo Limestone. Its thickness ranges from a few centimeters up to 4 m. Mineralization is represented by nodules, veins, and thin interbeds of manganese oxides replacing fine- and medium-grained clastic rocks or the matrix of coarse-grained types. The ore is relatively lean.

The lower and upper ore-bearing horizons are localized within the Charco Redondo unit but the mineralization is associated with interbeds of medium-grained volcano-fragmental rocks within the limestone. These interbeds are located 5-6 and 9-12 m respectively above the base of the Charco Redondo Limestone. Their thickness is about 1 m. Manganese oxides are distributed unevenly through the beds, but in certain parts they almost completely replace the enclosing rocks. The ores are rich, with the content of manganese in the commercial varieties 30-50%. The extent of the lower and upper ore beds is about 2000 m (including lean, non-commercial ores). At the base of the ore deposits lenses, pockets, and interbeds of siliceous rocks are often present, which are developed not only in clastic deposits but also project as pockets into the underlying limestone. This imparts an odd, sinuous line to the lower boundary of the ore-containing bed. Individual cases of embayment-like penetrations of the ore mass at the base of the seam into the underlying carbonate are seen. The upper contact of the ore "beds" is quite distinctly expressed: It is completely determined by the contact plane of the volcanogenic-fragmental rocks with the overlying limestone.

**2. Ponupo Deposit.** Mineralization is associated with beds of volcanogenic-fragmental rocks directly underlying the Charco Redondo Limestone. The thickness of the limestone unit in the area of the deposit ranges from 2 to 12 m. The thickness of the ore seam is as much as 2.5 m. Its length is about 1 km with an exposure width of 250-300 m. The rich ore (44-45% manganese) is typically located in the upper part of the deposit (approximately the uppermost 0.5 m) at the contact with limestone. Several centimeters of the basal limestone have been replaced by manganese oxides. Over a large part of the area of their development the ore-bearing clastic rocks are underlain by siliceous material, which grades downward into volcanogenic-fragmental deposits with no signs of mineralization. The siliceous material forms a bed-like body exposed over an area of 430 × 300 m with a thickness of up to 30 m in the central part. With an overall bed-like configuration of the body of siliceous rocks, its contacts with the enclosing rocks is, as a rule, complex: Only in certain areas are they determined by actual bedding; more often they have a more or less sharply expressed cross-cutting nature.

**3. Quinto Deposit (El Cristo Region).** The ore occurs within volcanogenic-fragmental deposits, localized into three bed-like bodies, of which the two upper are the main ones.

These ore bodies have a considerable extent (on the order of 1 km) and thickness (up to 12-15 m), but are composed of relatively lean ore, the manganese content of which averages 16-17%. The ore "beds" are separated by barren clastic rocks, which underlie and overlie the productive sequence as a whole. The uppermost ore is separated from the Charco Redondo Limestone by a sequence of clastic rocks up to 15 m thick. The total thickness of the productive interval is variable: In the southern and central parts of the ore field it reaches 40-50 m; to the north it is noticeably less. This change in thickness is due to a gradual convergence of the ore "beds" from south to north, with a corresponding decrease in the interval between the ores down to a complete pinchout. At the base of the ore deposits there are, as a rule, siliceous jasper-like rocks of extremely uneven thickness.

4. Boston Deposit (El Cristo Region). The sole ore "bed" in the Boston deposit is localized in coarse- and medium-grained volcanogenic-fragmental deposits. Within the ore-bearing sequence of clastic rocks there are some thin limestone interbeds, under one of which (with a thickness of about 3 m) is located the ore deposit. The maximum thickness of the productive layer is about 3 m. The ore is associated with siliceous rocks which form lenticular bodies 450 x 150 m with a maximum thickness of 12 m. The siliceous rocks underlie the productive layer, but their relationship with the ore-bearing clastic rocks is very complex. In addition to the fact that the ore penetrates into the siliceous rocks in deep embayments and pockets, cases of penetration of the mineralized layers into steep faces or sharp projections of siliceous lenses have been observed. The ore-bearing deposits can be traced some distance beyond the area of development of the siliceous rocks, but the amount of manganese mineralization in them drops sharply.

5. Espania Deposit (El Cristo Region). The absence of limestone is a characteristic feature of the productive section and also the deposits in which it is contained. Predominant in area of the ore deposit are coarse-grained volcanogenic-fragmental rocks, two beds of which contain ore mineralization. The beds are separated by ore-free clastic deposits 6-9 m thick. The ore is closely associated with siliceous jasper-like material. It is localized along the upper contact of siliceous lenses and even within them. The richest ore is characteristically found in the jasperoids themselves. Of the two ore occurrences present in the deposit, the lower is the more significant. The thickness of the clastic bed enriched in manganese oxides is as much as 3 m. The ore is underlain by a jasperoid lens about 200 m long and 6-9 m thick. Beyond this lens the ore body rapidly pinches out. The second lens of siliceous rocks, extending 60 m and having a maximum thickness of 6 m, is related to the upper productive horizon. Only an insignificant amount of manganese mineralization is associated with this horizon, usually in the form of small accumulation of manganese oxides localized in jasperoid, or clastic rocks that are weakly mineralized at the contact with the underlying siliceous material.

**TULSEQUAH CHIEF and BIG BULL PROJECTS, NORTHWESTERN  
B.C.**

**1994 EXPLORATION PROGRAM:  
DIAMOND DRILLING, GEOLOGY,  
GEOCHEMISTRY and GEOPHYSICS**

**OF THE  
BIG BULL MINE AND BANKER AREA**

**NTS 104K/12  
Latitude: 58°40' N, Longitude: 133°35' W**

**for**

**REDFERN RESOURCES LTD.  
205-10711 Cambie Road  
Richmond, B.C.  
V6X 3G5**

**R.G. Carmichael, P.Eng., Redfern Resources Ltd.  
R.B. March, Redfern Resources Ltd.  
B.T. McGrath, Redfern Resources Ltd.**

**January 16, 1995**

**FILMED**

**VOLUME 2.0**

**FILMED**

**LOGIC  
ASSESSMENT  
REPORT**

**24,188**



## 2.0 BIG BULL PROPERTY GEOLOGY

### 2.1 DEPOSIT AREA STRATIGRAPHY

The Big Bull stratigraphy has been divided into five main lithologic units: unit 1 mafic volcanic rocks, unit 2 dacite tuffs and minor flows, unit 3 maroon andesite tuffs, unit 4 basalt tuffs, and unit 5 mafic intrusives (Figure 2.0). These subdivisions represent a modification of previous work by Dawson and Harrison (1993) and Carmichael and Curtis (1994). Feldspar-phyric mafic dikes and a distinctive quartz feldspar porphyry dike postdate all other lithologies, and are thought to be related to the Eocene Sloko Group.

#### *UNIT 1: MAFIC VOLCANIC ROCKS*

The oldest unit in the Big Bull mine stratigraphy is only exposed to the east of the deposit, and has not been intersected in drill core. It is characterized by mixed mafic lapilli and ash tuffs, with occasional fine-grained, massive, homogeneous, feldspar-phyric sections which are interpreted as flows. Lapilli tuffs typically contain quartz-amygdaloidal basalt fragments, and tend to be massive. Ash tuffs are thinly (1-2 cm) bedded to massive.

#### *UNIT 2: FELSIC TUFFS AND FLOWS*

Felsic crystal, crystal lithic, and lapilli tuffs host the ore at the Big Bull deposit. This unit is primarily grey to greenish grey, laminated to chaotically banded dacites, which have been petrographically identified as metamorphosed and deformed dacite tuff and crystal tuff. The tuffs are commonly weakly porphyritic, with plagioclase phenocrysts in a compositionally layered plagioclase-sericite-rich groundmass. Magnetite and/or hematite occurs as disseminations and disrupted bands forming up to 15% of the unit locally. Unit 2 typically shows chaotic banding on a 2 to 5-millimetre scale, although fragmental textures are rare. Locally well preserved bed forms show grain-size grading which helps to establish local structural relationships. Occasional massive, feldspar-phyric flows have been identified within this unit.

#### *UNIT 2a: QUARTZ-SERICITE-PYRITE*

Unit 2a represents parts of unit 2 which were hydrothermally altered during the formation of the Big Bull deposit. The rock comprises a strongly foliated sericite-quartz-pyrite assemblage, containing 5 to 20% disseminated and stringer pyrite, with local base metal sulphides and tetrahedrite. The quartz-sericite-pyrite alteration appears to form a stratiform layer near the top of the felsic tuffs, but may in places be discordant to stratigraphy.

#### *UNIT 2b: MASSIVE SULPHIDE*

Unit 2b includes mineralization that ranges from massive, banded sulphides, to 30 to 40% disseminated and stringer sulphides in a matrix of barite, sericite and silica. The mineralogy comprises pyrite, sphalerite, galena, chalcopyrite and tetrahedrite, in a matrix of barite and sericitized lithic fragments. The sulphides are recrystallized, with well developed annealed textures that have obliterated any primary features. The sericitic fragments within the mineralized lenses may represent altered lithic fragments that were incorporated in the mineralized interval.

#### *UNIT 3: ANDESITE TUFF*

Grey to maroon, fine to coarse-grained, locally phyllitic andesitic fragmental rocks conformably overlie unit 2 felsic tuffs. The maroon colour is typically due to fine-grained disseminated red hematite, and hematite-discoloured fragments that range in size from 0.5 to 50 millimetres. This unit is variably calcareous, with some sections containing up to 30% pervasive white calcite. The tuffs range from massive to very well bedded, with graded bedding and scour marks commonly, but not exclusively, indicating an overturned section.

### *UNIT 3a: IRON / MANGANESE CHEMICAL SEDIMENT*

Massive, black, fine-grained manganese silicates typically occur near the stratigraphic base of unit 3. They reach a maximum known thickness of 31 metres in drill hole BB94020. Interbeds of red mudstone occur locally within the manganese unit, as do breccia and replacement textures. XRD work by the Mineral Deposit Research Unit at the University of British Columbia has identified braunite and piemontite as the main manganese minerals in this unit. Lithogeochemical samples from this unit indicate that it is a mixture of manganese and iron minerals, with two samples from adjacent massive manganese\hematite layers in DDH BB94017 (179.2 m and 218.2 m) returning values of 20.3%  $\text{Fe}_2\text{O}_3$ , 23.1% MnO and 68.8%  $\text{Fe}_2\text{O}_3$ , 1.7% MnO respectively.

### *UNIT 3b: INTERBEDDED TUFF AND HEMATITE / MANGANESE*

This distinctive unit often occurs at the stratigraphic top of unit 3. Its bedded nature and unique appearance make it useful as a marker interval. Maroon to pink crystal and ash tuff are interbedded with black, massive manganese silicates and/or hematite on a 1 to 10-centimetre scale. Iron / manganese beds are contorted and disrupted, and appear to represent thinly bedded equivalents of unit 3a.

### *UNIT 4: BASALT TUFF*

Unit 4 comprises dark green, chlorite-epidote-rich, mafic lapilli, ash and crystal tuffs. Patches and streaks of black hematite (1 to 20 mm) characterize this unit. Sausseritized feldspar crystals and crystal fragments are common, locally forming up to 30% of the rock. This unit is in gradational contact with unit 3.

### *UNIT 5: MAFIC INTRUSIVES*

Mafic intrusives occur as both dark green, fine-grained chloritic diabase, and as coarser grained diorite. They are included as one unit here, although lithogeochemical data suggests there are more than one intrusive suite. Diabase sills and dykes are typically massive to moderately well foliated, contain abundant chlorite and biotite, and are devoid of primary textures. Their interpretation as intrusive is based largely on contact relations and stratigraphic position. However, they can be difficult to differentiate from massive intervals of unit 4, particularly when they are intrusive into that unit. A large body of blocky weathering diorite outcrops northwest of the glory hole area; the diorite is massive, equigranular to weakly feldspar phyric, and medium to fine grained.

# NATURAL ZEOLITES

## Occurrence, Properties, Use

Edited by

L. B. SAND

and

F. A. MUMPTON

## GEOLOGICAL OCCURRENCES OF ZEOLITE IN MARINE ENVIRONMENTS

AZUMA IJIMA

*Geological Institute, University of Tokyo, Japan*

**Abstract** – Twenty-two species of zeolites have been found in marine deposits of Quaternary through Devonian age which are now on land areas. Fresh-water non-marine deposits contain the same species plus faujasite. Geological occurrences of these zeolites are classified into five genetic types: burial diagenesis, contact metamorphism, hydrothermal alteration, submarine hydrothermal alteration, and percolating groundwater alteration. Rock-interstitial water interaction is prevalent during the zeolitization, and migration of chemical components occurs to some degree in all of the types.

Zeolite deposits of burial diagenesis origin in a thick sedimentary column of marine deposits are characterized by regional vertical zoning. In silicic tuff sequences, an unaltered glass zone without zeolites (Zone I) is successively followed by an alkali clinoptilolite-mordenite zone (Zone II), an analcime zone (Zone III), and an albite zone (Zone IV) in silica-saturated environments. Zone III is subdivided into analcime-heulandite (IIIa) and analcime-laumontite (IIIb) subzones, though the occurrences of calcium zeolites are generally local. The downward succession of authigenic silicates represents decreasing hydration. Both field and laboratory evidence prove that the alkali zeolites-albite reaction series is dependent upon temperature. Subsurface data obtained from deep wells show that it is 84–91°C at the boundary Zone II/Zone III and 120–125°C at Zone III/Zone IV. Na<sup>+</sup> is the predominant cation of interstitial water in marine deposits and alkali-saline lake deposits probably causes drastic lowering of the equilibrium temperature of the alkali zeolites-albite reaction series. For example, the reaction analcime + SiO<sub>2</sub> → albite + H<sub>2</sub>O occurs at a P<sub>H<sub>2</sub>O</sub> less than 2 kb at 180–190°C in pure water; 120–125°C in interstitial water of 1.5–2.5 × 10<sup>4</sup> ppm Na<sup>+</sup> in marine deposits; and 55–65°C in water of 10<sup>5</sup> ppm Na<sup>+</sup> in alkali-saline lake deposits.

Compositional changes of zeolites within diagenetic zones are still not fully understood. In the heulandite group, high-silica, alkali-rich clinoptilolite in Zone II is replaced by high-silica heulandite in Zone III, probably via intermediate Ca-rich clinoptilolite. In the mordenite group, Na-rich varieties in Zone II tends to be replaced by Ca-rich varieties in Zone II. Systematic changes in analcime composition have not been recognized in Zone III. Albite derived from analcime seems to be richer in Ca and K than that from plagioclase grains.

Statistics of 812 deep-sea zeolite samples collected from Initial Reports of the Deep Sea Drilling Project, Volumes 1 through 32 except 30, reveal that phillipsite concentrates in pelagic brown clay and calcareous sediments of younger age in the Pacific proper, while clinoptilolite concentrates in terrigenous mud, silicic volcanic sediments, and calcareous sediments in the Pacific margin, and in the Atlantic and the Indian Oceans. Most phillipsite may be derived from mafic glass,

whereas most clinoptilolite formed from silicic glass or from mafic glass, with excess free silica being of biogenic or weathering origin. This hypothesis can easily explain why phillipsite does not occur in the silicic tuff sequences of marine deposits which are now on land. Temperature seems to be insufficient to promote the reaction clinoptilolite-analcime in deep-sea sediments at a sub-bottom depth less than 1000 m.

### Geologic age and abundance

Most zeolite species occur predominantly in marine and fresh-water non-marine deposits of Cenozoic and Mesozoic ages. The oldest zeolite-containing deposits (laumontite) are Devonian in age in Siberia (Buryanova, 1960) and in New South Wales (Packham and Crook, 1960); they are Jurassic in age in Japan (Fukuda, 1972). Laumontite has also been reported in Pre-cambrian volcanic sediments in Georgia, U.S.A. (Ross, 1958).

### Genetic types of zeolitization

The occurrences of zeolites in marine deposits on land are classified into five genetic types, as illustrated schematically in Fig. 1:

- Burial diagenesis.
- Contact metamorphism.
- Hydrothermal alteration.
- Submarine hydrothermal alteration.
- Percolating groundwater alteration.

**Burial diagenesis.** Zeolites are formed as sediments are successively buried by overlying, younger sediments. As a result, zeolites occur in a progressive zonal arrangement in a thick sedimentary column (Iijima and Utada, 1971). This phenomenon is very similar to or the same as the burial metamorphism of Coombs (1954, 1971); however, the term burial diagenesis is preferable because alkali zeolites such as clinoptilolite, mordenite, and analcime are almost always present in the marine deposits and Coombs (1971) excluded these alkali zeolites from the metamorphic régime.

**Contact metamorphism.** Zeolites are formed in contact aureoles of granite intrusives, resulting in a zonal arrangement around the intrusive body. This type of occurrence seems to be limited to younger orogenic belts where relatively small-scale intrusions occur at shallow

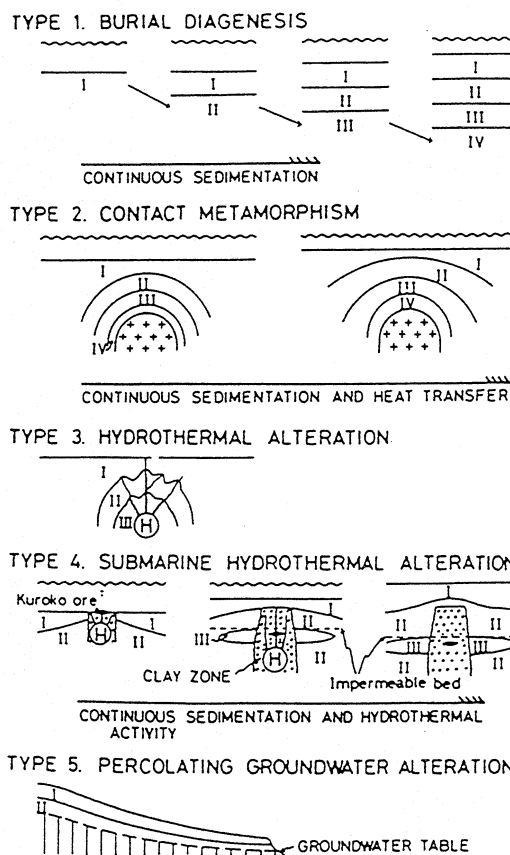


Fig. 1. Five genetic types of the occurrences of zeolites in marine and non-marine fresh-water sediments.

depths below the surface or sea-floor into incompletely consolidated, Tertiary volcanic sediments, e.g., in the Green Tuff region of Japan (Seki *et al.*, 1969; Motojuku Rock Alteration Research Subgroup, 1970; Utada, 1973, 1974) and Bulgaria (Kostov, 1969). Calcium zeolites, such as stilbite, heulandite, mordenite, laumontite, wairakite, and yugawaralite, are characteristic in this type.

**Hydrothermal alteration.** Zeolites are formed by hydrothermal alteration in active geothermal areas such as Wairakei in New Zealand (Steiner, 1953), Onikobe (Seki *et al.*, 1969), and Otake (Hayashi, 1973) in Japan, Yellowstone (Honda and Muffler, 1970), etc. Calcium zeolites, such as mordenite, laumontite, and wairakite, are characteristic of this type.

**Submarine hydrothermal alteration.** Zeolites are formed by submarine hydrothermal alteration which is commonly related to the Kuroko Pb-Zn-Cu sulfide-ore mineralization, e.g., in the Odate (Iijima, 1974) and Aizu (Utada *et al.*, 1974) districts in the Green Tuff region of northeast Honshu. A lenticular analcime zone is

characteristic, which overlies and grades laterally into the argillaceous ore-bearing zones. Analcime formed by reaction of precursor clinoptilolite and mordenite with Na-rich solution permeating penecontemporaneous, porous, pumiceous sediments beneath the Miocene sea-floor from the argillaceous zones.

Ferrierite, a magnesium zeolite, is locally associated with mordenite and clinoptilolite in the Kuroko mineralization areas (Hayakawa and Suzuki, 1970; Utada *et al.*, 1974). It is also found in veins in the Kuroishi Mg-bentonite deposit of Aomori which is an alteration product of Miocene dacite pumiceous tuffs due to penecontemporaneous submarine hydrothermal activity.

Laumontite occurs locally in a deeper level of the Odate district (Iijima, 1974). To the east, laumontite and wairakite are common in the Hanawa mining district (Seki *et al.*, 1968) where gypsum and anhydrite are abundant with the Kuroko-type ore deposits. Laumontite forms an irregularly shaped zone around the gypsum ore deposits of the Wanibuchi mine in Shimane, southeast Honshu (Miura, 1969; Yanagimoto, 1970). These calcium zeolites may have formed by submarine hydrothermal alteration at deeper levels below the sea floor than the sodium and magnesium zeolites. Alternatively, they may have formed by hydrothermal alteration on land at a later stage.

*Percolating groundwater alteration.* Zeolites are formed by reaction of volcanic glass with percolating groundwater through porous tuffs. Zeolitization occurs at a depth of 200 m below the surface in silicic tuffs of the John Day Formation of Oregon (Hay, 1963) and at a depth of about 5-50 m in ultramafic palagonite tuffs of the Honolulu Group on Oahu Island, Hawaii (Hay and Iijima, 1968 a, b).

Rock-interstitial water reactions take place during zeolitization. In addition to alkalis and alkali earths, silica and alumina are also dissolved from glass during palagonitization of ultramafic tuffs of Oahu; most of the elements are precipitated as zeolites and carbonates in cement, but some are leached from the system (Hay and Iijima, 1968b). The percolating groundwater type is really an open-system as classified by Munson and Sheppard (1974). In other types also, significant migration of chemical components occurs on various scales (Utada, 1965, 1971; Utada *et al.*, 1967, 1974; Iijima, 1974; Iijima and Utada, 1967).

L42

## M - SKARNS AND SKARN DEPOSITS IN THE CANADIAN CORDILLERA

Gerald E. Ray, British Columbia Geological Survey

Ray, G.E. (1998): Skarns and Skarn Deposits in the Canadian Cordillera; in *Metallogeny of Volcanic Arcs*, B.C. Geological Survey, Short Course Notes, Open File 1998-8, Section M.

### ABSTRACT

The Canadian Cordillera contains more than 1000 skarn occurrences, and some of its Au, Cu and W skarn deposits are of world-class size and grade. These major deposits include the Nickel Plate Au skarn, the Whitehorse Copper Belt, Ingerbelle, Craigmont and Phoenix Cu skarns and the Mactung, Lened and Cantung W skarns.

The more than 1000 recorded skarns can be broadly separated into three groups. One small group of 27 occurrences is associated with Cu, Mo or W porphyry deposits; in most cases the skarn alteration represents only a minor part of the porphyry system although the significant Cu-Au skarn components of the Ingerbelle, Stikine Copper and Mount Polley porphyry Cu deposits are notable exceptions. Another group of 37 skarns occurs as barren wallrock alteration that hosts or halos large AuCu-bearing quartz and/or sulphide vein systems. Economically important examples include the vein deposits at the Second Relief and Evening Star mines in southern BC.

The third and largest group comprises more than 960 occurrences. On the basis of their chemistry or dominant minerals, these include 436 Cu, 147 Fe, 142 Pb-Zn, 117 W, 33 Au, 29 Mo, 19 Sn and 19 industrial mineral skarns; the latter are a potential source of minerals such as wollastonite, garnet, fluorite, tremolite or rhodonite. In addition, 4 occurrences represent uranium or RRE skarns and a further 16 skarns are of unknown class.

Although the Yukon is substantially smaller in area than B.C., it contains a significantly greater number of Sn and W skarns, and a smaller number of Fe, Au and Cu skarns. The abundance of chalcophile skarns in B.C reflects the relative predominance of oceanic island arc-related plutonic rocks in that province, whereas the Yukon contains a greater proportion of intrusions derived from continental crust and consequently the associated skarn deposits are lithophile in character.

Skarns are found in at least 24 different tectono-stratigraphic terranes (as defined by Wheeler et al., 1991), but most are concentrated in just five terranes, namely Wrangellia, Stikinia, Quesnellia, Cassiar and Yukon-Tanana, as well as in the Ancestral North American craton. A spatial and temporal relationship exists between certain skarn classes, their metal production, and the character and origin of the host terranes. Over 80% of the skarns in B.C. are hosted by terranes dominated by island-arc rocks and these have accounted for virtually all the Fe, Cu and Au metal produced from skarns in the province. By contrast, only 5% of the skarns in B.C. are hosted by the North American craton and basement, yet these have been responsible for all the province's W production.

Most skarns in the region were formed during three major plutonic episodes that had distinctly different metallogenies. The oldest and most economically important was during the Early to Middle Jurassic

when most of the regions Au, Fe, Cu and Mo skarns were developed, as well as many Cu-Au and Cu-Mo porphyry deposits. The next most important skarn-forming plutonic event was during the Cretaceous. This resulted in many of the regions W and Sn skarns, as well as the Whitehorse Copper Belt deposits and some Cu skarns in the Greenwood camp of B.C. The third and youngest episode, during the Eocene-Oligocene, was less important and only resulted in a small number of W, Cu and Pb-Zn skarns.

The size and diversity of skarns in the Canadian Cordillera, together with their significant reserves and past metal production indicate that the region has a high potential for the discovery of new economic deposits. Moreover, the recognition that specific geological terranes in the region are prospective hosts for certain economic skarns, and the recent discovery elsewhere of major Cu and/or Au-rich skarn deposits in geological settings that are analogous to parts of the Canadian Cordillera, should spur exploration. In addition to the prospective island arc terranes, other targets include: re-evaluating many of the larger Cu skarns( such as those in the Whitehorse Copper and Greenwood camps) for distal Au skarns or Au-bearing mantos, exploring various Ca-rich volcanic belts for deposits similar to the QR Au skarn in B.C. or the Candelaria Cu-Au skarn in Chile, and examining areas with platformal, dolomitic carbonates for deposits resembling either the Butte Highlands Au skarn in Montana or the Big Gossan-IOZ Cu-Au skarns in Indonesia. In addition, parts of the eastern and northern Cordillera have many of the favorable geological features that characterize other Pb-Zn-Ag skarn or manto districts elsewhere in the world.



## PATHWAYS '98 SHORT COURSE NOTES

## TABLE OF CONTENTS

## SKARNS AND SKARN DEPOSITS IN THE CANADIAN CORDILLERA

by G.E. Ray

Abstract.....	1
Introduction.....	4
Skarn Terminology and Classification.....	5
Number and Distribution of Skarns.....	6
Tectonic Setting of Skarn-related Plutonism.....	7
Skarn Deposits	
Introduction.....	8
Iron (Magnetite) Skarns - General Synopsis.....	11
Iron Skarns in the Canadian Cordillera.....	12
Copper Skarns - General Synopsis.....	13
Copper Skarns in the Canadian Cordillera.....	14
Gold Skarns - General Synopsis.....	16
Gold Skarns in the Canadian Cordillera.....	18
Molybdenum Skarns - General Synopsis.....	20
Molybdenum Skarns in the Canadian Cordillera.....	21
Tungsten Skarns - General Synopsis.....	23
Tungsten Skarns in the Canadian Cordillera.....	24
Lead-Zinc Skarns - General Synopsis.....	25
Lead-Zinc Skarns in the Canadian Cordillera.....	27
Tin Skarns - General Synopsis.....	28
Tin Skarns in the Canadian Cordillera.....	29
Industrial Mineral Skarns.....	30
Chemistry of the Skarn-related Intrusions.....	31
Conclusions.....	33
Acknowledgments.....	34
References.....	35

# SKARNS AND SKARN DEPOSITS IN THE CANADIAN CORDILLERA

Gerald E. Ray

*B.C. Geological Survey, Box 9320 Stn Prov Govt, Victoria, B.C. Canada, V8W 9N3*

## INTRODUCTION

These short course notes are based, in part, on a forthcoming paper by Ray and Dawson (1998, in press). In the short course, we will examine the distribution, age and tectonic setting of skarns throughout the Canadian Cordillera, together with the mineralogical and chemical characteristics of various Au, Cu, Fe, Mo, W, Pb-Zn, and Sn skarn deposits.

The Canadian Cordillera has had a long history of mining metal from skarn, and some of its Au, Cu and W deposits are of world-class size and grade (Fig. 1; Tables 1A and B). The recently closed Nickel Plate mine at Hedley, B.C., for example, represented a 13.4 Mt deposit grading 5.3 g/t Au. The largest Cu skarns are associated with porphyry Cu systems; they include Ingerbelle (> 200 Mt of 0.4 % Cu) and Mount Polley (> 100 Mt of 0.38 % Cu). Other major Cu skarns include Craigmont (c. 29 Mt of 1.18 % Cu) and Phoenix (c. 21 Mt of 1.1 % Cu) in southern B.C., and the Whitehorse Copper Belt (10.1 Mt of 1.5 % Cu) in the Yukon. The world-class W skarns of the northern Cordillera include Mactung (Yukon) with reserves of 57 Mt grading 0.95 %  $\text{WO}_3$  and Cantung (N.W.T) with production plus reserves of 9 Mt of 1.42 %  $\text{WO}_3$ .

The British Columbia and Yukon geoscience information systems, MINFILE, indicate there are more than 1000 recorded occurrences of skarn, as defined by Burt (1977), in the Canadian Cordillera. Of these, 735 are in British Columbia, 291 in Yukon (Fig. 2) and a small number in the NWT. Most are believed to be infiltration skarns related to magmatic hydrothermal fluids. The majority have calcic mineral assemblages (i.e. garnet-clinopyroxene-epidote-wollastonite); the comparative rarity of magnesian skarns with olivine-serpentine-phlogopite gangue assemblages reflects the absence of major plutonism in areas with extensive platformal dolomites. Most of the skarns are associated with varying amounts of metallic minerals, and they range from small occurrences to large deposits that contain more than 30 million tonnes of ore (Tables 1A and B).

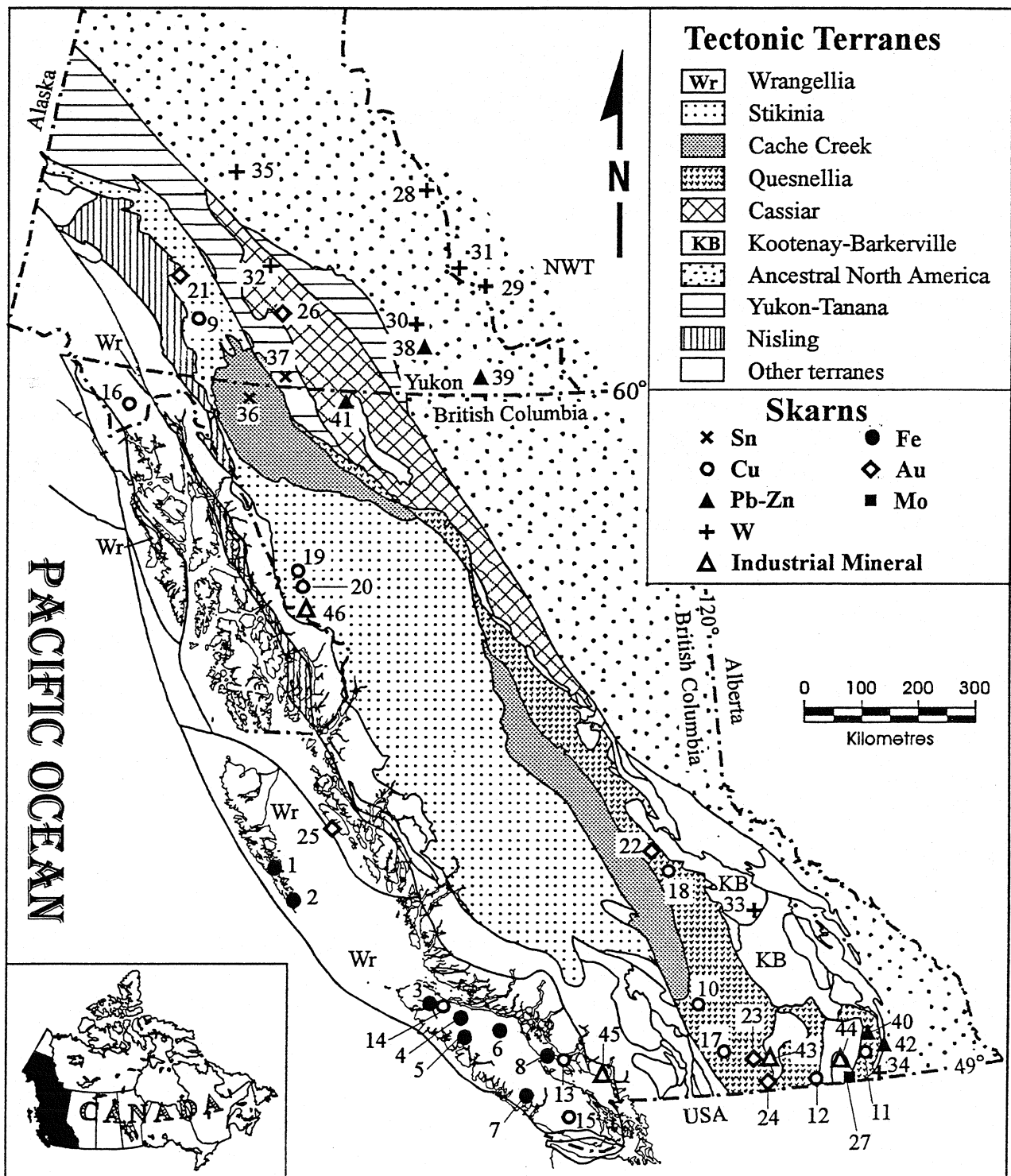


Figure 1. Simplified terrane map of the Canadian Cordillera (after Wheeler *et al.* (1991) showing locations of significant skarns or mantos.

## LEGEND FOR FIGURE 1

### SIGNIFICANT SKARNS IN THE CANADIAN CORDILLERA (*References in italics*)

#### Fe SKARNS

- 1 Tasu (*Sutherland Brown, 1968; Sangster, 1969*)
- 2 Jessie-Jedway (*Sutherland Brown, 1968; Sangster, 1969*)
- 3 Merry Widow, Kingfisher (*Eastwood, 1965; Haug, 1977; Ray and Webster, 1991*)
- 4 Iron Crown (*Sangster, 1969; Meinert, 1984*)
- 5 Ford (*Sangster, 1969*)
- 6 Iron Hill (*Sangster, 1969; Meinert, 1984*)
- 7 Brynnor (*Sangster, 1969*)
- 8 Texada Island (Prescott, Paxton, Yellow Kid, Lake) (*Bacon, 1957; 1984; Webster and Ray, 1990a and b*)

#### Cu SKARNS

- 9 Whitehorse Cu (Little Chief, Arctic Chief, War Eagle etc.) (*Morrison, 1981; Tenney, 1981; Meinert, 1986*)
- 10 Craigmont (*Morrison, 1980; Webster et al., 1992*)
- 11 Queen Victoria (*Little, 1960; Webster et al., 1992; Ray and Webster, 1997*)
- 12 Greenwood (Phoenix, Motherlode, Emma etc.) (*Church, 1986; Ettlinger and Ray, 1989; Ray and Webster, 1997*)
- 13 Texada Island (Marble Bay, Cornell, Little Billie) (*Ettlinger, 1990; Webster and Ray, 1990a and b*)
- 14 Old Sport, Benson Lake (*Eastwood and Merrett, 1962; Ettlinger and Ray, 1989; Ray and Webster, 1991*)
- 15 Blue Grouse (*Fyles, 1955; BC Minfile*)
- 16 Rainy Hollow (Maid of Erin, State of Montana) (*Webster et al., 1992*)
- 17 Ingerbelle (Porphyry-related) (*Fahrni et al., 1976; Preto, 1972*)
- 18 Mount Polley (Porphyry-related) (*Fraser et al., 1995*)
- 19 Galore Creek (Porphyry-related) (*Enns et al., 1995*)
- 20 McLymont NW (*Ray et al., 1991*)

#### Au SKARNS

- 21 Guder (*Yukon MINFILE*)
- 22 Quesnel River (QR) (*Fox and Cameron, 1995*)
- 23 Hedley (Nickel Plate, French, Canty etc.) (*Billingsley and Hume, 1941; Ettlinger et al., 1992; Ray and Dawson, 1994*)
- 24 Dividend-Lakeview (*Ettlinger and Ray, 1989*)
- 25 Banks Island (*Ettlinger and Ray, 1989*)
- 26 Ketza River (Manto) (*Cathro, 1990; Dawson, 1996b*)

#### Mo SKARNS

- 27 Coxey, Novelty etc. (*Little, 1963; Fyles, 1984; Hoy et al., 1992; Webster et al., 1992*)

#### W SKARNS

- 28 MacTung (*Dick, 1976, 1980; Dick and Hodgson, 1982, 1983*)
- 29 CanTung (*Dick, 1980; Dick and Hodgson, 1983*)
- 30 Bailey (*DIAND, 1981; Yukon MINFILE*)
- 31 Lened (*Glover and Buson, 1988*)
- 32 Risby (*Northern Miner July 8, 1982, p. 30*)
- 33 Dimac (*Dawson et al., 1983; Webster et al., 1992*)
- 34 Salmo Camp (Emerald Tungsten, Dodger etc.) (*Fyles & Hewlett, 1959; Mulligan, 1984; Ray & Webster, 1997*)
- 35 Ray Gulch (*Lennan, 1986; Yukon MINFILE*)

#### Sn SKARNS

- 36 Atlin (*Ray et al., 1997*)
- 37 JC (Viola) (*Layne and Spooner, 1986, 1991*)

#### Pb-Zn SKARNS

- 38 Sa Dena Hes (*Dawson, 1964*)
- 39 Quartz Lake (*Vaillancourt, 1982*)
- 40 Piedmont (*Webster et al., 1992*)
- 41 Midway (Manto) (*Bradford, 1988; Nelson, 1991*)
- 42 Bluebell (Manto) (*Hoy, 1980*)

#### INDUSTRIAL MINERAL SKARNS

- 43 Mount Riordan-Crystal Peak (Garnet) (*Grond et al., 1991; Ray et al., 1992*)
- 44 Rossland Wollastonite (Wollastonite) (*Stinson, 1995*)
- 45 Mineral Hill (Wollastonite) (*Ray and Kilby, 1996*)
- 46 Isk-Zippa Mountain (Wollastonite) (*Jaworski and Dipple, 1996*)

Table 1A: Tonnage, grade and metal ratios of some skarn deposits in B.C. listed by tectonic terrane.

WRANGELLIA							
Skarn class	Skarn & Minfile No.	Size (t)**	Au g/t	Ag g/t	Cu %	Cu/Au	Ag/Au
Cu (Au)	Benson Lake 092L091	24 905	0.98	7.59	1.92	19592	8
Cu	Cornell 092F112	40 687	11.58	53.94	3.36	2902	5
Cu (Fe)	Indian Chief 092E011	73 608	0.31	23.20	1.50	48387	76
Cu	Lily 103B028	13 410	3.82	64.32	4.28	11204	17
Cu	Little Billie 092F105	47 693	5.70	18.81	1.29	2263	3
Cu	Marble Bay 092F270	284 728	5.46	44.33	2.38	4359	8
Cu (Au)	Old Sport 092L035	2 631 155	1.46	4.41	1.55	10616	3
Cu	Yreka 092L052	133 572	0.34	31.22	2.71	79706	91
Fe	Brynnor 092F001	3 909 001	-	-	-	-	-
Fe	Ford 092L028	1 578 396	-	-	-	-	-
Fe	Glengary 092E001	56 700	-	-	-	-	-
Fe	Iron Crown-Nimkish 092L034	1 050 887	-	-	-	-	-
Fe	Iron Hill-Argonaut 092F075	3 655 773	-	-	-	-	-
Fe	Iron Mike 092K043	135 772	-	-	-	-	-
Fe	Jessie-Jedway 103B026	3 747 350	-	-	-	-	-
Fe	Kingfisher 092L045	380 525	-	-	-	-	-
Fe	Merry Widow 092L044	3 371 813	-	-	-	-	-
Fe	Prescott-Paxton-Yellow Kid-Lake	20 179 709	0.04	1.17	0.12	30000	27
Fe	Tasu 103C003	16 190 923	0.06	2.42	0.37	61667	38
QUESNELLIA							
Au	Canty 092HSE064	1 483	11.11	0.02	-	-	0.002
Au	Dividend-Lakeview 082ESW001	94 531	4.53	0.78	0.08	177	0.2
Au	French Mine 092HSE059	82 046	19.85	2.45	0.02	10	0.1
Au	Good Hope 092HSE060	11 115	14.93	10.76	0.01	7	0.7
Au	Nickel Plate-Mascot	13 438 358	5.30	c. 0.6	c. 0.1	25	0.3
Au	Tillicum 082FNW234	226	234.03	242.64	-	-	1
Au	QR (Quesnel River) 093A121	1 300 000	c. 4.7	c. 4.0	-	-	1
Cu	***Ingerbelle 092HSE004	c. 216 000 000	0.16	0.63	0.40	25000	4
Cu	***Galore Creek 104G090	c. 280 000 000	c. 0.4	7.70	0.67	16750	19
Cu	***Mount Polley 093A008	c. 100 000 000	0.55	4.50	0.38	6909	8
Cu	B.C. 082ESE060	93 874	0.33	71.00	4.36	132121	215
Cu	Craigmont 092ISE035	29 325 342	0.003	0.01	1.18	3933333	3
Cu	Emma 082ESE062	240 948	0.88	10.10	0.98	11136	11
Cu	Greyhound 082ESE050	221 200	0.07	1.58	0.27	38571	23
Cu	Mother Lode-Sunset 082ESE034	5 049 201	1.07	4.31	0.70	6542	4
Cu	Oro Denoro 082ESE063	124 001	0.94	7.69	1.36	14468	8
Cu	Phoenix 082ESE020	21 552 283	1.30	8.49	1.09	8385	7
Cu	Queen Victoria 082FSW082	45 352	0.17	20.95	1.48	87059	123
Cu	Rawhide 082ESE026	852 849	1.24	8.10	0.99	7984	7
Cu	Snowshoe 082ESE025	545 129	2.36	9.08	1.16	4915	4
Pb-Zn	Piedmont 082FNW129	479	-	149.15	-	-	-
KOOTENAY							
Au	Jumbo 082FSW111	30 794	14.15	0.40	-	-	0.03
Pb-Zn	Goldfinch 082ESE004	1 258	29.25	2602.00	-	-	89
Mo (W)	Coxey 082FSW110	1 035 509*	-	-	-	-	-
Mo (Au)	Giant 082FSW109	4 131	27.41	5.63	0.03	11	0.2
W	Dimac 082M123	18 350*	-	-	-	-	-
ALEXANDER							
Cu	Maid of Erin 114P007	3 285	0.10	452.54	7.42	742000	4525
ANCESTRAL N. AMERICA							
W	Salmo Camp (Emerald Tungsten, Dodger, Invincible, Feeney 082FSW010, 011, 218, 247)	1 500 000*	-	-	-	-	-

\*\* Deposit size based on either tonnage mined or milled, or on reserves.

\*\*\*Skarns associated with large alkalic porphyry systems.

\*Note: Coxey camp grades c. 0.17% Mo, Dimac grades c. 0.57 % WO<sub>3</sub>, Salmo Camp grades c. 0.50 % WO<sub>3</sub>

Data from B.C. MINFILE, Dawson and Kirkham (1996), Ray and Webster (1997) and Enns et al., (1995).

**Table 1B: Tonnage and grade of some skarn deposits in the Yukon and NWT listed by tectonic terrane.**

Skarn class	Deposit	Production (t)	Reserves (t)	Au g/t	Ag g/t	Cu %	WO <sub>3</sub> %
<b>NORTHERN STIKINE</b>							
<b>(Whitehorse Cu Belt)</b>							
Cu	Little Chief	8 536 400	-	0.75	9.10	1.5	NA
Cu	Keewenaw	159 000	202 000	NA	NA	1.0	NA
Cu	Arctic Chief	201 800	-	1.03	17.10	1.4	NA
Cu	Kodiak Cub	-	57 000	NA	NA	1.2	NA
Cu	Cowley Park	-	1 552 000	0.20	3.80	1.0	NA
Cu	Best Chance	-	447 000	0.03	NA	0.7	NA
Cu	Gem	-	625 000	NA	NA	1.0	NA
Cu	Black Cub N.	-	156 000	NA	NA	0.8	NA
Cu	Black Cub S.	187 000	20 000	0.20	12.30	1.3	NA
Cu	War Eagle	899 900	-	0.20	8.60	1.2	NA
Cu	Pueblo	127 635	-	0.17	NA	3.5	NA

Total Production from 11 deposits in Whitehorse Cu Belt (1898-1982) = 10.1 Mt grading c. 1.5% Cu

<b>NORTHERN STIKINE</b>							
Au	Guder (Goldstar)	-	123 800	4.10	48.00	NA	NA
<b>SELWYN BASIN</b>							
Au	Marn	-	275 000	8.60	17.00	1.0	0.1
<b>MACKENZIE PLATFORM</b>							
W	MacTung	-	57 200 000	NA	NA	NA	0.95
W	CanTung	-	9 000 000 *	NA	NA	NA	1.42
<b>CASSIAR PLATFORM</b>							
W	Risby	-	2 700 000	NA	NA	NA	0.81
W	Bailey	-	272 160	NA	NA	NA	1.00
<b>MCQUESTON PLUTONICS</b>							
W	Ray Gulch (Garnet)	-	7 260 000	NA	NA	NA	0.87

Skarn class	Deposit	Production (t)	Reserves (t)	Pb %	Zn %	Ag g/t	Sn %
<b>YUKON-TANANA</b>							
Sn	JC (Viola)	-	1 250 000	NA	NA	NA	0.54
<b>ANCESTRAL N. AMERICA</b>							
Pb-Zn	Sa Dena Hes	c. 527 000	c. 2 940 000	8.4	12.9	65.0	NA

Data compiled from Yukon MINFILE, Dick (1980), Watson (1984), Dawson (1996a, b and c), Layne and Spooner (1991), Dawson and Kirkham (1996), MacKay et al. (1993).

\* Cantung data includes reserves and production figures.

NA = data no available

## SKARN TERMINOLOGY AND CLASSIFICATION

The term *skarn* describes Ca or Mg silicate alteration formed by the replacement of Ca or Mg-rich sedimentary, volcanic or intrusive rocks; the silicates are commonly also rich in Fe, Al, and possibly Mn. As a skarn is defined by its gangue mineralogy, it is not necessarily mineralized and many skarns are barren. Skarn is mostly coarse grained, although fine to medium-grained textures may occur. It commonly forms at relatively high temperatures by either of the following two processes:

1. Localized metasomatic reaction, during regional or contact metamorphism, between different lithologies, such as between argillite and limestone. This alteration is often called "*reaction skarn*" (Magnusson, 1960).
2. Infiltration metasomatism involving the entry, generally into calcareous rocks, of hydrothermal fluids of either magmatic or metamorphic origin. Such alteration is commonly called "*replacement*" or "*infiltration skarn*".

Mineralization may occur with either reaction or infiltration skarns. However, most of the world's major metallic skarn deposits are believed to be infiltration skarns related the introduction of magmatic hydrothermal fluids. The alteration commonly overprints the genetically related intrusion to produce *endoskarn*, as well as the adjacent country rocks to form *exoskarn*. Most of the world's economic skarn deposits occur in exoskarn (Einaudi and Burt, 1982), although in many deposits the alteration may be so intense that the original protolith is unrecognizable.

Based on alteration assemblages, skarns are separable into two broad groups: *magnesian skarns*, where the replacement of Mg-rich volcanic or sedimentary rocks results in assemblages containing olivine, phlogopite, serpentine, spinel, Mg-rich clinopyroxene and chlorite, orthopyroxene, garnet, pargasite and humite group minerals; and *calcic skarns*, where the replacement of limestone or other Ca-rich sedimentary or volcanic rocks produces assemblages dominated by garnet, clinopyroxene, epidote, calcic amphibole and wollastonite.

Metal deposits associated with a skarn gangue are termed *skarn deposits* (Burt, 1972, 1977). On the basis of the dominant economic metal, at least seven major classes of metallic skarn deposit are recognized: Fe, Cu, Mo, W, Pb-Zn, Sn and Au skarns (Knopf, 1942; Burt, 1972, 1977; Einaudi *et al.* 1981; Orris *et al.*, 1987; Ray *et al.*, 1990; Meinert, 1988, 1989, 1992; Ettlinger and Ray, 1989a; Theodore *et al.*, 1991). In addition, some skarns are a source of wollastonite, garnet, rhodonite and other products and these can be classed as Industrial Mineral Skarns.

## NUMBER AND DISTRIBUTION OF SKARNS

The more than 1000 skarns recorded in the Canadian Cordillera can be broadly separated into three groups. One small group of 27 occurrences is associated with Cu, Mo or W porphyry deposits (Fig. 2), although in most cases the skarn alteration represents only a minor part of the overall porphyry system. However, the significant Cu-Au skarn components of the Ingerbelle, Stikine Copper and Mount Polley porphyry Cu deposits are notable exceptions.

Another group, comprising 37 occurrences, is characterized by generally barren wallrock skarn assemblages that are associated with large Au±Cu-bearing quartz and/or sulphide vein systems (Fig. 2). In many cases, the genetic and temporal relationship between the veins and the skarn envelopes is not specified. However, those in the Rossland area of southern British Columbia, for example, appear to be related and coeval (Höy *et al.*, 1992).

The third and largest group comprises 962 occurrences of which 695 are in B.C. and 267 in the Yukon (Fig. 2). On the basis of their chemistry or dominant minerals, these are classed as follows: 436 Cu, 147 Fe, 142 Pb-Zn, 117 W, 33 Au, 29 Mo, 19 industrial mineral and 19 Sn skarns, as well as a further 16 occurrences of unknown class. An additional 4 occurrences in the Yukon can also be classed as Uranium or rare earth element (REE) skarns. Although the Yukon is substantially smaller in area than B.C., it contains a significantly greater number of Sn and W skarns, and a smaller number of Fe, Au and Cu skarns (Fig. 2; Tables 1A and B). This difference is ascribed to the relative abundance of island arc-related plutonic rocks and associated chalcophile deposits in B.C, whereas in the Yukon a greater proportion of intrusions is derived from the anatexis of continental crust, and the associated skarn deposits are lithophile in character.

Skarns are found in at least 24 different tectono-stratigraphic terranes and subterrane (as defined by Wheeler *et al.*, 1991), but most are concentrated in just five, namely Wrangellia, Stikinia, Quesnellia, Cassiar and Yukon-Tanana, as well as in the Ancestral North American craton (Tables 2A and B). The 24 terranes vary considerably in character. They include those dominated by island-arc rocks (e.g. Wrangellia, Stikinia and Quesnellia), those with abundant ocean-floor material (e.g. Cache Creek and Slide Mountain), those with pericratonic or displaced platformal rocks deposited at or relatively close to the ancestral continental margin (e.g. Nisling, Kootenay, Yukon-Tanana and Cassiar) or rocks representing either cratonic basement (e.g. Monashee) or supracrustals deposited on Ancestral North America (e.g. Selwyn Basin, Mackenzie Platform).

A spatial and temporal relationship exists between certain skarn classes, their metal production, and the character and origin of the host terranes. Skarns are poorly developed in terranes composed



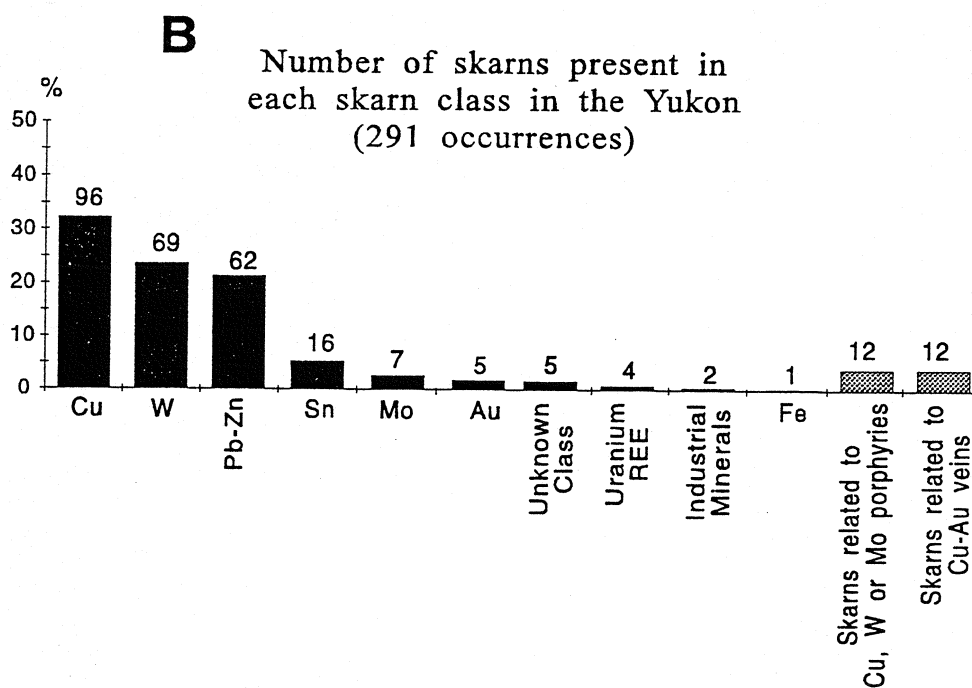
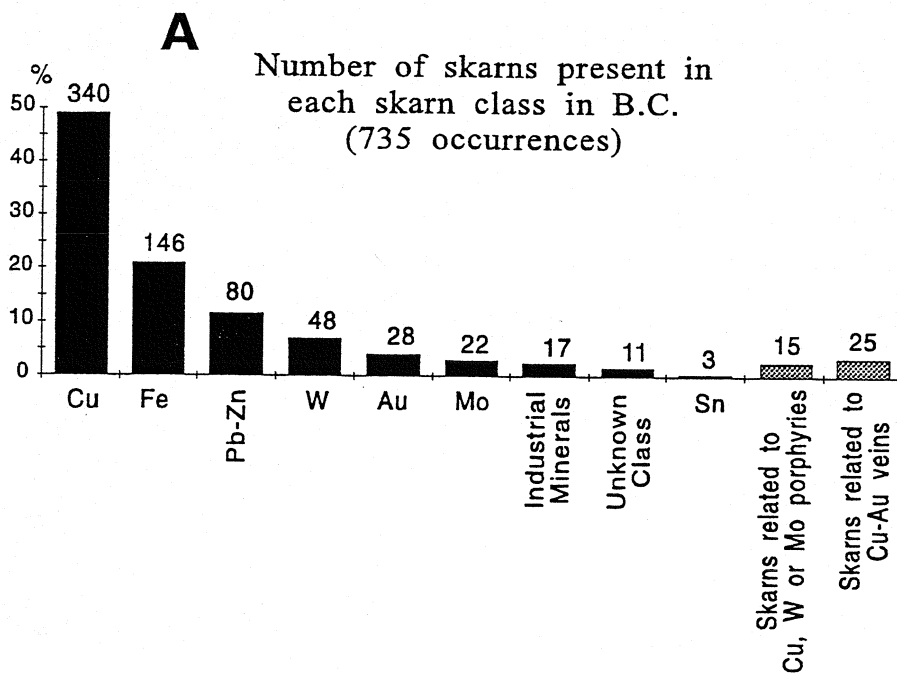


Figure 2. Bar charts showing percentage of occurrences in each skarn class in;  
A: British Columbia, and  
B: the Yukon. Number above each bar = number of skarn occurrences.

Table 2A: Number of skarns in B.C. listed by class and tectonic terrane

Skarn class	Cu	Fe	Pb-Zn	W	Au	Mo	Sn	Porphyry-related	Vein-related	IM*	Unknown class	BC TOTAL
Total No.	340	146	80	48	28	22	3	15	25	17	11	735
% of Total	46.3	19.9	10.9	6.5	3.8	3.0	0.4	2.0	3.4	2.3	1.5	100
No. of Producers	63	18	12	7	9	3	0	-	-	3	0	115
<b>TERRANE</b>												
Cassiar	-	-	8	12	-	3	-	-	-	-	-	23
Cache Creek	3	-	-	1	-	-	3	-	-	-	-	7
Coast/ undiv met complex	8	-	-	-	-	-	-	-	-	-	-	8
Stikine	47	6	11	2	1	1	-	7	3	-	2	80
Nisling	-	1	-	-	2	-	-	-	-	-	1	4
Wrangellia	173	136	25	-	1	-	-	-	5	7	-	347
Alexander	19	1	8	-	4	1	-	-	1	1	-	35
Gambier	2	-	2	-	-	-	-	-	-	-	-	4
Kootenay	7	1	1	5	2	8	-	1	-	3	-	28
Unknown	-	1	-	-	-	1	-	-	-	-	-	2
Chilliwack	2	-	-	-	-	-	-	-	-	-	-	2
Bridge River	4	-	1	2	-	-	-	-	-	-	2	9
Cadwallader	3	-	1	1	-	-	-	-	-	-	1	6
Quesnellia	64	-	10	1	18	4	-	7	15	2	5	126
Slide Mountain	4	-	2	-	-	-	-	-	-	-	-	6
Dorsey	1	-	1	3	-	-	-	-	1	-	-	6
Barkerville	1	-	-	4	-	-	-	-	-	-	-	5
Monashee	-	-	-	2	-	1	-	-	-	1	-	4
Harper Ranch	-	-	-	-	-	1	-	-	-	1	-	2
Ancestral N. America	2	-	10	15	-	2	-	-	-	2	-	31
SUM	340	146	80	48	28	22	3	15	25	17	11	735

IM\* = Industrial mineral skarns

Table 2B: Number of skarns in the Yukon listed by class and tectonic terrane

Skarn class	Cu	W	Pb-Zn	Sn	Mo	Au	Fe	U/REE*	Porphyry-related	Vein-related	IM*	Unknown class	YUKON TOTAL
Total No.	96	69	62	16	7	5	1	4	12	12	2	5	291
% of Total	33.0	23.7	21.3	5.5	2.4	2	0.3	1.4	4.1	4.1	0.7	1.7	100
No. of Producers	7**	0	1	0	0	0	0	0	0	1	1	0	10
<b>TERRANE</b>													
Mackenzie Platform	1	10	3	-	-	-	1	1	-	-	-	-	16
Selwyn Basin*	19	26	33	2	2	2	-	2	3	4	-	1	94
Tombstone Plutonics	-	-	-	-	-	-	-	-	1	-	-	-	1
Cassiar Platform*	4	20	12	1	2	-	-	-	2	7	-	1	49
Yukon Tanana	8	9	8	13	1	-	-	1	2	-	1	-	43
Nisling	8	2	3	-	1	-	-	-	-	-	-	-	14
Northern Stikine	47	-	2	-	1	1	-	-	2	-	-	3	56
Whitehorse Trough	2	-	-	-	-	-	-	-	-	-	-	-	2
Cache Creek	1	-	-	-	-	-	-	-	-	-	-	-	1
Coast Plutonic Complex	1	-	-	-	-	1	-	-	-	-	-	-	2
Wrangellia	5	-	-	-	-	1	-	-	-	-	1	-	7
McQueston Plutonics	-	1	-	-	-	-	-	-	2	-	-	-	3
Devonian Intrusion	-	1	-	-	-	-	-	-	-	-	-	-	1
Billings Batholith	-	-	1	-	-	-	-	-	-	-	-	-	1
Cretaceous Intrusions	-	-	-	-	-	-	-	-	-	1	-	-	1
SUM	96	69	62	16	7	5	1	4	12	12	2	5	291

\*\* includes multiple producers in the Whitehorse Cu belt

\*Selwyn Basin includes plutonic suites

\*Cassiar Platform includes Cassiar Batholith

\*U/REE = Uranium/rare-earth-element skarns

\*IM = industrial mineral skarns

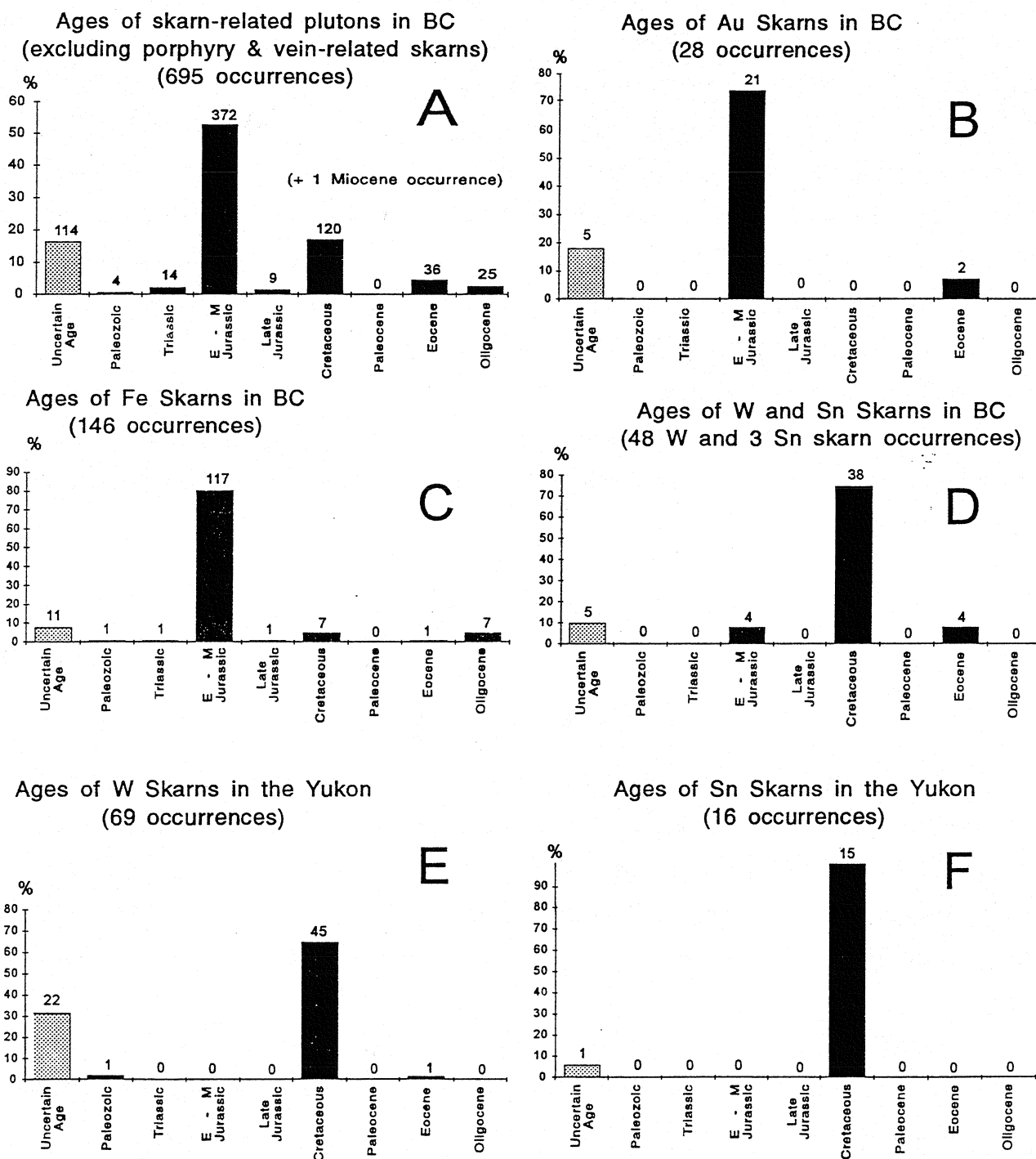
primarily of ocean-floor material. However, over 80 % of the skarns in B.C. are hosted by terranes dominated by island-arc rocks and these have accounted for virtually all the Fe, Cu and Au metal produced from skarns in the province (Ray *et al.*, 1995). By contrast, only 5 % of the skarns in B.C. are hosted by the North American craton and basement, yet these have been responsible for all the provinces W production as well as some Zn, Pb and Ag. Although the terranes of the Coast Plutonic Belt (e.g. Chilliwack, Cadwallader, Bridge River and undivided metamorphic complex) have the greatest concentration of plutonic rocks in the Canadian Cordillera, they host less than 4 % of the skarns, all with negligible metal production.

## TECTONIC SETTING AND AGE OF SKARN-RELATED PLUTONISM

Most skarns in the Canadian Cordillera were formed during three time periods (Fig. 3A) that had distinctly different metallogenies. The oldest and most important in B.C. was during the Early to Middle Jurassic when over half of the skarns were developed. The other two periods were during the Cretaceous and the Eocene-Oligocene.

These periods of skarn development coincide with three major plutonic episodes, two of which were associated with magmatism related to eastward-subducting oceanic crust (Armstrong, 1988), and one with trans-tensional tectonics and anatectic melting of the miogeocline (Woodsworth *et al.*, 1991). The first, an Early to Middle Jurassic episode of alkalic and calc-alkalic I-type plutonism was commonly cogenetic with volcanic rocks in several island-arc terranes. It involved intrusion both prior to, and during, terrane amalgamation and subsequent accretion to ancestral North America. It was concentrated largely in the accretionary island-arc terranes of Wrangellia, Stikinia and Quesnellia at a time when they lay outboard of North America, and was the most economically important metallogenic epoch in the Canadian Cordillera. This plutonism resulted in most of the Au, Fe (Fig. 3B and C) and Cu skarns as well as many of the Cu-Au and Cu-Mo porphyry deposits in the region (Preto, 1972; Preto *et al.*, 1979; Dawson *et al.*, 1991). Notable exceptions however, include the Whitehorse Copper Belt deposits and some Cu skarns in the Greenwood camp of B.C., which are related to the subsequent Cretaceous plutonic episode (Morrison, 1981; Tenney, 1981; Meinert, 1986; Church, 1986).

The Cretaceous plutonism was concentrated in two major metamorphic zones (Monger *et al.*, 1982; Woodsworth *et al.*, 1991), the easternmost of which resulted in mostly felsic, S-type intrusions with initial  $^{87}\text{Sr}/^{86}\text{Sr}$  ratios greater than 0.706 (Armstrong, 1988). This eastern zone was an indirect result of collision, during the Middle Jurassic, between the Intermontane Superterrane and ancestral North America, which produced thickening of the continental crust in the outer part of the miogeoclinal



**Figure 3.** Bar charts showing relative ages of the plutonic rocks associated with skarns in the Canadian Cordillera.

A: Plutons related to all 695 skarn occurrences in B.C.

B: Plutons related to Au skarns in B.C.

C: Plutons related to Fe skarns in B.C.

D: Plutons related to W and Sn skarns in B.C.

E: Plutons related to W skarns in the Yukon.

F: Plutons related to Sn skarns in the Yukon.. Note: Figure 3A includes 11 skarn occurrences of unknown class.

sedimentary wedge. This was followed by melting and the generation of mainly S-type plutonism which culminated in mid-Cretaceous time (Woodsworth *et al.*, 1991). These Cretaceous plutons, which are commonly, but not exclusively, peraluminous two-mica granites, were responsible for most of the W and Sn skarns (Fig. 3D, E and F) located in the eastern part of the region (Fig. 1). These include the plutons of the Surprise Lake suite with their associated Atlin Sn skarns, as well as the intrusions related to the Cassiar W and Sn occurrences (Cooke and Godwin, 1984; Ray *et al.*, 1995, 1997). Contemporaneous I-type plutons responsible for the Whitehorse Belt Cu skarns are part of an extensive continental-margin arc that formed in mid-Cretaceous to early Tertiary time. This resulted from collision and subduction of the Gravina-Gambier arc and its Wrangellia-Alexander basement with previously accreted arc and pericratonic terranes (Monger and Nokleberg, 1995).

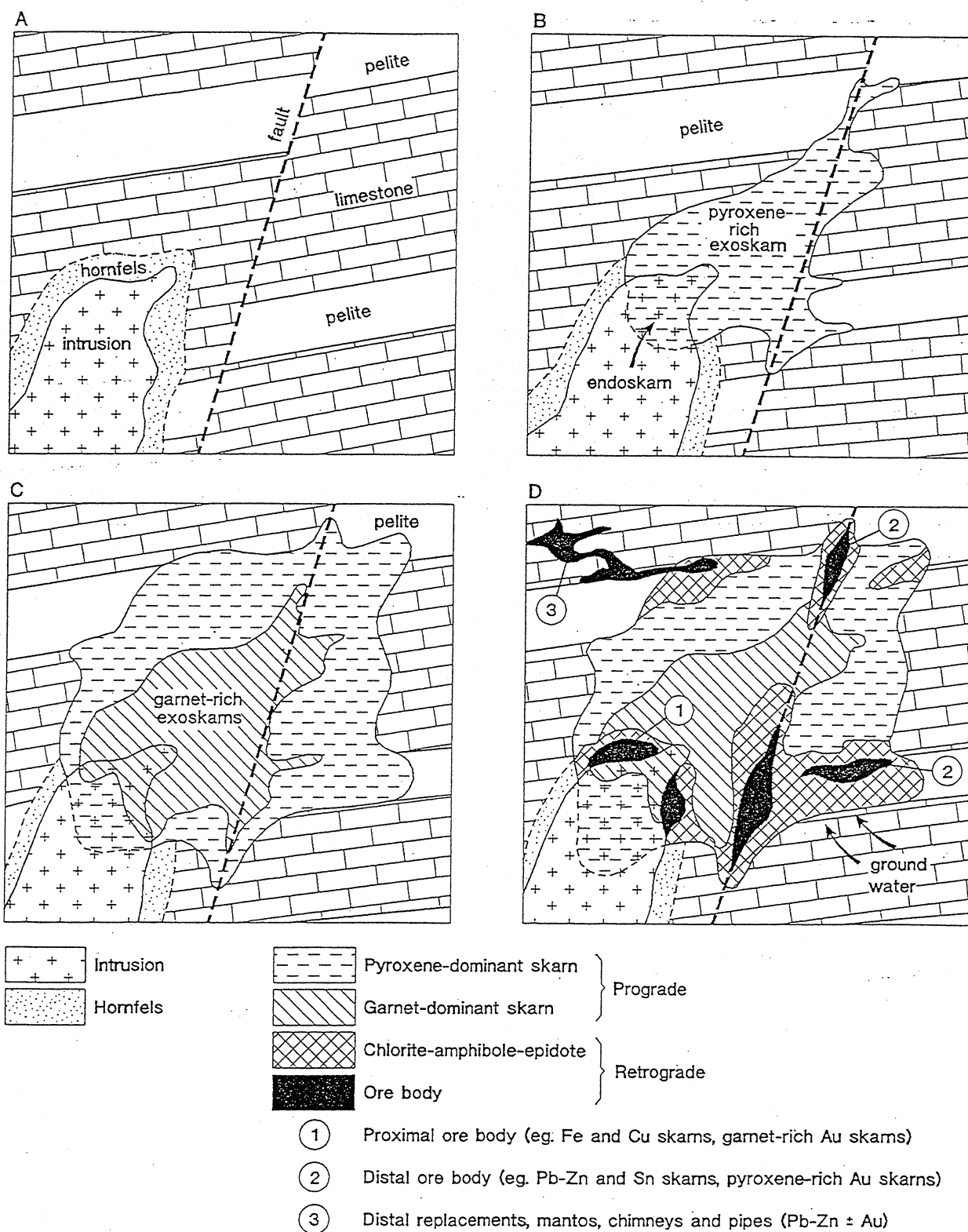
Compared to the Jurassic and Cretaceous episodes, the Eocene-Oligocene magmatism was less important for skarn development (Fig. 3A) and it only resulted in a relatively small number of Pb-Zn, Cu and W skarns.

## SKARN DEPOSITS

### INTRODUCTION

Economic deposits associated with a skarn gangue are termed skarn deposits (Burt, 1972, 1977). At least seven major classes of metallic skarn deposit are recognized in the Canadian Cordillera: Fe, Cu, Au, Mo, Pb-Zn, W and Sn skarns. In addition, a few skarns are enriched in U and rare earth elements (REE), and others represent industrial mineral skarns because they are an economic source of minerals or commodities such as fluorite, wollastonite, garnet, borates, rhodonite, tremolite or marble (Figs. 2A and 2B).

Many Fe, Cu, Mo and W skarn deposits form close to their related plutons, whereas the ore in some Au, Sn and Pb-Zn skarns tends to develop in the outer parts of the exoskarn envelope (Fig. 4; Table 3). In certain circumstances, the late, metal-carrying hydrothermal fluids may migrate considerable distances to produce deposits outside the main exoskarn halo. Depending on such physiochemical conditions as the lithology, porosity and permeability of the hostrocks and the chemistry of the fluids, the distal magmatic fluids may generate either sulphide-poor Carlin-type Au orebodies (Sillitoe and Bonham, 1990) or sulphide-rich veins, replacement bodies or mantos containing Pb, Zn, Ag, Au or Cu (Fig. 4).



**Figure 4.** Schematic evolution of a calcic skarn deposit.

**Figure 4. Schematic evolution of a calcic skarn deposit.**

- A. Intrusion of magma into faulted, carbonate-pelite sequence and formation of a contact hornfels or skarnoid.**
- B. Infiltration of hydrothermal fluids to produce endoskarn and pyroxene-dominant exoskarn.**
- C. Continued infiltration of fluids, with progressive expansion of exoskarn envelope and development of a proximal garnet-rich exoskarn. Skarn development is controlled partly by factors such as rock porosity, bedding planes, fractures and rock lithologies. Some mineralization may take place late in this stage.**
- D. The hydrothermal system wanes and cools, leading to retrograde overprinting. During this stage metals may be introduced, or scavenged and redeposited to form orebodies. The structural/lithological controls and influence of meteoric water may result in irregularly distributed orebodies that are notoriously difficult to delineate in skarn. In the exoskarn envelope, ore bodies may form proximally (as with some Cu, Fe and garnet-rich Au skarns) or more distally (as with pyroxene-rich Au skarns and Sn skarns). Some mineralizing fluids may also travel well beyond the skarn to form replacement-type orebodies such as mantos, chimneys and pipes.**



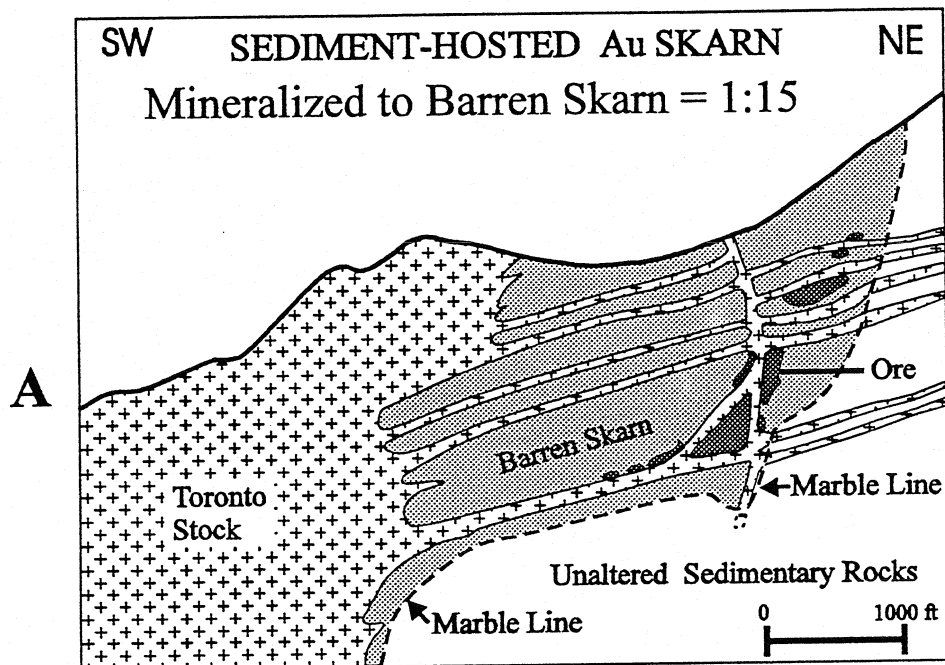
Although skarn envelopes and their contained deposits commonly display a complex morphology and mineralogy, each deposit class tends to have certain identifying characteristics (Tables 3 and 4). The chemistry and mineralogy of both the skarn gangue assemblage and the ore are influenced by factors such as hostrock lithology, depth of formation and the composition and oxidation state of the related intrusion and hydrothermal fluids. Dolomitic rocks are favorable hosts for some Fe and Sn skarns but tend to inhibit the development of W skarns (Zharikov, 1970; Einaudi *et al.*, 1981). Calcareous siltstones, tuffs or volcanic rocks are more commonly altered to pyroxene, actinolite or epidote-rich assemblages, whereas impure limestones generally result in skarns dominated by grossular garnet. The oxidation state of the hydrothermal fluids and the oxidizing or reducing capacity of the hostrocks also influences the skarn mineralogy and metal chemistry. Reduced fluids or hostrock tend to result in high pyrrhotite/pyrite ratios, magnetite rather than hematite, and low  $\text{Fe}_2\text{O}_3/\text{FeO}$  ratios in the silicates. It may also influence garnet/pyroxene ratios in the exoskarn.

Skarn deposits form throughout a wide range of depths, including shallow subvolcanic regimes, as indicated by the presence of Cu skarns associated with the high-level Copper Mountain, Mount Polley and Galore Creek alkaline Cu-Au porphyries in B.C. (Preto, 1972; Dawson and Kirkham, 1996). At shallow depths, the exoskarn envelopes tend to be more extensive, are increasingly controlled by brittle structures and may include hydrothermal breccias. They also have more oxidized mineral assemblages than skarns formed at greater depths and are liable to have undergone more intense retrograde alteration by convecting ground water. Deeper level systems (e.g. some W and Sn skarns) are characterized by higher temperature mineral assemblages and relatively reduced states (Newberry, 1983; Newberry and Swanson, 1986) as well as increased metamorphism and ductile deformation, and decreased alteration of the stock.

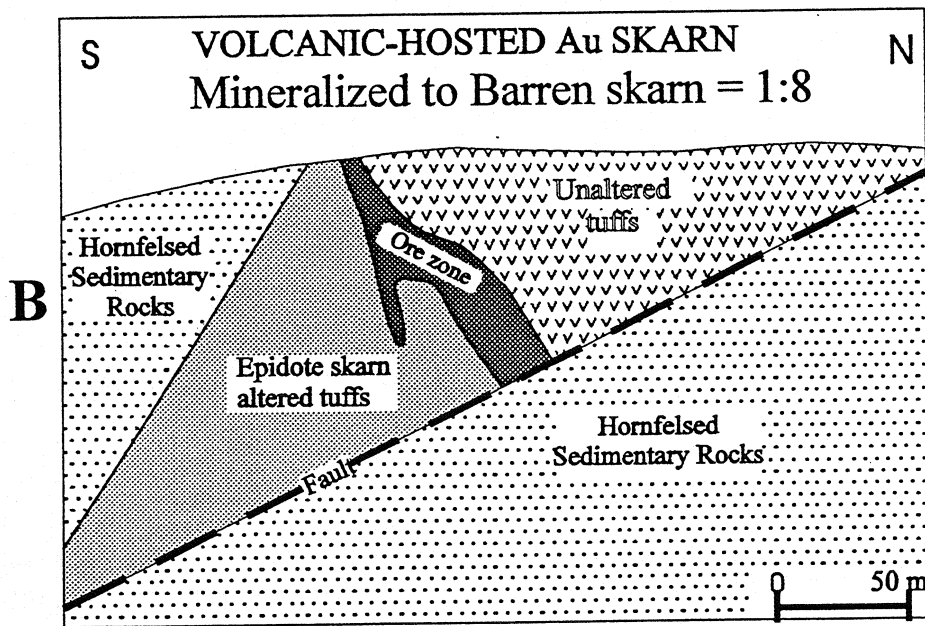
The presence of hostrocks that are both chemically reactive and physically capable of maintaining long-lived permeability and porosity is vital for the formation of an economic skarn deposit. Structures such as faults, fold-hinges, dike-sill margins and lithologic contacts often channel the hydrothermal fluids and control subsequent development of the skarn and its orebodies. By geological mapping and sampling, it is possible to recognize mineralogical and chemical zoning throughout a skarn envelope; these data can be used to identify and locate both the original hydrothermal conduits and any associated orebodies.

Variations in the permeability of the hostrocks can partly control the size and morphology of both the overall skarn and its contained orebodies, and the thickness of the barren alteration halo surrounding the ore zones. These points are demonstrated in Figure 5, which shows cross-sections of three Au skarn deposits whose hostrocks have different chemical and physical characteristics. The well bedded and highly permeable calcareous sedimentary rocks hosting the Nickel Plate Au deposit have allowed the

development of a large skarn (Fig. 5A) that is estimated to exceed 0.75 cubic kilometres of alteration (Ray and Dawson, 1994). However, the orebodies represent only a minor part of the system, and the ratio of mineralized to barren skarn is at least 1:15 (Fig. 5A). Likewise, the high permeability of the tuffaceous rocks hosting much of the QR deposit enabled the formation of an extensive skarn that has a mineralized to barren skarn ratio of approximately 1:8 (Fig. 5B). By contrast, the volcanic country rocks at the Diamond Hill deposit in Montana were relatively impermeable, and the hydrothermal fluids were restricted to zones of brittle shearing. This resulted in high grade ore bodies that are surrounded by very narrow alteration envelopes (Fig. 5C); the ratio of mineralized to barren skarn at Diamond Hill is estimated to range between 1:1 and 1:0.5. The contrasting gold grades at Diamond Hill and QR may also partly reflect the differences in their hostrock permeability; the hydrothermal fluids at the former deposit were tightly confined whereas at the QR skarn they were able to disperse widely through the tuffs, resulting in lower grade ore.

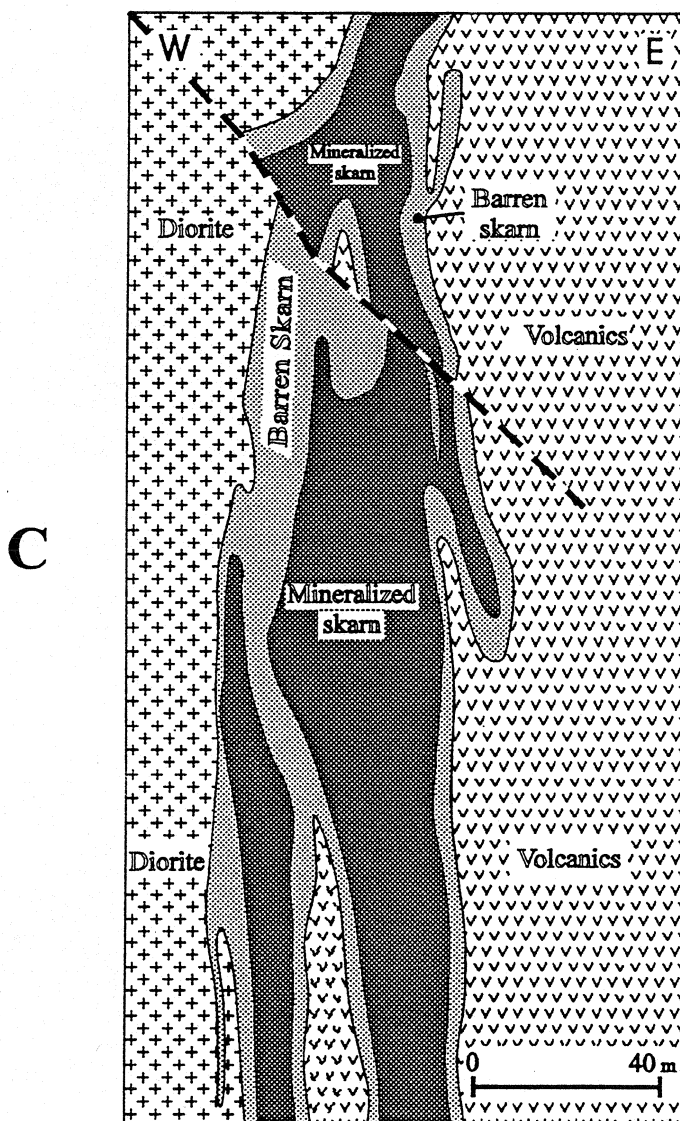


**Fig. 5A.** Geological cross section through the Nickel Plate Au skarn (after Dolmage and Brown, 1945)



**Fig. 5B.** Geological cross section through the Main Zone, QR Au skarn (after Fox and Cameron, 1995)

**VOLCANIC-HOSTED Au SKARN**  
Mineralized to Barren skarn = 1:1



**Fig. 5C. Geological cross section through the Glory Hole zone  
Diamond Hill Au skarn, Montana  
(data courtesy of Pegasus Gold Corp.)**

**Figure 5.** Geological cross sections of three Au skarn illustrating the strong relationship between the permeability of the hostrocks and the size, morphology and ore:gangue ratios of the deposits:

A: Nickel Plate deposit, Hedley, B.C. (after Dolmage and Brown, 1945).

B: QR deposit, Quesnel River, B.C. (after Fox and Cameron, 1995).

C: Diamond Hill deposit, Montana (data courtesy of Pegasus Gold Corp.)

**Note:** the highly permeable hostrocks at the Nickel Plate and QR deposits have allowed the formation of large skarn envelopes with low ore:gangue ratios. The Diamond Hill skarn is confined to brittle structures that cut impermeable rocks. Consequently, the skarn envelope is of limited extent and has a high ore:gangue ratio.

**Table 3: Characteristic controls and examples of skarn deposits in the Canadian Cordillera.**

Skarn Class	CHARACTERISTIC CONTROLS	TYPICAL OREBODY MORPHOLOGY AND EXAMPLES
Fe	Pluton margins, stratigraphic contacts and local structures are important. Economic Fe deposits are confined to the Wrangellia Terrane and are mostly concentrated along the upper and lower contacts of the Quatsino Formation or equivalent limestone units.	Stratiform orebodies, sheets, massive lenses, irregular veins and rarely (e.g. <i>Kingfisher</i> ) as vertical, sub-circular pipes. Examples: (B.C.) <i>Tasu, Jessie, Merry Widow, Iron Crown, Prescott, Lake.</i>
Cu	Preskarn structures and hostrock permeability are important. Many orebodies are controlled by intrusive margins, sedimentary lithologies and fault structures. Ore bodies tend to be proximal to plutons.	Highly variable morphology: stratiform and tabular orebodies, vertical pipes and irregular lenses. Examples: (B.C.) <i>Ingerbelle, Craigmont, Phoenix</i> (Yukon) <i>Whitehorse Copper Belt (Copper King, Carlisle, Pueblo, Valerie, Grafters, Arctic Chief and War Eagle).</i>
Au	Strong stratigraphic and structural controls. Preskarn structures (faults, fold axes, sill-dike contacts) are important. The pyroxene-rich Nickel Plate deposit is developed distal to the Toronto stock (although the higher grade orebodies commonly lie close to sills & dikes). Garnet-rich Au skarn orebodies tend form proximal to the igneous source-rocks.	Variable from irregular lenses and veins to tabular or stratiform orebodies with lengths and widths ranging up to many hundreds of metres. Examples: (B.C.) <i>Nickel Plate-Hedley Mascot, French, Canty, Hood Hope, QR (Quesnel River).</i> (Yukon) <i>Marn, Ketza River, Newry, Guder.</i>
Mo	Deposits commonly develop in carbonate or calcareous rocks within thermal aureoles adjacent to intrusive margins.	Irregular orebodies along, and controlled by intrusive contacts. Examples: (B.C.) <i>Coxey, Novelty.</i> (Yukon) <i>Molly.</i>
W	Deposits favour calcareous rocks within extensive thermal aureoles of intrusions. However, dolomites tend to inhibit W skarn development. Controls include: gently inclined bedding, intrusive contacts, structural and stratigraphic traps in sedimentary rocks or in irregular parts of the pluton-hostrock contacts.	Stratiform, tabular and lens-like orebodies. Deposits can be continuous for hundreds of metres, following intrusive contacts. Examples: (B.C.) <i>Emerald Tungsten, Feeney, Dodger, Invincible, Dimac (Silence Lake).</i> (Yukon) <i>MacTung, Bailey, Risby, Ray Gulch.</i> (NWT) <i>CanTung, Lened.</i>
Pb-Zn	Carbonate rocks, particularly along structural and/or lithological contacts (e.g. shale-limestone contacts or pre-ore dikes). Deposits may form considerable distances (>500m) from the source intrusions.	Variable: subvertical chimneys or veins along faults and fissures to subhorizontal blankets or mantos along igneous and stratigraphic contacts or along flat lying structures. Examples: (B.C.) <i>Piedmont, Contact.</i> (Yukon) <i>Silver Hart, Sa Dena Hes, Quartz Lake.</i>
Sn	Differentiate, peraluminous plutons intruding carbonates. Dolomites form favourable hostrocks. Ore bodies controlled by fractures, lithological or structural contacts, and may form some distance (up to 500m) from the related pluton.	Variable: stratiform, stockwork, pipe-like or irregular vein-like orebodies. Example: (B.C.) <i>Daybreak, Atlin Magnetite.</i> (Yukon) <i>JC (Viola), Can, Mulligan,</i>

**Table 4 Characteristic mineralogies of skarn deposits in the Canadian Cordillera.**

Skarn Class	ORE MINERALOGY & GEOCHEMISTRY (Principal and Subordinate)	EXOSKARN & ENDOSKARN ALTERATION
<b>Fe</b>	<p>Magnetite, <i>chalcopyrite</i>, <i>pyrite</i>, <i>sphalerite</i>, <i>cobaltite</i>, <i>pyrrhotite</i>, <i>arsenopyrite</i>, <i>galena</i>, <i>molybdenite</i>, <i>bornite</i>, <i>hematite</i>, <i>martite</i>, <i>gold</i>.</p> <p>Rarely, contain <i>tellurobismuthite</i>, <i>fluorite</i>, <i>scheelite</i>.</p> <p>Geochemical signature: Fe, Cu, Co, Au, Ag, As and Cr.</p>	<p><b>Exoskarn:</b> high Fe, low Mn, diopside-hedenbergite clinopyroxene (Hd0-70). Pyroxenes of Hd70-90 composition are generally absent (Ray &amp; Webster, 1997) although some include johannsenite-hedenbergite solid solutions (up to Jo50; Meinert, 1984).</p> <p>Low Mn grossular-andradite garnets (Ad 20-95).</p> <p>Fe skarns hosted by dolomitic rocks may include some Mg silicates; e.g. phlogopite, Mg-chlorite, serpentine.</p> <p><b>Endoskarn</b> extensive with Na-silicates <math>\pm</math> garnet <math>\pm</math> pyroxene <math>\pm</math> epidote <math>\pm</math> scapolite.</p>
<b>Cu</b>	<p>Chalcopyrite <math>\pm</math> pyrite <math>\pm</math> magnetite in inner garnet-pyroxene zone. Bornite <math>\pm</math> chalcopyrite <math>\pm</math> <i>sphalerite</i> <math>\pm</math> <i>tennantite</i> in outer wollastonite zone.</p> <p>Hematite, pyrite, pyrrhotite or magnetite may predominate (depending on the oxidation and sulphidation states).</p> <p><i>Scheelite</i>, <i>chalcocite</i>, <i>molybdenite</i>, <i>bismuthinite</i>, <i>galena</i>, <i>cosalite</i>, <i>arsenopyrite</i>, <i>enargite</i>, <i>tennantite</i>, <i>loellingite</i>, <i>cobaltite</i>, <i>goethite</i>, <i>tetrahedrite</i>, <i>covellite</i>, <i>digenite</i>, <i>electrum</i>, <i>native gold</i>, <i>native copper</i> and <i>rutile</i>.</p> <p>Geochemical signature: Cu-Au-Ag-rich inner zones grading outward through Au-Ag zones with high Au:Ag ratios to an outer Pb-Zn-Ag zone.</p> <p>Cobalt-As-Sb-Bi-Mo-W geochemical anomalies are present in the more reduced Cu skarn deposits</p>	<p><b>Exoskarn</b> commonly has high garnet:pyroxene ratios. High Fe, low Al, Mn andradite garnet (Ad35-100), and diopsidic clinopyroxene (Hd2-50). Other minerals include K-feldspar, biotite, amphibole, clinozoisite, epidote, wollastonite, scapolite and sericite.</p> <p>Mineral zoning from stock out to marble is commonly: diopside + andradite (proximal); wollastonite <math>\pm</math> tremolite/actinolite <math>\pm</math> garnet <math>\pm</math> diopside <math>\pm</math> vesuvianite (distal).</p> <p>Late minerals include actinolite, chlorite, montmorillonite, K-feldspar, epidote and sericite.</p> <p>Cu skarns hosted by mafic tuffs (e.g. Ingerbelle) have an exoskarn dominated by epidote, actinolite, biotite and chlorite.</p> <p>Cu skarns associated with alkalic porphyry Cu-Au deposits in British Columbia contains late scapolite.</p> <p>Cu skarns hosted by dolomitic rocks may include some Mg silicates; e.g. phlogopite, Mg-chlorite, brucite.</p> <p><b>Endoskarn</b> includes K-feldspar, epidote, sericite <math>\pm</math> pyroxene <math>\pm</math> garnet. Some retrograde actinolite, talc, chlorite and clay minerals.</p>
<b>Au</b>	<p><b>Pyroxene-rich type:</b> Native gold, pyrrhotite, arsenopyrite, <i>chalcopyrite</i>, <i>tellurides</i>, <i>bismuthinite</i>, <i>cobaltite</i>, <i>native bismuth</i>, <i>pyrite</i>, <i>sphalerite</i>, <i>maldonite</i>. Generally high sulphide content and high pyrrhotite:pyrite ratios.</p> <p><b>Garnet-rich type:</b> Native gold, pyrite, magnetite, <i>chalcopyrite</i>, <i>arsenopyrite</i>, <i>sphalerite</i>, <i>hematite</i>, <i>pyrrhotite</i>, <i>galena</i>, <i>tellurides</i>, <i>bismuthinite</i>.</p> <p>Generally low to moderate sulphide content and low pyrrhotite:pyrite ratios.</p> <p><b>Epidote-rich type:</b> Native gold, <i>chalcopyrite</i>, <i>pyrite</i>, <i>arsenopyrite</i>, <i>pyrrhotite</i>, <i>galena</i>.</p> <p>Moderate to high sulphide content with low pyrrhotite:pyrite ratios.</p> <p>Geochemical signature for pyroxene and garnet-rich types: Au, As, Bi, Te, Co, Cu, Zn or Ni.</p> <p>Very low Cu/Au, Ag/Au and Zn/Au ratios.</p>	<p><b>Pyroxene-rich type:</b> extensive exoskarn with high pyroxene:garnet ratios. Prograde minerals: K-feldspar, Fe-rich biotite, low Mn grandite garnet (Ad 10-100), wollastonite, diopsidic to hedenbergitic clinopyroxene (Hd 20-100) and vesuvianite.</p> <p>Trace rutile, axinite and sphene.</p> <p>Late minerals include epidote, chlorite, clinozoisite, vesuvianite, scapolite, tremolite-actinolite, sericite and prehnite.</p> <p><b>Garnet-rich type:</b> extensive exoskarn with low pyroxene:garnet ratios. Prograde minerals: K-feldspar, low Mn grandite garnet (Ad 10-100), wollastonite, diopsidic clinopyroxene (Hd 0-60), epidote, vesuvianite, sphene and apatite. Late minerals include epidote, chlorite, clinozoisite, vesuvianite, tremolite-actinolite, sericite, dolomite, siderite and prehnite.</p> <p><b>Epidote-rich type:</b> extensive exoskarn with abundant epidote and lesser chlorite, quartz and late carbonate. Epidote-pyrite and carbonate-pyrite veinlets and coarse aggregates are common.</p>

Table 4: Continued.

Skarn Class	ORE MINERALOGY & GEOCHEMISTRY (Principal and Subordinate)	EXOSKARN & ENDOSKARN ALTERATION
<b>Mo</b>	Molybdenite, <i>scheelite</i> , <i>powellite</i> , <i>chalcopyrite</i> , <i>arsenopyrite</i> , <i>pyrite</i> , <i>pyrrhotite</i> , <i>bismuthinite</i> , <i>sphalerite</i> , <i>fluorite</i> . Rarely, Mo skarns carry <i>galena</i> , <i>magnetite</i> , <i>uraninite</i> , <i>pitchblende</i> , <i>cassiterite</i> , <i>cobaltite</i> , <i>stannite</i> , and <i>gold</i> . Geochemical signature: Mo, Zn, Cu, Sn, Bi, As, F, Pb, U, Sb, Co (Au).	<b>Exoskarn:</b> hedenbergite pyroxene (Hd50-80, Jo-3) $\pm$ low Mn grossular-andradite garnet (Ad40-95) $\pm$ wollastonite $\pm$ biotite $\pm$ vesuvianite. Retrograde amphibole, epidote, chlorite and muscovite. <b>Endoskarn:</b> clinopyroxene, K-feldspar, hornblende, epidote, quartz veining and sericite.
<b>W</b>	Scheelite, molybdenite, chalcopyrite, pyrrhotite, sphalerite, arsenopyrite, pyrite, powellite. May contain trace wolframite, fluorite, cassiterite, galena, marcasite and bornite. Reduced types carry pyrrhotite, magnetite, bismuthinite, native bismuth and have high pyrrhotite:pyrite ratios. Variable amounts of quartz-vein stockwork (with local molybdenite) can cut both the exoskarn and endoskarn. The Emerald Tungsten skarns in B.C. include pyrrhotite-arsenopyrite pods that carry up to 9 g/t Au. Geochemical signature: W, Cu, Mo, As, Bi and B. Less commonly Zn, Pb, Sn, Be, F (Au).	<b>Exoskarn:</b> inner zone of diopside-hedenbergite (Hd60-90, Jo5-20) $\pm$ grossular-andradite (Ad 10-50, Spess5-50) $\pm$ biotite $\pm$ vesuvianite, with outer barren wollastonite-bearing zone. An innermost zone of massive quartz may be present. Late-stage spessartine $\pm$ almandine $\pm$ biotite $\pm$ amphibole $\pm$ plagioclase $\pm$ phlogopite $\pm$ epidote $\pm$ fluorite $\pm$ sphene. Reduced types characterized by hedenbergitic pyroxene, Fe-rich biotite, fluorite, vesuvianite, scapolite and low garnet:pyroxene ratios, whereas oxidized types are characterized by salitic pyroxene, epidote and andraditic garnet and high garnet:pyroxene ratios. Exoskarn can be associated with extensive areas of biotite hornfels. <b>Endoskarn:</b> pyroxene $\pm$ garnet $\pm$ biotite $\pm$ epidote $\pm$ amphibole $\pm$ muscovite $\pm$ plagioclase $\pm$ pyrite $\pm$ pyrrhotite $\pm$ trace tourmaline and scapolite; local greisen developed.
<b>Pb-Zn</b>	Sphalerite, galena, pyrrhotite, pyrite, magnetite, arsenopyrite, chalcopyrite, bornite. Fe-rich sphalerite predominate over galena in a ratio of about 3:2. Other trace minerals include <i>scheelite</i> , <i>bismuthinite</i> , <i>stannite</i> , <i>native gold</i> , <i>cassiterite</i> , <i>tetrahedrite</i> , <i>molybdenite</i> & <i>fluorite</i> . Rarely, boronsilicates such as <i>datolite</i> , <i>danburite</i> and <i>borospurrite</i> may occur (Dawson, 1996a). Proximal skarns tend to be richer in Fe, Cu & W, and more rarely in Au. Distal skarns contain higher amounts of Pb, Ag and Mn $\pm$ Sb $\pm$ As. Geochemical signature: Pb, Zn, Ag, Cu, Mn, As, Bi, W, F, Sn, Mo, Co, Sb, Cd and Au.	<b>Exoskarn:</b> Mn-rich hedenbergite-johannsenite pyroxene (Hd30-90, Jo10-50), andraditic garnet (Ad20-100, Spess2-10) $\pm$ wollastonite $\pm$ bustamite $\pm$ vesuvianite $\pm$ rhodonite. Late-stage Mn-rich actinolite $\pm$ epidote $\pm$ ilvaite $\pm$ chlorite $\pm$ dannermorite $\pm$ rhodochrosite $\pm$ axinite $\pm$ rhodonite $\pm$ fluorite. Yukon deposits have distinctive prograde assemblages of abundant epidote, rare andradite & intergrown diopside and Mn-hedenbergite (Dick, 1979). <b>Endoskarn:</b> in many distal Pb-Zn skarns the endoskarn is unknown but Zn-rich skarns formed near stocks are often associated with abundant endoskarn with epidote $\pm$ amphibole $\pm$ chlorite $\pm$ sericite and lesser rhodonite $\pm$ garnet $\pm$ vesuvianite $\pm$ pyroxene $\pm$ K-feldspar $\pm$ biotite and rare topaz. Marginal phases may contain greisen and/or tourmaline.

Table 4: Continued.

Skarn Class	ORE MINERALOGY & GEOCHEMISTRY (Principal and Subordinate)	EXOSKARN & ENDOSKARN ALTERATION
<b>Sn</b>	Cassiterite, scheelite, arsenopyrite, pyrrhotite, chalcopyrite, stannite, magnetite, <i>bismuthinite</i> , <i>sphalerite</i> , <i>pyrite</i> , <i>ilmenite</i> , <i>galena</i> & <i>stanniferous tetrahedrite</i> . Geochemical signature: Sn, W, F, Be, Bi, Mo, As, Zn, Pb, Cu, Rb, Li, Cs and Re.	<p><b>Exoskarn:</b> grandite garnet (Ad15-75, pyralisite 5-30) (sometimes Sn, F, and Be enriched), hedenbergitic pyroxene (Hd40-95) ± vesuvianite (sometimes Sn and F-enriched) ± malayaite ± Fe and/or F-rich biotite ± stanniferous sphene ± gahnite ± rutile ± Sn-rich ilvaite ± wollastonite ± adularia.</p> <p>Late minerals include axinite, wollastonite, vesuvianite, beryl, muscovite, Fe-rich biotite, chlorite, tourmaline, fluorite, sellaite, stilpnomelane, epidote and amphibole (latter two minerals can be Sn rich). Associated greisens carry quartz and muscovite ± tourmaline ± topaz ± fluorite ± cassiterite ± sulphides.</p> <p>Sn skarns hosted by dolomitic rocks may include some Mg silicates; e.g. olivine, serpentine, phlogopite, Mg-chlorite, brucite, spinel, ludwigite and talc.</p>



## IRON (MAGNETITE) SKARNS - GENERAL SYNOPSIS

**EXAMPLES:** (*Canadian Cordillera*): Tasu (103C003), Jessie (103B026), Merry Widow (092L044), Iron Crown (092L034), Iron Hill (092F075), Yellow Kid (092F258), Prescott (092F106), Paxton (092F107), Lake (092F259).

(*Elsewhere*): Shinyama (Japan), Cornwall (Pennsylvania), Iron Springs (Utah, USA) Eagle Mountain (California, USA), Perschansk, Dashkesan, Sheregesh and Teya (Russia), Daiquiri (Cuba), San Leone (Italy), El Romeral (Chile).

**DEPOSIT FORM:** Variable and includes stratiform orebodies, vertical pipes, fault-controlled sheets, massive lenses or veins, and irregular ore zones along intrusive margins.

**TEXTURES:** Igneous textures in endoskarn. Coarse to fine-grained, massive granoblastic to mineralogically layered textures in exoskarn. Some hornfelsic textures. Magnetite varies from massive to disseminated to veins.

**ORE MINERALOGY**(Principal and Subordinate): Calcic Fe skarns: Magnetite  $\pm$  *chalcopyrite*  $\pm$  *pyrite*  $\pm$  *cobaltite*  $\pm$  *pyrrhotite*  $\pm$  *arsenopyrite*  $\pm$  *sphalerite*  $\pm$  *galena*  $\pm$  *molybdenite*  $\pm$  *bornite*  $\pm$  *hematite*  $\pm$  *martite*  $\pm$  *gold*. Rarely, can contain *tellurobismuthite*  $\pm$  *fluorite*  $\pm$  *scheelite*. Magnesian Fe skarns: Magnetite  $\pm$  *chalcopyrite*  $\pm$  *bornite*  $\pm$  *pyrite*  $\pm$  *pyrrhotite*  $\pm$  *sphalerite*  $\pm$  *molybdenite*.

**EXOSKARN ALTERATION** (both calcic and magnesian): High Fe, low Mn, diopside-hedenbergite clinopyroxene (Hd20-80); however, some deposits include johannsenite-hedenbergite solid solutions (up to Jo50). Garnets are low Mn grossular-andradite solid solutions (Ad20-95),  $\pm$  epidote  $\pm$  apatite. Late stage amphibole  $\pm$  chlorite  $\pm$  ilvaite  $\pm$  epidote  $\pm$  scapolite  $\pm$  albite  $\pm$  K-feldspar. Magnesian Fe skarns can contain olivine, spinel, phlogopite, xanthophyllite, brucite, serpentine, and rare borate minerals such as ludwigite, szaibelyite, fluorborite and kotoite.

**ENDOSKARN ALTERATION:** Calcic Fe skarns: Extensive endoskarn with Na-silicates  $\pm$  garnet  $\pm$  pyroxene  $\pm$  epidote  $\pm$  scapolite. Magnesian skarns: Minor pyroxene  $\pm$  garnet endoskarn, and propylitic alteration.

**ORE CONTROLS:** Stratigraphic and structural controls. Close proximity to contacts between intrusions and carbonate sequences, volcanics or calcareous tuffs and sediments. Fracture zones near igneous contacts can also be important.

**ASSOCIATED DEPOSIT TYPES:** Porphyry Cu deposits; Cu and Pb-Zn skarns; small Pb-Zn veins. Regionally in British Columbia there is a negative spatial relationship between Fe and Au skarns.

**GEOCHEMICAL SIGNATURE:** Calcic Fe skarn: enriched in Fe, Cu, Co, Au, Ni, As and Cr. Overall Cu and Au grades are low (<0.2% Cu and 0.5 g/t Au).

**GEOPHYSICAL SIGNATURE:** Strong positive magnetic, electromagnetic and induced polarization anomalies. Possible gravity anomalies.

**OTHER EXPLORATION GUIDES:** Magnetite-rich float. In the Wrangellia Terrane of British Columbia, the upper and lower contacts of the Late Triassic Quatsino limestone (or equivalent units) are favorable horizons for Fe skarn development.

**GRADE AND TONNAGE:** Grades are typically 40 to 60 % Fe. Worldwide, calcic Fe skarns range from 3 to 150 Mt whereas magnesian Fe skarns can be larger (exceeding 250 Mt). In British Columbia, they reach 20 Mt and average approximately 4 Mt of mined ore.

**IMPORTANCE:** Worldwide, these deposits were once an important source of Fe, but in the last 40 years the market has been increasingly dominated by sedimentary Fe formation deposits. Nearly 90 % of British Columbia's historic Fe production was from skarns, most of which was derived from deposits in the Wrangellia Terrane.

## IRON SKARNS IN THE CANADIAN CORDILLERA

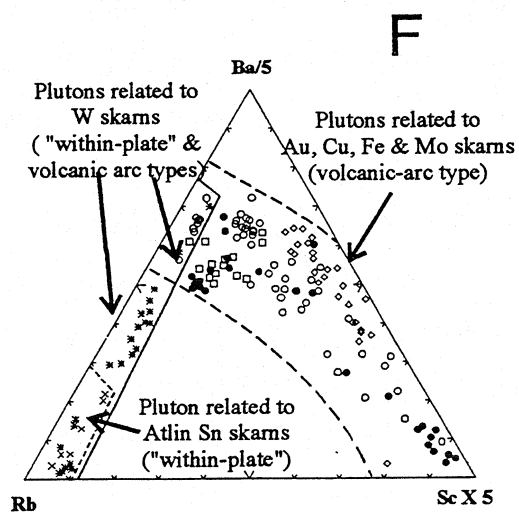
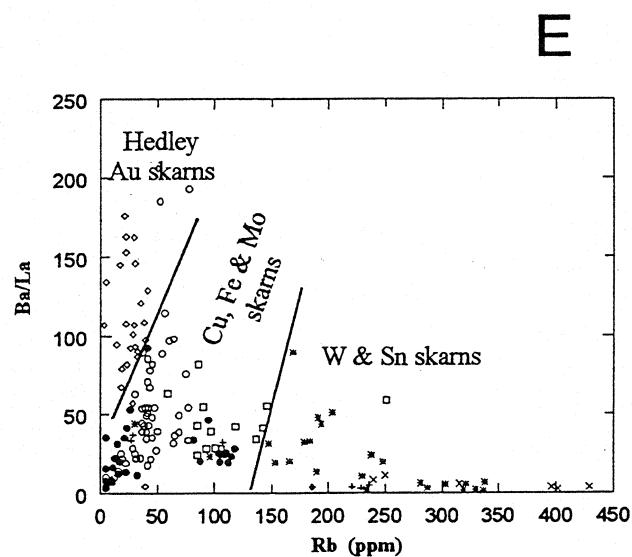
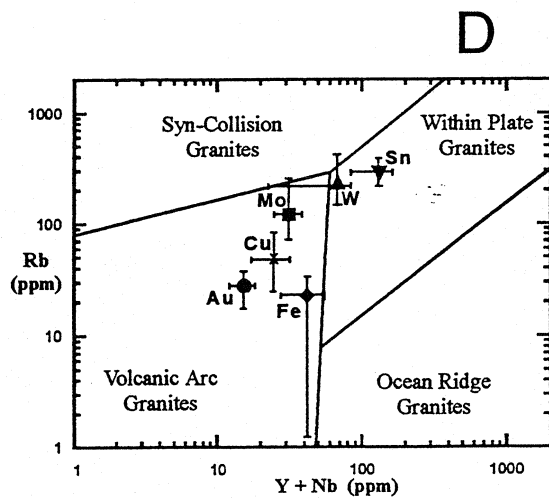
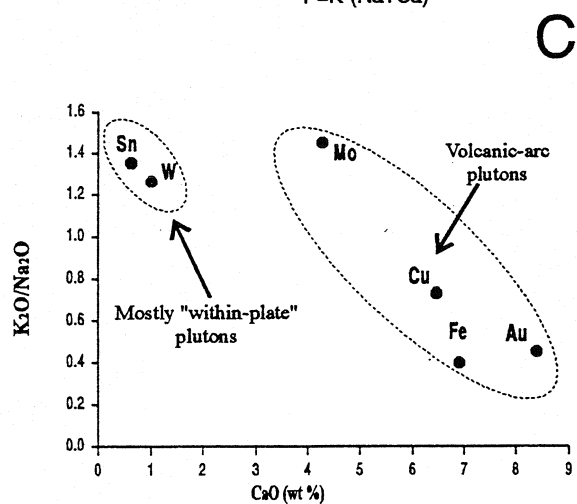
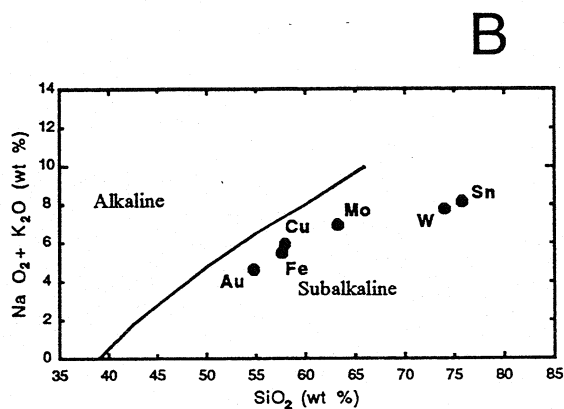
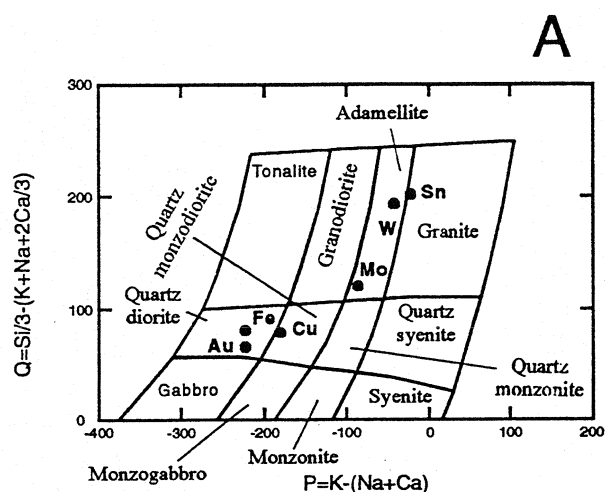
All of the significant Fe skarns in the Canadian Cordillera represent island-arc-related calcic skarns as defined by Einaudi *et al.*, (1981). They are characterized by extensive epidote-pyroxene or albite-scapolite endoskarn alteration (Table 4), and an Fe-rich calc-silicate gangue in the carbonate or volcanic exoskarn consisting of prograde epidote-grandite-ferrosalite with retrograde chlorite and actinolite. These mineral assemblages reflect an intermediate oxidation state (Einaudi *et al.*, 1981).

Most of the Fe skarns in the Canadian Cordillera lie in Wrangellia terrane (Fig. 1) where they are associated with calc-alkaline, island-arc-related, Early to Late Jurassic intrusions of gabbro-diorite composition (Figs. 3C and 6A; Woodsworth *et al.*, 1991; Anderson and Reichenbach, 1991). Most deposits are hosted by limestones of the Upper Triassic Quatsino Formation on Vancouver Island, and the equivalent Marble Bay and Kunga formations on Texada and the Queen Charlotte Islands, respectively. To a lesser degree, they may also be partly hosted by volcanic basalts of the underlying Karmutsen or Texada formations (Fig. 7).

Iron skarns have been described by Sangster (1969) and Meinert (1984), and the major deposits are listed in Table 1A and Figure 1. None are currently being mined, but they have accounted for nearly 90 % of the Fe production from skarn (Ray and Webster, 1997).

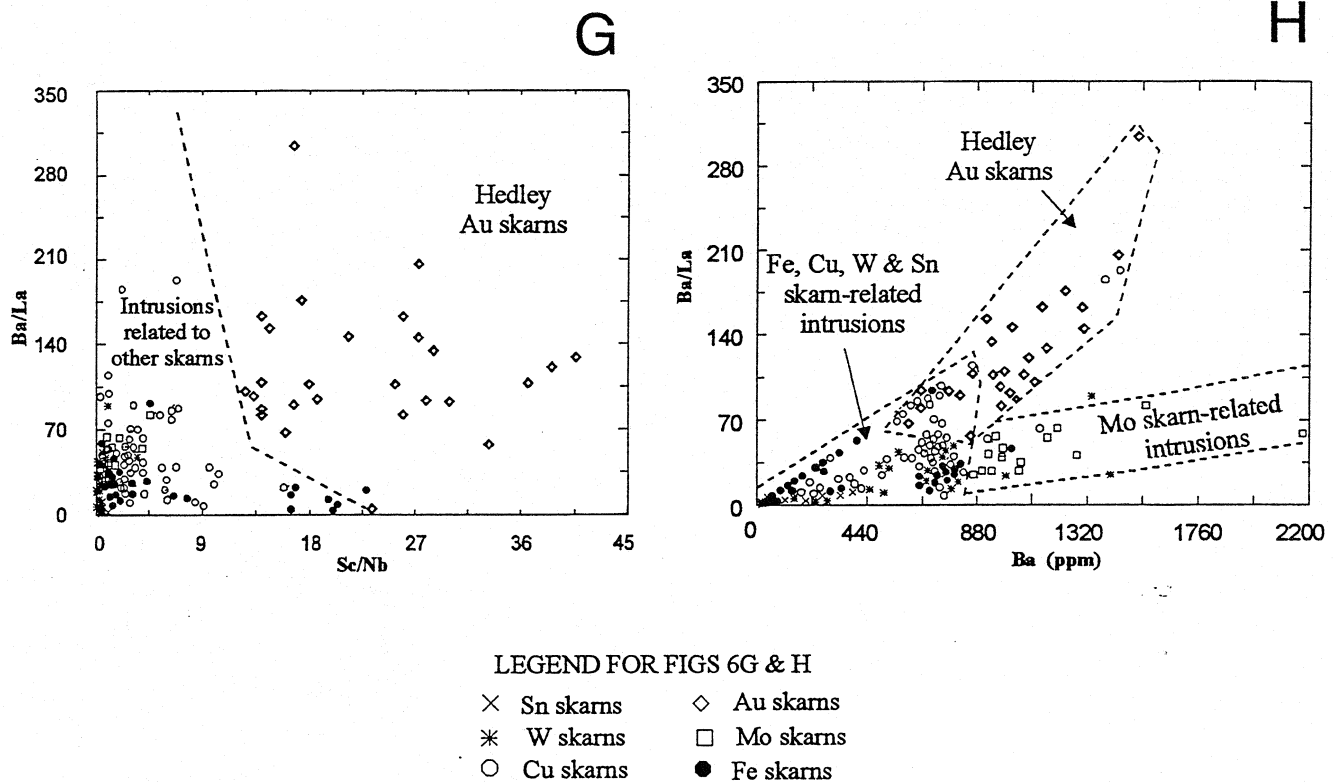
Many deposits are strongly controlled by both the pluton margins and stratigraphy in the country rocks (Figs 7 and 8). The Merry Widow and Texada Island skarns are hosted mainly by Triassic limestones of the Quatsino and Marble Bay formations, respectively. However, the former deposit lies at the top of the limestone formation (Haug, 1977; Ray and Webster, 1991) whereas the Texada Island skarns are concentrated at the base of the formation, along its contact with the underlying volcanics (Fig. 7; Webster and Ray, 1990a, 1990b). The Kingfisher deposits, which are close to the Merry Widow mine, have morphological, textural and mineralogical features that distinguish them from other Fe skarns in Wrangellia. They form sub-circular, pipe-like and replacement orebodies that sharply crosscut limestone hostrocks which show little evidence of skarn alteration (Haug and Farquharson, 1976). The magnetite is colloform textured (Stevenson and Jeffrey, 1964; Sangster, 1965), is cut by phlogopite veinlets, and has anomalously high F abundances (up to 1800 ppm F; Ray and Webster, 1997).

The magnetite-rich ore generally has a low Cu, Au and sulphide content (< 100 ppb Au and < 1000 ppm Cu). However, many deposits contain variable amounts of late pyrrhotite, pyrite and chalcopyrite which occur either as local disseminations in the magnetite or as more distal veins and pods. The sulphide-rich ore may have high Au, Ag and Cu (up to 32 ppm, 200 ppm and 17 % respectively;



LEGEND FOR FIGS 6E & F

- × Sn skarns
- \* W skarns
- Cu skarns
- ◇ Au skarns
- Mo skarns
- Fe skarns



**Figure 6.** Plots comparing the chemistry of plutonic rocks related to Fe, Cu, Au, Mo, W and Sn skarns in British Columbia (data from Ray *et al.*, 1995; Ray and Webster, 1997).

- A: Plot illustrating the mean composition of the various skarn-related igneous rocks. Plot after Debon and Le Fort (1983).
- B: Alkali vs. silica plot (using mean values) demonstrating the subalkaline affinity of the igneous rocks associated with all the metallic skarn classes. Plot after Irvine and Barager (1971).
- C:  $K_2O/Na_2O$  vs.  $CaO$  plot (using mean values) of the various skarn-related igneous rocks.
- D: Trace element discrimination plots (after Pearce *et al.* (1984), illustrating the "volcanic arc" character of intrusions related to Fe, Cu, Au and Mo skarns, and the "within-plate" character of those related to Sn and most W skarns. Points represent mean values; bar lines represent standard deviations.
- E: Ba/La vs. Rb plot.
- F: Triangular Rb-Ba/5-Sc X 5 discrimination plot.
- G: Ba/La vs. Sc/Nb plot.
- H: Ba/La vs. Ba plot.

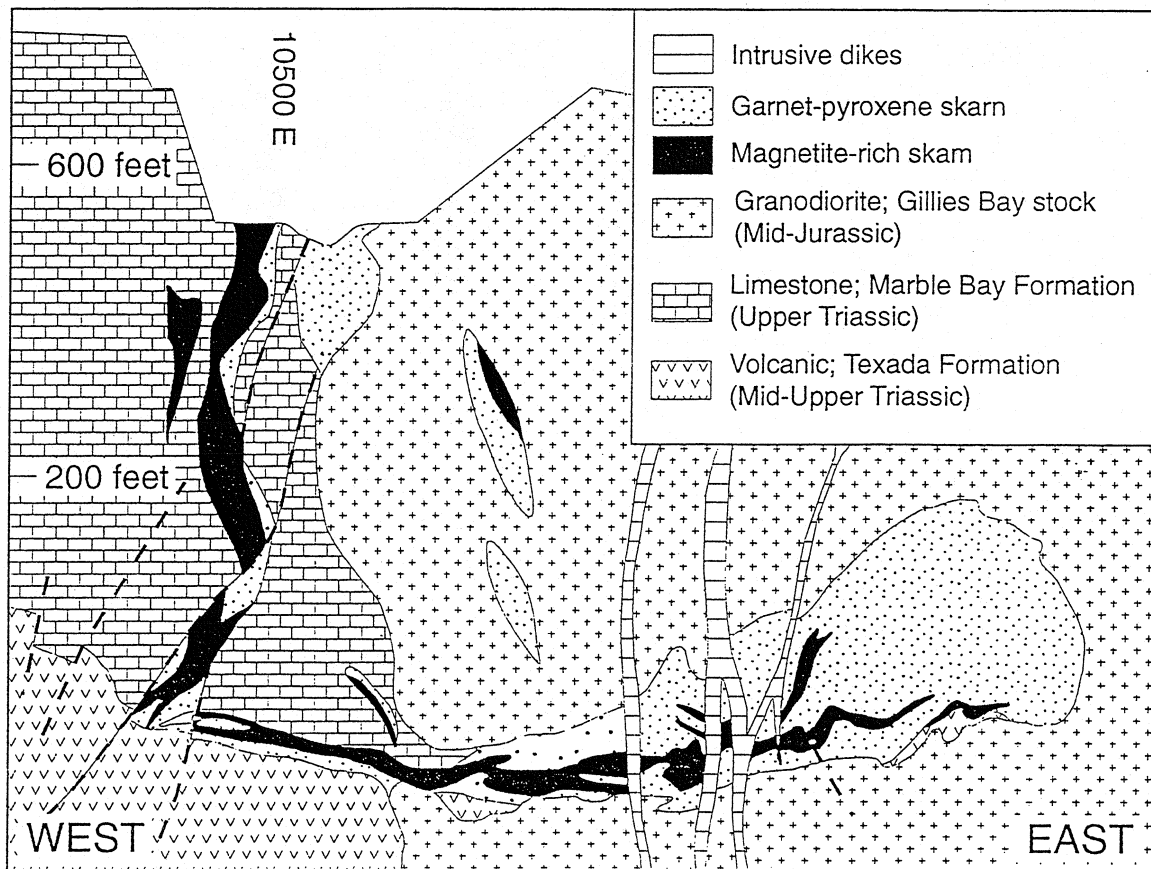
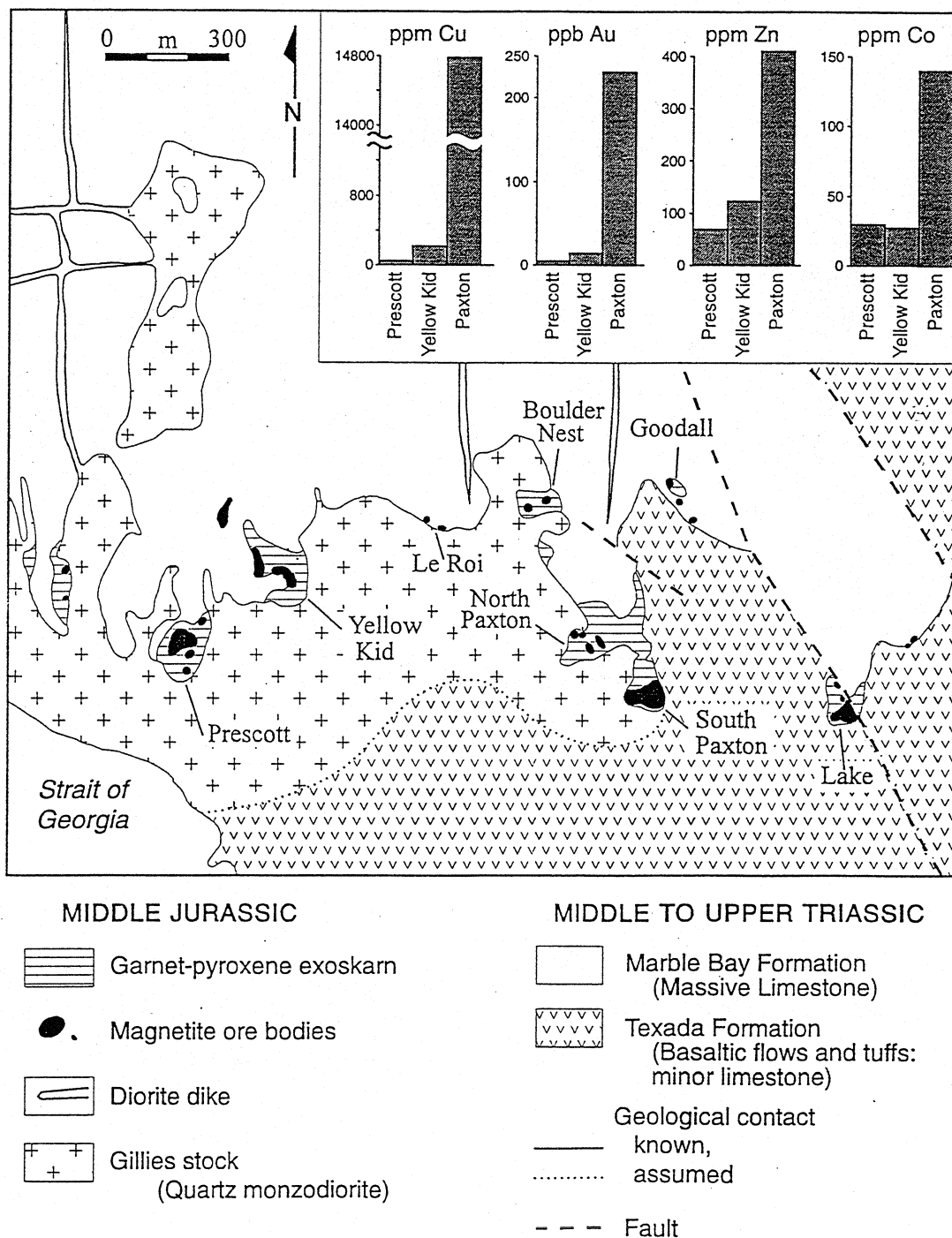


Figure 7. East-west geological cross-section through the Prescott Fe skarn deposit, Texada Island, B.C., showing the magnetite ore being controlled by stratigraphic contacts and high angle structures. From Webster and Ray (1990a); data courtesy of Ideal Cement Company, Texada Island.



**Figure 8.** Geology of the Texada Iron camp, Texada Island, B.C., showing distribution of the Fe skarn deposits along the margin of the Gillies stock. Inset bar charts show an easterly increases in Cu, Au, Zn and Co in the Fe skarn deposits. Geology and chemical data from Bacon (1957), Webster and Ray (1990a, b) and Ray and Webster (1997).

Ettlinger and Ray, 1989), and anomalous amounts of Co and Zn. A positive correlation between Cu, Au, Ag and S is apparent in these deposits (Ray and Webster, 1995). Many sulphide-rich Fe skarns have recently been explored for their Au potential but without economic success.

A metal zoning is apparent in some Fe skarn deposits or camps. In the Merry Widow camp, a vertical zoning probably occurs between the Cu±Au±magnetite-bearing Old Sport deposit, which lies along the base of the Quatsino limestone, and the overlying magnetite-dominant Merry Widow deposit at the top of the Quatsino unit. By contrast, there is a lateral metal zoning in the Texada Island Fe skarns where Cu, Au, Ag, Zn and Co abundances increase to the east (Fig. 8).

## COPPER SKARNS - GENERAL SYNOPSIS

**EXAMPLES:** (*Canadian Cordillera*): Numerous deposits in the Whitehorse Copper Belt (105D 053), Craigmont (092ISE 035), Phoenix (082ESE 020), Old Sport (092L 035), Queen Victoria (082FSW 082).

(*Elsewhere*): Mines Gaspé deposits (Québec, Canada), Ruth, Mason Valley and Copper Canyon (Nevada, USA), Carr Fork (Utah, USA), Ok Tedi (Papua New Guinea), Big Gossan, Ertsberg, Gunung Bijih Timor-IOZ-DOZ (Irian Jaya, Indonesia), Rosita (Nicaragua), Candelaria (Chile), Antamina (Peru).

**HOST/ASSOCIATED ROCK TYPES:** Alkalic and subalkalic porphyritic stocks, dikes and breccia pipes of quartz diorite, granodiorite, monzogranite and tonalite composition, intruding carbonate rocks, calcareous volcanics or tuffs. Copper skarns in oceanic island arcs tend to be associated with more mafic intrusions (quartz diorite to granodiorite), while those formed in continental margin environments are associated with more felsic rocks.

**DEPOSIT FORM:** Highly varied; includes stratiform and tabular orebodies, vertical pipes, narrow lenses, and irregular ore zones that are controlled by intrusive contacts, sedimentary host lithologies or structures.

**TEXTURES:** Igneous textures in endoskarn. Coarse to fine-grained, massive granoblastic to mineralogically layered textures in exoskarn. Some hornfelsic textures.

**ORE MINERALOGY** (Principal and *subordinate*): Moderate to high sulphide content. Chalcopyrite ± pyrite ± magnetite in inner garnet-pyroxene zone. Bornite ± chalcopyrite ± sphalerite ± tennantite in outer wollastonite zone. Hematite, pyrite, pyrrhotite or magnetite may predominate (depending on the oxidation and sulphidation states). Scheelite and traces of chalcocite, molybdenite, bismuthinite, galena, cosalite, arsenopyrite, enargite, tennantite, loellingite, cobaltite, goethite, tetrahedrite, covellite, digenite, electrum, native gold, native copper and rutile may be present. Distal to the skarn envelope, veins of pyrite, chalcopyrite, galena and sphalerite may occur.

**ALTERATION MINERALOGY:** Exoskarn alteration: usually high garnet:pyroxene ratios. High Fe, low Al, Mn andradite garnet (Ad35-100), and diopsidic clinopyroxene (Hd2-50). However, some deposits, such as the Candelaria skarn in Chile (Ryan *et al.*, 1996) include hedenbergitic pyroxenes.

Other minerals include K-feldspar, biotite, amphibole, clinozoisite, epidote, wollastonite, scapolite and sericite. The mineral zoning from stock out to marble is commonly: diopside + andradite (proximal); wollastonite ± tremolite/actinolite ± garnet ± diopside ± vesuvianite (distal). Retrograde alteration to actinolite, chlorite and montmorillonite is common. Other late alteration may include K-feldspar, epidote and minor sericite. The Candelaria Cu skarn in Chile includes scapolite (Ryan *et al.*, 1995), and skarn alteration associated with some of the alkalic porphyry Cu-Au deposits in British Columbia contains late scapolite veining. Magnesian Cu skarns also contain olivine, serpentine, monticellite and brucite.

Endoskarn alteration: Potassic alteration with K-feldspar, epidote, sericite  $\pm$  pyroxene  $\pm$  garnet. Retrograde phyllic alteration generates actinolite, talc, chlorite and clay minerals. The exoskarn may pass out to a highly altered or silicified marble zone.

**ORE CONTROLS:** Irregular or tabular orebodies tend to form in carbonate rocks and/or calcareous volcanics or tuffs near igneous contacts. Pre-skarn structures and hostrock permeability can be important. Some ore bodies (e.g. Ertsberg) form in pendants within the igneous stocks. Copper mineralization is present as stockwork veining and disseminations in both endoskarn and exoskarn; it commonly accompanies retrograde alteration.

**ASSOCIATED DEPOSIT TYPES:** Porphyry Cu deposits, Au, Fe and Pb-Zn skarns, and replacement Pb-Zn-Ag deposits.

**GEOCHEMICAL SIGNATURE:** Rock analyses may show Cu-Au-Ag-rich inner zones grading outward through Au-Ag zones with high Au:Ag ratios to an outer Pb-Zn-Ag zone. Cobalt-As-Sb-Bi-Mo-W geochemical anomalies are present in the more reduced Cu skarn deposits.

**GEOPHYSICAL SIGNATURE:** Magnetic, electromagnetic and induced polarization anomalies.

**GRADE AND TONNAGE:** Worldwide, average 1 to 2 % Cu and generally range from 1 to 100 Mt, although some exceptional deposits exceed 300 Mt (the Candelaria deposit in Chile, for example, contains 366 Mt grading 1.08% Cu (Ryan *et al.*, 1995).

**IMPORTANCE:** Historically, these deposits were a major source of Cu, although porphyry deposits have become much more important during the last 30 years. However, major Cu skarns are still worked throughout the world, including those in China, Indonesia and the U.S.

## COPPER SKARNS IN THE CANADIAN CORDILLERA

Copper skarns are widely distributed throughout the Canadian Cordillera and the greatest number of occurrences lie in Wrangellia (Table 2A). However, most of the larger deposits are hosted by Upper Triassic island-arc rocks of the Quesnellia and Stikine terranes (Tables 1A and B; Fig. 1). They can be broadly separated into two types: (1) those associated with generally alkaline porphyry Cu-Au stocks, which are commonly hosted by mafic tuffs or volcanics; and (2) those related to calc-alkaline plutons of diorite-quartz monzodiorite-granodiorite composition. The latter type are generally hosted by calcareous sedimentary rocks and porphyry-style mineralization is relatively uncommon.

Copper skarns associated with alkalic porphyry systems, such as the Ingerbelle deposit (Preto, 1972) tend to be large (>100 Mt), of lower grade (<0.7 % Cu), and their exoskarns are dominated by epidote-actinolite-biotite-K feldspar assemblages which partly reflect their mafic volcanic and tuffaceous hostrocks. At Galore Creek, prograde skarn ore constitutes about 80 % of the reserves (c. 280 Mt of 0.67 % Cu; Table 1A). It includes an assemblage of orthoclase and biotite in high-K volcanoclastic hostrocks, but changes to a calcic assemblage of andradite, diopside, epidote and vesuvianite in calcareous hostrocks (Enns *et al.*, 1995; Dawson and Kirkham, 1996).

Copper skarns related to calc-alkaline plutons tend to be more numerous, smaller (<30 Mt), of higher grade (> 1 % Cu), and are commonly associated with grandite garnet, diopsidic pyroxene and



epidote-rich exoskarn envelopes. Significant deposits of this type include the Craigmont and Old Sport skarns, the deposits of the Greenwood-Phoenix camps (Motherlode, Emma, Greyhound, Oro Denoro, Rawhide, Snowshoe, Idaho and Phoenix; Figs. 1 and 9), and the Marble Bay, Cornell and Little Billie Cu skarns on Texada Island (Morrison, 1980; Church, 1986; Ettlinger and Ray, 1989). In addition, there are the more than 30 orebodies comprising the Whitehorse Copper Belt (Figs. 1 and 10; Tenney, 1981; Morrison, 1981; Watson, 1984; Meinert, 1986; MacKay *et al.*, 1993).

Over half of the Cu skarn occurrences in B.C., whether related to calc-alkaline or alkaline plutonism, are Early to Middle Jurassic in age (Ray *et al.*, 1995). However, some deposits in the Greenwood camp, as well as those in the Whitehorse belt are Cretaceous (Morrison, 1981; Tenney, 1981; Church, 1986). Most Cu skarns have formed at high structural levels, are marked by high pyrite:pyrrhotite ratios and oxidized mineral assemblages. A mineral zoning is common in which pyrite-chalcopyrite-magnetite near plutonic contacts passes gradationally to bornite-chalcopyrite-wollastonite near the marble contacts. This reflects the trend both with time, and towards the periphery of the system, to a decrease in total Fe and an increase in the oxidation-sulphidation states (Table 4; Burt, 1972; Einaudi *et al.*, 1981). Deposits formed at deeper levels tend to have more reduced mineral assemblages, low pyrite:pyrrhotite ratios and are commonly enriched in W, Mo, Bi, Zn, As and Au. Deposits formed near the periphery of the system are enriched in sphalerite, pyrrhotite, tennantite and galena. Retrograde alteration assemblages include sulphides with actinolite, carbonates, clay, silica, Fe oxides and lesser amounts of chlorite, epidote and talc. Copper skarns associated with unmineralized stocks lack the intense stockwork fracturing typical of a porphyry system, and their retrograde alteration assemblages, together with significant concentrations of base and precious metals, are commonly restricted to widely spaced fractures, contact zones and vug fillings.

Ores at the Craigmont, Maid of Erin and Blue Grouse deposits (Fig. 1), have very low Au contents and correspondingly high Cu:Au ratios. However some deposits such as the Phoenix, Motherlode, Marble Bay and Old Sport have sufficiently high Au contents to allow its recovery as an important economic byproduct. The Greenwood-Phoenix camp (Figs. 1 and 9) represents a major concentration of productive Cu (Au) skarn deposits (Church, 1986; Ettlinger and Ray, 1989; Fyles, 1990). Extensive, stratigraphically controlled garnet and epidote-rich skarns are developed discontinuously over an 1.8 km by 1.4 km area (Fig. 9). Two narrow Au-bearing sulphide zones, the Jacinto and Sylvester K (Fig. 9), are located northwest of, and a short distance beyond the skarn envelope. These represent either massive replacements related to the Phoenix system (Church, 1986; Ray and Webster, 1997) or older VMS-type orebodies (M. Rasmussen, personal comm. 1997).

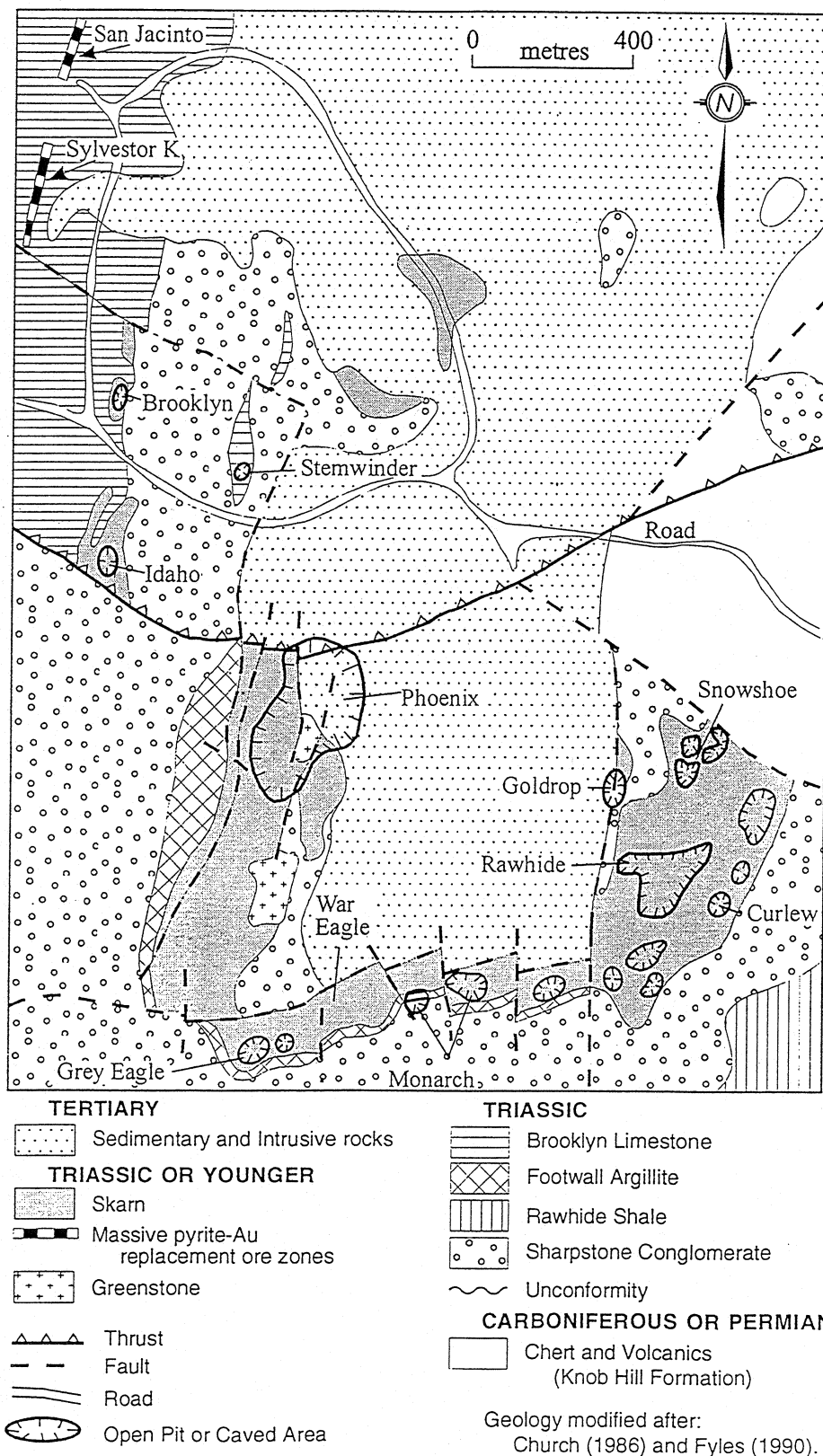
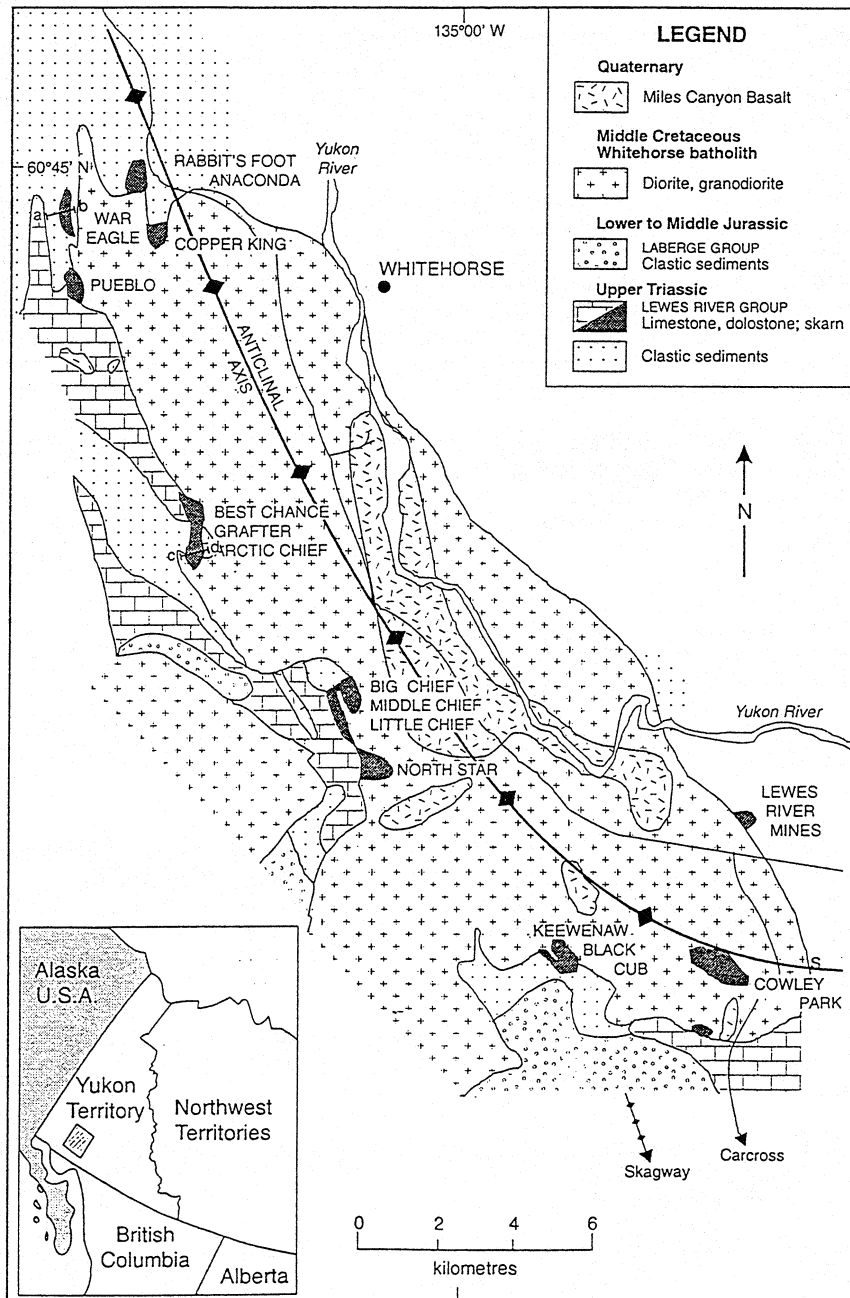


Figure 9. Geology of the Phoenix camp, southern B.C., showing the distribution of the Cu (Au) skarn and possible replacement deposits (adapted after Church, 1986; Fyles, 1990).



**Figure 10.** Regional geology of the Whitehorse Copper Belt showing distribution of the deposits around the margins of the Whitehorse batholith (after Morrison, 1981; Watson, 1984; Dawson and Kirkham, 1996).

## GOLD SKARNS - GENERAL SYNOPSIS

**EXAMPLES:** (*Canadian Cordillera*): Marn (116B 147), Guder (115I 053), Nickel Plate (092HSE038), French (092HSE059), Canty (092HSE 064), Good Hope (092HSE060), QR - Quesnel River (093A121).

(*Elsewhere*): Fortitude, McCoy and Tomboy-Minnie (Nevada, USA), Buckhorn Mountain (Washington, USA), Diamond Hill, New World district and Butte Highlands (Montana, USA), Nixon Fork (Alaska, USA), Thanksgiving (Philippines), Browns Creek and Junction Reefs-Sheahan-Grants (New South Wales, Australia), Mount Biggenden (Queensland, Australia), Savage Lode, Coogee (Western Australia, Australia), Nambija (Ecuador), Wabu (Irian Jaya, Indonesia).

**CAPSULE DESCRIPTION:** Gold skarns are defined as skarn deposits in which Au is the primary or dominant economic metal. The gold is often intimately associated with Bi or Au-tellurides, and commonly occurs as minute blebs (<40 microns) that lie within or on sulphide grains. The vast majority of Au skarns are hosted by calcareous sedimentary or volcanic rocks (calcic subtype). The much rarer magnesian subtype is hosted by dolomites or Mg-rich volcanics. On the basis of gangue mineralogy, the calcic Au skarns can be separated into either pyroxene-rich, garnet-rich or epidote-rich types; these contrasting mineral assemblages reflect differences in the host rock lithologies as well as the oxidation and sulphidation conditions in which the skarns developed.

**TECTONIC SETTINGS:** Most Au skarns form in orogenic belts at convergent plate margins, where they commonly exhibit a temporal and spatial association with Cu porphyry belts (Ray *et al.*, 1990). In the southwestern United States and Australia, Au skarns are commonly hosted in Paleozoic to lower Mesozoic shelf and basinal sedimentary rocks of cratonic origin and they range from Paleozoic to Tertiary in age. Gold skarns tend to be associated with syn to late island arc intrusions emplaced into calcareous sequences in arc or back-arc environments.

**DEPOSITIONAL ENVIRONMENT / GEOLOGICAL SETTING:** Most deposits are related to plutonism associated with the development of oceanic island arcs or back arcs, such as the Late Triassic to Early Jurassic Nicola Group in British Columbia.

**AGE OF MINERALIZATION:** Phanerozoic (mostly Cenozoic and Mesozoic); in the Canadian Cordillera are mainly of Early to Middle-Jurassic age. The unusual magnesian Au skarns of Western Australia are Archean.

**HOST/ASSOCIATED ROCK TYPES:** Gold skarns are hosted by sedimentary carbonates, calcareous clastics, volcanoclastics or (rarely) volcanic flows. They are commonly related to high to intermediate level stocks, sills and dikes of gabbro, diorite, quartz diorite or granodiorite composition. Economic mineralization is rarely developed in the endoskarn. The I-type intrusions are commonly porphyritic, undifferentiated, Fe-rich and calc-alkaline. However, the Nambija, Wabu and QR Au skarns are associated with alkalic intrusions.

**DEPOSIT FORM:** Variable from irregular lenses and veins to tabular or stratiform orebodies with lengths ranging up to many hundreds of metres. Rarely, can occur as vertical pipe-like bodies along permeable structures.

**TEXTURE/STRUCTURE:** Igneous textures in endoskarn. Coarse to fine-grained, massive granoblastic to layered textures in exoskarn. Some hornfelsic textures. Fractures, sill-dike margins and fold hinges can be an important loci for mineralization.

**ORE MINERALOGY (Principal and subordinate):** The gold is commonly present as micron-sized inclusions in sulphides, or at sulphide grain boundaries. To the naked eye, ore is generally indistinguishable from waste rock. Due to the poor correlation between Au and Cu in some Au skarns, the economic potential of a prospect can be overlooked if Cu-sulphide-rich outcrops are preferentially sampled and other sulphide-bearing or sulphide-lean assemblages are ignored. The ore in pyroxene-rich and garnet-rich skarns tends to have low Cu:Au (<2000:1), Zn:Au (<100:1) and Ag:Au (<1:1) ratios, and the gold is commonly associated with Bi minerals (particularly Bi tellurides).

**Magnesian subtype:** Native gold  $\pm$  pyrrhotite  $\pm$  chalcopyrite  $\pm$  pyrite  $\pm$  magnetite  $\pm$  galena  $\pm$  tetrahedrite.

**Calcic subtype:**

**Pyroxene-rich Au skarns:** Native gold  $\pm$  pyrrhotite  $\pm$  arsenopyrite  $\pm$  *chalcopyrite*  $\pm$  *tellurides* (e.g. *hedleyite*, *tetradymite*, *altaite* and *hessite*)  $\pm$  *bismuthinite*  $\pm$  *cobaltite*  $\pm$  *native bismuth*  $\pm$  *pyrite*  $\pm$  *sphalerite*  $\pm$  *maldonite*. They generally have a high sulphide content and high pyrrhotite:pyrite ratios. Mineral and metal zoning is common in the skarn envelope. At Nickel Plate for example, this comprises a narrow proximal zone of coarse-grained, garnet skarn containing high Cu:Au ratios, and a wider, distal zone of finer grained pyroxene skarn containing low Cu:Au ratios and the Au-sulphide orebodies.

**Garnet-rich Au skarns:** Native gold  $\pm$  *chalcopyrite*  $\pm$  *pyrite*  $\pm$  *arsenopyrite*  $\pm$  *sphalerite*  $\pm$  *magnetite*  $\pm$  *hematite*  $\pm$  *pyrrhotite*  $\pm$  *galena*  $\pm$  *tellurides*  $\pm$  *bismuthinite*. They generally have a low to moderate sulphide content and low pyrrhotite:pyrite ratios.

**Epidote-rich Au skarn:** Native gold  $\pm$  *chalcopyrite*  $\pm$  *pyrite*  $\pm$  *arsenopyrite*  $\pm$  *hematite*  $\pm$  *magnetite*  $\pm$  *pyrrhotite*  $\pm$  *galena*  $\pm$  *sphalerite*  $\pm$  *tellurides*. They generally have a moderate to high sulphide content with low pyrrhotite:pyrite ratios.

#### EXOSKARN MINERALOGY (GANGUE):

**Magnesian subtype:** Olivine, clinopyroxene (Hd2-50), garnet (Ad7-30), chondrodite and monticellite. Retrograde minerals include serpentinite, epidote, vesuvianite, tremolite-actinolite, phlogopite, talc, K-feldspar and chlorite.

#### Calcic subtype:

**Pyroxene-rich Au skarns:** Extensive exoskarn, generally with high pyroxene:garnet ratios. Prograde minerals include diopsidic to hedenbergitic clinopyroxene (Hd 20-100), K-feldspar, Fe-rich biotite, low Mn grandite garnet (Ad 10-100), wollastonite and vesuvianite. Other less common minerals include rutile, axinite and sphene. Late or retrograde minerals include epidote, chlorite, clinozoisite, vesuvianite, scapolite, tremolite-actinolite, sericite and prehnite.

**Garnet-rich Au skarns:** Extensive exoskarn, generally with low pyroxene:garnet ratios. Prograde minerals include low Mn grandite garnet (Ad 10-100), K-feldspar, wollastonite, diopsidic clinopyroxene (Hd 0-60), epidote, vesuvianite, sphene and apatite. Late or retrograde minerals include epidote, chlorite, clinozoisite, vesuvianite, tremolite-actinolite, sericite, dolomite, siderite and prehnite.

**Epidote-rich Au skarns:** Abundant epidote and lesser chlorite, tremolite-actinolite, quartz, K-feldspar, garnet, vesuvianite, biotite, clinopyroxene and late carbonate. At the QR deposit, epidote-pyrite and carbonate-pyrite veinlets and coarse aggregates are common, and the best ore occurs in the outer part of the alteration envelope, within 50 m of the epidote skarn front.

**ENDOSKARN MINERALOGY (GANGUE):** Moderate endoskarn development with K-feldspar, biotite, Mg-pyroxene (Hd 5-30) and garnet. Endoskarn at the epidote-rich QR deposit is characterized by calcite, epidote, clinozoisite and tremolite whereas at the Butte Highlands Mg skarn it contains argillic and propylitic alteration with garnet, clinopyroxene and epidote.

**WEATHERING:** In temperate and wet tropical climates, skarns often form topographic features with positive relief.

**ORE CONTROLS:** The ore exhibits strong stratigraphic and structural controls. Orebodies form along sill-dike intersections, sill-fault contacts, bedding-fault intersections, fold axes and permeable faults or tension zones. In the pyroxene-rich and epidote-rich types, ore commonly develops in the more distal portions of the alteration envelopes. In some districts, specific suites of reduced, Fe-rich intrusions are spatially related to Au skarn mineralization. Ore bodies in the garnet-rich Au skarns tend to lie more proximal to the intrusions.

**GENETIC MODEL:** Many Au skarns are related to plutons formed during oceanic plate subduction. There is a worldwide spatial, temporal and genetic association between porphyry Cu provinces and calcic Au skarns. Pyroxene-rich Au skarns tend to be hosted by siltstone-dominant packages and form in hydrothermal systems that are sulphur-rich and relatively reduced. Garnet-rich Au skarns tend to be hosted by carbonate-dominant packages and develop in more oxidising and/or more sulphur-poor hydrothermal systems.

**ASSOCIATED DEPOSIT TYPES:** Au placers, calcic Cu skarns, porphyry Cu deposits and Au-bearing quartz and/or sulphide veins. Magnesian subtype can be associated with porphyry Mo deposits and possibly W skarns. In British Columbia there is a negative spatial association between Au and Fe skarns at regional scales, even though both classes are related to arc plutonism. Fe skarns are concentrated in the Wrangellia Terrane whereas most Au skarn occurrences and all the economic deposits lie in Quesnellia.

**GEOCHEMICAL SIGNATURE:** Au, As, Bi, Te, Co, Cu, Zn or Ni soil, stream sediment and rock anomalies, as well as some geochemical zoning patterns throughout the skarn envelope (notably in Cu/Au, Ag/Au and Zn/Au ratios). Calcic Au skarns (whether garnet-rich or pyroxene-rich) tend to have lower Zn/Au, Cu/Au and Ag/Au ratios than any other skarn class (Fig. 13). The intrusions related to Au skarns

may be relatively enriched in the compatible elements Cr, Sc and V, and depleted in lithophile incompatible elements (Rb, Zr, Ce, Nb and La), compared to intrusions associated with most other skarn types.

**GEOPHYSICAL SIGNATURE:** Airborne magnetic or gravity surveys to locate plutons. Induced polarization and ground magnetic follow-up surveys can outline some deposits.

**OTHER EXPLORATION GUIDES:** Placer Au. Any carbonates, calcareous tuffs or calcareous volcanic flows intruded by arc-related plutons have a potential for hosting Au skarns. Favorable features in a skarn envelope include the presence of: (a) proximal Cu-bearing garnet skarn and extensive zones of distal pyroxene skarn which may carry micron Au, (b) hedenbergitic pyroxene (although diopsidic pyroxene may predominate overall), (c) sporadic As-Bi-Te geochemical anomalies, and, (d) undifferentiated, Fe-rich intrusions with low  $\text{Fe}_2\text{O}_3/\text{FeO}$  ratios. Any permeable calcareous volcanics intruded by high-level porphyry systems (particularly alkalic plutons) have a potential for hosting epidote-rich skarns with micron Au. During exploration, skarns of all types should be routinely sampled and assayed for Au, even if they are lean in sulphides.

**GRADE AND TONNAGE:** Worldwide, these deposits range from 0.4 to 13 Mt and from 2 to 15 g/t Au. Theodore *et al.* (1991) report median grades and tonnage of 8.6 g/t Au, 5.0 g/t Ag and 213 000 t. Nickel Plate produced over 71 tonnes of Au from 13.4 Mt of ore (grading 5.3 g/t Au). The 10.3 Mt Fortitude (Nevada) deposit graded 6.9 g/t Au whereas the 13.2 Mt McCoy skarn (Nevada) graded 1.5 g/t Au. The QR epidote-rich Au skarn has reserves exceeding 1.3 Mt grading 4.7 g/t Au.

**IMPORTANCE:** Recently, there have been some significant Au skarn deposits discovered around the world (e.g. Buckhorn Mountain, Wabu, Fortitude). Nevertheless, total historic production of Au from skarn (more than 1 000 t of metal) is minute compared to production from other deposit types. The Nickel Plate deposit (Hedley, British Columbia) was probably one of the earliest major Au skarns in the world to be mined. Skarns have accounted for about 16 % of British Columbia's Au production, although nearly half of this was derived as a byproduct from Cu and Fe skarns.

## GOLD SKARNS IN THE CANADIAN CORDILLERA

In the Canadian Cordillera, many of the most economically important Au skarns, such as those in the Hedley camp (Fig. 1; Nickel Plate, Canty, French, Good Hope), are Early to Middle Jurassic in age (Fig. 3B) and are related to syn- to post-tectonic plutons intruded into Triassic calcareous sequences in island-arc or back-arc environments (Ray *et al.*, 1996). Their principal setting is in accreted Quesnellia Terrane carbonate-clastic rocks that have a significant marine volcanic component. By contrast, the Au skarns at Banks Island, B.C. and Ketzia River, Yukon (Fig. 1), are hosted by displaced cratonic rocks of the Alexander and Cassiar terranes respectively, and are associated with Cretaceous granitoid plutons (Dawson, 1996b). The Marn Au skarn in the Yukon (Brown and Nesbitt, 1987) is also Cretaceous in age, but is hosted by Permian limestones in the Selwyn Basin (Table 1B).

The intrusions related to the Hedley Au skarns are I-type, porphyritic and sub-alkaline (Fig. 6B). They are mostly quartz diorite (Fig. 6A) but range in composition from gabbro to granodiorite. They tend to be undifferentiated, relatively depleted in LIL-elements such as Rb, Ce, Nb and La, and enriched in Cr, Sc, Sr and V (Fig. 6; Ray *et al.*, 1995). They are also characterized by having the highest Ba/La and Sc/Nb ratios, and the lowest mean Rb content of any skarn-related suite in B.C (Fig. 6E and 6G; Ray *et al.*, 1995). In B.C., a negative spatial association exists on a regional scale between Au and Fe skarns,

even though both classes are related to arc plutonism; Au skarns occur mostly in Quesnellia whereas Fe skarns are concentrated in Wrangellia (Fig. 1).

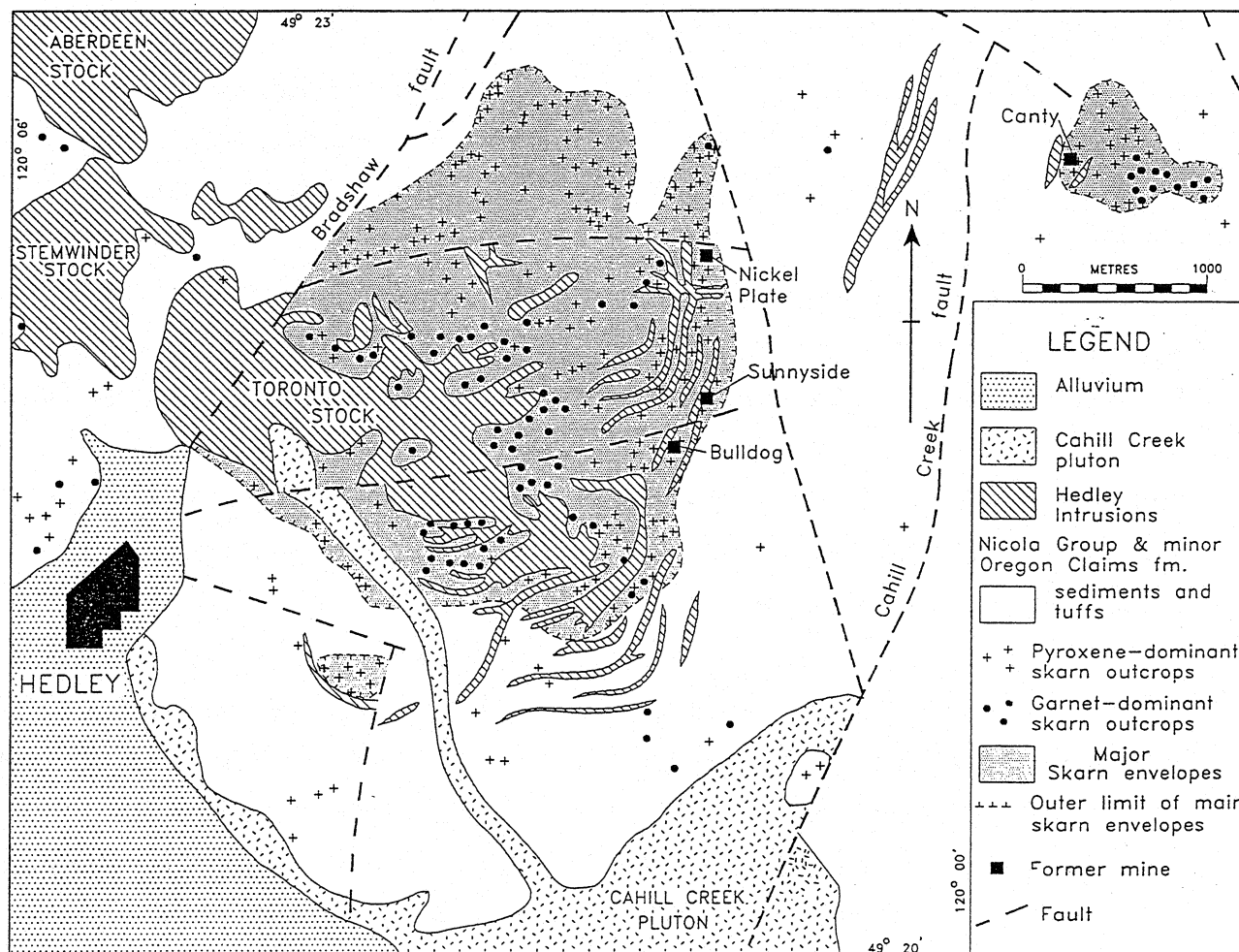
Worldwide, Au skarns include calcic and magnesian varieties; the latter, which are hosted by dolomites and Mg-rich volcanics, are extremely uncommon and have not been identified in the Canadian Cordillera. Examples include the Savage Lode and Butte Highlands deposits in Western Australia and Montana, respectively (Mueller, 1991; Ettlinger *et al.*, 1995).

Calcic Au skarns are hosted by calcareous rocks and, on the basis of gangue mineralogy, can be separated into pyroxene-rich, garnet-rich or epidote-rich types. These contrasting mineral assemblages reflect differences in the hostrock lithologies as well as the oxidation and sulphidation conditions in which each type of Au skarn developed.

*Pyroxene-rich Au skarns* are characterized by low garnet/pyroxene and pyrite/pyrrhotite ratios and the presence of hedenbergitic pyroxene and Fe-rich biotite (Table 4). The related intrusions have low  $\text{Fe}_2\text{O}_3/\text{FeO}$  ratios and the sulphide-rich orebodies tend to lie in the outer parts of the exoskarn envelopes (Table 3). Examples include the Marn skarn in the Yukon (Brown and Nesbitt, 1987) and the Nickel Plate, Canty, French and Good Hope deposits at Hedley, B.C. (Figs. 11 and 12; Billingsley and Hume, 1941; Ettlinger, 1990; Ray and Dawson, 1994). They favour siltstone-dominant hostrocks and their hydrothermal systems are relatively reduced.

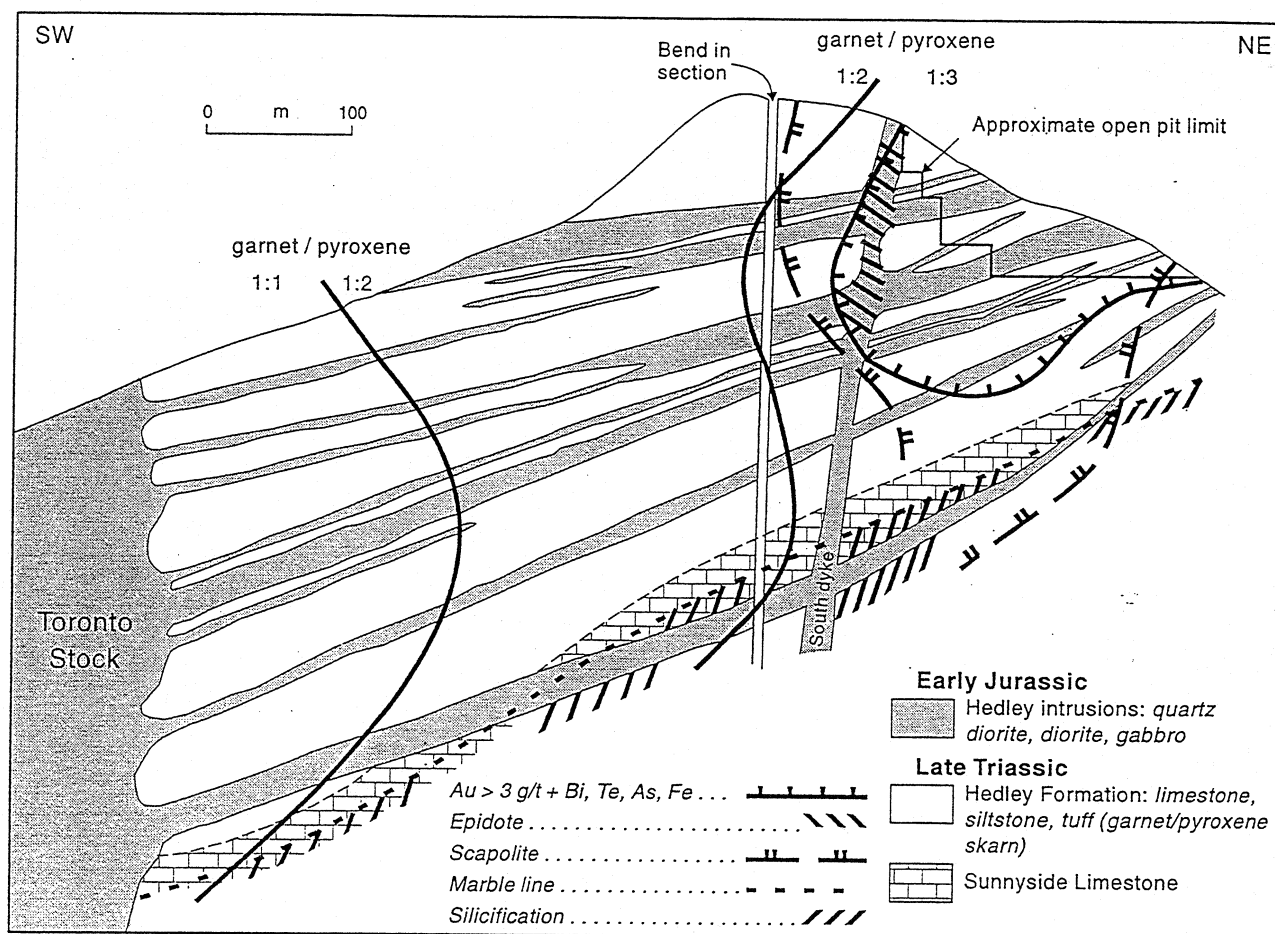
*Garnet-rich Au skarns:* large, economic garnet-rich Au skarns have not yet been identified in the Canadian Cordillera although the Guder skarn in the Yukon (Fig. 1) may be of this type and there a good potential elsewhere for these deposits. Foreign examples include the McCoy and Wabu skarns in Nevada and Indonesia, respectively (Brooks, 1994; Allen *et al.*, 1995). They are characterized by high garnet/pyroxene and pyrite/pyrrhotite ratios, and by the presence of diopsidic pyroxene, pyrite, magnetite and hematite (Table 4). Orebodies are generally sulphide poor and form closer to the intrusions. They can be Cu-poor (<200 ppm Cu), magnetite-rich, and locally contain anomalous amounts of Zn (>1000 ppm Zn). Some of the magnetite-bearing parts of the skarn may be associated with intense hydrothermal brecciation. They favour high-level, relatively oxidized hydrothermal systems and are commonly hosted by carbonate-dominant packages.

*Epidote-rich Au skarns* are uncommon. The QR (Quesnel River) skarn (Fig. 1; Table 1A; Fox and Cameron, 1995) is the only economic deposit known in the Canadian Cordillera, although two deposits in Montana, the McLaren and the Diamond Hill, are believed to be of this type (Johnson and Meinert, 1994; P.S. Mulholland and T. Stepp, personal communication, 1997). The QR skarn is related to a high-level, oxidized alkalic porphyry system and is hosted mainly by epidotized and chloritized mafic

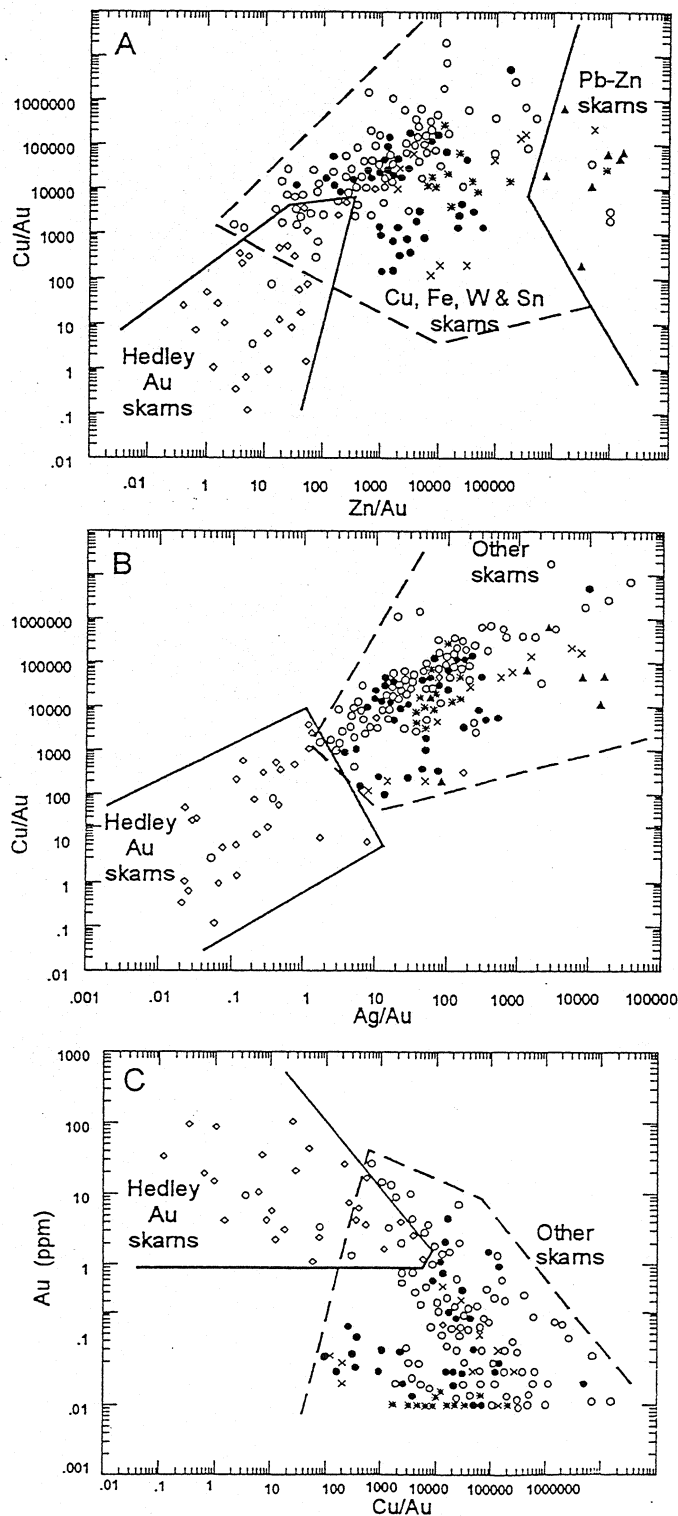


**Figure 11.** Geology of the Nickel Plate and Canty Au skarn deposits, Hedley, B.C., showing distribution of, and mineral zoning in the exoskarn envelopes (after Ray *et al.*, 1996). Note that most of the large Nickel Plate envelope comprises pyroxene skarn but a relatively narrow zone of garnet skarn is developed close to the Toronto stock





**Figure 12.** Cross-section, Nickel Plate Au skarn deposit, Hedley, B.C., after Ettlinger *et al.* (1992). Note the decreasing garnet/pyroxene ratios with increasing distance from the Toronto stock, and that the open pit Au ore lies in the distal, pyroxene-rich skarn.



**Figure 13.** Plots (using assay data from Ray and Webster, 1997) comparing the metal ratios of Au, Fe, Cu, W, Sn and Pb-Zn skarns in British Columbia; (Au skarns = open diamonds; Fe skarns = solid dots; Cu skarns = open circles; W skarns = asterisks; Sn skarns = crosses; Pb-Zn skarns = triangles). Skarn field classes are empirically drawn around main clustering of points. Note the comparatively low metal ratios in the Au skarns.

A: Log Cu/Au versus log Zn/Au. B: log Cu/Au versus log Ag/Au. C: log Au (in ppm) versus log Cu/Au.

volcanics and tuffs. Garnet is very uncommon, and the ore has high pyrite/pyrrhotite ratios and is locally rich in chalcopyrite.

To the naked eye, the ore in most Au skarns is indistinguishable from waste rock. Gold occurs as micron-sized inclusions in sulphides, or at sulphide grain boundaries. In the pyroxene-rich and garnet-rich Au skarns, it is commonly associated with various Bi minerals (including Bi tellurides) and arsenopyrite; in some deposits there is also an enrichment in Co (Table 4). Compared to the ore in other skarn classes (Fig. 13), Au skarn ore has distinctly low base metal/Au ratios ( $\text{Cu}/\text{Au} < 2000$ ;  $\text{Cu}/\text{Ag} < 1000$ ;  $\text{Zn}/\text{Au} < 100$ ,  $\text{Ag}/\text{Au} < 1$ ; Ray, 1996). Moreover, there is no correlation between Cu and Au in many pyroxene-rich and garnet-rich Au skarns (unlike the situation in most Fe and some Cu skarns where there is a good correlation between these metals). Thus, the Au potential of a prospect skarn can be overlooked if Cu sulphide rich outcrops are preferentially sampled and other sulphide-bearing or sulphide-lean assemblages ignored. By contrast, there is a positive Au:Cu correlation in the epidote-rich QR skarn (Fox and Cameron, 1995).

A mineral and metal zoning is common in many Au skarns. At the Nickel Plate deposit this consists of proximal, coarser grained garnet-dominant skarn ( Figs. 11 and 12) with high Cu/Au ratios and distal, finer grained pyroxene-dominant skarn with low Cu/Au ratios and the Au orebodies (Ettlinger *et al.*, 1992). District-wide zonation is also manifest at the Ketz River deposit in the Yukon, where Au-rich pyrrhotite-chalcopyrite manto orebodies apparently grade outward over 1 to 3 km to Ag-Pb-Zn replacements (Cathro, 1990). Mineral zoning is also present at the epidote-rich QR deposits and the richest ore occurs within 50 m of the distal epidote skarn front (Fox and Cameron, 1995).

## MOLYBDENUM SKARNS - GENERAL SYNOPSIS

EXAMPLES: (*Canadian Cordillera*): Coxey (082FSW110), Novelty (082FSW107).

(*Elsewhere*): Mount Tennyson (New South Wales, Australia), Little Boulder Creek (Idaho, USA), Cannivan Gulch (Montana, USA), Azegour (Morocco), Yangchiachangtze (China).

CAPSULE DESCRIPTION: Molybdenite-dominant mineralization genetically associated with a skarn gangue (includes calcic and magnesian Mo skarns). Molybdenum skarns are broadly separable into two types: polymetallic (containing molybdenite with other W, Zn, Pb, Bi, Sn, Co or U-rich minerals), and "molybdenite-only" (containing mainly molybdenite with no or few other sulphides).

TECTONIC SETTING: Late orogenic plutonism (derived from transitional crust) intruding continental margin carbonate sequences. Also, some are associated with Mo-bearing porphyry systems developed within intra-oceanic island arcs.

AGE OF MINERALIZATION: Mainly Mesozoic and Paleozoic, but may be any age. In the Canadian Cordillera, they are mainly Early to mid-Jurassic in age.

**HOST/ASSOCIATED ROCK TYPES:** Stocks and dikes of evolved, commonly leucocratic quartz monzonite to granite (some containing primary biotite and muscovite) intruding calcareous clastic rocks. Deposits tend to develop close to intrusive contacts. Some of the Mo skarns in British Columbia are associated with high-level intrusions that have explosive breccia textures.

**DEPOSIT FORM:** Irregular orebodies along, and controlled by, the intrusive contacts.

**TEXTURES:** Igneous textures in endoskarn; local explosive breccia textures. Coarse to fine-grained, massive granoblastic to mineralogically layered textures in exoskarn. Some hornfelsic textures.

**ORE MINERALOGY (Principal and subordinate):** Molybdenite  $\pm$  *scheelite*  $\pm$  *powellite*  $\pm$  *chalcopyrite*  $\pm$  *arsenopyrite*  $\pm$  pyrite  $\pm$  pyrrhotite  $\pm$  *bismuthinite*  $\pm$  *sphalerite*  $\pm$  *fluorite*. In rare instances Mo skarns carry *galena*  $\pm$  *magnetite*  $\pm$  *uraninite*  $\pm$  *pitchblende*  $\pm$  *cassiterite*  $\pm$  *cobaltite*  $\pm$  *stannite*  $\pm$  *Au*.

**EXOSKARN ALTERATION:** Calcic Mo skarns: Hedenbergite pyroxene (Hd50-80, Jo-3)  $\pm$  low Mn grossular-andradite garnet (Ad40-95)  $\pm$  wollastonite  $\pm$  biotite  $\pm$  vesuvianite. Magnesian Mo skarns: olivine (Fo96). Retrograde minerals: Calcic skarns: amphibole  $\pm$  epidote  $\pm$  chlorite and muscovite. Magnesian skarns: serpentine  $\pm$  tremolite  $\pm$  chlorite.

**ENDOSKARN ALTERATION:** Clinopyroxene, K-feldspar, hornblende, epidote, quartz veining, sericite, molybdenite.

**ORE CONTROLS:** Carbonate or calcareous rocks in thermal aureoles adjacent to intrusive margins.

**ASSOCIATED DEPOSIT TYPES:** Porphyry Mo deposits of quartz monzonite type, Mo-sulphide veins, and Zn-sulphide veins. Some Mo skarns in China are associated with distally-developed sphalerite-rich mineralization.

**GEOCHEMICAL SIGNATURE:** Enriched in Mo, Zn, Cu, Sn, Bi, As, F, Pb, U, Sb, Co (Au).

**GEOPHYSICAL SIGNATURE:** Positive magnetic and induced polarization anomalies.

**GRADE AND TONNAGE:** Worldwide, grades range from 0.1 to 2 % MoS<sub>2</sub>, and tonnages between 0.1 and 2 Mt. In British Columbia, the Coxey deposit produced 1 Mt of ore grading approximately 0.17 % MoS<sub>2</sub>.

**IMPORTANCE:** Worldwide, Mo skarns are usually smaller and of less economic importance than porphyry Mo deposits (Einaudi *et al.*, 1981).

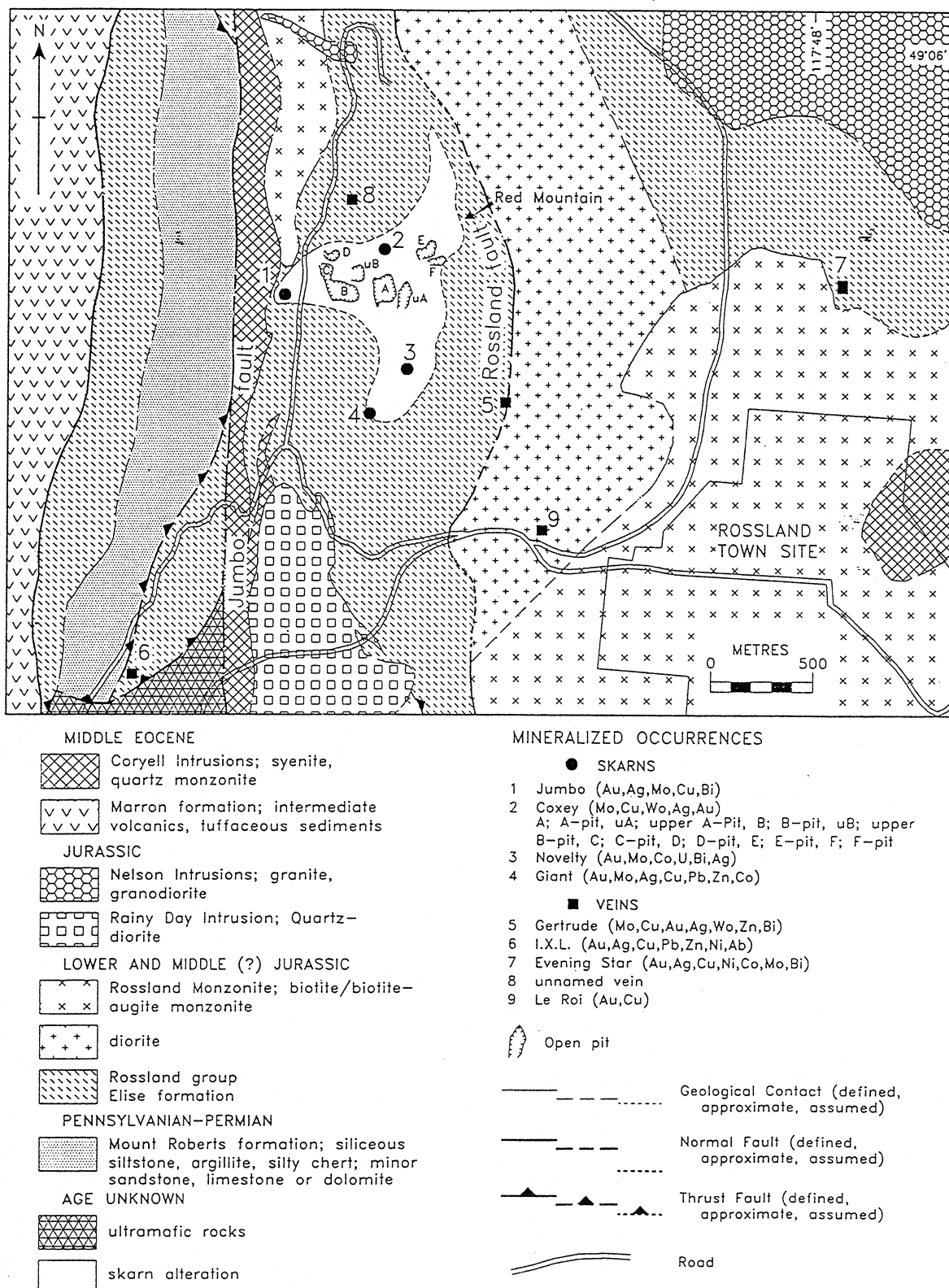
## MOLYBDENUM SKARNS IN THE CANADIAN CORDILLERA

British Columbia has 22 Mo skarn occurrences and the Yukon has another 7 (Fig. 2), but of these, only the Coxey and Novelty deposits at Rossland have been mined (Figs. 1 and 14; Fyles, 1984; Webster *et al.*, 1992). Most Mo skarns are hosted by cratonic, pericratonic and displaced continental margin rocks of the Kootenay and Cassiar terranes, and Ancestral North America (Tables 2A and B). They are mainly associated with Early to Middle Jurassic stocks and dikes of largely quartz monzonite to adamellite composition (Fig. 6A).

The high-level dikes and small stocks associated with the Coxey deposits locally display spectacular explosion breccia textures. The Coxey skarn is characterized by pyroxene and epidote with lesser garnet and actinolite, trace vesuvianite and some biotite hornfels (Webster *et al.*, 1992). The ore

consists primarily of molybdenite with minor scheelite, pyrite and pyrrhotite. Some mineralization occurs in the hydrothermally brecciated intrusives and in the adjacent brecciated sedimentary rocks. In contrast to the Coxey orebodies, no scheelite is reported in the nearby Novelty and Giant Mo skarn deposits (Fig. 14), which are unusual in containing abundant arsenopyrite, lesser molybdenite, and minor pyrrhotite, pyrite, chalcopyrite, cobaltite, bismuthinite and Au, (Fyles, 1984; Webster et al., 1992). The Novelty mineralization also includes uraninite. Grab samples from the Novelty and Giant skarns assayed up to 47 g/t Au, 3800 ppm Bi, 1.4 % Ni, 30 % As and 4.8 % Co; the ore also contain anomalous amounts of Te and Se (Ray and Webster, 1997). The Coxey, Novelty and Giant deposits probably lie within a single, large exoskarn envelope (Fig. 14) that may have mineralogical and metallic zoning.

Several deposits in Lower Paleozoic limestones of the Cassiar Terrane in the northern Cordillera are composite porphyry-skarn types in which Mo- and W-bearing veinlets are concentrated in the border phases of the pluton. However, molybdenite also overprints the adjacent scheelite-rich calc-silicate skarns at the Logtung, Boya and Mount Haskin properties (Dawson *et al.*, 1991; Kirkham and Sinclair, 1996).



**Figure 14.** Geology and location of vein and Coxey-Novelt Mo-skarn deposits in the Rossland camp, B.C. Geology after Höy *et al.* (1992).

## TUNGSTEN SKARNS - GENERAL SYNOPSIS

**EXAMPLES:** (*Canadian Cordillera*): Bailey (105A 017), Risby (105F 034), Mac Tung (105O 002), Ray Gulch - Garnet (106D 027), Emerald Tungsten (082FSW010), Dodger (082FSW011), Feeney (082FSW247), Invincible (082FSW218), Dimac (082M123), Lened, Can Tung.

(*Elsewhere*): Fostung (Ontario, Canada), MacTung (Yukon, Canada), Cantung (Northwest Territories, Canada), Pine Creek and Strawberry (California, USA), Osgood Range (Nevada, USA), King Island (Tasmania, Australia), Sang Dong (South Korea).

**CAPSULE DESCRIPTION:** Tungsten skarns are separable into two types (Newberry, 1982): reduced skarns (e.g. Cantung, Mactung), formed in carbonaceous rocks and/or at greater depths, and oxidized skarns (e.g. *King Island*), formed in hematitic or non-carbonaceous rocks, and/or at shallower depths. Late retrograde alteration is an important factor in many W skarns because, during retrogression, the early low-grade mineralization is often scavenged and redeposited into high-grade ore zones (e.g. Bateman, 1945; Dick, 1976, 1980).

**TECTONIC SETTING:** Continental margin, synorogenic to late orogenic plutonism intruding deeply buried sequences of eugeoclinal carbonate-shale sedimentary rocks. Can develop in tectonically thickened packages in back-arc thrust settings.

**AGE OF MINERALIZATION:** Mainly Mesozoic, but may be any age. Over 60 % of the W skarns in the Canadian Cordillera related to Cretaceous intrusions; the Fostung deposit in Ontario is Precambrian.

**HOST/ASSOCIATED ROCK TYPES:** Pure and impure limestones, calcareous to carbonaceous pelites. Associated with tonalite, granodiorite, quartz monzonite and granite of both I and S-types. Tungsten skarn-related granitoids, compared to Cu skarn-related plutonic rocks, tend to be more differentiated, more contaminated with sedimentary material, and have crystallized at a deeper structural level. Dolomitic rocks tend to inhibit the development of W skarns; consequently magnesian W skarns are less common than calcic W skarns.

**DEPOSIT FORM:** Stratiform, tabular and lens-like orebodies. Deposits can be continuous for hundreds of metres and follow intrusive contacts.

**TEXTURES:** Igneous textures in endoskarn. Coarse to fine-grained, massive granoblastic to mineralogically layered textures in exoskarn. Biotite hornfelsic textures common.

**ORE MINERALOGY (Principal and subordinate):** Scheelite  $\pm$  molybdenite  $\pm$  chalcopyrite  $\pm$  pyrrhotite  $\pm$  sphalerite  $\pm$  arsenopyrite  $\pm$  pyrite  $\pm$  powellite. May contain *trace wolframite, fluorite, cassiterite, galena, marcasite and bornite*. Reduced types are characterized by pyrrhotite, magnetite, *bismuthinite, native bismuth* and high pyrrhotite:pyrite ratios. Variable amounts of quartz-vein stockwork (with local molybdenite) can cut both the exoskarn and endoskarn. The Emerald Tungsten skarns in British Columbia include pyrrhotite-arsenopyrite veins and pods that carry up to 9 g/t Au.

**ALTERATION MINERALOGY:** Exoskarn alteration: Inner zone of diopside-hedenbergite (Hd60-90, Jo5-20)  $\pm$  grossular-andradite (Ad 10-50, Spess5-50)  $\pm$  biotite  $\pm$  vesuvianite, with outer barren wollastonite-bearing zone. An innermost zone of massive quartz may be present. Late-stage spessartine  $\pm$  almandine  $\pm$  biotite  $\pm$  amphibole  $\pm$  plagioclase  $\pm$  phlogopite  $\pm$  epidote  $\pm$  fluorite  $\pm$  sphene. Reduced types are characterized by hedenbergitic pyroxene, Fe-rich biotite, fluorite, vesuvianite, scapolite and low garnet:pyroxene ratios, whereas oxidized types are characterized by salitic pyroxene, epidote and andraditic garnet and high garnet:pyroxene ratios. Exoskarn envelope can be associated with extensive areas of biotite hornfels. Endoskarn alteration: Pyroxene  $\pm$  garnet  $\pm$  biotite  $\pm$  epidote  $\pm$  amphibole  $\pm$  muscovite  $\pm$  plagioclase  $\pm$  pyrite  $\pm$  pyrrhotite  $\pm$  trace tourmaline and scapolite; local greisen developed.

**ORE CONTROLS:** Carbonate rocks in extensive thermal aureoles of intrusions; gently inclined bedding and intrusive contacts; structural and/or stratigraphic traps in sedimentary rocks, and irregular parts of the pluton/country rock contacts.

**ASSOCIATED DEPOSIT TYPES:** Tin, Mo and Pb-Zn skarns. Wollastonite-rich industrial mineral skarns.

**GEOCHEMICAL SIGNATURE:** W, Cu, Mo, As, Bi and B. Less commonly Zn, Pb, Sn, Be and F geochemical anomalies.

**GRADE AND TONNAGE:** Worldwide, their grades range between 0.4 and 2 %  $\text{WO}_3$  (typically 0.7 %). Deposits vary from 0.1 to >30 Mt.

**IMPORTANCE:** Skarn deposits have accounted for nearly 60 % of the western world's production, and over 80 % of British Columbia's production.

## TUNGSTEN SKARNS IN THE CANADIAN CORDILLERA

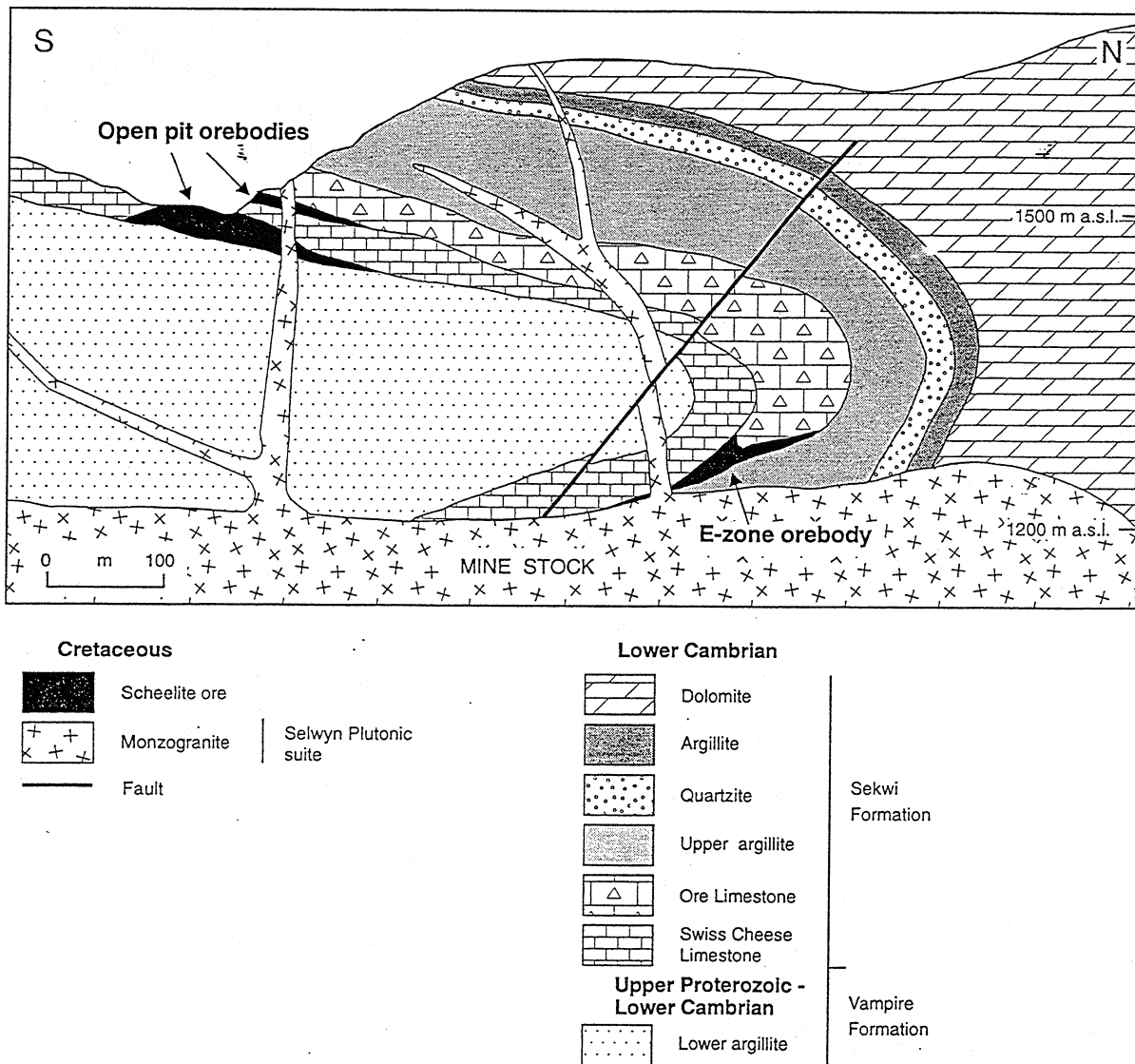
The northern Canadian Cordillera has several large W skarn deposits that define an arcuate belt flanking the Selwyn Basin (Fig. 1). They include the world-class Canada Tungsten (Cantung) mine in the N.W.T., and the Macmillan Tungsten (Mactung) developed prospect in the Yukon (Dick, 1976, 1980; Dick and Hodgson, 1982; Fig. 1; Table 1B). Significant mining has occurred only at Cantung (Fig. 15), and at the Emerald Tungsten (Fig. 16) and Dimac deposit in B.C. (Table 1A).

Most W skarns in the Canadian Cordillera are associated with mid-Cretaceous intrusions of the Omineca Crystalline Belt (Fig 3D and E), and are mainly hosted by Upper Proterozoic to Lower Paleozoic rocks of the cratonic shelf and its displaced equivalents (e.g. Cassiar, Kootenay, Yukon-Tanana, and Dorsey terranes; Tables 2A and B). Relatively thick and pure limestone beds in Lower Cambrian carbonate-pelite sequences are particularly favorable host rocks. Dolomitic carbonate rocks, although common in these settings, tend to be less favourable sites for W skarn development, hence magnesian W skarns are rare.

The associated plutonic rocks are, on average, of adamellite composition (Fig. 6A) and of both I and S-type, as exemplified by the calc-alkaline Selwyn Plutonic Suite (Anderson, 1983). The Nb, Y and Rb content (Fig. 6D) indicates that most represent "within-plate" plutons (as defined by Pearce *et al.*, 1984) although the intrusions at the Dimac deposit are of "volcanic arc" character (Ray and Webster, 1997). Granitoids related to W skarns tend to be more differentiated, more contaminated with sedimentary material, and have crystallized in more reduced and deeper structural levels than those associated with Cu skarns (Newberry and Swanson, 1986). They are commonly coarse grained, porphyritic and unaltered, but border phases are, in some cases, argillized, greisenized or tourmalinized. Stockwork quartz-scheelite-molybdenite veining is not extensive, and breccia pipes, intrusive and shatter breccias and other features indicative of high levels of emplacement are absent.

Calcic W skarns contain scheelite, commonly with pyrrhotite and either chalcopyrite or molybdenite, unevenly distributed throughout a prograde alteration assemblage of mainly hedenbergitic





**Figure 15** Schematic geological cross-section through the Canada Tungsten (Cantung) pit and E-zone orebodies (after Cummings and Bruce, 1977; Gordey and Anderson, 1993).

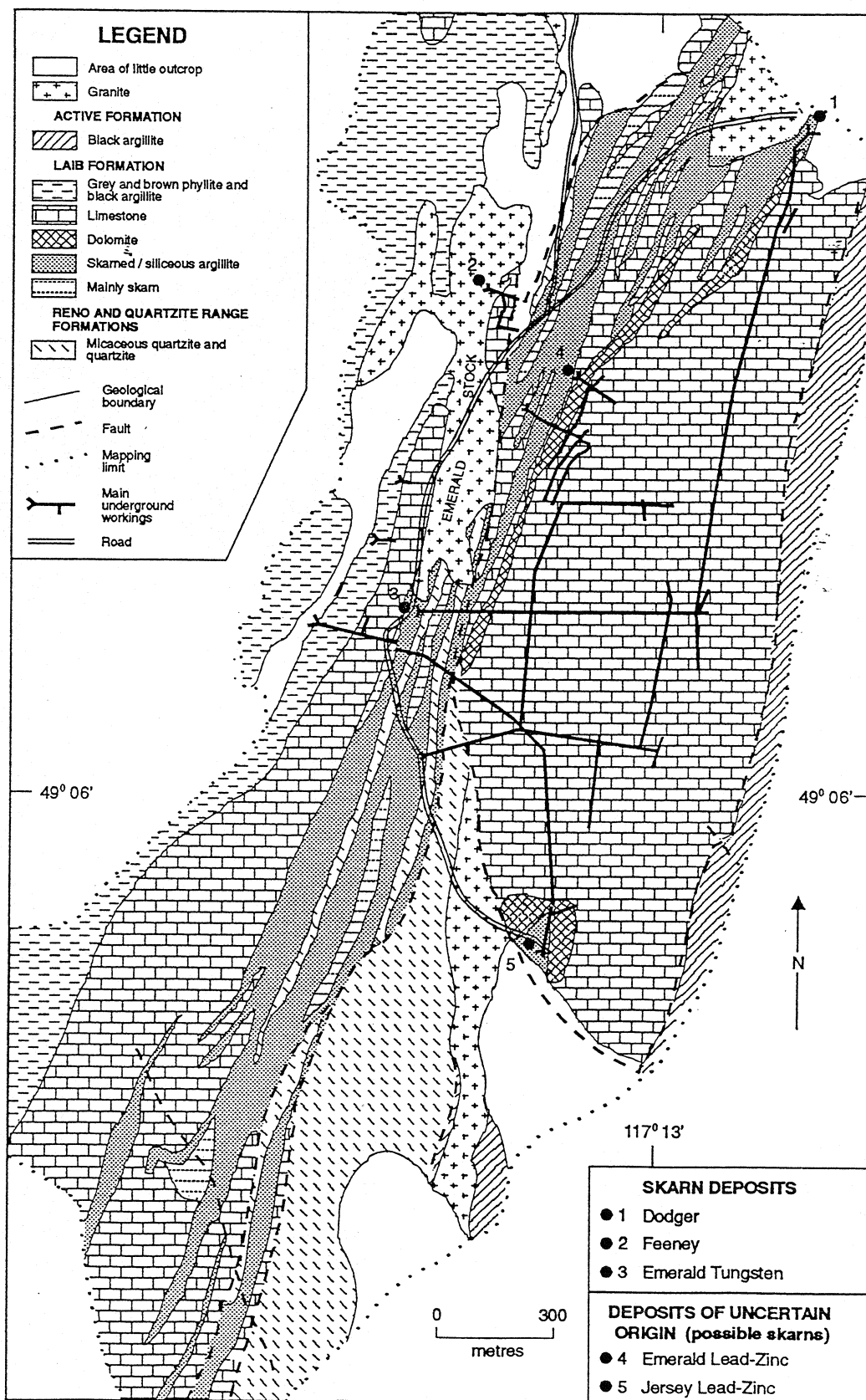


Figure 16 Geology of the Emerald Tungsten camp showing location of the W skarn deposits and enigmatic Pb-Zn orebodies (Geology after Fyles and Hewlett, 1959).

pyroxene, grossular-andradite-almandine garnet, and a hydrous retrograde assemblage of mainly hornblende and biotite. A typical calcic assemblage includes contemporaneously developed almandine-hedenbergite-scheelite exoskarn in calc-silicate hornfels, wollastonite-vesuvianite distal metamorphic skarn in marble, and hornblende-pyroxene-biotite-plagioclase endoskarn in the pluton and in pelitic hornfels. Cooling of the system and influx of meteoric water initiates hydrous retrograde alteration. This is accompanied by the deposition of most sulphides, and either primary deposition of scheelite or its redistribution, with both depletion and upgrading (Dick, 1976, 1980; Dawson, 1996c). Extensive areas of biotite hornfels are commonly associated with the larger deposits, and are a good exploration guide. Mineral zoning may be well developed and typically consists of sphalerite deposited peripherally to scheelite-rich skarn.

The scheelite ore at the Emerald Tungsten camp is generally sulphide poor and anomalously rich in F and Mo (Ray and Webster, 1995). However, some pyrrhotite and arsenopyrite-rich zones in the deposits lack scheelite and instead contain anomalous amounts of Au (up to 10 g/t), Bi, Sb, Te and Se, as well as a number of rare tellurides and selenide minerals (Ray and Webster, 1997). These auriferous sulphides suggests that other W skarns in the region have Au potential, although it is uncertain whether the sulphides at Emerald Tungsten were coeval with the skarn or result from a later epithermal event.

The enigmatic Jersey and Emerald Zn-Pb deposits lie adjacent to the Emerald, Feeney and Dodger W skarn orebodies (Fig. 16). They occur within the same anticlinal structure and are underlain by the same granitoid stock and related calc-silicate skarn horizon that hosts the W skarns. These features, plus their calc-silicate gangue have led to their interpretation as skarn Zn-Pb deposits distal to the proximal W-Mo (Au) skarns (Dawson, 1996a).

## LEAD-ZINC SKARNS - GENERAL SYNOPSIS

**EXAMPLES:** (*Canadian Cordillera*): Sa Dena Hes (Mt Hundere) (105A 012), Quartz Lake, Piedmont (082FNW 129), Contact (104P 004), Midway (104O 038).

(*Elsewhere*): Groundhog (New Mexico, USA), Darwin (California, USA) San Antonio, Santa Eulalia and Naica (Mexico), Yeonhwa-Ulchin deposits (South Korea), Nakatatsu deposits (Japan), Shuikoushan and Tienpaoshan (China).

**TECTONIC SETTING:** Along continental margins where they are associated with late orogenic plutonism. Pb-Zn skarns occur at a wide range of depths, being associated with subvolcanic aphanitic dikes and high-level breccia pipes, as well as deep-level batholiths. In British Columbia, some Pb-Zn skarns are found in oceanic island arcs where they form distally to larger calcic Fe or Cu skarn systems.

**AGE OF MINERALIZATION:** Mainly Mesozoic, but may be any age. In British Columbia, the 80 Pb-Zn skarn occurrences identified have a wide age range; over 40 % are Early to mid-Jurassic, 22 % are Cretaceous, and a further 17 % are Eocene-Oligocene in age.

**HOST/ASSOCIATED ROCK TYPES:** Variable; from high-level skarns in thick limestones, calcareous tuffs and sediment to deeper level skarns in marbles and calc silicate-bearing migmatites. Associated intrusive rocks are granodiorite to leucogranite, diorite to syenite (mostly quartz monzonite). Pb-Zn skarns tend to be associated with small stocks, sills and dikes and less commonly with larger plutons. The composition of the intrusions responsible for many distal Pb-Zn skarns is uncertain.

**DEPOSIT FORM:** Variable; commonly occurs along igneous or stratigraphic contacts. Can develop as subvertical chimneys or veins along faults and fissures and as subhorizontal blankets. Pb-Zn skarn deposits formed either at higher structural levels or distal to the intrusions tend to be larger and more Mn-rich compared to those formed at greater depths or more proximal.

**TEXTURES:** Igneous textures in endoskarn. Coarse to fine-grained, massive granoblastic to mineralogically layered textures in exoskarn.

**ORE MINERALOGY (Principal and subordinate):** Sphalerite  $\pm$  galena  $\pm$  pyrrhotite  $\pm$  pyrite  $\pm$  magnetite  $\pm$  arsenopyrite  $\pm$  chalcopyrite  $\pm$  bornite. Other trace minerals reported include scheelite, bismuthinite, stannite, cassiterite, tetrahedrite, molybdenite, fluorite, and native gold. Proximal skarns tend to be richer in Cu and W, whereas distal skarns contain higher amounts of Pb, Ag and Mn.

**ALTERATION MINERALOGY:** Many Pb-Zn skarn deposits have a distinctive Mn- and Fe-rich mineralogy. Exoskarn alteration includes Mn-rich hedenbergite (Hd30-90, Jo10-50), andraditic garnet (Ad20-100, Spess2-10)  $\pm$  wollastonite  $\pm$  bustamite  $\pm$  rhodonite. Late-stage Mn-rich actinolite  $\pm$  epidote  $\pm$  ilvaite  $\pm$  chlorite  $\pm$  dannemorite  $\pm$  rhodochrosite  $\pm$  axinite. Endoskarn alteration: Highly variable in development, and in many of the distal Pb-Zn skarns the nature of the endoskarn is unknown. However, Zn-rich skarns formed near stocks are often associated with abundant endoskarn that may equal or exceed the exoskarn (Einaudi *et al.*, 1981). Endoskarn mineralogy is dominated by epidote  $\pm$  amphibole  $\pm$  chlorite  $\pm$  sericite with lesser rhodonite  $\pm$  garnet  $\pm$  vesuvianite  $\pm$  pyroxene  $\pm$  K-feldspar  $\pm$  biotite and rare topaz. Marginal phases may contain greisen and/or tourmaline.

**ORE CONTROLS:** Tend to exhibit a pronounced structural control, forming in carbonate rocks along structural and/or lithological contacts (e.g. shale-limestone contacts, faults or pre-ore dikes). Deposits may occur considerable distances (100-1000+ m) from the source intrusions. A continuum is recognized from endoskarn and proximal exoskarn, through to distal manto and chimney deposits that are more stratigraphically or structurally controlled. There is also a progressively higher sulphide and lower calc-silicate gangue content with increasing distance from the intrusion. This passes ultimately to distal carbonate-hosted veins with Mn-rich silicate and carbonate gangue (Dawson, 1996a).

**ASSOCIATED DEPOSIT TYPES:** Pb-Zn-Ag veins, Cu skarns and Cu porphyries. In B.C., small Pb-Zn skarns occur distally to some Fe and W skarns.

**GEOCHEMICAL SIGNATURE:** Pb, Zn, Ag, Cu, Mn, As, Bi, W, F, Sn, Mo, Co, Sb, Cd and Au geochemical anomalies.

**GEOPHYSICAL SIGNATURE:** Generally good induced polarization response. Galena-rich orebodies may be marked by gravity anomalies whereas pyrrhotite-rich mineralization may be detected by magnetic surveys. CS-AMT may also be a useful exploration system.

**OTHER EXPLORATION GUIDES:** Thick limestones distal to small granitoid stocks; structural traps and lithological contacts; exoskarns with low garnet/pyroxene ratios.

**GRADE AND TONNAGE:** Worldwide, Pb-Zn skarns tend to be small (< 3 Mt) but can reach 45 Mt, grading up to 15 % Zn, 10 % Pb and > 150 g/t Ag with substantial Cd. Copper grades are generally < 0.2 %. Some deposits (e.g. Naica (Mexico) and Falun (Sweden)) contain Au.

**IMPORTANCE:** There are important past and current producers in Mexico, China, U.S.A (New Mexico and California), and Argentina.

## LEAD-ZINC SKARNS IN THE CANADIAN CORDILLERA

Because some distally developed mantos in the Canadian Cordillera lack a marked skarn gangue, their precise origin and relationship to skarn systems are uncertain. However, significant Pb-Zn skarn and/or manto deposits in the Cordillera include the Sa Dena Hes and Quartz Lake deposits in the Yukon (Fig. 1; Dawson, 1964; Vaillancourt, 1982), the Prairie Creek mantos in the N.W.T and the Bluebell, Midway, Ingenika and Piedmont orebodies in B.C. (Höy, 1980; Bradford, 1988; Nelson, 1991; Webster *et al.*, 1992). The enigmatic Mineral King, Jersey and Emerald Lead-Zinc (Fig. 16; Fyles, 1960; Fyles and Hewlett, 1959) deposits may also be of this type. In addition, small deposits such as the Magno D., Contact, Lucky Lake and Roy in the northern Cordillera lie adjacent to the Cassiar, Seagull and Mount Billings batholiths (McDougall, 1954; Aho, 1969; Dawson and Dick, 1978; Webster *et al.*, 1992; Dawson 1996a).

Lead-zinc skarn deposits in the Canadian Cordillera range from less than 1 Mt to about 8 Mt of ore at average grades of 10 to 15 % Zn+Pb, with Zn being dominant. Silver grades are variable, but average between 30 and 300g/t. By comparison, the large Ag-rich skarn and manto deposits of northern Mexico contain an average of more than 10 Mt Zn+Pb metal (Dawson, 1996a), and some Ag-rich skarns are mined for that commodity alone. Copper is recovered from some Pb-Zn skarns, at grades averaging 0.2 to 2 % Cu, and several Cordilleran deposits such as the Midway, Silver Hart, Roy and Magno D., contain minor amounts of W, Au, Cd and Sn (Dawson, 1996a).

Many Zn-Pb skarns in the Canadian Cordillera occur within the same Upper Proterozoic to mid-Paleozoic shelf sedimentary rocks that host many W skarns. The hosting sedimentary strata in the eastern Cordillera are underlain by basement lithologies dominated by thick, craton-derived clastic assemblages which, in the southeastern Cordillera, overlie crystalline Precambrian rocks. On Vancouver Island, however, the Pb-Zn skarns generally occur in Paleozoic and lower Mesozoic oceanic arc-type volcanic-carbonates.

Intrusive rocks associated with Zn-Pb skarns commonly are late orogenic to postorogenic, but may be synorogenic. They mostly are calc-alkaline felsic to intermediate batholiths, stocks, dikes and sills, and they span a wide range of compositions, from high-silica leucogranite and topaz granite, to syenite, through to diorite. However, small stocks of quartz monzonite composition are most common. In comparison with plutons associated with W, Cu and Au skarns, they show a broader range of composition, morphology and depth of emplacement. Age of intrusion and accompanying mineralization ranges from mid-Cretaceous to early Tertiary in the eastern Cordillera, but is Jurassic on Vancouver Island.

The Sa Dena Hes mine at Mount Hundere, near Watson Lake, Yukon (Fig. 1; Table 1B) is an example of a large Pb-Zn manto without an exposed igneous source. Distribution of abundant prograde actinolite-hedenbergite-grossularite and retrograde quartz-fluorite skarn assemblages over several manto orebodies is interpreted to reflect the influence of buried plutons (Dawson and Dick, 1978).

Between 1875 and 1971, the Bluebell deposit at Riondel, B.C. produced 5.2 Mt of ore grading approximately 6 % Zn, 5 % Pb and 45 g/t Ag (Höy, 1980). This exhibits characteristics of both early syngenetic and later, discordant epigenetic mineral deposition. Its distinctive mineral assemblage includes prograde knebelite (Fe, Mn-olivine) and retrograde minnesotaite (Fe-talc), Fe-, Mg-, and Mn-carbonates, chlorite, calcite, and quartz (Dawson, 1996a).

## TIN SKARNS - GENERAL SYNOPSIS

**EXAMPLES:** (*Canadian Cordillera*): JC (Viola) (105B 040) Silver Diamond, Atlin Magnetite and Daybreak (104N069, 126 and 134 respectively).

(*Elsewhere*): Moina, Mount Lindsay, Hole 16 and Mt. Garnet (Tasmania, Australia), Lost River (Alaska, USA).

**TECTONIC SETTINGS:** Late to post orogenic granites emplaced into thick and deeply buried continental margin sedimentary sequences, or sequences in rifted or stable cratonic environments.

**AGE OF MINERALIZATION:** Most economic deposits are Mesozoic or Paleozoic, but occurrences may be any age. The majority of Sn skarns in the Canadian Cordillera are Cretaceous.

**HOST/ASSOCIATED ROCK TYPES:** Carbonates and calcareous sedimentary sequences. Associated with differentiated (low Ca, high Si and K) ilmenite-series granite, adamellite and quartz monzonitic stocks and batholiths (of both I and S-type) intruding carbonate and calcareous clastic rocks. Tin skarns tend to develop in reduced and deep-level environments and may be associated with greisen alteration.

**DEPOSIT FORM:** Variable; can occur as either stratiform, stockwork, pipe-like or irregular vein-like orebodies.

**TEXTURES:** Igneous textures in endoskarn. Coarse to fine-grained, massive granoblastic to mineralogically layered textures in exoskarn; wrigglyite skarns contain thin rhythmic and alternating layers rich in either magnetite, fluorite, vesuvianite or tourmaline. Some hornfelsic textures.

**ORE MINERALOGY (Principal and subordinate):** Cassiterite  $\pm$  scheelite  $\pm$  arsenopyrite  $\pm$  pyrrhotite  $\pm$  chalcopyrite  $\pm$  stannite  $\pm$  magnetite  $\pm$  bismuthinite  $\pm$  sphalerite  $\pm$  pyrite  $\pm$  ilmenite.

**ALTERATION MINERALOGY:** Exoskarn alteration: Grandite garnet (Ad15-75, pyralspite 5-30) (sometimes Sn, F, and Be enriched), hedenbergitic pyroxene (Hd40-95)  $\pm$  vesuvianite (sometimes Sn and F-enriched)  $\pm$  malayaite  $\pm$  Fe and/or F-rich biotite  $\pm$  stanniferous sphene  $\pm$  gahnite  $\pm$  rutile  $\pm$  Sn-rich ilvaite  $\pm$  wollastonite  $\pm$  adularia. Late minerals include muscovite, Fe-rich biotite, chlorite, tourmaline, fluorite, sellaite, stilpnomelane, epidote and amphibole (latter two minerals can be Sn rich). Associated greisens carry quartz and muscovite  $\pm$  tourmaline  $\pm$  topaz  $\pm$  fluorite  $\pm$  cassiterite  $\pm$  sulphides. Magnesian Sn skarns may also contain olivine, serpentine, spinel, ludwigite, talc and brucite.

**ORE CONTROLS:** Differentiated, peraluminous plutons intruding carbonate rocks; fractures, lithological or structural contacts. Deposits may develop some distance (up to 500 m) from the related intrusions.

**ASSOCIATED DEPOSIT TYPES:** Tungsten skarns, Sn  $\pm$  Be greisens), Sn-bearing quartz-sulphide veins and mantos. In British Columbia, some of the Sn and W skarn-related intrusions (e.g. Cassiar batholith, Mount Haskin stock) are also associated with small Pb-Zn skarn occurrences.

**GEOCHEMICAL SIGNATURE:** Sn, W, F, Be, Bi, Mo, As, Zn, Cu, Rb, Li, Cs and Re geochemical anomalies. Borate-bearing magnesian Sn skarns may exhibit boron enrichment.

**GEOPHYSICAL SIGNATURE:** Magnetic, induced polarization and possible radiometric anomalies.

**GRADE AND TONNAGE:** Worldwide, deposits grade up to 1 % Sn, but much of the metal occurring in malayaite, garnet, amphibole and epidote is not economically recoverable. Worldwide, deposits reach 30 Mt, but most range between 0.1 and 3 Mt.

**IMPORTANCE:** Worldwide, Sn skarns represent a major reserve of tin. However, current production from skarn is relatively minor compared to that from placer Sn deposits and Sn-rich greisens and mantos. The Canadian Cordillera has had no Sn production from skarns.

## TIN SKARNS IN THE CANADIAN CORDILLERA

At least 19 Sn skarns are known in the Canadian Cordillera but none have been mined, due to their small size and subeconomic grade (much of the metal is unrecoverable in Sn silicates). Deposits occur peripheral to the Seagull batholith in southern Yukon, the Surprise Lake batholith near Atlin, B.C., and at Ash Mountain west of Cassiar, B.C. They are of mid- and Late Cretaceous age (Fig. 3F) and are mostly hosted by pericratonic carbonate-bearing rocks in the Cassiar and Yukon-Tanana terranes, and oceanic sedimentary and mafic rocks in the Cache Creek terrane (Tables 2A and B).

Plutons associated with Sn skarns are late to postorogenic stocks of S-type two-mica leucogranite (Fig. 6A). They are characteristically peraluminous and highly differentiated, with elevated contents of Rb, Nb, Y, F, Cl, B, Be and U (Fig. 6). Intrusive rocks adjacent to Sn skarns commonly are extensively greisenized, tourmalinized and may contain accessory topaz.

Cordilleran Sn skarns are characterized by a suite of Sn-rich prograde silicate minerals including green andradite garnet, sphene, malayaite and epidote (Table 4). Cassiterite overprints and replaces prograde Sn-rich silicates, in conjunction with other retrograde minerals. In comparison with W skarns, Sn skarns are deficient in sulphides and are more oxidized, being enriched in Si, F, Cl, B and ferric Fe. Skarns in the Seagull batholith and Ash Mountain areas have garnet compositions intermediate to grossular and andradite, and pyroxene compositions intermediate to diopside and hedenbergite (Dick and Hodgson, 1983). Strongly reduced Sn-skarn systems have low sulphidation states and tend to be characterized by high magnetite/sulphide ratios. Many are associated with Sn $\pm$ Be greisens, and biotite hornfelsic rocks are common in some deposits.

The largest Sn skarn in the Canadian Cordillera, the JC, lies within the Yukon-Tanana Terrane (Fig. 1) and is hosted by Mississippian limestones adjacent to the mid-Cretaceous Seagull batholith. A

resource of 1.25 Mt grading 0.54 % Sn has been identified. The skarn is a multi-stage assemblage of Sn-rich silicates overprinted and replaced by cassiterite, sphalerite and magnetite (Layne and Spooner, 1986, 1991).

In rare cases, F-rich Sn skarns may contain distinctive, thinly layered, wriggly textures. These are noteworthy because, unlike most Sn skarns which form at deeper levels, the wriggly skarns tend to develop in relatively near-surface conditions, such as over the cupolas of high-level granites (Kwak, 1987). The Daybreak skarn at Atlin, which is associated with the F-rich Surprise Lake batholith, has wriggly consisting of thin (< 1cm), alternating layers rich in either magnetite, fluorite, vesuvianite or garnet (Ray *et al.*, 1997).

## INDUSTRIAL MINERAL SKARNS

EXAMPLES: (*Canadian Cordillera*): Mount Riordan (Crystal Peak) (082ESW 102).

(Elsewhere): San Pedro (New Mexico, U.S.A) NYCO (New York, USA).

COMMENTS: Skarns and their associated altered hostrocks are a potential economic source of industrial minerals or commodities. In parts of the former USSR, some magnesian skarn deposits have produced coarse phlogopite and various borate minerals (Pertsev, 1991), and the Dalnegorsk B (datolite) skarn in Primor'ye, far eastern Russia provides 80 % of Russian borate production (Dawson, 1992). Skarn-related garnet and wollastonite are mined from several localities in the U.S.A. (Harben and Bates, 1990; Austin, 1991). The Canadian Cordillera also contains several important deposits (Fig. 1); in Yukon, the Marlin deposit has produced rhodonite, and the bleached carbonate haloes associated with some Fe skarns on Texada Island in southern B.C. are quarried for white ornamental marble. The Mount Riordan - Crystal Peak skarn at Hedley (Fig. 1) is the largest and highest grade garnet skarn yet identified in the Canadian Cordillera. It contains reserves of 40 Mt grading 78 % garnet (Grond *et al.*, 1991; Ray *et al.*, 1992).

The demand for industrial garnet in North America is growing and skarns such as the Mount Riordan deposit could be an important future source for the mineral. A very low content of non-silicate minerals, particularly sulphides is essential for economic viability. The garnet should have a high specific gravity and angularity, be free of inclusions, and occur as discrete grains that can be processed easily by conventional beneficiation techniques. Massive garnet skarns suitable for industrial mineral purposes tend to favour thick carbonate sequences intruded by granitic rocks in relatively oxidized conditions.

Commercial-grade wollastonite is increasingly used by the plastic, chemical and ceramic industries throughout North America. Although trace wollastonite has been identified in approximately 10 % of the skarns in the Canadian Cordillera, only a few occurrences have a demonstrated commercial potential for this mineral, and these are all in British Columbia (Fig. 1). They include the Mineral Hill, Rossland Wollastonite and Zippa Mountain-Isk skarns, where ongoing exploration is taking place to test their wollastonite potential (Ray and Kilby, 1996; Stinson, 1995; Jaworski and Dipple, 1996). The CO<sub>2</sub> content of the fluids is an important criteria in influencing the stability field of wollastonite (Greenwood, 1967). Because the wollastonite forming reaction produces CO<sub>2</sub> the development of large, high grade wollastonite deposits is enhanced where the CO<sub>2</sub> content is low. Such conditions prevail in open skarn systems that are either flushed by H<sub>2</sub>O-rich fluids, or where a dramatic lowering of the fluid pressure can periodically occur.



## CHEMISTRY OF THE SKARN-RELATED INTRUSIONS

Major element plots illustrate that the plutonic rocks associated with skarns in B.C. range in composition from gabbro and quartz diorite (Au skarns) to granite (Sn skarns; Fig. 6A). Virtually all skarns are related to subalkalic, calc-alkaline igneous rocks (Fig. 6B); noted exceptions include the Ingerbelle and QR deposits, which are associated with alkalic porphyry Cu-Au systems (Preto, 1972; Fox and Cameron, 1995).

Major element plots demonstrate there are systematic geochemical variations; the igneous rocks related to Fe, Au and Cu skarns generally contain the least Si and total alkalis and the most Ca, Mg, Al, ferrous Fe and total Fe (Fig. 6). By contrast, most plutons related to Sn and W skarns are mainly of granite-adamellite composition and have the highest average Si contents and the lowest overall amounts of total Fe, Mg, Al and Ca.

There is a relationship between the skarn deposit class, the peraluminous or metaluminous character of the intrusions, and the orogenic environment in which the melts were generated (Meinert, 1995; Ray and Webster, 1997). Gold, Fe, and Cu skarns are mostly associated with metaluminous intrusions that have a "pre-plate collisional" chemical signature (as defined by Batchelor and Bowden, 1985) whereas W and Sn skarns are related to fractionated, peraluminous leucogranitoids that are either "syncollisional" or "post-orogenic".

Systematic changes are also noted in the total alkali content and the  $K_2O/Na_2O$  and  $Fe_2O_3/FeO$  ratios of the intrusions. Gold and Fe skarn-related plutons generally have the lowest total alkali content (averaging <5.5 %), and those associated with Sn skarns have the highest (averaging >8 %; Ray *et al.*, 1995). Plutons related to Fe, Cu and Au skarns tend to also have low  $K_2O/Na_2O$  ratios (<0.7) compared to those related to Mo, W and Sn skarns which are characterized by ratios averaging between 1.1 and 1.4 (Fig. 6C). Igneous rocks associated with the more reduced W and Au skarn systems are characterized by low  $Fe_2O_3/FeO$  ratios (averaging <0.3), in contrast to plutons related to the more oxidized Cu skarns which have ratios averaging >0.8 (Ray *et al.*, 1995).

The plutonic rocks associated with Au, Fe and Cu skarns contain relatively higher amounts of Cr, Sc, Sr and V whereas those related to Sn and W skarns are enriched in large-ion lithophile elements such as Rb, Ce, Nb, Ta and La (Fig. 6D, E and F). Intrusions related to the Rossland Mo skarns and Hedley Au skarns contain larger quantities of Ba than the other skarn-related plutonic rocks in British Columbia (Fig. 6H), and the Hedley rocks are noteworthy for their higher Ba/La and Sc/Nb ratios (Fig. 6G).

The chemical signature and terrane setting of plutons responsible for Au, Fe and Cu skarns indicates they were derived from oceanic crust in a variety of oceanic arc and back-arc environments. This conclusion is supported by a trace element discrimination plot indicating these intrusions have a volcanic arc character, whereas plutons associated with Sn and most of the W skarns represent within-plate intrusions (Fig. 6D). The chemistry, predominant S-type affinity and high initial  $^{87}\text{Sr}/^{86}\text{Sr}$  ratios (Armstrong, 1988) of plutons associated with Sn and many W skarns suggests derivation by partial melting of sialic continental crust.

## CONCLUSIONS

The size and diversity of skarns in the Canadian Cordillera, together with their significant reserves and past metal production indicate that the region has a high potential for the discovery of new economic deposits. Exploration for these orebodies should be increased for a number of reasons, including:

- (a) the recognition that some geological terranes in the region (particularly island-arc terranes) are prospective hosts for such systems, and
- (b) the recent discovery and successful exploitation elsewhere of major Cu and/or Au-rich skarn deposits in geological settings that are analogous to parts of the Canadian Cordillera.

The Buckhorn Mountain deposit in Washington State (> 7.2 Mt of 5.5 g/t Au; Hickey, 1992) and the Candelaria skarn in Chile (366 Mt of 1.08 % Cu; Ryan *et al.*, 1995) for example, have similar mineralogies and island-arc settings to the Nickel Plate and Ingerbelle skarns, respectively. The QR, Ingerbelle, Diamond Hill and Candelaria skarns are all hosted by Ca-rich mafic volcanic rocks which suggests that many island-arc packages in the Cordillera (e.g. the Bonanza volcanics and Nicola and Stuhini groups) have potential for similar deposits.

Most of the major Cu and Au skarns found to date in the Canadian Cordillera are in terranes dominated by island-arc rocks. However, the Butte Highlands Au skarn in Montana (Ettlinger *et al.*, 1995) and the Big Gossan Cu-Au skarn in Indonesia (c. 37 Mt of 2.69 % Cu and 1 g/t Au; Meinert *et al.*, 1997) are hosted by platformal, dolomitic carbonates, indicating that miogeoclinal sedimentary rocks in the Canadian Cordillera should be explored for similar deposits.

Chemical and mineralogical zoning on both a deposit and district scale occurs in some Cu-Au skarn camps (e.g. Copper Canyon - Fortitude, Myers and Meinert, 1989; Hedley, Ettlinger *et al.*, 1992). In some cases, proximal Cu- and garnet-rich skarns merge out to distal, apparently barren pyroxene skarns that may contain micron Au mineralization. Thus, some of the mined-out proximal Cu skarns in the Cordillera, such as the Craigmont and Maid of Erin deposits, or those in the Greenwood and Whitehorse Copper camps (Figs. 1, 9 and 10), could be associated with distal Au skarns and therefore warrant re-evaluation.

Some base and ferrous metal skarns are also Au-bearing, which suggests that these types of skarn should be re-examined as an economic source of byproduct Au. For example, Au-As-Bi-Te mineralization in parts of the Emerald Tungsten deposits (Ray and Webster, 1997) suggests that other W skarns, including those hosted by Selwyn Basin and Cassiar terrane rocks of the Yukon, may be associated with Au-bearing orebodies. Likewise, the Au-rich Novelty and Giant deposits in Rossland,

B.C., (Fyles, 1984; Webster *et al.*, 1992; Höy *et al.*, 1992) show that other Mo-skarn occurrences in the Cordillera should be tested for Au.

Parts of the Canadian Cordillera have a potential for Pb-Zn-Ag mantos and skarns, particularly those underlain by North American or pericratonic assemblages. These areas contain many of the favorable geological features that characterize other Pb-Zn-Ag manto districts in the world (e.g. northern Mexico; Megaw *et al.*, 1988). Because many manto deposits lack a significant alteration halo, are often erratically distributed and may be blind, even large tonnage orebodies could have been overlooked during past exploration.

## ACKNOWLEDGMENTS

Thanks are expressed to: M.R. Burke and R.P. Deklerk of the Yukon Geology Program, Whitehorse, for providing data from the Yukon MINFILE; L.D. Jones of the B.C. Geological Survey, Victoria for assistance with the B.C. MINFILE; K.M. Dawson of Terra Geological Consultants for providing data on some of the regions Cu, W and Pb-Zn skarns; and M.E. Fournier and K. Hancock for drafting some of the figures. Other figure are provided by courtesy of the Geological Survey of Canada (Geology of Canadian Mineral Deposit Types, Geology of Canada, No. 8). Special thanks are due to Philip Mulholland and Steve Petroni of Pegasus Gold Corp., for permission to publish the geological section in Figure 5C.

Many of the data in these short course notes were compiled and researched during a study of the skarns in British Columbia funded by the Canada/British Columbia Mineral Development Agreement. The cooperation of the management and staff of the following companies are gratefully acknowledged: Banbury Gold Mines Ltd., Battle Mountain Gold Co., Cassiar Mining Corporation, Cambria Geological Ltd., Chevron Minerals Ltd., Corona Corporation, Cordilleran Engineering Ltd., Discovery Consultants, Esperanza Exploration Ltd., Echo Bay Mines Ltd., Freeport-McMoRan Gold Company, Freeport Indonesia Company, Gulf International Minerals Ltd., Geological Survey of Canada, Homestake Canada Inc., Kestrel Resources Ltd., Kettle River Resources Ltd., Mascot Gold Mines Ltd., Mineral Deposits Research Unit (MDRU), Orvana Resources Corp., Pamicon Developments Ltd., Pegasus Gold Corp., Santa Fe Pacific Gold, RTZ Mining and Exploration Ltd., Vananda Gold Ltd., Vangold Resources Ltd.

We are also grateful for the assistance and constructive comments of the following individuals:

Lloyd Addie, John Allen, John Bellemy, Noris Belluz, Jeff Brookes, Mike Burson, Gerry Carlson, Linda Caron, Garnet Dawson, Ken Dawson, Larry Dick, Art Ettlinger, Bob Flesher, Keith Glover, Colin Godwin, Brian Grant, Ian Hagemoen, Jan Hammarstrom, Brenda Harpring, Kris Hefton, Jim Laird, Dave Lefebure, Eric Lelacheur, Douglas MacKenzie, Mike Maslowski, Larry Meinert, Jim Monger, Philip Mulholland, Gary O'Connor, Jay Pennington, Steve Petroni, Dave Potter, Mike Rasmussen, Len Saleken, Paul Sarjeant, George Simandl, Ron Simpson, Tim Stepp, George Stewert, Wahyu Sunyoto, Ted Theodore, Steve Todoruk, Bill Wallis, and Bill Wilkinson.

## REFERENCES

- Aho, A.E. (1969): Base metal province of Yukon; *The Canadian Institute of Mining and Metallurgy, Bulletin*, April, 1969, 71-83.
- Allen, J.M., Artmont, G.J. & Palmer, K. (1995): Application of alluvial gold mineralogy to exploration of the Central Ranges, Irian Jaya, Indonesia, *PACRIM "95"*, 7-12.
- Anderson, R.G. (1983): Selwyn Plutonic Suite and its relationship to tungsten skarn mineralization, southeast Yukon and District of Mackenzie; in *Current Research, Part B; Geological Survey of Canada, Paper 83-1B*, 151-163.
- Anderson, R.G. & Reichenbach, I. (1991): U-Pb and K-Ar framework for Middle to Late Jurassic (172- >158 Ma) and Tertiary (46-27 Ma) plutons in Queen Charlotte Islands, British Columbia; in *Evolution and Petroleum Potential of the Queen Charlotte Basin*, editor G.J. Woodsworth, *Geological Survey of Canada, Paper 90-10*.
- Armstrong, R.L. (1988): Mesozoic and early Cenozoic magmatic evolution of the Canadian Cordillera; in *Processes in Continental Lithospheric Deformation*, editor Clark Jr., S.P. *Geological Society of America, Special Paper 218*, 55-91.
- Austin, G.T. (1991): Garnet (industrial); in *Mineral Commodity Summaries 1991, U.S. Dept. of Interior, Bureau of Mines*, January 1991, 58-59.
- Batchelor, R.A. & Bowden, P. (1985): Petrogenetic interpretation of granitoid rock series using multicationic parameters; *Chemical Geology*, **48**, 43-55.
- Bacon, W.R. (1957): Iron-ore deposits in coastal and southwestern British Columbia; Minister of Mines Annual Report 1956, *B.C. Ministry of Mines*, 129-136.
- Bateman, P.C. (1945): Pine Creek and Adamson Tungsten Mines, Inyo County, California; *California Journal of Mines Geology*, **41**, 231-249.
- Billingsley, P. & Hume, C.B. (1941): The ore deposits of Nickel Plate Mountain, Hedley, British Columbia; *Canadian Institute of Mining and Metallurgy, Bulletin*, **44**, 524-590.
- Bradford, J.A. (1988): Geology and genesis of the Midway silver-lead-zinc deposit, north-central British Columbia; unpublished M.Sc. thesis, *The University of British Columbia*, 280 pages.
- Brooks, J.W. (1994): Petrology and geochemistry in the McCoy gold skarn, Ladner County, Nevada; unpublished Ph.D. thesis, *Washington State University*, Washington, U.S.A.
- Brown, I.J. & Nesbitt, B.E. (1987): Gold-copper-bismuth mineralization in hedenbergitic skarn, Tombstone Mountains, Yukon; *Canadian Journal of Earth Sciences*, **24**, 2362-2372.

- Burt, D.M. (1972): Mineralogy and geochemistry of Ca-Fe-Si skarn deposits; unpububished Ph.D. thesis, *Harvard University*, 256 pages.
- Burt, D.M. (1977): Mineralogy and petrology of skarn deposits; Rendiconti, *Societa Italiana di Mineralogia e Petrologia*, 33 (2), 859-873.
- Cathro, M.S. (1990): Gold, silver and lead deposits of the Ketz River district, Yukon: Preliminary results of field work; in *Mineral Deposits of the Northern Canadian Cordillera, Yukon-Northeastern British Columbia (Field Trip 14)*, editors J.G. Abbott and R.J.W. Turner; 8th International Association on the Genesis of Ore Deposits Symposium, Ottawa, Field Trip Guidebook, *Geological Survey of Canada*, Open File 2169, 269-282.
- Church, B.N. (1986): Geological setting and mineralization in the Mount Attwood - Phoenix area of the Greenwood mining camp; *B.C. Ministry of Energy, Mines and Petroleum Resources*, Paper 1986-2, 65 p.
- Cooke, B.J. & Godwin, C.I. (1984): Geology, mineral equilibria, and isotopic studies of the McDame tungsten skarn prospect, north-central British Columbia; *Economic Geology*, 79, 826-847.
- Cummings, W.W. & Bruce, D.E. (1977): Canada Tungsten - change to underground mining and description of mine-mill practices; *The Canadian Institute of Mining and Metallurgy*, Bulletin, Volume 70, Number 784, 94-101.
- Dawson, K.M. (1964): Geology of the Mount Hundere lead-zinc-silver deposit, Watson Lake, Yukon Territory; unpublished B.Sc. thesis, *The University of British Columbia*, 53 pages.
- Dawson, K.M. (1992): Progress report on the project in comparative metallogenesis and tectonics of the U.S.S.R. Far East, Alaska, and the Canadian Cordillera; in *Current Research, Part A*, *Geological Survey of Canada*, Paper 92-1A, 173-177.
- Dawson, K.M. (1996a): Skarn zinc-lead-silver; in *Geology of Canadian Mineral Deposit Types*, editors O.R. Eckstrand, W.D. Sinclair & R.I. Thorpe, *Geological Survey of Canada*, Geology of Canada, 8, 448-459.
- Dawson, K.M. (1996b): Skarn gold; in *Geology of Canadian Mineral Deposit Types*, editors O.R. Eckstrand, W.D. Sinclair & R.I. Thorpe, *Geological Survey of Canada*, Geology of Canada, 8, 476-489.
- Dawson, K.M. (1996c): Skarn tungsten; in *Geology of Canadian Mineral Deposit Types*, editors O.R. Eckstrand, W.D. Sinclair, and R.I. Thorpe, *Geological Survey of Canada*, Geology of Canada, 8, 495-502.

- Dawson, K.M. & Dick, L.A. (1978): Regional metallogeny in the northern Cordillera: tungsten and base metal-bearing skarns in southeastern Yukon and southwestern Mackenzie; in *Current Research, Part A, Geological Survey of Canada, Paper 78-1A*, 289-292.
- Dawson, K.M. & Kirkham, R.V. (1996): Skarn copper; in *Geology of Canadian Mineral Deposit Types*, editors O.R. Eckstrand, W.D. Sinclair, and R.I. Thorpe, *Geological Survey of Canada, Geology of Canada*, 8, 460-476.
- Dawson, K.M., Friday, S.J. & McLaren, M.. (1983): Mineralogical and chemical zonation in the Silence Lake tungsten skarn, Clearwater, British Columbia; *Geological Association of Canada - Mineralogical Association of Canada, Abstracts with Programs*, 8, page A16, Annual meeting May 11-13 1983, Victoria, British Columbia.
- Dawson, K.M., Panteleyev, A., Sutherland Brown, A. & Woodsworth, G.J. (1991): Regional metallogeny, Chapter 19, in *Geology of the Cordilleran Orogen in Canada*, editors H. Gabrielse & C.J. Yorath, *Geological Survey of Canada, Geology of Canada, Number 4*, page 707-768 (also, *Geological Society of America, The Geology of North America*, volume G-2).
- Debon, F. & Le Fort, P. (1983): a chemical-mineralogical classification of common plutonic rocks and associations, *Royal Society of Edinburgh Transactions, Earth Sciences* 73 (for 1982), 135-149.
- D.I.A.N.D. (1981): Pat (Bailey) summary; in *Yukon Geology and Exploration 1979-80; Department of Indian Affairs and Northern Development (Canada)*, Northern Affairs Program, Exploration and Geological Services Division, Whitehorse, Yukon Territory, page 140.
- Dick, L.A. (1976): metamorphism and metasomatism at the Macmillan Pass tungsten deposit, Yukon and District of Mackenzie, Canada; unpublished M.Sc. thesis, *Queen's University*, Kingston, Ontario, 226 p.
- Dick, L.A. (1980): A comparative study of the geology, mineralogy, and conditions of formation of contact metasomatic mineral deposits in the northwest Canadian Cordillera; unpublished Ph.D. thesis, *Queen's University*, Kingston, Ontario.
- Dick, L.A. & Hodgson, C.J. (1982): The Mactung W-Cu(Zn) contact metasomatic and related deposits of the northeastern Canadian Cordillera; *Economic Geology*, 77, 845-867.
- Dick, L.A. & Hodgson, C.J. (1983): Contrasting environments of formation of W- and Sn-bearing skarns in the Canadian Cordillera; *Geological Association of Canada/Mineralogical Association of Canada, Joint Annual Meeting*, Victoria, B.C., Program and Abstracts, page A17.
- Eastwood, G.E.P. (1965): Replacement magnetite on Vancouver Island, British Columbia; *Economic Geology*, 60, 124-148.

- Eastwood, G.E.P. & Merrett, J.E. (1962): Nimpkish, Benson River and Old Sport; B.C. *Ministry of Energy, Mines and Petroleum Resources*, Annual Report 1961, 93-100.
- Einaudi, M.T., Meinert, L.D. & Newberry, R.J. (1981): Skarn deposits; in *Seventy-fifth Anniversary Volume, 1906-1980, Economic Geology*, editor B.J. Skinner: *Economic Geology Publishing Co.*, 317-391.
- Einaudi, M.T. and Burt, D.M. (1982): Introduction - Terminology, Classification and Composition of Skarn Deposits; *Economic Geology*, **77**, pages 745-754.
- Enns, S.G., Thompson, J.F.H., Stanley, C.R. & Yarrow, E.W. (1995): The Galore Creek porphyry copper-gold deposits, northwestern British Columbia; in *Porphyry Deposits of the Northwest Cordillera of North America*, editor T.G. Schroeter, *Canadian Institute of Mining, Metallurgy and Petroleum*, Special Volume 46, Paper 66, 630-644.
- Ettlinger, A.D. (1990): A geological analysis of gold skarns and precious metal enriched iron and copper skarns in British Columbia, Canada; unpublished Ph.D. thesis, *Washington State University*, 246 pages.
- Ettlinger, A.D. & Ray, G.E. (1989): Precious metal enriched skarns in British Columbia: An overview and geological study; *B. C. Ministry of Energy, Mines and Petroleum Resources*, Paper 1989-3, 128 pages.
- Ettlinger, A.D., Albers, D., Fredericks, R. & Urbisnov, S. (1995): The Butte Highlands project, Silver Bow County, Montana; An olivine-rich magnesian gold skarn; in *Symposium Proceedings of Geology and Ore Deposits of American Cordilleran*, *Geological Society of Nevada, U.S. Geological Survey and Geological Society of Chile*, April 10-13, 1995, Reno, Nevada.
- Ettlinger, A.D., Meinert, L.D. & Ray, G.E. (1992): Skarn evolution and hydrothermal fluid characteristics in the Nickel Plate deposit, Hedley District, British Columbia; *Economic Geology*, **87**, 1541-1565.
- Fahrni, K.C., Macauley, T.N. & Preto, V.A.G. (1976): Copper Mountain and Ingerbelle; in *Porphyry deposits of the Canadian Cordillera*, editor Sutherland Brown, A., *Canadian Institute of Mining and Metallurgy*, Special Volume 15, 368-375.
- Fox, P.E. & Cameron, R.S. (1995): Geology of the QR gold deposit, Quesnel River Area, British Columbia; in *Porphyry Deposits of the Northwest Cordillera of North America*, editor T.G. Schroeter, *Canadian Institute of Mining, Metallurgy and Petroleum*, Special Volume 46, Paper 66, 829-837.
- Fraser, T.M., Stanley, C.R., Nikic, Z.T., Pesalj, R. & Gorc, D. (1995): The Mount Polley alkaline porphyry copper-gold deposit, south-central British Columbia; in *Porphyry Deposits of the*



- Northwest Cordillera of North America, editor T.G. Schroeter, *Canadian Institute of Mining, Metallurgy and Petroleum*, Special Volume 46, Paper 66, 609-622.
- Fyles, J.T. (1955): Geology of the Cowichan Lake area, Vancouver Island, British Columbia; *B.C. Ministry of Energy, Mines and Petroleum Resources*, Bulletin 37, 72 pages.
- Fyles, J.T. (1960): Mineral King (Sheep Creek Ltd.); *B.C. Minister of Mines*, Annual Report, 1959, 74-89.
- Fyles, J.T. (1984): Geological setting of the Rossland Mining camp; *B.C. Ministry of Energy, Mines and Petroleum Resources*, Bulletin 74, 61 pages.
- Fyles, J.T. (1990): Geology of the Greenwood - Grand Forks area, B.C., (NTS 82E/1, 2); *B.C. Ministry of Energy, Mines and Petroleum Resources*, Open File 1990-25, 19 pages.
- Fyles, J.T. & Hewlett, C.G. (1959): Stratigraphy and structure of the Salmo Lead-Zinc Area; *B.C. Ministry of Energy, Mines and Petroleum Resources*, Bulletin 41, 162 pages.
- Glover, J.K. & Burson, M.J. (1986): Geology of the Lened tungsten deposit, Northwest Territories; in Mineral Deposits of the northern Canadian Cordillera, *Canadian Institute of Mining*, Special Volume 37, 255-265.
- Gordey, S.P. & Anderson, R.G. (1993): Evolution of the northern Cordilleran Miogeocline, Nahanni Map area (105I), Yukon and Northwest Territories; *Geological Survey of Canada*, Memoir 428, 214 pages.
- Greenwood, H.J. (1967): Wollastonite: Stability in H<sub>2</sub>O-CO<sub>2</sub> mixtures and occurrences in a contact metamorphic aureole near Salmo, British Columbia; *American Mineralogist*, Volume 52, 1669-1680.
- Grond, H.C., Wolfe, R., Montgomery, J.H. & Giroux, G.H. (1991): A massive skarn-hosted andradite deposit near Penticton, British Columbia; in Industrial Minerals of Alberta and British Columbia, Canada: *B.C. Ministry of Energy, Mines and Petroleum Resources*, Open File 1991-23, 131-133.
- Gross, G.A. (1996): Skarn iron; in Geology of Canadian Mineral Deposit Types, editors O.R. Eckstrand, W.D. Sinclair, & R.I. Thorpe; *Geological Survey of Canada*, Geology of Canada, 8, 489-495.
- Haug J.W. (1977): Geology of the Merry Widow and Kingfisher contact metasomatic skarn-magnetite deposits, northern Vancouver Island, British Columbia; unpublished M.Sc. thesis, *University of Calgary*, 117 pages.
- Haug, J. & Farquharson, R.B. (1976): Detailed textural and mineralogical study related to genesis of the Merry Widow and Kingfisher skarn deposits, northern Vancouver Island; *Geological Association of*

- Canada - Mineralogical Association of Canada, Joint Annual Meeting 1976, Program with Abstracts, page 57.*
- Harben, P.W. & Bates R.L. (1990): Garnet. wollastonite; in *Industrial Minerals, Geology and World Deposits, Industrial Minerals Division, Metal Bulletin Plc.*, London, pages 120-121 and 299-301.
- Hickey, R.J. (1992): The Buckhorn Mountain (Crown Jewel) gold skarn deposit, Okanogan County, Washington; *Economic Geology*, **87**, 125-141.
- Höy, T. (1980): Geology of the Riondel area, central Kootenay arc, southeastern British Columbia; *B.C. Ministry of Energy, Mines and Petroleum Resources, Bulletin 73*, 89 p.
- Höy, T., Dunne, K (nee Andrew) & Wehrle, D. (1992): Tectonic and stratigraphic controls of gold-copper mineralization in the Rossland Camp, southeastern British Columbia; in *Geological Fieldwork 1991, B.C. Ministry of Energy, Mines and Petroleum Resources, Paper 1992-1*, 261-272.
- Irvine, T.N. & Baragar, W.R.A. (1971): A guide to the chemical classification of the common volcanic rocks; *Canadian Journal of Earth Sciences*, **8**, 523-547.
- Jaworski, B.J. & Dipple, G.M. (1996): Zippa Mountain wollastonite skarns, Iskut River Map Area (104B/11); in *Geological Fieldwork 1995, B.C. Ministry of Energy, Mines and Petroleum Resources, Paper 1996-1*, 243-249.
- Johnson, T.W. & Meinert, L.D. (1994): Au-Cu-Ag skarn and replacement mineralization in the McLaren Deposit, New World District, Park County, Montana; *Economic Geology*, **89**, 969-993.
- Kirkham, R.V. & Sinclair, W.D. (1996): Porphyry copper, gold, molybdenum, tungsten, tin, silver; in *Geology of Canadian Mineral Deposit Types*, editors O.R. Eckstrand, W.D. Sinclair, & R.I. Thorpe; *Geological Survey of Canada, Geology of Canada*, **8**, 421-446.
- Knopf, A. (1942): Ore Deposition in the Pyrometamorphic Deposits; in *Ore Deposits as Related to Structural Features*, W.H. Newhouse, Editor, *Princeton University Press*, pages 63-72.
- Kwak, T.A.P. (1987): W-Sn skarn deposits and related metamorphic skarns and granitoids: in *Developments in Economic Geology*, **24**, Elsevier Publishing, 450 p.
- Layne, G.D. & Spooner, E.T.C. (1986): The JC Sn-Fe-F (Be-B-As) skarn, Wolf Lake area, Yukon Territory; in *Mineral Deposits of the Northern Cordillera*, editor J.A. Morin, *Canadian Institute of Mining and Metallurgy, Special Volume 37*.
- Layne, G.D. & Spooner, E.T.C. (1991): The JC tin skarn, southern Yukon Territory: I. Geology, Paragenesis, and Fluid Inclusion Microthermometry; *Economic Geology*, **86**, 29-47.
- Little, H.W. (1960): Nelson map-area, West half, British Columbia; *Geological Survey of Canada, Memoir 308*, 205 pages

- Little, H.W. (1963): Rossland map-area, British Columbia; *Geological Survey of Canada*, Paper 63-13 (Map 23-1963).
- Mackay, G., Diment, R. & Falkiner, J. (1993): Whitehorse Copper Belt - a simplified technical history; *Department of Indian Affairs and Northern Development (Canada)*, Open File 1993-2 (I), 48 pages.
- Magnusson, N.H. (1960): Iron and Sulfide Ores of Central Sweden; *21st International Geological Congress*, Copenhagen, Excursion Guides A26 and C21, 48 pages.
- Mcdougall, J.J. (1954): The telescoped silver-lead-zinc deposits of the Contact group mineral claims, McDame Map Area, B.C.; unpublished M.Sc. thesis, *The University of British Columbia*.
- Megaw, P.K.M., Ruiz, J. & Titley, S.R. (1988): High-temperature, carbonate-hosted Ag-Pb-Zn (Cu) deposits of northern Mexico; *Economic Geology*, **83**, 1856-1885.
- Meinert, L.D. (1984): Mineralogy and petrology of iron skarns in western British Columbia, Canada; *Economic Geology*, **79**, 869-882.
- Meinert, L.D. (1986): Gold in skarns of the Whitehorse Copper Belt, southern Yukon; in *Yukon Geology*, Volume 1, Exploration and Geological Services Division, *Department of Indian Affairs and Northern Development (Canada)*, 19-43.
- Meinert, L.D. (1988): Gold in Skarn Deposits - a Preliminary Overview; *Proceedings of the Seventh Quadrennial IAGOD Symposium*; *E. Schweizerbartische Verlagsbuchhandlung*, Stuttgart.
- Meinert, L.D. (1989): Gold skarn deposits - geology and exploration criteria; *Economic Geology*, Monograph 6, 537-552.
- Meinert, L.D. (1992): Skarns and Skarn Deposits; *Geoscience Canada*, Volume 19, No. 4, pages 145-162.
- Meinert, L.D. (1995): compositional variation of igneous rocks associated with skarn deposits - chemical evidence for a genetic connection between petrogenesis and mineralization; in *Magma, Fluids, and Ore Deposits*, editor Thompson, J.F.H., *Mineralogical Association of Canada*, Short Course Volume 23, 401-418.
- Meinert, L.D., Hefton, K.K. & Tasiran, I. (1997): Geology, zonation, and fluid evolution of the Big Gossan Cu-Au skarn deposit, Ertzberg district, Irian Jaya; *Economic Geology*, **92**, 509-534.
- Monger, J.W.H., Price, R.A. & Tempelman-Kluit, D.J. (1982): Tectonic accretion and the origin of two major metamorphic and plutonic belts in the Canadian Cordillera; *Geology*, **10**, 70-75.
- Monger, J.W.H. & Nokleberg, W.J. (1995): Evolution of the northern North American Cordillera: generation, fragmentation displacement and accretion of successive North American plate margin

- arcs; 1995 Geological Society of Nevada Symposium, Geology and Ore Deposits of the American Cordillera, Reno, Nevada.
- Morrison, G.W. (1980): Stratigraphic control of Cu-Fe skarn ore distribution and genesis at Craigmont, British Columbia; *Canadian Institute of Mining and Metallurgy, Bulletin*, 73, 109-123.
- Morrison, G.W. (1981): Setting and origin of skarn deposits in the Whitehorse Copper Belt, Yukon; unpublished thesis, *University of Western Ontario*, London.
- Mueller, A.G. (1991): The Savage Lode magnesian skarn in the Marvel Loch gold-silver mine, Southern Cross Greenstone Belt, Western Australia; Part I. Structural Setting, Petrography and Geochemistry; *Canadian Journal of Earth Sciences*, 28, No. 5, 659-685.
- Mulligan, R. (1984): Geology of Canadian tungsten occurrences; *Geological Survey of Canada*, Economic Geology Report 32, 121 pages.
- Myers, G.L. & Meinert, L.D. (1989): Zonation of the Copper Canyon - fortitude gold skarn system; *Geological Society of America*, Abstract 8095.
- Nelson, J.A. (1991): Carbonate-hosted lead-zinc ( $\pm$  silver, gold ) deposits of British Columbia; *B.C. Ministry of Energy, Mines and Petroleum Resources*, Paper 1991-4, 71-88.
- Newberry, R.J. (1982): Tungsten-bearing skarns of the Sierra Nevada. I. The Pine Creek Mine, California; *Economic Geology*, 77, 823-844.
- Newberry, R.J. (1983): The formation of subcalcic garnet in scheelite-bearing skarns; *Canadian Mineralogist*, 21, 529-544.
- Newberry, R.J. & Swanson, S.E. (1986): Scheelite skarn granitoids: An evaluation of the roles of magmatic source and process; *Ore Geology Reviews*, 1, 57-81.
- Orris, G.J., Bliss, J.D., Hammarstrom, J.M. & Theodore, T.G. (1987): Description and grades and tonnages of gold-bearing skarns; *U.S. Geological Survey*, Open File Report 87-273, 50 pages.
- Pearce, J.A., Harris, N.B.W. & Tindle, A.G. (1984): Trace element discrimination diagrams for the tectonic interpretation of granitic rocks; *Journal of Petrology*, 25, 956-983.
- Pertsev, N.N. (1991): Magnesian skarns; in Skarns - Their genesis and metallogeny, *Theophastrus Publications*, Athens, Greece, 299 -324.
- Preto, V.A. (1972): Geology of Copper Mountain; *B.C. Ministry of Energy, Mines and Petroleum Resources*, Bulletin 59, 87 pages.
- Preto, V.A., Osatenko, M.J., Mcmillan, W.J. & ARMSTRONG, R.L., (1979): Isotopic dates and strontium isotopic ratios for plutonic and volcanic rocks in the Quesnel Trough and Nicola Belt, south central British Columbia; *Canadian Journal of Earth Sciences*, 16, 1658-1672.

- Ray, G.E. (1996): The characteristics of gold skarns; in *New Mineral Deposit Models of the Cordillera*, Short Course organized by the *British Columbia Geological Survey and the Northwest Mining Association*, Spokane, Washington, December 2-3, 1996, Short Course Notes, B1-B51.
- Ray, G.E. & Dawson, G.L. (1994): The geology and mineral deposits of the Hedley gold skarn district, southern British Columbia; *B. C. Ministry of Energy, Mines and Petroleum Resources*, Bulletin 87, 156 pages.
- Ray, G.E. & Webster, I.C.L. (1991): Geology and mineral occurrences of the Merry Widow skarn camp, northern Vancouver Island, 92L/6; *B. C. Ministry of Energy, Mines and Petroleum Resources*, Open File 1991-8.
- Ray, G.E. & Webster, I.C.L. (1995): the geochemistry of mineralized skarns in British Columbia; in *Geological Fieldwork 1994*, *B.C. Ministry of Energy, Mines and Petroleum Resources*, Paper 1995-1, 371-383.
- Ray, G.E. & Webster, I.C.L. (1997): Skarns in British Columbia, *B.C. Ministry of Employment and Investment, Geological Survey Branch*, Bulletin 101, 260 pages.
- Ray, G.E., & Kilby, C.E. (1996): The geology and geochemistry of the Mineral Hill-Wormy Lake wollastonite skarns, southern British Columbia; in *Geological Fieldwork 1995*, *B.C. Ministry of Energy, Mines and Petroleum Resources*, Paper 1996-1, 227-241.
- Ray, G.E. & Dawson, K.M. (1998, in press): Mineralized skarns in the Canadian Cordillera; in *Mineralized intrusion-related skarn systems*, editor D.R. Lentz, *Mineralogical Association of Canada Short Course Series*, Short Course Volume 23.
- Ray, G.E., Dawson, G.L., & Webster, I.C.L. (1996): The stratigraphy of the Nicola Group in the Hedley District, British Columbia, and the chemistry of its intrusions and Au skarns; *Canadian Journal of Earth Sciences*, 33, 1105-1126.
- Ray, G.E., Ettlinger, A.D. & Meinert, L.D. (1990): Gold skarns: their distribution, characteristics and problems in classification; in *Geological Fieldwork 1989*, *B.C. Ministry of Energy, Mines and Petroleum Resources*, Paper 1990-1, 237-246.
- Ray, G.E., Grond, H.C., Dawson, G.L. & Webster, I.C.L. (1992): The Mount Riordan (Crystal Peak) garnet skarn, Hedley District, southern British Columbia; *Economic Geology*, 87, 1862-1876.
- Ray, G.E., Jaramillo, V.A. & Ettlinger, A.D. (1991): The McLymont Northwest Zone, northwest British Columbia: a gold-rich retrograde skarn? (104B); in *Geological Fieldwork 1990*, *B.C. Ministry of Energy, Mines and Petroleum Resources*, Paper 1991-1, 255-262.

- Ray, G.E., Webster, I.C.L., Ballantyne, S.B., Kilby, C.E. & Cornelius, S.B. (1997): Geology and mineral chemistry of tin-bearing skarns related to the Surprise Lake batholith, Atlin, northern British Columbia; *B.C. Ministry of Energy, Mines and Petroleum Resources*, Paper 1997-1, 233-254.
- Ray, G.E., Webster, I.C.L. & Ettlinger, A.D. (1995): The distribution of skarns in British Columbia and the chemistry and ages of their related plutonic rocks, *Economic Geology*, **90**, 920-937.
- Ryan, P.J., Lawrence, A.L., Jenkins, R.A., Matthews, J.P., Zamora, J.C., Marino, E.W. & Diaz, I.U. (1995): The Candelaria copper-gold deposit, Chile; in *Porphyry Copper Deposits of the American Cordillera*, editors Pierce, F.W. and Bolm, J.G, *Arizona Geological Society Digest*, **20**, 625-645.
- Sangster, D.F. (1965): Colloform magnetite in a contact metasomatic iron deposit; *Economic Geology*, **60**, 824-826.
- Sangster, D.F. (1969): The contact metasomatic magnetite deposits of British Columbia; *Geological Survey of Canada*, Bulletin 172, 85 pages.
- Sillitoe, R.H. & Bonham, H.F. (1990): Sediment-hosted gold deposits: distal products of magmatic-hydrothermal systems; *Geology*, **18**, 157-161.
- Stevenson, J.S. & Jeffrey, W.G. (1964): Colloform magnetite in a contact metasomatic iron deposit, Vancouver Island, British Columbia; *Economic Geology*, **59**, 1298-1305.
- Stinson, P.K. (1995): The structure and emplacement of the eastern part of the Coryell Batholith, southeastern British Columbia; unpublished M.Sc. thesis, *The University of Calgary*, 151 pages.
- Sutherland Brown, A. (1968): Geology of the Queen Charlotte Islands; *B.C. Ministry of Energy, Mines and Petroleum Resources*, Bulletin 54, 226 pages.
- Tenney, D. (1981): The Whitehorse Copper Belt: mining, exploration and geology (1967-1980); *Department of Indian and Northern Affairs*, Geology Section Yukon, Bulletin 1.
- Theodore, T.G., Orris, G.J., Hammarstrom, J.M. & Bliss, J.D. (1991): Gold bearing skarns; *United States Geological Survey*, Bulletin 1930, 61 pages.
- Vaillancourt, P. de G. (1982): Geology of the pyrite-sphalerite-galena concentrations in Proterozoic quartzite at Quartz Lake, southwestern Yukon; in *Yukon Exploration and Geology 1982*, *Department of Indian and Northern Affairs*, Exploration and Geological Services, Whitehorse, 73-77.
- Watson, P.H. (1984): The Whitehorse Copper Belt - A compilation; Exploration and Geological Services Division - Yukon, *Department of Indian and Northern Affairs*, Canada, Open File, 1:25000-scale map with marginal notes.

- Webster, I.C.L. & Ray, G.E. (1990a): Geology and mineral deposits of northern Texada Island; in Geological Fieldwork 1989, *B.C. Ministry of Energy, Mines and Petroleum Resources*, Paper 1990-1, 257-265.
- Webster, I.C.L. & Ray, G.E. (1990b): Geology and mineral deposits of northern Texada Island; *B.C. Ministry of Energy, Mines and Petroleum Resources*, Open File 1990-3.
- Webster, I.C.L., Ray, G.E. & Pettipas, A.R. (1992): An investigation of selected mineralized skarns in British Columbia; in Geological Fieldwork 1991, *B.C. Ministry of Energy, Mines and Petroleum Resources*, Paper 1992-1, 235-252.
- Wheeler, J.O., Brookfield, A.J., Gabrielse, H., Monger, J.W.H., Tipper, H.W. & Woodsworth, G.J. (1991): Terrane map of the Canadian Cordillera; *Geological Survey of Canada*, Map 1713A, scale 1:2 000 000.
- Woodsworth, G.J., Anderson, R.G. & Armstrong, R.L. (1991): Plutonic regimes, Chapter 15 in *Geology of the Cordilleran Orogen in Canada*, editors H. Gabrielse & C.J. Yorath; *Geological Survey of Canada*, *Geology of Canada*, 4, 491-531.
- Zharikov, V.A. (1970): Skarns; *International Geological Review*, 12, pages 541-559, 619-647, 760-775.

G.E. Ray

14th January 1998

## N - ARC-RELATED VOLCANOGENIC MASSIVE SULPHIDE DEPOSITS

J.M. Franklin, M.D Hannington, I.R. Jonasson and C.T. Barrie, Geological Survey of Canada

Franklin, J.M., Hannington, M.D., Jonasson, I.R. and Barrie, C.T. (1998): Arc-Related Volcanogenic Massive Sulphide Deposits; in Metallogeny of Volcanic Arcs, B.C. Geological Survey, Short Course Notes, Open File 1998-8, Section N.

### ABSTRACT

About 80% of the world's VMS deposits are in arc-related strata, with the remaining 20% in mid-ocean ridge ophiolitic settings (some are rifted marginal basins). Arc-related VMS may be broadly divided into four groups: Type 1 include deposits in arcs formed above ocean-floor dominated subduction (bimodal volcanic sequences). Type 2 are related to ocean-continent subduction (felsic-dominated bimodal sequences). Type 3 deposits are in basalt-sediment (back arc) sequences (Besshi-like). Type 4 deposits are in mature (epi-continental?) arcs and back-arcs, where felsic volcanic and/or sedimentary strata are dominant. The median sizes of each of the arc-related groups, along with those in the Besshi and ophiolite groups are roughly equal, at  $1\text{--}1.5 \times 10^6$  tonnes. Mature continental-arc or back-arc deposits have a median size of  $4 \times 10^6$  tonnes.

The convective genetic model for VMS deposits stipulates that metalliferous hydrothermal fluids were generated primarily in the sub-seafloor through heating of down-welling seawater and leaching of metals from the volcanic and sedimentary sub-strata. The size of convective metalliferous hydrothermal systems was a function of the abundance of heat in the upper two km of the sub-seafloor crust. Heat was supplied from a shallow-level subvolcanic intrusion. Evidence from modern seafloor examples indicates a direct magmatic component in deposits where melted continental crust (or hydrated oceanic crust) was involved in volcanism.

Any direct relationship between magma type and the abundance or composition of deposits is tenuous. Generally, for types 1 through 3, the felsic melts are quite high-temperature sodic dacite and rhyolite. Such high temperature environments promoted convective circulation and leaching. In the felsic-dominated and continental arc-related areas (type 4 and possibly 2), more-K-rich, continent-derived melts may be evident. In all, both the subvolcanic intrusions and related volcanic rocks have somewhat aberrant petrochemical trends, caused by unusually rapid heat removal to the hydrothermal system, assimilation of hydrated country rock, or interaction with seawater. Extensive fractionation may be evident in both major element and REE trends.

On reaching a critical reaction temperature (sustained acid pH) in convective systems, leached metals moved into the hydrothermal fluid. In basalt-dominated areas (types 1 and 3), leaching-related alteration of mafic "source" zones (lower semi-conformable alteration) formed the assemblage albite-epidote-actinolite-quartz. These zones are variably metal-depleted, and are characterized by patchy silicification and epidotization, with loss of calcium and addition of sodium. In felsic-dominated types 2 and 4, particularly in districts which formed at shallow seawater depths ( $<1500\text{m}$ ), laterally extensive carbonatization and aluminosilicate formation formed in the stratigraphic units immediately subjacent



to the deposits. The aluminous alteration resembles that near high sulfidation epithermal deposits, indicating that the altering fluids were very acid, and possibly magmatic.

Water depth controls aspects of deposit composition and alteration assemblages. Volcanoes associated with nascent ocean-dominated arcs and back-arcs settings tend to be of low elevation and deeply submerged (usually >2000m) shield volcanoes or elongate rifts. Felsic rocks rarely exceed 30% of the volcanic complement, and are usually cooled from high-temperature (sodic) melts. Volcanoes associated with arcs involving continents (Types 2 and 4) are more high standing, commonly emergent stratovolcanoes, consisting predominantly of subaqueous hydrovolcanic pyroclastic flows and tuff-cones, andesitic flows, and some felsic lava domes. Volcanological constraints can only provide cumulative evidence for water depth at depositional sites; generally speaking deposits in types 1 and 3 (and ophiolite-related deposits) provide deep water VMS depositional sites, whereas types 2 and 4 are in shallower water.

Hydrothermal systems that engender giant VMS deposits must discharge through only a few well-focused sites, be persistent, and be efficiently capped. Reservoir caps may be physical (impermeable sediments or well-sealed submarine ash flows), or may have formed through thermally induced chemical sealing, such as the aforementioned widespread carbonatization associated with types 2 and possibly 4. Silicification may also be an important reservoir-sealing process.

Faults that control hydrothermal discharge include rift-margin master faults and caldera ring-fault systems. Extensional regimes both in mid-ocean and back-arc systems engender VMS-producing structures. A second method for focusing discharge is the presence of sediment-submerged basement or volcanic highs. Alteration pipes associated with types 1 and 3 vary from those with cores of Fe-chlorite and silica and margins of Mg-chlorite (in part after smectite) to those associated with types 2 and 4, with silica-sericite  $\pm$  Fe-carbonate pipes. Deep-water systems (Types 1 and 3) are associated with high-velocity discharge, and highly fractured flows. Both promote local drawdown of cold seawater, promoting the cooling of the rising hydrothermal fluid and the rapid deposition of Mg-rich clays, and anhydrite, forming magnesian margins to pipes. Shallow water systems have lower-velocity discharge, and are associated with sediment caps and well-sealed subaqueous pyroclastic flows. Local drawdown was inhibited, and silicification prominent around these discharge zones, thus suppressing the formation of Mg-rich alteration.

Much sulfide precipitation occurs within sulfide mounds, where conductive cooling and circulation of heated seawater extensively modified the deposit's zoning and composition, and yield "replacement" paragenetic assemblages. Introduction of either residual brines or vapor phase fluids (boiling), or magmatic fluids can also modify the composition, with the addition/enrichment of hydride elements, copper, and gold. Continuation of seawater circulation also modifies the distribution of base and precious metals. Primary fluid compositions and the depositional environment control ore compositions. In felsic and sediment-dominated systems (Types 2 and 4) where buffering to acid pH may occur at any temperature, ore-forming fluids may contain more lead and zinc, relative to copper, than those high (>350°C)

temperature basalt-dominated systems (Types 1 and 3). Deposits of types 2 and 4, which tend to have formed in relatively shallow water, may be more lead, zinc, silver and gold rich simply because cooling (boiling) forced copper from the fluids during their ascent, and promoted the formation of bisulfide-complexing (and thus highly efficient transport) of gold. Separate, oxidized, magmatically generated brines may have been important in forming some high-sulfidation zones within a few deposits.

## ARC-RELATED VOLCANOGENIC MASSIVE SULFIDE DEPOSITS

J.M. Franklin, M.D. Hannington, I.R. Jonasson and C.T. Barrie  
Geological Survey of Canada\*

Volcanogenic massive sulfide (VMS) deposits have been classified on the basis of their composition (e.g. Cu-Zn-Pb triangle, Franklin et al. 1981; Au rich deposits, Poulsen and Hannington, 1995) or by geological setting (e.g. tectonic regime, e.g. Barrie and Hannington, 1997, or host rock composition, e.g. Divi et al. 1980). Compositional classification systems provide a test for specific compositional "anomalies", such as the multiple-population distribution of lead or gold. They are most useful as a basis for investigating the processes that control relative metal abundances in the members of a non-homogeneous population. Use of "geological settings", although more subjective than the compositional approach, may provide a better basis for establishing exploration criteria. The criteria used for geological setting, whether they are the composition of host rocks or the tectonic element represented by the host rocks in a district, are more difficult to assign. Scale of observation and quality of data are just two aspects that usually have some uncertainty, rendering the use of geological setting more difficult. However, the geological characteristics of VMS districts ultimately provide key indicators of the process that produced the deposits. Some of these indicators are useful as exploration guides. Ultimately the most useful guides are those attributes that have a well-established genetic role. For example, alteration pipes found primarily within the footwall sequences of VMS deposits are well established as attributes that formed as a direct consequence of the mineralization process, and thus are an excellent, albeit local, guide to economic mineralization. Other possible indicators, observed as recurring attributes but not necessarily as objectively explained in the context of a genetic model, may still be very useful guides for exploration.

Since the first discovery of an active seafloor hydrothermal system in 1977, research on VMS deposits has followed two tracks. Much work has proceeded on the examination of the setting of ancient deposits, particularly those in well established districts in Canada, Japan, Scandinavia and Iberia. Although excellent studies continue to document the immediate setting (ore mineralogy, alteration pipes, structure), more attention has been given to documenting the volcanological attributes of their settings, and the nature and role of intrusive rocks in these areas. Increasingly, research is focussing on the possible transitional processes that may be shared with epithermal and porphyry systems. Research has been progressing in parallel on modern hydrothermal systems. Although most of this work has been documenting hydrothermal systems associated with spreading-ridge environments, studies in the past five years have begun to document systems located in arc-related terrains. Research on modern systems provides an unprecedented opportunity to observe sulfide-forming processes, including the measurement of the compositions of fluids from which the metals are precipitated, and the compositions of the precipitated products. Deep drilling by the Ocean Drilling Program has provided new quantitative information on the deeper parts of the hydrothermal system in one area, Middle Valley in the NW Pacific. Although this area is

---

\* Geological Survey of Canada, 601 Booth St.,  
Ottawa, Ontario, CANADA K1A 0E8

a failed rift system, it resembles back-arc-spreading environment in most of its aspects, and thus provides some analogous data for arc-related VMS systems.

About 80% of the world's VMS deposits are in arc-related strata, with the remaining 20% in ophiolitic settings. Some of the latter are rifted marginal basins, and others are in preserved mid-ocean ridges, as noted below. Table 1 is an attempt to illustrate the range of tectonic settings in which hydrothermal systems develop, and in particular those environments which produce economic VMS deposits. The upper half of the table represents intra-ocean plate island arc environments, ranging from the primitive supra-subduction environment (volcanic front) through the more mature stage of island arc development, which includes an immature back-arc rift, ultimately to a mature arc with a fully developed back-arc spreading centre. In the intra-oceanic environment, melting of hydrated ridge-generated basalt formed felsic volcanic melts. The lower half of the diagram is a parallel scheme for arcs formed at ocean-continent collision zones. The lower half of the diagram is a parallel scheme for arcs formed at ocean-continent collision zones.

We subdivide VMS deposits into **five** types. The first three are dominated by volcanic rocks, the last two have a significant, and in some cases dominate sedimentary association. The deposit types are shown on Table 1, and their approximate positions in two generalized tectonic frameworks are shown in Figure 1. It is usually quite difficult to assign the settings of deposits to a specific tectonic element; this exercise is easiest in Phanerozoic sequences, where tectonic scheme have been developed following the Wilson Cycle. However, as we recognize that any assignment of deposits to tectonic elements is arguable, the presentation herein must be considered preliminary.

**Type 1** includes deposits in arcs formed above ocean-floor dominated subduction (bimodal volcanic sequences). These formed in an intra-oceanic environment, where basalt is dominant, but some melting of oceanic crust has generated a felsic component. The abundance of felsic rocks in this type of VMS district is usually less than 25%. Sedimentary rocks are confined to a few intraflow clastic units, and proximal epiclastic rocks. Pyroclastic strata are subordinate to flows, with pillow basalts, felsic flows and flow domes prominent.

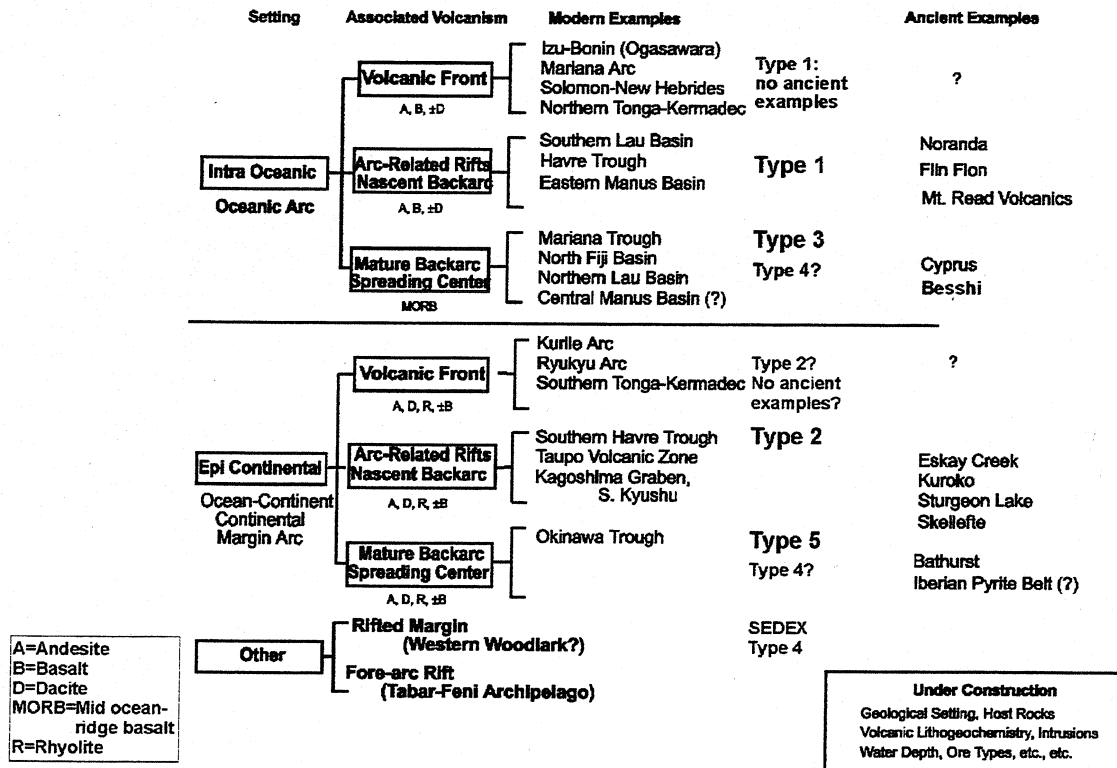
**Type 2** are related to ocean-continent subduction (felsic-dominated bimodal sequences). In these, felsic rocks typically form 35-70% of the volcanic strata, with basalt forming the remainder. Sedimentary strata are more abundant, but not dominant. Submarine pyroclastic strata are dominant, and mafic rocks are typically andesitic, with moderate vesicularity and hyaloclastite common. Some portions of these sequences may be subaerial.

Deposits of the third group (**Type 3**) are also dominated by volcanic strata, and are in ophiolitic sequences. Although ophiolites are most commonly ascribed to a mid-ocean ridge environment, Robertson (1990) presents convincing evidence that the Cyprus ophiolite-associated deposits formed above an intra-oceanic subduction zone. Other ophiolitic sequences are similarly in back-arc-related spreading environments. Thus, for comparison, ophiolite-associated deposits are included in our arc-related group of VMS deposits.

Most **Type 4** deposits are in basalt-sediment (back arc) sequences (Besshi-like). Basalt and sediment may be sub-equal in this type of environment, and although sedimentary strata are most prominent in the "type" examples at the Besshi Mine in

Shikoku Prefecture, Japan, although basalt may dominate. Felsic volcanic rocks are generally minor. The sediments are typically deep-water pelite, wacke and subordinate quartzite. **Type 5** deposits are in mature (epi-continental?) arcs and back-arcs, where

#### METALLOGENY OF SUBMARINE ARCS: EXAMPLES FROM THE WESTERN PACIFIC MARGIN

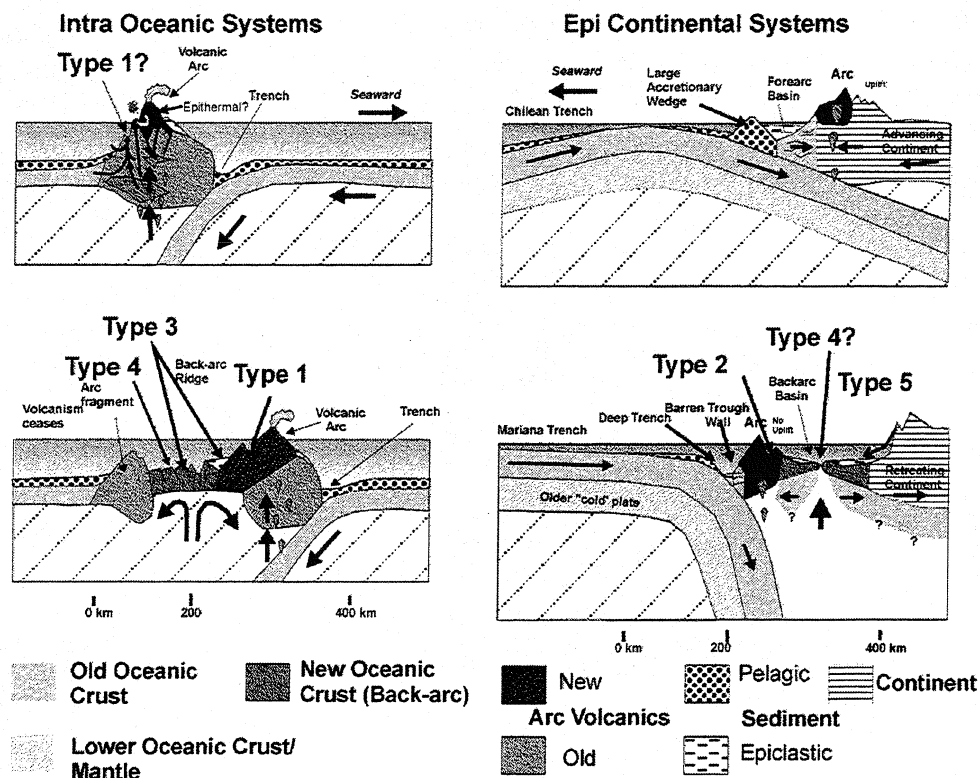


**Table 1: Tectonic settings of arc-related volcanogenic massive sulfide deposits**

felsic volcanic and/or sedimentary strata are dominant. Here, sedimentary strata (including epiclastic rocks) may form as much as 80% of the overall sequence, with felsic pyroclastic rocks much of the remainder. Basalt, if present, is minor, and typically is found in the hanging wall sequences.

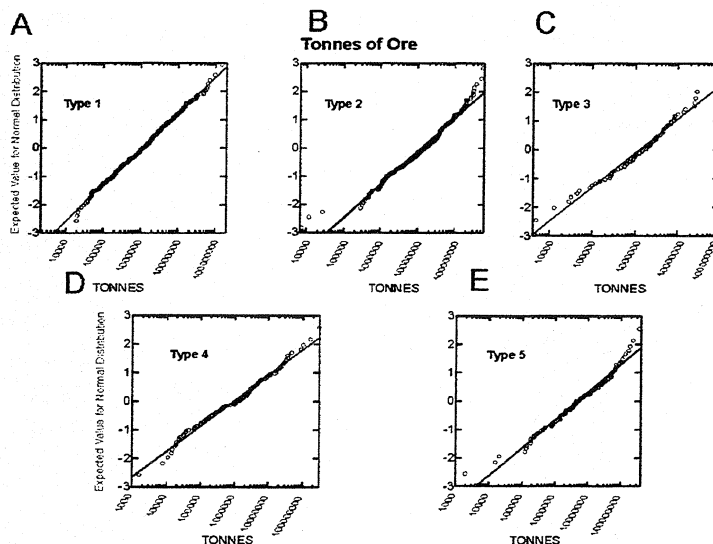
The size distributions of each of the VMS deposit types are displayed in Figure 2 and some relevant statistical measures are in Table 2. These data are based on a preliminary file of tonnage grade and age data for about 800 deposits. <sup>1</sup>All types of deposits have log-normally distributed populations (Figure 2). This distribution has been shown by Sangster (1981) to be true at the district scale, as well. The median sizes of each of the arc-related groups, along with those in the Besshi and ophiolite groups are roughly equal, at 1-1.5 million tonnes. Deposits in the mature continental-arcs or back-arcs (Type 5), where siliciclastic strata are prominent, are much larger (median size of about 4 million tonnes). As noted by Barrie and Hannington (1997), deposits of the bimodal siliciclastic group are only about 30% smaller than the average SEDEX deposit (see Lydon, 1996).

<sup>1</sup> Copies of this file may be obtained on request from the authors.



**Figure 1: Generalized tectonic environments of arc formation, with the possible positions of VMS deposit types**

The distribution of types by age provides some insight as to the state of development (or preservation) of various tectonic elements. Figure 3a shows that VMS deposits are by far the most abundant in the Paleozoic Era. Figure 4b illustrates that they



**Figure 2: Distribution of sizes of each type of VMS deposit**

contain even a greater proportion of the base metals than expected from their abundance. Paleozoic deposits account for 34% of the total in our file, but account for 58% of the total metal. Archean and Proterozoic deposits are very similar in metal content and abundance, by comparison, with 15% and 14% of the total metal, respectively, and 19% and 21% of the total number of deposits. Strata of the Paleozoic Era contain giant VMS districts, such as Ordovician Bathurst (New Brunswick) district,

the primarily Devonian Kazakhstan district, and the Mississippian Iberian Pyrite belt. In all of these districts, the continental mature back-arc spreading environments (Figure 4a). Compositional comparisons are similarly interesting. Figures 3 and 4 illustrate some differences with time and type. Felsic-dominant settings contain the most lead, as also noted by many reviewers, including Franklin et al. (1981) and Hannington and Barrie (1997). The latter authors note the similarity in metal distribution between the metal distribution of bulk continental crust and that of the deposits of Type 5, the siliciclastic VMS group. They also noted the similarity between early Phanerozoic mafic volcanic associated VMS deposits (types 1, 3 and 4), and the metal distribution in MORB. They imply that these trends reflect the source of the metals. Figure 4a illustrates that although the felsic siliciclastic deposits do have a very high lead content (24% of their total metal is Pb, on average), lead comprises 17% of the total metal content of the deposits in the bimodal felsic group (Type 2). Unfortunately there are few reliable data for lead in felsic volcanic rocks or for "average continental crust", and thus the comparisons of metal content in host rocks with those in the deposit class are somewhat unreliable.

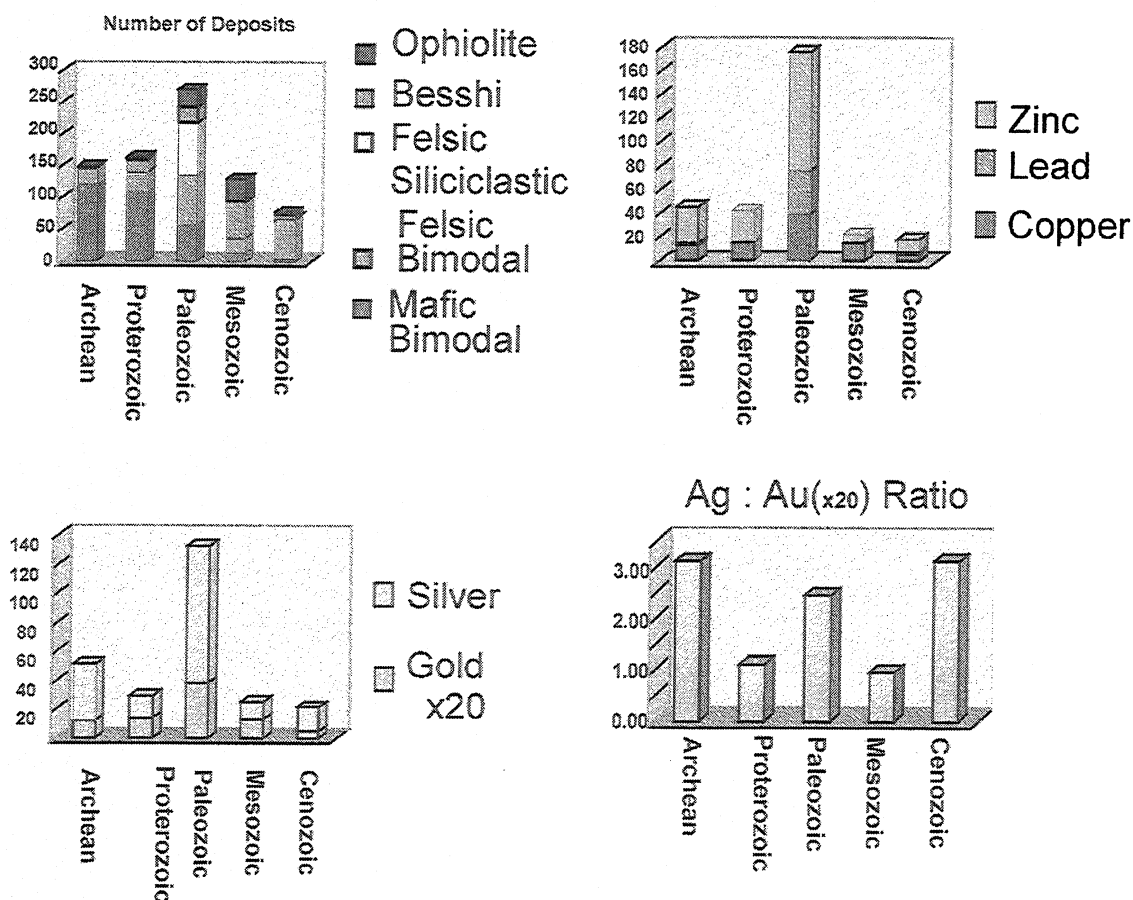


Figure 3: Size and composition of VMS deposits categorized by type and age

The silver content of felsic siliciclastic type of deposits (Type 5) is unusually high,

**Type 1 Bimodal Mafic (n=303)**

	Median	Mean		Median	Mean
TONNES	1,120,000	5,177,901	TONNES of METAL	46,769	246,154
Cu wt%	1.47	1.85	TONNES of Cu	12,600	92,184
Pb wt. %	0.30	0.73	TONNES of Pb	0	7,305
Zn wt. %	3.17	4.17	TONNES of Zn	21,482	148,086
Au g/t	0.90	1.61	KG of Au	37	4,527
Ag g/t	26.50	36.54	KG of Ag	9,631	146,258

**Type 2 Bimodal Felsic (n=211)**

	Median	Mean		Median	Mean
TONNES	1,506,334	4,718,232	TONNES of METAL	88,742	321,941
Cu wt%	1.23	1.50	TONNES of Cu	13,846	60,634
Pb wt. %	1.10	1.82	TONNES of Pb	7,223	54,242
Zn wt. %	4.99	6.00	TONNES of Zn	45,378	210,131
Au g/t	1.03	2.02	KG of Au	153	4,899
Ag g/t	72.20	103.98	KG of Ag	30,639	271,620

**Type 3 Ophiolite(n=70)**

	Median	Mean		Median	Mean
TONNES	1,650,000	5,079,578	TONNES of METAL	27,000	124,458
Cu wt%	1.70	2.13	TONNES of Cu	20,250	98,521
Pb wt. %	0.03	0.09	TONNES of Pb	0	1,267
Zn wt. %	1.00	1.54	TONNES of Zn	0	24,670
Au g/t	1.68	3.26	KG of Au	0	5,842
Ag g/t	11.00	20.23	KG of Ag	0	48,393

**Type 4 Besshi (n=107)**

	Median	Mean		Median	Mean
TONNES	998,185	10,731,804	TONNES of METAL	12,425	196,203
Cu wt%	1.40	1.67	TONNES of Cu	8,760	128,782
Pb wt. %	0.42	1.51	TONNES of Pb	0	1,383
Zn wt. %	1.10	2.42	TONNES of Zn	0	69,705
Au g/t	0.60	0.88	KG of Au	0	3,645
Ag g/t	14.00	18.79	KG of Ag	0	77,666

**Type 5 Bimodal Siliciclastic (n=93)**

	Median	Mean		Median	Mean
TONNES	4,400,000	28,335,039	TONNES of METAL	210,000	1,418,005
Cu wt%	0.76	1.21	TONNES of Cu	41,730	283,842
Pb wt. %	1.15	1.83	TONNES of Pb	50,250	336,950
Zn wt. %	3.90	4.25	TONNES of Zn	108,500	831,497
Au g/t	0.70	1.15	KG of Au	0	10,639
Ag g/t	34.29	69.00	KG of Ag	14,195	746,231

**Table 2: Metal content of volcanogenic massive sulfide deposits**

compared with their gold content. Deposits in bimodal felsic sequences are somewhat rich in gold, compared with silver; this is particularly true of the Proterozoic deposits. It was noted by Franklin (1996) that Proterozoic bimodal volcanic sequences, both felsic and mafic, contain anomalous abundances of VMS deposits per unit area of greenstone. For



example, the volcanic-dominated areas of the Trans Hudson orogen in central Canada contain over \$6 million in base metal content for km<sup>2</sup>, whereas the Archean volcanic strata in the Abitibi Belt of Ontario and Quebec contain only \$1 million per km<sup>2</sup>. Other Proterozoic greenstone belts also seem to contain abundant VMS deposits; the northern Wisconsin area, the Jerome, Arizona district and the Skellefte and Bergslagen districts in Sweden are examples. As GIS-based maps of these and other regions become available, this type of analysis will be undertaken with greater precision.

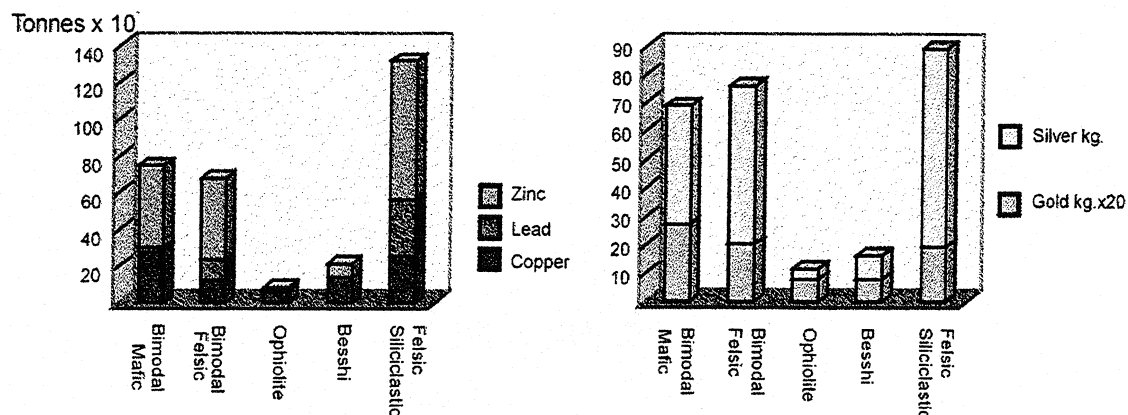


Figure 4: Composition of types of VMS deposits

#### Characteristics of each Type of VMS deposits in the context of a generalized model:

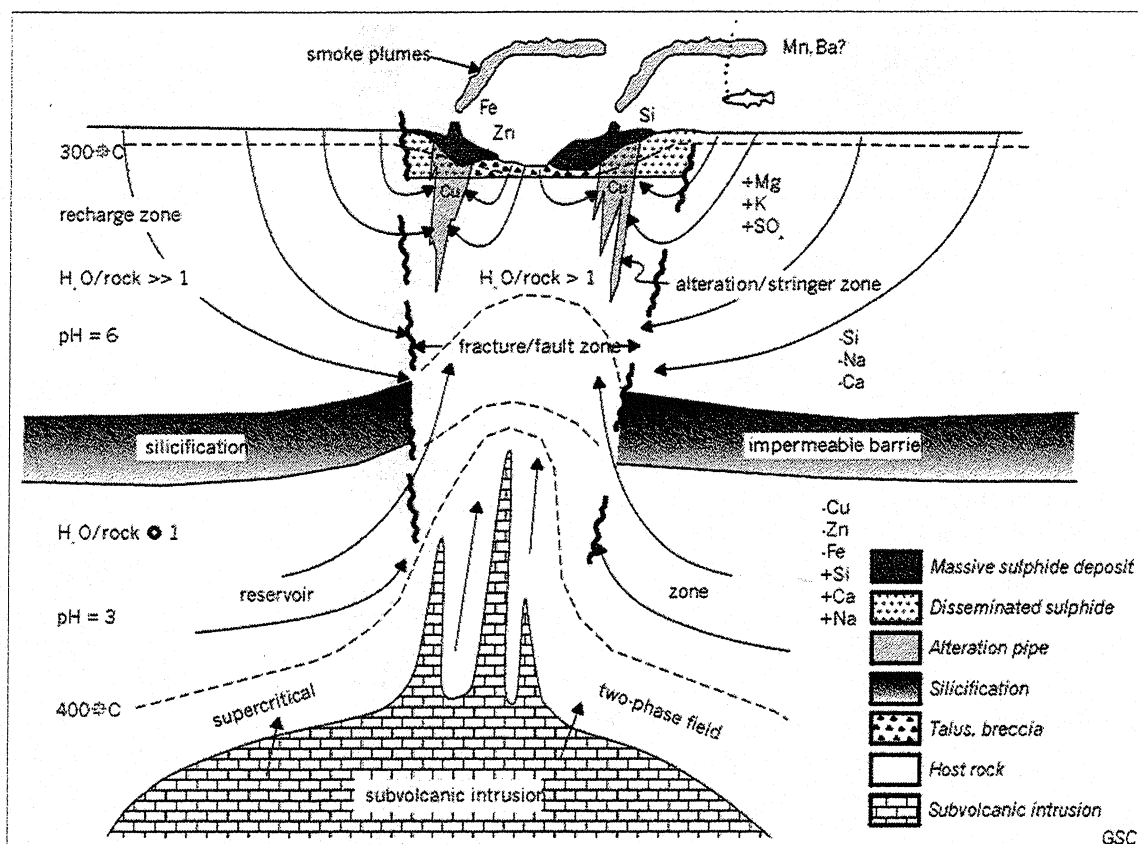
**Generalized model:** Evidence from field and analytical studies (summarized in Franklin et al., 1981, with additional data from Gibson et al, 1983, Skirrow and Franklin, 1994, and others), direct observation of vent fluid compositions (Von Damm, 1995) and experimental work (e.g. Seyfried et al, 1997) support a model for generation of metalliferous hydrothermal fluids by leaching of the substrata in a thermally driven convective system. A convective hydrothermal system was intersected in drilling on ODP Leg 139 (see Davis and Fisher, 1994). The convective model provides that metalliferous hydrothermal fluids were generated primarily in the sub-seafloor through heating of down-welling seawater and leaching of metal. The fundamental control on size of convective metalliferous hydrothermal systems is the abundance of heat in the upper two km of the sub-seafloor crust. Heat is usually supplied from a focused source (shallow-level subvolcanic intrusion). In some oceanic plateaus, hydrothermal systems may develop above mantle plumes (ocean islands).

Recent data (Fouquet et al., 1993) from the Valu Fa back arc region suggests that there may be a direct magmatic component in those deposits where melted continental crust (or hydrated oceanic crust) was involved in volcanism (see environment for Type 2, Figure 1, above). Crustally -derived (S-type?) calc-alkaline subvolcanic (or hypabyssal) intrusions may have generated magmatic-hydrothermal fluid in a manner similar to that attributed to epithermal gold-copper and copper porphyry deposits.

The principal elements of a convective hydrothermal system are:

1. Heat energy: subvolcanic intrusion
2. Metal sources:
3. High temperature reaction zone - convective system
4. Magmatic source
5. Insulating cap
6. Fluid conduit
7. Near surface interaction zone: alteration pipes
8. Vent sites: depositional mounds
9. "Distal" fallout and hydrothermal plumes

These elements are all shown schematically in Figure 5. Their principal characteristics for each of the VMS deposit types is described below.



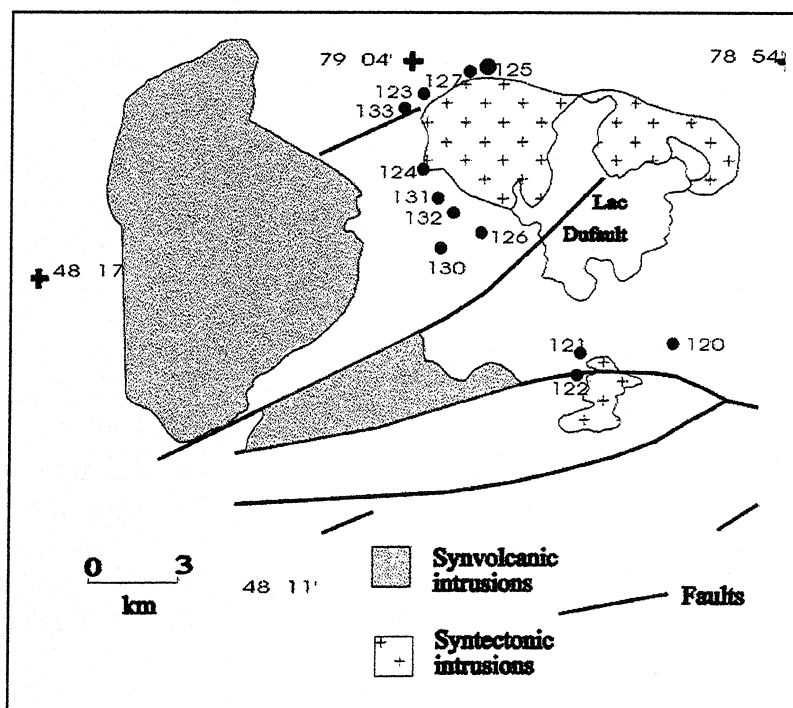
**Figure 5: Generalized model of a convective hydrothermal system for the production of VMS deposits (after Franklin, 1993).**

**Heat energy:** Convective heat transfer has been modeled quantitatively by Cathles (1981) and Barrie et al (1997). Fundamentally, a convective hydrothermal system will be sufficiently metalliferous to form VMS deposits at its discharge site if the convective zone can sustain an acid pH. Seyfried et al (1997) review experimental results (e.g. Bischoff and Seyfried, 1978; Seyfried and Janecky, 1985), and note that for basalt-seawater reactions, experimentally-derived compositions of high temperature fluids closely reflect measured seafloor hydrothermal fluids if the reactions occurred within a temperature range of 375-385°C. Such a temperature requires either a significantly enhanced geothermal gradient or a focused source of heat, i.e. a local intrusive system. Subvolcanic intrusions are a

manifestation of magmatically-supplied heat, although their exact role in driving a system is still under investigation (Barrie et al., 1997; Galley, current CAMIRO project).

Subvolcanic intrusions are prominent under deposits of types 1 and 3; syndeformational intrusions are documented for most of the other types, although they are less ubiquitous. An example of a subvolcanic intrusion associated with a Type 1 district is the Flavrian intrusion that stratigraphically underlies the deposits of the main Noranda caldera (Figure 6). This multiple intrusion is composed primarily of trondhjemite, with subordinate porphyritic and dioritic phases. It, and similar intrusions near the Snow Lake district in Manitoba, display the following typical characteristics:

- Typically about 30-60 km<sup>2</sup> in cross-sectional (typically map) area
- No surrounding contact metamorphic zone
- An extended emplacement history; it locally transects the stratigraphic succession, thus cutting the alteration pipe of the stratigraphically lowest deposits, as at the Ansil Mine at Noranda (Galley et al., 19 ) and the Anderson Mine at Snow Lake (Walford and Franklin, 1982).
- Contain disseminated, "porphyry-like" copper sulfides;
- Affected by all structural elements in the district
- Highly variable textures, some with miarolitic cavities



**Figure 6: Simplified map of the Noranda, P.Q. district, illustrating the distribution of synvolcanic and syntectonic intrusions (For deposit identification see Franklin, 1995).**

Not all subvolcanic intrusions of the Type 1 VMS group are felsic; the Bell River Complex, which stratigraphically underlies, and is pene-contemporaneous with, the deposits in the Mattagami Lake, P.Q. District, is a layered gabbro body. It also locally transects the strata, encompassing the Radiore deposit.

Subvolcanic intrusions that underlie the Type 2 deposits are similar to those under Type 1. The Beidelman Bay complex, which underlies the Sturgeon Lake District (Ontario), is an excellent example of such an intrusion.

The attributes of subvolcanic intrusions under ophiolite-associated deposits (Type 3) are amongst the best described for any VMS type. In Cyprus, the Cretaceous Troodos massif an elliptical body

of mafic and ultramafic rocks, has as its core a plutonic complex of tectonized harzburgite with irregular dunite pods, surrounded by cumulate gabbro and peridotite and capped by a highly differentiated gabbroic to trondhjemitic and tonalitic zone. Fractional crystallization in a magma chamber about 1-2 km below the sea floor; the upper, highly differentiated gabbroic zone is composed of high level intrusions, 50-800 m thick, that in part form the roof of the magma chamber and in part are the products of extreme fractional crystallization. These rocks underplate the Sheeted Dike Complex, a thick zone of feeder dikes to the overlying lava sequence that is rooted in the underlying gabbro. The upper part of the dike swarm, the Basal Group, consists of 90-100% dikes in screens of pillow lava, whereas the lower unit consists of multiple dikes and dike swarms intruded into screens of gabbro or quartz-diorite (Constantinou, 1980). Hall and Yang (1995) have demonstrated that the ore deposits occur stratigraphically about 100m above the zone where dyke density reaches 25%, implying a structural relationship to the dykes. Similar relationships exist in the Semail ophiolite and in Newfoundland (Hall and Yang, 1995).

The attributes of subvolcanic intrusions beneath deposits of Type 4 are poorly known. Slack (1993) noted that although large bodies of gabbro and serpentinite occur in the footwall to the Besshi district, these intrusions are in tectonic contact with the volcano-sedimentary sequence that hosts the deposits. Mafic sills are abundant in the footwall sequence to the Shimokawa district in Hokkaido, Japan, and Peter and Scott (1997) note abundant mafic sills in the footwall to the Windy Craggy deposit in British Columbia.

The most extensively studied modern example of a Besshi-like deposit is the Middle Valley area of the northern Juan de Fuca spreading ridge. Although this area is clearly not arc-related, the geological characteristics of the sulfide deposits are quite similar to those in Type 4 settings. The deposits and active vents are in pelagic, turbiditic sediments. Downwards from about 500m stratigraphically below the present seafloor, the sedimentary sequence contains about 25% mafic sills (see Stakes and Franklin, 1994, for a description). These sills have most of the characteristics of typical subvolcanic intrusions (no metamorphosed contacts, highly altered, superimposed base metal sulfide veins).

Although the exact roles of the intrusions under both the ophiolite (Type 3) and Besshi (Type 4) types of VMS deposits is unknown, it is clear that they are a manifestation of an anomalous heat source, and thus are useful exploration guides. All have interacted with the hydrothermal system, and clearly have an intimate role in VMS generation.

Synvolcanic intrusions within the footwall sequences to the felsic siliciclastic group of deposits (Type 5) are poorly documented. These areas are very structurally complex, and although intrusions have been noted in areas such as Bathurst and the Iberian Pyrite Belt, age determination and structural analyses are insufficient to permit their being identified as syn-volcanic.

**Igneous petrochemistry:** Any direct relationship between magma type and the abundance or composition of deposits is tenuous. Some generalized characteristics are shown in Table 3. Generally, for types 1 through 3, immobile element studies indicate that the felsic melts are sodic dacite and rhyolite, which were generated at quite high melting temperatures. This high temperature nature may have promoted convective circulation and leaching. In the felsic-dominated and continental arc-related areas (type 5 and possibly 2), more-K-rich, continent-derived melts may be evident. Acidic melts derived through anatexis

<b>Tectonic Environment</b>	<b>Mafic volcanics/intrusions</b>	<b>Felsic Volcanics/intrusions</b>	<b>Notes</b>
<b>Intra-oceanic</b>			
Volcanic front	Tholeiitic basalt dominant (75%); pillowed flows, sheet flows, low vesicularity; flat to slightly enriched LREE pattern	Felsic flows subordinate pyroclastics; Na-dacite, rhyolite. Derived from melting basaltic crust: Ti-enriched; flat REE pattern	Deeply submerged (~2500m)
Nascent Arc Rift	Basalt and andesite dominant (70%); mainly tholeiites, minor calc-alkaline: flat to slightly LREE enriched patterns	Tonalite/trondhjemite; dacite, less rhyolite: flows, minor pyroclastics; Sr/Rb high	Moderate (~2000m) to deep ocean
Mature backarc rift	LILE and LREE-enriched basalt flows, similar to ocean island alkalic and within plate tholeiites	Minor	
<b>Epi-continental</b>			
Volcanic Front	Minor: LREE enriched, alkaline to calc-alkaline or ocean-island, scoria	Calc-alkaline felsic ash flows, welded ashes, flow domes	Emergent, subaerial, continental
Nascent Rift	Mafic scoria, ash, flows; tholeiitic to calc-alkaline; <40%	Calc-alkaline pyroclastic flows; anatectic melting of continental crust	
Mature backarc	Subordinate (<30%), calc-alkaline to alkaline	Rhyolitic ash flows	

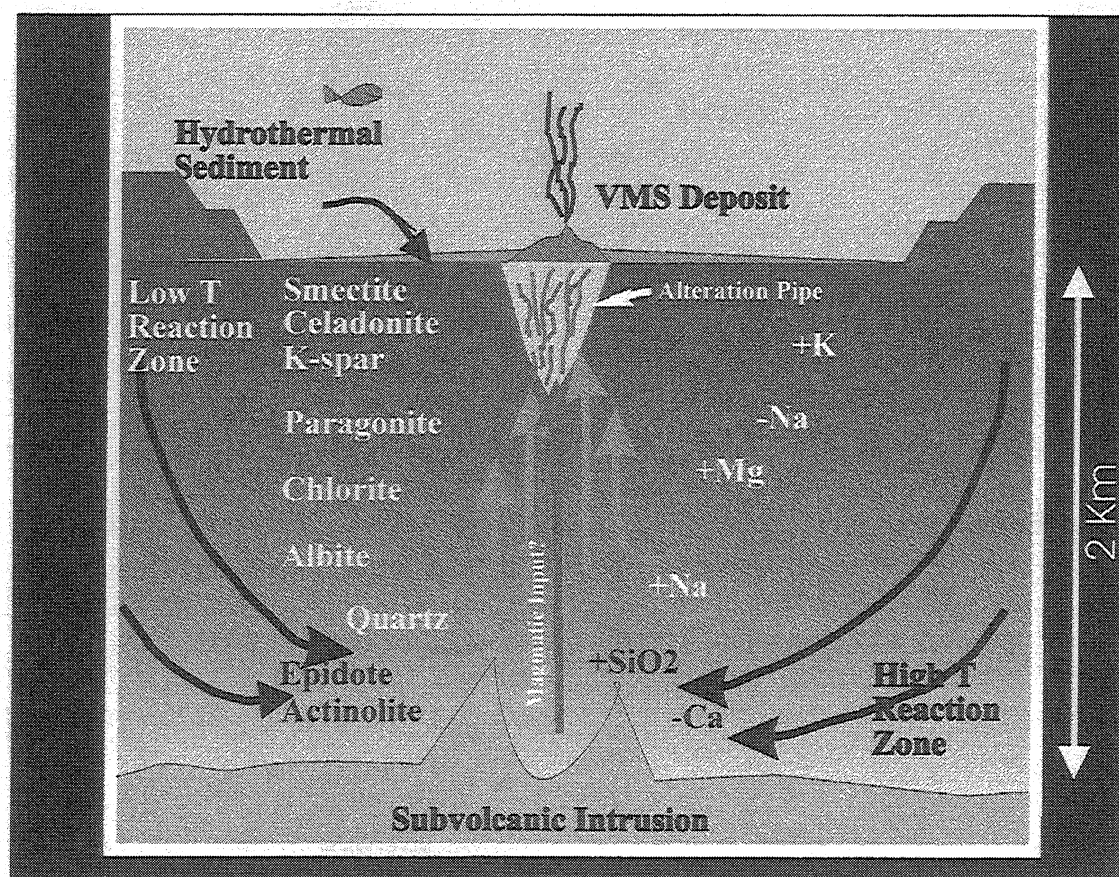
Table 3: Preliminary summary of the igneous petrogenesis of VMS districts

of subducted crust will be more volatile-rich than those associated with mantle-derived melts. The volatiles from such anatectic melts probably form a metal-rich magmatic fluid, which may participate in the formation of VMS deposits. Thus epi-continental systems potentially may have a direct magmatic component. Fouquet et al (1993) recorded vent fluid compositions that most likely contain a magmatic component. Such fluids, which may resemble the high-sulfidation fluids associated with epithermal gold deposits, may impart an unusual signature to the deposits, as discussed below.

Slack (1993) noted that the mafic igneous rocks that are contemporaneous with the Besshi deposits (Type 4) include some MORB, but alkalic and within-plate basalt compositions are present at many districts (Besshi, Windy Craggy, Namibia, Chile). One petrogenetic factor that could be a useful exploration guide, is the indication that the most prolific VMS systems in ophiolite-associated sequences (Type 3 deposits) are not in typical ocean-floor N-MORB, but in somewhat modified mafic compositions (E-MORB, more

alkalic basalt etc.). These unusual, light REE and light lithophile element – enriched compositions, as noted by Peter and Scott (1997), reflect melt generation in a regime where low degrees of partial melting of the mantle occurred. These compositions reflect a refractory upper mantle, and are typical of back-arc environments. Swinden (1996) also noted that basalts associated with VMS deposits in Newfoundland also display chemical characteristics of rifted arcs. Swinden, as others, noted that the relationship to VMS deposits is probably indirect, with the anomalous heat flow accompanying arc rifting being responsible for enhancing hydrothermal circulation. Such shifts in composition away from typical MORB may be also induced by assimilation of hydrated or seafloor-altered older basaltic crust into the mantle-derived melt. As part of such a crustal melting scenario, plagiogranites may be formed. Again, the anomalous heat flow associated with rift-related crustal thinning, in combination with the ready availability of hydrated crust for assimilation, generated the compositional trends that are atypical of ocean-floor rifting.

Perfit et al (1997) noted aberrant chemical compositions of basalts associated with the Galapagos rift VMS deposits. In the latter area, mid ocean-ridge basalt composition are unusually fractionated, with andesite present near the deposits. The more fractionated rocks contain high  $^{87}\text{Sr}/^{86}\text{Sr}$  ratios, relative to MORB, and elevated Cl and volatile contents. Perfit et al. (1997) suggest that these compositional attributes formed through partial assimilation of old hydrated crust. Such assimilation may have been induced because of a super-



**Figure 7: Distribution of alteration minerals, gains and losses for Type 1 VMS deposits.**



abundant magma supply, heat from which engendered a VMS-producing convective hydrothermal system.

The common feature of basaltic melts associated with Types 1 and 2 is that they are associated with nascent rifted arcs. In the case of types 3 and 4, rifting is more mature, and the melts have a typical back-arc petrogenetic signature.

Many mafic sequences associated with VMS districts have characteristic REE patterns that not only are LREE – enriched, but display negative europium anomalies. This feature, noted first by Campbell et al (1984) for Archean VMS districts, is a common, although not ubiquitous, attribute of VMS districts in non-Archean sequences. It may be ascribed either to removal of feldspar in a high-level subvolcanic magma chamber, or to hydrothermal alteration.

In summary, both the subvolcanic intrusions and related volcanic rocks associated with VMS deposits typically have somewhat aberrant petrochemical trends, caused by unusually rapid heat removal to the hydrothermal system, assimilation of hydrated country rock, or interaction with seawater. Extensive fractionation may be evident in both major element and REE trends.

**Lower Semiconformable Alteration:** Hydrothermal systems that engender giant VMS deposits must obtain their metals from the lower parts of the system, where heated seawater is able to react with the volcanic or sedimentary substrate. These systems must discharge through only a few well-focused sites, be persistent, and be efficiently capped. Thus lower semiconformable alteration may represent two important processes; metal source zones, and containment mechanisms for hydrothermal reservoirs. Reservoir caps may be physical (impermeable sediments or well-sealed submarine ash flows), or may have formed through thermally induced chemical sealing. Examples of the latter include the aforementioned widespread carbonatization (described below) associated with types 2 and possibly 4 and 5. Silicification may also be an important reservoir-sealing process, particularly in the latter two types.

On reaching a critical reaction temperature (a sustained acid pH) in convective

leaching systems, metals are leached and moved into the hydrothermal fluid. In basalt-dominated areas (types 1, 3 and 4), leaching-related alteration of mafic “source” zones (lower semiconformable alteration) formed the assemblage albite-epidote-actinolite-quartz. Silicification is local but prominent in these zones. It is most abundant adjacent to high-level subvolcanic intrusions (e.g. MacGeehan and MacLean, 1980, Skirrow and Franklin, 1994). Lower semiconformable alteration

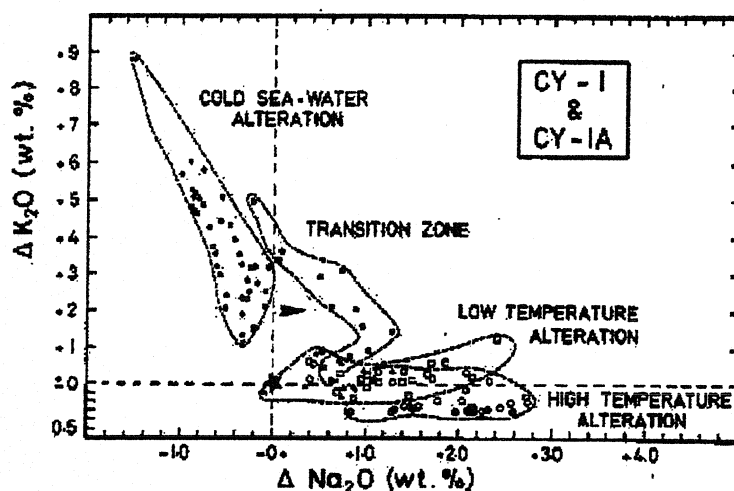
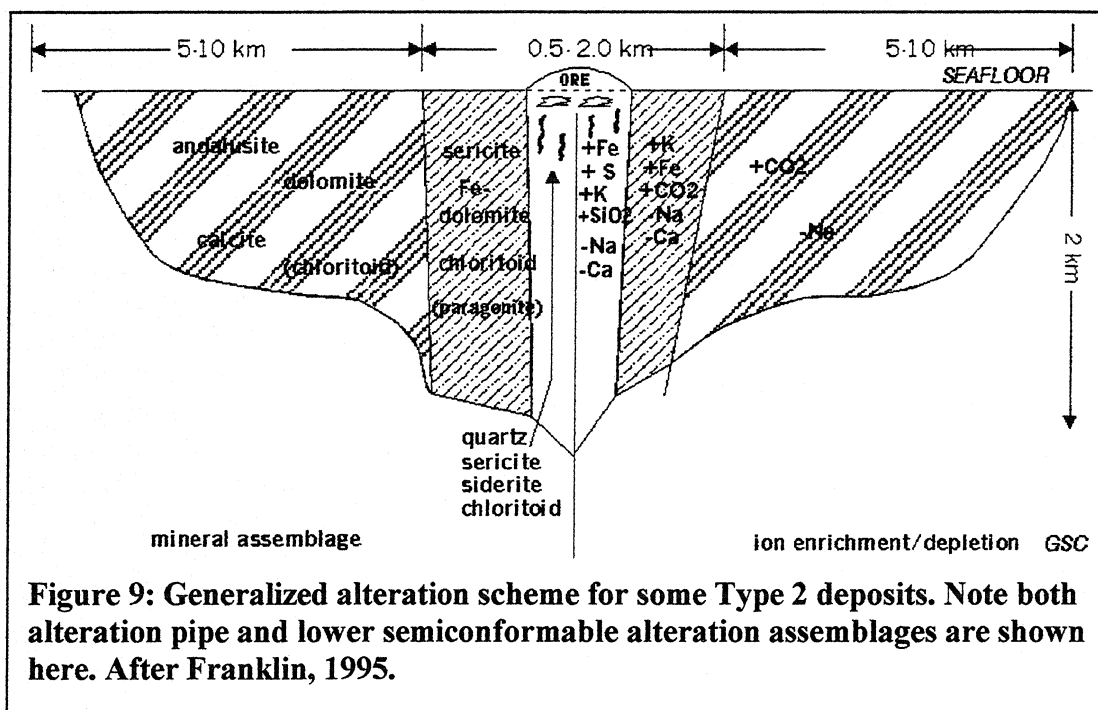


Figure 8: Change in  $\text{Na}_2\text{O}$  vs change in  $\text{K}_2\text{O}$  variation diagram for drill holes CY-1 and CY-1A discriminating the different alteration zones. From Bednarz and Schmincke, 1990.

zones associated with Type 1 deposits are well documented (see Galley, 1993 and references therein). Excellent examples of these may be found at Noranda P. Q and Snow Lake, Manitoba. The uppermost semiconformable alteration is usually locally Na-depleted. This feature is most pervasive near the deposits, and generally is thought to represent either recharge zones or local zones of advecting seawater, drawn down in response to nearby vigorous discharge. The lateral extent of Na depletion is probably dependent on the permeability of the volcanic rocks. The lower semiconformable alteration zones are variably metal-depleted (particularly in copper, see Skirrow and Franklin, 1993) and are characterized by patchy silicification and epidotization, with loss of calcium and addition of sodium (as albite). Their mineralogical and petrochemical characteristics are displayed in Figure 8.

Alteration under Type 3 districts is similar to that documented with Type 1 districts, and is similarly well documented (Spooner and Fyfe, 1973; Bednarz and Schmincke, 1990; Gillis and Robinson, 1990). This alteration is very similar to that described for the Type 1 deposits. Bednarz and Schmincke divide alteration into four zones (Figure 9): In the highest temperature alteration zone,  $K_2O$  is virtually completely lost,  $CaO$  depleted significantly, and  $Na_2O$  and  $MgO$  gained. In the lower alteration zones the opposite is true. In the cold seawater alteration zone, which is at the shallowest levels in the Cyprus drill holes, adularia and smectite have formed, and the rocks are more oxidized.



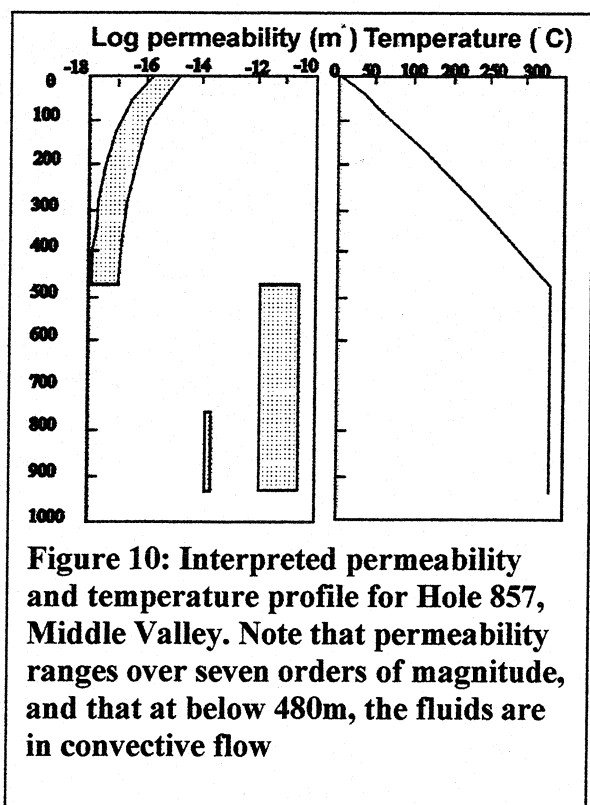
In more felsic-dominated areas (type 2 and possibly type 5), and particularly in those deposits which formed at shallow seawater depths ( $< \sim 1500\text{m}$ ), laterally extensive carbonatization may have occurred in the stratigraphic units immediately subjacent to the deposits. The  $CO_2$  source is enigmatic; organic-rich substrata, which provide methanogenic carbon, may be important. Such sequence may be more prevalent proximal to continental arcs, in fore-arcs or rifted marginal basins where a supply of carbonaceous detritus is readily



available. The carbonate species are more iron-rich (reaching siderite) as the orebody is approached. Sodium depletion and aluminous assemblages (andalucite) dominate semiconformable alteration associated with these deposits; metal depletion is not as evident. This alteration resembles that associated with high sulfidation epithermal deposits, perhaps indicating that the altering fluids were more acid than those in the deeper-water systems, and possibly of magmatic origin.

Lower semi-conformable alteration has been documented below other Type 2 VMS districts. Galley (1993) and Rickard (1988) describe a persistent downward change in the felsic sequence beneath the Bergslagen, Sweden district from quartz-microcline-biotite through chlorite-quartz-albite to quartz-albite-chlorite-epidote. This represents a transition for K metasomatism at the top of the section, through Na-Mg enrichment at intermediate levels, to Na enrichment at the bottom, presumably highest temperature part of the system. The overall zonation of alteration for Type two deposits is similar to that for the other volcanic-dominated regime, except that K-feldspar is more abundant in the uppermost parts of the system, whereas celadonite and K-micas are more common in the mafic-dominated systems.

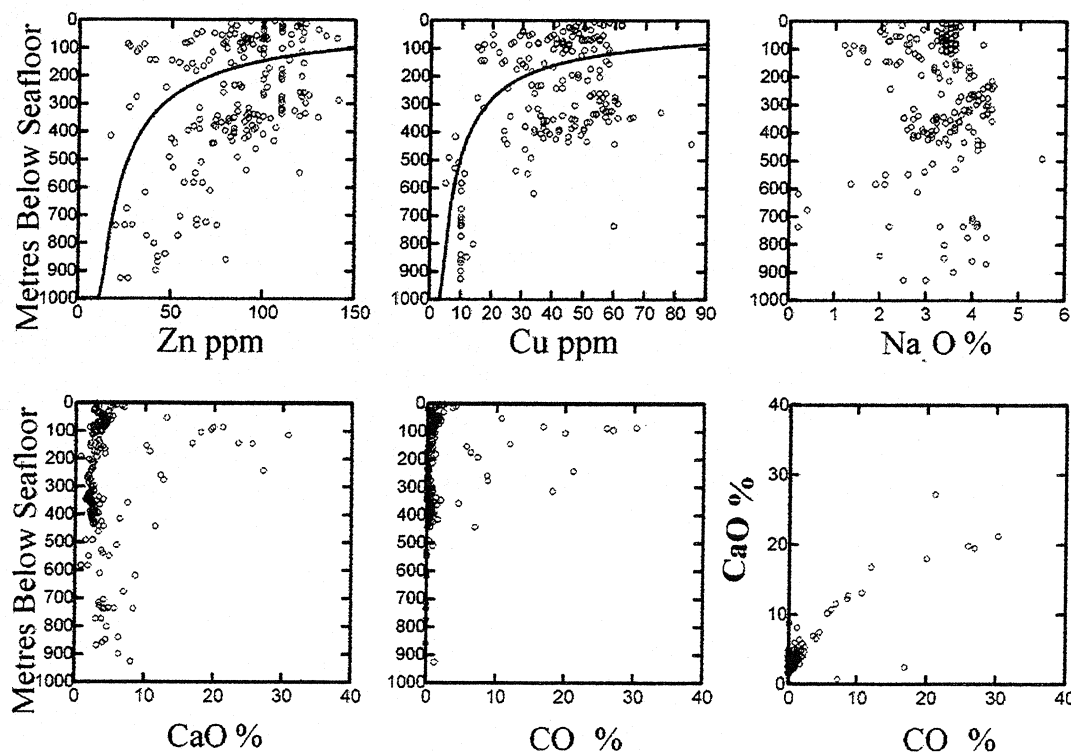
Regional scale alteration associated with Besshi deposits is not well documented. Peter (1992) noted extensive alteration in the Windy Craggy region, but few other studies are available. Work at Middle Valley may have direct application to this problem, and although it is forming in a failed rift, and thus is not arc-related, it has compositional characteristics that are very similar to a Besshi-type deposit. As described in Goodfellow and Franklin (1993), Mottl et al., (1994) and Goodfellow and Zierenberg (1997), the sulfide deposits occur as two mounds, about 400m apart. The more northerly and largest mound is 104 m thick and over 200m in diameter; collectively, the two deposits contain at least 20 million tonnes of sulfide. Each deposit is underlain by about 200m of stringer sulfide, including a deep copper zone that may be continuous between the two. The sedimentary sequence that contains these deposits, as well as a zone of active venting about 2.4 km to the north, occupies a failed or dormant rift. Seismic data (Rohr and Schmidt, 1994) indicate that there is in excess of 1000m of sediment in the centre of the Valley, and about 300m thick in the vicinity of the sulfide deposits. The margins of the basin are underlain by basalt, and the lowermost 500m of the sedimentary section in the centre of the valley contains many thin basaltic sills, as described above. The sediments are composed of intercalated turbiditic wacke and hemipelagic mud. The wacke content increases downwards. During leg 139, a deep hole was drilled near the centre of the basin to test for a "hydrothermal reservoir". Some of the salient geophysical interpretations are presented in Figure 10, and compositional data for the sedimentary strata are presented in Figures 11, 12 and 13.



Two remarkable observations regarding the physical state of Middle Valley are shown in Figures 11. For the first 480m below seafloor, the temperature increased linearly, indicating conductive heat transfer. Below that point, the temperatures measured in Hole 857D are isothermal, indicative of convective mixing. These observations are supported by the calculated changes in permeability, which increases by seven orders of magnitude. Thus, at about 480m, hole 857D entered the hydrothermal reservoir.

The geochemical data for this hole indicate that major metasomatism is (or has) occurring in the reservoir zone. In Figure 12 we can see that the copper content has dropped by about 75%, and the zinc content by one-half, in the reservoir zone. Metals have apparently been largely removed in this high

temperature zone, in a manner similar to that observed in preserved footwall deposits to

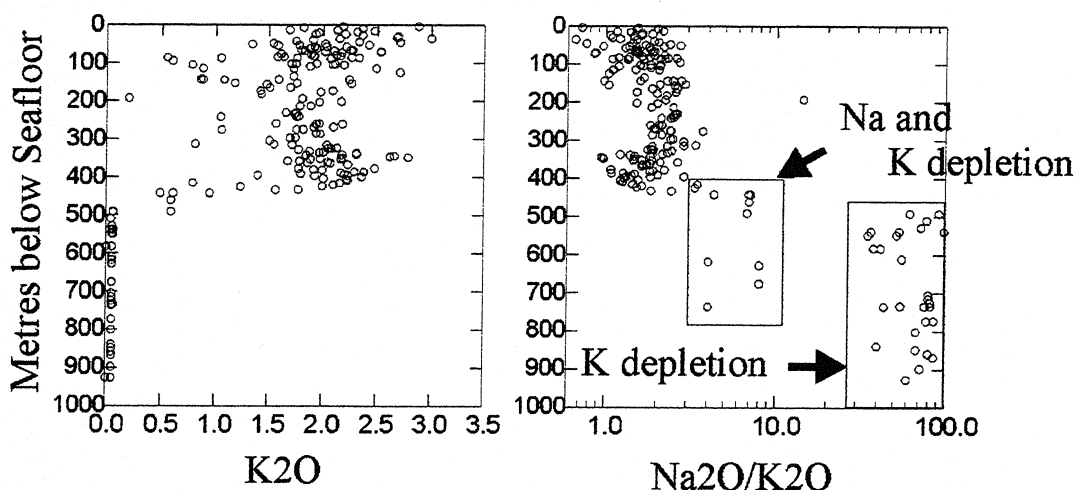


**Figure 11: Distribution of base metals and selected major elements in ODP Holes 857 C and D, Middle Valley, Juan de Fuca Ridge.**

ancient deposits.

The CaO-CO<sub>2</sub> data illustrate another aspect of the alteration. The CaO content of the uppermost 480m of the holes is very consistent (Figure 12c, except for a scattering of compositions to the right of the main trend. Figure 12e illustrates that these high CaO values correlate with high CO<sub>2</sub> values, a fact further demonstrated in Figure 12f. The uppermost 480m contain abundant carbonate nodules; these increase in abundance near the zones of hydrothermal discharge (see Baker et al., 1994). Isotopic data (Baker and Cross, 1994, Adshead, 1995) indicate that the carbonate for these nodules originated as methane, and that they are forming due to thermal diagenesis, whereby the methane is breaking down to CO<sub>2</sub>, and precipitating as carbonate in the cool, upper parts of the system. Adshead (1995) noted that these nodules increase in Mn and Cu content as the discharge zones are approached.

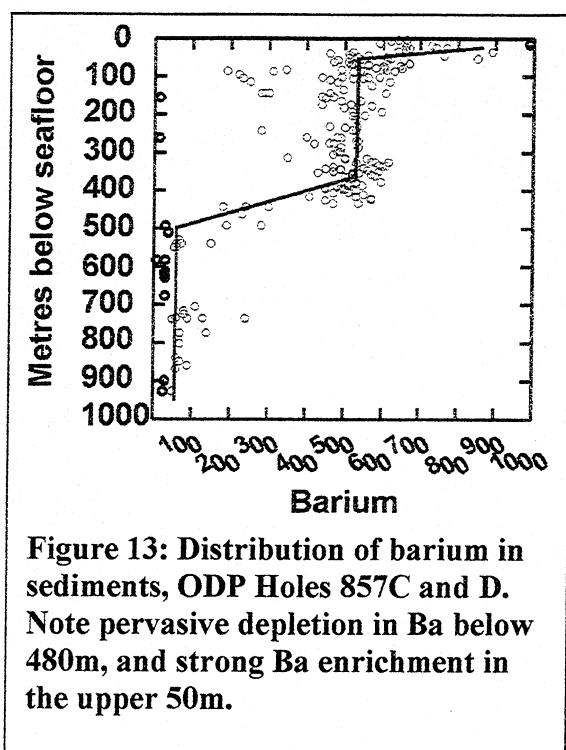
The data for Na<sub>2</sub>O reveal a difference in comparison with similar data for basalt-



**Figure 12 : Distribution of K<sub>2</sub>O and Na<sub>2</sub>O/K<sub>2</sub>O in ODP Hole 857 c and D. Note exceptional K<sub>2</sub>O depletion in lower part of section.**

dominated terrains. Na is not depleted in the low temperature part of the system. This is probably because of the very low permeability in the uppermost 480m. Immediately below the low permeability zone, Na is locally depleted, perhaps at the point where the temperature is not sufficiently high to maintain albite, and the water/rock ratio is high enough to remove Na. Below that zone, Na is retained.

Finally, K<sub>2</sub>O and Ba are pervasively depleted below 480m (Figure 12, 13). This depletion, accompanied by a parallel depletion in Rb and steady increase in Sr (not shown) in the same zone, indicate that mica (sericite) has been destroyed, and that feldspar (probably albite) has been formed. Mineralogical studies are in progress to test these hypotheses. The extensive depletion of K<sub>2</sub>O may serve as a useful indicator of VMS potential in ancient sediment-dominated sequences. Barium depletion in the lower 480m probably reflects the destruction of detrital K-feldspar. Potassium is enriched slightly near the top of the section, but this may be related to the increased content of pelagic clay. The barium enrichment that is so extensive near the top of the section was also noted near the discharge sites (piston core data, unpublished). Barite must have been extensively precipitated from unfocussed upwelling of hydrothermal fluids, under reducing conditions. This anomalous barium distribution is an excellent indicator of hydrothermal activity.



changes are accompanied by a downwards (stratigraphically) decrease in Mg/Ca, Mg/Na and Na/Ca ratios. The observation regarding K and carbonate enrichment near the top of the system is similar to that observed at Middle Valley and at Sturgeon Lake, Ontario (Types 4 and 2, respectively). The presence of metasomatically produced K-feldspar near the top of the Iberian system is similar to that observed in the Type 2 (bimodal felsic) systems in the Bergslagen, Sweden area. In summary, the lower semiconformable alteration patterns show some consistency between VMS deposit types (Table 5). These attributes should be useful regional-scale guides for VMS potential.

VMS Type	Mineral Assemblages	Chemical Change
Type 1	Upper zone: feldspar destroyed, K-mica +/- paragonite Lower zone: albite-actinolite-quartz-epidote	Upper zone: -Na, +K, +Mg (near ore) Lower zone: +Na, +Si (local), -Cu, -Zn
Type 2:	Upper zone: K-spar, carbonate added (Fe-carbonate increases towards ore). Albite destruction widespread, aluminosilicate abundant (andalucite) Lower zone: albite, epidote added	Upper zone: +CO <sub>2</sub> , -Na, +K Lower zone: +Na ?
Type 3	Same as Type 1	Same as Type 1

Type 4	<b>Upper zone;</b> carbonate, K-feldspar added; widespread barite, increasing near ore <b>Lower zone;</b> Complete loss of K-spar, carbonate, K-mica	<b>Upper zone:</b> +K, +Ba, +CO <sub>2</sub> <b>Lower Zone:</b> -K, -Rb, -Ba, -Cu, -Zn, +Ca, -CO <sub>2</sub>
Type 5	<b>Upper zone;</b> K-spar, mixed layer clays (smectite-chlorite), zeolite, carbonate <b>Lower zone:</b> albite-chlorite-actinolite-epidote	<b>Upper zone:</b> +K, +Mg <b>Lower zone;</b> +Na, +Ca

Table 5: Summary of mineralogical and compositional changes related to alteration in lower-semiconformable zones

### Discharge zones- alteration pipes:

Faults that control hydrothermal discharge include rift-margin master faults and caldera ring-fault systems. Extensional regimes both in mid-ocean and back-arc systems engender VMS-producing structures. The paucity of large deposits in either the modern or ancient volcanic fronts may be due to the very incipient nature of (or total lack of) extension in these environments. The deep-penetrating faults associated with the nascent backarc settings of Type 1 deposits (see the Noranda cross section, Figure 14, for example), or the

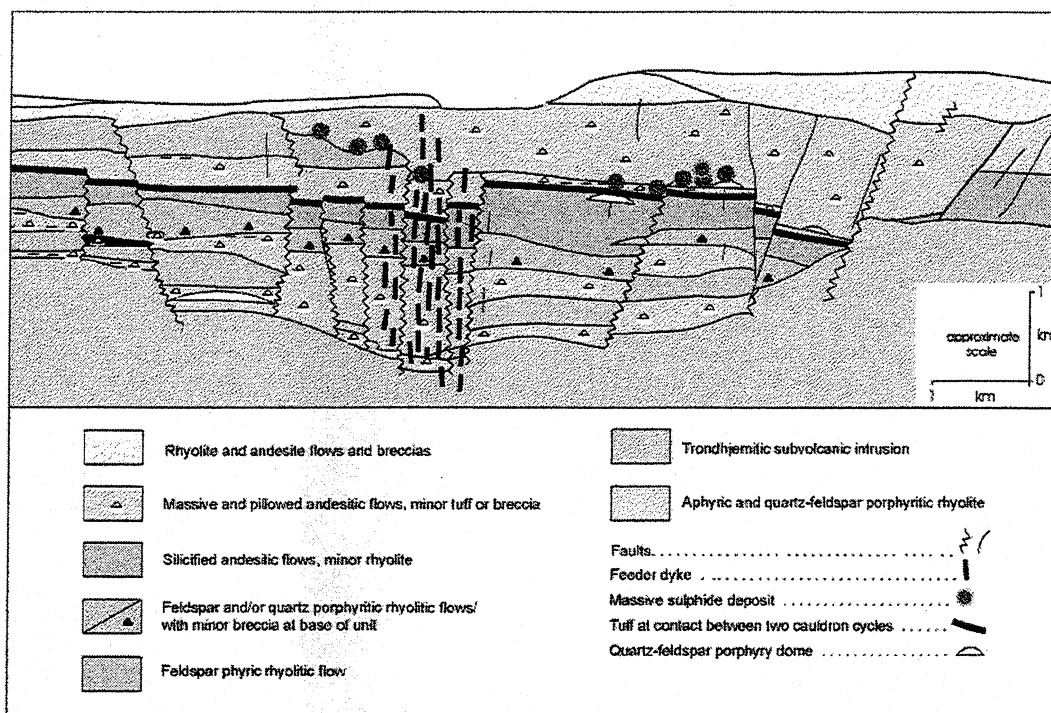
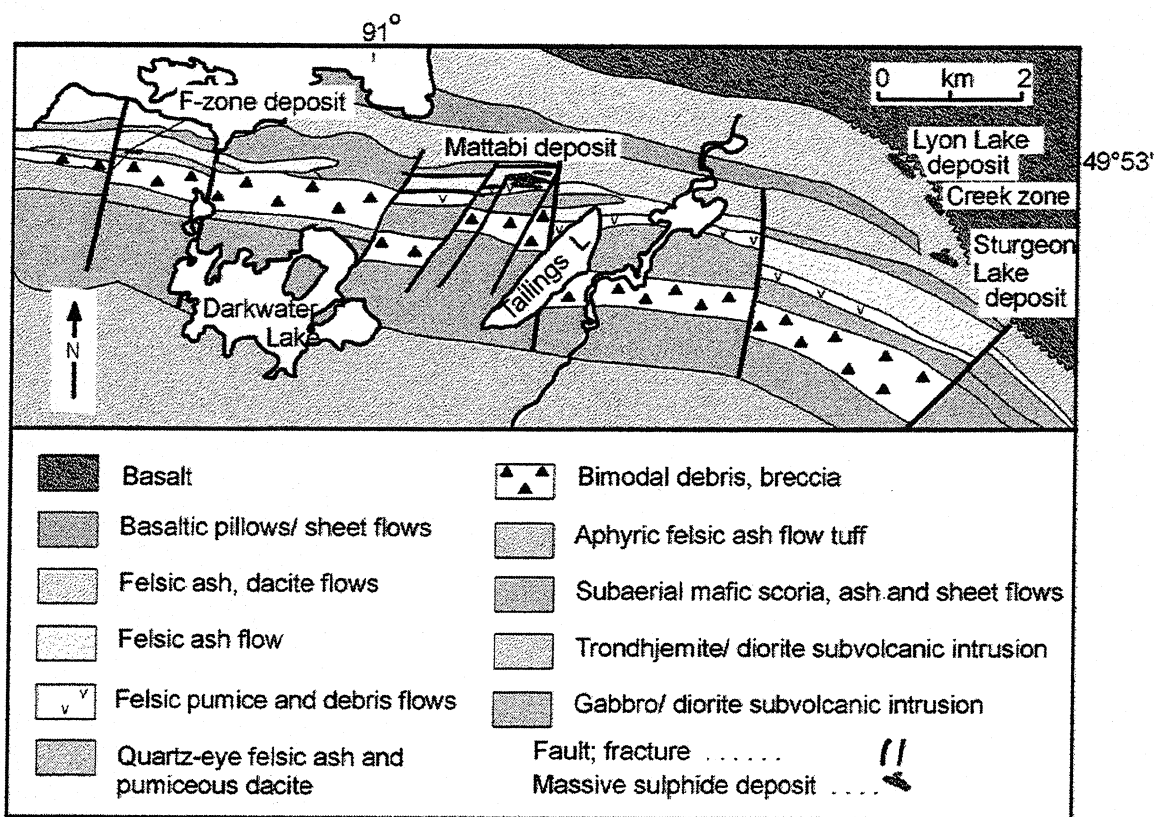


Figure 14: Cross-section of the main caldera, Noranda massive sulfide district (after Gibson and Watkinson, 1990). This section is oriented approximately north-south.

caldera margin faults associated with Type 2 deposits (see the Sturgeon lake map section for examples of synvolcanic faults: Figure 15). Fault systems that controlled hydrothermal discharge are useful guides for district-scale exploration, particularly for deeply buried ore deposits. Knuckey et al (1982) used the syn-volcanic fault pattern in the Noranda caldera to predict successfully where additional orebodies would be located. They noted that these

fault systems not only controlled hydrothermal discharge, but also were conduits for felsic



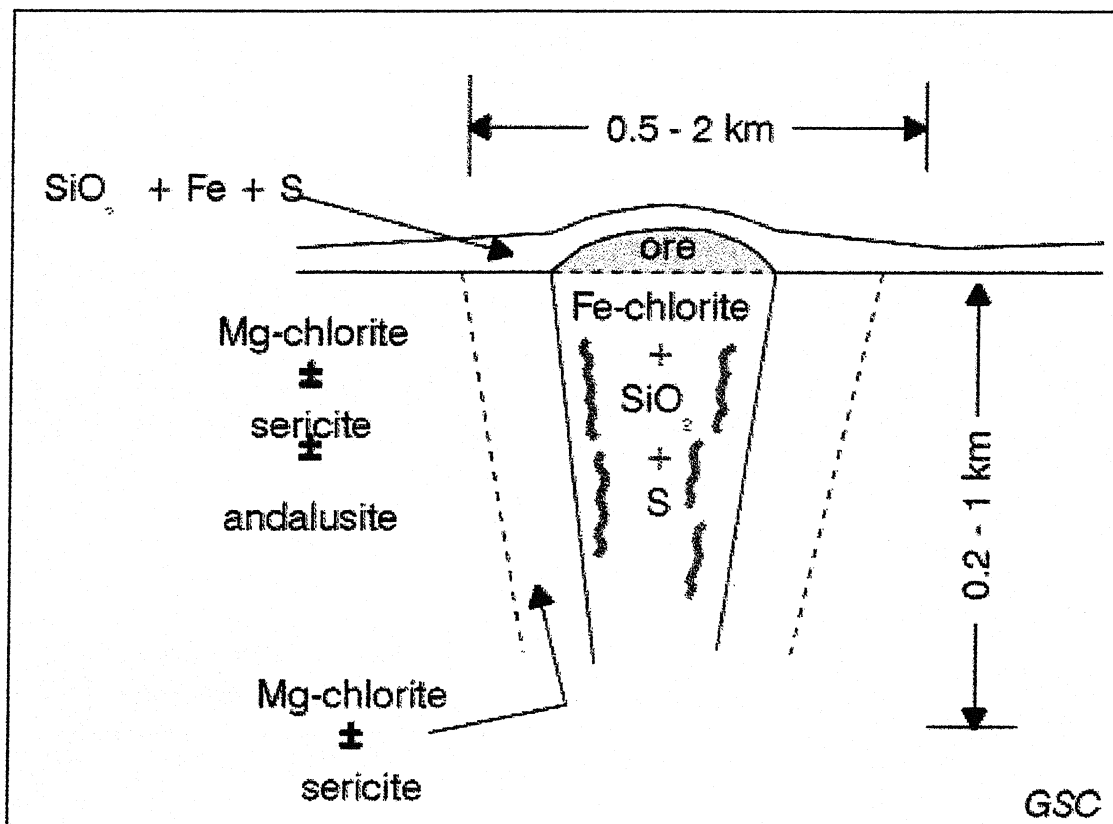
**Figure 15: map of the Sturgeon Lake massive sulfide camp, NW Ontario (after Morton et al., 1990). This map closely represents a cross-section through the Sturgeon Lake caldera, and is about the same scale as the Noranda cross-section (Figure 14).**

dykes that fed overlying flows. By mapping these dykes, as well as the distribution of synvolcanic faults (identified by their alteration and limited penetration of the stratigraphic section), drill targets can be identified. Presently, a major study of the distribution of oxygen and hydrogen isotopic ratios is showing promise as a tool for mapping those fault zones that were likely paleo-discharge conduits (A.G. Galley, B. Taylor, G. Holk, personal communication).

A second mechanism for focusing discharge is the channeling of interstratal or fault-controlled hydrothermal fluids along the margins of sediment-submerged basement horsts or volcanic highs. This is evident at the active discharge site at Middle Valley (ODP Site 858). Here, volcanic basement is only 265mbsf, in contrast with the areas only 100m to the west of the discharge site, where basement was not encountered in the full 400m extent of drilling (Site 858A). Rohr and Schmidt (1994) interpret the seismic data to suggest that the volcanic "high" under site 858 is a horst or volcanic promontory.

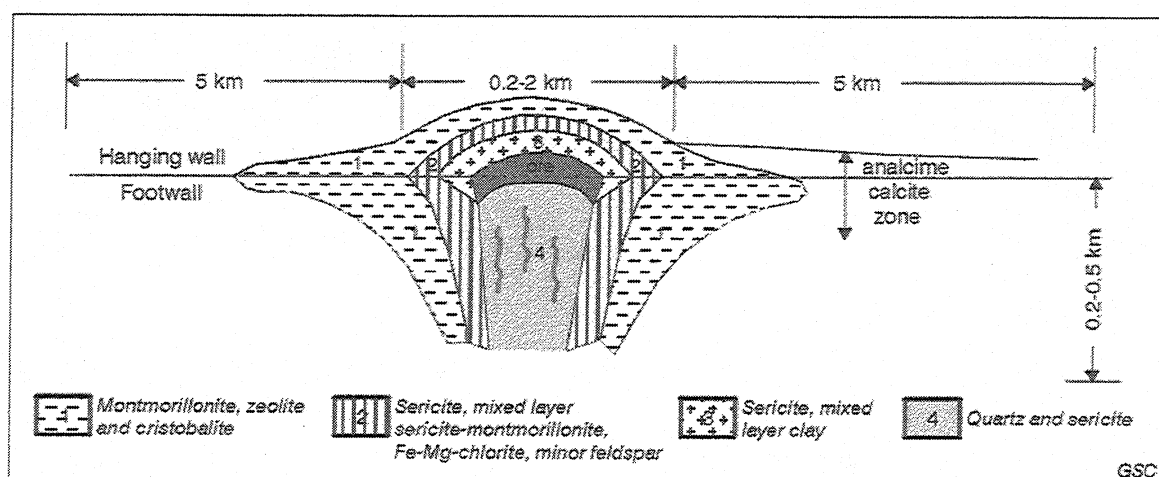
Regardless of fault origin, hydrothermal discharge sites are prominently altered. The alteration pipes are perhaps the best studied feature of VMS deposits, and thus they require less review here.

Pipes associated with types 1 and 3 vary from those with cores of Fe-chlorite and silica and rims of Mg-chlorite (in part after smectite) through Mg-chlorite core and sericite-rim pipes (products of a collapsed system) to those associated with types 2 and 4, with silica-sericite  $\pm$  Fe-carbonate pipes. All pipes associated with Types 1 through 3 are Na-, Ca-



**Figure 16: generalized scheme of pipe alteration associated with deposit Types 1 and 3. Note that this diagram is highly simplified, as the pipes are complex zones of overprinted and collapsed discharge and draw-down conduits.**

and Sr-depleted. Some in type 2 and 4 may be locally Na or K enriched (albite or paragonite), possibly through interaction with phase-separated (residual) saline brine or magmatic fluid. The mineral zonation can provide a locally useful directional guide to ore. Deep-water systems (Types 1 and 3) are associated with high-velocity discharge, and highly fractured flows. Both promote local draw-down of cold seawater, promoting the cooling of the rising hydrothermal fluid and the rapid deposition of Mg-rich clays, anhydrite and hydroxysulphate. Magnesian margins are thus prominent in this environment. Shallow water systems probably have lower-velocity discharge, and are associated with sediment caps and well-sealed subaqueous pyroclastic flows. Local draw-down may have been inhibited, and silicification more prominent around these discharge zones, thus suppressing the formation of Mg-rich alteration. Examples of the various types of pipes are illustrated in Figures 16 through 18.



**Figure 17: Idealized cross section of a Type 2 alteration pipe; this example is from the Kuroko deposits (after Shirozu, 1974). See also Figure 9 for another example of an alteration pipe associated with Type 2 deposits.**

### **Ore composition:**

Discussion of the composition of VMS deposits is largely beyond the scope of this review. Progress in understanding the processes attendant in spreading ridge systems is extensively reviewed in Hannington et al (1995) and Barrie and Hannington (1997). The latter authors note that both source rocks and physico-chemical conditions of the reaction zones and ascent paths affect the compositions of the ore-forming fluids. The two modern systems that have been investigated by ODP drilling, the TAG mounds on the Mid Atlantic Ridge and the Middle Valley deposits described above are both undergoing extensive in situ modification. Continuously refluxing seawater is modifying the TAG mound extensively, stripping out its metals, inducing precipitation of anhydrite in the mound, and enriching its upper portions in gold.

At Middle Valley, "metamorphic" fluid, considered (but not proven) possibly to be a terminal-phase hydrothermal product is modifying the composition of the ODP sulfide mound, south of Bent Hill. The main Bent Hill deposit has already been extensively modified, with much of its base metal stripped, and the sulfide assemblages extensively recrystallised.

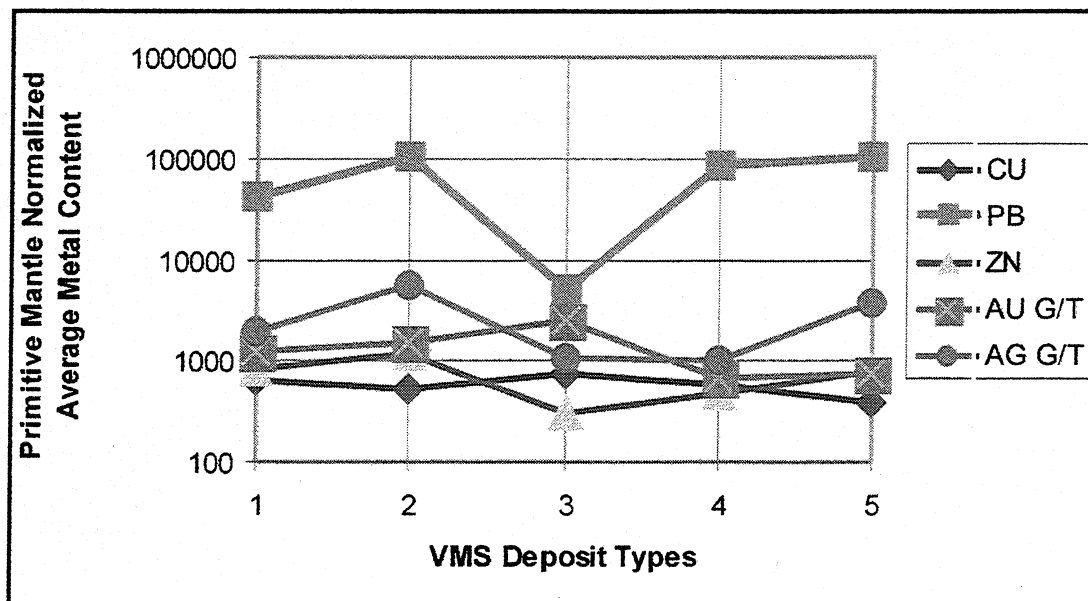
Added to the complexities of source rocks, fluid modification by cooling during ascent, and extensive remobilization within the hydrothermal mounds themselves, is the probability that some component of the mineralizing fluid was generated directly from a magmatic source.

### **Source rocks as control on composition:**

Barrie and Hannington (1997) compared the average contents of copper, zinc, lead, silver and gold for each of the five types of VMS deposits with the contents of these metals for primitive mantle and for average mid-ocean ridge basalt and continental crust. They also



examined temporal changes in metal contents for each of the five types. They then compared the metal contents of MORB and continental crust with those of primitive mantle. As noted in Table 2 and shown in Figure 18, the metal contents are reasonably similar for



**Figure 18: Average compositions of the five VMS types, normalized to primitive mantle (see Barrie and Hannington for PRIM compilation)**

most VMS types, except for Type 3 (ophiolite type), which has much lower lead content on average. As noted by Barrie and Hannington, the deposits associated primarily with mafic volcanic rocks have lower lead contents than the others. Surprisingly, the Besshi group of deposits, although closely associated with basalt, has lead contents that exceed types 1 and 3; perhaps some of their lead is being obtained from the sediments.

As noted in Table 2, Types 2 and 5 have high lead content. Barrie and Hannington suggest that this reflects a continentally-derived source rock. They use the values of Taylor and McLennan (1985) for comparison with average continental crust. The data provided by the latter authors are over-generalized with respect to the typical source rocks for VMS districts. Further, the lead data that they provide is suspect, as few data on the lead content of any rock type were available in 1985, due to analytical problems. For example, the average lead content of several thousand samples of MORB in the compilation of basalt analytical data provided by ODP is 2 ppm, but Doe (1995), using high precision analytical techniques, indicates that the true value is 0.35 ppm. Until accurate data are available for lead, such comparisons must be treated cautiously.

If the metal contents of the mineralizing fluids reflect the source rock compositions, and the fluids are therefore undersaturated with respect to most base metals, as suggested by Barrie and Hannington, then the metal contents of the source rocks should be reflected in the deposits. For example, a compilation of over 800 compositions of felsic rocks at Sturgeon Lake, Ontario (unpublished data) indicates that they have an average copper content of 31 ppm, and 67 ppm Zn. The unaltered portions of the Middle Valley sediment column contain 43 ppm Cu and 90 ppm Zn. (see Mottl et al, 1994). MORB contains 70 ppm Cu and 84 ppm Zn. The copper content of VMS deposits (Table 2) is quite similar (1.2-1.7%) for all types except Type 5 (0.76%). Perhaps the low content of copper in the bimodal siliciclastic

group of deposits reflects the low copper values in felsic volcanic strata. This analogy could be extended to ophiolite-associated (Type 3) deposits as they have the highest average content of copper (1.7%), coincident with their source rocks.

A second very important factor in controlling the composition of VMS deposits is the temperature of the mineralizing fluid. Franklin et al (1981), Lydon (1986) and many others have shown that copper is less soluble in a cooling hydrothermal fluid than are lead and zinc. Fractional precipitation of copper from a rising hydrothermal fluid will occur if boiling or mixing cools the fluid (see Franklin, 1986, Hannington et al, 1995 for data on T-boiling relationships and solubility data). Given the high velocity of the ascending fluids, cooling by boiling may be the most important controlling feature. Water depth controls this aspect of deposit composition and also may affect alteration assemblages. Volcanoes associated with nascent ocean-dominated arcs and back-arcs settings tend to be of low elevation and deeply submerged (usually >2000m) shield volcanoes. Felsic rocks rarely exceed 30% of the volcanic complement, and are usually cooled from high-temperature (sodic) melts (e.g. Noranda, Snow Lake, and Mattagami Lake districts). Fragmentation was usually caused by thermal shock, and formed hyaloclastite. Volcanoes associated with arcs involving continents (Types 2 and 5) are more high standing, commonly emergent stratovolcanoes. They consist predominantly of subaqueous hydrovolcanic pyroclastic flows and tuff-cones, andesitic flows, and some felsic lava domes. Pyroclastic fall deposits, and re-worked bedded tuff are also typical of these environments. Although volcanological constraints can only provide cumulative evidence for water depth at depositional sites, generally speaking deposits in types 1 and 3 (and ophiolite-related deposits) provide deep water VMS depositional sites, whereas types 2 and 5 are in shallower water. Water depth provides important constraints on ore composition and alteration facies.

Much sulfide precipitation occurs within sulfide mounds, where conductive cooling and circulation of heated seawater can extensively modify the deposit's zoning and composition, and yield "replacement" paragenetic assemblages. Introduction of either residual brines or vapor phase fluids, (boiling) or magmatic fluids can also modify the composition, usually with the addition/enrichment of hydride elements, copper, and gold. On cessation of hydrothermal flow, anhydrite dissolution collapse forms sulfide breccias. Continuation of seawater circulation also modified the distribution of base and precious metals. In some areas, sulfide precipitation in footwall sediments and permeable volcanic strata form "replacement" bodies (Kidd Creek; Hannington et al., 1997)

Ore compositions are related to primary fluid compositions and, importantly, the depositional environment. In felsic and sediment-dominated systems where buffering to acid pH may occur at any temperature, ore-forming fluids may contain more lead, relative to copper and zinc, than those high (>350°C) temperature basalt-dominated systems (Types 1 and 3). Critical factors in the precipitation environment include temperature (controlled by boiling, i.e. water depth), oxygen availability (atmospheric, basinal environment), organic activity, and aS<sub>2</sub> (controls speciation, important in gold transport). Temperature may effect a 10x variation in gold and silver content of the precipitate. Deposits of types 2 and 5, which tend to have formed in relatively shallow water, may be more lead, zinc, silver and gold rich simply because cooling (boiling) forced copper from the fluids during their ascent, and promoted the formation of bisulfide-complexing (and thus highly efficient precipitation) of gold. Separate, oxidized,

magmatically generated brines may have been important in forming some high-sulfidation zones within a few deposits.

### **Some concluding remarks**

1: A tectonically based classification system is a reasonable basis for characterizing specific attributes of VMS deposits. The compositional and alteration characteristics of each of the five types described herein are specific to each type, and indicate that there may be some essential differences in the genetic mechanisms for each. These could include different source rocks, differences in the sulfide depositional environment (e.g. boiling vs. non-boiling systems), or multiple metal sources (convective leaching sources vs. direct magmatic contributions).

2: From an exploration standpoint, the two most important characteristics of VMS deposits that provide vectors to possible ore are the attributes of large-scale "lower semiconformable" alteration zones, and the identification of anomalous paleo-heat generation, as reflected in specific subvolcanic intrusions. Many of these attributes are subtle, requiring careful mapping and petrographic analysis, along with judicious use of analytical and isotopic data.

3: Deposits associated with significant amounts of sediment in their depositional environment of source region are significantly larger than those in volcanic – dominated regimes. However, the combined grades of those in volcanic domains are higher. The lead content of those deposits that formed in a continent-ocean interaction zone are higher than those in ocean-dominant regimes. This may be a function of the metal content of source rocks or the fluid history. Continent-associated deposits are usually in shallower-water depositional setting, so fractional precipitation may have increased the lead and zinc content of their fluids relative to copper.

## References

- Baker, P.A. Cross S.L., and Burns, S.J. 1994. Geochemistry of carbonate nodules and cements and implications for hydrothermal circulation, Middle Valley, Juan de Fuca Ridge. . In Mottl, M.J., Davis, E.E., Fisher, A.T., and Slack, J.F. (Eds.), Proceeding of ODP, Sci. Results, 139. College Station, TX, p 212-328
- Baker, P.A. and Cross S.L., 1994. A note on the carbon, sulfur and noitrogen contents of hydrothermally altered sediments, Middle Valley, Juan de Fuca Ridge. . In Mottl, M.J., Davis, E.E., Fisher, A.T., and Slack, J.F. (Eds.), Proceeding of ODP, Sci. Results, 139. College Station, TX, p 307-312
- Barrie, C.T., and Hannington, M.D. 1997. Introduction: Classification of VMS deposits based on host rock compositions. In Volcanic-associated massive sulfide deposits: processes and examples in modern and ancient settings. GAC-MAC short course, May17-18, Ottawa p 1-12
- Bednarz, U., and Schmincke, H.-U., 1990. Chemical patterns of seawater and hydrothermal alteration in the northeastern Troodos extrusive series and sheeted dyke complex. . In ophiolites, Proceedings of the Symposium "Troodos 1987", Geological Survey Department, Nicosia, Republic of Cyprus p 639-654
- Bischoff, J.L., and Seyfried, W.E., 1978. Hydrothermal chemistry of seawater from 25° to 350oC. American Journal of Earth Science, v. 278, p 838-860.
- Campbell, I.H., Leshner, C.M., Coad, P., Franklin, J.M., Gorton, M.P., and Thurston, P.C., 1984. Rare earth element mobility in alteration pipes below massive Cu-Zn sulfide deposits. Chemical Geol vol.45, p181 -208
- Cathles, L.M., 1981. Fluid flow and genesis of hydrothermal ore deposits. In: Seventy-Fifth Anniversary Volume, 1905-1980, Economic Geology, p. 424-457.  
□
- Constantinou, G., 1980. Metallogensis associated with the Troodos ophiolite. In Panayiotou, A., ed. Ophiolites: Proceedings of the International Ophiolite Symposium, Cyprus, 1979. Cyprus Geological Survey Dept., p 663-673.
- Davis, E.E and Fisher, A.T., 1994 On the nature and consequences of hydrothermal circulation in the Middle Valley sedimented rift: inferences from geophysical and geochemical observation, Leg 139. In Mottl, M.J., Davis, E.E., Fisher, A.T., and Slack, J.F. (Eds.), Proceeding of ODP, Sci. Results, 139. College Station, TX, p 695-720
- Divi, S.R., Thorpe, R.I., and Franklin, J.M. 1979. Application of discriminant analysis to evaluate compositional controls of stratiform massive sulfide deposits in Canada: Mathematical Geology, volume 11, no. 4, p 391-406.
- Fouquet, Y., U. von Stackelberg, J.-L. Charlou, Erzinger, P. Herzig, R. Muhe, and M.

Wiedicke, 1993 Metallogenesis in back arc environments: The Lau Basin example, *Econ. Geol.* p 2154-2181

Franklin, J.M., Lydon, J.W., and Sangster, D.F., 1981. Volcanic-associated massive sulfide deposits. *Economic Geology 75th Anniversary Volume*, p. 485-627.

Franklin, J.M., 1995: Volcanogenic massive sulphide deposits; Geological Association of Canada, Special Paper no. 40, Mineral Deposit Modeling. R.V. Kirkham, D. Sinclair R.I. Thorpe and J.M. Duke, editors. p 315-334.

Galley, A.G., 1993: Characteristics of semi-conformable alteration zones associated with volcanogenic massive sulphide districts: *Journal of geochemical Exploration*, v. 48, p175-200.

Gibson, H.L., Watkinson, D.H., and Comba, C.D.A., 1983. Silicification: hydrothermal alteration in an Archean geothermal system within the Amulet Rhyolite Formation, Noranda, Quebec. *Economic Geology*, v. 78, p 954-971.

Gillis, K.M. and Robinson, P.T. 1990. Multistage alteration in the intrusive sequence of the Troodos ophiolite complex, Cyprus.. In ophiolites, *Proceedings of the Symposium "Troodos 1987"*, Geological Survey Department, Nicosia, Republic of Cyprus p 655-664

Goodfellow, W.D., and Franklin, J.M., 1993. Geology, mineralogy and geochemistry of massive sulfides in shallow cores, Middle Valley, Northern Juan de Fuca ridge. *Economic Geology*, vol 88, no. 8, p2037-2068.

Hall, J.M. and Yang, J.S., 1995 Constructional features of Troodos type oceanic crust: relationships between dike density, alteration, magnetization, and ore body distribution and their implications for in situ oceanic crust. *J. Geophysical Research*, vol. 100, no B10, p 19973-19989.

Hannington, M.D., Jonasson, I.R., Herzig, P.M., and Peterson, S. 1995. Physical and chemical processes of seafloor mineralization at mid-ocean ridges. In *Seafloor Hydrothermal Systems, Physical, Biological and Chemical Interactions* (Eds. S. Humphris, R.A Zierenberg, L.S. Mullineux, and R.E. Thompson) *Geophysical Monograph 91*, American Geophysical Union, p 115-157.

Hannington, M.D., Bleeker, W., and Kjarsgaard, I, 1997. Sulfide mineralogy, geochemistry and ore genesis of the giant Kidd Creek Deposit. *Society of economic geologists Neves Corvo Field Conference, Lisbon, Portugal, Abstracts and Program*, p55

Knuckey, M.J., Comba, C.D.A., and Riverin, G., 1982. Structure, metal zoning, and alteration at the Millenbach deposit, Noranda, Quebec. In: R.W. Hutchinson, C.D. Spence and J.M. Franklin, (eds.), "Precambrian Sulphide Deposits", *Geological Association of Canada Special Paper 25*, p. 255-295.

Lydon, J.W., 1984. Volcanogenic massive sulphide deposits Part 1: a descriptive model. Geoscience Canada, Vol.11, p. 195-202.

□

Lydon, J.W., 1988. Ore Deposit Models #14. Volcanogenic massive sulphide deposits Part 2: genetic models. Geoscience Canada, Vol. 15, No. 1, p.43-65.

Lydon, J.W. 1996 Sedimentary exhalative sulphides (SEDEX). In Geology of Canadian Mineral deposit Types (ed.) O.R. Eckstrand, W.D. Sinclair, and R.I. Thorpe. Geological Survey of Canada, no.8 p. 130-152

MacGeehan, P.J., and Maclean, W.H., 1978. Tholeiitic basalt-rhyolite magmatism and massive sulphide deposits at Matagami, Quebec. Nature, v. 283, p. 153-157.

Mottl, M.J., Davis, E.E., Fisher, A.T., and Slack, J.F. (Eds.), Proceeding of ODP, Sci. Results, 139. College Station, TX, 772p

Morton, J.L., and Franklin, J.M., 1987. Two-fold classification of Archean volcanic-associated massive sulfide deposits. Economic Geology, v. 82, p. 1057-1063.

□

Muhna, J., and Kerrich, 1980. Seawater – basalt interaction from the Iberian Pyrite belt. Contrib. Mineral. and Petrol vol 73, p191-200.

Peter, J.M. 1992. Comparative geochemical studies of the Upper Triassic Windy craggy and modern Guaymas Basin deposits. Unpublished Ph.D. Thesis, University of Toronto, 562p.

Peter, J. and Scott, S.D. 1997. Introduction: The Windy Craggy NW British Columbia massive sulfide deposit: the world's largest Besshi deposit. In Volcanic-associated massive sulfide deposits: processes and examples in modern and ancient settings. GAC-MAC short course, May17-18, Ottawa p295-330.

Perfit, M., Ridley, I., and Jonasson, I. . 1997. Magmatic and hydrothermal controls on seafloor venting In Volcanic-associated massive sulfide deposits: processes and examples in modern and ancient settings. GAC-MAC short course, May17-18, Ottawa p75-104

Poulsen, K.H. and Hannington, M.D. 1996. Volcanic-associated massive sulfide gold: in Geology of Canadian Mineral deposit Types (ed.) O.R. Eckstrand, W.D. Sinclair, and R.I. Thorpe. Geological Survey of Canada, no.8 p. 183-196

Rickard, D., 1988. Regional metamorphism of the Bergslagen Province., south central Sweden. Geol Mijnbouw, vol 67, p139-156.

Robertson, A.H.F., 1990. Tectonic evolution of Cyprus. In ophiolites, Proceedings of the Symposium "Troodos 1987", Geological Survey Department, Nicosia, Republic of Cyprus p 235-252

Rohr, K.M.M. and Schmidt, U. 1994. Seismic structure of Middle Valley near sites 855-858, leg 139, Juan de Fuca Ridge. . In Mottl, M.J., Davis, E.E., Fisher, A.T., and Slack, J.F. (Eds.), Proceeding of ODP, Sci. Results, 139. College Station, TX, p 3-18.

Seyfried, W.E., Jr., and Janecky, D.R., 1985. Heavy metal and sulfur transport during subcritical and supercritical hydrothermal alteration of basalt: Influence of fluid pressure and basalt composition and crystallinity. *Geochim. et Cosmochim. Acta*, v. 49, p 2545-2560.

Seyfried, W., Jr., Ding, M., Berndt, M., and Chen, X. 1997. Experimental and theoretical controls on metal mobility and Cl variability in mid-ocean ridge hydrothermal systems. In *Volcanic-associated massive sulfide deposits: processes and examples in modern and ancient settings*. GAC-MAC short course, May 17-18, Ottawa p 215-234

Seyfried, W.E., Jr., and Janecky, D.R., 1985. Heavy metal and sulfur transport during subcritical and supercritical hydrothermal alteration of basalt: Influence of fluid pressure and basalt composition and crystallinity. *Geochim. et Cosmochim. Acta*, v. 49, p 2545-2560.

Shirozo, H., 1974. Clay minerals in altered wall rocks of the Kuroko-type deposits. *Society of Mining Geologists Japan, Special Issue 6*, p 303-311.

Skirrow, R.G., and Franklin, J.M., 1994. Silicification and metal leaching in sub-concordant alteration zones beneath the Chisel Lake massive sulfide deposit, Snow Lake, Manitoba. *Economic Geology*. Vol 89, no1, p 31-50

Slack, J.F., 1993, Descriptive and grade-tonnage models for Besshi-type massive sulphide deposits. Geological Association of Canada, Special Paper no. 40, Mineral Deposit Modeling. R.V. Kirkham, D. Sinclair R.I. Thorpe and J.M. Duke, editors. p 343-372

Spooner, E.T.C., and Fyfe, W.S., 1973. Sub-sea floor metamorphism, heat and mass transfer. *Contributions to Mineralogy and Petrology*, v. 42, p. 287-304.

□

Stakes, D., and Franklin, J.M., 1994. Petrology of the Middle Valley igneous rocks. . In Mottl, M.J., Davis, E.E., Fisher, A.T., and Slack, J.F. (Eds.), Proceeding of ODP, Sci. Results, 139. College Station, TX, p 79-104.

Swinden, H.S. 1996. The application of volcanic geochemistry to the metallogeny of volcanic-hosted massive sulphide deposits in Central Newfoundland. In *Trace Element Geochemistry of Volcanic Rocks, Applications for Massive Sulphide exploration*

Geological Association of Canada Short Course Notes Vol 12, D.A Wyman, ed. p329-358.

Von Damm, K.L. 1995. Controls on the chemistry and temperature variability of seafloor hydrothermal fluids: in Seafloor Hydrothermal Systems, Physical, Biological and Chemical Interactions (Eds. S. Humphris, R.A Zierenberg, L.S, Mullineux, and R.E. Thompson) Geophysical Monograph 91, American Geophysical Union, p 222-247.

Walford, P.C., and Franklin, J.M., 1982. The Anderson Lake Mine, Snow Lake, Manitoba. in the Robinson Symposium Volume on Precambrian Mineral Deposits, R.W. Hutchinson, C.D. Spence and J.M. Franklin, editors, GAC Special Volume 25, p 481-524.



## O - GEOENVIRONMENTAL MODEL OF VOLCANOGENIC MASSIVE SULPHIDE DEPOSITS

Charles N. Alpers and Robert A. Zierenberg

Alpers, C.N. and Zierenberg, R.A. (1998): Geoenvironmental Model of Volcanogenic Massive Sulphide Deposits; in *Metallogeny of Volcanic Arcs*, B.C. Geological Survey, Short Course Notes, Open File 1998-8, Section O.

### ABSTRACT

Volcanogenic massive sulfide (VMS) deposits have a high potential for producing severe acid rock drainage and related environmental problems because of high concentrations of iron sulfides and relatively low acid buffering capacity. The iron sulfide mineralogy of most VMS deposits is dominated by pyrite, which can constitute 95% or more of the sulfide mass. Pyrrhotite dominates in some geologic settings, including deposits formed in more reducing environments associated with footwall sedimentary sequences such as black shales and deposits that have been affected by high-grade metamorphism. The trace elements of environmental concern most commonly associated with VMS deposits are Cu, Zn, Pb, and Cd; some deposits have anomalous As, Bi, Co, Hg, Mo, and/or Sn. These trace elements generally occur in primary ores as sulfide and sulfosalt minerals including chalcopyrite, sphalerite, galena, arsenopyrite, tennantite-tetrahedrite, cobaltite, and others, as well as in solid solution and/or mineral inclusions in pyrite and pyrrhotite. Trace metals are mobilized when sulfide minerals dissolve during weathering; in relatively dry periods, metals and acidity are commonly stored as metal-sulfate minerals, most of which are highly soluble. Lead is abundant as galena in many VMS deposits, particularly Kuroko-type and others associated with felsic volcanics and continentally derived sediments. Lead is often an environmental problem in solid mine wastes (e.g. waste rock, mill tailings) and smelter wastes (e.g. slag, flue dust), but is usually less mobile than other metals in acid (and near-neutral) rock drainage because of the low solubility of secondary minerals such as anglesite (Pb-sulfate).

Wall-rock mineralogy plays a critical role in determining the severity of acid rock drainage in VMS environments. The mineralogy of wall rocks is controlled by the original composition and the integrated effects of sea-floor hydrothermal alteration/metasomatism and any subsequent metamorphism. VMS deposits typically occur in Archean greenstone belts and Phanerozoic marine volcanic-sedimentary sequences that have typically been subjected to at least lower greenschist facies metamorphism. Common wall-rock alteration assemblages include chlorite, quartz, muscovite (sericite), albite, Fe-Mg-carbonates (dolomite, ankerite, siderite), tourmaline (generally in the footwall), and/or metamorphic minerals such as epidote, amphibole, and at high metamorphic grades, cordierite. Alteration associated with some VMS deposits can show a zonation from Fe-rich chlorite in the core of the hydrothermal upflow zone to Mg-rich chlorite and sericite on the periphery. Non-metamorphosed deposits contain smectites and mixed-layer clays at the outer fringes of the hydrothermal alteration zone. Barite, anhydrite and/or gypsum are found in some VMS deposits. Although anhydrite and gypsum have minimal effect on acid-buffering capacity, they may enhance weathering reactions due to increased permeability resulting from dissolution of these relatively soluble minerals.

The presence, composition, and distribution of carbonate minerals are important factors in determining the acid-neutralizing capacity of mine wastes and unmined deposits. Fe-bearing dolomite (ankerite) and siderite are reported in some VMS environments, and calcite may be deposited at low temperatures as the hydrothermal system collapses or may be formed as part of a metamorphic overprint. The extent to which Fe-bearing carbonates can neutralize acid is moderated by their iron content, because oxidation and hydrolysis of iron leads to a net production of hydrogen ions. Chemical reactions showing the effect of Fe substitution on acid neutralizing capacity can be conveniently represented on a tri-linear diagram of carbonate compositions in the  $\text{CaCO}_3\text{-MgCO}_3\text{-FeCO}_3$  system.

Examples of acid mine drainage affecting surface and ground water are presented for two deposits in California: Iron Mountain and Penn Mine. The Iron Mountain site is located at the southern end of the West Shasta mining district in northern California. The deposits in the West Shasta district do not fit readily into the existing USGS classification scheme for VMS deposits (Cyprus, Kuroko, and Besshi types) and show similarities to Noranda-style mineralization: low lead content; ore zones associated with felsic-intermediate volcanic rocks; mafic rocks in the footwall; and minimal sedimentary rocks in the sequence. Since 1983, the Iron Mountain site has been a high priority on the U.S. Environmental Protection Agency's National Priority List of contaminated sites, and is undergoing remediation under the "Superfund" program. The adit discharge from the Richmond Mine at Iron Mountain is among the most concentrated ever reported for a continuously flowing feature. A typical analysis of Richmond adit discharge during low-flow conditions in September 1990 had a pH of 0.48, and the following dissolved concentrations: copper of 290 mg/L, cadmium of 15.9 mg/L, zinc of 2,010 mg/L, aluminum of 2,210 mg/L, total iron of 20,300 mg/L (about 90 % ferrous), and sulfate of 118,000 mg/L. Drip waters in the underground workings of the Richmond mine have negative pH values, representing hydrogen ion activities greater than one. These extreme pH values can be measured with a combination pH electrode using concentrated sulfuric acid standards that are calibrated to the pH scale using specific-ion interaction (Pitzer) modeling. Season fluctuations in rainfall and evaporation result in cyclical precipitation and dissolution of efflorescent metal-sulfate salts in the Richmond mine workings. This seasonal flushing of soluble salts has dramatic effects on the water quality of adit discharge, causing increases in dissolved concentrations of some metals along with increased flows during the "first flush." Discharge of untreated and partially treated runoff from Iron Mountain has severely degraded surface waters in the area. Mixing of acidic drainage from Iron Mountain with dilute waters of the Sacramento River system results in precipitation of hydrous ferric iron and aluminum oxides with co-precipitated copper, zinc, and cadmium. More than 200,000 cubic meters of contaminated sediments have accumulated in a downstream reservoir, which is the subject of ongoing investigations of potential remedial measures.

At the Penn Mine, a VMS deposit in the Foothills Cu-Zn belt of central California classified as "Sierran Kuroko" by Singer (1992), acidic drainage from several different weathering and hydrologic environments can be distinguished by pH values, trace element concentrations, and stable isotope ratios. Water in the flooded underground mine workings has a pH value of about 4, elevated concentration of dissolved Zn (400 mg/L), relatively low concentrations of dissolved Cu (0.13 mg/L) and Cd (0.05 mg/L), and relatively heavy values of  $\text{d}_{18}\text{O}$  and  $\text{d}_{34}\text{S}$  in dissolved sulfate. The most likely

explanation for these characteristics is that sulfate reduction has occurred in this environment, causing preferential precipitation of Cu and Cd sulfides relative to Zn and leaving extremely high ratios of Zn/Cu and Zn/Cd. This interpretation is further supported by dissolved gas chemistry, which has little oxygen and traces of methane and hydrogen. Acidic drainage from waste rock and tailings piles which collects in unlined surface impoundments has pH values of 2.3 to 3.0, elevated concentrations of Cu (62 to 110 mg/L), Cd (0.9 to 1.7 mg/L), and Zn (200 to 570 mg/L), and relatively heavy values of d18O and dD caused by evaporation. Down-gradient from the lowermost impoundment, leakage of acidic drainage through fractured metavolcanic bedrock has resulted in formation of an acidic, metal-rich, ground-water plume, documented by drilling in an area overlain by a slag pile that is seasonally submerged by an adjacent fresh-water reservoir. Impacts on water-quality and aquatic life in the reservoir have mostly been associated with untreated surface-water discharges prior to 1993. The acidic ground-water plume has pH values as low as 3.5, elevated concentrations of Cu (up to 120 mg/L), Cd (up to 3 mg/L), and Zn (up to 630 mg/L), and d18O and dD values that form a linear mixing trend with the highly evaporated waters from the surface impoundments, indicating recharge of the acidic ground-water plume from the waste-water ponds. Waste rock, tailings, and unlined impoundments at the Penn Mine are scheduled for removal during site remediation planned for 1998-99.

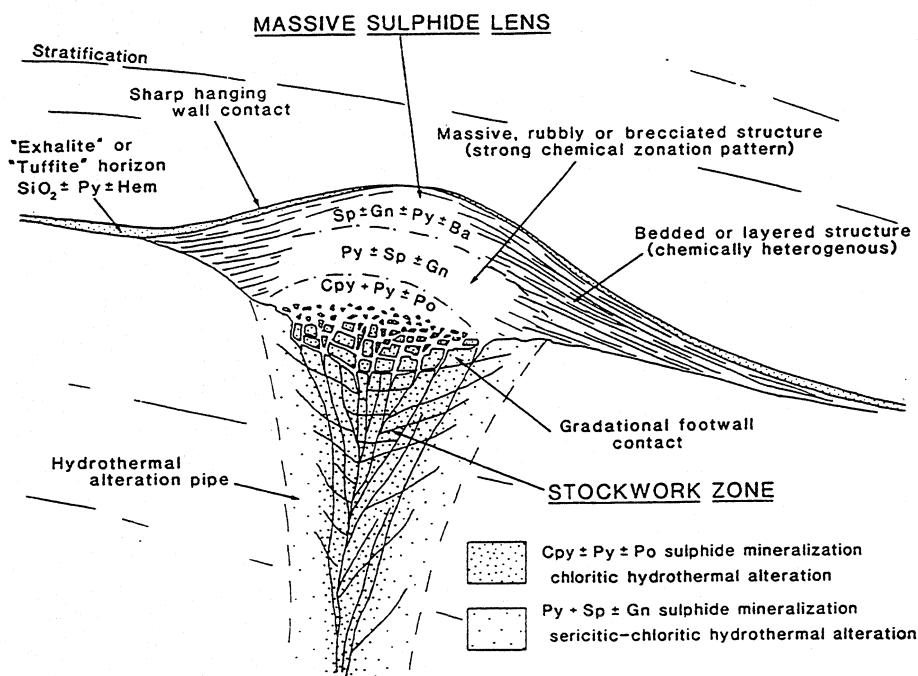
# VOLCANIC-ASSOCIATED MASSIVE SULFIDE DEPOSITS (MODELS 24a-b, 28a; Singer, 1986a,b; Cox, 1986)

by Cliff D. Taylor, Robert A. Zierenberg, Richard J. Goldfarb,  
James E. Kilburn, Robert R. Seal II, and M. Dean Kleinkopf

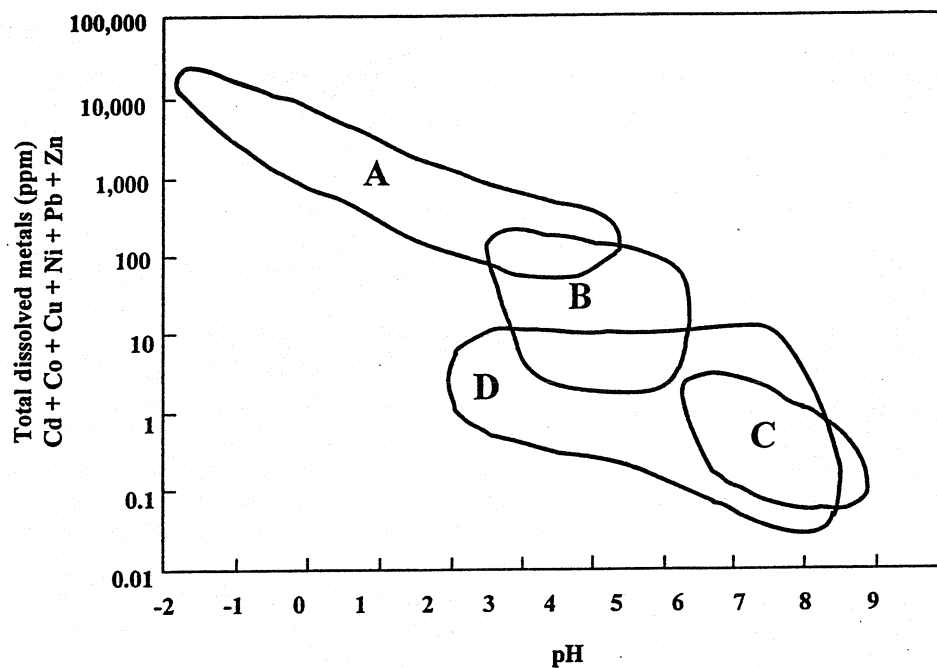
## SUMMARY OF RELEVANT GEOLOGIC, GEOENVIRONMENTAL, AND GEOPHYSICAL INFORMATION

### Deposit geology

Volcanic-associated massive sulfide (VMS) deposits range from lens shaped to sheet-like bodies of sulfide-mineral-rich rock spatially associated with volcanic rocks ranging in composition from basalt to rhyolite (fig. 1). VMS deposits can be divided into three general categories. Cyprus-type deposits (Model 24a; Singer, 1986a) tend to be small, medium-grade deposits rich in copper and zinc. They are generally lens or mound shaped accumulations of massive pyrite developed in ophiolite-related, extrusive basalt sequences. They are typically underlain by copper-rich "stringer-zones" composed of anastomosing quartz-sulfide mineral veins in extensively chloritized basalt. Kuroko deposits (Model 28a; Singer, 1986b) are typically developed in intermediate to felsic volcanic rock and are generally interpreted to have formed in extensional environments associated with arc volcanism. They are commonly high grade and can be very large. Relative to Cyprus-type deposits, they generally have much higher contents of zinc, lead, silver, and antimony, which reflects the composition of their felsic volcanic host rocks. They also have mound-like morphology and the abundance of coarse clastic sulfide minerals within many of these deposits attests to a moderately high energy, seafloor depositional setting. Kuroko-type deposits also tend to be underlain by copper-rich stringer zones and commonly have well developed geochemical zonation with progressive zinc, lead, and silver enrichment both vertically and laterally away from vent centers. Besshi-type deposits (Model 24b; Cox, 1986) are present in mixed volcanic-sedimentary environments. Deposits of this type are commonly hosted by turbidites that have been intruded by basaltic sills. These deposits are typically copper-rich and contain small abundances of lead and other lithophile elements. In contrast to other volcanic-hosted deposits, many Besshi-type deposits form thin, laterally extensive sheets of pyrrhotite- and (or) pyrite-rich massive sulfide rock; however, the characteristics of Besshi-type deposits vary considerably. Slack (1993) presents an expanded definition of Besshi-type deposits that includes deposits such as those in the Ducktown, Tenn., district and the large Windy Craggy deposit in British Columbia.



**Figure 1.** Essential characteristics of an idealized volcanogenic massive sulfide deposit (modified from Lydon, 1984). Mineral abbreviations as follows: Sp, sphalerite; Gn, galena; Py, pyrite; Ba, barite; Cpy, chalcopyrite; Po, pyrrhotite; and Hem, hematite.



**Figure 2.** Ficklin plot (Plumlee and others, 1993) showing aqueous metal contents and pH ranges of water associated with volcanic massive sulfide deposits. Fields A, B, and C (Plumlee and others, 1994), are those for West Shasta, Calif., district VMS deposits, sulfide-mineral-rich vein deposits in rocks with low buffering capacity, and sulfide-mineral-rich vein deposits in carbonate host rocks, respectively. Field D is the composite field for water draining Prince William Sound, Alaska, VMS deposits (Goldfarb and others, in press).

#### Examples

Cyprus-type: Skouriotissa, Cyprus; Betts Cove, Newfoundland; Turner-Albright, Oreg.; Big Mike, Nev.

Kuroko-type: Kidd Creek, Ontario; Iron King and Penn Mine, Calif.; Mokuroko district, Japan.

Besshi-type: Besshi, Japan; Windy Craggy, British Columbia.

#### Spatially and (or) genetically related deposit types

VMS deposits are associated with a number of other mineral deposit types (Cox and Singer, 1986). Some VMS deposits, especially the Besshi-type deposits as broadly defined by Slack (1993), are transitional in depositional setting with some sedex deposits (Model 31a), such as Sullivan, British Columbia. VMS deposits are commonly associated with regionally developed iron- and (or) manganese-rich metalliferous sediment and chert developed at the same time-stratigraphic horizon as the massive sulfide deposits. Some Archean VMS deposits may be transitional to volcanic-associated iron formation. VMS deposits, especially in Archean terranes, tend to be spatially associated with shear-hosted mesothermal lode gold deposits (Model 36a) and Algoma-type banded iron formation (Model 28b).

#### Potential environmental considerations

Volcanic-associated massive sulfide deposits are among the most likely of all deposit types to have associated environmental problems, particularly acid mine drainage. Analyses of water draining VMS deposits plot in the extreme metal-extreme acidity field (fig. 2). VMS deposits have high iron- and base-metal-sulfide mineral contents and are hosted by rocks with low buffering capacity. These minerals are unstable under normal oxidizing near surface conditions and represent potential sources of highly acid and metal-rich drainage, especially in areas disturbed by surface mining or tailings disposal. Associated high abundances of potentially toxic trace metals, including arsenic, bismuth, cadmium, mercury, lead, and antimony, are present in some deposits, particularly those associated with felsic volcanic or sedimentary source rocks.

#### Exploration geophysics

Electrical properties of sulfide minerals, combined with large sulfide mineral concentrations in VMS deposits, make this type of mineral deposit a particularly favorable target for location by a variety of geophysical techniques. Self-potential, induced polarization, and a wide range of electromagnetic methods have been successfully used to locate buried VMS deposits. Pyrrhotite-rich and magnetite-bearing massive sulfide deposits may be locatable by detailed magnetic surveys. Airborne multispectral remote sensing techniques have been used to identify areas that contain hydrothermally altered rock and stressed vegetation that may be associated with mineralized rock.

## References

Franklin and others (1981), Ohmoto and Skinner (1983), Fox (1984), Lydon (1984, 1988), Franklin (1993), and Slack (1993).

## GEOLOGIC FACTORS THAT INFLUENCE POTENTIAL ENVIRONMENTAL EFFECTS

### Deposit size

Historically, most economic deposits are in the 1-5 million tonnes range (Singer, 1986c,d; Singer and Mosier, 1986). Deposits of this size can still be developed in areas with an existing mining infrastructure; however, development of new deposits in frontier areas likely requires at least 10 million tonnes of reasonably high grade ore. Most Cyprus-type deposits contain less than 15 million tonnes of ore. Most Besshi-type deposits are also fairly small; notable exceptions include the >300 million tonne Windy Craggy, British Columbia, deposit. Kuroko-type deposits, especially those of Precambrian age, can be very large, such as the world class Kidd Creek, Ontario, deposit.

### Host rocks

Cyprus-type deposits are hosted by submarine mafic-volcanic rocks and their altered equivalents, typically in brecciated rocks commonly associated with pillow lavas, which have good buffering capacity. Host-rocks for Kuroko-type deposits range from basalt to rhyolite, which have high and low buffering capacities, respectively. Many deposits are associated with subaqueous dacitic-domes that have intermediate buffering capacity. Host rocks are commonly brecciated and are typically moderately to highly altered. Some deposits are hosted by associated volcanoclastic or hemipelagic sedimentary rocks that overly submarine volcanic sequences. Besshi-type deposits are typically hosted by turbiditic to hemipelagic graywacke interbedded with or intruded by basalt.

### Surrounding geologic terrane

Submarine volcanic activity is a defining characteristic of VMS deposits. Most VMS deposits, including many ophiolite-hosted deposits of the Cyprus-type, are associated with arc-related volcanism. Local extensional tectonic environments are particularly conducive to deposition of massive sulfide deposits. Many VMS deposits are in rocks that have undergone collisional tectonism and may be in structural contact with a wide variety of rock types.

### Wall-rock alteration

Footwall alteration is moderate to locally intense around most VMS deposits. Hanging-wall alteration is typically absent, but may be weakly developed in some deposits. Many deposits that have not been tectonically disrupted are underlain by "stringer-zone" mineralized and altered rock. Stringer-zones are characterized by anastomosing quartz-sulfide veins. Local zones of silicification are present near and within mineralized zones. The most common alteration is pervasive chloritization, which is less well developed with increasing depth and distance from hydrothermal upwelling zones, in the footwall of deposits. Deposits hosted by felsic rocks typically have extensively developed quartz sericite alteration in the footwall. Most altered rock associated with massive sulfide deposits has low to very low acid buffering capacity. Some massive sulfide deposits are associated with pervasive carbonate alteration in the footwall (for instance, Sturgeon Lake, Ontario; Morton and others, 1990). These carbonate alteration zones typically have low to moderate abundances of calcitic to ankeritic carbonate minerals. Massive sulfide deposits with associated carbonate alteration assemblages that are easily accessible to acid water are less likely to produce acid drainage.

### Nature of ore

Massive sulfide deposits, by definition, contain zones or lenses of massive sulfide minerals, many with sulfide mineral contents exceeding 90 volume percent. Most deposits also contain extensive zones of semi-massive sulfide rock (25 to 50 volume percent) that contain economically exploitable ore. Stringer zone ore zones typically contain 5 to 20 volume percent sulfide minerals, hosted in quartz veins and disseminated in chloritic wall rocks. Disseminated sulfide rock is extensively developed in footwall alteration zones; sulfide mineral abundances decrease with depth below the massive sulfide zone horizon. Lateral development of disseminated pyrite can be continuous for large distances at and immediately below the stratigraphic horizon of the massive sulfide lens.

### Deposit trace element geochemistry

Iron is nearly always the predominant metal in sulfide phases. Economically exploitable VMS deposits associated with mafic rocks are variably enriched in copper and zinc, whereas those that contain a significant component of

felsic volcanic or sedimentary rock are relatively enriched in zinc and lead. Deposits associated with mafic rocks can contain anomalous concentrations of gold, silver, and cobalt. Deposits associated with felsic volcanic and sedimentary rocks contain minor to significant concentrations of lead, silver, arsenic, antimony, cadmium, and locally bismuth, tin, and selenium.

#### Ore and gangue mineralogy and zonation

The dominant sulfide mineral in most VMS deposits is pyrite, but pyrrhotite is dominant in others. Marcasite, which is present either intergrown with fine grained pyrite or as a replacement product of pyrrhotite, is generally a minor constituent but can constitute a potential source of acidic drainage because of its high reactivity relative to pyrite. The other dominant phases include sphalerite and chalcopyrite, accompanied by galena in VMS deposits associated with felsic rock. Other ore minerals are present in much lower abundances, but constitute important potential heavy metal sources. The most common accessory sulfide and sulfosalt minerals are those of the tennantite-tetrahedrite series, arsenopyrite, and various lead-antimony-bismuth sulfosalt minerals, particularly in deposits associated with felsic rock. Deposits associated with mafic rock may contain cobalt sulfide or thiospinel. Magnetite is present in some deposits and barite can be very abundant in Kuroko-type VMS deposits, in which it commonly forms an important ore facies. Gypsum and anhydrite are also abundant in some Kuroko deposits. The most common silicate gangue minerals are quartz and chlorite, which are accompanied by sericite in deposits associated with felsic rocks. Other gangue phases are much less abundant, except in massive sulfide deposits that have been metamorphosed to greenschist or higher metamorphic grades. In these metamorphosed deposits, phases such as anthophyllite and cordierite form from chloritic protoliths.

Metal zoning is well developed in massive sulfide deposits. Copper abundances are elevated in footwall and stringer ore zones, and zinc content increases upward and outward from the core of hydrothermal upwelling zones. In felsic-associated deposits, lead, arsenic, and antimony abundances are enriched upward and outward from the zinc-rich zones. Barite and silica are also enriched toward the stratigraphic tops and distal edges of most Kuroko-type deposits.

#### Mineral characteristics

Grain size is highly variable and is generally controlled by primary sulfide mineralogy and the extent of metamorphic recrystallization. Primary sulfide minerals of most zinc-lead-copper deposits are fine grained and intergrown, whereas those of most copper-zinc deposits are coarser grained (Franklin, 1993). The extent of grain size changes depends upon pressure and temperature conditions attained during metamorphism, and on the ductility of sulfide minerals. For example, cataclastic deformation significantly reduces grain-size and therefore reactivity of brittle sulfide minerals such as chalcopyrite and pyrite, but plastically deforms ductile sulfide minerals such as galena. Thermal metamorphism commonly causes sulfide ore to become much coarser grained and develop mosaic or porphyroblastic sulfide textures (Stanton, 1972).

#### Secondary mineralogy

Both initial seafloor and later near surface oxidation of massive sulfide minerals results in the formation of iron-rich gossan. Intermediate stages of oxidation also can result in the formation of a wide range of iron- and base-metal sulfate and sulfate-hydrate minerals. These highly soluble minerals are potentially important reservoirs of heavy metals that can be easily mobilized and potentially can produce high peak loads of dissolved metals if hydrologic conditions are suddenly altered, for example, by surface mining of a deposit in a wet climate. Secondary minerals formed in temperate climates include goethite, crystalline and amorphous silica, jarosite, a variety of metal-bearing hydroxy-sulfate minerals (beudantite, plumbojarosite, argentojarosite, woodhouseite, beaverite, meta-aluminite, hinsdalite, and brochantite), scorodite, native gold, native silver, native bismuth, barite, anglesite, litharge, covellite, chalcocite, digenite, enargite, luzonite, and acanthite.

#### Topography, physiography

These deposits have no specific topographic or physiographic features.

#### Hydrology

These deposits exert no specific influence on the adjacent hydrologic regime, partly because of their relatively small size. The extent of mineralized outcrop and (or) mine-related excavations exposed to the atmosphere or oxidized groundwater, and their position relative to the water table, are hydrologic factors that can significantly influence the

intensity and scale of environmental problems related to VMS deposits. Availability of oxidizing water is a controlling factor for acid generating potential and dissolved metal carrying capacity of water interacting with massive sulfide deposits or their mine-related products.

#### Mining and milling methods

Mining methods have a large influence on the potential environmental impacts of massive sulfide deposits. Both open-pit and underground methods have been used to mine VMS deposits in historic and modern operations. Local climatic and hydrologic conditions influence the acid generating capacity of deposits. Most massive sulfide deposits contain a large excess of iron-sulfide minerals relative to valuable base-metal sulfide minerals. The nature of ore processing and the method of deposition of the sulfide-mineral-rich tailings and waste rocks are critical parameters that influence the scope of environmental impacts associated with mining massive sulfide deposits. Fine-grained and intergrown sulfide minerals may require very fine grinding, which can result in highly reactive tailings, for beneficiation. Many modern mines discharge fine-grained sulfide-mineral-rich tailings into surface tailings ponds underlain by a number of impermeable linings. Previous mining operations often discharged tailings in a manner that resulted in significant contamination of surface and shallow ground water. Some active underground mines are able to dispose of essentially all tailings by backfilling and cementing mined stopes; consequently, surface contamination is virtually eliminated. Base-metal sulfide minerals are typically separated by flotation; some surfactants used in the process are toxic. Most of these surfactants are recycled and relatively minor amounts are discharged to tailings ponds.

### ENVIRONMENTAL SIGNATURES

#### Drainage signatures

Natural drainage water: Published data concerning the chemistry of natural drainage associated with VMS deposits include: Goldfarb and others (in press), Prince William Sound, Alaska; Greens Creek Environmental Impact Statement (1983), Admiralty Island, Alaska; and Filipek and others (1987), West Shasta, Calif., district. Temperate rainforest climate--Water draining Cyprus- and Besshi-type VMS deposits in the Prince William Sound area is dilute calcium-bicarbonate-type water (5.8 mg/l Ca and 15 mg/l  $\text{HCO}_3^-$ ) that is slightly acidic to neutral (pH 6.4 to 7.6); the type of host rock, sedimentary or volcanic, does not seem to affect these generalizations. Specific conductance is <50 uS/cm. Metal abundances in this water include 20  $\mu\text{g/l}$  iron, 15  $\mu\text{g/l}$  aluminum, <2  $\mu\text{g/l}$  arsenic, 1.4  $\mu\text{g/l}$  zinc, and <1  $\mu\text{g/l}$  silver, copper, cobalt, chromium, lead, molybdenum, and antimony. Stream water flowing over undisturbed mineralized rock above several deposits has slightly elevated metal abundances, including as much as 40  $\mu\text{g/l}$  iron, 2  $\mu\text{g/l}$  copper, and 52  $\mu\text{g/l}$  zinc; pH varies from 5.6 to 7.3. Montaine, semi-arid climate--Natural water draining unmineralized areas above the West Shasta district (Filipek and others, 1987) also is calcium bicarbonate-type water (14 mg/l calcium and 22 mg/l  $\text{HCO}_3^-$ ) that has a pH of 6.15 and a specific conductance of 100 uS/cm. This water contains 8 mg/l iron, 18 mg/l aluminum, <12 mg/l copper, <10 mg/l zinc, and <1 mg/l arsenic.

Mine drainage water: Published data sources concerning the chemistry of mine drainage associated with VMS deposits include: Goldfarb and others (in press), Beatson and eight other mines in Prince William Sound, Alaska; Kilburn and others (1994, 1995), Holden mine, Wash.; Alpers and others (1991), Penn mine, Calif.; and Alpers and others (1991, 1994), Iron Mountain mine, Calif. Temperate rainforest climate--The most acidic and metal-rich mine water, draining from the base of well consolidated tailings piles of Besshi-type deposits, from two locations in the Prince William Sound, Alaska, has a pH of 2.6 to 2.7 and contains as much as 21,000  $\mu\text{g/l}$  iron, 3,600  $\mu\text{g/l}$  copper, 220  $\mu\text{g/l}$  lead, 3,300  $\mu\text{g/l}$  zinc, 30  $\mu\text{g/l}$  cobalt, 10  $\mu\text{g/l}$  cadmium, and 311 mg/l sulfate. The tailings are devoid of vegetation and the drainages support a rich growth of bright green, copper-loving, bryophyte algal mats. Slightly acidic (pH 4.3 to 6.6) mine water was identified at six other deposits. Maximum metal values are 310  $\mu\text{g/l}$  iron, 1,400  $\mu\text{g/l}$  copper, and 3,100  $\mu\text{g/l}$  zinc. Kilburn and others (1994) sampled acidic mine drainage from within adits and below consolidated tailings piles at the Holden Mine, a copper-zinc VMS in amphibolitic mafic volcanic rocks. Water within the adits has a pH of about 5 and metal concentrations of 370-580  $\mu\text{g/l}$  iron, 570-580  $\mu\text{g/l}$  copper, and nearly 5,000  $\mu\text{g/l}$  zinc. Effluent from tailings piles has a pH of 2.8 to 2.9 and contains 23,000 to 50,000  $\mu\text{g/l}$  iron, 21 to 53  $\mu\text{g/l}$  copper, and 130 to 3,800  $\mu\text{g/l}$  zinc. Montaine, semi-arid climate--The Iron Mountain mine contains the most acidic and metal-rich mine water ever recorded. Alpers and Nordstrom (1991) have reported pH values ranging between 1.5 and <1.0. The first ever occurrence of pH values less than one were obtained for dripping mine water that was actively precipitating melanterite and other efflorescent metal-sulfate salts. This water contains as much as 11 weight percent iron, 2.3 weight percent zinc, 0.5 weight percent copper, and 76 weight percent sulfate, with 340 mg/l arsenic, 211 mg/l cadmium, 12 mg/l lead, and 29 mg/l antimony.



### Metal mobility from solid mine wastes

Soluble sulfate salt minerals derived from weathering and oxidation of sulfide minerals in mine dumps and tailings piles represent a potential source of metal contamination and acid generation. As percolating surface and ground water evaporates during dry periods, efflorescent metal-sulfate salt minerals form encrustations around and below the base of the piles, which effectively stores acidity and metals released during sulfide mineral breakdown. Subsequent rainfall or snowmelt following a dry period is likely to release a highly concentrated pulse of acid mine water. Mine dumps associated with lead-rich VMS deposits (Kuroko-type) may be a source of lead contamination due to high concentrations of soluble secondary lead minerals.

Secondary minerals in tailings impoundments include a variety of iron oxyhydroxides (goethite, lepidocrocite, akaganeite, maghemite, and ferrihydrite), sulfates (gypsum, bassanite, jarosite, hydronium jarosite, melanterite, goslarite, ferrohexahydrite, epsomite, hexahydrite, siderotil, rozenite, anglesite, alunogen, and copiapite), and minerals such as marcasite, covellite, and native sulfur (Jambor, 1994). Pore water from tailings impoundments associated with the Heath Steele, New Brunswick, deposit are acidic (pH 1.8 to 5.2), have Eh of 280 to 580 mV, and contain significant dissolved metal abundances, including 0.3 to 600 mg/l copper, 0.8 to 11 mg/l lead, 23 to 4,880 mg/l zinc, 1,200 to 36,000 mg/l iron, and 600 to 67,600 mg/l sulfate (Boorman and Watson, 1976). Similarly, pore water from tailings impoundments associated with the Waite Amulet, Quebec, deposit are acidic (pH 2.5 to 6.0), have Eh of 200 to 700 mV, and contain significant dissolved metal abundances, including as much as 65 mg/l copper, as much as 5 mg/l lead, as much as 250 mg/l zinc, as much as 8,000 mg/l iron, and as much as 20,000 mg/l sulfate (Blowes and Jambor, 1990). Finally, pore water from tailings impoundments associated with the Kidd Creek, Ontario, deposit are acidic (pH 3.5 to 7.5), have Eh of 50-500 mV, and contain significant dissolved metal abundances, including 0 to 38 mg/l copper, 0 to 2 mg/l lead, 0 to 6,200 mg/l zinc, 0 to 350  $\mu$ g/l arsenic, 1 to 990 mg/l iron, and 1,860 to 27,000 mg/l sulfate (Al and others, 1994).

Extremely fine grinding required for beneficiation of VMS ore may enhance airborne transport of lead-arsenic-cadmium-antimony-bearing dust. This phenomenon is most probable in semi-arid to arid regions in which strong winds prevail.

### Soil, sediment signatures prior to mining

The elemental suite and magnitude of geochemical anomalies in soil and sediment collected from undisturbed VMS deposits depend upon a number of factors, including VMS deposit type, extent of ore outcrop or overburden, climate, topography, etc. Stream sediment samples collected below Kuroko-type deposits in temperate rain forest on Admiralty Island, Alaska, contain 5 to 10 weight percent iron, as much as 10,000 ppm barium, hundreds to several thousand ppm zinc, hundreds of ppm lead, tens to hundreds of ppm arsenic, copper, and nickel, as well as 0 to 20 ppm silver, bismuth, cadmium, mercury, molybdenum, and antimony (Kelley, 1990; Rowan and others, 1990; Taylor and others, 1992; C.D. Taylor, unpub. data, 1995).

Stream sediment geochemical signatures associated with undisturbed to variably disturbed Cyprus and Besshi VMS deposits in the Prince William Sound, Alaska, are similar to those just described. They contain 10 to 40 weight percent iron, several hundred ppm barium, hundreds of ppm arsenic and zinc, tens to hundreds of ppm lead, hundreds to thousands of ppm copper, and 0 to 20 ppm silver, bismuth, mercury, molybdenum, and antimony (R.J. Goldfarb, unpub. data, 1995).

### Potential environmental concerns associated with mineral processing

Tailings ponds below mills are likely to contain high abundances of lead, zinc, cadmium, bismuth, antimony, and cyanide and other reactants used in flotation and recovery circuits. Highly pyritic-pyrrhotitic orebodies that are exposed to oxidation by air circulating through open adits, manways, and exploration drill holes may evolve  $\text{SO}_2$  gas; in some cases, spontaneous combustion can cause sulfide ore to burn. Tailings that contain high percentages of non-ore iron sulfide minerals have extremely high acid-generating capacity. Surficial stockpiles of high-sulfide mineral ore are also potential sources of metal-rich mine water.

### Smelter signatures

Most base-metal rich ore concentrates are smelted. In most cases, concentrates are shipped to custom smelters, and therefore do not contribute to the environmental impact in the immediate mine vicinity. Larger districts are often served by a smelter co-located in the district. Data compiled by Gulson and others (1994) document the relationship between lead in soil near smelters and blood lead in children; similar data for the Leadville, Colo., area indicate similar trends. Additional data may be available for the Trail, British Columbia and El Paso, Tex. smelters.

### Climate effects on environmental signatures

Great differences between geochemical mine drainage data for deposits in the West Shasta, Calif., district, eastern Canada, and that for deposits in cooler and wetter Alaskan climates underscore the important role of climate with regard to acid mine drainage associated with VMS deposits. Acidity and total metal concentrations in mine drainage in arid environments are several orders of magnitude greater than in more temperate climates because of the concentrating effects of mine effluent evaporation and the resulting "storage" of metals and acidity in highly soluble metal-sulfate-salt minerals. However, minimal surface water flow in these areas inhibits generation of significant volumes of highly acidic, metal-enriched drainage. Concentrated release of these stored contaminants to local watersheds may be initiated by precipitation following a dry spell. In wet climates, high water tables may reduce exposure of abandoned orebodies to oxidation and continually flush existing tailings and mine dumps. Although metal-laden acid mine water does form, it may be diluted to benign metal abundances within several hundred meters of mixing with a higher order stream.

### Geoenvironmental geophysics

Self potential detects electrical potentials produced by ongoing redox reactions. The method is suitable for locating "hot spots" in tailings piles. Electromagnetic surveys are useful for tracing and monitoring metal-bearing ground water. In addition, detailed magnetic data can help delineate geologic contacts, strata, and fractures that may act as fluid conduits, especially in crystalline rocks.

### REFERENCES CITED

- Al, T.A., Blowes, D.W., and Jambor, J.L., 1994, A geochemical study of the tailings impoundment at the Falconbridge Limited, Kidd Creek division metallurgical site, Timmons, Ontario, in Jambor, J.L. and Blowes, D.W. eds., Short Course Handbook on Environmental Geochemistry of Sulfide Mine-wastes, Mineralogical Association of Canada, v. 22, p. 333-364.
- Alpers, C.N., and Nordstrom, D.K., 1991, Geochemical evolution of extremely acid mine waters at Iron Mountain, California--Are there any lower limits to pH?, in Proceedings, Second International Conference on the Abatement of Acidic Drainage: MEND (Mine Environmental Neutral Drainage), Ottawa, Canada, v. 2, p. 321-342.
- Alpers, C.N., Nordstrom, D.K., and Thompson, J.M., 1994, Seasonal variations of Zn/Cu ratios in acid mine waters from Iron Mountain, California, in Alpers, C.N., and Blowes, D.W., eds., Environmental geochemistry of sulfide oxidation, ACS Symposium Series 550: Washington D.C., American Chemical Society, p. 324-344.
- Blowes, D.W., and Jambor, J.L., 1990, The pore-water geochemistry and the mineralogy of the vadose zone of sulfide tailings, Waite Amulet, Quebec, Canada: Applied Geochemistry, v. 5, p. 327-346.
- Boorman, R.S., and Watson, D.M., 1976, Chemical processes in abandoned sulphide tailings dumps and environmental implication for northeastern New Brunswick, Canadian Institute of Mining and Metallurgy Bulletin, v. 69, no. 772, p. 86-96.
- Cox, D.P., 1986, Descriptive model of Besshi massive sulfide, in Cox, D.P., and Singer, D.A., eds., Mineral deposit models: U.S. Geological Survey Bulletin 1693, p. 136.
- Cox, D.P., and Singer, D.A., 1986, Mineral deposit models: U.S. Geological Survey Bulletin 1693, 379 p.
- Filipek, L.H., Nordstrom, D.K., and Ficklin, W.H., 1987, Interaction of acid mine drainage with waters and sediments of West Squaw Creek in the West Shasta mining district, California: Environmental Science and Technology, v. 21, no. 4, p. 388-396.
- Fox, J.S., 1984, Besshi-type volcanogenic sulphide deposits--a review, Canadian Institute of Mining and Metallurgy Bulletin, v. 77, no. 864, p. 57-68.
- Franklin, J.M., 1993, Volcanic-associated massive sulphide deposits, in Kirkham, R.V., Sinclair, W.D., Thorpe, R.I., and Duke, J.M., eds., Mineral deposit modeling, Geological Association of Canada Special Paper 40, p. 315-334.
- Franklin, J.M., Sangster, D.M., and Lydon, J.W., 1981, Volcanic-associated massive sulfide deposits, in Skinner, B.J., ed., Economic Geology 75th anniversary volume, p. 485-626.
- Goldfarb, R.J., Nelson, S.W., Taylor, C.D., d'Angelo, W.M., and Meier, A.L., in press, Acid mine drainage associated with volcanogenic massive sulfide deposits, Prince William Sound, Alaska, in Dumoulin, J.A., and Moore, T.E., eds., Geologic studies in Alaska by the U.S. Geological Survey, 1994: U.S. Geological Survey Bulletin 2152.
- Greens Creek Environmental Impact Statement, 1983.

- Gulson, B.L., Mizon, K.J., Law, A.J., Korsch, M.J., Davis, J.J., and Howarth, D., 1994, Source and pathways of lead in humans from the Broken Hill mining community--An alternative use of exploration methods: *Economic Geology*, v. 89, p. 889-908.
- Jambor, J.L., 1994, Mineralogy of sulfide-rich tailings and their oxidation products, *in* Jambor, J.L., and Blowes, D.W., eds., *Short Course Handbook on Environmental Geochemistry of Sulfide Mine-wastes: Mineralogical Association of Canada*, v. 22, p. 59-102.
- Kelley, K.D., 1990, Interpretation of geochemical data from Admiralty Island, Alaska--Evidence for volcanogenic massive sulfide mineralization, *in* Goldfarb, R.J., Nash, J.T., and Stoeser, J.W., eds., *Geochemical studies in Alaska by the U.S. Geological Survey, 1989*, U.S. Geological Survey Bulletin 1950, p. A1-A9.
- Kilburn, J.E., Sutley, S.J., and Whitney, G.C., 1995, Geochemistry and mineralogy of acid mine drainage at the Holden mine, Chelan County, Washington: *Explore*, Association of Exploration Geochemists newsletter, no. 87, p. 9-14.
- Kilburn, J.E., Whitney, G.C., d'Angelo, W.M., Fey, D.L., Hopkins, R.T., Meier, A.L., Motooka, J.M., Roushey, B.H., and Sutley, S.J., 1994, Geochemical data and sample locality maps for stream sediment, heavy-mineral-concentrate, mill tailing, water, and precipitate samples in and around the Holden mine, Chelan County, Washington: U.S. Geological Survey Open-File Report 94-680A, 33 p.
- Lydon, J.W., 1984, Volcanogenic massive sulphide deposits, Part 1--A descriptive model: *Geoscience Canada*, v. 11, p. 195-202.
- \_\_\_\_\_, 1988, Volcanogenic massive sulphide deposits, Part 2--Genetic models: *Geoscience Canada*, v. 15, p. 43-65.
- Morton, R.L., Hudak, G., Walker, J., and Franklin, J.M., 1990, Physical volcanology and hydrothermal alteration of the Sturgeon Lake caldera complex, *in* Franklin, J.M., Schneiders, B.R., and Koopman, E.R., eds., *Mineral Deposits in the western Superior province, Ontario: Geological Survey of Canada, Open File 2164*, p. 74-94.
- Ohmoto, H., and Skinner, B.J., 1983, The Kuroko and related volcanogenic massive sulfide deposits: *Economic Geology Monograph* 5, 604 p.
- Plumlee, G.S., Smith, K.S., Ficklin, W.H., Briggs, P.H., and McHugh, J.B., 1993, Empirical studies of diverse mine drainages in Colorado: Implications for the prediction of mine-drainage chemistry: *Proceedings, 1993 Mined Land Reclamation Symposium*, Billings, Montana, v. 1, p. 176-186.
- Plumlee, G.S., Smith, K.S., and Ficklin, W.H., 1994, Geoenvironmental models of mineral deposits, and geology-based mineral-environmental assessments of public lands: U.S. Geological Survey Open-File Report 94-203, 7 p.
- Rowan, E.L., Bailey, E.A., and Goldfarb, R.J., 1990, Geochemical orientation study for identification of metallic mineral resources in the Sitka quadrangle, southeastern Alaska, *in* Goldfarb, R.J., Nash, J.T., and Stoeser, J.W., eds., *Geochemical studies in Alaska by the U.S. Geological Survey, 1989*, U.S. Geological Survey Bulletin 1950, p. B1-B12.
- Singer, D.A., 1986a, Descriptive model of Cyprus massive sulfide, *in* Cox, D.P., and Singer, D.A., eds., *Mineral deposit models: U.S. Geological Survey Bulletin* 1693, p. 131.
- \_\_\_\_\_, 1986b, Descriptive model of Kuroko massive sulfide, *in* Cox, D.P., and Singer, D.A., eds., *Mineral deposit models: U.S. Geological Survey Bulletin* 1693, p. 189-190.
- \_\_\_\_\_, 1986c, Grade and tonnage model of Cyprus massive sulfide, *in* Cox, D.P., and Singer, D.A., eds., *Mineral deposit models: U.S. Geological Survey Bulletin* 1693, p. 131-135.
- \_\_\_\_\_, 1986d, Grade and tonnage model of Besshi massive sulfide, *in* Cox, D.P., and Singer, D.A., eds., *Mineral deposit models: U.S. Geological Survey Bulletin* 1693, p. 136-138.
- Singer, D.A., and Mosier, D.L., 1986, Grade and tonnage model of Kuroko massive sulfide, *in* Cox, D.P., and Singer, D.A., eds., *Mineral deposit models: U.S. Geological Survey Bulletin* 1693, p. 190-197.
- Slack, J.F., 1993, Descriptive and grade-tonnage models for Besshi-type massive sulfide deposits, *in* Kirkham, R.V., Sinclair, W.D., Thorpe, R.I., and Duke, J.M., eds., *Mineral deposit modeling*, Geological Association of Canada Special Paper 40, p. 343-372.
- Stanton, R.L., 1972, *Ore Petrology*, McGraw-Hill, New York, 713 p.
- Taylor, C.D., Cieutat, B.A., and Miller, L.D., 1992, A followup geochemical survey of base metal anomalies in the Ward Creek/Windfall Harbor and Gambier Bay areas, Admiralty Island S.E. Alaska, *in* Bradley, D., and Dusel-Bacon, C., eds., *1991 Geologic Studies in Alaska: U.S. Geological Survey Bulletin* 2041, p. 70-85.

# VOLCANIC-ASSOCIATED MASSIVE SULFIDE DEPOSITS (MODELS 24a-b, 28a; Singer, 1986a,b; Cox, 1986)

by Cliff D. Taylor, Robert A. Zierenberg, Richard J. Goldfarb,  
James E. Kilburn, Robert R. Seal II, and M. Dean Kleinkopf

## SUMMARY OF RELEVANT GEOLOGIC, GEOENVIRONMENTAL, AND GEOPHYSICAL INFORMATION

### Deposit geology

Volcanic-associated massive sulfide (VMS) deposits range from lens shaped to sheet-like bodies of sulfide-mineral-rich rock spatially associated with volcanic rocks ranging in composition from basalt to rhyolite (fig. 1). VMS deposits can be divided into three general categories. Cyprus-type deposits (Model 24a; Singer, 1986a) tend to be small, medium-grade deposits rich in copper and zinc. They are generally lens or mound shaped accumulations of massive pyrite developed in ophiolite-related, extrusive basalt sequences. They are typically underlain by copper-rich "stringer-zones" composed of anastomosing quartz-sulfide mineral veins in extensively chloritized basalt. Kuroko-type deposits (Model 28a; Singer, 1986b) are typically developed in intermediate to felsic volcanic rock and are generally interpreted to have formed in extensional environments associated with arc volcanism. They are commonly high grade and can be very large. Relative to Cyprus-type deposits, they generally have much higher contents of zinc, lead, silver, and antimony, which reflects the composition of their felsic volcanic host rocks. They also have mound-like morphology and the abundance of coarse clastic sulfide minerals within many of these deposits attests to a moderately high energy, seafloor depositional setting. Kuroko-type deposits also tend to be underlain by copper-rich stringer zones and commonly have well developed geochemical zonation with progressive zinc, lead, and silver enrichment both vertically and laterally away from vent centers. Besshi-type deposits (Model 24b; Cox, 1986) are present in mixed volcanic-sedimentary environments. Deposits of this type are commonly hosted by turbidites that have been intruded by basaltic sills. These deposits are typically copper-rich and contain small abundances of lead and other lithophile elements. In contrast to other volcanic-hosted deposits, many Besshi-type deposits form thin, laterally extensive sheets of pyrrhotite- and (or) pyrite-rich massive sulfide rock; however, the characteristics of Besshi-type deposits vary considerably. Slack (1993) presents an expanded definition of Besshi-type deposits that includes deposits such as those in the Ducktown, Tenn., district and the large Windy Craggy deposit in British Columbia.

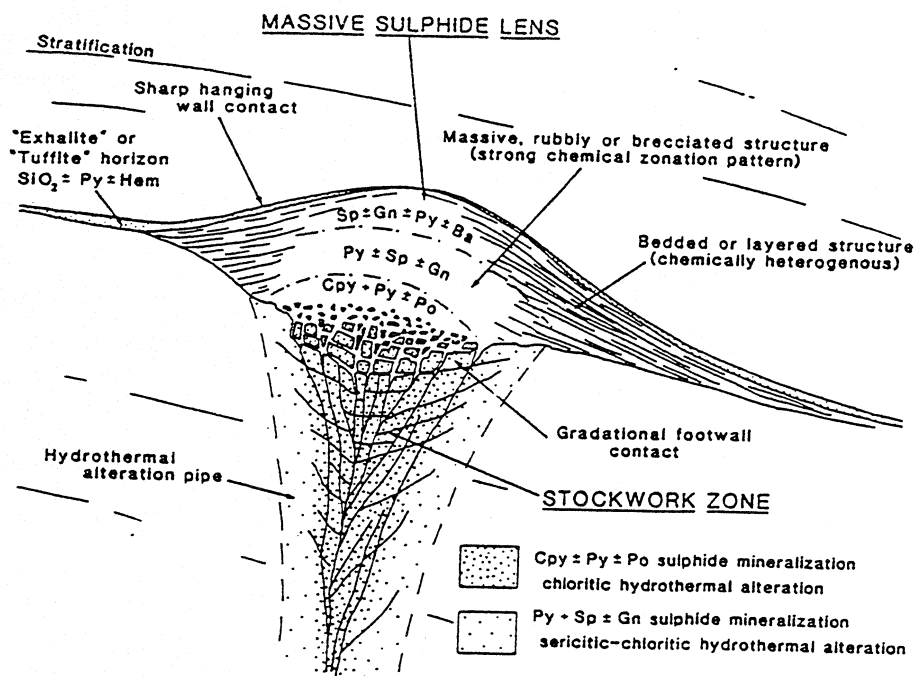
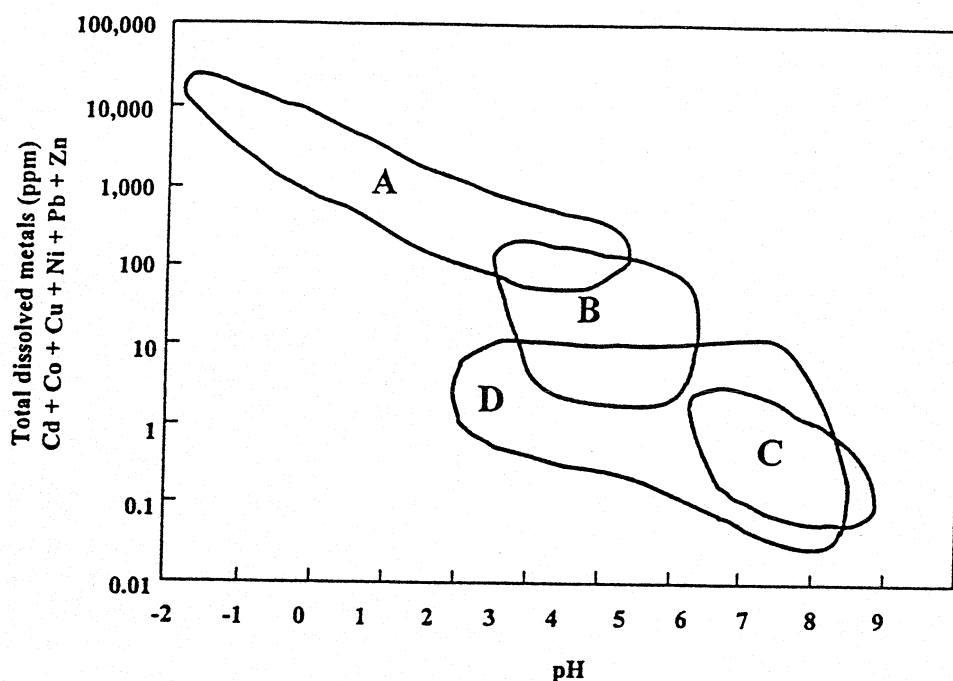


Figure 1. Essential characteristics of an idealized volcanogenic massive sulfide deposit (modified from Lydon, 1984). Mineral abbreviations as follows: Sp, sphalerite; Gn, galena; Py, pyrite; Ba, barite; Cpy, chalcopyrite; Po, pyrrhotite; and Hem, hematite.



**Figure 2.** Ficklin plot (Plumlee and others, 1993) showing aqueous metal contents and pH ranges of water associated with volcanic massive sulfide deposits. Fields A, B, and C (Plumlee and others, 1994), are those for West Shasta, Calif., district VMS deposits, sulfide-mineral-rich vein deposits in rocks with low buffering capacity, and sulfide-mineral-rich vein deposits in carbonate host rocks, respectively. Field D is the composite field for water draining Prince William Sound, Alaska, VMS deposits (Goldfarb and others, in press).

#### Examples

Cyprus-type: Skouriotissa, Cyprus; Betts Cove, Newfoundland; Turner-Albright, Oreg.; Big Mike, Nev.  
Kuroko-type: Kidd Creek, Ontario; Iron King and Penn Mine, Calif.; Mokuroko district, Japan.  
Besshi-type: Besshi, Japan; Windy Craggy, British Columbia.

#### Spatially and (or) genetically related deposit types

VMS deposits are associated with a number of other mineral deposit types (Cox and Singer, 1986). Some VMS deposits, especially the Besshi-type deposits as broadly defined by Slack (1993), are transitional in depositional setting with some sedex deposits (Model 31a), such as Sullivan, British Columbia. VMS deposits are commonly associated with regionally developed iron- and (or) manganese-rich metalliferous sediment and chert developed at the same time-stratigraphic horizon as the massive sulfide deposits. Some Archean VMS deposits may be transitional to volcanic-associated iron formation. VMS deposits, especially in Archean terranes, tend to be spatially associated with shear-hosted mesothermal lode gold deposits (Model 36a) and Algoma-type banded iron formation (Model 28b).

#### Potential environmental considerations

Volcanic-associated massive sulfide deposits are among the most likely of all deposit types to have associated environmental problems, particularly acid mine drainage. Analyses of water draining VMS deposits plot in the extreme metal-extreme acidity field (fig. 2). VMS deposits have high iron- and base-metal-sulfide mineral contents and are hosted by rocks with low buffering capacity. These minerals are unstable under normal oxidizing near surface conditions and represent potential sources of highly acid and metal-rich drainage, especially in areas disturbed by surface mining or tailings disposal. Associated high abundances of potentially toxic trace metals, including arsenic, bismuth, cadmium, mercury, lead, and antimony, are present in some deposits, particularly those associated with felsic volcanic or sedimentary source rocks.

#### Exploration geophysics

Electrical properties of sulfide minerals, combined with large sulfide mineral concentrations in VMS deposits, make this type of mineral deposit a particularly favorable target for location by a variety of geophysical techniques. Self-potential, induced polarization, and a wide range of electromagnetic methods have been successfully used to locate buried VMS deposits. Pyrrhotite-rich and magnetite-bearing massive sulfide deposits may be locatable by detailed magnetic surveys. Airborne multispectral remote sensing techniques have been used to identify areas that contain hydrothermally altered rock and stressed vegetation that may be associated with mineralized rock.

## References

Franklin and others (1981), Ohmoto and Skinner (1983), Fox (1984), Lydon (1984, 1988), Franklin (1993), and Slack (1993).

## GEOLOGIC FACTORS THAT INFLUENCE POTENTIAL ENVIRONMENTAL EFFECTS

### Deposit size

Historically, most economic deposits are in the 1-5 million tonnes range (Singer, 1986c,d; Singer and Mosier, 1986). Deposits of this size can still be developed in areas with an existing mining infrastructure; however, development of new deposits in frontier areas likely requires at least 10 million tonnes of reasonably high grade ore. Most Cyprus-type deposits contain less than 15 million tonnes of ore. Most Besshi-type deposits are also fairly small; notable exceptions include the >300 million tonne Windy Craggy, British Columbia, deposit. Kuroko-type deposits, especially those of Precambrian age, can be very large, such as the world class Kidd Creek, Ontario, deposit.

### Host rocks

Cyprus-type deposits are hosted by submarine mafic-volcanic rocks and their altered equivalents, typically in brecciated rocks commonly associated with pillow lavas, which have good buffering capacity. Host-rocks for Kuroko-type deposits range from basalt to rhyolite, which have high and low buffering capacities, respectively. Many deposits are associated with subaqueous dacitic-domes that have intermediate buffering capacity. Host rocks are commonly brecciated and are typically moderately to highly altered. Some deposits are hosted by associated volcanoclastic or hemipelagic sedimentary rocks that overly submarine volcanic sequences. Besshi-type deposits are typically hosted by turbiditic to hemipelagic graywacke interbedded with or intruded by basalt.

### Surrounding geologic terrane

Submarine volcanic activity is a defining characteristic of VMS deposits. Most VMS deposits, including many ophiolite-hosted deposits of the Cyprus-type, are associated with arc-related volcanism. Local extensional tectonic environments are particularly conducive to deposition of massive sulfide deposits. Many VMS deposits are in rocks that have undergone collisional tectonism and may be in structural contact with a wide variety of rock types.

### Wall-rock alteration

Footwall alteration is moderate to locally intense around most VMS deposits. Hanging-wall alteration is typically absent, but may be weakly developed in some deposits. Many deposits that have not been tectonically disrupted are underlain by "stringer-zone" mineralized and altered rock. Stringer-zones are characterized by anastomosing quartz-sulfide veins. Local zones of silicification are present near and within mineralized zones. The most common alteration is pervasive chloritization, which is less well developed with increasing depth and distance from hydrothermal upwelling zones, in the footwall of deposits. Deposits hosted by felsic rocks typically have extensively developed quartz sericite alteration in the footwall. Most altered rock associated with massive sulfide deposits has low to very low acid buffering capacity. Some massive sulfide deposits are associated with pervasive carbonate alteration in the footwall (for instance, Sturgeon Lake, Ontario; Morton and others, 1990). These carbonate alteration zones typically have low to moderate abundances of calcitic to ankeritic carbonate minerals. Massive sulfide deposits with associated carbonate alteration assemblages that are easily accessible to acid water are less likely to produce acid drainage.

### Nature of ore

Massive sulfide deposits, by definition, contain zones or lenses of massive sulfide minerals, many with sulfide mineral contents exceeding 90 volume percent. Most deposits also contain extensive zones of semi-massive sulfide rock (25 to 50 volume percent) that contain economically exploitable ore. Stringer zone ore zones typically contain 5 to 20 volume percent sulfide minerals, hosted in quartz veins and disseminated in chloritic wall rocks. Disseminated sulfide rock is extensively developed in footwall alteration zones; sulfide mineral abundances decrease with depth below the massive sulfide zone horizon. Lateral development of disseminated pyrite can be continuous for large distances at and immediately below the stratigraphic horizon of the massive sulfide lens.

### Deposit trace element geochemistry

Iron is nearly always the predominant metal in sulfide phases. Economically exploitable VMS deposits associated with mafic rocks are variably enriched in copper and zinc, whereas those that contain a significant component of

felsic volcanic or sedimentary rock are relatively enriched in zinc and lead. Deposits associated with mafic rocks can contain anomalous concentrations of gold, silver, and cobalt. Deposits associated with felsic volcanic and sedimentary rocks contain minor to significant concentrations of lead, silver, arsenic, antimony, cadmium, and locally bismuth, tin, and selenium.

#### Ore and gangue mineralogy and zonation

The dominant sulfide mineral in most VMS deposits is pyrite, but pyrrhotite is dominant in others. Marcasite, which is present either intergrown with fine grained pyrite or as a replacement product of pyrrhotite, is generally a minor constituent but can constitute a potential source of acidic drainage because of its high reactivity relative to pyrite. The other dominant phases include sphalerite and chalcopyrite, accompanied by galena in VMS deposits associated with felsic rock. Other ore minerals are present in much lower abundances, but constitute important potential heavy metal sources. The most common accessory sulfide and sulfosalt minerals are those of the tennantite-tetrahedrite series, arsenopyrite, and various lead-antimony-bismuth sulfosalt minerals, particularly in deposits associated with felsic rock. Deposits associated with mafic rock may contain cobalt sulfide or thiospinel. Magnetite is present in some deposits and barite can be very abundant in Kuroko-type VMS deposits, in which it commonly forms an important ore facies. Gypsum and anhydrite are also abundant in some Kuroko deposits. The most common silicate gangue minerals are quartz and chlorite, which are accompanied by sericite in deposits associated with felsic rocks. Other gangue phases are much less abundant, except in massive sulfide deposits that have been metamorphosed to greenschist or higher metamorphic grades. In these metamorphosed deposits, phases such as anthophyllite and cordierite form from chloritic protoliths.

Metal zoning is well developed in massive sulfide deposits. Copper abundances are elevated in footwall and stringer ore zones, and zinc content increases upward and outward from the core of hydrothermal upwelling zones. In felsic-associated deposits, lead, arsenic, and antimony abundances are enriched upward and outward from the zinc-rich zones. Barite and silica are also enriched toward the stratigraphic tops and distal edges of most Kuroko-type deposits.

#### Mineral characteristics

Grain size is highly variable and is generally controlled by primary sulfide mineralogy and the extent of metamorphic recrystallization. Primary sulfide minerals of most zinc-lead-copper deposits are fine grained and intergrown, whereas those of most copper-zinc deposits are coarser grained (Franklin, 1993). The extent of grain size changes depends upon pressure and temperature conditions attained during metamorphism, and on the ductility of sulfide minerals. For example, cataclastic deformation significantly reduces grain-size and therefore reactivity of brittle sulfide minerals such as chalcopyrite and pyrite, but plastically deforms ductile sulfide minerals such as galena. Thermal metamorphism commonly causes sulfide ore to become much coarser grained and develop mosaic or porphyroblastic sulfide textures (Stanton, 1972).

#### Secondary mineralogy

Both initial seafloor and later near surface oxidation of massive sulfide minerals results in the formation of iron-rich gossan. Intermediate stages of oxidation also can result in the formation of a wide range of iron- and base-metal sulfate and sulfate-hydrate minerals. These highly soluble minerals are potentially important reservoirs of heavy metals that can be easily mobilized and potentially can produce high peak loads of dissolved metals if hydrologic conditions are suddenly altered, for example, by surface mining of a deposit in a wet climate. Secondary minerals formed in temperate climates include goethite, crystalline and amorphous silica, jarosite, a variety of metal-bearing hydroxy-sulfate minerals (beudantite, plumbojarosite, argentojarosite, woodhouseite, beaverite, meta-aluminite, hinsdalite, and brochantite), scorodite, native gold, native silver, native bismuth, barite, anglesite, litharge, covellite, chalcocite, digenite, enargite, luzonite, and acanthite.

#### Topography, physiography

These deposits have no specific topographic or physiographic features.

#### Hydrology

These deposits exert no specific influence on the adjacent hydrologic regime, partly because of their relatively small size. The extent of mineralized outcrop and (or) mine-related excavations exposed to the atmosphere or oxidized groundwater, and their position relative to the water table, are hydrologic factors that can significantly influence the



intensity and scale of environmental problems related to VMS deposits. Availability of oxidizing water is a controlling factor for acid generating potential and dissolved metal carrying capacity of water interacting with massive sulfide deposits or their mine-related products.

#### Mining and milling methods

Mining methods have a large influence on the potential environmental impacts of massive sulfide deposits. Both open-pit and underground methods have been used to mine VMS deposits in historic and modern operations. Local climatic and hydrologic conditions influence the acid generating capacity of deposits. Most massive sulfide deposits contain a large excess of iron-sulfide minerals relative to valuable base-metal sulfide minerals. The nature of ore processing and the method of deposition of the sulfide-mineral-rich tailings and waste rocks are critical parameters that influence the scope of environmental impacts associated with mining massive sulfide deposits. Fine-grained and intergrown sulfide minerals may require very fine grinding, which can result in highly reactive tailings, for beneficiation. Many modern mines discharge fine-grained sulfide-mineral-rich tailings into surface tailings ponds underlain by a number of impermeable linings. Previous mining operations often discharged tailings in a manner that resulted in significant contamination of surface and shallow ground water. Some active underground mines are able to dispose of essentially all tailings by backfilling and cementing mined stopes; consequently, surface contamination is virtually eliminated. Base-metal sulfide minerals are typically separated by flotation; some surfactants used in the process are toxic. Most of these surfactants are recycled and relatively minor amounts are discharged to tailings ponds.

### ENVIRONMENTAL SIGNATURES

#### Drainage signatures

Natural drainage water: Published data concerning the chemistry of natural drainage associated with VMS deposits include: Goldfarb and others (in press), Prince William Sound, Alaska; Greens Creek Environmental Impact Statement (1983), Admiralty Island, Alaska; and Filipek and others (1987), West Shasta, Calif., district. Temperate rainforest climate--Water draining Cyprus- and Besshi-type VMS deposits in the Prince William Sound area is dilute calcium-bicarbonate-type water ( $5.8 \text{ mg/l Ca}$  and  $15 \text{ mg/l HCO}_3^-$ ) that is slightly acidic to neutral (pH 6.4 to 7.6); the type of host rock, sedimentary or volcanic, does not seem to affect these generalizations. Specific conductance is  $<50 \text{ uS/cm}$ . Metal abundances in this water include  $20 \text{ }\mu\text{g/l}$  iron,  $15 \text{ }\mu\text{g/l}$  aluminum,  $<2 \text{ }\mu\text{g/l}$  arsenic,  $1.4 \text{ }\mu\text{g/l}$  zinc, and  $<1 \text{ }\mu\text{g/l}$  silver, copper, cobalt, chromium, lead, molybdenum, and antimony. Stream water flowing over undisturbed mineralized rock above several deposits has slightly elevated metal abundances, including as much as  $40 \text{ }\mu\text{g/l}$  iron,  $2 \text{ }\mu\text{g/l}$  copper, and  $52 \text{ }\mu\text{g/l}$  zinc; pH varies from 5.6 to 7.3. Montaine, semi-arid climate--Natural water draining unmineralized areas above the West Shasta district (Filipek and others, 1987) also is calcium bicarbonate-type water ( $14 \text{ mg/l calcium}$  and  $22 \text{ mg/l HCO}_3^-$ ) that has a pH of 6.15 and a specific conductance of  $100 \text{ uS/cm}$ . This water contains  $8 \text{ mg/l}$  iron,  $18 \text{ mg/l}$  aluminum,  $<12 \text{ mg/l}$  copper,  $<10 \text{ mg/l}$  zinc, and  $<1 \text{ mg/l}$  arsenic.

Mine drainage water: Published data sources concerning the chemistry of mine drainage associated with VMS deposits include: Goldfarb and others (in press), Beatson and eight other mines in Prince William Sound, Alaska; Kilburn and others (1994, 1995), Holden mine, Wash.; Alpers and others (1991), Penn mine, Calif.; and Alpers and others (1991, 1994), Iron Mountain mine, Calif. Temperate rainforest climate--The most acidic and metal-rich mine water, draining from the base of well consolidated tailings piles of Besshi-type deposits, from two locations in the Prince William Sound, Alaska, has a pH of 2.6 to 2.7 and contains as much as  $21,000 \text{ }\mu\text{g/l}$  iron,  $3,600 \text{ }\mu\text{g/l}$  copper,  $220 \text{ }\mu\text{g/l}$  lead,  $3,300 \text{ }\mu\text{g/l}$  zinc,  $30 \text{ }\mu\text{g/l}$  cobalt,  $10 \text{ }\mu\text{g/l}$  cadmium, and  $311 \text{ mg/l}$  sulfate. The tailings are devoid of vegetation and the drainages support a rich growth of bright green, copper-loving, bryophyte algal mats. Slightly acidic (pH 4.3 to 6.6) mine water was identified at six other deposits. Maximum metal values are  $310 \text{ }\mu\text{g/l}$  iron,  $1,400 \text{ }\mu\text{g/l}$  copper, and  $3,100 \text{ }\mu\text{g/l}$  zinc. Kilburn and others (1994) sampled acidic mine drainage from within adits and below consolidated tailings piles at the Holden Mine, a copper-zinc VMS in amphibolitic mafic volcanic rocks. Water within the adits has a pH of about 5 and metal concentrations of  $370\text{--}580 \text{ }\mu\text{g/l}$  iron,  $570\text{--}580 \text{ }\mu\text{g/l}$  copper, and nearly  $5,000 \text{ }\mu\text{g/l}$  zinc. Effluent from tailings piles has a pH of 2.8 to 2.9 and contains  $23,000$  to  $50,000 \text{ }\mu\text{g/l}$  iron,  $21$  to  $53 \text{ }\mu\text{g/l}$  copper, and  $130$  to  $3,800 \text{ }\mu\text{g/l}$  zinc. Montaine, semi-arid climate--The Iron Mountain mine contains the most acidic and metal-rich mine water ever recorded. Alpers and Nordstrom (1991) have reported pH values ranging between 1.5 and  $<1.0$ . The first ever occurrence of pH values less than one were obtained for dripping mine water that was actively precipitating melanterite and other efflorescent metal-sulfate salts. This water contains as much as 11 weight percent iron, 2.3 weight percent zinc, 0.5 weight percent copper, and 76 weight percent sulfate, with  $340 \text{ mg/l}$  arsenic,  $211 \text{ mg/l}$  cadmium,  $12 \text{ mg/l}$  lead, and  $29 \text{ mg/l}$  antimony.



#### Metal mobility from solid mine wastes

Soluble sulfate salt minerals derived from weathering and oxidation of sulfide minerals in mine dumps and tailings piles represent a potential source of metal contamination and acid generation. As percolating surface and ground water evaporates during dry periods, efflorescent metal-sulfate salt minerals form encrustations around and below the base of the piles, which effectively stores acidity and metals released during sulfide mineral breakdown. Subsequent rainfall or snowmelt following a dry period is likely to release a highly concentrated pulse of acid mine water. Mine dumps associated with lead-rich VMS deposits (Kuroko-type) may be a source of lead contamination due to high concentrations of soluble secondary lead minerals.

Secondary minerals in tailings impoundments include a variety of iron oxyhydroxides (goethite, lepidocrocite, akaganeite, maghemite, and ferrihydrite), sulfates (gypsum, bassanite, jarosite, hydronium jarosite, melanterite, goslarite, ferroxahydrite, epsomite, hexahydrite, siderotil, rozenite, anglesite, alunogen, and copiapite), and minerals such as marcasite, covellite, and native sulfur (Jambor, 1994). Pore water from tailings impoundments associated with the Heath Steele, New Brunswick, deposit are acidic (pH 1.8 to 5.2), have Eh of 280 to 580 mV, and contain significant dissolved metal abundances, including 0.3 to 600 mg/l copper, 0.8 to 11 mg/l lead, 23 to 4,880 mg/l zinc, 1,200 to 36,000 mg/l iron, and 600 to 67,600 mg/l sulfate (Boorman and Watson, 1976). Similarly, pore water from tailings impoundments associated with the Waite Amulet, Quebec, deposit are acidic (pH 2.5 to 6.0), have Eh of 200 to 700 mV, and contain significant dissolved metal abundances, including as much as 65 mg/l copper, as much as 5 mg/l lead, as much as 250 mg/l zinc, as much as 8,000 mg/l iron, and as much as 20,000 mg/l sulfate (Blowes and Jambor, 1990). Finally, pore water from tailings impoundments associated with the Kidd Creek, Ontario, deposit are acidic (pH 3.5 to 7.5), have Eh of 50-500 mV, and contain significant dissolved metal abundances, including 0 to 38 mg/l copper, 0 to 2 mg/l lead, 0 to 6,200 mg/l zinc, 0 to 350 µg/l arsenic, 1 to 990 mg/l iron, and 1,860 to 27,000 mg/l sulfate (Al and others, 1994).

Extremely fine grinding required for beneficiation of VMS ore may enhance airborne transport of lead-arsenic-cadmium-antimony-bearing dust. This phenomenon is most probable in semi-arid to arid regions in which strong winds prevail.

#### Soil, sediment signatures prior to mining

The elemental suite and magnitude of geochemical anomalies in soil and sediment collected from undisturbed VMS deposits depend upon a number of factors, including VMS deposit type, extent of ore outcrop or overburden, climate, topography, etc. Stream sediment samples collected below Kuroko-type deposits in temperate rain forest on Admiralty Island, Alaska, contain 5 to 10 weight percent iron, as much as 10,000 ppm barium, hundreds to several thousand ppm zinc, hundreds of ppm lead, tens to hundreds of ppm arsenic, copper, and nickel, as well as 0 to 20 ppm silver, bismuth, cadmium, mercury, molybdenum, and antimony (Kelley, 1990; Rowan and others, 1990; Taylor and others, 1992; C.D. Taylor, unpub. data, 1995).

Stream sediment geochemical signatures associated with undisturbed to variably disturbed Cyprus and Besshi VMS deposits in the Prince William Sound, Alaska, are similar to those just described. They contain 10 to 40 weight percent iron, several hundred ppm barium, hundreds of ppm arsenic and zinc, tens to hundreds of ppm lead, hundreds to thousands of ppm copper, and 0 to 20 ppm silver, bismuth, mercury, molybdenum, and antimony (R.J. Goldfarb, unpub. data, 1995).

#### Potential environmental concerns associated with mineral processing

Tailings ponds below mills are likely to contain high abundances of lead, zinc, cadmium, bismuth, antimony, and cyanide and other reactants used in flotation and recovery circuits. Highly pyritic-pyrrhotitic orebodies that are exposed to oxidation by air circulating through open adits, manways, and exploration drill holes may evolve SO<sub>2</sub> gas; in some cases, spontaneous combustion can cause sulfide ore to burn. Tailings that contain high percentages of non-ore iron sulfide minerals have extremely high acid-generating capacity. Surficial stockpiles of high-sulfide mineral ore are also potential sources of metal-rich mine water.

#### Smelter signatures

Most base-metal rich ore concentrates are smelted. In most cases, concentrates are shipped to custom smelters, and therefore do not contribute to the environmental impact in the immediate mine vicinity. Larger districts are often served by a smelter co-located in the district. Data compiled by Gulson and others (1994) document the relationship between lead in soil near smelters and blood lead in children; similar data for the Leadville, Colo., area indicate similar trends. Additional data may be available for the Trail, British Columbia and El Paso, Tex. smelters.

### Climate effects on environmental signatures

Great differences between geochemical mine drainage data for deposits in the West Shasta, Calif., district, eastern Canada, and that for deposits in cooler and wetter Alaskan climates underscore the important role of climate with regard to acid mine drainage associated with VMS deposits. Acidity and total metal concentrations in mine drainage in arid environments are several orders of magnitude greater than in more temperate climates because of the concentrating effects of mine effluent evaporation and the resulting "storage" of metals and acidity in highly soluble metal-sulfate-salt minerals. However, minimal surface water flow in these areas inhibits generation of significant volumes of highly acidic, metal-enriched drainage. Concentrated release of these stored contaminants to local watersheds may be initiated by precipitation following a dry spell. In wet climates, high water tables may reduce exposure of abandoned orebodies to oxidation and continually flush existing tailings and mine dumps. Although metal-laden acid mine water does form, it is may be diluted to benign metal abundances within several hundred meters of mixing with a higher order stream.

### Geoenvironmental geophysics

Self potential detects electrical potentials produced by ongoing redox reactions. The method is suitable for locating "hot spots" in tailings piles. Electromagnetic surveys are useful for tracing and monitoring metal-bearing ground water. In addition, detailed magnetic data can help delineate geologic contacts, strata, and fractures that may act as fluid conduits, especially in crystalline rocks.

### REFERENCES CITED

- Al, T.A., Blowes, D.W., and Jambor, J.L., 1994, A geochemical study of the tailings impoundment at the Falconbridge Limited, Kidd Creek division metallurgical site, Timmons, Ontario, *in* Jambor, J.L., and Blowes, D.W. eds., *Short Course Handbook on Environmental Geochemistry of Sulfide Mine-wastes*, Mineralogical Association of Canada, v. 22, p. 333-364.
- Alpers, C.N., and Nordstrom, D.K., 1991, Geochemical evolution of extremely acid mine waters at Iron Mountain, California--Are there any lower limits to pH?, *in* *Proceedings, Second International Conference on the Abatement of Acidic Drainage: MEND (Mine Environmental Neutral Drainage)*, Ottawa, Canada, v. 2, p. 321-342.
- Alpers, C.N., Nordstrom, D.K., and Thompson, J.M., 1994, Seasonal variations of Zn/Cu ratios in acid mine waters from Iron Mountain, California, *in* Alpers, C.N., and Blowes, D.W., eds., *Environmental geochemistry of sulfide oxidation*, ACS Symposium Series 550: Washington D.C., American Chemical Society, p. 324-344.
- Blowes, D.W., and Jambor, J.L., 1990, The pore-water geochemistry and the mineralogy of the vadose zone of sulfide tailings, Waite Amulet, Quebec, Canada: *Applied Geochemistry*, v. 5, p. 327-346.
- Boorman, R.S., and Watson, D.M., 1976, Chemical processes in abandoned sulphide tailings dumps and environmental implication for northeastern New Brunswick, *Canadian Institute of Mining and Metallurgy Bulletin*, v. 69, no. 772, p. 86-96.
- Cox, D.P., 1986, Descriptive model of Besshi massive sulfide, *in* Cox, D.P., and Singer, D.A., eds., *Mineral deposit models: U.S. Geological Survey Bulletin 1693*, p. 136.
- Cox, D.P., and Singer, D.A., 1986, Mineral deposit models: U.S. Geological Survey Bulletin 1693, 379 p.
- Filipek, L.H., Nordstrom, D.K., and Ficklin, W.H., 1987, Interaction of acid mine drainage with waters and sediments of West Squaw Creek in the West Shasta mining district, California: *Environmental Science and Technology*, v. 21, no. 4, p. 388-396.
- Fox, J.S., 1984, Besshi-type volcanogenic sulphide deposits--a review, *Canadian Institute of Mining and Metallurgy Bulletin*, v. 77, no. 864, p. 57-68.
- Franklin, J.M., 1993, Volcanic-associated massive sulphide deposits, *in* Kirkham, R.V., Sinclair, W.D., Thorpe, R.I., and Duke, J.M., eds., *Mineral deposit modeling*, Geological Association of Canada Special Paper 40, p. 315-334.
- Franklin, J.M., Sangster, D.M., and Lydon, J.W., 1981, Volcanic-associated massive sulfide deposits, *in* Skinner, B.J., ed., *Economic Geology 75th anniversary volume*, p. 485-626.
- Goldfarb, R.J., Nelson, S.W., Taylor, C.D., d'Angelo, W.M., and Meier, A.L., in press, Acid mine drainage associated with volcanogenic massive sulfide deposits, Prince William Sound, Alaska, *in* Dumoulin, J.A., and Moore, T.E., eds., *Geologic studies in Alaska by the U.S. Geological Survey, 1994: U.S. Geological Survey Bulletin 2152*.
- Greens Creek Environmental Impact Statement, 1983.

- Gulson, B.L., Mizon, K.J., Law, A.J., Korsch, M.J., Davis, J.J., and Howarth, D., 1994, Source and pathways of lead in humans from the Broken Hill mining community--An alternative use of exploration methods: *Economic Geology*, v. 89, p. 889-908.
- Jambor, J.L., 1994, Mineralogy of sulfide-rich tailings and their oxidation products, *in* Jambor, J.L., and Blowes, D.W., eds., *Short Course Handbook on Environmental Geochemistry of Sulfide Mine-wastes: Mineralogical Association of Canada*, v. 22, p. 59-102.
- Kelley, K.D., 1990, Interpretation of geochemical data from Admiralty Island, Alaska--Evidence for volcanogenic massive sulfide mineralization, *in* Goldfarb, R.J., Nash, J.T., and Stoeser, J.W., eds., *Geochemical studies in Alaska by the U.S. Geological Survey, 1989*, U.S. Geological Survey Bulletin 1550, p. A1-A9.
- Kilburn, J.E., Sutley, S.J., and Whitney, G.C., 1995, Geochemistry and mineralogy of acid mine drainage at the Holden mine, Chelan County, Washington: *Explore*, Association of Exploration Geochemists newsletter, no. 87, p. 9-14.
- Kilburn, J.E., Whitney, G.C., d'Angelo, W.M., Fey, D.L., Hopkins, R.T., Meier, A.L., Motooka, J.M., Roushey, B.H., and Sutley, S.J., 1994, Geochemical data and sample locality maps for stream sediment, heavy-mineral-concentrate, mill tailing, water, and precipitate samples in and around the Holden mine, Chelan County, Washington: U.S. Geological Survey Open-File Report 94-680A, 33 p.
- Lydon, J.W., 1984, Volcanogenic massive sulphide deposits, Part 1--A descriptive model: *Geoscience Canada*, v. 11, p. 195-202.
- \_\_\_\_\_, 1988, Volcanogenic massive sulphide deposits, Part 2--Genetic models: *Geoscience Canada*, v. 15, p. 43-65.
- Morton, R.L., Hudak, G., Walker, J., and Franklin, J.M., 1990, Physical volcanology and hydrothermal alteration of the Sturgeon Lake caldera complex, *in* Franklin, J.M., Schneiders, B.R., and Koopman, E.R., eds., *Mineral Deposits in the western Superior province, Ontario: Geological Survey of Canada, Open File 2164*, p. 74-94.
- Ohmoto, H., and Skinner, B.J., 1983, The Kuroko and related volcanogenic massive sulfide deposits: *Economic Geology Monograph* 5, 604 p.
- Plumlee, G.S., Smith, K.S., Ficklin, W.H., Briggs, P.H., and McHugh, J.B., 1993, Empirical studies of diverse mine drainages in Colorado: Implications for the prediction of mine-drainage chemistry: *Proceedings, 1993 Mined Land Reclamation Symposium*, Billings, Montana, v. 1, p. 176-186.
- Plumlee, G.S., Smith, K.S., and Ficklin, W.H., 1994, Geoenvironmental models of mineral deposits, and geology-based mineral-environmental assessments of public lands: U.S. Geological Survey Open-File Report 94-203, 7 p.
- Rowan, E.L., Bailey, E.A., and Goldfarb, R.J., 1990, Geochemical orientation study for identification of metallic mineral resources in the Sitka quadrangle, southeastern Alaska, *in* Goldfarb, R.J., Nash, J.T., and Stoeser, J.W., eds., *Geochemical studies in Alaska by the U.S. Geological Survey, 1989*, U.S. Geological Survey Bulletin 1550, p. B1-B12.
- Singer, D.A., 1986a, Descriptive model of Cyprus massive sulfide, *in* Cox, D.P., and Singer, D.A., eds., *Mineral deposit models: U.S. Geological Survey Bulletin* 1693, p. 131.
- \_\_\_\_\_, 1986b, Descriptive model of Kuroko massive sulfide, *in* Cox, D.P., and Singer, D.A., eds., *Mineral deposit models: U.S. Geological Survey Bulletin* 1693, p. 189-190.
- \_\_\_\_\_, 1986c, Grade and tonnage model of Cyprus massive sulfide, *in* Cox, D.P., and Singer, D.A., eds., *Mineral deposit models: U.S. Geological Survey Bulletin* 1693, p. 131-135.
- \_\_\_\_\_, 1986d, Grade and tonnage model of Besshi massive sulfide, *in* Cox, D.P., and Singer, D.A., eds., *Mineral deposit models: U.S. Geological Survey Bulletin* 1693, p. 136-138.
- Singer, D.A., and Mosier, D.L., 1986, Grade and tonnage model of Kuroko massive sulfide, *in* Cox, D.P., and Singer, D.A., eds., *Mineral deposit models: U.S. Geological Survey Bulletin* 1693, p. 190-197.
- Slack, J.F., 1993, Descriptive and grade-tonnage models for Besshi-type massive sulfide deposits, *in* Kirkham, R.V., Sinclair, W.D., Thorpe, R.I., and Duke, J.M., eds., *Mineral deposit modeling*, Geological Association of Canada Special Paper 40, p. 343-372.
- Stanton, R.L., 1972, *Ore Petrology*, McGraw-Hill, New York, 713 p.
- Taylor, C.D., Cietat, B.A., and Miller, L.D., 1992, A followup geochemical survey of base metal anomalies in the Ward Creek/Windfall Harbor and Gambier Bay areas, Admiralty Island S.E. Alaska, *in* Bradley, D., and Dusel-Bacon, C., eds., *1991 Geologic Studies in Alaska: U.S. Geological Survey Bulletin* 2041, p. 70-85.

# GEOENVIRONMENTAL PROCESSES

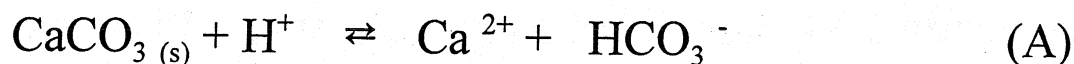
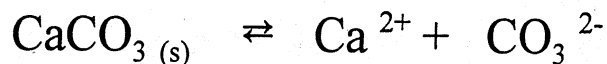
- 1) pyrite oxidation
- 2) oxidation of other sulfides
- 3) oxidation and hydrolysis of aqueous iron and other elements
- 4) neutralizing capacity of gangue minerals and country rock
- 5) neutralizing capacity of bicarbonate-buffered waters
- 6) oxygen transport
- 7) fluid transport of water and water vapor
- 8) form and location of permeable zones relative to flow paths
- 9) climatic variations (diel, storm events, seasonal)
- 10) evaporation, efflorescence, redissolution
- 11) heating by conduction and radiation (due to a variety of exothermic reactions including pyrite oxidation, dissolution of soluble salts, and dilution of concentrated acid)
- 12) temperature
- 13) microbial catalysis of reaction rates
- 14) microbial sorption and uptake of metals
- 15) mineral precipitation and dissolution during transport
- 16) adsorption and desorption of metals during transport
- 17) photoreduction of iron
- 18) organic complexing
- 19) microenvironmental processes (surface films, microbial films, mineral coatings)

TABLE 6.2—Environmental factors affecting acid mine water formation.

	Traditional Scientific Disciplines				
	Inorganic chemistry	Organic chemistry	Geology/ mineralogy	Hydrology	Microbiology
Sulfide oxidation	✓	✓	✓	✓	✓
$\text{Fe}^{(II)}_{(aq)} \rightarrow \text{Fe}^{(III)}_{(aq)}$	✓	✓		✓	✓
pH	✓	✓	✓	✓	✓
Temperature	✓		✓	✓	✓
Gangue dissolution	✓		✓	✓	
Rock type/structure	✓		✓	✓	
Porosity			✓	✓	
Permeability			✓	✓	
Flow paths	✓		✓	✓	
(recharge/discharge)					
Climate	✓			✓	
Evapoconcentration/ efflorescent salt formation	✓		✓	✓	
Efflorescent salt dissolution	✓		✓	✓	
Photochemistry	✓	✓		✓	✓

from Nordstrom and Alpers (1998, in press)

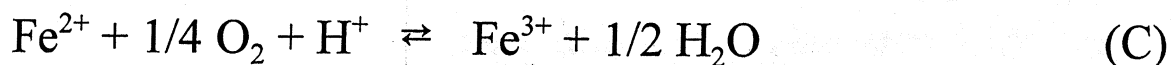
## CALCITE, ARAGONITE



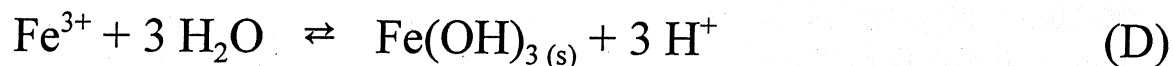
## SIDERITE



## OXIDATION

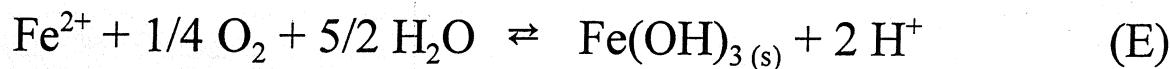


## HYDROLYSIS



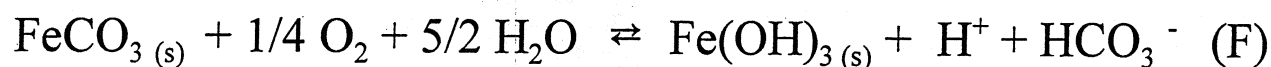
## “FERROLYSIS”

(C+D)=

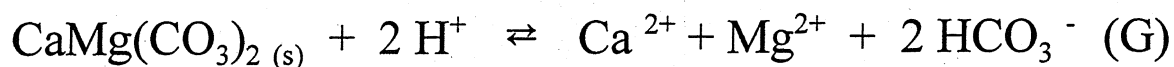


## SIDERITE “FERROLYSIS”

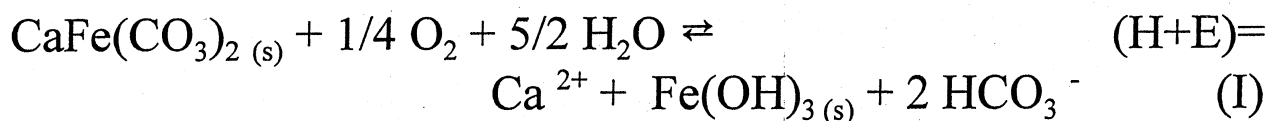
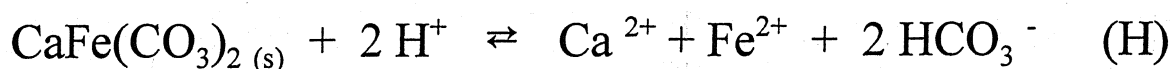
(B+E)=



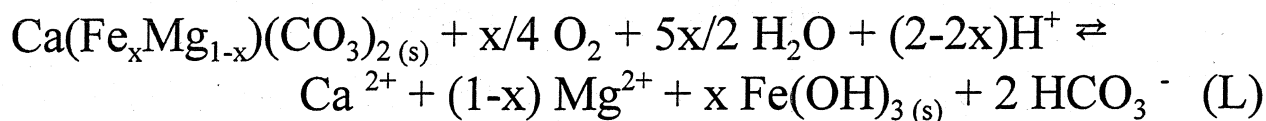
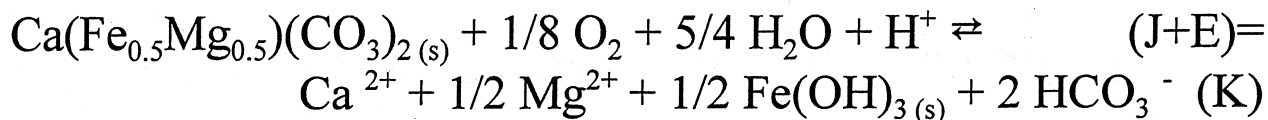
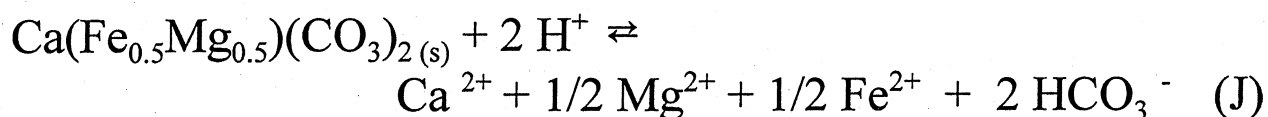
## DOLOMITE

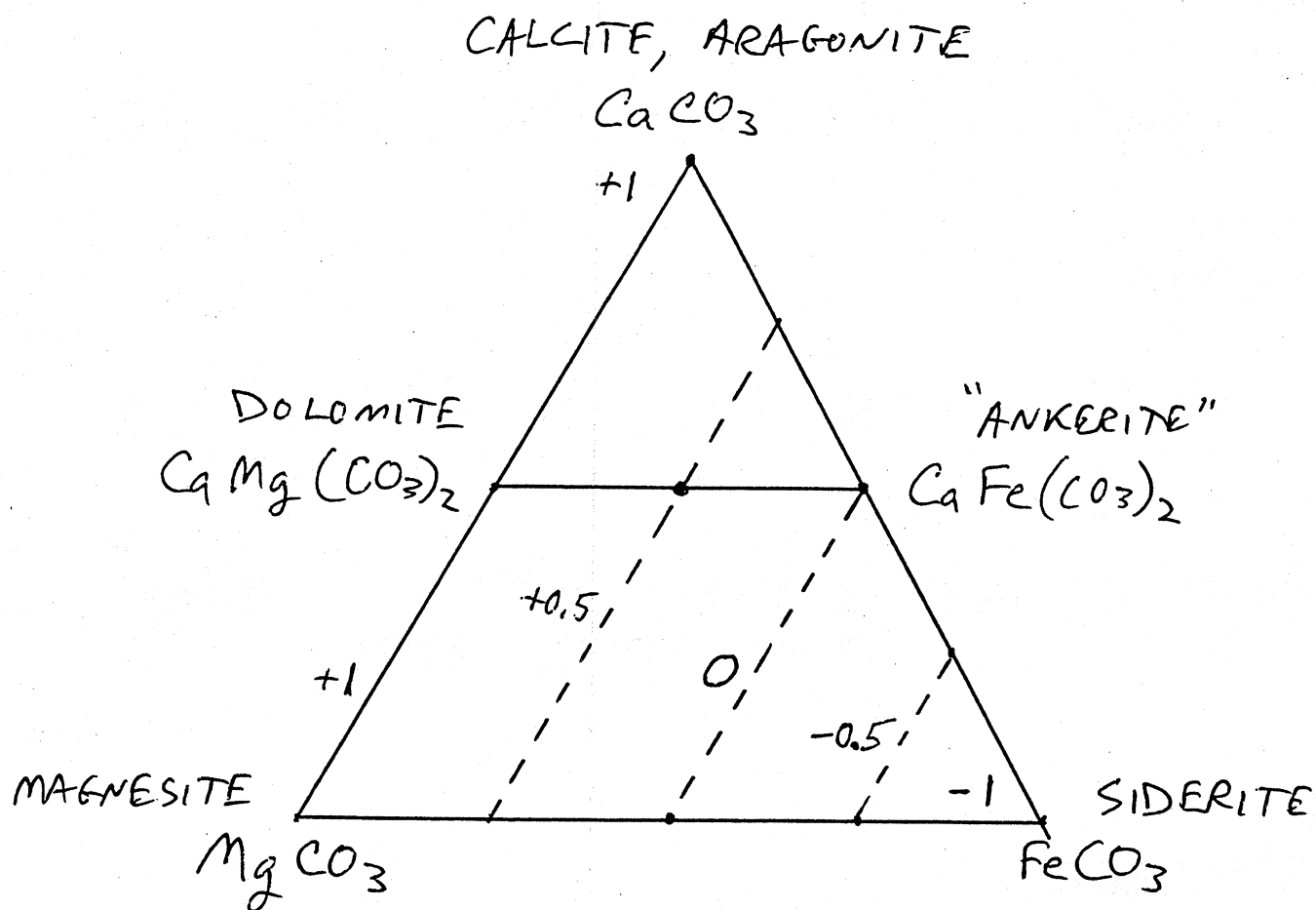


## ANKERITE



## Fe-DOLOMITE





NUMBERS DENOTE NEUTRALIZING  
POTENTIAL IN TERMS OF MOLES  $\text{H}^+$   
NEUTRALIZED (+) OR GENERATED (-)  
PER MOLE OF CARBONATE DISSOLVED,  
ASSUMING COMPLETE IRON OXIDATION  
AND HYDROLYSIS.

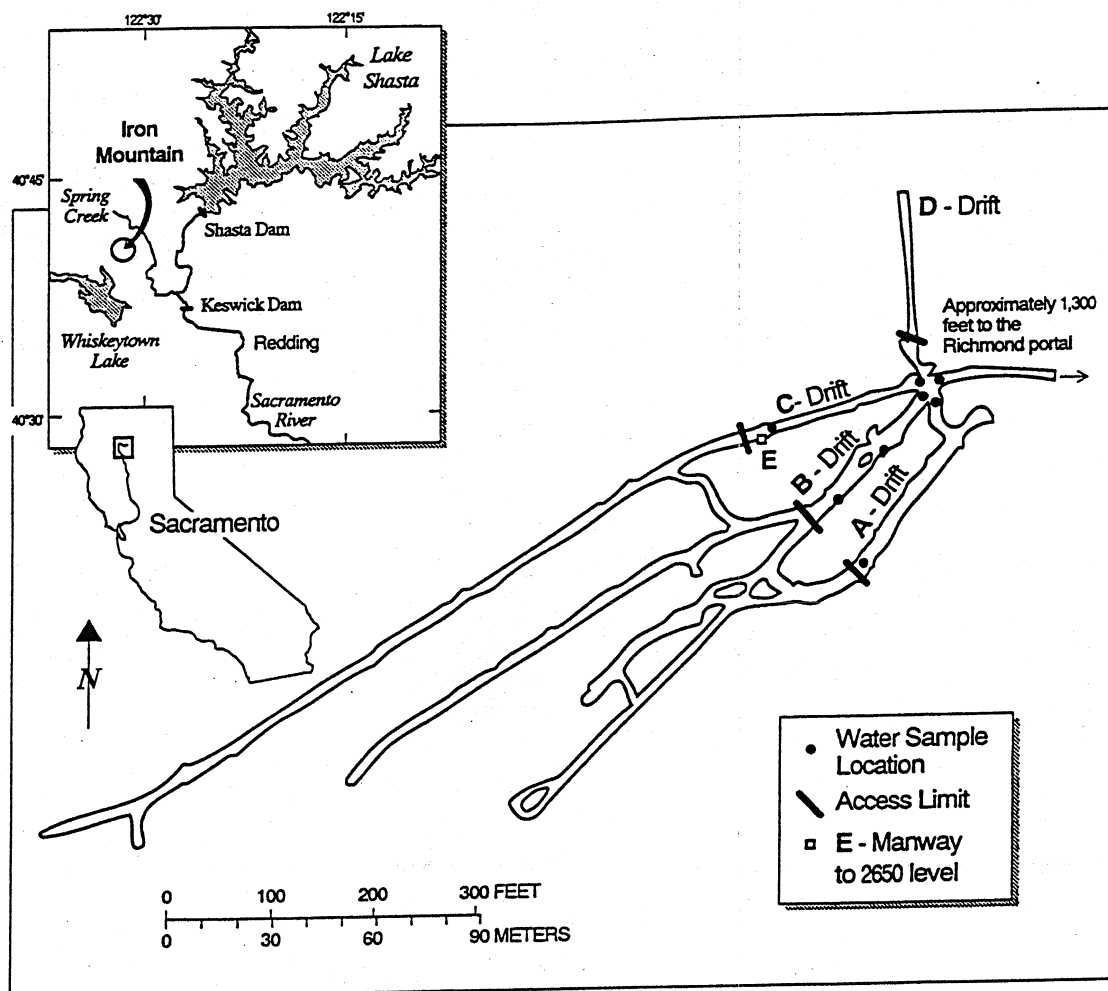


Figure 1. Location of Iron Mountain and plan view of mine workings on 2600 level of Richmond Mine.

from Alpers, Nordstrom, and Burchard (1992)

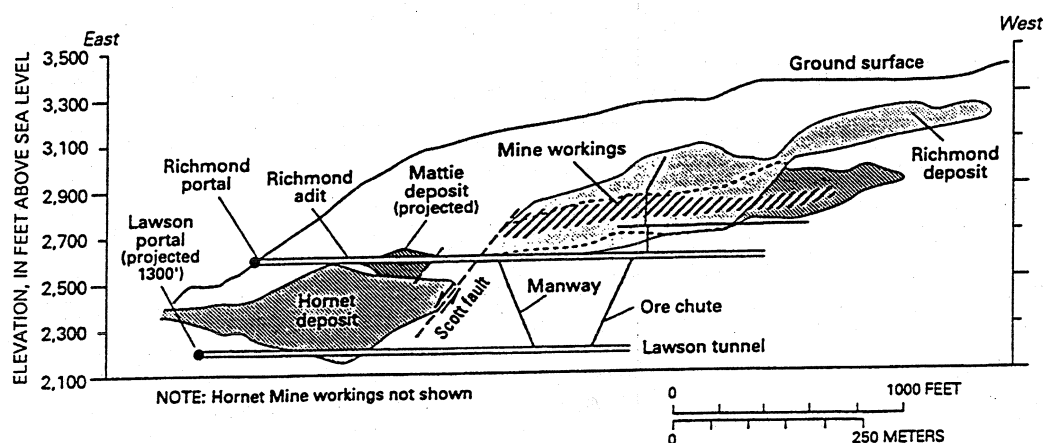


Figure 2. Cross section through Iron Mountain, showing location of Richmond and Hornet deposits, Richmond adit, and Lawson Tunnel.

from Alpers, Nordstrom, and Burchard (1992)



TABLE 14.1—Chemical data for four acid mine water samples. [Samples AMD-A and AMD-B correspond respectively to samples 82WA109 and 82WA110 from the Leviathan mine, Alpine County, California (Ball and Nordstrom, 1989); sample AMD-C corresponds to sample 76WA103 from the Hornet and Richmond mines, Iron Mountain, Shasta County, California (Nordstrom, 1977); sample AMD-D corresponds to sample 90WA103 from the Richmond mine at Iron Mountain (Alpers and Nordstrom, 1991).]

	AMD-A	AMD-B	AMD-C	AMD-D
Sample number	82WA109	82WA110	76WA103	90WA103
Water temperature (°C)	16.0	19.5	24.0	34.8
pH (field)	4.9	3.25	1.10	0.48
Constituent	(mg/l)			
Ca	44.7	82.2	240	183
Mg	13.5	23.6	720	821
Na	8.6	11.8	79.0	251
K	3.21	4.57	107	261
Cl	1.0	1.1	2.0	— <sup>1</sup>
SO <sub>4</sub>	206	483	50,000	118,000
HCO <sub>3</sub>	0	0	0	0
SiO <sub>2</sub>	42.6	46.4	140	165
Ba	0.042	0.048	—	0.068
Al	5.06	19.8	1,410	2,210
F	0.30	0.52	2.0	—
Fe (total)	4.72	18.4	11,000 <sup>3</sup>	20,300
Fe (II)	4.44	9.01	7,820	18,100
Fe (III) <sup>2</sup>	0.28	9.39	3,180	2,200
Mn	1.26	3.04	11.0	17.1
Cu	0.09	0.23	360	290
Zn	0.04	0.15	1,860	2,010
Cd	.004	0.01	14.0	15.9
As (total)	0.01	0.02	—	56.4
As (III)	—	—	—	8.14
As (V) <sup>4</sup>	—	—	—	48.3

<sup>1</sup>—, not determined.

<sup>2</sup>Fe (III) computed as difference of Fe (total) and Fe (II).

<sup>3</sup>Value uncertain by up to 15%.

<sup>4</sup>As (V) computed as difference of As (total) and As (III).

from Alpers and Nordstrom (1998, in press)

TABLE 6.1—Comparison of four of the most acidic mine waters at Iron Mountain, California with the most acidic and metal-rich mine waters reported in the world. (pH values in standard units, concentrations in grams per liter.)

	Iron Mountain (Nordstrom et al., 1991)				Other sites	References
pH	-0.7	-2.6	-2.6	-3.4	0.67	Goleva et al. (1970)
Cu	2.3	4.8	3.2	n.d.	48	Clarke (1916)
Zn	7.7	23.5	20	n.d.	50	Braeuning (1977)
Cd	0.048	0.21	0.011	n.d.	0.041	Lindgren (1928)
As	0.15	0.34	0.22	n.d.	0.40	Goleva (1977)
Fe (total)	86.2	124	141	16.3	48	Blowes et al. (1991)
Fe (II)	79.7	34.5	34.9	9.8	48	Blowes et al. (1991)
SO <sub>4</sub>	360	760	650	n.d.	209	Lindgren (1928)

from Nordstrom and Alpers (1998, in press)

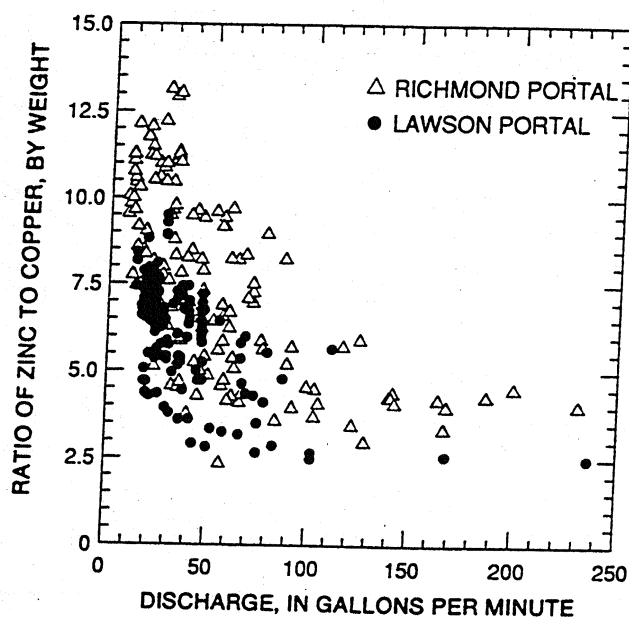


Figure 6. Concentration ratios of zinc to copper as a function of discharge. Richmond and Lawson portal effluents, 1983-91.

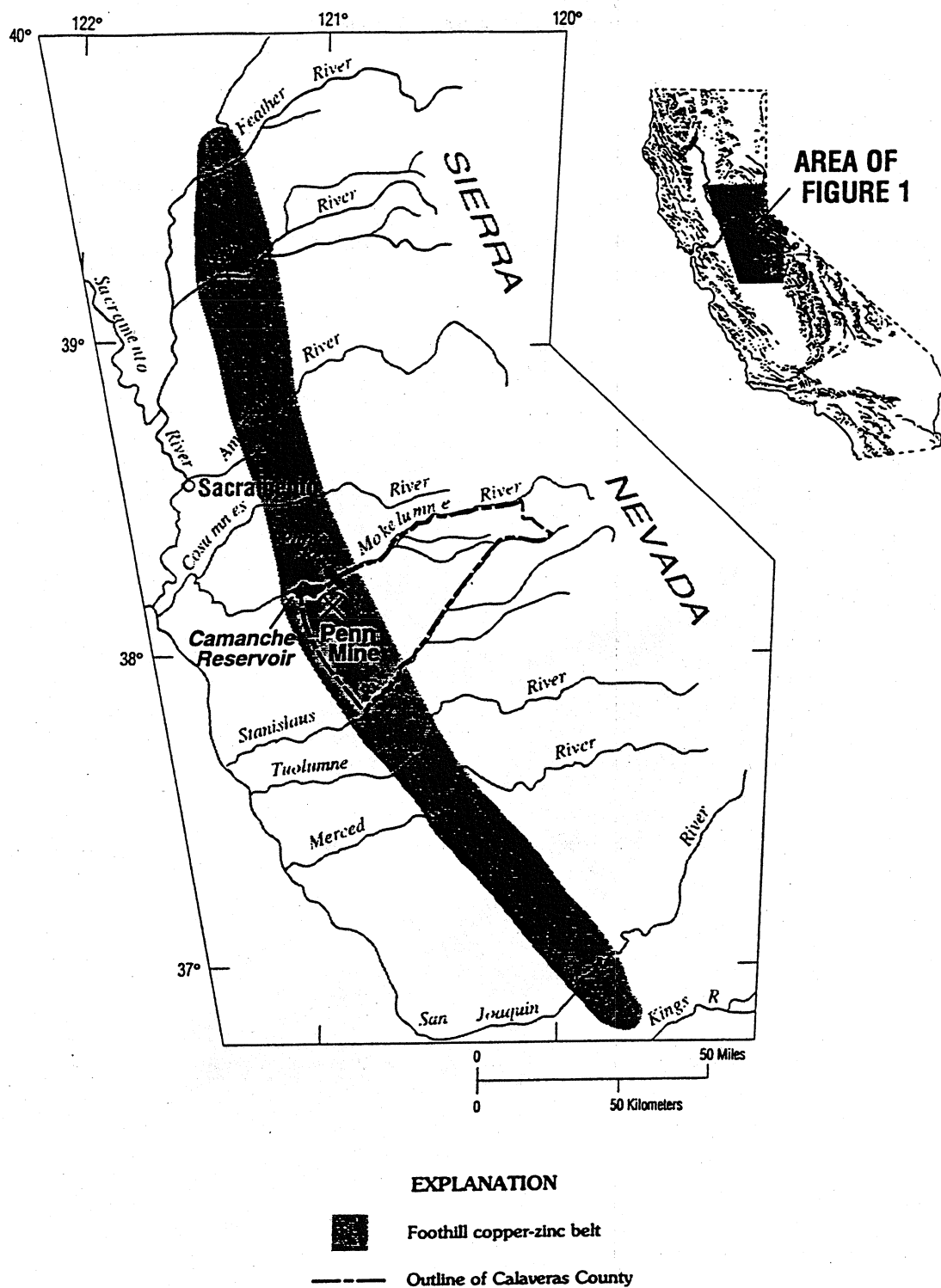
from Alpers, Nordstrom, and Burchard (1992)

Table 1. Characteristics of Lawson and Richmond portal effluents, 1983-91

[Source of data: See appendix B. gal/min, gallon per minute; mg/L, milligram per liter; —, no data]

	Lawson portal effluent		Richmond portal effluent	
	Mean	Range	Mean	Range
Overall				
Discharge (gal/min)	40	13 - 236	70	8 - 800
pH (units)	1.6	0.6 - 2.8	.8	0.02 - 1.5
Zinc (mg/L)	540	280 - 840	1,600	700 - 2,600
Copper (mg/L)	90	50 - 150	250	120 - 650
Zinc/copper (weight ratio)	6.2	2 - 10	7.5	2 - 13
Wet season				
Discharge (gal/min)	—	40 - 80	—	100 - 200+
Zinc/copper (weight ratio)	—	3 - 6	—	3 - 6
Dry season				
Discharge (gal/min)	—	~ 20	—	~ 10
Zinc/copper (weight ratio)	—	4 - 9	—	8 - 13

from Alpers, Nordstrom, and Burchard (1992)



**Figure 1.** Location of Penn Mine and Camanche Reservoir in the Foothill copper-zinc belt of California (after Peterson, 1985).

from Hamlin and Alpers (1996)

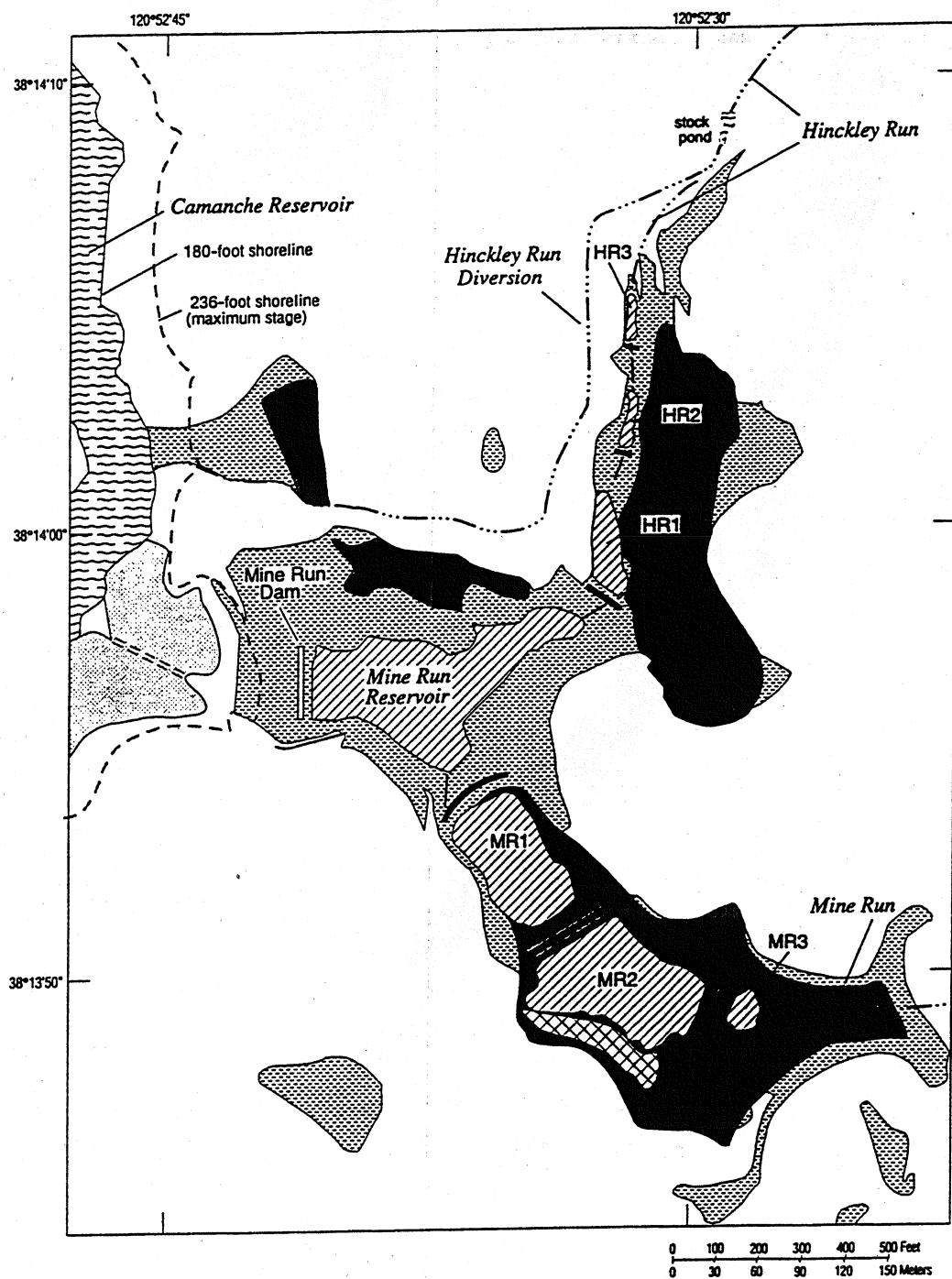
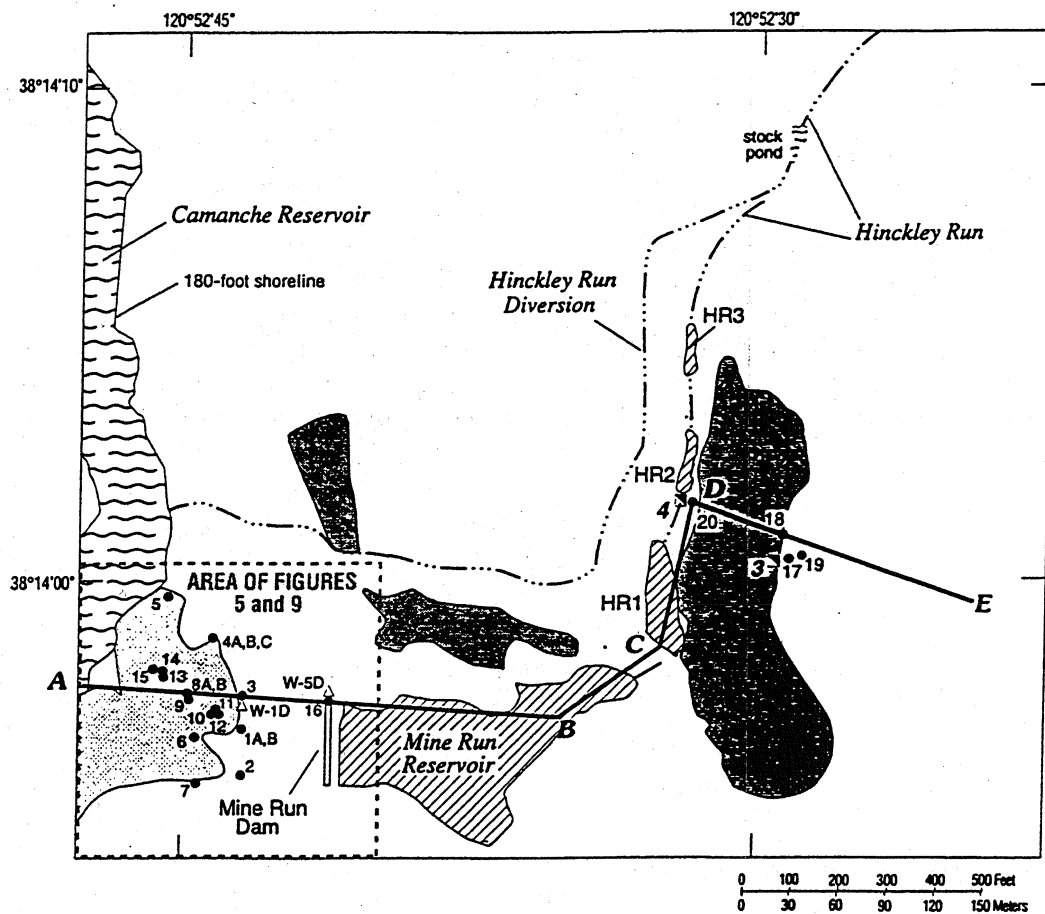


Figure 2. Penn Mine site and location of unlined wastewater impoundments, Calaveras County, California (modified from Davy Environmental, 1993).

from Hamlin and Alpers (1996)



#### EXPLANATION

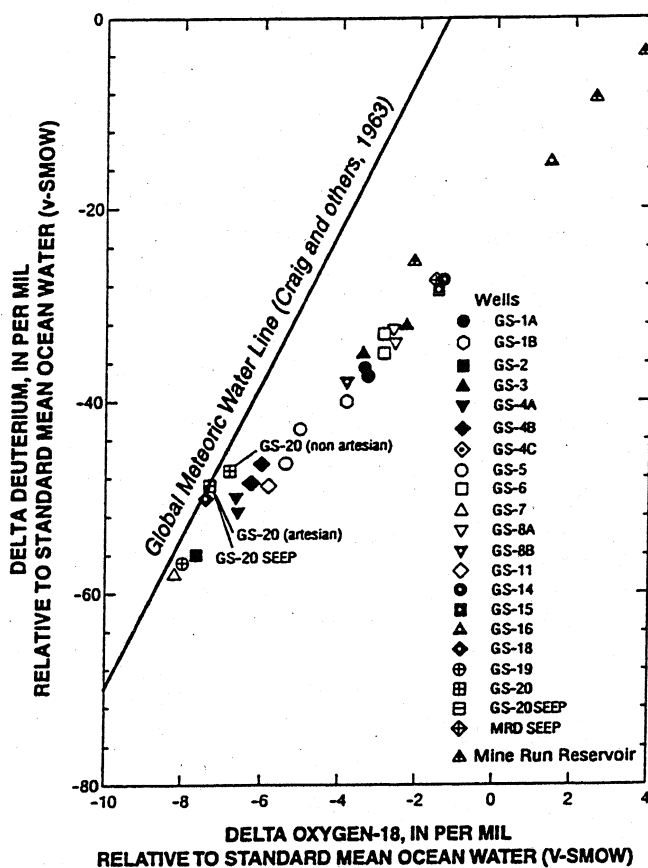
- |       |   |                        |
|-------|---|------------------------|
| A — E | Line of section   | Waste rock             |
| • 2   | USGS well and number — Letters denote depth intervals separated by inflatable packers | Wastewater impoundment |
| 4     | Mine shaft and number   | Slag                   |
| W-5D  | EBMUD well and number   |                        |

Figure 3. Location of monitoring wells and conceptual hydrogeologic section line, Calaveras County, California.

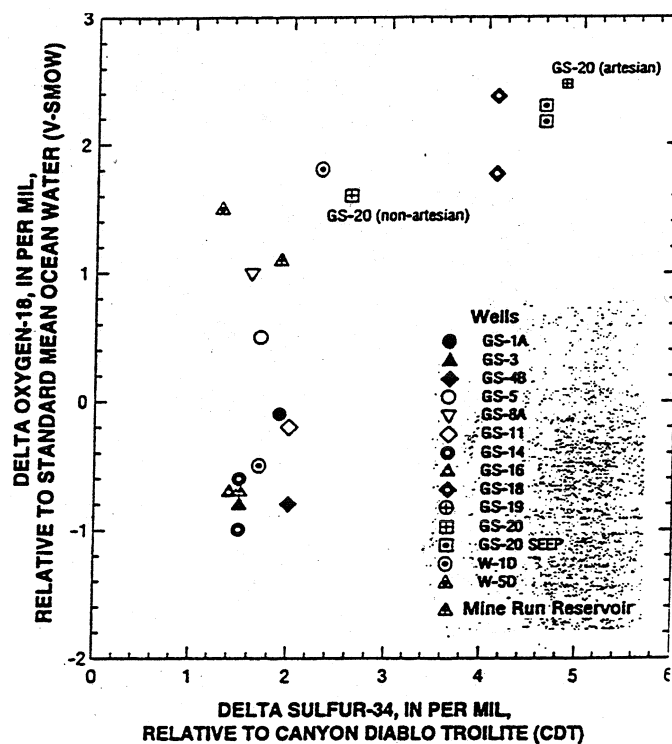
from Hamlin and Alpers (1996)



from Hamlin and Alpers (1996)



**Figure 11.** Stable-isotopic composition of water samples from wells, seeps, and Mine Run Reservoir at Penn Mine, Calaveras County, California, April and December 1992, and January and July 1993.



**Figure 12.** Relation between delta oxygen-18 and delta sulfur-34 in dissolved sulfate at Penn Mine, Calaveras County, California.

**Table 3.** Weight ratios of metals in ground-water and surface-water samples from Penn Mine, Calaveras County, California

[All ratios reported with two significant figures. MRR, Mine Run Reservoir; MRD, Mine Run Dam; Zn, zinc; Cd, cadmium; Cu, copper. —, not determined because one or both of the concentrations was below the detection level]

Well name or sample site	Date	Zn/Cd	Zn/Cu
GS-1A	4-17-92	67	14
	12-15-92	83	15
GS-1B	4-18-92	41	—
GS-3	4-15-92	58	13
	12-19-92	68	23
GS-4A	4-16-92	35	35
	4-16-92	34	31
GS-4B	4-16-92	23	92
	12-15-92	29	65
GS-4C	4-18-92	11	200
	4-13-92	26	30
GS-5	12-18-92	32	15
GS-6	4-15-92	180	10
	4-15-92	250	13
GS-7	4-14-92	130	5.9
GS-8A	12-04-92	310	5.3
GS-8B	4-17-92	310	56
GS-11	12-13-92	420	6.0
GS-14	12-14-92	310	5.5
GS-15	12-19-92	300	5.6
GS-16	12-16-92	330	5.3
GS-18	12-16-92	8,000	3,100
GS-19	12-16-92	23	1.1
GS-20	12-16-92	150	1.7
GS-20 <sup>1</sup>	1-28-93	2,100	680
GS-20-Seep	1-28-93	2,400	800
MRR-A <sup>2</sup>	12-22-92	340	5.2
MRR-A <sup>3</sup>	12-22-92	210	3.2
MRD-Seep	7-07-93	190	3.8
W-1D	12-19-92	300	13
W-5D	12-22-92	340	4.8

<sup>1</sup>Artesian flow.

<sup>2</sup>6 feet below water surface.

<sup>3</sup>1 foot below water surface.

## SELECTED REFERENCES

### GENERAL MINING-ENVIRONMENT GEOCHEMISTRY

- Alpers, C.N. and Blowes, D.W. (eds.), 1994, Environmental Geochemistry of Sulfide Oxidation. ACS Symposium Series, v. 550, American Chemical Society: Washington D.C., 681 p.
- Alpers, C.N., Blowes, D.W., Nordstrom, D.K., and Jambor, J.L., 1994, Secondary Minerals and Acid Mine-Water Chemistry: *In* Environmental Geochemistry of Sulfide Mine-Wastes, Jambor, J.L., and Blowes, D.W. (eds.), Mineralogical Association of Canada, Short Course Notes, v. 22, Waterloo, Ontario, p. 247-270.
- Alpers, C.N., and Nordstrom, D.K., 1998 (in press), Geochemical Modeling of Water-Rock Interactions in Mining Environments: *In* The Environmental Geochemistry of Mineral Deposits. Part A. Processes, Methods, and Health Issues, Plumlee, G.S., and Logsdon, M.J. (eds.) Society of Economic Geologists, Reviews in Economic Geology, v. 6, chapter 14.
- Jambor, J.L., and Blowes, D.W. (eds.), 1994, Environmental Geochemistry of Sulfide Mine-Wastes: Mineralogical Association of Canada, Short Course Notes, v. 22, Waterloo, Ontario.
- Nordstrom, D.K., and Alpers, C.N., 1998 (in press), Geochemistry of Acid Mine Waters: *In* The Environmental Geochemistry of Mineral Deposits. Part A. Processes, Methods, and Health Issues, Plumlee, G.S., and Logsdon, M.J. (eds.) Society of Economic Geologists, Reviews in Economic Geology, v. 6, chapter 6.

### IRON MOUNTAIN MINE, CALIFORNIA, U.S.A.

- Alpers, C.N., Bruns, T.R., Cunningham, K.M., Fujimura, R.W., Huang, C., and Finlayson, B.J., 1994, Geochemical, geophysical, and toxicological characterization of metalliferous bottom sediment from Keswick Reservoir, California: Geological Society of America, Abstracts with Programs, v. 26, No. 7, p. A-435.
- Alpers, C.N., and Nordstrom, D.K., 1991, Evolution of extremely acid mine waters at Iron Mountain, California: Are there any lower limits to pH?, *in* Proceedings, Second International Conference on the Abatement of Acidic Drainage, Montreal, Quebec, Canada, September 16-18, 1991, MEND (Mine Environment Neutral Drainage): Ottawa, Canada, v. 2, p. 321-342
- Alpers, C.N., Nordstrom, D.K., and Ball, J.W., 1989, Solubility of jarosite solid solutions precipitated from acid mine waters, Iron Mountain, California, U.S.A.: Sciences Géologiques, Bulletin, v. 42, p. 281-298.
- Alpers, C.N., Nordstrom, D.K., and Burchard, J.M., 1992, Compilation and interpretation of water-quality and discharge data for acidic mine waters at Iron Mountain, Shasta County, California, 1940-91. U.S. Geological Survey Water-Resources Investigations Report 91-4160.

- Alpers, C.N., Nordstrom, D.K., and Thompson, J.M., 1994, Seasonal variations in the Zn/Cu ratio of acid mine drainage from Iron Mountain, California: *In* Environmental Geochemistry of Sulfide Oxidation, Alpers, C.N. and Blowes, D.W. (eds.) ACS Symposium Series, v. 550, American Chemical Society: Washington D.C., p. 324-344.
- Kinkel, A.R., Jr., Hall, W.E., and Albers, J.P., 1956, Geology and base-metal deposits of the West Shasta copper-zinc district: U.S. Geological Survey Professional Paper 285, 156 p.
- Nordstrom, D.K., and Alpers, C.N., 1995, Remedial investigations, decisions, and geochemical consequences at Iron Mountain Mine, California: Proceedings of Sudbury '95 - Mining and the Environment. Hynes, T.P., and Blanchette, M.C. (eds.), May 28 - June 1, 1995, Sudbury, Ontario, Canada, CANMET, Ottawa. v. 2, p. 633-642.
- Nordstrom, D.K., Alpers, C.N., and Ball, J.W., 1991, Measurement of negative pH and extremely high metal concentrations in acid mine water from Iron Mountain, California. Geological Society of America, Abstracts with Programs, v. 23, No. 5, p. A383.
- Nordstrom, D.K., Alpers, C.N., Ptacek, C.J., and Blowes, D.W., 1996, Measurement of negative pH in ultra-acidic mine waters at Iron Mountain, California: Chapman Conference on Crater Lakes, Terrestrial Degassing, and Hyper-Acid Fluids in the Environment, Crater Lake, Oregon, September 4-9, 1996.

#### **PENN MINE, CALIFORNIA, U.S.A.**

- Alpers, C.N., Hamlin, S.N., and Rye, R.O., 1994, Stable isotopes (O,H,S) distinguish sources of acid drainage at Penn Mine, California: Abstracts of the Eighth International Conference on Geochronology, Cosmochronology, and Isotope Geology (ICOG-8), Berkeley, California, June 5-11, 1994, U.S. Geological Survey Circular 1107, Lanphere, M.A., Dalrymple, G.B., and Turrin, B.D. (eds.), p. 4
- Hamlin, S.N., and Alpers, C.N., 1995, Hydrogeology and Geochemistry of Acid Mine Drainage in Ground Water in the Vicinity of Penn Mine and Camanche Reservoir, Calaveras County, California: First-Year Summary: U.S. Geological Survey Water Resources Investigations Report 94-4040, 45 p.
- Hamlin, S.N., and Alpers, C.N., 1996, Hydrogeology and Geochemistry of Acid Mine Drainage in Ground Water in the Vicinity of Penn Mine and Camanche Reservoir, Calaveras County, California: Second-Year Summary, 1992-93: U.S. Geological Survey Water Resources Investigations Report 96-4257, 44 p.
- Hunerlach, M.P., and Alpers, C.N., 1994, Analysis of fracture orientations in surface outcrops and boreholes in the vicinity of an acidic ground-water plume at Penn Mine, Calaveras County, California. *In* EOS, Transactions American Geophysical Union, v. 75, no. 44, November 1, 1994 Supplement, p. 243.



## P - GEOENVIRONMENTAL CHARACTERISTICS OF EPITHERMAL AND PORPHYRY DEPOSITS

Geoffrey S. Plumlee, U.S. Geological Survey, Denver, CO 80225

Plumlee, G.S. (1998): Geoenvironmental Characteristics of Epithermal and Porphyry Deposits; in Metallogeny of Volcanic Arcs, B.C. Geological Survey, Short Course Notes, Open File 1998-8, Section P.

### ABSTRACT

The geologic characteristics of mineral deposits exert important and predictable controls on both the natural environmental signatures of mineralized areas prior to mining (such as natural acid-rock drainage and metal-bearing stream sediments) and the environmental signatures that result from mining and mineral processing (such as mine-drainage and tailings waters, mine wastes, and smelter emissions). A good understanding of the environmental geology of mineral deposits is therefore key to the development of effective mining-environmental prediction, mitigation, and remediation practices.

The environmental signatures of adularia-sericite epithermal deposits (such as Creede and Sunnyside, Colorado) can vary greatly within a district, deposit, and vein, due to the geologic complexity of the deposits (marked by strong mineral zoning, complex fracture-controlled ground water flow, and highly variable wallrock alteration). The abundance of carbonate in gangue and wallrock alteration in many of these deposits can lead to relatively near-neutral-pH mine- and natural-drainage waters; however, due to the enrichment of Zn and Mn in most ores and the relatively high mobility of these metals over a relatively broad pH range, near-neutral drainage waters frequently carry significant quantities of Zn and Mn in solution (as high as 100 ppm) and sorbed on suspended particulates (total concentrations as high as several hundreds of ppm). In contrast carbonate-poor, sulfide-rich ores, such as occur in some veins at Creede, can have quite acidic (pH 3-5) drainage waters with high levels of dissolved or particulate Fe, Al, Cu, Zn, Pb, As, and other metals (tens to hundreds of ppm).

The geoenvironmental characteristics of high-sulfidation (quartz-alunite, acid-sulfate) epithermal deposits (such as Summitville, Colorado, Round Mountain, Nevada, and Julcani, Peru) strongly reflect the intense pre-ore acid sulfate alteration of the deposit host rocks by magmatic gas condensates. The acid-sulfate alteration (which produced core zones of vuggy silica, quartz-alunite, and quartz-kaolinite, flanked by argillic and then propylitic assemblages) essentially removed all acid-buffering capacity from the host rocks in the cores of the deposits. Subsequent to the acid-sulfate alteration events, hydrothermal fluids deposited pyrite, marcasite, enargite, covellite, chalcocite, native sulfur, and barite in the intensely altered rocks. The net results of the alteration and mineralization processes are deposits which, unless completely oxidized during exposure and weathering, have extreme acid generating potential and minimal acid-buffering potential in their main ore zones. These characteristics are manifested in the compositions of mine waters and natural waters draining unmined deposits. In general, the mine waters draining the acid-sulfate alteration zones are highly acidic (pH 2-3), with high to extreme concentrations of dissolved metals such as: Fe and Al (thousands to several tens of thousands of ppm); Zn, Cu, and Mn (hundreds to low thousands of ppm); and As, Cr, Co, Ni, REE, U, Th, and Be (hundreds of ppb to several ppm). Natural waters draining unmined, mineralized, acid-sulfate-altered rocks tend to have generally similar ranges of pH values and Fe and Al concentrations to those of

the mine waters, but somewhat lower levels of Zn, Cu, and other metals, due to the lack of sulfide exposure at the ground surface. From an exploration and production standpoint, quartz-alunite epithermal deposits that will have the lowest potential environmental mitigation costs are those that either were completely oxidized prior to mining, or that occur in very dry climates where mining activity does not intersect the water table.

Porphyry-Cu and Cu-Mo deposits, as well as Climax-type porphyry-Mo deposits, tend to discharge quite acidic (pH 2-4), mine waters with elevated Al and Fe (hundreds to thousands of ppm), and Cu and Zn (several hundreds of ppm) from their core potassic and phyllic alteration zones; due to the low contents of Zn in the high-grade porphyry ores, the waters are generally enriched in Cu relative to Zn. Waters with near-neutral pH (6-7) and generally low levels of dissolved metals (less than several hundreds of ppm dissolved Zn, Cu, etc.) typically drain the distal, carbonate-bearing propylitic alteration zones of porphyry deposits. Natural waters draining the potassic and phyllic zones of unmined porphyry deposits can be quite acidic and Al- and Fe-rich. However, natural drainage waters tend to have lower concentrations of metals such as Cu and Zn than mine waters draining geologically similar ore types, unless the Cu-sulfides were exposed at the ground surface by rapid physical erosion or glaciation. Due to the abundance of U and F in the Climax-type porphyry Mo deposits, the mine drainage waters can have quite high dissolved concentrations of F (as high as 700-800 mg/L) and U (as high as 8-9 ppm).

#### USEFUL REFERENCES

- Alpers, C.N., and Blowes, D.W., eds., 1994, Environmental geochemistry of sulfide oxidation, ACS Symposium Series 550: Washington, D.C., American Chemical Society, 681 p.
- du Bray, E., 1995, Preliminary descriptive geoenvironmental mineral-deposit models: U.S. Geological Survey, Open-File Report 95-231, 272 p. (also available online at <http://minerals.cr.usgs.gov/>)
- Gray, J.E., Coolbaugh, M.F., Plumlee, G.S., and Atkinson, W. W., 1994, Environmental geology of the Summitville Mine, Colorado: Economic Geology, Special Issue on Volcanic Centers as Exploration Targets, v. 89, no. 8., p. 2006-2014.
- Jambor, J.L., and Blowes, D.W., eds., 1994, Short course on environmental geochemistry of sulfide-mine wastes: Mineralogical Association of Canada, Short Course Handbook, Volume 22, 438 p.
- Kwong, Y.T.J., 1993, Prediction and prevention of acid rock drainage from a geological and mineralogical perspective: MEND Project 1.32.1, 47 p.
- Nordstrom, D.K., and Alpers, C.N., 1998 in press, The geochemistry of acid mine waters, in Plumlee, G.S., and Logsdon, M.J., eds., The Environmental Geochemistry of Mineral Deposits-Part A; Processes, methods, and health issues: Society of Economic Geologists Reviews in Economic Geology, Volume 6A.
- Plumlee, G.S., 1998 in press, The environmental geology of mineral deposits, in Plumlee, G.S., and Logsdon, M.J., eds., The Environmental Geochemistry of Mineral Deposits-Part A; Processes,

methods, and health issues: Society of Economic Geologists Reviews in Economic Geology, Volume 6A.

Plumlee, G.S., and Edelman, P., 1995, An update on USGS studies of the Summitville Mine and its downstream environmental effects: U S. Geological Survey, Open-File Report 95-23, 9 p. (also available online at <http://minerals.cr.usgs.gov/>)

Plumlee, G. S., Gray, J. E., Roeber, M. M., Jr., Coolbaugh, M., Flohr, M., and Whitney, G., 1995, The importance of geology in understanding and remediating environmental problems at Summitville, in: Posey, H. H., Pendleton, J. A., and Van Zyl, D., eds: Summitville Forum Proceedings, Colorado Geological Survey, Special Publication 38, p. 13-22.

Plumlee, G.S., Smith, K.S., Montour, M.R., Ficklin, W.H., and Mosier, E.L., 1998 in press, Geologic controls on the composition of mine waters and natural waters draining diverse mineral-deposit types, in: Filipek, L.H., and Plumlee, G.S., eds., The Environmental Geochemistry of Mineral Deposits-Part B; Case studies and Research Topics: Society of Economic Geologists Reviews in Economic Geology, Volume 6B.

Plumlee, G. S., Smith, K. S., Mosier, E. L., Ficklin, W. H., Montour, M., Briggs, P. H., and Meier, A. L., 1995, Geochemical processes controlling acid-drainage generation and cyanide degradation at Summitville, in: Posey, H.H., Pendleton, J. A., and Van Zyl, D., eds: Summitville Forum Proceedings, Colorado Geological Survey, p. 23-34.

Smith, K.S., Plumlee, G.S., and Ficklin, W.H., 1994, Predicting water contamination from metal mines and mining waste: Notes, Workshop No. 2, International Land Reclamation and Mine Drainage Conference and Third International Conference on the Abatement of Acidic Drainage: U.S. Geological Survey, Open-File Report 94-264, 112 p.

## CREEDE, COMSTOCK, AND SADO EPITHERMAL VEIN DEPOSITS (MODELS 25b,c, and d; Mosier and others, 1986a,b, and c)

by Geoffrey S. Plumlee, Kathleen S. Smith, Byron R. Berger,  
Nora Foley-Ayuso, and Douglas P. Klein

### SUMMARY OF RELEVANT GEOLOGIC, GEOENVIRONMENTAL, AND GEOPHYSICAL INFORMATION

#### Deposit geology

These deposits consist of veins, stockwork veins, and mineralized breccias associated with intermediate to felsic volcanic centers in areas of regional faulting. Simple and complex sulfide minerals (those that contain arsenic, antimony, or bismuth), gold, electrum, silver,  $\pm$  telluride and selenide minerals are important ore constituents. Quartz, carbonate minerals, and adularia ( $\pm$  barite, chalcedony, and fluorite) are important gangue minerals. Mineral assemblages in many veins are characterized by well developed lateral and vertical zonation; this zonation may be present within an ore shoot, within a vein or vein system, or within entire districts. Most Creede-type veins are silver-rich, and are dominated by pyrite, sphalerite, galena, and chalcopryrite; variable amounts of carbonate minerals, quartz, and barite are present. Most Comstock-type veins are gold-rich, and are dominated by quartz and adularia  $\pm$  carbonate minerals; pyrite, sphalerite, galena, and other sulfide minerals comprise less than several percent of these veins. Sado-type veins are copper-rich equivalents of Comstock-type veins; quartz, adularia, and carbonate minerals are more abundant than chalcopryrite. Wall rock alteration assemblages, including silicic, propylitic, argillic, and advanced argillic assemblages, associated with all three epithermal vein deposit types display well developed lateral and vertical zonation. Intense silicification and pervasive argillic and advanced argillic alteration are common adjacent to shallow parts of veins, wall rock near deep parts of veins is moderately affected by silicification ( $\pm$  potassic alteration), and wall rock distal to veins contains propylitic mineral assemblages.

#### Examples

Creede-type: Creede, Silverton, Bonanza, Colo.; Worlds Fair, Ariz. Comstock-type: Comstock, Nev. Sado-type: Sado, Japan.

#### Spatially and (or) genetically related deposit types

Associated deposit types (Cox and Singer, 1986) include hot-spring Au-Ag (Model 25a); quartz alunite-epithermal (Model 25e); and, if carbonate-bearing rocks are present, polymetallic replacement (Model 19a) deposits.

#### Potential environmental considerations

- (1) Geoenvironmental signatures associated with different parts of epithermal vein deposits are highly variable on all scales due to well developed spatial zonation within vein and alteration mineral assemblages.
- (2) Pyrite contents of vein ore and carbonate contents of ore and wall rock principally determine the pH and metal content of water draining mines, mine waste piles, and tailings associated with epithermal vein deposits. Veins that contain abundant pyrite and base metal sulfide minerals, relative to carbonate minerals, and veins in rocks with low acid-buffering capacity, such as those affected by silicification and argillic or advanced argillic alteration, have enhanced potential for associated acidic drainage water that contains elevated abundances of dissolved iron, aluminum, manganese, zinc, copper, and lead. Water draining pyrite- and carbonate-rich ore or ore hosted by carbonate-bearing rocks tends to have near-neutral pH but elevated abundances of copper and zinc.
- (3) Historically, gold-rich ore was processed by crushing and mercury amalgamation; soil and stream sediment around historic mining and milling sites may be mercury contaminated. After the late 1800s or early 1900s, amalgamation was less common in ore processing; instead, sulfide-mineral-rich ore was roasted and gold was recovered by cyanidation. After milling, some of this ore was smelted. Soil in areas around roasting or smelting sites may be contaminated by elevated abundances of lead, zinc, copper, arsenic, or antimony.

Mitigation and remediation strategies for potential environmental concerns presented above are described in the section below entitled "Guidelines for mitigation and remediation."

#### Exploration geophysics

Geophysical expressions of precious-metal epithermal veins and stockworks have been reviewed by Allis (1990), Irvine and Smith (1990), Klein and Bankey (1992), and Watson and Knepper (1994). Silicic and carbonate alteration of volcanic rocks produces reflectance and thermal infrared contrasts and increases their resistivity and density; the extent of associated anomalies can be delineated with detailed gravity, multispectral remote sensing (Arribas and

others, 1989; Collins, 1989), and direct current and electromagnetic (Nishikawa, 1992) surveys, respectively. Gravity anomalies may be complicated by open fractures and brecciated rock, which reduce bulk density. Electrical and gravity anomalies associated with epithermal deposits may be difficult to distinguish from those caused by small intrusions or faults. Resistivity lows and reflectance contrasts associated with argillically altered rock can be delineated by electrical mapping (Bisdorf, 1995) and multispectral remote sensing, respectively. The distribution of clay zones and electrical chargeability associated with sulfide minerals can be mapped with induced polarization. Airborne photography and side-looking radar can identify topographic features that may be related to resistant silicic and carbonate zones and easily-weathered areas affected by argillic alteration. Areas that contain altered magnetite can be outlined by magnetic surveys. Rock affected by potassic alteration can be identified by spectral gamma-ray surveys. Regional gravity, aeromagnetic, and satellite or airborne remote sensing images may help identify linear, circular, and intersecting features associated with calderas and faulted volcanic terranes in which additional detailed surveys are warranted.

#### References

Geology: Becker (1882), Steven and Ratté (1965), Buchanan (1981), Berger and Eimon (1983), Hayba and others (1985), Heald and others (1987).

Environmental geology and geochemistry: Moran (1974), Plumlee and others (1993), Smith and others (1994).

### GEOLOGIC FACTORS THAT INFLUENCE POTENTIAL ENVIRONMENTAL EFFECTS

#### Deposit size

The size of most deposits is small (10,000 tonnes) to moderate (several million tonnes). However, a few districts are large to extremely large, including Casapalca, Peru, and Comstock, Nev. (10-20 million tonnes), and Pachuca-Real del Monte (Mexico) (>100 million tonnes).

#### Host rocks

Epithermal vein deposits are in intermediate to felsic volcanic rocks (andesite, dacite, quartz-latite, rhyodacite, and rhyolite) and associated volcanoclastic and sedimentary rocks (for example, those deposited in volcanic depressions such as caldera moats).

#### Surrounding geologic terrane

Most epithermal vein deposits are areas of regional faulting within intermediate to felsic volcanic fields, including volcanoes and caldera complexes from which volcanic rocks that host the deposits were erupted.

#### Wall-rock alteration

Wall rock alteration assemblages are characterized by strong vertical and lateral zonation between deep, central parts of veins and shallow and (or) distal parts of veins (fig. 1). In many (but not all) districts, host volcanic rocks are altered to propylitic assemblages, including chlorite, epidote, calcite, and pyrite, on a regional or district-wide basis; this type of alteration is distal to most veins. In the central parts of districts alteration varies as a function of depth. At deep levels, the alteration assemblage is characterized by quartz and chlorite  $\pm$  some potassic alteration (adularia). At intermediate levels the alteration assemblage consists of quartz; sericite; and illite, which may grade upward and distally to lower-temperature smectite;  $\pm$  zeolite minerals. At shallow levels, alteration is characterized by massive silicification, formation of chalcedonic sinter, and pervasive acid-sulfate alteration, including alteration to kaolinite and alunite. In laterally distal parts of districts, rock adjacent to veins may be locally silicified and (or) pyritized. In some places, wall rock along upper parts of veins may be altered to illite, smectite, and alunite or kaolinite.

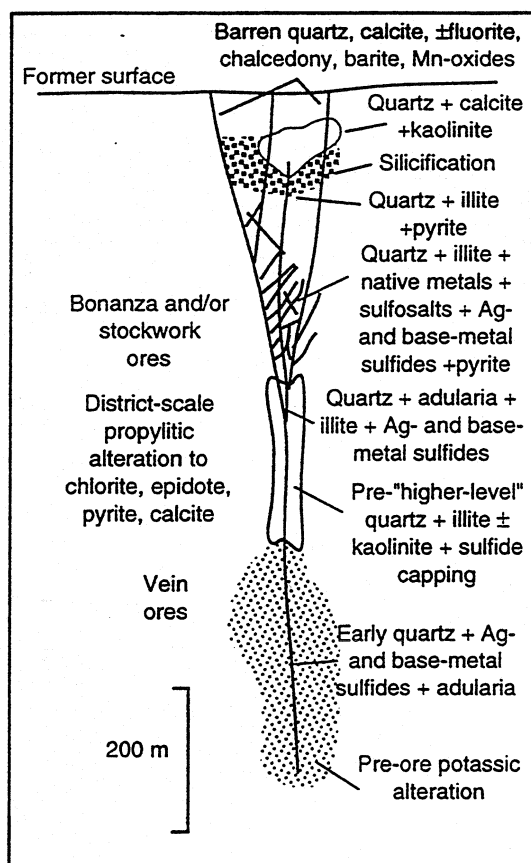
#### Nature of ore

Veins and stockwork veins fill fractures in intermediate to felsic volcanic rocks. Veins vary greatly in width, from less than several cm to more than 3 m. Most veins display banded layers characterized by substantial mineralogic differences; the veins can also be quite vuggy and include considerable open space.

#### Deposit trace element geochemistry

The geochemistry of epithermal veins varies laterally and vertically. Altered wall rock adjacent to veins can have significant enrichments in mineralization-related trace elements (Foley and Ayuso, 1993).

Creede-type: Specific parts of these veins are characterized by elevated abundances of various elemental suites as follows: Deep parts of central veins- Au, Cu, Pb, Zn,  $\pm$ Ag,  $\pm$ Te,  $\pm$ Se. Intermediate parts of central veins- Pb, Zn,



**Figure 1.** Schematic cross section through an epithermal vein deposit showing distribution of vein and wall rock alteration minerals. Modeled primarily after Creede-type veins; however, with the exception that base metal sulfide minerals are less abundant, the same general zoning patterns are present in Comstock-type vein ore. Figure modified from Mosier and others (1986a) and Berger and Eimon (1983).

Ag, Cu,  $\pm$ Mn. Intermediate to shallow parts of central and distal veins- As, Sb, Hg,  $\pm$ Au,  $\pm$ Mn,  $\pm$ Se. Distal, deep parts of veins- Ag, Pb, Zn,  $\pm$ Cu,  $\pm$ Ba,  $\pm$ As,  $\pm$ Sb,  $\pm$ Mn,  $\pm$ Se.

Sado and Comstock-type: Geochemical zonation within most Comstock-type veins is similar to that in Creede-type veins, except that lead and zinc are less abundant throughout all parts of veins.

#### Ore and gangue mineralogy and zonation

Minerals are listed in approximate decreasing order of abundance. Potentially acid-generating minerals are underlined; those that are acid-generating when oxidized by aqueous ferric iron are denoted by \*.

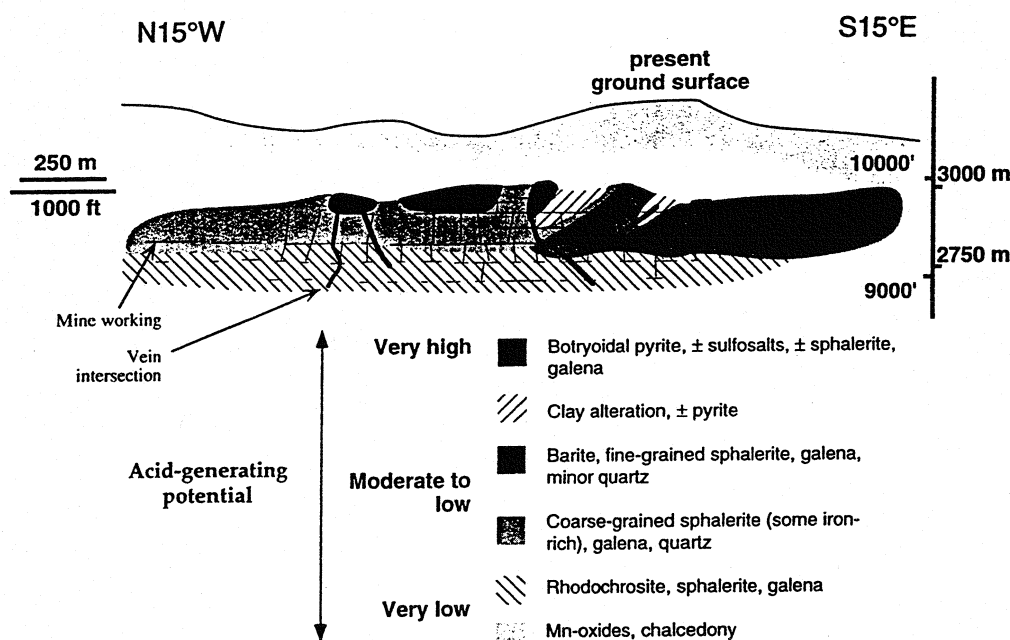
Creede-type veins are base-metal sulfide mineral rich. They contain abundant sphalerite\*, galena\*, chalcopryrite, and pyrite; lesser amounts of many other sulfide and sulfosalt minerals, such as argentite\*, tetrahedrite, pyrargyrite, ±marcasite, ±botryoidal pyrite; and variable but generally subordinate amounts of quartz, carbonate minerals (including rhodochrosite, calcite, Mn-siderite), adularia, fluorite, manganese silicate minerals (such as pyroxmangite), barite, and chalcedony.

Comstock- and Sado-type veins are dominated by quartz and adularia and contain variable amounts of carbonate minerals and generally subordinate amounts of sulfide minerals, including pyrite, sphalerite\*, galena\*, chalcopryrite, and arsenopyrite.

All three vein types tend to be enriched in manganese; abundances of rhodochrosite or manganese calcite are moderate to high, and manganese silicate minerals are also abundant. Well developed lateral and vertical vein mineralogy zonation is typical within ore shoots, within veins, and across districts (figs. 1 and 2). This zonation results from variations in the hydrologic and geochemical processes that prevailed during hydrothermal ore genesis.

#### Mineral characteristics

Textures: Mineral grains can vary from fine to coarse (<1 mm to >10 cm), depending upon the particular district



**Figure 2.** Longitudinal section of the A vein, Bulldog Mountain vein system, Creede district, Colorado, showing lateral and vertical vein mineral zoning patterns. The various mineralogic zones are ranked according to their potential to generate acid drainage water from mine workings or mine waste. A poorly-welded ash-flow tuff occurs immediately above the botryoidal pyrite zone. Fracture permeability in this ash flow tuff is very low, and so the botryoidal pyrite has largely escaped oxidation even though it occurs well above the present water table, which is within the deep rhodochrosite-dominant zone. Ground water that does penetrate beneath the ash flow tuff becomes highly acid, but evaporates, while still in the mine workings, and leaves behind melanterite and goslarite efflorescent salts. Figure modified from Plumlee and Whitehouse-Veaux (1994).

and location within the district. Textures range from euhedral to botryoidal to massive. Crustification sequences are often well developed; bands comprised of one mineral assemblage may be overgrown by one or more successive, mineralogically distinct bands.

Trace element contents: Sphalerite can have low to high iron contents (<1 to >15 mol percent), several tenths to 1 mol percent cadmium, and minor amounts of other trace elements, including silver. Galena can contain silver; <1 mol percent in most cases. Botryoidal pyrite and marcasite can have very high concentrations (as much as 15 weight percent, combined) of arsenic, antimony, silver, mercury, tellurium, selenium, and (or) gold. Carbonate minerals commonly form extensive solid solutions that include manganiferous calcite, kutnahorite, and siderite.

General weathering rates: Euhedral to massive, coarse-grained, interlocking sulfide minerals weather at very slow rates; samples of these crystals exposed on mine dumps in cool wet climates for >100 years can still appear fresh and unweathered. Most botryoidal pyrite and marcasite, especially if enriched in arsenic, antimony, and other trace elements, weather very rapidly, in some cases simply by atmospheric water vapor sorption. Rates at which carbonate minerals weather are variable, but increase with decreasing grain size and increasing trace element content. For example, iron-rich calcite and rhodochrosite weather more readily than equivalent minerals with low iron contents. Weathering rates for minerals can be quite high in warm, humid climates.

#### Secondary mineralogy

Readily soluble minerals underlined. Minerals formed by weathering prior to mining include goethite, jarosite, alunite, halloysite, anglesite, cerussite, smithsonite, manganese-oxide minerals (psilomelane, pyrolusite, braunite), and cerargyrite. Minerals formed by weathering subsequent to mining are primarily soluble sulfate minerals indicative of deposition from locally highly acidic water. Zinc sulfate minerals include goslarite. Iron sulfate minerals noted in published reports include melanterite, although other sulfate minerals, such as copiapite, are also probably present in pyrite-rich ore. Hydrated ferric oxide and iron hydroxysulfate minerals, such as ferrihydrite and schwertmanite, precipitate from acidic to near-neutral mine- and natural- drainage water. Aluminum hydroxysulfate minerals, including basaluminite and jurbanite, precipitate from water having pH between 4.5 and 5.

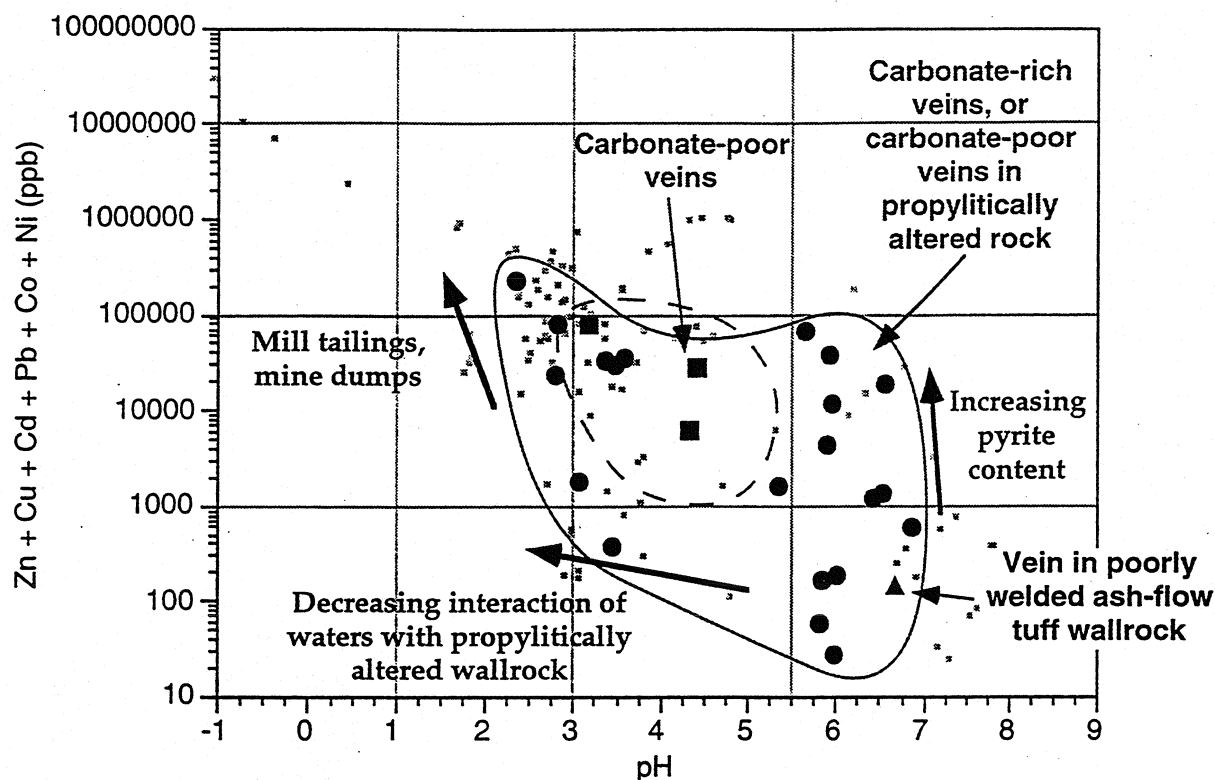


Figure 3. Ficklin plot showing variations in pH and sum of dissolved base metals Zn, Cu, Cd, Co, Ni, and Pb in mine and natural water draining epithermal veins of various geologic characteristics.

#### Topography, physiography

Silicified zones and quartz-chalcedony veins tend to form topographic highs. Clay altered zones probably erode more rapidly than adjacent less altered rocks, and form topographic lows.

#### Hydrology

Mine workings provide the most permeability for ground water flow. Faults, joints, and veins, which also focus ground water flow, provide the greatest natural permeability. Flow along unmineralized fractures and vuggy, open-space veins with continuous permeability is greatest; flow along veins completely filled by ore and gangue is minimal. Fracture permeability is also commonly reduced where fractures cross poorly welded ash flow tuffs, and in zones of intense clay alteration; these rocks and altered zones are aquitards or barriers to ground water flow. For example, epithermal ore at Creede is capped by poorly welded tuff that inhibited ascending hydrothermal fluids that formed the deposit and presently inhibits descending oxidized ground water. Most of a zone of botryoidal pyrite that formed directly beneath the cap rock is unoxidized even though it occurs well above the present-day water table; as a result, acid drainage from the botryoidal pyrite zone is very limited, and evaporates prior to exiting mine workings developed in the zone. Zones of hydrothermal brecciation can also be ground water conduits, provided sufficient open space remains; if no open space is present, these breccia zones may impede ground water flow.

#### Mining and milling methods

Historic: Most epithermal veins were mined in underground tunnels and stopes. However, open pits and glory holes developed in some districts. Mineral processing typically involved milling, gravity separation of coarse precious metals, mercury amalgamation to extract gold and silver, and flotation to extract lead, zinc, and copper. Sulfide concentrates were smelted in some historic districts.

Modern: Due to the potential for ore dilution by wall rock, vein ore is still largely extracted by underground mining. Deposits in which economic ore is disseminated through large volumes of near-surface rock, such as shallow stockwork vein systems or mineralized sedimentary rocks exposed in caldera moats, can be mined using open pit



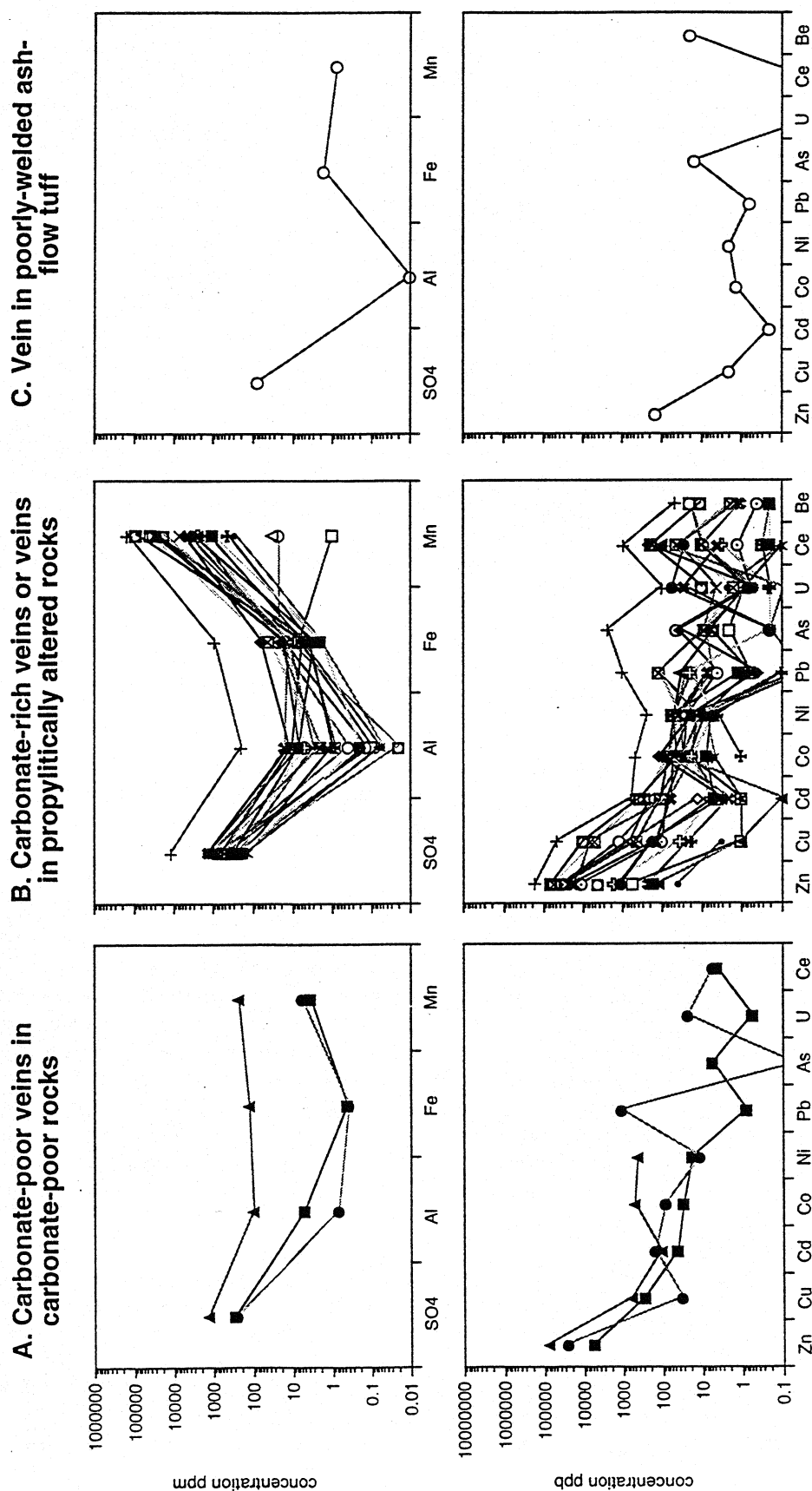


Figure 4. Plots showing concentrations of dissolved constituents in water draining epithermal veins of various geologic characteristics.

techniques. After the late 1800s to early 1900s, processing by amalgamation was increasingly replaced by cyanidation; most sulfide-mineral-rich ore has been roasted prior to cyanidation. Advances in mineral processing technology have recently led to a decline in roasting, however. Most modern processing involves milling, which is followed by cyanidation and extraction of precious metals via carbon-in-pulp or electrowinning. Stopes are backfilled with coarse tailings materials and fine tailings are stored in surface impoundments.

## ENVIRONMENTAL SIGNATURES

### Drainage signatures

Mine-drainage data: Mine drainage data (figs. 3 and 4) pertinent to the Creede, Silverton, and Bonanza, Colo., and Worlds Fair, Ariz., deposits are summarized from Moran (1974), Plumlee and others (1993), Smith and others (1994), and Plumlee and others (in press).

Mine water that drains underground workings in deposits that contain sphalerite, galena, and pyrite in ore with low carbonate mineral contents tends to be acidic, pH ranges from 3 to 5, and contain elevated dissolved metal abundances, including hundreds of mg/l iron, aluminum, and manganese; several to several tens of mg/l zinc and copper; and as much as 1 mg/l lead. Water draining arsenic- and pyrite-rich ore can potentially contain several hundreds of  $\mu\text{g/l}$  to several mg/l dissolved arsenic.

Water that drains pyrite-rich tailings and waste dumps can be quite acidic and contain elevated dissolved metal abundances, including thousands of mg/l iron, aluminum, and manganese; tens to hundreds of mg/l zinc and copper; and hundreds of  $\mu\text{g/l}$  to several mg/l lead, cadmium, arsenic, and other metals.

Mine water that drains underground workings in carbonate-rich ore, or ore in which water reacts with propylitically altered rock, tends to be near-neutral, pH values range from 5.5 to 7, and contain as much as tens of mg/l dissolved zinc and several mg/l dissolved copper, if ore is pyrite rich.

Mine water that drains underground workings in pyrite-rich veins hosted by propylitically altered rocks can be highly acidic and contain high dissolved metal contents if water flows along veins and does not react with wall rock carbonate minerals. As an example, in 1973, water in the Rawley drainage tunnel, which drains pyrite-sphalerite-galena veins in the Bonanza district, Colo., had a pH near 3.2 and contained high dissolved metal abundances (Moran, 1974). Subsequently, the adit collapsed, which eliminated interaction between ore and atmospheric oxygen and increased interaction between water and carbonate minerals in propylitically altered wall rock. Consequently, the water now has pH values near 6 (Plumlee and others, 1993; Smith and others, 1994) and contains significantly lower dissolved iron and aluminum contents; zinc and copper abundances are essentially unchanged.

Mine water that drains a vein hosted by poorly-welded ash-flow tuff (Creede, Colo.) has a near-neutral pH of 6.7 and contains low dissolved metal contents (Plumlee and others, 1993). The near-neutral pH may result from interaction between water and fine-grained, devitrified glass in poorly welded tuff. Low metals contents may reflect a lack of base metal sulfide minerals in the veins.

Manganese enrichments characteristic of epithermal vein ore cause mine drainage water to have elevated manganese abundances relative to those of iron and aluminum.

Natural-drainage data: Water draining broad areas of propylitically altered rocks can have near-neutral pH and relatively low dissolved abundances of aluminum, lead, arsenic, and copper. This water may have slightly elevated dissolved abundances of some metals, including as much as several mg/l zinc, iron, and manganese. Water draining sulfide-bearing fractures has significantly lower pH and contains correspondingly higher dissolved metal abundances.

### Metal mobility from solid mine wastes

Metals and acid are readily liberated from pyrite-rich mine waste and intermittently wet/dry mine workings due to the rapid dissolution of soluble secondary salts. Secondary salt dissolution (and resulting acid and metal generation) is much more rapid than acid consumption by carbonate minerals in dumps or surrounding mine workings. The soluble salts form coatings on mine waste, and fracture fillings in rocks and coatings on mine workings above the water table.

Storm water samples: No data available. However, vegetation kill zones downhill from pyrite-rich mine dumps indicate that highly acidic, metal-rich water can be generated, particularly by secondary salt dissolution, in spite of abundant carbonate-rich rocks on mine dumps.

### Soil, sediment signatures prior to mining

Elevated abundances of some metals, including Pb, Mn, Fe,  $\pm$  Zn, Cu, As, Sb, Hg?, are probably present downslope from vein outcroppings due to mechanical erosion of oxidized vein ore. Elevated abundances of elements

concentrated in oxidized vein ore, including Pb, Mn, Fe,  $\pm$  Zn, Cu, As, Sb, Hg?, are probably dispersed into nearby stream sediments.

#### Potential environmental signatures associated with mineral processing:

Historically, gold-rich ore was processed using crushing and mercury amalgamation. Consequently, soil around historic mining and milling sites may be contaminated with mercury. After the late 1800s or early 1900s, processing by amalgamation became less common; sulfide-rich ore was roasted and treated by cyanidation. Roaster particulates may potentially have contaminated soil and sediment in areas surrounding roasting sites with various metals, including lead, zinc, copper, arsenic, antimony, tellurium, and selenium.

#### Smelter signatures

Sulfide-rich ore was smelted in a number of historic districts. In districts with identified historic smelting activity, soil may contain locally elevated abundances of lead, zinc, copper,  $\pm$ arsenic,  $\pm$ antimony,  $\pm$ selenium,  $\pm$ tellurium.

#### Climate effects on environmental signatures

Currently available data mostly pertain to moderately wet, seasonally temperate climatic regimes of the Rocky Mountains; limited data are available for the Worlds Fair, Ariz., district in a relatively hot, dry climate. Mine drainage in the Worlds Fair district has significantly lower pH and higher metal contents than water draining geologically similar veins in a cooler climate at Creede, Colo. Lower pH and higher metal contents may reflect increased evaporation within mine workings, and periodic formation and flushing of soluble salts; however, more data are needed to verify this speculation. No data are available on effects relating to evaporation of near-neutral pH water draining carbonate-rich ore; evaporation of iron-poor water probably causes pH to increase. Mobilization of arsenic, uranium, and possibly selenium (if present in ore) may be enhanced in dry climates if drainage water is alkaline. Climate can strongly affect mineral weathering rates; rates are greatest in warm, humid climates.

#### Potential environmental effects:

Acid drainage from pyrite- and sulfide-rich veins may adversely affect ground water quality in either wet or dry climates.

(1) The greatest potential for deleterious downstream environmental effects pertain to deposits that consist of pyrite-, sphalerite-, galena-, ( $\pm$ chalcopyrite)-rich ore in carbonate-mineral poor veins; deposits in volcanic terranes minimally affected by propylitic alteration, in which associated water has low acid-buffering capacity; and deposits in which historic mining operations released significant volumes of fine-grained pyritic tailings, which have become part of the sediment column, into rivers or streams. Oxidation of associated tailings can facilitate long-term metal and acid releases, which result in water quality degradation. Downstream effects of acid drainage can be potentially extensive; copper, zinc, manganese, and lesser cadmium can remain mobile for significant distances downstream.

(2) Less significant downstream effects are most likely to be associated with deposits that principally consist of carbonate-bearing vein ore; veins in propylitically altered rock, which tend to have drainage water with near-neutral pH values; and deposits in dry climates, where water evaporates or seeps underground. Zinc and manganese are the principal elements that remain mobile, either in solution or as colloids (Kimball and others, 1995), for the greatest distances downstream. Some arsenic, uranium, selenium, and molybdenum may be mobilized if drainage water is alkaline.

(3) Zones that contain abundant botryoidal pyrite or marcasite have especially high acid drainage generation potential.

(4) Acidic, metal-rich water can develop in pyrite-rich tailings or waste dumps, even if carbonate minerals are present because secondary salt dissolution, and resulting acid and metal generation, is much more rapid than acid consumption by carbonate minerals.

(5) Arsenic and antimony, to a lesser extent, may pose health risks in water draining ore that contains abundant sulfosalt or sulfide minerals that contain elevated abundances of arsenic and antimony; arsenic and antimony abundances are greatest in acid water, but can be moderately high in near-neutral water.

#### Guidelines for mitigation and remediation:

Careful documentation of district- and mine-scale mineral zoning patterns; rock, soil, and water chemistry; and structural features is important to understand potential variability of environmental signatures.

(1) Acid water can be remediated successfully using lime addition and sodium-bisulfide precipitation of metals; a potentially acid-generating sludge is created. If drainage water is relatively iron-poor, such as most water having near-neutral pH, the amount of particulates formed by liming may be insufficient to effectively sorb all zinc,

cadmium, and nickel. Lime addition to iron-rich drainage water may generate sufficient suspended particulates onto which a major fraction of dissolved arsenic, lead, and copper can sorb, thereby reducing or eliminating need for sodium bisulfide addition; the resulting particulate sludge is non-acid-generating as well. If ore is arsenic-, selenium- or uranium-rich, liming to excessively high pH values may enhance mobility of these elements.

(2) The utility of carbonate-bearing, propylitically altered host rocks in acid drainage mitigation should be considered. For example, acid water could be channeled, away from veins, through these rocks via artificial or natural fractures to help reduce acidity.

(3) Constructed wetlands may be useful in mitigation of less acidic mine water.

(4) Careful mapping of fractures, which focus ground water flow, and poorly welded ash flow tuffs and clay alteration zones, which restrict ground water flow, is essential for an adequate understanding of site hydrology.

(5) Isolation of pyrite-rich waste from weathering and formation of soluble secondary salts is crucial in eliminating storm- and snowmelt-related pulses of acid and metals into surface water. High carbonate mineral content in dump material is not sufficient to prevent acid pulses because soluble secondary salts generate acid and metals much faster than carbonate minerals can consume acid.

(6) In modern milling operations, pyritic parts of mill tailings should be used as underground backfill to prevent accidental release of acid-generating material into downstream sediments.

#### Geoenvironmental geophysics

Geophysical applications to geoenvironmental investigations are reviewed by King and Pesowski (1993), Watson and Knepper (1994), and Paterson (1995). An example high-resolution airborne multispectral imagery applied to a geoenvironmental investigation is given by King (1995). Highly acidic and (or) metal-enriched ground water is highly conductive and may produce vegetation stress; associated anomalies can be identified by electrical and multispectral imaging methods, respectively. Surface water that contains suspended materials or has high conductivity can also be identified on multispectral imagery. Electrically conductive clay aquitards formed during mineralization or by weathering of ash-flow tuff can be delineated using electromagnetic and induced polarization/resistivity techniques. Distributions of electrically chargeable sulfide minerals can be mapped with induced polarization. Shallow mine workings may be located by electrical, seismic refraction, and gravity surveys, and may be identifiable on infrared thermal imagery. Low-resistivity fluids, whose flow is channeled by brecciated rock, faults, and joints, can be identified by gravity and electrical surveys.

#### REFERENCES CITED

- Allis, R.G., 1990, Geophysical anomalies over epithermal systems: *Journal of Geochemical Exploration*, v. 36, p. 339-374.
- Arribas, Antonio, Jr., Rytuba, J.J., Rye, R.O., Cunningham, C.G., Podwysocki, M.H., Kelly, W.C., Arribas, Antonio, Sr., McKee, E.H., and Smith, J.G., 1989, Preliminary study of the ore deposits and hydrothermal alteration in the Rodalquilar caldera complex, southeastern Spain: U.S. Geological Survey Open-file Report 89-327, 39 p.
- Becker, G.F., 1882, *Geology of the Comstock Lode and the Washoe district*: U.S. Geological Survey Monograph 3, 422 p.
- Berger, B.R., and Eimon, P.I., 1983, Conceptual models of epithermal metal deposits in Shanks, W.C., ed., *Cameron Volume on Unconventional Mineral Deposits*: Society of Mining Engineers, New York, p. 191-205.
- Bisdorf, R.J., 1995, Correlation of electrical geophysical data with lithology and degree of alteration at the Summitville mine site, in *Summitville Forum '95*: Colorado Geological Survey, Special Publication 38, p. 70-63.
- Buchanan, L.J., 1981, Precious metal deposits associated with volcanic environments in the southwest, in Dickinson, W.R., and Payne, W.D., eds., *Relations of Tectonics to Ore Deposits in the Southern Cordillera*: Arizona Geological Society Digest, v. XIV, p. 237-261.
- Collins, A.H., 1989, Thermal-infrared spectra of altered volcanic rocks in the Virginia Range, Nevada: *Proceedings of the 7th Thematic Conference on Remote Sensing for Exploration Geologists*, October 2-6, 1989, Calgary, Alberta, Canada, Environmental Research Institute of Michigan, Ann Arbor, Michigan, p. 1335-1340.
- Cox, D.P., and Singer, D.A., 1986, Mineral deposit models: U.S. Geological Survey Bulletin 1693, 379 p.
- Foley, N.K., and Ayuso, R.A., 1993, Trace element and Pb isotopic geochemistry of Au-Ag vein assemblages and volcanic wall rock, North Amethyst, Creede district, CO [Abs]: *Abstracts with Programs, Geological Society of America*, v. 25, p. A-164.

- Hayba, D.O., Bethke, P.M., Heald, P., and Foley, N.K., 1985, Geologic, mineralogic, and geochemical characteristics of volcanic-hosted epithermal precious metal deposits, *in* Berger, B.R., and Bethke, P.M., eds., *Geology and Geochemistry of Epithermal Systems: Society of Economic Geologists Reviews in Economic Geology*, v. 2, p. 129-168.
- Heald, P., Foley, N.K., and Hayba, D.O., 1987, Comparative anatomy of volcanic-hosted epithermal deposits; acid-sulfate and adularia-sericite types: *Economic Geology*, v. 82, p. 1-26.
- Irvine, R.J. and Smith, M.J., 1990, Geophysical exploration for epithermal gold deposits: *Journal of Geochemical Exploration*, v. 36, no. 1/3, p. 375-412.
- Kimball, B.A., Callender, E., and Axtmann, E.A., 1995, Effects of colloids on metal transport in a river receiving acid mine drainage, upper Arkansas River, Colorado, USA: *Applied Geochemistry*, v. 10, p. 285-306.
- King, T.V.V., 1995, Environmental considerations of active and abandoned mine lands: U.S. Geological Survey Bulletin 2220, 38 p.
- King, A. and Pesowski, M., 1993, Environmental applications of surface airborne geophysics in mining: *Bulletin of the Canadian Institute of Mining and Metallurgy Bulletin*, v. 86, no. 966, p. 58-67.
- Klein, D.P., Bankey, V.L., 1992, Composite geophysical model for continental volcanic-hosted epithermal mineralization: Cox and Singer mineral deposit models numbered 25b, 25c, 25d, and 25e: U.S. Geological Survey Open-file Report 92-389, 15 p.
- Moran, R.E., 1974, Trace element content of a stream affected by metal-mine drainage, Bonanza, Colorado: Austin, University of Texas, Ph.D. thesis, 167 p.
- Mosier, D.L., Berger, B.R., and Singer, D.A., 1986c, Descriptive model of Sado epithermal veins, *in* Cox, D.P., and Singer, D.A., eds., *Mineral Deposit Models: U.S. Geological Survey Bulletin 1693*, p. 154.
- Mosier, D.L., Sato, T., Page, N.J., Singer, D.A., and Berger, B.R., 1986a, Descriptive model of Creede epithermal veins, *in* Cox, D.P., and Singer, D.A., eds., *Mineral Deposit Models: U.S. Geological Survey Bulletin 1693*, p. 145-146.
- Mosier, D.L., Singer, D.A., and Berger, B.R., 1986b, Descriptive model of Comstock epithermal veins, *in* Cox, D.P., and Singer, D.A., eds., *Mineral Deposit Models: U.S. Geological Survey Bulletin 1693*, p. 150.
- Nishikawa, Nobuyasu, 1992, The use of electrical methods in recent exploration for epithermal gold deposits in Japan: *Exploration Geophysics*, v. 23, no.1 and 2, p. 249-254.
- Paterson, Norman, 1995, Application of geophysical methods to the detection and monitoring of acid mine drainage: *in* Bell, R.S., *Proceedings of the symposium on the application of geophysics to engineering and environmental problems: Orlando, Florida, April 23-26, 1995, Environmental and Engineering Geophysical Society*, p. 181-189.
- Plumlee, G.S., Smith, K.S., Ficklin, W.H., Briggs, P.H., and McHugh, J.B., 1993, Empirical studies of diverse mine drainages in Colorado: implications for the prediction of mine-drainage chemistry: *Proceedings, 1993 Mined Land Reclamation Symposium, Billings, Montana*, v. 1, p. 176-186.
- Plumlee, G.S., Smith, K.S., Montour, M., Mosier, E.L., Ficklin, W.H., *in press*, Geology-based models for the prediction of mine drainage composition: *Society of Economic Geology Reviews in Economic Geology*, v. 6B.
- Plumlee, G.S., and Whitehouse-Veaux, P.H., 1994, Mineralogy, paragenesis, and mineral zoning along the Bulldog Mountain vein system, Creede District, Colorado: *Economic Geology, Special Issue on Volcanic Centers as Exploration Targets*, v. 89, no. 8, p. 1883-1905.
- Smith, K.S., Plumlee, G.S., and Ficklin, W.H., 1994, Predicting water contamination from metal mines and mining waste: Notes, Workshop #2, International Land Reclamation and Mine Drainage Conference and Third International Conference on the Abatement of Acidic Drainage: U.S. Geological Survey Open-file Report 94-264, 112 p.
- Steven, T.A., and Ratte, J.C., 1965, Geology and structural control of ore deposition in the Creede district, San Juan Mountains, Colorado: U.S. Geological Survey Professional Paper 487, 90 p.
- Watson, Ken and Knepper, D.H., eds., 1994, Airborne remote sensing for geology and the environment - present and future: U.S. Geological Survey Bulletin 1926, 43 p.
- White, N.C., and Hedenquist, J.W., 1995, Epithermal gold deposits: styles, characteristics, and exploration: *Society of Economic Geologists Newsletter*, October, 1995, n. 23.

## EPITHERMAL QUARTZ-ALUNITE AU DEPOSITS (MODEL 25e; Berger, 1986)

by Geoffrey S. Plumlee, Kathleen S. Smith, John E. Gray, and Donald B. Hoover

### SUMMARY OF RELEVANT GEOLOGIC, GEOENVIRONMENTAL, AND GEOPHYSICAL INFORMATION

#### Deposit geology

Central advanced argillic zone has iron-, copper-, and arsenic-rich sulfide and sulfosalt minerals with high acid-generating capacity; deposits consist of vuggy veins and breccias in highly acid-altered volcanic rocks with very low acid-consuming capacity. Central advanced-argillic zone is flanked by argillic and distal propylitic zones with some acid-buffering capacity, decreased copper and arsenic abundances, and increased zinc and lead abundances.

#### Examples

Summitville and Red Mountain Pass, Colo.; Goldfield, Nev.; Paradise Peak, Nev.; Julcani, Peru.

#### Spatially and (or) genetically related deposit types

Associated deposit types (Cox and Singer, 1986) include porphyry copper (Model 17), porphyry gold-copper (Model 20c), and porphyry copper-molybdenum (Model 21a).

#### Potential environmental considerations

(1) Dominant mining activity is in sulfide-mineral-rich, strongly altered volcanic rocks with negligible acid-buffering capacity.

(2) Very high potential for the generation of acid-mine drainage (pH 1.5 to 3) that contains thousands of mg/l iron and aluminum; hundreds of mg/l copper and zinc (copper>zinc); hundreds of  $\mu\text{g/l}$  to tens of mg/l As, Co, Ni, Cr, U, Th, rare earth elements; tens to hundreds of  $\mu\text{g/l}$  beryllium; and anomalous abundances of bismuth, antimony, thallium, selenium, and (or) tellurium (Plumlee and others 1995a).

(3) Unoxidized sulfide minerals can persist in clay-rich alteration zones to within 10 m of ground surface. Exposure of these sulfide minerals during mining can further enhance potential for acid-drainage generation.

(4) In temperate or seasonally wet climates, soluble secondary iron, aluminum, and copper sulfate minerals dissolve during storm events and snowmelt, and lead to short term pulses of highly acidic, metal-bearing water from mine sites. The sulfate salts form by evaporation of acid mine water above the water table in open pits and underground mine workings during dry periods, even in wet climates.

(5) Potential downstream environmental effects of acid drainage can be significant in magnitude and spatial extent, especially if surrounding terrane is composed primarily of volcanic rocks with low acid-buffering capacity. Dominant downstream signatures include water having low pH, and high iron, aluminum, manganese, copper, and zinc abundances.

(6) Amalgamation-extraction of gold carried out during historic operations may be a residual source of mercury.

(7) Smelter emissions at historic sites have elevated abundances of arsenic, copper, and zinc, and possibly other elements such as beryllium and tellurium.

(8) Highly oxidized deposits and (or) deposits located in arid climates probably have lower potential for acid mine drainage and other environmental problems.

(9) Cyanide heap leach solutions are composed predominantly of copper-cyanide complexes and thiocyanate.

Mitigation and remediation strategies for potential environmental concerns presented above are described in the section below entitled "Guidelines for mitigation and remediation."

#### Exploration geophysics

Resistivity studies can be used to help map features such as alteration zones. Potassium contained in alteration alunite may be identified by gamma ray spectrometry. Alteration mineral assemblages and stressed vegetation can also be identified using multispectral scanning remote sensing techniques such as AVIRIS.

#### References

Geology: Stoffregen (1987), Vikre (1989), Ashley (1990), John and others (1991), Deen and others (1994), and Gray and Coolbaugh (1994).

Environmental geology, geochemistry: Koyanagi and Panteleyev (1993), Gray and others (1994), Smith and others (1994), and Plumlee and others (1995a,b).

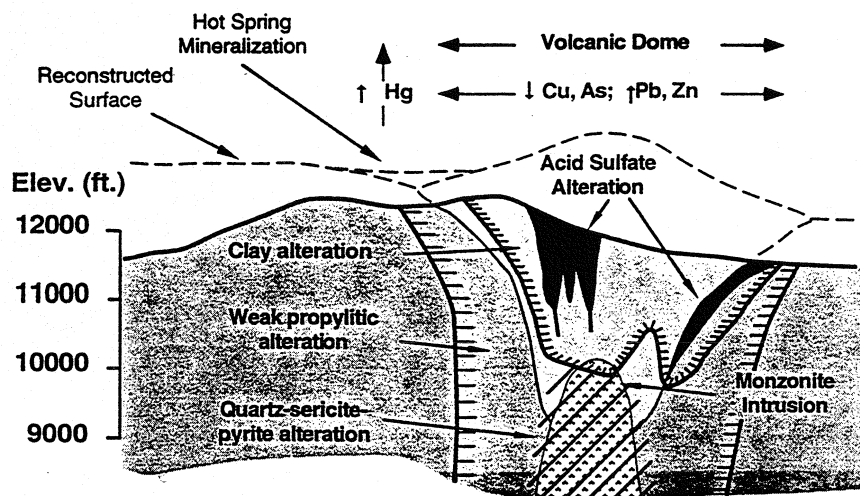


Figure 1. Simplified geologic cross section of an epithermal quartz-alunite Au deposit. Based on Summitville (Perkins and Neiman, 1982; Plumlee and others, 1995a) but modified to incorporate data from Julcani, Peru (Deen and others, 1994) and Paradise Peak, Nev., (John and others, 1991).

## GEOLOGIC FACTORS THAT INFLUENCE POTENTIAL ENVIRONMENTAL EFFECTS

### Deposit size

Deposit size is generally small (0.1 million tonnes) to intermediate (12 million tonnes).

### Host rocks

These deposits are hosted by felsic volcanic rocks, generally intrusions or lava domes (fig. 1), that have low acid-buffering capacity. Most of these volcanic rocks are part of composite stratovolcano complexes. Some ore may be hosted in older sedimentary or crystalline rocks surrounding lava domes.

### Surrounding geologic terrane

Surrounding geologic terrane is primarily volcanic but includes underlying sedimentary or crystalline rocks.

### Wall-rock alteration

Wall-rock alteration reflects progressive wall-rock neutralization of highly acidic magmatic gas condensates; alteration predates ore formation. Alteration zoning shown on figures 1 and 2.

Intermediate-level advanced-argillic zone: Innermost vuggy silica, grading outward into quartz-alunite ( $\pm$  pyrophyllite), quartz-kaolinite, and montmorillonite-illite-smectite alteration zones. Pyrite present in all zones. Phosphate minerals present primarily (?) in quartz-alunite zone.

Intermediate-level argillic zone: Montmorillonite-smectite-illite-clay minerals with pyrite.

Peripheral propylitic zone: Alteration of volcanic rocks to chlorite  $\pm$  epidote  $\pm$  pyrite  $\pm$  calcite.

Deep phyllic zone: Quartz-sericite-pyrite.

### Nature of ore

In some deposits (e.g. Summitville) disseminated sulfide minerals are focused primarily in vuggy silica, quartz-alunite, and quartz-kaolinite zones; however, significant pyrite and other sulfide minerals also are present in clay altered zones, as disseminations within breccia, and in altered wall-rock veinlets. See figure 2 for typical sulfide mineral-sulfur content ranges for Summitville alteration zones. Although sulfide mineral-sulfur content is relatively low (<5 percent), the alteration process effectively removes nearly all of the rock's capacity to buffer acid.

### Deposit trace element geochemistry

Deep: copper,  $\pm$  arsenic,  $\pm$  tungsten.

Intermediate inner: copper, arsenic, gold,  $\pm$  tellurium.

Intermediate peripheral: copper, lead, zinc.

Shallow, near surface: Mercury, arsenic, antimony, gold, thallium.

Ore at Paradise Peak contains elevated abundances of Au, Ag, Bi, Sb, Pb, Tl, Hg, S and Ba  $\pm$  Sn, Mo, Te, and Se. In addition to iron sulfide (mostly marcasite), sulfate (barite) and native sulfur were abundant throughout the deposit. Metal abundances in peripheral, argillically altered rock are essentially unchanged except that oxidized parts are

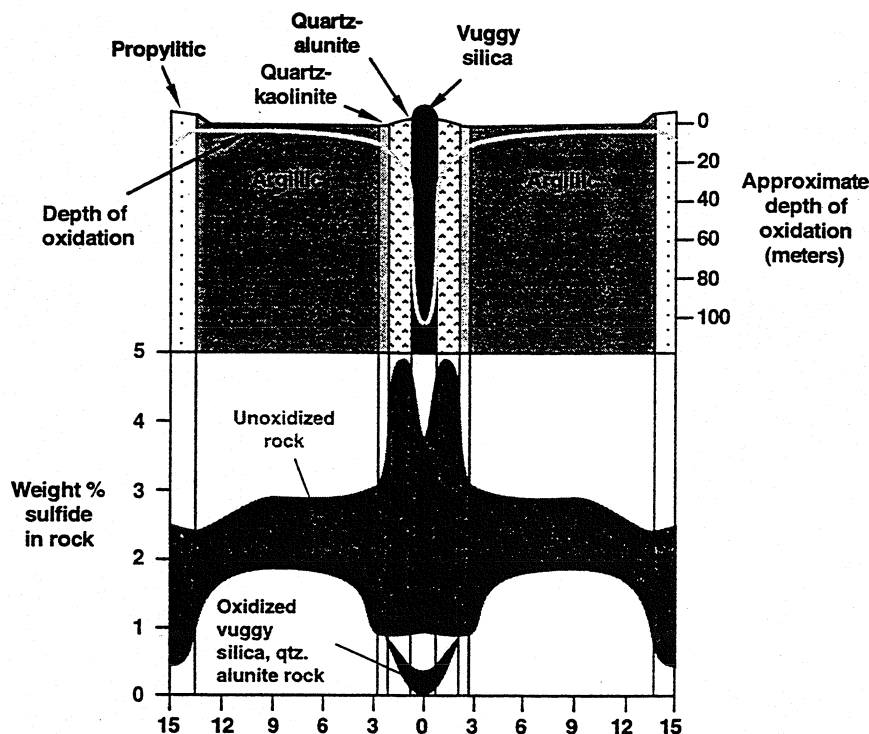


Figure 2. Schematic alteration zoning away from original fractures at Summitville, showing approximate depth of oxidation (upper plot) and range of oxidizable sulfide sulfur in sulfide minerals (lower plot). From Plumlee and others (1995a).

enriched in iron sulfide and unoxidized rocks contain gypsum and jarosite. Mineralized rock from the deepest part of this system tended to have elevated abundances of arsenic and copper but not as elevated as those characteristic of Goldfield, Nev. or Summitville, Colo.

#### Ore and gangue mineralogy and zonation

Minerals listed in decreasing order of abundance. Potentially acid-generating minerals underlined. In epithermal quartz-alunite gold deposits, ore deposition usually postdates development of argillic alteration.

Deep: Pyrite, chalcopryrite, tennantite,  $\pm$  wolframite-heubnerite (Julcani)

Advanced argillic, argillic alteration zones: Pyrite, enargite, covellite, chalcocite, chalcopryrite, native sulfur, marcasite, native gold, barite. Late barite, sphalerite, galena,  $\pm$  siderite (Julcani),  $\pm$  botryoidal pyrite.

Peripheral propylitic zone: Sphalerite, galena,  $\pm$  siderite, barite,  $\pm$  botryoidal pyrite

Shallow, near surface: Silica sinter, cinnabar, native mercury?, native gold, pyrite, marcasite, realgar, orpiment.

#### Mineral characteristics

Textures: Sulfide minerals form fine- to medium-grained (<5 mm), euhedral crystals and masses of very fine-grained, interlocking crystals. Some coarse-grained (as much as 4-5 cm) euhedral sulfide minerals also are present. Late-stage botryoidal pyrite and siderite are present in some deposits.

Trace element contents: Arsenic and antimony may be present in main-stage pyrite and (or) marcasite; late botryoidal pyrite, where present, is typically strongly enriched in arsenic, antimony, and other trace elements. Abundant stibnite-bismuthinite is the principal mineralogic site for antimony and bismuth in the Paradise Peak deposit.

General rates of weathering: Botryoidal, high trace elements > massive, fine >> coarse euhedral, low trace elements.

#### Secondary mineralogy

##### Readily soluble minerals underlined

Supergene minerals: Scorodite, goethite, limonite, K- and Na-jarosite, phosphate minerals, and plumbojarosite. Minerals formed by recent weathering: Jarosite (likely hydronium-enriched), chalcantite, brochantite, melanterite, alunogen, halotrichite, and phosphate minerals?. These minerals form by evaporation of acid water during dry periods, and then redissolve during wet periods. These minerals can also form by evaporation in overbank stream sediment downstream from mine sites.



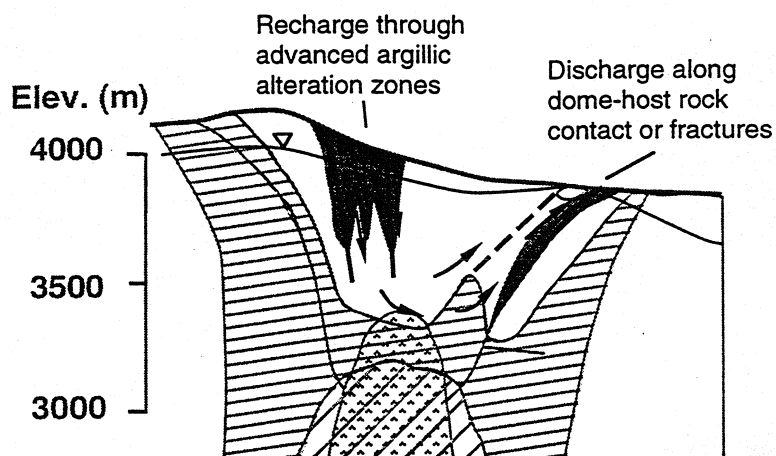


Figure 3. Inferred pre-mining hydrology at Summitville. Triangle marks position of water table.

#### Topography, physiography

Volcanic domes generally form topographic highs. Vuggy silica zones are resistant to weathering, and form prominent knobs and pinnacles. Because vuggy silica zones are highly resistant to weathering, physical erosion immediately surrounding clay alteration zones is minimal.

#### Hydrology

Pre-mining oxidation surfaces can help identify zones of high permeability within deposits. Ferricrete deposits mark pre-mining ground water discharge points. Vuggy silica alteration zones have the highest primary permeability and therefore focus ground water flow; most are oxidized to deep levels (100 meters) by pre-mining ground water. Clay alteration zones have the lowest permeability and therefore inhibit ground water flow; most are oxidized to only shallow levels (several meters to several tens of meters) by pre-mining ground water. Post-mineralization fractures can serve as conduits for ground water flow. Rock contacts between volcanic domes and surrounding rocks can be significant conduits for ground water flow and can also strongly influence distribution of alteration assemblages. In the vicinity of these deposits, the water table generally conforms to topography; the highest elevations are coincident with volcanic domes. At Summitville (fig. 3), ground water recharge is probably along vuggy silica zones. Ground water discharge prior to underground mining (marked by extensive ferricrete deposits) was primarily along contact between volcanic dome and host rocks, and at scarce locations where other fractures intersected the topographic surface of the volcanic dome. In the area around the Paradise Peak deposits, the water table is locally perched, which resulted in the presence of large blocks of unoxidized rock at shallow depths.

#### Mining and milling methods

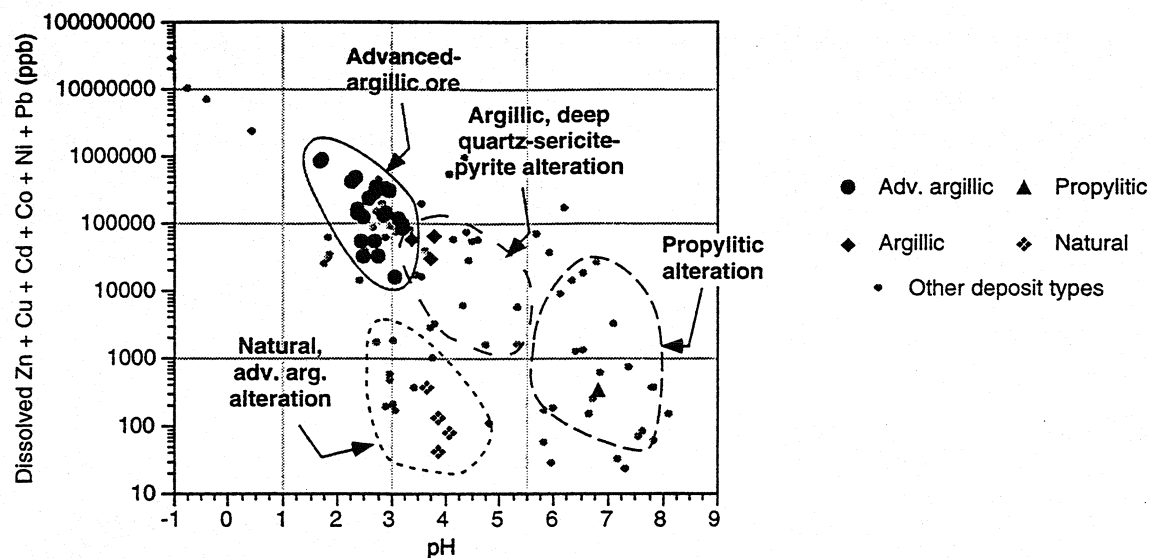
Historic: Underground mine workings followed vuggy silica alteration zones in most cases. Ore was processed using stamp mills and mercury amalgamation or cyanide vat leach.

Modern: Modern operations principally involve open-pit mining of vuggy silica and surrounding clay alteration zones but include some underground mining. Ore is processed primarily using cyanide heap leach techniques.

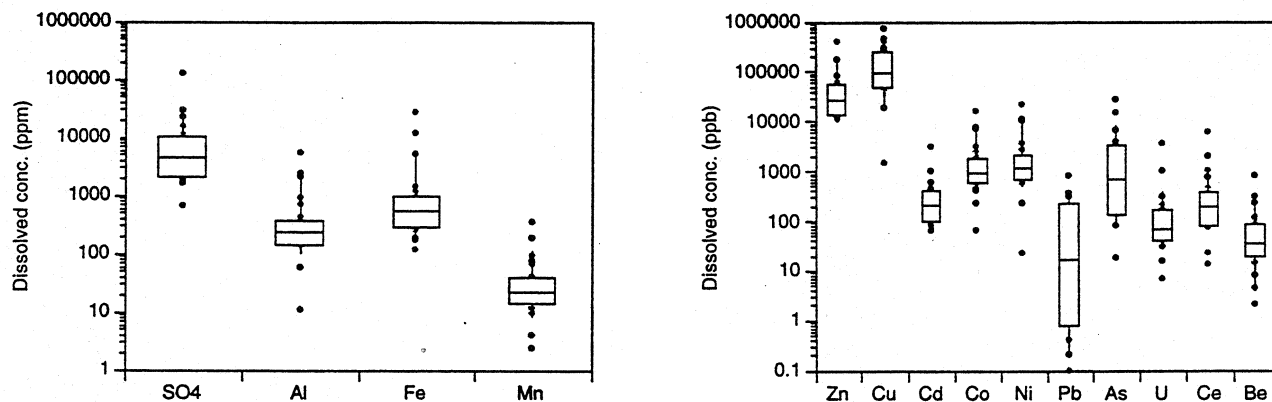
### ENVIRONMENTAL SIGNATURES

#### Drainage signatures

Mine-drainage data (figs. 4 and 5): Summitville and Red Mountain Pass, Colo. (Plumlee and others, 1993; Plumlee and others 1995a,b). Mine water draining ore hosted by advanced argillic altered rocks is highly acidic and contains high to extreme dissolved metal abundances, including hundreds to several thousands of mg/l iron, aluminum, and manganese; hundreds of mg/l zinc and copper; and hundreds of  $\mu\text{g/l}$  to several tens of mg/l As, Co, Ni, U, Th, Be, and REE. Water draining these deposits has elevated arsenic abundances; concentrations of uranium relative to zinc are unusual relative to those associated with many other deposit types. Preliminary data indicate that tellurium, mercury, and tungsten, though potentially enriched in advanced argillic ore, do not appear to be enriched in mine-



**Figure 4.** Plot of pH versus the sum of dissolved base metals Zn, Cu, Cd, Co, Ni, and Pb in mine and natural water draining epithermal quartz-alunite Au deposits. Lines show inferred likely ranges of metal content and pH for specific alteration zones. Samples are water draining adits and waste dumps, rain and snowmelt puddles, and seeps. Data from Koyanagi and Panteleyev (1993) and Plumlee and others (1995b).



**Figure 5.** Box plots showing ranges of selected dissolved constituents in mine water draining ore hosted by advanced argillic alteration zones of epithermal quartz-alunite Au deposits. For each constituent, the box encloses samples falling between the 25th and 75th percentiles, the line shows the range between the 10th and 90th percentiles, and the dots show actual concentrations for samples falling outside the 25th and 75th percentiles.

drainage water. Limited data indicate that mine water draining argillic alteration zones has slightly higher pH and lower metal content.

Mine water draining shallow hot spring ore: No data available. The best currently available data are for water draining advanced-argillic, native sulfur-rich parts of a hot spring sulfur deposit (Leviathan, Calif.), which is acidic (pH 2-3) and has relatively low base metal contents but elevated abundances of arsenic, antimony, and thallium (Ball and Nordstrom, 1989).

Natural-drainage data: Limited data for a relatively wet climate with high dilution rates (British Columbia) suggest low acidity (pH between 2 and 3) and elevated dissolved metal abundances, including hundreds of mg/l iron and aluminum; abundances of copper and zinc, tens to hundreds of  $\mu\text{g/l}$ , are lower than those measured in mine drainages. Potentially economically recoverable elements: High copper abundances in drainage water could be economically extracted.

#### Metal mobility from solid mine wastes

Metals and acid are readily liberated from sulfide-mineral-bearing mine wastes due to oxidation of sulfide minerals, mainly pyrite. During dry periods, secondary soluble salts form by evaporation. During wet periods, the soluble

salts are rapidly dissolved. These salts can be present as coatings on rock material. Metal and acid are probably not liberated in significant amounts from mine wastes associated with deposits oxidized extensively prior to mining. Storm water samples: The pH and metal contents of water in rain and snowmelt puddles, which contain dissolved soluble salts, is generally similar to that of water draining adits and waste dumps (Plumlee and others, 1995b). Water-rock leaching: The results of a few leaching experiments with advanced argillic waste rock material from Summitville (50 g sample in 1 liter of distilled water, Plumlee and others, 1995b) show that metal concentrations and pH values of leach water rapidly (within tens of minutes) approach those of water draining adits and mine dumps.

#### Soil, sediment signatures prior to mining

No data currently available.

#### Potential environmental concerns associated with mineral processing

Mercury amalgamation of ore during historic mining may provide a source of mercury contamination not directly attributable to epithermal quartz-alunite gold deposits.

Cyanide geochemistry: Heap leach and other cyanide processing solutions are likely to include copper-cyanide complexes (containing as much as several hundred mg/l copper), with lesser zinc and silver cyanide complexes (present as weak cyanide complexes with as much as several tens of mg/l contained metals), and strong gold-cyanide complexes. Arsenic, cobalt, nickel, and iron may be present at low mg/l abundances in cyanide heap leach solutions. Thiocyanate (SCN-) abundances may be quite high in ore containing unoxidized sulfide minerals. At Summitville, degradation of cyanide accidentally released into the environment may have been enhanced by mixing with acid-mine drainage and the resulting breakdown of copper-cyanide complexes; thiocyanate likely did not degrade rapidly.

#### Smelter signatures

Epithermal quartz-alunite gold ore from which copper and silver were extracted during historic mining were probably smelted. No data have been identified concerning the mineralogy or chemical composition of soil affected by emissions from smelters that processed epithermal quartz-alunite gold ore. The closest analogue is Butte, Mont., where enargite-chalcocite-bornite ore from cordilleran lode deposits were smelted. There, soil proximal to smelters is very highly enriched in copper, arsenic, zinc, and lead.

#### Climate effects on environmental signatures

Currently available data are from moderately wet, seasonally temperate climate (Rocky Mountains). However, water draining advanced argillic ore in all climates is likely to be quite acidic and metal rich. Evaporation of acid drainage water, which leads to significant increases in metal concentrations and acidity, is important in all climates in which wet periods are interspersed with prolonged dry periods. At Summitville, evaporation has been an important process during dry Summer and Fall seasons even though total precipitation at the site exceeds 125 cm per year (Plumlee and others, 1995b). No data are available for tropical-humid, very dry, or arctic climates. Intense chemical weathering that affects exposed deposits in humid tropical climates oxidizes sulfide minerals to significant depths. Unless the area is simultaneously subjected to high rates of mechanical erosion, oxidation products isolate or reduce the underlying sulfide minerals, which inhibits continued oxidation; the potential for additional acid drainage generation is thereby limited.

#### Potential environmental effects

Potential downstream environmental effects of acid drainage in moderately wet to moderately dry climates can be significant in magnitude and spatial extent, especially if the surrounding geologic terrane is primarily composed of volcanic rocks with low acid buffering capacity. Predominant downstream signatures include elevated abundances of acid, iron, aluminum, manganese, and copper. Iron and aluminum form hydrous oxide precipitates as a result of dilution by downstream tributaries, and help sorb some of the dissolved metals. However, if water remains sufficiently acidic (due to limited dilution by downstream tributaries or acid generation resulting from precipitation of hydrous oxide minerals), manganese, copper, and zinc can persist (at abundances of hundreds  $\mu\text{g/l}$ , or more) in solution well downstream from mine sites (Smith and others, 1995).

In very wet climates, dilution may significantly reduce downstream effects. In dry or seasonally wet and dry climates, off-site drainage is greatest during short-term storm events or longer-term wet periods; reactions between this water and surrounding alkaline sediment (caliche) and soil, and with alkaline water draining the

sediment and soil, probably help mitigate acid drainage. Downstream storm water evaporation, however, may lead to the formation of acid- and metal-bearing salts that can themselves generate off-site acid drainage during storms (K. Stewart, unpub. data).

#### Guidelines for mitigation and remediation

- (1) Acid drainage can be successfully remediated using lime addition and sodium-bisulfide precipitation of metals (which produce acid-generating sludge). Lime addition to iron-rich drainage water may generate sufficient suspended particulates onto which a major fraction of dissolved arsenic, lead, and copper can sorb, thereby reducing or eliminating the need for sodium-bisulfide addition; in addition, wastes are non-acid-generating.
- (2) Isolation of unoxidized sulfide minerals and soluble secondary salts from oxidation and dissolution is crucial to acid drainage mitigation.
- (3) Surrounding carbonate-bearing rocks, including carbonate sedimentary rocks or carbonate-bearing propylitically altered rock on the fringes of deposits, should be carefully considered for their utility in acid-mine drainage mitigation. For example, acid water could be channelled through underground fracture systems in propylitic rock to help reduce acidity.
- (4) Cyanide heap-leach solutions should be treated by peroxide addition or other standard techniques. Heap-leach pads should be decommissioned by rinsing or bioremediation.
- (5) Mixing cyanide heap-leach solutions with acid drainage may effectively neutralize both. Acid in drainage water breaks down copper-cyanide complexes, forming volatile free cyanide and copper-iron-cyanide particulates, which degrade photolytically. Because of the alkalinity of heap-leach solutions, iron in acidic drainage precipitates as particulates, which then effectively sorb other metals contributed from acid drainage and heap-leach solutions.

#### Geoenvironmental geophysics

Resistivity studies can be used to identify rocks saturated with metal-bearing ground water. Porous rocks that can focus ground water flow can be identified by microgravity studies. Heat generated by sulfide mineral oxidation may have an associated thermal anomaly measurable by borehole logging or shallow probes; measures of excess heat flux can provide an approximation of total acid generation potential. Induced polarization methods can provide qualitative estimates of sulfide mineral percentages and grain size. The position, volume and mineralogy of clay bodies can be identified by induced polarization.

#### REFERENCES CITED

- Ashley, R.P., 1990, The Goldfield gold district, Esmeralda and Nye Counties, Nevada, in Shawe, D.R., Ashley, R.P., and Carter, L.M.H., eds., *Geology and resources of gold in the United States*: U.S. Geological Survey Bulletin 1857-H, p. H1-H7.
- Ball, J.W., and Nordstrom, D.K., 1989, Final revised analyses of major and trace elements from acid mine waters in the Leviathan Mine drainage basin, California and Nevada, October 1981 to October 1982: *Water-Resources Investigations*, Report No. WRI 89-4138, 46 p.
- Berger, B.R., 1986, Descriptive model of epithermal quartz-alunite Au, in Cox, D.P., and Singer, D.A., eds., *Mineral deposit models*: U.S. Geological Survey Bulletin 1693, p. 158.
- Cox, D.P., and Singer, D.A., 1986, *Mineral deposit models*: U.S. Geological Survey Bulletin 1693, 379 p.
- Deen, J.A., Rye, R.O., Munoz, J.L., and Drexler, J.W., 1994, The magmatic hydrothermal system at Julcani, Peru: Evidence from fluid inclusions and hydrogen and oxygen isotopes: *Economic Geology*, v. 89, p. 1924-1938.
- Gray, J.E., and Coolbaugh, M.F., 1994, Summitville, Colorado-Geologic framework and geochemistry of an epithermal acid-sulfate deposit formed in a volcanic dome: *Economic Geology*, v. 89, p. 1906-1923.
- Gray, J.E., Coolbaugh, M.F., Plumlee, G.S., and Atkinson, W.W., 1994, Environmental geology of the Summitville Mine, Colorado: *Economic Geology*, v. 89, p. 2006-2014.
- John, D.A., Nash, J.T., Clark, C.W., and Wulftange, W., 1991, Geology, hydrothermal alteration, and mineralization at the Paradise Peak gold-silver-mercury deposit, Nye County, Nevada, in Raines, G.L., Lisle, R.E., Schafer, R.W., and Wilkinson, W.H., eds., *Geology and ore deposits of the Great Basin*, Symposium proceedings: Reno, Geological Society of Nevada and U.S. Geological Survey, p. 1020-1050.
- Koyanagi, V.M., and Panteleyev, Andre, 1993, Natural acid-drainage in the Mount McIntosh/Pemberton Hills area, northern Vancouver Island (92L/12), in Grant, B., and others, eds.: *Geological fieldwork 1992; a summary of field activities and current research*, Ministry of Energy, Mines and Petroleum Resources, Report No. 1993-1, p. 445-450.

- Perkins, M., and Nieman, G.W., 1982, Epithermal gold mineralization in the South Mountain volcanic dome, Summitville, CO: Denver Region Exploration Geologists Symposium on the genesis of Rocky Mountain ore deposits: Changes with time and tectonics, Denver, Colorado, Nov. 4-5, 1982, Proceedings, p. 165-171.
- Plumlee, G.S., Gray, J.E., Roeber, M.M., Jr., Coolbaugh, M., Flohr, M., Whitney, G., 1995a, The importance of geology in understanding and remediating environmental problems at Summitville, *in* Posey, H.H., Pendleton, J.A., and Van Zyl, D., eds.: Proceedings, Summitville Forum '95, Colorado Geological Survey Special Publication #38, p. 13-22.
- Plumlee, G.S., Smith, K.S., Ficklin, W.H., Briggs, P.H., and McHugh, J.B., 1993, Empirical studies of diverse mine drainages in Colorado-Implications for the prediction of mine-drainage chemistry: Proceedings, Mined Land Reclamation Symposium, Billings, Montana, p. 176-186.
- Plumlee, G.S., Smith, K.S., Mosier, E.L., Ficklin, W.H., Montour, M., Briggs, P.H., and Meier, A.L., 1995b, Geochemical processes controlling acid-drainage generation and cyanide degradation at Summitville, *in* Posey, H.H., Pendleton, J.A., and Van Zyl, D., eds.: Proceedings, Summitville Forum '95, Colorado Geological Survey Special Publication #38, p. 23-34.
- Smith, K.S., Plumlee, G.S., and Ficklin, W.H., 1994, Predicting water contamination from metal mines and mining wastes: Notes, Workshop #2, International Land Reclamation and Mine Drainage Conference and Third International Conference on the Abatement of Acidic Drainage: U.S. Geological Survey Open-File Report 94-264, 112 p.
- Smith, K.S., Mosier, E.L., Montour, M.R., Plumlee, G.S., Ficklin, W.H., Briggs, P.H., and Meier, A.L., 1995, Yearly and seasonal variations in acidity and metal content of irrigation waters from the Alamosa River, Colorado, *in* Posey, H.H., Pendleton, J.A., and Van Zyl, D., eds.: Proceedings, Summitville Forum '95, Colorado Geological Survey Special Publication #38, p. 293-298.
- Stoffregen, R.E., 1987, Genesis of acid-sulfate alteration and Au-Cu-Ag mineralization at Summitville, Colorado: *Economic Geology*, v. 82, p. 1575-1591.
- Vikre, P.G., 1989, Ledge formation at the Sandstone and Kendall gold mines, Goldfield, Nevada: *Economic Geology*, v. 84, p. 2115-2138.

## THE IMPORTANCE OF GEOLOGY IN UNDERSTANDING AND REMEDIATING ENVIRONMENTAL PROBLEMS AT SUMMITVILLE

by

Geoffrey S. Plumlee<sup>1</sup>, John E. Gray<sup>1</sup>, M. M. Roeber, Jr.<sup>2</sup>, Mark Coolbaugh<sup>3</sup>, Marta Flohr<sup>4</sup>, and Gene Whitney<sup>5</sup>

<sup>1</sup>U. S. Geological Survey, MS 973 Federal Center, Denver, CO 80225

<sup>2</sup>Environmental Chemical Corp., West Highway 160, Del Norte, CO 81132

<sup>3</sup>Carson Gold Corp., 355 Burrard St., Suite 1900, Vancouver, BC, Canada, V6C2G8

<sup>4</sup>U. S. Geological Survey, 959 National Center, Reston, VA 22092

<sup>5</sup>U. S. Geological Survey, MS 939 Federal Center, Denver, CO 80225

### ABSTRACT

Geologic characteristics of the Summitville mine and vicinity are an important control on the generation of acid-mine drainage, the dominant long-term environmental problem at the site. A good understanding of the environmental geology of the Summitville gold-silver-copper deposit is necessary to: (1) develop the most effective remediation strategies for the Summitville site; and (2) better predict, mitigate, and remediate potential environmental problems at future proposed mine sites with similar geologic characteristics.

Environmentally important geologic characteristics of the Summitville deposit include:

- A high acid-generating capacity resulting from the abundance of sulfide minerals such as pyrite, enargite, covellite, chalcocite, and chalcopyrite.
- A low acid-consuming capacity resulting from intense acid leaching of the volcanic host rocks that occurred prior to the formation of the deposit.
- Intensely altered vuggy silica alteration zones that provided permeability for (a) the mineralizing solutions that formed the deposit, and (b) post-mineralization groundwaters that oxidized sulfides in the vuggy silica zones to depths up to several hundred feet.
- Extensive sulfide-rich clay alteration zones with low permeabilities that were oxidized prior to mining to depths of only several tens of feet.
- Extensive areas of sulfide-rich rocks in clay alteration zones that were exposed to weathering by recent open-pit mining, and that led to increased generation of acid-mine drainage from the site.

Vuggy silica alteration zones and unmineralized faults predominantly controlled shallow groundwater movement prior to mining. Underground mine workings modified the hydrology so that the dominant water outflow occurred from mine-drainage tunnels. Open-pit mining further

affected the local hydrology by creating a snow and rain catchment basin that then funneled much greater quantities of water into sulfide rich rocks and mine workings beneath the pit. As a result of the plugging of the Reynolds Adit in late January, 1994, pre-adit hydrologic conditions are largely being re-established.

- Extensive deposits of ferricrete (precipitates of iron oxide and hydroxide minerals) mark the location of fossil acid groundwater springs that flowed prior to mining. The locations of ferricrete deposits can be used to help map likely outflow points of springs and seeps renewed by the plugging of the Reynolds adit.

The severe acid drainage problems at Summitville are a direct consequence of the site's geologic characteristics and its climatic setting. Effective remediation will require the isolation of both sulfide-bearing and secondary salt-bearing materials from weathering and oxidation, a formidable challenge given the wide distribution of such materials throughout the site. Future development of deposits geologically similar to Summitville will likely be economically and environmentally difficult unless adequate precautions can be made to mitigate acid-mine drainage.

### INTRODUCTION

Geologic characteristics of the Summitville mine and vicinity are an important control on the generation of acid-mine drainage, the dominant long-term environmental problem at the site (Plumlee et al., this volume). A good understanding of the environmental geology of the Summitville gold-silver-copper deposit is necessary to: (1) develop the most effective remediation strategies for the Summitville site; and (2) better predict, mitigate, and remediate potential environmental problems at future proposed mine sites with similar geologic characteristics. This paper summarizes key aspects of Summitville's

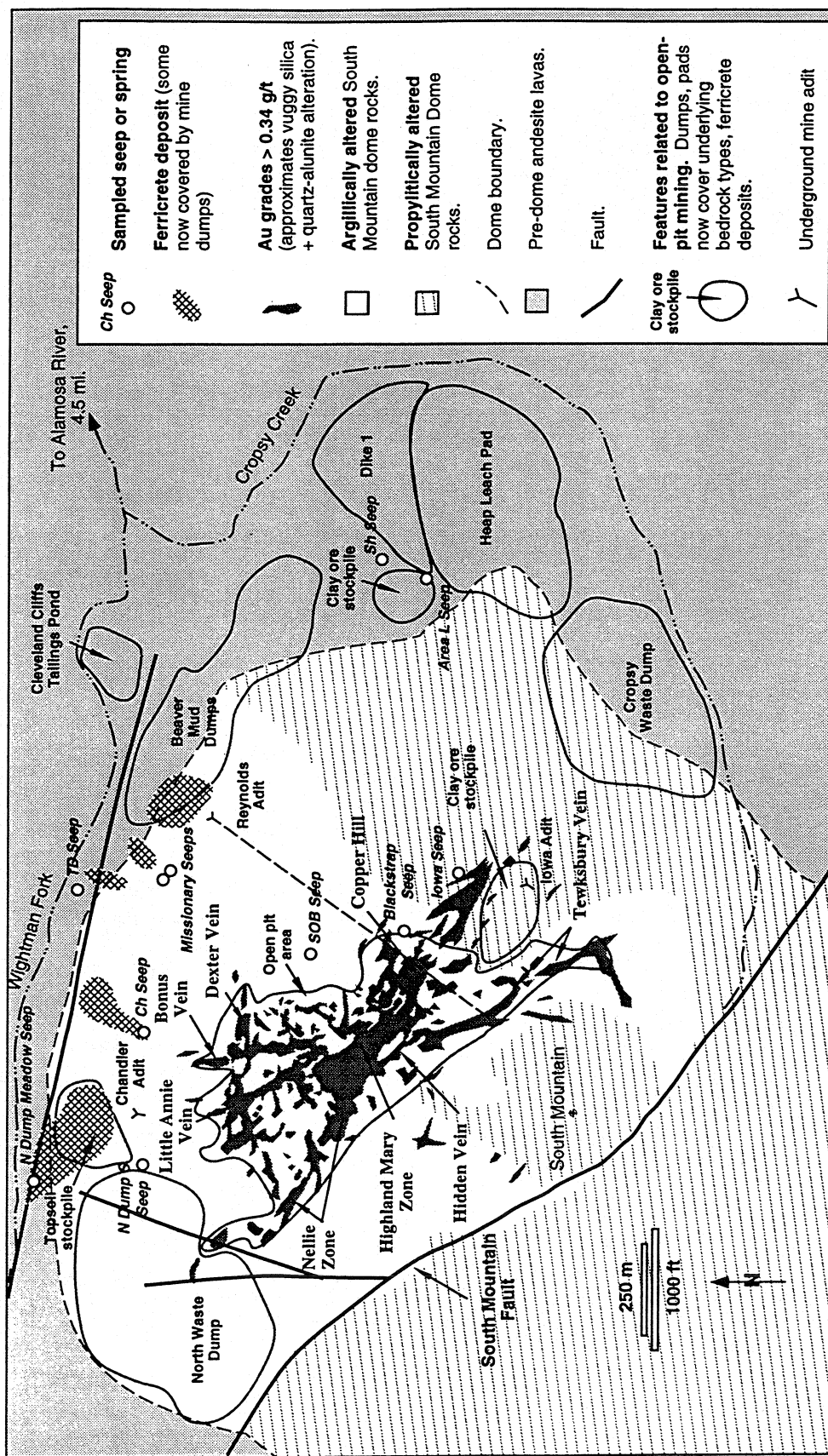


Figure 1. Generalized map of the Summitville mine site showing geologic features (major alteration and ore zones, ferricrete deposits) in relation to past and recent mine features. Also shown are the locations of active seeps sampled for chemical analysis (see Plumlee et al., this volume). The distribution of argillic and propylitic alteration was taken from a surficial geologic map prepared by Mike Perkins and Bill Nieman for the Anaconda Company in the early 1980's. The distribution of acid sulfate alteration (vuggy silica and quartz alunite zones) is approximated by gold grades greater than 0.34 grams per ton (after Gray and Coolbaugh, 1994 in press). The location of ferricrete deposits is approximate based on distributions observed in aerial photographs taken of the site in 1968 and 1980 by Intra-Search, Inc.; many of the deposits are now covered by material from the recent open pit mining operations.



environmental geology. For more detailed discussions, the reader is referred to Gray and Coolbaugh (in press), and Gray et al. (in press, 1993).

## GEOLOGY

The processes that formed the gold-silver-copper deposit at Summitville ultimately set the stage for the generation of both natural and mining-related acid drainage from the site. Summitville is located in the southeastern portion of the mid-Tertiary San Juan volcanic field, a thick section of volcanic rocks composed in its lower portions of andesitic volcanics and related rocks erupted from numerous stratovolcanoes, and in its upper portions of andesitic to rhyolitic ash flow sheets erupted from numerous calderas (Steven and Lipman, 1976). For a more detailed discussion of the regional geology, the reader is referred to Bove et al. (this volume).

### South Mountain volcanic dome

The 22.4 million-year old Summitville deposit is hosted by the South Mountain volcanic dome (Figs. 1, 2), and formed as a direct result of the magmatic processes that generated the dome (Gray and Coolbaugh, 1994 in press; Rye et al., 1990; Stoffregen, 1987; Perkins and Neiman, 1982; Steven and Ratté, 1960). The dome is composed of quartz latite volcanic lavas that are relatively rich in silica ( $\text{SiO}_2$ ) and have abundant coarse grained crystals of feldspar ( $\text{KAlSi}_3\text{O}_8$ ). The dome lavas were extruded from a narrow feeder zone (Steven and Ratté, 1960) and pushed outward to form a typical mushroom-shaped silicic lava dome (Fig. 2). Rocks along the contact between the dome

lavas and surrounding andesitic lavas were brecciated, creating a zone of higher permeability that is an important control on groundwater movement at the site.

### Alteration and Mineralization

As part of the dome-forming cycle, additional magmatic material was intruded into the area beneath the dome. As these magmas crystallized, they released hot gases rich in sulfur dioxide. The gases rose along fractures in the dome rocks and eventually condensed in the shallow portions of the dome, producing fluids rich in sulfuric acid that extensively leached and altered the dome rocks to an advanced argillic alteration assemblage (Figs. 2, 3; Table 1). The greatest amounts of leaching occurred near fractures and left only silica and pyrite in the rock; this alteration zone is called the vuggy silica zone because of the well-formed voids left by the removal of large feldspar crystals. Progressive neutralization of the acidic gas condensates outward from the vuggy silica zones altered the rocks (Fig. 3; Table 1) to successive quartz-alunite, quartz-kaolinite, clay (containing illite, montmorillonite, and pyrite), and propylitic (containing chlorite, pyrite, and some calcite) assemblages. The propylitically altered rocks are very rare in the open pit area, but are more common south and east of the mine.

The advanced argillic alteration event was important in the formation of the Summitville deposit because it provided open space porosity for subsequent sulfide and gold deposition. The advanced argillic assemblage rocks are also environmentally significant because they have a greatly reduced capacity (as compared to fresh, unaltered dome rocks) to consume acid in mine drainage.

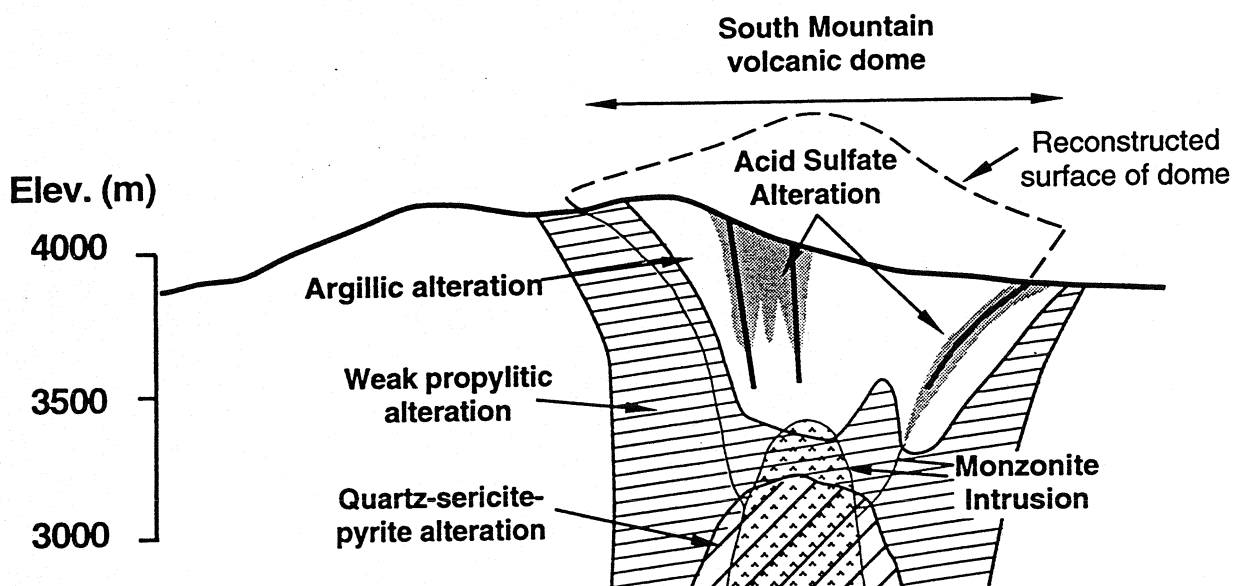


Figure 2. Generalized cross section of the South Mountain volcanic dome showing the geology and distribution of various alteration types. After Perkins and Nieman (1982).



**Table 1.** Minerals found at Summitville. Minerals listed in bold have the potential to generate acid during oxidation, weathering, or dissolution. Minerals followed by question marks are of uncertain time of origin.

*Minerals formed during advanced-argillic alteration*

Silica (quartz)	SiO <sub>2</sub>	<b>Alunite</b>	KAl <sub>3</sub> (SO <sub>4</sub> ) <sub>2</sub> (OH) <sub>6</sub>
Kaolinite	Al <sub>2</sub> Si <sub>2</sub> O <sub>5</sub> (OH) <sub>4</sub>	Illite	KAl <sub>4</sub> [Si <sub>7</sub> , Al]O <sub>20</sub> (OH) <sub>4</sub>
<b>Pyrite</b>	FeS <sub>2</sub>	Woodhouseite	CaAl(PO <sub>4</sub> )(SO <sub>4</sub> )(OH) <sub>6</sub>
Smectite	Na <sub>0.7</sub> (Al,Fe,Mg) <sub>4</sub> [(Si,Al) <sub>8</sub> O <sub>20</sub> ](OH) <sub>4</sub> •nH <sub>2</sub> O		
Chlorite	(Mg, Fe, Al) <sub>12</sub> [(Si, Al) <sub>8</sub> O <sub>20</sub> ](OH) <sub>16</sub>	Calcite	CaCO <sub>3</sub>

*Minerals formed during hydrothermal mineralization:*

<b>Pyrite</b>	FeS <sub>2</sub>	<b>Enargite</b>	Cu <sub>3</sub> AsS <sub>4</sub>
<b>Chalcocite</b> (?)	Cu <sub>2</sub> S	<b>Covellite</b>	CuS
Chalcopyrite	CuFeS <sub>2</sub>	<b>Marcasite</b>	FeS <sub>2</sub>
Native sulfur	S <sup>0</sup>	Gold	Au
Barite	BaSO <sub>4</sub>	<b>Sphalerite</b>	ZnS
<b>Luzonite</b>	Cu <sub>3</sub> AsS <sub>4</sub>	<b>Galena</b>	PbS
Kaolinite	Al <sub>2</sub> Si <sub>2</sub> O <sub>5</sub> (OH) <sub>4</sub>	<b>Tennantite</b>	(Cu,Fe,Zn) <sub>12</sub> As <sub>4</sub> S <sub>13</sub>
Hinsdalite	(Pb,Sr)Al <sub>3</sub> (PO <sub>4</sub> )(SO <sub>4</sub> )(OH) <sub>6</sub>		

*Secondary minerals formed during pre-mining weathering of the deposit:*

<b>Jarosite</b>	KFe <sub>3</sub> (SO <sub>4</sub> ) <sub>2</sub> (OH) <sub>6</sub>	Goethite	HFeO <sub>2</sub>
Limonite	FeO(OH)•nH <sub>2</sub> O	Scorodite	FeAsO <sub>4</sub> •2H <sub>2</sub> O
Hinsdalite (?)	(Pb,Sr)Al <sub>3</sub> (PO <sub>4</sub> )(SO <sub>4</sub> )(OH) <sub>6</sub>	<b>Chalcocite</b> (?)	Cu <sub>2</sub> S (below water table)

*Secondary minerals formed as a result of mining of the deposit (this list will likely expand with further study):*

Chalcanthite	Cu(SO <sub>4</sub> )•5H <sub>2</sub> O	Brochantite	Cu <sub>4</sub> (SO <sub>4</sub> )(OH) <sub>6</sub>
<b>Jarosite</b>	KFe <sub>3</sub> (SO <sub>4</sub> ) <sub>2</sub> (OH) <sub>6</sub>	Posnjakite	Cu <sub>4</sub> (SO <sub>4</sub> )(OH) <sub>6</sub> •5H <sub>2</sub> O
Hinsdalite (?)	(Pb,Sr)Al <sub>3</sub> (PO <sub>4</sub> )(SO <sub>4</sub> )(OH) <sub>6</sub>	Halotrichite	Fe <sup>+2</sup> Al <sub>2</sub> (SO <sub>4</sub> ) <sub>4</sub> •22H <sub>2</sub> O

Propylitically altered rocks contain minor amounts of carbonate minerals that can help consume acid in mine drainage; however, the propylitically altered rocks occur in such small amounts in the Summitville open pit that they likely have relatively little mitigative effect on acid-mine drainage at the site.

Following the period of intense acid leaching by magmatic gas condensates, Cu- and As-rich sulfide minerals were deposited in the highly altered dome rocks by hot hydrothermal fluids also derived from crystallizing magmas at depth. Minerals deposited in this assemblage include pyrite, marcasite, enargite - luzonite, native sulfur, covellite, chalcopyrite, tennantite, and minor barite, sphalerite, galena, and various phosphate minerals (Table 1; Gray and Coolbaugh, 1994 in press; Stoffregen, 1987). The greatest amounts of sulfide mineralization occurred within rocks altered to vuggy silica because hydrothermal fluid flow was focused in these highly permeable zones; however, appreciable Cu-As sulfide mineralization was also deposited in the quartz-alunite and quartz-kaolinite alteration zones. Multiple generations of hydrothermal brecciation, in which magmatic fluids were explosively released from depth into the dome rocks, also produced some sulfide mineralization. Finally, late-stage sulfide-rich veins were deposited in fractures cutting the highly altered

dome rocks (M. Roeber, unpub. data; Gray and Coolbaugh, in press).

Sulfides such as pyrite, marcasite, and enargite are capable of generating large amounts of acid as they weather (Plumlee et al., this volume). The end result of the alteration and mineralizing processes at Summitville was a low-grade gold-silver-copper deposit with the potential to generate large amounts of acid and metals during weathering, but with little capacity to consume this acid.

## Structure

The importance of dome-related structures as controls on the distribution of alteration and mineralization zones is illustrated by a map of gold grades of the Summitville mine (Fig. 1); the highest gold grades generally follow the vuggy silica zones of most intense alteration. Vuggy silica zones and coincident gold ore zones radiate outward from the core of the deposit (Fig. 1; Enders and Coolbaugh, 1987). Three northwest fracture trends are present that dip steeply from 65° to vertical. A N30°W ± 20° trend is typified by narrower zones with higher Au grades, such as the Little Annie and Tewksbury zones that were mined underground. A second strong NW structural trend is characterized by N60°W zones that are wider and longer but have lower than average Au grades; examples are the Highland Mary,

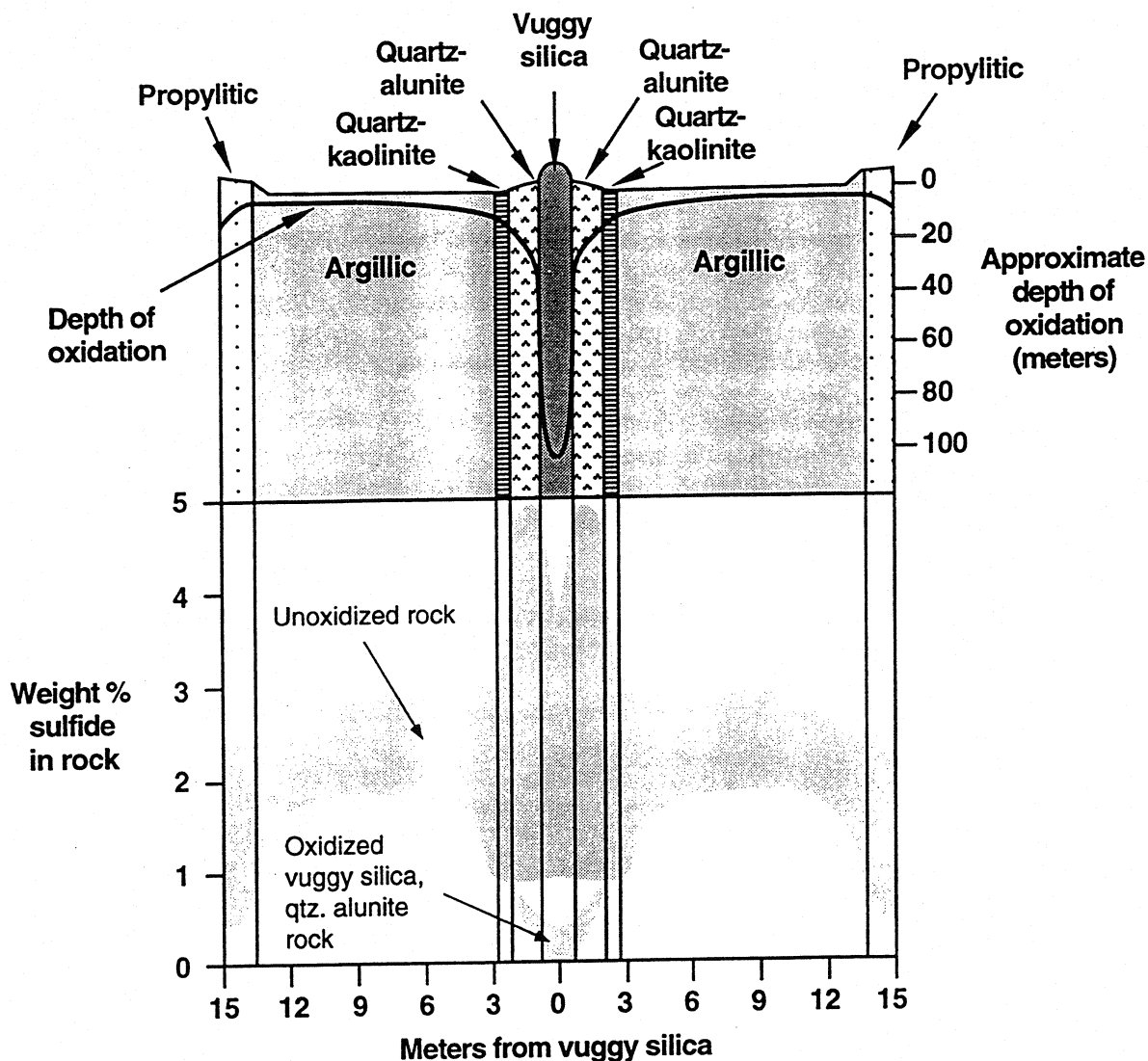


Figure 3. Schematic alteration zoning away from original fractures in the South Mountain dome rocks, showing approximate depth of oxidation (upper plot) and ranges of oxidizable reduced sulfur in weight percent (lower plot). After Gray et al. (1994 in press). Darker stipple shows reduced sulfur ranges in largely unoxidized rocks across all zones. Lightly stippled pattern shows reduced sulfur in oxidized vuggy silica, quartz alunite zones.

Nellie, and Copper Hill zones; these N60°W zones parallel the South Mountain fault on the southwest side of the deposit. A third, less well-developed NW trend strikes N5-10°W and is typified by the Bonus vein east of the Little Annie vein. These three trends intersected near the center of the deposit to form a large ore body approximately 150 by 400 m, the Highland Mary-Copper Hill zone. In addition, some west-trending arcuate ore zones such as the Dexter vein form concentric structures around the core of the deposit on its northern side (Fig. 1). The radial and arcuate structures probably resulted from emplacement of magmas at depth beneath the dome. The well-developed, N60°W-trending structures probably developed along pre-existing regional fractures that were reopened during the

#### Summitville alteration and mineralization.

Unmineralized structures of various orientations crosscut the alteration zones. Largely unmineralized structures mapped in the Reynolds adit (Anaconda Company, unpublished map) generally parallel one of the three northwest trends. These structures produce abundant water in the Reynolds adit, especially during spring snowmelt.

In summary, original dome structures focused alteration by magmatic gas condensates. The alteration zones and some later cross-cutting structures have, in turn, greatly influenced post-mineralization groundwater movement and the extent of weathering prior to mining.

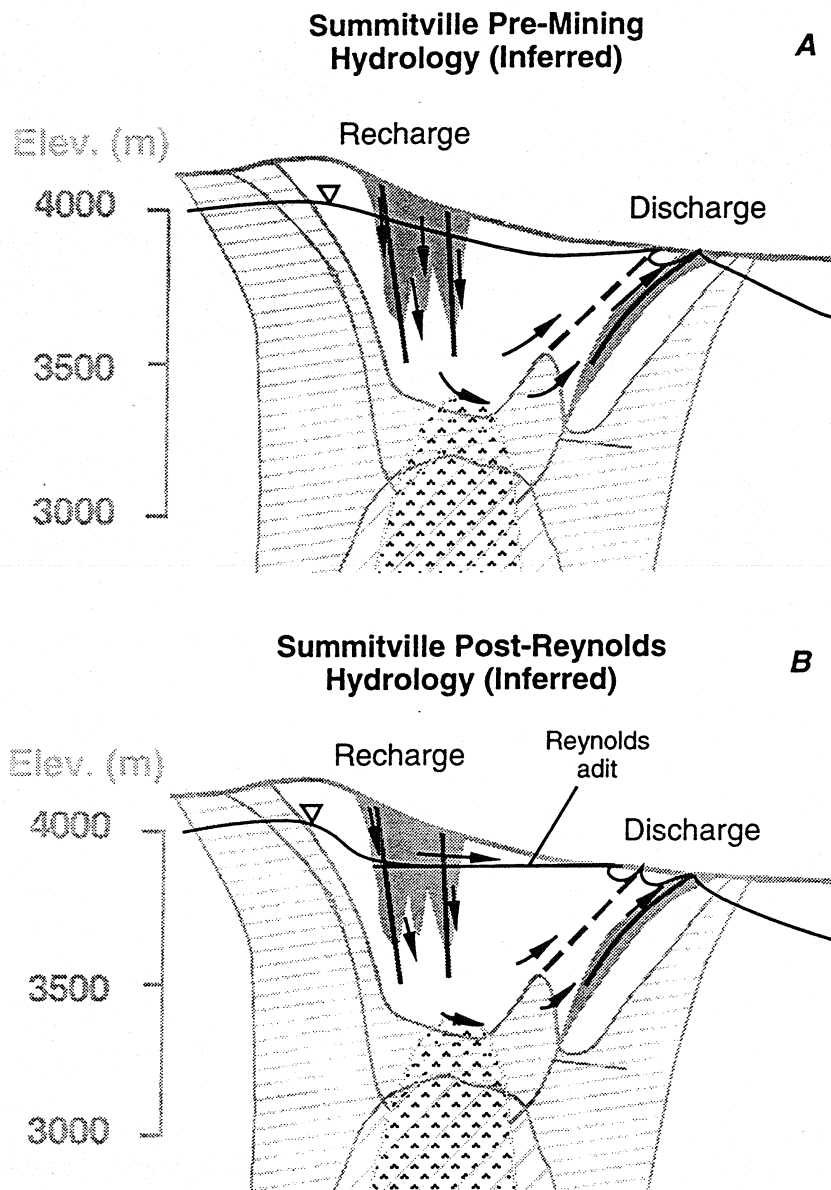


Figure 4. A. Schematic cross section showing inferred hydrology of the Summitville mine area prior to underground mining. Solid black line is water table. Arrows show postulated fluid flow paths. B. Schematic cross section showing inferred hydrology of the Summitville mine area resulting from underground mining. Solid black line is water table. Arrows show postulated fluid flow paths. Flow was reduced from natural discharge points due to increased flow from Reynolds adit. Triangles in each plot show inferred position of groundwater table.

### FEATURES OF WEATHERING AND OXIDATION

After the Summitville deposit formed, erosion gradually exposed the deposit to weathering and oxidation by oxygenated ground and surface waters. The most rapid erosion has occurred in the last 5 million years and resulted from a regional uplift of the San Juan Mountains (T. Steven, oral comm., 1993). Weathering and erosion are ongoing, and weathering has been greatly accelerated at the mine site by the recent mining activity.

### Pre-mining oxidation and weathering features

Prior to the mining, weathering of the Summitville deposit was focused along the high-permeability vuggy silica alteration zones; pre-mining oxidation of these zones occurred to depths as great as 300 feet below the ground surface (Gray et al., 1993); in fact, gold grades in the vuggy silica zones were enhanced by the oxidation and removal of sulfides. In contrast to the vuggy silica zones, oxidation of rocks in adjacent clay alteration zones occurred only to depths of several tens of feet below the ground surface, due

primarily to the greatly reduced permeability of the clay zones to groundwater flow. Some vuggy silica zones and late-stage sulfide veins escaped oxidation if groundwater flow was inhibited by clay-altered rock. Pre-mining weathering and oxidation removed sulfide minerals and left behind variable amounts of iron oxides (hematite and goethite), jarosite (a potassium-iron sulfate), alunite (a potassium-aluminum sulfate), scorodite (an iron arsenate), and gold (Table 1; Stoffregen, 1986). The highly variable nature of the pre-mining oxidation is readily apparent on color aerial photographs of the site (see color photo at front of this volume), with dark brown, highly oxidized vuggy silica zones occurring immediately adjacent to and within larger gray areas of unoxidized, clay-altered rocks.

### Features that result from mining

Recent open-pit mining at Summitville exposed to weathering large volumes of sulfide-bearing rocks in the clay alteration zones. It was this exposure of sulfide-bearing rocks in the pit and the storage of these rocks in waste dumps throughout the mine that has led to the increased acid drainage from the site. The acid waters are generated when oxygenated snowmelt and rain waters react with the sulfides to form waters with high contents of sulfuric acid and metals (Plumlee et al., this volume). As the acid waters evaporate during dry periods, they precipitate a complex suite of soluble secondary salts that store metals and acid in solid form until they dissolve during the next period of rain or snowfall. We have observed these salts as surficial coatings on rock materials within the open pit and waste dumps, as coatings on fractures in rocks forming the open pit walls, and as disseminations within sediments left after the evaporation of acid puddles throughout the mine site. In the area beneath the pit, these salts are likely most abundant near airways that allow for evaporation, such as in and near mine workings and in fractured rock immediately beneath the open pit.

Soluble secondary salts are a significant environmental concern at Summitville due to their abundance and the ease with which they can liberate metals and acid into the environment simply by dissolving in rain waters or snowmelt. The types and amounts of soluble secondary salts at Summitville are currently under investigation. Salts identified in limited studies to date include various copper sulfates (including chalcantite and brochantite), jarosite, and halotrichite. Several phosphate minerals (such as hinsdalite and woodhouseite) have been identified as intergrowths with and as late coatings on primary minerals, and as disseminations within mine-pond sediments. Although in some samples these phosphates are clearly related to the formation of the mineral deposit (Stoffregen and Alpers, 1987), textural evidence suggests that the same suite of phosphates may also be forming as a result of present-day weathering processes. Due to the potentially

large number of different salts that may be present, more detailed studies are needed on additional samples to adequately characterize secondary minerals at the site.

### Ferricrete deposits

Extensive ferricrete deposits occur primarily along the northern margins of the mine site. These deposits are composed of ferric oxide minerals that were precipitated by acidic, iron-rich groundwaters as they flowed onto the surface from springs. Many of the ferricrete deposits mark the locations of ancient iron springs that flowed prior to mining. The extent of these natural spring deposits can be mapped from aerial photographs taken prior to and during the recent open-pit mining. The ferricrete deposits are localized along the northern contact between the South Mountain dome and surrounding andesitic rocks, along the Missionary fault on the northeastern side of the deposit, and along the northern extensions of NW-trending ore zones such as the Little Annie vein and the Bonus vein (Fig. 1).

Numerous stalactites of hydrous ferric oxides (up to 10 cm long and 1 cm in diameter) were observed in June, 1993, to be actively forming in the Reynolds adit where crosscutting fractures leaked acid water from the adit back. These stalactites form as acidic waters flow from the fractures and become oxygenated; aqueous ferrous iron is then oxidized to ferric iron, which then precipitates as hydrous ferric oxides. As an aside, it is interesting to note that the copper-rich waters draining the Reynolds adit replaced the outer layers of mine rails and anything else made of iron with a thick layer of native copper; analysis of the copper reveals detectable levels of tellurium, indium, and other trace metals.

## GEOLOGIC CONTROLS ON HYDROLOGY AND GROUNDWATER FLOW

Summitville's hydrology can be understood qualitatively based on a knowledge of the site's geologic characteristics, limited pumping tests done in 1992, and the monitoring of water table elevations in the pit area since the plugging of the Reynolds adit. However, to adequately predict the long-term response of the site to remedial actions currently underway, more extensive hydrologic pumping tests, downhole geophysical characterization, and tracer and groundwater monitoring studies are required.

Older andesites that surround the South Mountain dome have very low permeabilities and limited groundwater flow near the current ground surface; drilling in the andesites encountered water at depths greater than five hundred feet. The low permeabilities of the andesites, coupled with the higher permeabilities of vuggy silica zones and other fractures in the dome rocks, led to the development of a shallow, perched groundwater system contained largely within the dome.

Prior to mining, vuggy silica zones, unmineralized

fractures, and the contact between the dome and surrounding andesites likely served as the dominant conduits for groundwaters at the site (Fig. 4A). Recharge for the groundwater system likely occurred primarily via surface outcrops of the vuggy silica zones. Groundwaters flowed downward along the vuggy silica zones and spread laterally through other intersecting vuggy silica zones and fractures not exposed at the surface. Groundwater discharge occurred primarily along the dome-andesite contact and along limited numbers of fractures that intersected the ground surface; discharge points are documented by the extensive ferricrete deposits discussed previously on the northern side of the mine site. The South Mountain fault west of the deposit was likely also a significant groundwater conduit, and may have fed springs on the northwest side of the South Mountain dome near the drainage divide between the Wightman Fork and Park Creek. It is likely that waters discharged along the dome andesite contact had followed rather deep flow paths (possibly as much or more than 1 km) to reach the contact, and therefore may have had an artesian component.

Inception of underground mining significantly altered the hydrology. Groundwater flow was shifted largely to underground mine workings, which short-circuited the deep flow system along the dome-andesite contact and allowed groundwaters to discharge at a higher elevation along the Reynolds adit (Fig. 4B). Open-pit mining further affected the local hydrology by creating a snow and rain catchment basin that funneled much greater quantities of water into sulfide rich rocks and mine workings beneath the pit and then out the Reynolds adit.

As a result of the plugging of the Reynolds adit in late January, 1994, hydrologic conditions that existed prior to the driving of the Reynolds Adit are largely being re-established. Monitoring by the Environmental Chemical Corporation has shown that water levels beneath the open pit area rose substantially in the months following the plugging and then declined somewhat after spring snowmelt was complete. Reduced flow still continued from the Reynolds adit due to leakage from fractures outside the plug; these fractures are also likely to be feeding active seeps located near the Reynolds Adit (such as the Missionary and TD seeps, Fig. 1). In May, 1994, a plug on the Chandler adit (located approximately 50 m higher than and 800 m northwest of the Reynolds Adit) failed and water began flowing from the adit opening. The flow from the Chandler shows, as expected, that the underground mine workings are much more conducive to fluid flow than the pre-mining fracture systems. However, seeps east and north of the open pit area have also either started flowing or have increased in flow since the Reynolds adit plugging. These seeps typically occur near or within old ferricrete deposits and are located near the dome-andesite contact, along the Missionary fault, or near structures within the dome that intersect the ground surface (Fig. 1). In addition to the

seeps located on Figure 1, an intermittent seep on the South Mountain fault (located northwest of the mine at the drainage divide between the Wightman Fork and Park Creek) started flowing again in summer, 1994. The renewed or increased seep activity indicates that groundwaters are once again utilizing natural conduits and flowing from natural discharge points. A number of other seeps are present on the northeastern and eastern side of the deposit; some of these are fed by waters flowing through bedrock fractures (such as the Ch, Missionary, TD, N Dump Meadow, and Iowa seeps), but many are fed by waters flowing through waste material left by the recent open pit mining (such as the N Dump S seep, and seeps from the Beaver mud dumps, clay ore stockpile, and Cropsy waste dump). Chemical compositions of the various seeps are discussed in Plumlee et al. (this volume).

## IMPLICATIONS FOR PREDICTION, MITIGATION, AND REMEDIATION

A good understanding of the environmental geology of the Summitville deposit is crucial to: (1) develop the most effective remediation strategies for the Summitville site; and (2) better predict, mitigate, and remediate potential environmental problems at future proposed mine sites with similar geologic characteristics.

### Remediation at Summitville

The most significant long-term remedial action needed at Summitville is the mitigation of acid-mine drainage from the site. This requires the isolation of both sulfide-bearing and secondary salt-bearing materials from weathering and oxidation, a formidable challenge given the wide distribution of such materials throughout the site. The current effort to backfill the open pit with acid-generating material and then cap the pit should help significantly reduce acid drainage from the site. However, geologic considerations indicate further efforts and precautions:

- The cap on the pit area must be as impermeable as possible, given the abundance of soluble salts and oxidizable sulfides in the backfill material and the fact that the pit area will continue to drain (although at a greatly reduced level) into the Wightman Fork from reactivated seeps.
- Surface outcrops of vuggy silica zones and faults that are not in the backfilled and capped pit area (Fig. 1) may permit groundwater recharge into the area beneath the cap; these should be identified and, if possible, sealed or capped.
- Seep activity north of the deposit will probably continue and may spread to other areas in which old ferricrete deposits mark pre-mining discharge points (Fig. 1), and to areas where fractures intersect the surface.
- Given the lower-level but pervasive occurrence of acid-generating material throughout the site (on roads, in

soils, windblown into forested areas, etc.), it is likely that some level of surficial acid drainage will bleed from the site over the long term even after the bulk of the waste dump materials have been relocated into the pit. Geochemical and mineralogical surveys of solids from throughout the site are needed to help assess the potential levels of this non-point acid drainage.

- Long-term, field-oriented hydrogeologic, mineralogic, and groundwater monitoring studies are needed to adequately assess the long-term response of the site to remedial actions.

### Lessons for the future

The severe acid drainage problems at Summitville were dictated by the site's geologic characteristics (high acid-generating capacity but low acid-consuming capacity of the deposit and its highly altered host rocks) and its climatic setting. The extent of Summitville's downstream effects (acidic, metal-bearing waters persisting more than 60 km downstream; Smith et al., this volume) was also a direct consequence of the surrounding volcanic terrane, which has extensive natural acid drainage from other mineralized areas and relatively small amounts of carbonate minerals to help naturally mitigate the effects of acid drainage. Summitville holds many lessons for the future development and remediation of geologically similar deposits:

- Future development of such deposits will likely be economically and environmentally difficult unless adequate precautions can be made to mitigate the acid-mine drainage.
- At sites in wet climates, extreme care must be taken to adequately isolate mine wastes from surface waters and oxygenated groundwaters. Similarly, the occurrence of alternating wet and dry cycles in mine wastes and workings must be reduced or stopped to prevent the formation of soluble salts and the large-scale flushing of these salts during storm or snowmelt events.
- Unless the climate is so dry as to preclude significant surficial drainage, development of similar deposits in geologic terranes containing rocks with little or no acid buffering capacity will likely be difficult environmentally. These terranes have little nearby material that can be used to mitigate problems on site, and allow the environmental effects of the site to reach much farther downstream without natural mitigation.
- The location of active seeps and fossil seeps (i.e., ferricrete deposits) should be carefully mapped prior to mining, so that acid-generating mine wastes will not be dumped onto active or potentially active springs.
- A detailed knowledge of site geology, hydrology, and the location of potential groundwater outflow points is necessary to better understand the potential effects resulting from plugging of underground mine workings. Mapping of active seeps and fossil seep deposits would help indicate where potential leakage could occur.

## ACKNOWLEDGMENTS

The authors wish to thank the U.S. EPA, U.S. Bureau of Reclamation, and Environmental Chemical Corporation (ECC) for their cooperation in this project. Shane Birdsey (ECC) provided significant help in locating seeps and ferricrete deposits.

## REFERENCES

- Enders, M.S., and Coolbaugh, M.F., 1987, The Summitville gold mining district, San Juan Mountains, Colorado, in Gee, W.R., and Thompson, T.B., eds., *Gold mineralization of Colorado's Rio Grande Rift*: Denver, Denver Region Exploration Geologists Society Fall Field Guidebook 19-20 Sept. 1987, p. 28-36.
- Gray, J. E., and Coolbaugh, M. F., 1994 in press, *Geology and geochemistry of Summitville, Colorado: An epithermal acid-sulfate deposit in a volcanic dome*: Economic Geology, Special Issue on Volcanic Centers as Exploration Targets, v. 89, no. 4.
- Gray, J. E., Coolbaugh, M. F., and Plumlee, G. S., 1993, *Geologic framework and environmental geology of the Summitville acid-sulfate mineral deposit*: U. S. Geological Survey Open-file Report 93-677, 29 p.
- Gray, J. E., Coolbaugh, M. F., Plumlee, G. S., and Atkinson, W. W., 1994 in press, *Environmental geology of the Summitville Mine, Colorado: Economic Geology, Special Issue on Volcanic Centers as Exploration Targets*, v. 89, no. 4.
- Perkins, M., and Nieman, G.W., 1982, *Epithermal gold mineralization in the South Mountain volcanic dome, Summitville, Colorado*: Denver Region Exploration Geologists Symposium on the genesis of Rocky Mountain ore deposits: Changes with time and tectonics, Denver, Colorado, Nov. 4-5, 1982, Proceedings, p. 165-171.
- Rye, R.O., Stoffregen, R., and Bethke, P.M., 1990, *Stable isotope systematics and magmatic and hydrothermal processes in the Summitville, CO gold deposit*: U.S. Geol. Survey Open-File Report 90-626, 31 p.
- Smith, K. S., Mosier, E. L., Montour, M. R., Plumlee, G. S., Ficklin, W. H., Briggs, P. H., and Meier, A. L., this volume, *Yearly and seasonal variations in acidity and metal content of irrigation waters from the Alamosa River, Colorado*: Summitville Forum Proceedings.
- Steven, T.A., and Lipman, P.W., 1976, *Calderas of the San Juan volcanic field, Southwestern Colorado*: U.S. Geol. Survey Prof. Paper 958, 35 pp.
- Steven, T.A., and Ratté, J.C., 1960, *Geology and ore deposits of the Summitville district, San Juan Mountains, Colorado*: U.S. Geol. Survey Prof. Paper 343, 70 p.
- Stoffregen, R. E., 1986, *Observations on the behavior of gold during supergene oxidation at Summitville, Colorado, and implications for electrum stability in the*

weathering environment: Applied Geochemistry, v. 1,  
p. 549-558.

Stoffregen, R. E., 1987, Genesis of acid-sulfate alteration  
and Au-Cu-Ag mineralization at Summitville, Colorado:  
Econ. Geol., v. 82, p. 1575-1591.

Stoffregen, R.E., and Alpers, C.N., 1987, Woodhouseite  
and svanbergite in hydrothermal ore deposits: Products  
of apatite destruction during advanced argillic alteration:  
Canadian Mineralogist, v. 25, p. 201-211.

## Q - PORPHYRY GOLD DEPOSITS OF THE ANDEAN CORDILLERA

John L. Muntean

Muntean, J.L. (1998): Porphyry Gold Deposits of the Andean Cordillera; in *Metallogeny of Volcanic Arcs*, B.C. Geological Survey, Short Course Notes, Open File 1998-8, Section Q.

### ABSTRACT

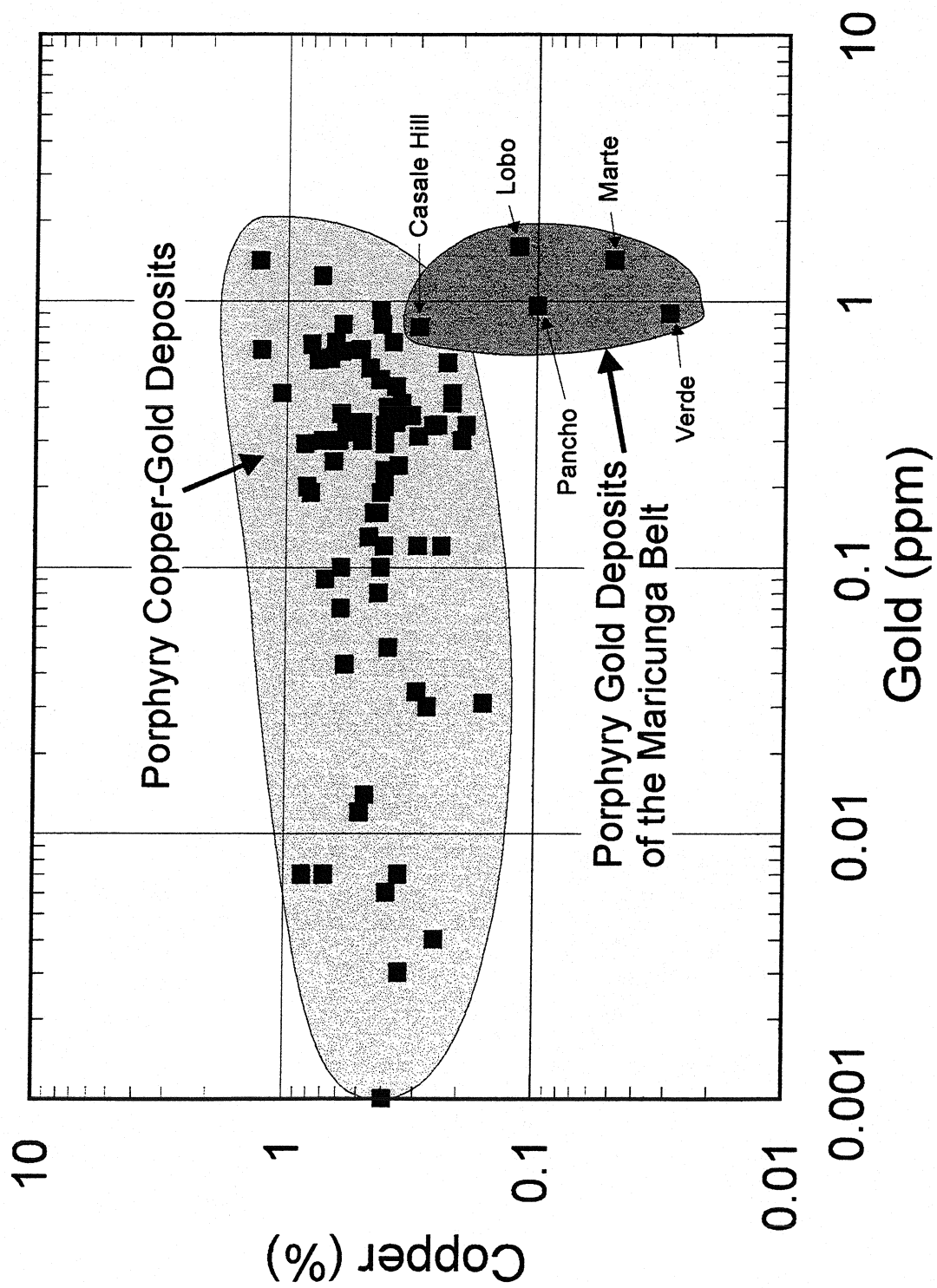
Porphyry gold deposits are large-tonnage (50-1000 MT), low-grade (0.5-2 g/t) deposits associated with narrow (1cm) quartz veinlets that are hosted mainly by subvolcanic porphyry intrusions of andesitic to dacitic composition. They have lower Cu:Au ratios than any known porphyry-type deposit and appear to be the result of shallow depths of formation. They are present throughout the Andean Cordillera and are best exemplified in the Maricunga belt of Northern Chile. A descriptive occurrence model is presented based on detailed studies of 4 deposits (Verde, Pancho, Casale Hill, Cavanha) in 3 districts (Refugio, Aldebaran, La Pepa). In addition, zones of advanced argillic alteration locally host high-sulfidation (HS) epithermal gold mineralization in close proximity to the porphyry-style mineralization.

Mineralization is characterized by 4 main vein types that are representative of specific zonal positions, both in time and space. The earliest, deepest veins are A quartz veinlets which range in character from hairline streaks of magnetite-biotite with minor quartz and chalcopyrite and K-feldspar alteration envelopes to sugary quartz veinlets with magnetite and chalcopyrite and no alteration envelopes. A veinlets, typical of porphyry copper deposits, are restricted to zones of potassic alteration in intrusive rocks. Lack of internal symmetry and non-matching vein walls suggest ductile conditions under lithostatic pressures. Hypersaline brine inclusions with multiple daughter minerals coexisting with vapor-rich inclusions indicate temperatures as high as nearly 700°C and depths <2 km. Banded veinlets, which are unique to porphyry gold deposits, occur mostly above and cross-cut A veinlets. Dark gray bands, whose color is due to increased density of vapor-rich fluid inclusions and m-scale grains of magnetite, commonly occur as symmetric pairs near the vein walls. The bands formed by flashing of hypersaline brines during episodic transitions from lithostatic to hydrostatic pressure. Loss of sulfur during flashing inhibited formation of Cu-sulfides. Rare liquid-rich fluid inclusions indicate temperatures 350°C at depths of 0.2-1.5 km. Pyrite, and local chlorite, calcite, and K-feldspar are found outside or cut the dark bands. Alteration envelopes are lacking. Banded veinlets do not form true stockworks and exhibit structural patterns that include steeply-dipping radial and shallowly-dipping concentric patterns. Zones of abundant banded veinlets generally contain 0.5-2 g/t Au and <0.1% Cu (hypogene), whereas zones of abundant A veinlets contain mostly <1 g/t Au and 0.1-0.4% Cu (hypogene). D veins are pyrite veins with sericitic alteration envelopes. They are widespread and cross-cut A and banded quartz veinlets. Silica ledges, typical of HS epithermal mineralization, are replacement veins of quartz+alunite alteration with local core zones of residual vuggy silica. They are mostly limited to overlying volcanic rocks.

A and banded quartz veinlets cut and are cut by intrusions indicating several cycles of intrusion-potassic alteration. A veinlets-banded veinlets during formation of porphyry-style mineralization. There is a spectrum of porphyry gold deposits ranging from the Casale Hill deposit at Aldebaran, fairly typical of gold-rich porphyry copper deposits, to the Verde deposit at Refugio -- a true porphyry gold deposit.



Potassic alteration and A veinlets are strongly developed at Casale Hill, whereas they are absent at Verde. Banded quartz veinlets and propylitic alteration are dominant at Verde, whereas they only occur at the upper levels of Casale Hill. The Pancho deposit at Refugio and the Cavancho deposit at La Pepa are telescoped systems in which banded veinlets overprint and spatially overlap zones of potassic alteration and A veinlets. D veins represent an irreversible temporal transition to temperatures <400°C, brittle fracturing, hydrostatic fluid pressures, and higher sulfide contents. D veins are nowhere truncated or cross-cut by intrusions, A veinlets, or banded veinlets.  $^{40}\text{Ar}/^{39}\text{Ar}$  data indicate alunite in silica ledges forms both synchronously with (Casale Hill) or later than (La Pepa, 140,000 to 900,000 year gap at the 95% confidence level) porphyry-style mineralization. Of the 3 districts studied, only at La Pepa has HS epithermal-style mineralization been mined from silica ledges at an average gold grade of about 20 g/t. At La Pepa gold-bearing D veins appear to be feeders to the silica ledges that zone upward from enargite- to barite-bearing near the surface. Timing of the irreversible switch to brittle, hydrostatic conditions relative to the life of the hydrothermal system determines how much porphyry-style mineralization forms relative to HS epithermal mineralization. Formation of HS epithermal mineralization appears to be dependent upon the ability of residual hypersaline brines to reach the surface during the late brittle, hydrostatic conditions or the ability of late, deeply sourced magmatic fluids to avoid hitting the two-phase field (and condensing a brine) upon ascent to the surface.



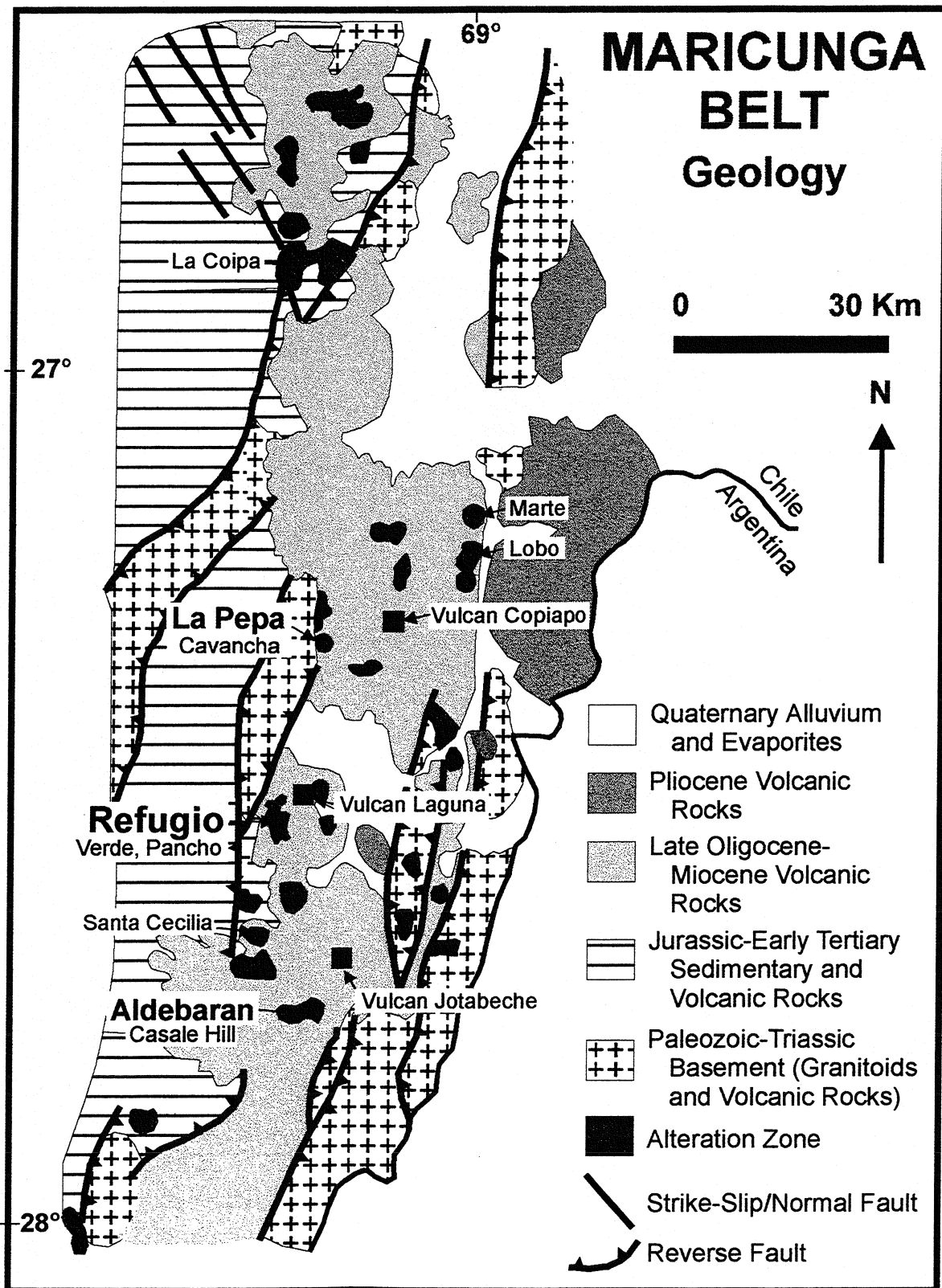


Table 1. Summary of Vein Types

Vein Types	Vein Minerals	Alteration Halo	Structural Style	Texture of Quartz and Fluid Inclusions
A Quartz Veinlets	Qtz+mgt±bio±cpy <u>Verde (Refugio)</u> absent <u>Pancho (Refugio)</u> 1. bio+qtz+mgt±(pyr, spl) 2. mgt+qtz+cpy±(chl, apa, ilm, rut) 3. qtz+mgt+cpy±spc±(chl, bio, bar, bor) 4. qtz+cpy±(py) <u>Casale Hill (Aldebaran)</u> 1. bio±(mgt, qtz, cpy) 2. mgt±qtz±(cpy) 3. qtz+mgt+bio±(cpy) 4. qtz+mgt+cpy±(ksp, spc, bio, chl, ser, tou, gyp, gal) 5. qtz+ksp+spc±cpy 6. qtz+cpy±(tou) <u>Cavancha (La Pepa)</u> 1. mgt±(bio, qtz) 2. qtz+py+mgt±(cpy)	Common ksp-rich envelope with narrow subtypes. <u>Pancho (Refugio)</u> Subtype 1 has local narrow envelope enriched in bio or ksp. Subtype 2 commonly has narrow envelope of ksp-qtz. Subtypes 3 and 4 do not have alteration envelopes. <u>Casale Hill (Aldebaran)</u> Subtypes 1-3 commonly have ksp-rich envelope. Subtypes 4-6 have local ksp-rich envelope. <u>Cavancha (La Pepa)</u> no envelopes	Lack of internal symmetry, walls commonly do not match up. ≤2cm, mostly <1mm. Early veinlets are irregular, narrow, and discontinuous; later veinlets are wider, more continuous, and straighter. <u>Pancho (Refugio)</u> Subtypes 1 and 2 are mostly <0.2 mm, discontinuous, and have wavy walls. Subtypes 3 and 4 are mostly <1-2 mm wide, continuous, and have slightly wavy walls. <u>Casale Hill (Aldebaran)</u> Subtypes 1 and 2 are mostly <0.1mm, discontinuous, irregular walls. Subtype 3 is mostly <0.2mm, slightly more continuous, wavy to slightly wavy walls. Subtypes 4-6 are ≤1cm, mostly < 1 mm, continuous, wavy to slightly wavy walls <u>Cavancha (La Pepa)</u> Subtype 1 is mostly < 0.2 mm, discontinuous, irregular walls. Subtype 2 is ≤2 cm wide, mostly < 1mm, continuous, slightly wavy walls.	Anhedral granular vitreous quartz with common "sugary" appearance. Hypersaline liquid-rich inclusions with multiple daughter minerals coexisting with more abundant vapor-rich inclusions.

Table 1. Summary of Vein Types (continued)

Vein Types	Vein Minerals	Alteration Halo	Structural Style	Texture of Quartz and Fluid Inclusions
Banded Quartz Veinlets	<p>Qtz+mgt+py (mgt in dark bands; py post-dates dark bands)</p> <p><u>Verde and Pancho (Refugio)</u>  banded portion: qtz+mgt±(cpy, bor, spl);  unbanded portion: qtz, py, mgt, cal, ksp,  spn, chl, cly, (ill, cpy, spl, gal, mol, cas,  ilm, epi, gar, gyp)</p> <p><u>Casale Hill (Aldebaran)</u>  banded portion: qtz+mgt±(cpy, bor)  unbanded portion: qtz, py, tou, ill, spc</p> <p><u>Cavancha (La Pepa)</u>  banded portion: qtz+mgt±(cpy)  unbanded portion: qtz, py</p>	None	<p>Slightly wavy walls that match up.  ≤2cm, mostly &lt;2mm.  Commonly occur as sheeted sets.  Dark bands commonly occur as  symmetric pairs near the vein walls.  Local vuggy centers.</p> <p><u>Pancho (Refugio)</u>  Bands are commonly discontinuous and  "streaked", local gradations with AB  veinlets.</p> <p><u>Cavancha (La Pepa)</u>  Bands are commonly discontinuous and  "streaked", commonly gradational with  AB veinlets.</p>	<p>Fine-grained granular quartz, locally elongated perpendicular to vein walls.  &gt;99% vapor-rich inclusions, &lt;1% liquid-rich inclusions with common halite daughter minerals.  No difference between banded and unbanded portion except for very high abundance of μm-sized vapor-rich inclusions in banded portions.</p>

Table 1. Summary of Vein Types (continued)

Vein Types	Vein Minerals	Alteration Halo	Structural Style	Texture of Quartz and Fluid Inclusions
D Veins	<p>Py+qtz±(cpy, mol)</p> <p><u>Verde</u> absent</p> <p><u>Pancho</u> py+qtz±(cpy, mol)</p> <p><u>Casale Hill (Aldebaran)</u> py+qtz±cpy±(spc) polymetallic subtype: qtz+bar+py+cpy+spl+ten/tet+gal+ser</p> <p><u>Cavanacha (La Pepa)</u> py+qtz±(cpy, mol, ten, bor, ena, gal, cas)</p>	Qtz+ser+py±(tou)	<p>Fairly straight walls. mm to cm-scale widths. Locally vuggy.</p>	<p>Common growth-zoned quartz with crystal terminations. Liquid-rich inclusions with halite daughter minerals coexisting with vapor-rich inclusions. Inclusions have irregular shapes.</p>

Vein Types	Vein Minerals	Alteration Halo	Structural Style	Texture of Quartz and Fluid Inclusions
Silica Ledges	Qtz+alu+py+rut  <u>Verde, Pancho, Refugio</u> qtz+alu+py+rut±(kao/dic, dia, pyo)  <u>Aldebaran</u> 1. qtz+alu+py+rut±pyo (near Casale Hill) 2. vuggy silica±alu±barite (above 4800m)±(ena, dia, pyo) (near Cathedral Peak)  <u>La Pepa</u> upper zone: qtz-alu±vuggy silica±chd silica+py+rut+bar±(ena, ida) lower zone: qtz-alu±vuggy silica+py+rut+chd silica+ena±(bar, cov)	Local inner qtz+kao+py to local outer qtz+ser+pyr	<5m wide replacement veins	Fine-grained granular to jigsaw-like quartz. Local coexisting irregular-shaped liquid-rich inclusions coexisting with vapor-rich inclusions in late quartz crystals lining vuggy silica.

Abbreviations: alu: alunite; apa: apatite, bar: barite, bio: biotite, bor: bornite, cal: calcite; cas: cassiterite, chd: chalcocite, cpy: chalcopyrite, chl: chlorite, cly: clay, cov: covellite, dia: diasporite, dic: dickite, ena: enargite, epi: epidote, gal: galena, gar: garnet, gyp: gypsum, ida: idaite, ill: illite, ilm: ilmenite, ksp: K-feldspar, lxn: leucosene, mgt: magnetite, mol: molybdenite, olg: oligoclase, py: pyrite, pyo: pyrophyllite, qtz: quartz, rut: rutile, ser: sericite, spc: specular hematite, spl: sphalerite, spn: sphene, ten: tennantite, tet: tetrahedrite, tou: tourmaline

Table 1. Summary of Vein Types (continued)

Table 2. Summary of the Characteristics of Early Mineralization

Deposit	Gold Grade (ppm) <sup>a</sup>	Estimated Hypogene Copper Grade (%) <sup>b</sup>	Copper %/ Gold (ppm) Ratio	Potassic Alteration	A Quartz Veinlets	Banded Quartz Veinlets	Propylitic Alteration	Magnetite/ Hematite	Total Sulfide
Verde (Refugio)	0.88	0.03	0.03	absent	absent	abundant	central	1-4%	<1%
Pancho (Refugio)	0.85	0.1	0.1	central mgt- ksp-olg out to bio-mgt	moderate, lower levels	abundant	peripheral	2-5%	<1%
Cavancha (La Pepa)	1	0.1	0.1	bio-mgt	moderate	moderate	absent?	<2.5%	<2.5%
Casale Hill (Aldebaran)	0.78	0.3	0.4	strong	abundant, lower levels	minor, higher levels	peripheral	4-7%	<1%

<sup>a</sup> Verde: geological reserve (Brown and Rayment, 1991); Pancho: geological reserve (Flores, 1993); Cavancha: crude estimate based on inspection of drill hole assays; Casale Hill : resource (Bema Gold news release, May 15, 1997)

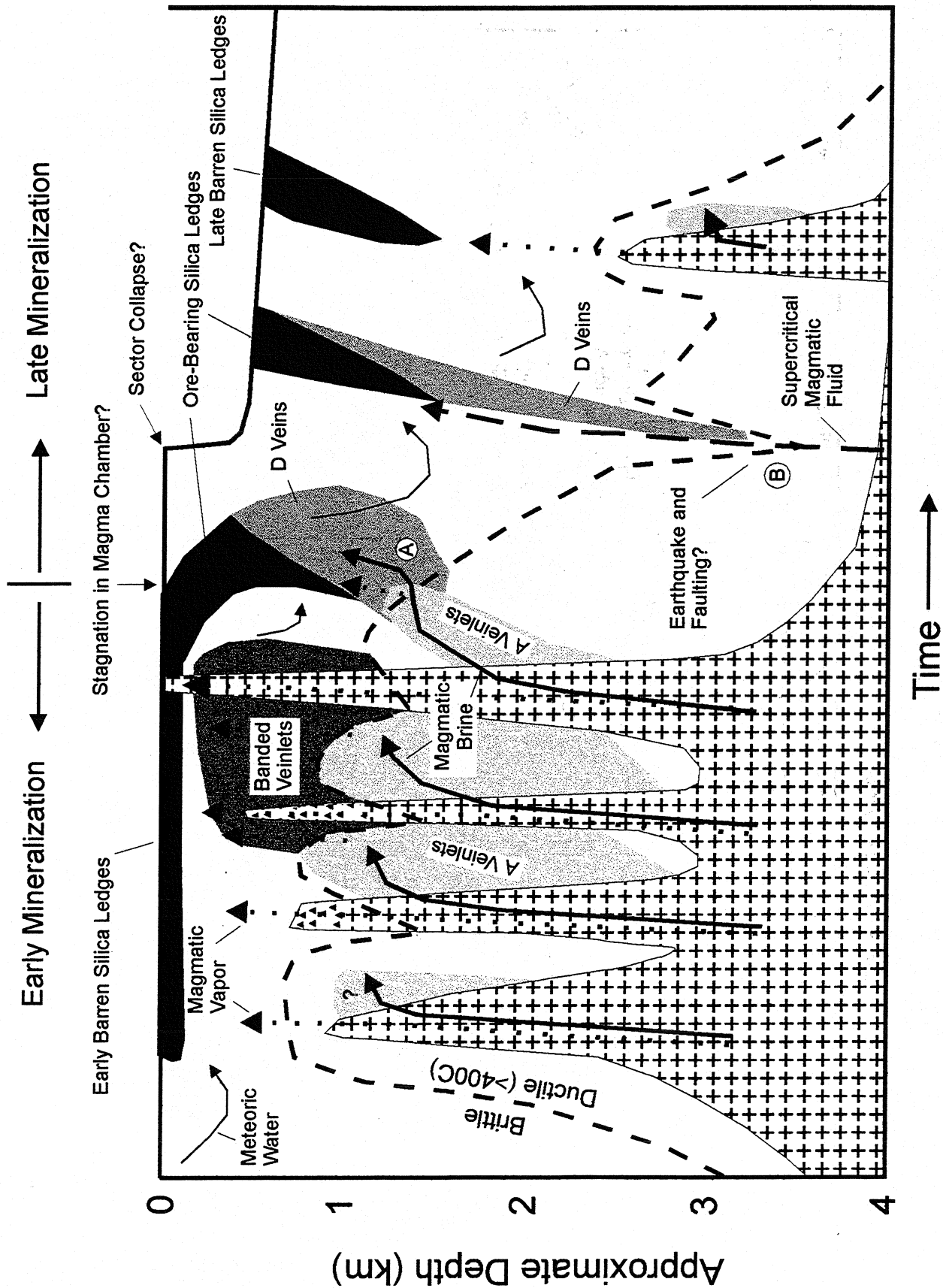
<sup>b</sup> Verde: (Flores, 1993); Pancho and Cavancha: crude estimate based on inspection of drill hole assays; Casale Hill : resource (Bema Gold news release, May 15, 1997)

Mineral abbreviations are found in Table 1.



Deposit	Pyrite-Albite-Clay Alteration	D Veins	Total Sulfide <sup>a</sup>	Silica Ledges	Supergene Effects
Verde (Refugio)	peripheral	absent	2-4%	qtz-alu, < 1ppm Au	deeper oxidation underneath late volcanic rocks
Pancho (Refugio)	peripheral, higher levels	very minor	2-4%	qtz-alu, < 1ppm Au	shallow oxidation; minor covellite
Cavancha (La Pepa)	widespread, higher levels	moderate (Au-bearing)	3-6%	(district) qtz-alu/vuggy silica/chd silica; local high grade Au-(Cu)	shallow oxidation; 15-70m thick chalcocite blanket, (0.1-0.5% Cu)
Casale Hill (Aldebaran)	peripheral, higher levels	moderate; local polymetallic veins	2-4%	(district) qtz-alu, local vuggy silica; mostly < 1ppm Au	variable oxidation; 30-40m thick chalcocite blanket, (0.5-1.5% Cu)

<sup>a</sup> Total sulfide refers to zones of pervasive pyrite-albite-clay alteration with or without D veins; it does not include silica ledges. Mineral abbreviations are found in Table 1.



Downloaded from https://www.cambridge.org/core

